

# nature

INTERNATIONAL WEEKLY JOURNAL OF SCIENCE

Volume 320 No 6058 13-19 March 1986 £1.90

INVESTIGATING  
THE PARANORMAL

A. Batter  
OH-S. S.  
311

✓ 4912

# Mass ion

## The new force in b.

ZetaPrep® Technology. Engineered for mass ion exchange. Powered with a unique solid matrix. Thrusting you into a new age of upstream purification. Boosting mass flow and volume flow with results that outdate every other known separation method. Giving you quantum savings in time and money.

### Unique solid matrix!

Designed for highly efficient, ultra-fast extraction of proteins, peptides and enzymes, the ZetaPrep solid matrix comes in a cartridge that's completely self-contained. With its unique, multi-directional radial flow, this patented rigid format offers optimal surface area for rapid bulk binding, plus the strength to withstand high flow rates.

*All ZetaPrep housings and cartridges are completely sterilizable and compatible with standard equipment. Shown here is the ZetaPrep 100 for laboratory separations.*

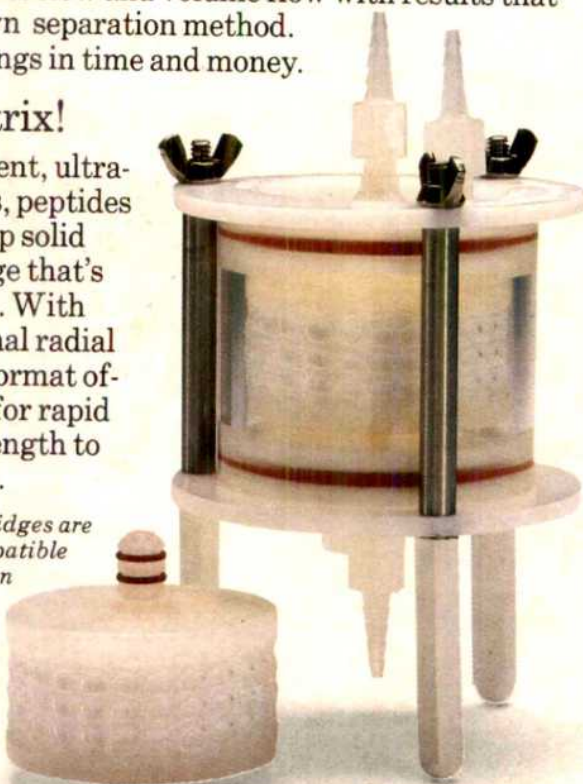
### Economics you just can't ignore!

Capable of one-step purification and concentration with up to 80% purity or more, ZetaPrep will slash your production costs to a fraction of what they are today. Because ZetaPrep is so easy to operate, simple to automate and efficient in use, you'll cut expensive man hours to a minimum.

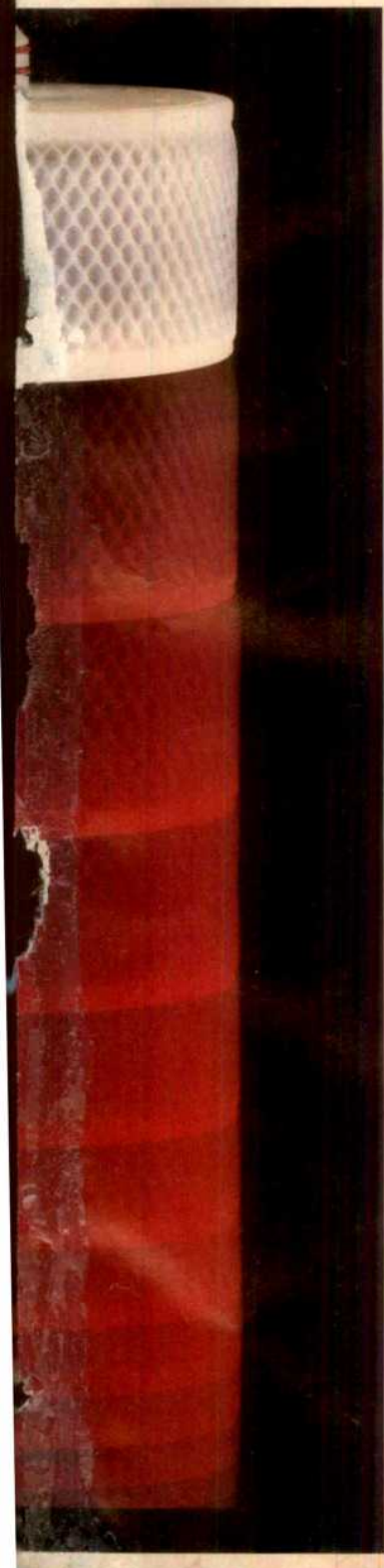
ZetaPrep's incredible flow lets you radically reduce total processing time. Gets you fast binding, wash and elution flow rates. And at least 10 times higher throughput. With no more packing problems. No more fines removal. Just all the benefits of a totally enclosed system—and yields that are truly astounding.

### Amazing scale-up potential

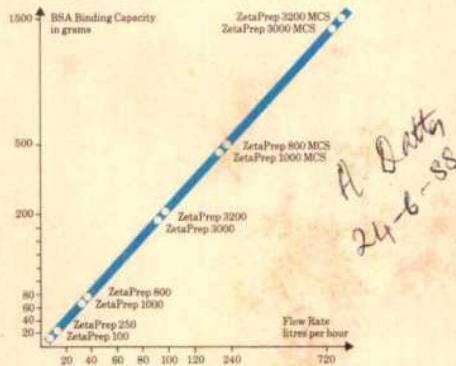
LKB's comprehensive range of ZetaPrep cartridges and Multi-Cartridge Systems lets you select different sizes, extend in series or even couple in parallel for virtually unlimited flow rate and process capacity. With DEAE, QAE and SP functional groups, you can now exploit this amazing scale-up potential from lab, through pilot to fullscale industrial production. In biotechnology, pharmaceuticals or any other process that needs cost-effective purification of proteins and biopolymer products.



# exchange process engineering!

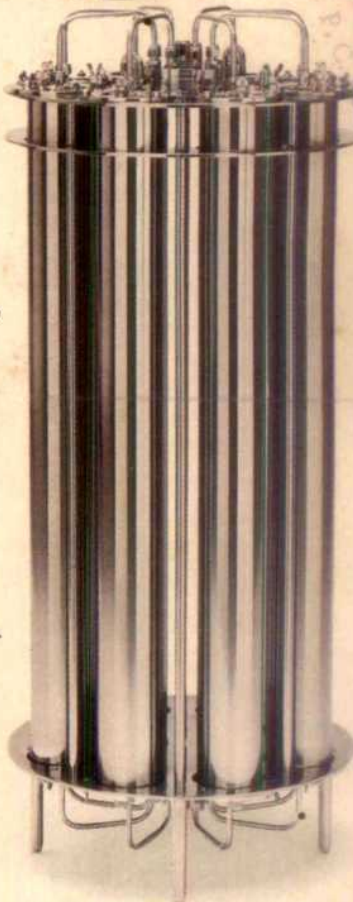


Scale up to 720 liters per hour



Seeing is believing!

Find out how much you can win. That'll convince you just why ZetaPrep Technology has been so successful in such a short time. Why many of the world's leading biotech and drug companies have gone from initial trials to routine industrial processing in just a few months. Why you should try ZetaPrep yourself. Post this coupon today, and we'll send you technical information, full details on test kits available and all prices. Your nearest LKB office delivers fast.



Available also in plastic housing, this ZetaPrep 3000 Multi-Cartridge System, is used for full-scale industrial bioprocessing.



Reader Service No. 40

LKB-Produkter AB, Box 305, S-161 26 Bromma, Sweden. Tel. +46(8)98 00 40, telex 10492  
Antwerp (03) 218 93 35 · Athens-Middle East +30(1) 894 73 96 · Copenhagen (01) 29 50 44 · Hongkong (852) 5-555555  
London (01) 657 88 22 · Lucerne (041) 57 44 57 · Madras (044) 45 28 74 · Moscow (095) 256-9002 · Munich (089) 85 830  
Paris (06) 928 65 07 · Rome (06) 39 90 33 · Stockholm (08) 98 00 40 · Tokyo (03) 293-5141 · Turku (021) 678 111  
Vienna +43 (222) 92 16 07 · Washington (301) 963 3200 · Zoetermeer (079) 31 92 01  
Over 60 qualified representatives throughout the world.

## Get more facts fast!

- Please send me more information    I'd like to try ZetaPrep in my lab  
 Have your technical representative contact me

Name \_\_\_\_\_

Title/Dept \_\_\_\_\_

Organization \_\_\_\_\_

Address \_\_\_\_\_

Tel. No. \_\_\_\_\_

Although very few people have actually seen a Giant Panda, it is probably the world's most familiar and lovable animal.

Unfortunately, it has a very low reproduction rate. And there is an acute shortage of its bamboo food supply. So the Giant Panda is threatened with extinction.

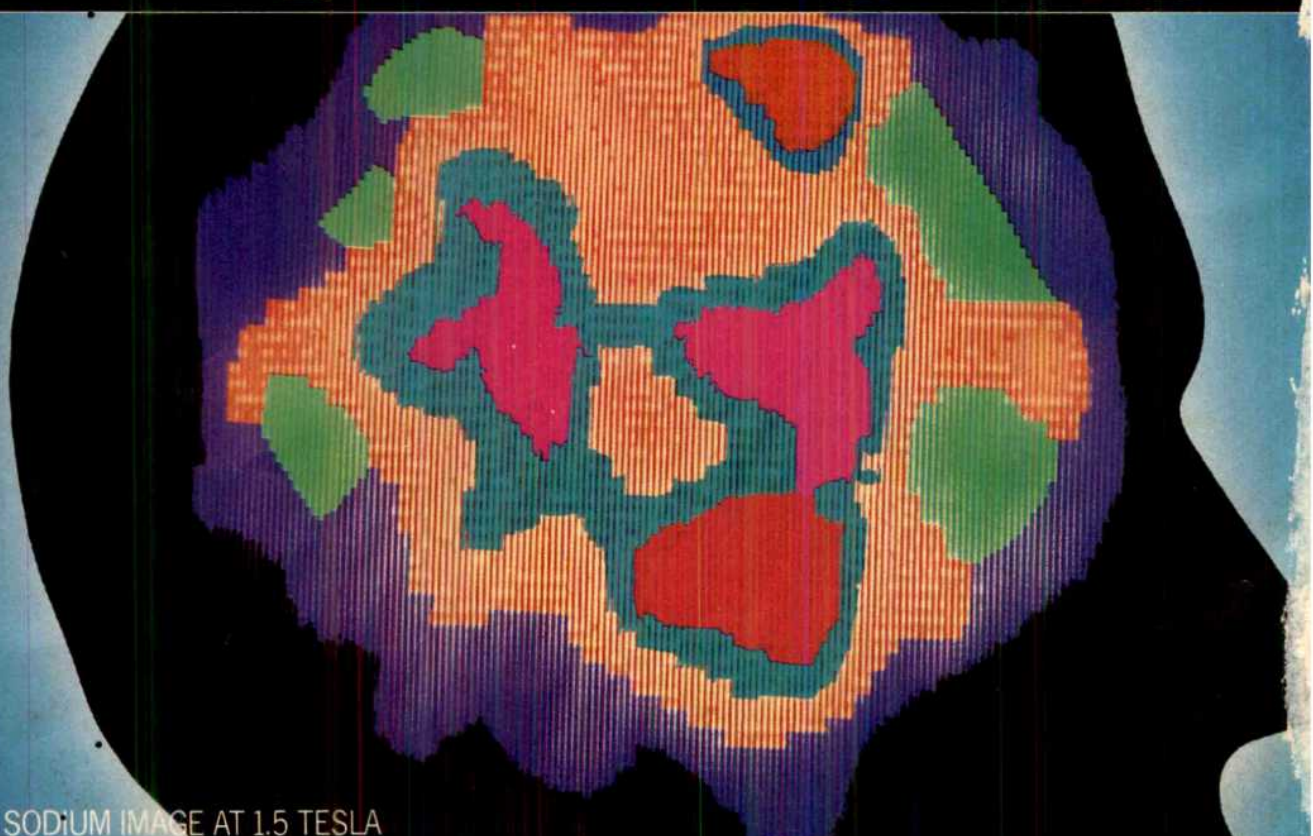
To solve these and other problems, the World Wildlife Fund and the Peoples Republic of China are cooperating in a major Panda Conservation Programme. Philips is helping, too.

At Wolong Natural Reservation in Sichuan Province, a Philips atomic absorption spectrophotometer is used to research alternative areas for growing bamboo, and to analyse the nutritional value of its edible shoots.

Panda blood and faeces, too, are analysed to monitor the vitamins and minerals necessary for their survival.



# Philips - helping re



IN-VIVO SODIUM IMAGE AT 1.5 TESLA

CUL-H06855-311-PP3438

# nature

NATURE VOL. 320 13 MARCH 1986

LIBRARY COMPLEX

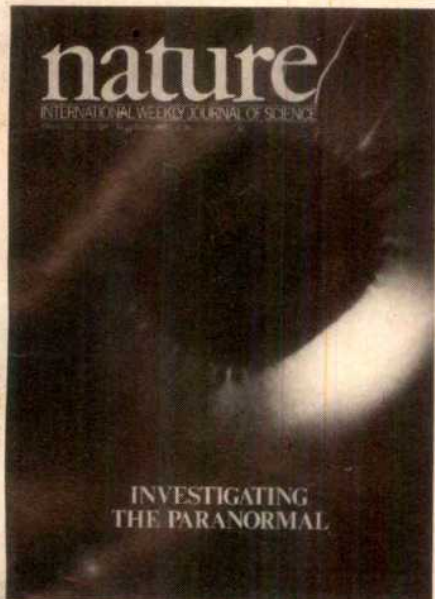
Departments of:

Chemical Engineering

Chemical Technology

Plastics &amp; Rubber Technology

92, A.P.C. Road, Calcutta



A Kirlian photograph showing coronal streamers around a finger tip and key induced by a high voltage, high frequency electrical field. The particularly bright streamers bridge the 0.25 cm distance between the finger tip and the key. Although the corona has a simple physical explanation it has been erroneously interpreted as the 'aura' or 'psychic energy' reported by clairvoyants. See page 119. Photo: Jerry Andrus.

## OPINION

- Tough talk on surrogate birth 95  
Future for the birds

## NEWS

- AIDS 96  
Halley's comet 97  
Biotechnology 100  
Swiss prize shared  
Plutonium dumping? 101  
Prizes 101  
US science and technology  
Strategic Defense Initiative 102  
SSC in doubt  
Canadian budget  
Nuclear winter 103

## CORRESPONDENCE

- South African science/Chinese forest/  
Bigfoot/etc. 104

## NEWS AND VIEWS

- A child's guide to Soviet science 105  
Laser fusion turned inside out  
R G Evans & M H Key 106  
Antigen binding and T cells  
N A Mitchison 106

## Biomarkers for ancient climates

- Erwin Suess 107  
A *Drosophila* 'clock' protein? 108  
John Merriam  
Visual cortex: cholinergic input  
and plasticity 109  
A M Sillito  
Prehistoric life in the  
Lake Victoria basin 110  
David W Phillipson  
Carnivore dominance and herbivore  
coexistence in Africa 112  
Jared M Diamond

## SCIENTIFIC CORRESPONDENCE

- Aids therapy by blocking CD4<sup>+</sup> cells 113  
A Singer & G M S Shearer  
Serotherapy of AIDS and pre-AIDS  
syndrome 113  
H F Sewell & F Walker  
Immunosuppressants in patients  
with AIDS 114  
A Hausen, M P Dierich, D Fuchs,  
P Hengster, G Reibnegger,  
T Schulz, E R Werner & H Wachter  
Genetic prediction of cystic fibrosis 114  
M E Pembrey & S Malcom

## BOOK REVIEWS

- Victorians abroad — three books on  
exploration and natural history  
in the nineteenth century 115  
David E Allen  
Surgeons at the Bailey: English  
Forensic Medicine to 1878 116  
By T Rogers Forbes  
H R F Keating  
Annual Review of Cell Biology,  
Vol. 1 1985  
G E Palade, B M Alberts  
and J A Spudich, eds  
Dennis Bray  
About Science  
by B Barnes 117  
Philip Gummell  
The Thalamus  
by E G Jones  
K E Webster  
Biochemistry of Dioxygen  
by L L Ingraham and D L Meyer  
Irwin Fridovich

## COMMENTARY

- Investigating the paranormal 119  
D F Marks

## REVIEW ARTICLE

- Heavy-electron metals 124  
Z Fisk, H R Ott,  
T M Rice & J L Smith

## ARTICLES

- Molecular stratigraphy: a new tool  
for climatic assessment 129  
S C Brassell, G Eglinton,  
I T Marlowe, U Pflaumann  
& M Sarnthein

- Human oestrogen receptor cDNA:  
sequence, expression and  
homology to v-erb-A 134  
S Green, P Walter, V Kumar,  
A Krust, J-M Bornert,  
P Argos & P Chambon

## LETTERS TO NATURE

- Strong breathing of the hydrogen  
coma of comet Halley 140  
E Kaneda, K Hirao, M Takagi,  
O Ashihara, T Itoh & M Shimizu

- Electromagnetic angular momentum  
transport in Saturn's rings 141  
C K Goertz, G E Morfill, W-H Ip,  
E Grün & O Havnes

- Plasmatization and recondensation of  
the saturnian rings 143  
W-H Ip

- Random fluctuations versus  
Poynting-Robertson drag  
on interplanetary dust grains 146  
M K Wallis

- Geomagnetic reversal spurs and  
episodes of extraterrestrial  
catastrophism 148  
P C Pal & K M Creer

- Aluminium/silicon disordering and  
melting in sillimanite at  
high pressures 151  
T J B Holland & M A Carpenter

- Rapid pressurization experiments  
on a liquid Al-Mn alloy 153  
J A Sekhar & T Rajasekharan

- Phenol and HC1 at 550 °C yield a large  
variety of chlorinated toxic compounds 155  
G Eklund, J R Pedersen  
& B Strömberg

- Measurement of organic carbon in  
polar snow samples

- M S Twickler, M J Spencer,  
W B Lyons & P A Mayewski 156

- Significance of atmospheric-derived  
fixed nitrogen on productivity  
of the Sargasso Sea 158  
A Knap, T Jickells,  
A Pszenny & J Galloway

Contents continued overleaf

# At last! An easy to use gene machine at an affordable price.



Now any laboratory working with oligonucleotides can perform automated DNA synthesis simply, reliably and affordably—whatever the volume demand—with the new Pharmacia Gene Assembler™. This high-quality system combines state-of-the-art technology and chemistry with simplicity of design and operation.

#### Integral

The Gene Assembler is a complete system. The compact, bench-top unit contains everything you need to synthesize active DNA: hardware, software, Pharmacia's own reagents, and a comprehensive handbook. It even includes automatic colorimetric monitoring and a built-in printer/plotter that gives you a permanent record of each synthesis in both peaks and print.

#### Simple

The Gene Assembler was designed for maximum ease of operation. You just insert a ready-to-use cassette of unique, new Mono Beads™ into one of the two column reactors, type in the desired sequence, and let the machine do the rest. It's not only self-contained, it's very nearly self-sufficient!

#### Flexible

You don't need any peripheral hardware (an expensive "option" with some competitors).

The Gene Assembler is preprogrammed for everything from standard syntheses to sophisticated mixed bases. And it's versatile enough to allow user-determined reprogramming—e.g. for modified nucleotides. It can also easily interface with a variety of other microcomputers for even greater capacity.

#### Reliable

As with all Pharmacia equipment, the Gene Assembler consists of high-quality components, each designed to give you years of dependable service. Of course, it's also backed by Pharmacia's established, worldwide service network and warranty.

#### Affordable

Pharmacia's expertise in biotechnology enabled us to optimize components to form a dedicated system. Therefore, designing and manufacturing the Gene Assembler cost substantially less than competitive machines. That saving is passed along to you. All in all, this high-quality, high-performance system is the most cost-effective and efficient DNA synthesizer you can buy.

#### Available

To find out more, ask your Pharmacia representative to send you the comprehensive, illustrated brochure. Do it today.

Pharmacia Headquarters: Pharmacia AB,  
S-751 82 Uppsala, Sweden. Tel: (018) 16 30 00.

In North America: Pharmacia Inc.,  
800 Centennial Avenue, Piscataway,  
NJ 08854, USA. Tel: (201) 457-8121.

Reader Service No.46



**Pharmacia**

Molecular Biology Division

Your Link With The Future

RPA38

## CONTENTS

**That important research article you've been looking for located instantly!**



If you store your copies of *Nature* for future reference, then the annual index of subject and author is an essential part of your collection. These comprehensive annual indexes are available for all issues of *Nature* from 1971 to 1985.

Prices and address for orders are set out below.

**Annual Subscription Prices**

UK & Irish Republic	£104
USA & Canada	US\$240
Australia, NZ & S. Africa	
Airspeed	£150
Airmail	£190
Continental Europe	£125
India	£120
Japan	£190
Rest of World	Y90000
Surface	£120
Airmail	£180

**Orders (with remittance) to:**

USA & Canada	UK & Rest of World
Nature	Nature
Subscription Dept	Circulation Dept
PO Box 1501	Brunel Road
Neptune	Basingstoke
NJ 07753	Hants RG21 2XS, UK
USA	Tel: 0256 29242

(The addresses of *Nature*'s editorial offices are shown facing the first editorial page)

**Japanese subscription enquiries to:**

Japan Publications Trading Company Ltd  
2-1 Sarugaku-cho 1-chome  
Chiyoda-ku, Tokyo, Japan

Tel: (03) 292 3755

**Personal subscription rates:** These are available in some countries to subscribers paying by personal cheque or credit card. Details from:

**USA & Canada**

Nature                   UK & Europe  
65 Bleecker Street     Felicity Parker  
New York               Nature  
NY 10012, USA        4 Little Essex Street  
Tel: (212) 477-9600   London WC2R 3LF, UK  
Tel: 01-836 6633

**Back issues:** UK, £2.50; USA & Canada, US\$6.00 (surface), US\$9.00 (air); Rest of World, £3.00 (surface), £4.00 (air)

**Binders**

Single binders: UK, £5.25; USA & Canada \$11.50; Rest of World, £7.75. Set of four: UK, £15.00; USA & Canada \$32.00; Rest of World, £22.00

**Annual indexes (1971-1985)**

UK, £5.00 each; Rest of World, \$10.00

**Nature First Issue Facsimile**

UK, £2.00; Rest of World (surface), \$3.00; (air) \$4.00

**Nature in microform**

Write to University Microfilms International, 300 North Zeeb Road, Ann Arbor, MI 48106, USA

**Isoprenoid thiophenes: novel products of sediment diagenesis?**

S C Brassell, C A Lewis,  
J W de Leeuw, F de Lange,  
& J S Sinninghe Damsté      160

**Floral evidence for Cretaceous chloranthoid angiosperms**

E M Friis, P R Crane & K R Pedersen      163

**Early forest clearance and environmental degradation in south-west Uganda**

A Hamilton, D Taylor & J C Vogel      164

**A lethal mutation in mice eliminates the slow calcium current in skeletal muscle cells**

K G Beam, C M Knudson  
& J A Powell      168

**Spermatogenic failure in male mice lacking H-Y antigen**

P S Burgoine, E R Levy  
& A McLaren      170

**Modulation of visual cortical plasticity by acetylcholine and noradrenaline**

M F Bear & W Singer      172

**T-cell recognition of antigen and the Ia molecule as a ternary complex**

J D Ashwell & R H Schwartz      176

**T-cell-mediated association of peptide antigen and major histocompatibility complex protein detected by energy transfer in an evanescent wave-field**

T H Watts, H E Gaub  
& H M McConnell      179

**Specific interaction between the p53 cellular tumour antigen and major heat shock proteins**

O Pinhasi-Kimhi, D Michalovitz,  
A Ben-Ze'ev & M Oren      182

**Product of per locus of *Drosophila* shares homology with proteoglycans**

F R Jackson, T A Bargiello,  
S-H Yun & M W Young      185

**Existence of distinct sodium channel messenger RNAs in rat brain**

M Noda, T Ikeda, T Kayano,  
H Suzuki, H Takeshima,  
M Kurasaki, H Takahashi  
& S Numa      188

**Multiple conformations of a protein demonstrated by magnetization transfer NMR spectroscopy**

R O Fox, P A Evans & C M Dobson      192

**MATTERS ARISING****Predisposition to helminth infection in man**

A W Cheever  
Reply: R M Anderson,  
J A Crombie & R M May      195

**Cause of the 'inhibitor' phenotype in the haemophilias**

F Giannelli & G G Brownlee      196

**MISCELLANY**

100 years ago      111

Books received      197

**NATURE CLASSIFIED****Professional appointments —****Research posts — Studentships —****Fellowships — Conferences —****Courses — Seminars — Symposia:**

Back Pages

**Next week in *Nature*:**

- Comet as rubble
- Solar System deuterium
- Half-life of rhenium-187
- Poincaré conjecture proved
- Palaeotemperatures still here
- Visual pathway development
- New prochlorophyte
- Rapid bacterial recognition
- Novel ribosomes
- Retroviruses for gene therapy
- Gene therapy ethics

**GUIDE TO AUTHORS**

Authors should be aware of the diversity of *Nature*'s readership and should strive to be as widely understood as possible.

**Review articles** should be accessible to the whole readership. Most are commissioned, but unsolicited reviews are welcome (in which case prior consultation with the office is desirable).

**Scientific articles** are research reports whose conclusions are of general interest or which represent substantial advances of understanding. The text should not exceed 3,000 words and six displayed items (figures plus tables). The article should include an italic heading of about 50 words.

**Letters to *Nature*** are ordinarily 1,000 words long with no more than four displayed items. The first paragraph (not exceeding 150 words) should say what the letter is about, why the study it reports was undertaken and what the conclusions are.

**Matters arising** are brief comments (up to 500 words) on articles and letters recently published in *Nature*. The originator of a Matters Arising contribution should initially send his manuscript to the author of the original paper and both parties should, wherever possible, agree on what is to be submitted.

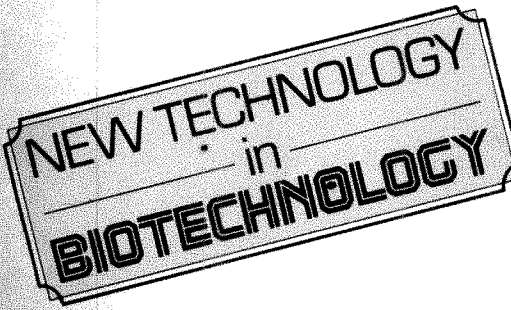
Manuscripts may be submitted either to London or Washington. Manuscripts should be typed (double spacing) on one side of the paper only. Four copies are required, each accompanied by copies of lettered artwork. No title should exceed 80 characters in length. Reference lists, figure legends, etc., should be on separate sheets, all of which should be numbered. Abbreviations, symbols, units, etc. should be identified on one copy of the manuscript at their first appearance.

References should appear sequentially indicated by superscripts, in the text and should be abbreviated according to the *World List of Scientific Periodicals*, fourth edition (Butterworth 1963-65). The first and last page numbers of each reference should be cited. Reference to books should clearly indicate the publisher and the date and place of publication. Unpublished articles should not be formally referred to unless accepted or submitted for publication, but may be mentioned in the text.

Each piece of artwork should be clearly marked with the author's name and the figure number. Original artwork should be unlettered. Suggestions for cover illustrations are welcome. Original artwork (and one copy of the manuscript) will be returned when manuscripts cannot be published.

*Requests for permission to reproduce material from *Nature* should be accompanied by a self-addressed (and, in the case of the United Kingdom and United States, stamped) envelope.*

# WHAT IMPACT ARE NEW BIOTECHNOLOGY TECHNIQUES HAVING ON MEDICINE WORLDWIDE TODAY?



Come to Nature's 7th International Conference in London on Molecular Biology in Medicine 1986 for all the up to date facts – and a look into the near future.

## MOLECULAR BIOLOGY IN MEDICINE

a survey of its achievements and its potential  
JUNE 18-20 1986 – LONDON

It is clear that the modern techniques of biotechnology are set to have a major impact on medicine. Over the next few years many new opportunities will emerge. This important conference will provide a wide-ranging survey of the most recent research in the fast changing field of molecular biology in medicine, and a look into the future. If you want an opportunity to see and hear for yourself what leading exponents have achieved in recent years – and to learn what new opportunities are on the horizon, come and join us.

### JOIN US AT NATURE'S 7TH INTERNATIONAL CONFERENCE, TO BE HELD AT THE LONDON WEST HOTEL, JUNE 18-20 1986.

REGISTER NOW TO ENSURE YOUR PLACE – SPACE IS LIMITED.

The CONFERENCE FEE is just £189 plus VAT for the three days of the conference. This includes entrance

to all sessions, mid-morning coffee, afternoon tea and reading material. Group discounts are available on application to Janine Slipman, see booking form for address and phone no.

**ACCOMMODATION** has been reserved in the London West Hotel for conference participants. A booking form will be sent to you as soon as we receive your registration.

**TECHNICAL SEMINARS** and **POSTER SESSIONS** will be held each day. Anybody wishing to present a poster should send a title and a brief synopsis.

OUR THREE DAY PROGRAMME ENABLES YOU TO ASSESS IMPORTANT NEW BIOTECHNOLOGY TECHNIQUES IN MEDICINE, MEET INTERNATIONAL RESEARCH SPECIALISTS, AND DISCUSS WHAT YOU LEARN WITH NEW CONTACTS FROM AROUND THE WORLD.

## CONFERENCE PROGRAMME

### Wednesday, June 18: Immune System

- 9.15 Opening
- 9.20 **Vaccines – viral diseases** G. Schild, National Institute for Biological Standards & Control, London
- 10.15 **Vaccines – parasitic diseases** A. Capron, Institut Pasteur, Lille
- 11.15 **Coffee**
- 11.45 **Lymphokines** S. Gillis, Immunex Corporation, Washington
- 12.45 **Lunch**
- 2.00 **Engineered immunoglobulins** M. Neuberger, LMB, Cambridge
- 3.00 **AIDS** L. Montagnier, Institut Pasteur, Paris
- 4.00 **Tea**
- 4.30 **Technical seminar**

### Thursday, June 19: Cancer

- 9.15 **Oncogenes – diagnostic value** K. Sikora, Royal Postgraduate Medical School, London
- 10.15 **Oncogenes – therapeutic possibilities** R. Gerety, Merck Sharp & Dohme, Pennsylvania
- 11.15 **Coffee**

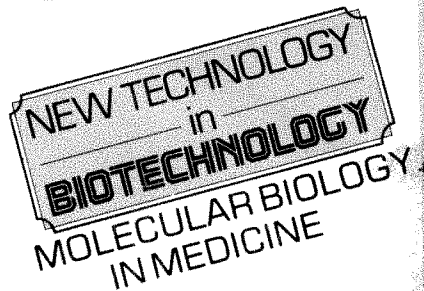
- 11.45 **Gene amplification and drug resistance** G. Stark, Imperial Cancer Research Fund, London
- 12.45 **Lunch**
- 2.00 **Gene probes for tumour progression** T. Waldmann, National Institutes of Health, Maryland
- 3.00 **Immunotoxins** R. Baldwin, University of Nottingham
- 4.00 **Tea**
- 4.30 **Technical seminar**.

### Friday, June 20: Genetic Disease

- 9.15 **Single gene disease** D. Weatherall, University of Oxford
- 10.15 **Polygenic disease** J. Scott, MRC Clinical Research Centre, Middlesex
- 11.15 **Coffee**
- 11.45 **Haemophilia** E. Tuddenham, Royal Free Hospital, London
- 12.45 **Lunch**
- 2.00 **Human gene therapy** W. F. Anderson, National Institutes of Health, Maryland
- 3.00 **Panel discussion: Detection and prevention of genetic diseases**
- 4.00 **Close**

Reader Service No.325

## CONFERENCE BOOKING FORM



To register for the conference, please return to Janet Mulhall Macmillan Conferences and Exhibitions, 4 Little Essex Street, London WC2R 3LF, UK

Full name \_\_\_\_\_

Full job title \_\_\_\_\_

Address \_\_\_\_\_  
\_\_\_\_\_  
\_\_\_\_\_

Tel/no: work \_\_\_\_\_ home \_\_\_\_\_

Please tick appropriate boxes

I wish to make a firm reservation for the full duration of the conference, at £217.35 (£189 + VAT)

I wish to attend the Conference Dinner on the evening of June 19th at £14.95 per person.

I enclose a cheque made payable to Macmillan Journals

Please charge my  Visa  Mastercard account no. \_\_\_\_\_  
expiry date \_\_\_\_\_

signature \_\_\_\_\_

Please bill my organisation (please attach address and contact name if different from above)

Please send me details of your group discounts.

Several social events will be organised offering a chance to chat informally with speakers and fellow delegates.

Cancellations received before May 23rd 1986 will be refunded less a processing charge. No refunds can be made after this date.

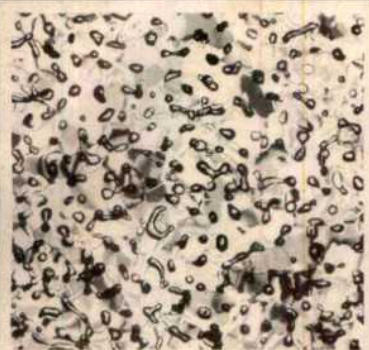
NOTES: Please complete one form per person. Extra booking forms can be obtained from the address above or by telephoning Janine Slipman on (01) 836 6633

# nature

NATURE VOL. 320 20 MARCH 1986

## nature

INTERNATIONAL WEEKLY JOURNAL OF SCIENCE



### ANTARCTIC CLUES TO ATMOSPHERIC HISTORY

MICROGRAPH  
Peter Lutz

A thin section of Antarctic ice from a depth of about 70 m, showing gas bubbles formed during the compaction of surface snow into ice. The gas content of these bubbles gives a measure of the make-up of past atmospheres, so levels of the gases implicated in the 'greenhouse effect' can be determined back to the year 1600. See page 248. (Photo, in polarized light, by D. Whillas of CSIRO's Division of Atmospheric Research.)

### OPINION

- Turning point for nuclear power 199  
Organization of research 200

### NEWS

- Space shuttle 201  
US space programme  
Halley's comet 202  
Book conservation 203  
Nuclear reprocessing 204  
Fusion in Japan  
US acid rain 205  
Soviet spacecraft  
German gigaflops  
Data protection 206  
Pesticide toxicity  
West German universities 207  
French elections

### CORRESPONDENCE

- Embryo research/Star wars/Women back to work 208

### NEWS AND VIEWS

- Heavy-ion positrons explained 209  
Axon growth in vertebrate embryos P H Taghert & J W Lichtman 210  
Beginnings of English village life Richard Hodges 211  
Origins of chloroplasts A E Walsby 212

### Gene therapy: Desperate appliances

Miranda Robertson 213

### Temperature of the ice sheets

G S Boulton 214

### Cell motility: Regulation by phosphorylation

J M Scholey 215

### Molecular biology: Brevity is the soul of wit

Roger H Pain 216

### Topology: The Poincaré conjecture proved

Ian Stewart 217

### SCIENTIFIC CORRESPONDENCE

#### Origins of human T-lymphotropic viruses

R C Gallo, A H Siski, C M C De Noronha & F De Noronha 219

#### Bovine leukaemia virus and multiple sclerosis

A S Cunningham 219

#### Endogenous retrovirus in multiple sclerosis?

R Kurth 219

#### Archaeabacterial status quo is defended

W Zillig, H Lederer 220

### BOOK REVIEWS

#### Niels Bohr: A Centenary Volume

A P French and P J Kennedy, eds R H Dalitz 221

#### Functions of the Brain

C W Coen, ed. Oliver Braddick 223

#### Ada: A Life and a Legacy by D Stein

Richard Gregory 224

#### Glycoprotein and Proteoglycan Techniques

by J G Beeley Tim Hardingham 224

### COMMENTARY

#### The ethics of human gene therapy

L Walters 225

### ARTICLES

#### Transitional field behaviour from Southern Hemisphere

lavas: evidence for two-stage reversals of the geodynamo K A Hoffman 228

#### Transfer of specificity by murine $\alpha$ and $\beta$ T-cell receptor genes

Z Dembić, W Haas, W Weiss, J McCubrey, H Kiefer, H Von Boehmer & M Steinmetz 232

### LETTERS TO NATURE

#### Very Large Array observations of rapid non-periodic variations in OJ 287

J W Dreher, D H Roberts & J Lehár 239

#### Are cometary nuclei primordial rubble piles?

P R Weissman 242

#### Deuterium in the outer Solar System: evidence for two distinct reservoirs

T Owen, B L Lutz & C De Bergh 244

#### Direct laboratory determination of the $^{187}\text{Re}$ half-life

M Lindner, D A Leich, R J Borg, G P Russ, J M Bazan, D S Simons & A R Date 246

#### Evidence of changing concentrations of atmospheric $\text{CO}_2$ , $\text{N}_2\text{O}$ and $\text{CH}_4$ from air bubbles in Antarctic ice

G I Pearman, D Etheridge, F De Silva & P J Fraser 248

#### Palaeotemperatures still exist in the Greenland ice sheet

D Dahl-Jensen & S J Johnsen 250

#### Geophysical modelling of the thermal history of foreland basins

M A Kominz & G C Bond 252

#### $^{36}\text{Cl}$ in a halite layer from the bottom of the Dead Sea

M Magaritz, A Kaufman, Y Levy, D Fink, O Meirav & M Paul 256

#### Carbon-isotope events across the Precambrian-Cambrian boundary on the Siberian Platform

M Magaritz, W T Holser & J L Kirschvink 258

#### Radiolarian and silicoflagellate response to oceanographic changes associated with the 1983 El Niño

N G Pisias, D W Murray & A K Roelofs 259

#### A new prokaryote containing chlorophylls *a* and *b*

T Burger-Wiersma, M Veenhuis, H J Korthals, C C M Van den Wiel & L R Mur 262

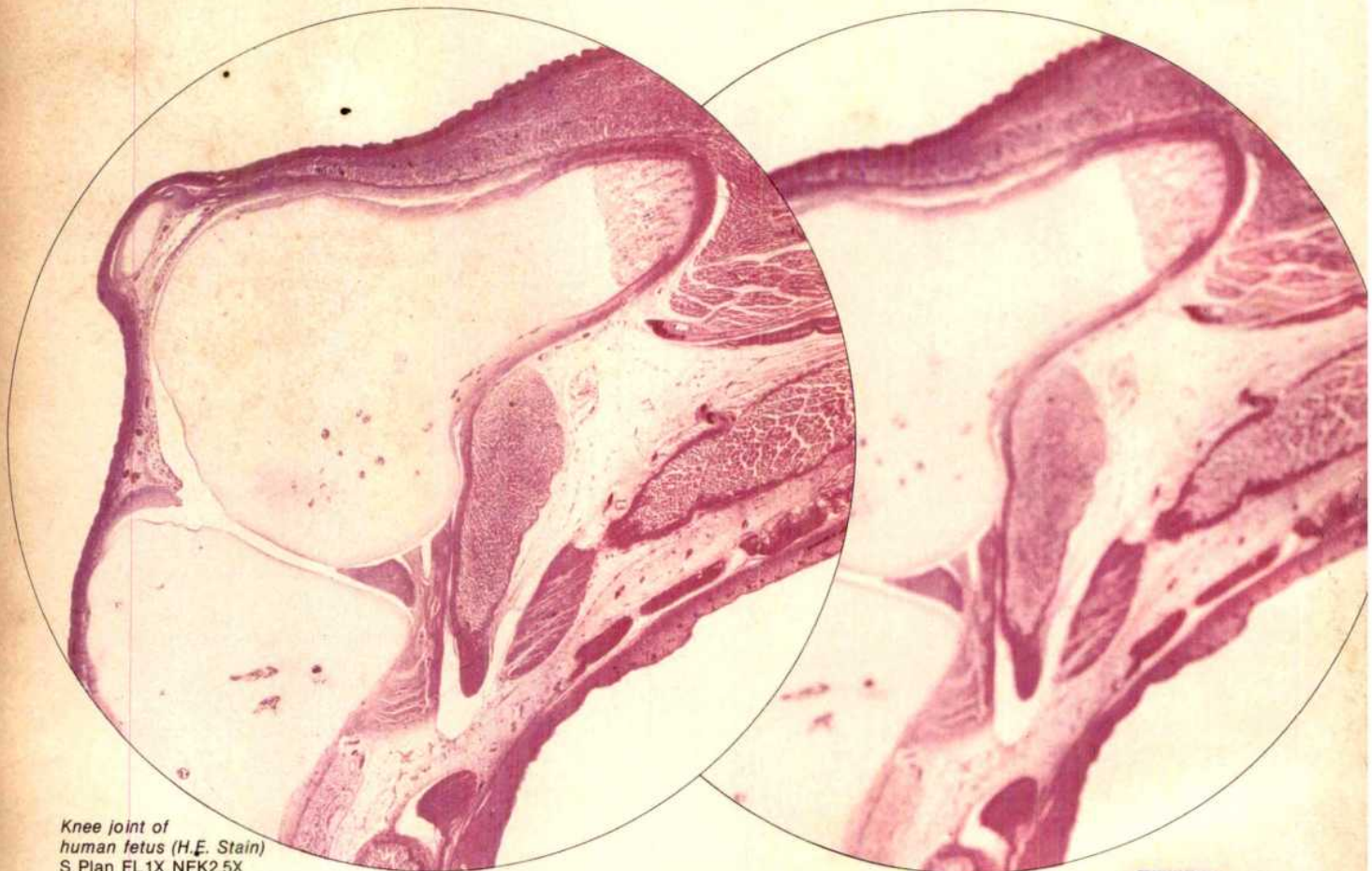
#### Serial and parallel processing of visual feature conjunctions

K Nakayama & G H Silverman 264

Contents continued overleaf

AF

# Focus on Accuracy



## Olympus autofocus photomicrography takes the error out of focusing

What the naked eye perceives as sharp and clear often translates into a blurred image on film or paper.

Now Olympus brings you the Vanox-S—the world's first autofocus photomicroscope system—designed to eliminate focusing error in low magnification photomicrography (objectives from 1X to 10X), and ensure needle-sharp imagery throughout the entire magnification range. All you have to do is push the AF button.

And the Vanox-S also enables the use of two 35mm cameras and a large-format camera, incorporated into the body, together with automatic exposure and four photo eyepieces. Light intensity is adjusted with neutral density filters, maintaining color temperature consistency.

The new Vanox-S research photomicroscope system lets you reproduce the actual image you see accurately and with high quality. More easily and consistently than ever before.



VANOX-S

# OLYMPUS®

**OLYMPUS OPTICAL CO., LTD.**

San-Ei Building, 22-2, Nishi Shinjuku 1-chome, Shinjuku-ku, Tokyo, Japan

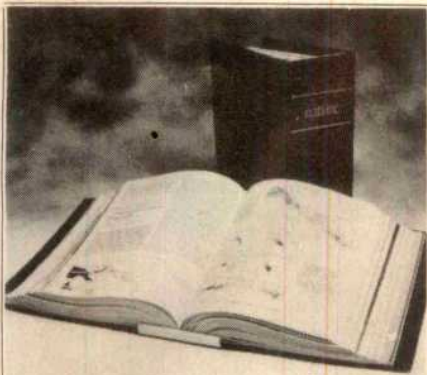
**OLYMPUS OPTICAL CO. (EUROPA) GMBH**

Postfach 104908, Wendenstrasse 14-16, 2 Hamburg 1, West Germany

**OLYMPUS CORPORATION**

4 Nevada Drive, Lake Success, N.Y. 11042-1179, U.S.A.

## CONTENTS



## NATURE BINDERS

Your copies of Nature are invaluable for future reference so why not give them the treatment they deserve and file them neatly in our special Nature binders?

**Ordering address and prices for one or a set of four are listed below.**

### Annual Subscription Prices

UK & Irish Republic	£104
USA & Canada	US\$240
Australia, NZ & S. Africa	Airspeed £150 Airmail £190
Continental Europe	Airspeed £125
India	Airspeed £120 Airmail £190
Japan	Airspeed Y90000
Rest of World	Surface £120 Airmail £180

### Orders (with remittance) to:

USA & Canada	UK & Rest of World
Nature	Nature
Subscription Dept	Circulation Dept
PO Box 1501	Brunel Road
Neptune	Basingstoke
NJ 07753	Hants RG21 2XS, UK
USA	Tel: 0256 29242

(The addresses of Nature's editorial offices are shown facing the first editorial page)

### Japanese subscription enquiries to:

Japan Publications Trading Company Ltd  
2-1 Sarugaku-cho 1-chome  
Chiyoda-ku, Tokyo, Japan  
Tel: (03) 292 3755

**Personal subscription rates:** These are available in some countries to subscribers paying by personal cheque or credit card. Details from:

USA & Canada	UK & Europe
Nature	Felicity Parker
65 Bleecker Street	Nature
New York	4 Little Essex Street
NY 10012, USA	London WC2R 3LF, UK
Tel: (212) 477-9600	Tel: 01-836 6633

**Back issues:** UK, £2.50; USA & Canada, US\$6.00 (surface), US\$9.00 (air); Rest of World, £3.00 (surface), £4.00 (air)

### Binders

Single binders: UK, £5.25; USA & Canada \$11.50; Rest of World, £7.75. Set of four: UK, £15.00; USA & Canada \$32.00; Rest of World, £22.00

### Annual indexes (1971-1985)

UK, £5.00 each; Rest of World, \$10.00

### Nature First Issue Facsimile

UK, £2.00; Rest of World (surface), \$3.00; (air) \$4.00

### Nature in microform

Write to University Microfilms International, 300 North Zeeb Road, Ann Arbor, MI 48106, USA

### Homing behaviour of axons in the embryonic vertebrate brain

W A Harris 266

### Pathway selection by growth cones of identified motoneurones in live zebra fish embryos

J S Eisen, P Z Myers & M Westerfield 269

### A T3-like protein complex associated with the antigen receptor on murine T cells

H C Oettgen, C L Pettey, W L Maloy & C Terhorst 272

### Retrovirus-mediated transfer and expression of drug resistance genes in human haematopoietic progenitor cells

R A Hock & A D Miller 275

### Structural alteration of viral homologue of receptor proto-oncogene fms at carboxyl terminus

L Coussens, C Van Beveren, D Smith, E Chen, R L Mitchell, C M Isacke, I M Verma & A Ullrich 277

### Genomic diversity correlates with clinical variation in Ph'-negative chronic myeloid leukaemia

C M Morris, A E Reeve, P H Fitzgerald, P E Hollings, M E J Beard & D C Heaton 281

### Sequence homology of the yeast regulatory protein ADR1 with Xenopus transcription factor TFIIIA

T A Hartshorne, H Blumberg & E T Young 283

### Eukaryotic ribosomes that lack a 5.8S RNA

C R Vossbrinck & C R Woese 287

## PRODUCT REVIEW

### Agglutination methods for rapid analysis

M Thomas 289

### Taking a closer look at microbiology

290

## MISCELLANY

100 years ago 212

## NATURE CLASSIFIED

### Professional appointments —

### Research posts — Studentships —

### Fellowships — Conferences —

### Courses — Seminars — Symposia:

Back Pages

## Next week in Nature:

- A star is born
- A place for teleology?
- Storing sea-level rise
- Colloidal glass phase
- Non-halogen oscillator
- Last de-glaciation dated
- Mantle transition region
- Natural radionuclide gatherer
- New homoeo box
- Spatial vision
- Retrovirus in gene inactivation
- Synthetase/tRNA interaction
- AIDS virus replication

## GUIDE TO AUTHORS

Authors should be aware of the diversity of *Nature's* readership and should strive to be as widely understood as possible.

**Review articles** should be accessible to the whole readership. Most are commissioned, but unsolicited reviews are welcome (in which case prior consultation with the office is desirable).

**Scientific articles** are research reports whose conclusions are of general interest or which represent substantial advances of understanding. The text should not exceed 3,000 words and six displayed items (figures plus tables). The article should include an italic heading of about 50 words.

**Letters to Nature** are ordinarily 1,000 words long with no more than four displayed items. The first paragraph (not exceeding 150 words) should say what the letter is about, why the study it reports was undertaken and what the conclusions are.

**Matters arising** are brief comments (up to 500 words) on articles and letters recently published in *Nature*. The originator of a *Matters Arising* contribution should initially send his manuscript to the author of the original paper and both parties should, wherever possible, agree on what is to be submitted.

Manuscripts may be submitted either to London or Washington. Manuscripts should be typed (double spacing) on one side of the paper only. Four copies are required, each accompanied by copies of lettered artwork. No title should exceed 80 characters in length. Reference lists, figure legends, etc., should be on separate sheets, all of which should be numbered. Abbreviations, symbols, units, etc., should be identified on one copy of the manuscript at their first appearance.

References should appear sequentially indicated by superscripts, in the text and should be abbreviated according to the *World List of Scientific Periodicals*, fourth edition (Butterworth 1963-65). The first and last page numbers of each reference should be cited. Reference to books should clearly indicate the publisher and the date and place of publication. Unpublished articles should not be formally referred to unless accepted or submitted for publication, but may be mentioned in the text.

Each piece of artwork should be clearly marked with the author's name and the figure number. Original artwork should be unlettered. Suggestions for cover illustrations are welcome. Original artwork (and one copy of the manuscript) will be returned when manuscripts cannot be published.

*Requests for permission to reproduce material from Nature should be accompanied by a self-addressed (and, in the case of the United Kingdom and United States, stamped) envelope.*

TAKE A FRESH LOOK AT BIOTECHNOLOGY

# BIOTECH 86

This is no ordinary event. Biotech '86 features new personalities with fresh ideas. The programme balances formal presentations, panel discussions, technical workshops and specialist seminars. There

are conference options to suit your interests, plus an industry exhibition and plenty of opportunity to talk with colleagues and make new contacts.

## APPLIED BIOTECHNOLOGY – STREAM 1

### Chemical & Enzyme Technology

Opening Address: Alexander Klibanov, MIT, USA

#### Biotransformations in the chemical industry

Chair: Peter Baker, DTI  
Chris Drew, Specialised Organics Information Service  
Doug Ribbons, Imperial College of Science & Technology  
Geoff Walker, DTI (on secondment from ICI)  
Noel Rouy, Rhône-Poulenc, France

#### Production & processing of fine chemicals

Chair: Howard Dalton, University of Warwick  
Sol Barer, Chem Systems, USA  
Stephen Taylor, ICI  
David Crout, University of Warwick  
Peter Cheetham, Tate & Lyle

#### Protein engineering

Chair: Brian Hartley, Imperial College of Science & Technology

Barry Robson, University of Manchester  
Michael Courtney, Transgene, France  
Peter Murray-Rust, Glaxo Group Research  
Steffen Petersen, Novo Industri, Denmark

#### Crop protection strategies

Chair: Peter Haskell, UCW Cardiff  
Martin Wolfe, Plant Breeding Institute  
Richard Bond, Shell Research Centre  
Barry Baldwin, Microbial Resources  
Dale Shaner, American Cyanamid

#### Toxic & environmental waste

Chair: Chris Knowles, University of Kent  
Martin Davies, University of York  
Howard Slater, BioTechnica  
Stanley Sojka, Occidental Chemicals, USA  
Frank Holt, ICI

## APPLIED BIOTECHNOLOGY – STREAM 2

### Healthcare

Opening Address: David Tyrrell, MRC Common Cold Unit

#### Standardisation of control requirements

Chair: Geoffrey Schild, Nat. Inst. for Biological Standards and Control  
David Secher, MRC Laboratory of Molecular Biology  
Tony Meager & Robin Thorpe, NIBSC  
Julian Peetersmans, Smith Kline-Rit, Belgium

#### Status report on AIDS

Chair: David Tyrrell, MRC Working Party on AIDS  
Philip Mortimer, Virus Reference Laboratory PHLSC  
Patricia Hewitt, North London Transfusion Centre  
Tony Whitehead, The Terrence Higgins Trust  
Simon Wain-Hobson, Institut Pasteur, France  
Jonathan Weber, Institute of Cancer Research

#### Biosensing systems

Chair: Robert Brown, Royal Signals & Radar Est.  
Elizabeth Hall, University of Cambridge  
Martin Smith, Unilever Research  
David Clarke, CAMR, Porton Down

#### Computers in processing

Chair: Norman Sawyer, Drew Scientific  
Jeremy Court, CAMR, Porton Down  
Derek Fletcher, Glaxo Group Research  
Ron Leigh, Polytechnic of Central London  
Les Spark, Biotechnology Process Services

#### Formation & recovery of biologicals

Malcolm Rhodes, Celltech  
Nigel Webb, Damon Biotech, USA  
John Ptak, LKB, Sweden  
Tony Atkinson, CAMR, Porton Down

## APPLIED BIOTECHNOLOGY – STREAM 3

### Two specialist seminars

#### NATURAL 'BIOGENIC' MATERIALS

##### Structure & function relationships

Chair: Gwyn Humphreys, Apcel  
Julian Vincent, University of Reading  
George Jeronimidis, University of Reading  
Andrew Yule, University College of North Wales

##### Novel materials for industry

Chair: Trevor Jarman, PA Technology  
Nigel Uttley, Marlborough Biopolymers  
Arthur J Hale, Genzyme  
Janice Light, PA Technology

##### New industrial applications

Chair: Brian Sagar, Shirley Institute  
Derek Ellwood, Fermentech  
William Bonfield, Queen Mary College  
Tom Burrow, Courtaulds Research  
Peter Lilford, Unilever Research

##### VACCINES

##### Enabling technologies

Chair: Fred Brown, Wellcome Biotechnology  
John Skehel, NIMR  
David Bishop, NERC Institute of Virology  
Ivan Roitt, Middlesex Hospital Medical School  
Duncan Stewart-Jull, Glasgow University

##### Commercial perspectives

Chair: Jack Meling, CAMR, Porton Down  
Ian Furninger, Evans Medical  
Stuart Wren, Wellcome Biotechnology  
Sir John Badenoc, DHSS Joint Committee on Vaccination and Immunisation  
David Tyrrell, MRC Common Cold Unit

## INTERNATIONAL BUSINESS FORUM

Opening address: Julian Davies, Institut Pasteur, France

#### Business trends & forecasts

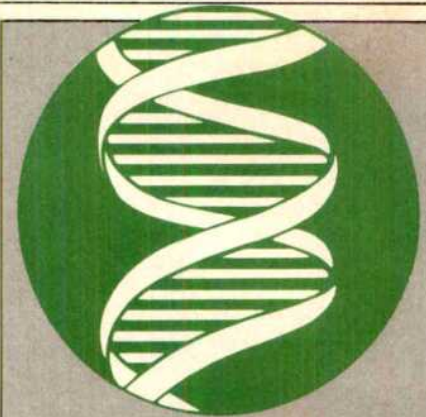
Chair: Steve Burrill, Arthur Young, USA  
Peter Drake, Kidder Peabody, USA  
Richard Freeman, PA Technology  
Robert Riley, Arthur D Little, USA

#### The regulation of biotechnology

Chair: David Sakura, Arthur D Little, USA  
Roger Nourish, HSE  
Tom Garvey, DG III, CEC  
Solomon Wald, OECD, France

#### Doing business in China

Chair: Ronald Coleman, UK Government Chemist  
Norman Garrett, APV International  
Gerard Fairtlough, Celtech  
Michael Leyburn, International Embryos  
Financial, corporate & company management  
Chair: Robert Riley, Arthur D Little, USA  
Count Albrecht Matuschka, TRV Group, FRG  
William Baker, California Biotechnology, USA  
Rolf Hickmann, Procede  
Rafaat El-Sayed, Fermenta, Sweden  
Rashid Domingo, Biocyte  
Donald Murfin, Lubrizol Enterprises, USA  
Ian Keenan, The Coverdale Organisation



INTERNATIONAL  
CONFERENCE  
AND  
EXHIBITION

WEMBLEY  
CONFERENCE  
CENTRE  
LONDON

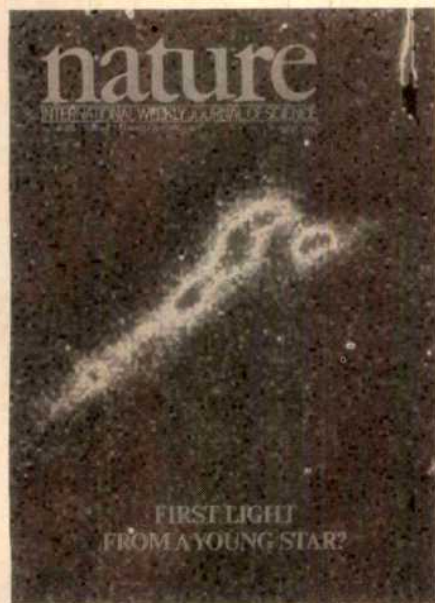
13 - 15 MAY 1986

The full  
conference programme  
is now available.  
Phone Pam Howard  
for your copy . . .  
01-868 4466

Online International Ltd  
Pinner Green House, Pinner,  
Middlesex, UK

# nature

NATURE VOL. 320 27 MARCH 1986



The Object 50 nebula in Orion. In this CCD image, taken on 9 January 1985, a pulse of light illuminates the jet. The pulse was emitted in late 1984 and by September 1985 had propagated 1 arc minute to the south. This burst of light may be the first optical radiation to have emerged from this newborn star. See page 336.

## OPINION

- Chirac's newly won winning ways 293

## NEWS

- SDI 294

- Waving the star (wars) and stripes 295

- French elections 295

- Nuclear energy 296

- Japan's research 296

- Japanese space programme 297

- US research costs 297

- British astronomy 298

- US Office of Naval Research 298

- No help on AIDS 299

- Medical Research Council 299

- British farm research 300

- West German environment 300

- Polish agriculture 300

- US agriculture 301

- Soviet education 301

- Environmental pollution 301

- Europe's optical telescope for 1990 301

## CORRESPONDENCE

- Sakharov's science/Archaeology 302

- congress/Matter 302

## NEWS AND VIEWS

- New ways with crystal growth 303

- Model crystals: Penny plain, tuppence coloured 304

- Robert W Cahn 304

## Do plants evolve differently?

- William J Sutherland & Andrew R Watkinson 305

## Palaeoclimatology: Bears versus beetles

- Peter D Moore 305

## Archaean mantle models

- E G Nisbet 306

## Tropical plant research in South-East Asia

- Barry Osmond 307

## Creationism: On the tracks of men and money

- Tony Thulborn 308

## Applications of microemulsions

- B H Robinson 309

## Visual cortex: What layer 6 tells layer 4

- Simon LeVay 310

## Low-luminosity stars: How no(w) brown dwarfs?

- Virginia Trimble 311

## SCIENTIFIC CORRESPONDENCE

### Major groove or minor groove?

- S Arnott 313

### X chromosomes and dosage compensation

- M F Lyon 313

### Scotophobin resurrected as a neuropeptide

- D Wilson 313

### Origin of anti-parallelism in $\beta$ -keratin

- M Feughelman 314

## BOOK REVIEWS

### The Anthropic Cosmological Principle

- by J D Barrow and F J Tipler 315

### Intermediate Filaments: A Review

- by P Traub 316

### Keith Burridge

- 316

### The Evolutionary Process: A Critical Review of Evolutionary Theory

- by V Grant 317

### J S Jones

- 317

### Virus Structure and Assembly

- S Casjens, ed. 318

### P J G Butler

- A Machine Called Indomitable

- by S Kleinfield 318

### Peter Newmark

- 318

## COMMENTARY

### The management of sea-level rise

- WS Newman & R W Fairbridge 319

## REVIEW ARTICLE

### Transition region of the Earth's upper mantle

- D L Anderson & J D Bass 321

## ARTICLES

### Spatial restriction in expression of a mouse homoeo box locus within the central nervous system

- A Awgulewitsch, M F Utset, C P Hart, W McGinnis & F H Ruddle 328

## LETTERS TO NATURE

### First light from a young star?

- B Reipurth & J Bally 336

### Occurrence of liquid-crystalline mesophases in microemulsion dispersions

- J Tabony 338

### Phase behaviour of concentrated suspensions of nearly hard colloidal spheres

- P N Pusey & W van Megen 340

### Bubble raft model for indentation with adhesion

- J M Georges, G Meille, J L Loubet & A M Tolen 342

### A novel, non-halogen-based chemical oscillator

- A Nagy & L Treindl 344

### Intensity modulation in SAR images of internal waves

- D R Thompson & R F Gasparovic 345

### Direct indication of pore-water advection from pore pressure measurements in Madeira

- Abyssal Plain sediments P J Schultheiss & S D McPhail 348

### Direct dating of the oxygen-isotope record of the last deglaciation by $^{14}\text{C}$ accelerator mass spectrometry

- J-C Duplessy, M Arnold, P Maurice, E Bard, J Duprat & J Moyes 350

### Extensive deposition of banded iron formations was possible without photosynthesis

- L M Francois 352

### High levels of natural radionuclides in a deep-sea infaunal xenophyophore

- D D Swinbanks & Y Shirayama 354

### Perception of apparent motion by commissurotomy patients

- V S Ramachandran, A Cronin-Golomb & J J Myers 358

### Sampling in spatial vision

- D M Levi & S A Klein 360

Contents continued overleaf

# At last! An easy to use gene machine at an affordable price.



Now any laboratory working with oligonucleotides can perform automated DNA synthesis simply, reliably and affordably—whatever the volume demand—with the new Pharmacia Gene Assembler™. This high-quality system combines state-of-the-art technology and chemistry with simplicity of design and operation.

#### Integral

The Gene Assembler is a complete system. The compact, bench-top unit contains everything you need to synthesize active DNA: hardware, software, Pharmacia's own reagents, and a comprehensive handbook. It even includes automatic colorimetric monitoring and a built-in printer/plotter that gives you a permanent record of each synthesis in both peaks and print.

#### Simple

The Gene Assembler was designed for maximum ease of operation. You just insert a ready-to-use cassette of unique, new Mono Beads™ into one of the two column reactors, type in the desired sequence, and let the machine do the rest. It's not only self-contained, it's very nearly self-sufficient!

#### Flexible

You don't need any peripheral hardware (an expensive "option" with some competitors).

The Gene Assembler is preprogrammed for everything from standard syntheses to sophisticated mixed bases. And it's versatile enough to allow user-determined reprogramming—e.g. for modified nucleotides. It can also easily interface with a variety of other microcomputers for even greater capacity.

#### Reliable

As with all Pharmacia equipment, the Gene Assembler consists of high-quality components, each designed to give you years of dependable service. Of course, it's also backed by Pharmacia's established, worldwide service network and warranty.

#### Affordable

Pharmacia's expertise in biotechnology enabled us to optimize components to form a dedicated system. Therefore, designing and manufacturing the Gene Assembler cost substantially less than competitive machines. That saving is passed along to you. All in all, this high-quality, high-performance system is the most cost-effective and efficient DNA synthesizer you can buy.

#### Available

To find out more, ask your Pharmacia representative to send you the comprehensive, illustrated brochure. Do it today.

Pharmacia Headquarters: Pharmacia AB,  
S-751 82 Uppsala, Sweden. Tel: (018) 1630 00.

In North America: Pharmacia Inc.,  
800 Centennial Avenue, Piscataway,  
NJ 08854, USA. Tel: (201) 457-8121.

Reader Service No.46



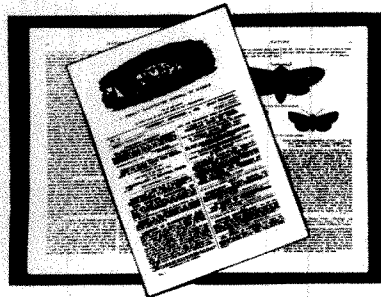
**Pharmacia**

Molecular Biology Division

Your Link With The Future

## CONTENTS

# NATURE'S FIRST ISSUE FACSIMILE



..... 40-PAGES OF INTRIGUING SCIENTIFIC HISTORY REPRODUCED.

ORDER YOUR OWN COPY AND DISCOVER HOW SCIENCE HAS ADVANCED SINCE 1869!

PRICES AND ADDRESS FOR ORDERS ARE SET OUT BELOW.

#### Annual Subscription Prices

UK & Irish Republic	£104
USA & Canada	US\$240
Australia, NZ & S. Africa	Airspeed £150 Airmail £190
Continental Europe	Airspeed £125 Airmail £120
India	Airspeed £120 Airmail £190
Japan	Airspeed Y90000
Rest of World	Surface £120 Airmail £180

#### Orders (with remittance) to:

USA & Canada      UK & Rest of World  
 Nature                Nature  
 Subscription Dept    Circulation Dept  
 PO Box 1501          Brunel Road  
 Neptune              Basingstoke  
 NJ 07753             Hants RG21 2XS, UK  
 USA                   Tel: 0256 29242  
 (The addresses of Nature's editorial offices are shown facing the first editorial page)

#### Japanese subscription enquiries to:

Japan Publications Trading Company Ltd  
 2-1 Sarugaku-cho 1-chome  
 Chiyoda-ku, Tokyo, Japan  
 Tel: (03) 292 3755

**Personal subscription rates:** These are available in some countries to subscribers paying by personal cheque or credit card. Details from:

USA & Canada      UK & Europe  
 Nature                Felicity Parker  
 65 Bleecker Street    Nature  
 New York             4 Little Essex Street  
 NY 10012, USA       London WC2R 3LF, UK  
 Tel: (212) 477-9600   Tel: 01-836 6633

**Back issues:** UK, £2.50; USA & Canada, US\$6.00 (surface), US\$9.00 (air); Rest of World, £3.00 (surface), £4.00 (air)

#### Binders

Single binders: UK, £5.25; USA & Canada \$11.50; Rest of World, £7.75. Set of four: UK, £15.00; USA & Canada \$32.00; Rest of World, £22.00

#### Annual indexes (1971-1985)

UK, £5.00 each; Rest of World, \$10.00

#### Nature First Issue Facsimile

UK, £2.00; Rest of World (surface), \$3.00; (air) \$4.00

#### Nature in microform

Write to University Microfilms International, 300 North Zeeb Road, Ann Arbor, MI 48106, USA

## Generation of end-inhibition in the visual cortex via interlaminar connections

J Bolz & C D Gilbert      362

## Retrovirus insertion inactivates mouse $\alpha 1$ (I) collagen gene by blocking initiation of transcription

S Hartung, R Jaenisch & M Breindl      365

## The trans-activator gene of HTLV-III is essential for virus replication

A G Fisher, M B Feinberg, S F Josephs, M E Harper, L M Marselle, G Reyes, M A Gonda, A Aldovini, C Debouk, R C Gallo & F Wong-Staal      367

## A model of synthetase/transfer-RNA interaction as deduced by protein engineering

H Bedouelle & G Winter      371

## Upstream activator sequences are present in the promoters of nitrogen fixation genes

M Buck, S Miller, M Drummond & R Dixon      374

## Tertiary structural similarity between a class A $\beta$ -lactamase and a penicillin-sensitive $\alpha$ -alanyl carboxypeptidase-transpeptidase

B Samraoui, B J Sutton, R J Todd, P J Artymiuk, S G Waley & D C Phillips      378

## MATTERS ARISING

### Estimation of scrapie nucleic acid MW from standard curves for virus sensitivity to ionizing radiation

R G Rohwer      381

## MISCELLANY

### 100 years ago

Author index, Vol. 319      xxi

## NATURE CLASSIFIED

### Professional appointments — Research posts — Studentships — Fellowships — Conferences — Courses — Seminars — Symposia:

Back Pages

## Next week in *Nature*:

- Cosmogenic helium on Earth
- Galactic nuclei
- Late Miocene salinity
- Fossil  $\alpha$ -particle tracks
- Fractal cracks
- Radar picture of hail
- Lanthanum-138 clock
- Tolerance to monoclonals
- New oncogene — v-kit
- Immunoglobulin genes
- Endoplasmic reticulum  $\text{Ca}^{2+}$
- Biological control of screwworm

## GUIDE TO AUTHORS

Authors should be aware of the diversity of *Nature*'s readership and should strive to be as widely understood as possible.

**Review articles** should be accessible to the whole readership. Most are commissioned, but unsolicited reviews are welcome (in which case prior consultation with the office is desirable).

**Scientific articles** are research reports whose conclusions are of general interest or which represent substantial advances of understanding. The text should not exceed 3,000 words and six displayed items (figures plus tables). The article should include an italic heading of about 50 words.

**Letters to Nature** are ordinarily 1,000 words long with no more than four displayed items. The first paragraph (not exceeding 150 words) should say what the letter is about, why the study it reports was undertaken and what the conclusions are.

**Matters arising** are brief comments (up to 500 words) on articles and letters recently published in *Nature*. The originator of a Matters Arising contribution should initially send his manuscript to the author of the original paper and both parties should, wherever possible, agree on what is to be submitted.

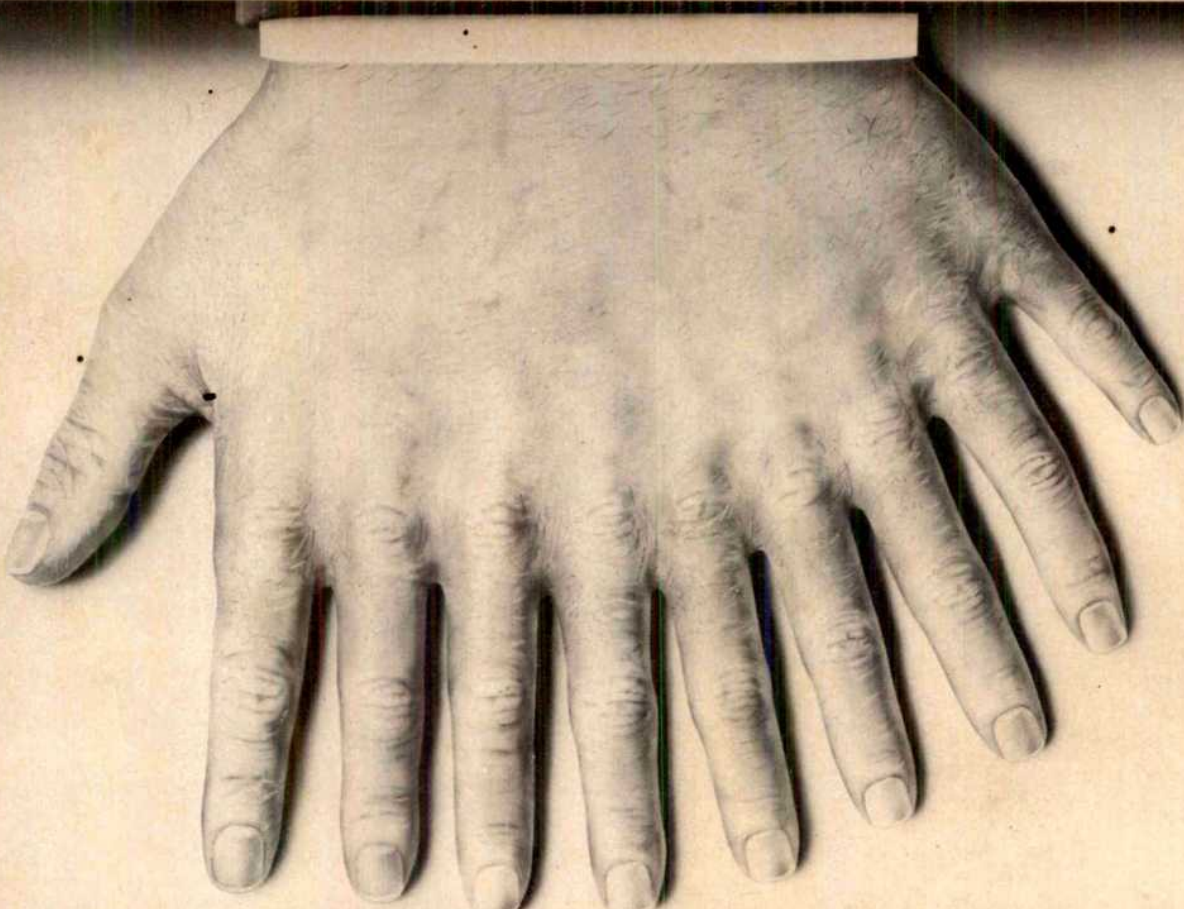
Manuscripts may be submitted either to London or Washington. Manuscripts should be typed (double spacing) on one side of the paper only. Four copies are required, each accompanied by copies of lettered artwork. No title should exceed 80 characters in length. Reference lists, figure legends, etc., should be on separate sheets, all of which should be numbered. Abbreviations, symbols, units, etc., should be identified on one copy of the manuscript at their first appearance.

References should appear sequentially indicated by superscripts, in the text and should be abbreviated according to the *World List of Scientific Periodicals*, fourth edition (Butterworth 1963-65). The first and last page numbers of each reference should be cited. Reference to books should clearly indicate the publisher and the date and place of publication. Unpublished articles should not be formally referred to unless accepted or submitted for publication, but may be mentioned in the text.

Each piece of artwork should be clearly marked with the author's name and the figure number. Original artwork should be unlettered. Suggestions for cover illustrations are welcome. Original artwork (and one copy of the manuscript) will be returned when manuscripts cannot be published.

**Requests for permission to reproduce material from Nature** should be accompanied by a self-addressed (and, in the case of the United Kingdom and United States, stamped) envelope.

LIBRARY COMPLEX  
UNIVERSITY OF CALIFORNIA  
BERKELEY  
1000 BANCROFT ROAD, BERKELEY, CA 94720



# COUNT YOUR BLESSINGS!

1. LABORATORY's annual outing to the North West ensures that there is intelligent regional exposure of the industry's latest apparatus, equipment, instrumentation and services.

2. The best companies in the business have fully supported the LABORATORY MANCHESTER concept in the only way that really counts – by deciding to be there. Go along and see for yourself!

3. LABORATORY MANCHESTER is therefore the largest regional event for a variety of scientific disciplines in the United Kingdom, and its success may be measured by seven years' uninterrupted growth.

4. This year, there is 25 percent more exhibition space than there was at the 1985 event – and over 100 exhibitors, representing our first (unbeaten!) century at the New Century Hall.

5. Our popular venue is conveniently situated alongside Victoria Station, with ample car parking available nearby for those who prefer to travel to LABORATORY '86 in Manchester by car.

6. Visitors who take a break during their tour of the exhibition – or require

refreshment when they have completed it – can take full advantage of catering facilities that don't cost the earth!

7. The prestige of LABORATORY MANCHESTER is enhanced by the sponsorship of the people who matter: The Royal Society of Chemistry; Chromatographic Society; Scientific Instrument Manufacturers' Association; British Laboratory Ware Association.

8. The exhibition attracts the top quality visitors – Heads of Department, key buyers, specifiers (over 3,000 of them last year!). If that sounds like you you'll be in good company.

9. Unlimited free tickets for LABORATORY MANCHESTER are available, simply by completing and returning the coupon below – so order for your colleagues too. And valuable free catalogues will await your arrival.

10. The event is an important part of Britain's premier showcase for the industry – the Laboratory Series of events. It's your absolute guarantee of a worthwhile occasion.

## LABORATORY '86

NEW CENTURY HALL, CORPORATION STREET, MANCHESTER.  
MANCHESTER 16-17 APRIL 1986

The Laboratory Series is organised by Curtis Steadman & Partners, The Hub, Emson Close, Saffron Walden, Essex CB10 1HL, United Kingdom.  
Telephone: Saffron Walden (0799) 26699. Telex: 81653 INFORM G. Fax: (0799) 26088. Reader Service No.60

To: Pat Rusted, Laboratory '86 Tickets, The Hub, Emson Close, Saffron Walden, Essex CB10 1HL, United Kingdom.

PLEASE SEND ME

FREE TICKETS FOR LABORATORY '86 IN MANCHESTER

NAME \_\_\_\_\_

(Please print clearly)

COMPANY/ORGANISATION \_\_\_\_\_

MAILING ADDRESS \_\_\_\_\_

# nature

NATURE VOL. 320 3 APRIL 1986

DEPARTMENTS  
Chemical Engineering  
Chemical Technology  
Plastics & Rubber Technology  
92, A P C Road, Calcutta



Subtropical desert scrub in the Sonoran Desert in California, at an altitude of 900 metres. The scrub is dominated by chainfruit cholla, paloverde and saguaro cactus. A fossil packrat midden from a rock shelter in the hill in the background documents a pinyon pine-juniper-sagebrush woodland during the last glacial maximum, with the present warm-desert flora becoming established here only during the last 8,000 years. See page 441.

## OPINION

- |                          |     |
|--------------------------|-----|
| No way to welcome spring | 383 |
| Nuclear virulence        | 384 |
| Good luck strikes back   |     |

## NEWS

- |                                     |     |
|-------------------------------------|-----|
| AIDS research                       | 385 |
| NSF tests mini-supercomputer        |     |
| US patents                          | 386 |
| UK SDI contracts                    |     |
| Mars mission                        |     |
| US research                         | 387 |
| US engineering                      |     |
| EPA bars AGS test                   |     |
| French science                      | 388 |
| Aleksandrov stays at Soviet Academy |     |
| Polish nuclear power                |     |
| Fermilab                            | 389 |

## CORRESPONDENCE

- |   |     |
|---|-----|
| West German universities/Japanese psychiatry/Infectious AIDS/Complex forests/etc. | 390 |
|---|-----|

## NEWS AND VIEWS

- |                                      |     |
|--------------------------------------|-----|
| Icosahedral frustrations ahead       | 393 |
| Hot stars: Breaking through the wall |     |
| James B Kaler                        | 394 |
| GTP and calcium release              |     |
| P F Baker                            | 395 |

## Growing stromatolites

- |  |     |
|--|-----|
| Peter J Smith                                    | 396 |
| <b>Transposon tricks revealed</b>                |     |
| Andy Flavell                                     | 397 |
| <b>Contrasuppressor cells and oral tolerance</b> |     |
| R B Taylor                                       | 398 |
| <b>A hidden quasar revealed</b>                  |     |
| C Martin Gaskell                                 | 398 |
| <b>Deformation of continents</b>                 |     |
| Philip England                                   | 399 |
| <b>How did eurypterids swim?</b>                 |     |
| D E G Briggs                                     | 400 |

## SCIENTIFIC CORRESPONDENCE

- |   |     |
|---|-----|
| <b>Outlook brighter on weather forecasts</b>          |     |
| S Lovejoy, D Schertzer & P Ladoy                      | 401 |
| <b>Are arguments against archaeabacteria valid?</b>   |     |
| C R Woese, N R Page & G J Olsen                       | 401 |
| <b>Link between lamins and intermediate filaments</b> |     |
| K Weber   | 402 |
| <b>The mechanics of visual acuity</b>                 |     |
| T Nash  | 402 |
| <b>The human factor in mammoth extinction</b>         |     |
| S Cachel  | 402 |

## BOOK REVIEWS

- |  |     |
|--|-----|
| <b>Nuclear Politics: The History of Nuclear Power in Britain</b><br><i>by T Hall</i>                 |     |
| David Pearce   | 403 |
| <b>William Hunter and the Eighteenth-Century Medical World</b><br><i>W F Bynum and R Porter, eds</i> |     |
| Michael Shortland  | 404 |
| <b>Amazonia</b><br><i>G T Prance and T E Lovejoy, eds</i>  |     |
| Norman Myers   | 405 |
| <b>Fundamentals of Insect Physiology</b><br><i>M S Blum, ed.</i>                                     |     |
| Timothy J Bradley  |     |
| <b>Marine Mammals and Fisheries</b><br><i>J R Beddington et al., eds</i>                             |     |
| T J Pitcher  | 406 |

## COMMENTARY

- |  |     |
|--|-----|
| <b>Screwworm eradication a grand delusion?</b> |     |
| J L Readshaw                                   | 407 |

## ARTICLES

- |  |     |
|--|-----|
| <b>Latest Miocene benthic <math>\delta^{18}\text{O}</math> changes, global ice volume, sea level and the 'Messinian salinity crisis'</b> |     |
| D A Hodell, K M Elmstrom & J P Kennett   | 411 |
| <b>Expression of N-cadherin adhesion molecules associated with early morphogenetic events in chick development</b>                       |     |
| K Hatta & M Takeichi   | 447 |

Contents continued overleaf



---

## ARE YOU FOLLOWING THE LEADER?

Throughout the world, Celltech's immunoprocessing activities are followed with interest.

Immunopurification is the breakthrough that allows high recovery rates of highly-purified interferon for the first time.

Celltech developed the only complete range of immunopurification reagents (the Reselute™ range) and process assays for interferons alpha, beta and gamma. Interferons produced using these reagents are now in clinical trials/product registration worldwide.

Now we are the first company to launch immunopurification reagents and process assays for interleukin-2.

Just what you'd expect from the world's largest producer of monoclonal antibodies.

So make sure your organisation is included on our mailing list.

Just complete and send the coupon below.

---

Please send me further details.

Name \_\_\_\_\_

Position \_\_\_\_\_

Company \_\_\_\_\_

Address \_\_\_\_\_

Telephone/Telex \_\_\_\_\_

**CELLTECH** LEADERS IN  
INTERFERON/INTERLEUKIN-2 PURIFICATION  
AND ASSAY



Celltech Limited, 228 Bath Road,  
Slough SL1 4EN, Berkshire, UK

Tel: UK (0753) 77866

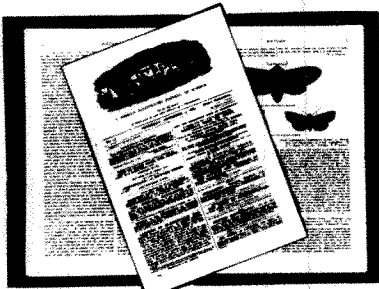
International + 44 753 77866

Telex: 846 701 CELTEC G

Represented in Japan by: Sumitomo Corporation  
Tel: Tokyo 03(294)1611. Osaka 06(220)6894

## CONTENTS

# NATURE'S FIRST ISSUE FACSIMILE



.....40-PAGES OF INTRIGUING SCIENTIFIC HISTORY REPRODUCED.

ORDER YOUR OWN COPY AND DISCOVER HOW SCIENCE HAS ADVANCED SINCE 1869!

PRICES AND ADDRESS FOR ORDERS ARE SET OUT BELOW.

#### Annual Subscription Prices

UK & Irish Republic	£104
USA & Canada	US\$240
Australia, NZ & S. Africa	Airspeed £150 Airmail £190
Continental Europe	Airspeed £125 India Airspeed £120 Airmail £190
Japan	Airspeed Y90000
Rest of World	Surface £120 Airmail £180

#### Orders (with remittance) to:

USA & Canada	UK & Rest of World
Nature	Nature
Subscription Dept	Circulation Dept
PO Box 1501	Brunel Road
Neptune	Basingstoke
NJ07753	Hants RG21 2XS, UK
USA	Tel: 0256 29242

(The addresses of Nature's editorial offices are shown facing the first editorial page)

#### Japanese subscription enquiries to:

Japan Publications Trading Company Ltd  
2-1 Sarugaku-cho 1-chome  
Chiyoda-ku, Tokyo, Japan  
Tel: (03) 292 3755

**Personal subscription rates:** These are available in some countries to subscribers paying by personal cheque or credit card. Details from:

USA & Canada	UK & Europe
Nature	Felicity Parker
65 Bleecker Street	Nature
New York	4 Little Essex Street
NY 10012, USA	London WC2R 3LF, UK
Tel: (212) 477-9600	Tel: 01-836 6633

**Back issues:** UK, £2.50; USA & Canada, US\$6.00 (surface), US\$9.00 (air); Rest of World, £3.00 (surface), £4.00 (air).

#### Binders

Single binders: UK, £5.25; USA & Canada \$11.50; Rest of World, £7.75. Set of four: UK, £15.00; USA & Canada \$32.00; Rest of World, £22.00.

#### Annual indexes (1971-1985)

UK, £5.00 each; Rest of World, \$10.00

#### Nature First Issue Facsimile

UK, £2.00; Rest of World (surface), \$3.00; (air) \$4.00

#### Nature in microform

Write to University Microfilms International, 300 North Zeeb Road, Ann Arbor, MI 48106, USA

#### Induction of tolerance by monoclonal antibody therapy

R J Benjamin & H Waldmann 449

#### Abrogation of oral tolerance by contrasuppressor T cells suggests the presence of regulatory T-cell networks in the mucosal immune system

I Suzuki, H Kiyono, K Kitamura, D R Green & J R McGhee 451

#### Superoxide anion is involved in the breakdown of endothelium-derived vascular relaxing factor

R J Gryglewski, R M J Palmer & S Moncada 454

#### Dispersed human immunoglobulin κ light-chain genes

E Löttscher, K-H Grzeschik, H G Bauer, H-D Pohlenz, B Straubinger & H G Zachau 456

#### Increased phosphorylation of ribosomal protein S6 following micro-injection of insulin receptor-kinase into *Xenopus* oocytes

J L Maller, L J Pike, G R Freidenberg, R Cordera, B J Stith, J M Olefsky & E G Krebs 459

#### Ca<sup>2+</sup> release from endoplasmic reticulum is mediated by a guanine nucleotide regulatory mechanism

D L Gill, T Ueda, S-H Chueh & M W Noel 461

## MATTERS ARISING

#### New evidence for the dendrochronological dating of Netherlandish paintings

D Eckstein, T Wazny, J Bauch & P Klein 466

#### Dating of art-historical artefacts

J M Fletcher 466

## NEW ON THE MARKET

#### Familiar sights in fresh relief

467

## EMPLOYMENT

#### Training for competitiveness

R Pearson 470

## NATURE CLASSIFIED

#### Professional appointments —

#### Research posts — Studentships —

#### Fellowships — Conferences —

#### Courses — Seminars — Symposia:

Back Pages

## Next week in Nature:

- Seeing in colour
- Microscopy of viruses
- Slime mould traction
- AIDS virus expressed in vaccinia virus
- c-ras in oncogenic transformation
- Immunoglobulin evolution
- Streptavidin-avidin techniques
- Bending DNA
- DNA mismatch repair
- Chaotic Hyperion
- ULF waves in ionosphere
- Atmospheric sulphur cycle
- Mexico City earthquake damage

## GUIDE TO AUTHORS

Authors should be aware of the diversity of *Nature's* readership and should strive to be as widely understood as possible.

**Review articles** should be accessible to the whole readership. Most are commissioned, but unsolicited reviews are welcome (in which case prior consultation with the office is desirable).

**Scientific articles** are research reports whose conclusions are of general interest or which represent substantial advances of understanding. The text should not exceed 3,000 words and six displayed items (figures plus tables). The article should include an italic heading of about 50 words.

**Letters to Nature** are ordinarily 1,000 words long with no more than four displayed items. The first paragraph (not exceeding 150 words) should say what the letter is about, why the study it reports was undertaken and what the conclusions are.

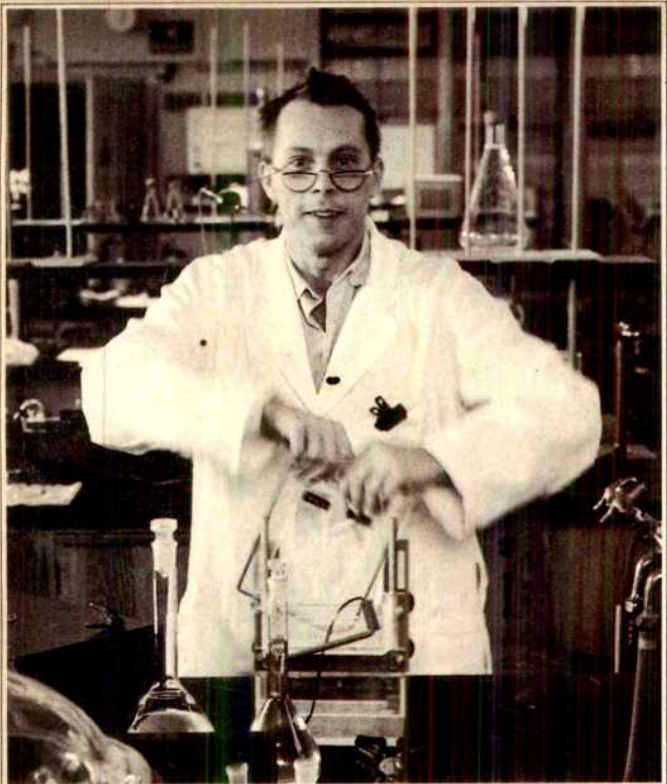
**Matters arising** are brief comments (up to 500 words) on articles and letters recently published in *Nature*. The originator of a Matters Arising contribution should initially send his manuscript to the author of the original paper and both parties should, wherever possible, agree on what is to be submitted.

Manuscripts may be submitted either to London or Washington. Manuscripts should be typed (double spacing) on one side of the paper only. Four copies are required, each accompanied by copies of lettered artwork. No title should exceed 80 characters in length. Reference lists, figure legends, etc., should be on separate sheets, all of which should be numbered. Abbreviations, symbols, units, etc., should be identified on one copy of the manuscript at their first appearance.

References should appear sequentially indicated by superscripts, in the text and should be abbreviated according to the *World List of Scientific Periodicals*, fourth edition (Butterworth 1963-65). The first and last page numbers of each reference should be cited. Reference to books should clearly indicate the publisher and the date and place of publication. Unpublished articles should not be formally referred to unless accepted or submitted for publication, but may be mentioned in the text.

Each piece of artwork should be clearly marked with the author's name and the figure number. Original artwork should be unlettered. Suggestions for cover illustrations are welcome. Original artwork (and one copy of the manuscript) will be returned when manuscripts cannot be published.

**Requests for permission to reproduce material from Nature** should be accompanied by a self-addressed (and, in the case of the United Kingdom and United States, stamped) envelope.



## Electrophoresis then and now

Then, in the early 70's, this was the latest thing in electrophoresis.

Now, it's the mid 80's, and there's a powerful new concept in high-resolution electrophoresis.

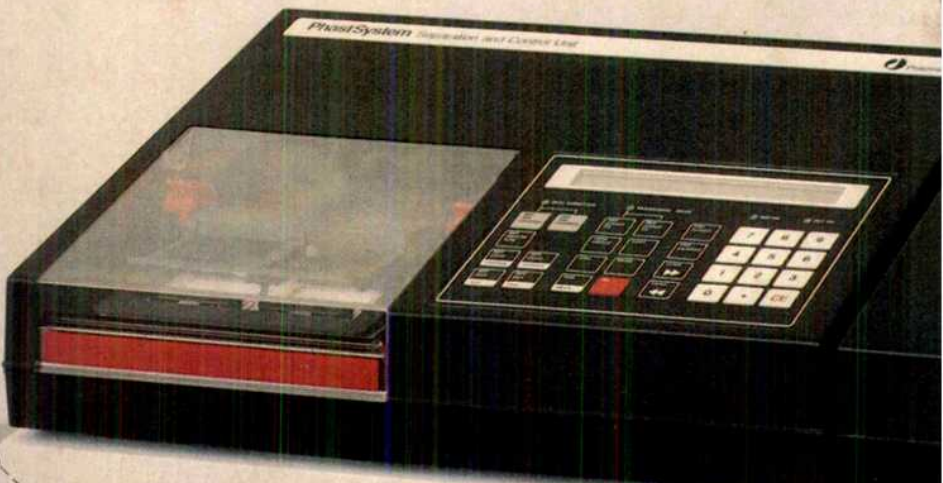
# Phast<sup>S</sup>

## Run and stain SDS-PAGE

**PhastSystem**, a new class of electrophoresis, gets you fast, high-resolution, reproducible results.

**PhastSystem** combines precision equipment and new high-performance media to give you:

- **Fast results** from short separation times and quick protein staining. SDS-PAGE, including staining, takes about 1 hour. IEF about the same. So you get results when you need them.
- **Four separation techniques** to choose from: SDS-PAGE, native PAGE, IEF and titration curves. All run and stained with the same system.



Yes, I want to get fast electrophoresis results.  
Send me more information about PhastSystem.

Name  
Title  
Address  
City  
State  
Zip  
Position

**Find out more about fast electrophoresis**  
Contact Pharmacia today and find out how to  
get fast electrophoresis results.

A. Salle  
21-6-88  
4917

## Tough talk on surrogate birth

*Is it wholly wrong that married couples unable to conceive children naturally should pay others to perform that service? Mistakenly, Britain is behaving as if there were no doubts.*

It was always on the cards that the British government, by its failure to legislate more quickly on the recommendations of the Warnock committee, would allow a muddle to develop. It seems to have a useful ally in that cause in the British Parliament. The most urgent need is that the position of those wishing to make observations of living embryos should be clarified; the Warnock committee advocated experiments under licence with embryos up to 14 days, whereafter any experiment would become the cause of a criminal prosecution. It would be good to think that the government has recognized the unwise of that proposal, and that it plans to legislate for licensing, coupled with supervision by independent committees, allowing researchers more flexibility, but there is no way of telling. Meanwhile, research limps along uncertainly, under the non-statutory supervision of a committee established by the Medical Research Council and the Royal College of Obstetricians and Gynaecologists — and the Houses of Parliament chip away piecemeal at what should be the government's responsibility. The dangers of this approach are well illustrated by the fate of last year's instant legislation, begun in the House of Commons, when the sale of surrogacy services became an offence. One consequence appears to have been that British couples who are infertile are seeking the service overseas, which the House of Lords will this week attempt to ban by law, making it illegal for agencies in Britain to offer to provide such services even with the help of surrogate mothers elsewhere. Presumably the result will be that the agencies concerned will operate offshore.

This is the inevitable result of attempts to prevent well-intentioned people from using what seems to them a natural way of meeting a natural need. Procreative instincts have an adaptive significance for all species and, while they may become a nuisance in long-lived human societies, cannot be repressed by legislation. Moreover, it is natural that couples should prefer genetically related to unrelated children: Dawkin's concept of the selfish gene, not to mention a great deal of sociobiology, refers. The Warnock committee, after eighteen months of careful study, was itself divided on the issue; the majority would have made surrogacy a criminal offence when money changes hands, partly by analogy with the law covering the adoption of children in Britain. But a minority wisely argued that circumstances might arise in which paid surrogacy is justified. (It seems to be common ground that the willingness of some women to bear children for close relatives, another illustration of the selfishness of genes, should not be prevented by law if no money changes hands.) What, for example, if a woman is infertile as a result of a hysterectomy? This is one of the questions raised last weekend by Dr Robert Edwards and Mr Patrick Steptoe, the pioneers of *in vitro* fertilization in Britain. It is hard to deny their case for surrogacy, ideally based on a fertilized egg from the infertile woman, but the British Parliament would even stop that.

The weakness in the British Parliament's position on surrogacy is that it confuses two quite unrelated emotional issues. Some people believe simply that unfamiliar practices are wicked, and should be stopped. This is, after all, the Parliament that required that men with red flags should walk in front of the

early motorcars. The other cause for anxiety, legitimate as it happens, is that surrogacy might become a vehicle for the exploitation of those concerned, either surrogate mothers or the putative genetic parents. So what the House of Lords should have been doing this week, and what the House of Commons will in due course have to decide, is how to protect the vulnerable parties to these transactions without denying remedies to those determined to have children.

The best solution, for which there is already a good working model, is that arrangements for surrogacy should be made not by commercial agencies but by corporations with the legal status of charities (which, in Britain, is what adoption societies are). But since it is wrong to hazard the lives of women by childbirth on behalf of others, it is quite wrong to insist that the surrogate mothers should not be paid. On the contrary, they should be insured financially against risk, while compensation for the considerable time and trouble is the opposite of outrageous. Further, all those concerned in a surrogacy arrangement should have the benefit of independent counselling, of a kind unlikely to be fully convincing if provided by an agency with a profit to make. That constructive course, not futile repression, is the wise course to follow. □

## Future for the birds

*The future of the US shuttle is still in doubt, but the causes of what went wrong are clear.*

THE reappointment of Dr James C. Fletcher as administrator of the US National Aeronautics and Space Administration (NASA) is one step towards the agency's rehabilitation (see p.100), but there is a long way to go. Although the technical cause of the failure of *Challenger* two months ago has not been finally pinpointed by the US President's commission of inquiry, it stands out a mile that the fault within the agency was simply the failure of bad news about the risk of rocket failure to travel upwards to those most in need of it, the people responsible for deciding how quickly to push ahead with the shuttle programme. No doubt before the commission's inquiry is over, it will become clear that the chief inhibition was the familiar phenomenon that the bearers of bad news usually win less than meagre credit. The shuttle pilots were probably right to have complained, earlier this week, that the shuttle should have been grounded at least since last summer.

Dr Fletcher's immediate problem is technical, how to get the shuttle safely off the ground again. He will have to say quite openly that he will not be able to do that on a shoestring, which may make him the bearer of bad news in the year when the Gramm-Rudman act comes into effect. He will also need to develop, or otherwise procure, an unmanned satellite launcher that can be used for the routine business of putting routine satellites into routine orbits, when it is pointless to risk people's lives. Meanwhile, the ambitious scheme for building a permanent space station should be postponed at least until the shuttle is made safe. But further ahead, he must find a way of encouraging constructive fault-finding within the agency. □

## AIDS

# Pasteur plans to pursue patent suit on virus

THE US Justice Department has told the Institut Pasteur in Paris, where virologist Luc Montagnier discovered the virus that causes acquired immune deficiency syndrome (AIDS), that "there is no case to answer" over the laboratory's complaint that the US National Institutes of Health (NIH) pirated Montagnier's discovery — and now profits from it by the sale of AIDS blood tests.

The French laboratory has, however, discovered what could be damning new evidence against NIH, and is now considering placing it before the Washington judge investigating whether NIH used the French-discovered virus for commercial gain, in breach of contract between NIH and the Pasteur.

Nobody disputes that Montagnier sent a sample of serum containing the AIDS virus, which he called LAV, to NIH virologist Robert Gallo in September 1983, but NIH claim that Gallo was unable to propagate LAV, and that he subsequently and independently isolated the virus he called HTLV-III. This and a blood test based upon it were rapidly patented and approved for use. HTLV-III tests are now marketed by five US companies, while the Pasteur's test (Elavia) based on Montagnier's virus is still awaiting US patent approval. This is despite the fact that the Pasteur applied for a patent for LAV and its associated test well before NIH applied for a similar patent for HTLV-III.

Pasteur sources claimed last week that the institute has new evidence, in the form of a letter describing research results, that Gallo's laboratory was making electron micrographs of the LAV virus in December 1983, three months after it was first received in a sample from the Pasteur. If this is confirmed, it would seem to contradict the NIH position that Gallo was unable to propagate LAV, and would strengthen at least the circumstantial evidence that HTLV-III is indeed derived from the French isolate. (HTLV-III and LAV have almost identical genetic sequences, but NIH have argued that this is merely because both viruses came from the same population of patients in New York.) According to the Pasteur, the letter in question describes December 1983 micrographs as pictures of LAV which indicate that it might be a form of lentivirus.

The electron micrographs in question were taken at the National Cancer Institute's Frederick Cancer Research Center. But Gallo and his colleagues scoff at the idea this constitutes evidence of skuldug-

gery. Gallo says the letter, along with all other "evidence", was supplied by his own laboratory to Montagnier. He achieved transient growth (evidenced by the electron microscope observations and reverse transcriptase activity) of the LAV sample supplied by Montagnier in a HUD-78 cell line, but for one week only and in small quantity: subsequent tests showed no evidence of viral replication. Attempts to grow LAV in the high-yielding H9 cell line were totally unsuccessful.

As for the significance of the timing, Dr Peter Fischinger of the National Cancer Institute points out that virus can be frozen and re-examined later, so the interval between the sample arriving and the date of the electron micrograph means nothing. Fischinger remarked that it would be surprising if Gallo had not made micrographs of his attempts to culture the virus. And on the charge that Gallo's isolate was in some way derived from LAV, Fischinger referred to recent results obtained using cytolitic antibodies that kill cells infected with HTLV-III but not those infected with LAV or other isolates and so establish conclusively a real biological difference between the isolates.

In a further and ironic twist to the tale, the US Food and Drug Administration (FDA) last month approved the Pasteur's Elavia test as safe to use, but because of the lack of a patent, Pasteur sources are now concerned at the possibility of legal action against them if Genetic Systems Inc., the company due to market Elavia in the United States, actually sells any tests. According to the Pasteur, while Elavia lacks an independent patent, the five companies selling tests based on HTLV-III — and paying royalties under licence to NIH — could complain that Elavia was a "counterfeit" of the NIH test designed to avoid royalty payments, even though the French say the real case is the reverse.

Meanwhile, Elavia is said to be performing very well in tests at the British Public Health Laboratory in London, with results close to those of the Dutch (Organon) and British (Wellcome) tests approved for use "with flying colours" a few months ago. This may leave Elavia with some room on the British market, but in the United States the primary market in blood banks and hospitals is now thought to be effectively tied up by the five companies whose tests are now approved there. The French test shows fewer "false positives" (false indications that a patient has AIDS antibody) than most of the US tests, thus avoiding expensive follow-up

tests, but this may not now be enough to win a market share.

British scientists also have a small interest in Elavia, but their work also threatens to displace whatever hold the French test may have in the United States. Elavia's technical advantage can be traced to the virus cultivated in a line of white blood cells, the CCRF-CEM line (or CEM for short) of T cells, that does not express certain antigens (HLA class two antigens) that can interfere with the results of blood tests.

The use of the CEM line was developed in London's Institute of Cancer Research. The director, Robin Weiss, says that "we have no claim on the CEM line", but his laboratory does have an agreement with the Pasteur that half of any royalties accruing to the Pasteur from use of the CEM line to prepare AIDS tests would return to Britain.

The Pasteur has made further developments "but we would still expect a proportion of the royalties" Weiss said last week, though "our goal has not been to make money but to develop a reliable test for public health". Weiss's laboratory has however developed its own more rapid test, using a British viral isolate and a completely different (and shorter) analysis technique, "competition assay", distinct from the enzyme-linked immunosorbent assay (ELISA) used by all other tests. This test is the one now approved and marketed by Wellcome in Britain. And according to Weiss, "we have not had one false positive in a million tests". Moreover, since the competition assay is complementary to other techniques, Weiss considers it a good follow-up test to check the results of others.

The conclusion is that whatever the result of the Pasteur's legal action in the United States, any mopping-up of the US market may go not to Genetic Systems and Elavia but to what are now more advanced tests such as Wellcome's, or to second-generation tests, now under development, based on the production of pure AIDS virus antigens by recombinant DNA techniques. It now seems clear that if the Pasteur wants to profit at all from tests for AIDS in the United States, it will have to prove that HTLV-III is derived from that sample of LAV that Montagnier sent Gallo back in 1983, and aim for a fraction of royalties on tests now on the market and derived from HTLV-III.

**Robert Walgate & Tim Beardsley**

## Halley's comet data

By agreement with the European, Japanese and Soviet groups, *Nature* will publish on 15 May the first formal accounts of the data gathered by the four encounters with Halley's comet, together with related US observations. □

**Halley's comet**

## Vega spacecraft reveal more dust than expected

*Moscow*

THE successful flight of the two Soviet space probes past the nucleus of Halley's comet showed that even from a distance of less than 8,000 km the nucleus of the comet was mostly obscured by dust. Estimates of the quantity of water being evaporated from the comet last week, a month after perihelion, range up to  $2 \times 10^{30}$  molecules per second. The three separate dust recorders in the first Vega package have shown that the mass of dust being lost is roughly a sixth that of the water. In round numbers, the water loss on 6 March was 30 tonnes an hour, that of dust roughly 5 tonnes an hour.

One practical consequence is that images from the two cameras on Vega 1 were unable to distinguish the nucleus of the comet within its dust cocoon. By the time of the encounter by Vega 2 on 10 March, the quantity of dust had fallen by a factor of two, for reasons not necessarily connected with the increasing distance of the comet from the Sun. But the camera images on this occasion are not as easily interpreted because of a pointing error, corrected only 10 minutes before the encounter. Even so, the Hungarian team working on the processing of images says it has extracted the information that the nucleus has a dumbbell shape and is less than 10 km across at the maximum.

The dust measurements have provided most of the surprises. Both Vega craft encountered the main dust sheet at about 100,000 km from the nucleus of the comet, in line with the expectation that the dust is responsible for the coma caused by the scattering of solar radiation. But some of the experimenters have been surprised to find recordings of dust particles from the comet as far away as 150,000 km.

Others say it is surprising that the dust recorders show the appearance of fine dust ( $10^{-15}$  grams or smaller) before that of more substantial grains. On the present view of the formation of the coma and the cometary tail, dust is carried from the solar side of the nucleus by the stream of evaporated water molecules until driven away from the Sun by radiation pressure, which leads to the prediction that larger grains should form the outermost sheath of the coma and the tail.

The sheer size of the dust particles has also been surprising. The Soviet originators of the photon experiment, an ingenious device by which the holes caused by dust particles penetrating the thin outer shell of the Vega spacecraft are measured optically and the accompanying plasma jet is detected electronically in such a way as to provide both the energy and momen-

tum of the incident particle, say the largest particle recorded by Vega 2 had a mass of  $2 \times 10^{-5}$  grams. It left a hole in the outer skin nearly half a centimetre across.

The approach to the comet by both spacecraft has also provided a wealth of information about the transition between the region dominated by the solar wind and that in which ions from the comet are predominant. At this stage, it is not clear



Image of comet Halley on 17 December 1985, taken with a 1-m reflector at the Alma-Ata Observatory by K.I. Churyumov and Rspayev. North is up and East to the left.

whether either of the spacecraft detected the expected bow shock, representing the interaction between the solar wind and the cometary environment. Vega 1 may have passed through the bow shock before the instruments were switched on just over three hours before the encounter on 6 March; alternatively, the transition region may be more diffuse than expected.

At the second encounter on 10 March, both the intensity of the solar wind and the concentration of gas and dust from the comet were reduced by a half. The plasma detectors on Vega 2 have clearly shown how, on the inward passage towards the comet, ions (mainly protons) characteristic of the solar wind are gradually replaced by heavier ions, chiefly those of water and its photolysis products, between 150,000 km and 50,000 km from the nucleus.

Magnetic field measurements in the hours before the two encounters, essentially with similar results, also show the steady transition from the interplanetary to the cometary environment. On both occasions, the magnetic field increased (but with an apparent periodicity which is not yet explained) from the

12–15 nT (1 nT =  $10^{-4}$  gauss) characteristic of the interplanetary solar wind regime to 75 nT within the cometary environment.

Some of the most striking data are those from the time-of-flight mass spectrometer designed at the Max-Planck-Institut für Kernphysik at Heidelberg, built with French funds and operated jointly with Soviet specialists. The instrument provides an instant mass spectrogram of the content of the plasma produced by the impact of individual dust particles on a silver target. Vega 1 provided more than 1,000 records, Vega 2 nearly half as many. Although many particles appear to have been composed largely of light elements with atomic number less than 20, there is a substantial fraction with components of atomic number between 30 and 50. The interest will be to see whether the second group shows the presence of silicon and iron, expected constituents of primordial dust.

The two encounters have also provided an extremely accurate determination of the orbit of Halley's comet, chiefly through the work of the Pathfinder project designed so as to provide the basis for guiding the European spacecraft Giotto to its encounter with Halley's comet on Thursday this week. On the basis of the data from Vega 1, the Pathfinder project says that it has been able to define the position of the comet in its orbit with an uncertainty of only 15 km.

One of the team responsible says that ground-based observations in the past few years have refined the orbital elements of the comet by a factor of 100, while triangulation based on accurate radio-interferometric measurements of the position of the Vega spacecraft and a knowledge of their pointing angles towards the Halley nucleus have made possible a further refinement by a factor of 30.

Elaborate arrangements have been made to communicate this information to those at the Darmstadt centre of the European Space Agency in West Germany, from where the Giotto encounter is being controlled. It is especially relevant that the uncertainty of the position of the comet along its orbit has been reduced from several hundred kilometres to a few tens of kilometres, given the ambition to send Giotto within 500 km of the nucleus.

A final decision about the direction of Giotto was due to be made on Tuesday this week. According to Dr Roger-Maurice Bonnet, the French scientific director of the Giotto project, the decision is certain to have been difficult. Five of the nine experiments on Giotto would prefer to get even closer to the nucleus than 500 km, but the other four wish to survive beyond the closest approach while two would like to survive by several days. One complicating factor is that nobody at

present understands why there has been such a rapid decrease of dust production in the three days between the two Vega encounters.

Dust appears to have played havoc with several of the Vega experiments. A low-frequency plasma detector, based on an antenna stretched between one of the booms projecting from the spacecraft and the solar panels, went out of action just before the first encounter, to the resigned annoyance of the group responsible. On the less successful encounter of Vega 2, several instruments went out of action before the encounter. One speculation is that the spacecraft may have become electrically charged in such a way as to affect the operation of instruments requiring a stable reference voltage.

The encounter of Vega 2 was also complicated by a pointing error, which for most of the approach had the cameras locked on to a bright patch of scattered sunlight offset from the nucleus of the comet. The most serious consequence was that the automatic microprocessor-based program relating the exposure of each frame to the brightness of the aiming point consistently over-exposed the nucleus. In a nail-biting emergency, the error was corrected only ten minutes before the encounter with the help of a back-up guidance system.

The general opinion of experimenters and managers is that the project has been outstandingly successful. Those gathered at the Institute of Space Science of the Soviet Academy of Science, which has mounted the exercise, have been quick to pay tribute to the international collaboration on which the project has been based.

Collaborators come from France and West Germany in Western Europe and from Czechoslovakia, Hungary and Yugoslavia in Eastern Europe. Although the United States is not formally involved in a project mounted when relations between the Soviet Union and the United States were in the doldrums, Professor J.A. Simpson from the University of Chicago has flown a novel dust detector on the identical Vega spacecraft at the invitation of Professor R.Z. Sagdeev, the director of the Soviet project and the institute at which it is based.

By common consent, the Deep Space Tracking Network of the US National Aeronautics and Space Administration (NASA) had also provided invaluable assistance both during the preliminary encounters of the Vega spacecraft with the gravitational field of Venus at the end of last year and in refining the trajectory of the vehicles.

Sagdeev recalls the Jet Propulsion Laboratory in California calling up one night with the question why one of the two Vegas had apparently vanished from the radio sky. □

## Halley's comet

# Telling the truth in real time

Moscow

As this monumental city last Wednesday watched its four-month covering of snow turn to grey slush, the builders of the first of four probes to Halley's comet were celebrating (mostly in the abstemious Gorbachev style) their successful first look at that eroding dirty snowball in the sky. But the more striking achievements may be the informality of the international collaboration on which the Vega project was based and the frankness with which all the details of the project were displayed.

To say that the outcome confirms the dirty snowball picture of a comet, that of a lump of frozen water with embedded dust, true though it might be, would be to diminish the occasion. Getting within 8,000 km of an object nine light-minutes away may be child's play these days, while Voyager has shown that instruments can be made to function at least a decade after being built, but who can suppress childish pleasure that five years of planning for an hour or so of proximity to Halley should, in the end, succeed?

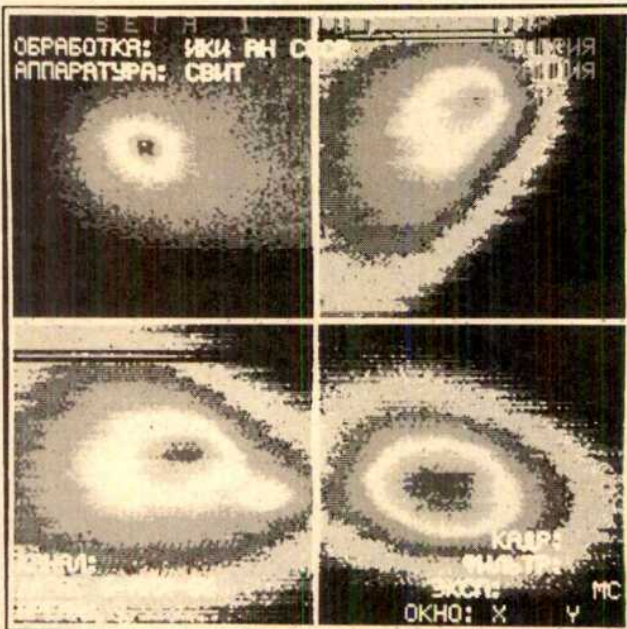
There were, in fact, two Vagas and thus two close encounters, on Wednesday last week and on Sunday. As launched (in December 1984), the two spacecraft were identical. Each of them dropped a balloon into the atmosphere of Venus before being deflected towards the retrograde orbit of Halley, still last week between the orbits of the Earth and Venus (but with the Earth on the other side of the Sun). At the Soviet Academy of Science's Institute of Space Sciences, the interval was spanned by a kind of perpetual polyglot symposium interrupted only by visits to other laboratories and the need for lunch.

Strictly, there have been two on-going

symposia. The experimentalists have been crammed with their microprocessors into a ground-floor room about 30 m<sup>2</sup> dominated by a full-scale model of Vega. Each experiment has been able to monitor its own data stream in real time; most, almost as a matter of pride, have thought it seemly to produce an instant analysis and interpretation as well. The Hungarian image processors were back-to-back with the Austrian recorders of the magnetic field. The Czechoslovak and US dust particle experiments were within whispering distance of each other (with the West Germans across the corridor). The French team taking ultraviolet spectra have been almost inaccessible in their corner.

The other symposium, on the floor above, has been for dignitaries, and has been recognizable by the bottles of mineral water on the tables. (Local opinion holds that "something is going to happen" when the bottles are changed; "they know we'd drink them if they left them there too long".) The dignitaries have included Dr Fred Whipple, lately retired from the Harvard-Smithsonian Astrophysical Observatory, the originator of the dirty snowball picture, Dr Thomas Donahue, chairman of the US National Academy's Space Sciences Board, delegations from the European Space Agency (ESA), the US National Aeronautics and Space Administration (NASA) and from the Space Sciences Institute at the University of Tokyo and vice-presidents of the Soviet Academy, who dropped in from time to time.

During both encounters with Halley's comet, this symposium has been kept thoroughly up to date by a display on two substantial video screens of data as re-



False-colour images of Halley's comet (shown here in black and white) from Vega 1 at around the time of closest approach at 07.20 GMT on 6 March, with four different filters. Although the top left-hand image shows a small peak of intensity (which appears white) near the centre, this cannot be identified with the nucleus of the comet, but is rather an artefact of the colour-coding system. The double structure immediately below, in the near infrared, may signify the jet of dust encountered by Vega 1. The distance across each frame is about 1,500 km.

ceived and analysed by the experimenters in virtually real time. Professor Albert Galeev provided a running commentary, doing his best to interpret data as they appeared and succeeding reasonably well except when the projectionists switched displays in the middle of a sentence. (A Hungarian image processor says he had not been asked to provide this frill until a month ago.) It is an interesting and moving experience to see mass spectrograms of the products of the impact of single cometary dust particles on a silver target literally before the West Germans who built this ingenious apparatus had a chance to censor them.

Formally, the six-day symposium was a meeting of the inter-agency coordinating group bringing together the US and European space agencies, an amalgam of the two agencies in Japan and that from the Soviet Union. Academician R.Z. Sagdeev, the driving force behind Vega and the manner of its public presentation, wanted to use the occasion for hammering out a further programme of collaboration, offering to form a working group to say what should be done next before everybody took flight for Darmstadt and the Giotto encounter. But neither NASA nor ESA was ready for this proposal, suggesting instead a formal discussion at a meeting planned for Padua in November.

Apparently there is a plan to move from Padua to Rome for a public presentation of the Halley data, including an audience with the Pope, to whom each agency is expected to provide its four best pictures of the comet, possibly on 7 November. Those making the arrangements appear to have overlooked the significance of the date, the anniversary of the October Revolution. Sagdeev wondered whether the Pope might be persuaded to celebrate mass for the occasion.

For the rest, the dignitaries behaved as dignitaries do on these occasions. Their congratulations have been full-throated, not merely for the success of the two Vegas but for the openness of the proceedings of which they have been a part. The institute's staff has been surprised to find the proceedings televised live from the "data analysis room", which is said to be unprecedented. But what about the Party Congress? "That's the other exception."

The good-humoured meeting has also been sadly depressed about the shuttle tragedy, wondering what the effect will be on the US space programme. NASA officials say that it has been decided to plan on the assumption that the shuttle will be operating again after a delay of twelve months, and that priority will then be given to launching the Galileo mission to Jupiter and the Hubble space telescope. The snag, it seems, is that "it's costing us \$10 million a month to keep things on hold".

John Maddox

## NEWS

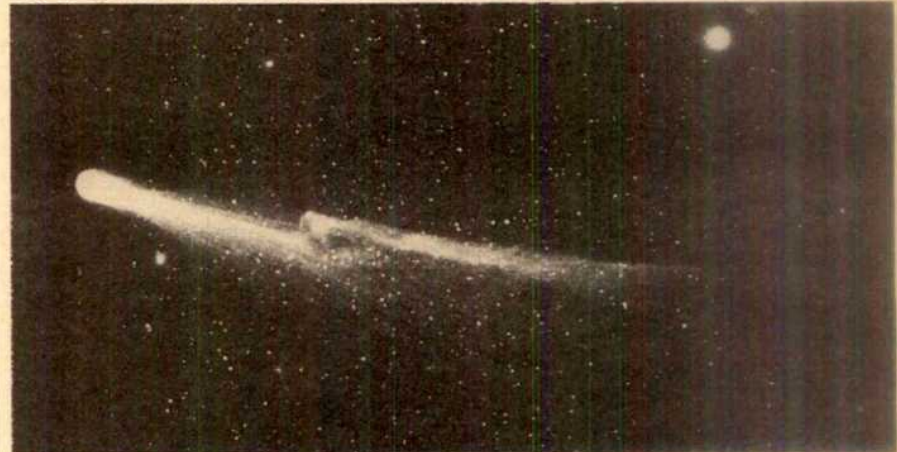
### Halley's comet

## Japan's probe rocked by dust

Tokyo

"It's great" was how researchers at Japan's Institute of Space and Astronautical Science (ISAS) reacted to news that their space probe *Suisei* (comet) had safely passed its point of closest approach to Halley's comet. *Suisei* was twice shaken by collision with high-velocity dust particles as it came within 150,000 km of the

some rapid calculations as to just how big the particles must have been to rock the 135-kg probe, bearing in mind that their relative velocity is something like 73 km per second. Initial estimates were that the dust weighed about 10 µg; but recalculation came up with a figure of 1–2 mg, giving the particles diameters of 1–2 mm. If this proves correct it is a very big sur-



Sun side of Halley at 22.06 on Saturday, 8 March (Japan time) but in neither case was it thrown sufficiently out of orientation to affect data collection.

News of the collisions and data from the encounter did not reach Japan until Sunday, for the probe was on the wrong side of the Earth to communicate with ISAS's new deep-space observation centre at Usuda in Nagano Prefecture, west of Tokyo. Last commands sent to *Suisei* on Saturday were for the probe to continue to make observations with its ultraviolet camera and its ion-energy analyser according to programme. From Saturday evening until Sunday morning, signals were picked up at the US National Aeronautics and Space Administration (NASA)'s space observation centres in Spain and California, suggesting that all was going well. Then when *Suisei* came back round to the Japan side of the Earth, all data collected during the encounter were taken out of memory and transmitted to Japan.

The first and biggest surprise was that the probe had been shaken by collisions with dust particles just before the point of closest approach. The first collision at 20.54 knocked the rotation axis of the probe relative to the Sun out by 0.48°; the second at 21.26 added another 0.24° deviation. But neither was sufficient to affect observations of the comet. The first impact was also powerful enough to slow down the satellite's spin period of 9.184 seconds by 0.027 seconds; the second, presumably to a different part of the structure, had a scarcely noticeable effect.

News of the dust collision triggered

prise and may be bad news for the European spacecraft, Giotto, which is going very much closer to Halley later this week. "We don't know whether to call it good luck or bad", said one ISAS scientist of the collisions — bad luck to have been hit or good luck to have discovered something quite unexpected; no dust particles this large were expected to be thrown off by the comet.

Not unsurprisingly, there has been no time yet to analyse data in any detail. But results from the Lyman-alpha ultraviolet imaging camera confirms the variability in the hydrogen coma of Halley's comet that the Japanese team report in this issue of *Nature* (see p. 140). Detailed study should make it possible to measure the period of rotation of the comet. Preliminary results from the ion-spectrum analyser also indicate that a shock-like region forms on the Sun side of the comet as the solar wind is displaced around it. Ions from the comet were detected as far as 400,000 km away.

*Suisei* will continue to make observations of Halley for as long as possible. Over the next few days, *Sakigake*, the test probe launched in advance of *Suisei*, will come into position downwind of Halley to complement its observations. On board are instruments to measure plasma waves, ion temperature, velocity and density and the interplanetary magnetic field. But scientists at ISAS are already beginning to wonder what can be done next with *Suisei*. One of ISAS's satellites continued to function for six years and it is hoped that further useful observations can be made with the probe as it continues to circle the Sun.

Alun Anderson

## Biotechnology

# All systems go in Britain

It has been a fortnight of activity at the business end of biotechnology in Britain. First Genentech, the Californian company, was granted a British patent for its tissue plasminogen activator (TPA), which is expected to find a place in the treatment of myocardial infarction. Then the British pharmaceutical company Wellcome plc, while awaiting Genentech's announced intention to file suit against Wellcome for infringement of the newly granted TPA patent, set in motion an attempt to revoke the patent. And finally, the first British licences for a clinical use of interferon were granted.

The interferon licences are less of a coup than they might seem, since they are only for the treatment of hairy-cell leukaemia, of which there are fewer than 100 new cases a year in Britain. Interestingly, the Committee on Safety of Medicines, which grants the licences, has chosen not to discriminate between Wellcome's interferon (trade name Wellferon), which is purified from a cultured cancer cell line and is a mixture of the many slightly different  $\alpha$ -interferons, and Intron A, which is a single  $\alpha$ -interferon produced in bacteria by recombinant DNA technology by Schering-Plough (the licence goes to the company's British subsidiary Kirby-Warrick Pharmaceuticals Limited). Hoffmann-La Roche has

also applied for product licences for its recombinant DNA-produced  $\alpha$ -interferon (Roferon A).

It remains to be seen, said Wellcome officials last week, whether there will be conditions in which their broad-spectrum product is advantageous or disadvantageous compared with single interferons. So far, both Schering and Hoffmann-La Roche have each concentrated on only one  $\alpha$ -interferon. Dr Daniel Catovsky of the Royal Postgraduate School of Medicine in London, who has carried out a trial of Wellcome's interferon, said this week that it seems as if all cases of hairy-cell leukaemia seem to benefit in a predictable way from treatment.

Schering's interferon- $\alpha_2$  started life as a clone in Dr Charles Weissmann's laboratory at the University of Zurich and was developed by Biogen for Schering, which now has a variety of product licences in the Philippines, Belgium and Ireland but none yet in the United States. Hoffmann-La Roche's interferon- $\alpha_2$  was originally cloned by Genentech.

In contrast with its policy on interferon, Genentech has chosen to be much more independent with TPA, although it does have marketing agreements with some overseas companies. From the first cloning of TPA's DNA at Genentech in 1982 (starting with a TPA-producing cell line characterized by Dr Désiré Collen, see below), the company had reached the stage last year of converting a car park into a fermentation plant dedicated to the culture of the mammalian cells that produce TPA after its DNA has been genetically engineered into them; several European patents have already been granted and clinical trials are far advanced.

By contrast, Wellcome's TPA is still at preclinical stage and is far from being a home-bred product. The original cloning was carried out by Joe Sambrook at Cold Spring Harbor Laboratory in conjunction with the Cell Biology Corporation which was a collaboration between the laboratory and Baxter Travenol. Pre-production development was carried out for Travenol by the biotechnology company Genetics Institute, based in Cambridge, Massachusetts. And Wellcome then took over for the production stages, because of its expertise in the large-scale culture of mammalian cells gained during its interferon work.

The hope is that TPA will be a better thrombolytic agent, particularly in the removal of clots in the coronary arteries, than the currently favoured streptokinase. Commenting on the clinical trials in *New England Journal of Medicine* last October, Dr Sol Sherry of Temple University School of Medicine concluded that "se-

# Plutonium dumping?

REPORTS of plutonium on the seabed near the Loviisa nuclear power station in Finland have been greatly exaggerated, according to Erkki Ikuus of the Finnish Centre for Radiation and Nuclear Safety. But the reports have come at an embarrassing moment for Finland's nuclear energy industry. The two nuclear power companies, Teollisuuden Voima (TVO), which has two nuclear power stations at Olkiluoto, and Imatran Voima (IVO), which operates the two stations at Loviisa, are at present negotiating a cooperation arrangement in order to increase their combined generating capacity by 1,000 MW.

According to Ikuus, the Centre for Radiation and Nuclear Safety monitors the whole Finnish coastline, but concentrates, naturally, on the vicinity of Olkiluoto and Loviisa. The reports about Loviisa referred, he said, to a plutonium concentration of about 100–300 becquerels per m<sup>2</sup>, which, he said, is "typical for all our coastal stations". Helsinki radio, which first carried the story, had, he said, simply mistaken its newsworthiness.

In any case, Ikuus said, the plutonium in question came, not from Loviisa, but from the fallout from nuclear tests in the past. When asked about reports reaching Sweden from Estonian dissidents that nuclear waste from the Paltiski submarine base is being dumped in the forest near Tallinn or discharged directly into the Baltic, Ikuus said that he was "sure on scientific grounds" that this was not the case with the plutonium found in the Finnish sediments.

Vera Rich

## Swiss prize shared

DÉSIRÉ Collen of the University of Louvain, Luc Montagnier of the Institut Pasteur and Michael Berridge of the University of Cambridge have shared this year's £600,000 prize awarded by the Louis Jeanet Foundation for Medicine.

The prize, named after a resident of Geneva who died in 1981, is awarded annually to up to three "outstanding and productive research workers" to provide them "with substantial funds to pursue their researches".

Collen, whose work on the mechanisms of thrombus dispersal forms the basis of the British patent for tissue plasminogen activator, awarded to Genentech two weeks ago, will use the prize money to apply genetic engineering to the production of new clot inhibiting or dissolving substances. The award to Montagnier, who discovered the virus that causes acquired immune deficiency syndrome (AIDS), is to be used to continue his research into this and other human retroviruses. And Berridge will continue to explore the presence and function in cells of substances related to inositol trisphosphate, the work for which his share of the prize was awarded.

Peter Newmark

rious questions remain about how much of a therapeutic advance it will represent as compared with the agents already available". Undeterred, Genentech and Wellcome are prepared to foot the bills for what might be a protracted test case for the patentability of the products of biotechnology. "If litigation does proceed", says Stephen Crespi, controller of patents for the British Technology Group, "it will shed some much-needed light in patentability in this very untested field."

Peter Newmark



DR James C. Fletcher, administrator of the US National Aeronautics and Space Administration between 1972 and 1977, who has been invited to resume the post in succession to Mr James Beggs, who has resigned. The appointment is subject to approval by the US Senate. □

**Prizes**

# US winners for Israeli prizes

**Rehovot**

US CITIZENS walked off with most of this year's Wolf Prizes, just as they did with most of the Nobel Prizes (although the prize categories are not identical).

In mathematics, for example, the \$100,000 Israel-based international award went to a pair of European-born Americans, Professor Samuel Eilenberg of Columbia University and Professor Alte Selberg of the Institute for Advanced Study at Princeton. Eilenberg was chosen for his fundamental work in algebraic topology and homological algebra, while Selberg was honoured for his profound and original work on number theory and on discrete groups and automorphic forms.

Opening up a new field of research, the study of chaos won Wolf Prizes in Physics for an American, Professor Mitchell Jay Feigenbaum of Cornell University, and a Frenchman working in the United States, Professor Albert Joseph Libchaber of the University of Chicago.

Professor Elias James Corey of Harvard University and Professor Albert Eschenmoser of the Swiss Federal Institute of Technology (ETH) share the Wolf Prize in Chemistry, in recognition of their research on the synthesis, stereochemistry and reaction mechanisms for the formation of complex natural products, particularly vitamin B<sub>12</sub>. Eschenmoser is the first Swiss national to receive a Wolf Prize.

In agriculture, the prize is shared by Dr Ernest R.R. Sears of the University of Missouri and Sir Ralph Riley of the UK Agricultural and Food Research Council. The two cytogeneticists were cited for their independent research in basic plant breeding, which has permitted the insertion into wheat of genes representing desirable characteristics from alien plants so as to improve wheat germ plasms and cultivars.

The Wolf Prize in Medicine, the last to be announced, went this year to a Japanese researcher, Professor Oshmu Hayaishi, president of the Osaka Medical College, for his discovery of oxygenases, a group of enzymes that are catalysts in the use of oxygen by living organisms. They also, as the citation noted, play a crucial role in the metabolic disposal of foreign compounds such as drugs and insecticides.

The Wolf Foundation, which has been awarding annual prizes since 1978, was established by the late Dr Ricardo Wolf, a German-born chemist and philanthropist who lived for many years in Cuba. Appointed Cuban Ambassador to Israel in the 1960s by his friend Fidel Castro, he remained in Israel after Cuba broke off diplomatic relations in 1967 until his death in 1981.

**Nechemia Meyers****US science and technology**

# McTeague looks to the future

**Washington**

CONTEMPLATING the future of your agency when it is faced with a 28 per cent budget cut is not a cheerful prospect. But that is the plight of John McTeague in his first weeks as acting director of the White House Office of Science and Technology Policy (OSTP). "We can operate with a budget at almost any level, the question is which activities the office will undertake", says McTeague. "That is a matter of consideration by the Congress."

Last month McTeague was on Capitol Hill before a Senate appropriations subcommittee. While he did not appeal for more money for his agency, McTeague did say that he would be very happy with a 10 per cent cut in his budget, considering the alternative he is faced with.

McTeague is not behaving like a temporary incumbent marking time while waiting to be replaced. Before the congressional committee he was quick to point out the need for a stronger hand in guiding science and technology policy by the federal government. He plans to provide some of that guidance through his own role as chairman of the dozen committees making up the Federal Coordinating Council on Science, Engineering and Technology (FCCSET). While he refuses to state explicitly that he favours a cabinet level department, he clearly feels the present system is awkward.

McTeague considers that most people fail to appreciate the scope of OSTP's activities. "OSTP is a little like an impressionist painting", said McTeague. "If you don't stand back, you miss the picture."

One FCCSET committee, formed last December, is attempting to place renewed emphasis on international cooperative agreements in which the United States is involved.

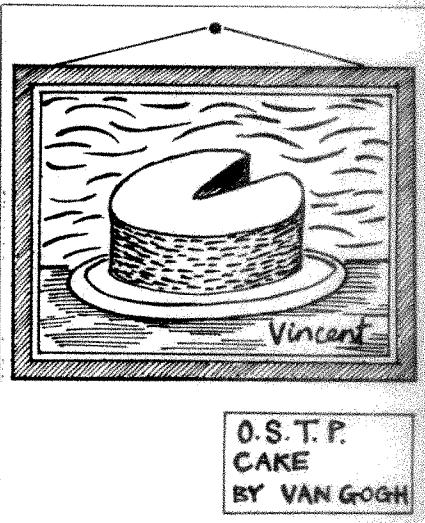
"It's not an effort to dictate individual programmes", says McTeague. But this does not mean that OSTP will support US participation in international programmes that do not fall in line with domestic priorities or international policies. McTeague believes that the most effective international interactions are those that take place informally, with government maintaining a hands-off policy.

One project with enormous international implications is the proposed Superconducting Supercollider (SSC). With a price tag approaching \$6,000 million, there is a natural reluctance to forge ahead, although McTeague maintains that the present administration firmly supports high-energy physics.

"We have to take a good hard look at it [SSC] and see how it fits in at this time with national priorities and budget exigencies", says McTeague. Although

greater cooperation with the European Organisation for Nuclear Research (CERN) may be a practical alternative to building SSC, it seems to fly in the face of a strong commitment by the government to maintaining "this nation's forefront role in high-energy physics".

OSTP has also recently become embroiled in the question of how to proceed with the US space programme following the shuttle disaster. The administration is faced with an expensive problem of whether to buy a new shuttle orbiter in a year when budgets are austere all round. While the administration has not yet officially made a decision, McTeague says expanded use of expendable rocket launch vehicles will provide a solution only "in the short run".



**O.S.T.P.  
CAKE  
BY VAN GOGH**

McTeague feels that the most effective federal role in science and technology "is not to attempt to drive specific commercial technologies, but to support forefront basic research, which will have payoffs not foreseeable at the time of funding". At the same time, he supports "problem focused" science centres at universities, aimed at areas of "broad national needs and relevant to industrial technology". McTeague explains this apparent contradiction by pointing out that it will be scientists, not the government, who will identify these "problems". The government's role will be to nurture these centres once their direction has been plotted.

McTeague has had three years in Washington to watch and participate in the workings of OSTP. He clearly intends to continue pressing for federal support of science, although he is anxious that industry should contribute its share to the financial burden. With the Gramm-Rudman cloud hanging over the United States and the federal budget, running OSTP will not be an easy job. Perhaps it never is.

**Joseph Palca**

## Strategic Defense Initiative

# Grilling for Abrahamson

**Washington**

A RARE glimpse of progress and problems with President Reagan's Strategic Defense Initiative (SDI) was offered last week by Lt General James A. Abrahamson, chief of the SDI organization, baited by a feisty Senator William Proxmire (Democrat, Wisconsin), who kicked off the congressional SDI appropriation hearing by declaring "if you expect a 75 per cent budget increase you're in for a rude awakening".

Abrahamson exercised commendable restraint as he outlined changes to the programme since his last appearance before the defence subcommittee of the Senate Appropriation Committee. Space-based chemical lasers, once one of the SDI organization's high hopes, are out; spaced-based kinetic kill vehicles are in. And point missile defence, a more restricted goal than President Reagan's concept of a shield covering the whole United States, will "need study".

The administration's proposed budget for SDI in fiscal year 1987, which starts next October, is \$4,800 million: the current budget is \$2,760 million, 25 per cent less than the President had requested. The rough treatment meted out to Abrahamson by some members of the subcommit-

tee last week owes something to the fact that, alone among military programmes, SDI has been totally exempted from cutbacks in the current financial year resulting from the Gramm-Rudman deficit reduction law.

But Proxmire — who dominated the proceedings though not formally in charge — also ridiculed the SDI organization's decision to classify a report on SDI contracts prepared by the General Accounting Office entirely from unclassified sources.

Declaring that all the information in the now classified report was readily available through other official and private publications, Proxmire demanded whether Abrahamson thought "the Soviets haven't got \$625 (the cost of the documents) and a calculator". Abrahamson thought it was not in the national interest to have details of SDI contracts and contractors listed in a single, easily obtained volume.

Abrahamson went on to unburden himself with some admissions of greater than expected technical problems that have been encountered in discriminating real warheads from decoys. The SDI organization's "red team" (set up to think of ways in which the Soviet Union might counter SDI) has made US versions of Soviet warheads and possible decoys so successfully that the blue team was forced to conclude that "passive discrimination is not quite sufficient" to tell them apart. Undeterred, Abrahamson explained how he now hopes to use low-power neutral particle beams and "cheap" detectors for "interactive discrimination" — although "more research is needed at this time".

Research on space-based lasers has been slowed "with a profound sense of technical regret" because of budget pressures, Abrahamson explained, in order to avoid accepting slippage in the more promising parts of the programme.

Proxmire was unforgiving. After reminding Abrahamson that the organization had cancelled a \$62 million contract for space-based infrared sensors because costs had exceeded estimates (and settled for a less capable sensor), he demanded to know "why Congress should believe the priorities won't change again" and whether it was not that the SDI organization had come to realize that space-based weapons were militarily vulnerable. Abrahamson replied with an allegory: just because aircraft are vulnerable to attack they have not become militarily useless, he said. Anyway, satellites could be defended but details were classified.

Abrahamson averred that in other areas research had been more successful than expected. (Very fast rockets in pods in space apparently look good.) But he did

provide one hint of where the SDI organization might be going if indeed, as many critics contend, an overall missile defence shield over the United States proves technically too daunting, although this was not a possibility Abrahamson thought at all likely.

While a decision on the feasibility of the population shield should be possible by the mid-1990s, according to Abrahamson, a decision on a more restricted goal of point missile defence should be possible somewhat earlier, perhaps as soon as the early 1990s.

Tim Beardsley

## Canadian budget

# New twist

CANADA has introduced a "brand new twist" to the budget process in an attempt to increase money for research, and provide university research councils with "stability of funding for the next five years". But many, not least the research councils themselves, are not too clear on how this stability is to be achieved.

The new scheme is designed to increase private sector support for research. Starting in fiscal year 1987, the government will match dollar for dollar contributions from private industry to research councils, up to a total of 5 per cent of an individual council's budget. The problem is that nobody is sure how the matching scheme will operate in practice, and the government is still working on an explanation.

Moreover, after increases for Canada's three research councils in the first year of the five-year plan, the government's core contribution drops, and any increase will have to come from the matching funds scheme. Uncertainties about how much this will amount to has forced the Natural Sciences and Engineering Research Council (NSERC) to cancel plans for expansion, and even at current levels NSERC will have to cut back its programme.

If the private sector does embrace the plan, the budgets of the research councils will increase by \$1,000 million over the next five years. The government is in the process of overhauling the tax structure to encourage private investment in research council projects.

A joint statement issued by the Canadian Association of University Teachers and the Association of Universities and Colleges of Canada expressed "grave concern" about the government's plan. While not opposed to closer cooperation with business, the university groups worry about how the relationship with industry will be defined.

A big loser in the budget battle is the Science Council of Canada. The council's budget was cut by half to \$2.5 million, and its full time staff was reduced from 68 to thirty.

Joseph Palca

## SSC in doubt

**Washington**

OBSERVERS on Capitol Hill are becoming suspicious that the US Department of Energy's possible mammoth accelerator project, the 60-mile-around Superconducting Supercollider (SSC), may be a hostage to the Gramm-Rudman deficit reduction act and perhaps to the cost of replacing the space shuttle *Challenger*. Recent testimony given by representatives of the department makes clear that no decision has yet been taken even to support continuing research in fiscal year 1987 (which starts next October).

The department insists that a decision on whether to build SSC, estimated to cost \$6,000 million, will be made only after it reviews a comprehensive technical report due from the Central Design Group on 1 April.

But the tone is decidedly less enthusiastic than in previous years. Project managers had hoped for \$65 million to conduct research on SSC next year, but even if all goes well the total is likely to be rather less than \$40 million, to be obtained by reprogramming from elsewhere in the high-energy physics budget. In any event, the project is big enough to require cabinet level approval before it goes ahead. Actual construction funds could not be expected before fiscal year 1988. Tim Beardsley

## Nuclear winter

# Has winter become fall?

**Blackburg, Virginia**

Two years of intensive computer modelling have substantially refined the concept of "nuclear winter" but the diverse opinions on its strategic and diplomatic implications suggest that any real impact on US defence policy is still some years away. A conference\* last week that included representatives from universities, government and the military heard sharply differing views on the importance that should be attached to the results so far obtained.

There was a consensus that although models have become increasingly sophisticated and useful, there is still great uncertainty about the source terms for the quantity of dust and smoke that would be injected into the atmosphere following a nuclear exchange. Beyond that, pre-established positions dominated. Colonel Terry Hawkins, representing the Pentagon, agreed that the possibility of nuclear winter was a "sideshow" that was simply another reason to avoid nuclear war, and repeated the familiar Pentagon line that the present policy of deterrence through strength is the best interim policy. But Hawkins did use the idea of nuclear winter to support a transition to defensive weapons as a long-term aim through the Strategic Defense Initiative (SDI). Others, believing SDI to be destabilizing, argued exactly the opposite.

Robert Simmons of the Arms Control and Disarmament Agency agreed that the threat of nuclear winter was a further reason for disarmament. Maurice Roesch III, assistant director of the White House Office of Science and Technology Policy (OSTP), said that it was necessary to understand the phenomenon "before we go too far trying to understand policy implications" and made clear his view that understanding had not yet been reached.

Others, such as Thomas Malone, former secretary-general of the International Committee of Scientific Unions' Scientific Committee on Problems of the Environment (SCOPE), emphasized that nuclear winter had attracted much interest in non-combatant countries such as India, which would in future take a much greater interest in nuclear war doctrines of the superpowers and catalyse "worldwide moral indignation" over nuclear weapons.

SCOPE last year produced the most thorough study yet of climatic effects of nuclear weapons. But George Rathjens of Massachusetts Institute of Technology strongly criticized "irresponsible" misrepresentation of the science of nuclear winter ("the worst example in my memory"), while making it clear that he was referring to popular press coverage and public statements by the populist scientists rather than to the research papers themselves.

And some pointed out that a nuclear war between the superpowers would be quite damaging enough to developing countries because of the loss of trade, even without nuclear winter.

Ambassador Richard Butler, Australia's representative at the Geneva arms talks, made an impassioned plea for the superpowers to live up to their commitment to abandoning nuclear weapons altogether and said the changes now occurring in the Soviet bureaucracy make it possible to start work on "a new fabric of security for the forthcoming post-nuclear age".

More sophisticated recent three-dimensional interactive global circulation models tend to predict smaller temperature drops in continental interiors than the one-dimensional model of Turco, Toon, Ackerman, Pollack and Sagan (*Science* **222**, 1283–1292; 1983).

The latest results from the global circulation model at the National Center for Atmospheric Research at Boulder, Colorado, continue the trend. Preliminary results reported by Stephen Schneider and Starley Thompson at a Defense Nuclear Agency technical review from a model incorporating microphysics effects to coagulate smoke and dust particles, remove them by precipitation and allow the changed particle size distribution to affect radiative transfer terms, predicted an average temperature drop in the Northern Hemisphere for a 180 terragram smoke injection at close to 12 degrees centigrade, about 3 degrees less than a similar model without the microphysics package. The results are likely to be referenced in a forthcoming but delayed report on nuclear winter requested by Congress from the Department of Defense.

Russell Seitz, currently at Harvard University, quoted Schneider as referring to the new simulations (together with new estimates of fuel loading by George Bing of Lawrence Livermore Laboratory that suggest 60 terragrams would be a more plausible smoke injection for a medium-sized conflict) as indicating that "nuclear fall" would be a more appropriate description of climatic changes after a nuclear exchange.

Richard Small of Pacific Sierra Research Corporation presented an analysis of fuel loadings resulting from a strictly counterforce exchange that predicted a maximum of 3 terragrams of smoke in the atmosphere, not enough to produce any nuclear winter effect. But Small agreed it was "prudent" to consider policy implications.

George Carrier of Harvard University said that trends in modelling suggest that for a nuclear exchange in the Northern

Hemisphere to devastate agriculture in the Southern Hemisphere "almost all the as yet unknown parameters will have to come out on the serious side", unless agricultural systems are even more sensitive to climate effects than is now recognized.

Others drew attention to other possible long-term consequences of a nuclear exchange. Michael McCracken of Lawrence Livermore Laboratory said that precipitation over land might be significantly reduced by even relatively small smoke injections, possibly leading to a failure of the monsoon.

Mark Harwell of Cornell University, a co-author of last year's SCOPE report on nuclear winter, reiterated that even the more modest temperature drops predicted by the latest models would still have disastrous consequences for agriculture given the effects of spatio-temporal variation, and pleaded for more research support for biological effects. The great majority of US federal support for nuclear winter research (nominally \$5.5 million in the current fiscal year) is for geophysics work, although the National Science Foundation still has \$100,000 uncommitted that could be diverted to biology.

Much discussion centred on the proposal, put forward by Senators Proxmire and Hatfield, that the United States and the Soviet Union should establish a joint commission to study nuclear winter. Alan Hecht of the National Oceanic and Atmospheric Administration, who drew up the US research plan before the topic was taken over by OSTP, spoke favourably of the potential of Soviet scientists to contribute to nuclear winter research, although the disappearance a year ago of Soviet researcher Vladimir Aleksandrov had done nothing to make collaboration easier. But he complained of the difficulty of gaining access to top Soviet scientists.

Large-scale experiments on fires are thought to be one area where collaboration might be fruitful; observations of deliberate forest burns are also being planned with the Canadian Forestry Service. Work on computer modelling is complicated by the Department of Defense's insistence that Soviet citizens should not have access to US supercomputing expertise, currently a source of friction between the Pentagon and the National Science Foundation. Administration officials strongly prefer to work on developing lower level contacts than a commission would imply, however, most probably under the auspices of the 10-year old US/Soviet bilateral agreement on environmental cooperation, which has a working group on atmospheric research chaired by Hecht. A final decision on whether to pursue that option has yet to be made.

Tim Beardsley

\* Nuclear Winter: strategic implications. Virginia Polytechnic Institute and State University, Blacksburg, Virginia, 6 March 1986.

## CORRESPONDENCE

NATURE VOL. 320 13 MARCH 1986

**South Africa and science for all**

SIR—Certain critics of South Africa are now threatening to invade the arena of the natural sciences. The objects of this vociferous minority, in essence a congeries of ill-informed scientists and non-scientists, are to isolate our scientific community by impairing the free flow of scientists and scientific information to and from South Africa. The latest manifestation of this campaign is the attempt to preclude the attendance of South African scientists at the World Archaeological Congress.

I am the president of the South African Council for Natural Scientists, an autonomous body created by statute, which consists of eminent scientists nominated by their peers from all the branches of the natural sciences.

The council's terms of reference are to register adequately qualified natural scientists and to promote the interests of their profession; to protect public health, safety and interests generally against actions by inadequately qualified or non-qualified persons who venture into the natural scientist's field; and to administer a code of professional conduct for all registered natural scientists.

The council, which is totally non-racial, issued a policy statement early in 1985 in which it reaffirmed its attitude in support of the universality of science. It further expressed itself in favour of the free and unfettered pursuit of science and reasserted its constant aim to promote the interests of all natural scientists, irrespective of race, colour, creed or sex.

The proponents of South Africa's scientific isolation find justification (*sic*) for their actions in convoluted political arguments which are spurious in the very context of what science is all about: the pursuit of knowledge and the advancement of human capabilities. Surely scientific contribution or discovery cannot in the least be discounted or deemed irrelevant or less cogent merely because it emanates from a particular individual or country.

International boundaries and ideological barriers are totally irrelevant in the pursuit and exchange of knowledge. Scientific genius crops up without regard for country, language and race. The laws of nature are identical in all lands: they are there to be discovered and applied, accessible to the researchers of all nations. The natural scientist constantly endeavours to think in terms of realities that transcend parochial interests and personal aggrandizement: he is, in fact, a member of an international community. This we believe, and would commend to those attempting to disrupt the community of natural scientists.

It is common cause that scientists worldwide are, by and large, men and women who are intelligent, objective and fair-minded. In the particular context of the

subject matter of this appeal, these attributes have significantly come to the fore of late: large numbers of letters are being received by scientists in this country from their colleagues worldwide in which the pernicious activities of our would-be isolationists are severely slated.

V. PRETORIUS

*South African Council  
for Natural Scientists,  
Private Bag 11303, Brooklyn,  
Pretoria 0011, South Africa*

**Chinese forest**

SIR—In the article "South China's germplasm tank" (*Nature* 318, 220; 1985) there is a reference to what must be the Ding-hushan Forest Nature Reserve, an out-station of the South China Institute. It is not, as described, a 1,200-hectare arboretum and if it were, it would be by far the largest arboretum (tree collection) in the world. It is a largely untouched relic of natural subtropical forest which has remained so because it surrounded a temple and was regarded as sacred ground. Nor is it 1,200 hectares, but 300 hectares surrounded by 900 hectares of recent *Pinus massoniana* plantation buffer zone.

Your article says that Dinghushan may become one of the UNESCO Man and the Biosphere projects. It has been one for some time and this is proudly proclaimed at the entrance to the reserve.

E.H.M. HARRIS

*Royal Forestry Society,  
102 High Street,  
Tring, Hertfordshire HP23 4AH, UK*

**Bigfoot no joke**

SIR—As the leader of the "Bigfoot conservation group" that threatened to disrupt Mark Keller's armed Bigfoot hunt in 1984 (see *Nature* 313, 418; 1985) as well as a Loch Ness monster investigator (1982 and 1983), I should like to comment on what you say. First, our group wanted to stop Keller because we had no faith that he would not shoot some unarmed hiker in error. Then, we (Project Bigfoot) found almost no commercial interest in Bigfoot by chambers of commerce in the northwest. The local citizens simply wanted to stop hikers and others from running any risk in their woods from trigger-happy Bigfoot hunters. Bigfoot himself and his tribe seem to be able easily to avoid armed men, as Keller found after four months of no results.

But your main complaint seems to be that too much money and public commission time is being spent on what the writer feels is wasted effort. He wants that money/time spent on serious science, such as anti-pollution studies. In response, let

me suggest that Bigfoot/Nessie/Chessie research may in time uncover some serious scientific information on the nature of energy-forms that we occasionally see but cannot catch or kill. The borderlands of science are often seen as a waste to study, but today's nonsense can often become tomorrow's serious scientific achievement.

ERIK BECKJORD

*The Cryptozoology Museum,  
18711 Pacific Coast Highway,  
Malibu, California 90265, USA*

**Animal intelligence**

SIR—If man can be separated from animals only because he shows foresight, what can we make of the squirrel burying nuts in advance of the cold weather? Or the ants that show true agriculture with their fungus gardens? Andrejs Baidins' rule of thumb (*Nature* 319, 172; 1986) is as shaky as any other.

R. POWERS

*Department of Palaeontology,  
British Museum (Natural History),  
Cromwell Road, London SW7 5BD, UK*

**Acid rain from jets?**

SIR—Any motorist knows how corrosive exhaust fumes are on metal. No doubt aeroplane exhaust gases have much the same property, but since much of the emission from modern civil aircraft occurs at high altitudes, the vapour trails of droplets of ice containing any corrosive material must travel hundreds of miles to reach ground level. Where they eventually arrive will be governed by the variable weather conditions that they will encounter in falling, or being washed down in rain.

It would be of considerable interest and practical importance to take samples of air containing water vapour and dissolved substances from the vapour trail area of the flight path of one of the large civil jets and to analyse the samples for "corrosive" content.

The present conventional hypothesis for the "acid rain effect" puts the blame on the water vapour contamination from the smoke stacks of industrial plant. But present coal consumption is only a little more than one-third of what it was in the 1900s, and even though oil firing is much increased since then, it seems unlikely that this source could be the main factor responsible for the quite recent rapid worsening of the mortality of trees due to acid rain. If this was the main cause, why were not its effects much more severe in the early years of this century? Atmospheric pollution on a large scale due to aircraft exhaust fumes is a much more recent phenomenon; this may be the cause.

FRANK PYGOTT

*Navigation Cottage, Willoughby,  
Rugby, Warwickshire CV23 8AG, UK*

# A child's guide to Soviet science

*The openness with which the Soviet Vega project was conducted at the weekend is both a pointer to the nature of Soviet science and a sign of how fruitful collaboration might be extended.*

## Moscow

WHAT can be learned about Soviet science in a mere five days in Moscow? Not much, of course. But the way in which the Vega project has been conducted in the past week, with quite astonishing frankness and friendliness, points to some important questions about the nature of the enterprise, and suggests some cheerful answers. The legend, in the West, that Soviet science is locked from sight of others behind a veil of paranoid secrecy is plainly, at best, a half truth.

The Vega project is the creation of one man, 54-year-old Academician R.Z. Sagdeev, who has been director of the Soviet academy's Institute of Space Sciences since 1973. He is Russian in the energetic mould, small, wiry and with a wry tongue. Part of the way through an account last week of how his laboratory has been simulating the effects of dust particles on metal targets, he could not suppress a reference to "other people's" interest in accelerating particles to high velocities "for other purposes". Last November, Sagdeev was the only scientist among the party of Soviet advisers at the Geneva summit.

The origins of the Vega project are interesting in themselves. Several people claim part of the credit. The Vega launches were originally scheduled chiefly as vehicles for a collaborative experiment with the French for the exploration of the atmosphere of Venus by means of balloons. In the event, it seems to have fallen to the then director of science at the European Space Agency (ESA), at a three-hour meeting at Moscow airport, to persuade Sagdeev "to fly to Halley as well".

The project has been thoroughly international, with no trace of chauvinism. Collaborators from elsewhere have been invited on the basis that their instruments have a valuable contribution to make. J.A. Simpson, from the University of Chicago, for example, says that his instrument (which records dust particles penetrating an electrically anisotropic dielectric between two metal foils by means of the nanosecond voltage pulses they generate) is on board because a Soviet scientist heard him describe the instrument at a meeting; the invitation to Vega followed quickly, and was irresistible.

Other collaborators speak warmly of the informality of the collaboration. Dr Jochen Kissel from Heidelberg, whose dust detector is a mass spectrometer of novel design, says that Sagdeev's institute

has been easier to deal with than the US Aeronautics and Space Administration (NASA) and even ESA, both of which require more paperwork. This is especially interesting because relations between the Soviet and West German governments do not officially exist (although there is an agreement on scientific collaboration between the Soviet academy and its West German counterpart, the Deutsche Forschungsgemeinschaft), which is why the collaboration has had to be laundered through France.

Kissel also says that the Soviets have been more daring than other agencies would have been in their willingness to fly instruments not previously used. This applies both to his present instrument and to that on which he is collaborating with Sagdeev's institute to produce a chemical analysis of the surface of the martian satellite Phobos by firing a powerful laser at the surface and collecting samples of the plasma thus generated, all this in the few minutes during which the instrument will be near the satellite, ideally a few metres up.

Not all Soviet institutes have this reputation for daring, of course. Part of the explanation at Sagdeev's institute is Sagdeev himself; his colleagues say that he has made a tremendous difference to the spirit of the place, especially by the recruitment of able scientists from elsewhere. (Even so, people say, there remains some of the dead wood that is the bane of the Soviet research system.) Another is the literal nature of the Soviet regard for the material world, of which science is a description; if there are good theoretical reasons for supposing that some phenomenon should occur, what reason can there be for behaving as if it will not? The Soviet educational system may also help; the way that the better university students spend two or three years at an institute before their first degree, often in the expectation of staying on, while frequently the reason for the accumulation of dead wood, can be in the hands of a daring director a way of finding firebrands.

Sagdeev's successful pursuit of international collaboration seems also to be an illustration of the independence that the director of a Soviet institute can enjoy. I have no means of knowing what the chauvinistic pressures may be, although the Soviet space programme has traditionally made a point of involving others through its "Interkosmos" programme.

So too has the US programme in its time. But the West is now mostly in the cost-sharing mode; collaborators pay their share of the overheads as well as their direct costs. Sagdeev has obviously been able to make the most of Soviet readiness to be flexible on these points. Other institute directors could no doubt follow suit if they were so inclined. It will be interesting to see if Sagdeev's example rubs off.

The other striking feature of the past week has been the frankness with which the details of the Vega project have been displayed. Visiting dignitaries were at first somewhat startled to find themselves expected to discuss where collaboration should go next (solar-terrestrial physics seems to be the favourite) in the presence of journalists. Most experimenters took well to the notion that they should provide virtually a kind of running commentary on their data.

The proceedings have been starkly in contrast with the way that even NASA handles these affairs. (The NASA official who said in public that "even we have something to learn" knew that he had blundered before the word "even" had escaped his lips.) But this is not the first time that the Soviets have startled the West by frankness. In 1958, for example, V.A. Kurchatov astounded a British audience at the Atomic Energy Research Establishment at Harwell with a full account of the Soviet thermonuclear programme, from which stemmed the still-continuing international collaboration in that field. Kurchatov was succeeded as director of the Soviet establishment at Dubna by the even more outspoken Artsimovich, himself a one-time colleague of Sagdeev.

It is far from fanciful to think this lineal connection between people who know the value of frankness is significant. Moreover, it is not necessary to suppose that there has been a high-level decision by the Soviet government that the scientific part of the space programme should be made "open". As the French have known for some time, it has always been more accessible than it may have seemed. On this occasion, Sagdeev's personal interest, and his success, seem to have been the mainsprings of what appears to have been a change (but which may be simply a mark of a neglected opportunity). This, obviously, is another example that other Soviet directors, and potential partners in the West, may follow. John Maddox

**Lasers**

# Fusion turned inside out

from R.G. Evans and M.H. Key

A GROUP of researchers from Osaka University and a compatriot at Bell Laboratories have recently proposed a rather novel approach to controlled fusion (Hasegawa, A. et al. *Phys. Rev. Lett.* **56**, 139; 1986). They have sought to combine the advantages (or perhaps the pessimists would say, the disadvantages) of both laser-driven inertial confinement and magnetic confinement fusion, and their approach makes use of the highly efficient CO<sub>2</sub> laser. This type of laser has been increasingly dismissed as a fusion driver because of its long wavelength, as we recently discussed in these columns (*Nature News and Views* **313**, 94; 1985).

Impressed by the ease with which lasers produce megagauss magnetic fields when they interact with solid targets (for an explanation, see Key, M.H. *Nature News and Views* **276**, 210; 1978), the authors seek to harness these fields in much the same way as a conventional magnetic confinement device such as a Tokamak. The magnetic field *B* in a Tokamak or mirror

Alamos National Laboratory in the United States, has been devoted to devising a fusion scheme that makes use of CO<sub>2</sub> lasers, which have the necessary efficiency and energy capability for a fusion driver, but no satisfactory solution has yet been proposed. The present novel target design perhaps offers such a solution.

The figure illustrates the principle in which a CO<sub>2</sub> laser is fired into a hollow target. The copious energetic electrons produced by the CO<sub>2</sub> laser form current loops (as shown) and produce magnetic fields of several megagauss which spread along the walls as electrons are driven outward by a force caused by perpendicular electric fields *E* and *B* (Forslund, D.W. & Brackbill, J.U. *Phys. Rev. Lett.* **48**, 1614; 1985). Both laser radiation and electron heat conduction inside the cavity ablate material from the inside walls and the relatively cold material flows towards the centre. Here the temperature is higher because of the laser heating and it is suggested that fusion temperatures (10–100 million degrees) could be produced. As the density can be quite high, perhaps 10<sup>21</sup> cm<sup>-3</sup>, because of the enormous magnetic pressure (1 Mbar), the required confinement time is relatively small, 10<sup>-7</sup> s. Cru-

cial to the success of the scheme is the requirement that the magnetic field persists for some time after the laser pulse, and that the central hot plasma is able to refuel itself by ablation of cold material from the inside walls.

Unlike laser fusion there is no need to compress the fuel with the attendant problems of symmetry and fluid instability. There might be magneto hydrodynamic instabilities in the magnetic field that is used to sustain a large temperature difference between the reacting fuel and the walls, but the authors suggest that the system is stable against these effects because of its uniform total pressure.

In support of their rather radical proposals the authors present results obtained with a modest CO<sub>2</sub> laser at Osaka University. Using a 1.5-ns laser pulse focused inside hollow plastic spheres up to 3 mm in diameter they show that the hot plasma lifetime exceeded the duration of the laser pulse by up to 10 times.

It is too early to assess the prospects of this approach to fusion, as many details of the scheme have not been analysed and experiments are at an early stage. But the work is indicative of substantial Japanese involvement in all branches of fusion research and shows their increasing commitment to this research at a time when the United States and Europe are reducing their fusion programmes. □

R.G. Evans and M.H. Key are at the Rutherford Appleton Laboratory, Didcot OX11 0QX, UK.

**Immunology**

# Antigen binding and T cells

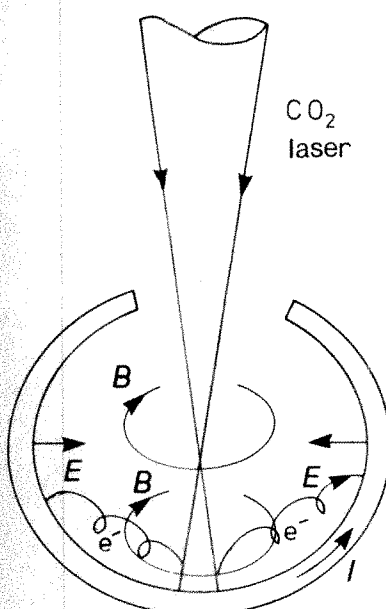
from N.A. Mitchison

LYMPHOCYTE recognition of antigens is a crucial feature of the immune response and occurs by means of receptor molecules. Although these receptors have fundamentally the same structure on the two major types of lymphocytes they work in very different ways. B cells, which use immunoglobulin molecules as their receptors, can bind antigen without the intervention of other molecules. This is not the case for T cells which normally bind antigen only when it is associated with a glycoprotein encoded by the major histocompatibility complex (MHC) on the surface of another cell. The evolutionary reasons for this 'dual recognition' are by now well understood. It provides a mechanism for ensuring that T cells come into action only when they touch another cell, which is important because they regulate or kill other cells through cell-to-cell contacts or at short range, unlike B cells whose secretions act far off. Two papers in this issue, Watts, T.H. et al. (*Nature* **320**, 179; 1986) and Ashwell, J.O. & Schwartz,

R.H. (*Nature*, **320**, 176; 1986) take us a step forward in understanding how T cells recognize antigen.

Any mechanism of this sort needs to be adjusted so that free antigen cannot block the T-cell receptor and MHC molecules do not activate on their own. Part of the adjustment seems to be pre-programmed in the receptor structure, but also selection of suitable receptors occurs in the thymus — hence 'restriction', the ability of T cells to recognize antigen only in the context of the MHC molecules to which they were exposed in the thymus.

Clearly an arrangement of two entirely separate receptors would have difficulty in meeting these requirements and would in any case be incompatible with current knowledge of receptor molecular genetics, so other possibilities have been canvassed. The simplest is a trimolecular complex, in which receptor, MHC molecule and antigen all interact with one another. It would still seem difficult to adjust the affinities so as to prevent



Schematic of Japanese hybrid laser-magnetic confinement target showing *B*, *E*, electron trajectory *e*<sup>-</sup> and current flow *I*.

machine is limited not only by the electrical power needed to drive the magnets but also by the sheer material strength needed to contain the magnetic pressure, which is proportional to *B*<sup>2</sup>. As the contained plasma pressure cannot exceed the magnetic pressure, this limits the plasma density in a magnetic machine and requires that it contains the plasma for a time of the order of one second for an efficient fusion reaction.

Much effort, particularly at the Los

bimolecular binding of receptor to antigen or MHC molecule (remember that we are dealing not with single molecules in solution, but with membrane-bound arrays in which high avidity could easily build up). So a good guess is that binding of two of the molecules may induce a conformational change that permits binding of the other to take place.

The answers may come from experiments in which these molecules are freed of their membrane-binding domains by genetic engineering and allowed to interact in solution, as several groups are currently trying to do. Watts *et al.* use fluorescence to study energy transfer from a peptide antigen to an MHC molecule in an artificial lipid membrane, and find that the two bind together only in the presence of specific T cells. Ashwell and Schwartz use less direct methods to address a similar problem. In previous experiments, by reading out activation of T-cell clones, they have been able to measure independently the potency of antigen–MHC combinations (from the concentration of antigen needed) and avidity for a receptor (from the ability of cells bearing the receptor to compete with one another). In the present study they show that switching an MHC molecule can change potency without affecting the avidity, and attribute this to a change in the strength of binding between MHC molecule and antigen. Certainly no other interpretation seems at all obvious.

Does the fluorescence signalling result contradict either this interpretation of potency/avidity or the earlier claim of Babbitt *et al.* (*Nature* **317**, 359; 1985) to have demonstrated direct binding of anti-

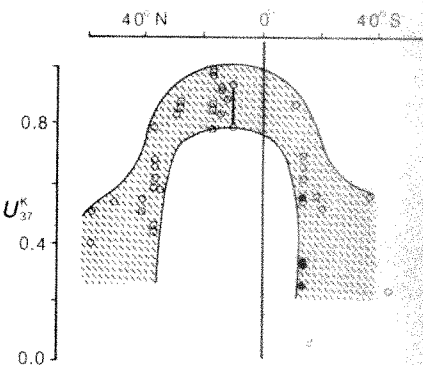
gen by MHC molecules? As Schwartz himself pointed out in these columns (*Nature News and Views* **317**, 284; 1985), the observed affinity did seem rather high, and it would be hard to reconcile such a value with the failure of MHC molecules to bind antigen in the absence of T cells as observed here. The direct binding experiment needs to be repeated in a criss-cross, using two MHC molecules predicted to bind two peptides reciprocally. On the other hand the new pieces of evidence do not contradict one another, because the MHC–antigen binding postulated to account for the potency change could well be small enough to have been missed by fluorescence signalling; and as the signals showed that MHC molecules and antigen ended up in tight proximity, they support the possibility of some degree of specific binding.

The outcome is to have strengthened the evidence of direct binding between antigen and MHC molecule. This in turn will strengthen the belief that immune response (and immune suppression) effects of MHC genes can result from such binding, and hence that this is what controls disease susceptibility in human and animal populations. But it should be emphasized that a very strong case can also be made for other forms of immune response control by MHC molecules, for example, through self-tolerance perturbing the T-cell repertoire (Müllbacher, A. *et al.* *J. exp. Med.* **157**, 1324; 1983), and that the forms of control are likely therefore to be multiple. □

*N.A. Mitchison is Professor of Zoology at University College, Gower St, London WC1E 6BT, UK.*

to be sensitive mainly to temperature, but it later turned out to be a stratigraphic parameter recording a mixed signal of temperature and ocean volume change. The new report raises the intriguing prospect that a combination of the  $C_{37}$  alkenone unsaturation index with  $\delta^{18}\text{O}$  data will eventually allow the portion of the oxygen-isotope signal caused by temperature to be separated from that related to ocean volume change.

As with most novel approaches, molecular stratigraphy also faces old problems. The deteriorating correlation between  $U^K$  indices and oxygen-isotope signals before 270,000 years ago, plus the lack of agreement in sediments more than 550,000 years old, provide clear evidence that conditions in the contemporary and ancient oceans are not analogous. One may surmise that a change in source organisms occurred at these times and that alkenone undersaturation may not be synthesized to the same degree by different species under the same environmental conditions. This hinders accurate temperature calibration more than stratigraphic correlation.



Alkenone unsaturation index for contemporary marine sediments and some sediment trap material from different latitudes. The distribution envelope corresponds to the pattern of global sea-surface temperature. Unsaturation index,  $U^K_{37} = [C_{37,2}]/[C_{37,2} + C_{37,3}]$ , where  $C_{37}$  denotes the total number of carbon atoms and :2 and :3 the number of double bonds per molecule. The greater the proportion of  $C_{37,2}$  molecules, the higher the unsaturation index that corresponds to higher water temperatures. ○, Sediments; \*, sediment traps.

## Palaeoceanography

# Biomarkers for ancient climates

from Erwin Suess

ENVIRONMENTAL conditions of growth, particularly ocean temperature, are faithfully recorded by the coccolithophorids — widely distributed marine phytoplankton. The record lies in the relative abundance of long-chain alkenones — complex organic molecules of the lipid bilayer which control the fluidity of cell membranes and thus respond to temperature stress. Elsewhere in this issue (*Nature* **320**, 129; 1986), S.C. Brassell and colleagues report that the chemical unsaturation of alkenones (the ratio of more saturated to less saturated ketone molecules among the isomers of  $C_{37}$  alkenones, here called the  $U^K$  index) in contemporary marine sediments varies directly with the present-day temperature of the ocean surface over the sites from which sediments and some suspended-matter samples were collected. These samples span wide latitudes

on both sides of the equator and bracket most of the global spectrum of sea-surface temperatures (see figure).

The authors show that the abundance of these molecular marker compounds in ancient sediments of the tropical Atlantic Ocean also varies with the expected ancient ocean climate. Glacial to interglacial fluctuations in climate, recorded by global oxygen isotope variations in calcareous shells of near-surface dwelling foraminifera, correspond to synchronous changes in  $C_{37}$  alkenone unsaturation indices. Such clear correlation provides a powerful new stratigraphic tool even in conditions where the temperature calibration is more tricky.

In the new approach, there are certain similarities to conventional oxygen-isotope stratigraphy. Using the latter,  $\delta^{18}\text{O}$  of foraminifera was thought at first

to search for palaeoceanographic biomarkers — in the sense that earth scientists use index fossils, assemblages and ecological data of organic skeletons — appears to equal in difficulty that of finding needles in a haystack. There are an almost infinite number of known and unknown natural organic compounds that are potential biomarkers and which have to be explored and catalogued. Often they occur in minute quantities in sediments overwhelmed by other more abundant compounds that are of less diagnostic value. Recently, improved analytical techniques using computerized capillary gas chromatography and mass spectrometry have greatly improved the

chances of finding organic compounds diagnostic for either particular organisms or specific environmental conditions of growth (Mackenzie, A.S. *et al.* *Science* **217**, 491; 1982).

Evaluating the sources of biomarkers, their physiological functions in key organisms and their chemical stability over geological time will be major tests for the success of organic molecular stratigraphy. Detailed surveys of organisms are only one step towards the identification of sources. For example, dinoflagellate algae contain a unique sterol molecule, dinosterol, which also survives burial (Boon, J.J. *et al.* *Nature* **277**, 125; 1979). These marine algae attain peculiarly high blooms under particular oceanographic conditions during coastal upwelling. Dinosterol marks the presence of algal residues in marine sediments that might otherwise be devoid of fossils. Similarly, proteins of calcareous and siliceous marine plankton contain diagnostic assemblages of amino acids (Mueller, P.J., Suess, E. & Ungerer, C.A. *Deep-Sea Res.* in the press). Acidic amino acids dominate the proteins that secrete calcareous skeletons; basic amino acids dominate those secreting siliceous skeletons. Again, such organic compounds are the imprint of the biosphere in contemporary sediments.

A third type of organic molecular marker consists of those compounds diagnostic for certain environmental conditions such as temperature or pressure (deLong, E.F. & Yayanos, A.A. *Science* **228**, 1101; 1985). Organisms which adapt their cellular composition of phospholipids to temperature changes have long been known to biologists. Such organisms increase the proportion of unsaturated fatty acids, which have lower melting points and greater molecular flexibility than saturated isomers at lower temperatures. There is much effort now being made to identify the saturation indices of fatty acids of cell membrane phospholipids in marine microorganisms and benthic macro-organisms. The giant benthic communities at hydrothermal vents, which thrive at spectacularly high temperatures, are favourite targets for this research.

There is a problem in the poor chemical stability of amino acids and these lipid compounds. Their usefulness as biomarkers is restricted largely to young sediments. More complex and larger molecular structures appear more resistant to biodegradation and physico-chemical diagenesis, and thus have greater potential for survival in the geological record. The success of Brassel *et al.* in studying biomarkers lies in resolving the complexity and diversity of the large organic molecular structures.

A collaborative effort is now needed to understand the mechanism of stabilization of biomarkers in the geological record to exploit them fully, in particular if dissolu-

tion has severely decimated the conventional skeletal carriers of palaeoceanographic information in sediments, as in the vast red clay deposits of the central Pacific Ocean, which contain few or no microfossils. Fortunately, complex organic molecules may be stabilized and survive diagenesis by sorption to clays. It is of high priority to intensify the search for biomarkers in those sediments which are devoid of microfossils. Encouraged by the

new results of Brassel *et al.*, such efforts could unlock imprints of the past biosphere and environmental conditions of growth that are normally hidden from palaeoceanographic interpretation. □

*Erwin Suess is visiting the Geological Institute, University of Kiel, 2300 Kiel, FRG, and is permanently at the College of Oceanography, Oregon State University, Corvallis, Oregon 97331, USA.*

### Behaviour rhythms

## A *Drosophila* 'clock' protein?

from John Merriam

THOSE of us who have experienced jet lag are aware that biological rhythms, including daily, or 'circadian', rhythms affect our behaviour. There are thus commercial as well as academic benefits to be gained from understanding the biology of clocks and the gene products that are essential for their activity. One such gene, the *period* (*per*) locus of the fruitfly *Drosophila*, has been extensively studied, most recently by molecular cloning<sup>1</sup>. Now Jackson *et al.* on page 185 of this issue<sup>2</sup> describe this potential clock gene, whose sequence predicts the amino-acid sequence of an unexpected protein which seems to be a proteoglycan. This is the first biochemical step in the identification of the biological clock, and helps to clarify a previously confused field.

Discovery of the *per* locus was one of the more remarkable sagas in applying genetics to biology<sup>3</sup>. The first three 'rhythm' mutants discovered were all alleles of the *per* locus, although they exhibited different phenotypes. The *per*-bearing flies have a long period rhythm, *per*<sup>+</sup> flies a short period and *per*<sup>0</sup> flies no circadian rhythm. Thus, in one step both the existence and the non-essential nature of an endogenous clock, as opposed to externally generated behaviour rhythms, was demonstrated. The *per* length mutants also affect the ability of flies to reset their clocks. These aspects of the *per* locus suggest that its gene product is close to, perhaps part of, the clock mechanism.

The location of the *per* gene mutants on the *Drosophila* X chromosome was established by standard recombination and cytogenetic techniques to be at the salivary chromosome bands 3B1-2 (see figure). By coincidence this also happens to be one of the most heavily studied genetic regions in the species: several chromosome deletions (termed deficiencies, or *Df*) which remove this region also remove the normal *per* function. Among the most useful *per*<sup>0</sup>-deleted chromosomes are two that overlap only around the *per* gene. Female heterozygotes with *Df(1)62d18* on one X chromosome and *Df(1)64j4* on the other

are viable, although *per*<sup>0</sup> in phenotype. The overlapping endpoints of the two deletions are markers of the left and right sides of the chromosome region responsible for the *per* function activity.

Another chromosome rearrangement with a breakpoint at 3B1-2, the translocation *JC43*, causes flies to exhibit an abnormal circadian rhythm which has a long period. This is consistent with the break causing a weak or 'hypomorphic' mutant allele, and thus represents another molecular marker of the *per* gene. Because the *JC43* translocation separates the X chromosomes into a left and a right part, the residual *per* activity can be mapped and is shown to be carried by the left fragment.

Working independently, groups at Rockefeller<sup>4</sup> and at Brandeis' universitites cloned chromosome bands 3B1-2 and identified these left and right deficiency endpoints. They turn out to be separated by about 15 kilobases (kb); therefore the *per* gene is thought to be located within this region of sequence — but where? The *JC43* break divides the 15 kb into a left (*per-L*) and a right region (*per-R*). Several transcript-coding regions are found within these regions. Most attention has focused on a 4.5-kb head-specific transcript originating largely from *per-L*, but Reddy *et al.*<sup>5</sup> have also identified a 1-kb transcript from the same region of *per-L* and a 0.9-kb transcript originating just to the right of the *HindIII* restriction site in *per-R*. (Restriction enzymes such as *HindIII* are used to cut DNA into fragments at specific regions of the sequence, as shown in the figure.) This last transcript is novel in that its abundance shows rhythmic behaviour and is reduced in the *per*<sup>0</sup> mutants.

The simplest assumption is that the 4.5-

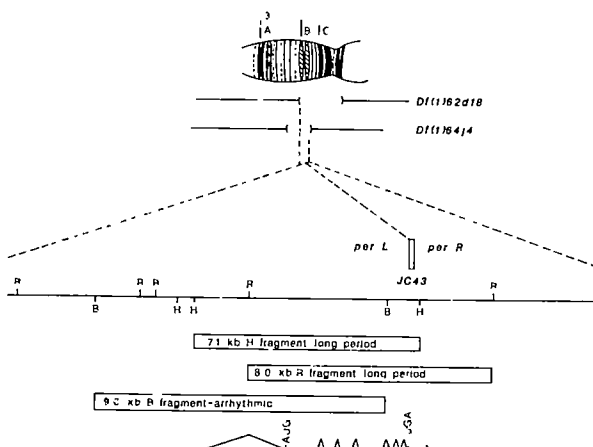
- Rosbash, M. & Hall, J.C. *Cell* **43**, 3 (1985).
- Jackson, F.R. *et al.* *Nature* **320**, 185 (1986).
- Konopka, R.J. & Benzer, S. *Proc. natn. Acad. Sci. U.S.A.* **68**, 2112 (1971).
- Bargiello, T.A. & Young, M.W. *Proc. natn. Acad. Sci. U.S.A.* **81**, 2142 (1974).
- Reddy, P. *et al.* *Cell* **38**, 701 (1984).
- Bargiello, T.A., Jackson, F.R. & Young, M.W. *Nature* **312**, 752 (1984).
- Zehring, W.A. *et al.* *Cell* **39**, 369 (1984).

The salivary chromosome bands 3B1-2 (top of figure) contains breakpoints for deleted (*Df*) and translocated chromosomes (JC43). Location of these breakpoints on the restriction map (middle) of about 15 kb of cloned DNA from this region permits the identification of restriction fragments and a transcript (bottom) thought to represent the *per* gene product. R, EcoRI; B, BamH; H, HindIII.

kb transcript (or the 1-kb transcript) alone represent the *per* gene product. What does not explain is why *per-L* (JC43 left fragment) does not restore completely normal circadian behaviour, or indeed why the adjacent 0.9-kb transcript normally shows rhythmic behaviour. One scenario advanced by the Brandeis group is that the 0.9-kb transcript is also part of the clock. In this view both the 4.6- and 0.9-kb transcripts are necessary for normal clock activity.

DNA transformation experiments with cloned portions of the 15-kb interval have not completely settled this issue. In one case a 7.1-kb *HindIII* fragment, largely originating from *per-L* (see figure), when transformed, restored weak long-period activity<sup>6</sup>. In another case an 8.0-kb *EcoRI* fragment also restored weak long-period activity but a 9.0-kb *BamH* fragment from *per-L* did not restore any rhythmic behaviour<sup>7</sup>. The inability of any of these fragments completely to restore wild-type activity could mean either that the *per* gene is complex and includes several components or that none of these fragments, including the *per-L* region of JC43, completely encodes a rather long transcript.

On the basis of transcript mapping and DNA sequencing of the more than 7,000 bases in this interval it now appears that the latter alternative is more likely. Starting with a complementary DNA clone hybridizing to the 1.5-kb *BamH/HindIII* interval of *per-L*, Jackson *et al.*<sup>2</sup> succeeded in placing the transcript map onto the DNA restriction map. The transcript they describe includes eight exons originating over a slightly longer region than the 7.1-kb *HindIII* fragment previously used in transformation. The sequence is consistent with a single open reading frame with an AUG start codon in exon 2 and a UGA stop codon in exon 8. Of significance is the finding that none of the fragments used in transformation, or the *per-L* region of JC43, could be expected to encode a completely normal full-length transcript. For example, the JC43 breakpoint, thought to fall about 170 base pairs upstream of the poly(A) addition site, is within the 502 base pairs forming the downstream un-



translated part of the messenger RNA. This strengthens the view that the 4.5-kb transcript alone forms the *per* gene. With this knowledge we can expect that transformation with a suitably longer fragment will completely restore wild-type rhythms. Understanding of the DNA alterations associated with the *per'*, *per'* and *per* mutations, which should soon be forthcoming, will further pinpoint the gene. But none of this explains the behaviour or the role of the 0.9-kb transcript.

The predicted translation product of the open reading frame determined from the

*per-L* DNA sequence is a polypeptide of 1,127 amino acids. The amino-acid composition is somewhat unusual in that nearly half (47 per cent) comprises the amino acids serine, threonine, glycine, alanine and proline. Polyglycine and polyalanine repeats of up to 17 residues long are found at several positions. The putative *per* protein includes a potential site for phosphorylation by a cyclic AMP-dependent protein kinase. The amino-acid sequence at this site is homologous with the phosphorylation site in the calcium regulatory protein troponin I isolated from rat skeletal muscle. Other homologies with sequences found in the Dayhoff and Doolittle databases include the core protein of a rat chondroitin sulphate proteoglycan, predominantly in the alternating Ser-Gly residue series. These series, and the Thr-Gly repeats, may serve as sites for glycosylation. Nobody has speculated on the role of glycosylation sites in clock function, but site-directed mutagenesis techniques that alter the numbers or locations of these sites should permit the experimental test of their significance. □

John Merriam is Associate Professor of Genetics in the Biology Department, University of California, Los Angeles, California 90024, USA.

## Visual cortex

# Cholinergic input and plasticity?

from A.M. Sillito

THERE is a growing controversy in developmental neurobiology centred on the role of noradrenaline in the plasticity of the visual cortex of young mammals. One group maintains that depletion of noradrenaline results in a loss of plasticity, which can be restored by microperfusion (see refs 1,2), while others claim that there is no correlation between cortical noradrenaline levels and the presence or absence of plasticity in early life<sup>3-5</sup>. Now, on page 172 of this issue<sup>6</sup>, Mark Bear and Wolf Singer offer at least a partial resolution to the controversy.

In the so-called 'critical period' during the first three months of life, the visual cortex of cat or monkey shows a remarkable capability to reorganize its patterns of functional connectivity. The experimental model generally used to demonstrate this is that of monocular deprivation. Although both eyes normally influence an equal proportion of cells in the visual cortex, monocular deprivation (produced by suturing closed the lids of one eye) in the critical period results in an almost complete takeover of the visual cortex by the non-deprived eye<sup>7-9</sup>, concomitant with a corresponding loss in the capability of the deprived eye to drive cortical cells. These processes involve a major change in the

cortical distribution of the thalamic fibres that relay the inputs from the eyes and occurs only within the critical period. Even a few days of monocular deprivation can precipitate a major change in cortical organization<sup>9</sup>, whereas in the mature animal extended periods of deprivation over many months have no effect. The relatively sharp transition in the capability of the cortex to reorganize its patterns of connectivity has provoked considerable interest.

The involvement of noradrenaline was suggested by the imaginative experiments of Kasamatsu and Pettigrew<sup>2</sup>, who used 6-hydroxydopamine (6-OHDA), a neurotoxin that is apparently selective for catecholaminergic terminals, to deplete cortical noradrenaline levels either by intraventricular injection or direct microperfusion of the cortex. Both procedures were found to block plasticity within the critical period — that is, monocular deprivation apparently fails to cause any redistribution of the pattern of influence of the two eyes over the population of visual cortical cells studied. Subsequent microperfusion with noradrenaline was reported to render the cortex again susceptible to monocular deprivation. These data broadly support the view that

the noradrenergic input to the cortex exerts an important control over plasticity.

There is general agreement that microperfusion of the visual cortex with 6-OHDA blocks plasticity in the critical period<sup>10,11</sup>. But if cortical noradrenaline levels are depleted to comparable levels by any one of a range of other procedures, plasticity is unaffected. These include neonatal injection of 6-OHDA; electrolyte or 6-OHDA lesions to the dorsal noradrenergic bundle carrying fibres from the locus coeruleus; and intraventricular injection of another neurotoxin, DSP-4, also with fairly selective effects on noradrenergic fibres<sup>3,5,12</sup>. Furthermore it now seems difficult to produce a convincing loss of plasticity by intraventricular injection of 6-OHDA. Taken together, these data make it hard to maintain the view that the noradrenergic input to the cortex is responsible for plasticity, but the data of Kasamatsu and colleagues are difficult to explain if the case for noradrenaline is dismissed<sup>2,13</sup>.

The new report by Bear and Singer<sup>6</sup> confirms that lesions affecting the noradrenergic input to the visual cortex have no effect on plasticity, but that there is a loss of plasticity when the noradrenergic lesions are paired with lesions to the cholinergic input. The authors also show that 6-OHDA apparently blocks the facilitatory effects of the neurotransmitter acetylcholine on the visual responses of cortical cells, which implies that 6-OHDA is effective because it causes both a depletion of noradrenaline and blocks the action of the cholinergic input. (Destruction of the cholinergic input alone does not block the plasticity.)

How does the new evidence relate to plasticity within the critical period? The visual cortex receives a series of non-specific modulatory inputs, most notably the noradrenergic input from the locus coeruleus, a cholinergic input from the magnocellular nuclei of the basal forebrain and a serotonergic input from the raphe nuclei. In the normal adult cortex these inputs influence potassium channels, cyclic AMP, cortical metabolism and possibly blood flow<sup>14-19</sup>. It is not easy to determine which of these effects in the adult cortex are relevant to plasticity in the critical period of young mammals. The most parsimonious explanation is that any procedure that severely disrupts the normal functioning of the cortex will block the processes underlying plasticity. In support of this view, it is found that microperfusion of the cortex with glutamate (which probably disrupts cortical activity either by direct excitatory action on cortical cells or as a consequence of neurotoxin effects) also blocks plasticity<sup>20</sup>.

Thus, the debate still turns on one group of observations indicating that plasticity can be partially restored by microperfusion with noradrenaline or electrical stimulation of the locus coeruleus<sup>1,2</sup>. If, as

Bear and Singer indicate, plasticity is disrupted only when both the cholinergic and the noradrenergic inputs to the cortex are blocked, it seems that either of these inputs can compensate for the loss of the other and that future efforts should be directed to some process that is influenced by both inputs.

There is evidence that both acetylcholine and noradrenaline can enhance the responsiveness of cortical cells to an excitatory input by inhibiting the potassium currents that underlie the after-hyperpolarization built up during a burst of action potentials<sup>16,18,19</sup>. Acetylcholine seems to affect both a slow voltage-dependent potassium channel, as recently discussed in these columns<sup>18</sup>, and a slow calcium-activated potassium channel, whereas noradrenaline seems only to affect the calcium-activated channel. If the potassium-channel effects are important, one implication is that they raise the excitatory response to a given visual input above some critical threshold required for plasticity to occur. But acetylcholine exerts a much more potent and widespread facilitation of stimulus-driven responses in the visual cortex than noradrenaline, hence the cholinergic system should be more important to plasticity than the noradrenergic. The data of Bear and Singer do not suggest that damage to the cholinergic system has a significantly greater effect than the noradrenergic, so the action on potassium channels is unlikely to be the critical factor. Nonetheless it would be interesting to ascertain whether microperfusion experiments, with the aim to enhance or mimic the cholinergic influ-

ence, would restore plasticity in the way that is claimed for noradrenaline.

The potential role of the serotonergic input should not be neglected<sup>17</sup>—any two of the modulatory influences may be able to sustain the conditions necessary for plasticity in the critical period. One might infer that the critical period is distinguished either by a heightened sensitivity of cortical processes (or some element of these) to the modulatory inputs or by a heightened output from these inputs. At present there is a notable lack of evidence for either possibility and therefore an urgent need for further corroboration of the conditions that can restore plasticity. □

1. Kasamatsu, T. & Pettigrew, J.D. *Science* **194**, 206 (1976).
2. Kasamatsu, T., Pettigrew, J.D. & Arey, M.J. *Neurophysiol.* **45**, 254 (1981).
3. Bear, M.F. & Daniels, J.D. *J. Neurosci.* **3**, 407 (1983).
4. Afrien, J.P. et al. *C.R. Acad. Sc. Paris III* **295**, (1982).
5. Daw, N.W., Videen, T.O., Parkinson, D. & Rader, R.K. *J. Neurosci.* **9**, (1985).
6. Bear, M.F. & Singer, W. *Nature* **320**, 172 (1986).
7. Wiesel, T.N. & Hubel, D.H. *J. Neurophysiol.* **26**, 1303 (1963).
8. Hubel, D.H. & Wiesel, T.N. *J. Physiol., Lond.* **206**, 419 (1970).
9. Sherman, S.M. & Spear, P.D. *Physiol. Rev.* **62**, 738; (1982).
10. Paradiso, M.A., Bear, M.F. & Daniels, J.D. *Expl Brain Res.* **51**, 413 (1983).
11. Daw, N.W., Rader, R.K., Robertson, T.W. & Ariel, M.J. *Neurosci.* **3**, 907 (1983).
12. Trombley, P. et al. *J. Neurosci.* **6**, 266 (1986).
13. Kasamatsu, T., Watabe, K., Heggelund, P. & Scholler, E. *Neurosci. Res.* **2**, 365 (1985).
14. Magistretti, P.J. & Schorderet, M. *J. Neurosci.* **5**, 362 (1985).
15. Videen, T.O., Daw, N.W. & Radar, R.K. *J. Neurosci.* **4**, 1607 (1984).
16. Madison, D.V. & Nicoll, R.A. *Nature* **299**, 636 (1982).
17. Foote, S.L. & Morrison, J.H. *J. Neurosci.* **4** 2667 (1984).
18. Brown, D. *Nature News and Views* **319**, 358 (1986).
19. Sillito, A.M. & Kemp, J.A. *Brain Res.* **289**, 143 (1983).
20. Trombley, P. et al. *J. Neurosci.* **6**, 266 (1986).

A.M. Sillito is Professor of Physiology at University College, Cardiff CF1 1XL, UK.

## African pre-history

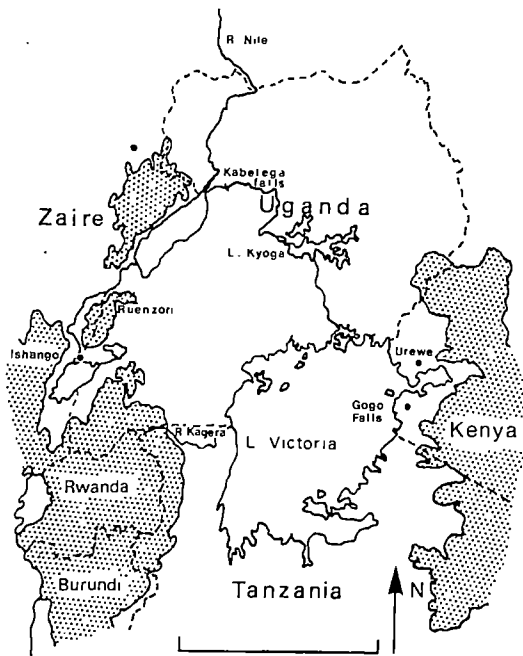
# Life in the Lake Victoria basin

from David W. Phillipson

THE East African interlacustrine region, in particular the western part, has occupied a key position in Africa's later prehistory. Here, at the headwaters of the White Nile are well-watered plains, 1,000–1,500 m above sea level, which support a dense human population practising, in the recent past, various traditional lifestyles. Today, the greater part of the area consists of savannah with patches of dense forest which, even within living memory, were more extensive than at present. Before human interference, this would have been the natural vegetation over the greater part of the region<sup>1</sup>. Recent research, reported on page 164 of this issue<sup>2</sup>, indicates that the process of forest clearance began earlier than previously thought, extending back over some five millennia. Further, it appears that preparation of land for cultivation was the prime cause of forest clearance, initially in the valleys,

which were clear by about 2,200 years ago (2,200 BP), and subsequently at progressively higher altitudes.

The interlacustrine region (see map) is a contact zone between diverse African agricultural traditions. Cereals are cultivated, notably the millets, including sorghum. But in much of the relatively low-lying country north and west of Lake Victoria, bananas are the staple food, accompanied by other vegetatively propagated food-plants, notably yams and sweet potatoes. These food crops arise from four distinct origins. The millets are indigenous African cereal crops which appear to have been brought under cultivation in what is now the Sahel or, in the case of finger millet (*Eleusine coracana*), in an area centred on Ethiopia and perhaps extending into northern Uganda<sup>3</sup>. Bananas, which grow at altitudes below 1,950 m, are generally believed to be of trans-Indian



The East African interlacustrine region bounded in the west by the Ruenzori mountains and equatorial forest. Scale bar, 300 km; shaded area, land over 1,500 m.

Ocean origin, introduced via the East African coast sometime in the first millennium AD. The yams and sweet potatoes are diverse, including not only African species of *Dioscorea* which may have been the first cultivated on the West African forest fringes, but also those of New World and trans-Indian Ocean origin.

Cattle occupy an important place in the traditional lifestyle of many of the region's inhabitants where this is not precluded by tsetse-fly infestation. Herding is a savannah activity that may be assumed to have begun following forest clearance.

Although the beginning of cultivation in the region may have been the reason for the onset of substantial clearance of the native forest, today the main reasons are the quest for firewood and the production of charcoal. Charcoal production may, however, have been a more significant early factor than is commonly realized, as recent archaeological investigations<sup>4</sup> have revealed that this area, including the western Lake Victoria shore, saw the emergence of a sophisticated iron-smelting technology (2,500–2,000 BP) — the earliest in sub-equatorial Africa. Experimental reconstructions of the prehistoric smelting process<sup>5</sup> have confirmed the substantial amounts of hardwood charcoal that were used; the long-term effect on forest cover is thus clear.

Archaeological investigations do not yet reveal a comprehensive picture of human settlement in this region throughout the Holocene. At Ishango on the western (Zaire) shore of Lake Edward, a specialized harpoon-fishing settlement<sup>6</sup> has been dated to probably 11,000–6,000 BP. Elsewhere, presumed hunter-gatherers maintained a mainly microlithic technology.

Although the herding of domestic animals and possible plant cultivation had begun in the Lake Turkana basin of northern Kenya by approximately 4,500 BP<sup>7</sup>, and in the Rift Valley and adjacent highlands further to the south by about 3,000 BP<sup>8</sup>, there is no direct evidence that farming and pottery-making peoples were established west of Lake Victoria at this time. The earliest form of pottery recognized in the latter area is called Kansyore ware, named after an island site in the Kagera River, which was being made by about 2,500 BP<sup>9</sup>. It is associated with chipped stone stools rather than with iron, but the mode of subsistence of its makers remains unknown. The people who inhabited the sites where Kansyore ware has been found are a prime focus for future archaeological research in the Lake Victoria region.

By about 2,500–2,000 BP a distinct pottery tradition was widespread in the region, its northernmost occurrence being near Kabelega (Murchison) Falls. The tradition as a whole has been named after a site at Urewe in south-western Kenya, but several local sub-styles may be recognized<sup>10</sup>. There may have been some chronological overlap between the production of Kansyore and Urewe pottery, but at Gogo Falls east of Lake Victoria an Urewe deposit is stratified over one which contains Kansyore ware<sup>11</sup>. It is at sites of this period in Rwanda that there is the first clear local evidence for food production<sup>12</sup> — teeth of goats (or sheep) and seeds of sorghum and finger millet. Urewe pottery is of particular interest in being associated with the smelting of metals, noted above. The Urewe settlement of the Lake Victor-

ia region is generally seen as a source from which derived the metal-using, mixed-farming lifestyle adopted by about 1,900–1,600 BP over much of the southern half of the continent<sup>13</sup>. This change to a food-producing economy is widely accepted as having accompanied the introduction of Bantu languages into southern Africa<sup>14</sup>.

It was probably about 1,200 BP that a distinct roulette-decorated pottery type first appears in the archaeological record of the region<sup>15</sup>; its connections are almost certainly with pastoral areas further to the north. It is more widespread than its predecessors, suggesting that more land was available for human settlement. The cereal cultivation and iron-smelting of Urewe peoples would, as the palynological evidence confirms, have led to significant reduction in the forest cover, permitting the eventual growth of herds of cattle. It remains for archaeology to demonstrate the human populations responsible for the earlier stages of forest clearance now suggested in the Lake Victoria region.

1. Hamilton, A. *Vegetatio* 29, 21 (1974)
2. Hamilton, A., Taylor, D. & Vogel, J.C. *Nature* 320, 164 (1986).
3. Harlan, J.R., de Wet, J.M.J. & Stemler, A.B.L. (eds) *Origins of African Plant Domestication* (Meuton, The Hague, 1976)
4. Schmidt, P.R. *Tanzania Notes & Records* 84–5, 77 (1980)
5. Schmidt, P.R. in *Proceedings of Pan-African Congress of Prehistory & Quaternary Studies* (eds Leakey, R.F. & Ogot, B.A.) 335 (Leakey Memorial Institute, Nairobi, 1980).
6. de Haenzel, J. *Les Fouilles d'Ishango* (Brussels, 1957)
7. Owen, R.B. et al. *Nature* 298, 521 (1982)
8. Ambrose, S.H. in *From Hunters to Farmers* (eds Clark, J.D. & Brandt, S.A.) 212 (University of California Press, Berkeley, 1984).
9. Soper, R.C. & Golden, B. *Azania* 4, 15 (1969)
10. Van Noten, F. *Azania* 14, 61 (1979)
11. Collet, D.P. & Robertshaw, P.T. *Azania* 15, 131 (1980)
12. Van Noten, F. *Histoire Archéologique du Rwanda* (Musée Royal de l'Afrique Centrale, Tervuren, 1983)
13. Phillipson, D.W. *African Archaeology* (Cambridge University Press, 1985)
14. Ehret, C. & Posnansky, M. (eds) *Archaeological and Linguistic Reconstruction of African History* (University of California Press, Berkeley, 1982)

David W. Phillipson is Curator of the University Museum of Archaeology and Anthropology, Downing St, Cambridge, CB2 3DZ.

### 100 years ago



The *La France* above Paris. Facsimile of an instantaneous photograph executed at the Observatory of Physical Astronomy, Meudon.

From *Nature* 33 422, 4 March 1886.

## Ecology

# Carnivore dominance and herbivore coexistence in Africa

from Jared M. Diamond

Most concepts of temperate-zone ecology are derived from studies in Europe and North America, but are such concepts really appropriate to the temperate zone of southern Africa? This issue was debated at two meetings last year in South Africa: a symposium on competition and coexistence, held by the Zoological Society of South Africa at Pietermaritzburg (23–25 July, 1985); and a workshop on terrestrial ecology at Houw Hoek organized by the Foundation for Research Development (1–3 August, 1985). Two studies of large mammals discussed at these meetings illustrate some of the special problems of southern African ecology.

The first is an unintended natural experiment on a large scale (Hugh Berry, Etosha National Park: *Madoqua* 12, 242, 255, 1981; 13 151, 1982). The gravel pits excavated in Etosha during road construction produced entirely unexpected large-scale changes in the mammal community of the plains. The trophic relationships and size structure of this community are outlined in *a* in the figure. As a result of the seemingly modest disturbance there were crashes in the wildebeest and zebra populations; declines in cheetah, brown hyaena and eland; and increases in lions, spotted hyenas, jackal and springbok.

Berry reconstructed the causal sequence of these changes as follows (*b* in the figure): rainwater standing in the alkaline gravel pits became a reservoir for anthrax bacteria, to which wildebeest and zebra are especially susceptible; and the resulting abundance of sick or dead prey more than offset the effects of the decline in healthy prey, causing a population surge of the two dominant and largest species of carnivores/scavengers, the lion and the spotted hyaena, which are immune to anthrax. The lions reduced the population of eland, which suffered little from anthrax but are a favourite alternative prey of lions. The lions and spotted hyenas competitively suppressed the next largest species of cat and hyaenid, the cheetah and brown hyaena, respectively. Relief from competing cheetahs and brown hyenas, together with the abund-

ance of carcasses, permitted the next-largest carnivore/scavenger, the black-backed jackal, to increase. Competitive release was also seen among herbivores—the wildebeest and zebra crashes permitted the smaller and more anthrax-resistant springbok (which also profited from the decline of cheetah, its major predator) to increase.

Berry's work illustrates the unique insights that careful study of the natural environment can yield. Ecologists will never be permitted to kill 25,000 wildebeest out of curiosity, but the same result produced by anthrax has illustrated how predation and competition control population sizes of mammals on the Etosha plains.

The second study concerned species coexistence among Africa's diverse large herbivorous mammals, which include 78 species of bovids. Several species often feed right next to each other and Richard Emslie (University of Witwatersrand) has examined the niche specializations that permit this coexistence among five large grazers in Umfolozi Game Reserve—white rhinoceros, buffalo, zebra, wildebeest and impala,

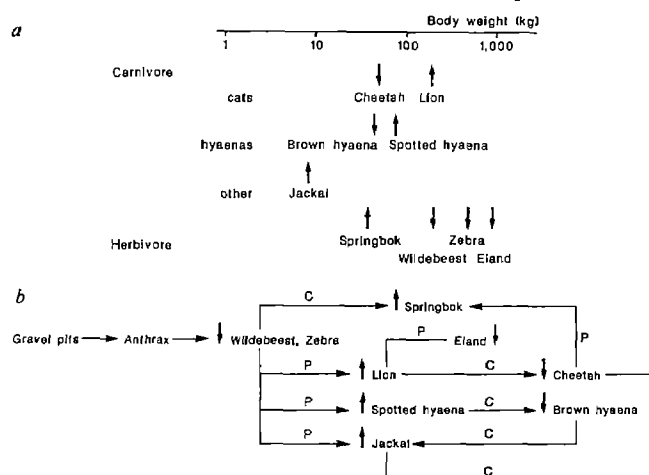
adding a new level of detail to previous analyses.

After individual animals had finished grazing, Emslie searched their feeding sites for freshly defoliated surfaces, measuring the vegetation available within a 0.25 m<sup>2</sup> hoop and recording what had been eaten and how it had been eaten. Every plant in the hoop was examined and every tiller (the unit of a grass tuft) of the two key grass species *Themeda triandra* and *Panicum coloratum* was measured. He also monitored the availability of vegetation over an area of 33.25 km<sup>2</sup> by measuring within each 25-hectare block. This yielded data on resource selection over a hierarchy of levels, ranging from 25-hectare areas to parts of individual plants.

At the coarsest level, buffalo selected areas (25 hectares) with a high biomass of tall grass, whereas the other four species

chose areas of shorter grass. In the short grass areas, impala selected feeding patches dominated by *P. coloratum*, whereas wildebeest, often only a few metres away, sought patches with short *T. triandra*. Within feeding patches, the different species selected different tillers of the same grass species—the short erect tillers in the centre of *P. coloratum* plants grazed preferentially by wildebeest and white rhino, with their lawnmower-like wide muzzle and lips, and the longer, more prostrate tillers at the edge of tufts were eaten by the narrower-muzzled zebra and impala. Buffalo rejected tall *T. triandra* but selected medium-height tillers (40–75 cm), whereas wildebeest favoured short leafy tillers with no stem. Clearly, ecological studies that list only the species eaten omit considerations that are important to grazers.

Previous studies have revealed ecological differences among herbivores related to their differing body sizes and digestive anatomies (Bell, R. in *Animal Populations in Relation to Their Feeding Resources* ed. Watson, A. p. 111; British



*a*, Trophic relationships and size structure of mammals from the Etosha National Park. *b*, Inferred causal sequences of changes in the community. ↑, Increased abundance; ↓, decreased abundance; P, predator/prey interaction; C, competitive interaction.

Ecological Society, 1970 and Jarman, P. *Behaviour* 48, 215; 1974). Big animals cannot afford to be as selective about food as their related smaller species. On one hand, the non-ruminant zebra processes large quantities of low-quality plant matter quickly and inefficiently; on the other, ruminants process smaller quantities of higher-quality matter more slowly and efficiently. Emslie's studies now emphasize the importance of differing mouth anatomy as well. It is these differences that give rise to the familiar African scene of diverse large herbivores grazing next to each other, apparently in contempt of Gause's competitive exclusion principle but actually exploiting habitat heterogeneity at many scales. □

## Corrigendum

The article by Jeremy Berg (*Nature* 319 264; 1986), which discussed the repeated domains in the TFIIIA protein described by Miller *et al.* (*EMBO J.* 4 1609; 1986), should have mentioned that the repeating nature of the TFIIIA sequence has been independently noted by R.S. Brown and coworkers (Brown, R.S., Sander, C. & Argos, P. *FEBS Lett.* 186, 271; 1985).

Jared M. Diamond is Professor of Physiology at the University of California Medical School, Los Angeles, California 90024, USA.

## AIDS therapy by blocking CD4<sup>+</sup> cells

SIR—In a recent *News and Views* article<sup>1</sup>, Klatzmann and Montagnier discussed approaches to therapy of patients with acquired immune deficiency syndrome (AIDS), including immunosuppressive drug therapy, and, in particular, the case in which AIDS patients were treated with the drug cyclosporin A<sup>2</sup>. Since AIDS results in an immune-deficient state, most efforts to restore immune function have involved immune-enhancing therapy<sup>3</sup>. However, the rationale for immunosuppressive drug therapy is that the development of AIDS involves a progression of immune disorders of which an early phase may be autoimmune<sup>4</sup>.

We suggest an alternative therapeutic approach based on the observation *in vitro* that the virus associated with AIDS, HTLV-III/LAV, is produced in activated but not resting T cells<sup>5</sup>. It seems logical to design therapy that would diminish the pool of CD4<sup>+</sup> cells with the potential to produce virus efficiently. This could be accomplished by treating patients as early as possible in the course of the syndrome's development with either monoclonal anti-CD4 or anti-class II HLA reagents, either of which would block the activation of CD4<sup>+</sup> T cells. The administration of CD4-specific antibodies would have the added advantage of interfering with the binding of HTLV-III/LAV to the CD4<sup>+</sup> cell<sup>6,7</sup>.

The mechanism by which HTLV-III/LAV causes the destruction of infected CD4<sup>+</sup> T cells is unknown. If the virus is directly cytopathic, addition of CD4-specific reagents should prevent further infection of healthy cells, while permitting the infected cells to be lysed. It is likely that at least part of the destruction of infected CD4<sup>+</sup> cells is due to cytotoxic T lymphocytes (CTL) that recognize HTLV-III/LAV antigenic determinants in association with self-HLA products and lyse infected cells<sup>8</sup>. In this case, treatment with antibodies that inhibit CD4<sup>+</sup> helper T cell function should block further help provided by anti-HTLV-III/LAV-specific helper cells, but should permit the lysis of infected targets by CTL effectors that have already been activated.

From this perspective, it could be reasoned that immune-enhancing therapy such as administration of interleukin-2 (IL-2) would activate CD4<sup>+</sup> cells and increase the number of T cells that would be susceptible to infection with the AIDS virus. Furthermore, since many HTLV-III/LAV infected individuals do not exhibit symptoms<sup>8</sup>, it appears that cofactors such as other infectious agents<sup>9</sup>, drugs<sup>10</sup>, or HLA allogenic stimulation<sup>11,12</sup> contribute to the appearance of the syndrome. A common mechanism by which these various potential cofactors could operate is

by the activation of CD4<sup>+</sup> T cells, thereby increasing the HTLV-III/LAV target cell pool size.

A therapeutic protocol that blocks CD4<sup>+</sup> T cell activation would probably limit the number of CD4<sup>+</sup> cells infected by HTLV-III/LAV and subsequently destroyed. However, because these antibodies function to prevent activation of helper T cells, they would be likely to induce immune deficiency, but one that is reversible upon cessation of treatment. Thus, therapy that blocks CD4<sup>+</sup> T cell function differs from treatment with immunosuppressive drugs (which can have severe side effects and can be difficult to control) in that it is readily reversible. If therapy that blocks CD4<sup>+</sup> T cells were to be attempted, it should be administered as early as possible in the development of AIDS, before depletion of CD4<sup>+</sup> T cells has occurred, and probably with agents that have anti-retroviral activity<sup>13,14</sup>.

ALFRED SINGER  
GENE M. SHEARER

*Immunology Branch,  
National Cancer Institute,  
Bethesda, Maryland 20892, USA*

1. Klatzmann, D. & Montagnier, L. *Nature* **319**, 10 (1986).
2. Walgate, R. *Nature* **318**, 3 (1985).
3. Fauci, A.S. *et al.* *Ann. intern. Med.* **100**, 92 (1984).
4. Shearer, G.M. *Mt Sinai J. Med.* (in the press).
5. McDougal, J.S. *et al.* *J. Immun.* **135**, 3151 (1985).
6. Dalgleish, A.G. *et al.* *Nature* **312**, 763 (1984).
7. Klatzmann, D. *et al.* *Nature* **312**, 767 (1984).
8. Blattner, W.A. *et al.* *Ann. intern. Med.* **103**, 665 (1985).
9. Frederick, W.R. *et al.* *J. infect. Dis.* **152**, 162 (1985).
10. Marmot, M. *et al.* *Lancet* **i**, 1083 (1982).
11. Mavligit, G.M. *et al.* *J. Am. med. Ass.* **251**, 237 (1984).
12. Tung, K.S. *et al.* *J. Immun.* **135**, 3163 (1985).
13. Mitsuya, H. *et al.* *Science* **226**, 172 (1984).
14. Rozenbaum, W. *et al.* *Lancet* **i**, 450 (1985).

## Serotherapy for AIDS and pre-AIDS syndrome

SIR—Acquired immune deficiency syndrome (AIDS) and the related pre-AIDS syndrome continue to spread<sup>1</sup> with as yet no effective treatment. Vaccines are a hope for the future, but it is generally acknowledged that vaccines are unlikely to prove useful in established AIDS. Recent suggestions of using methods of inhibition of gene expression to treat AIDS are theoretically attractive but also somewhat futuristic<sup>2</sup>. There is another and more immediate approach to treating these diseases. McDougal *et al.*<sup>3</sup> and others (including our unpublished observations) have shown that lymphadenopathy-associated virus/human T-lymphotropic virus type III (LAV/HTLV-III) infected T cells and T cell lines established from AIDS patients express the interleukin-2 (IL-2) receptor. This membrane receptor is an 'activation' marker of mitogen and antigen stimulated normal lymphocytes. The virus LAV/HTLV-III causing AIDS on gaining access to T lymphocytes via their CD4 receptors<sup>4</sup> remains within a protected intracellular environment, avoiding the effects of neutralizing

antibodies. Such antibodies have been detected in the blood of AIDS and AIDS-risk patients<sup>5,6</sup>. Present indications are that such neutralizing antibodies seem not to influence the course of the disease. This is probably due to the privileged intracellular location of the virus mainly within the helper/inducer T lymphocytes. This is indicated in the experiments of Robert-Guroff *et al.*<sup>6</sup>, showing that absorption with virus-infected and uninfected H9 cells do not substantially affect neutralizing antibody titres, in contrast to cell-free virus preparations.

We suggest that the expression of the IL-2 receptor by the LAV/HTLV-III infected cells provides an extremely useful target (with a fairly high degree of tissue selectivity) for antibody-directed destruction of such cells. A high affinity anti-IL-2 receptor antibody (several monoclonals exist) selected from the appropriate species and of the appropriate isotype would be lytic-destructive for the LAV/HTLV-III infected target cells. The released virus would then be exposed to the neutralizing antibodies in blood. A good candidate for the anti-IL-2 receptor antibody would be a rat monoclonal of the IgG2b isotype. Such a monoclonal immunoglobulin with pre-defined specificity for membrane molecules of human and mouse T cells has already been shown *in vivo* and *in vitro* to be highly destructive to target lymphocytes. The antibody activates the recipient's own serum complement and operates in antibody-dependent cell cytotoxicity to give lysis of the targets<sup>7</sup>.

The AIDS and pre-AIDS patients' sera may contain enough neutralizing antibody to be effective against the exposed virus following the lysis of IL-2 receptor bearing infected targets. Alternatively, passive anti-LAV/HTLV-III human antibodies could also be infused to boost the patient's own antibody. Passive anti-LAV/HTLV-III antibody for administration can be obtained from pooled AIDS sera by ethyl alcohol fractionation which inactivates the virus<sup>8</sup> without reducing antibody activity.

The combined serotherapeutic approach outlined above can now be put to the test using the recently developed *in vitro* model systems<sup>6,9</sup>. Passive administration of antibodies is a time proven method of therapy, and the side effects are well documented and amenable to prophylaxis and treatment. Ideally this form of therapy should be introduced early after the diagnosis of AIDS and pre-AIDS syndrome, and possibly for patients shown to be LAV/HTLV-III antibody positive, with or without the secondary lymphocyte subset changes. Serotherapy could also be combined with drug treatment with agents such as suramin, which by itself in early clinical trials has proved to be ineffective in the long term, with marked toxic side effects. The early introduction of the ther-

## SCIENTIFIC CORRESPONDENCE

apy described may ensure protection from infection of new T lymphocytes generated from the patient stem cells under thymic influence. Such cells could contribute to significant degrees of immune reconstitution of the individual.

H.F.SEWELL  
F. WALKER

*Department of Pathology,  
University of Aberdeen,  
Foresterhill, Aberdeen AB9 2XD, UK*

1. Curran, J.W. et al. *Science* **229**, 1352 (1985).
2. Mariman, E.C.M. *Nature* **318**, 414 (1985).
3. McDougal, J.S. et al. *J. Immun.* **135**, 3151 (1985).
4. Dagleish, A.G. et al. *Nature* **312**, 763 (1984).
5. Weiss, R.A. et al. *Nature* **316**, 69 (1985).
6. Robert-Guroff, M. et al. *Nature* **316**, 72 (1985).
7. Cobbold, S.P. et al. *Nature* **312**, 548 (1984).
8. Spire, B. et al. *Lancet* ii, 899 (1984).
9. Hoxie, J.A. et al. *Science* **220**, 1400 (1985).

## Immunosuppressants in patients with AIDS

SIR—An interesting rationale for the treatment of acquired immune deficiency syndrome (AIDS) with the immunosuppressive cyclosporin A is based on the view that AIDS is an autoimmune disease<sup>1</sup>. Immunosuppressive drugs would be designed to reduce virus replication and autoimmune processes triggered by retroviral envelope proteins that are bound to T4 molecules. Klatzmann and Montagnier state, however, that there is still no firm basis for such a therapeutic approach.

To this point, we are able to present a contribution that is experimentally corroborated by studies on neopterin excretion: measurement of neopterin levels provides a sensitive tool able to quantify activation of T-lymphocytes *in vivo*. Elevated neopterin levels are observed in virtually all diseases where activation of T-cells is apparent. *In vitro*, neopterin is released exclusively from macrophages in response to specific stimulation with  $\gamma$ -interferon (IFN- $\gamma$ ) secreted by activated T-cells<sup>2</sup>.

Studies of neopterin excretion have demonstrated an activated cellular immune system in patients with AIDS, with AIDS related complex (ARC) and in risk-group members<sup>3–5</sup>. The frequency of elevated neopterin levels in risk groups is significantly correlated to the known AIDS risk factors: receptive anal intercourse, parenteral drug abuse and clotting factor substitution therapy in haemophiliacs. This elevation is observed also in recipients of multiple blood transfusions, infant children and in LAV/HTLV-III seronegative, apparently healthy risk-group members<sup>6</sup>. Although the activation of the cellular immune system seems to contrast with the clinical presentation of AIDS, the high serum levels of  $\alpha_1$ -thymosin and of acid-labile IFN- $\alpha$  in AIDS and ARC patients and elevated cytotoxic T-lymphocyte activity against allogeneic lymphoblasts in homosexual

men are consistent with activation<sup>6</sup>. These data argue for the view that T-cell-activation plays a crucial role in the development of AIDS. We conclude that conditions linked with T-cell activation are prerequisite for the development of AIDS. Permanent or multiple stimulations of the cellular immune system might represent the often discussed cofactor for progressive syndrome.

According to this concept, and as suggested by Klatzmann and Montagnier<sup>1</sup> and demonstrated *in vitro*<sup>7</sup>, the activation and proliferation of T4-cells will determine how much and how fast virus replication will ensue.

Consequently, T-cell activation should be strictly avoided particularly in LAV/HTLV-III seropositive individuals. Application of immunostimulative drugs such as interleukin-2 (IL-2), will exacerbate the course of disease by accelerating virus spreading and T4-depletion; the failure of IL-2 treatment is well known<sup>1</sup>. Regimens preventing activation of T-cells and applications of immunosuppressive agents (such as cyclosporin A) that inhibit secretion of IL-2 from T-cells, should be tested with adequate caution.

Finally, the activation of T-cells by treatment can be readily assessed by measurement of serum or urinary neopterin concentrations which rise with immunostimulatory therapy and fall with immunosuppression.

Financial support by the Jubiläumsfonds der Österreichischen Nationalbank, P2591, is gratefully acknowledged.

A. HAUSEN  
M.P. DIERICH  
D. FUCHS  
P. HENGSTER  
G. REIBNEGGER  
T. SCHULZ  
E.R. WERNER  
H. WACHTER

*Institute of Medical Chemistry  
and Biochemistry,  
Institute of Hygiene,  
University of Innsbruck,  
A-6020 Innsbruck, Austria*

1. Klatzmann, D. & Montagnier, L. *Nature* **319**, 10 (1986).
2. Huber, C. et al. *J. exp. Med.* **160**, 310 (1984).
3. Wachter, H. et al. *Hoppe Seyler's Z. physiol. Chem.* **364**, 1345 (1983).
4. Fuchs, D. et al. *Lancet* II, 1130 (1985).
5. Wachter, H. et al. *Lancet* I, 97 (1986).
6. Tung, K.S.K. et al. *J. Immun.* **135**, 3163 (1985).
7. McDougal, J.S. et al. *J. Immun.* **135**, 3151 (1985).

## Genetic prediction of cystic fibrosis

SIR—Brock and van Heyningen (*Nature* **319**, 184; 1986) have reason to be a little indignant about the way their current prenatal test for cystic fibrosis was ignored, but they are wrong to state that first trimester prenatal diagnosis by gene tracking with linked DNA probes suffers from a major problem due to the inability to confirm cystic fibrosis in the aborted

embryo. Their "cardinal requirement of prenatal testing, namely that some method of confirmation of diagnosis on the abortus be available" only really applies to tests based on empirical correlations between the level of some factor in amniotic fluid, for example, and fetal genotype (tests such as Brock's current prenatal cystic fibrosis test and his earlier important contribution, the  $\alpha$ -fetoprotein test for open neural tube defects like spina bifida). This is not so for genetic prediction using linked probes.

The reliability of gene tracking using linked DNA probes depends on both exclusion of non-allelic genetic heterogeneity and the frequency of recombination between disease locus and marker(s). Careful linkage studies in a large number of families from different populations will allow exclusion of significant non-allelic heterogeneity and provide a mean recombination frequency. These studies are already well advanced. The recombination frequency combined with the prior genetic risk will allow a reliable prediction of the false positive and false negative rates for first trimester diagnosis; and the false negatives will also be observed after birth. Thus, the information required to assess the reliability of the prenatal test is available from studying living family members.

Our unit has probably had the greatest experience in Britain of using linked and gene specific probes for early prenatal diagnosis of haemophilia A, a disorder for which there is a reliable second trimester test by fetal blood sampling. Our experience shows that couples at risk understand the inherent errors in using linked probes, and yet almost always opt for the earlier test based on chorionic villus sampling; often followed, in the case of a negative result, by fetal blood sampling. We cannot over-emphasize the advantages of early diagnosis as perceived by the family. These include the psychological benefits of an early result and an earlier and safer therapeutic abortion, if they choose that option. A consequence seems to be a shorter gap before trying again if unlucky. Furthermore, there is the opportunity to keep the pregnancy private until the matter is decided.

MARCUS E. PEMBREY  
SUE MALCOLM  
*Mothercare Unit of Paediatric Genetics,  
Institute of Child Health,  
University of London,  
30 Guilford Street,  
London WC1N 1EH, UK*

### Scientific Correspondence

Scientific Correspondence is intended to provide a forum in which readers may raise points of a rather technical character which are not provoked by articles or letters previously published.

# Victorians abroad

David E. Allen

**Explorers Extraordinary.** By John Keay. *John Murray, London/Tarcher, Los Angeles: 1985. Pp. 195. £10.95, \$7.95.*

**The Travelling Naturalists.** By Clare Lloyd. *Croom Helm/University of Washington Press: 1985. Pp. 156. £13.95, \$19.95.*

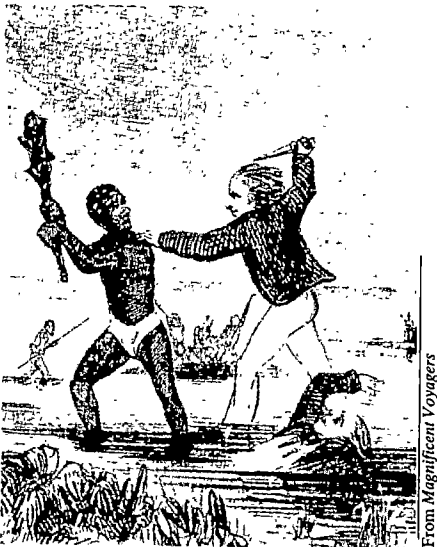
**Magnificent Voyagers.** Edited by Herman J. Viola and Carolyn Margolis. *Smithsonian Institution Press: 1985. Pp. 304. Hbk £35; pbk £17.50. To be distributed in Britain from May by Eurospan, hbk £37.95; pbk £18.95.*

EXPLORERS have always felt a need to find justifications for their efforts, and adding to scientific knowledge has long been one of the most popular of them. The Victorians, in particular, were fond of making out that the only reason why they hauled themselves up precipices or hacked their way through jungles was to make observations of unrecorded phenomena or to add to the tally of the Earth's known species. It was just not done to admit that other and less lofty motives lay behind their efforts: the physical challenge maybe, the thrill of the chase, or the glory of getting there first. A new literary genre came into being as a result: the scientific travel book. In addition to experiencing vicariously all the wonders and the perils of the untrodden wilds, the armchair reader wanted the reassurance that it had all been in a worthwhile cause, that the enjoyment and the suffering had had an underpinning of usefulness. And as the supply of scientists who had travelled interestingly was strictly limited, many who were barely scientific rushed in to fill the gap.

In his entertaining, light-hearted romp of a book — originally a series of radio talks — John Keay has disinterred a choice handful of the often rich and varied characters, a few of them frauds, most of them engagingly eccentric, from among whom the outer fringe of this literature acquired many of its inhabitants. Three with scientific pretensions feature among the seven whose exploits he recounts. The claim of one of them, H. Savage Landor, to have been contributing to science, however, is evidently to be taken no more seriously than the title *Everywhere* that he had the effrontery to give to the published narrative of his journeys. The other two, though, did make useful collections. Ludwig Leichhardt, one of a series of impossibly prickly Central Europeans who lend added colour to the history of the early exploration of Australia, had undoubtedly talents as a botanist and his eventual, still-unsolved disappearance was a definite loss to that discipline. For Mary Kingsley, niece of the author of the *Water Babies*, on the other hand, collecting was a sideline: it was to carry on her late father's researches into primitive religion that she braved the depths of the African rain-forest. Spe-

cializing in creatures that did not need to be taken with a gun, she brought back for the British Museum many valuable specimens of beetles and fish.

John Keay is a practised, professional writer, addressing with confidence what might almost be termed the professional



From *Magnificent Voyagers*

*Perils of adventure: the Malolo incident of July 1840 in which Fijians attacked members of the US Exploring Expedition, killing Midshipman Wilkes Henry, nephew of the Expedition's leader.*

reader. Clare Lloyd, by contrast, is a professional zoologist more obviously having to strain in writing for the less sophisticated audience on which she has set her sights. Her book, however, is reprehensibly mistitled: botanists and geologists, the other members of the trinity that ostensibly forms her subject, scarcely feature at all in its pages. It is hardly tactful of her, either, in a work whose readers will presumably be amateurs in the main, to let slip the suggestion here and there that genuine science can be done only by those who have received an academic training. Nor is the bibliography all that it should be, for much of the historical scene-setting is recognizably drawn from a source that she fails to mention.

Nevertheless *The Travelling Naturalists* is a book which, besides being read with pleasure, will prove of particular value for its helpful bringing together of accounts of the far-flung fieldwork of three late-Victorian naturalists: Howard Saunders

and Henry Seebohm, wealthy ornithologists who respectively followed their pursuit into the Andes and Siberia, and William Spotswood Green, who went a long way down as well as up, organizing the Royal Irish Academy's deep-sea dredging programme of 1885–1887 and notching up first ascents in Canada's Selkirk Mountains and in the Southern Alps. More familiar figures occupy more than half of the rest of the book: Mary Kingsley (again), Waterton, Bates, Speke and Franklin. While the tales of these certainly stand a re-telling, it is a pity the opportunity was missed to exhume rather more of the second division.

Bundling together biographies like this is one sure way of recapturing that age of the great pioneers: another is the portrait-in-depth of a single expedition. The sumptuous form in which the voyage of the *Beagle* was recently commemorated seems to have started a welcome fashion in this line of publishing; in the past year or two we have been treated to an even finer volume on the voyage of the *Endeavour*, complete with Sydney Parkinson's long-unpublished drawings, and now the Smithsonian Institution has surpassed even that with a yet more magnificent book on the Wilkes Expedition of 1838–1842. Just as the *Endeavour* volume was the product of a team of specialists drawn mainly from the ranks of the British Museum (Natural History), so their Smithsonian counterparts have turned out in force to provide us with a definitive account based on exhaustive historical and taxonomic research.

The United States Exploring Expedition (to give it its official title) was the largest voyage ever undertaken expressly for the purpose of scientific discovery. It was designed to demonstrate to the world that the youthful Republic was able to bring muscle to such work that was in no way inferior to that of the longer-established nations, and to the extent that the collections brought home proved as important as they were massive it can be said to have succeeded in its aim. The emphasis on national prestige, however, was very much a mixed blessing. On the one hand it wrung out of Congress — admittedly, only after many years of lobbying — funding on a scale generous enough to allow a staff of seven scientists to be recruited, foremost among them the 25-year-old James Dwight Dana, the effective founding father of American geology. It also decreed a certain showy expansiveness in the Expedition's itinerary, enabling a wide spread of territories to be visited and for collecting in these to extend in certain cases (most notably in Fiji) to spells of up to several months. The placing at its disposal of as many as half-a-dozen ships was a further piece of unheard-of lavishness. ▶

On the other hand these were necessarily naval ships and as such quite unsuited to the scientists' requirements. The fact that the Navy held command, moreover, meant that surveying was accorded priority throughout. Worst of all, the Expedition's leader was high-handed and officious, even forbidding the conchologist member to take specimens below decks, thereby compelling him to restrict his collections severely.

Lieutenant Charles Wilkes, indeed, is both hero and villain of the story. But for his forcefulness and determination the Expedition would never have accomplished so much; yet, ever-conscious of the political purpose its research was meant to serve (not for nothing was he the great-nephew of the English politician of the same surname), he boxed in the taxonomists appointed to work up the collections with stultifying edicts. The reports, he insisted, must all be written by Americans in America — and, what is more, only in its capital city. Yet Washington at that date had no scientific library or reference collections of any consequence. Only after repeated protests did he consent to material being referred to specialists overseas.

Even when the scientific work was completed, its publication was ludicrously botched: the 19 volumes of reports and atlases in which it was embodied were limited to a print run of only 100 copies. The collections meanwhile were left without a home for all of 16 years, subjected to pilfering by Congressmen and other public figures who helped themselves to specimens as souvenirs. First offered to the Smithsonian in 1846, only to be rejected as too expensive to curate, they were finally consigned there in 1858 by a Congress bereft of further patience or ideas. Even then their fate was not necessarily happy. Most of the crustacean material perished while on loan to Chicago in the great fire of 1871. Symptomatically, too, the unpublished report on the fishes produced by Louis Agassiz was lost in the bowels of the museum for well over a century.

Despite all this, impressive additions to knowledge resulted. The zoological specimens alone turned out to contain nearly 2,000 new species. Dana's geological work, in particular, was to have an enduring influence, his observations in the Pacific anticipating the recent discoveries of plate tectonics. Many years were to pass, too, before the survey findings were superseded. Appropriately, indeed, even as late as the Second World War when the US marines came to invade Tarawa it was the chart made by the Wilkes Expedition that proved to be the only one available to guide them. □

David E. Allen, *Lesney Cottage, Middle Road, Winchester, Hampshire SO22 5EJ*, is a past President of the Society for the History of Natural History and author of *The Naturalist in Britain: A Social History* (Allen Lane, 1976).

## Curiosities of crime in medicine

H.R.F. Keating

**Surgeons at the Bailey: English Forensic Medicine to 1878.** By Thomas Rogers Forbes. Yale University Press: 1986. Pp. 255. \$26, £20.

HISTORY has a terrible habit of lapsing into anecdote, and one never knows whether to cry or to laugh. This ambivalence applies just as firmly when the history is the history of science. Thomas Rogers Forbes, Professor Emeritus of Anatomy and advisor in medical memorabilia at Yale, has had the worthily academic notion of outlining a history of forensic medicine in Britain. He uses chiefly the Old Bailey Sessions Papers, records of trials at what is now the Central Criminal Court from 1684 up to an arbitrary finishing point of 1878.

These papers are one of the few sources we have for seeing what doctors or embryo medical scientists did and thought when they were brought into rough contact with the varied forms of human criminality. So far so good. Professor Forbes has delved into them with persistence and, with footnotes and bibliography (13 small-print pages), he has laid down what could have been a formidable account.

But, alas, there is a falling-away from the ideal. Fundamentally, the material for a proper account of the gradual introduction of scientific method into English criminology is not available in the Sessions Papers nor in such other accounts as Professor Forbes from time to time quotes. Furthermore he has chosen to present what evidence he has, not in one sweep, but piecemeal, with potted histories of advances in the detection of blunt instrument injuries, of asphyxia, of sexual offences, of poisoning, of insanity and of a score of other minor aspects.

So it is hard to get much sense of the development of forensic medicine as a whole. On the other side of the coin, the book is simultaneously a tremendous hotch-potch of curiosities and comicalities. Bedside reading for a month, if you can take the odd references to inflammation of the ileum and, indeed, to *peine forte et dure*, an early scientific approach to finding the truth by squashing a suspect till he talked.

The fact is that murder is as much risible as it is horrific, I suppose because for many of us the funny side is the only way we dare look on the possible prospect of our own violent demise. So we get the so-called Resurrection Men who supplied bodies for anatomical study by digging them up or on occasion doing in the living. Thus the poet Thomas Hood wrote,

Don't go and weep upon my grave  
And think that there I be.  
They haven't left an atom there  
Of my anatomicie.

We get, too, such curiosities as cruentation. Cruentation is the belief that if a murderer can be made to touch the corpse of his victim the wounds will at once bleed. "See", wrote Shakespeare, "dead Henry's wounds Open their congeal'd mouths and bleed afresh". And in 1658 a Major Strangeways was put to this test, passed it triumphantly — and then succumbed under the *peine forte*, thus sacrificing himself to prevent his property being forfeit to the Crown.

Other speculation-causing titbits include the fact that Addison's Disease is named after Dr Thomas Addison, who actually confused that malady with another (read the footnotes). Or some vicious textbook reviewing in the early 1800s in which accusations of bad grammar played as dominant a part as challenges to experimental conclusions.

But perhaps the most savourable pages come in the various accounts of attempts on the life of Queen Victoria. There was Edward Oxford, a mulatto pot-boy who, in 1840, shot twice at Her Majesty, probably with pistols without bullets, and, out of a contradictory plethora of medical evidence, was found insane. (Because he was tried for treason rather than attempted murder he was allowed Counsel without payment.) In the Bethlehem Hospital he learnt six languages, chess, carpentry, the violin and knitting, as well as meeting George Hadfield who, convinced he was King George III and wanting to commit suicide, had fired at the real George III and missed.

Robert Pate, who in 1850 merely whammed Her Majesty on the head with a walking-stick, inflicting only a cut, was luckier. Life being odder than fiction, he was arrested by the selfsame policeman who had seized M'Naughten, the error-prone assassin of Robert Peel's secretary and origin of the long-held M'Naughten Rules for defining insanity. Pate was found guilty and not insane — the Judge happened to disagree with the M'Naughten formulations — but was merely sentenced to seven years' transportation. A mad world, my masters — in every sense. □

H.R.F. Keating, 35 Northumberland Place, London W2 5AS, UK, is a crime novelist and creator of Inspector Ghote of the Bombay CID. His most recent book is *Under a Monsoon Cloud* (Hutchinson, 1986).

### New in paperback

- *The Limits of Science*, by Peter Medawar, a characteristically short, incisive and elegant account of the place of science in the modern world. Publisher in Britain is Oxford University Press, price is £3.95. The hardback edition was reviewed by Lewis Thomas in *Nature* 312, 203 (1984).

## Cells come of age

Dennis Bray

**Annual Review of Cell Biology, Vol. 1 1985.** Edited by George E. Palade, Bruce M. Alberts and James A. Spudich. *Annual Reviews Inc., 4139 El Camino Way, Palo Alto, California 94306, USA: 1985. Pp. 580. \$27 (North America), \$30 (elsewhere).*

REVIEWING reviews can be a vertiginous business, especially in a field such as cell biology in which any single experimental observation may be caught up and reflected from a ramifying literature, like images in a Hall of Mirrors. On the red blood cell cytoskeleton, for example, you will have a choice of a dozen or more reviews written in the past four years. All have the same viewpoint (no spicy controversies here) and offer more or less the same litany of facts. It is reasonable to ask how useful they are: do we need more reviews?

Well, yes, we do, at least when they are as authoritative and critical as those published by Annual Reviews Inc. Founded in 1929, the company is a non-profit-making organization and produces volumes of reviews of scientific subjects at a remarkably low price. The directors, editors and authors all contribute their energies and talents for free, and in the interests of their science they are very conservative in starting new series. Beginning with the *Annual Review of Biochemistry* in 1931, the company now produces 27 volumes annually: a remarkably small number when one considers the range of subjects covered and the awesome increase in published literature in 55 years. New volumes are introduced only reluctantly, so that when one does appear it is a mark of recognition — a coming of age.

Some material in the new *Annual Review of Cell Biology* inevitably overlaps other disciplines. The articles on intermediate filaments, fibronectin, acetylcholine receptors and actin-binding proteins could as well have stayed in the parental *Annual Review of Biochemistry*. But the main part of the volume is distinctive in content and deals with a higher level of organization. Accounts of structures such as the brush border, the membrane cytoskeleton and microtubule organizing centres, and of organelles such as peroxisomes and Golgi apparatus, are complemented by refreshing, integrative reviews of the processes of protein targeting, endocytosis and membrane traffic, and the establishment of cell polarity in eukaryotes and prokaryotes.

The emphasis is still strongly molecular, and only one article — an excellent account of cell migration in the embryo by Thiery, Duband and Tucker — treats cells

as the sentient creatures we all know them to be. Obviously molecules are easier to study and generate more data. But cell biology and molecular biology are not the same (despite some confused statements to this effect in the preface), and it is a pity that such an influential volume does not have more on the lineage, differentiation, behaviour and tissue interactions of the eponymous cell.

Within the rigidly defined format of the *Annual Review* volume, many excellent features are to be found in the book. There are more illustrations than usual, adding greatly to the interest and comprehensibility of a subject that deals in organization and structure (line diagrams are probably more effective than halftones in such an economically produced volume). It is also pleasant to discover how readable

many of the articles are. Back in 1950, the first volume of the *Annual Review of Physical Chemistry* regaled its readers with sentences several pages long, containing lists of references and chemical names and one verb. We have come a long way since then. Many of the reviews in this new volume could be enjoyed by informed readers outside the immediate area of specialization, especially where authors have ventured to bring the facts together in a hypothesis. The marvellously complete account of mitosis and meiosis by Murray and Szostak creates calm in a tormented universe; right or wrong, intelligent models of this kind certainly make facts easier to remember.

Dennis Bray is in the Medical Research Council's Cell Biophysics Unit, 26–29 Drury Lane, London WC2B 5RL, UK.

## Scientific anatomy

Philip Gummell

**About Science.** By Barry Barnes. *Basil Blackwell: 1985. Pp. 163. Hbk £19.50, \$24.95; pbk £6.50, \$8.95.*

SCIENCE is the dominant form of cognitive knowledge in all modern societies. What counts as empirical knowledge in these societies is very close to being what scientists and associated experts allow so to count. How this state of affairs came about, and what it entails for both science and society, are the main themes of this book.

These themes are the bread and butter of the social studies of science, a field which developed largely from the 1960s, when there was a flurry of interest in the possibility of a "science of science". Although that goal has long been abandoned, we do now have a richer understanding of science as a social institution. Unfortunately, much of the relevant literature is written only for the *cognoscenti*. Barnes redresses the balance well with this extremely lucid book. His intended audience is undergraduates and sixth-formers who are studying natural science and wish to learn more about science as an activity. But the book is so well written that it should attract a much wider readership.

Barnes describes how science became central to society during the Industrial Revolution. This was not because there were large numbers of scientists, nor because of any misplaced belief in its usefulness. Rather, science was for the rising commercial and industrial classes what the Bible and the classics had been for the old landed gentry and aristocracy. As science developed so did specialization, and with it came social processes for authenticating scientific knowledge and granting admis-

sion to the body of acknowledged scientists. Within this new social institution, recognition by one's peers served the purpose that money served in the wider society: scientists sought recognition of their work, not as an end in itself, but because with it they could more readily advance their careers in the ways that they wanted.

The unequal distribution of recognition among the scientific community means that the word of some scientists counts more than that of others. This has the useful consequence that the authority of the most highly-regarded scientists acts as a filter for the mass of data which scientists encounter daily, and so allows them to survive without having constantly to go back to basics. This portrait of scientific activity contradicts, of course, the popular picture of scientists as always questioning everything.

The authority structures that arise within science extend into the wider society. This did not happen by accident. As part of their campaign in the nineteenth century for social acceptance, scientists fought the church for recognition as the authoritative voice on issues to do with natural phenomena. Their victory is now more or less complete, and this raises the question today of the possible political domination of society by experts. Barnes is sceptical of this argument. For him, society is dominated through science and technology rather than by them. He also disputes the proposition that, if only all citizens were properly informed about the issues of the day, rationally correct decisions would be made by simple aggregation of individual preferences. Such aggregation is neither simple nor even necessarily rational. The science of society remains as remote as the science of science.

Philip Gummell is in the Department of Science and Technology Policy, University of Manchester, Manchester M13 9PL, UK

## At the threshold of consciousness

K.E. Webster

**The Thalamus.** By Edward G. Jones. Plenum: 1985. Pp. 935. \$135, £114.09.

SOME 50 years ago, Sir Wilfrid Le Gros Clark described the thalamus as "at the threshold of consciousness". The phrase conveys vividly the peculiarity of an organization common to all vertebrates: the flow of sensory information to the cerebral cortex and basal ganglia (or their homologues) in the forebrain is, with few — and largely peculiar — exceptions, strikingly interrupted in the nuclei of the thalamus. And yet the effects of the destruction of the thalamus, even in human beings, are seemingly either obviously predictable (for example blindness) or spectacularly unpredictable (for example the changes in pain sensibility associated with the thalamic syndrome). This crude summary indicates, I hope, why the thalamus has fascinated so many distinguished neuroscientists for so long.

Nonetheless, this beautifully produced book is the first large-scale monograph on the thalamus to be published since the 1930s. Its scope is wide: it includes an introductory historical chapter — which lends an admirable perspective to the whole — and ranges from cytoarchitecture through synaptology, connectivity, physiology and histo-pharmacology, to ontogeny and comparative studies of the vertebrate thalamus. In general, the functional groups of nuclei are dealt with together. In many cases, when the sources of afferents and the targets of efferents are referred to, the discussion of the organization of the sources and targets is commendably extensive and well-researched: comparable in fact, to that on the subject matter *sensu strictu*. The reader can thus turn to the book as a useful source of references and informed discussion on, for example, the organization of the cerebral cortex.

The text is very readable, yet exhaustively referenced, and the numerous illustrations are of high quality. The book imparts a clear sense that the overall objective is to explain the significance of the vertebrate thalamus. That, in the last analysis, the account fails in this endeavour is a reflection not so much upon the author as upon the ultimately intractable nature of his subject matter. Professor Jones makes us well aware that, vast as our knowledge may now be, our understanding remains small: a truly all-embracing synthesis is as little possible now as it was 50 years ago.

Inevitably, in a book of this size and compass, there are details of interpreta-

tion with which one might disagree, or information at the omission of which one might complain. In my view such omissions are virtually always trivial, and represent but minor blemishes on a successful and accomplished work, while the contentious emphases and interpretations are, for me at least, the spice in a generous meal. This book is at once stimulating and useful: the earlier monographs of Le Gros Clark and of Walker have a worthy successor. □

*K.E. Webster is Professor in the Department of Anatomy and Human Biology, King's College London (KQC), Strand, London WC2R 2LS, UK.*

## Brief encounter

Irwin Fridovich

**Biochemistry of Dioxygen.** By Lloyd L. Ingraham and Damon L. Meyer. Plenum: 1985. Pp. 287. \$45, £39.13.

THIS volume, fourth in a series entitled *Biochemistry of the Elements*, might have had as its subtitle: *Once Over Lightly*. Dioxygen, its singlet states and reduction products, and the enzymes which produce and act upon them, has been under intense investigation for several decades and is the subject of a vast and rich literature. Unfortunately the authors have tried to cover it all in a small-format book of only 287 pages. They would have been better advised to have chosen some modest fraction of this broad field and to have tilled it more diligently. Probably the cause for the less than satisfactory outcome was faulty planning; if selenium deserved one volume (Vol. 2 in the series), then dioxygen should have commanded at least four volumes.

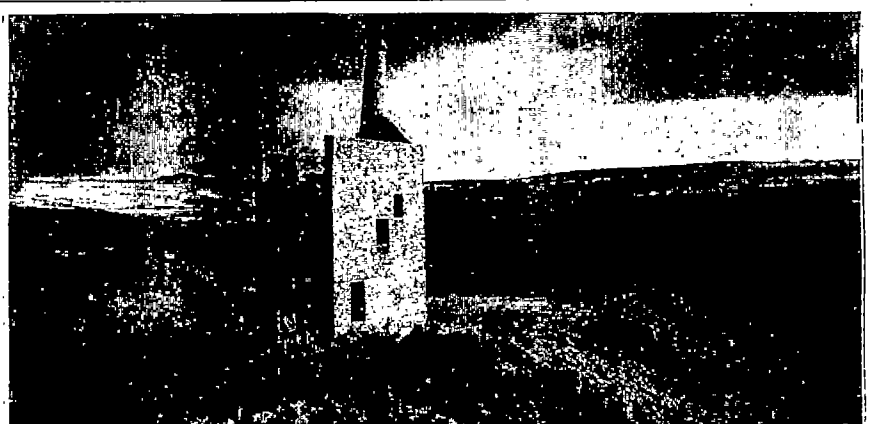
The collision between the enormity of the subject matter and the paucity of space has yielded a book which does not bear up well under close scrutiny. The results of

the past five years of research are almost entirely ignored; illuminating equations, chemical structures and diagrams are too few; typographical errors are numerous; explanations are sometimes so compressed that their import will be opaque to most readers; and the facts stated are sometimes erroneous. Some specific examples are required to give substance to these charges.

Thus, sulphite is prone to oxidation by a free radical chain reaction, but sulphite does not reduce  $O_2$  to  $O_2^-$ . The iron-containing superoxide dismutase of *Escherichia coli* was once thought to reside in the periplasm, but this claim was withdrawn on the basis of subsequent work. Some evidence for the existence of an essential persulphide in xanthine oxidase was once presented, but more recent work identifies the essential sulphur as a terminal ligand of the molybdenum, which in turn is attached to a novel pterin prosthetic group called molybdopterin; this pterin, whose discovery is the most exciting development of the past decade of study of xanthine oxidase, is nowhere mentioned. D-Amino acid oxidase catalyses the oxidation of the nitroethane anion, not of ethyl nitrate. The chapter on catalases and peroxidases makes no reference to the bacterial catalases, such as the manganese-catalase, and the chapter on "Biological Iron Dioxygen Carriers" fails to mention the Bohr effect and the influence of 2,3-diphosphoglycerate on the oxygen-binding curve of haemoglobin. The cooperativity of dioxygen binding to haemoglobin is discussed but not its physiological significance.

There is much more, but this will suffice. One may sum up the book by saying that the authors tried too much and hence were doomed to fail. We must hope that another attempt by several authors, spread over several volumes, will one day do justice to this important subject. □

*Irwin Fridovich is James B. Duke Professor of Biochemistry at Duke University Medical Center, Durham, North Carolina 27710, USA.*



*Tin decline: an abandoned mine, near Lydford, Devon, UK. The picture is taken from the paperback edition of Landscape in Britain, with photographs by Charlie Waite and commentary by Adam Nicolson, to be published in Britain on 24 March by Pavilion.*

# Investigating the paranormal

from David F. Marks

*Parascience has so far failed to produce a single repeatable finding and, until it does, will continue to be viewed as an incoherent collection of belief systems steeped in fantasy, illusion and error.*

FEW fields of inquiry capture the attention of the public as much as the paranormal. Newspapers, books, films and television have all cashed in and promoted it. Yet after millennia of experience and more than a century of controlled investigation, since the founding in 1882 of the Society of Psychical Research, the paranormal remains as controversial as ever. While credence in extrasensory perception (ESP) and precognition is widespread, parapsychology has failed to produce a single repeatable demonstration. In the face of such a dearth of hard evidence, how can such widespread belief in the paranormal be accounted for?

The importance of rigorous analysis of the evidence for parascientific claims cannot be underestimated. The establishment of ESP could conceivably require a paradigm shift (in Kuhn's sense) of the most fundamental kind and our concepts of mind-brain relationships and consciousness would need radical alteration. Our whole approach to psychology as an empirical science, based as it is on the time-honoured assumption that perception can result only from sensory activity, would be brought into question.

The conventional response of many scientists to the paranormal is to ignore the evidence on *a priori* grounds, believing it to be of basically poor quality. This attitude is allied to the Humean stance that a lie is more probable than a miracle. Although this scepticism is certainly justified, it could be argued that such a blanket response is counterproductive. First, it is hardly scientific to reject a claim purely because of its *a priori* improbability. Second, a division is created between aligned groups of committed 'believers' and 'sceptics' and the resulting adversarial positions inhibit proper discourse and the possibility of an account which satisfies all parties. Third, it leaves the field open for undisciplined exploitation, which is irresponsible; there are many examples of financial loss, suffering and even death resulting from fraudulent paranormal claims (for example, the Jonestown massacre, psychic surgery, the Transcendental Meditation levitation programme, firewalking, scientology and other pseudo-scientific cults). For scientists passively to

ignore such developments is, to say the least, uncharitable.

The Committee for the Scientific Investigation of Claims of the Paranormal (CSICOP) was established in 1976 with the aim of increasing the quality of scientific investigations into the paranormal by constructive criticism and the exposure of invalid or fraudulent claims. Over this 10-year period, an inordinate amount of fraud, error and incompetence in paranormal investigations has been brought to light<sup>1-11</sup>. But pseudo-sciences are remarkably stable and tradition-bound; their presence on the edges of science can be expected indefinitely<sup>12</sup>.

Areas of experimental psychology can shed light on the paranormal, especially the study of consciousness and cognition. Such investigation indicates that the many anomalies of putatively paranormal experience are an inevitable consequence of normal selective and constructive processes in perception, memory and imagery. I summarize here what seem to be the common assumptions on which claims of the paranormal are based.

## Theoretical assumptions

**Paranormal phenomena are negatively defined.** A phenomenon is defined as paranormal only if it contravenes some fundamental and well-founded assumption of science. Hence, to establish an effect as paranormal, all possible 'normal' explanations must be shown to be invalid. Any paranormal claim thus also remains provisional; a normal explanation, not previously thought of, may be discovered at some future time.

Mysteriousness *per se* is a necessary but insufficient condition for adjudging an event as paranormal. There will always be limits to knowledge, so that new phenomena that initially appear anomalous will be given a natural explanation following systematically controlled observations. *Bona fide* paranormal effects, on the other hand, are supposed to contravene established assumptions as though from another order of existence and not simply for lack of explanation. 'Contranormal' would be a more precise technical term.

Examples of effects which until recently

were claimed to be paranormal but which can now be explained from within orthodox science include:

(1) Kirlian photography, the photographic recording of coronal discharges around living or non-living objects produced by high-voltage, (20–100 kV), high-frequency (75 kHz–3 MHz) electrical fields<sup>13,14</sup>. Variations in the images of the corona can be explained in terms of normal physical factors such as moisture, pressure or distance, all of which influence circuit resistance.

(2) Fire-walking, if conducted briskly on hot materials of low thermal capacity and poor thermal conductivity, does not produce burns<sup>15,16</sup>. The Leidenfrost effect created by an insulating layer of water or sweat may also reduce energy transfer to the surface of the body.

(3) Dowsing is based on sensory cues, expectancy effects and probability. Controlled trials fail to produce above-chance results<sup>8,17-19</sup>.

(4) Psychic surgery, thought photography and metal bending all involve sleight-of-hand and can be duplicated by skilled magicians<sup>8,20-22</sup>. The first differs from the others in respect of the associated false hopes and financial loss, but all three are fraudulent.

(5) 'Gellerized' watches<sup>21,22</sup>, thought to be broken, are purportedly repaired by illusionist Uri Geller by 'psychic concentration'. In about 50% of cases, simply holding the watch in a clenched fist and shaking it provides a sufficient stimulus to free the mechanism<sup>23</sup>.

(6) Astrology, graphology, tea-leaf and tarot card readings, the I Ching and other forms of divination are all types of 'cold reading' or 'sleight-of-mouth'<sup>24</sup>. They depend upon ambiguous, wish-fulfilling and general advice, the use of prior or presented information and cues obtained by verbal 'fishing'. A strong feeling of personal validation often accompanies such readings. Various forms of 'mediumship' and 'psychometry' as practised by D. Collins and D. Stokes are also examples of cold reading.

In some cases, field observations can be checked under laboratory conditions and the sensori-motor features of the original performance reproduced using a delayed

control group of non-psychic subjects; for example, Geller's watch-starting procedure and ability to draw the contents of sealed and apparently opaque envelopes were matched by that of non-psychic controls<sup>23</sup> (Fig. 1). Clearly, the tendency to judge a mysterious event as paranormal in the absence of controlled observations can be quite misleading.

The most dramatic evidence for the paranormal has been based on either fraud or methodological error. Apparent frauds that have been uncovered include University of London mathematician S. G. Soal's manipulation of his recording sheets<sup>25-27</sup>, University of Utrecht Professor Tanhaeff's evidence on Croiset, the Dutch 'psychic' detective<sup>28</sup>, and the description by C. Castaneda (University of California at Los Angeles) of the paranormal teachings of Don Juan<sup>29</sup>. C. E. M. Hansel<sup>3</sup> has provided a valuable review of the history of trickery, fraud and error in parapsychology. However, outright fraud is not the only vehicle in which the paranormal cause can travel, and it is a serious mistake to assume it is a necessary part of any paranormal investigation.

**There are no theories to account for paranormal effects or their properties.** There are some undesirable implications of this aspect. First, investigators are unable to conduct properly controlled experiments on the properties of psi phenomena because they have no idea what the relevant variables are. In particular, there is no procedure by which psi can be deliberately switched on or off, and so there is no possibility of examining the effects of psi on other variables. All that can be done is to establish whether a given performance in some particular set of circumstances differs from a baseline; if so, psi is assumed to be the cause.

Oddly, neither the subject nor the experimenter can state which of the successful trials in a psi experiment result purely from chance guessing and which are generated by psi, so that there is no basis for distinguishing between a high score in a psi experiment and a lucky run in a game of chance. Also, the persistence of psi investigators in the face of variable but mainly negative results could have a similar motivational basis to that of addicted gamblers; both show high resistance to extinction following variable ratio schedules of reinforcement<sup>30</sup>.

A more fundamental problem with the paranormal's atheoretical status is that of untestability. Failure to observe a particular effect can be readily attributed to a host of *ad hoc*, hypothetical factors. Vivid imagination is no substitute for testability, however, and if *ad hoc* hypotheses are not independently testable, nor is the original claim<sup>31</sup>.

It has been stated that the participants in any experiment may unconsciously determine the results according to whether

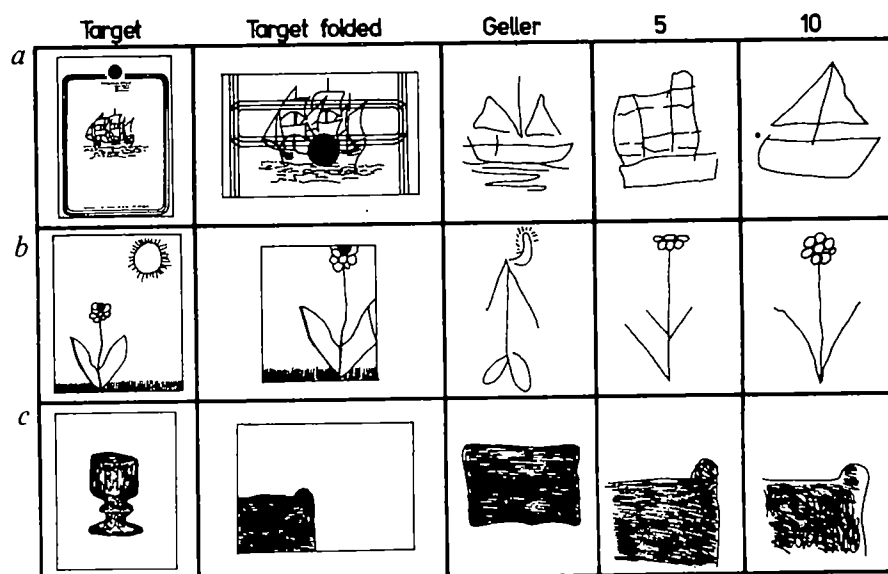


Fig. 1 Drawings presented to Geller and to non-psychic controls. The targets were inside envelopes, and Geller and the controls were allowed to see the sealed envelopes. The first and second columns show targets as they appeared in unfolded and folded states. Geller's final attempts at reproducing the drawings, which were folded and sealed inside envelopes, are shown in column 3. Columns 4 and 5 show the best results obtained from the control subjects after only 5 and 10 s of close visual inspection. The drawings were presented inside the same envelopes under similar lighting conditions. Geller, who claimed to use ESP, had taken 11.5, 85 and 18 min for a, b and c, respectively, but he was being observed, albeit discontinuously (see ref. 23).

they themselves believe in psi, the so-called 'sheep-goat' effect<sup>32</sup>. Hence, psi can be held to be present whatever the results, unless the belief of the investigators is itself independently controlled.

In an extreme version of the 'sheep-goat' hypothesis, some investigators have even proposed that the participants in an experiment need not be restricted to the individuals in the laboratory but could also include all of the readers of the journal which subsequently publishes the results<sup>33</sup>! In this case the proportion of sceptics and believers among the eventual readership would determine the experimental outcome through backward causality. Similar in kind is the 'shyness effect', the tendency of metal not to bend psychically while it is being observed<sup>34</sup>.

**Evidence of the paranormal is held to be incompatible with materialism.** Investigators throughout history have been convinced that evidence of the paranormal proves that materialism must be wrong. This was assumed by the Society of Psychological Research, one of whose early presidents, Sir William Barrett, spoke of parapsychology 'as the most valuable handmaid to religion'<sup>35</sup>. J. B. Rhine<sup>36</sup>, the founder of the Parapsychology Association and C. Tart<sup>37</sup>, a former president, have both reiterated the religio-spiritual motive for pursuing psi research.

An immaterial 'soul' has passed out of the formal language of parapsychology, but anti-materialism is still the backbone of the underlying philosophy. A. Flew has described the profound logical difficulties with an immaterial, immortal entity which

somewhat discriminates its own mental experiences from that of all others<sup>38</sup>. But even putting that issue to one side, it is curious how seldom the anti-materialist assumption has been properly explained. D. E. Cooper indicated one way in which the anti-materialist argument can be constructed as a *reductio ad absurdum*, but he found this to be incoherent<sup>39</sup>. In fact, it seems doubtful that materialism and ESP would be incompatible, should real evidence of ESP ever be found. As M. Scriven has pointed out, materialism can always be enlarged to absorb newly substantiated phenomena, "since the very act of substantiation demonstrates that the phenomena are indeed part of the material world, and hence that a current version of materialism must embrace them"<sup>40</sup>.

### Methodological problems

The failure of paranormal investigators to produce a single repeatable effect despite 100 years of published research is a serious matter. The hoped-for results have been described in thousands of reports, but not one can be repeated in a properly controlled replication. Yet in addition to the huge literature of unrepeatable findings, there is an inestimable number of unpublished and presumably negative results.

The most systematically investigated area is undoubtedly parapsychology. The field is professionally organized, with its own associations of accredited members and journals. Since 1969 the Parapsychological Association has been an affiliated division of the American Association for the Advancement of Science. On the sur-

face, the research sophistication of many parapsychologists seems to be as high as that of other professional researchers. The University of Edinburgh now has its own Koestler Chair of Parapsychology. Yet parapsychology is unique in that it remains permanently in search of a reliable finding. In spite of the long history of error, fraud and negative results, the practitioners remain confident that a positive result will soon be obtained. While many abortive leads have been reported in its major publications (for example, *Advances in Parapsychological Research*, *Handbook of Parapsychology*<sup>41</sup>, *Journal of Parapsychology*), there is no paradigmatic experiment in the Kuhnian sense, and every new investigator must start afresh, as though he or she is the first worker in the field.

Leading parapsychologists acknowledge the unrepeatability and admit that no single experiment has been free of error. J. Beloff<sup>42</sup> and R. Morris<sup>43</sup> have concluded that the best case for psi rests on collections of experiments which, although individually flawed, reveal the undeniable presence of psi. But badly controlled experiments prove nothing, no matter how large the collection.

If any genuinely repeatable effect is ever discovered, then existing science would be modified to accommodate the new finding, which would then become an integral part of materialist science. The continued existence of 'parascience' as a separate field depends upon the investigators' creativity in searching for new, unexplained anomalies of a singularly unrepeatable kind.

How close are we to a repeatable paranormal finding? Examination of the literature suggests, not very. In systematic reviews of parapsychological experiments, C. Akers<sup>44</sup> and R. Hyman<sup>45</sup> have independently come to the same conclusion: that the research methods and evidence are too weak to establish the existence of a paranormal phenomenon.

Akers reviewed a representative sample of 54 published experiments which used unselected subjects and reported significant results. The sample included 11 experiments using the ganzfeld technique (in which the eyes and ears receive unpattered sensory inputs), 12 hypnosis experiments, 12 studies of personality correlates, 10 studies of attitude correlates, 5 relaxation experiments and 4 meditation experiments. Akers identified seven sources of methodological error and the majority of experiments included one or more errors (see Table 1).

Hyman's analysis included 42 ganzfeld experiments reported during 1974-81. Twenty-three (55%) claimed significant evidence of psi on at least one performance measure. Giving consideration to what can be counted as an independent study, Hyman concluded that the true suc-

**Table 1** Flaw analyses of representative parapsychological experiments: proportions of samples containing each flaw

Flaw	Akers' sample (ref. 44)	Hyman's sample (ref. 45)
Sensory cues	22/54	23/42
Inadequate randomization	13/54	31/42
Inappropriate statistics or multiple testing	11/54	12/42
Potential fraud	12/54	10/42
Recording errors	10/54	—
Classification or scoring errors	9/54	—
Reporting failures	10/54	25/42
One or more errors	46/54	42/42

cess rate was at most 31%. Moreover, many studies had conducted multiple statistical testing by analysing more than one performance measure and Hyman suggested that a more realistic significance level would have been as high as 0.25 instead of the nominal 0.05 level. Hence, the effective significance level and percentage of significant results are approximately equal.

Hyman's tally of procedural flaws is shown in Table 1. None of his sample was judged to be free of flaws, while Akers adjudged only eight of his sample to be flawless, but stated that none could be considered ideal.

The much-publicized experiments on remote viewing by Puthoff and Targ<sup>46</sup> are also invalid because of the many sensory cues<sup>47</sup>, non-randomization<sup>47</sup> and inappropriate statistics<sup>48</sup>. Tart organized a re-analysis of this research and claimed to have removed all of the sensory cues and obtained the same highly significant results<sup>49</sup>. However, he did not in fact remove all of the cues as he had stated. Attempted replications of the remote-viewing research are either flawed or, in the case of well-controlled studies, show no evidence of ESP<sup>50</sup>.

This review leads to only one conclusion: there is no scientific evidence of ESP. Yet millions of people throughout the world believe in the reality of ESP and other paranormal phenomena. How can these two facts be reconciled? Is science mistaken, or are folk beliefs manufactured from error and illusion?

### Psychological factors

Many factors of a psychological nature foster paranormal beliefs and make them a common feature of human thinking and behaviour. Our cultural traditions are steeped in religion and magic, many features of which lend themselves to belief in supernatural agencies. Scientific thinking is a recent departure in human history and scientific ideas have had little time to affect the magical thinking from which science itself evolved.

Sociologist D. O'Keefe argues that paranormal research has evolved from within the traditions of magic which themselves evolved from religion<sup>51</sup>. The current

occult revival is seen as a reaction to the excessive rationalism which many perceive in science. O'Keefe argues that religion created the 'cloud-cuckoo land' in which magic, and thence the paranormal, can flourish. Yet scientists are often ill-prepared to provide the necessary counterbalancing rational account of the paranormal. Against this background of magico-religious entrenchment, there are some extra psychological processes that make paranormal beliefs an inevitable characteristic of human consciousness and thinking.

**Mental imagery.** A mental image is a quasi-perceptual experience in the absence of an objective stimulus. There are huge individual differences in the reported vividness and controllability of images. In Western cultures 1-5% of the population appears regularly to experience fantasies which seem as real as actual events even though they are entirely fictional<sup>52</sup>. Such individuals often experience vivid, uncontrollable 'eidetic' images of almost hallucinatory quality<sup>53</sup>, are highly suggestible and can be easily hypnotized<sup>54</sup>. They report more putatively paranormal experiences, such as telepathy, precognition, ghosts and out-of-the-body experiences. While mental imagery has a large number of practical uses in thinking, memory and problem solving, it can also occur in altered states of consciousness in which the normal level of lucidity is no longer present<sup>55</sup>.

Research conducted a century ago by E. Gurney and F. W. H. Myers described 27 cases of 'spirit communication' from deceased persons<sup>56</sup>. Eighteen of the apparitions occurred in sleep-related states normally associated with highly vivid and autonomous images which are easily mistaken for reality. The remaining cases occurred in subjects who were fully awake and these could easily have been structural eidetic images stimulated by thought-processes of the daydreaming kind<sup>57</sup>. H. Sidgwick noted that 9.9% of 17,000 subjects had experienced at least one vivid visual, auditory or tactile image of a living being or object while completely awake<sup>58</sup>. The appearance of ghosts is shaped by cultural expectancies and beliefs about what a ghost should look like<sup>59</sup>. Mental

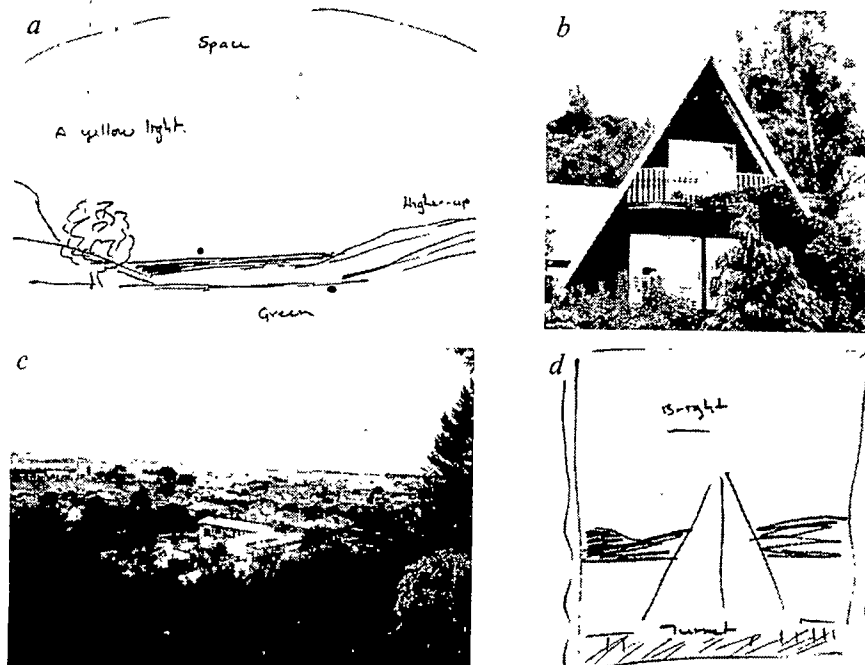


**Fig. 2** *a*, A remote viewer's drawing of the target site shown in *b*, an A-frame house and steps, purportedly using ESP. When taken to the target area, the subject was delighted when he discovered the view from above the house, halfway up the steps (*c*). When an independent judge visited the target he was convinced that the correctly matching drawing was *d*. This had actually been produced for another target site, a railway station (see ref. 4).

images can be easily misinterpreted in terms of pre-existing beliefs<sup>57</sup>.

**Expectancy** or mental set provides the framework within which we organize new experience. Human cognition is not a simple copying process but entails a constructive striving or 'effort after meaning'. What we experience is often more a confirmation of belief than a matter of plain fact. Beliefs are not automatically updated by the best evidence available, but have an active life of their own and fight tenaciously for their own survival. They tell us what to read, what to listen to, who to trust and how to rationalize contray information<sup>4,5,57</sup>.

Selective exposure protects beliefs from more dramatic forms of contradiction. When the mentalist U. Geller visited the city of Dunedin in New Zealand there were seven different opportunities to obtain information about his alleged psychic abilities: four media interviews, two newspaper stories and one stage performance. Of 17 subjects who, before Geller's visit, were already 'believers', 15 selected three or more of the available exposures. Of 20 'non-believers', only 10 selected as many as three exposures ( $\chi^2(1) = 6.13$ ;  $P < 0.02$ ).

A further problem is that when we are exposed to relevant information, our opinion revisions are often less than optimal, and we act like conservative Bayesians<sup>58</sup>, with a confirmation bias<sup>59</sup>. In a recent 'ESP' demonstration to a class of 226 psychology students, presented as an exercise in observation, I performed five

mentalists's tricks consisting of: (1) correctly naming a colour written out of sight; (2) correctly transmitting a colour name to a volunteer who, like me, had not previously seen it; (3) helping a volunteer correctly to read messages sealed inside envelopes or to appear to transmit messages to me; (4) producing bent keys which I had not previously touched; and (5) moving or stopping the hands of a watch in a mysterious manner.

Although at no time did I claim to be psychic, 90% of the class stated that I had demonstrated psychic ability. When the results from subjects who had previously been classified as 'believers' and 'sceptics' were analysed separately, 79% of believers thought at least three of the five effects were psychic compared with only 43% of sceptics ( $P < 0.001$ ).

Naturally, we often encounter information that is unexpected or ambiguous. In such instances, there is a second line of defence: the data can be selectively perceived or even misperceived so that they still appear to support our beliefs by 'subjective validation'<sup>4</sup>. One illustration of this powerful cognitive defence in the context of ESP research is the strong conviction that one has successfully viewed a complex target site by ESP in a remote-viewing experiment even when one is completely wrong (Fig. 2).

There are many now-classic examples of subjective validation: the prophecies of the Delphic Oracle and Nostradamus<sup>60</sup>, the discovery of N-rays<sup>61</sup>, phlogiston, Vulcan, the canals on Mars, flying saucers,

Freud's interpretation of dreams, prejudice, faith-healing, the placebo effect, bone pointing and the 'evil eye'. Beliefs of all kinds tend to be self-perpetuating. **Coincidences.** Psi phenomena consist of an experience, image or thought matched by some other similar experience, image or thought. Collections of such coincidences have been published by A. Koestler<sup>62</sup>, L. Rhine<sup>63</sup> and others based on the assumption that odd-matches of events cannot occur purely by chance.

Probability theory shows that an event which is improbable over a short run can become highly probable over the long run. If five coins are tossed all at once on a single occasion the probability of obtaining five heads is  $2^{-5}$  or approximately 0.03. If the coin tossing is repeated 100 times the probability of five heads somewhere in the series is approximately 0.96.

The principle of the long run is easy to grasp in simple situations but much less visible in the more chaotic world of spontaneous human experience. Calculation shows how easily Koestler could obtain his 40-plus odd-match anecdotes. Assuming that in an ordinary day a person can recall 100 distinct events, there are  ${}^{100}C_2$  or 4,950 pairs of events per day. Odd-matches can be remembered for years, perhaps 10 yr or 3,650 days. If Koestler knew 1,000 people, he could draw upon a total pool of  $4,950 \times 3,650 \times 1,000$ , or more than  $18 \times 10^9$  pairs of events. That Koestler obtained 40 striking odd-matches seems hardly surprising.

Koestler's fallacy (see ref. 4) is certainly not unique to him, although he was one of a small group of analysts who wanted to make a scientific revolution out of it. The fallacy is widespread and several biases contribute to it. First, we notice and remember odd-matches. Second, we do not notice non-matches. This triggers the short-run illusion that makes the odd-match seem improbable. Third, we are normally poor estimators of probabilities, especially for combinations of events.

**Unseen causes.** Another class of psychic-looking experiences is generated by invisible chains of cause and effect which bias the probabilities away from chance levels. Failure to randomize target stimuli properly in ESP experiments is a good example of this. Thus, Tart reported a successful ESP experiment in which his subjects learned to score above chance in guessing which of 10 digits was displayed by an apparatus in another room following the presentation of feedback<sup>4</sup>. The random number generator mistakenly avoided using the same digit twice in succession, a bias which is matched by the pervasive 'gambler's fallacy'. When Tart removed this bias, the 'ESP' also disappeared<sup>65</sup>.

Another unseen factor, used by illusionists, is the 'population stereotype'. The performer 'sends a message' to the

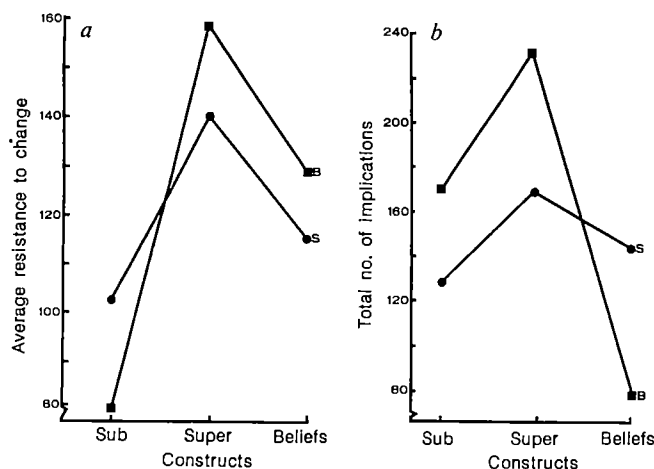


**Fig. 3** *a*, The average resistance to change scores for 'believers' (B) and 'sceptics' (S) for subordinate (Sub), superordinate (Super) and belief constructs. Believers showed a significantly higher resistance to change for superordinate constructs than sceptics. *b*, The total number of implications for the same sets of constructs. The interaction between group and construct-type was highly significant ( $F(2, 42) = 9.14, P < 0.005$ ). Believers saw significantly more implications in changing positions on superordinate constructs than did the sceptics, while sceptics saw significantly more implications in changing their beliefs than believers ( $P < 0.05$  for both comparisons).

audience, saying "I am thinking of a number between 1 and 50, both digits are odd, and different". Controlled experiments show that the most common response for the 1-50 problem is 37, which accounts for 30-35% of all responses, and the second most common response is 35 (20-25%)<sup>4</sup>. If the performer always says he had been thinking of 35 and then changed his mind to 37, at least 50% of the audience will be thinking of the 'correct' number.

Human beings never behave randomly. Our experiences contain many culturally shared elements such that particular items are associated with particular verbal contexts. This causes associative networks to be set up and a tendency towards non-random, stereotypical responses even when there is freedom to choose.

Other unnoticed causes of putatively psychic effects include subliminal and non-verbal sensory cues<sup>66</sup> which may lead to common thought patterns in different people, presenting the illusion of telepathy.

**The 'will to believe'.** What factors differentiate believer from sceptic? Psychologists down the ages have puzzled over the question of what motivates different world-views and the so-called will to believe. Research conducted by J. Waugh used Kelly's personal construct theory. In this framework<sup>67</sup>, people vary in the quality and extent of their investigatory procedures so that, while some may be working to establish an ordered and meaningful world which is not highly predictable or readily explained, others may be content that they already have all the necessary explanatory constructs.

In Kelly's theory, each individual deals with the world in terms of a hierachial

system of constructs with which people, objects and events are compared, contrasted and predicted. Core constructs have relatively superordinate positions and a large range of convenience while peripheral constructs are relatively subordinate and more easily altered. Waugh compared the personal construct systems of sceptics and believers in the paranormal using a belief questionnaire. Ten subordinate and ten superordinate<sup>67</sup> constructs were generated using standard procedures and each subject's constructs were tested for their relative resistance to change and the number of implications entailed by changing the subject's preferred pole on the 20 constructs and 10 paranormal beliefs (Fig. 3).

Believers' core constructs were significantly more resistant to change and there was a parallel difference in the number of implications resulting from changes at the superordinate level. Compared with sceptics, believers seem to possess much tighter construct systems in which any change at the core level implies a significantly greater upheaval or threat. Waugh also found that believers had significantly higher neuroticism scores than sceptics (see also ref. 68). These data are congruent with those reported by Zusne and Jones<sup>57</sup> who found that believers are less flexible than sceptics when confronted with disconfirming evidence. Content analyses of believers' construct systems indicate the presence of spiritual, non-materialist constructs at superordinate level. Such core constructs are not easily shaken because they are closed off from empirical considerations and appear to be impermeable to rational persuasion. Hence the feeling of futility experienced in trying to hold rational discussion

between believer and sceptic; one could well be arguing about the existence of God. Belief in the paranormal is metaphysical and therefore not subject to the constraints of empirically based science.

Parascience has all the qualities of a magical system while wearing the mantle of science. Until any significant discoveries are made, science can justifiably ignore it, but it is important to say why: parascience is a pseudo-scientific system of untestable beliefs steeped in illusion, error and fraud.

I thank Jerry Andrus, Bob Audley, Ray Hyman, A. R. Jonckheere, Peter McKellar, J. Randi, Christopher Scott, Jean Waugh and many colleagues in CSICOP for useful discussions and information. The late Richard Kammann contributed substantially in the earlier stages of this research.

**David F. Marks** is at the Department of Psychology, University of Otago, PO Box 56, Dunedin, New Zealand.

1. Kurtz, P. *Skeptical Inquirer* 3, 14-32 (1978).
2. Diaconis, P. *Science* 201, 131-136 (1978).
3. Hansel, C. E. M. *ESP and Parapsychology: A Critical Re-evaluation* (Prometheus, Buffalo, 1980).
4. Marks, D. & Kammann, R. *The Psychology of the Paranormal* (Prometheus, Buffalo, 1980).
5. Alcock, J. E. *Parapsychology: Science or Magie?* (Pergamon, Oxford, 1981).
6. Frazier, K. (ed.). *Paranormal Borderlands of Science* (Prometheus, Buffalo, 1981).
7. Gardner, M. *Science Good Bad and Bogus* (Prometheus, Buffalo, 1981).
8. Randi, J. *Flim-Flam! Psychics, ESP, Unicorns, and Other Delusions* (Prometheus, Buffalo, 1981).
9. Kurtz, P. *Skeptical Inquirer* 8, 239-246 (1984).
10. Frazier, K. (ed.) *Science Confronts the Paranormal* (Prometheus, Buffalo, 1985).
11. Kurtz, P. (ed.) *A Skeptics Handbook of Parapsychology* (Prometheus, Buffalo, 1985).
12. Bunge, M. *Skeptical Inquirer* 9, 36-46 (1984).
13. Tiller, W. A. *New Scientist* 62, 160-163 (1974).
14. Pehek, J. O., Kyler, H. J. & Faust, D. L. *Science* 194, 263-270 (1976).
15. Houdini *Miracle Mongers and Their Methods* (Prometheus, Buffalo, 1981).
16. Leikind, B. J. & McCarthy, W. J. *Skeptical Inquirer* 10, 23-34 (1985).
17. Vogt, E. H. & Hyman, R. *Waterwitching USA* 2nd edn (Chicago University Press, 1979).
18. Randi, J. *Skeptical Inquirer* 8, 329-333 (1984).
19. Martin, M. *Skeptical Inquirer* 8, 138-140 (1983).
20. Randi, J. *The Magic of Uri Geller* (Ballantine, New York, 1975).
21. Fuller, U. *Confessions of a Psychic* (Kari Fulves, Box 423, Teaneck, New Jersey, 1975).
22. Fuller, U. *Further Confessions of a Psychic* (Kari Fulves, New Jersey, 1980).
23. Marks, D. & Kammann, R. *Zetetic* 1(2), 9-17 (1977).
24. Hyman, R. *Zetetic* 1(2), 18-37 (1977).
25. Soal, S. G. & Goldney, K. M. *Proc. Soc. Psychical Res.* 47, 21-150 (1943).
26. Scott, C. & Haskell, P. *Nature* 245, 52-54 (1974).
27. Marwick, B. *Proc. Soc. Psychical Res.* 56, 250-281 (1978).
28. Hoebens, P. H. *Skeptical Inquirer* 6, 32-40 (1981).
29. De Mille, R. *Castaneda's Journey* 2nd ed (Capra, Santa Barbara, 1978).
30. Skinner, B. F. *Science and Human Behavior* (Macmillan, New York, 1953).
31. Bunge, M. *Method, Model and Matter* (Reidel, Dordrecht, 1973).
32. Schmeidler, G. R. & McConnell, R. A. *ESP and Personality Patterns* (Yale University Press, 1958).
33. Collins, H. M. & Pinch, T. J. *Frames of Meaning: The Social Construction of Extraordinary Science* (Routledge & Kegan Paul, London, 1982).
34. Taylor, J. *Superminds: An Inquiry into the Paranormal* (Macmillan, London, 1975).
35. Barratt, W. *Proc. Soc. Psychical Res.* 34, 275-297 (1924).
36. Rhine, J. B. *The Reach of Mind*, 209-214 (Sloane, New York, 1947).
37. Tart, C. T. *PSI: Scientific Studies of the Psychic Realm*, viii-vii (Dutton, New York, 1977).
38. Flew, A. in *Science, Pseudo-Science and Society* (eds Hanan

- M. P., Osler, M. J. & Weyant, R. G.) 55–75 (Wilfrid Laurier University Press, Waterloo, 1980).
39. Cooper, D. E. in *Philosophy and Psychical Research* (ed. Thakur, S. C.) 59–80 (Allen & Unwin, London, 1976).
40. Scriven, M. in *Philosophy and Psychical Research* (ed. Thakur, S. C.) 181–194 (Allen & Unwin, London, 1976).
41. Wolman, B. J. (ed.) *Handbook of Parapsychology* (Van Nostrand, New York, 1977).
42. Beloff, J. *Zetetic Scholar* 6, 90–94 (1980).
43. Morris, R. L. *J. Am. Soc. psychical Res.* 74, 425–443 (1980).
44. Akers, C. in *Advances in Parapsychological Research* Vol. 4 (ed. Krippner, S.) 112–164 (McFarland, Jefferson, North Carolina, 1984).
45. Hyman, R. J. *Parapsychol.* 49, 3–49 (1985).
46. Targ, R. & Puthoff, H. E. *Nature* 252, 602–607 (1974).
47. Marks, D. F. & Kammann, R. *Nature* 274, 680–681 (1978).
48. Hyman, R. *Skeptical Inquirer* 9, 125–145 (1984–5).
49. Tart, C. T., Puthoff, H. E. & Targ, R. *Nature* 284, 191 (1980).
50. Marks, D. F. *Skeptical Inquirer* 6, 18–29 (1982).
51. O'Keefe, D. *Stolen Lightning* (Robertson, Oxford, 1982).
52. Wilson, S. C. & Barber, T. X. in *Imagery: Current Theory, Research and Application* (ed. Sheikh, A. A.) 340–387 (Wiley, New York, 1983).
53. Marks, D. & McKellar, P. J. *mental imagery* 6, 1–124 (1982).
54. Gurney, E. & Myers, F. W. H. *Proc. Soc. psychical Res.* 5, 403–485 (1889).
55. Sidgwick, H. *Proc. Soc. psychical Res.* 10, 25–422 (1894).
56. Finucane, R. C. *Appearances of the Dead* (Prometheus, Buffalo, 1985).
57. Zusne, L. & Jones, W. H. *Anomalistic Psychology* (Erlbaum, Hillsdale, New Jersey, 1982).
58. Edwards, W. in *Formal Representation of Human Judgement* (ed. Kleinmuntz, B.) 17–52 (Wiley, New York, 1968).
59. Nisbett, R. & Ross, L. *Human Inference: Strategies and Shortcomings of Social Judgment* (Prentice-Hall, Englewood Cliffs, 1980).
60. Hoebens, P. H. *Skeptical Inquirer* 1, 38–45 (1982).
61. Klass, P. J. *Zetetic* 2, 57–61 (1977).
62. Koestler, A. *The Roots of Coincidence* (Hutchinson, London, 1972).
63. Rhine, L. E. J. *Parapsychol.* 15, 164–190 (1951).
64. Tart, C. T. *Learning to Use Extrasensory Perception* (University of Chicago Press, 1976).
65. Tart, C. T., Palmer, J. & Redington, D. J. *J. Am. Soc. psychical Res.* 73, 151–165 (1978).
66. Dixon, N. F. *Preconscious Processing* (Wiley, Chichester, 1981).
67. Fransella, F. & Bannister, D. *A Manual for Repertory Grid Technique* (Academic, London, 1977).
68. Windholz, G. & Diamant, L. *Bull. psychon. Sci.* 3, 125–126 (1974).

## REVIEW ARTICLE

# Heavy-electron metals

**Z. Fisk, H. R. Ott\*, T. M. Rice\* & J. L. Smith**

Center for Materials Science, Los Alamos National Laboratory, Los Alamos, New Mexico 87545, USA

*A new class of metals has been found in which the electrons have effective masses orders of magnitude larger than the free-electron mass. Some of these metals are superconducting at low temperatures. This superconductivity seems to be unconventional, with an underlying mechanism different from that in all other known superconductors.*

AMONG the main developments in physics since the 1930s have been the discovery and exploration of new ground states of condensed matter. Each of these discoveries opened a new chapter in the physics of condensed matter; recent examples are spin- and charge-density waves in metals, the superfluid state of liquid  $^3\text{He}$  and the quantized Hall effect. Very recently an exciting new class of metallic materials has been discovered with remarkable properties and showing signs of further new ground states. (A general compilation of data, with references current as of mid-1984, can be found in ref. 1.)

The terms 'heavy-electron metal' and 'heavy-fermion system' have been introduced to describe materials in which the electronic states have a characteristic energy orders of magnitude smaller than in ordinary metals. If we write the energy  $\varepsilon(k)$  in a free-electron form ( $\varepsilon(k) = \hbar^2 k^2 / 2m^*$ ), then since the wave-vectors  $\mathbf{k}$  of the electron determined by the interatomic spacing are not much different, the effective mass  $m^*$  must be orders of magnitude larger than the free-electron value and in some cases  $m^*$  is a fair fraction of the proton mass. These materials are intermetallic compounds in which one of the constituents is a rare-earth or actinide atom, with partially filled 4f- or 5f-electron shells. At high temperatures these materials behave as if the f-electrons were localized on their atomic sites, as in conventional rare-earth and actinide compounds, where any itinerant electrons are in states derived from loosely bound atomic s-, p- and d-orbitals. As the conventional materials are cooled, the atomic moments due to the f-electrons order spontaneously, mostly antiferromagnetically, less often ferromagnetically. By contrast, in the heavy-electron systems some of the f-electrons become itinerant at low temperatures and form a metallic state with the characteristics described above.

Recently the exciting discovery was made that in some of these new materials the heavy electrons form a superconducting state at very low temperatures<sup>3,4,6</sup>. Superconductivity in ordinary metals is associated with an instability of itinerant electrons; thus it was surprising that it should also occur where normal-

state properties are dominated by nearly localized electrons. Various features of this superconducting state are unusual, leading theorists to speculate that not only is the mechanism driving this superconducting transition unconventional, but also that the configuration of the superconducting state is different from that of an ordinary superconductor. Instead of an interaction between electrons that is mediated by phonons (lattice-vibrational quanta), which leads to an essentially isotropic gap in the spectrum of electronic excitations, it is envisaged that a Coulomb interaction between heavy electrons induces a superconducting state in which the energy gap is strongly anisotropic. If this could be definitely established, it would be the culmination of a long search for this phenomenon.

There is no doubt that a proper understanding of this superconducting state requires a clear understanding of the preceding normal state with its remarkable properties. Early theories of the properties of metals always assumed that, whereas the conduction electrons interact with the ionic lattice forming the solid, they do not interact at all among themselves. Quantum statistics then determine the low-temperature properties of this electron gas, two of which are of particular importance in the context of our discussion. The specific heat of this electron gas  $c_p$  varies linearly with temperature as  $T \rightarrow 0$  K (that is,  $c_p = \gamma T$ ). The low-temperature magnetic susceptibility,  $\chi$ , is independent of temperature. In this simple theory the ratio

$$\chi/\gamma = 3 \mu_B^2 / \pi^2 k_B^2 \quad (1)$$

is obviously a universal number.  $\mu_B = 9.27 \times 10^{-21}$  erg G<sup>-1</sup> is the Bohr magneton and  $k_B = 1.38 \times 10^{-16}$  erg K<sup>-1</sup> is the Boltzmann constant. The factor which determines the magnitude of both  $\chi$  and  $\gamma$  is the density of electronic states per unit energy,  $N(E_F)$ , at the Fermi energy  $E_F$ . ( $E_F$  is the energy up to which all possible states of the electron gas are occupied at  $T = 0$  K.) Hence  $N(E_F)$  varies inversely with the characteristic energy of the electrons, leading  $N(E_F)$  to be proportional to  $m^*$ . This simple concept is quite adequate to describe the qualitative low-temperature features of simple metals, for which  $\gamma$  is of the order of 1 mJ mol<sup>-1</sup> K<sup>-1</sup>,  $\chi \approx 10^{-5}$  e.m.u. mol<sup>-1</sup> and  $T_F = E_F/k_B$ , the Fermi temperature, is  $\sim 10^4$ – $10^5$  K. The experimental facts quoted in

\* Permanent address: Eidg. Tech. Hochschule, ETH-Hönggerberg, CH-8093 Zürich, Switzerland.

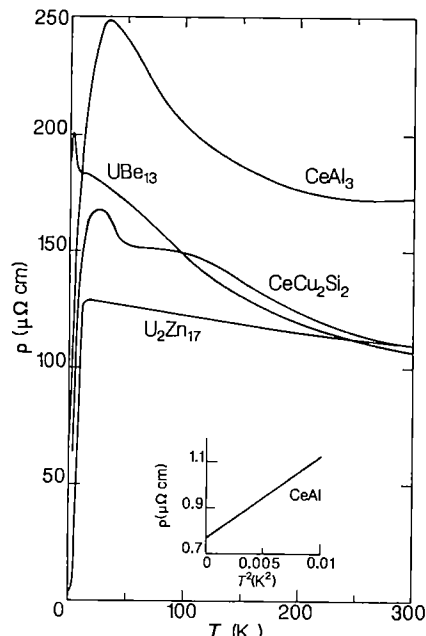


**Fig. 1** Temperature dependence of the electrical resistivity  $\rho$  of four different heavy-electron compounds below room temperature. The high values indicate very strong scattering of the electrons but the distinct features and the resistivity decrease at low temperatures demonstrate that these are not simply 'dirty' metals. The inset reveals the  $T^2$  dependence of the  $\rho$  of CeAl<sub>3</sub> at very low temperatures.

the next section should not only make it clear that these parameters are very different in this new class of materials but also demonstrate the intriguing transition from localized to itinerant behaviour of these heavy electrons.

### Normal-state properties

First we consider the electrical resistivity  $\rho$ . In ordinary metals  $\rho$  decreases rapidly with decreasing temperature below 300 K, from values that are  $\sim 1\text{--}10 \mu\Omega \text{ cm}$ . In heavy-electron materials  $\rho = 100 \mu\Omega \text{ cm}$  at room temperature. It often increases with decreasing temperature and only after passing over a maximum at  $T \leq 50 \text{ K}$  does  $\rho$  decrease to low values as  $T \rightarrow 0 \text{ K}$ . Figure 1 shows examples of this behaviour in CeAl<sub>3</sub>, CeCu<sub>2</sub>Si<sub>2</sub>, UBe<sub>13</sub> and U<sub>2</sub>Zn<sub>17</sub>. CeAl<sub>3</sub> was the first to be identified as a heavy-electron metal<sup>2</sup>. It stays normal to the lowest temperature investigated ( $\sim 10^{-2} \text{ K}$ ) and therefore can be used to study the heavy electrons in their normal state. For CeAl<sub>3</sub> it is found that although  $\rho$  reaches a maximum value of the order of  $200 \mu\Omega \text{ cm}$  at 35 K, it drops to less than  $1 \mu\Omega \text{ cm}$  at  $T = 0 \text{ K}$ , where this residual value of the resistivity is determined by impurities and imperfections of the crystal lattice as in ordinary metals. As an intriguing fact it was noted that  $\rho \propto T^2$  at the lowest temperatures with a remarkably large pre-factor of  $35 \mu\Omega \text{ cm K}^{-2}$ , indicating a very effective, temperature-dependent scattering mechanism even at these very low temperatures. (See inset, Fig. 1.)

The first observation of superconductivity in heavy-electron metals was made in CeCu<sub>2</sub>Si<sub>2</sub> (ref. 3), and this was quite unexpected. As shown in Fig. 1, its  $\rho(T)$  is very anomalous in the normal state. The increase of  $\rho$  seems to saturate below 100 K but reaches a pronounced maximum in the vicinity of 10 K before it decreases rapidly and finally vanishes discontinuously at the superconducting transition around 0.5 K. UBe<sub>13</sub> is a 5f-electron-based heavy-electron system, and is also becomes superconducting below 1 K (ref. 4). Its  $\rho(T)$  is indeed very much like that of CeCu<sub>2</sub>Si<sub>2</sub>, but the characteristic structures (shoulder and peak) are shifted to lower temperatures. The decrease of  $\rho$  below 2.5 K is interrupted by the superconducting transition at

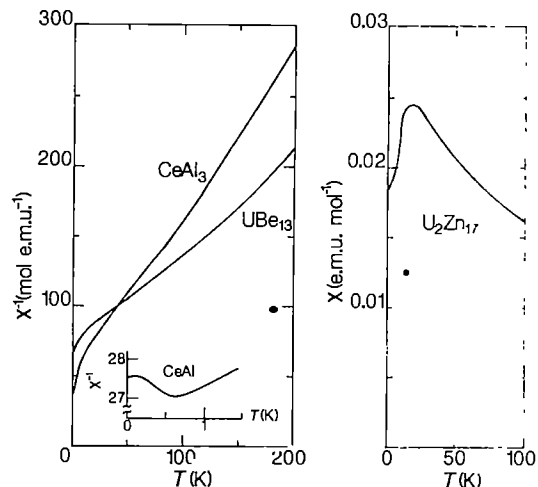


**Fig. 2** The Curie-Weiss behaviour of the magnetic susceptibilities  $\chi$  of CeAl<sub>3</sub> and UBe<sub>13</sub> above 100 K is evidence for localized f-electron moments. The low-temperature saturation (inset) for CeAl<sub>3</sub>, however, demonstrates the itinerancy of the f-electrons below 1.5 K. For U<sub>2</sub>Zn<sub>17</sub>, the tendency to saturation is interrupted by a sharp drop of  $\chi$  due to antiferromagnetic ordering.

0.9 K. Finally we consider the  $\rho(T)$  of U<sub>2</sub>Zn<sub>17</sub>, a substance that orders magnetically from a heavy-electron state<sup>5</sup>. Here the maximum resistivity is observed at 17 K and the rapid decrease of almost two orders of magnitude occurs below 10 K.

Magnetic moments that are due to partially filled 5f-electron shells of individual atoms give rise to the familiar Curie-Weiss-type behaviour of the magnetic susceptibility  $\chi$  with varying temperature; that is,  $\chi^{-1} \propto (T - \theta_p)$  where  $\theta_p$  is the paramagnetic Curie-Weiss temperature. This type of behaviour is clearly reflected in the plots of  $\chi^{-1}$  versus  $T$  for CeAl<sub>3</sub> and UBe<sub>13</sub> in Fig. 2. Deviations from this simple behaviour are apparent at  $T < 100 \text{ K}$  but they can still be ascribed to local f-electron configurations. In both materials  $\chi$  saturates only at  $T \leq 1.5 \text{ K}$  (see inset, Fig. 2). In UBe<sub>13</sub>,  $\chi$  jumps discontinuously to the ideal diamagnetic value of  $(4\pi)^{-1}$  at the superconducting transition (at  $T_c \sim 0.9 \text{ K}$ ). For U<sub>2</sub>Zn<sub>17</sub>, we show  $\chi(T)$  below 100 K; note the trend to saturation and the broad maximum at 17 K. The sharp decrease just below 10 K is due to an antiferromagnetic phase transition. The saturation values of  $\chi$  for all three materials are very large compared with those of normal metals ( $3.6 \times 10^{-2} \text{ emu mol}^{-1}$  CeAl<sub>3</sub>;  $1.5 \times 10^{-2} \text{ emu mol}^{-1}$  UBe<sub>13</sub>,  $2.45 \times 10^{-2} \text{ emu mol}^{-1}$  U<sub>2</sub>Zn<sub>17</sub>).

As mentioned above, the electronic specific heat of ordinary metals can be described by a single term,  $c_p^{el} = \gamma T$  at temperatures below 10 K. That this is not the case for heavy-electron materials is shown in Fig. 3, where we plot  $c_p/T$  against  $T$  for CeAl<sub>3</sub>, CeCu<sub>2</sub>Si<sub>2</sub> and UBe<sub>13</sub> for temperatures between 1 and 10 K (Fig. 3a) and for UPt<sub>3</sub> (ref. 6) between 1 and 17 K (Fig. 3b). For ordinary metals, such a plot would result in a straight line with a positive slope and an ordinate  $\approx 1 \text{ mJ mol}^{-1} \text{ K}^{-2}$  at  $T = 0 \text{ K}$ . For heavy-electron materials in general, the ratio  $c_p/T$  rises considerably with decreasing temperature in this temperature range, starting from values of about  $100 \text{ mJ mol}^{-1} \text{ K}^{-2}$ . The temperature dependence itself might be loosely interpreted by stating that the  $\gamma$  parameter is no longer constant but is strongly temperature-dependent. Below 1 K, the  $c_p/T$  of CeAl<sub>3</sub> rises to a maximum of more than  $2 \text{ J mol}^{-1} \text{ K}^{-2}$  at about 0.5 K and finally saturates at  $\sim 1.6 \text{ J mol}^{-1} \text{ K}^{-2}$  as  $T$  approaches 0 K. For both CeCu<sub>2</sub>Si<sub>2</sub> and UBe<sub>13</sub>,  $c_p/T$  rises in a very similar way but then saturates around 1 K and remains almost constant until a specific-heat anomaly indicates the transition to the superconducting state, as is shown, for example, for UBe<sub>13</sub> in Fig. 3c.

As outlined in the introduction, these very large values of the  $c_p^{el}/T$  ratio (or  $\gamma$  value) as  $T$  approaches 0 K must be

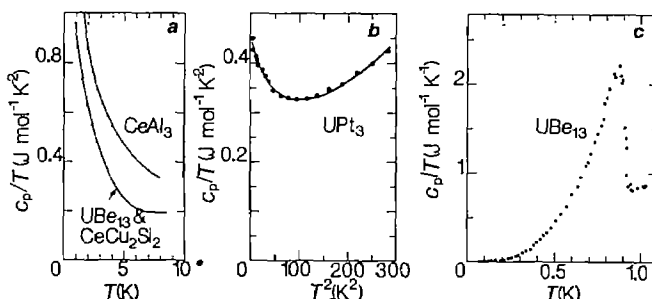


**Fig. 3** The low-temperature specific heat  $c_p$  of these materials is unusually large. The values of  $T=1\text{ K}$  are more than a hundred times larger than for ordinary metals and originate in the strong interactions between electrons. An analytic form describing the experimental data has been found only for  $\text{UPt}_3$ ; this is indicated by the solid line in *b*. The specific-heat anomaly of  $\text{UBe}_{13}$  (*c*) below 1 K is due to the transition to the superconducting state.

interpreted as evidence for enormous densities of states at  $E_F$  in the electronic spectrum of these substances. This in turn implies very large effective masses for these electrons, and hence provides the name now generally used for these systems. Although both  $\gamma$  and  $\chi$  are enhanced in these materials above the values seen in ordinary metals, their ratio  $\chi/\gamma$  is comparable to that defined in equation (1).

### Phase transitions within heavy-electron state

**Superconductivity.** The discovery of superconductivity in  $\text{CeCu}_2\text{Si}_2$  by Steglich *et al.*<sup>3</sup> was surprising because it violated many long-held beliefs in the field. In particular, the Curie-Weiss-type high-temperature magnetic susceptibility suggested local magnetic moments on the Ce atoms, and these are known to depress conventional s-state (or singlet) superconductivity by breaking up the Cooper electron pairs.

The specific-heat anomaly (shown for  $\text{UBe}_{13}$  in Fig. 3*c*) at the superconducting transition temperature (critical temperature,  $T_c$ ) scales with the normal-state value, giving not only convincing proof of bulk superconductivity but also hard evidence that  $\gamma (= c_p/T)$  is really due to a large density of states of itinerant electrons. The superconducting energy gap opens in the large-mass band; the f-electrons are therefore intimately involved in the superconductivity. It is important to distinguish this behaviour from that of the Chevrel-phase and ternary-boride magnetic superconductors<sup>7</sup>. In these latter we have an independent sublattice of magnetic ions, the magnetic order parameter of which competes with the superconducting order parameter of the essentially separate conduction electron system; in the heavy-electron materials it is one and the same set of electrons which deliberates between superconductivity and magnetism.

Arguments given below suggest the possibility that the superconductivity observed in these materials may not be of the s-state, isotropic type usual in the Bardeen-Cooper-Schrieffer (BCS) theory of superconductivity<sup>8</sup>. It may instead be an anisotropic p-, or possibly d-state type also possible in a generalized BCS theory, and now quite firmly established as the pairing state in superfluid  $^3\text{He}$  (ref. 9) but previously unknown in metals. Anisotropic superconducting states may have zeroes of the superconducting energy gap on the Fermi surface and these lead to non-exponential temperature dependences below  $T_c$  in experimental measurements such as specific heat, ultrasonic attenuation, thermal conductivity and NMR relaxation rates.

The experimental situation can be illustrated with data for  $\text{UBe}_{13}$  and  $\text{UPt}_3$ . In  $\text{UBe}_{13}$ , the superconducting specific-heat jump at  $T_c$  (see Fig. 3*c*) is  $\sim 50\%$  larger than the weak-coupling BCS prediction, placing it very squarely in the strong-coupling regime. Below  $T_c$ , the specific heat varies with a power law close to  $T^3$  (ref. 10). Ultrasonic attenuation<sup>11</sup> and NMR relaxation rates<sup>12</sup> also follow power laws, as shown in Fig. 4. Deviations

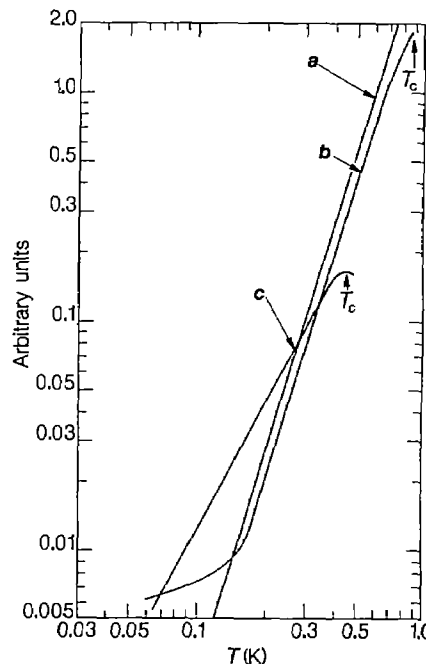


**Fig. 4** Examples of the power-law-type temperature dependence of various properties in the superconducting state of  $\text{UBe}_{13}$  and  $\text{UPt}_3$ , indicating anisotropic gaps in the electronic excitation spectrum. Conventional isotropic superconductivity would result in exponential temperature dependences for all these physical quantities. *a*, Specific heat of  $\text{UBe}_{13}$  ( $\propto T^3$ ); *b*, inverse spin-lattice relaxation rate of  $^9\text{Be}$  in  $\text{UBe}_{13}$  ( $\propto T^3$ ); *c*, ultrasonic attenuation in  $\text{UPt}_3$  ( $\propto T^2$ ).

from exponential behaviour are found in conventional superconductors containing many magnetic impurities, but the behaviour of the heavy-electron superconductors cannot be explained in this way. In addition, ultrasonic attenuation experiments on  $\text{UBe}_{13}$  (ref. 13) reveal a peak in attenuation just below  $T_c$ , a feature not observed previously in any other superconductor, again suggesting an unconventional form of superconductivity.

The effect of substitutional impurities on the  $T_c$  of superconductors is often informative, because impurities carrying local magnetic moments depress  $T_c$  in conventional superconductors in a way which varies from impurity to impurity in a predictable way. Local moments are, as mentioned above, strongly pair-breaking for s-state superconductors. In  $\text{UBe}_{13}$ , the substitution for U of rare-earth impurities with local moments leads to fairly rapid depressions of  $T_c$ , but there is no observable difference between those rare-earths which carry local moments and those which do not. Lutetium, for example, at a concentration of 3 atom per cent (at. %) in  $\text{UBe}_{13}$  has pushed  $T_c$  to below 20 mK.

Thorium substitution for U is quite peculiar (Fig. 5). Instead of a monotonic depression of  $T_c$  as observed for the rare-earth substitutions in  $\text{UBe}_{13}$ , an initial depression is followed by a plateau or even a slight rise in  $T_c$  at 0.6 K between 2 and 4 at. % Th, after which  $T_c$  again decreases, the specific-heat jump being sizeably reduced by the time the Th concentration reaches 6 at. %. Completely unexpected was the finding that there are actually two consecutive second-order phase transitions of comparable magnitude in the plateau region, the lower-temperature one being at approximately 0.4 K (ref. 15). Experiment shows that these samples remain superconducting below the second transition.

This second transition involves an ultrasonic-attenuation anomaly that is two orders of magnitude larger than the first, superconducting one<sup>16</sup>. The similarity to anomalies observed by this technique at magnetic transitions led these authors to suggest that it might be a spin-density-wave transition. The ordered

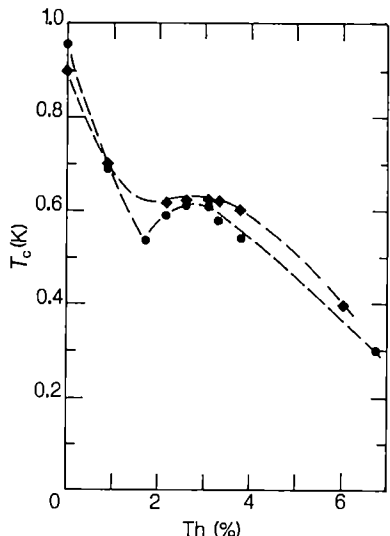


Fig. 5 Influence of small amounts of Th substitution for U in UBe<sub>13</sub> (ref. 15). Non-magnetic impurities in superconductors usually lead to smooth depressions of the critical temperature  $T_c$ . For  $0.02 < x_{\text{Th}} < 0.04$ , a second phase transition occurs at about 0.4 K. Its nature is still not well established. ●,  $T_c$  obtained from magnetic susceptibility; ◆,  $T_c$  obtained from specific heat.

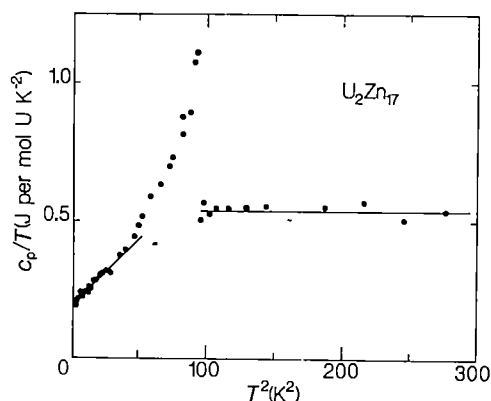


Fig. 6 Electronic specific heat of U<sub>2</sub>Zn<sub>17</sub> at low temperatures. The anomaly is due to the antiferromagnetic ordering. The finite ordinate at  $T=0$  K indicates that 40% of the large electronic density of states is unaffected by the transition.

magnetic moment would be  $\sim 0.01 \mu_B/U$ , consistent with the upper limit set by both NMR and neutron scattering experiments. However, there appears to be no theory at present which can explain how a spin-density wave and superconductivity could co-exist in the same large-mass band.

Another possibility is that the second phase transition is to a second superconducting state. This certainly would require some kind of unconventional superconductivity. The remaining possibility of a simple structural phase transition is unlikely because, by experience, impurities tend to suppress, not enhance, such transitions.

**Magnetism.** We illustrate the occurrence of magnetic order in heavy-electron metals with the example of U<sub>2</sub>Zn<sub>17</sub>. It orders at a transition temperature  $T_N = 9.8$  K into a simple antiferromagnetic structure with an ordered moment of approximately  $0.8 \mu_B$  (ref. 17). This value is considerably smaller than the Curie-Weiss effective moment of  $3.3 \mu_B$ . Just above  $T_N$ ,  $\gamma = 504 \text{ mJ per mol UK}^{-2}$ , falling to a limiting value of  $198 \text{ mJ per mol UK}^{-2}$  as  $T \rightarrow 0$  K as shown in Fig. 6.

The specific-heat anomaly at  $T_N$  shows that the magnetism

involves the heavy electrons. Also note that the residual  $\gamma$  is still very large, indicating that some heavy electrons survive in the magnetically ordered state. The magnetic transition can be thought of as removing 60% of the Fermi surface, and this seems to be a general feature of the other known magnetically ordering heavy-electron systems. These systems resemble itinerant-electron magnets such as chromium, not local-moment magnets. This resemblance is strengthened by the fact that the magnetic order in U<sub>2</sub>Zn<sub>17</sub> is strongly affected by substitution on the Zn sites, completely unlike usual local-moment behaviour and very reminiscent of what is observed in Cr.

### Theoretical understanding

The fascinating and unusual properties of the heavy-electron metals have attracted the attention of many theorists. Their work can be divided into two broad categories: first, attempts to construct a microscopic theory of the normal-state properties, and second, the use of phenomenological models to examine the experimental consequences of, and the tests for, unconventional superconductivity. Several summaries of current theories have recently been published<sup>18-20</sup>.

**Normal state.** The starting point for the microscopic theories is a periodic version of the model hamiltonian introduced many years ago by P. W. Anderson<sup>21</sup>, which serves to describe a single rare-earth or actinide impurity in a conventional metal. There are three parts to this model. One part describes the conduction-electron states derived from s- and p-states as free-electron states and all effects of the Coulomb interaction among these electrons are ignored. In the second part the f-atomic states are described as a set of degenerate energy levels, but because these f-states are spatially localized in the vicinity of the atomic core, the Coulomb interaction between electrons in these states is large and must be included. Consider what will happen if the energy of the degenerate set of f-levels is considerably below the Fermi energy  $E_F$ , but the strong Coulomb interaction prevents the f-states from being completely filled. There are now several ground states of the system, because the partially filled f-level can have more than one configuration. The third and complicating part of the Anderson model is the term which describes so-called hybridization, or electron transfer between the f-states and the conduction states. This hybridization is in general a small term, but it allows the possibility of making transitions within this degenerate (in energy) set of ground states, so that one particular combination becomes the true ground state. This process has been extensively studied for the single-site impurity case, where it is known as the Kondo effect, after J. Kondo, who posed the problem more than twenty years ago<sup>22</sup>. After many years of theoretical work, exact analytic solutions for this case have been obtained. The solution is characterized by a non-degenerate ground state in which the magnetic susceptibility  $\chi$  is finite and the entropy associated with the partially filled f-states vanishes linearly in temperature so that the excess specific heat (associated with the impurity) is  $\sim \gamma T$ . The ratio  $\chi/\gamma$  can be enhanced by up to a factor of 2 from the universal form in equation (1). The mixing between the conduction states and the f-states leads to a very large electrical resistance in the limit as  $T \rightarrow 0$  K.

In the heavy-electron metals the f-state atoms sit on periodic lattice sites and the problem is no longer exactly soluble. Some authors (see refs 18-20) have suggested simply applying what is known about the single-site impurity problem by considering a set of single-site impurities on the lattice. The lattice problem differs from the single-site problem in that coherent states (in solid-state physics terms, Bloch states) can be formed. In other words, the electrons can coherently propagate through the lattice in the same way that wave propagation is possible through coherent diffraction in any periodic set of scatterers. This picture has many attractive features. The coherence of the electronic state causes the resistivity to vanish, thus explaining the low residual resistivity quoted earlier. Secondly the energy scale on

which this coherence occurs would be the single-site Kondo energy, which is determined by the weak hybridization process and is therefore small (typically 10–100 K). Because all the entropy associated with the degeneracies of the f-electron configurations is on the scale of the small Kondo energy, the coefficient  $\gamma$  is much larger than usual and can reach the desired value of  $\sim 1 \text{ J mol}^{-1} \text{ K}^{-2}$ . The magnetic susceptibility is correspondingly large because the opposition to the development of a magnetic moment in the ground state has as its characteristic energy the small Kondo energy.

There are, however, objections to describing these systems as simple collections of single-site Kondo impurities. The description lacks a clear microscopic derivation, and when one tries such a derivation the interaction effects between the sites do not seem to be negligible. An alternative approach is to consider that the essence of the lattice problem is the formation of the coherent Bloch states and that this comes about through the transfer of f-electrons from site to site. However, such transfer processes are severely inhibited by the strong Coulomb intra-site interaction which forbids extra f-electrons on a site. Therefore the only way to obtain f-electron transfer is to remove some f-electrons from the f-levels and place them in the higher energy states near the Fermi energy. This costs energy but it allows coherent hybridization processes to take place, which gain energy. The balance between these two processes leads to a small number of f-electrons being promoted to the higher energy states and a characteristic energy for the coherent state which has a form similar to the single-site Kondo energy. Again  $\chi$  and  $\gamma$  are determined by this small coherent energy and are large, but the ratio  $\chi/\gamma$  may now be larger than the value given by equation (1). A feature common to all approaches is that the large  $\gamma$  values arise from the entropy associated with the degeneracy of the f-configurations or, in other words, the spin degeneracy of the f-states. Another way of describing this feature is that spin fluctuations of the f-electrons are the dominant electronic excitations responsible for the large values of  $\chi$  and  $\gamma$  at low temperatures.

There is another possible ground state for the lattice problem, namely a state with integral f-electron atomic configurations and ordered local moments on the f-sites. The energy comparison between such a state and the heavy-electron state is an open theoretical question and until it is solved no theoretical predictions can be made as to which of these intermetallic compounds are the more usual antiferromagnetic metals and which are heavy-electron metals.

**Superconductivity.** There is one condensed-matter system with strong spin fluctuations and a superfluid state: this is liquid  $^3\text{He}$ . (Note that  $^3\text{He}$  atoms have spin-1/2 and are fermions, whereas  $^4\text{He}$  atoms have spin 0 and are bosons. The  $^3\text{He}$  ground state is called superfluid rather than superconducting simply because  $^3\text{He}$  atoms are neutral.) Liquid  $^3\text{He}$  solidifies at a modest pressure, so that in the liquid state the  $^3\text{He}$  atoms are almost localized and therefore can flip their spins easily. In  $^3\text{He}$  the superfluid state is known to be an anisotropic p-state (that is, the Cooper pairs of  $^3\text{He}$  atoms responsible for the superfluid state are in a relative p-state). It has been shown theoretically that the interactions mediated through spin fluctuations favour p-state superfluidity<sup>23</sup>. Also a relative p-state means a much reduced overlap between the fermions and so is favoured when there is a very strong short-range repulsion as is the case for  $^3\text{He}$  atoms. The analogy has been made by many authors on both grounds (that is, strong spin fluctuations and strong short-range repulsion) for the heavy-electron systems. In normal metals there is an attractive interaction, mediated by the exchange of phonons, between electrons in states within a Debye energy,  $k_B\theta_D$ , of the Fermi energy, where  $\theta_D$  is the Debye temperature. The repulsive Coulomb interaction is reduced for these states because of the mismatch of the energy scale of the Coulomb energy, which is  $E_F$  and  $k_B\theta_D$ . Typically  $k_B\theta_D/E_F = 10^{-2}$ , but in the heavy-electron metals  $k_B\theta_D \geq E_F$  so there is no mismatch. Nevertheless

some authors continue to argue for the dominance of phonon-mediated interactions, and therefore for an isotropic or relative s-state pairing. The microscopic theory of the electron pairing necessary to obtain superconductivity in these systems is as yet only qualitative.

Much effort has been put into obtaining a proper description of p-state superconductivity in these crystalline materials which also have important spin-orbit interactions. By the use of group-theoretical techniques the allowed forms can be correctly specified, and there are many possible states which differ in the detailed form of the energy gap which is associated with the electron pairing. In usual s-state pairing the gap is simply isotropic in  $\mathbf{k}$ -space and the electrons are in a relative spin-singlet state. However the global antisymmetry of fermions requires non-trivial structure for the gap in other pairing states where electrons are in spin-parallel or triplet states. As a result, in many of these states, the energy gap vanishes along specific directions in  $\mathbf{k}$ -space.

Clearly the very-low-energy excitations in superconductors with isotropic gaps will differ from those in superconductors with anisotropic gaps which vanish in certain directions. In the former, properties such as specific heat are exponential as  $T \rightarrow 0 \text{ K}$ , whereas in the latter they exhibit power-law behaviour (as shown in Fig. 4) as  $T \rightarrow 0 \text{ K}$ . The observation of such power-law behaviour, as discussed above (Fig. 4), is taken by many as evidence for anisotropic superconductivity. Unfortunately we lack a decisive way to determine the detailed symmetry of the superconducting state: the equivalent of X-ray and neutron scattering for lattice and magnetic transitions does not exist here. Therefore we must proceed by inference, which can lead, and indeed has led, to differing interpretations.

## Conclusions

It is clear from the above that the heavy-electron metals represent an exciting new class of materials. They do not fit into the traditional classifications of materials with partially filled atomic shells; namely, metals, semiconductors or Mott insulators. At high temperatures they are essentially indistinguishable from a host of other rare-earth or actinide intermetallic compounds with local moments arising from the partially filled f-shells. But as the temperature is lowered, instead of forming magnetically ordered structures as is usually the case, these materials unexpectedly form an itinerant or delocalized metallic state. The electrons in this state have a much compressed energy scale and correspondingly high effective mass. The theoretical understanding of how such a state arises out of the f-electrons with their strong Coulomb interactions is today a very active problem and will undoubtedly lead to new insights into the general many-body problem. In particular we would like to know what the material parameters are which determine whether, and under what conditions, a material exhibits this heavy-electron state; we would also like to understand the nature of the residual interactions which characterize this metallic state. It is clear from the discussion above that the heavy-electron metallic state can display the phase transitions seen in many other traditional metals; namely, superconductivity (as in  $\text{UBe}_{13}$ ) and weak (or itinerant) magnetism (as in  $\text{U}_2\text{Zn}_{17}$ ). But, as we have stressed, there are many intriguing signs that the superconductivity is not simply the usual isotropic (or s-state) kind. As we have also stressed, this anisotropic superconductivity is expected theoretically when the mechanism responsible for the superconductivity is not the usual electron-phonon interaction. Thus it appears that at last such superconductivity has been found in metals. The confirmation of a second mechanism for superconductivity will spur the search for yet other mechanisms. One of the motivations in this long search was the hope that by achieving superconductivity through unconventional mechanisms, new and possibly higher energy scales would apply, leading to higher values of  $T_c$ . This has not yet been obtained, but two important areas must continue to be explored. Materials scientists must

## ARTICLES

continue the search for a higher  $T_c$ , while theorists strive for an improved understanding of the factors which determine and limit  $T_c$ . Even modest rises in  $T_c$  in these materials might have important technical consequences in the generation of very high magnetic fields, as their superconducting state is extremely stable with respect to magnetic field intensity.

1. Stewart, G. R. *Rev. mod. Phys.* **56**, 755–787 (1984).
2. Andres, K., Graebner, J. E. & Ott, H. R. *Phys. Rev. Lett.* **35**, 1779–1782 (1975).
3. Steglich, F. et al. *Phys. Rev. Lett.* **43**, 1892–1896 (1979).
4. Ott, H. R., Rudiger, H., Fisk, Z. & Smith, J. L. *Phys. Rev. Lett.* **50**, 1595–1598 (1983).
5. Ott, H. R., Rudiger, H., Delsing, P. & Fisk, Z. *Phys. Rev. Lett.* **52**, 1551–1554 (1984).
6. Stewart, G. R., Fisk, Z., Willis, J. O. & Smith, J. L. *Phys. Rev. Lett.* **52**, 679–682 (1984).
7. Maple, M. B. & Fischer, Ø. (eds) *Superconductivity in Ternary Compounds II* (Springer, Berlin, 1982).
8. Bardeen, J., Cooper, L. N. & Schrieffer, J. R. *Phys. Rev.* **108**, 1175–1204 (1957).
9. Leggett, A. J. *Rev. mod. Phys.* **47**, 331–414 (1975).
10. Ott, H. R. et al. *Phys. Rev. Lett.* **52**, 1915–1918 (1984).
11. Bishop, D. J. et al. *Phys. Rev. Lett.* **53**, 1009–1011 (1984).
12. MacLaughlin, D. E. et al. *Phys. Rev. Lett.* **53**, 1833–1836 (1984).
13. Golding, B. et al. *Phys. Rev. Lett.* **55**, 2479–2482 (1985).
14. Maple, M. B. et al. *Phys. Rev. Lett.* **54**, 477–480 (1985).
15. Ott, H. R., Rudiger, H., Fisk, Z. & Smith, J. L. *Phys. Rev. B* **31**, 1651–1652 (1985).
16. Batlogg, B. et al. *Phys. Rev. Lett.* **55**, 1319–1323 (1985).
17. Cox, D. E. et al. *Phys. Rev. B* (in the press).
18. Varma, C. M. *Comments Solid St. Phys.* **11**, 221–240 (1985).
19. Kasuya, T. & T. Saso (eds) *Theory of Heavy Fermions and Valence Fluctuations* Proc. 8th Taniguchi Symp. (Springer, Berlin, 1985).
20. Lee, P. A., Rice, T. M., Serene, J. W., Sham, L. J. & Wilkins, J. W. *Comments. Con. Matter Phys.* **12**, 99–130 (1986).
21. Anderson, P. W. *Phys. Rev.* **124**, 41–53 (1961).
22. Tsvetkov, A. M. & Wiegmann, P. B. *Adv. Phys.* **32**, 453–713 (1983).
23. Anderson, P. W. & Brinkman, W. F. *Phys. Rev. Lett.* **30**, 1108–1111 (1973).

## ARTICLES

## Molecular stratigraphy: a new tool for climatic assessment

S. C. Brassell\*, G. Eglinton\*, I. T. Marlowe\*, U. Pflaumann† & M. Sarntheim\*

\* Organic Geochemistry Unit, University of Bristol, School of Chemistry, Cantock's Close, Bristol BS8 1TS, UK  
 † Geologisch-Paläontologisches Institut und Museum, Universität Kiel, Olshausenstrasse 40/60, D-2300 Kiel, FRG

*Variations in sea-surface temperatures over the past 500,000 years are inferred from the relative abundance behaviour of two organic compounds,  $C_{37}$  alkenones over the upper 8 metres of a sediment core from the eastern equatorial Atlantic. This molecular record, ascribed to contributions from prymnesiophyte algae, correlates well with the variations in the  $\delta^{18}\text{O}$  signal for the calcareous skeletons of certain planktonic foraminifera, thus providing the first demonstration of a new stratigraphical technique, which may be especially valuable where methods based on carbonate  $\delta^{18}\text{O}$  fail.*

THE ubiquitous unicellular marine coccolithophorid *Emiliania huxleyi* (Prymnesiophyceae)<sup>1</sup> contains long-chain ( $C_{37}$ – $C_{39}$ ) di-, tri- and tetra-unsaturated methyl and ethyl ketones (alkenones)<sup>2–4</sup> whose unsaturation changes with growth temperature in laboratory cultures<sup>5</sup>. These compounds also occur in contemporary bottom sediments<sup>6,7</sup>, presumably derived from phytoplankton in the photic zone of the overlying water column<sup>8</sup>. Differences in the alkenone unsaturation of contemporary sediments from two different climatic regimes<sup>9</sup> suggest that this feature might reflect, and thereby provide a measure of, water temperatures in the euphotic zone<sup>10</sup>. Accordingly, the distribution of alkenones in many Quaternary marine sediments from various latitudes of different mean sea-surface temperatures (SST) has been examined. We now report the alkenone unsaturation in a gravity core from the eastern equatorial Atlantic ocean, covering the past million years, and compare this record with that of the  $\delta^{18}\text{O}$  of planktonic foraminifera, an established indicator of a combination of global ice sheet variations and local SST in the euphotic zone<sup>11,12</sup>.

### Organic compounds

Improved chromatographic and spectrometric methods for the analysis of complex mixtures have greatly extended the number and variety of organic compounds identified in geological materials<sup>13</sup> and have aided the better understanding of their origins and sedimentary fate<sup>13,14</sup>. Often, such marker compounds in bottom sediments can be directly related to their source organisms<sup>14</sup>; a record that can survive passage through food web processes<sup>8</sup> and, subsequently, consolidation and the effects

of diagenesis<sup>15</sup>. Such signals best escape disturbance by post-depositional heterotrophic (notably microbial) activity<sup>16</sup> in areas of high sediment accumulation rates and low geothermal gradient<sup>15</sup>, as in the deep sea.

The search for organic compounds that are diagnostic of their biological origins in marine sediments<sup>17</sup> and sediment traps<sup>18</sup> has led to the recognition of specific lipid markers for many different types of organisms, including algae such as dinoflagellates<sup>19,20</sup>, bacteria, notably methanogens<sup>21</sup>, and terrestrial higher plants, such as conifers<sup>22</sup>. In addition, there is the possibility that their distribution patterns may depend on growth conditions; indeed, aquatic organisms can biosynthetically tailor their lipid composition to match environmental conditions of stress<sup>23</sup>. Specifically, they maintain the fluidity of their membranes by changing the molecular composition of the lipid bilayer, either in chain length or in unsaturation<sup>23</sup>. Laboratory culturing experiments show changes in lipid unsaturation, notably for carboxylic acids<sup>24</sup> and wax esters<sup>25</sup>, in response to temperature variations. These observations are likely to reflect the behaviour of phytoplankton populations in the natural environment, which may also be preserved in the underlying sedimentary record.

### Long-chain alkenones

The less labile constituents of marine phytoplankton include series of long-chain ( $n\text{-}C_{37}$  to  $n\text{-}C_{39}$ ) alkenones<sup>2,7</sup> which appear to be restricted to a few species of the class Prymnesiophyceae, notably coccolithophorids<sup>3,4</sup> of the family Gephyrocapsaceae. The unsaturation of such compounds shows a temperature dependence (more at lower temperatures) in laboratory cultur-

Table 1 Alkenone unsaturation index ( $U_{37}^K$ ) values for Quaternary marine sediments and for sediment trap material

Site*	Location	Codes	Samples	No.	$U_{37}^K$	Ref.
<b>Sediments</b>						
A	North Sea	IGS SLN33, SP333CS		2	0.40–0.51	2
B	Porcupine Seabight	D51704		1	0.54	6†
C	Japan Trench	DSDP 440		4	0.51–0.55	2, 47†
D	Ionian Sea	10103		5	0.44–0.79	52
E	Cretan Basin	DSDP 378		1	0.66	53
F	Messina Abyssal Plain	DSDP 374		1	0.47	53
G	San Miguel Gap	DSDP 467		1	0.58	54
H	Orca Basin	DSDP 618		1	0.84	†
I	Gulf of California	DSDP 479, 481		3	0.86–0.95	†
J	Middle America Trench	DSDP 487, 491, 493		5	0.78–0.98	9†
K	Middle America Trench	DSDP 494, 495, 496		3	0.84–0.92	†
L	Cariaco Trench	DSDP 147		1	0.89	†
M	Kane Gap	M16415-2		72	0.76–0.94	This paper
N	Sierra Leone Rise	M13519		3	0.88–0.97	†
O	Peruvian Shelf	110		1	0.87	55
P	Peruvian Shelf	BC7		5	0.23–0.70	44
Q	Walvis Ridge	DSDP 532		1	0.56	17
R	Walvis Bay	IOS 1/75		2	0.52	2
S	Corner Inlet	—		1	0.56	56
T	South Atlantic	DSDP 513		1	0.33	†
<b>Sediment traps</b>						
P	Peruvian Shelf	—		8	0.26–0.56	43

Codes refer to sample sites (DSDP 440 denotes Deep Sea Drilling Project Site 440) as specified in the refs.  $U_{37}^K$  denotes the alkenone unsaturation index. The terminology [ $U$  = unsaturation,  $K$  = ketone (alkenone), 37 = chain length of ketone] will allow for future use with different molecular parameters.

$$U_{37}^K = \frac{[C_{37:2}] - [C_{37:4}]}{[C_{37:2} + C_{37:3} + C_{37:4}]}$$

where, for example,  $C_{37:2}$  represents the quantity of the  $C_{37}$  alkadienone, as measured by GC peak integration.  $U_{37}^K$  can have values between −1.0 (all  $C_{37:4}$ ) and +1.0 (all  $C_{37:2}$ ), but varies between +0.23 and +0.98 in Quaternary marine sediments, and between −0.2 and +1.0 for marine sediments of Albian to Holocene age<sup>6,28</sup>.

\* Letters A to T relate to sample latitudes shown in Fig. 1.

† I.T.M., S.C.B. and G.E., unpublished data.

ing experiments with *E. huxleyi* and *Isochrysis galbana*<sup>5</sup>. The distribution patterns of these compounds appear largely unaltered by food web processes, surviving digestion by copepods<sup>8</sup> and mussels<sup>26</sup>. Alkenones are easily recovered from sediments by routine extraction procedures and can be readily recognized at subnanogram levels by capillary gas chromatography (GC) and gas chromatography/mass spectrometry (GC/MS)<sup>2,6</sup>.

Since their first description<sup>27</sup>, these alkenones have been found in numerous Quaternary marine sediments<sup>6,7</sup> (Table 1), although they vary in their unsaturation. Here, this variation is expressed as an alkenone unsaturation index,  $U_{37}^K$  (Table 1), defined as:

$$U_{37}^K = [C_{37:2}] - [C_{37:4}] / [C_{37:2} + C_{37:3} + C_{37:4}]$$

For most sediments the absence of  $C_{37:4}$  simplifies  $U_{37}^K$  to  $[C_{37:2}] / [C_{37:2} + C_{37:3}]$  which varies inversely with unsaturation. Replicate GC analyses suggest that  $U_{37}^K$  values are accurate to ±0.02. In Quaternary marine sediments (Table 1), the greater values for  $U_{37}^K$ , which we interpret as corresponding to higher water temperatures, are seen in low latitudes, and the lowest values for  $U_{37}^K$  are those for the highest latitudes (Fig. 1). This broad relationship suggests mutual trends due to the inherent global and regional variations in SST resulting from oceanic circulation features, such as gyres and upwelling of cooler intermediate water masses in subtropical latitudes. The overall correspondence, however, suggests that alkenone unsaturation in oceanic bottom sediments is an indirect measure of SST. The same series of alkenones has also been recognized in sediments of Pliocene, Miocene, Oligocene and Eocene age<sup>6,7</sup> and, recently, in Cretaceous black shales<sup>28</sup>.

## Kane Gap sediments

The direct assessment of water temperatures (and hence palaeoclimates) from molecular data requires testing by relating  $U_{37}^K$  to an established technique, namely the oxygen isotope ( $\delta^{18}\text{O}$ ) signal for the carbonate tests of foraminifera. Herein, the correlation between the alkenone distributions (as  $U_{37}^K$  values) and  $\delta^{18}\text{O}$  ( $\text{CaCO}_3$ ) values for both planktonic and benthic foraminifera, is explored for a 13-m sediment core from near the Kane Gap, eastern equatorial Atlantic (Fig. 2). The core (M16415-2), collected during *Meteor* cruise 65 in 1983 (ref. 29), possessed many features appropriate for this study. First, it provided an almost complete record of glacial/interglacial cycles over the past million years. Second, examination of a gravity core (M13519) from the nearby Sierra Leone Rise<sup>30</sup> (Table 1; Fig. 2) revealed sufficient quantities of alkenones to permit their evaluation by GC (Fig. 3) in 2–3-cm sections of sediment cores from this region. Third, the oxygen isotope records of the planktonic and benthic foraminifera were determined, using a new MAT 251 instrument capable, for the first time, of measuring single specimens (one or two), using modified standard procedures<sup>12,31</sup> from throughout the sequence, except where precluded by carbonate dissolution. When combined with magnetic stratigraphy, oxygen isotope stratigraphy provides a high-resolution timescale for the past 3 Myr, correlated on a global scale<sup>32,33</sup>.

The down-core variations in oxygen isotope compositions of the three species of foraminifera and in alkenone unsaturation (Fig. 4) show generally similar trends for the glacial/interglacial

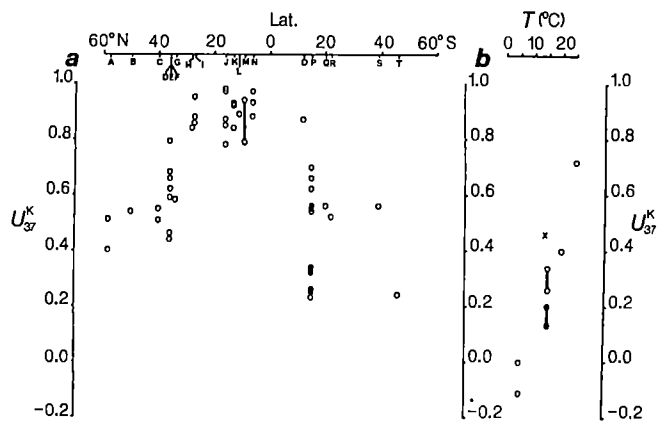


**Fig. 1** Alkenone unsaturation index ( $U_{37}^K$ ) values (Table 1) for: *a*, Quaternary marine sediments at sites A to T (○) and sediment traps (●) plotted against latitude; and *b*, laboratory cultures of *E. huxleyi*<sup>5</sup> strain 92 (○) and strain 92d (●) and a plankton tow (×) off Cape Finisterre, plotted against water temperature. The vertical bars indicate where numerous samples fall within that particular range of values of  $U_{37}^K$ . The sediment trap data in *a*, which display a considerable range of values, would become a single, time-averaged value on sedimentation.

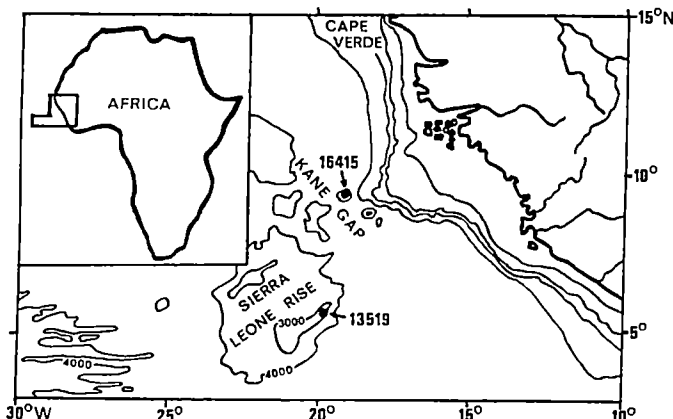


**Fig. 2** Locations of Meteor site M13519 on the Sierra Leone Rise and site M16415 in the Kane Gap (partly redrawn from ref. 28). Water depths are in metres.

stages, that is, higher values of  $\delta^{18}\text{O}$ , corresponding to cooler glacial episodes, are observed at those horizons with lower values of  $U_{37}^K$ , and vice versa. The coccolithophorids held to be the principal organisms biosynthesizing the alkenones in the oceans inhabit the upper 150 m of the water column<sup>34</sup>, although they can occur at greater depths<sup>35</sup>. Thus, the  $\delta^{18}\text{O}$  record for the planktonic foraminifera *Globigerinoides sacculifer* and *Globigerinoides ruber* should parallel that of alkenone unsaturation. These species occur in tropical warm waters where the  $\delta^{18}\text{O}$  values for their carbonate tests reflect ice volumes and local SST<sup>30</sup>, with the former more significant. By contrast, the benthic foraminifer, *Cibidelloides wuellerstorfi*, inhabits deeper water masses and its  $\delta^{18}\text{O}$  principally reflects the waxing and waning of ice sheets rather than sea temperatures<sup>30</sup>; it is therefore less relevant to  $U_{37}^K$  than the planktonic foraminifera. Furthermore, its sampling intervals are greater and the effects of its ecological disappearance are more pronounced, being significant as recent as Stage 6 (Fig. 4). Similarly,  $\delta^{18}\text{O}$  data for *G. ruber* are less complete than those for *G. sacculifer*, chosen for detailed comparison with the alkenone unsaturation.

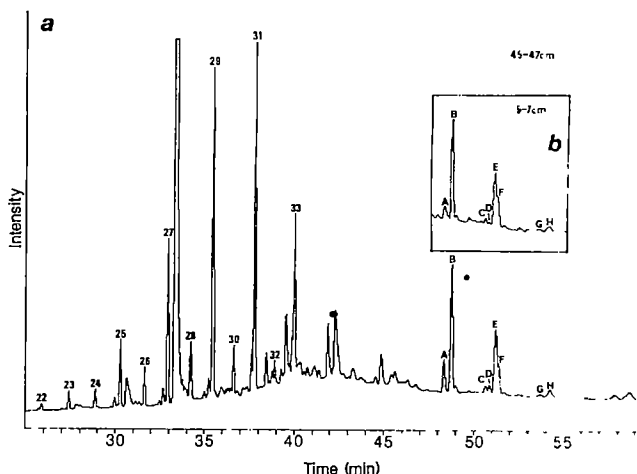


**Fig. 3** *a*, Gas chromatogram of total extract ( $\text{CH}_3\text{OH}$ , then  $\text{CH}_2\text{Cl}_2/\text{CH}_3\text{OH}$  with sonication) of sample collected at 45–47 cm depth interval from core M16415-2 recovered from the Kane Gap (Fig. 2). Numbered peaks are *n*-alkanes; the number indicates the chain length; those designated A–H are alkenones<sup>2–7</sup>. A, Heptatriaconta-8,15,22-trien-2-one[ $\text{CH}_3(\text{CH}_2)_{13}\text{CH}=\text{CH}(\text{CH}_2)_5\text{CH}=\text{CH}(\text{CH}_2)_5\text{CH}=\text{COCH}_3$ ]; B, heptatriaconta-15,22-dien-2-one[ $\text{CH}_3(\text{CH}_2)_{20}\text{CH}=\text{CH}(\text{CH}_2)_5\text{CH}=\text{CH}(\text{CH}_2)_5\text{COCH}_3$ ]; C, octatriaconta-9,16,23-trien-3-one; D, octatriaconta-9,16,23-trien-2-one; E, octatriaconta-16,23-dien-3-one; F, octatriaconta-16,23-dien-2-one; G, nonatriaconta-10,17,24-trien-3-one; H, nonatriaconta-17,24-dien-3-one. The relative proportions of  $\text{C}_{37:3}$  and  $\text{C}_{37:2}$  alkenones (peaks A and B, respectively) are typical of the lower  $U_{37}^K$  values (0.78) for core M16415-2. *b*, Partial gas chromatogram of total extract of 5–7 cm depth interval from core M16415-2, illustrative of the higher  $U_{37}^K$  values (0.89) determined in this study. GC conditions: Carlo Erba 4160 instrument with on-column injection, fitted with 50-m CPSil 5CB flexible silica WCOT capillary column, temperature programmed from 60 to 300 °C at 6 °C min<sup>-1</sup>.  $U_{37}^K$  values were calculated from the peak areas of A and B, determined using a VG Minichrom data system. Compound identifications were confirmed by GC/MS (Carlo Erba Mega chromatograph equipped with 25-m OV-1 flexible silica column, programmed as above, and coupled to a Finnigan 4000 mass spectrometer). Data acquisition by INCOS 2300 data system, scanning  $m/z$  50–600 at 1-s intervals.

$\delta^{18}\text{O}$  for *G. sacculifer* and  $U_{37}^K$  correlate well ( $r = 0.932$ ; Fig. 5*a*) to almost 2 m and are broadly parallel ( $r = 0.676$ ; Fig. 5*b*) to 8 m. Below 8 m they show little agreement. The discrepancies in Fig. 4 may stem from the low sampling frequency due to  $\text{CaCO}_3$  dissolution, from bioturbation and core disturbance, or from the different intervals of  $\delta^{18}\text{O}$  and alkenone determinations. The excellent correlation between  $\delta^{18}\text{O}$  for *G. sacculifer* and  $U_{37}^K$  for the upper 2 m is striking, and includes the temperature profile characteristic of a gradual cooling and subsequent rapid warming over the interglacial/glacial cycle<sup>11,30,36</sup> of the past 120,000 yr. A general correspondence between the two data sets holds to 8 m, that is the past 550,000 yr. Such similarity of  $\delta^{18}\text{O}$  and  $U_{37}^K$  data suggests a common causality, namely the systematic variations in the Earth's orbit, described by Milankovitch's theory<sup>36,37</sup>. Such orbital changes affect global ice volumes and the temperature of oceanic water masses, which are both reflected in the oxygen isotope composition of planktonic foraminifera, such as *G. sacculifer*, whereas the alkenones produced by phytoplankton should reflect SST, but not any direct effects due to changes in global ice volumes. Fluctuations in alkenone unsaturation should therefore, be an indirect manifestation of the Earth's orbital cycles<sup>33,38</sup>. The discrepancies in the  $U_{37}^K$  and  $\delta^{18}\text{O}$  profiles raise the intriguing prospect that interpretation of their combination may constitute a general method for assessing the relative contributions of ice

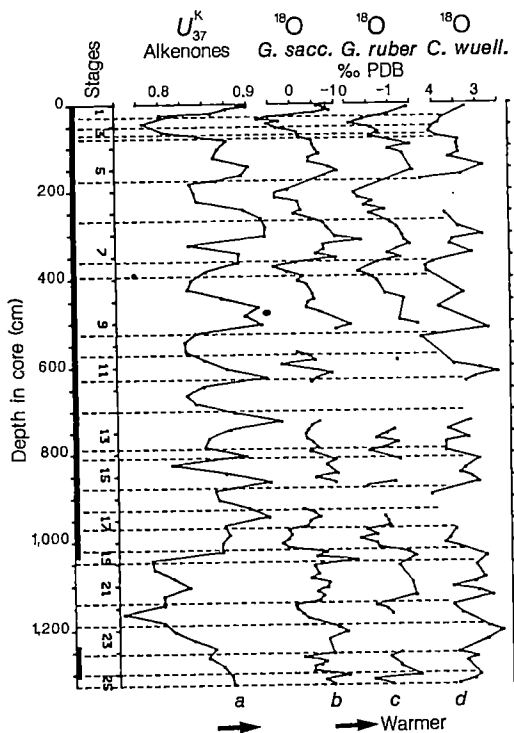


**Fig. 4** Downhole plots of the direct measures of alkenone unsaturation index ( $U_{37}^K$ ) for sediment extracts and of  $\delta^{18}\text{O}$  values for foraminifera in Meteor core 16415-2. *a*, Alkenone unsaturation index ( $U_{37}^K$ ; Table 1). *b-d*,  $\delta^{18}\text{O}$  values of  $\text{CaCO}_3$  of foraminifera: planktonic *G. sacculifer* and *G. ruber* and benthic *C. wuellerstorfi*. Gaps between the  $\delta^{18}\text{O}$  data indicate complete dissolution of  $\text{CaCO}_3$ . The sampling intervals for *d* are greater than those for *a*, *b* and *c*. The oxygen isotope stages<sup>30</sup> are indicated by numbers between the ordinates and their boundaries are designated by broken lines (Stage 3 is probably reduced due to an hiatus). The magnetic stratigraphy (thickening of ordinate) for the core is that determined by U. Bleil (personal communication). The general trends reflecting cooler and warmer temperatures are indicated.

volume and SST within the oxygen isotope signal. Indeed, the direct correspondence between  $U_{37}^K$  and  $\delta^{18}\text{O}$  values to 2 m suggests that  $\delta^{18}\text{O}$  values may reflect SST more closely than originally thought—at least in this part of the ocean.

The behaviour pattern of  $U_{37}^K$  below 8 m (down to 1 Myr BP) differs significantly from that above 8 m. Diagenetic alteration of alkenone distributions and/or changes in the processes affecting alkenone degradation before burial, are unlikely to be responsible; a transition in the source organisms of the alkenones seems more probable. Such factors cannot be distinguished at present, but a possible source species<sup>39</sup>, the coccolithophorid *Pseudoemiliania lacunosa*, became globally extinct at a time<sup>40,41</sup> corresponding to a depth of ~6.5 m within this core, and *E. huxleyi* first appeared <270,000 yr BP (at ~4 m)<sup>41</sup>. Some ancestor/predecessor species of *E. huxleyi*, such as *Gephyrocapsa marginata*<sup>40</sup>, must show similar alkenone compositional behaviour back to at least 550,000 yr BP (that is, 8 m). If variations in alkenone unsaturation are indeed related to membrane fluidity and hence temperature, then this behaviour should be a general feature of such organisms. The extent of alkenone unsaturation of different species, however, need not be uniform at a given temperature.

### $U_{37}^K$ temperature calibration

The molecular record of SST requires a defined link between the alkenone unsaturation index for relevant organisms and that for bottom sediments. There is a need to evaluate  $U_{37}^K$  for natural

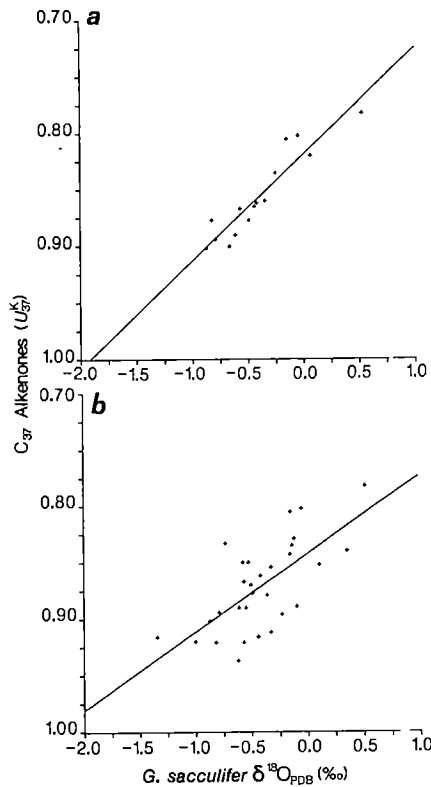


**Fig. 5** Regression plots of the alkenone unsaturation index ( $U_{37}^K$ ) for sediment extracts against  $\delta^{18}\text{O}$  for the carbonate of *G. sacculifer*. *a*, Interpolated data for 5–185 cm depth in Meteor core M16415-2;  $r = 0.932$ . *b*, Original data, 0–800 cm depth in Meteor core M16415-2;  $r = 0.676$ .

populations of phytoplankton, principally coccolithophorids such as *E. huxleyi*, collected from present-day oceanic water masses of known temperature at depths comparable to those where appropriate planktonic foraminifera produce their tests, and at times of maximum primary productivity. In the eastern equatorial Atlantic, the standing crop of *E. huxleyi* is probably highest during the winter months, by analogy with waters around Bermuda<sup>42</sup>. A plankton tow taken off Cape Finisterre (43°11' N, 09°33' W) in early July, from waters of 14 °C containing *E. huxleyi* and *Coccolithus pelagicus*, yielded small amounts of alkenones with a  $U_{37}^K$  of 0.46 (Fig. 1); a value comparable to those of sediments from similar latitudes. A broader base of alkenone data, however, exists for laboratory cultures of *E. huxleyi* grown at several temperatures<sup>5</sup> (Fig. 1), although these show discrepancies compared with those for sediments. For example, tetra-unsaturated alkenones (alkatetraenones) occur in the cultured algae<sup>4,6</sup> at all temperatures<sup>5</sup>, but are rarely detected in oceanic sediments<sup>6</sup>, even when  $U_{37}^K$  is <0.4 (Table 1). Indeed,  $U_{37}^K$  values of *E. huxleyi* grown at a given temperature are lower (Fig. 1) than those of sediments deposited beneath waters of similar temperature. However, the strains of *E. huxleyi* in culture were collected originally from the south-west approaches to the English Channel (~50° N; J. C. Green, personal communication) and their tolerance to higher growth temperatures (20 or 25 °C) may be limited. The influence of sedimentation processes on  $U_{37}^K$  values, where zooplankton faecal pellets may facilitate rapid transportation of alkenones to bottom sediments<sup>8</sup>, has not been tested. The amounts of alkenones in the plankton tow off Cape Finisterre suggest that they may have been derived, in part, from semi-digested phytoplankton in the guts of zooplankton within this sample (I.T.M., S.C.B. and G.E., unpublished data). Certainly, the range of  $U_{37}^K$  values in sediment traps from Peru<sup>43</sup> (Table 1; Fig. 1) requires

explanation, and the low  $U_{37}^K$  value for the surface sediment in this locality<sup>44</sup> is also unexpected. The sedimentary record, however, represents a time-averaged signal, so that short-term fluctuations and extremes in  $U_{37}^K$  values may make little ultimate impact.

The  $U_{37}^K$  values of sediments from the Kane Gap (Fig. 4) where SST remain at  $\sim 26^\circ\text{C}$  throughout the year<sup>45,46</sup> are greater than those of *E. huxleyi*<sup>5</sup> grown at temperatures up to  $25^\circ\text{C}$  in the laboratory. For M16415-2 the extreme values of  $U_{37}^K$  differ by 0.18 over the entire core sequence and by 0.12 over the last warming episode, that is, Termination I. Laboratory cultures of *E. huxleyi* (Fig. 1) indicate that the latter value corresponds to a temperature change of  $2-5^\circ\text{C}$ . Despite the obvious uncertainties in such calibration based on culture experiments this value is comparable to the  $4^\circ\text{C}$  reported for Termination I, based on February SST values for 18,000 yr BP and for the present day, estimated from foraminiferal assemblages<sup>45</sup>.

Additional influences on  $U_{37}^K$  values will include the geological and evolutionary succession of species<sup>40,41</sup> that contributed alkenones to sediments<sup>39</sup>. Clearly, species-related effects on the distributions of alkenones need to be assessed, yet their biosynthesis is likely to be more conservative than the morphology of the algae. Diagenetic effects may also affect the  $U_{37}^K$  record, but the notable absence of mono-unsaturated homologues in all sediments that contain alkenones suggests that chemical reduction of alkenones does not occur, and argues against any effects on  $U_{37}^K$  stemming from diagenetic conversion of alkatrienones into alkadienones.

## Molecular geochemical indicators

Future applications of molecular geochemical indicators of water temperatures will include evaluation of sediment sequences deposited below the calcite compensation depth (CCD), where planktonic foraminiferal tests are not preserved. In core

M16415-2, alkenone data cover intervals lacking such tests, due to dissolution, for example, in Stage 12 (Fig. 4). In addition, alkenones occur as abundant constituents of diatomaceous oozes from the Japan Trench (Table 1) deposited below the CCD<sup>2,47,48</sup> and, consequently, bereft of calcareous foraminiferal tests. The alkenone unsaturation index may be a uniquely useful stratigraphical tool in such instances. Alkenones have also been detected in lacustrine sediments<sup>49</sup>, with  $U_{37}^K$  values of +0.16 to -0.58, and could therefore serve as palaeoclimatic indicators in such environments. Future improvements in alkenone detection limits will reduce sample sizes and thereby increase stratigraphical resolution—although this, inevitably, is limited by the extent of bioturbation.

The alkenones are independent of isotopic factors, although subject to effects related to biochemical evolution and diagenesis. They are a single type of organic compound among the thousands known to occur in sediments<sup>13,14</sup>. We anticipate that  $U_{37}^K$  is the forerunner of a substantial number of molecular parameters<sup>50</sup> for assessment of environmental conditions of sediment deposition<sup>51</sup>. To this end, we are now exploring correlations between molecular and other data using principal-component and spectral analysis and are investigating evidence for Milankovitch cycles in sedimentary alkenone data<sup>50</sup>.

We thank the NERC (GR3/2951 and GR3/3758) for support and a studentship (I.T.M.), and the Royal Society for funds towards the VG Minichrom system. We thank Dr J. C. Green (MBA, Plymouth) for collaboration with studies of alkenones in living algae and Dr H. Erlenkeuser (Kiel University  $^{14}\text{C}$  laboratory) for access to new preparation facilities of a MAT 251 mass spectrometer for measurements of foraminiferal  $\delta^{18}\text{O}$ . Professor U. Bleil (Bochum) provided unpublished magnetostratigraphy for core M16415-2. We also thank Drs R. G. Brereton and J. Grimalt for helpful discussions during the final preparation of this paper and other colleagues at Bristol for access to unpublished data.

Received 14 August; accepted 30 December 1985.

1. Hay, W. W. & Mohler, H. P. *Trans. Gulf-Coast Ass. geol. Soc.* (eds Hay, W. W. et al.) 17, 426-480 (1967).
2. Volkman, J. K., Eglington, G., Corner, E. D. S. & Sargent, J. R. in *Advances in Organic Geochemistry 1979* (eds Douglas, A. G. & Maxwell, J. R.) 219-227 (Pergamon, Oxford, 1980).
3. Volkman, J. K., Eglington, G., Corner, E. D. S. & Forsberg, T. E. V. *Phytochemistry* 19, 2619-2622 (1980).
4. Marlowe, I. T. et al. *Br. phycol. J.* 19, 203-216 (1984).
5. Marlowe, I. T., Green, J. C., Brassell, S. C., Eglington, G. & Course, P. A. *Phytochemistry* (submitted).
6. Marlowe, I. T., Brassell, S. C., Eglington, G. & Green, J. C. *Org. Geochem.* 6, 135-141 (1984).
7. de Leeuw, J. W., van der Meer, F. W. & Rijpstra, W. I. C. in *Advances in Organic Geochemistry 1979* (eds Douglas, A. G. & Maxwell, J. R.) 211-217 (Pergamon, Oxford, 1980).
8. Volkman, J. K., Corner, E. D. S. & Eglington, G. in *Colloq. int. CNRS no. 293* (ed. Daumas, R.) 185-197 (Editions CNRS, Paris, 1980).
9. Brassell, S. C., Eglington, G. & Maxwell, J. R. *Init. Rep. DSDP* 66, 557-580 (1981).
10. Brassell, S. C. & Eglington, G. in *Heterotrophic Activity in the Sea* (eds Hobbie, J. E. & Williams, P. J. leB.) 481-503 (Plenum, New York, 1984).
11. Shackleton, N. J. & Opdyke, N. D. *Quat. Res.* 3, 39-55 (1973).
12. Duplessy, J. C. in *Climatic Change* (ed. Gribbin, J.) 46-67 (Cambridge University Press, 1978).
13. Mackenzie, A. S., Brassell, S. C., Eglington, G. & Maxwell, J. R. *Science* 217, 491-504 (1982).
14. Brassell, S. C., Eglington, G. & Maxwell, J. R. *Biochem. Soc. Trans.* 11, 575-586 (1983).
15. Brassell, S. C. & Eglington, G. in *Advances in Organic Geochemistry 1981* (eds Björk, M. et al.) 684-697 (Wiley, New York, 1983).
16. Boon, J. J., de Leeuw, J. W. & Schenck, P. A. *Geochim. cosmochim. Acta* 39, 1559-1565 (1975).
17. Brassell, S. C. & Eglington, G. in *Coastal Upwelling: Its Sediment Record* (eds Suess, E. & Thiede, J.) 545-571 (Plenum, New York, 1983).
18. Gagopian, R. B., Nigrelli, G. E. & Volkman, J. K. in *Coastal Upwelling: Its Sediment Record* (eds Suess, E. & Thiede, J.) 241-272 (Plenum, New York, 1983).
19. Boon, J. J. et al. *Nature* 277, 125-127 (1979).
20. Robinson, N., Eglington, G., Brassell, S. C. & Cranwell, P. A. *Nature* 308, 439-441 (1984).
21. Brassell, S. C., Wardrop, A. M. K., Thomson, I. D., Maxwell, J. R. & Eglington, G. *Nature* 290, 693-696 (1981).
22. Simoneit, B. R. T. *Geochim. cosmochim. Acta* 41, 463-476 (1977).
23. Harwood, J. R. & Russell, N. J. *Lipids in Plants and Microbes* (George Allen & Unwin, London, 1984).
24. Holton, R. W., Blecker, H. H. & Onore, M. *Phytochemistry* 3, 595-602 (1964).
25. Russell, N. J. & Volkman, J. K. *J. gen. Microbiol.* 118, 131-141 (1980).
26. Rowland, S. J. & Volkman, J. K. *Mar. envir. Res.* 7, 117-130 (1982).
27. Boon, J. J., van der Meer, F. W., Schuyl, P. J. W., de Leeuw, J. W. & Schenck, P. A. *Init. Rep. DSDP* 40, 627-637 (1978).
28. Farrimond, P., Eglington, G. & Brassell, S. C. in *Advances in Organic Geochemistry 1985* (eds Leythaeuser, D. & Rullkötter, J.) (Pergamon, Oxford, in the press).
29. Sarnthein, M., Kögl, F. C. & Werner, F. *Geolog. Paläontol. Inst. Univ. Kiel Ber* No 2 (1983).
30. Sarnthein, M., Erlenkeuser, H., von Grafenstein, R. & Schröder, C. *Meteo: Forsch.-Ergebn.* C38, 9-24 (1984).
31. Ganssen, G. *'Meteo' Forsch.-Ergebn.* C37, 1-46 (1983).
32. Shackleton, N. J. & Opdyke, N. D. *Mem. geol. Soc. Am.* 145, 449-464 (1976).
33. Specmap 1984 in *Milankovitch and Climate* (eds Berger, A. & Imbrie, J.) (Reidel, New York, 1984).
34. McIntyre, A., Bé, A. W. H. & Roche, M. B. *Trans. N.Y. Acad. Sci. Ser. II* 32, 720-731 (1970).
35. Raymont, J. E. G. *Plankton and Productivity in the Oceans* (Pergamon, Oxford, 1980).
36. Hays, J. D., Imbrie, J. & Shackleton, N. J. *Science* 194, 1121-1132 (1976).
37. Milankovitch, M. K. *Serb. Akad. Beogr. Spec. Publ.* 132 (1941) (Transl. by Israel Prog. for Scientific Translations, Jerusalem, 1969).
38. Herterich, K. & Sarnthein, M. in *Milankovitch and Climate* (eds Berger, A. L. & Imbrie, J.) 447-466 (Reidel, New York, 1984).
39. Marlowe, I. T., Brassell, S. C., Eglington, G. & Green, J. C. *Oceanologica Acta* (submitted).
40. Samtleben, C. *Palaion. Z.* 54, 91-127 (1980).
41. Thierstein, H. R., Geitzenauer, K. R., Molino, B. & Shackleton, N. J. *Geol.* 5, 400-404 (1977).
42. McIntyre, A. & Bé, A. W. H. *Deep-Sea Res.* 14, 561-597 (1967).
43. Wakeham, S. G., Farrington, J. W. & Gagopian, R. B. *Org. Geochem.* 6, 203-215 (1984).
44. Volkman, J. K., Farrington, J. W., Gagopian, R. B. & Wakeham, S. G. in *Advances in Organic Geochemistry 1981* (eds Björk, M. et al.) 228-240 (Wiley, New York, 1983).
45. Gardner, J. V. & Hays, J. D. *Mem. geol. Soc. Am.* 145, 211-246 (1976).
46. Sarnthein, M. et al. in *Geology of the Northwest African Continental Margin* (eds von Rad, U., Hinze, K., Sarnthein, M. & Seibold, E.) 545-604 (Springer, Berlin, 1982).
47. Brassell, S. C. et al. *Init. Rep. DSDP* 56/57, 1367-1390 (1980).
48. Brassell, S. C. et al. in *Advances in Organic Geochemistry 1979* (eds Douglas, A. G. & Maxwell, J. R.) 375-392 (Pergamon, Oxford, 1980).
49. Cranwell, P. A. *Geochim. cosmochim. Acta* 49, 1545-1551 (1985).
50. Brassell, S. C. et al. in *Advances in Organic Geochemistry 1985* (eds Leythaeuser, D. & Rullkötter, J.) (Pergamon, Oxford, in the press).
51. Didyk, B. M., Simoneit, B. R. T., Brassell, S. C. & Eglington, G. *Nature* 272, 216-222 (1978).
52. Smith, D. J., Eglington, G. & Morris, R. J. *Phil. Trans. R. Soc.* (in the press).
53. Comet, P. A. thesis, Univ. Bristol (1982).
54. McEvoy, J. thesis, Univ. Bristol (1983).
55. Smith, D. J., Eglington, G. & Morris, R. J. *Geochim. cosmochim. Acta* 47, 2225-2232 (1983).
56. Volkman, J. K., Gillan, F. T., Johns, R. B. & Eglington, G. *Geochim. cosmochim. Acta* 45, 1817-1828 (1981).

# Human oestrogen receptor cDNA: sequence, expression and homology to v-erb-A

Stephen Green\*, Philippe Walter\*, Vijay Kumar\*, Andrée Krust\*, Jean-Marc Bornert\*, Patrick Argos† & Pierre Chambon\*\*‡

\* Laboratoire de Génétique Moléculaire des Eucaryotes du CNRS, Unité 184 de Biologie Moléculaire et de Génie Génétique de l'INSERM, Faculté de Médecine, 11 rue Humann, 67085 Strasbourg Cedex, France

† European Molecular Biology Laboratory, Postfach 10.2209, Meyerhofstrasse 1, 6900 Heidelberg, FRG

We have cloned and sequenced the complete complementary DNA of the oestrogen receptor (ER) present in the breast cancer cell line MCF-7. The expression of the ER cDNA in HeLa cells produces a protein that has the same relative molecular mass and binds oestradiol with the same affinity as the MCF-7 ER. There is extensive homology between the ER and the erb-A protein of the oncogenic avian erythroblastosis virus.

THE oestrogen receptor (ER) is found in a wide variety of species and is involved in the programming and regulation of gene expression in vertebrate female sex-accessory tissues (for reviews see refs 1 and 2). It has been suggested that the ER is localized predominantly in the nucleus<sup>3,4</sup> and that, following the binding of oestrogen, there is an increase in its affinity for some promoter elements of oestrogen-regulated genes (refs 2, 5, 6 and references therein). Very little is known about the underlying molecular mechanism.

Significant levels of ER have been detected in more than 50% of human breast cancers. Approximately 70% of these ER-positive tumours respond to anti-oestrogen therapy compared with only ~5% of ER-negative tumours, suggesting a strong correlation between the growth of breast tumours *in vivo* and the presence of the ER<sup>7</sup>. Oestrogens have been shown to be mitogenic in the ER-positive breast cancer cell line MCF-7 (ref. 8). The mechanism by which the binding of oestradiol to the ER results in stimulation of cell division is unknown, but several gene products are known to be induced (ref. 9 and references therein). Their role in promoting cell growth is unknown.

We have described previously the isolation of complementary DNA clones corresponding to the human ER messenger RNA present in MCF-7<sup>10</sup> and we have now isolated and sequenced additional cDNA clones that cover the entire ER mRNA. We report here the sequence of the complete ER cDNA and its expression in HeLa cells, and show that there is extensive homology between the ER cDNA and the erb-A gene of the oncogenic avian erythroblastosis virus (AEV).

## Sequence of the ER mRNA and gene

We have described previously the isolation of a 2.1-kilobase (kb) ER cDNA clone ( $\lambda$ OR8, see Fig. 1) using synthetic oligonucleotides corresponding to ER peptide sequences<sup>10</sup>. Sequencing of  $\lambda$ OR8 showed that it contains a large open reading frame of 1,785 nucleotides, sufficient to encode the ER (relative molecular mass ( $M_r$ ) ~65,000; ref. 10). Since the most 5' ATG is commonly used to initiate translation in eukaryotes<sup>11</sup>, we expected  $\lambda$ OR8 to correspond to the 5' end of the ER mRNA, which is ~6.2 kb long<sup>10</sup>. An oligo(dT)-primed  $\lambda$ gt10 cDNA library, prepared from MCF-7 cell poly(A)<sup>+</sup> RNA enriched in ER mRNA<sup>10</sup>, was screened with  $\lambda$ OR8 and the isolated clones were mapped. A probe corresponding to the 3' end of one of these clones,  $\lambda$ OR15 (see Fig. 1), was used to re-screen the library. This process was continued in order to isolate clones representing the entire ER mRNA (Fig. 1). No clones extending

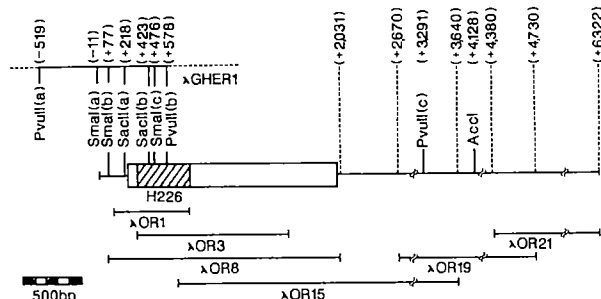


**Fig. 1** cDNA clones representing the complete ER mRNA. The MCF-7 ER mRNA is represented by a solid line beginning at nucleotide +1 (the cap site) and ending at nucleotide +6,322. The open reading frame is denoted as a box beginning at nucleotide +233 and ending at nucleotide +2,018. The region which contains the epitope recognized by the MCF-7 ER monoclonal antibody H226 is shown as a hatched box. This region was determined from the overlapping portions of the two  $\lambda$ gt11 cDNA clones ( $\lambda$ OR1 and  $\lambda$ OR3) which react with the H226 antibody<sup>10</sup>. Only those restriction enzyme sites referred to in the text are shown.  $\lambda$ GHER1 was isolated from a human genomic library and is shown above the ER mRNA. The region between the cap site and the  $Pvu$ II(b) site at +578 is homologous to the ER mRNA. The dotted lines upstream and downstream of the  $Pvu$ II/ $Pvu$ II region of  $\lambda$ GHER1 represent sequences in the  $\lambda$  clone which have not been analysed. The  $\lambda$ OR8,  $\lambda$ OR15,  $\lambda$ OR19 and  $\lambda$ OR21 clones were isolated from MCF-7 cDNA libraries<sup>10</sup> (also see below).

**Methods.** An oligo(dT)-primed cDNA library, prepared using sucrose gradient fractions of MCF-7 cell poly(A)<sup>+</sup> RNA enriched in ER mRNA, was constructed in  $\lambda$ gt10 as described previously<sup>10</sup>. The extremities of each of the inserts contain an EcoRI site due to the addition of EcoRI linkers during the cloning procedure. The insert of  $\lambda$ OR8 was purified on sucrose gradients, nick-translated and used to screen this library. The  $Pvu$ II(c)/EcoRI (3' end) fragment of one of the isolated clones,  $\lambda$ OR15, was purified on a 5% polyacrylamide gel, electroeluted, nick-translated and used to rescreen the library which resulted in the isolation of  $\lambda$ OR19. This process was repeated using the 3' AccI/EcoRI fragment of  $\lambda$ OR19 to obtain  $\lambda$ OR21. The 400-bp  $Sma$ I(b)/ $Sma$ I(c) fragment, corresponding to the 5' end of  $\lambda$ OR8, was similarly used to screen a genomic library constructed from human leukocyte DNA partially digested with  $Sau$ 3A and inserted into the  $Bam$ HI site of  $\lambda$ EMBL3<sup>39</sup>. The 13-kb insert of one of the clones isolated,  $\lambda$ GHER1, contains a 1.1-kb  $Pvu$ II(a)/ $Pvu$ II(b) fragment (solid line) representing the 5'-flanking sequence and part of the first exon of the ER.

‡ To whom all correspondence should be addressed.

**Fig. 2** Full-length nucleotide sequence and deduced amino-acid sequence of the MCF-7 ER mRNA. The 5'-flanking sequence of the human ER gene is shown from -128 to the cap site at nucleotide +1 (arrow). The ER mRNA sequence begins at nucleotide +1 and ends at the start of the poly(A) tail at nucleotide +6,322. The numbers on the left refer to the position of the nucleotides and those on the right to that of the amino acids. The CAT (GCCAATG) and TATA (TACTTAAA) boxes homologies in the 5'-flanking sequence, the three putative polyadenylation signal sites (AATAAA), the two potential cAMP-dependent kinase phosphorylation sites (basic-basic-X-Ser), the potential nuclear transfer signal (Arg-Pro-Gln-Leu-Lys), the most 5' ATG codon and the TGA termination codon 20 codons downstream, are all underlined. No potential N-linked glycosylation sites are present. The sequence which is complementary to the 17-mer primer A (5'-CGAGCTTGA-GCCCTGAA-3') used in the experiments to map the 5' end of the ER mRNA is boxed.

**Methods.** The cDNA clones (see Fig. 1) were digested with a range of restriction enzymes, the fragments were subcloned in both orientations into the M13 sequencing vector mp8 and sequenced using the dideoxy technique. Any gaps or ambiguous regions in the sequence were resequenced using synthetic oligonucleotide primers. The 5'-flanking sequence and that corresponding to the first 70 nucleotides of the ER mRNA were determined from the 1.1-kb *Pvu*II fragment of

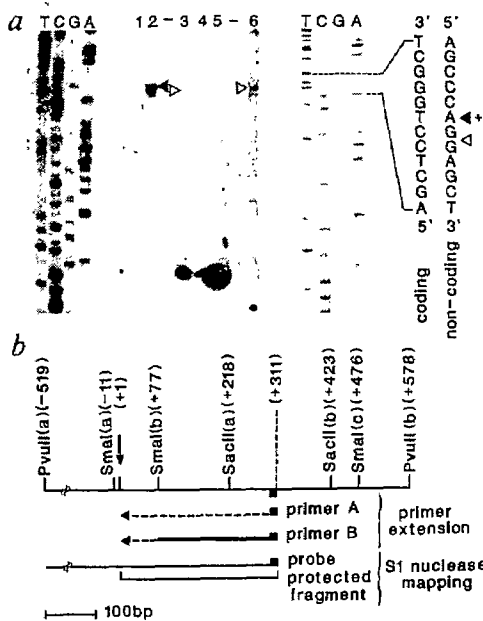


**Fig. 3** Mapping of the ER mRNA cap site. *a*, The 1.1-kb *Pvu*II/*Pvu*II fragment of  $\lambda$ GHER1 (Fig. 1) was subcloned into M13mp18. A single-stranded DNA probe (*b*) corresponding to this genomic fragment was prepared and used for  $S_1$ -nuclease mapping with (lane 2) or without (lane 1) sucrose gradient fractions of MCF-7 poly(A)<sup>+</sup> RNA enriched in ER mRNA<sup>10</sup>. Primer extension mapping was performed using primers A and B (*b*), reverse transcriptase and poly(A)<sup>+</sup> RNA enriched in ER mRNA. Primer A is a 17-mer oligonucleotide (5'-TCAGGGGCTCCAGCTG-3') corresponding to positions +295 to +311 of the ER mRNA sequence (Fig. 2); it was elongated and electrophoresed without treatment with  $S_1$  nuclease (lane 6). Primer B (lane 5) is 232 nucleotides long, from the *Sma*I(b) site to position +311. It was extended in the presence (lane 3) or absence (lane 4) of ER mRNA and treated with  $S_1$  nuclease before electrophoresis. The arrowheads show the position of the 5' end of the ER mRNA as defined by either  $S_1$ -nuclease mapping (closed arrowheads) or primer extension (open arrowheads). The four lanes (TCGA) show the sequence of the mRNA coding strand of the *Pvu*II/*Pvu*II fragment of  $\lambda$ GHER1 (dideoxy sequencing using the 5'-end-labelled primer A).

**Methods.** For both the  $S_1$ -nuclease and primer extension mapping, the 17-mer oligonucleotide, primer A, was 5'-end-labelled with [ $\gamma$ -<sup>32</sup>P]ATP and polynucleotide kinase. The  $S_1$ -nuclease mapping was carried out as follows. The labelled primer A was used for second-strand synthesis using the *Pvu*II/*Pvu*II M13mp18 clone as a template with cold nucleotides (500  $\mu$ M) and all other conditions as for dideoxy sequencing. The DNA was cut at the *Eco*RI site in the M13mp18 polylinker and the 830-nucleotide single-stranded probe was purified by polyacrylamide gel electrophoresis. This probe (600,000 c.p.m., 0.12 pmol) was hybridized to sucrose gradient fractions of MCF-7 poly(A)<sup>+</sup> RNA containing ~500 pg ER mRNA (40 mM PIPES pH 6.5, 400 mM NaCl, 50% formamide, 2 min at 80 °C, 2 min at 100 °C and overnight at 42 °C), and then digested with 60 U of  $S_1$  nuclease (BRL) for 2 h at 25 °C in 50 mM Na-acetate pH 4.5, 100 mM NaCl, 1 mM ZnCl<sub>2</sub>. Primer B was prepared as described for the  $S_1$ -nuclease mapping probe except that the synthesized DNA was cut at the *Sma*I(b) site (see *b*). This 232-nucleotide single-stranded primer (800,000 c.p.m., 0.16 pmol) was hybridized with the same MCF-7 RNA as above using the same conditions. After precipitation with ethanol, the primer was elongated with 25 U of reverse transcriptase for 10 min at 42 °C (50 mM Tris-HCl pH 8.3, 40 mM KCl, 8 mM MgCl<sub>2</sub>, 0.5 mM dNTP, 0.4 mM dithiothreitol).  $S_1$ -nuclease treatment before gel electrophoresis was as described above. For primer extension mapping with primer A, the primer (5  $\times$  10<sup>6</sup> c.p.m., 1 pmol) was hybridized as for primer B, except that the formamide concentration was reduced to 10%. Primer A was elongated with reverse transcriptase as described for primer B, but was not treated with  $S_1$  nuclease. Both the  $S_1$ -nuclease-protected and primer-extended fragments were electrophoresed on a standard 6% sequencing gel.

farther 5' than  $\lambda$ OR8 were obtained when the 5' *Sma*I(b)/*Sma*I(c) fragment of  $\lambda$ OR8 (see Fig. 1) was used as a probe to screen the randomly primed  $\lambda$ gt10 library, which has been described previously<sup>10</sup>. Clones  $\lambda$ OR8,  $\lambda$ OR15,  $\lambda$ OR19 and  $\lambda$ OR21 (Fig. 1) were subcloned into the M13 sequencing vector mp8, yielding a series of overlapping fragments suitable for sequencing by the dideoxy technique. The complete sequence is shown in Fig. 2.

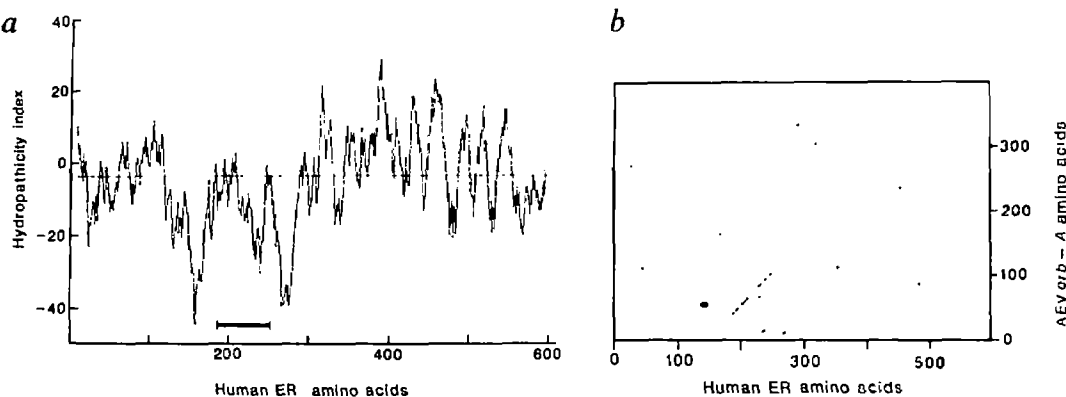
The 400-base pair (bp) *Sma*I(b)/*Sma*I(c) fragment of  $\lambda$ OR8 was also used to screen a human leukocyte genomic  $\lambda$  library. The 1.1-kb *Pvu*II/*Pvu*II fragment of one of the isolated clones ( $\lambda$ GHER1), which contains the *Sma*I(b)/*Sma*I(c) region of  $\lambda$ OR8 together with ~500 bp of 5'-flanking sequence, was subcloned into M13mp18 (Fig. 1). A single-stranded DNA probe, corresponding to the coding strand of the ER gene, was prepared from this *Pvu*II fragment using the 5' end-labelled synthetic oligonucleotide primer A (5'-TCAGGGGCTCCAGCTG-3'; see Figs 2 and 3b legends). This probe was used in an  $S_1$ -nuclease mapping assay with sucrose gradient fractions of MCF-7 poly(A)<sup>+</sup> RNA enriched in ER mRNA<sup>10</sup>. The ER mRNA remained homologous to this genomic probe as far as an adenine located 77 bp upstream from the *Sma*I(b) site of  $\lambda$ OR8 (see Figs 2 and 3b, arrow +1, and Fig. 3a, lane 2, arrowhead; the faint bands which are larger than the major protected fragment may correspond to minor transcription start sites). Primer extension experiments, using two different primers, were performed to show that this site corresponds to the 5' end of the ER mRNA rather than to an intron-exon boundary. Primer A was hybridized to the ER mRNA-enriched RNA and elongated with reverse transcriptase. Primer B was prepared from the *Pvu*II/*Pvu*II M13 clone, exactly as described above for the  $S_1$ -nuclease mapping experiment, except that the primer was cut at the *Sma*I(b) site so as to generate a 232-nucleotide fragment which was completely homologous to ER mRNA (Fig. 3a, lane 5, and b). Primer B was hybridized to ER mRNA-enriched RNA and elongated as for primer A (see Fig. 3 legend). After incubation with reverse transcriptase, both primers A (Fig. 3a, lane 6, open arrowhead) and B (lane 3, open arrowhead; the band in the control lane 4 may correspond to a self-primed elongation product of the probe) were extended to one of the two guanine nucleotides located at positions +2 and +3 (Fig. 3a). We conclude from these results and similar experiments not shown that the A indicated by +1 in Figs 2 and 3 probably corresponds to the 5' end of the ER mRNA. This conclusion is supported by the presence of a TATA box-like sequence, 5'-TACTTAAA-3', located 27 bp upstream from this putative start site (Fig. 2). The sequence 5'-GCCAATGT-3' situated at -103 (Fig. 2) may correspond to a CAT box<sup>12</sup>.

The MCF-7 ER mRNA is 6,322 nucleotides long and has a 5'-untranslated region of 232 nucleotides (Figs 1, 2). The most 5' ATG codon, at position +119, is followed 20 codons downstream by a TGA stop codon. A second ATG codon, at position +233, is in the same translational reading frame as the first and is flanked by nucleotides which have a closer homology to the Kozak's consensus sequence<sup>11</sup>. This codon represents the start of an open reading frame of 1,785 nucleotides which codes for a 595-amino-acid protein of  $M_r$  66,182. It is common for translation in eukaryotes to initiate at the most 5' ATG codon of the mRNA<sup>11</sup>. However, the presence of an upstream ATG codon is not unique to the ER mRNA<sup>13</sup>, although usually only a few codons are present between the ATG and stop codons. It is not known whether this first 20-codon open reading frame is expressed and has any physiological role. In this respect, it will be of interest to compare the human and other ER cDNA sequences to determine whether this region is conserved. Whether the presence of this upstream ATG codon affects the translational efficiency of the ER mRNA is also unknown, but this region does not appear to have the potential to form any stable secondary structure as is observed in some other mRNA sequences<sup>14</sup>. A long 3'-untranslated region (4,305 nucleotides)

**Fig. 4** Hydropathicity plot of the MCF-7 ER amino-acid sequence and sequence homology with *v-erb-A*. *a*, A computer program, using the algorithm described by Kyte and Doolittle<sup>40</sup>, was used to display the hydropathic nature of the MCF-7 ER using a window of 15 amino acids. Negative values represent hydrophilic regions and positive values hydrophobic regions. The numbers on the horizontal axis refer to the amino-acid sequence beginning at the N-terminus. The region of the ER sequence (residues 185–251) possessing the greatest homology with *v-erb-A* is indicated by a bar.

*b*, The amino-acid sequences of the MCF-7 ER and *erb-A* were compared by a matrix analysis using a window of six residues and a dot plotted for a match of four or more identical residues. The program therefore generates a diagonal line where any homology between the two sequences is found. The numbers along the axes for both sequences are as described in *a*. *c*, The alignment between the sequence of the MCF-7 ER and *v-erb-A* protein was determined using a search procedure based on the amino-acid physical characteristics<sup>41,42</sup>. There are 378 aligned residues for the ER and *v-erb-A* proteins, of which 27% are identical (boxed amino acids) and 41% conserved according to the following scheme: (P, G), (M, C), (Y, W, F, H), (L, V, I, A), (K, R), (E, Q, N, D) and (S, T) (denoted by a line both above and below the amino acid). The average correlation coefficient between the two sequences, using six amino-acid physical characteristics, was 0.37. The mean correlation, maximum correlation and standard deviation for control protein sequences (see below) were 0.00, 0.20 and 0.04, respectively. The ER-*v-erb-A* correlation was 9.2 s.d. above the control mean and 4.2 s.d. above the control maximum. The control protein sequence consisted of a group of 63 proteins of unrelated tertiary structure (see ref. 43 for examples) whose sequence was expanded to contain 1,000 residues. Segments of 378 amino acids were randomly selected (using a random generator seeded with a number based on the time of day) and an average correlation coefficient calculated. This procedure was repeated at 10 different times and the mean s.d. and maximum correlations were calculated for the resulting 19,530 average correlations over six amino-acid characteristics. To determine whether the homology between the ER and *v-erb-A* is significant throughout the entire *v-erb-A* sequence, the ER sequence was subdivided into three regions (I, residues 146–255; II, residues 256–467; III, residues 468–595) and each aligned with *v-erb-A* as shown in *c*. The correlation coefficients were 5.8, 6.2 and 3.2 s.d. above the control mean, respectively.

(E, Q, N, D) and (S, T) (denoted by a line both above and below the amino acid). The average correlation coefficient between the two sequences, using six amino-acid physical characteristics, was 0.37. The mean correlation, maximum correlation and standard deviation for control protein sequences (see below) were 0.00, 0.20 and 0.04, respectively. The ER-*v-erb-A* correlation was 9.2 s.d. above the control mean and 4.2 s.d. above the control maximum. The control protein sequence consisted of a group of 63 proteins of unrelated tertiary structure (see ref. 43 for examples) whose sequence was expanded to contain 1,000 residues. Segments of 378 amino acids were randomly selected (using a random generator seeded with a number based on the time of day) and an average correlation coefficient calculated. This procedure was repeated at 10 different times and the mean s.d. and maximum correlations were calculated for the resulting 19,530 average correlations over six amino-acid characteristics. To determine whether the homology between the ER and *v-erb-A* is significant throughout the entire *v-erb-A* sequence, the ER sequence was subdivided into three regions (I, residues 146–255; II, residues 256–467; III, residues 468–595) and each aligned with *v-erb-A* as shown in *c*. The correlation coefficients were 5.8, 6.2 and 3.2 s.d. above the control mean, respectively.



is not unique to the ER; other receptor mRNAs<sup>15,16</sup>, including that of the human glucocorticoid receptor<sup>17</sup>, have a similar structure. The putative polyadenylation signal 'AATAAA' is found 15 bp upstream from the polyadenylation site. Two other such sequences, found in the 3'-untranslated region of the ER mRNA at positions 4,422 and 5,497, are used weakly, if at all, as only the 6.3-kb transcript was detected<sup>10</sup>.

### ER sequence and homology to *v-erb-A*

The ER amino-acid sequence is shown in Fig. 2 and its hydrophaticity is analysed in Fig. 4*a*. The human ER can apparently be subdivided into at least three hydrophatic domains. The first domain, containing the first 120 amino acids, is followed by a region between amino acids 120 and 300 which is rich in cysteine, lysine and arginine and poor in leucine and proline. This hydrophilic region is likely to be exposed on the surface of the receptor and, being rich in positively charged amino acids, may bind to nucleic acids. In this respect, we note that this region may contain the epitope for the monoclonal antibody, H226, which

is believed to interact with the DNA-binding domain of the receptor<sup>18</sup> (Fig. 1). A characteristic feature of prokaryotic DNA-binding proteins is the helix-β-turn-helix secondary structure, in which the two helices provide the DNA specificity of the binding through intimate contact with the major groove of the B-form of the DNA helix<sup>19</sup>. We compared the ER amino acid sequence with those of the prokaryotic proteins that are either believed or known to contain DNA-binding domains, and with that of the protein thought to be encoded by the *Drosophila* segmentation gene *fushi tarazu* (*ftz*), and the yeast MAT $\alpha$ 1 and MAT $\alpha$ 2 proteins which may contain such domains (ref. 20 and references therein). No structural similarities between any of these proteins and the ER were found, and no similar helix-β-turn-helix secondary structure is predicted from the ER sequence. The third domain corresponds to the C-terminal half of the receptor from approximately amino acid 300 onwards. Being mostly hydrophobic, this domain may contain the oestrogen-binding site.

The ER in MCF-7 cells is predominantly nuclear<sup>3</sup>. The yeast

**Fig. 5** Expression of the ER cDNA in HeLa cells. *a*, The size of the protein coded by the cloned ER cDNA is identical to that of the MCF-7 ER. The ER cDNA sequence was inserted into the eukaryotic expression vector pKCR2 (ref. 29), yielding pKCR2-ER. This recombinant was transfected into HeLa cells and the proteins labelled with  $^{35}\text{S}$ -methionine. Cytoplasmic proteins were immunoprecipitated with ER antibodies, separated by SDS-polyacrylamide gel electrophoresis (7%) and revealed by fluorography. Lane 1, wild-type HeLa cells; lane 2, HeLa cells transfected with pKCR2; lane 3, HeLa cells transfected with pKCR2-ER; lane 4, wild-type MCF-7 cells. The arrowhead shows the position of the 65,000- $M_r$  protein. Lane M,  $^{14}\text{C}$ -labelled protein markers: phosphorylase b, bovine serum albumin, ovalbumin,  $\alpha$ -chymotrypsinogen. Numbers on the right indicate their respective  $M_r$ s ( $\times 10^{-3}$ ).

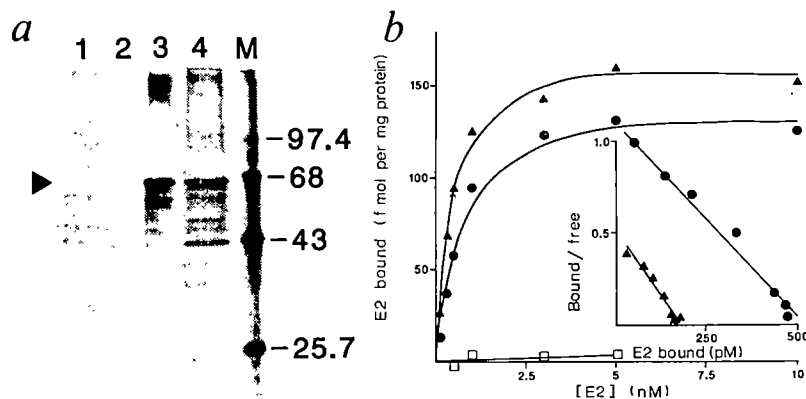
*b*, The ER cDNA-encoded protein binds oestradiol with the same affinity as the MCF-7 ER. Cytosol extracts, prepared from MCF-7 cells (●) or HeLa cells transfected with pKCR2 (□) or pKCR2-ER (▲), were incubated overnight at 0 °C in the presence of  $^3\text{H}$ -17 $\beta$ -oestradiol (E2) with or without a 100-fold excess of unlabelled 17 $\beta$ -oestradiol. The unbound steroid was removed using dextran-coated charcoal and the receptor-bound steroid counted in a scintillation counter. The number of moles of steroid bound per milligram of cytosolic protein was calculated after subtraction of the nonspecific binding. Each point was performed in duplicate and line-fitting was by computer<sup>44</sup>. The inset shows a Scatchard plot of these data.

**Methods.** *a*, For construction of vector pKCR2-ER, the ER cDNA clone λOR8, which had been subcloned into the EcoRI site of pBR322, was partially digested with *Sac*II to remove the upstream ATG codon, which is followed by a stop codon (see Fig. 2). The extremities of the DNA were blunt-ended with T4 DNA polymerase and EcoRI linkers added. The DNA was digested with EcoRI, cutting both in the newly added linker and in the EcoRI site present at the 3' end of the pOR8 insert. The 1.8-kb EcoRI fragment was then inserted into the EcoRI site of pKCR2<sup>29</sup>. This vector contains the SV40 early promoter and  $\beta$ -globin splicing donor and acceptor sites upstream of the inserted ER sequence, and downstream from it the  $\beta$ -globin and SV40 polyadenylation sites. Transfection of 30–50% confluent HeLa cells (in 9-cm Petri dishes) with calcium phosphate-precipitated supercoiled plasmid DNA (10  $\mu\text{g}$  per dish) was performed as described previously<sup>45</sup>. All the serum was stripped of endogenous steroid hormones by charcoal treatment. The medium was replaced 48 h after transfection with 3 ml of methionine-free and serum-free Dulbecco's medium containing 100  $\mu\text{Ci}$  of  $^{35}\text{S}$ -methionine (1,500 Ci mmol<sup>-1</sup>). After 5 h, the cells were washed with ice-cold phosphate-buffered saline (PBS), resuspended for 5–10 min at 4 °C in 200  $\mu\text{l}$  of 1% Nonidet-P40, 50 mM Tris-HCl pH 7.5, and centrifuged at 12,000g for 1 min. SDS (22  $\mu\text{l}$  of 10%) and EDTA (3  $\mu\text{l}$  of 0.2 M) were added to the supernatant and the protein denatured by boiling for 5 min. The ER protein present in HeLa cells ( $10 \times 10^6$  c.p.m. total protein radioactivity) or MCF-7 cells ( $18 \times 10^6$  c.p.m.) was immunoabsorbed to protein A/Sepharose using 5  $\mu\text{g}$  each of the monoclonal antibodies H226 and D75 as described previously<sup>10</sup>, before electrophoresis. *b*, HeLa cells were transfected as described in *a*. The cells from 10 Petri dishes were washed twice with ice-cold PBS and homogenized on ice in 1 ml of buffer (20 mM Tris-HCl pH 7.3, 1 mM EDTA, 2 mM  $\beta$ -mercaptoethanol, 50 mM NaCl, 0.3 mM phenylmethylsulphonyl fluoride, 10 mM Na-molybdate and 10% glycerol), using 50 strokes of a 5-ml glass-glass homogenizer. The cytosol was prepared by centrifugation of the homogenate at 105,000g at 4 °C for 1 h. Aliquots (50  $\mu\text{l}$ ) were incubated in duplicate with different concentrations of  $^3\text{H}$ -17 $\beta$ -oestradiol (153 Ci mmol<sup>-1</sup>) with (nonspecific binding) or without (total binding) a 100-fold excess of unlabelled 17 $\beta$ -oestradiol. After incubation overnight at 0 °C, 100  $\mu\text{l}$  of dextran-coated charcoal (DCC) solution (0.5% Norit-A, 0.05% dextran T70 in 10 mM Tris-HCl, pH 7.5) was added for 15 min on ice to remove the free steroid. DCC was removed by centrifugation and the amount of  $^3\text{H}$ -17 $\beta$ -oestradiol remaining in 100  $\mu\text{l}$  of supernatant counted. Cytosol preparation and determination of the ER content of MCF-7 cells grown in stripped medium<sup>9</sup> were carried out as described above for HeLa cells. Cytosolic protein contents were estimated using the Bradford assay.

protein, MAT $\alpha$ 2, contains a sequence of three hydrophobic amino acids (one being proline) with a basic amino acid at each side which may be responsible for the transfer of a MAT $\alpha$ 2- $\beta$ -galactosidase fusion protein to the nucleus<sup>21</sup>. A similar region (Arg-Pro-Gln-Leu-Lys<sup>32</sup>) is present near the N-terminus of the ER (Fig. 2). No region homologous to those sequences responsible for nuclear transfer of the simian virus 40 (SV40) large-T antigen<sup>22</sup> or the yeast ribosomal protein L3 (ref. 23) was found.

It has been suggested that tyrosine phosphorylation of the calf uterine ER by a cytoplasmic kinase potentiates the binding of oestrogen<sup>24</sup>. The selection of the tyrosine phosphorylation site may require the presence of basic (lysine or arginine) and acidic (glutamate or aspartate) amino acids on the N-terminal side of the phosphorylated tyrosine<sup>25</sup>. Several of the tyrosine residues (positions 43, 184, 219, 526) of the MCF-7 ER sequence exhibit this general feature. Two potential cyclic AMP-dependent phosphorylation sites<sup>26</sup> (basic amino acid-basic amino acid-X-Ser/Thr) are present in the ER sequence at positions 236 and 305 (see Fig. 2).

The ER amino-acid sequence was used in a computer search of the NBRF protein database for related sequences. Only one sequence, that of the AEV gag-erb-A fusion protein<sup>27</sup>, showed significantly homology (Fig. 4*b*, *c*). This homology is particularly striking in the cysteine-rich region of the ER between amino acids 185 and 251, where each of the 9 cysteine residues in this region is conserved in the erb-A protein. This high degree of conservation suggests that the tertiary structure of this region is an important feature of the ER. Although less striking than that within the cysteine-rich region, the homology between the ER and erb-A protein extends throughout the erb-A sequence (see Fig. 4*c*). Very little, if any, homology was observed between



the MCF-7 ER sequence and the rat prostatic steroid-binding proteins or rabbit uteroglobin<sup>28</sup>, which bind weakly androgens and progesterone, respectively (data not shown).

### Expression of ER cDNA in HeLa cells

The ER cDNA insert of λOR8 was partially digested with *Sac*II so as to remove the most 5' ATG codon together with the stop codon located 20 codons downstream (Figs 1, 2). The 1.8-kb fragment, containing the complete ER open reading frame, was inserted in the eukaryotic expression vector pKCR2 downstream from the SV40 early promoter<sup>29</sup>. HeLa cells transfected with this construct (pKCR2-ER) were labelled with  $^{35}\text{S}$ -methionine and the proteins immunoprecipitated with the two ER monoclonal antibodies H226 and D75 (ref. 18) (Fig. 5*a*, lane 3). The endogenous MCF-7 cell ER was similarly labelled and precipitated, and the proteins were separated on a 7% SDS-polyacrylamide gel (Fig. 5*a*, lane 4). In both cases a protein of  $M_r$  ~65,000 was observed. No such protein was seen in either wild-type HeLa cells (Fig. 5*a*, lane 1) or HeLa cells transfected with the pKCR2 vector (lane 2). Other smaller proteins, which appear to be specific to the HeLa cells transfected with pKCR2-ER, may be due to either proteolysis of the ER or premature termination of translation.

Cytosol extracts were prepared from either HeLa cells, transfected with pKCR2 or pKCR2-ER, or from MCF-7 cells. A dextran-coated charcoal assay was then used to determine both the number and affinity for oestradiol of any oestrogen-binding protein present in HeLa cells and in MCF-7 (Fig. 5*b*). HeLa cells transfected with the pKCR2 vector had only background oestradiol-binding activity, whereas HeLa cells transfected with pKCR2-ER contained significant amounts of oestradiol-binding activity (Fig. 5*b*). The affinity of the corresponding protein for

oestradiol ( $K_D = 0.4$  nM) was very similar to that of the MCF-7 ER ( $K_D = 0.5$  nM) (Fig. 5b, inset). We conclude that the expression of the cloned ER cDNA in HeLa cells yields a protein which, using these criteria, is indistinguishable from the MCF-7 cell ER.

## Discussion

We have isolated and sequenced cDNA clones corresponding to the complete sequence of the human ER mRNA. When expressed in HeLa cells, this cDNA codes for a protein that has the same apparent relative molecular mass and binds oestradiol with the same affinity as the MCF-7 cell ER.

It is extremely interesting that the predicted human ER sequence shares strong sequence homology with the *erb-A* gene of the oncogenic AEV. The AEV genome contains two cell-derived genes termed *v-erb-A* and *v-erb-B* (for review see ref. 30). The *v-erb-A* gene is expressed as a cytoplasmic *gag-erb-A* fusion protein of ~75,000  $M_r$ , which is not itself oncogenic<sup>31</sup>. Instead it appears that its action is to increase the oncogenic potential of *v-erb-B*<sup>31</sup>, which is homologous to the epidermal growth factor (EGF) receptor, although it lacks the EGF-binding domain<sup>32</sup>. The function of *c-erb-A*, the cellular counterpart of the *v-erb-A* gene, is unknown; it is also unknown whether the *erb-A* protein binds to either DNA or steroid hormones. The chicken ER does not correspond to *c-erb-A*, since its sequence is more closely homologous to that of the human ER than to *v-erb-A* (our unpublished results). The human *c-erb-A* has been mapped to chromosome 17 and part of its amino-acid sequence (residues 226–312) is 96% homologous to *v-erb-A*<sup>27</sup>; in contrast, the human ER maps<sup>10</sup> to chromosome 6 and shares only a 6.7% homology with *v-erb-A* in this region. Although the non-cysteine-rich domain 2 (ref. 27) of the *v-erb-A* protein shares some homology with human carbonic anhydrase<sup>27</sup>, no such homology exists between carbonic anhydrase and the human ER (1.3 s.d. above the control mean).

Two *v-erb-A*-related human genomic clones have been isolated<sup>33</sup>. The sequences of these two clones are only distantly related<sup>33</sup> and both appear to map<sup>34</sup> to human chromosome 17. Southern analysis with human DNA using one of these clones,  $\lambda$ he-A2, suggests the presence of at least an additional related gene showing that *c-erb-A* belongs to a multigene family.

Southern analysis of the human MCF-7 ER gene using  $\lambda$ OR8 as a probe<sup>10</sup> shows that neither  $\lambda$ he-A1 nor  $\lambda$ he-A2<sup>33</sup> corresponds to ER sequence.

It is probable that the conserved cysteine-rich domain, common to the human ER and *v-erb-A* proteins, has some important biological function. It will be interesting to investigate whether it is common to all members of the *erb-A* family. Site-directed *in vitro* mutagenesis of the ER cDNA sequence in the expression vector pKCR2-ER should help to elucidate its function, as well as to localize those regions involved in the multiple functions of the ER. In this respect, a comparison of the ER and *v-erb-A* sequences with that of the glucocorticoid receptor, which has recently been cloned<sup>17,35,36</sup>, should also be very informative.

There is a strong correlation between the growth of breast cancers and their ER content<sup>7</sup>, and although the mechanism by which the ER increases the growth rate of these tumours is unknown, it may involve the induction of either growth factors or their receptors<sup>37,38</sup>. The mechanism by which *v-erb-A* potentiates the action of *v-erb-B* is also unknown, but it is possible that the ER may similarly potentiate a human oncogene in breast cancer. In this respect, it will be interesting to investigate whether the sequence of the MCF-7 breast cancer cell line ER differs in some way from that of the ER from non-malignant tissues.

We thank G. L. Greene (University of Chicago) and L. S. Miller (Abbott Laboratories) for providing the D75 and H226 ER monoclonal antibodies, respectively; A. Staub for synthesis of the oligonucleotides; the Michigan Cancer Foundation for providing MCF-7 cells; Transgene for providing the human genomic library; I. Issemann for technical assistance; L. Heydler for growing the cells; and C. Werlé and B. Boulay for the preparation of the figures. This research was supported by INSERM, CNRS (ATP Etats-Unis) and the Ministère de la Recherche et de la Technologie (84VO803). S.G. is a recipient of a Royal Society European Exchange fellowship.

*Note added in proof:* After this manuscript was submitted, the sequence of the human glucocorticoid receptor and its homology with *v-erb-A* were reported<sup>46,47</sup>. A comparison of the human and chicken oestrogen receptor, the human glucocorticoid receptor and *v-erb-A* shows that the cysteine-rich and hydrophobic regions are conserved in all four sequences, supporting the view that they correspond to important functional domains<sup>48</sup>.

Received 6 December 1985; accepted 20 January 1986.

1. Knowler, J. T. & Beaumont, J. M. *Essays Biochem.* **20**, 1–39 (1985).
2. Yamamoto, K. R. A. *Rev. Genet.* **19**, 209–252 (1985).
3. King, W. J. & Greene, G. L. *Nature* **307**, 745–747 (1984).
4. Welshons, W. V., Lieberman, M. E. & Gorski, J. *Nature* **307**, 747–749 (1984).
5. Dean, D. C., Gope, R., Knoll, B. J., Risner, M. E. & O'Malley, B. W. *J. biol. Chem.* **259**, 9967–9970 (1984).
6. Jost, J.-P., Geiser, M. & Seldman, M. *Proc. natn. Acad. Sci. U.S.A.* **82**, 988–991 (1985).
7. Edwards, D. P., Chamness, G. C. & McGuire, W. L. *Biochim. biophys. Acta* **560**, 457–486 (1979).
8. Lippman, M. E., Bolan, G. & Huff, K. K. *Cancer Res.* **36**, 4595–4601 (1976).
9. Masiakowski, P. *et al.* *Nucleic Acids Res.* **10**, 7895–7903 (1982).
10. Walter, P. *et al.* *Proc. natn. Acad. Sci. U.S.A.* **82**, 7889–7893 (1985).
11. Kozak, M. *Nucleic Acids Res.* **12**, 857–872 (1984).
12. Benoit, C., O'Hare, K., Breathnach, R. & Chambon, P. *Nucleic Acids Res.* **8**, 127–142 (1980).
13. Hunt, T. *Nature* **316**, 580–581 (1985).
14. Dickson, L. A., de Wet, W., Di Liberto, M., Weil, D. & Ramirez, F. *Nucleic Acids Res.* **13**, 3427–3438 (1985).
15. Yamamoto, T. *et al.* *Cell* **39**, 27–38 (1984).
16. Schneider, C., Owen, M. J., Banville, D. & Williams, J. G. *Nature* **311**, 675–678 (1984).
17. Govindan, M. V., Devic, M., Green, S., Gronemeyer, H. & Chambon, P. *Nucleic Acids Res.* **13**, 8293–8304 (1985).
18. Greene, G. L., Sobel, N. B., King, W. J. & Jensen, E. V. *J. Steroid Biochem.* **20**, 51–56 (1984).
19. Pabo, C. O. & Saenger, R. T. A. *Rev. Biochem.* **53**, 293–321 (1984).
20. Laughon, A. & Scott, M. P. *Nature* **310**, 25–31 (1984).
21. Hall, M. N., Hereford, L. & Herskowitz, I. *Cell* **36**, 1057–1065 (1984).
22. Kalderon, D., Roberts, B. L., Richardson, W. D. & Smith, A. E. *Cell* **39**, 499–509 (1984).
23. Moreland, R. B., Nam, H. G., Hereford, L. M. & Fried, H. M. *Proc. natn. Acad. Sci. U.S.A.* **82**, 6561–6565 (1985).
24. Migliaccio, A., Rotondi, A. & Auricchio, F. *Proc. natn. Acad. Sci. U.S.A.* **81**, 5921–5925 (1984).
25. Patschinsky, T., Hunter, T., Esch, F. S., Cooper, J. A. & Sefton, B. M. *Proc. natn. Acad. Sci. U.S.A.* **79**, 973–977 (1982).
26. Krebs, E. G. & Beavo, J. A. *A. Rev. Biochem.* **48**, 923–959 (1979).
27. Debuire, B. *et al.* *Science* **224**, 1456–1459 (1984).
28. Baker, M. E. *Biochem. biophys. Res. Commun.* **114**, 325–330 (1983).
29. Breathnach, R. & Harris, B. A. *Nucleic Acids Res.* **11**, 7119–7136 (1983).
30. Graf, T. & Beug, H. *Cell* **34**, 7–9 (1983).
31. Frykberg, L. *et al.* *Cell* **32**, 227–238 (1983).
32. Ullrich, A. *et al.* *Nature* **309**, 418–425 (1984).
33. Jansson, M., Philipson, L. & Vennström, B. *EMBO J.* **2**, 561–565 (1983).
34. Spurr, N. K. *et al.* *EMBO J.* **3**, 159–163 (1984).
35. Miesfeld, R. *et al.* *Nature* **312**, 779–781 (1984).
36. Weinberger, C. *et al.* *Science* **238**, 740–742 (1985).
37. Sirbasku, D. A. & Leland, F. E. in *Biochemical Actions of Hormones* Vol. 9 (ed. Litwack, G.) 115–140 (Academic, New York, 1982).
38. Mukka, V. R. & Stancel, G. M. *J. biol. Chem.* **260**, 9820–9824 (1985).
39. Frischaufer, A.-M., Lehrach, H., Pousta, A. & Murray, N. *J. molec. Biol.* **170**, 827–842 (1983).
40. Kyte, J. & Doolittle, R. F. *J. molec. Biol.* **157**, 105–132 (1982).
41. Argos, P., Hanei, M., Wilson, J. M. & Kelley, W. N. *J. biol. Chem.* **258**, 6450–6457 (1983).
42. Argos, P. *EMBO J.* **4**, 1351–1355 (1985).
43. Rosmann, M. G. & Argos, P. *A. Rev. Biochem.* **50**, 497–532 (1981).
44. Green, S., Field, J. K., Green, C. D. & Beynon, R. J. B. *Nucleic Acids Res.* **10**, 1411–1421 (1982).
45. Banerji, J., Rusconi, S. & Schaffner, W. *Cell* **27**, 299–308 (1981).
46. Hollenberg, S. M. *et al.* *Nature* **318**, 635–641 (1985).
47. Weinberger, C., Hollenberg, S. M., Rosenfeld, M. G. & Evans, R. M. *Nature* **318**, 670–672 (1985).
48. Krust, A. *et al.* *EMBO J.* (in the press).

## Strong breathing of the hydrogen coma of comet Halley

E. Kaneda\*, K. Hirao†, M. Takagi‡, O. Ashihara§,  
T. Itoh§ & M. Shimizu§

\* Geophysics Research Laboratory, University of Tokyo, Hongo, Bunkyo-ku, Tokyo 113, Japan

† Department of Aeronautics and Astronautics, Tokai University, 1117, Kita-kaname, Hiratsuka-shi, Kanagawa Prefecture 259-12, Japan

‡ Institute of Industrial Science, University of Tokyo, Roppongi, Minato-ku, Tokyo 106, Japan

§ Institute of Space and Astronautical Science, Komaba, Meguro-ku, Tokyo 153, Japan

**Strong breathing of the hydrogen coma of comet Halley was observed by the Lyman- $\alpha$  imager of the Japanese interplanetary spacecraft, Suisei. Measurement of the peak-to-peak variation of central brightness yields a preliminary value of  $2.2 \pm 0.1$  days for the period. Two outbursts from the active regions on the comet's surface could be the cause of this variation. A shell structure in the hydrogen coma was also detected. The outbursts appear to contribute overwhelmingly to the Lyman- $\alpha$  activity of this comet, at a pre-perihelion heliocentric distance of  $\sim 1.5$  AU.**

Comet Halley has a reddish dark nucleus with a radius of  $3 \pm 1$  km (refs 1, 2). Various observations of OH, H and other volatiles suggest that the core beneath this dark mantle could be the usual dirty ice. Water, the main constituent of the coma, is photodissociated into OH and H by solar ultraviolet radiation, resulting in a high-velocity component ( $\sim 20$  km s $^{-1}$ ) of the hydrogen coma. Further photodissociation of OH creates a low-velocity component ( $\sim 8$  km s $^{-1}$ ). In addition to these major processes, there are many minor photochemical processes which produce hydrogen atoms with various velocities<sup>3</sup>.

The analysis of the dust behaviour of comet Halley in the 1910 apparition<sup>4,5</sup> suggested that water production was not necessarily uniform, a significant contribution arising from outbursts (with velocities of several hundred metres per second) at three locations on the surface (two point sources and one crack at almost the same longitude). It appears that an outburst occurs when, due to the rotation of the comet nucleus, one of these sources faces the Sun. If this assumption is correct, it can be expected that analysis of the intensity variation of the hydrogen coma will determine the rotational period of the comet.

The Lyman- $\alpha$  (1216Å) imager onboard Suisei, the first Japanese interplanetary spacecraft, is a charge-coupled device (CCD) imaging detector with a field of view of  $2.0^\circ \times 1.8^\circ$  ( $153 \times 122$  pixels) (ref. 6 and E.K., K.H. and M.T., in preparation). This imager took several hundred faint ultraviolet images of comet Halley during the 3 weeks following 26 November 1985 (see Fig. 1). Figure 2 shows the synthesized images of Halley at 00:00 30 November UT (active phase) and 04:00 28 November UT (inactive phase), respectively, obtained by superposing seven images on its first position, after adjusting for the comet's subsequent motion.

The time-sequential analysis of the images showed the following activity of comet Halley (see also Fig. 1): During an inactive phase (Fig. 2b), the images were quite faint (04:00 28 November). After that phase, an expansion of the hydrogen coma was observed, possibly arising from the photodissociation of a weak outburst. About 20 h after the blasting of this weak outburst, a bright pixel (which corresponds to a linear size of about 40,000 km) appeared suddenly adjacent to the ephemeris position of the comet. The transit time over this distance of a hydrogen atom with a velocity of 10 km s $^{-1}$  is about 1 h; thus,

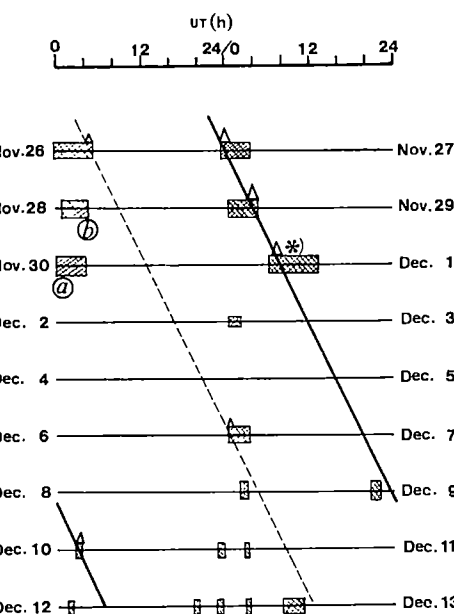
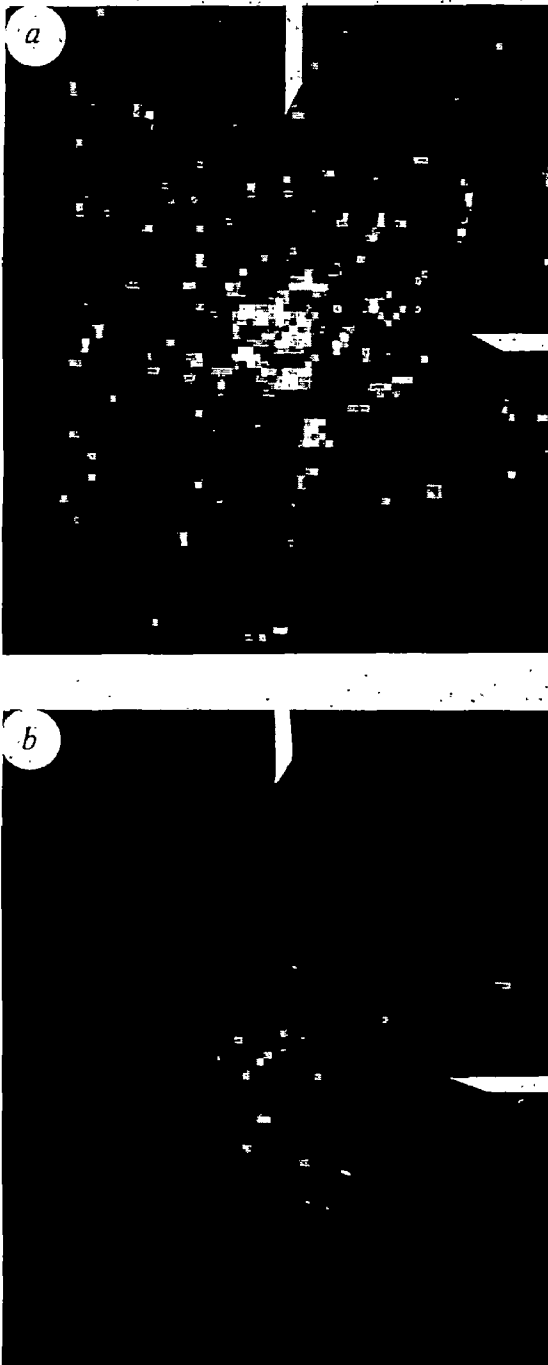


Fig. 1 Time-sequential plot of observation intervals and activities of the hydrogen coma. Cross-hatched sections represent the observational time intervals. Triangular spikes indicate the times when the images taken included central bright pixels, suggesting the appearance of a jet. Diagonal lines crossing the figure have a slope of 2.2 days periodicity (solid line, strong outburst; broken line, weak outburst). The asterisk indicates that the images on this interval are taken in a compressed mode (to save data transmission time). The times when the images in Figs 2 and 3 were taken are indicated (@, B).

the phenomenon could be interpreted as the occurrence of a strong outburst. These events are observed repeatedly at 23:00 26 November, 04:00 29 November and 09:00 1 December. With the appearance of this new hydrogen atom source, the images become brighter (Fig. 2a), then gradually fade away as the hydrogen atom density decreases with the expansion of the hydrogen coma. The ultimate image is similar to Fig. 2b. A very similar sequence of events was observed during the week starting 9 December. In particular, the flash at 04:00 10 December was essential in determining the period of the Lyman- $\alpha$  radiance variation.

The difference between the active and inactive phases of the hydrogen coma suggests that the outburst phenomena overwhelm the other activity of this comet, at a heliocentric distance of  $\sim 1.5$  AU. The time interval between flashes (strong outbursts) suggests a preliminary value of  $2.2 \pm 0.1$  days for the period of this activity. The rotational period of comet Halley is still controversial, but the above value is close to 2.23 days, the value derived by Sekanina and Larson<sup>4,5</sup> from the analysis of dust behaviour in the 1910 apparition. It is also about five times the period of 10 h estimated by Whipple<sup>7</sup>, and about twice the value proposed by Le Fevre *et al.*<sup>8</sup>. This last value has been criticized by West and Pedersen<sup>9</sup>.

Expansion of the hydrogen atoms produced from photodissociation of the water outburst will form a shell structure, propagating with time in the hydrogen coma, because the velocity of the hydrogen atoms is much higher than that of the parent molecules. The image in Fig. 2a shows such a shell, with a radius of about  $0.58 \times 10^6$  km. At the comet's present location, the photodissociation time of water is about 2 days, comparable to the characteristic travel time of the hydrogen atoms in the coma; therefore, the width of the shell is very large. When Suisei



**Fig. 2** Lyman- $\alpha$  images of the hydrogen coma of comet Halley taken at *a*, 00:00 30 November UT (active phase) and *b*, 04:00 28 November UT (inactive phase). The vertical and horizontal dimensions of the photographs are both  $2.5 \times 10^6$  km (at the comet's position). The comet nucleus (located at the intersection of the white marker wedges) is at (right ascension, declination) = (01 h 41 m, 15° 50') on the 1950.0 star atlas in *a* and (01 h 56 m, 16° 50') in *b*. The distances of comet Halley from the Sun and Suisei are *a*, 1.50 and 0.84 AU, and *b*, 1.53 and 0.83 AU. The faintness of this image suggests that the outburst phenomena overwhelm the other activity of this comet.

encounters the comet, on 8 March 1986, we would expect the shell to have a more sharply defined form due to the shorter photodissociation time. Our continuous observations over the next several months will allow detailed spatial and temporal studies of the hydrogen coma in comet Halley.

We thank the many people in ISAS engaged in the Planet-A mission project; in particular, Professor M. Oda for valuable discussions; also Dr J. Hughes (Harvard-Smithsonian Center for Astrophysics) for his linguistic help.

Received 31 December 1985; accepted 23 January 1986.

1. Wyckoff, S. *et al.* *Nature* **316**, 241–242 (1985).
2. Wallis, M. K. & Wickramasinghe, N. C. *Mon. Not. R. astr. Soc.* **216**, 453–458 (1985).
3. Keller, H. U. *Space Sci. Rev.* **18**, 641–684 (1976).
4. Sekanina, Z. & Larson, S. M. *Astr. J.* **89**, 1408–1425 (1984).
5. Sekanina, Z. *Proc. Interagency Consulting Group*, Working Group 1, 5 (IACG, Pasadena, 1985).
6. Hirao, K. & Kaneda, E. *Adv. Space Res.* **2**, 167–169 (1983).
7. Whipple, F. L. in *Comets* (ed. Wilkening, L. L.) 227–250 (University of Arizona Press, 1982).
8. Le Fevre, O. *et al.* *Astr. Astrophys.* **138**, L1–L4 (1984).
9. West, R. M. & Pedersen, H. *Astr. Astrophys.* **138**, L9–L10 (1984).

## Electromagnetic angular momentum transport in Saturn's rings

C. K. Goertz\*,†, G. E. Morfill†, W. Ip‡,  
E. Grün§ & O. Havnes||

\* Department of Physics and Astronomy, University of Iowa, Iowa City, Iowa 52242, USA

† Max-Planck-Institut für Physik und Astrophysik, Institut für extraterrestrische Physik, 8046 Garching, FRG

‡ Max-Planck-Institut für Aeronomie, D-3411 Katlenburg-Lindau, FRG

§ Max-Planck-Institut für Kernphysik, D-6900 Heidelberg, FRG

|| Aurora Observatory, University of Tromsø, P.B. 953, N-9001, Tromsø, Norway

The observed 'spokes' in Saturn's rings have been interpreted as consisting of elevated, sub-micrometre sized dust particles<sup>1</sup>. Arguments in favour of this interpretation are, for example, the photometric properties (spokes are dark in backscattered, bright in forward scattered light), the dynamics (approximate keplerian rotation) and lifetime (less than half an orbital period). We show here that submicrometre dust particles sporadically elevated above the ring are subject to electromagnetic forces which will reduce their angular momentum inside synchronous orbit and increase it outside. When the dust is reabsorbed by the ring the angular momentum of the ring is decreased (increased) inside (outside) of synchronous orbit. For the case of the spokes in Saturn's B-ring we estimate that the timescale for transporting ring material due to this angular momentum coupling effect is comparable to the viscous transport time or even smaller. We suggest that the minimum in the optical depth of the B-ring at synchronous orbit is due to this effect.

The temporal evolution of Saturn's rings is believed to be primarily determined by the angular momentum transport as a consequence of collisions between the differentially rotating ring particles<sup>2</sup>. In addition, mass erosion effects, meteor impacts, resonances with satellites and moonlets and density waves<sup>3–5</sup> are important. So far, electromagnetic effects have not been considered to be important because the electromagnetic forces on the typical big ( $\sim 1$  m) ring particles are small compared with the gravitational force of the planet<sup>6</sup>. Only submicrometre dust particles are significantly influenced by electromagnetic effects. We now discuss a potentially very important indirect mechanism whereby electromagnetic forces can affect the angular momentum transport in the ring and hence its long-term evolution. This indirect mechanism works through the small dust particles constituting the spokes. Note that if the spokes do not consist of elevated dust, but only of a rearrangement of dust particles in the ring plane, our mechanism would probably not be relevant. However, as mentioned earlier, the available evidence favours elevated dust, and then it is easily demonstrated that the effect is important. The spokes of Saturn have an optical depth of

$\tau \approx 0.1$ , and cover a fraction  $\eta \approx 0.05$  of the B-ring between  $1.7 R_p$  and  $1.9 R_p$  (planetary radii). The mean particle size is  $s = 3 \times 10^{-5}$  cm. The total mass in the spokes is thus

$$M_s = 0.7 \frac{4\pi}{3} s t \rho_s \eta R_p^2$$

For a nominal material density of the spoke particles  $\rho_s = 1 \text{ g cm}^{-3}$  we obtain  $M_s \approx 3 \times 10^{15} \text{ g}$  (see also ref. 6). We argue below that during the time a spoke particle is elevated it has an average radial velocity of  $\sim 10^2 \text{ cm s}^{-1}$ . Thus the total mass of the B-ring ( $7 \times 10^{21} \text{ g}$ ) could be transported over a distance of  $0.2 R_p$  in  $10^8 \text{ yr}$ .

Consider a dust particle of mass  $m$  ejected at a radial distance  $r$  out of the ring plane. It has a charge  $Q$ . Its velocity is  $v_r \hat{r} + v_\phi \hat{\phi}$ . If the planetary magnetic field corotates, the particle will be subject to a Lorentz force

$$\vec{F} = m \frac{d\vec{v}}{dt} = Q[v_r \hat{r} + (v_\phi - \Omega_p r) \hat{\phi}] \times \frac{\vec{B}}{c} - \frac{GM_p m}{r^2} \hat{r} \quad (1)$$

where  $\Omega_p$  is the rotation rate of the planet,  $G$  the gravitational constant and  $c$  the speed of light. From the  $\phi$  component of equation (1), we get ( $\phi$  is in the direction of the ring particle rotation)

$$\frac{d}{dt} \mathcal{L} = v_r \frac{a}{r^2} \quad (2)$$

where  $\mathcal{L} = rv_\phi$  is the specific angular momentum of the particle. We have assumed a dipole field, near the equatorial plane this is

$$\vec{B} = -B_0 \left( \frac{R_p^3}{r^3} \right) \hat{z} \quad (3)$$

and have introduced

$$a = \left( \frac{QB_0}{mc} \right) R_p^3$$

For Saturn  $B_0 = 0.2 \text{ G}$ , and the planetary radius is  $R_p = 6 \times 10^9 \text{ cm}$ . When the particle is reabsorbed by the ring after a mean time,  $t_L$ , it has changed its specific angular momentum by an amount

$$\Delta \mathcal{L} = \int_0^{t_L} \frac{d\mathcal{L}}{dt} dt \quad (4)$$

Since we are concerned here with particle populations, it is convenient to introduce the angular momentum per unit surface area

$$\tilde{\mathcal{L}} = \sigma \mathcal{L} \quad (5)$$

where  $\sigma$  is the surface density. In the following, we shall use subscripts R and S for rings and spokes, respectively. The rate of change of ring angular momentum can then be easily calculated.

Since in the absorption process of spoke material the total angular momentum must be conserved, the only angular momentum lost by the system is that calculated from equations (2)-(5). Hence,

$$\frac{d\tilde{\mathcal{L}}_R}{dt} = \frac{d\tilde{\mathcal{L}}_S}{dt} \quad (6)$$

The rate of change of the specific ring angular momentum is then

$$\frac{d\mathcal{L}_R}{dt} = \frac{\sigma_S v_r a}{\sigma_R r^2} \quad (7)$$

from which we may compute the timescale for angular momentum change of the ring

$$\tau_R = \mathcal{L}_R \left( \frac{d\mathcal{L}_R}{dt} \right)^{-1} = \frac{\sigma_R r^2 \mathcal{L}_R}{\sigma_S v_r a} \quad (8)$$

For all practical purposes, we may put  $\mathcal{L}_R = \mathcal{L}_K$ , the Kepler

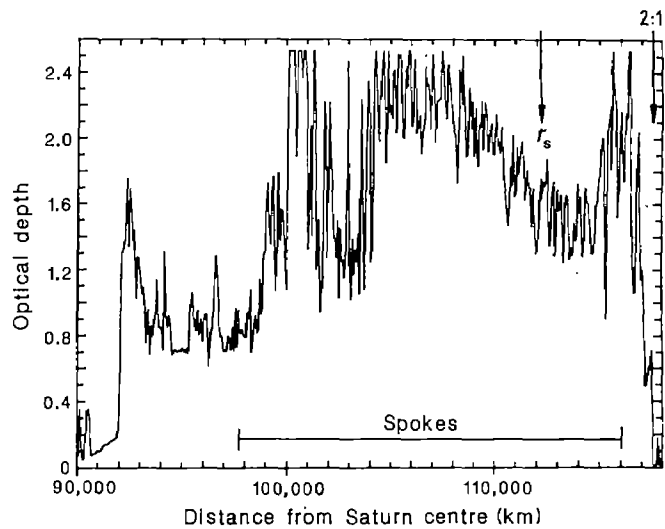


Fig. 1 Optical depth variation in Saturn's B-ring<sup>10</sup>. The horizontal line indicates the observed extent of spoke activity. The synchronous radius and the Mimas 2:1 resonance positions are also shown.

value  $\sqrt{GM_p r}$ . The radial evolution of the ring material is characterized by a velocity

$$w = \frac{2r}{\mathcal{L}_R} \frac{d\mathcal{L}_R}{dt} = \frac{2\sigma_S v_r a}{\sigma_R r \mathcal{L}_R} \quad (9)$$

The radial velocity at impact can be calculated from equation (1).

$$v_r \approx - \left( \frac{QB_0}{mc} \right) \frac{R_p^3}{r^2} \left( \frac{v_\phi - \Omega_p}{r} \right) t_L \quad (10)$$

To simplify matters we assume that the azimuthal velocity of the particle is everywhere the keplerian velocity. This is a good approximation as long as  $\Delta r/r \ll 1$ . Thus the effective radial mass transport velocity is (we use  $L = r/R_p$ )

$$w \approx - \left( \frac{QB_0}{mc} \right)^2 \frac{R_p}{L_S^5} \frac{\sigma_S}{\sigma_R} \left[ \left( \frac{L_S}{L} \right)^5 - \left( \frac{L_S}{L} \right)^{7/2} \right] t_L \quad (11)$$

Inside the synchronous orbit ( $r_s = R_p L_S$ , where  $\Omega_k = \Omega_p$ ) the mass transport is inwards, it is zero at synchronous orbit and outwards beyond  $r_s$ .

We note that the direction of the mass transport is independent of the charge sign. The reason is that inside synchronous orbit keplerian dust particles move faster than the corotating magnetic field and, therefore, always lose angular momentum to the planet (irrespective of the charge sign) whereas they gain angular momentum from the planet outside synchronous orbit. This change of angular momentum of one component determines the evolution of the whole ring material. If the small particles remained in the ring they would quickly collide with, and be absorbed by, the large ring particles. In that case  $t_L$  would be small. If the elevated particles were bigger  $\sigma_S = 4/3 \rho_s s r$  increases. However, if the charge is proportional to particle radius,  $s$ , (implying constant potential),  $w$  is inversely proportional to  $m$ , and the significance of the effect is reduced accordingly. The angular momentum coupling to the planet is thus most significant if small dust particles can be elevated above the ring plane, that is, where spoke-like activity occurs in the ring. These considerations suggest that the spokes in Saturn's B-ring, so far regarded as a curious phenomenon without major consequences, may significantly affect the long term evolution of the B-ring itself.

To make some numerical estimates of the effect, we consider the following. The spokes in Saturn's B-ring presumably consist of ice grains with an average size of  $s = 3 \times 10^{-5}$  cm ( $m = 10^{-13}$  g).

The azimuthally-averaged mass density is  $\sigma_s = \tau_s \eta m / \pi s^2 = 1.5 \times 10^{-6} \text{ g cm}^{-2}$  for  $\tau_s = 0.1$  and the fractional area covered,  $\eta = 0.05$  (ref. 6). If spokes exist below the Voyager contrast or resolution level, which seems likely, then our estimates can be regarded as a conservative lower limit. The lifetime of a spoke is  $t_L = 9 \times 10^3 \text{ s}$  (ref. 7). The average charge of a spoke particle is not well known. Goertz<sup>8</sup> argues that  $Q = -200 e$  whereas Eplee and Smith<sup>9</sup> suggest that  $Q$  can be as large as  $Q = -10,000 e$ . Here  $e$  is the electronic charge. The ring surface density  $\sigma_R$  is taken to be  $60 \text{ g cm}^{-2}$  (ref. 2). The effective radial mass transport velocity is

$$w \approx -1.2 \times 10^{-10} \left( \frac{Q}{e} \right)^2 \left[ \left( \frac{L_s}{L} \right)^5 - \left( \frac{L_s}{L} \right)^{7/2} \right] \text{ cm s}^{-1}$$

At  $L = 1.8$  the velocity  $w$  is  $7.0 \times 10^{-12} (Q/e)^2 \text{ cm s}^{-1}$ . The transport velocity due to the ring viscosity is given by  $-\nu/r$  with  $\nu \approx 20 \text{ cm}^2 \text{ s}^{-1}$  a typical value in the B-ring<sup>1</sup>. At  $L = 1.8$  this is  $\sim 2 \times 10^{-9} \text{ cm s}^{-1}$ . Thus mass transport due to electromagnetic angular momentum coupling to Saturn is of comparable importance even for  $Q/e = 30$  except very close to the synchronous orbit ( $L = L_s = 1.86$ ). We note that the radial velocity of the spoke particles  $v_r = -4.3(Q/e) \text{ cm s}^{-1}$  at  $L = 1.8$ . The electromagnetic angular momentum timescale, as defined by equation (8), becomes

$$\tau_R = 2.2 \times 10^{18} \left( \frac{Q}{e} \right)^{-2} L^6 \left[ 1 - \left( \frac{L}{L_s} \right)^{3/2} \right]^{-1} \text{ s}$$

At  $L = 1.8$ , and for  $Q/e = 100$ , this yields about  $5 \times 10^9 \text{ yr}$ . Viscous time scales,  $\tau_{vis} = r^2/\nu$ , on the other hand give  $\sim 2 \times 10^{11} \text{ yr}$ .

The viscosity of a particulate disk is a complex and not well understood function of the ring mass density<sup>2</sup>. In general, there will always be some particle diffusion due to collisions, as well as the systematic radial drift  $-\nu/r$ . We will discuss this elsewhere. Here we just note that a steady-state solution of the transport problem, including viscous and electromagnetic effects, will display a minimum in the B-ring near, but outside of the synchronous orbit. Figure 1 shows the optical depth variation of the B-ring on a linear scale. It clearly shows such a minimum. If the optical depth of the B-ring was originally constant at  $-2.5$ , corresponding to the values outside the 'synchronous minimum', then the equivalent displaced mass corresponds to  $9 \times 10^{20} \text{ g}$ , about 13% of the current ring mass. The timescale for displacing this mass can be estimated from the above considerations, and is significantly less than the lifetime of Saturn. If the electromagnetic angular momentum transport process really works as efficiently as we have calculated (this depends on the charge, mass and elevation of spoke particles) this implies that Saturn's ring system is not primordial, or that spoke activity has not been continuous.

We have shown that the sporadic elevation of small dust particles above Saturn's ring, and their subsequent reabsorption, provides a mechanism for angular momentum coupling to the planet, provided the dust particles are charged. There is clear evidence that the spoke particles are, indeed, charged. Then the ring loses angular momentum inside synchronous orbit and thus moves towards the planet, whereas it gains angular momentum and moves away from the planet outside synchronous orbit. In this picture, the outer boundary of the B-ring follows quite naturally.

At  $L = 1.9485$ , angular momentum is transferred by strong gravitational torques to the moon Mimas (2:1 resonance). In this way, excess angular momentum is removed, and the ring material is clamped in place. The positional agreement between the outer B-ring boundary and the Mimas 2:1 resonance is very good.

One may even speculate that the A-ring has evolved away from this resonance under the past influence of spoke-like

phenomena, or even due to the current action of weak activity below the Voyager observational threshold.

Using reasonable values for the charge of the spoke particles, and observed ring and spoke properties, we have shown that the timescales for B-ring evolution due to the momentum coupling discussed here are comparable with, or even smaller than, viscous evolution timescales.

This effect, combined with some stochastic spreading, should produce a minimum in the optical depth of the ring near, but just outside synchronous orbit. Such a minimum seems, indeed, to exist. We also note that the transport due to the momentum coupling should affect the viscous instability discussed in connection with the formation of ringlets<sup>2</sup> as well as the resonantly driven density and bending waves. Since spokes are observed only in the outer B-ring this may be less important for the waves in the A and C rings.

In addition, the momentum coupling introduced across the ring by the processes discussed here, may lead to instabilities by themselves. This will be discussed elsewhere (C.K.G. and G.E.M., in preparation).

C.K.G. thanks the NSF for support under grant ATM 81-11112 and NASA contracts NSC-7632, NGL-16-001-043 and NAGW-364. The hospitality of the Auroral Observatory, University Tromsø, in organizing a 'midnight sun' workshop on 'dust plasmas' is gratefully acknowledged.

Received 5 August 1985; accepted 10 January 1986.

1. Terrile, R. J., Yagi, G., Cook, A. F. & Porco, C. C. *Bull. Am. astr. Soc.* 13, 728 (1981)
2. Stewart, G. R., Lin, D. N. C. & Bodenheimer, P. in *Planetary Rings* (eds Greenberg, R. & Brahic, A.) 447 (University of Arizona Press, Tucson, 1984)
3. Durisen, R. M. in *Planetary Rings* (eds Greenberg, R. & Brahic, A.) 416 (University of Arizona Press, Tucson, 1984)
4. Shu, F. H. in *Planetary Rings* (eds Greenberg, R. & Brahic, A.) 413 (University of Arizona Press, Tucson, 1984)
5. Dermott, S. in *Planetary Rings* (eds Greenberg, R. & Brahic, A.) 589 (University of Arizona Press, Tucson, 1984)
6. Grün, E., Morfill, G. E. & Mendis, D. A. in *Planetary Rings* (eds Greenberg, R. & Brahic, A.) 275 (University of Arizona Press, Tucson, 1984)
7. Grün, E., Garneau, G. W., Terrile, R. J., Johnson, T. V. & Morfill, G. *Adv. Space Res.* 4, 143-xxx (1984)
8. Goertz, C. K., *Adv. Space Res.* 4, 137-xxx (1984)
9. Eplee, E. & Smith, B. *Icarus* 63, 304 (1985)
10. Esposito, L. W. et al. *J. geophys. Res.* 88, 8643 (1983)

## Plasmatization and recondensation of the saturnian rings

W.-H. Ip

Max-Planck-Institut für Aeronomie, D-3411 Katlenburg-Lindau, FRG

**One major puzzle from the ground-based and Voyager observations of the saturnian system concerns the presence of the E ring and its possible relationship to the icy satellite, Enceladus<sup>1-3</sup>.** Several issues concerning the surface property and interior condition of Enceladus remain unresolved if it is the main supplier of the E-ring particulate matter. Here we explore the intriguing alternative that the mass supply and orbital configuration of the E ring may be derived from a mass and momentum coupling between the A ring and the tenuous E ring a process of plasmatization and recondensation of the A-ring icy material. In the same way, the C ring could be replenished by the B ring. In this new view, plasma transport has a very important role in the dynamical evolution of the saturnian ring system.

The possible importance of plasma transport in the redistribution of the mass of Saturn's rings has been discussed elsewhere<sup>4-8</sup>. The basic idea is that charged particles situated at the ring plane would be lost to the planetary surface by field-aligned motion if the radial distance is smaller than a certain critical value. For charged particles initially in co-rotation, for which the magnetic moment is negligibly small, the critical radius is  $R_c = 1.625R_s$  (where  $R_s$  is the radius of Saturn); and for

keplerian-launched charged particles with their magnetic moments defined by the difference between the co-rotational speed and the keplerian speed, the critical radius is  $R_c = 1.525 R_s$ , as determined by Northrop and Hill<sup>5</sup> using the Z3 magnetic model<sup>9</sup> and the  $J_2$  and  $J_4$  terms<sup>10</sup> of the gravitational field of Saturn.

The critical radius  $R_c$  is located near a sharp transition in brightness in the B ring at  $R = 1.64 R_s$ , and the second critical radius  $R'_c$  is situated only 20 km away from the inner edge of the B ring<sup>4,7</sup>. Plasma transport could therefore be instrumental in defining the ring mass distribution. Note that although Northrop and Hill considered the relevant charged particles to be tiny icy grains with a very large value of  $q/m$  (where  $q$  and  $m$  are, respectively, the charge and mass of the particles), I stressed the role of large water cluster ions in the mass-loss process (or siphon flow)<sup>6</sup>. In principle, these two types of charged particle are the same as long as the charge-to-mass ratio is effectively very large. In the following we refer to the charged particles under discussion as water cluster ions and their parent neutral particles as water clusters, to distinguish their ring origin. If the loss rate of the water cluster ions remains the same throughout the existence of the ring system, which may be as short as  $10^8$  yr from dynamical considerations<sup>11-14</sup>, the average mass injection rate from the ring plane for  $R < 1.63 R_s$  to the planetary atmosphere would be  $\dot{\sigma} = \sigma/10^8$  yr  $\approx 3.2 \times 10^{-14}$  g cm $^{-2}$  s $^{-1}$  or  $\dot{M} \approx 4 \times 10^6$  g s $^{-1}$  if the surface density is  $\sigma \approx 100$  g cm $^{-2}$ . This large influx of water ions and molecules could be very important in modifying the ionosphere of Saturn (by electron depletion), as discussed elsewhere<sup>6,15,16</sup>.

One consequence of the ionization of the ring material is that the water cluster ions will be accelerated or decelerated to co-rotational motion depending on where they are produced. For those stably trapped in field-aligned motion (that is, not lost to the planetary atmosphere because of the siphon flow effect), they may be directly reabsorbed by the rings during their bounces across the ring plane. As the water clusters recondense on the surfaces of larger ring particles, they will be decelerated or accelerated to keplerian motion. This implies a very efficient method of exchange of angular momentum between the rings and Saturn. For orbital distances larger than the co-rotation distance ( $R_{syn} = 1.86 R_s$ ), there will be an acceleration effect with angular momentum transfer from Saturn to the rings, whereas the opposite effect holds for  $R < R_{syn}$  (ref. 8). It can be estimated that the ring torque from ionization and recycling of the ring material is of the order of  $\dot{L} \sim 5 \times 10^{-21}$  g cm $^2$  s $^{-1}$  as far as the A ring is concerned<sup>17</sup>; this value is comparable to the torque in the opposite direction from gravitational interaction with the shepherding satellites and the co-orbital satellites<sup>11,18</sup>. It is thus clear that the electrodynamic effect from ring plasmatization could be of importance in holding the A ring in place.

In addition to direct recondensation of the water (ion) clusters, another way to transfer mass and angular momentum is through accretion of the particles flung into elliptical keplerian orbits or ballistic escape orbits after their neutralization from the ring plasma. For cold ring plasma (as indicated by the brightness variation at  $1.63 R_s$ ), the keplerian orbit of a neutralized particle will be determined by the radial distance ( $R_o$ ) at neutralization and the angular momentum ( $L_o$ ). From conservation of angular momentum and the condition of force balance of a particle in circular keplerian motion, the radial position of this 'projected' particle ( $R_k$ ) can then be determined.

Because the planet itself represents a perfect absorber, particles with flight paths intercepting Saturn will be lost after the first launch. This condition then defines the inner limit of the inward projection of the plasmatized ring matter (originating from  $R < R_{syn}$ ). Our computation, taking into account the  $J_2$  and  $J_4$  terms of the gravitational field, indicates that this limit is given as  $R_{k,min} = 1.258 R_s$  for  $R_{o,min} = 1.691 R_s$ . If the C ring forms by the accretion of ring material injected from the B ring to balance the loss through siphon flow, the consideration of

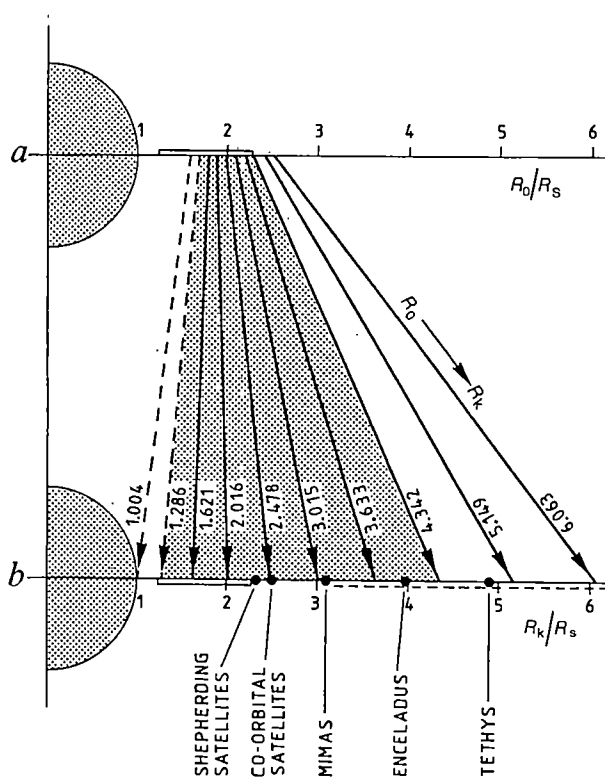


**Fig. 1** Angular momentum projection of the ionized ring material in the form of charged particles with  $q/m \rightarrow \infty$  after their neutralization. Conservation of angular momentum allows the determination of the orbital radius ( $R_k$ ) of a particle flung into keplerian orbit (b) from its radial distance ( $R_o$ ) at neutralization (a). Because of the absorption effect of the planet, neutral particles ejected inside  $R = 1.69 R_s$  from co-rotating motion will be lost after the first launch. This process may define the inner edge of the C ring. At the same time, material ejected from the A ring would define the spatial extension of the E ring via angular momentum redistribution.

the angular momentum budget would imply that the inner boundary of the C ring should be given approximately by  $R_{k,min}$ . The value of  $R_{k,min}$  is indeed almost the same as the observed inner edge of the C ring taken to be at  $1.235 R_s$ . The slight discrepancy could be explained, for example, by the thermal spread of the water cluster ions or collisional scattering effects.

The E ring, which has a peak brightness near the orbit of Enceladus, has generally been thought to be the product of mass ejection from the surface of this icy satellite<sup>1-3</sup>. The E-ring particles, with an average size determined to be a few micrometres<sup>19</sup>, have very short lifetimes against energetic charged particle sputtering and plasma drag (outward) transport<sup>20,21</sup>. Both mechanisms typically have timescales of the order of  $10^3$ - $10^4$  yr. If the E-ring system is to be maintained as a permanent structure, it will require a steady source<sup>22</sup>. Below, we consider the possible contribution from the material ejected from the main ring system.

As shown in Fig. 1, the particles neutralized from the ring plasma at different locations in the A ring will have angular momentum corresponding to  $R_k$  between  $3.0 R_s$  and  $4.0 R_s$ . This means that interception of these particles in ballistic flight by the E ring beyond  $4 R_s$  will lead to braking of the outward motion of the charged E-ring particles as a result of interaction with co-rotating thermal plasma. Furthermore, accretion of these water clusters will lead to replenishment of the material lost by the surface sputtering effect. The mass erosion rate of the E ring may be estimated as follows. For an average optical depth of

$\tau_E = 3 \times 10^{-7}$ , a total area of  $S_E \approx 1.7 \times 10^{21} \text{ cm}^2$  and an average particle size of  $d = 3 \mu\text{m}$ , the total mass erosion rate can be given as  $\dot{M}_E \approx -0.6 \text{ g s}^{-1}$  if the sputtering timescale is  $10^4 \text{ yr}$ .

The injection rate and accretion rate of the water clusters from the A ring are more difficult to derive because the whole sequence of ionization, neutralization and final collisional assimilation must be very complicated. But we could use the C ring as a reference point in the sense that the maintenance of the C ring is conditioned by balancing the mass loss rate (through siphon flow) with the mass accretion rate (from the B ring):

$$\frac{\tau_c S_c}{t_s} = \frac{\tau_B S_B}{t_a} \quad (1)$$

where  $t_s$  is the loss timescale and  $t_a$  the accretion timescale. From equation (1),  $t_a \approx (\tau_B/\tau_c)t_s$  or  $t_a \approx 20t_s$  (for equal areas:  $S_c \approx S_B$ ) as the optical depth of the C ring is  $\tau_c = 0.1$  and that of the B ring  $\tau_B = 2$ . When applied to the E ring, the effective value of the accretion timescale of matter injected from the A ring should be scaled by the probability of interception ( $P$ ). As  $P_c \approx 0(1)$  and  $P_E \approx 0(10^{-5})$ , the total mass accretion rate will be

$$\dot{M}_E^* \sim \frac{10^{-5} f \tau_A S_A}{t_a} \quad (2)$$

where  $f = 100 \text{ g cm}^{-2}$  is the factor converting optical depth to surface density,  $\tau_A = 0.5$ , and  $S_A = 10^{20} \text{ cm}^2$ . Thus, for  $t_a \approx 2 \times 10^9 \text{ yr}$ ,  $\dot{M}_E^* \approx 0.8 \text{ g s}^{-1}$ ; and it can be seen that  $\dot{M}_E^* \approx |\dot{M}_E|$ . This much simplified calculation therefore shows that the E-ring complex could be partially maintained by accretion of the A-ring water grains as well as acquisition of the corresponding angular momentum. Thus, the E ring could have a lifetime much larger than  $10^4 \text{ yr}$  as estimated before.

In general, the plasmatization model of the rings requires the presence of many water clusters in the ring system. To maintain the loss rate of  $\dot{M} \approx 4 \times 10^6 \text{ g s}^{-1}$  and with photoionization as the only net ionization effect (timescale assumed to be  $\sim 10^9 \text{ s}$ ), the average number density of the water clusters (assumed to contain 1,000  $\text{H}_2\text{O}$  molecules each) would be  $n_{\text{cluster}} \approx 10^7\text{--}10^8 \text{ cm}^{-3}$  in the ring plane with a thickness  $\leq 10^2 \text{ km}$ . Their existence can be tested by remote sensing methods or by *in situ* measurements. Neglecting the interception effect by the E ring, from equation (2) we have the total escape flux  $N \approx 10^5 \dot{M}_E/m_{\text{cluster}} \approx 2 \times 10^{24} \text{ s}^{-1}$ . It is of interest to search for these water clusters and ions (after their re-ionization) in the magnetosphere of Saturn using appropriate ion and neutral detectors/analyzers.

Let us consider the physical constraints on the generation of cluster ions. Hypervelocity impact experiments have shown that tiny condensates form as part of the impact ejecta (E. Grün, personal communication). One reason for their formation may be related to the supersaturation (and hence recondensation) effect in the adiabatically cooling outflow of the expanding impact vapour. Secondary cluster ions have also been detected and analysed in ion sputtering experiments<sup>23</sup>. In the D-region of the Earth's ionosphere, water cluster ions are very abundant as a result of ion-neutral reactions<sup>24</sup>. As for the required number density of such large cluster ions, we shall adopt the assumption that there is a population of cool plasma stored in the so-called 'free-zone' just above the ring plane<sup>25</sup>. Taking the vertical displacement of the centre of the azimuthally symmetrical magnetic field to be  $\sim 0.04 R_s$  (ref. 9), the total volume of the plasma disk so formed can be estimated to be  $V \approx 1-8 \times 10^{28} \text{ cm}^3$ . Assuming that the ring plasma contains mainly electrons and singly ionized cluster ions, we have the total mass loss rate caused by electronic recombination given as  $\dot{M}_c \approx \alpha_e m_e (n_e^+)^2 V$ , with  $\alpha_e$  as the electronic recombination coefficient and  $n_e^+$  as the number density

of the cluster ions in the free-zone. In laboratory studies<sup>26</sup>,  $\alpha_e$  for water cluster ions  $\text{H}_3\text{O}^+(\text{H}_2\text{O})_n$  with  $n = 0-6$  has been determined to be rather large ( $\sim 10^{-5} \text{ cm}^3 \text{ s}^{-1}$ ). Now, equating  $\dot{M}_c$  to  $10^5 \dot{M}_E$  we find  $n_e^+ \approx 2-11 \text{ cm}^{-3}$ , which is reasonably small. (Taking the larger value of  $n_e^+ \approx 11 \text{ cm}^{-3}$ , which may be more appropriate for a thin plasma disk, the corresponding electronic recombination time is of the order of  $10^4 \text{ s}$ , which is a fraction of the bouncing period of the cluster ions and the planetary rotation period.)

In the estimate of the accretion probability  $P_E$ , it was assumed that the water clusters pass through the E ring only once. In fact, in the present scenario, the water clusters emitted at radial distance less than  $2.34 R_s$  will be in periodic elliptical orbits, and they could return to the E-ring region repeatedly until lost by ionization or impact. For instance, for  $R_o = 2.20 R_s$  (and  $R_k = 3.70 R_s$ ), there will be about 10 returns if the ionization time is about  $2 \times 10^6 \text{ s}$ . This effect will increase the  $P_E$  value by a factor of 10 and leads to a reduction of the total recombination rate by a similar factor. This means the momentum coupling between the A ring and the E ring should require only a moderate amount of mass ejection from the A ring. Note that, besides water clusters, atoms and molecules like H, O and  $\text{H}_2\text{O}$  (and thus their ionized counterparts) could in principle perform the same function in mass and momentum transfer. The role of large water clusters and cluster ions is emphasized here, as they would imply a very small value of electron number density ( $n_e \lesssim 10 \text{ cm}^{-3}$ ) along the magnetic flux tubes in the siphon flow process, whereas for atomic and molecular ions,  $n_e \approx 10^3\text{--}10^4 \text{ cm}^{-3}$  is required. More quantitative work should clarify this point further.

Finally, we note that the proposed scenario of the plasmatization and recondensation of the saturnian ring system is reminiscent of the model of Alfvén<sup>27</sup> which relates the mass distribution of the rings to the condensation process in a rotating plasma. The important difference is that the present model applies to the redistribution of ring matter after the initial formation of the ring system. We also note that other electromagnetic angular momentum transfer processes such as that discussed in the case of charged dust particles<sup>28</sup> could be important and complementary to the one described here.

Received 23 July 1985; accepted 14 January 1986.

1. Baum, W. A. *et al.* *Icarus* **47**, 84–96 (1980).
2. Larson, S. M., Fountain, J. W., Smith, B. A. & Reitsema, H. J. *Icarus* **47**, 288–290 (1981).
3. Smith, B. A. *et al.* *Science* **215**, 504–537 (1982).
4. Northrop, T. G. & Hill, J. R. *J. geophys. Res.* **87**, 6045–6051 (1982).
5. Northrop, T. G. & Hill, J. R. *J. geophys. Res.* **88**, 6102–6108 (1983).
6. Ip, W.-H. *J. geophys. Res.* **88**, 819–822 (1983).
7. Ip, W.-H. *J. geophys. Res.* **89**, 395–398 (1984).
8. Ip, W.-H. *Adv. Space Res.* **4**, 53–62 (1984).
9. Connerney, J. E. P., Ness, N. F. & Acuna, M. H. *Nature* **298**, 44–46 (1982).
10. Null, G. W., Lau, E. L., Biller, E. D. & Anderson, J. D. *Astr. J.* **86**, 456–468 (1981).
11. Lissauer, J. J., Peale, S. J. & Cuzzi, J. N. *Icarus* **58**, 159–168 (1984).
12. Henon, M. in *Planetary Rings* (ed. Brahic, A. 361–384 (Capadouze, Toulouse, 1984).
13. Morfill, G. E., Fechtig, H., Grün, E. & Goertz, C. K. *Icarus* **55**, 439–457 (1973).
14. Ip, W.-H. *Icarus* **60**, 547–552 (1984).
15. Shimizu, H. *Moon Planets* **22**, 521–522 (1980).
16. Connerney, J. E. P. & Waite, J. H. *Nature* **312**, 136–138 (1984).
17. Ip, W.-H. in *Proc. Charged Particle Transport in Plasmas*, Spring College on Plasma Physics, Int. Center for Theoretical Physics, Trieste (World Scientific, Singapore, in the press).
18. Lissauer, J. J. & Cuzzi, J. N. *Astr. J.* **87**, 1051–1058 (1982).
19. Pang, K. D., Voge, C. C. & Rhoads, J. W. in *Planetary Rings* (ed. Brahic, A.) 607–614 (Capadouze, Toulouse, 1984).
20. Morfill, G. E., Grün, E. & Johnson, T. V. *J. geophys. Res.* **88**, 5571–5579 (1983).
21. Lanza, L. J. *et al.* *J. geophys. Res.* **88**, 8765–8770 (1983).
22. Haff, P. K., Eviatar, A. & Siscoe, G. L. *Icarus* **56**, 426–438 (1983).
23. Lancaster, G. M., Honda, F., Fukuda, Y. & Rabalais. *J. Am. chem. Soc.* **101**, 1951–1953 (1979).
24. Arnold, F., Krankowsky, D. & Marien, K. H. *Nature* **267**, 30–32 (1977).
25. Ip, W.-H. *Nature* **302**, 599–601 (1983).
26. Smith, D., Adams, N. G. & Church, M. J. *Planet. Space Sci.* **24**, 697–703 (1976).
27. Alfvén, H. *On the Origin of the Solar System* (Clarendon, Oxford, 1954).
28. Goertz, C. K. *et al.* *Nature* **320**, 141–143 (1986).

## Random fluctuations versus Poynting–Robertson drag on interplanetary dust grains

Max K. Wallis

Department of Applied Mathematics and Astronomy, University College, Cathays Park, Cardiff CF1 1XL, UK

A particle moving through a sea of stochastic impulses gains energy from the sea; this is a long-established property of Brownian motion, given theoretical backing in the fluctuation-dissipation theorem<sup>1</sup>. However, this energy gain is generally neglected in describing circumstellar dust grains as slowly spiralling into the central star under Poynting–Robertson (P–R) drag. Stochastic forces on circumsolar grains arise from low-frequency fluctuations in surface charge and interplanetary fields, as has long been recognized<sup>2,3</sup>, but previous studies have treated the mean orbital energy as constant<sup>4,5</sup> or slowly decreasing<sup>6</sup>. I show here that stochastic heating can balance and indeed overwhelm the dissipative P–R drag for small grains ( $\leq 1 \mu\text{m}$  scale radius). Furthermore, the consequent drift to the outer Solar System may cancel the strong collisional source inferred<sup>7</sup> for micrometre and sub-micrometre fragments, explaining how their present distribution is stable in time. More generally, the stochastic heating mechanism combined with collisional fragmentation sets limits on dust accretion onto cool stars.

The stochastic forces  $\mathbf{F}^{\sim}$  are formally included in the Langevin equation of motion of a mass  $m$  in the gravitational field of a large mass  $M_0$  as

$$m\ddot{\mathbf{r}} = mM_0G\mathbf{V}\left(\frac{1}{r}\right) - \mathbf{F}^{\text{PR}} - \mathbf{F}^{\sim} \quad (1)$$

This generalized Kepler problem has been studied for other damping and stochastic forces; stationary solutions do exist in which, on average, energy gain compensates orbital damping, as demonstrated by Marshall and Claverie<sup>8</sup> in the stochastic electrodynamic model of atoms. Following these authors, we start from the corresponding Fokker–Planck equation in the hamiltonian variables<sup>9</sup> for the distribution function  $f$

$$\frac{\partial f}{\partial t} = \frac{\partial}{\partial w_i} \left( -a_i f + \frac{1}{2} b_{ij} \frac{\partial f}{\partial w_j} \right) \quad (2)$$

This depends on assuming the fluctuations to be markovian and adopting the narrow-line approximation<sup>9</sup>. Then diffusive terms remain in the action variables, but not in the hamiltonian angles. The generalized force and diffusion coefficients are

$$a_j = \langle F_i^{\text{PR}} \partial w_j / \partial p_i \rangle, \quad b_{ij} = \tau^{-1} \langle \Delta w_i \Delta w_j \rangle \quad (3)$$

averaged around the slowly-changing Kepler orbits,  $b_{ij}$  being averaged also over the spectrum of fluctuations  $\Delta w$  arising from  $\mathbf{F}^{\sim}$ . In the Kepler problem, the  $w_i$  are equivalent to total energy  $w_1 = p_i p_i / 2m - m M_0 G / r$ , total angular momentum  $w_2 = \sqrt{(p_i p_i)}$  and angular momentum in a given direction  $w_3 = p_2$ ; an alternative formulation<sup>4,6</sup> employs the orbital elements instead of the above  $w_j$ .

Stationary solutions of equation (2) are not available for the Kepler problem<sup>8</sup>. However, the principle and the physical scale involved are illustrated by the one-dimensional analogue including source  $Q$  and loss terms  $L$ :

$$\frac{\partial f}{\partial t} = \frac{\partial}{\partial \varepsilon} \left( -af + \frac{1}{2}b \frac{\partial f}{\partial \varepsilon} \right) + Q(\varepsilon) - L(\varepsilon) \quad (4)$$

for purely circular orbits of scaled energy

$$\varepsilon = 2w_1/m = -2 M_0 G / r + p_\theta^2 / m^2, \quad (5)$$

$$p_\theta^2 / m^2 = M_0 G / r$$

The Poynting–Robertson drag on a spherical grain of radius  $s$  (valid down to  $0.3 \mu\text{m}$  radius in general, down to  $0.1 \mu\text{m}$  for iron and graphite grains) is<sup>10</sup>

$$\mathbf{F}^{\text{PR}} = -(s_0/s) M^0 G p_\theta / r^2 c, \quad \text{where } s_0 = 0.19 \mu\text{m}$$

so the damping force from equations (3) and (5) is

$$a = F^{\text{PR}} d\varepsilon / dp_\theta = -(s_0/s) 2p_\theta^2 / m^2 r^2 \quad (6)$$

The Fokker–Planck coefficient arising from the fluctuating electromagnetic impulse is

$$b = \tau^{-1} \langle \Delta \varepsilon \Delta \varepsilon \rangle = 4 \left\{ \frac{q\Omega}{mc} \right\}^2 P_{nn} P_\theta^2 / m^2 r^2 \quad (7)$$

where  $q$  is the grain charge,  $\Omega$  is a constant (solar angular speed),  $c$  is the velocity of light and  $P_{nn}(\omega; i, \theta)$  is the power spectrum of the fluctuating fields, to be averaged around orbital positions  $\theta$ . Compare equation (7) with equation (20) of ref. 6, scaled by eccentricity; also  $\langle \Delta a^2 \rangle$  of ref. 4 with arithmetical correction of a factor of 10 in equation (9). In the interplanetary medium, the mean  $P_{nn}$  is probably larger around orbits of small inclination  $i$  to the ecliptic plane than on highly inclined orbits (because reversals in the magnetic field direction which are confined to within  $\pm 15^\circ$  contribute strongly). For the present spherically symmetric analogue, we take as representative the rough value<sup>4</sup>

$$P_{nn} = 5 \times 10^{48} \text{ G}^2 \text{ cm}^4 \text{ s} \quad (8)$$

corresponding to  $1 \times 10^6 \text{ nT}^2 \text{ Hz}^{-1}$  power in field fluctuations ( $1 \text{ nT} = 10^{-5} \text{ G}$ ). This value lies between values measured at small and large heliolatitudes, and is good to a factor of 2–3 (see ref. 6).

The stationary solution to equation (4) with no source or loss terms and vanishing at large  $r$  is trivial:

$$f \propto \exp \int (2a/b) d\varepsilon - 1 = e^{-a\varepsilon} - 1 \quad \text{for } \alpha = -2a/b \quad (9)$$

since the parameters  $a$  and  $b$  have identical dependence ( $\propto \varepsilon^3$ ). In terms of radial distance,  $f \sim \exp(-R/r) - 1$  with the scale radius

$$R = M_0 G \alpha = (s_0/s)(M_0 G m / q\Omega)^2 c / P_{nn} = R_0 \rho^2 s^3 \quad (10)$$

Taking the grain charge  $q$  to correspond to a 5-V potential ( $q = (s V_0 / 300)$  e.s.u. for radius  $s$  in  $\mu\text{m}$ ) and  $P_{nn}$  from equation (8), the scale  $R_0$  is:

$$R_0 = 1.0 \text{ AU } \mu\text{m}^{-3} \text{ g}^{-2} \text{ cm}^{-6} \quad (11)$$

The exponential behaviour shows that stochastic heating is vigorous enough in  $r > R$  to readily compensate the P–R damping; also, the inner region where damping dominates is smaller for smaller grains.

In the Solar System, grains are destroyed by evaporation near the Sun ( $\varepsilon \approx -\infty$ ) or lost from loosely-bound orbits ( $\varepsilon \approx 0$ ); comets and asteroids are sources of new grains, while both losses and gains result from fragmenting collisions<sup>11</sup>. For simplicity, we follow ref. 7 by taking a source  $Q = \Phi k |\varepsilon|^{k-1}$  with power index  $k > 2$  and allow some loss  $L_0 \delta(\varepsilon)$  at  $\varepsilon = 0$ . Then the stationary form of equation (4) integrates once to give the flux

$$J = af - \frac{1}{2}b \frac{\partial f}{\partial \varepsilon} = L_0 - \Phi |\varepsilon|^k \quad (12)$$

The distribution satisfying equation (12) is

$$f(\varepsilon) = 2 \int_{-\varepsilon}^0 e^{\alpha(\varepsilon - \varepsilon')} \frac{d\varepsilon'}{b(\varepsilon')} (L_0 - \Phi |\varepsilon'|^k) \quad (13)$$

where  $b \sim |\varepsilon|^3$  from equations (5) and (7). Formally, the loss integral is singular at  $\varepsilon = 0$  and we should take  $L_0 \rightarrow 0$ . This is in part a consequence of the diffusion approximation, overcome in stochastic models having finite step size (as for comet orbit

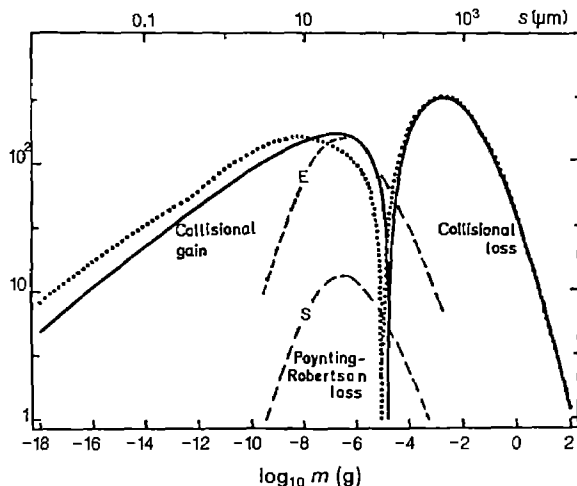


**Fig. 1** Net gain and loss rates (arbitrary units) due to collisions evaluated in ref. 7 at 1 AU for two different grain density models (solid line from interplanetary dust collection; dotted line from lunar microcrater counts), compared with the differential P-R loss<sup>7</sup> for spherical grains (S) and estimated enhanced loss for elongated grains (E), which assume spatial density variation as  $r^{-1.3}$ . The upper size scale is for spherical grains of density  $2.4 \text{ g cm}^{-3}$ .

'diffusion'; see, for example, ref. 12), but in part results because  $b \sim r^{-2}$ , so that particles accumulate in the outer Solar System until removed by accretion or fragmenting collisions. Indeed, at a distance of order 100 AU, where the solar wind degrades or terminates,  $b$  would fall off still faster and produce stronger accumulation. As this aspect is not modelled here, dropping the loss integral and taking  $f_0$  as finite is legitimate. Thus we have

$$f(\varepsilon) = e^{\alpha\varepsilon} \left\{ f_0 - \frac{2}{\beta} \Phi \int_0^{|\varepsilon|} s^{\alpha y} y^k \frac{dy}{y^3} \right\} \quad (14)$$

where the constant  $\beta = b|\varepsilon|^{-3}$  depends strongly on grain size ( $\beta \propto s^{-4}$ ). No cutoff in the source is needed at small  $\varepsilon$  for  $k > 2$ . Evidently for  $k = 3$ , the integral takes the simple form of equation (9). An inner boundary condition could be imposed corresponding to evaporation of grains near the Sun, but all we need is to ensure that  $J < 0$  at 0.1 AU. The explicit solution available for  $k = 3$  is

$$f = f_0 + \frac{2}{\alpha\beta} \Phi \exp \left( \frac{6 \text{ AU}}{r} s [\mu\text{m}]^3 \right)^{-1} \quad (15)$$

after using equations (10) and (11), and setting  $\rho$  equal to  $2.4 \text{ g cm}^{-3}$ . The combined multiplicative factors do not vary strongly with grain size: the dependence is roughly  $\Phi \sim s^{-2}$  for  $s < 2 \mu\text{m}$  (or  $10^{-10} \text{ g}$ ; see Fig. 1),  $\Phi/\alpha\beta \sim s^{-1}$ . But the exponential factor in equation (15) can be huge, for example  $\exp(6,000)$  for  $10\text{-}\mu\text{m}$  grains, because diffusion is very weak and sources and sinks dominate. Thus, the zodiacal light indicates that  $10\text{-}100\text{-}\mu\text{m}$  grains are confined to the ecliptic plane, as collisions and P-R forces dominate<sup>7</sup>. For  $0.2\text{-}\mu\text{m}$  grains, on the other hand, the diffusive solution varies relatively slowly, as  $\exp(0.6 \text{ AU}/r)$ , and diffusive processes dominate. The boundary of applicability of the simple stochastic solution (14) is thus plausibly  $s = 0.5 \mu\text{m}$  ( $10^{-12} \text{ g}$ ).

The scales are changed if damping forces operate that exceed the classical P-R force. Sputtering of grains by the solar wind, the direction of which is a few degrees from radial, gives<sup>13</sup> a pseudo-P-R force with doubled parameters  $a$  (of equation (6)) and  $R_0$  (of equation (11)) for prograde orbiting dust particles. A second variant covers highly-elongated grains partially aligned by the magnetic field, which scatter photons anisotropically and

suffer a mean tangential force many times higher than the P-R force<sup>14</sup>. In the absence of particular analysis and knowledge of actual shapes, this may justify increasing P-R loss rates by an order of magnitude to balance the net collisional gains, as in Fig. 1 (dashed line E). Because the enhancement depends little on grain size<sup>14</sup>, it cannot explain the increasing divergence evident in Fig. 1 between gains and losses of grains smaller than a few micrometres.

We have demonstrated that the stochastic energy addition ignored in previous studies can, in principle, overcome the spiralling in of dust grains due to P-R drag. The one-dimensional model explored here should be an adequate description of the problem. Variation with orbit eccentricity and inclination are not directly important, because orbital periods are unaffected and mean stochastic rates depend only weakly on them<sup>6</sup>. Insofar as  $P_{nn}$  is up to 3 times higher for low-orbit inclinations, diffusive speeds may be higher and densities lower by a factor  $\sqrt{3}$  in the ecliptic plane. The systematic electromagnetic effects that strongly deflect grains smaller than  $\sim 0.3 \mu\text{m}$  in the inner Solar System reverse sign with solar polarity every 11 yr; diffusive behaviour is thus valid outside Jupiter's orbit, although periodic effects would be evident in the Earth's neighbourhood. The  $\mu\text{m}$ -sized grains released mainly in the ecliptic plane would diffuse initially in inclination<sup>4-6</sup>. Grains of a few micrometres have mean P-R drag reduced by energy gains, and so continue to orbit along P-R spirals; their space density depends primarily on diffusion out of the plane, not modelled here. Observations of the particle spectrum at 1 AU do show evidence of a new mechanism operating on submicrometre grains; the break or 'knee' at around  $0.5\text{-}1 \mu\text{m}$  in the size distribution<sup>11</sup> would correspond to the change from source-dominated to stochastic diffusive-type solutions. The steeper spectrum of grains of  $s < 1 \mu\text{m}$  inferred by Lamy and Perrin<sup>15</sup>, if confirmed to exist, would constitute the diffusion-dominated population.

One longstanding issue concerning the zodiacal cloud is the nature of the source which replaces the estimated 10–20 tonnes  $\text{s}^{-1}$  lost within 1 AU through fragmenting collisions<sup>16</sup>. Short-period comets have been thought inadequate, but there are uncertainties in the estimates and other possible sources exist for the required sub-millimetre meteoroids<sup>7</sup>. The more pressing issue concerns removal of the fragments from collisions that we know must occur. Whipple<sup>16</sup> supposed that one third of the fragments would go immediately into hyperbolic orbits, but found that the removal rate through P-R forces is only 5–10% of the production rate. Grün *et al.*<sup>7</sup> estimate a 50% loss to hyperbolic orbits but, excluding the counteracting stochastic effects, still only 5% through P-R drag (see Fig. 1). If, however, P-R forces were  $\sim 10$  times stronger, as appears plausible from the calculations for cylindrical grains<sup>14</sup>, they could remove the excess in the  $10\text{-}100\text{-}\mu\text{m}$  range ( $10^{-8}\text{-}10^{-5} \text{ g}$ ). Nevertheless, the strong excess production of micrometre and smaller grains remains (Fig. 1), so that their density would be increasing over the relatively short timescale of 10,000 yr. The present analysis identifies a new removal mechanism that can solve this conundrum. The stochastic forces add energy on the average, ejecting grains towards the outer Solar System. These grains might accumulate there over long periods of time and eventually perhaps accrete onto meteoroids and comets.

I thank Trevor Marshall and Ajoy DasGupta for helpful discussions.

Received 21 June 1985; accepted 13 January 1986.

1. Kubo, R. *Rep. Prog. Phys.* **29**, 255–285 (1966).
2. Parker, E. N. *Astrophys. J.* **139**, 951–958 (1963).
3. Morfill, G. E. & Grün, E. *Planet. Space Sci.* **27**, 1283–1292 (1979).
4. Consolmagno, G. *Icarus* **38**, 398–410 (1979).
5. Barge, P., Pellet, R. & Millet, J. *Astr. Astrophys.* **115**, 8–19 (1982).
6. Wallis, M. K. & Hassan, M. H. A. *Astr. Astrophys.* **151**, 435–441 (1985).
7. Grün, E., Zook, H. A., Fechtig, H. & Giese, R. H. *Icarus* **62**, 244–272 (1985).
8. Marshall, T. W. *Claverie, P. J. math. Phys.* **21**, 1819–1825 (1980).
9. Marshall, T. W. *Physica* **103A**, 172–182 (1980).

10. Burns, J. A., Lamy, Ph. L. & Soter, S. *Icarus* **40**, 1–48 (1979).
11. Leinert, C., Röser, S. & Buitrago, J. *Astr. Astrophys.* **118**, 345–357 (1983).
12. Yabushita, S. *Astr. Astrophys.* **85**, 77–79 (1980).
13. Mukai, T. & Yamamoto, T. *Astr. Astrophys.* **107**, 97–100 (1982).
14. Voschinikov, N. V. & Il'in, V. B. *Pis'ma Astr. Zh.* **9**, 188–192 (1983). (*Soviet Astr. Lett.* **9**, 101–103; 1983).
15. Lamy, Ph. L. & Perrin, J. M. in *Solid Particles in the Solar System* (eds Halliday, I. & McIntosh, B. I.) 75–80 (Reidel, Dordrecht, 1980).
16. Whipple, F. L. in *Zodiacal Light and the Interplanetary Medium* 409–326 (NASA SP-150 1967).

## Geomagnetic reversal spurs and episodes of extraterrestrial catastrophism

Poorna C. Pal\* & Kenneth M. Creer†

\* Department of Geology & Mineral Sciences, University of Ilorin, PMB 1515, Ilorin, Nigeria

† Department of Geophysics, University of Edinburgh, Edinburgh EH9 3JZ, UK

The possibility that the observed 26–32-Myr periodicity in the records of extinction events<sup>1</sup> and astrobleme ages<sup>2</sup> was caused by periodic episodes of physical bombardment of the planetary surface has raised the likelihood that such an astronomical clock also affects geomagnetic reversals<sup>3,4</sup>. However, the detection<sup>5</sup> of a comparable 30-Myr harmonic in the geomagnetic reversal record has now been found<sup>6</sup> to be an accident of data length while the earlier-reported<sup>7</sup> 32–34-Myr harmonic of the reversal record may well be an artefact of the data base. Here we examine the temporal relation between geomagnetic reversals and those catastrophic episodes which occurred during periods of frequent reversals. As geomagnetic history comprises long intervals of frequent reversals, alternating with intervals of fixed polarity, our rationale is that the geomagnetic field should be most susceptible to catastrophe during its relatively unstable periods of frequent reversals. We find spurs in the frequency of geomagnetic reversals at approximately 30-Myr intervals, correlated with catastrophic episodes. These spurs can be seen as the geomagnetic signatures of terrestrial catastrophe, and we tentatively ascribe them to enhanced core turbulence during episodes of bombardment. The absence of reversal spurs during long intervals of fixed polarity is attributed to the failure during these intervals of the geomagnetic dynamo's bi-stable oscillations.

Polarity reversals of the geomagnetic field have occurred often in the geological record<sup>8</sup>, although with varying frequency. The durations of the individual normal (N) and reversed (R) regimes have thus ranged from 0.02–0.03 Myr for the early Pleistocene (Olduvai) N-polarity intervals ('subchrons') to 20–70 Myr for the late Palaeozoic R- and early and late Mesozoic N-polarity intervals (Kiaman, Balkan and Gubbio 'superchrons'). Figure

1 shows the variation of reversal frequency since the late Palaeozoic as seen through 5-Myr rectangular windows at 2.5-Myr intervals, based on a largely marine-derived magnetic record for the post-Callovian period<sup>8</sup> and magnetostratigraphic data<sup>9</sup> for earlier times. A rhythmic variation in reversal frequency with time is readily apparent here, with periods of few or no reversals (the fixed-polarity superchrons) lasting 20–70 Myr, alternating with equally long periods of frequent reversals (the mixed-polarity superchrons). The N and R interval lengths tend to increase towards the fixed polarity superchrons; however, the likely significance of this trend, reported in several recent studies<sup>10–12</sup>, is obscured by an abrupt rise in reversal frequency following the late Triassic–early Jurassic N-polarity superchron. Similarly, although the lengths of the superchrons appear to decrease with age, this observation may be dramatically affected by any improvement in resolution and detection threshold, particularly as the Norian–Callovian reversal sequence remains far from complete.

The time distribution of reversals is thus enigmatic. Fourier spectrum<sup>13</sup>, maximum entropy<sup>9,14</sup>, Walsh sequency<sup>7</sup>, minimum dispersion<sup>5</sup> and autocorrelation<sup>11</sup> analyses, for example, have been used to demonstrate the presence in the reversal spectrum of harmonics with periods of approximately 700, 250–300, 100–120, 45–70, 30–34 and 15 Myr. The incompleteness of the record casts doubt on the significance of the longer-period harmonics cited; even the proposed 30- and 15-Myr harmonics are controversial<sup>6,15,16</sup>. As for the 32–34-Myr harmonic<sup>7</sup>, the tentativeness of the database and the inclusion of fixed-polarity superchrons in the analysis (one of which is of ~35-Myr duration) make its identification rather suspect. Its correlation with the 26–32-Myr periodicity of catastrophic episodes is hindered by the failure to identify the associated geomagnetic signatures, as these episodes occurred during mixed- as well as fixed-polarity superchrons. From a theoretical standpoint, the postulated<sup>12,17</sup> random nature of the geomagnetic reversal process rules out the presence of well-defined harmonics in the reversal frequency spectrum. Thus, if there is a link between geomagnetic reversals and global catastrophe<sup>5,7</sup>, it is not revealed as a common periodicity.

What then is the geomagnetic signature of a catastrophic episode? One possibility is that the reversal record is totally free of any such signatures. Another is that catastrophic episodes are expressed only in mixed-polarity superchrons. The post-Callovian record<sup>8</sup>, the most reliable segment of the data in Fig. 1, comprises two such superchrons: the post-Santonian sequence (from 83 Myr to the present) and the Oxfordian–Barremian sequence (~163–119 Myr). The first of these is analysed here, the latter having been too brief for a detailed analysis.

Figure 2 shows the variations in reversal frequency since early Campanian based on the Lowrie–Alvarez (LA-81) timescale<sup>18</sup> as seen through a 15-Myr window sliding at 1-Myr intervals. The reversal rate curve (a) shows clear fluctuations, with peaks in reversal frequency at about 65–75, 35–45 and <8–12 Myr

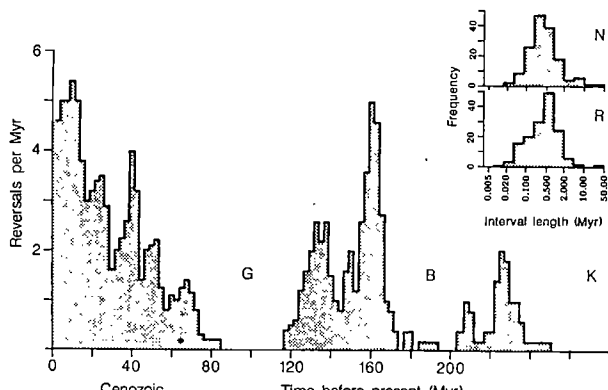


**Fig. 1** Geomagnetic reversal frequency as a function of geological time since the late Permian computed for successive 5-Myr segments in 2.5-Myr overlaps using the timescale of Harland *et al.*<sup>8</sup> for the post-Callovian (<163 Myr) interval and magnetostratigraphic data<sup>9</sup> for earlier times. The inset shows that the N and R interval lengths in this chronology are log-normally distributed (about means of 0.387 and 0.367 Myr, respectively), implying that intervals shorter than about 0.1 Myr have been almost as uncommon as those longer than about 2 Myr. Long periods of few or no reversals (fixed-polarity superchrons) are indicated by letters: G, Gubbio (Mercatton) N interval; B, Balkan (Graham) N interval; K, Kiaman R interval.

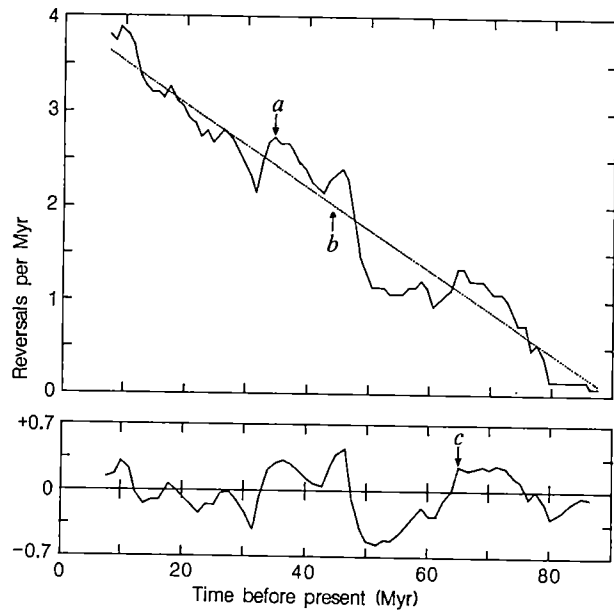


**Fig. 2** Geomagnetic reversal frequency (*a*) during the present (post-Santonian) mixed-polarity superchron, obtained by viewing the LA-81 timescale<sup>18</sup> through a 15-Myr rectangular window, chosen in order to remove the 15-Myr harmonic of Mazaud *et al.*<sup>11</sup>. The overall trend of decreasing frequency with age is modelled here using a straight line fit (*b*):  $RF(T) = 3.96 - 0.0445 T$ , where  $RF(T)$  is reversal frequency (per Myr) at any time  $T$  (Myr) during the past 90 Myr. The residual curve (*c*) is obtained by removing this linear fit from the reversal rate curve and clearly emphasizes the rhythmicity in the reversal rate curve, with spurs during the intervals 65–75, 35–45 and 8–12 Myr.

superposed on a linear decrease with age. When we detrend this by removing a straight line fit (*b*), the residual curve (*c*) is found from the Fourier and maximum entropy analyses (Fig. 3) to be dominated by a 26–32-Myr harmonic. While the data length analysed here is too short to be able to call this a basic harmonic of the reversal record, these results do confirm the presence of three reversal spurs separated by ~30 Myr.

The assumption that these 30-Myr spurs in the reversal frequency are otherwise masked by a 15-Myr harmonic, which prompted our selection of a 15-Myr window, is amply demonstrated by the following analysis of the post-Santonian reversal record. Figure 4 shows the reversal frequency histogram obtained when the LA-81 scale<sup>18</sup> is viewed through a 5-Myr window, along with the corresponding power spectrum (inset). An overwhelming proportion of the power ( $\geq 80\%$ ) is accounted for by the 45-Myr and longer-period harmonics; the remainder is dominated by the 28–36- and 14–18-Myr harmonics. Also shown in Fig. 4 (dotted curve) is the reversal rate curve obtained by deleting harmonics of period  $\leq 18$  Myr. Reversal spurs centred at about 12, 38 and 67 Myr appear distinctly in this curve, corroborating the reversal rate curve obtained in Fig. 2 by a 15-Myr smoothing.

Our results thus suggest that the presently continuing superchron of frequent reversals is characterized by three clearly defined reversal spurs spaced about 30 Myr apart. If the geomagnetic reversal process were characterized by a 30-Myr periodicity, we would expect to see a reversal spurt ~30 Myr before the oldest of these three; that is, in Cenomanian or late Albian times. There was no such spurt; indeed, the field remained fixed in the N-polarity state throughout the 35-Myr Aptian–Santonian interval<sup>8</sup>. The preceding Oxfordian–Barremian mixed-polarity superchron did contain two such spurs at 130–140 and 155–165 Myr (ref. 5) (see Fig. 1), but this superchron was too short to allow detailed analysis.

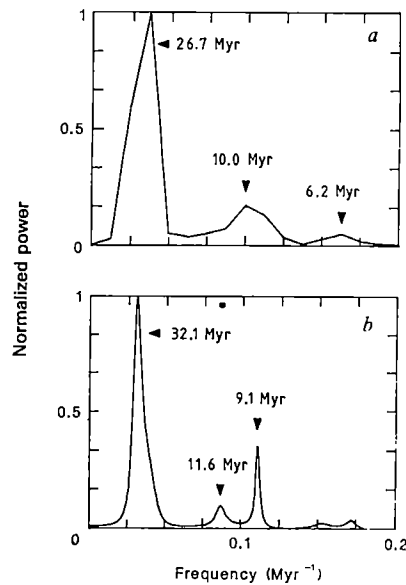


**Fig. 3** Fourier (*a*) and maximum entropy (*b*) spectra for the residual curve of Fig. 2. Note the dominance of a 26.7–32.1-Myr harmonic, reflecting the removal of shorter-period harmonics by the 15-Myr smoothing, and of longer-period harmonics by linear detrending. The 6.2–11.6-Myr periods in these spectra indicate leftovers from the smoothing process used to compute the reversal-rate curve shown in Fig. 2.

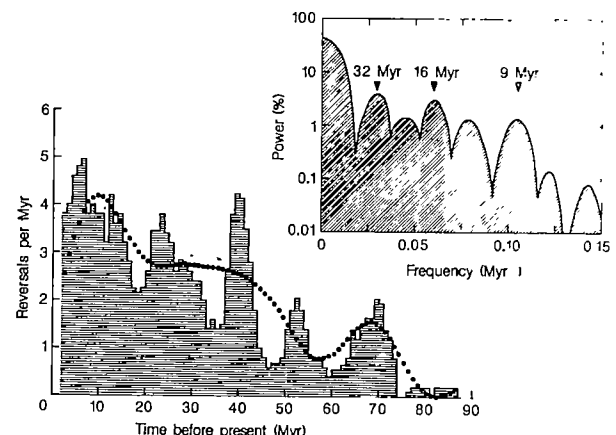


**Fig. 4** The reversal frequency plot obtained by viewing the LA-81 scale<sup>18</sup> through a 5-Myr rectangular window, before (histogram) and after (dotted curve) filtering the 18-Myr and shorter-period harmonics. The inset shows the power spectrum obtained from the unfiltered data.

Our finding that reversal spurs indeed characterized the mixed-polarity superchrons, occurring approximately once every 30 Myr since ~165 Myr except during the Cretaceous N-polarity superchron, prompts a search for a chronological link between these spurs and suspected catastrophic events. Evidence for the occurrence of global-scale catastrophic events includes impact craters, tektites and impactites signifying bombardment episodes, coeval geochemical anomalies implying an extraterrestrial origin for the bombardment, and the chronologically correlated extinction events as their attendant environmental repercussions. The terminal-Cretaceous and

Table 1 Correlation of reversal spurs and catastrophic episodes

Geological time	Reversals			Evidences of catastrophism				Extinction event
	Polarity superchron	Reversal - spur	Astroblemes	Impactites	Tektites	Geochemical anomalies		
Late-middle Miocene	Mixed	×	×	×	×			×
Early Oligocene-late Eocene	Mixed	×	×	×	×	×		×
Palaeocene-late Cretaceous	Mixed	×		×	×	×		×
Middle Cretaceous	Fixed		×	×				×
Early Cretaceous	Mixed	×	×	×				×
Late Jurassic	Mixed	×	×					×
Early-middle Jurassic	Fixed		×					×
Late Triassic	Mixed	?	×					×
Late Permian	Fixed						×	×

terminal-Eocene catastrophic episodes are thus inferred from the presence of iridium and osmium anomalies associated with extinction events<sup>19,22</sup>, and from the discoveries of coeval astrobleme structures<sup>2</sup>, impactites<sup>23</sup> and microtektites<sup>24,25</sup>. The middle-late Miocene boundary is similarly characterized by a major extinction event<sup>1</sup>, several impact structures<sup>2</sup> and the East European tektite strewn field<sup>25,26</sup>. Palaeontological and crater-age data also indicate catastrophic episodes in the middle (Cenomanian) and early (Hauterivian) Cretaceous, late (Callovian-Tithonian) and early-middle (Bajocian-Pliensbachian) Jurassic, late Triassic (Norian) and late Permian (Guadalupian-Dzhulfian), yielding an estimate of about 30 Myr for the periodicity of catastrophic episodes since the end of the Palaeozoic<sup>1-3</sup>.

Table 1 summarizes a chronological correlation of reversal spurs and catastrophic episodes since the late Palaeozoic. Except for the late Permian and middle Cretaceous episodes, which occurred during the Permian R and Cretaceous N fixed-polarity superchrons respectively, all the other catastrophic episodes are associated with reversal spurs. Questions remain about the presumed periodicity in the palaeontological record<sup>27</sup>, but Raup's<sup>28</sup> re-analysis has confirmed its statistical significance. Similarly, tektites are not universally regarded<sup>29</sup> as indicative of extraterrestrially caused catastrophism, although the inference that they represent the reworking of terrestrial material attendant upon bolide collisions is widely accepted. Note that Fig. 1 suggests an element of cyclicity in the occurrences of the alternate mixed- and fixed-polarity superchrons. The power spectrum in Fig. 4 reflects this, with a concentration of  $\geq 80\%$  of the total power in the 45-Myr and longer-period harmonics. Superposed on this pattern, the reversal spurs are so located in the mixed-polarity superchrons as if a basic 30-Myr harmonic in the reversal spectrum, extending back to at least 165 Myr and probably to the late Permian, is masked during the fixed-polarity superchrons. In view of the correlations shown in Table 1, we suggest that the approximately periodic recurrences of catastrophic episodes caused reversal spurs during the mixed-polarity superchrons. It would thus seem likely that these reversal spurs had little to do with any stochastic behaviour intrinsic to the geomagnetic dynamo mechanism and possibly represent an additive factor superposed on the otherwise random occurrences of reversals.

The geomagnetic field is thought to arise from magnetohydrodynamic motions in the Earth's fluid outer core<sup>31</sup>, and reversals in polarity are likely to be caused by core turbulence<sup>30</sup>. The correlation of reversal spurs and catastrophic episodes can be explained in terms of enhanced turbulence in the core motions resulting from intensified physical bombardments of the planetary surface during the catastrophic episodes. The observed<sup>32-34</sup> diminution of field strength and departure from axial symmetry during a polarity reversal is consistent with a core turbulence model for reversals. Similarly, evidence from lunar magnetism<sup>35</sup> supports our suggestion that extraterrestrially

induced catastrophism can drastically affect geomagnetic behaviour.

If catastrophic episodes indeed caused reversal spurs, we need to explain why fixed-polarity superchrons remained unaffected by them and why the spurs are of such long duration (relative to the duration of the catastrophic episodes). The first of these results from the likelihood that the geomagnetic dynamo is locked into a frozen state during a fixed-polarity superchron, implying an occasional failure of its random bi-stable oscillations<sup>12</sup>, from which a catastrophism-induced resonance cannot readily free it. As for the second, the explanation lies partly in the broadening effect of smoothing (Fig. 2) and filtering (Fig. 4), and partly in the possibility that the corresponding catastrophic episodes comprised multiple pulses, not isolated events. The latter suggestion is supported by the discovery<sup>24</sup> of several microtektite layers spanning a 10-Myr interval near the Eocene-Oligocene boundary.

We thank David Raup and Timothy Lutz for constructive reviews and Bill Napier and Victor Clube for helpful discussions. P.C.P. also acknowledges the facilities provided by Universidad Nacional Autónoma de México and University of California, Los Angeles.

Received 12 August 1985; accepted 23 January 1986.

- Raup, D. M. & Sepkoski, J. J. *Proc. natn. Acad. Sci. U.S.A.* **81**, 801-805 (1984).
- Alvarez, W. & Müller, R. A. *Nature* **308**, 718-720 (1984).
- Rampino, M. R. & Strothers, R. B. *Nature* **308**, 709-712 (1984); *Science* **226**, 1427-1431 (1984).
- Clube, S. V. M. & Napier, W. M. *Nature* **311**, 635-636 (1984); *Mon. Not. R. astr. Soc.* **208**, 575-588 (1984); *Earth planet. Sci. Lett.* **57**, 251-262 (1982).
- Raup, D. M. *Nature* **314**, 341-343 (1985).
- Lutz, T. M. *Nature* **317**, 404-407 (1985).
- Negi, J. G. & Tiwari, R. K. *Geophys. Res. Lett.* **10**, 713-716 (1983).
- Harland, W. B. *et al.* *A Geologic Time Scale* (Cambridge University Press, 1982).
- Irving, E. & Pulliaiah, G. *Earth Sci. Rev.* **12**, 35-64 (1976).
- Lowrie, W. & Kent, D. V. *Earth planet. Sci. Lett.* **62**, 305-313 (1983).
- Mazaud, A., Laj, C., de Seze, L. & Verosub, K. L. *Nature* **304**, 328-330 (1983).
- McFadden, P. L. & Merrill, R. T. *J. geophys. Res.* **89**, 3354-3362 (1984).
- Crain, I. K., Crain, P. L. & Plaunt, M. S. *Nature* **223**, 282-283 (1969).
- Ulrich, T. J. *Nature* **235**, 218-219 (1972).
- McFadden, P. L. *Nature* **311**, (1984).
- Mazaud, A., Laj, C., de Seze, L. & Verosub, K. L. *Nature* **311**, 396 (1984).
- Cox, A. *Phys. Earth & planet. Int.* **24**, 178-190 (1981).
- Lowrie, W. & Alvarez, W. *Geology* **9**, 393-397 (1981).
- Alvarez, L. W. & Alvarez, W. *Science* **223**, 1174-1186 (1983).
- Ganapathy, R. *Science* **216**, 885-886 (1982); *Science* **209**, 921-922 (1980).
- Kyte, F. T., Smit, J. & Wasson, J. T. *Earth planet. Sci. Lett.* **73**, 183-195 (1985).
- Luck, J. M. & Turekian, K. K. *Science* **222**, 613-615 (1983).
- Bohor, B. F., Foord, E. E., Modreski, P. J. & Triplehorn, D. M. *Science* **224**, 867-868 (1984).
- Keller, G., D'Hondt, S. & Vallier, T. L. *Science* **221**, 150-152 (1983).
- Glass, B. P., Swincki, M. B. & Zwart, P. A. *Proc. 10th lunar planet. Sci. Conf.* Vol. 3, 2535-2545 (Pergamon, Oxford, 1979).
- Barnes, V. F. in *Tektites* (ed. O'Keefe, J. A.) 25-50 (University of Chicago Press, 1963).
- Hoffman, A. *Nature* **315**, 659-661 (1985).
- Raup, D. M. *Nature* **317**, 384-385 (1985).
- Crawford, A. R. Q. *Hil. R. astr. Soc.* **26**, 53-55 (1985); *Geol. Mag.* **116**, 261-283 (1979).
- Olson, P. *Phys. Earth planet. Inter.* **33**, 260-274 (1983).
- Parker, E. N. *Cosmical Magnetic Fields* (Clarendon, Oxford, 1979).
- Prevot, M., Maniken, E. A., Gromme, C. S. & Coe, R. S. *Nature* **316**, 230-234 (1985).
- Dagley, P. & Lowley, E. *Geophys. J. R. astr. Soc.* **36**, 577-598 (1974).
- Pal, P. C. J. *Ind. Acad. Geosci.* **16**, 81-96 (1973).
- Runcorn, S. K. Q. *Jl R. astr. Soc.* **26**, 137-146 (1985); *Nature* **304**, 589-596 (1983).

## Aluminium/silicon disordering and melting in sillimanite at high pressures

T. J. B. Holland & M. A. Carpenter

Department of Earth Sciences, University of Cambridge,  
Downing Street, Cambridge CB2 3EQ, UK

Naturally occurring polymorphs of  $\text{Al}_2\text{SiO}_5$  (andalusite, kyanite and sillimanite) have assumed a special significance for geologists because of their value as indicators of the pressures ( $P$ ) and temperatures ( $T$ ) experienced by metamorphic rocks<sup>1,2</sup>, and for materials scientists because the binary system  $\text{Al}_2\text{SiO}_5-\text{Al}_2\text{O}_3$  contains the important refractory mineral, mullite<sup>3</sup>. The equilibrium stability field of sillimanite in natural rocks and the process by which it can be transformed to mullite for ceramic materials (mullitization) have received particular attention because of the role of cation ordering ( $\text{Al}^{3+}/\text{Si}^{4+}$ ) in stabilizing these structures<sup>1-7</sup>. Here we present the results of annealing experiments undertaken to determine the disordering behaviour of sillimanite crystals at high confining pressures. At  $P \approx 18-20$  kbar and  $T = 1,300-1,700^\circ\text{C}$ , they undergo partial melting to give a  $\text{SiO}_2$ -rich melt. The residual crystals become progressively more disordered as they become enriched in  $\text{Al}_2\text{O}_3$  until they transform to a higher-symmetry structure. Our observations shed new light on previous thermochemical studies of Al/Si order-disorder in sillimanite and on the phase relationships between sillimanite and mullite.

In principle, sillimanite should show an Al/Si disordering transformation at high temperature<sup>8,9</sup>. To study such a transformation experimentally, however, high pressures must be applied to suppress the breakdown reaction sillimanite  $\rightarrow$  mullite +  $\text{SiO}_2$  and incongruent melting<sup>10,11</sup>. The disordering reaction would result in a halving of the  $c$  unit-cell repeat and a space group change from Pbnm to Pbam<sup>6,10,12</sup>, and should be readily detect-

able by single crystal diffraction methods. Reflections of the type  $l=\text{odd}$  are absent in diffraction patterns from disordered crystals<sup>6,10,12</sup>, but are present and sharp in ordered sillimanite diffraction patterns<sup>2</sup>. (The incommensurate superlattice of mullite gives pairs of reflections about these  $l=\text{odd}$  positions<sup>2,4</sup>). The original intention of the present experiments was to bracket the  $\text{Pbam} \rightleftharpoons \text{Pbnm}$  transformation in sillimanite by the use of high- $P$  and - $T$  annealing experiments and transmission electron microscopy (TEM).

Natural sillimanite crystals from Connecticut, USA (Cambridge mineral collection no. 3076) were annealed in sealed Pt capsules at pressures of 18–20 kbar and temperatures of 1,300–1,690 °C for 0.3–10 h in a piston-cylinder apparatus. The product crystals were examined at 100 kV in an AEI EM6G or a JEM100C electron microscope, as crushed grains deposited on carbon film and as ion-beam-thinned slices. The starting material had no pervasive microstructure and gave strong, sharp  $l=\text{odd}$  reflections in electron diffraction patterns. The product crystals contained abundant dislocations, both isolated and in subgrain boundaries (Fig. 1), features resembling antiphase boundaries (APBs) in dark-field images formed with  $l=\text{odd}$  reflections (Fig. 1a, b) and small inclusions on a scale of  $\sim 200-2,000$  Å (Fig. 1c–e). In addition, the intensity of  $l=\text{odd}$  reflections in the electron diffraction patterns showed considerable variation. The observations are summarized in Table 1.

The APBs were commonly observed to end at dislocations (Fig. 1a), but in some cases formed quite regular domain textures (Fig. 1b). Antiphase domains (APDs) with a stacking vector of  $\frac{1}{2}[001]$  would be expected to appear during an ordering transformation from Pbam to Pbnm in sillimanite. The same stacking mistakes can also be generated by the passage of partial dislocations, however, since deformed sillimanites commonly contain [001]-type dislocations which dissociate into partials  $\frac{1}{2}[001] + \frac{1}{2}[001]$  (refs 13–16). Stacking faults between partials of this type also have a displacement vector of  $\frac{1}{2}[001]$  and cause the juxtaposition of Si next to Si and Al next to Al where, in defect-free regions, the Al and Si would alternate in a fully

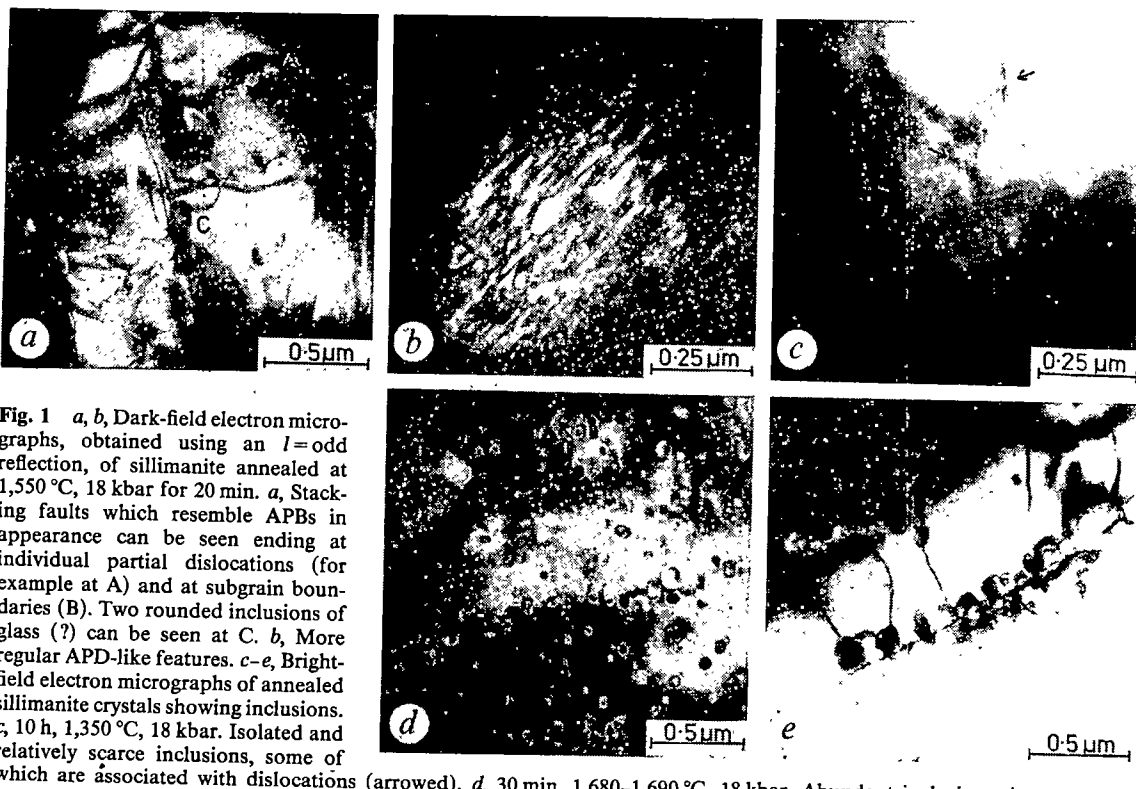


**Fig. 1** *a, b*, Dark-field electron micrographs, obtained using an  $l=\text{odd}$  reflection, of sillimanite annealed at 1,550 °C, 18 kbar for 20 min. *a*, Stacking faults which resemble APBs in appearance can be seen ending at individual partial dislocations (for example at A) and at subgrain boundaries (B). Two rounded inclusions (?) can be seen at C. *b*, More regular APD-like features. *c–e*, Bright-field electron micrographs of annealed sillimanite crystals showing inclusions. *c*, 10 h, 1,350 °C, 18 kbar. Isolated and relatively scarce inclusions, some of which are associated with dislocations (arrowed). *d*, 30 min, 1,680–1,690 °C, 18 kbar. Abundant inclusions, interpreted as consisting of silica-rich glass. *e*, 30 mins, 1,680–1,690 °C, 18 kbar. Large inclusions apparently formed by nucleation at a subgrain boundary. Electron diffraction patterns from the inclusion-free zone have  $l=\text{odd}$  reflections absent.

**Table 1** Annealing conditions and microstructures of heat-treated sillimanite crystals

Run no.	T (°C)	P(kbar)	Annealing time (h)	Product*
S10	1,680-1,690	20	0.5	~15-20% inclusions; $l = \text{odd}$ reflections generally weak, but absent in inclusion-free zones.
S5	1,650	18	0.5	Abundant inclusions; $l = \text{odd}$ reflections generally weak, but absent in inclusion-free zones.
S7	1,620	20	0.66	Abundant APBs; many inclusions; $l = \text{odd}$ strong.
S2	1,550	18	0.33	Many inclusions; abundant APBs; $l = \text{odd}$ strong.
S1	1,450	20	1.0	Inclusions scarce; abundant APBs; $l = \text{odd}$ strong.
S4	1,350	18	10	Relatively scarce inclusions; abundant APBs; $l = \text{odd}$ strong.
S3	1,350	20	0.5	Relatively scarce inclusions; abundant APBs; $l = \text{odd}$ strong.
S12	1,300	20	9	Inclusions scarce; abundant APBs; $l = \text{odd}$ strong.

\* All products also contained abundant dislocations.

ordered manner<sup>13-16</sup>. Once formed, these stacking defects would be free to migrate, and configurations resembling true APD textures might result. The common association of APB-like features with dislocations suggests that a deformation origin is the most likely explanation for their occurrence in the present case.

We interpret the small inclusions in Fig. 1c-e as silica-rich glass resulting from partial melting of the sillimanite crystals. They are typically associated with dislocations and subgrain boundaries, suggesting heterogeneous nucleation of the melt. In some cases they are slightly elongate, with flat sides parallel to  $c$  and rounded ends. Their amorphous character has been deduced from the absence of any diffraction maxima other than those of sillimanite and from the lack of diffraction contrast within the inclusions. Small fragments of isotropic material were also observed by high-magnification optical microscopy in the 1,680-1,690 °C run product.

Crystals from runs at 1,300-1,550 °C gave diffraction patterns with strong  $l = \text{odd}$  reflections and had relatively few inclusions, which were less homogeneously distributed (Fig. 1c). Crystals annealed at 1,620 °C had a higher density of inclusions but the  $l = \text{odd}$  reflections were still strong. Crystals from the two highest-temperature runs contained significantly more inclusions (up to 15-20% at 1,680-1,690 °C; Fig. 1d), and diffraction patterns from these contained obviously weakened (but still sharp)  $l = \text{odd}$  reflections. One relatively inclusion-free region from the 1,680-1,690 °C run (Fig. 1e) gave diffraction patterns with  $l = \text{odd}$  absent. In this case, a subgrain boundary had evidently provided suitable sites for heterogeneous melt nucleation; diffusion of Si and Al between the liquid and residual crystal then occurred on a sufficient scale to leave an inclusion-free zone. Small inclusions of glass were spread more homogeneously throughout the rest of the crystal. It is clear, therefore, that partial melting at the highest temperatures was accompanied by substantial Al/Si disordering.

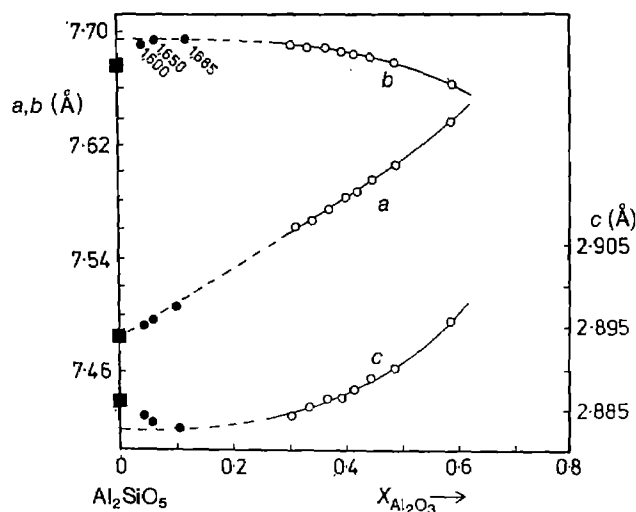


**Fig. 2** Lattice parameters of mullites from ref. 4 (open circles) extrapolated to pure  $\text{Al}_2\text{SiO}_5$ . Filled squares are lattice parameters of sillimanite used as starting material. Filled circles indicate  $a$ ,  $b$  and  $c$  parameters for residual sillimanite after annealing at 1,600 °C, 1,650 °C and 1,685 °C. Approximate fits of the experimental data to the extrapolated curves give rough estimates of the compositions of the residual sillimanites. The most aluminous product (~1,685 °C) fits with  $X_{\text{Al}_2\text{O}_3} \approx 0.1$  and a composition of  $\sim \text{Al}_2[\text{Al}_{2.2}\text{Si}_{1.8}\text{O}_{9.9}]$ .

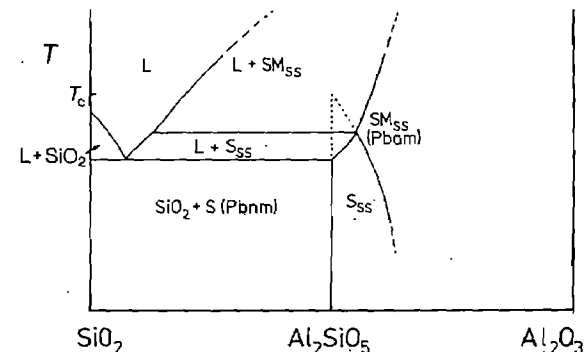


**Fig. 3** Postulated phase relations (schematic) of a part of the  $\text{SiO}_2\text{-Al}_2\text{O}_3$  system close to  $\text{Al}_2\text{SiO}_5$  for high temperatures at 18-20 kbar. The  $\text{Pbnm} \rightleftharpoons \text{Pbam}$  transition is shown as having non-first-order character, and a stability field for a sillimanite-mullite solid solution with disordered Al/Si (Pbam) is suggested. L, liquid; S, sillimanite; S<sub>ss</sub>, sillimanite solid solution; SM<sub>ss</sub>, sillimanite-mullite solid solution. Dotted lines indicate metastable extensions up to the equilibrium order-disorder transformation temperature ( $T_c$ ) of pure sillimanite. At lower temperature there is a miscibility gap between sillimanite and mullite<sup>4,5,22-24</sup>.

The siliceous nature of the melt was suggested initially by the low-pressure melting relations for the system  $\text{SiO}_2\text{-Al}_2\text{O}_3$ , in which the combination of silica-rich liquid and alumina-rich solid predominates<sup>17</sup>. Al-enrichment of the residual sillimanite in our runs is also suggested by changes in lattice parameters (determined from X-ray powder diffraction data) towards those of mullite. Specifically, the sillimanite showed an increase in  $a$  and  $b$  dimensions with increasing annealing temperature, while  $c$  decreased very slightly. Similar changes have been reported in previous high-pressure experiments<sup>10,11,18,19</sup>, although some authors have attributed them to variations in Al/Si order at

constant composition<sup>10,11,19</sup>. A very rough estimate of the composition of the final sillimanite after heating at 1,680–1,690 °C can be made by extrapolating the mullite parameters<sup>4</sup> to pure sillimanite (Fig. 2). Given the short annealing time, this approximate composition does not necessarily represent an equilibrium state.

These experimental observations shed light on the process of mullitization at high pressures, on interpretations of thermochemical data for Al/Si disordering in sillimanite, and on the relationship between sillimanite and mullite. First, when sillimanite is heated at atmospheric pressure it breaks down by a solid-state reaction to mullite +  $\text{SiO}_2$  (ref. 6). Our TEM observations suggest that mullitization at 18–20 kbar would occur by partial melting. The total melting interval (from ~1,300 °C to at least ~1,700 °C) is rather large for a simple binary system ( $\text{Al}_2\text{O}_3$ – $\text{SiO}_2$ ). The apparent melting at 1,300–1,500 °C may depend on the presence of impurities and trace amounts of water, especially since natural sillimanite can contain significant amounts of structural OH groups<sup>20</sup>. The only impurity detected by electron microprobe analysis of this sample was iron (~0.9 wt %  $\text{Fe}_2\text{O}_3$ , assuming all Fe present as  $\text{Fe}^{3+}$ ).

Second, annealing sillimanite at high  $P$  and  $T$  induces a significant enthalpy change relative to untreated natural crystals<sup>11</sup>. Navrotsky *et al.*<sup>11</sup> found that the lattice parameters and heats of solution in lead borate of sillimanite crystals heated at 1,400–1,500 °C (16–23 kbar) show relatively small changes, but more substantial effects were found for crystals heated at 1,600–1,700 °C (16–23 kbar). In both temperature ranges, at 18–20 kbar, our annealed products show high dislocation densities, APB-like defects, and inclusions. Some degree of Al/Si disorder at 1,400–1,550 °C may be implied by the calorimetric results and is certainly present at the APB-like defects. Because enthalpies of vitrification are usually substantial compared with enthalpies of ordering<sup>21</sup>, however, it is possible that at least part of the heat-of-solution changes might be attributed to the presence of glass in the annealed products. Moreover, the break in behaviour observed by Navrotsky *et al.* at 1,550–1,600 °C appears to coincide with a change in the proportion of inclusions present in our material. We have examined some of the original samples prepared for the calorimetric study (generously lent to us by Professor R. C. Newton) and, although we were unable to characterize them fully because they were too finely ground to prepare for TEM by ion-beam thinning, they did appear to have similar microstructures to those described above.

By analogy with order-disorder transformations in other mineral solid solutions<sup>9</sup>, the equilibrium order-disorder temperature,  $T_{\text{ord}}$ , for the  $\text{Pbnm} \rightleftharpoons \text{Pbam}$  transformation should have a maximum value for pure  $\text{Al}_2\text{SiO}_5$ . At this composition the ratio of tetrahedral Al to Si in sillimanite is 1:1; as the composition deviates from this stoichiometry,  $T_{\text{ord}}$  should decrease.  $\text{Pbam}$  crystals have been produced in the present experiments at 1,680–1,690 °C by partial melting; that is, they crossed the  $\text{Pbnm} \rightleftharpoons \text{Pbam}$  transition by changing composition.  $T_{\text{ord}}$  for pure sillimanite must, therefore, be at a higher temperature (at 18–20 kbar), in agreement with a value of ~1,740 °C estimated on the basis of a statistical mechanical model of the disordering<sup>8</sup>.

Figure 3 shows a schematic phase diagram illustrating the order-disorder and melting relations as interpreted here. Many uncertainties remain but there are some interesting contrasts with solid-solution behaviour at lower pressures. From observations of two-phase assemblages<sup>4,22</sup> and of sillimanite–mullite intergrowths which developed from initially homogeneous crystals by exsolution<sup>23,24</sup>, it is clear that there is a miscibility gap between mullite and sillimanite at geological pressures and temperatures<sup>4,5</sup>. Some natural crystals have been found to have intermediate compositions, but these are ordered, with sillimanite-type ordering reflections<sup>5,25</sup>. Disordered crystals have not yet been found in nature. We suggest, on the basis of our experiments, that an equilibrium stability field for a  $\text{Pbam}$  sillimanite–mullite solid solution may exist between ordered sil-

imanite (commensurate,  $\text{Pbnm}$ ) and ordered mullite (incommensurate) at high pressures and temperatures. Further experiments are under way to test this hypothesis and to bracket the order-disorder transformations within the solid solution.

We thank NERC for financial support (grants GR3/4404 to J. D. C. McConnell and GR3/5246 to T.J.B.H. and A. Putnis). This paper is Cambridge Earth Sciences contribution ES 653.

Received 22 October 1985; accepted 22 January 1986.

1. Day, H. W. & Kumin, H. J. *Am. J. Sci.* **280**, 265–287 (1980).
2. Ribbe, P. H. *Rev. Miner.* **5** (2nd edn), 189–214 (1982).
3. Cameron, W. E. *Bull. Am. Ceram. Soc.* **56**, 1003–1007, 1011 (1977).
4. Cameron, W. E. *Am. Miner.* **62**, 747–755 (1977).
5. Cameron, W. E. *Phys. & Chem. Miner.* **1**, 265–272 (1977).
6. Guse, W., Saalfeld, H. & Tjandra, J. *Neues Jb. Miner. Mh.* 175–181 (1979).
7. McConnell, J. D. C. & Heine, V. *Phys. Rev. B* **31**, 6140–6142 (1985).
8. Greenwood, H. J. *Memo. geol. Soc. Am.* **132**, 553–571 (1972).
9. Carpenter, M. A. *Rev. Miner.* **14**, 187–223 (1985).
10. Beger, R. M., Burnham, C. W. & Hays, J. F. *Geol. Soc. Am. Abstr. Prog.* **2**, 490–491 (1970).
11. Navrotsky, A., Newton, R. C. & Kleppa, O. J. *Geochim. cosmochim. Acta* **37**, 2497–2508 (1973).
12. Burnham, C. W. *Carnegie Inst. Wash. Yb.* **63**, 227–228 (1964).
13. Menard, D. & Doukhan, J.-C. *J. Phys. (Fr.)* **39**, L19–L22 (1978).
14. Doukhan, J.-C. & Christie, J. M. *Bull. Minér.* **105**, 583–589 (1982).
15. Lefebvre, A. & Paquet, J. *Bull. Minér.* **106**, 287–292 (1983).
16. Doukhan, J.-C., Doukhan, N., Koch, P. S. & Christie, J. M. *Bull. Minér.* **108**, 81–96 (1985).
17. Aksay, I. A. & Pask, J. A. *J. Am. Ceram. Soc.* **58**, 507–512 (1975).
18. Hariya, Y., Dollase, W. A. & Kennedy, G. G. *Am. Miner.* **54**, 1419–1441 (1969).
19. Chatterjee, N. D. & Schreyer, W. *Contr. Miner. Petro.* **36**, 49–62 (1972).
20. Beran, A., Hafner, St. & Zemann, J. *Neues Jb. Miner. Mh.* 219–229 (1983).
21. Navrotsky, A. *Rev. Miner.* **14**, 225–275 (1985).
22. Cameron, W. E. *Geol. Mag.* **113**, 497–592 (1976).
23. Cameron, W. E. *Nature* **264**, 736–738 (1976).
24. Wenk, H.-R. *Neues Jb. Miner. Abh.* **146**, 1–14 (1983).
25. Cameron, W. E. *Am. Miner.* **61**, 1025–1026 (1976).

## Rapid pressurization experiments on a liquid Al–Mn alloy

J. A. Sekhar & T. Rajasekharan

Defence Metallurgical Research Laboratory,  
Hyderabad-500258, India

Rapid pressurization of liquid metals has been shown both theoretically and experimentally to yield appreciable undercooling<sup>1,2</sup>. With the aim of demonstrating metastable phase formation by this technique, we have now performed a rapid pressurization experiment on an  $\text{Al}_{80}\text{Mn}_{20}$  alloy and studied the product thus obtained. This was found to contain the metastable icosahedral phase first reported by Shechtman *et al.*<sup>3</sup> and studied extensively by many authors<sup>4–9</sup>. (Pauling<sup>8</sup> has recently suggested that the same phase can also be indexed to a large cubic cell. However, our conclusions on the formation of metastable phases will be unaffected by the outcome of this controversy.) We have also found that a new metastable cubic ferromagnetic phase of composition  $\text{Al}_3\text{Mn}$  coexists along with the icosahedral phase. The rapid pressurization technique shows promise of becoming a method for obtaining rapidly solidified microstructures and phases in large volumes.

Concomitantly with pressure application on a liquid alloy contained inside a die, three important processes occur: (1) the liquidus rises for all metals that contract on solidification; (2) there is an adiabatic heat release; and (3) the thermal contact at the metal/die interface improves (see ref. 2). If the rise in liquidus temperature exceeds the rise in temperature due to the adiabatic heat, a net undercooling results which can drive rapid solidification. These undercoolings are high, for example >130 K for aluminium when pressurized to 5.7 GPa (which is adequate for complete solidification purely by pressure application). If the adiabatic heat is dissipated by the efficient thermal contact, then the resultant undercooling will be even greater than given above<sup>2</sup>.

Rapid pressurization of the  $\text{Al}_{80}\text{Mn}_{20}$  alloy was carried out in a simple piston cylinder apparatus made of 'maraging' (high-

Table 1 Observed  $d$ -spacings and intensities from  $\text{Al}_{80}\text{Mn}_{20}$  rapidly pressurized alloy

$I_{\text{obs}}$	$d$ (nm)	Icosahedral indices	Observed ( $d/d(100000)^{-1}$ )	Expected ( $d/d(100000)^{-1}$ )	$\mu$ phase d (nm)	Intensity	$\text{Al}_6\text{Mn}$ ( $hkl$ )	Cubic phase ( $hkl$ )	$\text{Al}_2\text{O}_3$ ( $hkl$ )
(1)	(2)	(3)	(4)	(5)	(6)	(7)	(8)	(9)	(10)
W	0.638				0.636	MW			
VW	0.610				0.607	VW			
VW	0.555				0.549	VW			
VW	0.505				0.505	VW			
W	0.487				0.492	VW	(110) (002)	(111)	
VW	0.438				0.412	VW			
VW	0.413				0.371	W	(020)		
W	0.374	(110001)	0.58	0.56	0.334	W			
VW	0.331	(111010)	0.65	0.65	0.299	MW		(220)	
VW	0.295								
VVV	0.286						(022)		
W	0.268				0.269	W			
W	0.261						(202)		
St	0.252				0.249	W	(113)	(311)	(104)
W	0.244				0.241	M		(222)	(110)
M	0.232				0.231	MW	(130)		
St	0.226				0.225	MW	(131)		
St	0.215	(100000)	1	1	0.215	M			
St	0.209				0.208	VSt	(310)	(400)	(113)
St	0.204	(110000)	1.058	1.051	0.203	St	(311)		
St	0.201				0.201	M			
MW	0.188				0.189	W	(223)		
VW	0.184						(133)		
VW	0.177				0.177	VW			
VW	0.173						(042)	(422)	(024)
VW	0.169								
VVV	0.164						(224)		
VW	0.161							(333)	
VW	0.160								(116)
VVV	0.153				0.152		(242)		
VVV	0.151								
M	0.148	(111000)	1.45	1.45	0.148	VW	(006)	(440)	
VW	0.147								
VW	0.145	(111100)	1.49	1.49	0.145	VW			
M	0.143				0.143	VW	(243)		
VW	0.140				0.140	M		(531)	(124)
VW	0.137								(030)
W	0.131								
M	0.1272	(101000)	1.69	1.70	0.1272	St			
M	0.1258				0.1260	W			
W	0.1248				0.1254	W			
W	0.1238				0.1248	VW			
W	0.1226				0.1236	M			
VW	0.1169	(211000)	1.84	1.82	0.1228	VW			
VVV	0.1140								
VVV	0.1123				0.1121	MW			
VW	0.1117				0.1115	VW			
VW	0.1093	(110010)	1.97	1.97					
M	0.1070	(200000)	2.01	2.00	0.1070	MW			
VVV	0.1056				0.1067	MW			
VVV	0.1035				0.1056	W			
VVV	0.1013	(220000)	2.13	2.10	0.1036	MW		(226)	
VVV	0.0996				0.1010	VW			(1,2,10)

A long-exposure (12 h) Debye-Scherrer photograph obtained with Fe K $\alpha$  radiation was used. The icosahedral phase was indexed as explained in the text, the indices for  $\text{Al}_6\text{Mn}$  and  $\alpha\text{-Al}_2\text{O}_3$  were obtained from the JCPDS<sup>12</sup> powder data file (card nos 06-665 and 10-173) and the d-spacings of the  $\mu$  phase were obtained as described in the text. St, Strong; M, medium; W, weak; V, very.

strength) steel. The alloy was melted in air at 1,245 K in a 3-mm diameter (4-mm height) cylindrical cavity and was rapidly pressurized by forge hammer application on the cold piston. The piston and the liquid alloy were thermally isolated by a hot 1-mm asbestos cloth placed on the liquid metal. We estimate that the sample was pressurized to  $\sim 2$  GPa in  $< 200$  ms (refs 1, 2).

The product of the rapid pressurization experiment was magnetic. A vibrating sample magnetometer measurement of the sample showed the presence of a ferromagnetic phase with a Curie temperature of 800 K. The sample was then analysed by X-ray powder diffraction. The observed d-spacings with their assignment to various phases are shown in Table 1. The diffraction pattern from the icosahedral phase (we have used the



Fig. 1 Microstructure of the rapidly pressurized sample. The compositions of phases A, B, C and D are given in Table 2.

Table 2 Chemical composition (in atomic %) of the various phases shown in Fig. 1

	Al	Mn	Fe	O
Phase A	74.99	24.81	0.20	—
Phase B	78.53	20.58	0.89	—
Phase C	82.41	17.20	0.39	—
Phase D	32.70	1.01	0.09	66.20

icosahedral indexing rather than the cubic indexing of Pauling<sup>8</sup>) was indexed on the basis of six independent vectors  $(1, \pm\tau, 0)$ ,  $(0, 1, \pm\tau)$  and  $(\pm\tau, 0, 1)$ , pointing to the vertices of an icosahedron as done by Bancel *et al.*<sup>9</sup>, where  $\tau = 1.618$ , the golden mean. In addition to the icosahedral phase, the X-ray powder pattern shows the presence of a cubic phase ( $a = 0.838$  nm), the  $\mu$  phase of the Al-Mn system<sup>10</sup>, small amounts of  $\text{Al}_6\text{Mn}$  and a little contamination of  $\text{Al}_2\text{O}_3$ . The X-ray powder pattern after magnetic separation of part of the material showed a clear reduction in intensity of the lines from the cubic phase. The material, when heated at 1,180 K for 3 h in an evacuated quartz ampule (at  $\sim 10^{-6}$  torr), was no longer ferromagnetic and X-ray photographs showed a complete transformation of the material to the  $\mu$  phase (with a little  $\text{Al}_2\text{O}_3$ ), showing conclusively that the cubic phase is a new metastable ferromagnetic phase formed by the rapid pressurization process in the Al-Mn system. The transformed phase is the same as that obtained on heating a rapidly quenched  $\text{Al}_{78}\text{Mn}_{22}$  alloy at 700 °C for 3 h. A comparison of the X-ray photographs from the rapidly pressurized and rapidly cooled alloys after transformation shows a one-to-one correspondence between the X-ray lines, except for the presence of a few weak lines of  $\text{Al}_2\text{O}_3$  contaminant in the pressurized sample. Figure 1 shows the typical microstructure of the alloy. The presence of four distinct phases, A, B, C and D, was observed after initially etching mildly with a  $(\text{FeCl}_3 + \text{ethanol} + \text{HCl})$  solution followed by a deep etch with Keller's reagent ( $1 \text{ cm}^3 \text{ HF} + 1.5 \text{ cm}^3 \text{ HNO}_3 + 2.5 \text{ cm}^3 \text{ HCl} + 95 \text{ cm}^3 \text{ H}_2\text{O}$ ). The compositions of these phases were determined using an electron microprobe. Results obtained from the microprobe were corrected for fluorescence, beam absorption and atomic number against pure standards (99.99 wt% pure) and are shown in Table 2. Microprobe results indicate that a small amount of iron from the steel dies had contaminated the material. The dark chain marked D was found to be an  $\text{Al}_2\text{O}_3$  stringer left over from the melting experiment.

Because the extreme brittleness of the sample precluded transmission electron microscopy, our evidence for correlating the phases to the microstructure is as follows. Phase A could be pitted completely with the  $\text{FeCl}_3$  etch when etched for a long time. The other phases were relatively stable to this etch. We melt-spun alloys with compositions from  $\text{Al}_{75}\text{Mn}_{25}$  to  $\text{Al}_{84}\text{Mn}_{16}$  but could not find any phase that was similarly etched. However, as expected, we found that the icosahedral phases in these

ribbons and those with compositions from  $\text{Al}_{84}\text{Mn}_{16}$  to  $\text{Al}_{80}\text{Mn}_{20}$  etched similarly to phase C. The pressurization experiments were repeated with a 1-mm die cavity where a higher pressure than that applied earlier could be achieved. The sample thus obtained showed larger areas that would etch with  $\text{FeCl}_3$  and also showed higher X-ray intensities of the cubic phase;  $\mu$ -phase X-ray lines were also then much weaker. We conclude that phase A is the magnetic cubic phase. The  $\mu$  phase from the equilibrium phase diagram of the Al-Mn system<sup>10</sup> contains  $\sim 22$  atom% Mn, and of phases B and C in Fig. 1, phase B must correspond to the  $\mu$  phase because of its composition. Phase C is therefore the icosahedral phase. The measured composition of phase C supports this conclusion.

We conclude that the undercooling resulting from rapid pressurization can yield metastable phases, as is shown for the  $\text{Al}_{80}\text{Mn}_{20}$  alloy where the icosahedral phase and a new cubic ferromagnetic phase are obtained. The only other ferromagnetic phase in the Al-Mn binary exists at equi-atomic concentration<sup>11</sup>. The rapid pressurization technique is important because of the possibility of scaling it up to make near net shape components, which have rapidly solidified structures, without relying on rapid heat extraction.

We thank Dr P. Rama Rao for critical discussions and for permission to publish this work.

Received 19 November; accepted 30 December 1985.

1. Sekhar, J. A., Mohan, M., Divakar, C. & Singh, A. K. *Scr. metallurg.* **18**, 1327–1330 (1984).
2. Sekhar, J. A. *Scr. metallurg.* **19**, 1429–1433 (1985).
3. Shechtman, D., Blech, I., Gratias, D. & Cahn, J. W. *Phys. Rev. Lett.* **53**, 1951–xxxx (1984).
4. Levine, D. & Steinhardt, P. J. *Phys. Rev. Lett.* **53**, 2477–XXXX (1984).
5. Maddox, J. *Nature* **314**, 575 (1985).
6. Mackay, A. L. & Kramer, P. *Nature* **316**, 17–18 (1985).
7. Bursill, L. A. & Peng, Ju Lin *Nature* **316**, 50–51 (1985).
8. Pauling, L. *Nature* **317**, 512–514 (1985).
9. Bancel, P. A. *et al.* *Phys. Rev. Lett.* **54**, 2422–2425 (1985).
10. Taylor, M. A. *Acta metall.* **8**, 256–262 (1960).
11. Vlasova, N. I. *et al.* *Physics Metals Metallogr., N.Y.* **51** (6), 1–35 (1981).
12. Joint Committee on Powder Diffraction Standards, *Powder Diffraction Data for Metals and Alloys* (International Center for Diffraction Data, Swarthmore, 1978).

## Phenol and HCl at 550 °C yield a large variety of chlorinated toxic compounds

Göran Eklund, Jörgen R. Pedersen & Birgitta Strömberg

Studsvik Energiteknik AB, S-611 82 Nyköping, Sweden

During the past decade it has been shown conclusively that the incineration of municipal and industrial wastes gives rise to emissions of chlorinated dibenzodioxins and dibenzofurans. However, the mechanism by which these toxic compounds are formed has not yet been fully established. Some researchers believe that the presence of organically bound chlorine is necessary<sup>1</sup>, but others consider that inorganic forms of chlorine may also participate in the process<sup>2</sup>. We now report the synthesis of a large number of chlorinated environmental pollutants in a simple high-temperature experiment. The results show that phenol and HCl are the most likely precursors of the chlorinated dibenzodioxins and dibenzofurans formed in the combustion of wastes. The dependence of the reaction on the concentration of HCl indicates a way of controlling the formation of these toxic compounds during incineration.

Phenol (1 mg) was mixed in quartz tubes with an aqueous solution (10  $\mu\text{l}$ ) containing a constant amount of  $\text{Cl}^-$  (3.7 mg), and variable  $[\text{H}^+]$  ( $\text{pH} = 0.75$ –14). The tubes were sealed and heated to 550 °C for 5 min. After cooling, the residues were extracted with 100  $\mu\text{l}$  of *n*-hexane. The extracts were analysed by gas chromatography-mass spectroscopy (GC-MS) and gas chromatography with electron capture detection. Aliquots (2  $\mu\text{l}$ ) of each extract were injected in splitless mode into a Hewlett-Packard 5880 A gas chromatograph with a fused silica column

Table 1 Chlorinated organic compounds produced by reaction of phenol with HCl

GC separate no.	MS identification	No. of isomers	Relative concentration	GC separate no.	MS identification	No. of isomers	Relative concentration
1	Monochlorobenzene	2	m	29	Tetrachlorchromone	1	t
2	Chlorophenol	2	m	30	Dichlorodibenzofuran	2	m
3	Dichlorobenzene	3	m	31	Trichloronaphthoquinone	1	t
4	Tetrachloropropene	1	m	32	Tetrachloronaphthoquinone	1	t
5	Pentachloropropene	2	m	33	Monochloroxanthrone	1	t
6	Trichlorobenzene	3	M	34	Pentachlorodihydroxy-cyclohexane	2	m
7	Dichlorophenol	2	M	35	Trichlorodibenzofuran	5	m
8	Dichlorobenzofuran	1	M	36	Trichlorodibenzodioxin	5	m
9	Tetrachlorobenzene	3	M	37	Dichloroxanthrone	1	t
10	Trichlorophenol	2	M	38	Tetrachlorodibenzofuran	12	t
11	Trichlorocresol	1	m	39	Tetrachlorodibenzodioxin	>10	m
12	Dichloroindene	3	t	40	Trichlorobiphenyl	1	t
13	Trichlorobenzofuran	2	m	41	Trichloroxanthrone	1	t
14	Pentachlorobenzene	1	m	42	Pentachlorobiphenyl	2	m
15	Tetrachlorophenol	2	M	43	Pentachlorochromone	2	t
16	Tetrachlorocresol	1	m	44	Pentachlorodibenzofuran	5	t
17	Tetrachlorobenzofuran	3	m	45	Pentachlorodibenzodioxin	5	t
18	Trichloroindene	3	m	46	Tetrachloroxanthrone	1	m
19	Trichloromethylbenzoquinone	1	m	47	Hexachlorocoumarone	1	t
20	Hexachlorobenzene	1	m	48	Hexachlorodibenzodioxin	5	m
21	Monochlorodibenzofuran	2	t	49	Hexachlorodibenzofuran	4	m
22	Dichloronaphthoquinone	1	t	50	Tetrachlorodihydroxytetrahydrophenanthrene	1	t
23	Pentachlorophenol	1	m	51	Heptachlorodibenzofuran	1	t
24	Tetrachlorobenzodihydroquinone	1	m	52	Dichlorotriphenylbenzene	1	t
25	Dichlorohydroxyindene	1	t	53	Octachlorodibenzodioxin	1	t
26	Dichlorochromone	1	t	54	Octachlorodibenzofuran	1	t
27	Tetrachlorobenzoquinone	2	m	55	Hexachlorotriphenylbenzene	1	t
28	Trichlorochromone	1	t				

M, m and t denote major, minor and trace reaction products, respectively.

(SE-54, 30 m, 0.22 mm i.d.). The GC-MS analyses were performed on a Finnigan 1020 GCMS, and the mass spectra were tentatively identified by comparison with standard mass spectra libraries. Table 1 contains the result of the GC-MS analysis of the extract from the experiment at highest [HCl]; the list of identified chlorinated organic compounds is very similar to lists of pollutants found in flue gases from municipal incinerators.

Figure 1 shows the amount of phenols produced, as a function of [HCl]; clearly, the reaction is very sensitive to [HCl]. At  $[HCl] < 10^{-3}$  M no chlorinated compounds could be detected.

Although the reaction time in these experiments was substantially longer than the residence time of fuels during incineration, the temperatures and HCl concentrations were such as may be achieved locally in a typical waste incinerator. Phenol and precursors to phenol are ubiquitous in household wastes. A reasonable hypothesis is that chlorinated organic compounds are produced from phenols, acids and any chlorine source in

the combustion zone. This hypothesis can easily be tested in a full-scale experiment in which acids from the fuels are neutralized during combustion.

We believe that production of chlorinated dibenzodioxins and dibenzofurans is a probable, though not a necessary result of waste incineration. The high sensitivity of the chlorination reaction to [HCl] suggests that the emissions of these pollutants can be significantly reduced at low cost. Reduction of [HCl] in the combustion zone should be possible by injection of a suitable alkaline sorbent along with the fuel.

Received 28 October 1985; accepted 24 January 1986.

- Rappe, Ch., Markland, S., Buser, H. R. & Bosshard, H. P. *Chemosphere* 7, 269–277 (1978).
- Bumb, R. R. et al. *Science* 210, 385–390 (1980).

## Measurement of organic carbon in polar snow samples

Mark S. Twickler, Mary Jo Spencer,  
W. Berry Lyons & Paul A. Mayewski

Glacier Research Group and Department of Earth Sciences,  
University of New Hampshire, Durham,  
New Hampshire 03824, USA

Glaciers provide a unique medium for the study of palaeoatmospheric chemistry<sup>1–3</sup>, particularly in polar glaciers where chemical records may extend for at least several hundred thousand years. Glaciochemical records from remote, high-latitude areas provide a regional- to global-scale integration of past atmospheric chemistry. These records yield information regarding climate change<sup>4–7</sup>, volcanic events<sup>8,9</sup> and solar activity<sup>10</sup>, as well as the effect of human activities<sup>11,12</sup>. Although gaseous forms of organic carbon have been analysed in polar ice<sup>13,14</sup>, we present here the first measurements, to our knowledge, of organic carbon from

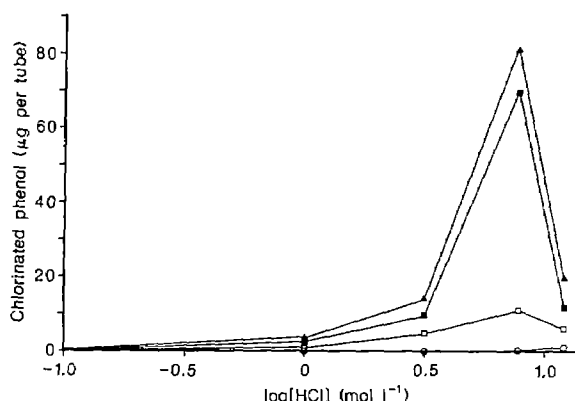
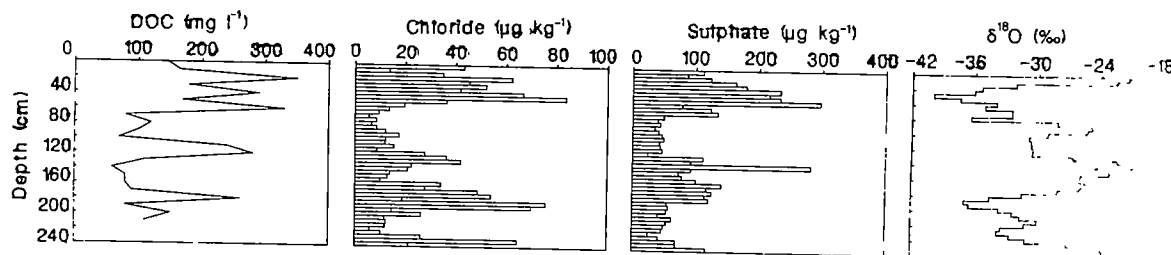


Fig. 1 The formation of chlorinated phenols as a function of HCl concentration. At  $[HCl]$  lower than  $10^{-3}$  M, no chlorinated compounds could be detected. ○, Pentachlorophenol, ■, tetrachlorophenols; □, trichlorophenols; ▲, total chlorophenols. Reaction conditions are specified in the text.

Fig. 1 Concentrations of DOC, chloride, sulphate and  $\delta^{18}\text{O}$  in snowpit.

polar firm samples. Our measurements are among the lowest reported for organic carbon in precipitation. The data indicate that dissolved organic carbon in Greenland snow has a seasonal deposition pattern, with higher concentrations observed in the winter/spring period. Although we are unable to establish the source of the organic carbon in Greenland snow, three possibilities are discussed.

The burning of fossil fuels and the clearing of forests have led to the increase in inorganic carbon input into the atmosphere that has been documented recently in polar ice cores<sup>15</sup>. These processes introduce organic carbon and elemental carbon into the atmosphere as well<sup>16,17</sup>. It is also evident that natural processes may introduce quantities of gases and particulate organic carbon into the atmosphere<sup>18-23</sup>. We now compare organic carbon data for snow from a remote, high-latitude location with values from other, lower latitude locations and evaluate the feasibility of using ice core samples to monitor the historic record of both natural and anthropogenic organic carbon emissions into the atmosphere.

In June 1984, a 2.3-m snowpit was carefully excavated ~40 km south-west of Dye 3, Greenland ( $65.01^\circ\text{N}$ ,  $44.87^\circ\text{W}$ ). The snowpit sampling was part of a larger programme that involved the electrochemical drilling of a 115-m core at this location and the collection of snow samples from several 1.5-m snowpits between the drilling site and Dye 3. The sampling was carefully undertaken by individuals wearing polyethylene gloves, non-particulating clean-suits and particle masks. Samples for organic carbon analysis were collected at 10-cm intervals by pushing Pyrex tubes (previously combusted at  $500^\circ\text{C}$ ), horizontally into a cleanly scraped side of the snowpit. A tube was taken into the field, opened and closed and returned to our laboratory, filled with organic-carbon-free water and analysed as a blank. This blank was below our detection limit of  $0.01\text{ mg l}^{-1}$ . The mean of organic carbon values from 19 snow samples collected in snowpits from the depth range 0–150 cm between the primary sampling site and Dye 3 was  $0.11\text{ mg l}^{-1}$  with a range between  $0.03$  and  $0.32\text{ mg l}^{-1}$ . All samples were kept frozen until a few hours before analysis. Samples were analysed by injecting  $10\text{ cm}^3$  of melted snow into a Barnstead Photochem organic carbon analyser with a glass syringe. Potassium hydrogen phthalate was used as a standard. All glassware and syringes were cleaned and/or rinsed several times in Chromerge before use. Duplicate analyses of four samples gave the following results:  $0.145 \pm 0.005$ ,  $0.165 \pm 0.055$ ,  $0.10 \pm 0.01$  and  $0.07 \pm 0.01\text{ mg l}^{-1}$ .

We report the values as dissolved organic carbon (DOC) even though the samples were not filtered before analysis. A few minutes before the samples were extracted from their containers, the tubes were swirled in order to homogenize the samples; this may have resuspended any particulate matter present. Samples were then drawn from the top of the liquid. Although colloidal organic material present in the samples was undoubtedly collected and analysed by this technique, much of the particulate carbon present in these samples remained in the sample containers. Recent work at Dye 3 indicates that only a very small percentage of the tropospheric aerosol collected in the spring season is composed of organic carbon<sup>24</sup>. In addition, owing to the nature of our analytical technique (ultraviolet oxidation of

the sample), it is highly unlikely that the measurement includes any elemental carbon (soot) present in the sample. No attempt was made to assess possible adsorption of DOC onto the container walls during the thawing procedure.

Figure 1 shows a plot of the DOC concentration versus depth in the snowpit. In addition, the values for  $\text{Cl}^-$  and  $\text{SO}_4^{2-}$  (measured by ion chromatography) are also shown. The DOC values are the lowest ever reported for precipitation (Table 1). In general, the DOC profile resembles those of  $\text{Cl}^-$  and  $\text{SO}_4^{2-}$ . Busenberg and Langway have demonstrated that the highest  $\text{Cl}^-$  values in Dye 3 precipitation occur in the winter/spring period<sup>25</sup>. Examination of the  $\delta^{18}\text{O}$  data from this snowpit (Fig. 1) suggest that the high DOC values are generally associated with lower temperatures (the correlation between  $\text{Cl}^-$  and  $\delta^{18}\text{O}$  is negative and significant at the 95% confidence level). Because the major source of  $\text{Cl}^-$  to this area is thought to be sea-salt aerosol<sup>19,25</sup>, the DOC probably has a similar source, or is transported along the same pathway.

One explanation for the increased marine aerosol component in the winter/spring snows of south-central Greenland is that it reflects increased storm activity, wave action and sea-salt entrainment in the ocean and atmosphere surrounding Greenland at this time of year. 'Clean' marine aerosols at  $\sim 41^\circ\text{S}$  latitude contain a considerable amount of organic matter<sup>26</sup>. Another explanation of this seasonal pattern of DOC deposition is that the sources of these chemical species ( $\text{Cl}^-$ ,  $\text{SO}_4^{2-}$  and DOC) may be distinct, but common atmospheric transport and removal processes lead to a similarity in depositional pattern. For example, the continental derived element aluminium also shows a strong late winter/spring peak in central Greenland snow<sup>27</sup> similar to that of marine-derived species such as  $\text{Cl}^-$ . Therefore, a long-travelled continental biogenic source of the DOC is also possible. Andreae has shown that most organic carbon present in the tropospheric aerosol over the Atlantic Ocean has a terrestrial source<sup>16</sup>. These compounds could be the products of gas-to-particle conversion of continental derived gaseous precursors<sup>28</sup>. Finally, a local to regional terrestrial source of the DOC is highly unlikely as higher values would be expected primarily during the summer<sup>29</sup>. High  $\text{SO}_4^{2-}$

Table 1 Mean dissolved organic carbon values for remote precipitation

Location	Concentration of DOC ( $\text{mg l}^{-1}$ )	Ref.
Carrol Glacier, Alaska	0.15	31
Hubbard Brook, New Hampshire	1.09	32
Ithaca, New York	1.88	27
Como Creek, Colorado	1.52	33
Enewetak Aroll	0.27 (rainy season) 1.18 (dry season)	34
Alberta	1.6	35
Colorado Rockies†	0.5	36
Amsterdam Island	As high as 0.4*	23
Katherine, Australia	As high as 0.6*	23

\* Values only for acetic and formic acid carbon.

† Subsurface values.

concentrations in Arctic aerosols and snows during the winter/spring period are due to meteorological conditions that allow transport of air masses from anthropogenically impacted mid-latitude areas to the Arctic<sup>30</sup>. The observed winter/spring DOC maxima may then also represent deposition of a continental derived aerosol which has been affected by fossil fuel burning.

Obviously, we lack the data to determine the origin of the DOC at this time and we cannot rule out the possibilities that the DOC may: (1) reflect an input of marine organic carbon and be similar in source to  $\text{Cl}^-$ ; (2) represent a natural continental source similar to Al; or (3) have its origin from an anthropogenic source similar to the winter/spring  $\text{SO}_4^{2-}$  signal. Only by the detailed investigation of the specific organic compounds present in polar snows will a unique solution to the origin of DOC be found. It does appear, however, no matter what the source, that DOC may be useful as a seasonal indicator in Greenland ice.

Owing to the small number of samples analysed, the short time period represented by the snowpit and the lack of identification of specific organic compounds, we cannot comment with any certainty on the effect of human activities on the DOC concentrations found in the Greenland snow. More detailed studies using ice-core samples could provide detailed information regarding historic organic carbon emissions as well as the ultimate source of the DOC.

This work was supported by a contract from the US Environmental Protection Agency administered through North Carolina State University (APP-0306-1983). We thank W. Dansgaard and H. Clausen for the oxygen isotope analyses and J. V. James and T. Hinkley for help with sample collection.

Received 19 August; accepted 30 December 1985.

1. Boutron, C. & Lorius, C. *Ambio* 9, 210–215 (1980).
2. Herron, M. M. & Herron, S. L. *J. Sci. Hydrol.* 28, 139–153 (1983).
3. Wolff, E. W. & Peel, D. A. *Nature* 313, 535–540 (1985).
4. Thompson, L. G. & Mosley-Thompson, E. *Science* 212, 812–815 (1981).
5. Mayewski, P. A. & Lyons, W. B. *Geophys. Res. Lett.* 9, 190–192 (1982).
6. Palais, J. M. & Legrand, M. *J. geophys. Res.* 90, 1143–1154 (1985).
7. Finkel, R. C. & Langway, C. C. Jr *Earth planet. Sci. Lett.* 73, 196–206 (1985).
8. Hammer, C. U., Clausen, H. B. & Dansgaard, W. *Nature* 288, 230–235 (1980).
9. Herron, M. M. *J. geophys. Res.* 87, 3052–3060 (1982).
10. Raisbeck, G. M. et al. *Nature* 293, 825–826 (1982).
11. Ng, A. & Patterson, C. *Geochim. cosmochim. Acta* 45, 2109–2121 (1981).
12. Boutron, C. F., Patterson, C. C. *Geochim. cosmochim. Acta* 47, 1355–1368 (1983).
13. Craig, H. & Chou, C. C. *Geophys. Res. Lett.* 9, 1221–1224 (1982).
14. Rasmussen, R. A. & Khalil, M. A. K. *J. geophys. Res.* 89, 11599–11605 (1984).
15. Neftel, A., Moor, E., Oeschger, H. & Stauffer, B. *Nature* 315, 45–47 (1985).
16. Andreae, M. O. *Science* 220, 1148–1151 (1983).
17. Hansel, A. D. A. & Rosen, H. *Geophys. Res. Lett.* 11, 381–384 (1984).
18. Rasmussen, R. A. & Went, F. W. *Proc. natn. Acad. Sci. U.S.A.* 53, 215–220 (1965).
19. Lewis, W. M. Jr *Wat. Resour. Res.* 17, 169–181 (1981).
20. Andreae, M. O. & Raemdonck, H. *Science* 221, 744–777 (1983).
21. Cline, J. D. & Bates, T. S. *Geophys. Res. Lett.* 10, 949–952 (1983).
22. Hov, Ø., Penkett, S. A., Isaksen, I. S. A. & Semb, A. *Geophys. Res. Lett.* 11, 425–428 (1984).
23. Galloway, J. M., Likens, G. E., Keene, W. C. & Miller, J. M. *J. geophys. Res.* 87, 8771–8786 (1982).
24. Davidson, C. I., Santhanam, S., Fortmann, R. C. & Olson, M. P. *Atmos. Environ.* (submitted).
25. Busenberg, E. & Langway, C. C. Jr *J. geophys. Res.* 84, 1705–1709 (1979).
26. Andreae, M. O. *J. geophys. Res.* 87, 8875–8885 (1982).
27. Langway, C. C. Jr, Cragin, J. H., Klouda, G. A. & Herron, M. M. *Proc. IUGG Symp. Isotopes and Impurities in Snow and Ice*, 302–306 (International Association of Hydrological Sciences, 1977).
28. Chesselet, R., Fontugne, M., Buat-Menard, P., Ezat, U. & Lambert, C. E. *Geophys. Res. Lett.* 8, 345–348 (1981).
29. Likens, G. E., Edgerton, E. S. & Galloway, J. M. *Tellus* 35B, 16–24 (1983).
30. Rahn, K. A. *Atmos. Environ.* 15, 1447–1455 (1981).
31. Loder, T. C. & Hood, D. W. *Limnol. Oceanogr.* 17, 349–355 (1972).
32. Likens, G. E., Bornmann, F. H., Pierce, R. S., Eaton, J. S. & Johnson, N. M. *Biogeochemistry of a Forested Ecosystem* (Springer, New York, 1977).
33. Grant, N. C. & Lewis, W. M. Jr *Tellus* 34, 74–88 (1982).
34. Zafriou, O. V., Gagosian, R. B., Peltzer, E. T., Alford, J. B. & Loder, T. C. *J. geophys. Res.* 90, 2409–2423 (1985).
35. Wallis, P. M., Hynes, H. B. N. & Telang, S. A. *Hydrobiologia* 79, 77–90 (1981).
36. Thurman, E. M. *Organic Geochemistry of Natural Waters* (Nijhoff/Junk, Dordrecht, 1985).

## Significance of atmospheric-derived fixed nitrogen on productivity of the Sargasso Sea

Anthony Knap & Timothy Jickells\*

Marine and Atmospheric Programme, Bermuda Biological Station for Research, Inc., Ferry Reach 1–15, Bermuda

Alex Pszenny & James Galloway

Department of Environmental Studies, University of Virginia, Charlottesville, Virginia 22903, USA

Recently, it has been suggested that marine primary productivity can be influenced by direct inputs of fixed inorganic nitrogen ( $\text{NO}_3^-$ ,  $\text{NO}_2^-$  and  $\text{NH}_4^+$ ) from atmospheric deposition, and that this may be important in shaping trends of productivity in coastal areas<sup>1</sup>. It is known that anthropogenic contaminants are transported from North America to the Sargasso Sea, affecting the chemistry of rain water over this oligotrophic ocean area. Here we present data collected between 1982 and 1984 as part of the Western Atlantic Ocean Experiment (WATOX) by a wet-only precipitation collector on Bermuda. Our measurements of the anthropogenic fixed nitrogen in the rainwater samples are discussed in the context of the amount of nitrogen required to support 'new' primary production in the Sargasso Sea. We show that the effects of atmospheric deposition are insignificant.

The suggested influence of precipitation on primary productivity was derived using sea water diluted with nutrient-rich deionized water and/or one or two natural local rainwater samples of unspecified composition. As this suggestion has severe implications for oceanic nutrient budgets, we felt it

required further consideration, especially as the nitrogen content of rain water has increased over the past 100 years because of anthropogenic emissions<sup>2</sup>.

We have chosen the Sargasso Sea as a useful area in which to evaluate the effects of rain-derived fixed nitrogen sources for four main reasons:

- (1) It is a central ocean gyre, removed from coastal sources, with low rates of primary productivity<sup>3</sup> and therefore potentially susceptible to.
- (2) It has been shown to be 'downwind' of the North American continent which is a source of acid rain containing fixed nitrogen from anthropogenic emissions; long-range transport of this material can deposit this anthropogenic fixed nitrogen in the Sargasso Sea<sup>4</sup>.
- (3) There is a large database available on the precipitation chemistry on Bermuda which can be extrapolated to estimate wet deposition in the Sargasso Sea<sup>5,6</sup>. There is also a considerable database of precipitation events monitored by ships in the Sargasso Sea<sup>7</sup>.
- (4) There is a long-term (31-yr) database on the hydrography of this area<sup>8</sup> and considerable data on primary productivity collected periodically at 32° N, 65° W over the same time period<sup>3,9</sup>.

We have therefore attempted to assess the relative significance of the atmospheric fixed nitrogen source on the primary productivity of the Sargasso Sea using the considerable data available.

From September 1982 to May 1984 we collected rain water on an event basis at High Point, Bermuda. Samples were spiked immediately after collection with a biocide ( $\text{CHCl}_3$ ) to prevent chemical changes. Samples were analysed at the University of Virginia for  $\text{NO}_3^-$  and  $\text{NH}_4^+$  ions using colorimetric and ion chromatographic techniques<sup>10</sup>. The results for 126 samples are summarized in Table 1 as deposition rates, in  $\mu\text{mol N per m}^2$  per event, calculated from the measured  $\text{NH}_4^+$  and  $\text{NO}_3^-$  concentrations and the amount of precipitation for each event<sup>11</sup>. There is negligible  $\text{NO}_2^-$  in Bermuda rain<sup>4,5</sup>. Ranges and

\* Present address: School of Environmental Science, University of East Anglia, Norwich NR4 7TJ, UK.

Table 1 Wet deposition of  $\text{NH}_4^+$ -N and  $\text{NO}_3^-$ -N at High Point, Bermuda from September 1982 to May 1984

Component	Minimum	Geometric mean ( $\mu\text{mol N per m}^2 \text{ per event}$ )	Maximum	Volume-weighted average* ( $\mu\text{mol N m}^{-2} \text{ d}^{-1}$ )
$\text{NH}_4^+$ -N	1	32	470	13
$\text{NO}_3^-$ -N	3	42	500	17
$(\text{NH}_4^+ + \text{NO}_3^-)$ -N†	7	77	860	30

For details of analyses, see ref. 10.

\* Calculated as volume-weighted average of  $\text{NH}_4^+$ -N or  $\text{NO}_3^-$ -N multiplied by the average precipitation in Bermuda of  $152.5 \text{ cm yr}^{-1}$  (ref. 4), then divided by 365.25.

† These values are different from the sum of  $\text{NH}_4^+$  and  $\text{NO}_3^-$  because the minimum and maximum values of  $\text{NH}_4^+$  and  $\text{NO}_3^-$  occurred in different events, thus affecting the totals.

geometric means are listed as well as the deposition rate in  $\mu\text{mol m}^{-2} \text{ day}^{-1}$ , calculated from the volume-weighted average and the average annual precipitation for Bermuda ( $152.5 \text{ cm}$ )<sup>4</sup>. The  $\text{NO}_3^-$  appears to have a predominantly anthropogenic source in Bermuda precipitation<sup>4</sup> and can therefore be assumed to have increased over the past 100 yr because of increased anthropogenic emissions<sup>2</sup> from North America. Sources of ammonium are probably related to agricultural practices in North America<sup>2</sup> and appear to travel with the acids in Sargasso Sea precipitation<sup>3,7</sup>. There is little information on the concentrations of organic nitrogen in rain, its form or whether it can be used for primary productivity. The organic nitrogen values that are available represent total digestions and are therefore overestimates<sup>12</sup>. The concentration of organic nitrogen has been calculated to be  $7.5 \mu\text{mol l}^{-1}$ , which corresponds to a flux of  $31.2 \mu\text{mol m}^{-2} \text{ d}^{-1}$ , or approximately equal to the  $\text{NH}_4^+$  and  $\text{NO}_3^-$  input.

Estimates of total primary production rates in the Sargasso Sea have been calculated as  $72 \text{ g C m}^{-2} \text{ yr}^{-1}$  (ref. 3), and more recent measurements by our group yielded a similar value of

$90 \text{ g C m}^{-2} \text{ yr}^{-1}$  (S. R. Smith, T.J. and A.K., unpublished data). Using the 'Redfield ratio'<sup>13</sup> of C/N of 106:16 or the more recent ratio of 122:16 (ref. 14), and assuming that 10–20% of net productivity is new production<sup>15</sup>, there is a nutrient requirement of  $\sim 0.08$ – $0.23 \text{ mol N m}^{-2} \text{ yr}^{-1}$  or  $220$ – $630 \mu\text{mol N m}^{-2} \text{ d}^{-1}$ . The rates of primary productivity in the Sargasso Sea have recently been critically reviewed<sup>9</sup>; based on oxygen budget analysis, it is estimated that new (not 'net') productivity may be far greater than the proposed 10–20% of the net productivity rates<sup>15</sup>. It is probable that new productivity is as high as  $50 \text{ g C m}^{-2} \text{ yr}^{-1}$  (ref. 9) which would then require  $1,700 \mu\text{mol N m}^{-2} \text{ d}^{-1}$ .

We have created an inventory of nitrogen sources to the Sargasso Sea based on our work and that of others (Table 2). Even with the inclusion of organic nitrogen sources, nitrogen input due to precipitation ranges from  $16$  to  $80 \mu\text{mol N m}^{-2} \text{ d}^{-1}$ . The 'low' of  $16 \mu\text{mol N m}^{-2} \text{ d}^{-1}$  is based on the possibility that organic nitrogen is not a usable source of nitrogen.

This 'new' production may be supported by nutrient injection from below the euphotic zone. Klein and Coste's 1984 model<sup>16</sup> suggests that nutrients are injected in pulses with frequencies in hours in response to wind stress interaction with surface currents. Klein and Coste's average value for an oligotrophic area in the Mediterranean Sea is  $\sim 900 \text{ mmol N m}^{-2} \text{ yr}^{-1}$ , which corresponds to an average of  $2,500 \mu\text{mol N m}^{-2} \text{ d}^{-1}$ . Although we cannot extrapolate this result to the oligotrophic Sargasso Sea, it does serve to illustrate the range and magnitude of fixed nitrogen that could be provided by this source. Even if there was one major precipitation event, and assuming this lasted 1 day and contained the maximum amount of fixed nitrogen that we have found (Table 1), it could supply only half the nitrogen required for new production<sup>9</sup>.

As the Sargasso Sea is, in our opinion, an extreme case because of the significant anthropogenic component in North American rain, and because this anthropogenic component only reaches Bermuda during favourable meteorological events, we feel we can generalize about other marine oligotrophic areas. We therefore conclude that precipitation plays a minor part in the provision of nutrients for primary productivity in oligotrophic ocean areas<sup>17,18</sup> even though there has been a considerable increase in nitrogen in rain water caused by anthropogenic sources over the past 100 years.

We thank J. Tokos and W. Keene for collection and analysis of the rain water, S. R. Smith for the primary productivity data, and J. Goldman and R. Duce for valuable comments on the manuscript. This work was supported by the US NOAA under the WATOX funding. Additional support was provided by the Bermuda Government. This is contribution no. 1081 from the Bermuda Biological Station for Research, Inc.

Table 2 Average fixed nitrogen inputs to the Sargasso Sea

Input	Range of values ( $\mu\text{mol N m}^{-2} \text{ d}^{-1}$ )	Ref.
<b>Atmosphere</b>		
a, Wet deposition		
$\text{NO}_3^-$ -N	6–29	5–7, 10, 17
$\text{NH}_4^+$ -N	10–21	5–7, 10, 18, 19
Organic N	~30	12
Total wet deposition	16–80	
b, Dry deposition*		
Aerosols		
$\text{NO}_3^-$ -N	1–2	6
$\text{NH}_4^+$ -N	0.1–2	6
Organic N	?	
Gases		
$\text{HNO}_3$	0.4–2	6
$\text{NH}_3$	0.04–40	
$\text{NO}_x$	0.03–2	6
Organic N	?	
<b>Ocean</b>		
In situ $\text{N}_2$ fixation	0.1	19
From deep-water $\text{NO}_3^-$ -N†	22–112	19
Required for 'new' production	~1,700	8
Estimated from 10–20% net production‡	220–630	

\* Estimates of dry deposition rates to the Sargasso Sea have not been made; these represent estimates of global averages.

† Recalculated based on ref. 19. (Originally calculated as  $225$ – $1,350 \mu\text{mol N m}^{-2} \text{ d}^{-1}$ , however a mathematical error in conversion of nitrate flux to  $\text{m}^{-2} \text{ h}^{-1}$  resulted in an order-of-magnitude overestimate.)

‡ S. R. Smith, T.J. and A.K., unpublished data.

Received 11 October 1985; accepted 15 January 1986.

- Paerl, H. W. *Nature* **315**, 747–749 (1985).
- Brimblecombe, P. & Stedman, D. H. *Nature* **298**, 460–462 (1982).
- Menzel, D. & Ryther, J. *Deep-Sea Res.* **6**, 351–367 (1960).
- Jickells, T. D., Knap, A. H., Church, T., Galloway, J. N. & Miller, J. *Nature* **297**, 55–57 (1982).
- Church, T. M., Galloway, J. N., Jickells, T. D. & Knap, A. H. *J. geophys. Res.* **87**, 11013–11018 (1982).

6. Galloway, J. N. in *The Biogeochemical Cycling of Sulfur and Nitrogen in the Remote Atmosphere* (eds Galloway, J. N., Charlson, R. J., Andrae, M. O. & Rodhe, H.) (Reidel, Dordrecht, in the press).
7. Galloway, J. N., Knap, A. H. & Church, T. M. J. *Geophys. Res.* **88**, 10859–10864 (1983).
8. Wright, W. R. & Knap, A. H. *Intergovt oceanogr. Commun Tech. Ser.* **24** (1983).
9. Jenkins, W. J. & Goldman, J. C. *J. mar. Res.* **43**, 465–491 (1985).
10. Galloway, J. N., Likens, G. E., Keene, W. C. & Miller, J. J. *Geophys. Res.* **87**, 8771–8786 (1982).
11. Keene, W. C., Pszenny, A. A. P., Galloway, J. N. & Hawley, M. E. *J. Geophys. Res.* (submitted).
12. Jickells, T. D. & Hillier, G. B. in *Bermuda Biol. Sta. Spec. Publ.* No. 18, 63–66 (1982).
13. Redfield, A. C., Ketchum, B. H. & Richards, F. A. in *The Sea* Vol. 2 (ed. Hill, M. N.) (Interscience, London, 1963).
14. Takahashi, T., Broeker, W. S. & Langer, S. *J. Geophys. Res.* **90**, 6907–6924 (1985).
15. Dugdale, R. C. & Goering, J. J. *Limnol. Oceanogr.* **12**, 196–206 (1967).
16. Klein, P. & Coste, B. *Deep Sea Res.* **31**, 21–37 (1984).
17. Carpenter, E. D. & McCarthy, J. J. *Limnol. Oceanogr.* **20**, 389–401 (1975).
18. Menzel, D. W. & Spaeth, J. P. *Limnol. Oceanogr.* **7**, 159–162 (1962).
19. McCarthy, J. J. & Carpenter, E. D. *Nitrogen in the Marine Environment* (eds Carpenter, E. J. & Capone, D. G.) 487–512 (Academic, New York, 1983).

phytanes or their diagenetic products. Its recognition suggests a novel diagenetic pathway for acyclic isoprenoids involving the introduction of sulphur into specific lipid moieties. Similar, but intermolecular, sulphur incorporation might give rise to sulphur-linked macromolecular materials and thereby contribute significantly to the formation of kerogens.

Significant developments have recently occurred in the understanding of the biological origins of sedimentary acyclic isoprenoids and their subsequent diagenetic fate. It is now evident that such compounds, which were among the first clearly related to natural products to be recognized in sediments and petroleums<sup>14,15</sup>, are not wholly derived from the phytol side-chain of chlorophyll, but may also originate from the free and ether-bound lipids of archaeabacteria<sup>16–18</sup> and from the tocopherols<sup>19</sup> of photosynthetic organisms. Here we further expand the range of such compounds with the characterization of acyclic isoprenoid thiophenes in sediments.

In addition to a thiophene-containing hopane<sup>6</sup>, many immature sediments, notably those recovered by the Deep Sea Drilling Project (DSDP), contain a number of components tentatively identified as thiophenes from their mass spectra<sup>7–10</sup> (Table 1, Fig. 1). These spectra are dominated by cleavages and rearrangements associated with the thiophene ring<sup>20,21</sup>, a feature that simplifies the recognition of the size of their alkyl substituents, although providing no indication of the structure of these alkyl groups (whether straight-chain or branched). The widespread occurrence and relative abundance of the C<sub>20</sub> alkyl thiophenes I and II suggested to us that these compounds might be related to acyclic isoprenoids. Certainly their occurrence in several sediments (for example, in the Japan Trench, Walvis Ridge and Cariaco Trench) with high concentrations of phytanes<sup>22</sup> and phytol<sup>23</sup> provided circumstantial evidence for this relationship.

If I (Table 1, Fig. 1) is an acyclic isoprenoid thiophene, then its mass spectrum<sup>9</sup> might correspond to that expected for 3-methyl-2-(3,7,11-trimethyldodecyl)-thiophene (Fig. 2). Synthesis of this compound (together with its 4-methyl isomer, III; Fig. 3) followed by gas chromatograph (GC) and gas chromatograph-mass spectrometer (GC-MS) coinjection (OV-1 methyl silicone fluid columns) confirmed this assignment. Such a structure might arise from the incorporation of sulphur into a phytadiene or phytol, a process also observed in heating experiments with H<sub>2</sub>S and carbohydrates<sup>24</sup>. The recognition of alkyl

## Isoprenoid thiophenes: novel products of sediment diagenesis?

S. C. Brassell\*, C. A. Lewis\*, J. W. de Leeuw†,  
F. de Lange† & J. S. Sinninghe Damsté†

\* Organic Geochemistry Unit, University of Bristol,  
School of Chemistry, Cantock's Close, Bristol BS8 1TS, UK  
† Organic Geochemistry Unit, Delft University of Technology,  
Department of Chemistry and Chemical Engineering,  
de Vries van Heystplantsoen 2, 2628 RZ Delft, The Netherlands

Sulphur is a significant component of the organic matter in recent and ancient sediments and in petroleums<sup>1,2</sup>, yet the precise nature of its association and incorporation is poorly understood. Various sulphur-containing compounds have been recognized in petroleums<sup>2–4</sup>, but little is known about their origins and mode of generation during sediment burial, and for only a few organo-sulphur compounds with >15 carbon atoms have the structures been determined<sup>5,6</sup>. Here we identify one of the alkyl thiophenes which occur widely in both recent and ancient deep-sea sediments<sup>7–13</sup> as 3-methyl-2-(3,7,11-trimethyldodecyl)-thiophene, occurring as a limited number of the possible stereoisomers. This compound is presumed to originate from the incorporation of sulphur into chlorophyll-derived phytol, or archaeabacterial

Table 1 Occurrence of alkylthiophenes in oceanic and other sediments

Location	DSDP Leg-Site	Age	I	II	Others*	Ref.
Cariaco Trench	15–147	Quaternary	✓	✓	—	‡
Japan Trench	56–436	Pliocene	—	—	F	‡
	57–440	Pleist.-Mio.	✓	✓	E, F	‡
San Miguel Gap	63–467	Plio.-Mio.	✓	✓	F	7
Gulf of California	64–474	Pleistocene	—	—	F	8
	64–478	Pleistocene	—	—	G, H	8
	64–479	Pleistocene	✓	✓	G, H	‡
	64–481	Pleistocene	—	—	Unspecified†	8
Middle America Trench	67–496	Quaternary	✓	✓	—	‡
Walvis Ridge	75–532	Quat.-Plio.	✓	✓	A-F	9,‡
Angola Basin	75–530	Miocene	✓	✓	F	9
Mazagan Escarpment	79–545	Cenomanian	✓	—	—	10
	79–547	Eocene	✓	✓	—	10
Livello Bonarelli	NA	Cen./Tur.	✓	✓	—	11
Namibian Shelf	NA	Quaternary	✓	✓	—	12
Sarcina	NA	Miocene	✓	✓	B, C and others	13

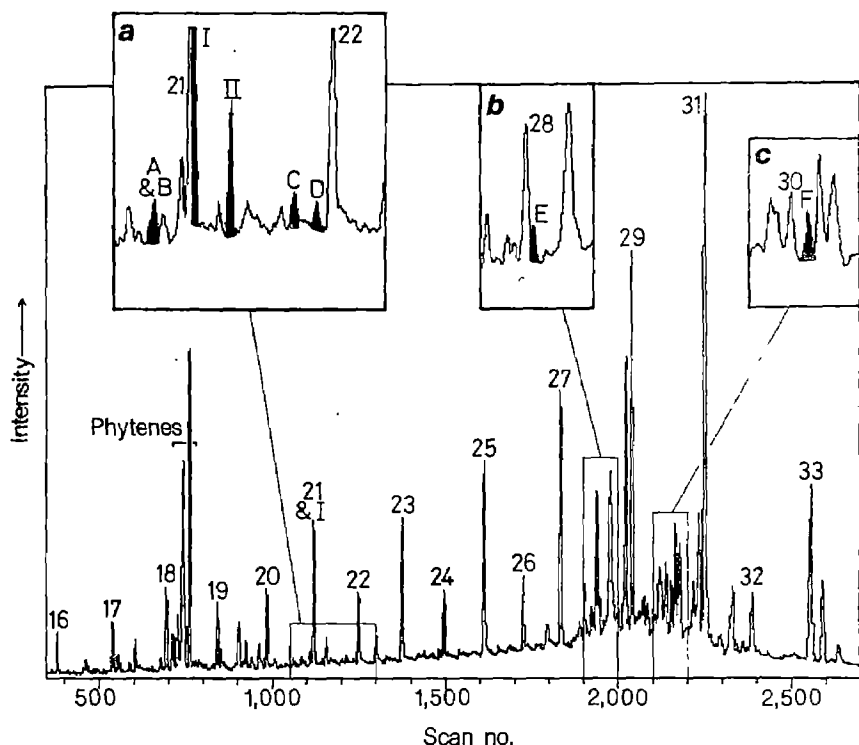
—, Not observed or reported; NA, not applicable. Pleist., Pleistocene; Mio., Miocene, Quat., Quaternary; Plio., Pliocene; Cen., Cenomanian; Tur., Turonian.

\* The identities of compounds A to F are given in the legend of Fig. 1; G and H are isomeric C<sub>25</sub> alkylthiophenes ( $M^+ = 378$ , prominent ions with mass/charge ratios  $m/z = 265$  and 125 (ref. 8)) of unknown structure.

† Range of mono-, di- and trialkylated thiophenes.

‡ S.C.B., unpublished data.

**Fig. 1** Reconstructed ion chromatogram from GC-MS analysis of the extractable aliphatic hydrocarbon fraction of a diatomaceous ooze from Walvis Ridge (DSDP 75-532-42-3, 173-m sub-bottom depth). Insets *a*, *b* and *c* are expansions of the scan regions 1,050–1,300, 1,900–2,000 and 2,100–2,200, respectively. This sample contains a number of alkyl thiophenes distinguished by the prominence of  $m/z = 97$ , 98, 111 or 125 in their mass spectra. Compounds I and II are discussed in the text; their mass spectra for molecular ion fragment mass ( $M^+$ ) 308 are dominated by  $m/z$  of 111 and 98, respectively, and are published in ref. 10. A, D, E and F appear to be  $C_{18}$ ,  $C_{19}$ ,  $C_{25}$  and  $C_{27}$  *n*-alkyl substituted thiophenes. The mass spectrum of F ( $M^+ = 406$ ) is given in ref. 9. The minor constituents B and C are probably 2,3-dimethyl-5-(2,6,10-trimethylundecyl)-thiophene<sup>13</sup> and 3,5-dimethyl-2-(3,7,11-trimethylundecyl)-thiophene, respectively (Fig. 2). Peaks corresponding to *n*-alkanes are designated by their carbon numbers; among other significant components note the abundance of three phytene isomers between scans 700 and 800. The GC-MS conditions were similar to those previously reported<sup>29</sup>.



thiophenes in shallow, immature sediments (Table 1) suggests, however, that elevated temperatures are not required for their formation. Rather, their occurrence in oceanic sediments is more closely analogous to that of various low-molecular-weight organo-sulphur compounds, including dimethylsulphide and volatile thiophenes<sup>23</sup>, which are deemed to be direct metabolic products. A biosynthetic origin of higher-molecular-weight thiophenes, such as I, cannot be fully excluded.

A useful method for assessing the origins and extent of thermal maturation of acyclic isoprenoids is the evaluation of the steric configuration at their chiral centres. Comparative GC on a

diethylene glycol succinate/polyethylene glycol succinate (DEGS/PEGS)-coated column<sup>26</sup> showed that the naturally occurring compound in a calcareous clay from the Cariaco Trench was composed of a maximum of two of the four possible stereoisomers (Ia-d, Fig. 4) found in the all-isomer synthetic product. It also seems probable from this analysis that the naturally occurring I in the Cariaco Trench sediment is composed, at least in part, of the isomer (3R, 7R; Ia in Fig. 4) expected to derive from isoprenoid biosynthesis, although proof of this requires stereospecific synthesis in the laboratory. The structure and limited stereochemistry of I is consistent with sulphur incorporation into phyt-a-1,3-diene (IV in Fig. 2) or phytol.

By analogy with the mass spectrum of I (ref. 9), compound II (Table 1, Fig. 1) would correspond to 3-(4,8,12-trimethyltridecyl)-thiophene, which might arise from sulphur incorporation into phyt-a-1,3(17)-diene (V in Fig. 2) or phytol. Such phytadienes, and hence isoprenoid thiophenes, cannot be artefacts generated during sample preparation because wet extraction methods were used<sup>27</sup>. Given the widespread occurrence of I and II, and other *n*-alkyl and isopranyl substituted thiophenes (ref. 13 and S.C.B., unpublished data), in oceanic sediments (Table 1), there appears to be a general metabolic or diagenetic process which results in the introduction of sulphur into lipid moieties. The precise mechanism and biological or chemical agents of this process are unclear, but H<sub>2</sub>S or polysulphides may be involved. Perhaps it is a side reaction associated with bacterial sulphate reduction, which certainly occurs or has occurred in the sediments found to contain thiophenes.

For the thiophenes discussed here, the sulphur introduced into the acyclic isoprenoids is bonded intramolecularly. Similar reactions operating in an intermolecular fashion would give rise to sulphur-linked polymeric material within kerogens. Such bonding may survive in petroleums and occur in both their aromatic and asphaltene fractions; especially the latter since it is rich in sulphur. Alternatively, thermal breaking of carbon-sulphur bonds may be a significant contributory process in the generation of petroleum from kerogen. The clear indication that sulphur incorporation can affect organic compounds during early diagenesis represents a major advance in the understanding of interactions at the molecular level between the sulphur and

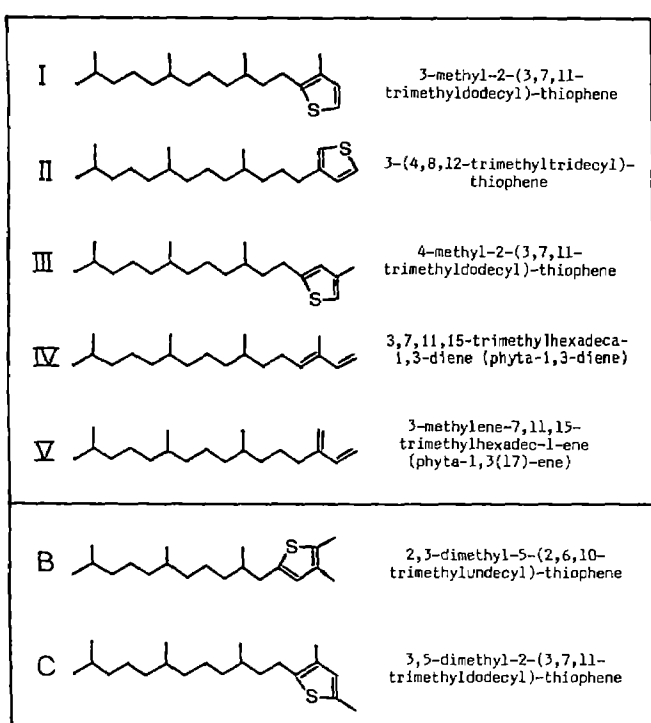


**Fig. 2** Structures of compounds cited in the text and figures.

**Fig. 3** Summary scheme for synthesis of all-isomer 3-methyl-2-(3,7,11-trimethyldodecyl)-thiophene (**I**) together with their 4-methyl isomers (**III**). The methyl substitution at C-3 and C-4 can be distinguished by mass spectrometry, since the compounds show base peaks at  $m/z = 111$  and 112, respectively. Proton-NMR ( $\text{CDCl}_3$ , 200 MHz) proved the presence of the different methyl isomers: **I** gave  $\delta_{\text{H}5} = 6.984$  p.p.m.,  $J = 5.1$  Hz and  $\delta_{\text{H}4} = 6.766$  p.p.m.,  $J = 5.1$  Hz and **III** gave  $\delta_{\text{H}3} = 6.589$  p.p.m. and  $\delta_{\text{H}5} = 6.657$  p.p.m. with very small splitting, possibly caused by coupling with the C-4 methyl of the thiophene ring.

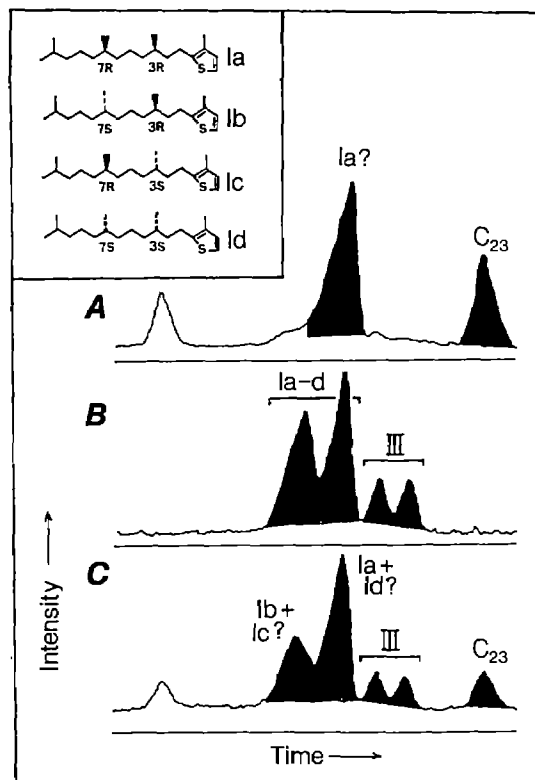
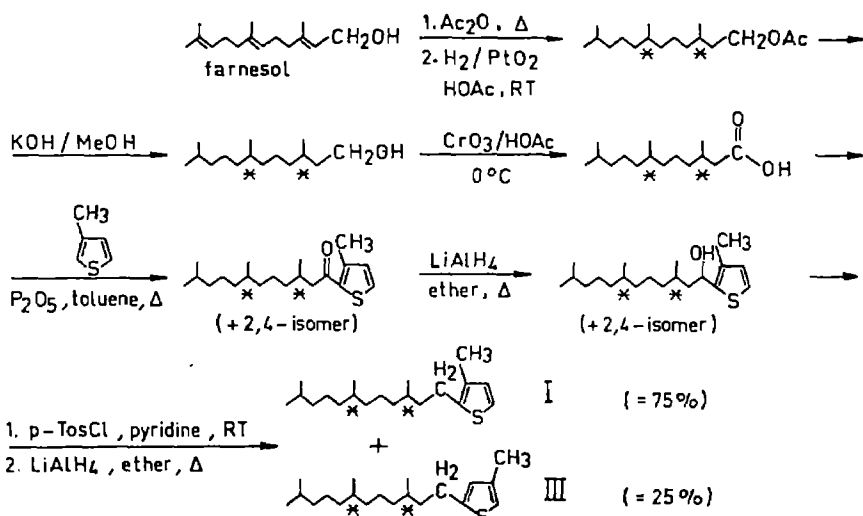


**Fig. 4** Partial GC traces using a DEGS/PEGS column of the  $n$ -tricosane ( $n$ -C<sub>23</sub>) region of: **A**, aliphatic hydrocarbon fraction of a Pleistocene calcareous clay from the Cariaco Trench (DSDP 15-147C-3-3, 138-m sub-bottom depth). **B**, Products (**I** and **III**) of the synthesis shown in Fig. 3. **C**, Coinjection of **A** and **B**. The naturally occurring thiophene enhances the latter peak attributed to **I**. This evidence can be compared with that from similar GC analyses of acyclic isoprenoids where the isomer with the stereochemistry corresponding to both that of the phytol moiety in chlorophyll- $\alpha$ <sup>30</sup> and archaeabacterial phytanyl ether moieties<sup>31</sup> occurs in the peak with the greater elution time (for example 7R, 11R in dihydrophytol<sup>31-34</sup> and phytanic acid<sup>32,34</sup>, and 6R, 10S in phytane<sup>35</sup>).

**Methods.** 34-m DEGS/PEGS (3:1) glass capillary column fitted in Carlo Erba FTV2150 chromatograph programmed from 20–109 °C at 4 °C min<sup>-1</sup> and held isothermally at 109 °C. Data are acquired and processed using a VG Minichrom data system. Assignment of  $n$ -C<sub>23</sub> was made by comparison with the elution position of a reference standard. Note that the elution times of the thiophenes relative to  $n$ -alkanes are markedly greater with this column than with that (OV-1) employed in the GC-MS analysis (Fig. 1).

carbon cycles within sediments. Also, the occurrence of organo-sulphur compounds indicates that organic matter, like iron<sup>28</sup>, can act as a sink for sedimentary sulphur. Thus, the identification of acyclic isoprenoid thiophenes in sediments demonstrates a new, significant process in the diagenetic alteration of lipids, and presumably other compound classes.

S.C.B. and C.A.L. are grateful to NERC for GC-MS facilities (grants GR3/2951 and GR3/3758 to Professor G. Eglinton), to the Royal Society for an instrument grant (VG Minichrom system) and to British Petroleum PLC for a studentship (C.A.L.).

Received 2 September 1985; accepted 23 January 1986.

- Tissot, B. P. & Welte, D. H. *Petroleum Formation and Occurrence* (Springer, Berlin, 1984).
- Orr, W. L. *Amer. chem. Soc. Div. Fuel. Chem. Preprints* 22, 86–99 (1977).
- Speers, G. C. & Whitehead, E. V. in *Organic Geochemistry: Methods and Results* (eds Eglinton, G. & Murphy, M. T. J.) 638–675 (Springer, Berlin, 1969).
- Ho, T. Y., Rogers, M. A., Drushel, H. V. & Koons, C. B. *Bull. Amer. Ass. Petrol. Geol.* 58, 2338–2348 (1974).
- Payzant, J. D., Cyr, T. D., Montgomery, D. S. & Strausz, O. P. *Tetrahedron Lett.* 26, 4175–4178 (1985).
- Valisalalao, J., Perakis, N., Chappe, B. & Albrecht, P. *Tetrahedron Lett.* 25, 1183–1186 (1984).
- Rulkötter, J., von der Dick, H. & Welte, D. H. *Init. Rep. DSDP* 63, 819–836 (1981).
- Rulkötter, J., von der Dick, H. & Welte, D. H. *Init. Rep. DSDP* 64, 837–853 (1982).
- Rulkötter, J., Mukhopadhyay, P. K. & Welte, D. H. *Init. Rep. DSDP* 75, 1069–1087 (1984).
- Rulkötter, J., Mukhopadhyay, P. K., Schaefer, R. G. & Welte, D. H. *Init. Rep. DSDP* 79, 775–806 (1984).
- van der Graas, G. thesis, Delft Univ. Technol. (1982).
- Klok, J. thesis, Delft Univ. Technol. (1984).
- ten Haven, H. L., de Leeuw, J. W. & Schenck, P. A. *Geochim. cosmochim. Acta* 49, 2181–2191 (1985).
- Dean, R. A. & Whitehead, E. V. *Tetrahedron Lett.* 768–770 (1961).
- Bendoraitis, J. G., Brown, B. L. & Hepner, L. S. *Analyt. Chem.* 34, 49–53 (1962).
- Brassell, S. C., Wardrop, A. M. K., Thomson, I. D., Maxwell, J. R. & Eglinton, G. *Nature* 290, 693–696 (1981).
- Chappe, B., Michaelis, W. & Albrecht, P. in *Advances in Organic Geochemistry 1979* (eds Douglas, A. G. & Maxwell, J. R.) 265–274 (Pergamon, Oxford, 1980).
- Risatti, J. B., Rowland, S. J., Yon, D. A. & Maxwell, J. R. *Org. Geochem.* 6, 93–104 (1984).
- Goossens, H., de Leeuw, J. W., Schenck, P. A. & Brassell, S. C. *Nature* 312, 440–442 (1984).
- Kinney, I. W. & Cook, G. L. *Analyt. Chem.* 24, 1391–1396 (1952).
- Ponomis, J. G., Fatland, C. L. & Zaylskie, R. G. *J. chem. Engng Data* 21, 380–385 (1976).
- Brassell, S. C. & Eglinton, G. in *Advances in Organic Geochemistry 1981* (eds Bjordal, M. et al.) 684–697 (Wiley, Chichester, 1983).
- Brassell, S. C. et al. in *Advances in Organic Geochemistry 1979* (eds Douglas, A. G. & Maxwell, J. R.) 375–392 (Pergamon, Oxford, 1980).
- Margo, F. D. *Geochim. cosmochim. Acta* 47, 1433–1441 (1983).
- Whelan, J. K., Hunt, J. M. & Berman, J. *Geochim. cosmochim. Acta* 44, 1767–1785 (1980).
- McKenzie, A. S., Patience, R. L., Yon, D. A. & Maxwell, J. R. *Geochim. cosmochim. Acta* 46, 783–792 (1982).
- de Leeuw, J. W. et al. in *Advances in Organic Geochemistry 1975* (eds Campos, R. & Goni, J.) 61–79 (Enadis, Madrid 1977).
- Berner, R. A. *Geochim. cosmochim. Acta* 48, 605–615 (1984).
- Brassell, S. C., Gowar, A. P. & Eglinton, G. in *Advances in Organic Geochemistry 1979* (eds Douglas, A. G. & Maxwell, J. R.) 421–426 (Pergamon, Oxford, 1980).
- Burrell, J. W. K., Garwood, R. F., Jackman, L. M., Oskay, E. & Weedon, B. C. L. *J. chem. Soc. C*, 2144–2154 (1966).
- Anderson, R., Kates, M., Baedecker, M. J., Kaplan, I. R. & Ackman, R. G. *Geochim. cosmochim. Acta* 41, 1381–1390 (1977).
- Brooks, P. W. & Maxwell, J. R. in *Advances in Organic Geochemistry 1973* (eds Tissot, B. P. & Biernier, F.) 977–991 (Technip, Paris, 1974).
- Van Vleet, E. S. & Quinn, J. G. *Geochim. cosmochim. Acta* 43, 289–303 (1979).
- Prahl, F. G., Eglinton, G., Corner, E. D. S. & O'Hara, S. C. M. *Science* 224, 1235–1237 (1984).
- Patience, R. L., Yon, D. A., Ryback, G. & Maxwell, J. R. in *Advances in Organic Geochemistry 1979* (eds Douglas, A. G. & Maxwell, J. R.) 287–293 (Pergamon, Oxford, 1980).

## Floral evidence for Cretaceous chloranthoid angiosperms

E. M. Friis\*, P. R. Crane† & K. R. Pedersen\*

\* Department of Geology, University of Aarhus,  
DK-8000 Aarhus C, Denmark

† Department of Geology, Field Museum of Natural History,  
Chicago, Illinois 60605, USA

The hypothesis that multiparted magnoliaceous flowers retain the largest number of primitive floral characters among living angiosperms has received support from almost 80 years of comparative studies with extant plants<sup>1–3</sup>. Accumulating fossil data suggest, however, that large *Magnolia*-like flowers were probably preceded in the fossil record by smaller and simpler floral types, some of them perhaps related to the Chloranthaceae, a family generally regarded as being advanced within the Magnoliidae<sup>2–4</sup>. The presence of chloranthoid plants early in the history of the angiosperms has been suggested by studies of dispersed pollen<sup>4–7</sup> and fossil leaves<sup>8</sup>, but the information on floral structure crucial to assessing the biology of these plants and their relationships within the Chloranthaceae, has so far been unavailable. We now provide new evidence of Cretaceous chloranthoid angiosperms based on fossil androecia, with pollen *in situ*, from the Lower Cretaceous of eastern North America and the Upper Cretaceous of southern Sweden. The Cretaceous material clarifies the homologies of chloranthoid androecial structures and provides an improved basis for interpreting the pollination biology in this enigmatic group of early angiosperms.

The earliest well-documented angiosperm fossils include pollen grains of *Clavatipollenites hughesii*, originally described from the late Barremian and Aptian of southern England<sup>5,9,10</sup>. Couper<sup>5</sup> noted the resemblance of these pollen grains to those of the extant chloranthaceous genus *Ascarina*, and detailed similarities in pollen wall structure have subsequently been demonstrated by transmission and scanning electron microscopy of fossil and Recent material<sup>4</sup>. Two other Lower Cretaceous angiosperm pollen types, *Stephanocolpites fredericksburgensis* and *Asteropollis asteroides*, are also closely similar to pollen of extant Chloranthaceae and have been compared to the genera *Chloranthus* and *Hedyosmum*, respectively<sup>4</sup>. Certain Lower Cretaceous leaves also exhibit strong epidermal and architectural similarities to extant Chloranthaceae<sup>8</sup>, although these are not sufficiently well marked to permit an assignment to the modern family.

The material described here provides the first direct evidence of floral structure in early chloranthoid angiosperms. It com-

prises two kinds of androecial structure obtained by sieving from the Lower Cretaceous Patapsco Formation (Potomac Group) of eastern North America and from the Upper Cretaceous of Scania, southern Sweden. The Lower Cretaceous material was recovered from a clay lens at the West Brothers locality in Maryland, dated on palynological evidence as probably early late Albian (Pollen Subzone II-B)<sup>11</sup>. The associated flora includes wood fragments, logs and numerous angiosperm leaf fossils<sup>8,12</sup> as well as conifer shoots, cones and seeds, and a variety of angiosperm fruits, seeds, anthers and flowers. The Upper Cretaceous material was recovered from clays and sands in the Höganäs AB kaolin quarry near Åsen, Scania, dated on palynological evidence as of late Santonian or early Campanian age. A diverse assemblage of angiosperm flowers, fruits, seeds and seeds has already been reported from the Åsen locality<sup>13,14</sup>.

The androecial structures from both localities are three-dimensionally preserved as charcoal, and scanning electron microscopy reveals both morphological details and *in situ* pollen. Both androecia are three-lobed with the lateral lobes slightly shorter than the central lobe. In the Lower Cretaceous material each lobe consists of a fully developed stamen with two pairs of small, elongated pollen sacs borne laterally on a fleshy and almost cylindrical connective that is slightly expanded at the apex. The three stamens are fused only at the base (Fig. 1a). The central lobe is ~0.7 mm long, and the total width of the androecium is ~0.5 mm. The anthers contain small, coarsely reticulate pollen grains, ~10 µm long. The pollen apparently has three (or four) colpi, but the precise number of apertures is obscured by folds in the grains and by a thick coating resembling pollenkitt (Fig. 1b). In the Upper Cretaceous fossils only the central lobe of the androecium has four pollen sacs, and the two lateral lobes each bear a single pair of pollen sacs on the adaxial surface (Fig. 1c). The connectives of all three lobes are broad and fleshy, with a short apical expansion. They are fused immediately below the pollen sacs and form a broad laminar structure, ~1–2 mm long and 1–2 mm wide. Pollen grains observed *in situ* are small (~13 µm in diameter), reticulate and spiraperturate (Fig. 1d).

Extant Chloranthaceae comprise approximately 70 species distributed among four genera. *Ascarina* (including *Ascarinopsis*) and *Hedyosmum* have unisexual flowers and an arborescent or shrubby habit, while *Chloranthus* and *Sarcandra* have bisexual flowers and a suffrutescent or herbaceous habit. All genera produce reticulate pollen grains, but within the family there is considerable variation in the number and arrangement of apertures<sup>4,15,16</sup>. The three-lobed arrangement of both the Lower and Upper Cretaceous androecia, combined with the expanded connectives, small pollen sacs and reticulate pollen, constitutes a unique combination of characters that occurs today

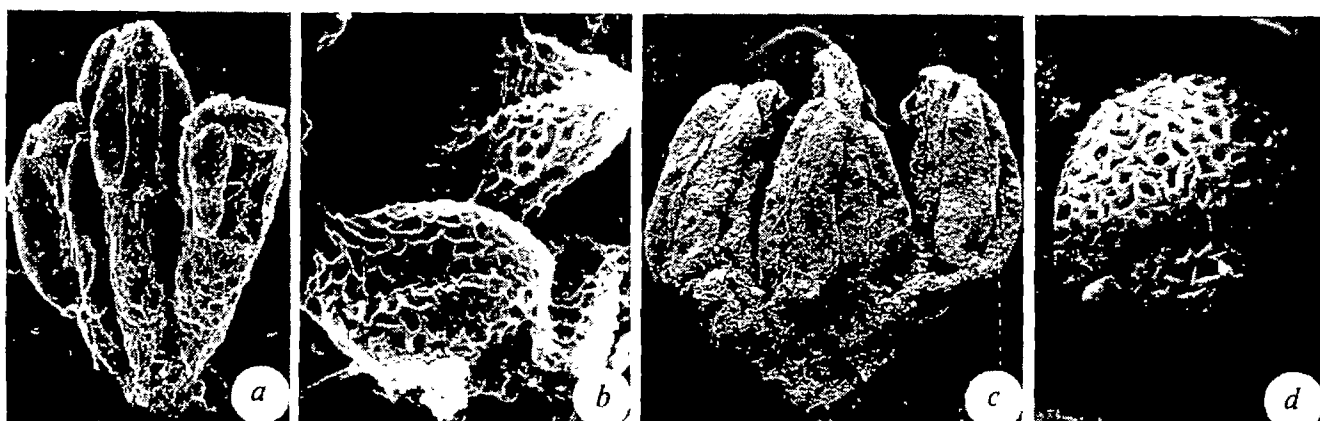


Fig. 1 Scanning electron micrographs of fossil chloranthoid androecia and pollen from the Cretaceous. *a*, Chloranthoid androecium from the Lower Cretaceous (Upper Albian of eastern North America) ( $\times 80$ ). *b*, Pollen grains from the androecium shown in *a*, adhering to the anther by means of a substance resembling pollenkitt ( $\times 3,300$ ). *c*, Chloranthoid androecium from the Upper Cretaceous (Upper Santonian/Lower Campanian) of southern Sweden ( $\times 50$ ). *d*, Pollen grains from the androecium shown in *c*; note the spiral aperture ( $\times 3,300$ ).

only in the genus *Chloranthus*. The androecia of modern *Chloranthus* are more or less laminar and identical to that of the Upper Cretaceous form in the arrangement and number of pollen sacs, with one pair on the lateral lobes and two pairs on the central lobe. Owing to lack of information on the gynoecium, however, the fossils cannot be included with certainty in the extant genus *Chloranthus*. The Lower Cretaceous androecium has a more generalized morphology, and there are no extant species of *Chloranthus* that have lateral lobes with a full complement of four pollen sacs, or that have laterally positioned pollen sacs borne on a more or less cylindrical connective. In *Sarcandra*, however, the androecium consists of a single stamen, closely resembling each lobe of the Lower Cretaceous fossil. The Lower Cretaceous form may thus be related to the ancestral chloranthoids that may have given rise to both *Chloranthus* and *Sarcandra*.

The nature of the *Chloranthus* androecium is the subject of much controversy. Some authors have suggested an origin by lateral fusion of three stamens, one with a fully developed anther consisting of two pairs of pollen sacs, and two with half-anthers each consisting of a single pair of pollen sacs<sup>3,15</sup>. Other authors have suggested an origin by division of a single stamen that bore four pairs of pollen sacs<sup>15</sup>. The structure of the Lower Cretaceous androecium reported here supports the more straightforward view that the *Chloranthus* androecium originated by simple lateral fusion of three normally developed stamens, each of which originally bore four pollen sacs. This notion is also consistent with the available anatomical and ontogenetic data on extant *Chloranthus*<sup>15</sup>. The loss of the two pollen sacs in each of the lateral stamens may have occurred with increasing fusion, and a shift to adaxially positioned pollen sacs may have been established as the androecium became more laminar. Both changes may have occurred as part of a trend towards increasingly efficient pollination.

Extant Chloranthaceae include both insect- and wind-pollinated taxa. The bisexual flowers of *Chloranthus* and *Sarcandra* are apparently pollinated by beetles or occasionally flies<sup>17</sup>. Insects are attracted to the flowers by the enlarged, fleshy connectives, which become coloured and glossy at anthesis and produce a fruit-like aroma. Pollen production is low and the pollen grains are covered by sticky pollenkitt<sup>17</sup>. In *Ascarina* and *Hedyosmum* the flowers are unisexual and apparently anemophilous<sup>17,18</sup>. The pollen grains are dry and produced in large quantities.

The two fossil androecia reported here strongly suggest pollination by insects. In addition to the probable relationship to *Chloranthus* and *Sarcandra*, the presence of fleshy connectives, small pollen grains and a coating of pollenkitt all support this interpretation. The number of apertures in the pollen from the Lower Cretaceous androecium is not fully clear, but no tri- or polycolpate pollen of comparable size and sculpture has been recognized among the dispersed pollen described from the Potomac Group. Similarly, spiraperturate pollen comparable to that from the Upper Cretaceous androecia has not been observed in the dispersed pollen flora from Åsen; this also suggests the possibility of low pollen production in our Cretaceous material. In contrast, the relative abundance of *Clavatipollenites* (similar to *Ascarina*) and *Asteropollis* (similar to *Hedyosmum*) in some Lower Cretaceous samples has been used to infer that the plants producing these grains were probably anemophilous<sup>4</sup>. If this interpretation is correct, then chloranthoid angiosperms had already differentiated into anemophilous and entomophilous taxa before the end of the late Cretaceous. This supports the suggestion of an early differentiation of insect- and wind-pollination systems in the angiosperms, based on slightly younger material<sup>19</sup>.

The evidence now available on Cretaceous Chloranthaceae demonstrates conclusively the importance of this family in the earliest phases of angiosperm diversification. At least some early angiosperms had small, inconspicuous flowers and evidence

suggests that both wind and insect pollination were established very early in angiosperm evolution.

We thank Professor W. L. Crepet, Professor D. L. Dilcher, Dr P. K. Endress and Dr K. Nixon for helpful discussion. We acknowledge the receipt of a Niels Bohr fellowship (E.M.F.) and support from the NATO Senior Fellowship Scheme (E.M.F.), the Field Museum Department of Geology Visiting Scientist Program (K.R.P.) and NSF grant BSR-8314592 (P.R.C.).

Received 17 October 1985; accepted 27 January 1986.

1. Arber, E. A. N. & Parkin, J. J. Linn. Soc. 38, 29–80 (1907).
2. Takhtajan, A. *Flowering Plants, Origin and Dispersal*, 1–310 (Oliver & Boyd, Edinburgh, 1969).
3. Cronquist, A. *An Integrated System of Classification of Flowering Plants*, 1–1262 (Columbia University Press, 1981).
4. Walker, J. W. & Walker, A. G. Ann. M. bot. Gdn 71, 464–521 (1984).
5. Couper, R. A. *Palaeontographica* B103, 77–179 (1958).
6. Doyle, J. A. J. Arnold Arbor. 50, 1–35 (1969).
7. Muller, J. Bot. Rev. 47, 1–142 (1981).
8. Upchurch, G. R. Ann. M. bot. Gdn 71, 522–550 (1984).
9. Kemp, E. M. *Palaeontology* 11, 421–434 (1968).
10. Hughes, N. R., Drewry, G. E. & Laing, J. F. *Palaeontology* 22, 513–535 (1979).
11. Doyle, J. A. & Hickey, L. J. in *Origin and Early Evolution of Angiosperms* (ed. Beck, C. B.) 139–206 (Columbia University Press, 1976).
12. Hickey, L. J. in *Cretaceous and Tertiary Stratigraphy, Paleontology and Structure, Southwestern Maryland and Northeastern Virginia* (eds Frederiksen, N. O. & Kraft, K.) 193–209 (U.S. Geological Survey, Reston, 1984).
13. Friis, E. M. Ann. M. bot. Gdn 71, 403–418 (1984).
14. Friis, E. M. Biol. Skr. 25, 1–37 (1985).
15. Swamy, B. G. L. J. Arnold Arbor. 34, 375–408 (1953).
16. Erdtman, G. *Pollen Morphology and Plant Taxonomy*, 1–539 (Almqvist & Wiksell, Stockholm, 1952).
17. Endress, P. K. *Pl. Syst. Evol.* (in the press).
18. van der Hammen, T. & Gonzales, E. *Leid. geol. Meded.* 25, 261–315 (1960).
19. Dilcher, D. L. *Rev. Palaeobot. Palynol.* 27, 291–328 (1979).

## Early forest clearance and environmental degradation in south-west Uganda

Alan Hamilton\*, David Taylor\* & J. C. Vogel†

\* Department of Environmental Studies, University of Ulster, Coleraine, Co. Londonderry BT52 1SA, UK

† National Physical Research Laboratory, PO Box 395, Pretoria 001, South Africa

Evidence for early agriculture can be obtained from pollen profiles indicating forest clearance<sup>1</sup>. The practice of cultivation is widely believed to have been introduced into the interlacustrine region of central Africa by Bantu-speaking iron-workers<sup>2</sup>, present by 2,000 yr BP (ref. 3) or, disputedly<sup>2–4</sup>, 2,600 yr BP (ref. 5). There are, however, archaeological and linguistic indications that cultivation may have begun earlier<sup>3,4,6,7</sup>. Published pollen diagrams which clearly show forest clearance in East Africa are either poorly dated<sup>8</sup> or place forest destruction<sup>1</sup> after 2,000 yr BP; possible palynological signs of previous clearance<sup>9,10</sup> are open to other interpretations, notably climatic change<sup>1</sup>. We have now analysed the pollen and charcoal of a peat core from Ahakagyezi Swamp in south-west Uganda using radiocarbon for dating. The results suggest a history of forest clearance stretching back beyond 4,800 yr BP. This is the earliest evidence for cultivation reported from tropical Africa.

Ahakagyezi Swamp (1,830 m; Fig. 1) is surrounded by steep hillsides, covered today with a patchwork of small fields and short pasture<sup>11</sup>. Few indigenous woody plants remain, but the rainfall is 1,125 mm yr<sup>-1</sup> (ref. 12) and the natural vegetation has been reconstructed as moist lower montane forest<sup>13</sup>, similar to that in early Bwindi Forest<sup>11</sup>. Erosion of the infertile soils developed from Precambrian argillitic rocks<sup>12</sup> is a major agricultural problem<sup>14</sup>. The swamp vegetation is *Syzygium* forest with a marginal zone of sedges or *Typha*<sup>11</sup>.

The 10-m core, collected with a Hiller borer, is mainly wood peat, with herbaceous macrofossils and clay common in two horizons towards the base and herbaceous fossils also present

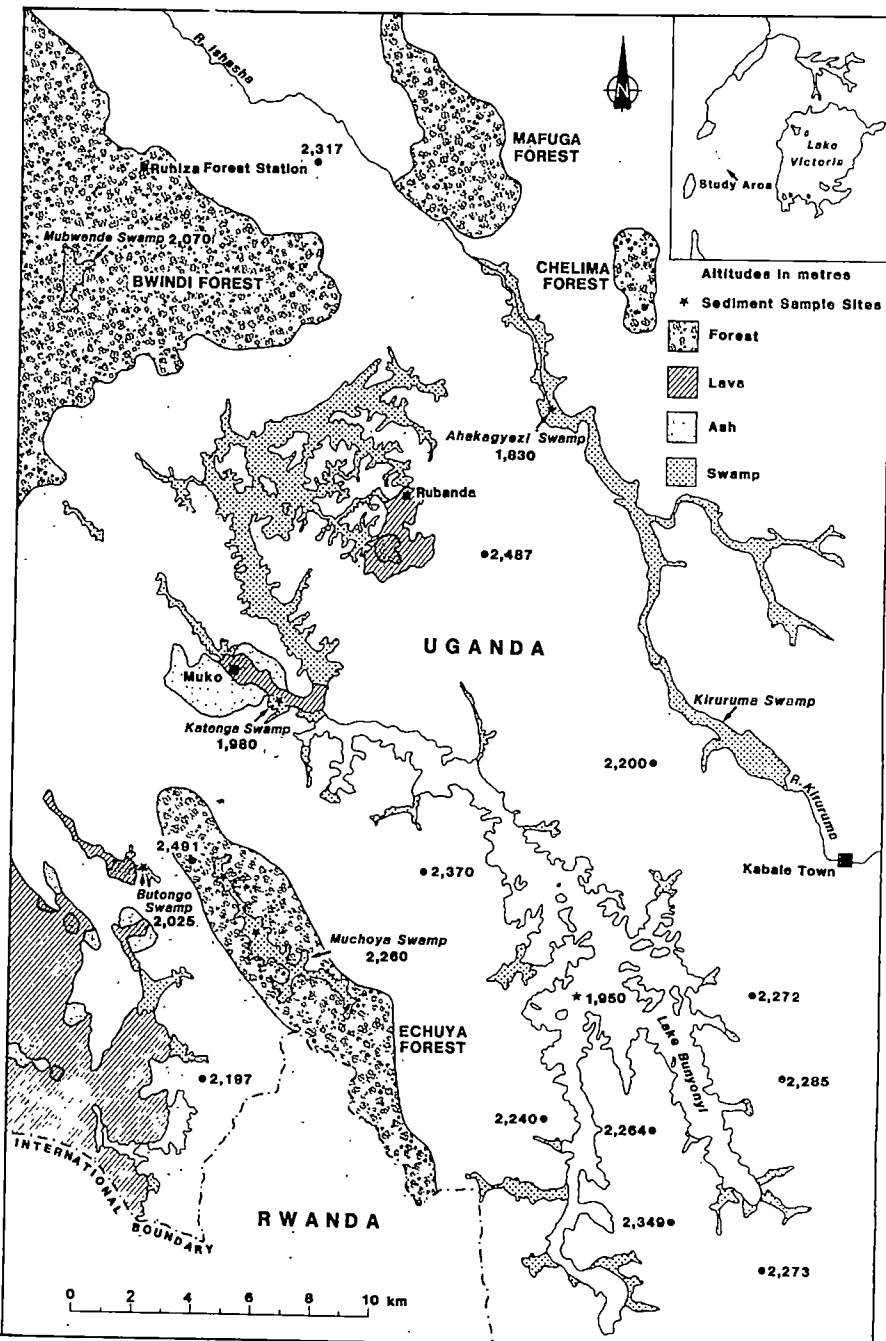


**Fig. 1** Part of the Rukiga Highlands, southwest Uganda, showing Ahakagyezi and other sites<sup>8,23</sup> used for pollen analysis. Bwindi is moist lower montane forest, grading into lowland forest towards the north-west; the vegetation varies topographically and altitudinally<sup>11</sup>. Other forests shown are secondary.

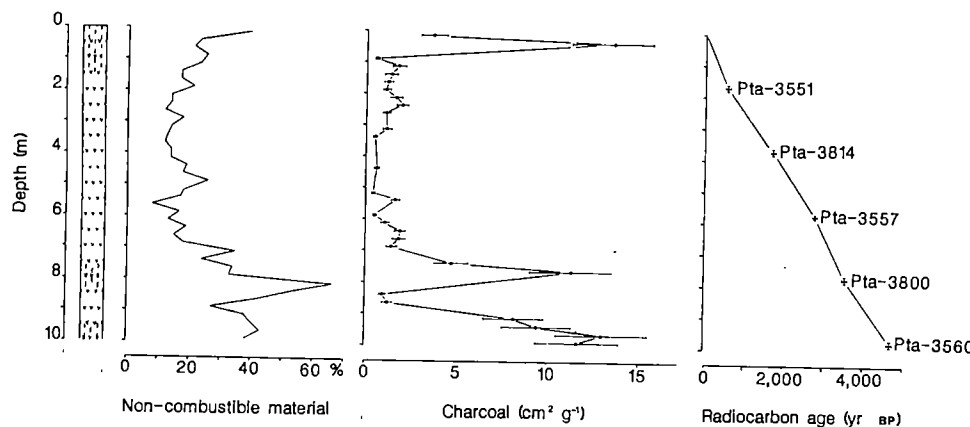


**Fig. 2** Stratigraphy and sediment properties of a core from Ahakagyezi Swamp. Non-combustible material determined by ignition of dried samples at 550°C. Charcoal abundance estimated by the point-count method<sup>24</sup>; bars indicate 95% confidence limits of the counts. Radiocarbon determined on whole peat samples, pretreated with dilute acid; dates calculated using a half-life of 5,568 yr, corrected for isotopic fractionation. □, Wood peat; ▨, herbaceous peat; ▨, clay.

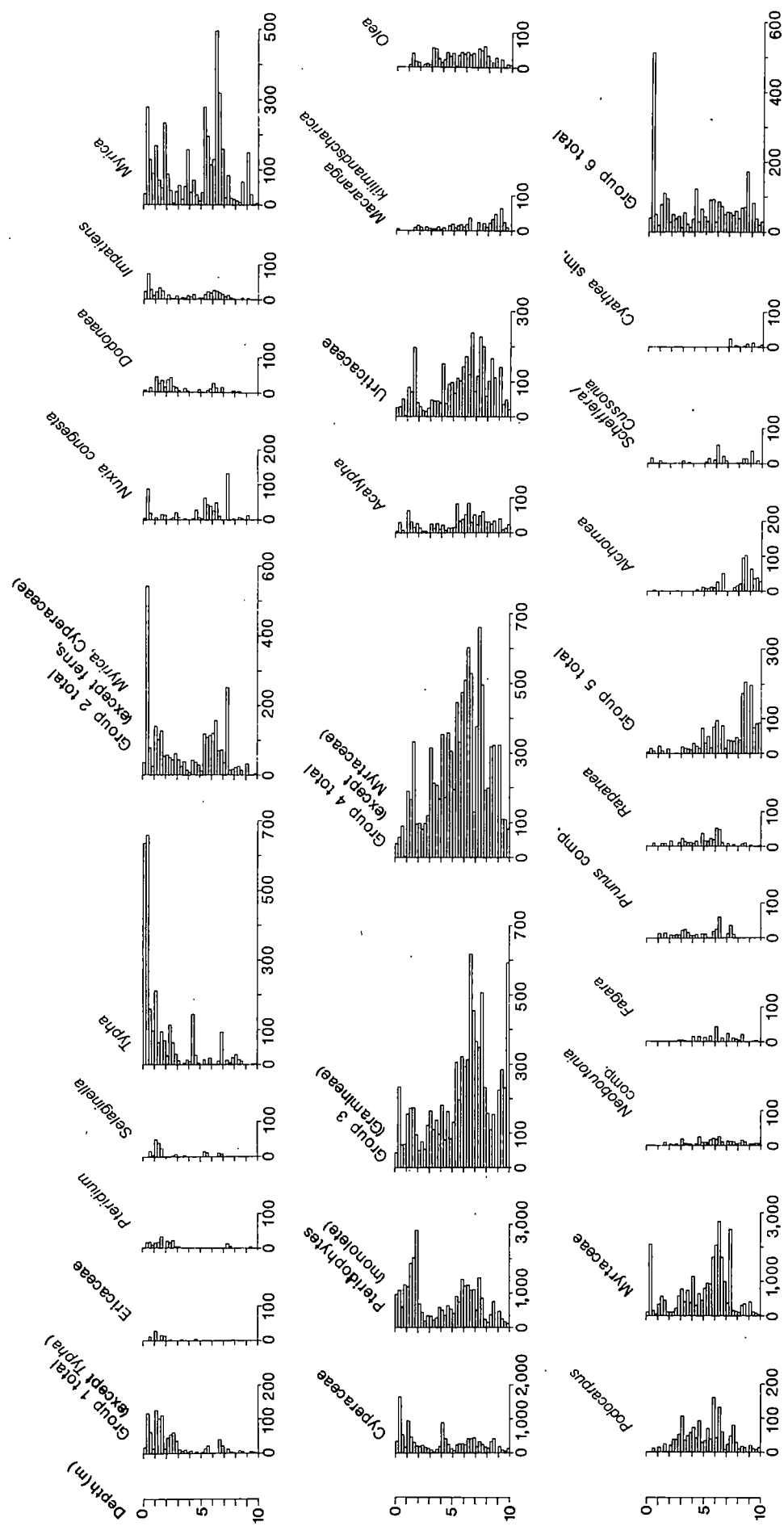


**Fig. 3** Ahakagyezi: pollen diagram with group totals and selected individual taxa. Pollen abundance expressed as grains deposited per  $\text{cm}^2$  per yr. Level 8.85–8.90 m omitted because of suspected error in estimating pollen concentration. The group totals omit *Typha* (group 1), *Cyperaceae*, *Myrica*, pteridophytes (monoletes) (group 2) and *Myrtaceae* (group 4), all of which attain high values; if included, they would unduly dominate the group totals. All identified pollen types with an abundance of >0.4% of total pollen at any one level are on the figure or listed below. Additional pollen types: group 1, *Clematis*, *Trilete* spores (smooth); group 2, *Bidens* sim., *Crassulaceae* comp., *Polyscias*, *Rumex*, *Stephania*; group 4, *Celtis* sim., *Maesa* comp., *Polypodium* sim., *Umbelliferae*; group 5, *Anthoceros*, *Anthocleista*, *Ebenaceae*, *Loranthaceae*, *Musanga*/*Myrianthus*, *Parinari*; group 6, *Acanthaceae*, *Achyranthes* comp., *Begonia*, *Faurea* comp., *Helichrysum* sim., *Hydrocotyle* sim., *Ilex*, *Laurembergia*, *Olinia*, *Potamogeton*. Ecological interpretation of group 6, characterized by little directional change, is not given.

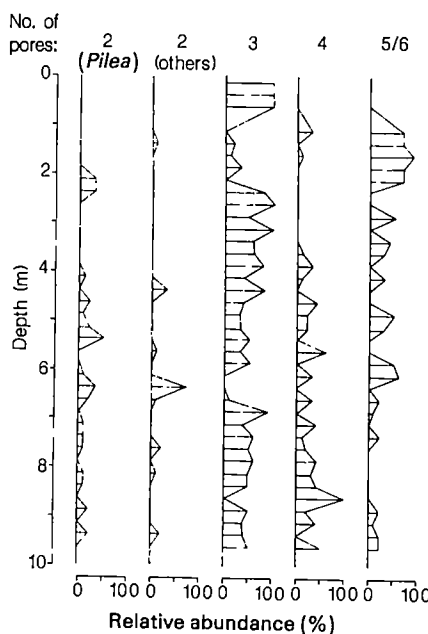


Fig. 4 Urticaceae pollen: percentage abundance of various types in the Ahakagyezi core. Those most clearly indicative of forest are *Pilea* and four-porate grains (produced mainly by *Urtica hypselodendron*)<sup>25</sup>.

above 1.5 m (Fig. 2). The horizons containing clay or herbaceous fossils are associated palynologically with periods of forest clearance or intensified agriculture and are believed to signify enhanced soil erosion. Microscopic charcoal is abundant at some levels, especially in and just above the clay-rich strata. Radiocarbon measurements provide excellent dating control (Table 1).

Samples were prepared for pollen analysis by a standard procedure including HF treatment and acetolysis<sup>15</sup>; pollen influx rates were estimated using the *Lycopodium* spore method<sup>16</sup>. Pollen preservation is generally excellent. Pollen types are grouped here according to patterns of change in accumulation rate, regardless of absolute values (Fig. 3).

Group 1, increasing above ~3 m (1,300 yr BP), includes pollen types derived from plants of agricultural land and scrub<sup>1,17</sup> (*Ericaceae*, *Pteridium*, *Vernonia*) and from swamp species associated with heavy siltation<sup>18</sup> (*Selaginella*, *Typha*). This suggests marked disturbance of terrestrial vegetation, leading to soil erosion and consequent vegetational change in the swamp.

Group 2, with two peaks, one similar to that of group 1 and the other at ~5.25–7.5 m (2,500–3,400 yr BP), contains pollen types of plants associated with human disturbance (*Bidens*, *Dodonaea*, *Nuxia*, *Polyscias*, *Rumex*) and pollen of swamp margin plants (*Cyperaceae*, *Impatiens*, ferns). This indicates a phase of marked human disturbance preceding that already noted.

Gramineae is the only member of group 3, with high values at 5.25–8 m (2,500–3,700 yr BP) and 9–10 m (4,200–4,800 yr BP). Although grasses grow in many habitats<sup>10,19</sup>, they are rare in the swamp today and these peaks are probably due to spread of secondary grassland replacing forest. Indicators of disturbance in groups 1 and 2 are uncommon at 9–10 m, perhaps because ruderals found establishment difficult under luxuriant grass growth on undegraded forest soils; the low grass values above 5.25 m could be due to declining soil fertility. Increases<sup>10</sup> and decreases<sup>1</sup> of Gramineae pollen with human disturbance in East Africa have been reported, but not previously sequentially at one site.

Group 4 shows an early increase and a later decline. Most parent species are forest trees. Increases in the swamp forest Myrtaceae (*Syzygium*) and the upper slope trees *Olea* and *Podocarpus* suggest a drier climate after 3,500–3,600 yr BP. *Podocarpus* expansion elsewhere in eastern Africa at about this

Table 1 Dating control provided by  $^{14}\text{C}$  measurements

Depth (m)	Age (yr BP)	$\delta^{13}\text{C}$ (‰)	Laboratory reference
1.65–1.85	$580 \pm 50$	-27.0	Pta-3551
3.65–3.85	$1,690 \pm 40$	-26.0	Pta-3814
5.70–5.85	$2,800 \pm 60$	-26.9	Pta-3557
7.65–7.85	$3,520 \pm 50$	-18.2	Pta-3800
9.65–9.85	$4,670 \pm 60$	-15.9	Pta-3560

time has been interpreted as due to decreased rainfall<sup>1</sup>. Increases in various early successional trees (*Fagara*, *Maesa*, *Neoboutonia*, *Prunus*) could be due to forest disturbance. The falls in abundance of group 4 pollen types towards the surface provide further evidence for forest destruction; lower-slope plants (for example, *Fagara*) tend to decline before upper-slope plants (such as *Podocarpus*), with final clearance of ridge forest at 900 yr BP. Forest Urticaceae pollen becomes rare above 3.5–4 m (1,600–1,800 yr BP) (Fig. 4).

Group 5, with high values at ~8.25–9.25 m (3,800–4,400 yr BP) and a secondary peak at ~4.75–6.75 m (2,200–3,200 yr BP), comprises mainly pollen types of lower-slope forest trees. Little valley forest remained after 2,200 yr BP.

The first two phases of forest reduction were associated with soil erosion and burning. Lightning or volcanism are unlikely causes of such major destruction<sup>20,21</sup> and in any case volcanism was earlier in this area<sup>8</sup>. Hunting in moist African forests does not involve burning<sup>22</sup> and the forest destruction is attributed to the clearance of land for cultivation. Unfortunately, as with other East African pollen diagrams<sup>1,9</sup>, pollen grains from cultivated plants have not been definitely identified. Charcoal manufacture for iron smelting consumes large quantities of wood<sup>5</sup> and this could have contributed to the destruction of trees, perhaps including *Syzygium*<sup>5</sup>, during the past two millennia.

This record shows a long history of forest clearance and soil erosion, interrupted by periods of partial forest recovery. Major degradation of the environment by man occurred early at this locality.

We thank the Government of Uganda for permission to undertake this research. We also thank H. Taligoola, A. Katende, D. Baziya, F. Butera, M. Byamugisha, D. Mutigah, A. Mwesigye and C. Sabiiti for help in Uganda and W. Magowan, K. McDade, N. McDowell, B. O'Kane, S. Tinkler and C. Todd for assistance at Coleraine. This work was supported by the NERC, the Royal Society and the University of Ulster.

Received 19 June 1985; accepted 6 January 1986.

- Hamilton, A. C. *Environmental History of East Africa* (Academic, London, 1982).
- van der Merwe, M. J. in *The Coming of the Iron Age* (eds Wertime, T. A. & Muhly, J. D.) 463–506 (Yale University Press, New Haven, 1980).
- van Noten, F. *Azania* 14, 61–80 (1979).
- Ehret, C. & Posnansky, M. (eds) *The Archaeological and Linguistic Reconstruction of African History* (University of California Press, Berkeley, 1982).
- Schmidt, P. R. *Tanzania Notes & Records*, 84–85, 77–94 (1980).
- Robertshaw, P., Collett, D., Gifford, D. & Mbae, N. B. *Azania* 18, 1–43 (1983).
- Robertshaw, P. & Collett, D. P. *Wld Archaeol.* 15, 67–78 (1983).
- Morrison, M. E. S. & Hamilton, A. C. J. *Ecol.* 62, 1–31 (1974).
- Kendall, R. L. *Ecol. Monogr.* 39, 121–176 (1969).
- Livingstone, D. A. *Ecol. Monogr.* 37, 25–52 (1967).
- Hamilton, A. C. *Uganda J.* 33, 175–199 (1969).
- Atlas of Uganda* 2nd edn (Department of Lands and Surveys, Entebbe, 1967).
- Langdale-Brown, I., Osmaston, H. A. & Wilson, J. G. in *The Vegetation of Uganda and its Bearing on Land-Use* (Government Printer, Uganda, 1964).
- Kururagire, A. R. *Uganda J.* 33, 59–64 (1969).
- Faegri, K. & Iversen, J. *Textbook of Pollen Analysis* 2nd edn (Munksgaard, Copenhagen, 1964).
- Stockmarr, J. *Pollen Spores* 13, 615–621 (1971).
- Hamilton, A. C. *Palaeoecol. Afr.* 7, 45–149 (1972).
- Deuse, P. *Inst. natn. tech. Scienc. Publ.* 4 (I.N.R.S., Butare, Rwanda, 1966).
- Coetzer, J. A. *Palaeoecol. Afr.* 3, 1–146 (1967).
- Dubois, C. G. B. *Uganda J.* 23, 118–123 (1959).
- Rose Innes, R. *Proc. 11th Tall Timbers Fire Ecology Conf.*, 147–173 (Tall Timbers Research Station, Tallahassee, Florida, 1972).
- Turnbull, C. M. *The Forest People* (Cape, London, 1961).
- Morrison, M. E. S. *J. Ecol.* 56, 363–384 (1968).
- Clark, R. L. *Pollen Spores* 24, 523–535 (1982).
- Hamilton, A. C. *Pollen Spores* 18, 27–66 (1976).

## A lethal mutation in mice eliminates the slow calcium current in skeletal muscle cells

Kurt G. Beam, C. Michael Knudson  
& Jeanne A. Powell\*

Department of Physiology and Biophysics, University of Iowa,  
Iowa City, Iowa 52242, USA

\* Department of Biological Sciences, Smith College, Northampton,  
Massachusetts 01063, USA

**Contraction of a vertebrate skeletal muscle fibre is triggered by electrical depolarization of sarcolemmal infoldings termed transverse-tubules (t-tubules), which in turn causes the release of calcium from an internal store, the sarcoplasmic reticulum (SR)<sup>1,2</sup>. The mechanism that links t-tubular depolarization to SR calcium release remains poorly understood. In principle, this link might be provided by the prominent slow calcium current that has been described in skeletal muscle cells of adult frogs<sup>3,4</sup> and rats<sup>5</sup>. However, blocking this current does not abolish the depolarization-induced contractile responses of frog muscle<sup>6</sup>, and the function of this slow calcium current is unknown. Here we describe measurements of calcium currents in developing skeletal muscle cells of normal rats and mice, and of mice with muscular dysgenesis, a mutation<sup>7</sup> that causes excitation-contraction (E-C) coupling to fail<sup>8</sup>. We find that a slow calcium current is present in skeletal muscle cells of normal animals but absent from skeletal muscle cells of mutant animals. The effect of the mutation is specific to the slow calcium current of skeletal muscle; a fast calcium current is present in developing skeletal muscle cells of both normal and mutant animals, and slow calcium currents are present in cardiac and sensory neurones of mutant animals. We believe this to be the first report of a mutation affecting calcium currents in a multicellular organism. The effects of the mutation raise important questions about the relationship between the slow calcium current and skeletal muscle E-C coupling.**

Calcium currents were recorded using the whole-cell patch-clamp technique<sup>9</sup> in skeletal muscle, cardiac and neuronal cells obtained from fetal and newborn rats and mice. Figure 1a illustrates the presence of two kinetically distinct inward currents in a rat myotube grown in primary tissue culture. Test potentials in the range -40 to -10 mV elicited a fast, transient, inward current ( $I_{fast}$ ). Test pulses to potentials of  $\geq 0$  mV activated an additional, slower, maintained, inward current ( $I_{slow}$ ), which resembles the slow calcium current of adult skeletal muscle. Both  $I_{fast}$  and  $I_{slow}$  are calcium currents as they are: (1) observed in Na-free solutions containing 10  $\mu$ M tetrodotoxin (TTX), (2) abolished by removing calcium from the bathing medium, and (3) blocked by cadmium (see below).  $I_{fast}$  and  $I_{slow}$  are seen not only in myotubes in primary tissue culture, but also in enzymatically dissociated fibres of muscles that have been acutely removed from neonatal rats (Fig. 1b). The two calcium currents of developing muscle are kinetically similar to the fast and slow calcium currents previously described in cardiac muscle<sup>10,11</sup>, smooth muscle<sup>12</sup>, neuronal cell lines<sup>13,14</sup> and sensory neurones<sup>15-18</sup>. In most of the myotubes we examined, both  $I_{fast}$  and  $I_{slow}$  were present, although their magnitudes varied considerably between cells. In 20 rat and mouse myotubes examined in 10 mM external calcium, the peak  $I_{fast}$  averaged  $0.7 \pm 0.6$  pA  $pF^{-1}$  (mean  $\pm$  s.d.) and the peak  $I_{slow}$   $8.2 \pm 4.9$  pA  $pF^{-1}$  (currents normalized by linear cell capacitance). For 13 myotubes in 50 mM external calcium, peak  $I_{fast}$  and  $I_{slow}$  were  $2.1 \pm 1.6$  and  $6.6 \pm 4.4$  pA  $pF^{-1}$ , respectively. In 7 of these 33 cells,  $I_{fast}$  was too small to be detected, whereas in only 2 of them was  $I_{slow}$  undetectable.

$I_{fast}$  and  $I_{slow}$  can be distinguished not only by kinetics and voltage-dependence of activation, but also by the effects of

holding potential. Figure 1b illustrates, for an enzymatically dissociated fibre, that changing the holding potential from -90 to -40 mV inactivates the transient  $I_{fast}$  elicited by a test pulse to -20 mV; a similar change in holding potential (from -90 to -30 mV) has essentially no effect on  $I_{slow}$  elicited by a test pulse to +30 mV. The effects of holding potential on  $I_{fast}$  and  $I_{slow}$  in myotubes were similar to those illustrated in Fig. 1b.

Calcium channel antagonists provide another means of distinguishing between  $I_{fast}$  and  $I_{slow}$ . High concentrations ( $\geq 1$  mM) of cadmium block both  $I_{fast}$  and  $I_{slow}$ , but lower concentrations ( $\leq 100$   $\mu$ M) produce a significantly greater block of  $I_{slow}$  than of  $I_{fast}$ . Similarly, 5  $\mu$ M nitrendipine (a dihydropyridine Ca-channel antagonist) causes a ~75% reduction in  $I_{slow}$ , with little effect on  $I_{fast}$ . A greater cadmium and dihydropyridine sensitivity has also been described for the slow calcium currents in cardiac cells<sup>10,11</sup>, a neuronal cell line<sup>14</sup> and sensory neurones<sup>17,18</sup>. Thus, the voltage-dependence, kinetics and antagonist sensitivity of the fast and slow calcium currents in skeletal muscle all resemble those of fast and slow calcium currents in heart and nerve.

Muscular dysgenesis is a single, recessive, lethal, autosomal mutation (*mdg*) in mice<sup>7</sup>. In dysgenic muscle the sarcolemma can still generate action potentials<sup>8</sup>, and the SR retains the ability to sequester calcium and release it in response to caffeine<sup>19</sup>, but sarcolemmal depolarization fails to elicit SR calcium release<sup>20</sup>. Figure 2 demonstrates that this genetic defect of E-C coupling is associated with the specific absence of  $I_{slow}$ . Figure 2a shows calcium currents obtained from a dysgenic myotube. As in normal muscle cells, relatively weak depolarizations elicit  $I_{fast}$ ; however, stronger depolarizations fail to elicit  $I_{slow}$ , so that even for these strong depolarizations only  $I_{fast}$  is present. Altogether, we examined calcium currents in 15 dysgenic myotubes; in none of these was a measurable  $I_{slow}$  present. In these same cells the peak  $I_{fast}$  was  $1.0 \pm 0.5$  ( $n = 8$ ) in 10 mM external calcium and  $1.8 \pm 1.3$  pA  $pF^{-1}$  ( $n = 7$ ) in 50 mM  $Ca^{2+}$ , values similar to those in normal myotubes (see above). Figure 2b illustrates the effect of changing the holding potential on the currents elicited in a dysgenic myotube by test pulses to either -10 or +30 mV. When the holding potential was -80 mV, both test pulses elicited  $I_{fast}$  (prominent at -10 mV; partially obscured by noise at +30 mV). The same test pulses failed to elicit  $I_{fast}$  when the holding potential was -30 mV. Thus, the inactivation of  $I_{fast}$  with holding potential is similar in dysgenic myotubes to that in normal skeletal muscle cells. Importantly, the steady-state current for the +30-mV test pulse is in quite good agreement for the -80 and -30 mV holding potentials, which argues against the possibility that large nonlinearities in leak current disguise the presence of  $I_{slow}$  in dysgenic myotubes. Thus, the *mdg* mutation seems specific in its effect:  $I_{slow}$  is absent but  $I_{fast}$  is present with normal properties. Additionally, dysgenic myotubes possess sodium currents of normal appearance (data not shown).

The many similarities between calcium currents in skeletal muscle and those in sensory neurones and cardiac cells prompted us to determine whether the *mdg* mutation also eliminates slow calcium current in these tissues. In control experiments on heart and nerve from non-mutant animals, we observed two clearly distinct components of current resembling  $I_{fast}$  and  $I_{slow}$  of developing skeletal muscle. (A third calcium current, termed N, has been described for sensory neurones<sup>18</sup>, but in our experimental conditions this current was not prominent.) Figure 3 illustrates calcium currents recorded in cardiac myocytes and dorsal root ganglion neurones from mutant animals. In the dysgenic cardiac myocyte (Fig. 3a), a 0-mV test pulse applied from a -80-mV holding potential activated both  $I_{fast}$  and  $I_{slow}$ ; when the same test pulse was used but the holding potential was changed to -40 mV,  $I_{fast}$  was inactivated but  $I_{slow}$  was little affected. This change in holding potential also had little effect on the much larger  $I_{slow}$  that was activated by a test pulse to +30 mV. Similarly, in the dysgenic neurone (Fig. 3b), a test pulse to -20 mV elicited a predominantly transient ( $I_{fast}$ )

**Fig. 1** Developing skeletal muscle cells possess two distinct calcium currents. *a*, Transient ( $I_{fast}$ ) and maintained ( $I_{slow}$ ) calcium currents in a rat myotube. The cell was held at a potential of  $-90$  mV from which it was depolarized to the test potentials indicated to the right of each trace. Test depolarizations of  $-40$  to  $-10$  mV selectively activate  $I_{fast}$ ; test potentials of  $0$  mV and above activate an additional current,  $I_{slow}$ . Owing to its much larger size,  $I_{slow}$  masks the presence of  $I_{fast}$  for test potentials  $\geq 20$  mV. Rat myotube (A07), 12 days in culture,  $10$  mM Ca +  $10$   $\mu$ M TTX, holding potential (HP)  $-90$  mV, linear capacitance (C) =  $340$  pF. *b*, Depolarized holding potentials selectively inactivate  $I_{fast}$ . Single fibre (D18), enzymatically dissociated<sup>28</sup> from the flexor digitorum brevis muscle of a 13-day rat,  $10$  mM Ca +  $10$   $\mu$ M TTX, C =  $290$  pF. Test potentials of  $-20$  and  $+20$  mV were applied.

**Methods.** Currents were recorded with the whole-cell variant of the patch-clamp technique<sup>9</sup>. Unless otherwise indicated, illustrated test currents have been corrected digitally for linear components of capacitative and leak current. The pipette contained (in mM):  $140$  Cs-aspartate,  $5$  Mg-aspartate<sub>2</sub>,  $10$  Cs<sub>2</sub>EGTA,  $10$  HEPES (adjusted to pH 7.4 with CsOH). External solutions, designated by their divalent cation, contained (in mM)  $10$  Ca:  $145$  tetraethylammonium ion (TEA),  $10$  Ca;  $50$  Ca:  $85$  TEA,  $50$  Ca; isotonic Ba:  $105$  Ba. All external solutions contained  $10$  mM HEPES (pH 7.4 with CsOH) and Br and/or Cl as anions. Experiments were done at room temperature ( $20$  °C). Primary cultures of myoblasts were prepared from fore- and hindlimbs of late-term fetal or newborn rats and mice. The limb muscles were minced finely and incubated at  $37$  °C for  $40$  min in physiological saline<sup>5</sup> containing collagenase ( $2$  mg ml<sup>-1</sup>, Sigma Type I). After filtration and centrifugation to remove large debris, the cell suspension was pre-plated for  $1$  h in glass to remove rapidly adhering cells and then plated onto  $35$ -mm Falcon 'primaria' dishes in 'plating medium' containing (v/v)  $80\%$  Dulbecco's modified Eagle's medium with  $4.5$  g l<sup>-1</sup> glucose (DMEM),  $10\%$  horse serum, media contained penicillin ( $1,000$  U ml<sup>-1</sup>) and streptomycin ( $1$  mg ml<sup>-1</sup>). Cardiac myocytes were prepared from hearts of newborn mice essentially as described in ref. 29, suspended in plating medium supplemented with  $0.1$  mM 8-bromo-cyclic AMP, and plated onto polylysine-coated culture dishes. Dorsal root ganglia were removed from either  $14$ -day-old fetuses or newborn animals, and incubated for  $20$  min at  $37$  °C in physiological saline containing  $0.25\%$  trypsin (Sigma type IIIS). The ganglia were washed, disaggregated, suspended in plating medium enriched with  $50$  ng ml<sup>-1</sup>  $7S$  nerve growth factor (Collaborative Research), and plated onto polylysine-coated culture dishes. Cultures were maintained at  $37$  °C in a  $95\%$  air- $5\%$  CO<sub>2</sub>, water-saturated atmosphere.

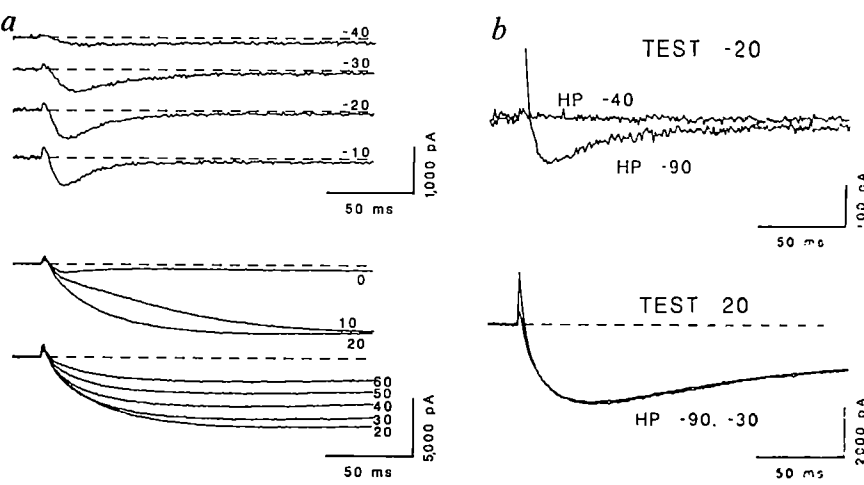
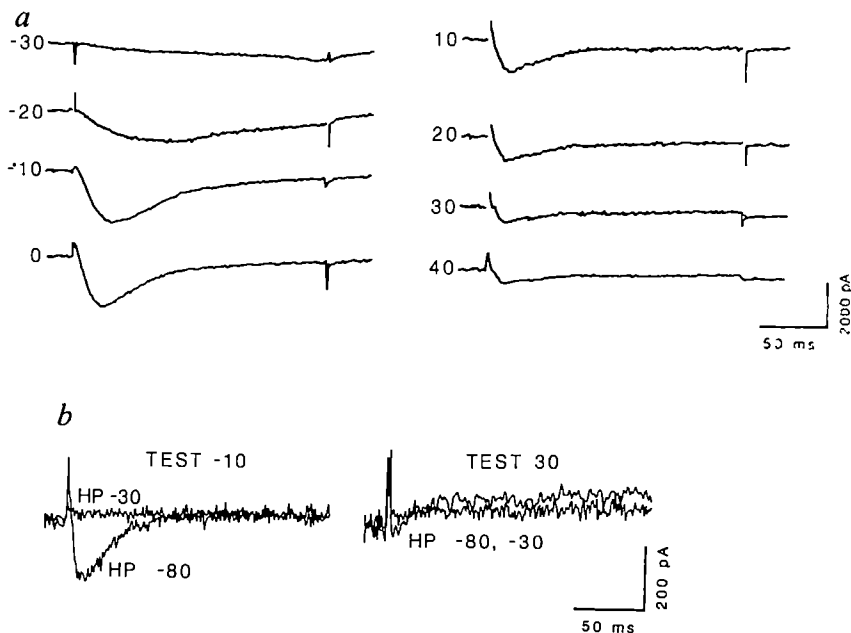


**Fig. 2** Skeletal muscle cells of mutant animals specifically lack  $I_{slow}$ . *a*, Presence of  $I_{fast}$  and absence of  $I_{slow}$  in dysgenic myotube. Cell MD158, 6 days in culture,  $50$  mM Ca, HP =  $-90$  mV, C =  $675$  pF. *b*, Inactivation of  $I_{fast}$  with holding potential in a dysgenic myotube. Cell E11, 10 days in culture,  $10$  mM Ca +  $10$   $\mu$ M TTX, C =  $100$  pF.



inward current that was inactivated at a holding potential of  $-40$  mV, whereas a test pulse to  $+20$  mV elicited a predominantly maintained ( $I_{slow}$ ) inward current that was similar for holding potentials of  $-80$  and  $-40$  mV. Thus, both an  $I_{fast}$  and an  $I_{slow}$  component of current are present in cardiac and neuronal cells of mutant animals, and the effect of the *mdg* mutation seems to be specific for the slow calcium current of skeletal muscle.

The results of recent biochemical experiments<sup>21</sup> agree with our electrophysiological measurements in demonstrating that the *mdg* mutation affects skeletal muscle but not cardiac cells. Thus, in cardiac tissue the number of binding sites for PN 200-110 (a dihydropyridine calcium-channel blocker) is the

same in normal and dysgenic animals. By contrast, in skeletal muscle of mutant animals, the number of PN 200-110 binding sites is reduced about fivefold relative to the control. The identity of the substantial number of dihydropyridine binding sites that remain in dysgenic skeletal muscle is uncertain. If they represent functional slow calcium channels, the dysgenic myotubes would have an  $I_{slow}$  about one-fifth the size of  $I_{slow}$  in normal cells, which should have been detectable by our electrophysiological measurements. Our failure to detect  $I_{slow}$  suggests that the dihydropyridine binding sites in dysgenic skeletal muscle represent non-functional slow calcium channels or an unrelated component of the muscle membrane.

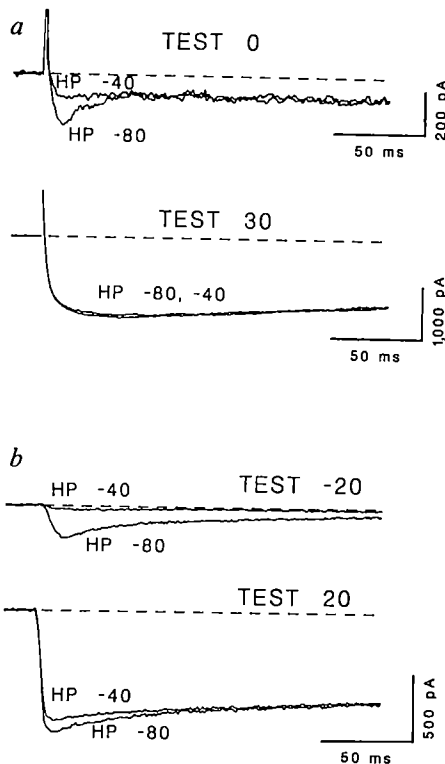


**Fig. 3** Cardiac and neuronal cells of mutant animals possess both  $I_{fast}$  and  $I_{slow}$ . *a*, Dysgenic cardiac myocyte (B59), 8 days in culture, isotonic Ba + 10  $\mu$ M TTX, C = 46 pF, no leak subtraction. *b*, Dorsal root ganglion neurone (C44) from a 15-day dysgenic fetus, 3 days in culture, 10 mM Ca + 10  $\mu$ M TTX, C = 40 pF.

Why does the *mdg* mutation result in the absence of slow calcium current in skeletal muscle? Among the possibilities are that the mutation directly alters the structural gene for the slow calcium channel, that it interferes with transcription of the gene, that it disrupts the post-translational processing and/or insertion of the channel protein, or that it affects a soluble regulatory protein necessary for channel function. The last of these has been shown to be the case for the paramecium mutant *cnrC*, which lacks the calcium current present in wild-type animals<sup>22</sup>. The presence of slow calcium currents in dysgenic cardiac and neuronal cells suggests the possibility that slow calcium channels in these tissues are encoded by different structural genes from those in skeletal muscle, even though the currents are similar in the three tissues. Alternatively, if the same gene codes for the slow calcium channel in all three tissues, the expression of the slow current in skeletal muscle must involve tissue-specific processes that do not occur in cardiac or neuronal cells.

A second major question raised by our results is the relationship between the absence of  $I_{slow}$  and the failure of E-C coupling. One explanation would be to suppose that calcium entry via  $I_{slow}$  is a necessary trigger for SR calcium release, but this seems unlikely considering the current's slow activation kinetics. Moreover, as mentioned earlier, blocking the slow current in adult frog muscle does not abolish E-C coupling<sup>6</sup>. Further, both brief electrical stimuli and K-depolarization elicit vigorous mechanical responses of non-mutant myotubes and neonatal muscle fibres bathed in concentrations of cadmium sufficient to block both  $I_{fast}$  and  $I_{slow}$  (S. Jay and K.G.B., unpublished). Even though the actual current through the slow calcium channel seems unlikely to be directly involved in E-C coupling, the channel protein itself might still be intimately involved. For example, it has been suggested that the slow calcium-channel protein serves as the 'voltage-sensor' for the process governing SR calcium release<sup>23</sup>. Accordingly, a mutation affecting slow

calcium current would also affect E-C coupling. It is also possible that the absence of  $I_{slow}$  and the failure of E-C coupling are only coincidentally related. The slow calcium channels in skeletal muscle are believed to be localized within the t-tubules<sup>4,24-26</sup>, and in dysgenic muscle cells the normal morphological association between t-tubules and SR develops incompletely<sup>21,27</sup>. Thus, this defect in t-tubular development may be the cause of both the absence of  $I_{slow}$  and the failure of E-C coupling.

We thank Dr Bruce Bean for many valuable discussions. This work was supported by NIH grant NS-14901 (K.G.B.) and grants from the Muscular Dystrophy Association of America (K.G.B. and J.A.P.), and the Blakeslee Fund of Smith College (J.A.P.). K.G.B. is the recipient of Research Career Development Award NS-00840.

Received 15 October 1985; accepted 20 January 1986.

1. Constantin, L. L. *Prog. Biophys. molec. Biol.* **29**, 197-224 (1975).
2. Endo, M. *Physiol. Rev.* **57**, 71-108 (1977).
3. Sanchez, J. A. & Stefani, E. *J. Physiol., Lond.* **283**, 197-209 (1978).
4. Almers, W., Fink, R. & Palade, P. T. *J. Physiol., Lond.* **312**, 177-207 (1981).
5. Donaldson, P. L. & Bean, K. G. *J. gen. Physiol.* **82**, 449-468 (1983).
6. Gonzalez-Serratos, H., Valle-Aguilera, R., Lathrop, D. A. & del Carmen Garcia, M. *Nature* **298**, 292-294 (1982).
7. Gluecksohn-Waelsch, S. *Science* **142**, 1269-1276 (1963).
8. Powell, J. A. & Fambrough, D. M. *J. cell. Physiol.* **82**, 21-38 (1973).
9. Hamill, O. P., Marty, A., Neher, E., Sakmann, B. & Sigworth, F. J. *Pflügers Arch. ges. Physiol.* **391**, 85-100 (1981).
10. Bean, B. P. *J. gen. Physiol.* **86**, 1-30 (1985).
11. Niijima, B., Hess, P., Lansman, J. B. & Tsien, R. W. *Nature* **316**, 443-446 (1985).
12. Bean, B. P., Sturek, M., Puga, A. & Hermansmeyer, K. *J. gen. Physiol.* **86**, 23a (1985).
13. Armstrong, C. M. & Matteson, D. R. *Science* **277**, 65-67 (1985).
14. Tsunoo, A., Yoshii, M. & Narahashi, T. *Biophys. J.* **47**, 433a (1985).
15. Carbone, E. & Lux, H. D. *Nature* **310**, 501-502 (1984).
16. Fedulova, S. A., Kostyuk, P. G. & Veselovsky, N. S. *J. Physiol., Lond.* **359**, 431-446 (1985).
17. Bossu, J. L., Feltz, A. & Thomann, J. M. *Pflügers Arch. ges. Physiol.* **403**, 360-368 (1985).
18. Nowicky, M. C., Fox, A. P. & Tsien, R. W. *Nature* **316**, 440-443 (1985).
19. Bowden-Essien, F. *Dev. Biol.* **27**, 351-364 (1972).
20. Klaus, M. M., Stylianou, P. S., Rapalus, J. M., Briggs, R. T. & Powell, J. A. *Dev. Biol.* **99**, 152-165 (1983).
21. Pincon-Raymond, M., Rieger, F., Fosset, M. & Lazdunski, M. *Dev. Biol.* **112**, 458-466 (1985).
22. Haga, N. *et al. Cell* **39**, 71-78 (1984).
23. Rios, E., Brum, G. & Stefani, E. *Biophys. J.* **49**, 13a (1986).
24. Nicola Siri, L., Sanchez, J. A. & Stefani, E. *J. Physiol., Lond.* **305**, 87-96 (1980).
25. Fosset, M., Jaimovich, E., Delpont, E. & Lazdunski, M. *J. biol. Chem.* **258**, 6086-6092 (1983).
26. Grossman, H., Ferry, D. R. & Boschek, C. B. *Naunyn-Schmiedebergs Archs Pharmak.* **323**, 1-11 (1983).
27. Powell, J. A. & Briggs, R. T. *J. Cell Biol.* **99**, 24a (1984).
28. Bekoff, A. & Betz, W. J. *J. Physiol., Lond.* **271**, 25-40 (1977).
29. Harary, I., Hoover, F. & Farley, B. *Meth. Enzym.* **32**, 740-745 (1974).

## Spermatogenic failure in male mice lacking H-Y antigen

Paul S. Burgoyne, Elaine R. Levy & Anne McLaren

MRC Mammalian Development Unit, Wolfson House,  
4 Stephenson Way, London NW1 2HE, UK

The mammalian Y chromosome carries a factor that initiates male sexual development by directing the fetal gonads to form testes. Wachtel and his colleagues<sup>1</sup> proposed that this testis-determining function of the Y is mediated by the male-specific cell-surface antigen H-Y, originally defined by skin grafting<sup>2</sup>. This attractive hypothesis, which has been widely accepted, was based on the assumption that serological tests using antisera raised against male cells were recognizing H-Y antigen. Although disputed<sup>3</sup>, this assumption is supported by some recent studies<sup>4-6</sup>. However, mice have been described<sup>7</sup> which develop testes but lack the cell-surface H-Y antigen as defined by T-cell-mediated transplantation tests. Thus, although it remains possible that a serologically detected male-specific antigen is responsible for testis determination, it seems that H-Y, as originally defined, is not. We show here that H-Y-negative male mice, in losing the genetic information that encodes H-Y, have also lost genetic information required for spermatogenesis. This result identifies a gene on the mouse Y,

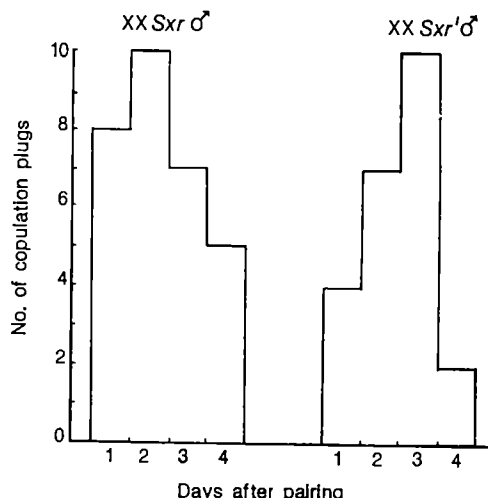


Fig. 1 Copulatory activity of  $XX\ Sxr'$  compared with  $XX\ Sxr$  males. Four males of each type were each paired with three females (MF1 strain; Olac) and the females were examined for copulation plugs on the following four mornings. This was repeated for four successive weeks. The histograms show the total numbers of plugs found on days 1–4 after pairing.

distinct from the testis-determining gene, which is necessary for spermatogenesis, and raises the intriguing possibility that the product of this 'spermatogenesis gene' is H-Y antigen.

Cattanach *et al.*<sup>8</sup> originally described a sex reversal factor (*Sxr*) in mice which caused XX individuals to develop as males with testes. It is now known that *Sxr* is a small segment of the Y chromosome which is transferred to the X during meiosis in XY *Sxr* carriers<sup>9,10</sup>. *Sxr* includes the genetic information for testis determination and for the expression of H-Y<sup>11</sup>. However, McLaren *et al.*<sup>7</sup> found a variant *Sxr* (designated *Sxr'*) that still carried the testis-determining information, but did not confer H-Y antigenicity. Our objective here was to determine whether loss of H-Y antigenicity was correlated with any impairment of male reproductive function, as it seemed likely that this male-specific antigen would have a male-specific role. Initially, we compared  $XX\ Sxr'$  males with  $XX\ Sxr$  males. The H-Y-negative  $XX\ Sxr'$  males were not detectably less proficient than  $XX\ Sxr$  males at mating or at inducing synchronization of mating behaviour (Fig. 1), suggesting that testosterone and pheromone production are unaltered in the absence of H-Y antigen.

Adult  $XX\ Sxr'$  mice, like  $XX\ Sxr$  mice, have sterile testes due to the perinatal loss of germ cells (E.R.L. and P.S.B., unpublished observations), characteristic of male mice carrying two X chromosomes. Presumably the expression of a double dose of X-linked genes in the germ cells is incompatible with their survival beyond the perinatal period. Adult  $X0\ Sxr$  mice, in contrast to  $XX\ Sxr'$  and  $XX\ Sxr$  mice, have all stages of spermatogenesis represented in their testes. They are nonetheless sterile because the later stages are defective, and only a few grossly abnormal sperm are produced<sup>8</sup>. These defects may result from the absence of a pairing partner for the X chromosome, since X-Y pairing during pachytene seems to be necessary for the successful completion of spermatogenesis<sup>12</sup>.

We produced  $X0\ Sxr'$  mice and compared them with  $X0\ Sxr$  mice to see if the loss of H-Y antigenicity is correlated with any additional defect of spermatogenesis. One  $X0\ Sxr$  and four  $X0\ Sxr'$  mice were checked for their H-Y status (Table 1). For each mouse designated H-Y-negative (final column), the target cells were shown to be negative with appropriate H-2-restricted H-Y-specific cytotoxic T cells but positive with the corresponding anti-H-2 cytotoxic T cells. Each of the  $X0\ Sxr'$  mice was H-Y-negative by these criteria. By contrast, the  $X0\ Sxr$  male typed positive, like the XY control male and the previously

Table 1 H-Y typing of  $X0\ Sxr'$ ,  $X0\ Sxr$  and control XX and XY mice with H-2<sup>a</sup>- and H-2<sup>a</sup>-restricted H-Y-specific T cells

Mouse	H-2 <sup>†</sup>	Karyotype	Sex	% Specific lysis at E:T = 10:1 T <sub>c</sub> *		H-Y summary
				Anti-H-2 <sup>a</sup>	Anti-H-Y <sup>a</sup>	
555	bq	X0 Sxr'	Male	28	1	-
556	bq	X0 Sxr'	Male	27	0	..
SWR	qq	XY	Male	38	46	+
SWR	qq	XX	Female	31	9	-
				Anti-H-2 <sup>k</sup>	Anti-H-Y <sup>k</sup>	
557	kk	X0 Sxr	Male	20	22	+
558	kb	X0 Sxr'	Male	17	1	-
559	kb	X0 Sxr'	Male	29	6	-
CBA	kk	XY	Male	29	38	+
CBA	kk	XX	Female	38	9	-

\* Cytotoxic T cells ( $T_c$ ) were from 5-day mixed lymphocyte cultures (MLC) of (B10 × BALB/c)F<sub>1</sub> anti-SWR (anti-H-2<sup>a</sup>), (B10 × SWR)F<sub>1</sub> ♀ anti-SWR ♂ (anti-H-Y<sup>a</sup>), BALB/B anti-CBA (anti-H-2<sup>k</sup>) and (B10 × CBA)F<sub>1</sub> ♀ anti-CBA ♂ (anti-H-Y<sup>k</sup>). The anti-H-2 were primary, the anti-H-Y secondary *in vitro* MLC and were used as attacker  $T_c$  as described previously<sup>7</sup> with 5-day concanavalin A-stimulated spleen cells from the mice to be typed as <sup>51</sup>Cr-labelled targets. Four effector/target (E:T) ratios were tested for each target using serial threefold dilutions of the effector  $T_c$  starting at E:T = 30:1, and a fixed number ( $10^4$ ) of target cells. The data were analysed by regression analysis; the values given are from the titration curves, at E:T = 10:1. Numbers underlined are positive values, and lie on curves with  $r^2 > 0.80$  ( $r$  = coefficient of correlation, a measure of goodness of fit of the data on the regression line).

† H-2 typing with monoclonal antibody plus rabbit complement, as described previously<sup>7</sup>.

reported  $XX\ Sxr$  males<sup>13</sup>, with both H-2-restricted H-Y-specific cytotoxic T cells and the corresponding anti-H-2 cytotoxic T cells. Histological analysis revealed that spermatogenesis is much more severely affected in  $X0\ Sxr'$  than  $X0\ Sxr$  mice. There is almost total elimination of spermatogenic cells beyond the spermatogonial stage in adult  $X0\ Sxr'$  testes, and this block is evident prepubertally, at the onset of meiosis (Fig. 2). Although grossly the block to spermatogenesis is clearcut, it is hard to define the point at which it acts. Spermatogonia appear to be few in number and spermatogonial divisions are rare: this could result from either an intrinsic defect of proliferation in the spermatogonial compartment, or some inhibition of proliferation in response to a block in spermatogonial differentiation and commitment to meiosis. Even the block to meiosis is not absolute, because very occasionally patches of cells enter meiosis (Fig. 3), only to arrest and degenerate early in the pachytene stage.

Our results, together with those of McLaren *et al.*<sup>7</sup>, show that when *Sxr'* arose from *Sxr*, genetic information needed for H-Y expression and spermatogenesis was lost, while genetic information required for testis determination was retained. Incidentally, the fact that  $X0\ Sxr'$  mice are H-Y-negative, just like T16H/X *Sxr'* mice<sup>7</sup>, rules out Ohno's recent suggestion that spreading of X-inactivation into *Sxr'* is responsible for the non-expression of H-Y<sup>14</sup>.

Levy and Burgoine<sup>15</sup> found that there is an early spermatogenic failure of  $X0$  germ cells in  $X0/XY$  mosaic mice, and concluded that since the  $X0$  germ cells are not 'rescued' by the mosaic testicular soma, there must be a 'spermatogenesis gene' on the Y chromosome which is expressed in the germ line. Histologically, the arrested spermatogenesis that occurs in patches in these  $X0/XY$  mosaic testes is indistinguishable from that in  $X0\ Sxr'$  testes; this suggests that it is the loss or mutation of this 'spermatogenesis gene' which leads to the spermatogenic arrest in  $X0\ Sxr'$  mice.

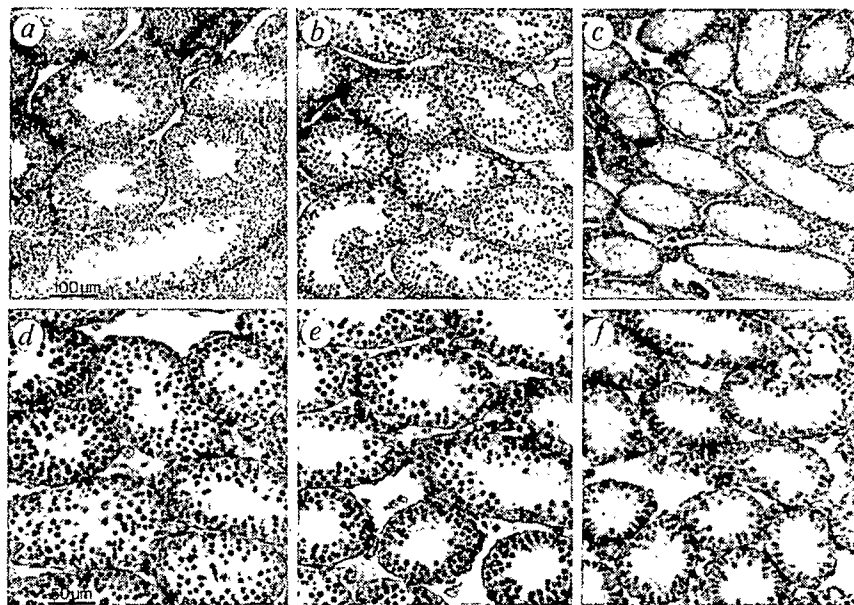
As the loss of spermatogenesis in  $X0\ Sxr'$  mice is correlated with the loss of H-Y expression, it is tempting to conclude that H-Y antigen is the product of the spermatogenesis gene, thus reinstating a male-specific function for this evolutionarily conserved male antigen. The same correlation of H-Y antigen negativity and spermatogenic failure was seen in the  $X0$  male mouse described by Melvold *et al.*<sup>16</sup>. However, it remains possible that there are separate genes for spermatogenesis and H-Y

**Fig. 2** Spermatogenic failure in X0 Sxr' male mice. *a*, Complete spermatogenesis in a testis from an adult (49-day-old) XY mouse. *b*, Abnormal spermatogenesis with a marked deficiency of condensing spermatid stages in the testis of a 49-day-old X0 Sxr mouse (H-Y-positive). *c*, An almost total block of spermatogenesis in the testis of a 49-day-old X0 Sxr' mouse (H-Y-negative). Although some spermatogonia are present, almost all tubules lack spermatocytes and spermatids. *d-f*, Testes from 13-day-old XY, X0 Sxr and X0 Sxr' mice showing that the defect in X0 Sxr' spermatogenesis is already present prepubertally when meiosis begins.

**Methods.** X0 Sxr and X0 Sxr' mice were produced by mating XY Sxr or XY Sxr' males to females heterozygous for the inversion In(X)1H. These females generate some nullo-X eggs following crossing-over within the inversion. The testes from 15 X0 Sxr' and 9 X0 Sxr males together with those from their male littermates, at 2–50 days post partum, were examined during this study. All mice were karyotyped. Testes were fixed in Bouin's fixative. The sections were stained with periodic acid-Schiff's reagent and counterstained with haematoxylin.

expression which are tightly linked. It may be pertinent that spermatogonia have been identified as the only adult male cells which type negative for male-specific antigen using serological tests<sup>17</sup>. Later spermatogenic stages are increasingly positive. If serological tests do recognize H-Y antigen, this pattern of expression would be consistent with H-Y antigen being the spermatogenesis gene product.

The possibility that H-Y antigen is the product of the spermatogenesis gene leads to predictions about the H-Y status of human XX males and XY females. A human spermatogenesis gene, which we presume is homologous to that on the mouse Y, is located on the human Y long arm close to the centromere<sup>18</sup>. Human XX males that have acquired testis-determining sequences from the Y short arm<sup>19–21</sup> will lack Y long arm sequences including the spermatogenesis gene, and hence should type H-Y-negative if H-Y is the spermatogenesis gene product. Conversely, XY females that have lost testis-determining sequences from the Y short arm should type H-Y-positive because the spermatogenesis gene on the Y long arm should have been retained. H-Y typing of human sex-reversed individuals is now possible using histocompatibility locus antigen (HLA)-restricted H-Y-specific T-cell clones. All five XX males so far typed are H-Y-negative, in line with our predictions (ref. 22 and E. Goulimy and E. Simpson, personal communication).



We thank Dr Elizabeth Simpson of the Clinical Research Centre, Harrow, for H-Y typing. E.R.L. is a recipient of an SERC studentship.

Received 20 November 1985; accepted 29 January 1986.

- Wachtel, S., Ohno, S., Koo, G. C. & Boyse, E. A. *Nature* **257**, 235–236 (1975).
- Eichwald, E. J. & Silms, C. R. *Transplant Bull.* **2**, 154–155 (1955).
- Silvers, W. K., Gasser, D. L. & Eicher, E. M. *Cell* **28**, 439–440 (1982).
- Wiberg, U. H. *Hum. Genet.* **69**, 15–18 (1985).
- Wiberg, U. H. & Günther, E. *Immunogenetics* **21**, 91–96 (1985).
- Wiberg, U. H. & Mayerova, A. J. *Immunogenet.* **12**, 55–63 (1985).
- McLaren, A., Simpson, E., Tomonari, K., Chandler, P. & Hogg, H. *Nature* **312**, 552–555 (1984).
- Cattanach, B. M., Pollard, C. E. & Hawkes, S. G. *Cytogenetics* **10**, 318–337 (1971).
- Singh, L. & Jones, K. W. *Cell* **28**, 205–216 (1982).
- Evans, E. P., Burtsenshaw, M. D. & Cattanach, B. M. *Nature* **300**, 443–445 (1982).
- Bennett, D. *et al.* *Nature* **265**, 255–257 (1977).
- Burgoyne, P. S. & Baker, T. G. in *Controlling Events in Meiosis* (eds Evans, C. W. & Dickinson, H. G.) 349–362 (Company of Biologists, Cambridge, 1984).
- Simpson, E., Edwards, P., Wachtel, S., McLaren, A. & Chandler, P. *Immunogenetics* **13**, 355–358 (1981).
- Ohno, S. *Endocrine Rev.* **6**, 421–431 (1985).
- Levy, E. R. & Burgoyne, P. S. *Cytogenet. Cell Genet.* (submitted).
- Melvold, R. W., Kohn, H. I., Yeriganian, G. & Fawcett, D. W. *Immunogenetics* **5**, 33–41 (1977).
- Zenzen, M. T., Müller, U., Aschmoneit, I. & Wolf, U. *Hum. Genet.* **45**, 297–303 (1978).
- Tiepolo, L. & Zuffardi, O. *Hum. Genet.* **34**, 119–124 (1976).
- de la Chapelle, A., Tippett, P. A., Wetterstrand, G. & Page, D. *Nature* **307**, 170–171 (1984).
- Guellau, G. *et al.* *Nature* **307**, 172–173 (1984).
- Page, D. C., de la Chapelle, A. & Weissenbach, J. *Nature* **315**, 224–226 (1985).
- Goulimy, E., van Leeuwen, A., Blokland, E., Sachs, E. S. & Geraedts, J. P. M. *Immunogenetics* **17**, 523–531 (1983).

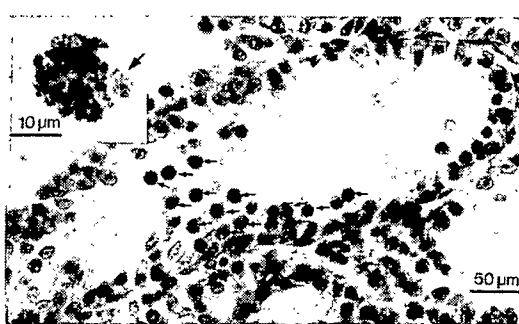


**Fig. 3** Meiotic cells in X0 Sxr' testes. Occasionally tubules are seen in X0 Sxr' testes which contain patches of meiotic cells (arrowed) that degenerate during the early pachytene stage. These pachytene cells have a clear sex vesicle in air-dried preparations (arrowed in inset), showing that this structure can form in the absence of H-Y antigen.

## Modulation of visual cortical plasticity by acetylcholine and noradrenaline

Mark F. Bear\* & Wolf Singer

Max Planck Institute for Brain Research, Deutschordensstrasse 46, 6000 Frankfurt 71, FRG

During a critical period of postnatal development, the temporary closure of one eye in kittens will permanently shift the ocular dominance (OD) of neurones in the striate cortex to the eye that remains open<sup>1</sup>. The OD plasticity can be substantially reduced if the cortex is infused continuously with the catecholamine neurotoxin 6-hydroxydopamine (6-OHDA) during the period of monocular deprivation<sup>2–5</sup>, an effect that has been attributed to selective depletion of cortical noradrenaline<sup>6</sup>. However, several

\* Present address: Center for Neural Science, Box 1953, Brown University, Providence, Rhode Island 02912, USA.

**Fig. 1** *a, b*, Coronal sections through the forebrain of a 44-day-old kitten (K125) at the approximate frontal planes A14.0 and A 11.75, respectively. Projected onto the right side of *a* and *b* is the distribution of cells in the basal telencephalon that were back-filled after 1  $\mu$ l of 30% horseradish peroxidase (HRP) was injected into the visual cortex of a 4-week-old kitten. For each drawing, five contiguous 50- $\mu$ m thick sections were pooled; each dot represents approximately two HRP-labelled neurones. (?????) The extrinsic cholinergic innervation of the striate cortex arises from these cells<sup>20</sup>. This unilateral projection derives from neurones scattered within the internal capsule (IC), the substantia innominata (SI), the diagonal band of Broca and the medial septal nucleus (SMN). Reconstructed on the left side of *a* and *b* are the regions of cell loss (crosshatching) after NMA was injected into the telencephalon of K125. Also indicated (●—) are the two needle tracks along which NMA was delivered, one (*a*) targeting cells in the vertical limb of the diagonal band (50  $\mu$ g) and SMN (50  $\mu$ g), the other (*b*) targeting cells in the horizontal limb of the diagonal band (DBH, 125  $\mu$ g), SI (75  $\mu$ g) and IC (50  $\mu$ g). This lesion produced a drastic and widespread depletion of AChE-positive axons in the neocortex. In addition to the cholinergic basal forebrain neurones, cells in the caudate, globus pallidus, ventral pallidum and rostral pole of the dorsal thalamus were also destroyed by the NMA injections. The cell loss in the thalamus was confined to the reticular, ventral anterior and ventral lateral nuclei. The portions of the claustrum (Clau) and intralaminar thalamus that project to the visual cortex were spared by the NMA injections. AC, anterior commissure; Ca, caudate nucleus. *c*, Coronal section through the forebrain of K152 at the approximate frontal plane A 16.25 to illustrate a cingulate gyrus lesion. The blackened region was surgically removed by subpial aspiration. The lesion produced a depletion of AChE-positive axons in the striate cortex comparable to that observed with basal forebrain lesions. Analysis of cortical tissue using HPLC confirmed that NA was also reduced in area 17 to <50% of control levels (Table 1). *d*, Anterior-posterior extent of the lesion in *c* in a mid-sagittal view of a kitten brain, showing the approximate level of each of the sections illustrated. Also indicated is the extent of the cingulate gyrus lesion in K152 (black area). Scale bars, 5.0 mm.

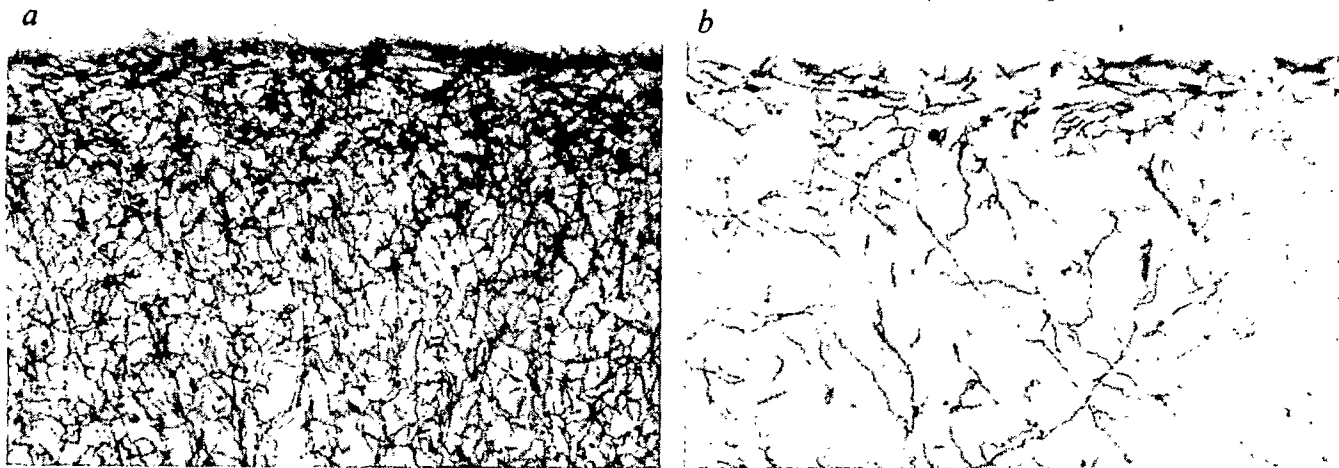


**Fig. 2** Photomicrographs of AChE-containing axons in the striate cortex of a 47-day-old kitten. *b*, Layers I-IV in the hemisphere that had received a chemical lesion of the cholinergic basal telencephalon 18 days earlier. *a*, A homotypic region in the contralateral control hemisphere. A unilateral loss of ocular dominance plasticity accompanies this reduction in the density of cholinergic axons if cortical noradrenaline is depleted concurrently. Magnification,  $\times 150$ .

other methods causing noradrenaline (NA) depletion leave the plasticity intact<sup>7-10</sup>. Here we present a possible explanation for the conflicting results. Combined destruction of the cortical noradrenergic and cholinergic innervations reduces the physiological response to monocular deprivation although lesions of either system alone are ineffective. We also find that 6-OHDA can interfere directly with the action of acetylcholine (ACh) on cortical neurones. Taken together, our results suggest that intracortical 6-OHDA disrupts plasticity by interfering with both cholinergic and noradrenergic transmission and raise the possibility that ACh and NA facilitate synaptic modifications in the striate cortex by a common molecular mechanism.

Our study was designed to assess the contribution of the extrathalamic cortical afferents to OD plasticity in the striate

cortex. Our attention was focused initially on the cholinergic projection for three reasons. First, there is converging biochemical<sup>11,12</sup> and anatomical<sup>13</sup> evidence suggesting that the striate cortex receives a dense cholinergic innervation during the critical period. Second, the facilitatory action of ACh on excitatory transmission in striate cortex<sup>14,15</sup> increases the probability of postsynaptic activation, a condition that is required for the experience-dependent modification of many excitatory synapses<sup>16</sup>. Third, the cholinergic projection is thought to be an important component of the ascending reticular activating system<sup>17</sup>, and there is evidence that reticular activation of striate cortex may be necessary for OD plasticity<sup>18,19</sup>.

The cholinergic innervation of striate cortex arises from cells scattered through the basal telencephalon (Fig. 1*a, b*; ref. 20).

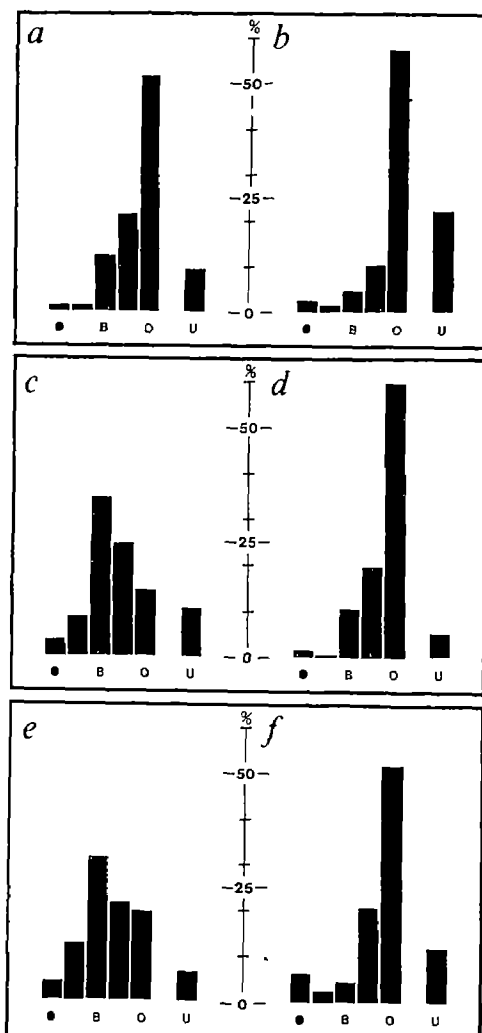


**Fig. 3** Percentages of cells in each of the five ocular dominance groups in the experimental (*a*, *c*, *e*) and control (*b*, *d*, *f*) hemispheres. Open circles, monocular open eye groups; filled circles, monocular closed eye groups; B, strictly binocular groups (group 3); U, % of unclassifiable neurones. *a*, *b*, Composite ocular dominance histograms from kittens that received unilateral NMA lesions of the cholinergic basal forebrain before 7–11 days of monocular deprivation (see Table 1). The ocular dominance distribution is shifted to the open eye both in the ACh-depleted left hemispheres (*a*, 126 cells) and in the control right hemispheres (*b*, 66 cells). *c*, *d*, Composite OD histograms from kittens that received unilateral 6-OHDA lesions of the dorsal noradrenergic bundle 1 week before the NMA lesions of the forebrain (see Table 1). *c*, OD distribution in the experimental hemispheres (110 cells) is significantly more binocular and less shifted than in *d*, showing the distribution in the control hemispheres (97 cells). *e*, *f*, Composite OD histograms from kittens that received unilateral lesions of the cingulate gyrus before 8–9 days of monocular deprivation (see Table 1). The OD histogram from the cingulate-damaged hemispheres (*e*, 94 cells) is also significantly more binocular and less shifted than that from the control hemispheres (*f*, 64 cells). The striate cortex in both the 6-OHDA+NMA-injected and cingulate-damaged hemispheres was depleted of its normal complement of cholinergic and noradrenergic axons. Other than OD, the visual-response properties of the cells recorded in these hemispheres did not differ from the controls. Histological reconstruction of the electrode tracks was not possible because the area centralis representation of area 17 was dissected for HPLC analysis. However, our sampling methods were the same in both hemispheres and no obvious laminar bias was indicated by the relative percentages of simple or complex cells encountered.

**Table 1** Rearing histories of kittens and physiological results

Animal	Lesion	Age at lesion (days postnatal)	Monocular deprivation (days postnatal)	Control hemispheres			Experimental hemispheres			% NA
				N	B	OED	N	B	OED	
K125	BF	29	33–43	21	0.06	0.94	30	0.46	0.61	—
K127	BF	29	40–47	20	0.25	0.81	30	0.38	0.77	—
K128	BF	29	44–55	25	0.33	0.67	36	0.52	0.59	—
K142	BF	32	32–40	—	—	—	30	0.26	0.83	—
K149	DNAB/BF	32/39	39–48	30	0.39	0.71	35	0.84	0.31	16
K151	DNAB/BF	32/39	41–50	30	0.33	0.80	35	0.78	0.39	49
K156	DNAB/BF	32/39	39–49	37	0.31	0.72	40	0.74	0.26	40
K152	C	39	39–47	31	0.19	0.89	31	0.69	0.40	30
K157	C	39	39–47	—	—	—	33	0.70	0.32	40
K158	C	39	39–48	33	0.42	0.60	30	0.79	0.30	31
K160	DNAB	32	39–49	—	—	—	30	0.33	0.82	33
K164	C*	35	35–45	—	—	—	30	0.33	0.64	—

BF, basal forebrain; DNAB, dorsal noradrenergic bundle; DNAB/BF, DNAB followed by BF; C, surgical aspiration of the cingulate gyrus; C\*, NMA lesion of cingulate cortex. N, number of cells recorded in each hemisphere; B, binocularity; OED, open-eye dominance for each hemisphere. Binocularity is defined as the number of cells in OD groups 2–4 divided by the total number of cells recorded. OED (after Paradiso *et al.*<sup>28</sup>) is defined as the number of cells in group 5 plus 0.5 times the number of cells in group 4 divided by the total number of cells (group 5, by convention, is the monocular group dominated by the open eye). In all cases except K142 the lesions were unilateral so that the opposite hemispheres could serve as controls. The cortical NA content in hemispheres with DNAB and C lesions (expressed as a per cent of the control cortex) is also shown. In these cases, saline-perfused samples of visual cortex were rapidly dissected from both hemispheres and frozen at  $-70^{\circ}\text{C}$ . The samples were subsequently homogenized in 0.1 M perchloric acid containing EDTA ( $60\text{ mg l}^{-1}$ ) and sodium metabisulphite ( $100\text{ mg l}^{-1}$ ) and then centrifuged to remove denatured protein. Aliquots of the supernatant were applied directly to an HPLC column (ALTEX ODS 5  $\mu\text{m}$ ) and the catechol compounds were measured relative to an internal dihydroxybenzylamine standard using electrochemical detection as described elsewhere<sup>7,26</sup>. The NA content of the control visual cortex was  $73.67 \pm 7.26$  (mean  $\pm$  s.e.m.) ng per g tissue, wet weight.

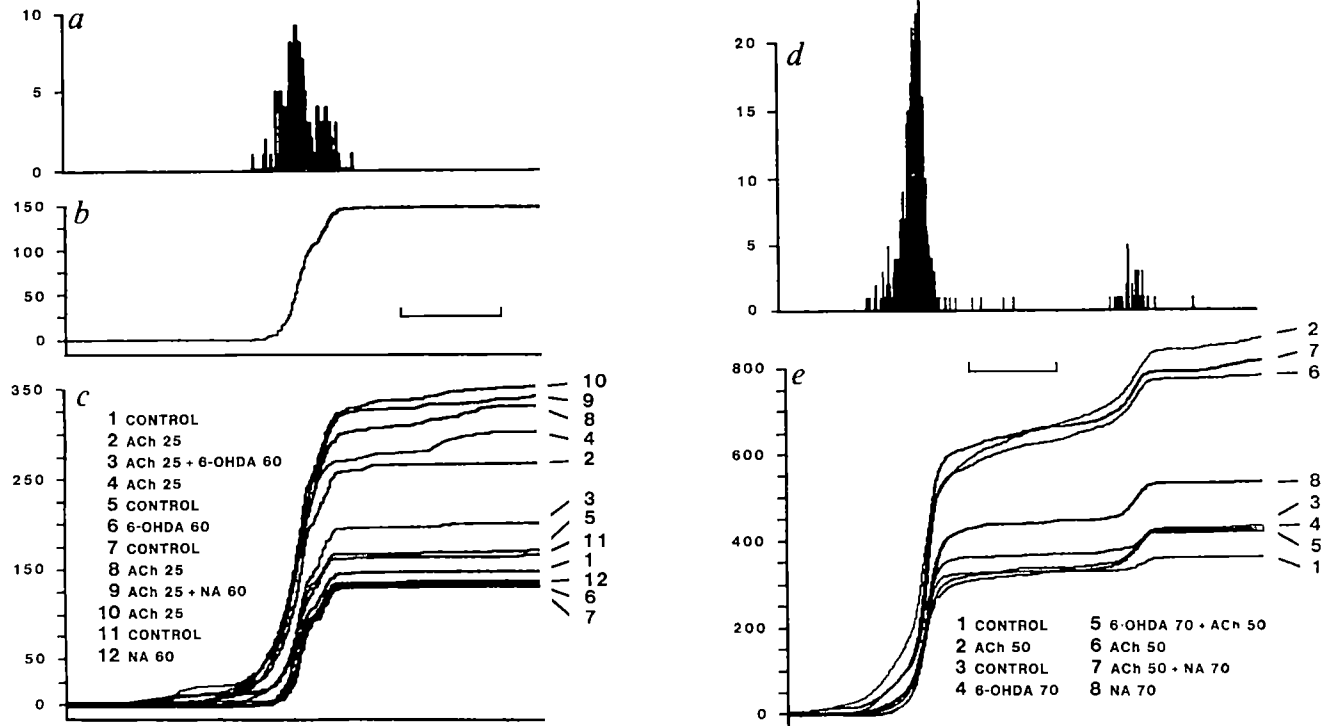


**Fig. 4** Antagonistic effect of iontophoretically applied 6-OHDA on ACh-evoked responses. *a*, Peri-stimulus time histogram of the control response of a simple cell in the striate cortex to an optimally oriented bar of light swept at a constant speed over the receptive field of the neurone. The ordinate shows the number of spikes per bin accumulated in 10 trials; bin width, 20 ms. *b*, To facilitate quantitative comparisons, the same data are expressed as total spikes accumulated as a function of sweep time. In this example, the cell responded to 10 stimulus presentations with 148 spikes. Scale bar, 1.0 s. *c*, Response of this cell to visual stimulation is plotted as in *b*, under the 12 test conditions listed in chronological order. The interval between tests ranged from 1 to 1.5 min. Indicated after each drug tested is the iontophoresis current (nA). The visual response of this cell was reliably enhanced each time ACh was applied by itself (tests 2, 4, 8 and 10). However, this enhancement was reduced considerably when 6-OHDA was applied concurrently (test 3). In contrast, NA applied in the same way had no effect on the ACh response (test 9); 6-OHDA application by itself had little apparent effect (test 6) compared with the control responses (tests 1, 5, 7 and 11). *d*, Peri-stimulus time histogram of the control response of a complex cell in the striate cortex to a bar of light swept first in the preferred direction, then in the opposite direction. *e*, Data from this complex cell expressed as in *b* and *c*. Test conditions are listed in chronological order and the interval between tests ranged from 1 to 7 min. In this example, the facilitation of the visual response by ACh (tests 2 and 6) was completely blocked by 6-OHDA (test 5). Noradrenaline did not have a similar action (test 7) and 6-OHDA had no effect on the cellular response when applied alone (test 4). Scale bar, 1.0 s. Excitation of this cell with glutamate was not antagonized by the concurrent application of 6-OHDA (data not shown).

**Methods.** All the records were made with a micropipette containing 1.5 M potassium citrate ( $R = 15 \mu\text{m}$ ) that protruded  $\sim 50 \mu\text{m}$  from an attached 7-barrel micropipette. Two of these barrels contained acetylcholine chloride (2.0 M, pH 4.5), two contained 6-OHDA-HCl (0.2 M) in 0.1% ascorbate (pH 3), one was filled with noradrenaline-HCl (0.2 M), also in 0.1% ascorbate, and one contained glutamic acid (0.3 M, pH 8). Currents of 5 nA were applied to retain the drugs in the barrels; positive for glutamate and negative for all others. Tip potentials were automatically balanced by passing currents of equal and opposite polarity through an additional barrel containing 2.0 M NaCl.

We destroyed these cells with the excitotoxin *N*-methyl-DL-aspartate (NMA) in 4–5-week-old kittens, and then tested for a deficit in the OD shift after brief periods of monocular deprivation. All lesions were made in the left hemisphere. The right eyelids were closed and, 7–10 days later, a standard physiological assay of OD was performed in the striate cortex on both sides<sup>18</sup>. As the normal OD shift is nearly symmetrical in the two hemispheres<sup>8,9</sup>, the cortex on the right (unoperated) side served as an internal control. The effectiveness of the lesions was monitored by acetylcholinesterase (AChE) histochemistry. Most, if not all, of the AChE-positive axons in the cat striate cortex arise from cholinergic cells in the basal telencephalon<sup>20</sup>.

A typical basal forebrain (BF) lesion, illustrated in Fig. 1*a*, *b* (left side), resulted in a drastic reduction in the density of AChE-stained axons in striate cortex (Fig. 2). Nevertheless, subsequent monocular deprivation shifted the OD of cortical neurones dramatically to the open eye (Fig. 3*a*, *b*, Table 1). These data indicate that a substantial depletion of ACh alone is not sufficient to block plasticity. However, when cortical NA was depleted by >50% (Table 1) before the basal forebrain lesions, the normal OD shift was prevented (Fig. 3*c*, *d*; Table 1). The noradrenergic projection was destroyed unilaterally in these animals by injecting 6–10 µg of 6-OHDA into the left dorsal noradrenergic bundle (co-ordinates A7, L3, DO). Daw

*et al.*<sup>9</sup> have shown, and we have confirmed (K160, Table 1), that dorsal noradrenergic bundle lesions do not normally affect the plastic response to monocular deprivation, even with a 70–90% depletion of cortical NA. Thus, although basal forebrain and dorsal noradrenergic bundle lesions alone are ineffective, they cause a significant loss of OD plasticity in the striate cortex when they are combined.

These data suggest that the combined depletion of cortical ACh and NA is a sufficient condition to retard experience-dependent synaptic modifications in the striate cortex. This notion was tested further by using a second experimental approach. Anatomical studies in this laboratory indicate that cholinergic and noradrenergic axons en route to area 17 travel together within the white matter of the cingulate gyrus. Thus, surgical lesions of the cingulate gyrus also effectively deplete striate cortex of both NA and ACh. Such a lesion (Fig. 1*c*, *d*) drastically reduces the density of AChE-positive axons, depletes endogenous NA (Table 1) and prevents the normal OD shift after monocular deprivation in area 17 on the lesioned side (Fig. 3*e*, *f*; Table 1). In one kitten (Table 1, K164), an extensive lesion of the cingulate cortex was made with multiple injections of NMA, which spares axons of passage. This treatment did not significantly alter the normal OD shift after monocular deprivation, thus confirming that the effects of the surgical lesions are

caused by the interruption of pathways passing through the cingulate gyrus.

These results predict that any treatment that simultaneously blocks noradrenergic and cholinergic transmission in the cortex is effective in slowing the OD shift after monocular deprivation. The work of Furness<sup>21</sup> on intestinal smooth muscle indicates that continuously applied 6-OHDA has exactly this effect—noradrenergic denervation and blockade of muscarinic cholinergic transmission. We explored this possibility in the striate cortex by assessing the effects of 6-OHDA iontophoresis on the neuronal responses induced by applying ACh from a piggyback microelectrode assembly<sup>22</sup>. We studied 30 ACh-sensitive neurones in the striate cortex of three adult cats. The effects of ACh iontophoresis were generally in agreement with those of Sillito and Kemp<sup>14</sup>. In most cases (26 cells), the visual responses were enhanced by ACh. However, in 85% of these cells the enhancement was significantly attenuated when ACh was applied concurrently with 6-OHDA (Fig. 4).

Our iontophoretic data are consistent with the hypothesis that the continuous application of 6-OHDA to the cortex affects cholinergic transmission, suggesting that intracortical 6-OHDA disrupts cortical plasticity by a combined action on the noradrenergic and cholinergic projections. In this context, note that the threshold concentration of 6-OHDA to block muscarinic transmission in the gut is ~5 μM (ref. 21). This is the same tissue concentration of 6-OHDA that Kasamatsu *et al.*<sup>23</sup> calculated to be the threshold for preventing plasticity in the striate cortex of kittens.

It is not yet clear whether these data indicate a special role for NA and ACh in the control of cortical plasticity. Many experience-dependent synaptic modifications seem to require the activation of cortical neurones<sup>16</sup> and there are indications that this activation must exceed the threshold of voltage-sensitive Ca<sup>2+</sup> channels in order to be effective<sup>24</sup>. Thus, removal of enough facilitatory extrageniculate inputs could lower cortical excitability below the threshold for synaptic modifications. Both ACh and NA reduce K<sup>+</sup> permeability<sup>25,26</sup> and hence both could enhance depolarization in response to visual input<sup>15</sup>. On the other hand, the actions of these neuromodulators may be related more specifically to the control of synaptic plasticity in the cerebral cortex. For example, both stimulate the production of cyclic nucleotides and the mobilization of intracellular Ca<sup>2+</sup> in target neurones<sup>27</sup>. Thus, it is plausible that ACh and NA regulate, via second-messenger-dependent phosphorylation, a common set of proteins that are involved in the modification of synaptic transmission.

We thank Dr P. Zöphel for performing the HPLC analysis, Dr J. Dann for critically reading the manuscript, C. Ziegler for making the electrodes, E. Kastl and A. Franke for assistance with the histology, and G. Trauten for typing the manuscript.

Received 27 June; accepted 12 November 1985.

1. Wiesel, T. N. & Hubel, D. H. *J. Neurophysiol.* **26**, 1003–1017 (1963).
2. Kasamatsu, T. & Pettigrew, J. D. *Science* **194**, 206–209 (1976).
3. Kasamatsu, T. & Pettigrew, J. D. *J. comp. Neurol.* **185**, 139–162 (1979).
4. Kasamatsu, T., Pettigrew, J. D. & Ary, M. *J. comp. Neurol.* **185**, 163–182 (1979).
5. Pettigrew, J. D. & Kasamatsu, T. *Nature* **271**, 761–763 (1978).
6. Kasamatsu, T. *Prog. Psychobiol. physiol. Psychol.* **10**, 1–112 (1984).
7. Bear, M. F. *et al.* *Nature* **302**, 245–247 (1983).
8. Daw, N. W., Robertson, T. W., Rader, R. K., Videen, T. O. & Coscia, C. J. *J. Neurosci.* **4**, 1354–1360 (1984).
9. Daw, N. W., Videen, T. O., Parkinson, D. & Rader, R. K. *J. Neurosci.* **5**, 1925–1933 (1985).
10. Adrién, J. *et al.* *J. Physiol., Lond.* **367**, 73–98 (1985).
11. Potempaska, A., Skangiel-Kramarska, J. & Kossut, M. *Dev. Neurosci.* **2**, 38–45 (1979).
12. Shaw, C., Needler, M. C. & Cynader, M. *Dev. Brain Res.* **14**, 295–299 (1984).
13. Bear, M. F., Carnes, K. M. & Ebner, F. F. *J. comp. Neurol.* **237**, 519–532 (1985).
14. Sillito, A. M. & Kemp, J. A. *Brain Res.* **289**, 143–155 (1983).
15. Sillito, A. M. *Nature* **303**, 477–478 (1983).
16. Rauschecker, J. P. & Singer, W. *Nature* **280**, 58–60 (1979).
17. Singer, W. in *The Neurosciences: 4th Study Program*, 1093–1110 (MIT Press Cambridge, 1979).
18. Singer, W. *Expl. Brain Res.* **47**, 209–222 (1982).
19. Singer, W. & Rauschecker, J. P. *Expl. Brain Res.* **47**, 223–233 (1982).
20. Bear, M. F., Carnes, K. M. & Ebner, F. F. *J. comp. Neurol.* **234**, 411–430 (1985).
21. Furness, J. B. in *6-Hydroxydopamine and Catecholamine Neurons*, 205–214 (North-Holland, Amsterdam, 1971).
22. Francesconi, W., Müller, C. M. & Singer, W. *Neurosci. Lett.* **18**, 309 (1984).

23. Kasamatsu, T., Itakura, T. & Jonsson, G. *J. Pharmac. exp. Ther.* **217**, 841–850 (1981).
24. Geiger, H. & Singer, W. *Expl. Brain Res. Suppl.* (in the press).
25. Madison, D. V. & Nicoll, R. A. *Nature* **299**, 636 (1982).
26. Halliwell, J. V. & Adams, P. R. *Brain Res.* **250**, 71 (1982).
27. Nestler, E. J., Walas, S. I. & Greengard, P. *Science* **225**, 1357–1364 (1984).
28. Paradiso, M. A., Bear, M. F. & Daniels, J. D. *Expl. Brain Res.* **51**, 413–422 (1983).

## T-cell recognition of antigen and the Ia molecule as a ternary complex

Jonathan D. Ashwell & Ronald H. Schwartz

Laboratory of Immunology, National Institute of Allergy and Infectious Diseases, National Institutes of Health, Bethesda, Maryland 20892, USA

T-lymphocyte co-recognition of antigen and major histocompatibility complex (MHC)-encoded molecules (such as murine Ia molecules) is thought to be mediated by a single cell-surface receptor, although the molecular mechanism by which this occurs is controversial (reviewed in ref. 1). One possibility is that the antigen molecule and the Ia molecule interact physically, either before or after encountering the T-cell antigen-specific receptor<sup>1,2</sup>. Alternatively, both molecules could bind to the receptor independently of one another, accounting for the dual specificity of the receptor without postulating a physical interaction between a limited number of Ia molecules present in any given animal and the myriad antigens to which T cells can respond. Here, we used a recently described approach for analysing the relative avidity of the T-cell receptor for different ligands<sup>3</sup> to address these two possibilities. We describe a T-cell clone whose response to a single antigen, presented in the context of two different Ia molecules, strongly suggests that the antigen and the Ia molecule interact physically.

Receptor-bearing cells in culture compete with each other for ligand. For a fixed concentration of ligand, as the number of responding cells in an assay increases, at some point the number of receptors occupied per cell will decrease as the free ligand becomes significantly depleted by binding to the receptor. If the response of the cell to the ligand is proportional to the number of receptors occupied, at least in the dose-sensitive portion of the response, then the average cellular response, or the probability that a cell will respond in the case of a proliferation assay, will also decline<sup>4–6</sup>. Furthermore, the point at which the cells bind sufficient ligand to result in a decrease in the average cellular response is dependent upon two variables: the number of receptors per cell and the affinity of the receptors for the ligand. We have used this phenomenon to analyse the interaction of the T-cell antigen-specific receptor with its ligand, which is a combination of antigen and Ia molecule (antigen-Ia)<sup>3</sup>. The fraction of T cells stimulated by antigen-Ia to incorporate <sup>3</sup>H-thymidine varied as a function of the number of responding T cells, best displayed by plotting the response of the T cells as a fraction of the maximum response achieved (Fig. 1). In a previous study we used this technique to compare the ability of four synthetic analogues of moth cytochrome c to activate a T-cell clone when presented in association with a single Ia molecule, E<sub>B</sub><sup>k</sup>E<sub>A</sub><sup>k</sup> (ref. 3). In the present study, we assessed the effect of changing the allelic form of the Ia molecule while keeping the antigen constant.

The T-cell clone designated F1.A.2 can recognize the moth cytochrome c synthetic fragment 86–89; 93–103(93E) (moth fragment) in association with either E<sub>B</sub><sup>k</sup>E<sub>A</sub><sup>k</sup> or E<sub>B</sub><sup>b</sup>E<sub>A</sub><sup>k</sup>. These two Ia molecules differ by only four amino acids in the N-terminal domain of their β-chains (ref. 7 and P. Jones, personal communication). The moth fragment was 13-fold more potent (defined in Fig. 1) when recognized in association with E<sub>B</sub><sup>k</sup>E<sub>A</sub><sup>k</sup> than with E<sub>B</sub><sup>b</sup>E<sub>A</sub><sup>k</sup> (one representative experiment is shown in Fig. 2, an

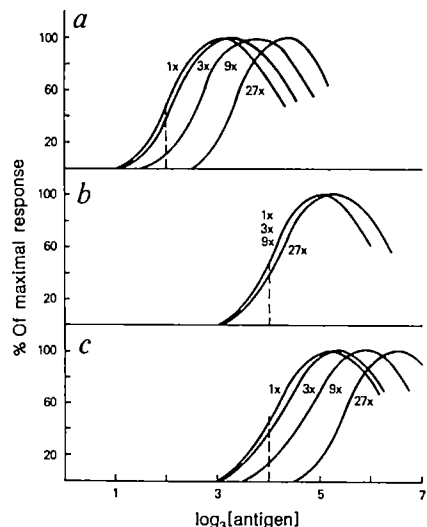


**Fig. 1** Schematic representation of shifts in the antigen dose-response for various numbers of responding T cells. *a*, The proliferative response of a T-cell clone to varying concentrations of antigen in the presence of a fixed number of antigen-presenting cells (that is, the number of Ia molecules is constant). Each curve represents a different number of responding T cells, shown in threefold increments ( $1\times$ ,  $3\times$ ,  $9\times$ ,  $27\times$ ). Because receptor-bearing cells compete with each other for ligand, as the number of responding cells in culture is increased, the fractional response will decrease<sup>3-6</sup>. When this results in an observable shift in the dose-response curves, the 'transition point' is said to have been reached<sup>3</sup>. In *a*, by inspection, the transition point is found to occur between the  $1\times$  and  $3\times$  increments. *b*, Illustration of a potency difference due to avidity. In the example shown, an antigen analogue exhibits a ninefold lower potency than the parent molecule. The relative potency of different antigen analogues (indicated here by a broken line perpendicular to the abscissa) is determined by comparing the concentrations of antigen required to achieve 50% of the maximal response for a specific responding cell number at or below the transition point. An alteration in the antigen that reduces the affinity of the antigen-specific receptor for antigen-Ia will result in a loss in potency. Furthermore, the lower affinity will also result in a decrease in the ability of the antigen-specific receptors to compete for ligand. Therefore, the number of responding cells required to achieve the transition point will increase (*b*). Alternatively, other modifications to the antigen might not affect the affinity of the antigen-specific receptor for the antigen-Ia, but would still cause a loss of potency (for example, by altering the way in which the antigen is processed, its solubility in the lipid membrane of the APC, its ability to interact with the Ia molecule) as shown in *c*. *c*, Dose-response curves using such an antigen analogue that differs in potency by ninefold from the analogue in *a*. In this case there is no difference in the affinity of the antigen-specific receptor for either the analogue or the original molecule. Therefore, the number of responding T cells needed to achieve the transition point is identical. The two different patterns shown here could also be generated by altering the affinity of the Ia molecule for either the receptor (*b*) or the antigen (*c*). Note that the descending portion of each of these schematic dose-response curves represents the phenomenon of 'high-dose suppression' seen on antigen activation of T cells<sup>16</sup>. This is not the result of antigen toxicity, but rather of receptor occupancy, and the shifts in the descending portions of the dose-response curves roughly parallel the shifts in the ascending portions.

average of four experiments is given in Table 1). We investigated the way in which varying the responding number of this T-cell clone affected its response to antigen in association with either Ia molecule. Despite the difference in potency, we found no significant difference in the degree to which the antigen dose-response curves shifted when antigen-presenting cells bearing either Ia molecule were used (Table 1). The unlikely possibility that the number of  $E_\beta E_\alpha$  molecules present on the two types of antigen-presenting cells differed by 13-fold, thus accounting

**Table 1** Summary of shifts in the antigen dose-response curve using moth 86-89; 93-103(93E) in association with  $E_\beta^k E_\alpha^k$  or  $E_\beta^b E_\alpha^k$

APC	Expt	[Ag] <sub>50%</sub> ratio No. of responding T cells ( $\times 10^{-3}$ )			
		2	6	18	54
B10.A ( $E_\beta^k E_\alpha^k$ )	1	1 [0.00036]*	1.56	2.19	5.0
	2	1 [0.00018]	1.11	2.22	3.11
	2	1 [0.00014]	1.0	1.14	2.14
	4	1 [0.00075]	1.19	1.77	3.16
Geometric mean:		1 [0.00029]†	1.20 (1.10)	1.77 (1.17)‡	3.20 (1.19)‡
B10.A(5R) ( $E_\beta^b E_\alpha^k$ )	1	1 [0.0056]	1.27	2.32	5.36
	2	1 [0.0018]	1.39	3.11	3.94
	3	1 [0.0018]	1.0	1.39	2.50
	4	1 [0.011]	1.06	1.59	2.38
Geometric mean:		1 [0.0038]†	1.17 (1.08)	2.00 (1.20)‡	3.15 (1.21)‡

T-cell proliferation assays were performed as described in Fig. 2 legend. The concentration of antigen required to achieve 50% of the maximal stimulation of the clone F1.A.2 ([Ag]<sub>50%</sub>) in the presence of either B10.A antigen-presenting cells (APC) (bearing the Ia molecule  $E_\beta^k E_\alpha^k$ ) or B10.A(5R) APC (bearing  $I_\beta^b E_\alpha^k$ ) at varying numbers of responding cells was determined in four separate experiments. A ratio was then calculated for each group by comparing the concentration of antigen required for a 50% response with the concentration required for a 50% response by the lowest number of responding T cells,  $2 \times 10^3$  per well. Values in parentheses are  $\times/\div$  s.e.m. of the geometric means.

\* The concentration of antigen ( $\mu\text{M}$ ) required to achieve 50% of the maximal response at  $2 \times 10^3$  responding T cells.

† The ratio of these two numbers ( $0.0038/0.00029 = 13.1$ ) defines the potency difference for the two different antigen-Ia molecule ligands.

‡ Significantly different from 1 at the 5% level (two-tailed Student's *t*-test).

for the difference in potency, was ruled out by quantitative flow microcytometric analysis using a monoclonal antibody (14.4.4) that binds to the  $E_\alpha$  chain; the levels of  $E_\alpha^k$  expressed on the spleen cells from the two strains were comparable (data not shown).

A potency difference that results from an alteration in the affinity of the T-cell receptor for any component of its ligand (either the antigen or the Ia molecule) would be seen as a difference in avidity of the T-cell receptor for the entire ligand, and should be reflected in the antigen dose-response curve shifts that occur as the number of responding T cells is increased. As the ligand recognized with lower avidity must be present in greater amounts than the ligand recognized with higher avidity in order to achieve the same degree of activation, the competition that occurs between receptor-bearing cells should result in a greater fractional depletion of the ligand recognized with higher avidity. In the case where the Ia molecule has been altered, the shifts of the antigen dose-response curve would occur at lower numbers of responding T cells for the Ia molecule requiring less antigen than for the Ia molecule requiring more antigen. In contrast, if the functional difference between the two Ia molecules were a consequence of their interaction with the antigen, no difference would be expected between them in the way the antigen dose-response curve shifted. In this case, although the amount of soluble antigen would vary at the same degree of cellular response, the amount of the true ligand (antigen-Ia) would be the same. For the antigen-Ia molecule combination studied here (moth fragment plus  $E_\beta^k E_\alpha^k$  and moth fragment plus  $E_\beta^b E_\alpha^k$ ), no difference was seen in the shifts of the antigen dose-response curve, despite a 13-fold difference in the observed potency. This result suggests that there is no avidity difference between the T-cell antigen-specific receptor and these two ligands. The most likely mechanism by which a change in the molecule could cause the potency difference is through a change in the interaction between the Ia molecule and the antigen. Although altering the Ia molecule did not result in a change in avidity in this particular case, the possibility exists that, with other T-cell clones, making such a change will alter a site on the Ia molecule that makes contact with the T-cell receptor, and hence alter the affinity of the antigen-specific receptor for the Ia molecule.

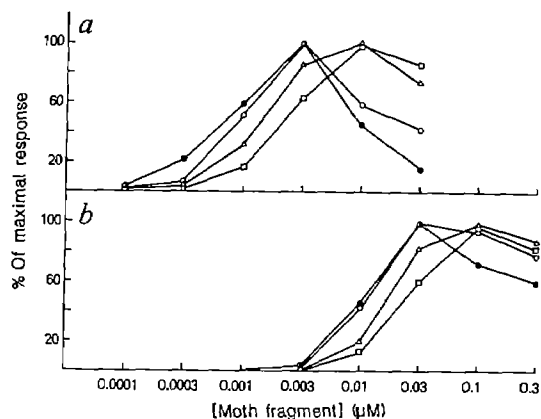


**Fig. 2** The proliferative response of varying numbers of a T-cell clone to the antigen moth cytochrome *c* in the presence of the  $E_\beta^k E_\alpha^k$  Ia molecule (B10.A APC; *a*) or the  $E_\beta^b E_\alpha^k$  Ia molecule (B10.A(5R) APC; *b*). The T-cell clone F1.A.2 was obtained by Dr Gen Suzuki of our laboratory from [B10.A × B10.A(3R)]F<sub>1</sub> mice immunized with pigeon cytochrome *c* in Freund's complete adjuvant (Difco). Cell lines were established from T cells taken from the draining lymph nodes and T-cell clones prepared by limiting dilution as described previously<sup>3</sup>. The clone F1.A.2 was found to respond to a variety of cytochrome *c* species variants in association with either  $E_\beta^k E_\alpha^k$  or  $E_\beta^b E_\alpha^k$ , as determined by its proliferative response to irradiated (3,300 rad) spleen cells from congenic C57BL/10 mice in the presence or absence of anti-Ia monoclonal antibodies specific for products of the *I-A* or *I-E* subregion (data not shown). The nomenclature used to describe the Ia molecules in this study is as follows: the *E* denotes the subregion of the mouse *H-2* complex that encodes the protein, the subscripts refer to the two chains that make up the Ia heterodimer, and the superscripts refer to the allelic forms of the two chains. The T-cell clone was maintained by periodic stimulation with pigeon cytochrome *c* plus irradiated B10.A spleen cells (for 4 days), followed by a period of rest (9–17 days) in the absence of antigen. Concanavalin A-stimulated rat spleen-cell supernatant (as a source of interleukin-2) was occasionally added to the cultures 48 h after stimulation with antigen to promote optimal expansion of the cells. After a rest period, F1.A.2 T cells were titrated into 96-well flat-bottomed plates (3596, Costar) at  $2 \times 10^3$  (●),  $6 \times 10^3$  (○),  $18 \times 10^3$  (△) or  $54 \times 10^3$  (□) cells per well. Each well contained  $5 \times 10^5$  irradiated (3,300 rad) spleen cells from B10.A (*a*) or B10.A(5R) (*b*) mice as a source of APC bearing the Ia molecules, and varying concentrations of the synthetic peptide moth cytochrome *c* 86–89; 93–103(93E)<sup>17</sup>. Each well was brought to a final volume of 200  $\mu$ l with complete medium, a 50:50 (v/v) mixture of RPMI 1640 medium (Biofluids, Rockville, Maryland) and Eagle's Hank's Amino Acids (Biofluids), supplemented with 10% fetal calf serum,  $5 \times 10^{-5}$  M 2-mercaptoethanol, 4 mM glutamine, 100 U ml<sup>-1</sup> of penicillin and 150  $\mu$ g ml<sup>-1</sup> gentamicin. After 48 h of culture at 37 °C in a humidified atmosphere containing 5% CO<sub>2</sub>, the wells were pulsed with 1  $\mu$ Ci of <sup>3</sup>H-thymidine (6.7 Ci mmol<sup>-1</sup>; ICN); 16 h later the plates were harvested (PHD Cell Harvester, Cambridge Technologies, Cambridge, Massachusetts) and the amount of thymidine incorporation assessed by liquid scintillation counting. The results of duplicate cultures were averaged and plotted as a percentage of the maximal response achieved for each responding cell number. The maximum responses in this experiment were as follows. B10.A APC:  $2 \times 10^3$ , 19,200 c.p.m.;  $6 \times 10^3$ , 55,400 c.p.m.;  $18 \times 10^3$ , 126,700 c.p.m.;  $54 \times 10^3$ , 350,300 c.p.m. B10.A(5R) APC:  $2 \times 10^3$ , 23,000 c.p.m.;  $6 \times 10^3$ , 63,400 c.p.m.;  $18 \times 10^3$ , 157,100 c.p.m.;  $54 \times 10^3$ , 263,300 c.p.m.

The data presented here can be used to discriminate between some of the models proposed to explain the molecular basis of T-lymphocyte co-recognition. One model hypothesizes that the three molecular elements physically interact to form a stable complex that ultimately leads to signal transduction (the trimolecular complex model<sup>8</sup>; Fig. 3*a*). In this model, the T-cell antigen-specific receptor, along with the antigen and the Ia molecule, combine to deliver a stimulatory signal to the T cell. A change in affinity at any one of the potential interaction sites

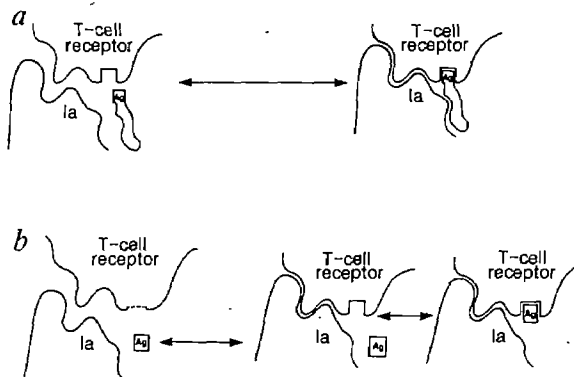


**Fig. 3** Two models for antigen-specific T-cell receptor recognition of antigen and an Ia molecule. *a*, The trimolecular complex model. The three elements of the trimolecular complex (antigen-specific receptor, antigen and Ia molecule) are in equilibrium with a ternary complex. There are three potential sites of interaction: T-cell receptor/antigen, T-cell receptor/Ia molecule, and antigen/Ia molecule<sup>8</sup>. Each bimolecular interaction in the complex can be considered as a discrete reaction with its own kinetic constants. *b*, The allosteric or induced-fit model. In an allosteric model, the T-cell antigen-specific receptor has two binding sites: one for the antigen and the other for the Ia molecule. In an induced-fit model, a binding site exists for only one of the elements in the absence of the other. In either case, the affinity for one of these elements (the antigen, in this example) is so low that at equilibrium, insufficient binding occurs to lead to activation. The antigen-binding portion of the T-cell receptor is depicted by a shallow dotted depression to indicate that the antigen-binding site might not exist before the binding of the Ia molecule, or that it might exist predominantly in a low-affinity state (left). In this example, when the Ia molecule occupies its portion of the receptor, a conformational change occurs (or an alternative state is stabilized) (middle) such that the receptor can now bind the antigen with high affinity (right). This results in signal transduction. There is no postulated direct contact between the antigen and the Ia molecule. Note that a completely allosteric model requires two alternative states after Ia molecule binding to account for the differences we have observed previously in the fine specificity of antigen binding in the presence of  $E_\beta^k E_\alpha^k$  as opposed to  $E_\beta^b E_\alpha^k$  Ia molecules<sup>18</sup>.

would alter the potency of the ligand by virtue of the effect on the stability of the final trimolecular complex. If only the interaction between the Ia molecule and the antigen were altered, the affinity of the T-cell antigen-specific receptor for its ligand (antigen-Ia) could be unchanged, and the antigen dose-response curves would shift identically regardless of which Ia molecule was used to stimulate the T cell; this was the result obtained for clone F1.A.2. In contrast, the present results are not consistent with a simple allosteric or induced-fit model (Fig. 3*b*) of T-cell recognition. In such a model, differences in the ability of one antigen to stimulate a T-cell clone in the presence of two different Ia molecules must result from a difference in the affinity of the T cell's antigen-specific receptor for either the two Ia molecules or the antigen (the latter due to different states of the receptor induced or stabilized by the two Ia molecules)<sup>9,10</sup>.

The results presented here argue only that the Ia molecule and the antigen interact physically, thus they do not exclude a third model, that of 'altered self', in which the antigen induces a conformational change in the Ia molecule which is detected by the T cell's antigen-specific receptor<sup>11,12</sup>. This particular model seems unlikely in view of the accumulating data which suggest that the antigen-specific receptor can bind antigen in the absence of an Ia molecule under certain circumstances<sup>13–15</sup>.

We thank Drs Ronald Germain and Barbara Fox for critical review of the manuscript, and Ms Shirley Starnes for preparation of the manuscript.

Received 15 October 1985; accepted 27 January 1986.

1. Schwartz, R. H. *Adv. Immun.* **38**, 31–201 (1986).
2. Babbitt, B. P., Alien, P. M., Matsueda, G., Haber, E. & Unanue, E. R. *Nature* **317**, 359–361 (1985).
3. Ashwell, J. D., Fox, B. S. & Schwartz, R. H. *J. Immun.* **136**, 757–768 (1986).
4. Cuatrecasas, P. & Hollenberg, M. D. *Adv. Protein Chem.* **30**, 251–451 (1976).
5. Moyle, W. E., Lee, E. Y., Bahl, O. P., Garfink, J. E. & Rodbard, D. *Am. J. Physiol.* **232**, E274–E285 (1977).
6. Moyle, W. R., Lee, E. Y., Bahl, O. P. & Rodbard, D. in *Receptors and Hormone Action* (Academic, New York, 1978).
7. Mengle-Gaw, L., McDevitt, H. O. A. *Rev. Immun.* **3**, 367–396 (1985).
8. Heber-Katz, E., Hansburg, D. & Schwartz, R. H. *J. molec. cell. Immun.* **1**, 3–14 (1983).
9. Schwartz, R. H., Heber-Katz, E. & Hansburg, D. in *Intercellular Communication in Leukocyte Function* (Wiley, Chichester, 1983).
10. Cleveland, W. L. & Erlanger, B. F. *Molec. Immun.* **21**, 1037–1046 (1984).
11. Zinkernagel, R. M. & Doherty, P. *Nature* **251**, 547–548 (1974).
12. Sherman, L. *Nature* **292**, 511–513 (1982).
13. Carel, S., Bron, C. & Corradin, G. *Proc. natn. Acad. Sci. U.S.A.* **80**, 4832–4836 (1983).
14. Rao, A., Weng-Ping, W., Faes, S. J. & Cantor, H. *Cell* **36**, 879–888 (1984).
15. Siliciano, R. F., Keegan, A. D., Dintzis, R. Z., Dintzis, H. M. & Shin, H. S. *J. Immun.* **135**, 906–914 (1985).
16. Matis, L. A., Glimcher, L. H., Paul, W. E. & Schwartz, R. H. *Proc. natn. Acad. Sci. U.S.A.* **80**, 6019–6023 (1984).
17. Schwartz, R. H., Fox, B. S., Fraga, E., Chen, C. & Singh, B. *J. Immun.* **135**, 2498–2608 (1985).
18. Schwartz, R. H. A. *Rev. Immun.* **3**, 237–261 (1985).

## T-cell-mediated association of peptide antigen and major histocompatibility complex protein detected by energy transfer in an evanescent wave-field

Tania H. Watts, Hermann E. Gaub\* & Harden M. McConnell

Stauffer laboratory for Physical Chemistry, Stanford University, Stanford, California 94305, USA

**Helper T cells recognize foreign antigen displayed on antigen-presenting cells which also express self-molecules of the major histocompatibility complex (MHC)<sup>1</sup>.** A single T-cell receptor mediates recognition of both MHC and foreign antigen<sup>2,3</sup>. A proposed ternary complex between T-cell receptor, foreign antigen and MHC antigen has not yet been demonstrated (see ref. 1 for review). Here, we show that a fluorescein-labelled synthetic peptide, together with Texas red-labelled class II MHC antigen, I-A<sup>d</sup>, stimulates the production of interleukin-2 by a peptide-specific I-A<sup>d</sup>-restricted T-cell hybridoma when reconstituted in a lipid membrane on a glass substrate. Under the same conditions, resonance-energy transfer from donor peptide to acceptor I-A can be stimulated in an evanescent wave-field only in the presence of the specific T-hybrid. Our results show that the T cell stabilizes an association between peptide antigen and class II MHC protein to within a distance of about 40 Å.

The T-cell hybridoma 3DO-54.8 recognizes a 17-residue tryptic peptide representing residues 323–339 of ovalbumin when processed ovalbumin is presented by I-A<sup>d</sup>-bearing antigen-presenting cells<sup>4</sup>. Previous work has shown that when phospholipid vesicles are allowed to interact with a clean glass slide, the vesicles fuse to form a continuous membrane<sup>5,6</sup>. When these vesicles contain MHC antigens, the resulting planar membranes are effective in stimulating T-cell responses<sup>5,6</sup>. When synthetic peptide 323–339 is presented by I-A<sup>d</sup>-containing planar membranes, the midpoint of the dose-response curve occurs at 2 μM antigen and the response saturates at 20 μM antigen<sup>7</sup>. The N-terminal three residues and the C-terminal three residues of this peptide can be removed with only a small shift in the dose-response curve<sup>7</sup>. In the present study, the amino-terminus of peptide 323–339 was modified with fluorescein 5-isothiocyanate (FITC). The resulting peptide was indistinguishable from unlabelled peptide in stimulating interleukin-2 (IL-2) production from 3DO-54.8 cells (data not shown). The I-A<sup>d</sup> was

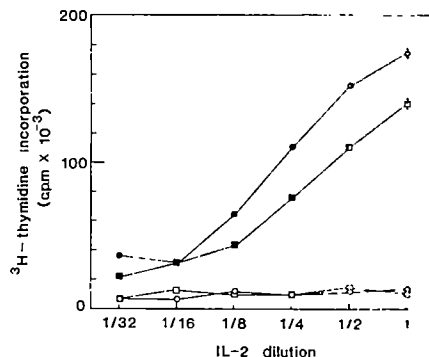


**Fig. 1** T-cell stimulation by Texas red-labelled I-A<sup>d</sup> in supported lipid membranes. IL-2 production from 3DO-54.8 cells in contact with supported planar membranes containing purified unlabelled I-A<sup>d</sup> was measured using the IL-2-dependent cell line CTLL as described previously<sup>6</sup>. Planar membranes contained unlabelled I-A<sup>d</sup> (●, ○) or Texas red-labelled I-A<sup>d</sup> (five Texas red molecules per I-A molecule) (■, □). Filled symbols, fluorescein-labelled peptide antigen added to a final concentration of 2 μM; open symbols, no antigen. Peptide labelling was carried out for 2 h at room temperature in 0.1 M sodium bicarbonate/carbonate buffer pH 9.0 using a fivefold molar excess of FITC (isomer 1, Molecular Probes Inc., Junction City) over peptide. Labelled peptide was purified using HPLC<sup>7</sup>. Texas red (Molecular Probes Inc.) labelling of I-A was carried out for 2.5 h on ice in 0.5% (w/v) sodium deoxycholate in 0.1 M sodium bicarbonate/carbonate pH 9.5 using a 1,000-fold molar excess of Texas red to I-A. Excess Texas red was removed by exhaustive dialysis. The Texas red-labelled I-A was reconstituted with egg phosphatidylcholine/cholesterol as described previously<sup>6</sup>. Dialysis of a lipid sample containing free Texas red showed that all the noncovalently linked Texas red could be removed by the exhaustive dialysis.

modified with the fluorescent probe Texas red<sup>8</sup>. Usually, the product contained five Texas red molecules per I-A molecule. Figure 1 shows IL-2 release by 3DO-54.8 cells in contact with planar membranes containing purified unlabelled or Texas red-labelled I-A. The results shown are for 2 μM fluorescein peptide 323–339. Although there is a decrease in the stimulatory ability of I-A after modification with Texas red, the overall response is still high.

I-A was incorporated into planar membranes on two classes of glass (or quartz) substrates. The experiments described in Fig. 1 were carried out on hydrophilic supports as described previously<sup>6,7</sup>. In addition, planar membranes were prepared by fusing I-A<sup>d</sup>-containing phospholipid vesicles on supports that had been alkylated with hexadecyltrichlorosilane (C<sub>16</sub> supports). (Alkylated supports have been described elsewhere<sup>9</sup>.) The resulting membranes contain I-A<sup>d</sup> as measured by Texas red fluorescence. IL-2 production by 3DO-54.8 cells in contact with planar membranes on C<sub>16</sub> supports requires ~10-fold more peptide antigen than the same membranes on hydrophilic supports (data not shown). A preliminary experiment indicates that the reconstituted I-A on C<sub>16</sub> supports exhibits slow lateral diffusion ( $10^{-10} \text{ cm}^2 \text{ s}^{-1}$ ) whereas lateral diffusion of MHC antigens in lipid bilayers on hydrophilic supports is below the limits of detection ( $<10^{-11} \text{ cm}^2 \text{ s}^{-1}$ )<sup>5,6</sup>. These values were determined by using fluorescein-labelled anti-I-A antibody and measuring fluorescence recovery after photobleaching<sup>10</sup>.

The apparatus for observing resonance energy transfer at the T-cell/lipid membrane interface is shown in Fig. 2a. Essential features are the use of evanescent wave excitation<sup>11,12</sup> and the use of a monochromator to record fluorescence emission spectra. Energy transfer between donor peptide and acceptor MHC molecules will be stimulated only if these molecules are within 40 Å of one another (for a review of Förster energy transfer see refs 13, 14). Only those donor-labelled peptide molecules that are within 800 Å of the planar membrane surface are excited; this has the effect of reducing the fluorescein background in our samples by three orders of magnitude and also greatly reduces

\* Present address: Institute for Biophysics E22, Department of Physics, Technische Universität München, 8046 Garching, FRG.

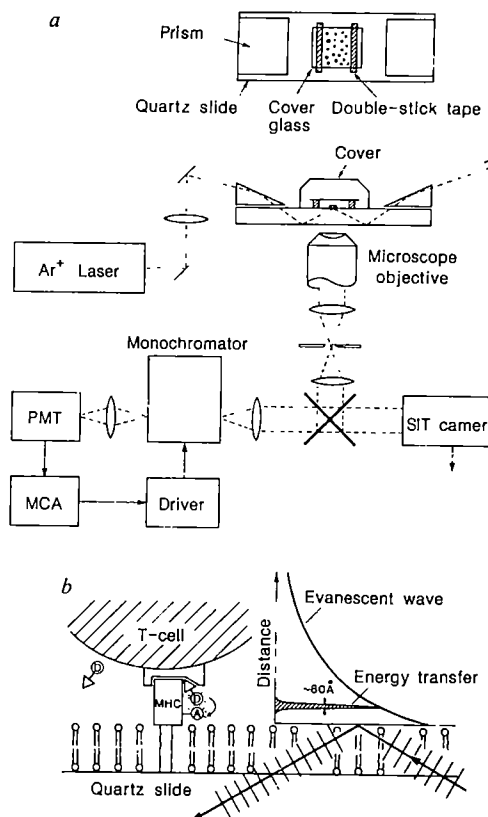


**Fig. 2** *a*, Experimental design; *b*, schematic representation of the molecular problem. *a*, The microfluorometer is based on an inverted microscope (Nikon Diaphot TMD) on an optical isolation table. The beam of an argon ion laser (Spectra Physics Ar 2000) is attenuated to <10 mW by a set of partially reflecting mirrors and a halfwave plate followed by a Glan-Thompson prism. The *p*-polarized beam is focused ( $f=600$  mm) and coupled by a high-refractive-index prism ( $n=1.8$ ) into a quartz microscope slide. The prism is positioned so that the first reflection on the upper side of the slide is in the sample area. Fine adjustment of the mirrors positions the excitation spot (~200  $\mu\text{m}$  diameter) in the field of view of the microscope. A  $\times 40$  variable correction 0.55 NA Nikon objective was used for all measurements. A variable diaphragm in the image plane limits the area from which fluorescence is detected to a spot of  $<150 \times 150 \mu\text{m}$ . The image of this diaphragm is focused ( $f=600$  mm) with the same aperture angle as that on the entrance slit of the monochromator (Spex 1681). The output slit is enlarged threefold and projected on the cathode of a photomultiplier (RCA 31034 cooled housing,  $-30^\circ\text{C}$ ). Photons are counted with a multichannel analyser (MCA; LeCroy 3500) with an EG&G 436 discriminator and an EG&G 535 preamplifier module. The monochromator is driven by a Spex Compudrive. PMT, photomultiplier tube; SIT silicon-intensified target. A plane wave hitting the boundary to an optically less dense medium is totally internally reflected if the incidence angle exceeds the critical angle (see ref. 12 for review). Lipid and the quartz have a very similar refractive index and are treated as one medium. The reflected wave creates an exponentially decaying evanescent electrical field in the optically less dense medium, the  $1/e$  distance is  $\sim 800 \text{\AA}$ . Only those molecules that are close to the interface are excited. The acceptor fluorophore (designated A) is attached to the MHC molecule, confined to the planar membrane, as indicated. The donor fluorophore (D) is attached to the peptide antigen. If the T-cell receptor brings about a significant enhancement in the probability that the donor and acceptor groups are within 40  $\text{\AA}$  of each other, then energy extracted from the evanescent wave field and absorbed by the donor group D leads to an enhancement in the fluorescence of A through resonance energy transfer. An enhancement of emission from A does not distinguish between a model for a ternary complex in which there are two closely apposed, but separate, sites for antigen and MHC on the T-cell receptor, from one in which there is one continuous site for binding the two molecules.

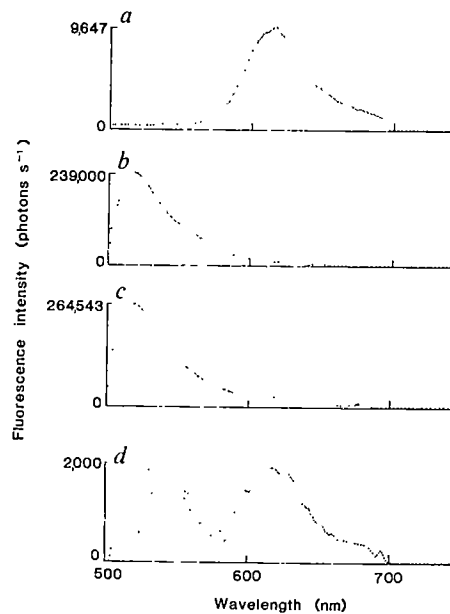


**Fig. 3** Energy transfer from fluorescein-labelled peptide to Texas red-labelled I-A<sup>d</sup> in the presence of 3DO-54.8 cells. Shown are typical raw data obtained from the apparatus described in Fig. 2. *a*, Spectrum of a planar membrane containing Texas red-I-A<sup>d</sup> and lipid alone; *b*, reference spectrum of fluorescein-labelled peptide antigen and 3DO-54.8 cells in contact with unlabelled I-A<sup>d</sup>-containing planar membranes; *c*, 3DO-54.8 cells in contact with the planar membrane shown in *a* in the presence of 20  $\mu\text{M}$  fluorescein-labelled peptide; *d*, difference spectrum *c* - *b* - *a*. Spectra *b* and *c* were scaled before subtraction using the integrals of the curves from 500 to 544 nm. The Texas red signal is negligible at these wavelengths. From this difference spectrum the Texas red-I-A signal was then subtracted directly. The noise in the difference spectrum in the wavelength region 500–580 nm arises from the subtraction of two large numbers, which can be caused by 1% fluctuations in laser intensity. In the region of the Texas red emission, this noise is less because the overall intensities used in the subtraction are 10-fold smaller. The fact that the double difference spectrum has the characteristic line shape of the Texas red emission shows the fidelity of the subtraction procedure. The double difference spectrum in the region from 500 to 580 nm is random noise. Cells and peptide were suspended in buffer consisting of 10 mM HEPES, 120 mM NaCl, 5.4 mM KCl, 5.6 mM glucose, 2.0 mM CaCl<sub>2</sub>, 1.5 mM MgCl<sub>2</sub>, 0.5–2% FCS. Cells were allowed to settle for 7 min at room temperature before the spectrum was recorded.

the problem of cell autofluorescence. From the overlap integral between the emission of fluorescein and the absorption of Texas red, the energy-transfer distance is calculated to be 40  $\text{\AA}$  (ref. 13).

As a positive control, energy transfer from fluorescein-labelled anti-I-A antibodies was examined. When specific anti-I-A<sup>d</sup> antibody (MKD6)<sup>2</sup> was used, a 90% enhancement of the Texas red signal was observed with antibody labelled with 8 fluorescein molecules per antibody. A 25% enhancement of the Texas red signal was observed when the antibody was labelled at a ratio of 1:1. No enhancement of Texas red fluorescence was observed with nonspecific fluorescein-labelled antibody (anti-I-A<sup>k</sup> antibody 10-12.6 (ref. 15) labelled with 5 fluorescein molecules per protein) (data not shown).

Texas red/I-A-containing planar membranes were prepared as described previously<sup>6</sup> and their fluorescence emission spectra recorded (Fig. 3*a*). Without moving the sample on the microscope stage, cells and peptide were added. Fluorescein-labelled peptide antigen was pre-mixed with T cells to give a final concentration of 20  $\mu\text{M}$  peptide, 0.5–2% fetal calf serum (FCS) and sufficient cells to produce a confluent layer. In some experiments anti-I-A antibody or a 10-fold excess of unlabelled peptide was included in the solution (see Fig. 3*c*). The spectrum of a control sample consisting of fluorescein-labelled peptide

Table 1 Summary of energy transfer results

Expt	No. of trials	Support*	Concentration FITC-peptide ( $\mu\text{M}$ )†	Concentration unlabelled peptide ( $\mu\text{M}$ )‡	Antibody§	Cells	Increase in Texas red emission † s.d.¶
a	4	H, $\text{C}_{16}$	20	—	—	—	0 ± 0
b	4	H	1	—	—	3DO-54.8	-13 ± 15
c	10	H	20	—	—	3DO-54.8	18 ± 8.5
d	3	H	20	200	—	3DO-54.8	4 ± 6
e	10	$\text{C}_{16}$	20	—	—	3DO-54.8	28 ± 10
f	4	$\text{C}_{16}$	20	200	—	3DO-54.8	-0.8 ± 15
g	2	$\text{C}_{16}$ , H	20	—	MKD6	3DO-54.8	-20 ± 28
h	3	$\text{C}_{16}$ , H	20	—	—	FS11-72.3	6 ± 10
i	1	H	20	—	—	CTL	0

\* H, hydrophilic support, resulting in a supported lipid bilayer;  $\text{C}_{16}$ , a support alkylated with hexadecyltrichlorosilane, resulting in a supported lipid monolayer.

† FITC-peptide, fluorescein-labelled synthetic peptide representing residues 323–339 of ovalbumin, modified and purified as described in Fig. 1.

‡ Unlabelled peptide, the same peptide without the fluorescein tag. The competing unlabelled peptide was added in 10-fold molar excess to the mixture of T cells and fluorescent peptide before adding them to the planar membrane.

§ Sufficient MKD6 antibody was added to the mixture of T cells and peptide to saturate the I-A with antibody.

|| 3DO-54.8, specific T cell (see text); FS11-72.3, self-reactive T-cell hybridoma which recognizes I-A<sup>k</sup>; CTL is the cytotoxic IL-2 indicator line.

¶ The per cent enhancement of the Texas red signal was determined from a comparison of the double-difference spectrum described in Fig. 3d with the original Texas red spectra.

plus 3DO-54.8 cells in contact with a planar membrane containing unlabelled I-A was recorded in a separate experiment (Fig. 3b). To subtract the fluorescein component from spectrum c to obtain the signal resulting from Texas red alone, spectra b and c were scaled using the integral of the curve between 500 and 544 nm. The signal obtained in spectrum a (obtained before addition of cells and peptide) was subtracted from the difference spectrum (c - b) to give the double difference spectrum d. This spectrum (d = c - b - a) is the enhancement of the Texas red signal caused by the addition of cells and peptide.

From the experiments summarized in Table 1, we conclude that: (1) In the absence of cells, there is no observed energy transfer between peptide and I-A at the same concentrations used in the experiments with cells (expt a), irrespective of whether the support is  $\text{C}_{16}$  or hydrophilic. (2) At peptide concentrations representing the midpoint of the dose-response curve for IL-2 release, there is no detectable energy transfer in the presence of cells (expt b). (3) We always observe an increase in Texas red emission when peptide is added to a concentration of 20  $\mu\text{M}$  together with the specific T cells. The magnitude of this enhancement is 10–30% on hydrophilic supports and 20–50% on  $\text{C}_{16}$  supports (expt c). (4) When the energy transfer experiment is performed in the presence of a 10-fold molar excess of unlabelled peptide, we always observe a smaller enhancement of the Texas red emission signal (expts d, f). Each competition experiment was carried out immediately following a positive experiment and always showed a decrease in the effect, excluding the possibility that the enhancement of Texas red fluorescence is caused by a change in its quantum yield on complexation. (5) Anti-I-A<sup>d</sup> antibody abolishes T-cell-mediated energy transfer (expt g). (6) Other T cells, not specific for I-A<sup>d</sup> and ovalbumin, show little or no energy transfer (expts h, i). When a small amount of transfer was observed, this could not be diminished by addition of unlabelled peptide (data not shown). Recent experiments indicate that nonspecific trapping of the peptide between the two membranes leading to energy transfer, can be decreased by increasing the concentration of FCS. The only exception to the above statements was obtained with the T cell 3DO-18.3. This T cell comes from the same fusion as 3DO-54.8, responds to I-A<sup>d</sup> and ovalbumin, but does not respond to the 17-residue synthetic peptide<sup>16</sup>. This cell mediates some energy transfer between I-A and peptide and there was competition with excess unlabelled peptide.

Our results provide compelling evidence that a specific T-helper cell stabilizes the proximity of peptide antigen and I-A<sup>d</sup> incorporated in a lipid membrane. This result is particularly

significant in that it was obtained under conditions where a physiological response can be demonstrated. The results support theoretical models (see ref. 1 for review) of MHC-restricted recognition of antigen involving a T-cell receptor-mediated association of antigen and class II MHC molecules to within distances of the order of 40 Å. Without a clonotypic antibody against 3DO-54.8 cells we cannot say that the T-cell receptor  $\alpha/\beta$  heterodimer (see ref. 17 for review) is responsible for this effect. In the absence of cells, no interaction between antigen and MHC was detected. Either there is no complex between antigen and MHC in the absence of the specific T cell or the affinity is too low to measure using this approach for this particular antigen/MHC combination.

At present we cannot distinguish whether the observed energy transfer arises from many antigen-MHC associations at relatively large distances (40 Å) where energy transfer is inefficient or whether there are a few associations where the energy transfer is efficient. We anticipate that these and other questions can be answered by extension of the techniques described here.

We thank J. Gariépy and G. Schoolnik for peptide synthesis and P. Marrack and J. Kappler for T cells. This work was supported by NIH grant 5RO1 A113587, Department of Defense equipment grant N00014-84-G-0210 and San Francisco Laser Center grant UC-SC-32072 (H.M.M.); the MRC of Canada and the Alberta Heritage Foundation for Medical Research (T.H.W.); and by the Deutsche Forschungsgemeinschaft (H.E.G.).

Received 28 October 1985; accepted 10 January 1986.

- Schwartz, R. A. *Rev. Immun.* **3**, 237–261 (1985).
- Kappler, J. W., Skidmore, B., White, J. & Marrack, P. *J. exp. Med.* **153**, 1198–1214 (1981).
- Yagüe, J. *et al.* *Cell* **42**, 81–87 (1985).
- Shimonkevitz, R., Colon, S., Kappler, J. W., Marrack, P. & Grey, H. M. *J. immun.* **133**, 2067–2074 (1984).
- Brian, A. A. & McConnell, H. M. *Proc. natn. Acad. Sci. U.S.A.* **81**, 6159–6163 (1984).
- Watts, T. H., Brian, A. A., Kappler, J. W., Marrack, P. & McConnell, H. M. *Proc. natn. Acad. Sci. U.S.A.* **81**, 7564–7568 (1984).
- Watts, T. H., Gariépy, J., Schoolnik, G. & McConnell, H. M. *Proc. natn. Acad. Sci. U.S.A.* **82**, 5480–5484 (1985).
- Titus, J., Haugland, R., Sharrow, S. O. & Segal, D. M. *J. immun. Meth.* **50**, 193–204 (1982).
- Seul, M., Subramanian, S. & McConnell, H. M. *J. phys. Chem.* **89**, 3592–3595 (1985).
- Smith, L. M., Rubenstein, J. L. R., Parce, J. W. & McConnell, H. M. *Biochemistry* **19**, 5907–5911 (1980).
- Weis, R. M., Balakrishnan, K., Smith, B. A. & McConnell, H. M. *J. biol. Chem.* **257**, 6440–6445 (1982).
- Axelrod, D., Burghardt, T. P. & Thompson, N. L. A. *Rev. Biophys. Bioengng* **13**, 247–268 (1984).
- Lakowicz, J. R. *Principles of Fluorescence Spectroscopy*, 303–339 (Plenum, New York, 1985).
- Stryer, L. A. *Rev. Biochem.* **47**, 819–846 (1978).
- Oi, V. T., Jones, P. P., Godding, J. W., Herzenberg, L. A. & Herzenberg, L. A. *Curr. Topics Microbiol. Immun.* **81**, 115–129 (1978).
- Shimonkevitz, R., Kappler, J., Marrack, P. & Grey, H. M. *J. exp. Med.* **158**, 303–316 (1983).
- Haskins, K., Kappler, J. & Marrack, P. A. *Rev. Immun.* **2**, 51–66 (1984).

## Specific interaction between the p53 cellular tumour antigen and major heat shock proteins

Orit Pinhasi-Kimhi\*, Dan Michalovitz\*, Avri Ben-Zeev† & Moshe Oren\*

Departments of Chemical \* Immunology and † Genetics, Weizmann Institute of Science, Rehovot 76100, Israel

The protein p53 is capable of participating in neoplastic transformation<sup>1–3</sup> and can form specific complexes with the large-T antigen of simian virus 40 (SV40)<sup>4–6</sup>. This interaction probably results in the stabilization of p53 (refs 7, 8) and may contribute to SV40-mediated transformation<sup>9,10</sup>. Several non-SV40-transformed cells also exhibit a stabilized p53 which is present in elevated levels<sup>11–13</sup>. Recently, this stabilization was shown to coincide with the ability to precipitate a polypeptide (p68) of relative molecular mass ( $M_r$ ) 68,000–70,000 by anti-p53 monoclonal antibodies<sup>13–15</sup>. We now report that this co-precipitation indeed represents a specific complex between the two proteins; the complex sediments on a sucrose gradient as a relatively broad peak of 10–14S and can be dissociated *in vitro*. Furthermore, p68 is the HSP70 heat shock protein cognate, found in elevated levels in a p53-overproducing cell line. On heat-shock treatment of such overproducers, p53 also forms a complex with the related highly inducible HSP68.

The present studies used clone 6, a cell line derived by co-transformation of rat embryo fibroblasts with murine p53 and activated Ha-ras (D. Eliyahu *et al.*, in preparation). In such cells, p53 is both overproduced and stabilized (D. Eliyahu *et al.*, in preparation). Immunoprecipitation of labelled clone 6 proteins with anti-p53 monoclonal antibodies (Fig. 1a, lane 2) produces a prominent p53 band, along with a co-precipitating band of  $M_r \sim 70,000$ , previously<sup>15</sup> referred to as p68. The precipitation of p68 could be explained in one of the following ways: (1) p68 is an irrelevant protein accidentally sharing an epitope with p53; (2) p68 is a modified more slowly migrating form of p53; (3) p68 forms a specific physical association with p53. In the first case one would not expect p68 to react with two different anti-p53 monoclonal antibodies. However, p68 is brought down by both PAb421<sup>16</sup> and RA3-2C2<sup>17</sup> antibodies, which bind to different domains of the p53 molecule<sup>18,19</sup> (Fig. 1a, lanes 4, 5).

To elucidate the relationship between p53 and p68, a labelled clone 6 extract was denatured before incubation with anti-p53 monoclonal antibodies, to dissociate non-covalent complexes. This totally abolished the immunoprecipitation of p68 while having no effect on the reactivity of p53 (Fig. 1a, lane 3), as expected if p68 forms a physical complex with p53 rather than reacting directly with the monoclonal antibodies. Finally, comparison of the partial proteolytic patterns of p53 and p68<sup>20</sup> showed the patterns to be totally different, demonstrating that these are not closely related polypeptides (data not shown). Hence, the presence of p68 in the immunoprecipitate can be accounted for only if it is in physical association with p53, forming part of an anti-p53 reactive complex.

Figure 1a shows that there seems to be much more p53 than p68 in the precipitate, suggesting that only a minor fraction of p53 is tightly associated with p68. However, when immunoprecipitated proteins were visualized by Coomassie-blue staining (Fig. 1b, lane 1), large quantities of p68 were indeed seen, consistent with the notion that most of the p53 molecules are involved in the interaction.

The finding of a p53-p68 complex raised the possibility that the latter protein is related to the transforming activity of p53. It was therefore of interest to characterize p68, and for this, an immunoprecipitate of clone 6 cells was subjected to two-dimensional electrophoresis. A preliminary experiment (not

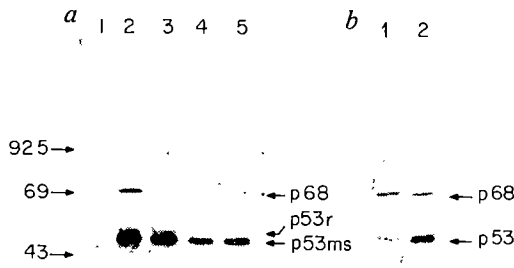


**Fig. 1** Analysis of p53-p68 interaction. *a*, Immunoprecipitation with different antibodies.  $^{35}\text{S}$ -labelled proteins were extracted from cells of clone 6, derived by transformation of rat embryo fibroblasts by p53 plus Ha-ras. Equal amounts of trichloroacetic acid (TCA)-insoluble radioactivity ( $1.4 \times 10^6$  c.p.m.) were reacted with either non-immune serum (lane 1) or anti-p53 monoclonal antibody PAb421 (lane 2). An identical sample was subjected to heat denaturation in reducing conditions<sup>33</sup> and similarly reacted with PAb421 (lane 3). The supernatant (unreacted material) of the immunoprecipitate shown in lane 2 was divided in half and incubated again with either the anti-p53 monoclonal antibody RA3-2C2 (lane 4) or PAb421 (lane 5). The autoradiograms are shown. Numbers on the left denote the sizes and positions of co-electrophoresed  $M_r$  markers. p53ms, mouse p53; p53r, endogenous rat p53. *b*, Comparison of stained and radiolabelled p53 and p68. A radiolabelled extract of clone 6, derived from one-quarter of a 90-mm dish, was reacted with PAb421 and the reacting polypeptides were resolved on a 12.5% SDS-polyacrylamide gel. The Coomassie blue-stained gel section (lane 1) and the autoradiogram of the same section (lane 2) are shown. Autoradiography was performed without prior fluorography.

**Methods.** Clone 6 is a cell line established from a transformed focus generated by co-transformation of rat embryo fibroblasts with activated Ha-ras and the p53-specific plasmid pLTRp53cG (refs 1, 26 and D. Eliyahu *et al.*, in preparation). For the experiment shown in *a*, a confluent 60-mm dish was labelled with 50  $\mu\text{Ci}$   $^{35}\text{S}$ -methionine for 3 h and extracts were prepared and analysed by immunoprecipitation followed by SDS-polyacrylamide gel analysis and autoradiography as previously described<sup>39</sup>. The aliquot analysed in lane 3 was first made 5% in  $\beta$ -mercaptoethanol and 0.5% in SDS, heated to 100 °C for 5 min, cleared at 12,500g for 10 min and the supernatant was taken for immunoprecipitation. For experiment *b*, the material to be analysed was derived from one-quarter of a 90-mm dish, labelled with 50  $\mu\text{Ci}$  of  $^{35}\text{S}$ -methionine for 3 h. Other details were as for *a*.

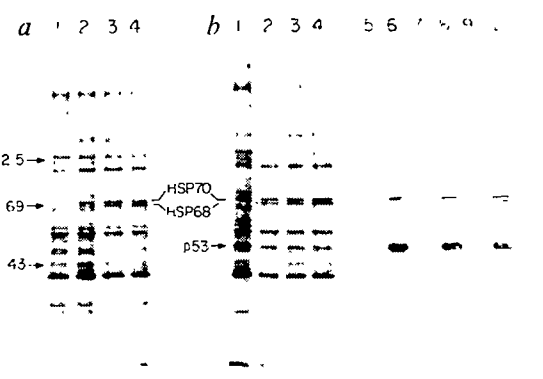
shown) revealed that the position of p68 coincided with that of an abundant cellular polypeptide, migrating similarly to the  $\sim 70,000$ - $M_r$  rodent heat shock proteins (HSPs). Furthermore, at least in one system, two polypeptides of  $M_r \sim 68,000$  and  $\sim 70,000$  co-precipitated with p53<sup>15</sup>, reminiscent of the HSP doublet reported in various mammalian species<sup>21–24</sup>. To determine the relationship between p68 and HSPs, clone 6 cells were subjected to brief periods of hyperthermia<sup>22</sup>, followed by radio-labelling and protein analysis. A similar treatment was performed on Rat-1 established rat fibroblasts<sup>25</sup>, which produce low amounts of p53<sup>26</sup>. As Fig. 2 shows, p68 indeed co-migrated with a major HSP, the semi-inducible HSP70. Moreover, on increased hyperthermia, increasing amounts of a slightly faster-migrating polypeptide became prominent in the immunoprecipitate. This polypeptide co-migrated exactly with the highly inducible HSP68. Both polypeptides were absent from immunoprecipitates of denatured samples (data not shown), indicating that this second protein also complexed with p53. Neither of the two  $\sim 70,000$ - $M_r$  bands was convincingly detectable in immunoprecipitates of heat-shocked Rat-1 cells, although the existence of minute amounts of the complex with p53 could not be excluded (data not shown). To confirm the identity between p68 and HSP70, immunoprecipitates were resolved on two-dimensional gels and compared with total extracts from cells

**Fig. 2** Analysis of p53 co-precipitating proteins following heat shock. Non-transformed Rat-1 cells (*a*) or clone 6 cells (*b*) were subjected to increasing temperatures followed by radiolabelling and extraction. Equal amounts of TCA-insoluble radioactivity (31,000 c.p.m.) were analysed directly by gel electrophoresis (lanes 1-4). Parallel but larger aliquots ( $7.2 \times 10^5$  c.p.m.) were reacted with either non-immune serum (lanes 5, 7, 9, 11) or anti-p53 monoclonal antibody PAb421 (lanes 6, 8, 10, 12). Hyperthermia was performed at the following temperatures: 37 °C (lanes 1, 5, 6), 44 °C (lanes 2, 7, 8), 45 °C (lanes 3, 9, 10) or 46 °C (lanes 4, 11, 12). The positions of the major rat heat-shock proteins HSP70 and HSP68 are indicated.

**Methods.** Subconfluent 60-mm dishes of either Rat-1<sup>25</sup> or clone 6 cells were pre-starved for 45 min in non-radioactive methionine-free medium. For the last 10 min of this period, the dishes were subjected to hyperthermia as described previously<sup>22</sup>. Incubation was then resumed at 37 °C for 4 h in methionine-free medium containing either 30 µCi (37–45 °C dishes) or 60 µCi (46 °C dish) of <sup>35</sup>S-methionine. Extracts were prepared as described previously and small aliquots analysed directly by SDS-polyacrylamide gel electrophoresis. Most of the extracts were used for immunoprecipitation and analysed as for Fig. 1.

either exposed to hyperthermia or kept at 37 °C (Fig. 3). The pertinent heat-shock proteins are most easily identified in total extracts from Rat-1 cells (Fig. 3e, f): HSP70 is easily detectable at 37 °C but is several-fold overproduced at 46 °C, whereas HSP68 is seen only after hyperthermia. On the other hand, clone 6 shows hardly any increase in HSP70 after heat shock (Fig. 2, Fig. 3c, d), while HSP68 displays the same pattern as in Rat-1. Most importantly, comparison of the total cell extracts with the immunoprecipitates reveals that p68 indeed co-migrates precisely with HSP70, while the other polypeptide corresponds to HSP68. This is shown most clearly in Fig. 3g, in which an immunoprecipitate was mixed and co-electrophoresed with a small amount of total cell extract, to allow a better alignment of the co-precipitating polypeptides with the HSPs.

To characterize the complex better, a clone 6 extract was subjected to sucrose gradient sedimentation (Fig. 4). While most cellular proteins were in monomeric form (fractions 20–23), there was hardly any monomeric p53. Rather, p53 was found in oligomers sedimenting as a relatively broad peak of 10–14S, with a small proportion of larger complexes. HSP70 was clearly

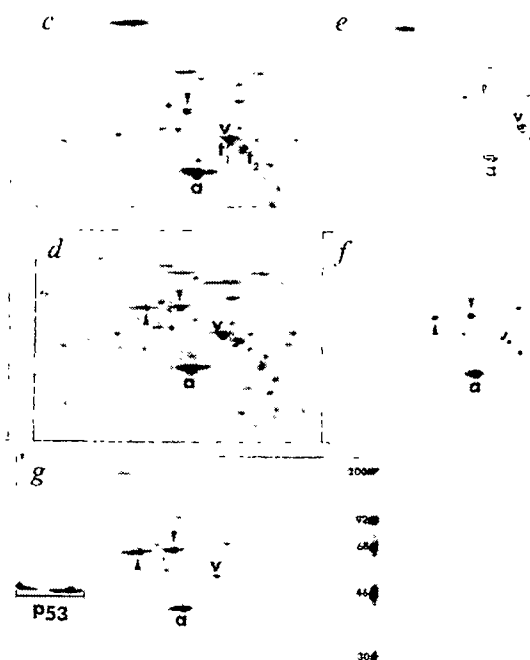


associated with p53 throughout the gradient, and the ratio between the two polypeptides appeared to be constant. Unlike p53, a substantial fraction of HSP70 was in monomers or low- $M_r$  oligomers (Fig. 4b).

In conclusion, p53 can associate specifically with at least two rat HSPs, HSP68 and HSP70. A similar interaction seems to exist in transformed mouse cells that overproduce p53 because of a naturally occurring event rather than to *in vitro* transfection<sup>13,14</sup>. It is therefore plausible that this complex is of physiological importance and may even be related to the transformation process.

One obvious concern is that the p53-HSP70 complex may be an extraction artefact. Although this is hard to disprove, the inability to detect a comparable complex in heat-shocked Rat-1 cells (data not shown) strongly militates against it. Interestingly, a specific association has also been shown between another heat shock protein, HSP90, and pp60<sup>32C</sup> (ref. 27). It is tempting to speculate that this is not mere coincidence, but rather may reflect a more general involvement of HSPs in the regulation of cell proliferation.

**Fig. 3** Two-dimensional polyacrylamide gel comparison of heat shock proteins and p53-co-precipitating polypeptides. Clone 6 and Rat-1 cells were either maintained at 37 °C (*a*, *c*, *e*) or exposed to 46 °C for 10 min (*b*, *d*, *f*, *g*). Clone 6 lysates containing equal amounts of acid-insoluble radioactivity ( $2 \times 10^6$  c.p.m.) were immunoprecipitated with monoclonal antibody PAb421 and analysed by two-dimensional gel electrophoresis (*a*, *b*). Aliquots of the radiolabelled total cell extracts ( $3.7 \times 10^5$  c.p.m.) were also taken directly for a similar analysis. *c*-Clone 6, 37 °C; *d*, clone 6, 46 °C; *e*, Rat-1, 37 °C; *f*, Rat-1, 46 °C; *g*, a mixture of an immunoprecipitate identical to that in *b* with an aliquot of unprocessed clone 6, 46 °C lysate (similar to that shown in *d* but representing only 35,000 acid-insoluble c.p.m.). Upward-pointing arrow, HSP68; downward-pointing arrow, HSP70; *a*, actin; *t<sub>1</sub>*, α-tubulin; *t<sub>2</sub>*, β-tubulin; *v*, vimentin. Direction of migration in the first dimension (isoelectric focusing) was from left to right. Numbers on the right of *g* indicate the positions and sizes ( $\times 10^{-3}$ ) of co-electrophoresed protein  $M_r$  markers. **Methods.** Cells were labelled and processed as described in Fig. 2 legend. Samples to be analysed were made 9.5 M in urea and 2% in β-mercaptoethanol and subjected to two-dimensional gel electrophoresis according to O'Farrell *et al.*<sup>36</sup>. The first dimension used isoelectrofocusing in the presence of 2% ampholites (1.6% pH 5.0–7.0, 0.4% pH 3.5–10.0). The second dimension was an 8% SDS-polyacrylamide gel.



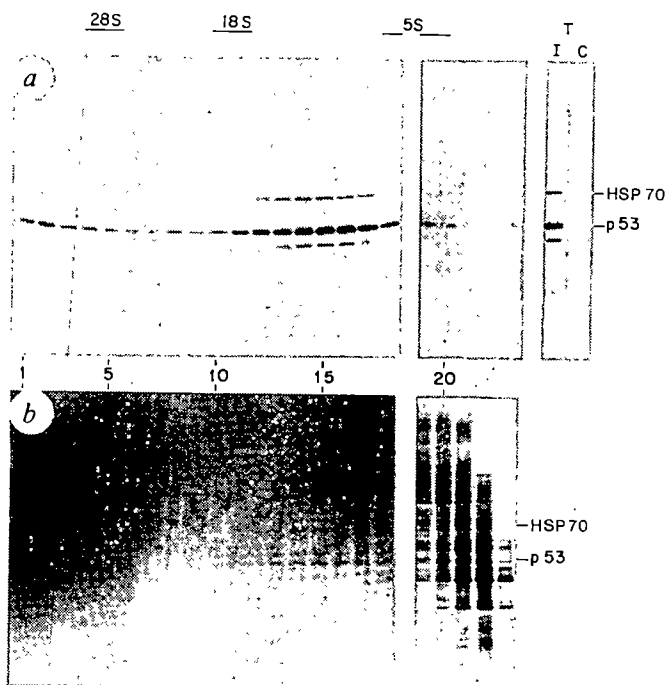


**Fig. 4** Co-sedimentation of p53 and HSP70 on a sucrose gradient. A labelled cellular extract was fractionated on a sucrose gradient and each fraction was assayed for the presence of p53 and co-precipitating HSP70. *a*, Polypeptides immunoprecipitated with an anti-p53 monoclonal antibody. Fraction numbers are shown at the bottom; the positions of ribosomal RNA markers, sedimented in a parallel tube, are shown on top. T represents the proteins precipitated from an aliquot of the total (unfractionated) extract by either control (C) or anti-p53 monoclonal antibodies (I). *b*, Electrophoretic pattern of aliquots of each fraction subjected directly to gel analysis. The identification of HSP70 and p53 is tentative. Note that fractions 19–23 were electrophoresed on a separate gel and that the migration distances of individual polypeptides differed slightly between the two gels; we attempted to align the gels at the tentative position of the p53 band. The bands migrating ahead of p53 probably represent proteolytic cleavage products of this protein, present in variable quantities in different experiments and generated at least in part during the immunoprecipitation process<sup>37</sup>. **Methods.** A 60-mm dish of clone 6 cells was labelled at 37 °C with 200 μCi <sup>35</sup>S-methionine for 4 h, extracted (see Fig. 1 legend) and sedimented through a 4.7-ml 5–20% (w/v) sucrose gradient containing 0.14 M NaCl, 10 mM Tris-Cl pH 8, 10 mM dithiothreitol, 1% aprotinin and 300 μg ml<sup>-1</sup> phenylmethylsulphonyl fluoride, including a 0.4-ml 60% sucrose pad. Sedimentation was in a Beckman SW 50.1 rotor at 48,000 r.p.m. for 3 h at 4 °C. Fractions (0.21 ml, 23 fractions per gradient) were collected from the bottom of the tube following puncturing with a needle. Fraction 1 represents the fastest-sedimenting material. Aliquots (10 μl) were mixed with sample buffer and directly analysed on a 12.5% SDS-polyacrylamide gel (*b*). The rest of the material underwent immunoprecipitation with monoclonal antibody PAb421 and was analysed similarly (*b*). Rat rRNA was sedimented through a parallel gradient and the positions of the respective size species determined using a spectrophotometer and confirmed by electrophoresis on a formaldehyde-agarose gel. Autoradiographic exposure time for both *a* and *b* was 1.5 h.

We have been unable to detect similar complexes convincingly in normal cells. In heat-induced cells both these HSPs are predominantly nuclear<sup>28,29</sup>. If a nuclear site is necessary for the specific association, the apparent absence of p53 from nuclei of normal cells<sup>30</sup> may account for the inability of a complex to form. The nuclear accumulation of p53 in a variety of transformed cells<sup>30</sup> may thus lead to complex formation. Alternatively, the association between p53 and HSP70 may be a normal process, except that in such conditions the complex is very unstable and accumulates only in abnormal situations. Such abnormal conditions might simply be the overproduction of

p53, or structural changes in either HSP70 or p53 resulting in a more stable complex. The latter may pertain to Meth A cells, which contain strongly elevated p53 levels while possessing only twice the amount of the corresponding messenger RNA<sup>12</sup>. Such cells exhibit a p53-HSP70 complex<sup>13,15</sup>, and a relatively stable p53<sup>12,13</sup>, and indeed seem to carry a mutated p53 gene encoding an altered protein product<sup>38</sup>. It is not known whether this mutant p53 has a higher affinity for HSP70.

Stabilization of p53 in transformed cells may involve complex formation with HSP70, although it is equally conceivable that accumulation of the complex may in fact be a consequence of the stabilization. In this respect, the SV40 large-T antigen could be mimicking the action of a normal cellular protein, HSP70. This is also suggested by studies using the expression of mouse p53 in SV40-transformed monkey COS cells<sup>15</sup>, where anti-p53 monoclonal antibodies brought down both complexed large-T antigen and a ~70,000-M<sub>r</sub> doublet, presumably HSP68 and HSP70. However, antibodies to SV40 large-T antigen efficiently co-precipitated only p53, with very little evidence for HSPs, suggesting that HSP70 and large-T antigen may be competing for the same or very close sites on the p53 molecule. Other similarities exist between HSP70 and the SV40 large-T antigen. Aside from having a nuclear affinity<sup>28,29,31</sup>, both proteins are able to bind ATP<sup>24,31</sup>. The SV40 large-T antigen possesses ATPase activity<sup>31</sup>, and although no activity has been demonstrated for HSP70<sup>24</sup>, it is exhibited by the structurally related *Escherichia coli* DNA K protein<sup>32,33</sup>. Interestingly, this bacterial protein is involved in the replication of bacteriophage DNA<sup>33</sup>, as is large-T antigen in the replication of SV40<sup>31</sup>. Finally, clone 6 possesses a markedly elevated level of HSP70 without heat induction. The relationship between this apparent overproduction of HSP70 and the specific oncogenes activated in clone 6 remains unknown.

The data presented here raise the possibility that HSP70 is involved in cell proliferation, which is in keeping with the apparent cell-cycle-dependent expression of the human *hsp70* gene(s)<sup>34</sup>. However, the significance of these findings can only be assessed when more is known about the molecular functions of HSP70.

We thank M. Tainovich for technical assistance and Drs O. Bensaude and B. Geiger for stimulating discussions. This work was supported by USPHS grant R01 CA 40099-01 from the National Cancer Institute, DHHS, and by a grant from the USA-Israel Binational Science Foundation. M.O. is a Scholar of the Leukemia Society of America, Inc.

Received 14 November 1985; accepted 13 January 1986.

1. Eliyahu, D., Raz, A., Gruss, P., Givol, D. & Oren, M. *Nature* **312**, 646–649 (1984).
2. Parada, L. F., Land, H., Weinberg, R. A., Wolf, D. & Rotter, V. *Nature* **312**, 649–651 (1984).
3. Jenkins, J. R., Rudge, K. & Currie, G. A. *Nature* **312**, 651–654 (1984).
4. Crawford, L. V. *et al.* *Cold Spring Harb. Symp. quant. Biol.* **44**, 179–187 (1980).
5. McCormick, F. & Harlow, E. *J. Virol.* **34**, 213–224 (1980).
6. Lane, D. P., Gannon, J. & Winchester, G. *Adv. viral Oncol.* **2**, 23–39 (1982).
7. Oren, M., Maltzman, W. & Levine, A. J. *Molec. cell. Biol.* **1**, 101–110 (1981).
8. Mora, P. T., Chandrasekaran, K., Hoffman, J. C. & McFarland, V. W. *Molec. cell. Biol.* **2**, 763–771 (1982).
9. May, E., Lasne, C., Prives, C., Borde, J. & May, P. J. *Virol.* **45**, 901–913 (1983).
10. Montenarh, M., Kohler, M., Aggeler, G. & Henning, R. *EMBO J.* (in the press).
11. Oren, M., Reich, N. C. & Levine, A. J. *Molec. cell. Biol.* **2**, 443–449 (1982).
12. Reich, N. C., Oren, M. & Levine, A. J. *Molec. cell. Biol.* **3**, 2143–2150 (1983).
13. Gronostajski, R. M., Goldberg, A. L. & Pardee, A. B. *Molec. cell. Biol.* **4**, 442–448 (1984).
14. Ruscetti, S. K. & Scolnick, E. M. *J. Virol.* **46**, 1022–1026 (1983).
15. Pinhasi, O. & Oren, M. *Molec. cell. Biol.* **4**, 2180–2186 (1984).
16. Harlow, E., Crawford, L. V., Pin, D. C. & Williamson, N. M. *J. Virol.* **39**, 861–869 (1981).
17. Rotter, V., Witte, O. N., Coffman, R. & Baltimore, D. *J. Virol.* **36**, 547–555 (1980).
18. Crawford, L. V. *Adv. viral Oncol.* **2**, 3–21 (1982).
19. Rotter, V., Friedman, H., Katz, A., Zervitz, K. & Wolf, D. *J. Immun.* **131**, 329–333 (1983).
20. Cleveland, D., Fisher, S., Kirshner, M. & Laemmli, U. K. *J. biol. Chem.* **252**, 1102–1106 (1977).
21. Bensaude, O. & Morange, M. *EMBO J.* **2**, 173–177 (1983).
22. Morange, M., Diu, A., Bensaude, O. & Babinet, C. *Molec. cell. Biol.* **4**, 730–735 (1984).
23. Lowe, D. G. & Moran, L. A. *Proc. natn. Acad. Sci. U.S.A.* **81**, 2317–2321 (1984).
24. Welch, W. J. & Feramisco, J. R. *Molec. cell. Biol.* **5**, 1929–1937 (1985).
25. Steinberg, B., Pollack, R., Topp, W. & Botchan, M. *Cell* **13**, 19–32 (1978).
26. Eliyahu, D., Michaelovitz, D. & Oren, M. *Nature* **316**, 158–160 (1985).
27. Opperman, H., Levinson, W. & Bishop, J. M. *Proc. natn. Acad. Sci. U.S.A.* **78**, 1067–1071 (1981).
28. Welch, W. J. & Feramisco, J. R. *J. biol. Chem.* **259**, 4501–4513 (1984).
29. Velasquez, J. M. & Lindquist, S. *Cell* **36**, 655–662 (1984).
30. Rotter, V., Abutbul, H. & Ben-Ze'ev, A. *EMBO J.* **2**, 1041–1047 (1983).

31. Tooze, J. (ed.) *DNA Tumor Viruses Pt 2* (Cold Spring Harbor Laboratory, New York, 1982).  
 32. Bardwell, J. C. A. & Craig, E. *Proc. natn. Acad. Sci. U.S.A.* **81**, 848–852 (1984).  
 33. Zylizc, M. & Georgopoulos, C. P. *J. biol. Chem.* **259**, 8820–8825 (1984).  
 34. Kao, H. T., Capassa, D., Heintz, N. & Nevins, J. R. *Molec. cell. Biol.* **5**, 628–633 (1985).  
 35. Curran, T., Van Beveren, C., Ling, N. & Verma, I. M. *Molec. cell. Biol.* **5**, 167–172 (1985).  
 36. O'Farrell, P. Z., Goodman, H. M. & O'Farrell, P. H. *Cell* **12**, 1133–1142 (1977).  
 37. Oren, M. & Levine, A. J. *Proc. natn. Acad. Sci. U.S.A.* **80**, 56–59 (1983).  
 38. Blen, B., Zakut-Houri, R., Givoli, D. & Oren, M. *EMBO J.* **3**, 2179–2184 (1984).  
 39. Mattzman, W., Oren, M. & Levine, A. J. *Virology* **112**, 145–156 (1981).

## Product of *per* locus of *Drosophila* shares homology with proteoglycans

F. Rob Jackson\*, Thaddeus A. Bargiello,  
 Suk-Hyeon Yun & Michael W. Young†

The Rockefeller University, 1230 York Avenue, New York,  
 New York 10021, USA

Genes controlling biological rhythms have been identified in *Drosophila*<sup>1,2</sup>. The best characterized of these genes is called *period* (*per*). Although wild-type flies have daily (circadian) rhythms with a periodicity of ~24 h, *per*<sup>s</sup> and *per*<sup>l</sup> mutants have 19-h and 29-h rhythms, respectively, and *per*<sup>0</sup> mutants are arrhythmic<sup>1</sup>. The *per*<sup>s</sup> mutation also enhances the sensitivity of the circadian clock to resetting by light stimuli<sup>3</sup>, and all three types of *per* mutations affect a much shorter period ultradian rhythm, the 55-s rhythm of the *Drosophila* courtship song<sup>4</sup>. A fragment of DNA of ~7 kilobases (kb) encoding a 4.5-kb poly(A)<sup>+</sup> RNA restores rhythmicity when transduced into *Drosophila* carrying mutations<sup>5,6</sup> or chromosomal deletions<sup>5</sup> of the *per* locus. Here we report the sequence of this biologically active segment of DNA. The transcription unit that encodes the 4.5-kb RNA has been mapped, permitting a conceptual translation of a protein of 1,127 amino acids. Several abnormal phenotypes characterized by long-period rhythms are associated with changes in the sequence of untranslated portions of the transcription unit. The structure of some segments of the predicted protein suggests that it is a proteoglycan.

The structure of the 4.5-kb transcript was analysed by ribonuclease mapping of a series of RNA/RNA heteroduplexes. For each experiment, RNA complementary to a predetermined region of the 4.5-kb transcript was synthesized *in vitro* from a corresponding DNA segment of known sequence, cloned in pSP64 or pSP65 (ref. 7). Heteroduplexes were digested with RNase T<sub>2</sub> or a combination of RNase T<sub>1</sub> and RNase A, and resistant material was denatured and size-separated on acrylamide sequencing gels. Figure 1 shows the structures of most of the synthetic RNAs used to map the 4.5-kb transcript. Figure 2a–d shows the results of several of the mapping experiments.

To confirm the proposed structure of the 5' RNA coding region, two primer extension experiments were performed. The sequences of the two chemically synthesized primers, P1 and P2, are shown in Fig. 1. P1 corresponds to a DNA sequence that begins in RNA coding region 1, 81 base pairs (bp) from the putative 5' terminus, and P2 includes a sequence that starts in coding region 1, 167 bp from this expected terminus. Both primer extension experiments map the 5' end of the transcription unit to position 179 of Fig. 1. The result of the P1 primer extension experiment is shown in Fig. 2e.

Complementary DNA clones were produced by oligo(dT) priming of total adult poly(A)<sup>+</sup> RNA as described in Fig. 3 legend. A 1.7-kb cDNA chosen for sequence analysis includes a poly(A) segment at its 3' terminus, allowing the 3' end of the transcription unit and a polyadenylation signal (position 7,370) to be identified (see Fig. 3, and legend). The cDNA contains most of coding region 5, beginning at position 5,524 of Fig. 3, and all of coding regions 6–8, as indicated at the top of Fig. 1.

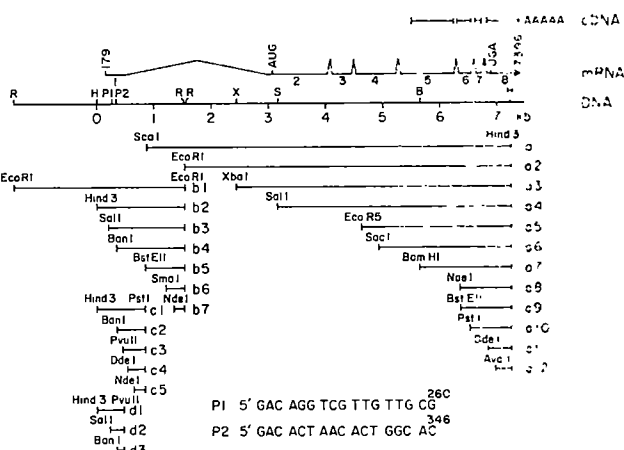


Fig. 1 Transcription map of the *per* locus. The structures of the restriction fragments cloned in pSP64 or pSP65 Riboprobe vectors (Promega Biotech) are indicated in the bottom half of the figure. For each fragment, <sup>32</sup>P-labelled, single-stranded RNA was synthesized from plasmid DNA after digestion with the restriction enzyme used to form the left end of each region depicted. Synthetic RNAs a1–12 extend leftward from a *Hind*III site, while b1–7, c1–5 and d1–3 extend leftward from *Eco*RI, *Pst*I and *Pvu*II sites, respectively. P1 and P2 represent the sequences and locations on the transcription unit of two primers used to map the transcription start site. The positions of transcription initiation (179) and termination (7,396) and of translation initiation (AUG) and termination (UGA) are indicated. For the restriction map in the centre of the figure, H = *Hind*III, R = *Eco*RI, X = *Xba*I, S = *Sal*I and B = *Bam*HI.

A comparison of this cDNA sequence with that of cloned genomic *per* DNA (presented below) has allowed us to locate several splice junctions, all of which agree with those established by ribonuclease mapping experiments. The cDNA sequence contains a single open reading frame that encodes 391 amino acids.

Figure 3 shows the DNA sequence of the interval containing the transcription unit that encodes the 4.5-kb *per* RNA. The length of the transcription unit is 7.217 kb. Also shown in Fig. 3 are the boundaries of the eight RNA coding regions which form the 4.5-kb messenger RNA. For those coding regions located only by ribonuclease mapping, splice junctions are predicted according to the consensus sequence rules of Mount<sup>8</sup>. The predicted size of the mRNA encoded by this transcription unit (minus a poly(A) tail) is 4.290 kb; this is in good agreement with a size of 4.5 kb determined previously by comparison with DNA and RNA size standards after electrophoresis of poly(A)<sup>+</sup> RNA on formaldehyde/agarose gels<sup>9,10</sup>.

Figure 3 shows a conceptual translation of the spliced mRNA. Accordingly, RNA coding region 1 is not translatable. Translation is initiated near the beginning of RNA coding region 2, 2.909 kb from the beginning of the transcription unit (position 3,088; see also map in Fig. 1). All open reading frames are blocked upstream of this position. Translation could be initiated at the methionine codon at position 3,050 but a protein beginning at this position would be terminated 39 bp downstream (position 3,089). Translation of the predicted *per* protein terminates near the beginning of coding region 8 (position 6,891), so that 505 untranslated bases are found at the 3' end of the mRNA. The predicted *per* protein contains 1,127 amino acids.

A sequence analysis of the *per* locus allows a better understanding of a number of irregular clock phenotypes. A transcription study has been reported previously for several *per* locus mutations<sup>9,10</sup>. Among these was a mutation associated with a chromosome translocation, *T(1;4)JC43*. Flies carrying this mutation have long-period rhythms (35 h), or can be arrhythmic<sup>11,12</sup>. The 4.5-kb *per* transcript is absent in *T(1;4)JC43* flies, but a new transcript, of 11.5 kb, is synthesized in its place<sup>9,10</sup>. Previous studies mapped the breakpoint of the translocation to

\* Present address: Worcester Foundation for Experimental Biology, 222 Maple Avenue, Shrewsbury, Massachusetts 01545, USA.

† To whom reprint requests should be addressed.

**Fig. 2** Mapping of *per* RNA coding regions. Labels at tops of panels *a-d* refer to transcribed segments depicted in Fig. 1.  $^{32}\text{P}$ -labelled synthetic RNAs were transcribed from regions of cloned *per* DNA as described in Fig. 1 legend, then hybridized to 5–10  $\mu\text{g}$  of total poly(A)<sup>+</sup> RNA from Oregon R adults at 45 °C for 8–12 h (56 °C for a1–12), and heteroduplexes were digested with ribonucleases (RNase T<sub>2</sub>, 50–100 U ml<sup>-1</sup> or RNase A and T<sub>1</sub>, 100  $\mu\text{g}$  ml<sup>-1</sup> and 10 U ml<sup>-1</sup>) at 37 °C for 1 h. Protected fragments were denatured in formamide and separated on acrylamide gels as indicated in the text. Numbers indicate sizes (in kb) of ribonuclease-resistant RNA measured against single-stranded RNAs of known length transcribed from Riboprobe vectors. Superscripts to these numbers in *a* indicate the RNA coding region. Three fragments, of 0.32, 0.18 and 0.11 kb, are protected with synthetic RNAs b1 and c1 (*d*, lane 3 shows the results with c1); this seems to indicate that three RNA coding regions map to this interval. The two smaller fragments must

be generated by secondary ribonuclease cleavage of the 0.32-kb fragment. RNA d1 (*d*, lane 2) protects all of the 0.11-kb region, but only part of the 0.32-kb region (0.30 kb) and part of the 0.18-kb region (0.16 kb). As both of the latter two regions are reduced to the same extent, they must end at the same position, about 20 bp to the right of the *Pvu*II site used to construct d1. This experiment also indicates that the 0.18-kb region is co-extensive with the right half of the 0.32-kb region. The 5' end of the 0.32-kb coding region must lie 0.30 kb to the left of the *Pvu*II site. RNA d2 protects most (0.085 kb) of the 0.11-kb region. The 5' end of the region, which is not protected, is therefore located ~25 bp to the left of a *Sal*I site used to form RNA d2; this is 0.30 kb to the left of the *Pvu*II site used to map the boundaries of the 0.32-kb coding region above. As the 5' end of the 0.32-kb coding region is also 0.30 kb to the left of this *Pvu*II site, both regions begin at the same position and are co-extensive for 0.11 kb. The site of secondary cleavage proposed for the 0.32-kb coding region is composed of 18 consecutive A-T base pairs (see also Fig. 3). This sequence probably forms a hypersensitive substrate for the ribonucleases used in this mapping procedure. For *e*, <sup>32</sup>P-end-labelled primers (1-5 ng) were hybridized with total poly(A)<sup>+</sup> RNA (10 µg) for 2-4 h at 42 °C and extended for 1 h with avian myeloblastosis virus (AMV) reverse transcriptase (50 U; BRL). DNA sequence ladders were produced by hybridizing the primers to cloned *per* DNA, followed by primer extension according to the dideoxy sequencing method<sup>24,25</sup>.

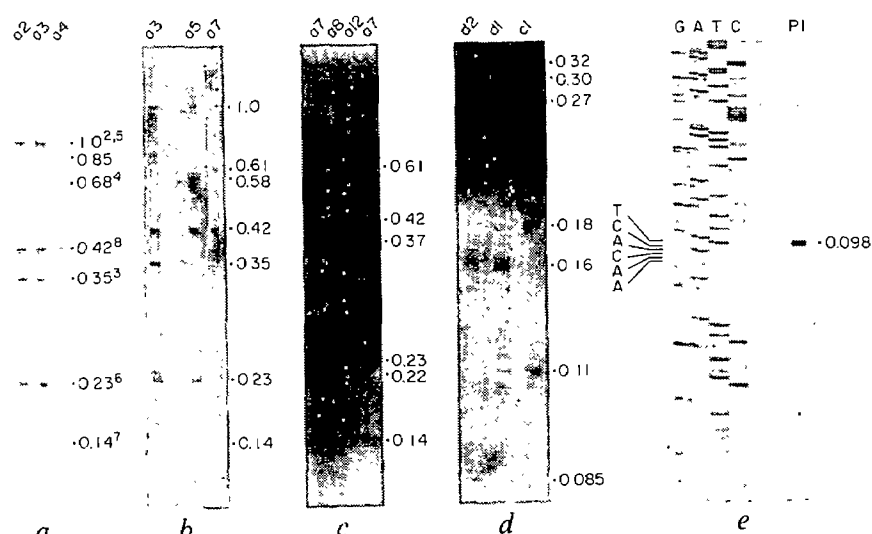
a *Bgl*II/*Hind*III fragment<sup>9</sup>. A sequence analysis of the gene now allows the boundaries of the affected restriction fragment to be mapped to positions 7,217 and 7,234 respectively; this places the breakpoint of the translocation within the 3'-untranslated region of the transcription unit. Approximately 0.17 kb of the 4.5-kb mRNA has been exchanged, because of the translocation, for about 7 kb of RNA transcribed from chromosome 4 sequences. Ribonuclease mapping experiments have shown that sequences upstream of this breakpoint are spliced in the same way as wild-type 4.5-kb RNA (T.A.B., unpublished results). Presumably, *T(1;4)JC43* flies can still produce biological rhythms because a full-length *per* protein can be translated from the 11.5-kb fusion transcript.

Long-period rhythms are also generated by some transformed flies<sup>5,6</sup>. In one study an attempt was made to construct transformants with a complete *per* transcription unit<sup>5</sup>. It is now apparent that these flies received DNA lacking 157 bp of the 3'-untranslated region. A 4.5-kb RNA is still produced by these long-period transformants, but at levels much lower than those found in wild-type flies<sup>5</sup>. The transcripts must terminate in vector sequences used to generate the transforming DNA.

In a second transformation study<sup>6</sup>, long-period rhythms were produced in flies transformed with DNA lacking sequences at the 5' end of the *per* transcription unit. From the sequence data presented here, these flies must lack the 5'-untranslated RNA coding region, but still retain all of the protein-coding sequence. Thus, if transcripts are produced by this DNA, a wild-type *per* protein would still be the expected translation product.

Thus, several long-period phenotypes can be associated with changes in the *per* transcription unit. In each case the change in DNA sequence fails to affect the structure of the *per* protein. Therefore, these long-period rhythms are probably generated by altered regulation of *per* protein synthesis.

Nearly half of the predicted *per* protein (47%) is composed of the five amino acids serine, threonine, glycine, alanine and proline, and these often form simple sequence tracts. For example, polyalanine and polyglycine tracts up to 17 residues long are found at positions 160, 801, 909 and 938. Given this



predominance of a small group of uncharged polar and nonpolar amino acids, the procedures of Kyte and Doolittle<sup>13</sup> and Eisenberg *et al.*<sup>14</sup> were used to perform a hydropathicity analysis of the protein. The protein contains no clearly hydrophobic regions, rather most protein segments have hydrophobicities and hydrophobic moment values that are characteristic of soluble proteins<sup>14</sup>.

The predicted *per* protein includes a potential site for phosphorylation by cyclic AMP-dependent protein kinase. This amino-acid sequence (Lys-His-Arg-Lys-Leu-Lys-Ser-Met) occurs near the carboxy terminus (residues 1,099-1,106) and resembles the phosphorylatable site in troponin I from rat skeletal muscle<sup>15</sup>. A synthetic peptide containing this sequence has been produced, and it appears to be an efficient substrate for phosphorylation *in vitro* (G. P. Gasic, unpublished). Various chemical agents commonly used to alter cyclic nucleotide levels induce a phase shift in circadian clocks<sup>16,17</sup>. Thus, agents that affect cyclic nucleotide levels could alter the phosphorylation of a *per* protein.

The predicted *per* protein sequence has been compared with all sequences currently available in the Dayhoff and Doolittle protein sequence libraries. Using the FASTP computer program and the algorithm of Lipman and Pearson<sup>18</sup>, we detected extensive regions of homology to the core protein of a rat chondroitin sulphate proteoglycan. The bases for these homologies are the alternating Ser-Gly and Thr-Gly repeats of the *per* protein (residues 592-670). DNAs homologous to these unusual protein-coding segments have been found in vertebrates<sup>19</sup>. The protein core of the homologous chondroitin sulphate proteoglycan, which is 104 amino acids long, contains 49 strictly alternating Ser-Gly residues. This repetitive amino-acid sequence forms a substrate for the extensive glycosylation of the core protein<sup>20</sup>. A partial analysis of the glycosylated region of a second proteoglycan, a rat heparin proteoglycan, has shown that it, too, is composed of only serine and glycine residues, many or all of which must form an alternating repeat<sup>21</sup>. Synthetic peptides containing alternating Ser-Gly residues behave as substrates for glycosyl transferases *in vitro*<sup>22</sup>.

**Fig. 3 Sequence of genomic *per* DNA.** The DNA sequence begins at coordinate 0 of the Fig. 1 map (a *Hind*III recognition sequence), and ends 91 bp downstream of the site of poly(A) addition, at coordinate 7,396. mRNA coding regions are indicated by upper case letters; intervening sequences, and 5' and 3' non-transcribed DNA, are indicated by lower case letters. A conceptual translation of the *per* protein is given above the DNA sequence, with gaps in the amino-acid sequence corresponding to the locations of intervening sequences. (The complete sequence of intervening sequence 1 is available from the authors on request.) Methods. Genomic DNA fragments were sequenced using the dideoxy method<sup>24,25</sup>. Fragments suitable for shotgun sequencing were generated by digesting Canton S, *per* locus DNA with one of four restriction enzymes, each of which cleaves a 4-bp recognition sequence (*Sau*3A, *Alu*I, *Fnu*DII and *Rsa*I). These smaller fragments were randomly subcloned in M13 (mp18 or mp19), and the database of sequences obtained was assembled into longer contiguous DNA sequences using the programs of Staden<sup>26</sup>. Gaps in the complete sequence of the genomic DNA were resolved by cloning selected subregions and generating ordered sets of overlapping deletions according to the method of Dale *et al.*<sup>27</sup>. 27 kb of DNA was sequenced to generate the complete sequence for both strands of *per*. Thus, each base was read twice on average. cDNA libraries were constructed from 1-2 µg of poly(A)<sup>+</sup> RNA isolated from adult Canton S *Drosophila melanogaster*. RNA was annealed to oligo(dT) primers which were elongated with AMV reverse transcriptase. Second-strand synthesis was done using the Klenow fragment of *Escherichia coli* DNA polymerase. The product was digested with S<sub>1</sub> nuclease, ends were repaired with DNA polymerase, and DNA was modified with *Eco*RI methylase. Synthetic *Eco*RI linkers were ligated, cut with *Eco*RI, and DNA fragments were size-selected on Bio-Gel A15 (Bio-Rad). DNA was cloned in λgt10. The *Eco*RI fragment from one *per*-homologous clone was ligated to M13mp18. Processive deletions were produced<sup>27</sup>, and the complete DNA sequence was obtained by conventional methods<sup>24,25</sup>.

Whereas serines are glycosylated in the Ser-Gly repeats of the two naturally occurring proteoglycans described above, threonine is glycosylated in other proteoglycans that are only just beginning to be characterized<sup>23</sup>. The modification of proteoglycans containing Ser-Gly repeats occurs through an *O*-glycosylation of serine. Aside from serine, only threonine can be modified in this way<sup>23</sup>. Thus, both of the unusual Ser-Gly and Thr-Gly repeat tracts in the *per* protein might serve as sites for glycosylation.

Although relatively little is known about the function of proteoglycans, their distribution has been well studied; they are found in extracellular locations or in association with cell surfaces. Given the similarities between *per* protein and known proteoglycans, this is where we would expect to find this clock protein and perhaps other components of the biological clock that it controls.

We thank Laurel Eckhardt, Simon Kidd, Peter Model and Norton D. Zinder for comments on the manuscript, and Peter Model for providing the synthetic oligonucleotide primers. This work was supported by grants to M.W.Y. from the NIH and the Andre and Bella Meyer Foundation.

Received 7 November; accepted 30 December 1985.

1. Konopka, R. J. & Benzer, S. *Proc. natn. Acad. Sci. U.S.A.* **68**, 2112–2116 (1971).

2. Jackson, F. R. *J. Neurogenet.* **1**, 3–15 (1983).
3. Konopka, R. J. *Fedn Proc.* **38**, 2602–2605 (1979).
4. Kyriacou, C. P. & Hall, J. C. *Proc. natn. Acad. Sci. U.S.A.* **77**, 6729–6733 (1980).
5. Bargiello, T. A., Jackson, F. R. & Young, M. W. *Nature* **312**, 752–754 (1984).
6. Zehring, W. A. *et al.* *Cell* **39**, 369–376 (1984).
7. Melton, D. A. *et al.* *Nucleic Acids Res.* **12**, 7035–7056 (1984).
8. Mount, S. M. *Nucleic Acids Res.* **10**, 459–472 (1982).
9. Bargiello, T. A. & Young, M. W. *Proc. natn. Acad. Sci. U.S.A.* **81**, 2142–2146 (1984).
10. Reddy, P. *et al.* *Cell* **38**, 701–710 (1984).
11. Young, M. W. & Judd, B. H. *Genetics* **88**, 723–742 (1978).
12. Smith, R. F. & Konopka, R. J. *Molec. gen. Genet.* **183**, 243–251 (1981).
13. Kyte, J. & Doolittle, R. F. *J. molec. Biol.* **157**, 105–132 (1982).
14. Eisenberg, D., Schwarz, E., Komaromy, M. & Wall, R. J. *molec. Biol.* **179**, 125–142 (1984).
15. Bramson, H. N., Kaiser, E. T. & Mildvan, A. S. *CRC Crit. Rev. Biochem.* **15** (No. 2), 93–124 (1984).
16. Eskin, A., Corrent, G., Lin, C.-Y. & McAdoo, D. J. *Proc. natn. Acad. Sci. U.S.A.* **79**, 660–664 (1982).
17. Eskin, A. & Takahashi, J. S. *Science* **220**, 82–84 (1983).
18. Lipman, D. J. & Pearson, W. R. *Science* **227**, 1435–1441 (1985).
19. Shin, H. S., Bargiello, T. A., Clark, B. T., Jackson, F. R. & Young, M. W. *Nature* **317**, 445–448 (1985).
20. Bourdon, M. A., Oldberg, A., Pierschbacher, M. & Ruoslahti, E. *Proc. natn. Acad. Sci. U.S.A.* **82**, 1321–1325 (1985).
21. Robinson, H. M., Horner, K. A., Hook, M., Ogren, S. & Lindahl, U. *J. biol. Chem.* **253**, 6687–6693 (1978).
22. Coudron, C., Loerner, T., Jacobson, I., Roden, L. & Schwartz, N. B. *Fedn Proc. Abstr.* **39**, 1671 (1980).
23. Kornfeld, R. & Kornfeld, S. in *The Biochemistry of Glycoproteins and Proteoglycans* (ed. Lennarz, W. J.) 1–34 (Plenum, New York, 1980).
24. Sanger, F., Nicklen, S. & Coulson, A. R. *Proc. natn. Acad. Sci. U.S.A.* **74**, 5463–5467 (1977).
25. Biggin, M. D., Gibson, T. J. & Hong, G. F. *Proc. natn. Acad. Sci. U.S.A.* **80**, 3963–3965 (1983).
26. Staden, R. *Nucleic Acids Res.* **10**, 4731–4751 (1982).
27. Dale, R. M. K., McClure, B. A. & Houchins, J. P. *Plasmid* **13**, 31–40 (1985).

## Existence of distinct sodium channel messenger RNAs in rat brain

Masaharu Noda, Takayuki Ikeda, Toshiaki Kayano, Harukazu Suzuki, Hiroshi Takeshima, Mika Kurasaki, Hideo Takahashi & Shosaku Numa

Departments of Medical Chemistry and Molecular Genetics, Kyoto University Faculty of Medicine, Kyoto 606, Japan

The sodium channel is a voltage-gated ionic channel essential for the generation of action potentials<sup>1–3</sup>. It has been reported that the sodium channels purified from the electric organ of *Electrophorus electricus* (electric eel)<sup>4,5</sup> and from chick cardiac muscle<sup>6</sup> consist of a single polypeptide of relative molecular mass ( $M_r$ ) ~260,000 (260K), whereas those purified from rat brain<sup>7</sup> and skeletal muscle<sup>8</sup> contain, in addition to the large polypeptide, two or three smaller polypeptides of  $M_r$  37–45K. Recently, we have elucidated the primary structure of the *Electrophorus* sodium channel by cloning and sequencing the DNA complementary to its messenger RNA<sup>9</sup>. Despite the apparent homogeneity of the purified sodium channel preparations, several types of tetrodotoxin (or saxitoxin) binding sites or sodium currents have been observed in many excitable membranes<sup>10–19</sup>. The occurrence of distinguishable populations of sodium channels may be attributable to different states of the same channel protein or to distinct channel proteins. We have now isolated complementary DNA clones derived from two distinct rat brain mRNAs encoding sodium channel large polypeptides and present here the complete amino-acid sequences of the two polypeptides (designated sodium channels I and II), as deduced from the cDNA sequences. A partial DNA sequence complementary to a third homologous mRNA from rat brain has also been cloned.

Figure 1 shows the nucleotide sequences of the cloned cDNAs encoding rat brain sodium channels I and II (for the cloning procedure, see Fig. 1 legend). The primary structures of the two sodium channel large polypeptides were deduced by using the reading frame corresponding to the amino-acid sequence of the *Electrophorus* counterpart. The assignment of the translation initiation sites was based on the fact that they represent the first ATG triplets that appear downstream of a nonsense codon found in-frame. Rat brain sodium channels I and II are composed of

2,009 (or 1,998 with the deletion in clone prSCH28) and 2,005 amino acids, with calculated  $M_r$ s of 228,758 (227,576) and 227,840, respectively; at positions where amino-acid differences are predicted by the nucleotide differences found among the individual clones used (see Fig. 1 legend), the amino acids given in Fig. 1 have been used to calculate the  $M_r$ . Nucleotide sequence analysis of the third type of cloned cDNA (clone prSCH203; see Fig. 1 legend) revealed that it encodes a sequence of 573 amino acids that is highly homologous with the carboxy-terminal sequences of sodium channels I and II (data not shown).

The amino-acid sequences of rat sodium channels I and II are compared with that of *Electrophorus* sodium channel in Fig. 1. The degree of sequence homology is 87%, 62% and 62% for the rat I/rat II, rat I/*Electrophorus* and rat II/*Electrophorus* pairs, respectively. Rat sodium channel I as well as II, like the *Electrophorus* sodium channel<sup>9</sup>, contains four homologous internal repeats with deletions (or insertions) (positions 111–456, 775–1,047, 1,239–1,553 and 1,562–1,860 in the aligned sequences). The regions corresponding to these repeats are highly conserved among the three sodium channels, whereas the remaining regions, all of which are assigned to the cytoplasmic side of the membrane (see below), are less well conserved, except for the region between repeats III and IV. A large insertion of 166–178 amino acids occurs in the region between repeats I and II of the rat sodium channels, as compared with the *Electrophorus* counterpart. The inserted segment contains several potential sites of phosphorylation by cyclic AMP-dependent protein kinase<sup>20–22</sup>, which are conserved in the two rat sodium channels.

Rat sodium channels I and II have hydrophobicity profiles<sup>23</sup> similar to that of the *Electrophorus* sodium channel<sup>9</sup> (data not shown). Each internal repeat has five hydrophobic segments (S1, S2, S3, S5 and S6) and one positively charged segment (S4), all of which exhibit predicted secondary structure<sup>24</sup>. Segments S1, S2 and S3 generally contain a few charged residues. S3 has a few negative charges, and S2 a few negative and positive charges, whereas S1 is not uniform in charge. Segment S4 contains four to eight arginine or lysine residues located at every third position, with mostly nonpolar residues intervening between the basic residues. Segments S5 and S6 are highly hydrophobic regions without any charged residues (except S6 in repeat II of sodium channel I).

We have previously assumed that the four repeated units of homology in the sodium channel are oriented in a pseudosymmetric fashion across the membrane and that its amino terminus is located on the cytoplasmic side of the membrane<sup>9</sup>. This model

**Fig. 1** Nucleotide sequences of cDNAs encoding rat sodium channels I (first row) and II (second row) and alignment of the deduced amino-acid sequences of rat sodium channels I (third row) and II (fourth row) and of the *E. electricus* sodium channel<sup>9</sup> (fifth row) (see overleaf)

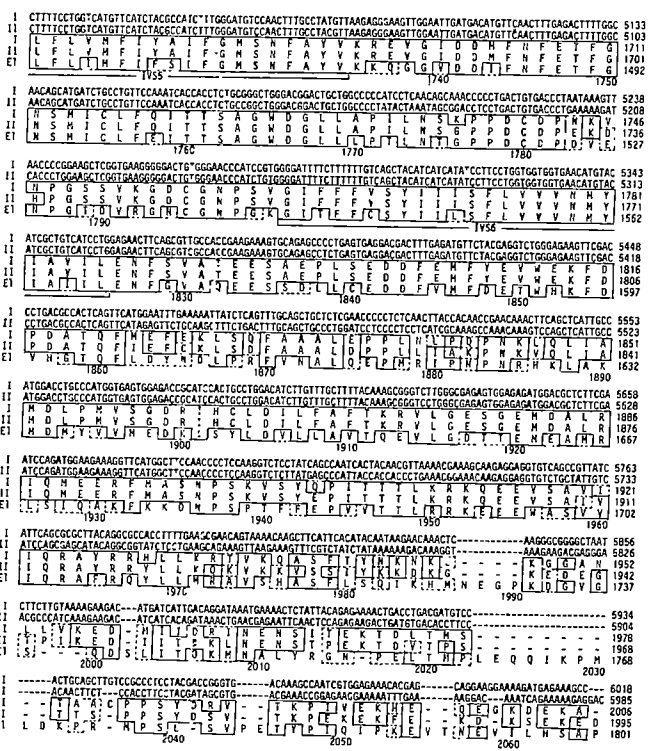
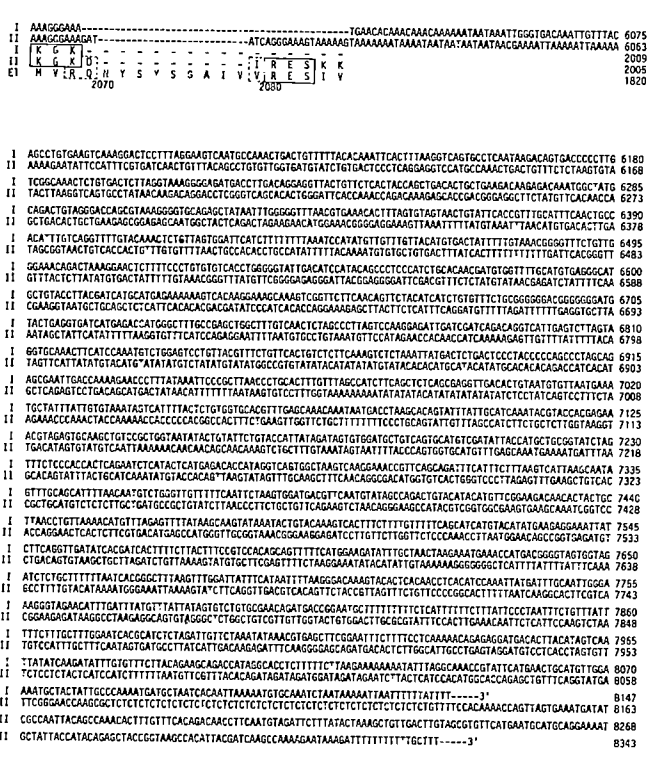


**Fig. 1** Nucleotide sequences of cDNAs encoding rat sodium channels I (first row) and II (second row) and alignment of the deduced amino-acid sequences of rat sodium channels I (third row) and II (fourth row) and of the *E. electricus* sodium channel<sup>9</sup> (fifth row). Nucleotide and amino-acid residues are numbered as in ref. 9; numbers of the last residues are given in the right-hand side. Identical amino-acid residues are boxed with solid-lines and conservative amino-acid residues<sup>35</sup> with broken lines. Gaps (-) have been inserted into the amino-acid and nucleotide sequences to achieve maximum amino-acid sequence homology. Numbers of positions in the aligned amino-acid sequences into which gaps have been introduced are given beneath the sequences. For evaluating amino-acid sequence homology (see text), a continuous stretch of gaps has been counted as one substitution regardless of its length. Segments S1–S6 in each of repeats I–IV are indicated. The potential *N*-glycosylation sites<sup>30,31</sup> conserved in all three sodium channels are the asparagine residues at positions 212, 285, 303, 340, 917, 1,417 and 1,431. Nucleotide 8,147 in prSCH109, nucleotide 7,682 in prSCH202 and nucleotide 8,343 in prSCH207 are followed by a poly(dA) tract which is connected with the vector DNA sequence<sup>36</sup>. A polyadenylation signal, AATAAA (ref. 37) or ATTAAA (ref. 38), is found at nucleotides 8,125–8,130 for prSCH109 and at nucleotides 7,662–7,667 and 8,320–8,325 for prSCH202 and prSCH207, respectively. The nucleotide differences observed among the individual clones are as follows. Sodium channel I cDNA: insertion (prSCH71) or deletion (prSCH28) of nucleotides 2,011–2,043 (underlined); G (prSCH74) or A (prSCH71) at nucleotide 1,441; G (prSCH28) or A (prSCH71) at 1,780; G (prSCH28) or A (prSCH71) at 2,467. Sodium channel II cDNA: A (prSCH93) or G (prSCH9) at nucleotide 1,149; G (prSCH78) or A (prSCH9) at 1,511; C (prSCH78) or T (prSCH11) at 2,688; G (prSCH78 and prSCH82) or A (prSCH11) at 3,065; G (prSCH11 and prSCH82) or A (prSCH78) at 3,313; G (prSCH82) or A (prSCH11 and prSCH78) at 3,357; T (prSCH82) or C (prSCH202) at 3,669; C (prSCH82) or G (prSCH202) at 3,671; A (prSCH82) or G (prSCH202) at 3,684. The resulting amino-acid substitutions are as follows. Sodium channel I: insertion/deletion of residues 671–681; Asp or Asn at residue 481; Glu or Lys at 594; Asp or Asn at 823. Sodium channel II: Arg or Lys at residue 504; Arg or His at 1,022; Val or Met at 1,105; Ala or Gly at 1,224. Wherever a nucleotide or amino-acid difference occurs, the former residue is shown in the sequences presented. S<sub>1</sub> nuclease mapping<sup>39</sup> of rat brain poly(A)<sup>+</sup> RNA with a probe containing the EcoRI (nucleotide 1,556)–BamHI(2,116) segment of prSCH71 indicated the presence of the sodium channel I mRNA both with and without the deletion of nucleotides 2,011–2,043.

**Methods.** Poly(A)<sup>+</sup> RNA was prepared<sup>40,41</sup> from the whole brain of male Wistar rats (~200 g body weight). A cDNA library, constructed<sup>42</sup> using 20 µg of oligo(dT)<sub>12–18</sub> and 20 µg of rat brain poly(A)<sup>+</sup> RNA, was screened by hybridization at 50 °C with an *E. electricus* sodium



channel cDNA probe, that is, an equimolar mixture of the *Hind*III(–250)–*Hind*III(1,777) fragment from pSCH411 and the *Hind*III(1,777)–*Ban*II(3,307) and *Ban*II(3,307)–*Xba*I(5,615) fragments from pSCH50 (ref. 9). Transformation and screening were done as described previously<sup>9</sup>. Of the 13 positive clones isolated from ~1 × 10<sup>5</sup> transformants, four (prSCH7, prSCH8, prSCH9 and prSCH11) hybridized with an RNA species of ~9,000–9,500 nucleotides when their cDNA inserts were used as probes for blot hybridization analysis<sup>43</sup> of rat brain poly(A)<sup>+</sup> RNA. The cDNA insert of prSCH7 was shown by restriction mapping to comprise part of that of prSCH8. Nucleotide sequence analysis<sup>44</sup> revealed that prSCH8, prSCH9 and prSCH11 carried cDNA sequences encoding amino-acid sequences homologous with different regions of the *E. electricus* sodium channel. Another cDNA library was constructed<sup>36</sup> using 12.6 µg of poly(A)<sup>+</sup> RNA and 5.6 µg of the vector-primer DNA. From ~2 × 10<sup>5</sup> transformants, five positive clones were isolated by hybridization at 60 °C with an equimolar mixture of the *Hinf*I(4,935)–*Hinf*I(5,658) fragment from prSCH8 and the *Hinf*I(2,568)–*Hinf*I(3,332) fragment from prSCH11. Restriction mapping indicated that all five clones were derived from an identical mRNA species. Sequence analysis showed that the 5'-terminal 219-nucleotide sequence of prSCH109, which harboured the largest cDNA insert, was similar but not identical to the 3'-terminal sequence of the cDNA insert of prSCH11, indicating that the two clones were derived from distinct mRNA species. Screening of an additional ~6 × 10<sup>5</sup> transformants from the same Okayama–Berg library by hybridization at 55 °C with the *Pst*I(4,350)–*Pvu*II(5,498) fragment from prSCH109 yielded 14 positive clones. These clones were classified into three groups by restriction mapping: nine clones belonged to the same group as prSCH109, three (for example, prSCH202 and prSCH207) to another group, and two (for example, prSCH203) to the third group. For cloning cDNA sequences further upstream, the oligodeoxyribonucleotide primer 5'-TCTGTGTTAACAGTTT-3', complementary both to nucleotides 3,375–3,389 in prSCH109 and to nucleotides 3,345–3,359 in prSCH11, was prepared using an automatic DNA synthesizer (Applied Biosystems) and was elongated by reverse transcription. Single-stranded cDNA was synthesized using 1 nmol of this primer and 100 µg of rat brain poly(A)<sup>+</sup> RNA and was converted to double-stranded cDNA, which was cloned in pBR322; the procedures were essentially the same as reported previously<sup>42</sup>, except that poly(A)<sup>+</sup> RNA was denatured using methylmercuric hydroxide<sup>45</sup>. From ~4 × 10<sup>4</sup> transformants, 46 positive clones were isolated by hybridization at 55 °C with an equimolar mixture of the *Hinf*I(1,144)–*Pst*I(1,396) fragment from prSCH9 and the *Bam*HI(2,440)–*Eco*RI(3,068) and *Eco*RI(3,068)–*Eco*RI(3,362) fragments from prSCH11. Restriction mapping of 23 of the clones indicated that 11 (for example, prSCH28, prSCH71 and prSCH74) were derived from the mRNA represented by prSCH109, and 9 clones (for example, prSCH78) from the mRNA represented by prSCH11. For isolating ▶

postulates the presence of an even number of transmembrane segments in each repeat because no additional hydrophobic segments are predicted outside the repeats. Thus, we have proposed that either four or all six of segments S1-S6 in each repeat traverse the membrane<sup>9</sup>. If four transmembrane segments are assumed, it seems likely that segments S5 and S6 and two of segments S1, S2 and S3 span the membrane. This transmembrane topology would be favoured if each of the four positively charged segments S4 interacted with each of the four negatively charged segments located between segment S6 of repeat II and segment S1 of repeat III<sup>9</sup>. However, the clusters of acidic residues in this region are not as conspicuous in the rat sodium channels as in the *Electrophorus* counterpart. Furthermore, the voltage-dependent gating of the sodium channel implies the presence of a voltage sensor, which is thought to be a collection of charges or equivalent dipoles moving under the influence of the membrane electric field<sup>1,25</sup>. In fact, this movement can be measured as a gating current<sup>26</sup>. The finding that the equivalent of four to six charges must move fully across the membrane to open one sodium channel<sup>1,25</sup> suggests the intramembranous location of many dipoles that move by smaller distances. These considerations favour the possibility that all of the six segments S1-S6 span the membrane (Fig. 2a), presumably forming  $\alpha$ -helical structures<sup>27-29</sup>. The ion selectivity of the sodium channel makes it unlikely that segment S4, which has many positive charges, constitutes the inner wall of the channel; it seems more reasonable for this segment to be localized within clusters of other segments (Fig. 2b). The formation of ion pairs between many of the positive charges in segment S4 and the negative charges in other segments such as S3 and S1 would stabilize the intramembranous location of the charged segments. The transmembrane topology shown in Fig. 2a is consistent with six of the seven potential N-glycosylation sites<sup>30,31</sup> that are conserved in all three sodium channels (see Fig. 1 legend) as well as with all the potential cyclic AMP-dependent phosphorylation sites<sup>20-22</sup>.

The unique structure of segment S4 in all repeats is strikingly well conserved among the three sodium channels. It seems probable that the positive charges present in this segment, many of which presumably form dipoles, represent the voltage sensor. They would move outward in response to depolarization, causing conformational changes and possible rearrangement of ion pairs. Segment S4 in repeats I, II, III and IV contains four, five, six and eight positive charges, respectively; this may underlie the proposal that the successive transitions among several closed states are fast and involve less charge movement than the slow transition from the last closed state to the open state<sup>32</sup>.

As the minimum cross-section of the sodium channel is thought to be  $3 \times 5 \text{ \AA}$  (refs 33, 34), at least one helical segment

prSCH82 and prSCH93, the synthetic oligodeoxyribonucleotide primers 5'-TTCCCCGTGGTGA-3' (complementary to nucleotides 4,105-4,119 in prSCH202) and 5'-ACTGACGAACTCTCC-3' (complementary to nucleotides 1,452-1,466 in prSCH9 and prSCH78) were elongated using a mixture of 3 nmol of the former primer and 2 nmol of the latter primer and 200  $\mu\text{g}$  of rat brain poly(A)<sup>+</sup> RNA (see above). Selection of the cloned cDNA transcripts ( $\sim 4 \times 10^4$  transformants) by hybridization at  $60^\circ\text{C}$  with the EcoRI(3,068)-EcoRI(3,362) fragment from prSCH11 and with the *Hinf*I(1,144)-*Pst*I(1,396) fragment from prSCH9 yielded two (for example, prSCH82) and five (for example, prSCH93) positive clones, respectively. DNA sequencing was done using the method of Maxam and Gilbert<sup>44</sup>; both strands were sequenced, except for a small portion of the 3'-noncoding sequence (nucleotides 8,309-8,343) of the sodium channel II cDNA. The clones that were subjected to DNA sequencing were as follows. Sodium channel I: prSCH74 (carrying nucleotides -251 to 1,624), prSCH71 (1,245-2,709), prSCH28 (1,724-3,389 with a deletion of 2,011-2,043), prSCH109 (3,234-8,147), prSCH8 (4,561-6,039). Sodium channel II: prSCH93 (-210 to 1,458), prSCH9 (979-1,511), prSCH78 (1,336-3,359), prSCH11 (2,139-3,428), prSCH82 (2,983-4,119), prSCH202 (3,669-7,682), prSCH207 (4,234-8,343; nucleotides 4,290-7,553 were not sequenced). The restriction maps and sequencing strategy are available from the authors on request.

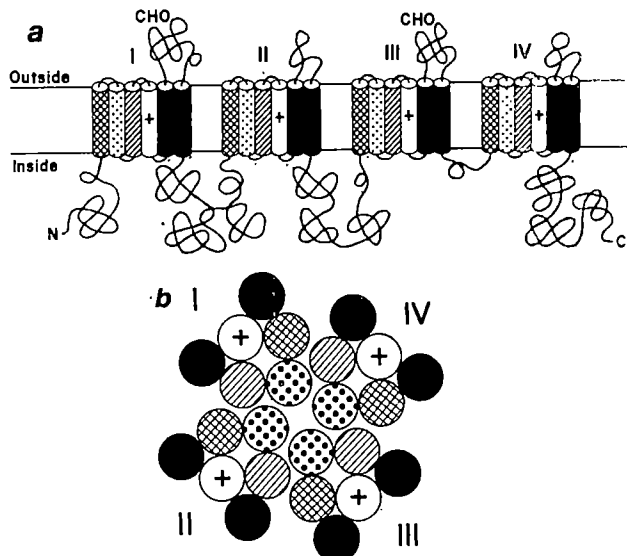
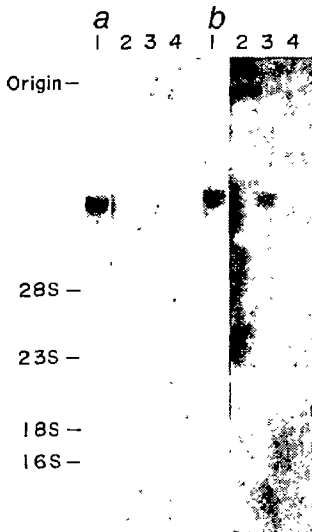


Fig. 2 a, Proposed transmembrane topology of the sodium channels; b, proposed arrangement of the transmembrane segments viewed in the direction perpendicular to the membrane. In a, the four units of homology spanning the membrane are displayed linearly. Segments S1-S6 in each repeat (I-IV) are indicated by cylinders as follows: S1, cross-hatched; S2, stippled; S3, hatched; S4, indicated by a plus sign; S5 and S6, solid. Putative sites of N-glycosylation (CHO) are indicated. In b, the ionic channel is represented as a central pore surrounded by the four units of homology. Segments S1-S6 in each repeat (I-IV) are represented by circles indicated as in a.

from each repeat would participate in forming the inner wall of the channel at the narrowest point. Remarkably, segment S2 in every repeat contains, at equivalent positions, a glutamic acid residue (positions 169, 839, 1,305 and 1,626 in the aligned sequences) and a lysine residue (positions 173, 843, 1,309 and 1,630), which are conserved in all three sodium channels. These acidic and basic residues are located on one side of the  $\alpha$ -helix. In addition, segment S2 in repeats I and III contains a conserved glutamic acid or aspartic acid residue (positions 159 and 1,295) located 10 residues from the above-mentioned glutamic acid on nearly the same side of the  $\alpha$ -helix; segment S2 in repeat III has two more conserved charged residues (glutamic acid at position 1,292 and lysine at position 1,296), which face another side of the  $\alpha$ -helix. In view of the high degree of conservation of the charged residues in segment S2, it is tempting to hypothesize that this segment forms the inner wall of the channel (Fig. 2b).

Segment S3 in every repeat also contains a conserved aspartic acid residue (positions 195, 861, 1,327 and 1,647) at an equivalent position. It is an intriguing speculation that this aspartic acid, which may be paired with a basic residue in segment S4 in the closed state of the channel, may be shifted by depolarization to interact with the lysine present in segment S2 of every repeat; this would cause a conformational change of the putative channel wall and simultaneously mask the positive charge on the channel lining to allow sodium ions to pass through the central pore. Clusters of positively charged residues (predominantly lysine) and of negatively charged residues are conserved in the regions preceding segment S1 and following segment S6 of repeat IV, respectively. It is conceivable that these segments, which are assigned to the cytoplasmic side of the membrane, are involved in the inactivation of the sodium channel<sup>32</sup>.

Poly(A)<sup>+</sup> RNA from adult rat brain, skeletal muscle and cardiac muscle was subjected to blot hybridization analysis with cDNA probes for rat brain sodium channels I and II (Fig. 3a, b). The brain contained RNA species of  $\sim 9,000$  and  $\sim 9,500$  nucleotides that were hybridizable with the sodium channel I



**Fig. 3** Autoradiogram of blot hybridization analysis of poly(A)<sup>+</sup> RNA from excitable tissues with sodium channel I (*a*) and II (*b*) cDNA probes. Poly(A)<sup>+</sup> RNA (20 µg) from whole brain (lane 1), skeletal muscle (lane 2), cardiac muscle (lane 3) and liver (lane 4) of male Wistar rats (~200 g body weight) was denatured with 1 M glyoxal and 50% dimethyl sulphoxide, electrophoresed on a 1.2% agarose gel and transferred to a nitrocellulose filter<sup>43</sup>. The filter was divided into two portions and subjected to hybridization with the HindIII(3,534)-HindIII(5,811) fragment from prSCH109 (*a*) or the SacI(3,931)-EcoRI(5,869) fragment from prSCH202 (*b*). The probes were labelled by nick-translation<sup>46</sup> with [ $\alpha$ -<sup>32</sup>P]dCTP. Autoradiography was performed for 10 h (lane 1) or 72 h (lanes 2-4). The size markers used were rat and *Escherichia coli* ribosomal RNAs.

and II cDNA probes, respectively, in comparable amounts (Fig. 3, lanes 1). These sizes are consistent with those expected from the cloned cDNAs. The cardiac muscle also contained two RNA species that were hybridizable with the respective cDNA probes and indistinguishable in size from the brain mRNAs, although the hybridization signals were much weaker (Fig. 3, lanes 3); note the difference in the duration of autoradiography (see Fig. 3 legend). No hybridizable RNA species were detected with the skeletal muscle RNA (lane 2) or with the liver RNA used as a control (lane 4). The weak or undetectable hybridization observed with the cardiac muscle and skeletal muscle RNAs may be accounted for either by their low content of the sodium channel mRNAs or by the presence of different sodium channel mRNAs in these tissues. It has been reported that adult rat cardiac muscle contains a sodium channel species with a low affinity for tetrodotoxin, in addition to a species of sodium channel that, like the brain counterpart, has a high affinity for the toxin, and that the concentration of the high-affinity sodium channel is much lower than that of the low-affinity sodium channel<sup>10,11</sup>. The structurally distinct sodium channels encoded by the mRNAs found may be responsible for the different types of sodium currents observed in excitable tissues<sup>14-19</sup>.

We thank Drs Paul Berg and Hiroto Okayama for providing us with their high-efficiency cloning system and Dr Takashi Miyata and Mr Hidenori Hayashida for computer analysis. This investigation was supported in part by research grants from the Ministry of Education, Science and Culture of Japan, the Mitsubishi Foundation and the Japanese Foundation of Metabolism and Diseases.

Received 15 October 1985; accepted 15 January 1986.

- Hodgkin, A. L. & Huxley, A. F. *J. Physiol., Lond.* **117**, 500-544 (1952).
- Agnew, W. S. *A. Rev. Physiol.* **46**, 517-530 (1984).
- Catterall, W. A. *Science* **223**, 653-661 (1984).
- Agnew, W. S., Levinson, S. R., Brabson, J. S. & Raftery, M. A. *Proc. natn. Acad. Sci. U.S.A.* **75**, 2606-2610 (1978).
- Miller, J. A., Agnew, W. S. & Levinson, S. R. *Biochemistry* **22**, 462-470 (1983).
- Lombet, A. & Lazdunski, M. *Eur. J. Biochem.* **141**, 651-660 (1984).

- Hartshorne, R. P. & Catterall, W. A. *Proc. natn. Acad. Sci. U.S.A.* **78**, 4620-4624 (1981).
- Barchi, R. L. *J. Neurochem.* **40**, 1377-1385 (1983).
- Noda, M. *et al. Nature* **312**, 121-127 (1984).
- Lombet, A., Renaud, J.-F., Chicheportiche, R. & Lazdunski, M. *Biochemistry* **20**, 1279-1285 (1981).
- Lombet, A., Kazazoglou, T., Delpont, E., Renaud, J.-F. & Lazdunski, M. *Biochem. biophys. Res. Commun.* **110**, 894-901 (1983).
- Renaud, J.-F. *et al. J. biol. Chem.* **258**, 8799-8805 (1983).
- Sherman, S. J. & Catterall, W. A. in *Regulation and Development of Membrane Transport Processes* (ed. Graves, J. S.) 237-263 (Wiley, New York, 1985).
- Barrett, J. N. & Crill, W. E. *J. Physiol., Lond.* **304**, 231-249 (1980).
- Gundersen, C. B., Miledi, R. & Parker, I. *Proc. R. Soc. B220*, 131-140 (1983).
- Jaimovich, E. *et al. Eur. J. Physiol.* **397**, 1-5 (1983).
- Eick, R. T., Yeh, J. & Matsuki, N. *Biophys. J.* **45**, 70-73 (1984).
- Gilly, W. F. & Armstrong, C. M. *Nature* **309**, 448-450 (1984).
- Benoit, E., Corbier, A. & Dubois, J.-M. *J. Physiol., Lond.* **361**, 339-360 (1985).
- Costa, M. R. C., Casanelle, J. E. & Catterall, W. A. *J. biol. Chem.* **257**, 7918-7921 (1982).
- Costa, M. R. C. & Catterall, W. A. *J. biol. Chem.* **259**, 8210-8218 (1984).
- Krebs, E. G. & Beavo, J. A. *Rev. Biochem.* **48**, 923-959 (1979).
- Kyte, J. & Doolittle, R. F. *J. molec. Biol.* **157**, 105-132 (1982).
- Chou, P. Y. & Fasman, G. D. *Adv. Biochem.* **47**, 251-276 (1978).
- Hille, B. *Ionic Channels of Excitable Membranes* (Sinauer, Sunderland, Massachusetts, 1984).
- Armstrong, C. M. & Bezanilla, F. *Nature* **242**, 459-461 (1973).
- Capaldi, R. A. & Vanderkooi, G. *Proc. natn. Acad. Sci. U.S.A.* **69**, 930-932 (1972).
- Engelman, D. M. & Steitz, T. A. *Cell* **23**, 411-422 (1981).
- Rice, C. M., Bell, J. R., Hunkapiller, M. W., Strauss, E. G. & Strauss, J. H. *J. molec. Biol.* **154**, 355-378 (1982).
- Hubbard, S. C. & Ivatt, R. J. *Adv. Rev. Biochem.* **50**, 555-583 (1981).
- Bause, E. *Biochem. J.* **209**, 331-336 (1983).
- Armstrong, C. M. *Physiol. Rev.* **61**, 644-683 (1981).
- Hille, B. *J. gen. Physiol.* **58**, 599-619 (1971).
- Hille, B. *J. gen. Physiol.* **59**, 637-658 (1972).
- Dayhoff, M. O., Schwartz, R. M. & Orcutt, B. C. in *Atlas of Protein Sequence and Structure* Vol. 5, Suppl. 3 (ed. Dayhoff, M. O.) 345-352 (National Biomedical Research Foundation, Silver Spring, Maryland, 1978).
- Okayama, H. & Berg, P. *Molec. cell. Biol.* **2**, 161-170 (1982).
- Proudfoot, N. J. & Brownlee, G. G. *Nature* **263**, 211-214 (1976).
- Goeddel, D. V. *et al. Nature* **290**, 20-26 (1981).
- Berk, A. J. & Sharp, P. A. *Cell* **12**, 721-732 (1977).
- Chirgwin, J. M., Przybyla, A. E., MacDonald, R. J. & Rutter, W. J. *Biochemistry* **18**, 5294-5299 (1979).
- Aviv, H. & Leder, P. *Proc. natn. Acad. Sci. U.S.A.* **69**, 1408-1412 (1972).
- Noda, M. *et al. Nature* **295**, 202-206 (1982).
- Thomas, P. S. *Proc. natn. Acad. Sci. U.S.A.* **77**, 5201-5205 (1980).
- Maxam, A. M. & Gilbert, W. *Meth. Enzym.* **65**, 499-560 (1980).
- Payvar, F. & Schimke, R. T. *J. biol. Chem.* **254**, 7636-7642 (1979).
- Weinstock, R., Sweet, R., Weiss, M., Cedar, H. & Axel, R. *Proc. natn. Acad. Sci. U.S.A.* **75**, 1299-1303 (1978).

## Multiple conformations of a protein demonstrated by magnetization transfer NMR spectroscopy

Robert O. Fox\*, Philip A. Evans  
& Christopher M. Dobson

Inorganic Chemistry Laboratory, University of Oxford,  
South Parks Road, Oxford OX1 3QR, UK

It is generally accepted that a globular protein in its native state adopts a single, well-defined conformation. However, there have been several reports that some proteins may exist in more than one distinct folded form in equilibrium. In the case of staphylococcal nuclease, evidence for multiple conformations has come from electrophoretic and NMR studies<sup>1-4</sup>, although there has been some controversy as to whether these are actually interconvertible forms of the same molecular species<sup>5,6</sup>. Recently, magnetization transfer(MT)-NMR has been developed as a means of studying the kinetics of conformational transitions in proteins<sup>7</sup>. In the study reported here, this approach has been extended and used to demonstrate the presence of at least two native forms of nuclease in equilibrium and to study their interconversion with the unfolded state under the conditions of the thermal unfolding transition. The experiments reveal that two distinct native forms of the protein fold and unfold independently and that these can interconvert directly as well as via the unfolded state. The spectra of the different forms suggest that they are structurally similar but the MT experiments show that the kinetics of folding and unfolding are quite

\* Present address: Department of Cell Biology, Stanford University Medical School, Stanford, California 94305, USA.

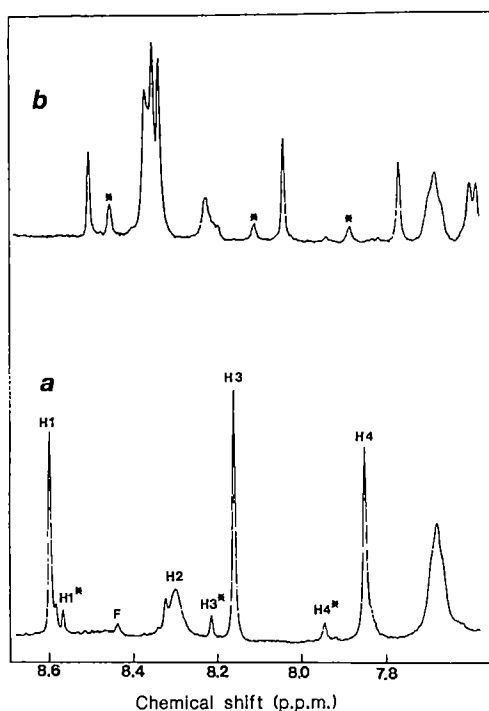


**Fig. 1** *a*, 500-MHz  $^1\text{H}$ -NMR spectrum of nuclease ( $100 \text{ mg ml}^{-1}$ ), pH 5.5 in 200 mM deuterated sodium acetate solution ( $37^\circ\text{C}$ ). Backbone amide protons have been exchanged for deuterons to reveal the resonances of the His  $\text{H}^{e_1}$  protons. The asterisks denote histidine resonances of minor folded forms of the protein. *F* denotes a non-protein impurity. *b*, Spectrum of nuclease; same sample as in *a* but at  $55^\circ\text{C}$ .

**Methods.** The nuclease used in these experiments was produced by a recombinant expression construct in which the nuclease gene cloned from *S. aureus* Foggi strain was under the control of the  $\lambda_{PL}$  promoter in the vector pAS1 (R.O.F., unpublished). The protein produced contains the additional N-terminal sequence fMet-Asp-Pro-Thr-Val-Tyr-Ser beyond the nuclease A sequence<sup>19</sup>. Nuclease produced in *E. coli* was isolated to >95% purity on a phosphocellulose column developed with a linear gradient of 0.3 M ammonium acetate, pH 6 to 1.0 M ammonium acetate, pH 8 (ref. 20).

**different. Characterization of this behaviour will, therefore, have important implications for our understanding of the relationship between structure and folding kinetics.**

The  $\text{Ca}^{2+}$ -dependent nuclease of *Staphylococcus aureus* (EC 3.1.4.7) has been used extensively in folding studies because of its small size (149 residues), the reversibility of unfolding *in vitro* and the absence of disulphide crosslinks (reviewed in refs 8–10). The structure of a crystal of the nuclease has been determined to 1.5-Å resolution, revealing extensive  $\alpha$ - and  $\beta$ -structure in the folded state<sup>11,12</sup>. In the present study we have used a protein obtained by expression of the recombinant nuclease gene in *Escherichia coli*. This protein includes additional residues at the N-terminus, part of a sequence which is cleaved from the mature protein in *S. aureus*.

Part of the  $^1\text{H}$ -NMR spectrum of the nuclease in native conditions is shown in Fig. 1*a*. The  $\text{H}^{e_1}$  ( $\text{C}_2\text{H}$ ) resonances of the four histidines are prominent and are accompanied by several smaller peaks. Each minor resonance has a chemical shift comparable to that of one of the major peaks and these relationships persist throughout the pH range over which the resonances titrate. This result suggests that the minor peaks are due to one or more folded forms which are native-like but distinct from the major form. Here we consider one pair of resonances (labelled  $\text{H}4$  and  $\text{H}4^*$  in Fig. 1) which are sufficiently well resolved to permit detailed NMR studies.

The relative intensities of the major ( $\text{H}4$ ) and minor ( $\text{H}4^*$ ) resonances change reversibly with temperature, which shows

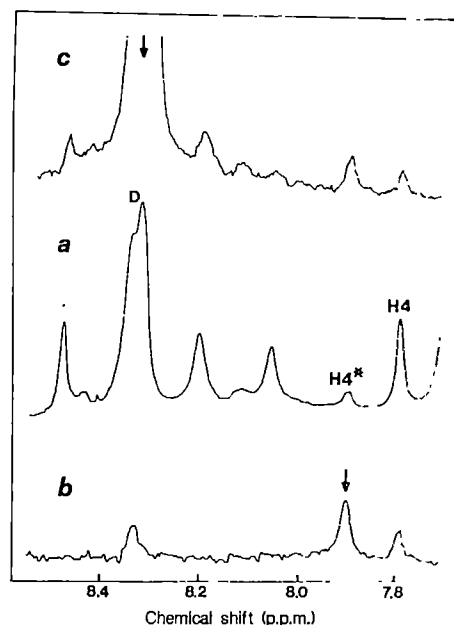


**Fig. 2** Single-saturation magnetization transfer experiments on nuclease, pH 5.5 ( $55^\circ\text{C}$ ). *a*, A 'blank' spectrum in which a pre-saturation pulse was applied at a frequency at which no protons resonate. *b*, *c*, Difference spectra obtained by subtraction from *a* of spectra acquired in an interleaved fashion in which individual resonances (denoted by the arrows) have been selectively saturated. The vertical scale of the difference spectra is four times that of spectrum *a*. In *b*,  $\text{H}4^*$ , a resonance of a minor folded state, was irradiated for 3 s before observation of the spectrum. In *c* the saturation pulse was applied to the resonances of the unfolded state. The selectivity of the saturation in these experiments was checked by carrying out control experiments at lower temperatures where there is no measurable magnetization transfer.

that they arise from different states of the same molecule in equilibrium. Moreover, on forming a ternary complex with  $\text{Ca}^{2+}$  and thymidine 3',5'-diphosphate,  $\text{H}4^*$  is lost from the nuclease spectrum, suggesting that the stabilization afforded by binding the ligands displaces the equilibrium in favour of the major folded form.

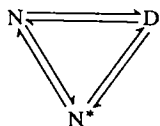
In the spectrum shown in Fig. 1*b*, the temperature has been raised to  $55^\circ\text{C}$ , which is in the transition zone of reversible thermal unfolding. The resonances of the folded forms are now accompanied by those of the unfolded protein, whose His  $\text{H}^{e_1}$  peaks are clustered between 8.3 and 8.4 parts per  $10^6$  (p.p.m.). We have studied the processes of interconversion of the different states through a series of MT experiments. If a resonance of the protein in one state is selectively perturbed, the corresponding resonances in the other states may in turn be affected as a result of chemical exchange between the states. Figure 2 presents difference spectra showing the effects of saturating individual resonances and allowing the system to equilibrate in the presence of the perturbation. In these conditions the resonance intensity of a site in exchange with that which has been irradiated will depend on the rate of magnetization transfer from this site compared with its spin-lattice relaxation rate<sup>7,13,14</sup>.

Figure 2*b* shows the effect of selective saturation of  $\text{H}4^*$  in the conditions of the thermal unfolding transition. Decreases in the intensities of  $\text{H}4$  and of the corresponding unfolded-state resonance, *D*, demonstrate directly that all three states are interconverting under these conditions. Figure 2*c* shows the effect of saturating the *D* resonance: as expected, both  $\text{H}4$  and  $\text{H}4^*$  are affected but the effect on  $\text{H}4^*$  is proportionately much greater. As the spin-lattice relaxation times of  $\text{H}4$  and  $\text{H}4^*$  are comparable, this result shows that the equilibrium unfolding rate of the minor species,  $\text{N}^*$ , is much greater than that of the major folded form, *N*. The effect on *D* of saturating  $\text{H}4$  is also much smaller than when  $\text{H}4^*$  is saturated, which shows that the overall rate of conversion of *D* to *N* is smaller than that to  $\text{N}^*$ ,

although further interpretation of this result is complicated by the possibility that the unfolded state is not kinetically homogeneous. We shall discuss this further below.

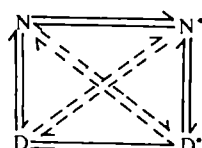
These single-saturation experiments alone do not reveal the pathways of interconversion in such a multi-site system. To address this problem we have extended the MT approach to measure the effects of simultaneous saturation of two resonances. Figure 3 compares the effect of saturating H4\* alone with saturating H4\* and D together. The difference spectrum shows clearly that the extent of saturation transfer to H4 increased when both resonances were saturated; this means that magnetization transfer can occur directly between N and D without the need to be relayed through N\*, excluding the possibility that N\* is a required intermediate for the folding and unfolding of N. Similarly, saturation of both D and H4 leads to a larger effect on H4\* than saturation of H4 alone, which reveals direct magnetization transfer from H4\* to D and thus confirms that the different native forms unfold independently. Furthermore, we found that while D was saturated, direct magnetization transfer between H4 and H4\* was detectable; this shows that the different folded forms can interconvert without the need to pass through the unfolded state. Magnetization transfer between H4 and H4\* was not measurable at significantly lower temperatures, however, showing that there is a substantial energy barrier to this process.

The above experiments have thus revealed mutual exchange between at least three states of nuclease under the experimental conditions:



This conclusion is based on the behaviour of one of the four histidines, H4. Minor resonances are also evident for the other histidines and elsewhere in the spectrum. At least some of these resonances show behaviour very similar to H4\* in a two-dimensional MT experiment and it seems likely that these arise from a common minor component. It has been possible, however, to observe that the intensity of another minor peak changes relative to that of H4\* on variation of the temperature. Further, unlike H4\*, it is still present in the spectrum of the inhibited nuclease. This result shows that there could, in fact, be more than a single equilibrium among folded species. Although it is not possible to define the conformations of the different states, they are clearly not very different. For example, each of the minor histidine resonances has a chemical shift similar to that of one of the major peaks, and their pH dependences demonstrate that the  $pK_a$  values in the different states are very similar.

Another aspect which must be considered concerns the possibility of spectroscopically unresolved heterogeneity of the unfolded state arising from *cis-trans* isomerism of proline peptide bonds<sup>15</sup>, which is of particular interest because this could also be the origin of the heterogeneity of the folded protein. It is known that RNase A, for example, has a metastable form which contains a non-native proline isomer<sup>16</sup>, and it is possible that in some circumstances such species could be sufficiently stable to be populated at equilibrium. In this case the scheme would be extended thus:



The MT experiment will allow us to test these models by examining the time course of development of the effects.

Globular proteins have usually been observed to equilibrate rapidly about a single average structure in solution. Evidence

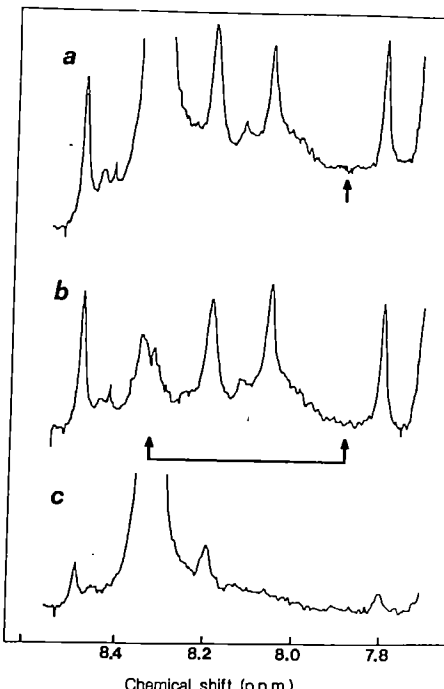


**Fig. 3** Double-saturation magnetization transfer experiment on nuclease, pH 5.5 (55 °C). In spectrum *a* the H4\* resonance was saturated for 3 s before observation. In spectrum *b*, which was acquired in an interleaved fashion, both H4\* and the resonances of the unfolded state were saturated. *c*, The differences between the two spectra. The simultaneous double saturation was achieved by applying a single selective 3-s pulse to H4\* in the normal way while simultaneously applying a DANTE pulse<sup>21</sup> of the same duration to the resonances of the unfolded state.

now exists, however, for multiple folded forms of similar stability in the cases of nuclease and some other proteins, including dihydrofolate reductase<sup>17,18</sup>. We have demonstrated here that MT studies constitute a powerful tool for the elucidation of pathways of conformational interconversion in these systems. We anticipate that the existence of alternative stable folded states will provide unique possibilities for elucidating the effects of single-site mutations on folding.

This work was supported by SERC. R.O.F. acknowledges a postdoctoral fellowship from the Jane Coffin Childs Memorial Fund for Medical Research whilst in Oxford and the encouragement and support of N. D. F. Grindley and his laboratory in carrying out the cloning and expression of the nuclease gene. C.M.D. is a member of the Oxford Enzyme Group.

Received 11 December 1985; accepted 14 January 1986.

1. Taniuchi, H. & Anfinsen, C. B. *J. biol. Chem.* **241**, 4366–4385 (1966).
2. Markley, J. L., Williams, M. N. & Jarde茨基, O. *Proc. natn. Acad. Sci. U.S.A.* **65**, 645–651 (1970).
3. Arata, Y., Khalifah, R. & Jarde茨基, O. *Ann. N.Y. Acad. Sci.* **222**, 230–239 (1973).
4. Tucker, P. W., Hazen, E. E. & Cotton, F. A. *Molec. cell. Biochem.* **22**, 67–77 (1978).
5. Cohen, J. S., Shrager, R. I., McNeil, M. & Schechter, A. N. *Nature* **228**, 642–644 (1970).
6. Marrakechi, N. & Cozzane, P. J. *C.r. hebdo. Séanc. Acad. Sci., Paris Ser. 3* **293**, 23–26 (1981).
7. Dobson, C. M. & Evans, P. A. *Biochemistry* **23**, 4267–4270 (1984).
8. Anfinsen, C. B., Schechter, A. N. & Taniuchi, H. *Cold Spring Harb. Symp. quant. Biol.* **36**, 243–249 (1971).
9. Anfinsen, C. B. *Science* **181**, 223–230 (1973).
10. Tucker, P. W., Hazen, E. E. & Cotton, F. A. *Molec. cell. Biochem.* **23**, 131–141 (1979).
11. Arnone, A. *et al.* *J. biol. Chem.* **246**, 2302–2316 (1971).
12. Cotton, F. A., Hazen, E. E. & Legg, M. J. *Proc. natn. Acad. Sci. U.S.A.* **76**, 2551–2555 (1979).
13. Forsén, S. & Hoffman, R. A. *J. chem. Phys.* **39**, 2892–2901 (1963).
14. Campbell, I. D., Dobson, C. M., Ratcliffe, R. G. & Williams, R. J. P. *J. magn. Reson.* **29**, 397–417 (1978).
15. Brandts, J. F., Halvorson, H. R. & Brennan, M. *Biochemistry* **14**, 4953–4963 (1975).
16. Cook, K. H., Schmid, F. X. & Baldwin, R. L. *Proc. natn. Acad. Sci. U.S.A.* **76**, 6157–6161 (1979).
17. Gronenborn, A. *et al.* *Molec. Pharm.* **20**, 145–153 (1981).
18. Mathews, C. R., Perry, K. M. & Touchette, N. A. *Am. chem. Soc. Abstr.* **186**, BIOL83 (1983).
19. Cone, J. L., Cusumano, C. L., Taniuchi, H. & Anfinsen, C. B. *J. biol. Chem.* **246**, 3103–3110 (1971).
20. Fuchs, S., Cuatrecasas, P. & Anfinsen, C. B. *J. biol. Chem.* **242**, 4768–4770 (1967).
21. Morris, G. A. & Freeman, R. *J. magn. Reson.* **29**, 433–462 (1978).

## Predisposition to helminth infection in man

I FIND it difficult to accept the basic assumptions made by Anderson and May<sup>1</sup> in their model of herd immunity, at least as it applies to schistosome infection. They initially assume that certain individuals are predisposed to heavy infections. In field studies of individuals with treated *Schistosoma mansoni* infections<sup>3</sup>, this was not the case. The supposition is supported by studies of hookworm infections<sup>4</sup>. Even if predisposition to heavy schistosome infection were shown to exist, it would be premature to attribute this to lack of immunity or to assume that such individuals cannot be successfully vaccinated.

Anderson and May also assume that immunity to schistosome infection is correlated with the intensity of infection and cite the more rapid decline in faecal egg counts in a heavily infected population examined by Siongok *et al.*<sup>5</sup> compared with more lightly infected persons examined by Abdel-Wahab *et al.*<sup>6</sup>. My objections here are that the difference in faecal egg counts between these populations was not great (464 eggs per g of faeces in 5–9-yr-old males in the study by Abdel-Wahab *et al.*<sup>6</sup> and 650 eggs per g in the groups examined by Siongok *et al.*<sup>5</sup>) and the report of Ongom and Bradley<sup>7</sup> is not cited. In this last study the decline in egg excretion was gradual although 5–9-yr-old boys excreted an average of 793 eggs per g faeces. In the very lightly infected populations in Puerto Rico and St Lucia (geometric means of 20–30 eggs per g faeces in 5–9-yr-olds), egg excretion was maintained at relatively stable levels for many years<sup>8,9</sup>. Resistance of mice to reinfection is clearly related to infection intensity<sup>10</sup>, but a large part of this resistance is nonspecific<sup>11</sup> and is related to infection intensities that generally are not relevant for humans<sup>12</sup>.

The experimental study by Crombie and Anderson<sup>13</sup> also presents problems and does not provide convincing evidence for the death of significant numbers of *S. mansoni* worms in mice. Although dead worms are visible in the livers of mice for months after treatment<sup>14</sup>, I rarely encounter them in the livers of untreated mice. Certainly, the more heavily infected mice die sooner than the less heavily infected ones, a point considered by the authors but dismissed, without presentation of data, as a cause of decreasing intensity of infection with time. The mouse model is an inherently difficult one in which to pursue this point, as nearly all chronically infected mice develop large portal-systemic collateral veins with resultant shunting of some worms into the pulmonary circulation (my unpublished data), where their survival is probably

limited. Such collaterals also develop in patients with severe disease, but such patients form a small part of the population and would not be important epidemiologically.

ALLEN W. CHEEVER

Laboratory of Parasitic Diseases,  
National Institute of Allergy  
and Infectious Diseases,  
National Institutes of Health,  
Bethesda, Maryland 20205, USA

1. Anderson, R. M. & May, R. M. *Nature* **315**, 493–496 (1985).
2. Mahmoud, A. A. F., Siongok, T. A., Ouma, J., Houser, H. B. & Warren, K. S. *Lancet* **i**, 849–851 (1983).
3. Sturrock, R. F. *et al.* *Trans. R. Soc. trop. Med. Hyg.* **77**, 363–371 (1983).
4. Shad, G. A. & Anderson, R. M. *Science* **228**, 1537–1540 (1985).
5. Siongok, T. K. A. *et al.* *Am. J. trop. Med. Hyg.* **25**, 273–284 (1976).
6. Abdel-Wahab, M. F. *et al.* *Am. J. trop. Med. Hyg.* **29**, 868–874 (1980).
7. Ongom, V. L. & Bradley, D. J. *Trans. R. Soc. trop. Med. Hyg.* **66**, 835–851 (1972).
8. Hiatt, R. A., Cline, B. L., Ruiz-Tiben, E., Knight, W. B. & Berrios-Duran, L. A. *Am. J. trop. Med. Hyg.* **29**, 1228–1240 (1980).
9. Barnish, G., Jordan, P., Bartholomew, R. K. & Grist, E. *Trans. R. Soc. trop. Med. Hyg.* **76**, 602–609 (1982).
10. Dean, D. A. *Expl. Parasit.* **55**, 1–104 (1983).
11. Dean, D. A., Minard, P., Murrell, K. D. & Vannier, W. E. *Am. J. trop. Med. Hyg.* **27**, 957–965 (1978).
12. Cheever, A. W. *Trans. R. Soc. trop. Med. Hyg.* **63**, 781–795 (1969).
14. Cheever, A. W., DeWitt, W. B. & Warren, K. S. *Am. J. trop. Med. Hyg.* **14**, 239–253 (1965).

**ANDERSON ET AL. REPLY**—The assumption of predisposition to heavy (or light) infection is not central to the framework of our model<sup>1</sup> of herd immunity to helminth infection (see equations (1) and (2) of ref. 1). It is simply an optional extension which can be used to investigate the potential influence of heterogeneity in either exposure to infection (that is, behavioural factors) or the host's ability to restrict parasite establishment and survival (that is, immunological factors which may be under genetic control) on the transmission and control of helminths in human communities. Such heterogeneity is a central feature of the epidemiology of helminths, as indicated by the high degrees of aggregation observed in parasite distributions within human populations<sup>2</sup>. However, the interesting issue raised by Cheever centres on the question of whether or not predisposition is an important component of the epidemiology of schistosome parasites. We believe it is. The two studies cited by Cheever do not address the statistical question of whether there is a positive association (in large samples of people, stratified according to age and sex) between faecal egg counts in individual patients before treatment and after an interval of reinfection following chemotherapy<sup>3,4</sup>. The first such analysis of this question<sup>7</sup> for *Schistosoma mansoni* infection in a rural community in Kenya<sup>5,6</sup>, reveals a highly significant positive

tive association (12-month period of reinfection in 8–15-yr-old children, Kendall's  $\tau = 0.347$ ,  $n = 117$ ,  $P < 0.0001$ ; ref. 7) between pretreatment egg counts (in eggs per g, e.p.g.) and counts following an interval of reinfection after chemotherapeutic treatment<sup>7</sup>. Whether this observed pattern is a consequence of differences in contact with infection, or in immunological competence of the host, is unclear at present. Work in progress (the same field study<sup>5,6</sup>) on individual patterns of contact with water and faecal egg output should improve our understanding of this issue. More broadly, recent field studies record evidence for predisposition to heavy infection with *Ascaris*<sup>8,9</sup>, hookworm<sup>10</sup> and *Trichuris*<sup>11</sup>.

We disagree with Cheever's interpretation of the relevant data on the question of a positive association between the force of transmission and the degree of convexity of age-intensity of infection profiles (Fig. 1b in ref. 1). In the 5–9-yr-old age classes in the two studies we cited<sup>12,13</sup>, the intensity of infection (mean e.p.g. per person sampled, including boys and girls) was 690 eggs per g faeces in the high transmission area and 144 eggs per g in the low transmission area. Furthermore, in the study of Ongom and Bradley<sup>14</sup> (within a high transmission area of Uganda), the average intensity of infection (boys and girls) fell from a maximum of 1,128 eggs per g of faeces in the 5–9-yr-old class to a minimum of 404 eggs per g of faeces in the 40–49-yr-old class; again, a marked convex pattern was associated with a high net force of transmission. The studies in Puerto Rico and St. Lucia<sup>15,16</sup>, cited by Cheever, further support our argument, as in these areas of low transmission intensity, mean faecal egg counts remain relatively stable over a wide range of age classes. More generally, a recent statistical study, using a range of epidemiology surveys for *S. mansoni* and *Schistosoma haematobium*, of the relationship between the maximum average intensity of infection (commonly in the child/teenage age groups) and the rate of decline in average intensity from child to adult groups reveals a highly significant positive correlation (J.A.C., unpublished).

With respect to our experimental studies<sup>17</sup>, juvenile and dead adult worms were recovered from mice throughout the long periods of repeated exposure to infection; this suggests that populations of adult parasites in individual mice are subject to continual recruitment and mortality. We discounted parasite-induced host mortality as the major cause of the convex profiles of change in mean parasite burden with duration of exposure (=mouse age) (Fig. 1a in ref. 17) as at all sampling points in the trickle studies, the distribution of worm numbers per mouse

in each sample remained Poisson in form (as predicted by stochastic models of immigration-death processes<sup>18</sup>). Within a cohort of inbred mice repeatedly exposed to the same level of infection, underdispersion in parasite numbers per host would have resulted, especially in the latter part of the experiment when mean worm burdens declined, if the host mortality were linked directly to worm burden<sup>19</sup> (the rapid elimination of heavily infected animals acting to decrease the variance within a sample).

More generally, we agree that mice are not ideal models for the study of schistosome infections of man. However, our aim was to show that experimental studies of immunity to helminth parasites, based on repeated exposure to low levels of infection (as is thought to occur in human communities within areas of endemic infection), produce results that are not always in accord with more conventional experimental designs based on primary infection and a single subsequent challenge.

R. M. ANDERSON  
J. A. CROMBIE

*Department of Pure and Applied Biology,  
Imperial College,  
University of London,  
London SW7 2BB, UK*

R. M. MAY

*Department of Biology,  
University of Princeton,  
Princeton,  
New Jersey 08540, USA*

## Cause of the 'inhibitor' phenotype in the haemophiliacs

Following the paper by Gitschier *et al.*<sup>1</sup>, we feel that a brief comment on their data and our earlier findings in haemophilia B<sup>2</sup> may help to clarify, or generate ideas that may lead to a better understanding of, the causes of the 'inhibitor' phenotype, a necessary step in the development of a completely successful treatment.

In 1983 we reported gross gene deletions in four out of five haemophilia B patients with the inhibitor phenotype, in support of the hypothesis that haemophilia B patients with inhibitors are predisposed to develop antibodies to factor IX as a result of mutations that prohibit the synthesis of a sufficiently normal factor IX protein and thus prevent the development of immune tolerance to normal factor IX. Of course, whether such a predisposition results in the inhibitor complication may depend on other factors such as the patient's genetic background and environmental experience: for example, the intensity and duration of treatment with normal coagulants. In four of our patients the predisposing mutation was a deletion of two-thirds or more of the factor IX coding sequence, but, of course, point mutations, frameshift mutations or shorter deletions could have had the same effect if they had occurred at positions which prevented the synthesis of a protein capable of inducing immune tolerance to normal factor IX. For example, the predisposing mutations might interfere with synthesis or processing of RNA, or might be mutations that affect the translation of messenger RNA into protein.

Previously, we predicted that gross changes of the factor VIII(c) gene might be found in haemophilia A patients with inhibitors. Now, Gitschier *et al.*<sup>1</sup> report a patient with a deletion involving exon 26 which codes for the last 51 amino acids of factor VIII, and another with an aberrant translation stop codon arresting translation of the factor VIII mRNA 26 amino acids prematurely, neither of which are associated with antibodies to factor VIII. Conversely, a patient with a different aberrant stop codon generating a truncated protein that is 124 amino acids short and another patient with a deletion comprising exons 23–25 which code for 157 amino acids, have both developed inhibitors. Such results seem in keeping with our observations in haemophilia B, since the loss of normal factor VIII epitopes in the latter two cases would be expected to be greater than in the first two cases of Gitschier *et al.*<sup>1</sup>, and hence more likely to result in defective immune tolerance to normal factor VIII.

In haemophilia B four further inhibitor patients have shown gross gene deletions: one in the United Kingdom<sup>3</sup> and three in Italy (H. J. Hassan *et al.*, F. Bernardi *et*

*al.* and M. Pecorara *et al.*, personal communications). These findings, of course, are at variance with the results of Gitschier *et al.* in haemophilia A, as many of their inhibitor patients did not show easily detectable gene defects. However, this is not the crux of the matter. What matters is whether the inhibitor complication arises in patients with mutations preventing the development of immune tolerance or not. In other words, is the discrepancy between the findings in haemophilia A and B principally a result of a more complex aetiology of the inhibitor complication in haemophilia A or caused by the plurality of factor VIII defects which can prevent the development of immune tolerance to normal factor VIII, in keeping with the example of haemophilia B?

We believe that the characterization of both the gene defects and the epitope specificity of the antibodies against factor VIII found in inhibitor patients would clarify the situation and reveal important immunological features of this coagulation factor.

F. GIANNELLI  
*Paediatric Research Unit,  
United Medical Schools of  
Guy's and St Thomas's Hospitals,  
Guy's Tower, London Bridge,  
London SE1 9RT, UK*

G. G. BROWNLEE  
*Sir William Dunn School of Pathology,  
South Parks Road,  
Oxford OX1 5RE, UK*

1. Gitschier, J. *et al.* *Nature* **315**, 427–430 (1985).
2. Giannelli, F. *et al.* *Nature* **303**, 181–182 (1983).
3. Peake, I. R., Furlong, B. L. & Bloom, A. L. *Lancet* **i**, 242–243 (1984).

### Copies of articles from this publication are now available from the UMI Article Clearinghouse.

Yes! I would like to know more about UMI Article Clearinghouse. I am interested in electronic ordering through the following system(s):

- DIALOG/Dialorder       ITT Dialcom  
 OnTyme       OCLC ILL Subsystem  
 Other (please specify) \_\_\_\_\_  
 I am interested in sending my order by mail.  
 Please send me your current catalog and user instructions for the system(s) I checked above.

Name \_\_\_\_\_

Title \_\_\_\_\_

Institution/Company \_\_\_\_\_

Department \_\_\_\_\_

Address \_\_\_\_\_

City \_\_\_\_\_ State \_\_\_\_\_ Zip \_\_\_\_\_

Phone (\_\_\_\_\_) \_\_\_\_\_

**UMI Article  
Clearinghouse**

Mail to: University Microfilms International  
300 North Zeeb Road, Box 91 Ann Arbor, MI 48106

## Mathematics

**Calculus.** By HARLEY FLANDERS. W.H. Freeman: 1985. Pp. 984. ISBN 0-7167-1643-7. Np.

**Graph Theory With Applications to Algorithms and Computer Science.** Y. ALVI, G. CHARTRAND, L. LESNIAK, D.R. LICK and G.E. WALL (eds). Wiley: 1985. Pp. 810. Hbk ISBN 0-471-81635-3. £46.

**Integration Theory.** Vol. 1. Measure and Integral. By CORNELIU CONSTANTINESCU and KARL WEBER. Wiley: 1985. Pp. 520. ISBN 0-471-04479-2. £50.65.

**Oxford Logic Guides, Vol. 12: Boolean-Valued Models and Independence Proofs in Set Theory,** 2nd Edn. By J.L. BELL. Clarendon Press: 1985. Pp. 165. ISBN 0-19-853241-5. £16.

**Principia Mathematica.** By ISAAC NEWTON. Christian Bourgois Editrice: 1985. Pp. 376. Pbk ISBN 2-267-00425-9. Np.

## Astronomy

**Anuario del Observatorio Astronómico 1985.** INSTITUTO GEOGRÁFICO NACIONAL. Talleres del Instituto Geográfico, Madrid: 1985. Pp. 502. ISBN 84-505-1088-0. Pts 400.

**Astronomy and Astrophysics Abstracts, Vol. 38.** S. BOHME et al. (eds). Springer-Verlag: 1984. Pp. 919. ISBN 3-540-15562-7/0-387-15562-7. DM 189.

**Astronomy and Astrophysics Publications from D. Reidel Publishing Company, Fall 1985.** D. Reidel: 1985. Pp. 200. Pbk np.

**The Atmosphere of Venus: Recent Findings.** G.M. KEATING, A.J. KLIORÉ and V.I. MOROZ (eds). Pergamon: 1985. Pp. 201. Pbk ISBN 0-08-033223-4. Np.

**Birth and Infancy of the Stars.** Proceedings of the Les Houches Summer School, Session XLI, 8 August–2 September, 1983. Elsevier: 1985. Pp. 846. Hbk ISBN 0-444-86917-4. Dfl. 430. \$159.25.

**Glimpsing an Invisible Universe: The Emergence of X-Ray Astronomy.** By RICHARD F. HIRSH. Cambridge University Press: 1985. Pp. 186. Pbk ISBN 0-521-31232-9. Pbk £8.95.

**Ices in the Solar System.** JÜRGEN KLINGER et al. (eds). Reidel: 1985. Pp. 954. ISBN 90-277-2062-2. Dfl. 290, \$99, £80.50.

**Planetary Landscapes.** By R. GREELEY. Allen & Unwin: 1985. Pp. 265. Hbk ISBN 0-04-551080-6. £44.95.

**Protostars and Planets II.** DAVID C. BLACK and MILDRED SHAPLEY MATTHEWS (eds). University of Arizona Press: 1985. Pp. 1293. Hbk ISBN 0-8165-0950-6. \$45.

**Venus: An Errant Twin.** By ERIC BURGESS. Columbia University Press: 1985. Pp. 160. Hbk ISBN 0-231-05856-X. \$29.95.

## Physics

**Advances in Infrared and Raman Spectroscopy, Vol. 12.** R.J.H. CLARK and R.E. HESTER (eds). Wiley: 1985. Pp. 360. ISBN 0-471-90674-3. £72.

**Applications of Plasma Processes to VLSI Technology.** TAKUO SUGANO (ed.). Wiley: 1985. Pp. 394. Hbk ISBN 0-471-86960-0. £46.

**Applied Classical Electrodynamics, Vol. 1: Linear Optics.** F.A. HOPF and G.I. STEGEMAN. Wiley: 1985. Pp. 262. Hbk ISBN 0-471-82788-6. £30.65.

**Classical Electrodynamics.** By ROMAN S. INGARDEN and ANDREJ Z. JAMIOLKOWSKI. Elsevier: 1985. Pp. 350. ISBN 0-444-99604-4. \$86.50.

**Computer Aided Chemical Thermodynamics of Gases and Liquids: Theory, Models, Programs.** By PAUL BENEDEK and FERENC OLTI. Wiley: 1985. Pp. 731. Hbk ISBN 0-471-87825-1. £86.95.

**Current Topics in Photovoltaics.** T.J. COUTTS and J.D. MEAKIN (eds). Academic: 1985. Pp. 279. ISBN 0-12-193860-3. £62, £50.

**Diffractive Processes in Nuclear Physics.** By W.E. FRAHN. Oxford University Press: 1985. Pp. 179. ISBN 0-19-851512-X. £22.50.

**Galaxies, Axisymmetric Systems and Relativity.** M.A.H. MACCALLUM (ed.). Cambridge University Press: 1985. Pp. 300. Hbk ISBN 0-521-30812-7. £25, \$49.50.

**High-energy Ion–atom Collisions, Second Workshop.** D. BERÉNYI and G. HOCK (eds). Akadémiai Kiadó, Budapest: 1985. Pp. 306. ISBN 963-05-4091-6. £28.50.

**Integral Systems in Statistical Mechanics.** G.M. D'ARIANO, A. MONTORSI and M.G. RASETTI (eds). World Scientific: 1985. Pp. 169. ISBN 9971-978-11-3. £29.65.

**Introduction to Magnetic Recording.** ROBERT M. WHITE (ed.). Institute of Electrical and Electronics Engineers: 1985. Pp. 307. ISBN 0-87942-184-3. Np.

**Memory Function Approaches to Stochastic Problems in Condensed Matter.** M.W. EVANS, P. GRIGOLINI and G. PASTORI PARRAVICINI (eds). Wiley: 1985. Pp. 556. Hbk ISBN 0-471-80482-7. £86.90.

**The Metallic and Nonmetallic States of Matter.** P.P. EDWARDS and C.N.R. RAO (eds). Taylor & Francis: 1985. Pp. 427. Hbk ISBN 0-85066-321-0. £40.

**Multiple Photon Infrared Laser Photophysics and Photochemistry.** By V.N. BAGRATASHVILI, V.S. LETOKHOV, A.A. MAKAROV and E.A. RYABOV. Harwood Academic Publishers: 1985. Pp. 512. Hbk ISBN 3-7186-0296-5. \$65.

**Nonequilibrium Phonon Dynamics.** WALTER E. BRON (ed.). Plenum: 1985. Pp. 679. ISBN 0-306-42008-2. \$97.50.

**Perspectives in Particles and Fields.** Cargese 1983. MAURICE LEVY, JEAN LOUIS BASDEVANT, DAVID SPEISER, JACQUES WEYERS, MAURICE JACO and RAYMOND GASTMANS (eds). Plenum: 1985. Pp. 598. Hbk ISBN 0-306-42067-8. Np.

**Phenomena Induced by Intermolecular Interactions.** Nato ASI Series. G. BIRNBAUM (ed.). Plenum: 1985. Pp. 792. Hbk ISBN 0-306-42071-6. Np.

**Physics of Disordered Materials.** DAVID ADLER, HELLMUT FRITZSCHE and STANFORD R. OVSHINSKY (eds). Plenum: 1985. Pp. 850. ISBN 0-306-42074-0. Np.

**Problems and Solutions in Electromagnetic Theory.** By C.M. LERNER. Wiley: 1985. Pp. 614. Pbk ISBN 0-471-88678-5. £35.75.

**Rates of Phase Transformations.** By R.H. DORE-MUS. Academic: 1985. Pp. 176. Hbk ISBN 0-12-220530-8. £26, \$29.

**Solid-State Sciences, Vol. 31. Statistical Physics II: Nonequilibrium Statistical Mechanics.** Springer-Verlag: 1985. Pp. 279. ISBN 3-540-11461-0/0-387-11461-0. DM 98.

**Spherical Harmonics and Tensors for Classical Field Theory.** By M.N. JONES. Research Studies Press: 1985. Pp. 230. ISBN 0-86380-028-9. £28.90.

**Springer Series in Optical Sciences: Integrated Optics.** H.P. NOLTING and R. ULRICH (eds). Springer-Verlag: 1985. Pp. 242. ISBN 3-540-15537-6/0-387-15537-6. DM 62.

**Tetrahedrally-Bonded Amorphous Semiconductors.** DAVID ADLER and HELLMUT FRITZSCHE (eds). Plenum: 1985. Pp. 564. ISBN 0-306-42076-7. Np.

**Theory of Heavy Fermions and Valence Fluctuations.** Springer Series in Solid-State Sciences 62. T. KASUYA and T. SASO (eds). Springer-Verlag: 1985. Pp. 287. Hbk ISBN 3-540-15922-3. DM 75.

**The Theory of Thermodynamics.** By J.R. WALDRAM. Cambridge University Press: 1985. Pp. 336. ISBN 0-521-24575-3. Np.

## Chemistry

**Advances in Organometallic Chemistry, Vol. 24.** Academic: 1985. Pp. 470. ISBN 0-12-031124-0. \$79.50, £69.

**Adventures with Atoms and Molecules: Chemistry Experiments for Young People.** By ROBERT C. MEBANE and THOMAS R. RYBOLD. Enslow: 1985. Pp. 82. ISBN 0-89490-120-6. £10.95.

**Aspects of Chemical Evolution.** By G. NICOLIS. Wiley: 1985. Pp. 286. ISBN 0-471-88405-7. £52.25.

**Handbook of Aqueous Electrolyte Solutions: Physical Properties, Estimation and Correlation Methods.** By A.L. HORVATH. Ellis Horwood: 1985. Pp. 631. Hbk ISBN 0-85312-894-4. £69.50.

**Heterogeneous Catalysis with Compounds of Rhodium and Iridium.** By RONALD S. DICKSON. D. Reidel: 1985. Pp. 278. Hbk ISBN 90-277-1880-6. Dfl. 135, £37.50, \$44.50.

**Improved Hollow Cathode Lamps for Atomic Spectroscopy.** SERGIO CAROLI (ed.). Ellis Horwood: 1985. Pp. 232. ISBN 0-85312-707-7. £35.

**Instrumental Methods in Electrochemistry.** SOUTHAMPTON ELECTROCHEMISTRY GROUP. Ellis Horwood: 1985. Pp. 443. ISBN 0-85312-875-8. \$49.50.

**Molecular Spectroscopy: Modern Research, Vol. III.** K. NARAHARI RAO (ed.). Academic: 1985. Pp. 452. ISBN 0-12-580643-4. \$85, £85.

**Structural Chemistry of Silicates: Structure, Bonding and Classification.** By FRIEDRICH LIEBAU. Springer-Verlag: 1985. Pp. 347. Hbk ISBN 3-540-13747-5. DM 163.

## Technology

**Dictionary of Robotics.** By HARRY WALDMAN. Collier Macmillan: 1985. Pp. 303. Hbk ISBN 0-02-948530-4. £35.

**Horticultural Engineering Technology: Field Machinery.** By R. BALLS. Macmillan, London: 1985. Pp. 216. Pbk ISBN 0-333-36434-1. Pbk £12.50.

**The Manufacture of Soaps, Other Detergents and Glycerine.** By EDGAR WOOLLATT. Ellis Horwood, Chichester, UK: 1985. Pp. 473. Hbk ISBN 0-85312-567-8. £55.

**Microcircuit Engineering 84.** A. HEUBERGER and H. BENEKING (eds). Academic: 1985. Pp. 563. ISBN 0-12-345750-5. \$35, £29.

**Process Engineering Developments: The Subject Groups Symposium, Multi-Stream 85.** INSTITUTION OF CHEMICAL ENGINEERS. Pergamon Press: 1985. Pp. 398. ISBN 0-08-031445-7. \$27, £22.50.

**Radioisotope Techniques for Problem-Solving in Industrial Process Plants.** J.S. CHARLTON (ed.). Leonard Hill: 1986. Pp. 320. Hbk ISBN 0-249-44171-3. £35.

**Research Techniques in Nondestructive Testing, Vol. VIII.** R.S. SHARPE (ed.). Academic: 1985. Pp. 479. ISBN 0-12-639058-4. \$99, £90.

**Rock Grouting, With Emphasis on Dam Sites.** By F.-K. EWERT. Springer-Verlag: 1985. Pp. 420. Hbk ISBN 3-540-15252-0. DM 175.

**Satellite Broadcasting Systems: Planning and Design.** By J.N. SLATER and L.A. TRINOGGA. Ellis Horwood: 1985. Pp. 168. Hbk ISBN 0-85312-864-2. £18.50.

## Computer Science

**How to Write a Usable User Manual.** By EDMOND H. WEISS. ISI Press: 1985. Pp. 197. Pbk ISBN 0-89495-052-5. Pbk £14.95.

**Interface Fundamentals in Microprocessor-Controlled Systems.** By CHRIS J. GEORGOPoulos. D. Reidel: 1985. Pp. 364. Hbk ISBN 90-277-2127-0. Dfl. 90, £24.95, \$32.

## Earth Sciences

**Discours Sur les Révolutions de la Surface du Globe.** By GEORGES CUVIER. Christian Bourgois Editore: 1985. Pp. 335. Pbk ISBN 2-267-00424-0. Np.

**Evolution of Archean Supracrustal Sequences.** L.D. AYRES, P.C. THURSTON, K.D. CARD and W. WEBER (eds). Geological Association of Canada: 1985. Pp. 380. ISBN 0-919216-24-2. \$45.

**Geological Factors and the Evolution of Plants.** BRUCE H. TIFFNEY (ed.). Yale University Press: 1985. Pp. 294. Hbk ISBN 0-300-03304-4. £25.

**Geology and Mineral Resources of West Africa.** J.B. WRIGHT (ed.). Allen & Unwin: 1985. Pp. 187. ISBN 0-04-556001-3. £30.

**Geology for Civil Engineers, 2nd Edn.** By A.C. MCLEAN and C.D. GRIBBLE. *Allen & Unwin*:1985. Pp.314. ISBN 0-04-624006-3. Hbk £20; pbk £9.95.

**Geology in Petroleum Production.** By A.J. DIK-KERS. *Elsevier*:1985. Pp.240. Hbk ISBN 0-444-42450-4. Dfl. 120, \$44.50.

**Historical Events and People in Geosciences.** WILFRIED SCHRÖDER (ed.). *Verlag Peter Lang, Postfach 277, CH-3000, Bern 15, Switzerland*:1985. Pp.220. Pbk ISBN 3-8204-7472-2. Pbk SwFr. 48, \$20.85.

**Ingenieur-geologische Probleme im Grenzbereich zwischen Locker und Festgestein.** KARL-HEINRICH HEITFELD (ed.). *Springer-Verlag*:1985. Pp. 695. Pbk ISBN 3-540-15366-7. DM 148.

**Phytogeomorphology.** By J.A. HOWARD and C.W. MITCHELL. *Wiley*:1985. Pp.222. Hbk ISBN 0-471-09914-7. £46.

**Soil Erosion and Conservation.** S.A. EL-SWAIFY, W.C. MOLDENHAUER and ANDREW LO (eds). *Soil Conservation Society of America*:1985. Pp.793. ISBN 0-935734-11-2. \$35.

**South African Ocean Colour and Upwelling Experiment.** L.V. SHANNON (ed.). *Sea Fisheries Research Institute, Capetown, South Africa*:1985. Pp.270. Hbk ISBN 0-621-07386-5. Np.

**Tectonic Geomorphology.** M. MORISAWA and J.T. HACK (eds). *Allen & Unwin*:1985. Pp.390. ISBN 0-04-551098-9. £25.

**Turbulence in the Ocean.** By A.S. MONIN and R.V. OZMIDOV. *D. Reidel*:1985. Pp.247. Hbk ISBN 90-277-1735-4. Np.

**A Stratigraphical Index of Conodonts.** A.C. HIGGINS and R.L. AUSTIN (eds). *Ellis Horwood, Chichester, UK*:1985. Pp.263. Hbk ISBN 0-85312-641-0. £27.50.

## Environmental Sciences

**Acid Rain: Economic Assessment.** PAULETTE MANDELBAUM (ed.). *Plenum*:1985. Pp.287. Hbk ISBN 0-306-42102-X. Np.

**Air Pollutants Effects on Forest Ecosystems. The Acid Rain Foundation**:1985. Pp.439. \$45.

**The Assessment and Control of Major Hazards.** INSTITUTION OF CHEMICAL ENGINEERS. *Pergamon*:1985. Pp.454. ISBN 0-08-031444-9. £30, \$36.

**Determination of Organic Substances in Water, Vol. 2.** By T.R. CROMPTON. *Wiley*:1985. Pp.518. ISBN 0-471-90469-4. £49.95.

**Environmental Policies: An International Review.** CHRIS C. PARK (ed.). *Croom Helm, Kent, UK*:1985. Pp.315. Hbk ISBN 0-7099-2062-8. £22.50.

**Mutagenicity Testing in Environmental Pollution Control.** F.K. ZIMMERMANN and R.E. TAYLOR-MAYER (eds). *Wiley*:1985. Pp.195. ISBN 0-85312-681-X. £27.50.

**Regulating Industrial Risks: Science, Hazards and Public Protection.** HARRY OTWAY and MALCOLM PELETU (eds). *The Butterworth Group, Kent, UK*:1985. Pp.181. Hbk ISBN 0-408-00740-0. £25.

**Selected Methods of Trace Metal Analysis. Biological and Environmental Samples.** By JON C. VAN LOON. *Wiley*:1985. Pp.357. Hbk ISBN 0-471-89634-9. £56.25.

## Biological Sciences

**Aphasia and Brain Organization.** By IVAR REIN-VANG. *Plenum*:1985. Pp.195. ISBN 0-306-41975-0. Np.

**Arbrégé de Zoologie. 2. Vertébrés.** By P.P. GRASSE. *Masson*:1985. Pp.184. Pbk ISBN 2-225-80576-8. F 100.

**Atherosclerosis Reviews. Arachidonic Acid Metabolites.** Vol. 13. RUTH JOHNSSON HEGYELI (ed.). *Raven Press*:1985. Pp.182. Hbk ISBN 0-88167-131-2. \$49.50.

**Behaviour and Pathology of Aging in Rhesus Monkeys.** ROGER D. DAVIS and CHARLES W. LEATHERS (eds). *Alan R. Liss*:1985. Pp.380. Hbk ISBN 0-8451-3407-8. £67.00.

**Biology of Invertebrate and Lower Vertebrate Collagens.** NATO ASI Series. A. BAIRATI and R. GARRONE (eds). *Plenum*:1985. Pp.583. Hbk ISBN 0-306-42078-3. Np.

**Biology of the Reptilia.** CARL GANS, FRANK BILLETT and PAUL F.A. MADERSON (eds). *Wiley*:1985. Pp.763. ISBN 0-471-81358-3. £86.90.

**Body and Self: Elements of Human Biology, Behaviour, and Health.** By GEORGE BLOCH, W.H. FREEMAN:1985. Pp.313. ISBN 0-86576-041-1. £17.95.

**Calcium and Cell Physiology.** DIETER MARME (ed.). *Spring-Verlag*:1985. Pp.390. ISBN 3-540-13841-2/387-13841-2. DM 128.

**Cancer Biology: Readings from Scientific American. Introductions by ERROL C. FREIDBERG, W.H. FREEMAN**:1985. Pp.156. Pbk ISBN 0-7167-1751-4. Pbk \$12.95.

**Cell Transformation.** J. CELIS and A. GRAESSMANN (eds). *Plenum*:1985. Pp.321. Hbk ISBN 0-306-42082-1. Np.

**Coléoptères Scarabaeoidea.** By J. BARAUD. *Editions Lechevalier, Paris*:1985. Pp.651. Hbk ISBN 2-7205-0517-X. Np.

**Common Seaweeds of China.** C.K. TSENG (ed.). *Science Press, Beijing/Kugler, Amsterdam, The Netherlands*:1985. Pp.316. ISBN 90-6299-012-6. Dfl. 400.

**Control of Leaf Growth.** N.R. BAKER, W.J. DAVIES and C.K. ONG (eds). *Cambridge University Press*:1985. Pp.350. ISBN 0-521-30480-6. £22.50.

**Developmental Biology.** By SCOTT F. GILBERT. *Blackwell*:1985. Pp.726. ISBN 0-87893-246-1. Np.

**Developmental Biology of Higher Fungi.** D. MOORE et al. (eds). *Cambridge University Press*:1985. Pp.615. ISBN 0-521-30161-0. Np.

**Developments in Biological Standardization.** R. SPIER, B. GRIFFITHS and W. HENNESSEN (eds). *Karger*:1985. Pp.546. Pbk ISBN 3-8055-4043-4. Pbk DM 168, \$59.75.

**Energetics of the Photosynthesizing Plant Cell.** By L.N. BELL. *Harwood*:1985. Pp.402. ISBN 3-7186-0195-8. \$175.

**Evolutionary Relationships Among Rodents: A Multidisciplinary Analysis.** W. PATRICK LUCKETT and JEAN-LOUIS HARTENBERGER (eds). *Plenum*:1985. Pp.721. ISBN 0-306-42061-9. \$110.

**Extracellular Matrix: Structure and Function.** A. HARI REDDI (ed.). *Alan R. Liss*:1985. Pp.462. Hbk ISBN 0-8451-2624-5. £73.00.

**Fat-Soluble Vitamins: Their Biochemistry and Applications.** ANTHONY T. DIPLOCK (ed.). *Heinemann*:1985. Pp.319. ISBN 0-434-90312-4. £22.

**Fish Immunology.** MARGARET J. MANNING and MARY F. TATNER (eds). *Academic*:1985. Pp.374. Hbk ISBN 0-12-469230-3. £27.00, \$32.50.

**Flying Squirrels: Gliders in the Dark.** By NANCY WELLS-GOSLING. *Smithsonian Institution Press*:1985. Pp.128. ISBN 087474-952-2. \$24.95.

**Form and Function in Birds, Vol. 3.** A.S. KING and J. McLELLAND (eds). *Academic*:1985. Pp.522. Hbk ISBN 0-12-407503-7. £90.00, \$99.50.

**Frankia and Actinorhizal Plants: Developments in Plant and Soil Sciences, Vol. 18.** M. LALONDE, C. CÁMIRE and J.O. DAWSON (eds). *Martinus Nijhoff/Dr W. Junk*:1985. Pp.208. Hbk ISBN 90-247-3214-X. Dfl.120, £33.25, \$45.00.

**From Laurel Hill to Siller's Bog. The Walking Adventures of a Naturalist.** By JOHN K. TERRES. *Algonquin Books of Chapel Hill, PO Box 2225, Chapel Hill, North Carolina, USA*:1985. Pp.227. Pbk ISBN 0-912697-26-1. \$12.95.

**Frontiers in Histamine Research: A Tribute to Heinz Schild.** C.R. GANELLIN and J.C. SCHWARTZ (eds). *Pergamon*:1985. Pp.442. ISBN 0-08-031989-0. \$80.

**Frontiers in Physiological Research.** D.G. GARLICK and P.I. KORNER (eds). *Cambridge University Press*:1985. Pp.391. ISBN 0-521-26838-9. £67.50, \$95.

**Fungal Dimorphism, with Emphasis on Fungi Pathogenic for Humans.** PAUL J. SZANISZLO (ed.). *Plenum*:1985. Pp.395. Hbk ISBN 0-306-42020-1. Np.

**Hormonal Regulation of Plant Growth and Development.** S.S. PUROHIT (ed.). *Martinus Nijhoff*:1985. Pp.412. ISBN 90-247-3198-4. Dfl. 200, \$69.50, £55.50.

**Hormones and Cell Regulation: European Symposium, Vol. 9.** J.E. DUMONT, B. HAMPRECHT and J. NUNEZ (eds). *Elsevier*:1985. Pp.430. ISBN 0-7204-0657-9. \$89.

**The Illustrated Encyclopedia of Dinosaurs.** By DR DAVID NORMAN. *Salamander Books, London, UK*:1985. Pp.208. Hbk ISBN 0-86101-225-9. £9.95.

**The Illustrated Tarka the Otter.** By HENRY WILLIAMSON. *Webb & Bower*:1985. Pp.207. £12.95.

**Immunological Methods, Vol. 3.** IVAN LEFKOVITS and BENVENUTO PERNIS (eds). *Academic*:1985. Pp.477. Hbk ISBN 0-12-442703-0. £48.50, \$54.50.

**Institute of Terrestrial Ecology: Annual Report 1984.** *Natural Environment Research Council*:1985. Pp.188. ISBN 0-904282-84-8. Np.

**International Review of Cytology, Vol. 93. Genome Evolution in Prokaryotes and Eukaryotes.** D.C. REANEY and P. CHAMBON. *Academic*:1985. Pp.367. ISBN 0-12-364493-3. \$49.50, £49.50.

**Islands in the Bush: A Natural History of the Kora National Reserve, Kenya.** By MALCOLM COE. *George Philip*:1985. Pp.240. ISBN 0-540-01086-3. £14.95.

**The Living Isles: A Natural History of Britain and Ireland.** By PETER CRAWFORD. *BBC Books*:1985. Pp.320. Hbk ISBN 0-563-20369-2. £14.95.

**Longman Illustrated Dictionary of Biology: Living Organisms in All Forms Explained and Illustrated.** By NEIL CURTIS. *Longman*:1985. Pp.256. ISBN 0-582-82554-4. £3.95.

**Longman World Guide to Mammals.** PHILIP WHITFIELD (ed.). *Longman*:1985. Pp.198. ISBN 0-582-89211-2. £12.95.

**Microenvironments in the Lymphoid System.** G.G.B. KLAUS (ed.). *Plenum*:1985. Pp.1080. ISBN 0-306-41917-3. Np.

**Multiple Choice Questions in Neurophysiology with Answers and Explanatory Comments.** By LYNN BINDMAN and PETER ELLAWAY. *Edward Arnold*:1985. Pp.93. Pbk ISBN 0-7131-4474-2. Pbk £3.95.

**The Natural History of Otters.** By PAUL CHANIN. *Croom Helm*:1985. Pp.179. ISBN 0-7099-3460-2. £7.95.

**The Nature Watchers: Exploring Wildlife with the Experts.** By R. BROWN and J. PETTIFER. *Collins*:1985. Pp.240. Hbk ISBN 0-00-219149-0. £12.00.

**The Neuropsychology of Individual Differences: A Developmental Perspective.** LAWRENCE C. HARTLAGE and CATHY F. TELZROW (eds). *Plenum*:1985. Pp.329. ISBN 0-306-41986-6. \$35.

**The New Theory of Respiratory Dynamics.** By A. GONZALEZ-BOGEN. *Universidad Central de Venezuela, Epociones de la Biblioteca, Caracas*:1985. Pp.141. Pbk ISBN 3125901. Np.

**Notes of an Anatomist.** By F. GONZEZ-CRUSSI. *Harcourt Brace Jovanovich*:1985. Pp.144. ISBN 0-15-167285-7. \$12.95.

**Nuclear Envelope Structure and RNA Maturation.** EDWARD A. SMUCKLER and GARY A. CLAWSON (eds). *Alan R. Liss*:1985. Pp.694. Hbk ISBN 0-8451-2625-3. £75.00.

**The Origins and Relationships of Lower Invertebrates.** S. CONWAY MORRIS, J.D. GEORGE, R. GIBSON and H.M. PLATT (eds). *Oxford University Press*:1985. Pp.397. ISBN 0-19-857181-X. £45.

**The Oxford Dictionary of Natural History.** MICHAEL ALLABY (ed.). *David Attenborough* (forward). *Oxford University Press*:1985. Pp.688. Hbk ISBN 0-19-217720-6. £20.00.

**Oxford Reviews in Reproductive Biology, Vol. 7.** J.R. CLARKE (ed.). *Clarendon Press*:1985. Pp.409. ISBN 0-19-857540-8. Np.

**People of the Desert and Sea. Ethnobotany of the Seri Indians.** By RICHARD FELGER and MARY BECK MOSER. *University of Arizona Press*:1985. Pp.435. \$65.

**The Physiological Development of Fetus and Newborn.** C.T. JONES and P.W. NATHANIELSZ (eds). *Academic*:1985. Pp.837. ISBN 0-12-389080-2. \$54, £49.

**Proteins of Iron Storage and Transport.** G. SPIK, J. MONTREUIL, R.R. CRICHTON and J. MAZURIER (eds). *Elsevier*:1985. Pp.380. Hbk ISBN 0-444-80722-5. Dfl. 198, \$73.25.

H-Battie  
94-8

## Turning point for nuclear power

*The British nuclear power programme is not alone by being in a mess, but its particular condition is a pointer to other faults in British industry — and to some general remedies.*

THAT British nuclear power has fallen on bad times is well known, but not on that account especially shameful; other nuclear power programmes are also in the doldrums. But the causes of the British condition may be different from those elsewhere, and may also typify the more general sense of being moribund that pervades a large part of British industry. That is one reading of the admirable report on radioactive waste produced last week by the House of Commons Environment Committee (HMSO, £9.85), which is a level-headed and perceptive account of one part of the problem. Particular recommendations apart, the document sustains the more general belief that the perennial faults of British heavy industry are mismanagement, indecisiveness and parsimony, all veiled from public scrutiny to such an extent that rational assessment of the zigzags of policy is virtually impossible.

The immediate British discontents have their origins in the well-documented sleep-walking decision of the first postwar British government to become, first, a military nuclear power and, then, a major producer of electricity from uranium. Then, two plutonium-producing reactors and a fuel reprocessing plant were built at a site called Windscale on the coast of Cumbria (as it now is) in north-west England. In 1957, less than two years after the Queen of Great Britain and Northern Ireland had opened on the same site the first of a chain of dual-purpose reactors (for making both electricity and plutonium), the fuel in one of the original reactors caught fire, releasing radioactivity (mostly iodine) in a much more serious nuclear accident than that at Three Mile Island a decade ago. Since then, Windscale has become a persistent source of public controversy about the leakage of radioactive materials, most but not all of which are inconsequential for the health of the general public and of those working at the plant. Much of this trouble is partly explained by the antiquity of the plant, the cramped condition of the Windscale site (now called Sellafield) and the degree to which its efficient management is hampered by the large amounts of radioactivity stored there, not merely in dedicated storage tanks and other facilities but in those patches of ground that have been contaminated by past accidents on the site. Yet within the past decade, the present owner of the site, nationalized British Nuclear Fuels Ltd, has embarked on the construction of a plant for reprocessing irradiated uranium oxide fuel, eventually to service British pressurized water reactors but, more immediately, to service reactors elsewhere in the world.

### Disposal

This state of affairs is one of the principal reasons why the House of Commons committee embarked on its inquiry in the first place, and why its inquiry is concerned chiefly with waste disposal. The first of the committee's recommendations, technical though it may seem, illustrates the temper of its report. Present practice at Sellafield, as elsewhere in the British nuclear industry, is to classify radioactive wastes as low-level, intermediate-level and high-level wastes; materials of the first kind are buried beneath earth in ground trenches, those of the second kind are stored in silos (but there are plans to compact them and embed them in retrievable concrete blocks) and those of the third kind

are stored in artificially cooled tanks pending incorporation into vitreous solids beginning in the 1990s. The distinction between the three categories is based on the instantaneous radioactivity of the materials, with some allowance for the separate properties of alpha and beta activity, as indeed radioactive waste materials have been classified for the past forty years in Britain. But why not, the committee asks, be more subtle and more sensitive, classifying materials according to the elemental source of their activity? For, as every schoolchild knows, there is a world of difference between the health hazard of a few microbecquerels of plutonium and of, say, strontium.

### Decisions

Much in the same vein, the committee argues that circumstances have changed since the decision to build the oxide-fuel plant at Windscale was taken in 1978. In particular, the market price of natural uranium has fallen sharply, chiefly as a reaction to the general slump of interest in nuclear power, so that the economic case for reprocessing nuclear fuel (for the sake of the plutonium that might itself be used as fuel in breeder reactors) has declined. This (see p.204) appears to be the basis for such opposition as remains to French activities of this kind, and the committee asks that the British government should mount an inquiry on the subject, reconsidering the decision to build the oxide plant if the economic case for going ahead is insubstantial. The committee's doubts are reasonable enough, but they have been given prominence in its report only because of the way in which each new reprocessing plant has come to seem a potential source of further unpredicted leaks of radioactivity, any one of which might be catastrophic. This, to the nuclear industry the most damaging of the committee's recommendations, is not so much an opinion about the economic justification of the reprocessing plant (whose builders say it will be paid for by contracts already signed) but a sign of diminished confidence in the managers of the plant to operate it safely.

But have not the dangers of reprocessing been exaggerated? That is the natural defensive reaction of the Sellafield managers. So they have, and the House of Commons committee implicitly agrees, especially in its condemnation of the role of the Greenpeace organization in giving public currency to an irresponsible newspaper fairy-tale (to the effect that the plant managers were planning a controlled experiment in which one group of children would be fed radioactive materials). Nor does the committee fall into the other familiar trap of supposing that because plutonium can be used for making nuclear weapons, it is somehow a contribution to a peaceful world if countries such as Britain refrain from extracting plutonium from their nuclear fuel (and which is part of the mistaken inspiration of the Carter Anti-Proliferation Act in the United States). The committee's unwillingness to be stampeded by exaggerations gives the general sense of its argument greater force.

The committee is at its best in its discussion of just this psychological point, the degree to which general opinions of an organization (or of a committee's report) are moulded by the spirit in which they are informed of it. The Sellafield managers have been given a rotten time, over the past several years, by the way

in which each tiny release of radioactivity, not necessarily to the environment at large, has been blown up by sensation-mongers. But the committee is right to imply that the industry has helped to bring these troubles on itself by being less than wholeheartedly informative about its own problems. It is one thing to respond truthfully and fully to inquiries about the radioactivity in the environment, which the British nuclear industry now does, and another to be actively concerned to see that the general public is fully aware not merely of the vast difference between the hazards of, say, radioactive argon emitted from all nuclear power station stacks and that of plutonium dust such as may be carried into the atmosphere from reprocessing works. What the committee says the industry should be doing is to help its taxpayer constituents appreciate both the subtleties of the biological effects of radiation and the difficulty of the technical problems it faces. If there is an unusual cluster of leukaemia cases on the Cumbrian coast, the Sellafield managers have every interest to be the first to investigate. If one of the reasons why the planned vitrification of high-level waste hangs fire is the likely exposure of workpeople to volatiles in the glass melt, there is nothing to be lost by saying so.

Timorousness of this kind is long since out of fashion, even in Britain, where traditionally it is born of the notion that the infallibility of organizations increases with their size and public importance. Especially because British Nuclear Fuels still handles military plutonium, and so is able to hug secrets to itself, it is especially prone to the tendency to believe that information about its affairs should be regulated by what it senses to be the need. Its perceptions have changed over the past decade, but there is still a long way to go before it will accept that to acknowledge the problems that exist is a necessary first step towards making the nuclear industry popular. Fair play, this is a trap into which many other British organizations have fallen.

How should the British government respond (as it must) to the committee's report? The first need is to decide whether there should be yet another inquiry into the proposal to build an oxide reprocessing plant. (That in the 1970s took two years.) The simple answer is that there need not be, but that it should not be beyond the wit of sensible people to devise clear lines of authority and responsibility within the nuclear fuel company to ensure that the plant is managed well — and that it will be evident whose head should roll if it is not. Second, the government should accept the committee's relatively minor proposals that sea dumping should be set aside for the time being, until the international diplomacy as well as the technical assessment of this procedure has been carried out. Most important, the government should decide (which seems to be its intention) that it will indeed sanction the building of more nuclear power stations once the report of the Layfield inquiry is available in the summer (five years after it was set up). There is nothing so likely to sap morale as to have nothing to do. But, even more important, the government must insist that the long-term problem of waste storage is tackled with the energy that it deserves. The nuclear industry has been talking of vitrification for years, and is especially eloquent when inquiries are being held, but British development on the process has hung fire while there is still no assurance that this process is the best.

How fair is it to generalize from the sad case of the nuclear industry, the feather in Britain's self-designed cap a mere thirty years ago, to British industry as a whole? The tendency towards secretiveness, especially about difficulties, is obvious. The habit of diluting both authority and responsibility for the successful management of important projects by allowing the intervention of boards of directors in matters outside their competence is commonplace. The general failure to recognize that long-term research may have a value that goes beyond the calculable economic return (in the nuclear case, by providing the public assurance without which nothing is possible) is another general failing. So, too, are the starts and stops of government policy, which ensure that successive governments change the economic

and social climate in which important industries must find a way to prosper. British nuclear engineers now envy their French colleagues and competitors. Should not British governments also seek to emulate the sense of continuity their French counterparts provide, not simply in the nuclear field? □

## Organization of research

*The chairman of Britain's smallest research council deserves an answer to an honest question.*

SIR Douglas Hague, the chairman of the British Economic and Social Research Council, will have lost more friends than he can have gained by his evidence to the House of Lords Select Committee on Science and Technology earlier this week (on 18 March) which is inquiring yet again into the organization of British civil science (perhaps because it had only a dusty answer from the government when it did so last, in 1981). For Hague is by reason of his office a member of the governing councils of British civil science, the Advisory Board for the Research Councils (which divides the civil science cake) in particular; there will be many who say that politeness requires people not to complain about the organizations to which they belong, as Hague did this week by saying publicly that the board has slipped into the habit of telling the research councils what to do, thus blunting the division of responsibility between them and itself.

Worse still, in the predictable opinion of some of those who will not be sending him Christmas cards in future, he endorsed a view put forward here at the end of last year that, in the interests of flexibility and of the academic research community which it exists to serve, the Science and Engineering Research Council should strive to make the Rutherford Appleton Laboratory a less conspicuous and costly part of its institutional overhead (see *Nature* 318, 587; 1985). Hague's particular anxiety is that the decision to spend £11 million on a new Cray computer for the laboratory will further enhance its permanence. In passing, he remarked on the anomaly that those who commit such sums to new projects, desirable though they may be, have rarely decided in advance which existing project they will axe in recompense.

It will be a great misfortune if this rough talk is set aside simply because it is rough. For the past decade, the British research community has been forced by an unsympathetic government to jump through a series of unwelcome and even damaging hoops, chiefly of a financial character. In many ways, the process of concentrating funds on fewer institutions and fewer people has been handled in such a way as to create diseconomies. The precipitate closing of laboratories has often, for example, meant that people who might have earned their salaries have instead been paid pensions for doing nothing. It is also probable that the attempt to drive academics into the arms of industry has been counterproductively vigorous. But none of these injustices can be welded into a case for supposing that the self-administration of science is beyond reproach. That is the essence of Hague's complaints this week.

What will the House of Lords make of it all? The case for nominating a political head of the research enterprise is as strong now as when the House of Lords made it five years ago. The greatest need is for some means of balancing the needs of civil and military research against each other. (Hague was asking, this week, why Britain has to spend 0.65 per cent of its Gross Domestic Product on public defence research and development when even France gets by on less.) There is also an urgent need to devise a mechanism for making sure that the research councils live up to their protestations, which have recently rightly tended to emphasize the importance and the need of support for academic science. Some, such as the agricultural and medical research councils, have made valiant if marginal efforts in this direction in the face of enormous difficulties, but for the system as a whole, run as it is by representatives of the research community, there is a long way to go. □

## Space shuttle

# No early prospects of decision on future flights

*Washington*

As the debate over how and whether to pay for a new space shuttle rages at the White House, the National Aeronautics and Space Administration (NASA) is trying to give shape to the agency's future in the post-Challenger era.

In testimony last week before the House Science and Technology Committee, NASA acting administrator William Graham made it clear that shuttle flights are unlikely to resume before next January. NASA estimates it will cost \$350 million over the next two years for "anomaly resolution activities".

NASA is already launched on an exhaustive safety analysis of shuttle systems. Although the presidential panel investigating the Challenger accident has yet to establish a cause, Graham conceded that changes in the solid rocket booster would probably be necessary and it would be "appropriate" to redesign the seal rings.

Even if the \$2,800 million needed for a new shuttle is found, \$750 million of which must come from the already tight 1987 budget, NASA will be able to operate only three shuttles between now and 1990. NASA plans to move slowly after shuttle flights resume, exacerbating the accumulating payload backlog. Graham hopes that commercial interests will operate expendable launch vehicles to relieve some of the burden on the shuttle, but he admitted that the current budget contains no money to help start such ventures.

Although members of the House committee are clearly anxious to allocate funds for building a new shuttle, a source close to the White House senior interagency group responsible for making a decision about the shuttle says no answer is likely until June, when the presidential panel makes its report. The interagency group is also wrestling with the thorny problem of which government agencies should be paying for shuttle services. The debate is being carried on by mid-level bureaucrats, but agency chiefs will soon be joining in.

Several members of the committee expressed concern that NASA might encourage potential shuttle customers to look elsewhere for launch services. But Graham confirmed that a proposal to carry the British Skynet satellites aboard the shuttle had already been terminated. With 32 launch commitments already on the books, Graham argued that NASA could not commit itself to others until the future of the shuttle was clear.

When flights do resume, priority will be

given to those carrying payloads "critical to national security priorities", followed by scientific launches with fixed launch windows, and finally all other flights specifically needing the capabilities of the shuttle. Both the Galileo mission (see below) and Ulysses, the European Space Agency (ESA) mission to explore the Sun's polar regions, have launch windows in June 1987, but Graham doubted that both could then be launched.

No matter what decisions are made about the shuttle, NASA plans to go ahead with the manned space station programme as scheduled. It is expecting to sign agreements shortly covering the parts of the space station on which Canada and Japan will work. Japan has been studying a multipurpose pressurized module, while Canada is developing a remote manipula-

tor system. But an agreement with ESA over European participation has hit a snag, and NASA administrators are working feverishly to hammer out an agreement before the end of March, when an engineering meeting will establish the space station baseline configuration.

As acting administrator, Graham has presided over NASA during its most difficult time. The agency's reputation has suffered as much of a setback as its flight schedule. The budget analyst whose July 1985 memorandum showed that NASA was aware of safety hazards in the solid rocket boosters said in a *Washington Post* article (16 March) that he had been asked to "deny the validity" of the memorandum, in ensuing press enquiries. In the article, the analyst denounces NASA for perpetuating a stubborn optimism that flies in the face of its employees' conscientious warnings.

James C. Fletcher, nominated by the White House to take over as permanent administrator of NASA, is said to have had little enthusiasm for the job, and agreed to accept it only after considerable persuasion.

Joseph Palca

## US space programme

### Delay not an unmixed curse

*Washington*

WHILE it will be for Washington to decide how the US space programme will be continued in the post-Challenger era, the managers of individual projects are having to arrange that spacecraft poised for launch later in this year will survive long and still unknown delays on the ground. But uncertainty about the likely launch time may bring some unexpected benefits.

This may be the case with the Hubble Space Telescope, which was to have been launched next August. The deadline for the submission of research proposals has now been put back, which may give the Space Telescope Institute time to resolve the dispute about allocations of observing time (see *Nature* 318, 591; 1985).

The extra ground-time will also give engineers a chance to reduce the risk of "infant mortality" among the components of the telescope. This term refers to the failure of electronic parts which is common in the early weeks of space missions. The remedy is to switch on instruments before the launching of a satellite or space-probe, to "burn in" the electronic circuits.

Even so, James Welch, the NASA (National Aeronautics and Space Administration) programme director for the space telescope, says it will "not be a trivial matter" to store "this beast" on the ground until shuttle flights can be resumed. Mechanical systems designed to function in microgravity environments may not fare so well at 1 g, while gyroscopes must be spun at regular intervals to

prevent the pooling of lubricants and so as to redistribute weight. Similarly, the light-amplification assemblage of the faint-object camera, which has been designed and built by the European Space Agency, will have to be powered up every 30 days so as to maintain the internal vacuum.

A further difficulty is that career advancement is unlikely while spacecraft sit on the ground, which means that project leaders may be tempted to try their luck elsewhere. The way in which long-term space projects may suffer, even after launch, is illustrated by the Voyager missions to the outer planets, which have had six project managers since their inception more than a decade ago.

Nevertheless, the hope is that professionals who have already devoted a large part of their career to a project will not be driven away by a delay of another year or two. Torrence Johnson, head of the Galileo mission to Jupiter, says that people working on such projects have learned to cope with the frustration of delay.

Part of the Galileo team will be kept busy recalculating the trajectory of the spacecraft. The next launch window will be in June 1987. The plan is that Galileo should make ten orbits around Jupiter in a period of 20 months, but all the orbits will be different from each other so as to maximize the number of jovian moons encountered. In a celestial version of a 12-cushion billiards shot, the spacecraft will be helped on its way by the gravitational influence of successive moons.

Joseph Palca

Halley's comet

## Giotto confirms reports of dumbbell-shaped nucleus

Darmstadt

THE notice DO NOT PANIC hung in one of the experimental areas here last week and, throughout a somewhat vertiginous approach by Giotto, the European Space Agency (ESA)'s spacecraft, to the core of comet Halley in the first few minutes of 14 March (GMT), and despite a loss of signal at closest approach, nobody did. And there, at last, was the nucleus. "It looks like a peanut", said one. "A potato", said another. And it is black.

It was the perfect day for an encounter. The solar wind was calm, with a speed of about  $380 \text{ km s}^{-1}$  with a steady interplanetary magnetic field of about 8 nanotesla. Earlier, there had been fears that solar activity might produce choppy electromagnetic conditions, in which case information from satellites such as the Solar Maximum Mission might have been essential to distinguish the effects of a gusty plasma environment from truly cometary phenomena.

Before the Giotto encounter, expectations were conditioned by the two Vega encounters the previous week (see *Nature* 320, 97; 1986). The Soviet chief scientist, Roald Sagdeev, had brought the news that Vega 2 had shown that the nucleus looked rather like a potato of maximum length 11 km. But there was some fear that the Vega detectors had been deceived by the variable brightness of the dust. "I'm convinced Vega saw the nucleus", said Fred Whipple, architect of the prevailing "dirty snowball" model; "there were earlier reports of a double nucleus, but the imaging people now say it's more like an irregular potato with two bright ends."

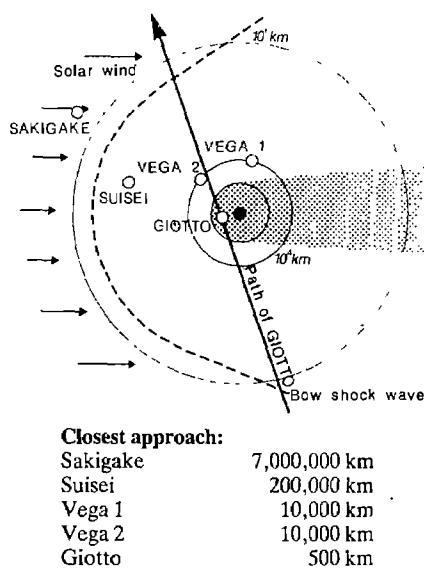
With its tenfold increase in resolution, Giotto could be expected to resolve the debate. Meanwhile, the dust specialists were perturbed but philosophical about reports from Japan of large and potentially disastrous dust particles detected by the Suisei spacecraft at the surprisingly large distance of more than 150,000 km from the nucleus (see *Nature* 320, 99; 1986).

In the event, Giotto first detected effects of the comet on its environment at a distance of 7.8 million km, with cometary ions and plasma waves becoming more and more noticeable. At this point, Giotto had entered the outer coma, a vast invisible cloud whose expansion is virtually unhindered by Halley's tiny gravity. Cometary hydrogen and oxygen atoms plus hydroxyl radicals began to be detected, the results of photodissociation of water vapour sublimed from the nucleus.

As the solar wind picks up such atoms, it is decelerated to a point (roughly corres-

ponding to a 25 per cent increase in mass loading) where a bow-shock should form, with a sudden change in flow conditions. There had been some debate whether such a shock had been detected at comet Giacobini-Zinner by the International Cometary Explorer. Pretty much on schedule, however, according to principal investigator Alan Johnstone, Giotto entered a weak bow-shock (or bow-wave) at 1.15 million km, extending along its trajectory over 0.5 million km or so. The spacecraft detected a shift in solar wind direction of about  $15^\circ$ , a slowing of helium ion speeds to  $260 \text{ km s}^{-1}$  and fluctuations in the magnetic field of up to 20 nanotesla.

The excitement became more noticeable with the first images from a distance



of 750,000 km though, with resolution of 50 km or so, the nucleus was not yet visible. The atmosphere was distinctly polyglot as collaborators from many parts of the globe began to pile into the surprisingly restricted space taken up by each of the ten experimental groups. By means of a direct link to Moscow, about 30 people there were also following the encounter.

At about 0.5 million km, the presence of cometary ions was much more pronounced. Here also, cometary chemistry began to be noticeable and, as its pick-up of heavy ions increased, the speed of the solar wind decreased further. "It's terrific, it's terrific", exclaimed one experimenter. But what about the dust? So far there was none, and principal investigator Tony McDonnell was discreetly beginning to wonder whether his impact detectors had failed. To his relief, the first particle finally arrived, detected on Giotto's front shield at about 200,000 km.

At about 48,000 km, the nucleus seemed to be resolved as an unchanging feature in the camera frame. A few minutes later came the first hint of trouble as the attitude sensor indicated a slight shift in the spin axis. But by now the instruments were working overtime as Giotto approached the nucleus from behind its left shoulder, as it were, and heading towards the Sun-side, from which most of the outflow of gas and dust occurs.

As Giotto's camera followed the changing relative position, its images were relayed live, every few seconds, to the watchers on the ground. A few minutes before the closest encounter, the region of the nucleus began rapidly to dominate the screen, and mottled features became apparent. It was a frankly emotional moment; the quiet voice of the scientific commentary began to shake with excitement and the assembly broke into applause. At about 5,000 km, the magnetometers saw the magnetic field vanish — Giotto had penetrated the ionopause where electrical currents carried by electrons and ions cancel the ambient field.

Almost to the second of closest encounter, at a distance of 605 km, the images ceased and the telemetry link at the 64-m Parkes radiotelescope in Australia lost contact with the spacecraft. Tony McDonnell later said, "we seemed to hit a wall of dust a few minutes before the encounter". The impact rate had then gradually increased from the already high rate of 120 per second to the point where the spacecraft suddenly went out of alignment. But in the belief that the spinning spacecraft had been knocked into a wobbling precession, damping manoeuvres were carried out and contact re-established after 30 min.

And the nucleus? According to the camera principal investigator Horst Uwe Keller, first indications are that it is 15 km long and at least 4 km wide, perhaps shaped like an indented potato or peanut shell. The loss of contact meant that only one side of the nucleus was seen, so that an accurate evaluation of the volume will not be possible, nor will the variation of the reflecting properties of nuclear material with Sun angle be fully known.

Nevertheless, surface features have been seen with a best resolution of 70 m. The nucleus is "blacker than coal", according to Keller, "similar to the lowest albedos yet seen in the Solar System". He says that the surface must be at least warm enough to melt ice. Fred Whipple believes that such an appearance could arise from ice embedded with a great deal of dust including carbon or organic material.

Perhaps the major surprise of the encounter, according to chief scientist R. Reinhard, was the great inhomogeneity of dust emission. To a much greater extent than expected, the dust outflow is concentrated in jets and there are indications of nozzle-like features on the surface. A

most important task will now be to match *in situ* observations of jets with those provided by the International Halley Watch network.

Analysis of mass spectrometry also proved exciting. "When we moved into the coma, we were overwhelmed by the richness of the neutral and ion spectra", said principal investigator D. Krarkowski. The major ions turned out to be those associated with water vapour,  $H_3O^+$  and  $H_2O^+$ , with a sharp increase in density to a plateau of about  $10^3$  per cubic centimetre at about 30,000 km; among the neutrals,  $H_2O$  reached  $10^8 \text{ cm}^{-3}$  at about 3,000 km. The total water outflow was estimated to be about  $2 \times 10^{30}$  molecules per second. Compounds of carbon, nitrogen and oxygen were also seen by optical spectrometry.  $C_2$  was found to be more abundant than  $CN$ , the latter and  $CO^+$  increasing from a distance of 150,000 km with a sharp rise in  $CO^+$  just before approach. Metal ions were also seen, though as H. Balsinger indicated, if the nucleus is a potato it is not a salty one; little sodium was seen.

The blackness of the nucleus may be linked to another surprise reported by Tony McDonnell — the presence of an unexpected population of dust with masses as small as  $10^{-17}$  grams. As Vega dust scientist J.S. Simpson remarked, most models predict a fall-off in dust masses below  $10^{-12}$  grams, but Vega and Giotto have indicated substantial numbers of smaller particles. It had been thought that such particles would have been expelled from the Solar System by radiation pressure before they could be incorporated into comets. The efficiency of such processes may now have to be re-evaluated in view of the photo-properties of the nucleus discovered by Giotto.

The density of each dust particle seems to have been less than that of water, indicating a porous structure, possibly with a solid core covered with an icy mantle.

Comparing the Giotto and Vega missions, Sagdeev said that the gas, dust and particle measurements showed very good correspondence while highlighting the variability of the neighbourhood of Halley's nucleus. The Giotto measurements of *in situ* chemistry should be matched with Vega's remote sensing spectrometers, whose resolution might permit investigation even closer to the nucleus than Giotto.

"The science was really great", he said. "After many sleepless nights, we have to part with the comet. We feel real nostalgia now which will last beyond Halley's next apparition."

Meanwhile, Giotto is still working, although with possible damage to the camera and altitude control. It is hoped to adjust its orbit, enabling it to use the Earth as a gravitational sling in 1990, perhaps to encounter comet Grigg-Skjellerup in 1992.

**Philip Campbell**

## NEWS

### Book conservation

## Red faces over US pilot plant

### Washington

An explosion and fire have raised design and safety questions about a book conservation process developed by the Library of Congress (LC) that supposedly presented "absolutely no safety risks to personnel or books". The process was designed to make book paper less acidic.

The explosion occurred at a pilot facility operated by Northrop Services Inc., under contract to the National Aeronautics and Space Administration (NASA) at the Goddard Space Flight Center in Greenbelt, Maryland. The facility was designed to support start-up of a \$11.5 million Mass Deacidification Facility for LC to be constructed at Fort Detrick, Maryland.

What started as a small leak of the chemical used in the deacidification process in early December ultimately resulted in the "controlled disassembly" of the entire system by a demolition team on 21 February.

Book deterioration caused by the high acid content of paper made from wood pulp is a serious problem for all libraries. To decrease the acid content, LC developed and patented a vapour phase process using diethyl zinc (DEZ). The process works by placing books in a vacuum chamber at 20 torr, removing most of the moisture from the books, then injecting gaseous DEZ into the chamber. The DEZ reacts with sulphuric acid in the paper, forming zinc sulphate and water, and the water then reacts with additional DEZ to form zinc oxide in the paper fibres. This provides an alkaline reserve against further acid degradation. Zinc carbonate, produced by adding carbon dioxide to the reaction, also buffers the paper, as well as providing some measure of protection against photodegradation of cellulose.

While the DEZ process has advantages over other liquid processes that have been developed, DEZ is a difficult material to work with. It is pyrophoric in its liquid state at room temperature, burning on contact with air and explosively decomposing on contact with water.

On 5 December, with the book chamber in the pilot facility empty, the system was put through its operational cycle. At the point where all DEZ should have either been recovered or vented, the door to the chamber was allowed to open. The technician on duty reports seeing approximately one litre of liquid DEZ spill out of the chamber onto the ground. Automatic sprinklers extinguished the resulting fire in 8 seconds, and only minor damage resulted, but project engineers immediately shut-down the system while they attempted to discover why liquid DEZ had formed in what was supposed to be a vapour phase of the process. The best

guess, according to James Robinson, acting associate director for institutional management at Goddard and chairman of the board of inquiry into the accident, is that some pipes in the gas delivery system had cooled to the point where DEZ would condense, even at low pressure.

When NASA and Northrop engineers returned to the facility early last month, they discovered a positive pressure in the recovery leg of the system. Assuming that additional DEZ or ethane, a reaction by-product, still remained in some of the process piping, they attempted to vent the remaining gas. During this process, a "significant" explosion occurred, destroying valves, pipes and instrumentation, and compromising the ability to "safe" the system with nitrogen gas.

NASA and Northrop engineers were unable to tell whether any DEZ remained in the process piping, and, if it did, how to remove it safely. Robinson says project engineers considered punching a hole in the remaining pipes from a distance with a rifle bullet, but rejected single-point venting because all remaining DEZ might not escape. NASA and Northrop ultimately concluded that the only way to make the facility safe was to destroy it. An army demolition team set off ten shaped charges on 21 February, "disassembling" the system. The DEZ released at this point burned off in 30 seconds, but this fire spread to the wooden structure housing the system, which burned for nearly an hour. Damage was estimated at \$30,000.

Both NASA and LC are satisfied that adequate safety procedures were followed in the design of the test facility. If anything, NASA and LC officials say the nature of DEZ prompted excessive safety concerns about its handling.

But safety issues have been raised in the past about how NASA and Northrop conducted the deacidification testing. In 1982, a Northrop safety engineer was fired for insubordination after bypassing his own superiors and reporting safety concerns about the project directly to NASA.

While Robinson would not rule out the possibility that safety issues may have been neglected, he contends "the safety review was adequate... but the fact is that we have had two accidents in three months".

LC has delayed opening of bids for construction of the Mass Deacidification Facility for at least a month until the board of inquiry makes its report.

Peter Sparks, director of preservation for LC, says the pilot system was designed to point out design problems. "We learned a lot from this, but it wasn't quite the way we wanted to learn it."

**Joseph Palca**

## Nuclear reprocessing

# France avoids British problem

Do the French do their reprocessing better than the British? The answer seems to be yes, at least by the criteria of leakage from and accidents at the principal French reprocessing plant at Cap de la Hague, on the English Channel coast near Cherbourg. Even opponents of the French nuclear programme admit that leakage is no longer a problem; environmentalists have turned their attention to other matters.

Even so, La Hague may be storing up problems for the future, for much of the low and medium level waste that British Nuclear Fuels discharges into the Irish Sea from Sellafield is stored on the land in Brittany. In short, the long-term nuclear waste problem has not been solved.

Nevertheless, French emissions of radioactivity from La Hague, the principal reprocessing plant, are low. The independently supported claim is that La Hague discharges into the English Channel 220 times less alpha emission, and seven times less beta emission, than does Sellafield into the Irish Sea. And despite the large amounts of waste stored on land, the average radiation exposure of a La Hague worker is 2.5 times less than that of workers at Sellafield.

But not everything has been rosy. La Hague suffered a series of setbacks in the 1970s. As in Britain, French nuclear power began with Magnox gas-cooled reactors, and early reprocessing of this fuel was very inefficient. Process pipes shielded in concrete had constantly to be broken open, exposing workers to high levels of Purex process (in which wastes are precipitated from a solution of the spent fuel in nitric acid). In the late 1970s, throughput at the plant was only a quarter of design capacity. La Hague also suffered a serious transformer fire which closed down pumps in the plant and raised questions about safety and the redundancy of equipment. (There was no second transformer to bring on line.)

Now, most of the limited amount of French Magnox reprocessing has been transferred to a new plant at Marcoule on the Rhone, and La Hague is concentrating on reprocessing the more highly irradiated oxide fuel from the huge French collection of pressurized water reactors (PWRs). This is the connection in which La Hague is proving efficient and relatively clean.

According to COGEMA, the French nuclear fuels company for which reprocessing is a third of turnover, La Hague is currently responsible for reprocessing 80 per cent of the world's reprocessed oxide fuel (most of it French but some from Japan, Belgium, West Germany and elsewhere). COGEMA has a clear commercial interest in proving itself better than Sellafield, with which it will be competing

directly in the 1990s, when the Sellafield "THORP" plant is due to be on stream.

COGEMA is a relatively secretive organization. French civil and military nuclear institutions overlap, and access to the La Hague plant is tightly controlled. But the doors have been opened, notably to a team of physicists, including nuclear opponents and headed by Professor Jacques Castaing, which reported on La Hague a couple of years ago. Moreover, many members of the antinuclear French trades union CFDT are workers at the plant, and are not slow to report accidents to their union. So although independent information on La Hague is not easy to come by, it is available. The general

impression is that La Hague does not leak.

This is why the French environmentalists' attack on reprocessing is directed at the prospect of a "plutonium economy" and at the costs of reprocessing. The company claims that costs have actually fallen by some five per cent over the past year because of the smooth operation of its UP II oxide reprocessing stream, which handled 418 tonnes of fuel last year, 18 tonnes (or nearly five per cent) more than the plant's targeted 400 tonnes. Reprocessing costs would now be some FF5,000–6,000 per kg of spent oxide fuel (£500–600) according to COGEMA, but its opponents say this figure involves some sleight of hand over discount accounting, and that the true costs will turn out to be twice as much. Indeed, the critics say that the electricity utility EDF would not be able to afford the true costs. **Robert Walgate**

## Fusion in Japan

# Plans for second major machine

### Tokyo

A NEW institute for basic studies in nuclear fusion seems likely to be built in Japan quite separately from that supporting the massive JT-60 tokamak project. An important step towards this goal was taken last week with the submission of an official recommendation from the Ministry of Education, Culture and Science (MESC)'s Science Council.

The institute is likely to be centred on the Nagoya University Institute of Plasma Physics, the largest university basic physics research facility, which has for some years been planning to move from the Nagoya University campus to more spacious grounds at Toki, in nearby Gifu prefecture. Parts of the land reserved for the move have already been bought with funds supplied by MESC.

Now that support has been gained from the Science Council (a twenty-seven member academic advisory board appointed by the ministry), MESC will spend some time considering whether an expanded institute should be built. A special committee will shortly be set up by the ministry.

The Institute of Plasma Physics has been Japan's chief plasma research institute for 25 years: it is an open institute at which scientists and engineers from all over Japan may come to do research and has helped give birth to several other large facilities, most notably Osaka University's laser fusion institute. After the move it could well undergo a change in status to that of a "national joint-use research institute". Such industries, like the High-Energy Physics Research Institute at Tsukuba and the Institute of Space and Astronautical Science in Tokyo, are quite independent and have been able to obtain research facilities that are often superior to those at universities. Conversion to

"national" status would almost certainly mean that Kyoto University's Heliotron group, as well as plasma physics groups elsewhere, would be incorporated into the institute.

The new institute, whatever its status, is to have a helical conductor system as its main facility, rather than a tokamak. Japan's giant JT-60 tokamak — on the same scale as the Joint European Torus at Culham (United Kingdom) and the fusion test reactor at Princeton (United States) — is run quite separately by the Science and Technology Agency.

At JT-60, expansion is also expected following the submission of a recommendation from the Atomic Energy Commission in the middle of February. Although there are tokamaks in the universities, it is overall variety rather than scale that has been aimed at in fusion machines; in laboratories around the country can be found heliotrons, stellarators and bumpy torus machines, open-ended "magnetic bottles", reversed-field pinch torus machines and compact toroids, including spheromaks.

A conceptual design for the new helical conductor system will be worked on by a committee in the Institute of Plasma Physics. Its nearest relatives are likely to be the Advanced Toroidal Facility under construction at Oak Ridge in the United States and the "Deep Well" project at Wendelstein in West Germany.

If all goes well, purchase of the land and clearing of the site will be completed in the next fiscal year. How quickly the new institute will then be built will depend on how quickly a consensus on its form can be reached by MESC among Japan's fusion research community — and on how quickly funds can be won from the Ministry of Finance. **Alun Anderson**

**US acid rain****Academy finds causal connection***Washington*

With a fine sense of timing, the National Academy of Sciences last week released the latest of its contributions to the study of acid rain. The academy's study\*, which provides the most conclusive evidence likely to be available for some time that emissions of sulphur dioxide from power stations acidify lakes and kill fish, comes the week before Canadian Prime Minister Brian Mulroney arrives in Washington for a summit meeting with President Reagan. Acid rain is at the top of the agenda.

The academy's study, chaired by James Gibson of Colorado State University, looks at time trends and regional variations in anthropogenic sulphur dioxide and nitrogen oxide emissions over the United States, reexamining original data to ensure consistency where necessary, and relates these to effects in the atmosphere and on the ground. It concludes, on the basis of consistency in the association and demonstration of intermediate steps, that in eastern North America a causal relationship exists between sulphur dioxide emissions and presence of sulphate aerosol, reduced visibility and wet deposition of sulphate. Regional changes in sulphate in streams are consistent with these changes, and so is acidification of lakes (assessed over time by diatom remains). Because "the observed acidification cannot be explained by other known disturbances . . . acid deposition is the most probable causal agent".

The clearest instances of environmental effects of acid rain were found in the Adirondack lakes of New York, although there were marked variations in the sensitivity of different lakes. Gibson characterized the results last week as establishing a "very significant linkage" between emissions and acidification. Furthermore, fish populations appear to decline concurrently with acidification. But geographically widespread reductions in tree-ring width and increased mortality of red spruce in the eastern United States, occurring concurrently with climatic anomalies and with high rates of acid deposition, could both be laid unambiguously at the door of acid rain. Members of the academy's committee said last week that the causes of tree mortality should be the next major acid rain research project. Because of poor time-trend data, few conclusions could be reached about nitrogen oxides.

Environmental groups, which have long been convinced of the damage caused by sulphur dioxide, saw the study as further confirmation of what they already knew; the basic hypothesis that sulphur dioxide emissions have caused acidification of lakes has been accepted by several academy and other studies since 1981. The

weight of the study would seem to lie in its demonstration that such effects are large in relation to natural processes and dominate them statistically. But however elegant and persuasive, it is unlikely to persuade the Reagan administration to accept immediate measures to reduce US emissions, which have begun to rise again and which under present policies are likely to go on rising until at least 2010, according to projections by the Environmental Protection Agency.

Fears about the federal budget deficit, which have reached a new pitch because of

unfavourable reaction on Capitol Hill to President Reagan's budget proposals for 1987, make large federal expenditures on control technologies difficult to contemplate, despite the apparent emergence of a new bipartisan consensus favouring control measures in Congress. The discussion with Mulroney this week is likely instead to focus on the recent recommendation of two US/Canadian special envoys that \$5,000 million be spent on demonstration projects to develop cheaper ways of burning coal cleanly. The sum currently proposed for this purpose in the United States in fiscal year 1987 is \$400 million.

**Tim Beardsley**

\**Acid deposition: long-term trends*, National Academy Press, 1986.

**Soviet spacecraft****Space station takes X-ray satellite**

A joint Soviet/West European study of X rays in space, originally planned for a Salyut-type spacecraft, will now be carried out aboard the new Mir space station, according to unofficial reports from Moscow. This could cause some rethinking of the project, if, as the Soviet media suggest, Mir, after a running-in period, will be permanently manned. For, in order to ensure the accurate pointing which the experiments demand, it was originally planned to carry out the study during a period when the host station was unmanned.

The joint project, known to the Soviet side as "Rentgen" and to the West Europeans as HEXE (High Energy X-ray Experiment), was originally scheduled for April 1986, but there was some delay in the construction of the instruments. Two pieces of apparatus, designed and made by the Max Planck Institute for extraterrestrial physics at Garching (West Germany), have already been delivered to Moscow, but are apparently still causing problems. The software for the project is also still being worked out, and it now seems doubtful that the August launch date can be met.

The Soviet space planners have not yet said when Mir is likely to be ready for full occupation (cosmonauts Leonid Kizim and Vladimir Solov'ev are at present activating the life-support systems and preparing it for habitation). Some 30 cosmonauts are believed to be in training for service aboard Mir, most of whom will be involved in research and "technological production". (The operation of the station itself will be virtually automatic.) Whether there will be any intervals between "shifts" in which HEXE could be deployed as first planned is doubtful.

The HEXE experiments, designed by teams from the Universities of Utrecht, Birmingham and Tübingen and from the European Space Agency, as well as from the Max Planck Institute, are intended to

study the X-ray stars of the Galaxy, the remnants of supernovae and the nuclei of other galaxies. This will require extremely accurate pointing and minimal perturbation of the station during the experiments. Hence the original stipulation that Salyut should be in its unmanned mode. The greater mass of Mir might, however, make it possible to attain the accuracy needed of HEXE, even if one or two people were on board the station. **Vera Rich**

**German gigaflops***Hamburg*

The West German government is to support a project for building a huge supercomputer designed around more than a thousand microprocessors. This was announced last week by Heinz Riesenhuber, the federal minister for research and technology, who said that Krupp Atlas Elektronik GmbH of Bremen and Stollmann GmbH of Hamburg will be joining with the existing Gesellschaft für mathematische Datenverarbeitung (GMD) with the intention of completing the prototype of the new computer by the end of 1988.

Riesenhuber's ministry, BMFT, has already appropriated DM27 million for the project, which will be carried out by a newly formed company based in Bonn. The total cost is estimated at DM130 million. The designers are aiming at a machine capable of 1,000 million operations a second, known as one gigaflop. Much of the incentive for the development has come from GMD, which has had some success in the development of programs and programming languages for computers based on parallel architecture.

The new machine will probably be used for the simulation of large-scale phenomena, among which Riesenhuber mentioned combustion processes and wind-tunnel experiments. **Jürgen Neffe**

## Data protection

# Swedish research under wraps

*Stockholm*

SWEDEN's Data Inspectorate has caused consternation among sociological researchers by ordering the removal of all personal identification from the records of a research project run by the Institute of Sociology at the University of Stockholm, and completed at the end of last year. The project, known as *Metropolit*, consisted of the longitudinal study of 15,000 people born in Stockholm in 1952, and had cost Skr7 million (roughly £700,000) over two decades. The university has until 1 May to comply with the inspectorate's ruling.

One consequence of the ruling will be that sociologists will not be able to add to the data now on file, either now or in the future. Indeed, even the potential value of the data so far gathered for control purposes is threatened by the mounting demand, which Swedish liberal newspapers are supporting, that the files should be scrapped completely.

This development may compromise the needs of sociologists and medical researchers elsewhere in Europe for access to the individual records of research projects. In the late 1970s, an attempt to win government approval for such access, accompanied by assurances of confidentiality, was mounted within the framework of the European Science Foundation, but not in the end pursued.

This turn of events is also an interesting pointer to the changed attitude of Swedish society towards the collection of confidential data about individuals. In 1966, Dr Carl Gunnar Jansson, the head of the *Metropolit* project, was able to recruit members of his study cohort by distributing study forms to teenagers in school classrooms; social surveys were a routine part of Swedish life in which openness was considered an unavoidable virtue.

At the outset of the project, the teenagers in the sample were told in general terms of the objectives. No direct approach was made to their parents, but Jansson says that there was enough information in the general press for them to know the project's aims. To the information provided by the members of the sample were added data on educational attainment, physical and mental health and infringements of the law derived from government records themselves regarded, in 1966, as "open".

Jansson's problems began only in the mid-1970s, with mounting public concern about the confidentiality of data stored in computers. Although the Swedish Data Protection Act, which came into effect in 1974, allowed existing research projects to continue, Jansson was told in 1976 that no further data could be added to the files without the informed consent of the sub-

jects, then in their twenties. Until the Data Inspectorate reversed that ruling in 1978, the result was a two-year hiatus in the addition of data to the files, on the grounds that consent would surely be withheld by those in the 15,000-strong cohort with criminal or other unflattering records, so biasing the sample.

Although *Metropolit* has now formally ended, Jansson had sought to make the files accessible to future researchers by depositing a key to the identity of the members of the sample in the national archives. Opposition to this proposal was stimulated by an enterprising journalist of *Dagens Nyheter* (which, ironically, was a strong supporter of the survey when it began). The result has been a general outcry against "Big Brother": 5,000 of the original sample of 15,000 have either asked that their names be withdrawn or that they should have access to their records.

The university will have three weeks in which to appeal against the new ruling

once it has been promulgated officially next month, but Jansson, now lecturing in the United States, is unsure whether he will follow this course for fear that an appeal would subject the *Metropolit* researchers (of whom his wife is one) to further stress. The appearances suggest that the Data Inspectorate will extend the basis of its new ruling to other projects, having also ruled that personal identification should be removed from a follow-up study of women who have had abortions.

Meanwhile, Swedish researchers needing to compile files of personal information may be tempted to follow what is called the "Evajo" option, named after Eva Johansson who, in the mid-1970s, carried out a study of the development and social adaptation of the children of former juvenile delinquents. Considering it unethical to interview the children for fear of the psychological damage that would be caused, but denied permission by the Data Inspectorate to compile a computer file from government records, she took her study outside the scope of the Data Protection Act by assembling the data manually, on index cards. **Vera Rich**

## Pesticide toxicity

# US Congress acts on compromise

*Washington*

LAGGARD federal safety testing of pesticides will be given an \$80 million boost from industry user fees, but also a strict new timetable, if Congress passes legislation put forward by industry and environmental groups. The proposals are meant by both sides in a long-running dispute over pesticide safety to ensure that testing is speeded and that efforts are concentrated on the chemicals of greatest concern.

Many of the 600 or more active ingredients in pesticides registered before 1978 were tested during the 1950s and 1960s, when requirements were less demanding. The Federal Insecticide, Fungicide and Rodenticide Act (FIFRA) was amended in 1972 to require the Environmental Protection Agency (EPA) to demand comprehensive industry health and safety studies, but in the intervening fourteen years, only six ingredients have been fully tested and approved; for 475, even the data needed have not been specified.

Under the amendments to FIFRA now proposed, all the unapproved active ingredients would have to be reregistered according to a strict timetable, with industry paying \$150,000 to EPA for each material considered. Pesticides previously registered with false or invalid data would be banned. "Special reviews", undertaken when a substance fails a potentially significant toxicity or carcinogenicity test, would be limited to one year's duration; testing of all pesticides on the market would have to be completed in seven years.

Besides the active ingredients, the bill would for the first time require EPA to test thoroughly so-called "inert ingredients", which include all those that do not actually kill the pest but that contain several substances (such as benzene and cadmium compounds) not normally thought of as inert. Because there are 2,000 inert ingredients in use, EPA would each year draw up a priority list of those most in need of more safety data, data which would have to be supplied within four years. The effect of this provision, according to Nancy Drabble of Public Citizen's Congress Watch, would be to put pressure on manufacturers to use those inert ingredients that are most likely to be safe. Other provisions would improve public access to information.

The new compromise has been hammered out over the past year by 41 environmental and consumer groups under the banner of the Campaign for Pesticide Reform and 92 agricultural companies represented by the National Agricultural Chemicals Association. A bill was introduced in both houses of Congress last week, and given the broad support is thought to have a good chance of passing. But the American Farm Bureau, representing the users of the chemicals, has still not put its name to the bill. It wants to see a clause to protect farmers from lawsuits arising from approved pesticide use, and it has considerable clout in Congress. Negotiations are said to be at a delicate stage.

**Tim Beardsley**

## West German universities

# Shortening of courses urged

**Hamburg**

A DRASIC shortening of university courses has been advocated by the Wissenschaftsrat, the standing committee of scientists and delegates from the federal and regional governments which functions as West Germany's senior science advisory board. In a 130-page document published earlier this month, Heinz Heckhausen, the chairman who is also the director of the Max Planck Institute for psychology at Munich, says that the average length of university studies in West Germany is much greater than in comparable countries. His report advocates a basic four-year course with only a few exceptions.

A century ago, most university students studied for only three years, but since then their courses have been lengthening steadily. The Heckhausen report says that the average length of study in social science and economics amounts to 11 half-year semesters. In mathematics, natural science and medicine, students spend an average of 12.8 semesters at university. Chemistry students, who usually finish up with a doctorate, spend no fewer than an average of 19 semesters at their universities, which means that they are usually 31 years old by the time they leave.

Under the new proposals, the content of university courses would be chosen to give students "a high degree of professional mobility" and would be complementary to professional practice. Courses would ordinarily last for four years, but there would be an extra three months of study for certain courses with exceptional needs.

The proposals fit in well with the recent discussions of the proposed new university law Hochschulerahmengesetz (see *Nature* 316, 96; 1985 and 317, 717; 1985). Significantly, however, they are addressed not to students but to academic boards, to universities and to professors. This may be the first time in the long discussion of this problem that responsibility has been shifted from students to officials.

The underlying difficulty is that the threefold increase of student entrants to West German universities, from 65,000 in 1950–61 to 155,000 in 1984–85, has not been accompanied by reorganization of university courses. As long ago as 1966, the then minister of education in the federal government, Hans Leussink, advocated that action should be taken, but almost the only tangible result was that

discussions of the problem were made more prominent.

The Keckhausen report is critical of proposals that have emerged from the Studienreform Kommission in the past few years, which has suggested ways of reducing the length of 10 university courses (excluding the time occupied by final examinations) to 10 semesters, a further four courses to nine semesters, but with courses in architecture remaining 12 semesters long. According to the new report, these are inappropriate recipes.

The Wissenschaftsrat's own proposals rely crucially on the assumption that a small proportion of the students completing first "four-plus" courses at universities would go on to graduate studies. The Heckhausen report, however, contains no specific proposals as to how the existing university courses would be shortened, and there are many who argue that shifting the problem to the universities is no solution.

Thus Theodor Berchem, the president of the Westdeutsche Rektorenkonferenz (the standing committee of university heads), has warned that too much should not be expected from the Wissenschaftsrat's proposals, which have been realized "only on paper". He points out that students whose employment prospects are not bright or who seek the high grades required for entry to the civil service will be tempted to prolong their studies to improve their grades by changing "the places after the decimal point".

According to WRK, there will be a change only if industrial companies are prepared to relax their demands of leaving students for high qualifications. Others point out that the universities have not yet been able to demonstrate that they can reduce the length or specialization of their courses, while the Gewerkschaft Erziehung und Wissenschaft calls the proposals "hollow" and "cobbled together", saying that the necessary conditions for their implementation must be a sufficiently generous payment to students and better professional prospects.

On the other hand, the federal minister for education, Dorothee Wilms, has praised the recommendations, emphasizing that the central and regional governments are in agreement on the issues raised by the report. She says that the federal government has already offered the regional governments assistance with the preparation of new graduate courses, but that it will be for the universities themselves to carry through the bulk of the reform. She hopes that the growing competition among universities for students will be a powerful incentive for change.

**Jürgen Neffe****Correction**

In last week's *Nature* (320, 101; 1986), the name of John McTague, the acting director of the White House Office of Science and Technology Policy, was misspelt. □

**French elections**

# Chevènement's last hurrah?

M. JEAN-PIERRE Chevènement, the architect of the French socialists' expansionary science policy, startled French voters on the eve of last Sunday's general election with the proposal that the *grandes écoles* should be doubled in size. Much of the interest of this proposal lies in its source. Chevènement is the leader of Ceres, the most substantial left-wing grouping within the Socialist Party, and as such might just as well have proposed that the *grandes écoles*, the training grounds of the French élite, should be abolished.

Since the beginning of his two-year spell as French minister of research and industry five years ago, Chevènement has been an ideas man. Now that the voters have proved the opinion polls right, and have robbed the socialists of their hold on the executive branch of the government, there will be no chance to tell whether the proposal was seriously intended or merely an election ploy. But this is not the first time that Chevènement has departed from the ideology of the left: as minister of education during the past two years, he has been responsible for a number of innovations — such as the singing of the *Marseillaise* every morning in the *lycées* — which are more popular with the right than the left.

This may not be as inconsistent as it sounds. Chevènement now calls himself a "republican élitist"; what he did last week was merely to endorse a report he had commissioned from Mme Josianne Serre, director of the École Normale Supérieure de Sèvres, whom he had asked to find ways of doubling the annual entry to the *grandes écoles*, now a meagre one per cent of the annual entry into higher education. What Serre (and Chevènement) now propose is that entry should not depend exclusively on success in the "baccalaureate C", with its emphasis on mathematics and physics, but on the results of a broader school-leaving examination.

The Serre report also advocated that the proposed doubling of the population of the *grandes écoles* should be brought about not only by increasing the size of existing institutions but by creating more of them, concentrating on technical fields other than the branches of conventional engineering to which most *grandes écoles* are at present dedicated. This coincides with the present inclinations of the *grandes écoles* themselves, for which reason there is a chance that these influential institutions could make the changes happen even if the new government declines Chevènement's offer to serve even in a right-wing government under suitable conditions.

**Robert Walgate**

## Embryo research

SIR—I cannot claim to have read every word submitted to the Warnock Committee of Inquiry into Human Fertilisation and Embryology, of which I was a member, but I am reasonably sure that at least in our discussions the word "pre-embryo" was never used. Certainly we were all well aware that the human embryo for the first two weeks of its existence, and even more, bears no visual resemblance whatever to the later embryonic and fetal stages, but I can recall no efforts either within or from outside the committee to redefine the early stages as not an embryo. Within the past year, however, the word "pre-embryo" has been creeping in. For instance Maxine Clarke (*Nature* 319, 349; 1986) reports that nine research councils in Europe agree that research should be restricted to the "pre-embryo" and that the British Medical Research Council is supporting research to develop a test to identify healthy pre-embryos.

If research on embryos were an uncontroversial matter, and if scientists were generally of the opinion that the new terminology helped their understanding, nobody would have many qualms at the name change. But those who are introducing "pre-embryo" into the vocabulary know full well that the research is indeed contentious and that fundamental issues have yet to be resolved. They complain, with justification, when embryos are described as "unborn children" in hostile parliamentary bills, but they are themselves manipulating words to polarize an ethical discussion.

The central issue is whether it is justifiable, once an egg has been fertilized, for anyone to perform experiments on the resulting embryo when those experiments are not in the best interests of that particular embryo. This is a complex and profound issue. The introduction of cosmetic words does not help.

DAVID DAVIES

*Wester Ground,  
Chittlehamholt, Umberleigh,  
North Devon EX37 9NU, UK*

David Davies was Editor of *Nature* from 1973 to 1980.

## Price of star wars

SIR—Joseph Hertzlinger (*Nature* 319, 8; 1986) has drawn attention to an aspect that I had overlooked in my letter (*Nature* 317, 470; 1985) about some of the consequences of the US Strategic Defense Initiative (SDI). However, the plutonium scattered into the atmosphere by the non-nuclear explosion of a Soviet missile will not only increase the background alpha-radiation by about 50 per cent; unlike naturally-occurring radon gas, it will be unevenly distributed in the troposphere

and, as plutonium oxide, it will be in solid form. A litre of inhaled air containing 1 µg of the oxide could be lethal; a litre of air free of the plutonium but with the average global proportion of radon gas would have less than one ten-millionth of the radioactivity of 1 µg of plutonium and be virtually harmless.

Probably more important than the scattering of radioactive debris in the atmosphere, however, are the consequences of the arrival at ground level of guidance-damaged missiles and parts of exploded warheads containing plutonium-239. The rumpus caused by that part of the recent report of the Australian Royal Commission dealing with the British A-bomb crash tests at Maralinga related to the scattering of a few kilograms of plutonium over a test site in the Australian desert. In the SDI scenario, the amount of plutonium could be thousands of kilograms and the "test site" could be populated Europe.

R.V. HARROWELL

*Devana, Cardinal's Green,  
Horseheath, Cambridge CB1 6QX, UK*

SIR—R.V. Harrowell (*Nature* 317, 470; 1985) raises an interesting question about a successful US defence system, but his conclusions may be misleading. Consider the more extreme case where 15,000 kg of plutonium-239 is uniformly dispersed throughout the  $2 \times 10^6 \text{ km}^2$  of Europe (bounded by  $5^\circ\text{W}$  to  $15^\circ\text{E}$  longitude and  $45^\circ\text{N}$  to  $55^\circ\text{N}$  latitude). It is assumed that an operable ATBM (anti-theatre ballistic missile) defence system intercepts 100 per cent of the incoming warheads at very low altitudes. A simplified pathway to human intake will be used in which only the effects on the lungs due to inhalation of insoluble plutonium-239 are considered. The particle size of the plutonium-239 will be assumed to be about  $1 \mu\text{m}$  AMAD (activity median aerodynamic diameter). The deposition velocity is taken to be about  $1 \text{ cm s}^{-1}$ , and the average breathing rate for humans is about  $20 \text{ m}^3 \text{ per day}$ . A rough estimate of the average mass of plutonium-239 that might be inhaled per person is

$$\frac{(15,000 \text{ kg}) (20 \text{ m}^3 \text{ d}^{-1})}{(2 \times 10^6 \text{ km}^2) (1 \text{ cm s}^{-1})} = 0.17 \mu\text{g.}$$

The committed dose per unit intake of inhaled plutonium-239 is  $16 \mu\text{Gy Bq}^{-1}$  (ref. 1) (which converts to  $37 \text{ mGy } \mu\text{g}^{-1}$ ). Thus, the dose commitment per person within the area of interest would be approximately  $6 \text{ mGy}$ . Since the ICRP (International Committee on Radiological Protection) limit for radiation workers is  $25 \text{ mGy}$  (ref. 2), the doses that most people would receive are not lethal. There would certainly be an increase in the long-term effects (for example, lung cancers), but the short-term mortality rate would not be significantly changed.

The question of whether one dies quick-

ly by nuclear annihilation or slowly by plutonium poisoning is not the central issue. The more realistic threats of future anti-ballistic missile (ABM) (and ATBM) defence systems deserve more attention.

The ABM Treaty of 1972 has recently raised a dilemma regarding the US Strategic Defense Initiative because it is only a bilateral measure and does not address the ATBM issues. This substantive deficiency must be addressed in the near future lest the heavens surely become the battleground of the twenty-first century.

BHUPENDRA JASANI  
GUY LETTEER

*Stockholm International  
Peace Research Institute,  
Pipers Väg 28,  
S-171 73 Solna, Sweden*

- United Nations Scientific Committee on the Effects of Atomic Radiation (UNSCEAR). *Ionizing Radiation: Sources and Biological Effects*, 1982 Report to the General Assembly, Annex E, p. 239.
- Recommendations of the International Commission on Radiological Protection. *Annals of the ICRP* ICRP Pub. 26, vol. 1, no. 3, January 1977.

## Women back to work

SIR—In his article on career breaks (*Nature* 319, 522; 1986), Richard Pearson remarks that "many more women would return if it could be to part-time work". The academic world has been slow to recognize this important condition, but the situation is changing. For example, the Science and Engineering Research Council has given positive support for part-time appointments to its fellowships and grant-funded positions.

I have initiated a scheme of part-time fellowships for women wishing to return to academic research in science and engineering. The first group of fellowships has been funded by British Gas, British Telecom, GEC, the Leverhulme Trust, the Institute of Physics, ICI and BICC. Donations have been received from Rank Xerox and British Aerospace.

Over a quarter of a million pounds has so far been raised and the first seven fellows have been appointed. Ninety applications have been received; well over half of the applicants have PhDs and well over a third have industrial experience. Two essential features of the scheme are that the fellowships are part-time and retraining is available. The university departments involved have been most helpful.

It is hoped that this scheme will serve as a pilot project for the return of qualified women to industry. It is clear that returners should be offered flexible working patterns and that contact must be made through local press and radio.

D.F. JACKSON

*Department of Physics,  
University of Surrey,  
Guildford, Surrey GU2 5XH, UK*

# Heavy-ion positrons explained

*The surprising observation of mono-energetic positrons in heavy-ion collisions may not be the signature of a novel particle but merely a sign that classical physics has been overlooked.*

THAT apparently small phenomena perceptively observed can lead to huge conceptual changes is a large part of the excitement of science. Newton's apocryphal falling apple is one example. Another is the recognition, by Meitner and Frisch (*Nature* **143**, 239; 1939) that the presence of barium in the products of the reaction of neutrons with uranium must mean something odd, such as the fission of heavy nuclei.

So it is inevitable that there should have been suppressed excitement for well over a year about an unexpected phenomenon associated with the collision of heavy ions which appears first to have been recognized at the heavy-ion accelerator at Darmstadt, the West German town just south of Frankfurt which, since last weekend, will briefly be best known as the site from which the European Space Agency coordinated the flight of the Giotto spacecraft to Halley's comet.

The circumstances are these. The Darmstadt laboratory, in German the Gesellschaft für Schwerionenforschung, has a longstanding (and successful) interest in the creation of artificial heavy nuclei, to which end it is equipped to collide heavy ions with each other so energetically that the Coulomb repulsion of their positive charges are overcome. The surprise, first reported in 1983, is that if the combined charge of the colliding ions is great enough (more than 163 units) the collisions are accompanied by the production of positrons with a precise energy (measured in the rest frame of the colliding ions).

Specifically, the energy distribution of the positrons appears to have a peak at an energy of 336 keV, which is itself apparently independent of the nature of the colliding ions. The width of the distribution is 75 keV or so, implying that the positrons are produced from a source whose lifetime is long by the yardstick of the time taken by the nuclear collision of the ions, estimated at  $10^{-21}$  seconds or so.

The excitement generated by these observations is easily imagined. The temptation has been irresistible to speculate about the properties of the unknown particles that are supposedly formed in the collision of heavy nuclei and which, by their radioactive decay, yield the positrons that are observed. One of the favourite candidates has been the axion, the particle that should exist if parity and isotopic spin are not conserved in weak

nuclear reactions (see *Nature* **319**, 717; 1986). There has even been the beginnings of a controversy on the subject, with some people saying that axions are produced because of their coupling to electrons, while others have held that the production process involves the interaction of hadronic particles, nuclear matter proper.

It now seems more probable that both camps are wrong, and that the unexpected observation of positrons in heavy-ion collisions is not so much evidence of a novel state of matter but rather a sign that even the people who should know much better have overlooked what should now be elementary physics. That, at least, is the implication of a modest article by Cheuk-Yin Wong, from the Oak Ridge National Laboratory in the United States, in the 10 March issue of *Physical Review Letters* (**56**, 1047; 1986).

Wong's argument is essentially quite simple. It turns on what should be by now Dirac's familiar description of what the vacuum is like. The point is merely that when Dirac first recognized more than half a century ago that a properly relativistic equation for the quantum motion of a free electron would admit of energies that are negative as well as positive, he was compelled to save the appearances by supposing that all the negative energy levels were in the real world completely occupied. If this were not the case, ordinary free electrons would forever be making the transition from a positive to a negative energy level, with the result that we would live in a world filled with radiation more energetic than the equivalent of 500 keV, which is half the smallest gap between a positive and negative electron energy level.

As the world knows, Dirac's view, strange though it may have seemed at the time, has been a great success. A positron is nothing but a hole in the sea of ordinary electrons with negative energy. The annihilation of positrons by ordinary electrons is the occupation of such a hole by an ordinary electron. The creation of an electron pair by a sufficiently energetic photon (whose energy must exceed the equivalent of twice 500 keV) consists simply of the promotion of an electron from the negative energy sea, leaving a hole that seems to be a positron, into an ordinary state of positive energy. Particle field theory is full of many more sophisticated applications of the same principle, under the banner of the "polarization of the vacuum" by suffi-

ciently strong fields of force. (Near a black hole, gravitational forces produce other particles than electrons in this way.)

In essence, what Wong now says is that the positrons observed in heavy-ion collisions arise in much the same way. Dirac's concept of a sea of electrons is valid only in the absence of electrical or magnetic forces, and must therefore be modified in the neighbourhood of a nucleus. Wong points out that the energy of the two electrons in the lowest bound state in an atom whose atomic number is greater than 150 is negative, which is another way of saying (a little crudely) that its binding energy to the nucleus of the atom is greater than its rest energy, that due to its mass.

Indeed, Wong argues that for a sufficiently heavy ion entirely devoid of electrons, it would be energetically favourable that there should be created two electron-positron pairs, each of them crammed into the ground state of the nucleus (which would not be forbidden by Pauli's exclusion principle).

The extension of the argument to heavy-ion collisions is straightforward. Electron-positron pairs created in this way in the ground states of colliding ions would be shaken loose during the collision and thus left to their own devices. In the centre of mass of the system, they would be virtually at rest. Only mutual annihilation would be feasible. So why should not the electrons and positrons annihilate each other in pairs? Sometimes, no doubt, they do, producing 500-keV radiation that will promptly be lost in the background. The more noticeable process, according to Wong, is that a single pair should annihilate each other, producing a single photon and transferring the excess momentum to a second positron that happens to be in the neighbourhood.

The surprise in this simple calculation is that the numbers turn out to be just right. The calculated kinetic energy of the surviving positron is 341 keV. Wong predicts that the accompanying photons (which might be detected by a coincidence experiment) should have an energy equivalent to 681 keV. There should also, he says, be observed the products of the inverse process in which excess momentum is transferred to an ordinary electron. That at least is something for which the experimentalists can hope to look, while they berate themselves (not to mention their theorist advisers) for having forgotten about Dirac.

John Maddox

## Developmental neurobiology

# Axon outgrowth in vertebrates

from P.H. Taghert and J.W. Lichtman

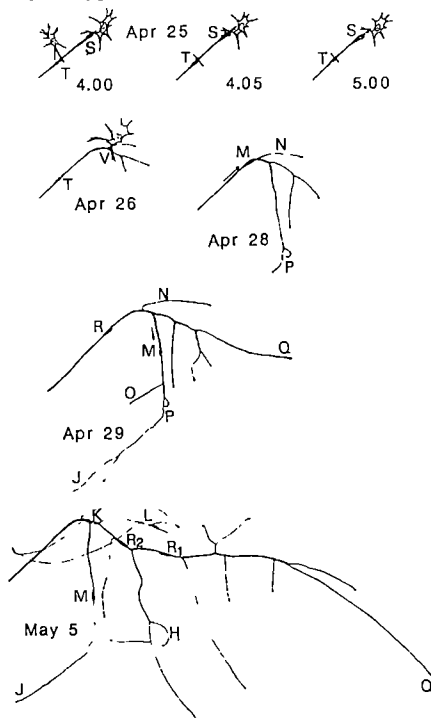
CARL Speidel observed the growth of single nerve fibres in the tails of living tadpoles more than fifty years ago<sup>1</sup>. Despite the ease with which he could watch axons over long time-periods (see figure) this line of enquiry lay more or less dormant until very recently. Perhaps one reason that *in situ* studies of axon outgrowth have been avoided is that it was not clear what such observations should explain — the relation between axon outgrowth and the specificity of neuronal connections was not always as evident as it now seems. Indeed, Paul Weiss promulgated for many years hypotheses arguing that axons either grow everywhere (resonance in the patterns of the activity of pre- and post-synaptic cells generated the specificity)<sup>2</sup>, or grow anywhere (the specificity occurring as a secondary step when central connections became specified by the targets axons contacted)<sup>3</sup>. Although it is now clear that at least some axons transiently project to multiple regions (see ref. 4 for review), recent work, including two reports in this issue<sup>5,6</sup>, shows that at least some axons are guided to their intended targets.

It is now generally agreed that the cellular and molecular mechanisms underlying the specificity of neuronal connections concern two general phenomena. The first is the guidance of developing axons to the neighbourhoods of the appropriate targets; the second is the formation and subsequent refinement of synaptic connections. The importance of axon guidance for synaptogenesis is obvious: neurones are capable of making synapses only with those targets that their growing axons can contact. It follows that to elucidate the basis of specific synaptic connections the mechanisms that guide developing axons through the embryonic cellular environment must be understood.

The articles by Harris<sup>5</sup> and by Eisen *et al.*<sup>6</sup> in this issue help to elucidate these mechanisms in vertebrate embryos at a time when we are becoming increasingly knowledgeable about axon outgrowth in invertebrates. The application of cellular techniques to the study of developing axons and growth cones *in situ* in insect embryos<sup>7-10</sup> generally support the hypothesis that the growth cones of individual neurones (via filopodia) actively select among many available cell substrates specific pathways on which to extend. Identified neurones make stereotyped choices of substrates at specific locations in the developing neuropil or periphery. These observations of normal growth-cone behaviour in developing embryos have

generated the view that the most critical environmental factor is the set of cell-surface 'markers' whose existence is inferred from the stereotyped and highly selective pathway choices made by individual growth cones<sup>9</sup> and the equally selective filopodial contacts at the precise times that pathway changes occur<sup>10</sup>.

These inferences (formalized as the labelled pathways hypothesis<sup>9</sup>) are in many ways analogous to Sperry's chemo-affinity hypothesis that sought to explain the precise connection between cells of the retina and the tectum in vertebrates. An experimental test of the labelled pathways hypothesis shows that specific



Extension of a growth cone and its branches over several weeks in a regenerating tadpole tail (from the original work of Speidel<sup>1</sup>).

ablation of particular neurones and mesodermal cells causes the growth cones of the neurones that normally choose the ablated cells as substrates either to stall or to select a different pathway. It is thought that the major factor controlling this directional movement of growth cones consists of specific interactions between a growth cone and its neighbouring substrates. In this view, pathway alterations result from sampling the cell surfaces of available substrates and substrate preference reflects the greatest adhesion between two cells whose membrane labels are most 'compatible'.

The study of axon guidance in insect embryos has been so fruitful because of

the accessibility and identifiability of embryonic neurones during the stages of development at which the critical events occur. It has been much more difficult to study vertebrate embryos. Recently, Lynn Landmesser and her colleagues have described the behaviour of chick motor neurones as they navigate out of the spinal cord towards their muscle targets both during normal development and following experimental manipulation<sup>11,12</sup>. Their interpretation of the events suggests that the vertebrate axons find their specific targets by growing along stereotyped pathways.

Eisen *et al.*<sup>6</sup> return to the approach initiated by Speidel by examining the growth of individual motor axons in the spinal cord of living zebra fish embryos. They have used the optical clarity of this embryo and the intracellular injection of fluorescent probes to describe the complete sequence of events as the growth cones of the motor neurones first navigate out of the spinal cord. Consistent with the behaviour of growth cones in insect embryos and the interpreted behaviour of chick spinal motor neurones, these cells appear to make cell-specific pathway choices. Similarly, within the developing fish spinal cord, the first interneurones to project axons do so along stereotyped substrates<sup>13</sup>. The stereotyped, precise and cell-specific nature of the axonal guidance suggests direct parallels with similar phenomena in insect embryos.

Harris<sup>5</sup> also examined the development of stereotyped axon pathways in the vertebrate nervous system. Once again, the novelty of the study arises from analysis performed not just after growth cones have finished navigating, but also during the formation of these pathways. Retinal neurones placed at ectopic locations in the developing brain of the South African clawed toad (*Xenopus*) appear to home-in to their normal target region in the developing tectum. Especially noteworthy is the evaluation of the trajectory of ectopic axons during their corrective action. Harris demonstrates that the axons do not fail to navigate correctly even at times soon after axonogenesis, and it is only when the primordium of the retina is placed at long ectopic distances from its prospective target that evidence of 'error' is found.

The ability of developing vertebrate neurones to correct experimental misplacement up to a certain spatial point as demonstrated by Harris is reminiscent of events in the chick spinal cord<sup>11</sup>. Interestingly, the interpretations differ slightly in their emphasis: Lance-Jones and Landmesser<sup>11</sup> suggest that motor neurones navigate under normal circumstances by deciphering some aspect(s) of the local environment at what are now called decision points<sup>12</sup>. Past a certain distance, access to the proper local environment is no longer possible and thus mistakes in axon projection occur with increasing regular-

## NEWS AND VIEWS

ity. Harris<sup>5</sup> emphasizes the fact that retinal neurones seem to show directional predilections almost anywhere when they are ectopically placed in the developing brain. Hence, he predicts that the positioning of cell-surface signals (or strength of a diffusible gradient) necessary for the guidance of particular axons are not restricted to decision points but are instead distributed to many neuronal locations.

Perhaps the two sets of interpretations could be reconciled by considering the absolute distances of the ectopically placed neurones from their normal targets. Are the dimensions of the developing *Xenopus* brain very much greater than those of the local environment deciphered by chick motor neurones?

In the examples we have described here (and in others; see, for example, ref. 13), the picture is beginning to emerge that the earliest neurones to project axons in the developing nervous system of vertebrates do so in a stereotyped manner. The mechanisms that underlie this form of

development, and their relationship to potentially analogous mechanisms of invertebrate systems, are fast becoming subjects of more than simple speculation. □

1. Speidel, C.C. *Am. J. Anat.* **52**, 1 (1933).
2. Weiss, P. *Ergebn. Biol.* **3**, 1 (1928).
3. Weiss, P. *Biol. Rev.* **11**, 494 (1936).
4. Cowan, W.M., Fawcett, J.W., O'Leary, D.D.M. & Stanfield, B.B. *Science* **225**, 1258 (1985).
5. Harris, W.A. *Nature* **320**, 266 (1986).
6. Eisen, J.S., Myers, P.Z. & Westerfield, M. *Nature* **320**, 269 (1986).
7. Goodman, C.S. & Bate, C.M. *Trends Neurosci.* **4**, 163 (1981).
8. Bentley, D. & Keshishian, H. *Trends Neurosci.* **5**, 354 (1982).
9. Raper, J.A., Bastiaiani, M.J. & Goodman, C.S. *Cold Spring Harb. Symp. quant. Biol.* **48**, 587 (1984).
10. Bastiaiani, M.J., du Lac, S. & Goodman, C.S. In *Model Neural Networks and Behavior* (ed. Selverston, A.I.) 149 (Plenum, New York, 1985).
11. Lance-Jones, C. & Landmesser, L. *Proc. R. Soc. B* **214**, 1, 19 (1981).
12. Tosney, K. & Landmesser, L. *J. Neurosci. Abstr.* **5**, 2345 (1985).
13. Kuwada, J. *Soc. Neurosci. Abstr.* **11**, 334 (1985).

P.H. Taghert and J.W. Lichtman are in the Department of Anatomy and Neurobiology, Washington University School of Medicine, Box 8108, St Louis, Missouri 63110, USA.

## Archaeology

## Beginnings of English village life

from Richard Hodges

TWENTY-FIVE years ago archaeologists generally believed that the first English villagers of the fifth to seventh century AD lived in 'pit-houses' in a primeval condition. Improved excavation techniques in the 1960s, however, brought a new image of the early English to light. By excavating large areas rather than trenches it became apparent that the remains of post-built halls existed alongside these sunken pit-houses. Moreover, the new excavation techniques revealed a material culture pertaining to daily life as opposed to the common picture of a barbaric society. Although contemporary cemeteries contained bodies inhumed with swords, shields and spears, the first excavated villages by contrast seem to have been places of rich tranquility. Such points have been revealed by one of the first of these village excavations, at West Stow, Suffolk<sup>1</sup>.

This village, one of several discovered from this era, was situated in the Lark Valley, north of Bury St Edmunds. Excavations and survey show that the Roman villas in the area were falling into decay by about AD 400, well before the imperial government left Britain; it is equally clear that West Stow, like several other communities, was founded in the wake of this traumatic decision<sup>2</sup>. The new report charts the sequence of the community from the early fifth and seventh centuries, when it was probably abandoned in favour of a nearby site. At any one time there were about three halls accompanied by up to about a dozen small

sunken huts. Each hall was constructed of posts set deeply into the ground with walls clad presumably with wattle and daub, whereas the sunken huts were smaller buildings, probably with lean-to roofs over a sunken floor. It is now thought that



Reconstruction of the West Stow village (courtesy of Suffolk County Council).

the halls were for accommodation, while the sunken huts were used for domestic crafts and storage. The halls, however, are unlike contemporary German long-houses and much closer in style to the peasant farms of Roman Britain<sup>3</sup>.

The absence, until the seventh century, of ditched enclosures around each farm unit is also strikingly at variance with continental village patterns in this period<sup>4,5</sup>. Yet the material culture is a classic early Anglo-Saxon assemblage. The stamp-decorated sixth century pottery, the bone combs and the jewellery are consistent, if poorer in quality, with the assemblage found in the cemetery at West Stow as well as other Anglian cemeteries. Faunal and botanical assemblages also show a pattern

of mixed farming with pigs making up a fairly high proportion of the livestock (about 20 per cent), while it appears that spelt, typical of Roman farms, had been replaced by wheats and rye (pages 86, 103 of ref. 1; and ref. 6). The subsistence strategy suggests a localized regime of low intensity compared with the more specialized, productive agrarian policies of Roman times. West Stow must have had a population numbering about 20–30 until the early seventh century when the village was abandoned. Note that ditches enclose the final-phase buildings, as if in the era of St Augustine and with the coming of Christianity, attitudes to property altered.

The survey of the Lark Valley indicates that West Stow was typical; similar villages existed at regular intervals following the desertion of the Romans. The material culture suggests that their occupants were English, whereas the buildings hint that they were descendants of Romano-British peasants adapting to the changes.

For almost two hundred years a largely domestic mode of production was sustained with involvement in regional exchange being only on a modest scale. At the same time, some elements of warrior status occur in the cemetery in the form of spears and shields despite the egalitarian agrarian character of the village buildings. Some time before AD 700 almost all the early Anglo-Saxon sites in the valley were deserted in favour of new loci, most of which are still occupied today (page 170 of ref. 1). These divisions look purely functional and economic, with river frontages, water meadows and arable land, backing onto high drier sheepwalks. However, other recent village excavations such as those at Raunds (Northamptonshire) and Wharram Percy (North Yorkshire) show that the parish church and its bounds were features of the tenth century and the socio-economic changes of that era<sup>7,8</sup>.

The excavations at West Stow provide an image of the transitory age between the collapse of Roman Britain and the formation of the Christian kingdoms of the seventh century. It is too soon to challenge the traditional history, yet, just as these excavations reveal that Anglo-Saxon farmers did not inhabit pit-houses, it is clear that their agrarian way of life constitutes a significant chapter in the evolution of English medieval life. □

1. West, S. *West Stow. The Anglo-Saxon Village* (East Anglian Archaeology, Ipswich, 1985).
2. Thompson, E.A. *Britannia* **8**, 303 (1977).
3. Dixon, P. In *Structural reconstruction* (ed. Drury, P.J.) 275 (BAR, Oxford, 1983).
4. Hvass, S. *Acta Archaeologica* **49**, 61 (1978).
5. van Es, W.A. *Berichten R.O.B.* **23**, 273 (1973).
6. Randsborg, K. In *Beyond Domestication in Prehistoric Europe* (eds Barker, G. & Gamble, C.) 233 (Academic, London, 1985).
7. Cadman, G.E. *Medieval Archaeol.* **27**, 207 (1983).
8. Hurst, J.G. *Medieval Archaeol.* **28**, 77 (1984).

Richard Hodges is Lecturer in Archaeology at the University of Sheffield, Sheffield S10 2TN, UK.

## Prochlorophytes

# Origins of chloroplasts

from A.E. Walsby

OUR Victorian forebears did such a good job of describing the major groups of plants, animals and microbes that it is now a particular delight to find even a new species, let alone a representative of a new family or higher order. A decade ago, R.A. Lewin's discovery of the Prochlorophyta<sup>1,2</sup>, a new division of photosynthetic microbes, was therefore quite momentous, particularly when it was realized that this might be the missing link in the evolution of chloroplasts. The study of prochlorophytes since then has been hampered because only symbiotic forms have been found, none of which can be grown in culture<sup>2</sup>. But on page 262 of this issue<sup>3</sup>, T. Burger-Wiersma and her colleagues report the discovery of the first free-living prochlorophyte from the Loosdrecht lakes of the Netherlands.

The *Prochloron* found by Lewin is an oxygen-evolving photosynthetic prokaryote that possesses both chlorophyll *a* and *b*, the photosynthetic pigments of green plants<sup>4</sup>. The serial endosymbiosis theory<sup>5</sup> claims that eukaryotes — all those organisms whose cells have a true nucleus and membrane-bound organelles — arose by the symbiotic merger of prokaryotic organisms, and that in eukaryotic plants the chloroplast developed from a cyanobacterium (blue-green alga). This particular aspect of the theory had one drawback: although cyanobacteria also perform a similar type of photosynthesis based on chlorophyll *a*, they lack chlorophyll *b*, the pigment that is involved in the second oxygenic photosystem of plants (photosystem II). They have instead a photosystem based on pigmented phycobiliproteins which, although functionally homologous, must have evolved by a different route. It is probable that cyanobacteria were the precursors of chloroplasts in red algae, which have almost identical phycobiliproteins, but what of chloroplasts in all the other plant groups? Did they develop from primitive red algae, evolving chlorophyll *b* to replace the phycobiliprotein pigments of photosystem II, or were they products of a separate endosymbiosis involving prochlorophytes<sup>6</sup> that had already adopted such a replacement? One might even ask which came the first, the cyanobacteria or the prochlorophytes?

In an attempt to answer such questions Lewin's *Prochloron* has been investigated from every conceivable angle. The first *Prochloron* was found on the surface of didemnid ascidians (sea squirts, sedentary hemichordates that produce sponge-like incrustations on rocks) in the intertidal region of Baja, California. Other pro-

chlorophytes that differed in size and other minor respects were soon discovered in tropical waters but they, too, were always present in association with these same animals. The failure to grow prochlorophytes in culture even produced some anxiety that they might not be complete organisms but chloroplasts, escaped from some unidentified algae and enslaved by their sea-squirt host. In the absence of cultures there was no option but to analyse the few prochlorophyte cells that could be obtained from the sea-squirts.

Structural and biochemical analyses of precious milligrams of material show *Prochloron* to be closely related to cyanobacteria<sup>7</sup>. The organism possesses a peptidoglycan wall, diagnostic of eubacteria, and polyhedral carboxysomes (stores of the CO<sub>2</sub>-fixing enzyme) peculiar to autotrophic prokaryotes. The carotenoids and lipids are similar to those in cyanobacteria, as are other features of the cytoplasm. The most telling comparison is that of their ribosomal RNA sequences, which indicate that *Prochloron* is phylogenetically closer to cyanobacteria than to the chloroplasts of green plants<sup>8</sup>. One important finding<sup>9</sup> was that the symbiotic *Prochloron* had a DNA genome size of relative molecular mass  $3.6 \times 10^9$ , similar to that of many cyanobacteria and 30 times greater than the residual genome of chloroplasts, which is insufficient to support an independent existence by these organelles.

In one respect the prochlorophytes did resemble green chloroplasts more closely than cyanobacteria: their thylakoids (photosynthetic membranes) were paired or stacked. However, this may be a quasi-

mechanical consequence of the presence of chlorophyll *b* and the absence of phycobilisome structures, which in cyanobacteria prevent the close juxtaposition of neighbouring thylakoids. It may not, therefore, be of any phylogenetic significance.

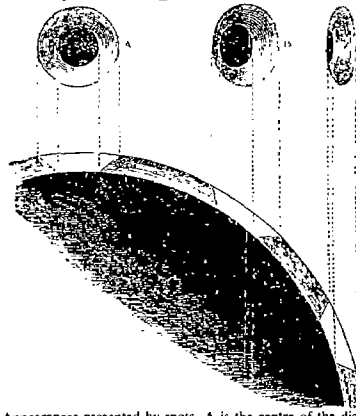
With the newly discovered free-living prochlorophytes, which morphologically resemble filamentous cyanobacteria, it will be possible to make even more fundamental comparisons. For example, although Burger-Wiersma *et al.* find no trace of phycobiliproteins in the cells, it would still be interesting to see if there are DNA base sequences homologous with the structural genes for these proteins that have been isolated from several cyanobacteria during the past year. Even more exciting is the prospect of using recombinant DNA technology to transfer the genes required for a chlorophyll *b* photosystem II into phycobilisome-disabled mutants of cyanobacteria (and vice versa). These experiments would define the amount of information required to evolve such a photosystem and in this way shed light on the origins and affinities of these photosynthetic prokaryotes.

In just one respect the discovery of the free-living prochlorophyte has done a disservice to biologists: previously, *Prochloron* could be obtained only by visiting a sun-drenched beach in Baja or a tropical island. A surprising number of biologists not noted for their field work found such visits worthwhile. Now they can investigate the biochemistry of a prochlorophyte in the comfort of the laboratory. □

1. Lewin, R.A. *Phycologia* **14**, 153 (1975).
2. Lewin, R.A. *Nature* **261**, 697 (1976).
3. Burger-Wiersma, T. *et al.* *Nature* **320**, 262 (1986).
4. Withers, N., Vidaver, W. & Lewin R.A. *Phycologia* **17**, 167 (1978).
5. Sagan, L. *J. theor. Biol.* **14**, 225 (1967).
6. Lewin, R.A. *Annals Inst. Pasteur, Paris* **134B**, 37 (1983).
7. Lewin R.A. *Phycologia* **23**, 03 (1984).
8. Seewaldt, E. & Stachebrandt, E. *Nature* **295**, 618 (1982).
9. Herdman, M. *Archs Microbiol.* **129**, 314 (1981).

A.E. Walsby is in the Department of Botany, University of Bristol, Bristol BS8 1UG, UK.

## 100 years ago



Appearances presented by spots. A is the centre of the disk; B between centre and limb; C, near the limb.

from *Nature* **33**, 469, 18 March 1886



Copy of part of a photograph taken at Dehra Dun in 1884, showing a sunspot passing over the Sun's edge.

In the large photographs now secured at Meudon and in India, showing the sunspots, I am glad to say almost every day now, on a scale of 8 inches to the sun's diameter, we get wonderful records of what a spot really is, and how it changes.

## Gene therapy

# Desperate appliances

from *Miranda Robertson*

It was widely prophesied last year that the first clinical trials of gene therapy would be under way before the end of 1985 if obstructive action by the US Food and Drug Administration (FDA) did not prevent them<sup>1</sup>. As it turns out, however, gene therapists have been thwarted not by the FDA but by the biology of the retroviruses on which they depend for gene transfer. That the paper published by Hock and Miller on p. 275 of this issue<sup>2</sup> constitutes a substantial advance in the development of retroviral vectors for human gene therapy is a measure of how far away it still is.

The paper reports the transfer of a drug-resistance gene to human bone marrow cells. What makes it important is that this is the first time that has been achieved in the absence of infectious helper virus (which could contaminate the bone marrow cells and preclude their use for gene therapy); and that the drug-resistance gene is expressed in the transfected cells. The ingenuity that has gone into the design and construction of the retroviral vectors that have made this possible is awe-inspiring; but it seems it is not enough. What are the problems of the technology, and what now are the prospects for putting it to use?

## Prospects

No-one expects in the foreseeable future to be interfering with human fetuses: the immediate hopes for gene therapy are concentrated on those diseases that could in principle be treated by the manipulation of haemopoietic cells of the bone marrow, which are relatively easily removed and replaced and provide a self-renewing population of cells for the propagation of transferred genes. (A comprehensive account of the prospects for gene therapy is given in ref. 3.) The diseases that are susceptible to this approach include disorders of the haemopoietic cells themselves — hereditary anaemias and immune deficiencies — and single-protein deficiencies such as haemophilia in which the release of the missing protein into the bloodstream would correct the defect.

Its success depends on the efficiency with which a normal copy of the defective gene can be introduced into bone marrow cells in such a way that it will be expressed as protein in their progeny. The efficiency of the vector is crucial because if the gene is to persist in the bone marrow after it has been returned to the patient it must enter the self-renewing stem cells that are responsible for replenishing the entire haemopoietic population. These stem cells have been estimated to com-

prise 0.01 per cent of bone marrow cells, and there is no guarantee that all of those transfected will express the gene; so to be certain of getting useful amounts of the normal gene product it may be necessary for the vector to enter virtually 100 per cent of the cells. Only retroviral vectors are capable of this order of efficiency; but an elaborate series of manoeuvres has been necessary to devise a vector that will deliver the gene without leaving the cells full of infectious virus. Briefly, the trick is as follows.

The vector contains only the gene to be transferred; the sequences necessary to insert itself into the DNA of the cell and ensure transcription of the gene it carries (both contained in the long terminal repeated sequences (LTRs) at its ends); and a packaging signal — an uncharacterized sequence that enables the viral genome to be packaged into its protein coat and escape the cell as an infectious particle. Because it does not contain the coat-protein genes, however, it is incapable on its own of generating infectious particles. Large quantities of infectious virus must nonetheless be generated for the efficient transfection of bone marrow cells, and this is made possible by introducing plasmids containing the vector sequences into cell lines that harbour what are known as helper viruses. The helper viruses still have their coat- and envelope-protein genes, so that when the vector genes are replicated in the cell, they can be packaged in the helper coat proteins. The packaging cell line is incubated with the bone marrow cells, which the vector particles are able to enter. Once in the bone marrow cells, the vector genome becomes integrated in the cellular DNA where, because it has no coat-protein genes of its own, it cannot give rise to further infectious particles. With an intact helper virus, helper particles are produced along with the vector particles; this is not acceptable for human gene therapy and can now be avoided by the use of helper viruses from which the packaging signal has been deleted so that they cannot package their own genomes and are trapped in the cell lines they are grown in.

Such a combination of packaging-defective helper and retroviral vector has been successfully used to introduce drug-resistance genes into mice, through transfection of the bone marrow<sup>4,5</sup>; but until now no-one had been able to get it to work in human bone marrow cells, and people were beginning to wonder if the systems that work for mouse cells are for some reason simply unsuitable for use in man.

Hock and Miller have now shown that this is not the case. They used a cell line, PA-12, which contains a packaging-defective helper with a wide host range, to produce a vector carrying the dihydrofolate reductase (*dfr*) gene, which confers resistance to methotrexate, and have been able to grow drug-resistant cells from transfected human bone marrow.

## Problems

The drug-resistant cells that they grew in this way were, as it happens, derived from CFU-GM cells, the progenitor cells for the myeloid lineage. How likely is it that if the system will work for CFU-GM it will also work for the self-renewing stem cell — a rarer and more elusive species? There is no completely satisfactory answer to this question, largely because there is no unequivocal assay for the self-renewing haemopoietic stem cell short of putting it back in the animal, which is not an option where the appropriate animal is man. But experiments with essentially similar systems in mice suggest that if it will work for a late progenitor like CFU-GM then it will work for earlier ones too. It would help to show that drug resistance can be conferred in the same way to other human precursor cells that can be assayed *in vitro* — namely, the erythroid precursor BFU-E and the earlier progenitor cell CFU-MIX, which is the precursor of both CFU-GM and BFU-E. Hock and Miller have almost but not quite done this.

Using two other vectors, they have succeeded in growing drug-resistant colonies of all three progenitor cell types, but only from cultures containing helper viruses. The helper virus in the cultures was an unpleasant surprise: it materialized through recombination between the packaging-defective mutant and the vector during co-incubation, because of a short region of homology between the vector and helper viral sequences (the vector that came out helper-free did not have this region of homology). This rather strikingly illustrates some of the hazards of working with retroviral vectors — people do worry about the possibility of recombination between vectors and endogenous viral sequences in human cells; but although the presence of the helper virus would be an absolute bar to the therapeutic use of the cells, it does not account for the essential observation that drug resistance can be transferred to three types of haemopoietic progenitor cells: expression of the transferred genes can be detected in the bone marrow immediately after transfection, when it can only be due to the activity of the vector.

Nor does the presence of helper virus seem materially to affect the efficiency of transfection, which Hock and Miller estimate at about 3–10 per cent for CFU-GM. This is almost certainly too low for practical purposes, partly because it is clear

from experiments with mice that only a small proportion of those cells containing the gene are likely to express it. Indeed, expression in general has been a major problem, especially in human bone marrow cells, which is another reason for the importance of the results reported by Hock and Miller. On the other hand, again, the fact that the drug-resistance genes are expressed even in the CFU-MIX does not necessarily mean they would be expressed in self-renewing haemopoietic stem cells. This is not a quibble: it is known that the viral sequences can induce permanent suppression of viral gene expression in embryonic cells, and although the mechanism is unknown it is suspected that the viral LTRs may be responsible. This raises the unwelcome possibility that the failures of stable gene expression in bone marrow are due to analogous mechanisms that cause stem cells to suppress everything under the control of the viral LTR. Re-engineering the LTR so as to retain its essential functions in vector replication and integration, but eliminate the suppressive effect, would not be trivial.

It is probably fair to say that problems of efficacy are for the moment taking precedence over questions of safety. If you cannot make a vector work, after all, you will not be tempted to endanger anyone with it. But it is acknowledged that only for the mortally ill would a treatment involving the random insertion of viral DNA in the chromosomes of proliferating bone marrow cells seem justified.

In an ideal world, the introduced gene would be targeted to replace precisely the defective one by site-specific recombination. This would not only eliminate the danger inherent in random insertion: it would also guarantee correctly regulated gene expression — a truly major advance. At present, the hereditary anaemias, which are the only really common genetic

disorders of the haemopoietic cells, are out of reach because precise regulation of globin gene expression is essential and no-one yet knows how globin gene regulation works, still less how to manipulate it.

There have recently been two reports of site-specific recombination of genes introduced into mammalian cells in plasmid vectors<sup>7,8</sup>, one of them involving a globin gene<sup>7</sup>. But in neither case is the recombination reliable or accurate enough to have any immediate implications for gene therapy (the implications of the globin gene experiment, and its limitations, have been very clearly laid out in these columns by Tom Maniatis<sup>9</sup>). Moreover its efficiency is vanishingly low: it is the specialized and indiscriminate nature of the viral LTR insertional mechanism that makes the retroviral vectors so efficient.

For the time being, therefore, the prospect of gene therapy is limited to those life-threatening genetic diseases that are due to a single gene defect whose effects can be corrected by the insertion of the normal gene into the bone marrow without the need for precise regulation of gene expression; and for which there is no other cure. The consensus is that clinical trials are very unlikely before next year. I can summarize more elegantly with the lines from which I borrowed the title of this article:

"Diseases desperate grown  
By desperate appliances are relieved,  
Or not at all."

(Shakespeare wrote them.) □

1. Beardsley, T. *Nature News* 316, 567 (1985).
2. Hock, R. & Miller, A.D. *Nature* 320, 275 (1986).
3. Anderson, W.F. *Science* 226, 401 (1984).
4. Williams, D.A., Lemischka, I.R., Nathan, D.G. & Mulligan, R.C. *Nature* 310, 476 (1984).
5. Dick, J.E. *et al.* *Cell* 42, 71 (1985).
6. Keller, G., Paige, C., Gilboa, E. & Wagner, E.F. *Nature* 318, 149 (1985).
7. Smithies, O. *et al.* *Nature* 317, 230 (1985).
8. Thomas, K.R., Folger, K.R. & Capecchi, M.R. *Cell* 44, 419 (1986).
9. Maniatis, T. *Nature News and Views* 317, 205 (1985).

Miranda Robertson is Biology Editor of Nature

tends to dull the cutting edge of our analytical tools. Whereas numerical and analytical methods should be kept as simple as possible for the job in hand, some empirical data, which appear opaque to simple techniques, can yield invaluable insights when analysed more thoroughly.

Dahl-Jensen and Johnsen now demonstrate that the measured temperature profile at the Dye-3 bore-hole in the southern dome of the Greenland ice sheet is significantly different from the profile calculated to be in equilibrium with modern conditions. Using a simple heat-transfer equation, the authors show that surface temperatures must have been colder in the past. Furthermore, by assuming constant surface temperature and accumulation through the last glacial cycle, they calculate the combination of the two which would be compatible with the measured profile. Assuming that surface temperatures lay in the range -30 to -35°C, the authors calculate an accumulation value of about 50 per cent of the modern values. The result is probably only the first step in deducing the significance of the temperature profile anomaly. It should be pursued further, as it represents a valuable piece in an important jigsaw puzzle.

Much work has been done on the reconstruction of environments in the North Atlantic region around South Greenland during the last glacial/interglacial cycle. The polewards heat flux in atmosphere and ocean are greater in this zone than any other comparable latitudinal zone of the Northern Hemisphere and the amplitude of change from glacial to interglacial has been greater here than elsewhere. Terrestrial and oceanic evidence has demonstrated strong environmental changes even within the last glacial episode, beginning at about 120 kiloyears ago (BP) and ending about 10 kiloyears BP.

The North Atlantic appears to have remained an 'interglacial' ocean with a circulation similar to that of the present until about 75 kiloyears BP, from when, until about 13 kiloyears BP, glacial circulation dominated, with an outward surface flow from the polar ocean (Ruddiman, B.F. *Bull. geol. Soc. Am.* 88, 1813; 1977). On land, a major arctic glacial episode appears to have coincided with the early period of interglacial circulation (Boulton, G.S. *et al.* *Nature* 296, 437; 1982), possibly associated with high accumulation rates on the North Greenland ice sheet (Andrews, J.T. *et al.* *Geology* 2, 355; 1974), suggesting particularly high moisture fluxes from a still-warm ocean surface into a cooling Arctic. The period between 75 and 13 kiloyears BP was associated with strong mid-latitude glacier growth and arctic glacial decay, reflecting possible drying and cooling of the Arctic as the polar front moved far south, producing deflection of major storm tracks towards the growing mid-latitude ice

## Palaeoenvironments

# Temperature of the ice sheets

from G.S. Boulton

CHANGES in the surface environment of the Earth on a timescale of  $10^3$ – $10^5$  years are determined by interactions between oceans, ice sheets and atmosphere in response to changes in incident solar radiation. There are two ways of reconstructing these changes: first, the classical geological approach, in which dated physical remains are used to infer past environments by empirical studies of modern controls on their character and distribution; and second, by the demonstration of the disequilibrium between the current state of a system and the factors which should control that state. A splendid illustration

of this 'memory effect' is described elsewhere in this issue (Dahl-Jensen, D. & Johnsen, S.J. *Nature* 320, 250; 1986).

The memory effect allows the reconstruction of past changes on a timescale of the order of the response time of the system. But the extent to which the memory can be recalled is limited by our theoretical comprehension of the behaviour of the system. The components of the Earth's hydrosphere are not simple systems which react in a simple way to single external causes, but are complex, interactive and intrinsically difficult to analyse explicitly without the excessive empiricism that

## NEWS AND VIEWS

sheets and starving arctic ice masses. South Greenland stands in the critical pivotal zone in this north/south see-saw. It would be surprising if the assumption of a stable glacial climate in Dahl-Jensen and Johnsen's model survived the relaxation of restrictions such as constant thickness and flow pattern.

There are probably many natural systems that are analysed in a highly constrained way which would appear very different if some of the constraints were relaxed. There is often much empirical data which can be used to define a boundary condition that can be satisfied by a properly posed, highly coupled, numerical solution in which the interactions are not artificially restricted. In the case of an

ice sheet such as that of Greenland, time-dependent thermomechanically coupled dynamic models, such as those currently being developed, should be applied to ice-sheet evolution to calculate the mass balance and flow changes that would satisfy boundary conditions such as temperature profiles, isotope composition, gas pressure, crustal rebound and glacial geology. But even such a solution would have to be considered for compatibility within a larger system of oceanic and atmospheric changes. □

G.S. Boulton is Reader in Environmental Sciences at the University of East Anglia, Norwich NR4 7TJ, UK, and Professor of Physical Geography at the University of Amsterdam, Spui 21, 1012 WX Amsterdam, The Netherlands.

## Cell motility

## Regulation by phosphorylation

from J.M. Scholey

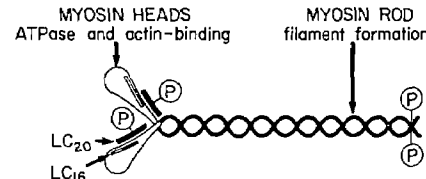
MANY motile activities of cells are believed to be driven by the actin-activated ATPase activity of myosin. In the decade since it was reported<sup>1</sup> that the phosphorylation of platelet myosin increases its actin-activated ATPase activity, similar results have been obtained with many different vertebrate non-muscle myosins. This suggests that changes in the degree of phosphorylation of myosin light chains represent a widespread regulatory mechanism that serves to switch on and off the actin-activated ATPase activity of myosin within vertebrate non-muscle cells. But this simple interpretation of the effects of phosphorylation has now been questioned by P.D. Wagner and J.N. George<sup>2</sup>, using calf thymus myosin.

Thymus myosin resembles other vertebrate non-muscle myosins in possessing two regulatory light chains (relative molecular mass,  $M_r \sim 20,000$ ), one on each head of the molecule, which can be phosphorylated, resulting in a stimulation of actin-activated ATPase activity (see figure)<sup>3,4</sup>. The actin-activated ATPase activity of thymus myosin varies as a function of the concentration of actin filaments (F-actin) according to Michaelis-Menten kinetics. Wagner and George have now measured the maximum rate of actin-activated ATPase activity ( $V_{max}$ ) and the actin concentration required to produce  $\frac{1}{2} V_{max}$  (called  $K_{app}$ ), for both phosphorylated and unphosphorylated thymus myosin<sup>2</sup>.

Surprisingly, they find that light-chain phosphorylation causes a 15- to 20-fold decrease in  $K_{app}$ , but does not affect the  $V_{max}$ , so that the unphosphorylated light chain can be described as a competitive inhibitor of the actin-activated ATPase. At low concentrations of actin, phosphorylation relieves the inhibition, thereby

stimulating the actomyosin ATPase activity. However, as the actin concentration increases, the capacity of this actin to 'compete' out and overcome the inhibitory effect of the unphosphorylated light chain also increases until, at sufficiently high actin concentrations ( $>6 \text{ mg ml}^{-1}$ ), both phosphorylated and nonphosphorylated myosin hydrolyse ATP at similar rates (close to  $V_{max}$ ).

Light-chain phosphorylation therefore seems to be a feasible mechanism for switching on and off the actin-activated



A vertebrate non-muscle myosin molecule, consisting of two heavy chains ( $M_r 200,000$ ) and two pairs of light chains ( $M_r 20,000$  and  $16,000$ ). The molecule is asymmetrical, comprising two pear-shaped heads attached to a fibrous rod. The heads contain the actin-binding and ATPase sites. Each one contains one of each type of light chain. The function of the  $M_r 16,000$  light chains (LC<sub>16</sub>) is unclear. The  $M_r 20,000$  light chain (LC<sub>20</sub>) has been implicated in the regulation of actin-myosin interaction. P, phosphorylation sites on LC<sub>20</sub> and on the heavy chains.

ATPase within thymus cells, but only at low cellular F-actin concentrations. About  $1-10 \text{ mg ml}^{-1}$  actin is thought to be present in non-muscle cells *in vivo*, but the effective concentration of actin filaments in localized regions of the cell is unknown.

Light-chain phosphorylation also stimulates the polymerization of thymus myosin into filaments *in vitro*, but it is not known whether the effect is physiologically relevant<sup>5</sup>. Whether thymus myosin,

like several other vertebrate non-muscle myosins, can also be phosphorylated on its heavy chains (see ref. 6) is not yet known, but if so, this modification would be another possible mechanism for regulating its activity<sup>7</sup>. For example, the stimulation of myosin assembly caused by changes in the level of heavy- or light-chain phosphorylation may be an important element in the pathway leading to the activation of cytokinesis<sup>8</sup>. But the protein may not need to assemble into filaments to translocate particles along actin filaments, a process which can be driven by myosin monomers<sup>9,10</sup>. A new procedure for visualizing myosin filaments in cells could be used to determine whether phosphorylation regulates myosin filament assembly *in vivo* as well as *in vitro*.

How similar is thymus myosin to the protein from other tissues<sup>9</sup>? Properties such as enzyme activity, immunological cross-reactivity, filament assembly and regulation of myosin isoenzymes differ, so thymus myosin could be a special case. Indeed, it differs from chicken gizzard smooth muscle myosin, where the major effect of light-chain phosphorylation is greatly to increase the  $V_{max}$  of the actin-activated ATPase activity<sup>11</sup>, suggesting that phosphorylation stimulates the actin-activation of this myosin even at very high concentrations of actin. Phosphorylation of skeletal muscle myosin light chains has a much smaller effect on the actin-activated ATPase activity, causing only a twofold decrease in  $K_{app}$  and no change in  $V_{max}$  (ref. 12). It would be interesting to know whether these differences reflect physiologically significant differences between non-muscle, smooth and skeletal muscle contractile systems.

Another question concerns whether phosphorylation of myosin from thymus and from other vertebrate non-muscle tissues can regulate motility (as opposed to enzyme activity and filament formation). An assay for the movement of myosin-coated beads along actin filament bundles<sup>13</sup> will be useful in addressing this question. Indeed, Sellers *et al.*<sup>14</sup> have shown that light-chain phosphorylation regulates translocation of gizzard myosin-coated beads along actin filaments and have demonstrated a high correlation between motility and ATPase activity.

Some of the actin-binding proteins present in non-muscle cells may also contribute to the regulation of motility. Interestingly, Wagner and George<sup>2</sup> report that tropomyosin seems to mimic light-chain phosphorylation, causing a large decrease in the  $K_{app}$  of unphosphorylated thymus myosin to a level similar to the  $K_{app}$  of phosphorylated myosin. This suggests that unphosphorylated and phosphorylated myosin are equally effective in causing movement in regions of the cell that contain tropomyosin, even if the actin concentration is low. Actin filaments con-

taining tropomyosin plus troponin (a skeletal muscle  $\text{Ca}^{2+}$ -binding regulatory protein) activate the ATPase activity of unphosphorylated myosin in the presence, but not in the absence (less than  $10^{-6}\text{M}$ ) of  $\text{Ca}^{2+}$ .

In contrast, activation of the ATPase activity of phosphorylated thymus myosin by actin-troponin-tropomyosin is insensitive to calcium. Therefore, light-chain phosphorylation stimulates the actin-tropomyosin-troponin-activated ATPase activity of thymus myosin independent of the actin concentration when the  $\text{Ca}^{2+}$  concentration is less than micromolar. But it is not known whether troponin is present in non-muscle cells.

To elucidate the functions of myosin in non-muscle cells, antibodies that specifically inhibit the actin-activated ATPase activity of myosin can be microinjected into living cells. Treatment of cells in this way causes an inhibition of cytokinesis but not mitosis<sup>15,16</sup>.

Analogous experiments, using probes that specifically inhibit myosin phosphory-

lation in living cells (such as antibodies to myosin kinases) might similarly illuminate the role of this modification in the regulation of actomyosin-based motile activities in many cells. □

1. Adelstein, R.S. & Conti, M.A. *Nature* **256**, 597 (1975).
2. Wagner, P.D. & George, J.N. *Biochemistry* **25**, 913 (1986).
3. Scholey, J.M. *et al.* *J. Biol. Chem.* **257**, 7737 (1982).
4. Wagner, P.D., Vu, N.-D. & George, J.N. *J. Biol. Chem.* **260**, 8084 (1985).
5. Smith, R.C. *et al.* *Phil. Trans. R. Soc. B* **302**, 73 (1983).
6. Trotter, J.A., Nixon, C.S. & Johnson, M.A. *J. Biol. Chem.* **260**, 14374 (1985).
7. Kuczmarski, E.R. & Spudich, J.A. *Proc. Natl. Acad. Sci. U.S.A.* **77**, 7292 (1980).
8. Yumura, S. & Fukui, Y. *Nature* **314**, 194 (1985).
9. Albanesi, J.P. *et al.* *J. Biol. Chem.* **260**, 8649 (1985).
10. Adams, R.J. & Pollard, T.D. *J. Cell. Biol.* **101**, 389a (1985).
11. Sellers, J.R., Eisenberg, E. & Adelstein, R.S. *J. Biol. Chem.* **257**, 13880 (1982).
12. Persechini, A. & Stull, J.T. *Biochemistry* **23**, 4144 (1984).
13. Sheetz, M.P. & Spudich, J.A. *Nature* **303**, 31 (1983).
14. Sellers, J.R., Spudich, J.A. & Sheetz, M.P. *J. Cell Biol.* **101**, 1897 (1985).
15. Mabuchi, I. & Okuno, M. *J. Cell Biol.* **74**, 251 (1977).
16. Kiehart, D.P., Mabuchi, I. & Inoue, S. *J. Cell Biol.* **94**, 165 (1982).

J.M. Scholey is in the Department of Molecular, Cellular and Developmental Biology, University of Colorado, Boulder, Colorado 80309, USA.

## Molecular biology

# Brevity is the soul of wit

from Roger H. Pain

IN HIGHER organisms, protein-coding genes are made up of exons, each of which encodes relatively short sections of the protein chain, and introns, intervening regions of DNA that are not translated into protein. This revolutionary discovery led to speculation that this sort of gene structure could provide the basis for rapid and radical steps in the evolution of proteins<sup>1</sup>. One development of this idea is the proposal that the sections of protein encoded by exons have particular biochemical functions within the whole molecule; in 1981 M. Gō assigned different functions of the haemoglobin molecule to the three exons of the globin gene<sup>2</sup>. In the 5 March issue of the *Journal of Molecular Biology*, De Sanctis and colleagues report that a polypeptide corresponding closely to one of these exons binds haem to form a 'mini-myoglobin' which exhibits the oxygen-binding function of whole myoglobin, providing experimental evidence for Gō's hypothesis.

The idea that one structural and functional domain of a protein is encoded by one exon has developed as the structures of more genes have become known. The function of a domain can range from specific antigen binding to the provision of small sections of peptide or 'beads' that can be strung together by exon multiplication to form a chain of a functionally appropriate length. But if the larger exons originally encoded 'ancestral' protein units (those that existed in isolation from

other exon-coded units), then the polypeptide must have been able to fold into a reasonably stable conformation to exercise the specific function on which its evolutionary selection would be based<sup>4</sup>.

Experimental confirmation of these proposals, in terms of the ability to fold and the expression of a biochemical function, is made difficult by the sophisticated and specialized mutational changes in the ancestral protein unit that have led to the present-day form of the protein. Changes in amino-acid composition that strengthen the interaction of the ancestral unit with other exon products, and which modify or supplement the original function, may decrease the ability of the original structure to function independently. Increasing the number of non-polar amino-acid residues on the surface of a protein, for example, can strengthen the interaction between two domains but at the same time make the isolated unit less stable in aqueous solution. Therefore, exon-coded domains may only be fossils, with no relevance to their intrinsic structure or function. But if it is true that, throughout evolutionary modification, the ability of the domains to fold into a very precise three-

dimensional conformation is retained or strengthened at all steps of development of each protein, an experimental test of the hypothesis should be possible.

The first protein structure to be determined in three dimensions was myoglobin. Watson and Kendrew showed that this protein consists largely of helical segments of backbone chain folded back on one another in such a way that one side of each helix points to the solvent and the other to the core of the molecule. A cleft in this structure, lined with appropriate amino-acid residues, receives the haem

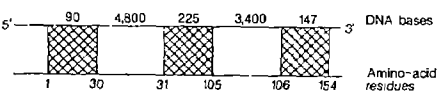


Fig. 1 The myoglobin gene of the grey seal<sup>7</sup>.

group like a coin entering a slot. The gene encoding myoglobin comprises three exons separated by long introns (Fig. 1). Gō performed a nearest-neighbour analysis of the amino-acid residues in the structure of globin and found that the peptides encoded by the two outer exons fold so as to fall naturally into two clusters (or domains) of amino acids, separate from each other and flanking the remaining peptide that folds to form the haem slot (Fig. 2). The bonds joining residues 30–31 and 105–106 each occur within helices, hence these exons do not encode neat domains that are immediately obvious to the eye, unlike those in immunoglobulins and nucleotide-binding enzymes.

In their new work, De Sanctis *et al.* excised a peptide from myoglobin that corresponds to that encoded by the central exon but which contains an additional 30 residues at the carboxy-terminal end. This peptide binds haem with high affinity and then behaves as a mini-myoglobin by combining reversibly both with carbon monoxide and with oxygen. Remarkably, the kinetics of these reactions are very similar to those of whole myoglobin.

These results provide strong evidence that the central exon encodes a functional unit, whose structure is very similar to that in the intact protein, in order that amino-acid residues that are essential for oxygen binding (such as histidines) may be oriented precisely towards the haem. A

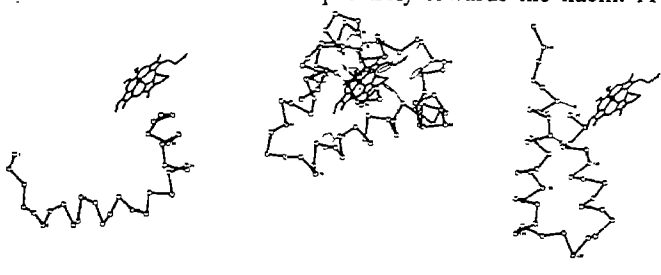


Fig. 2 Conformation of the three exon-coded peptides of the beta-chain of haemoglobin, which shares a common three-dimensional conformation with myoglobin<sup>2</sup>. Numbers, amino-acid residues.

## NEWS AND VIEWS

similar experiment using the precise central domain was only partly successful<sup>1</sup>, supporting the notion that, without additional stabilization, the domain of the present-day protein lacks the stability that is presumed to have existed in the ancestral exon product.

Despite the apparent evidence to the contrary from the globin gene structure, Gö proposed that the peptide encoded by the central exon comprises two structural domains<sup>2</sup>. Subsequent analysis of the gene encoding plant leghaemoglobin, which shares the globin family conformation, showed the presence of four exons with the additional intron exactly where Gö predicted.

Has the break been gained recently, by

insertion<sup>6</sup>, or does this reflect the primordial gene structure? If the latter is true, the experiment of De Sanctis *et al.* suggests that a functional role for either or both of these domains could be assigned. Who will have the wit to explore the ultimate brevity of micro-myoglobin? □

1. Gilbert, W.A. *Nature* **271**, 501 (1978).
2. Gö, M. *Nature* **291**, 90 (1981).
3. De Sanctis, G., Falcioni, G., Giardina, B., Ascoli, F. & Brunori, M. *J. molec. Biol.* **188**, 73 (1986).
4. Blake, C.C.F. *Nature* **273**, 267 (1978).
5. Craik, C.S., Buchman, S.R. & Beychok, S. *Nature* **291**, 87 (1981).
6. Rogers, J. *Nature News and Views* **315**, 458 (1985).
7. Blanchetot, A., Wilson, V., Wood, D. & Jeffreys, A.J. *Nature* **301**, 732 (1983).

*Roger H. Pain is Professor of Physical Biochemistry at the University of Newcastle upon Tyne, Newcastle upon Tyne NE1 7RU, UK.*

with fewest topological complications.

For a torus (or doughnut) two distinct winding numbers are required: the first representing the number of times the curve winds around the hole in the middle; the second the number of times it winds around the body of the torus (like the stripes on a barber's pole). The fundamental group therefore consists of pairs  $(m,n)$  of integers, and the operation of joining loops again corresponds to arithmetical addition:  $(m,n)+(p,q)=(m+p, n+q)$ . As this is a different algebraic object from the integers or the trivial group, it follows that a torus cannot be topologically deformed into a circle or a sphere. That a torus is not topologically equivalent to a circle is obvious on other grounds; that it is not deformable into a sphere is less obvious. For more complicated examples, the fundamental group plays a central role.

The fundamental groups of all surfaces can be calculated, and it can be seen that they are all non-trivial (that is, they contain loops that cannot be shrunk to a point), unless the surface is a two-sphere. In other words, any surface with a trivial fundamental group must be topologically equivalent to the two-sphere.

The Poincaré conjecture is the exact analogue of this fact for the next dimension of manifolds — three-dimensional manifolds. Once again there is a particularly simple three-dimensional manifold, the three-dimensional sphere, which can be thought of as ordinary three-dimensional space, but 'gathered together' at infinity so that it closes up on itself, much as a square of cloth can be gathered into a closed bag by pulling tight a loop of string around its edge. The three-sphere has a trivial fundamental group (every loop can be shrunk to a point). Poincaré's question (*Rendiconti del Circolo matematico di Palermo* **18**, 45; 1904, reprinted in *Oeuvres de Henri Poincaré* Vol. VI p.498; Gauthier-Villars, Paris, 1953), posed with the off-hand remark "this question would lead us too far astray", is the converse. If a (connected closed compact) three-dimensional manifold has a trivial fundamental group, then must it be topologically equivalent to the three-sphere? Poincaré's problem turned out to be one of the most baffling in mathematics, and it soon joined the ranks of other notorious and difficult unsolved problems, such as Fermat's last theorem or the Riemann hypothesis.

To explain why the problem turned out to be so difficult, and to explain how Rêgo and Rourke have now solved it, we need to look at the higher-dimensional analogues of the problem. The fundamental group, using as it does one-dimensional loops, is incapable of capturing certain features of higher-dimensional manifolds. For example it cannot distinguish between a solid ball and its two-sphere boundary.

## Topology

## The Poincaré conjecture proved

from Ian Stewart

A SOLUTION to the Poincaré conjecture, one of topology's biggest open questions which dates from 1904, was announced earlier this month by Eduardo Rêgo (Centro Matemática Ruy Luis Gomez, University of Oporto) and Colin Rourke (Mathematics Institute, University of Warwick). Their work sets the seal on some 80 years of intensive effort by mathematicians, and represents a fundamental advance in our understanding of three-dimensional topology.

Topology is the study of those properties of objects that are unchanged by continuous transformations. Its origins can be traced back to 1735 when Leonhard Euler solved the problem of the Königsberg bridges, but it first acquired mathematical significance around 1860 with the work of Georg Bernhard Riemann on Riemann surfaces. Over the past 50 years it has developed into a major area of mathematics, and its influence now extends throughout the subject. It is now starting to play an important role in applied science; for example there are topological questions in the same general area as the Poincaré conjecture that lie at the heart of current attempts to unify the fundamental forces of nature.

A major triumph of topology in the nineteenth century was the complete classification of (closed compact) surfaces. The orientable, or two-sided, surfaces are all equivalent to a sphere or a torus with one or more holes. (The number of holes is called the genus of the surface.) The non-orientable, or one-sided, surfaces are similarly classified by their genus. The genus is a topological invariant: if one surface can be transformed continuously into another, the number of holes does not change. This implies that all possible surfaces may be topologically classified by

just two items of data: orientability/non-orientability; and the number of holes.

One of the most important problems in topology is to extend these classical results on surfaces to their multidimensional analogues, called manifolds. (A surface is a two-dimensional manifold.) For example, it would be extremely useful to have a complete classification of (closed compact) manifolds of any given dimension. The main idea is to associate with each manifold various algebraic structures that capture key features of the topology. One of the most basic, introduced by Henri Poincaré in 1895, is the fundamental group. This determines the way in which closed loops in a manifold may be deformed into one another.

For example, consider a circle, the simplest one-dimensional manifold. Two loops round a circle may be deformed into each other if, and only if, they wind round the circle the same number of times. (Topologists then call them homotopic, meaning similarly situated.) The algebraic structure arises because loops can be 'added' by joining them end to end. If loops with winding numbers  $m$  and  $n$  are so joined, the result winds round  $m+n$  times. The fundamental group is thus the set of integers (representing the winding numbers) under the operation of addition (representing the joining of two loops in sequence).

For a two-dimensional sphere — the surface of a solid ball — the fundamental group is trivial, that is, it consists of a single element. This happens because any loop on a sphere may be shrunk to a point by sliding it over the sphere. The two-dimensional sphere is said to be simply connected. For this and other reasons topologists consider the two-sphere to be the simplest of all surfaces, that is, the one

## NEWS AND VIEWS

But analogous invariants may be constructed using 'loops' (actually spheres) of higher dimension. These objects are called the higher homotopy groups. In the subject of algebraic topology, many variations on this theme have been introduced, calculated and analysed. A major part of the research effort of the past 50 years has gone into refining such ideas.

It can be shown that if a three-dimensional manifold has a trivial fundamental group, then it is a homotopy three-sphere: that is, all of its higher homotopy groups (fundamental and higher) are the same as those of the three-sphere. Poincaré's problem now has an immediate generalization to all dimensions: must every homotopy sphere be a genuine sphere?

Ever since Poincaré stated his problem, it and its generalization have been under incessant (and largely unsuccessful) attack. Only for the two-dimensional case — surfaces — was the answer known to be 'yes', as a result of the classification theorem. While topology grew ever more powerful, Poincaré's problem remained almost totally intractable. It is not hard to see why. To calculate the higher homotopy groups of a given manifold is itself a difficult task; but the Poincaré conjecture asks the inverse question: given the groups, find the manifold. To prove it, one must start with a completely arbitrary manifold, and then somehow use the information on the higher homotopy groups to bring it into a recognizable form. For surfaces, a case-by-case analysis will do the trick, because the classification theorem lists all the cases. But in three dimensions or more, no classification is known, and to make matters worse, the unknown status of the Poincaré conjecture is to some extent responsible for that state of affairs. There is an air of Catch-22: before proving the Poincaré conjecture, one must first prove the Poincaré conjecture. The only way out is to develop totally new methods and bypass the unsolved problems of classification.

The first big breakthrough came in 1961 when Stephen Smale developed a method for breaking manifolds into nice pieces, called handles. By moving handles around he proved a far-reaching theorem, for dimensions five or higher, one of whose consequences is the truth of the Poincaré conjecture for dimensions  $n \geq 5$ . Originally, Smale's proof worked only for  $n \geq 7$ . John Stallings dealt with  $n=6$  and Christopher Zeeman with  $n=5$ . Smale subsequently extended his methods to these dimensions.

Another important tool for the study of higher dimensional manifolds was also developed in the early 1960s — the technique of surgery. This is in essence a systematic study of the effect of removing certain nice pieces of a manifold and gluing them back with a specific 'twist'.

Using surgery, John Milnor found a counterexample in dimension seven to the analogue of the Poincaré conjecture for a more specialized case. This is the 'differentiable' case where the topological equivalence is required to be differentiable as well as continuous. Milnor and Michael Kervaire obtained a complete understanding of this more specialized formulation of the conjecture in dimensions five and higher.

That left only the three-dimensional case (Poincaré's original problem) and the four-dimensional case unsolved; but here both handle theory and surgery fail to work. The number of dimensions is high enough to allow complicated behaviour, but too small to leave adequate room for manoeuvre in eliminating those complications. The general feeling was that something unusual happens in spaces of dimension three or four. But in the late 1970s the Cambridge mathematician Andrew Casson found a way to make handle theory start to work in four dimensions. In 1982 Michael Freedman used 'Casson-handles' to prove the four-dimensional case of the Poincaré conjecture (but not the more specialized differentiable case, which remains open).

This left just one case of the problem unsolved — the dimension three problem which Poincaré had originally posed! Here the more specialized differentiable case is known to have the same answer as the continuous case. It is this final question that has now been answered, affirmatively, by Rêgo and Rourke. Their results have been written up as three University of Warwick preprints (*A Characterization of Homotopy 3-Spheres I and II*; and *Characterizations of  $S^3$* ). The proof has been subjected to detailed scrutiny by several experts and no errors have yet been found; it was discussed at a special meeting in low-dimensional topology held at Warwick this month. Although it is wise to be cautious, it seems that the problem really has been solved at last.

The new proof is based on an ingenious combination of both methods used to solve the higher-dimensional problems — handle theory and surgery. In dimension three, handle theory was already a well-established tool dating back to the diagrams devised by the nineteenth century mathematician P. Heegaard. But despite many intensive efforts, little progress had been made in using Heegaard theory to prove the Poincaré conjecture. Surgery, on the other hand, was not exploited systematically in the analysis of three-dimensional manifolds until Robion Kirby introduced his 'Kirby calculus' in the 1970s (*Inventiones Mathematicae* 45, 35; 1979). The surgery description of a three-dimensional manifold can be seen as a complicated picture of linked curves. Unfortunately many distinct forms of the links can correspond to the same mani-

fold. The Kirby calculus attempts to deal with this difficulty by giving a complete list of 'moves' that can be made in the link picture, without altering the manifold obtained by surgery.

In 1977 Joan Birman and W. Powell observed that there is a useful class of surgery descriptions that corresponds at once to Heegaard decompositions. It is this class of surgery descriptions that is exploited by Rêgo and Rourke. They consider simultaneously three descriptions of a homotopy three-sphere. These comprise a surgery description of the Birman-Powell type in the standard three-sphere; the corresponding Heegaard decomposition; and the dual surgery description in the homotopy three-sphere. Rêgo and Rourke introduce 'moves' that alter all three descriptions in recognizable and predictable ways, and by using these moves they rearrange the three descriptions until the one based on handles — the Heegaard decomposition — is finally rendered accessible to the ordinary handle moves used by Smale. At this point the homotopy three-sphere is seen to be equivalent to the standard three-sphere.

The simultaneous moves of Rêgo and Rourke can be viewed either as complicated sequences of Smale moves, or as complicated sequences of Kirby moves and their duals. In fact they are related to these more elementary moves in approximately the same way that the complicated sequences of twists used to unscramble a Rubik cube are related to the elementary twists of which they are composed. (This is a loose analogy only; the Rubik cube is not relevant to the problem.)

Ironically, the work of Rêgo and Rourke goes against the prevailing wisdom. The main focus of recent work on three-manifolds has been directed towards the remarkable discovery by William Thurston of connections between three-manifolds and non-Euclidean geometry. One hoped-for end-result of Thurston's programme was to have been a proof of the Poincaré conjecture. The 'classical methods' of Heegaard decompositions or the Kirby calculus had been almost written off as too unsophisticated to tackle the Poincaré conjecture.

The results of Rêgo and Rourke put the finishing touches on many known results in topology, by removing unnecessary hypotheses. There are also important consequences in four-dimensional topology, particularly the existence of a four-dimensional manifold having no triangulation. And their pioneering effort paves the way, at last, for a detailed understanding not just of the three-sphere, but of three-manifolds in general. Of course the book of topology is by no means closed; but a major chapter is. □

## SCIENTIFIC CORRESPONDENCE

## Origins of human T-lymphotropic viruses

SIR—Joseph Rosenior finds it hard to understand why we have postulated that human T lymphotropic virus (HTLV-I) originated in Africa<sup>1</sup>. We were surprised by his belief that Japan did not have contact with Europeans until the eighteenth century. While it is true that "Japan was virtually cut off economically and politically from the rest of the world", it is striking that the initial contacts with Portuguese explorers during the sixteenth century occurred precisely in areas of Southern Japan where HTLV-I is endemic. The first Portuguese contact arrived in 1543<sup>2</sup>. In 1549, Saint Francisco Xavier, a Jesuit missionary, arrived in Kagoshima. He later gained Lord Omura Sumita's sanction to use the Port of Nagasaki. This port prospered and became a large commercial centre. The Portuguese established themselves throughout the southern portion of Japan and their influence and contact with the Japanese became frequent. It is known that the Portuguese took Africans with them to Japan. The Africans' presence can be seen in Portuguese pictorial records known as Nanban-Byobu, where the artist depicted Portuguese, Japanese and Africans together<sup>3,4</sup>.

Further, it is believed that the Portuguese came with African monkeys. The Japanese word for monkey *amakawa* is thought by Juijirō Cogā to be derived from the Portuguese word *macaco* also meaning monkey (ref. 5 and p. 92, ref. 1).

Recently, Hino *et al.* supported this conclusion by demonstrating that the proportion of HTLV-I disease was correlated with the incidence of Japanese Catholics<sup>6</sup>, again consistent with this hypothesis. A virus similar to HTLV-I was found in Japanese macaques, stimulating an alternative idea that HTLV-I entered Japan from a monkey. However, viruses like HTLV-I were also found in many African monkeys<sup>7</sup> and Yoshida, Seiki and colleagues recently found that the African monkey virus (STLV-I) is almost identical to the HTLV-I in man (African and Japanese)<sup>8</sup>.

Rosenior is also surprised that we think that HTLV-III, the virus which causes AIDS, also originated in Africa. He states "that HTLV-III occurs . . . in some flocks of European sheep." It is ironic that he refers to our own work (with M. Gonda), although he has misinterpreted the results. Visna virus of sheep is very distantly related to HTLV-III. Both viruses probably have a very ancient ancestral origin in common. HTLV-III is much more closely related to the simian virus STLV-III, the virus isolated by Essex and colleagues from African green monkeys. All current data from HTLV-I and HTLV-III support an African origin for these two human

retroviruses. Just as important, no alternative reasonable hypothesis has been presented.

Finally, the origin of the only other human retrovirus, HTLV-II, is unknown, but its relatedness (about 50% of the genome) to HTLV-I suggests that HTLV-II and HTLV-I have common ancestry.

ROBERT C. GALLO  
ANN H. SLISKI

Laboratory of Tumor Cell Biology,  
National Cancer Institute,  
National Institutes of Health,  
Bethesda, Maryland 20205, USA

CARLOS M.C. DE NORONHA  
FERNANDO DE NORONHA

Department of Veterinary Microbiology,  
Cornell University,  
Ithaca, New York 14853, USA

1. Rosenior, J. *Nature* **318**, 100 (1985).
2. Matsuda, K. *The Relations between Portugal and Japan*, (Junta de Investigações do Ultramar e Centro de Estudos Históricos Ultramarinos, Lisboa, 1965).
3. Boxer, C.R. *The History of Portuguese in Japan* 10–11 (Kegan Paul, London, 1929); *As viagens de Japão e os seus capitães-morres* (1550–1640), 17–18 (Escola Tipográfica do Oratório de S.J. Bosco Salesianos–Macau, 1949).
4. Nagayama, T. *Collection of Historic Materials Connected with the Roman Catholic Religion in Japan* (*Kirishitan Shirio-Sho*) Nagasaki, 13 (1924).
5. Norton, L. *Os Portugueses no Japão (1543–1640)* (Notas e Documentos) 35–36 (Agência Geral do Ultramar, Divisão de Publicações e Biblioteca, Lisboa 1952).
6. Hino, S., Kinoshita, K. & Kitamura, Y. *Lancet* **ii**, 572–573 (1984).
7. Miyoshi, I. *et al.* *Lancet* **ii**, 958–959 (1982).
8. Watanabe, T. *et al.* *Virology* **144**, 59–65 (1985).

## Bovine leukaemia virus and multiple sclerosis

SIR—Koprowski *et al.* provide evidence that the serum and spinal fluid of multiple sclerosis patients contain antibody which cross-reacts with human T-cell viruses and that cells from the spinal fluid contain RNA which hybridizes with human T-lymphotropic virus (HTLV) type I under low-stringency conditions<sup>1</sup>. But is it possible that the 'footprints' which they have found are actually those of bovine leukaemia virus (BLV)?

There are strong geographic correlations between production and consumption of dairy products and multiple sclerosis<sup>2</sup>. Moreover, milk from cows shedding BLV has caused leukaemia in chimpanzees<sup>3</sup> and there is epidemiological evidence linking cattle herds infected by this virus with human leukaemia<sup>4</sup>. Therefore, it seems likely that BLV can be transmitted in dairy products and cause disease in humans.

It also seems likely that the viral traces found in multiple sclerosis patients could have been left by BLV. Antisera to BLV proteins cross-react with those of human T-cell viruses. Amino acid microsequencing and statistical analysis reveal 9 common amino acid residues out of 24 possible comparisons when the NH<sub>2</sub>-terminal sequences from the core proteins of HTLV p24 are aligned. The probability

that this sequence homology is due to chance is only  $0.4 \times 10^{-10}$  (ref. 5). Nucleic acid hybridization experiments thus far reveal a sequence homology of 11% between the RNA of BLV and HTLV<sup>6</sup>.

Diets low in saturated fats (with sharp reduction in the use of dairy products) are said to help patients with multiple sclerosis<sup>7</sup> and the Guillain–Barré syndrome<sup>8</sup>. It is an interesting coincidence that one of the control subjects studied by Koprowski *et al.* was a patient with Guillain–Barré syndrome who also had antibody to HTLV.

In the aggregate, these facts should prompt some consideration of BLV infection in patients with multiple sclerosis and, perhaps, certain other neurological syndromes of unknown cause.

ALLAN S. CUNNINGHAM  
Mary Imogene Bassett Hospital,  
Cooperstown, New York 13326, USA

1. Koprowski, H. *et al.* *Nature* **318**, 154–160 (1985).
2. Agranoff, B. & Goldberg, D. *Lancet* **ii**, 1061–1066 (1974).
3. *Lancet* **ii**, 30–31 (1974).
4. Donham, K.J. *et al.* *Am. J. Epidemiol.* **112**, 80–92 (1980).
5. Oroszlan, S. *et al.* *Proc. natn Acad. Sci. U.S.A.* **79**, 1291–1294 (1982).
6. Reitz, M.S. Jr *et al.* *Proc. natn Acad. Sci. U.S.A.* **78**, 1887–1891 (1981).
7. Field, E.J. *J. R. Soc. Med.* **72**, 487–488 (1979).
8. Bower, B.D. & Newsholme, E.A. *Lancet* **i**, 583–585 (1978).

## Endogenous retrovirus in multiple sclerosis?

SIR—In their recent article<sup>1</sup> Koprowski *et al.* described the presence, in sera from some patients suffering from multiple sclerosis, of antibodies reactive with antigens of the human T-lymphotropic viruses HTLV-I, -II and -III. Although the authors did not distinguish between healthy blood donors possessing no anti-viral antibodies or those possessing antibodies only occasionally in lower titres (there was no definition of cut-off in the enzyme-linked immunosorbent assay), they cautiously suggested that infection by an exogenous, so far unknown retrovirus strain might be involved in the development of multiple sclerosis. The induction of antibodies that cross-react with such immunologically divergent strains as HTLV-I and -III and the inhibition by both HTLV-I and -III of antibody binding to HTLV-I p24 suggest that the putative multiple sclerosis strain must be very different from the two strains investigated. Testing of sera from multiple sclerosis patients against a variety of available animal retrovirus antigens may help to predict more precisely the antigenic composition of a putative multiple sclerosis retrovirus.

However, there is an alternative explanation for the data reported, namely the possible activation of a human endogenous retrovirus in cells of multiple sclerosis patients either directly by infection with viruses (such as measles, varicella, influenza) often associated with

the development of multiple sclerosis, or indirectly and more likely, by immunological response to such virus infected cells. It is well known that chromosomally integrated, endogenous or exogenous retroviruses can be induced to replicate by immunological mechanisms.

Evidence for the existence of a human endogenous retrovirus is slowly, but steadily accumulating. Retrovirus-like particles can regularly be observed budding from human placental trophoblasts (see ref.2 for review). Morphologically indistinguishable viruses have been detected in all investigated trophoblast-containing human teratocarcinoma cell lines. Animal retrovirus core (gag-) related antigens and corresponding antibodies have repeatedly been found in healthy individuals and in patients with autoimmune disorders (most recently in ref.4). Furthermore, naturally occurring antibodies to endogenous retroviruses are widespread in animals, including higher primates<sup>5</sup>.

Like exogenous retroviruses, induced endogenous strains insert their envelope glycoproteins into the host's cell membrane, rendering the cell vulnerable to immunological attack<sup>6</sup>. In astrocytes or other glial cells, this process may lead to immunological exposure of myelin basic protein (MBP) or other antigens, sensitizing and activating MBP-specific T cells. Thus, induction of endogenous retroviruses, either directly by horizontally transmissible viruses like measles, varicella or influenza or indirectly by the immune response to such virus infected cells, may turn out to explain anti-retroviral antibodies in multiple sclerosis patients.

REINHARD KURTH

*Paul-Ehrlich-Institut,  
Paul-Ehrlich-Str. 42-44,  
6000 Frankfurt am Main 70, FRG*

1. Koprowski, H. et al. *Nature* **318**, 154-160 (1985).
2. Löwer, R. et al. *J. gen. Virol.* **65**, 887-898 (1984).
3. Boller, K. et al. *J. gen. Virol.* **64**, 2549-2559 (1983).
4. Ruchton, M. et al. *Virology* **144**, 468-480 (1985).
5. Fine, D.L. & Arthur, L.O. *Virology* **112**, 49-61 (1981).
6. Kurth, R. et al. *Nature* **279**, 197-201 (1979).

## Archaeabacterial status quo is defended

SIR—In the interest of the young progressive field of molecular phylogeny the debate between Lake and the "orthodoxy of archaeabacteria" should be reduced to its factual basis. Lake *et al.* claim (1) that the urkingdom of the archaeabacteria<sup>1,2</sup> be divided into two distinct urkingdoms—the "eocytes", comprising the genus *Sulfolobus* and the *Thermoproteales* and the "archaeabacteria", comprising the rest<sup>4</sup>; and (2) that the *Halobacteriaceae* (or, rather, *Halobacterales*) be transferred from the urkingdom of the archaeabacteria into that of the eubacteria which they, after its expansion, rechristened "photocytes"<sup>5</sup>.

• Lake bases his claims on a comparison

## SCIENTIFIC CORRESPONDENCE

of details of the three-dimensional structure of ribosomes as revealed by electron microscopy. The phylogenetic usefulness of this feature, at the present level of resolution, has been profoundly queried by Stöffler-Meilicke *et al.* and Stöffler and Stöffler-Meilicke<sup>7</sup>.

• The division of the archaeabacteria into two branches, methanogens plus halophiles and sulphur-dependent archaeabacteria, had been recognized previously<sup>8,9</sup>. Yet the sequences of 16S rRNAs<sup>10,11</sup> and many other feature designs of both branches are clearly too similar to justify their promotion to kingdom level<sup>10</sup>.

• The alleged homology of the purple membrane of some halobacteria and the photosynthetic machinery of several groups of eubacteria, the only argument besides ribosome shape quoted in support of the creation of the "photocyte" kingdom, is at best an analogy in principle (light energy utilization). Homology (or identity of origin) must be proven before it can prove relatedness.

Lake *et al.* discount the features supporting the "orthodox" view of one kingdom of the archaeabacteria including the halophiles mainly in two ways:

• So-called plesiomorphic properties (shared by "archaeabacteria", "eocytes" and *Halobacteriaceae* but not eubacteria) are considered useless for cladistics in contrast to the "synapomorphic properties" which have served to establish the proposed tree. The reason for this astonishing conversion of good archaeabacterial features ("orthodox" meaning) into "shared" plesiomorphic properties is simply the proposed division of one phylum into three. Are there other "synapomorphic" features common to halobacteria and eubacteria? And, if the archaeabacterial properties are plesiomorphic, why are they not shared by any eubacteria? Such terms should only be assigned after analysis and not used in a dialectical and tendentious way.

• As Lederer explains below, the proposals of Lake *et al.* in contrast to the tree derived from rRNA sequences comparison, prove invalid when tested by the consistency criteria of Felsenstein<sup>12</sup>. The kingdom of the archaeabacteria remains a solid entity in our incomplete understanding of the early phase of biotic evolution.

WOLFRAM ZILLIG

*Max-Planck-Institut für Biochemie,  
8033 Martinsried bei München, FRG*

1. Woese, C.R. & Fox, G.E. *Proc. natn. Acad. Sci. U.S.A.* **74**, 5088-5090 (1977).
2. Woese, C.R., Magrum, L.J. & Fox, G.E. *J. molec. Evol.* **11**, 245-252 (1978).
3. Fox, G.E. *et al. Science* **209**, 457-463 (1980).
4. Lake, J.A., Henderson, E., Oakes, M. & Clark, M.W. *Proc. natn. Acad. Sci. U.S.A.* **81**, 3786-3790 (1984).
5. Lake, J.A. *et al. Proc. natn. Acad. Sci. U.S.A.* **82**, 3716-3720 (1985).
6. Stöffler-Meilicke, M., Böhme, C., Strobel, O., Böck, A. & Stöffler, G. *Science* (in the press).
7. Stöffler, G. & Stöffler-Meilicke, M. *System. appl. Microbiol.* (in the press).
8. Zillig, W., Schnabel, R., Tu, J. & Stetter, K.O. *Naturwissenschaften* **69**, 197-204 (1982).

9. Woese, C.R., Gupta, R., Hahn, C.M., Zillig, W. & Tu, J. *System. appl. Microbiol.* **5**, 97-105 (1984).
10. Woese, C.R. & Olsen, G.J. *System. appl. Microbiol.* (in the press).
11. Hummel, H., Jarsch, M. & Böck, A. *Microbiology* (in the press).
12. Felsenstein, J. *System. Zool.* **27**, 401-410 (1978).

SIR—In his letter "An alternative to archaeabacterial dogma" (*Nature* **319**, 626; 1986), Lake claims that the archaeabacterial tree proposed by Woese and Olsen (*System. appl. Microbiol.* in the press) is inconsistent because of unequal clock-rates in different branches of the tree, citing the work of Felsenstein (*Syst. Zool.* **27**, 401; 1978).

According to Felsenstein, in an unrooted tree with four branches the relevant sums of transition probabilities, which determine the branching of the tree, are not affected by the exact placement of the root and thus different clock-rates.

By alternatively omitting one branch of the two trees shown in Lake's letter, five trees with four branches are obtained in both cases. Taking the branch lengths to represent the transition probabilities, one can calculate Felsenstein's probability sums ( $P_{110} + P_{0011}$ ,  $P_{1010} + P_{0101}$ ,  $P_{1001} + P_{0110}$ ). All five trees with four branches deduced from the tree of Woese did not violate the consistency condition ( $P_{1100} + P_{0011}$  must be largest), whereas the five trees deduced from the tree of Lake violated the consistency condition in four out of five cases. In the one consistent case (a tree with eukaryotes omitted), the phylogenetic distance between methanogens and halobacteria used in Lake's tree was 30% greater than that found in Woese's tree.

Using Felsenstein's criteria it therefore seems inappropriate to depart from the "archaeabacterial dogma".

HERMANN LEDERER

*Max-Planck-Institut für Biochemie,  
8033 Martinsried bei München, FRG*

**nature  
is available in  
microform  
from University  
Microfilms  
International.**



Please send information about these titles:

Name \_\_\_\_\_

Company/Institution \_\_\_\_\_

Address \_\_\_\_\_

City \_\_\_\_\_

State \_\_\_\_\_ Zip \_\_\_\_\_

Phone (\_\_\_\_\_) \_\_\_\_\_

Call toll-free 800-521-3044. Or mail inquiry to:  
University Microfilms International, 300 North  
Zeeb Road, Ann Arbor, MI 48106.

## BOOK REVIEWS

# Beyond hope: Bohr and physics

R.H. Dalitz

**Niels Bohr: A Centenary Volume.** Edited by A.P. French and P.J. Kennedy. Harvard University Press: 1985. Pp. 403. \$27.50, £16.50 (£25.25 from 1 April).

NIELS BOHR was born on 7 October 1885; he died on 18 November 1962. His centennial year was the occasion for many meetings and addresses about his life and work, and its impact on science today. This collection of about 40 articles gives a broad coverage of these topics, together with a chronology, a full publication list and a substantial glossary (17 pages), all at a quite modest price.

It is a chastening experience for those of the present generation to look back into history and see how many parts Bohr played and how pervasive was his influence on physics in the twentieth century. Most of us, for example, know little of the genesis of Bohr's atomic theory, beyond the brief mention of the Bohr atom in today's textbooks. To follow his original arguments is a most instructive experience, and in the book J.L. Heilbron brings out well the tenacious way Bohr explored ideas, testing them in a flexible framework of physical principles which were in the course of becoming established. No wonder that Bohr's collaborator J.C. Slater could see him as "a remorseless fanatic" who persisted in pressing on beyond hope, until some link with other truths emerged or that line of thought became decisively excluded. He sought continually to link up half-formed ideas, building upon dimly glimpsed relationships. His correspondence principle was one such relationship, and very much his own — more a way of life than a principle, said some. In his contribution, H. Kragh traces out the steps Bohr took to achieve his semiclassical

theory of the periodic table, a product of great intuition and completed long before Pauli's exclusion principle.

Bohr's association with Rutherford was vital in this early period, not only because Rutherford's laboratory in Manchester was the centre for the exploration of nuclear aspects of atoms and molecules but also because of the fruitful interaction between their personalities. As Bohr worked and worked, waiting to convince himself that his atomic model covered the whole periodic table, Rutherford finally thundered "You explain hydrogen, you explain helium, and everybody will believe all the rest". And so Bohr's "Trilogy" of papers emerged, forwarded by Rutherford to the *Philosophical Magazine*, published there in 1913 and rewarded by the Nobel Prize for 1922.

A second phase of Bohr's life began with his appointment to a professorship in the University of Copenhagen in 1916 and blossomed when his Institute of Theoretical Physics was set up in 1921. This quickly became a Mecca for physicists from around the world. Bohr was readily accessible to all who went there, and years spent in Copenhagen left an indelible mark on those who had the good fortune to visit the Institute. Bohr continued to work on his atomic theory; element 78 was discovered there through its guidance and named hafnium, after the Latin for Copenhagen. The well-known "BKS" paper (with Kramers and Slater) was written there in 1923, but despite Compton's direct evidence for "light quanta" Bohr

was unwilling to relate his atomic transitions to the concept — this paper did not accept them as particles and implied that energy and momentum conservation were only statistical, as is recalled here in Slater's article. However, Heisenberg soon arrived at the ideas and relationships which quickly became "matrix-mechanics"; concepts and theoretical ideas developed rapidly at this point, stimulated by Dirac's interpretation of Heisenberg's non-commuting matrices as dynamical operators and Schrödinger's wave-function, with its probabilistic interpretation. Heisenberg's uncertainty relationship demonstrated that position and momentum could not both be known precisely, and this led Bohr to his notion of *complementarity*, a logical relationship required to express mutual exclusion between two physical quantities observable by different kinds of measurement on the same physical system.

Although holding much truth, complementarity has always been rather ill-defined. The eventual upshot was the "Copenhagen interpretation" of quantum mechanics, which holds the measuring apparatus to be an essential part of the system in the process of observation, and which Bohr used in a disarming way. For example, the dramatic discussions between Bohr and Einstein at the Solvay Conferences of 1927 and 1930 are here recalled by long extracts from Bohr's own account of these breakfast-time dialogues. Each morning, Einstein would propose a new paradox to confound quantum theory, which Bohr was able to meet at the end of the day by showing that the quantum uncertainties inherent in the measuring devices were just sufficient to annul Einstein's contradiction. These sequences of challenge and riposte represent one of the most remarkable episodes in the history of scientific thought; although Einstein was not ever convinced, Bohr's success



The Solvay Conference of 1927, held in Brussels between the 23rd and 29th of October. As well as Bohr, among those present in the photograph are H.A. Kramers, P.A.M. Dirac, W. Heisenberg, E. Schrödinger, A. Einstein and W. Pauli.

## BOOK REVIEWS

**PLENUM:  
MACROCOSMIC  
MICROBIOLOGY**

**THE MOLECULAR  
BIOLOGY OF  
*PHYSARUM*  
*POLYCEPHALUM***

edited by William F. Dove,  
Jennifer Dee, Sadashi Hatano,  
Finn B. Haugli, and Karl-Ernst  
Wohlfarth-Bottermann

Presents a variety of current molecular genetic studies of *Physarum polycephalum*.

0-306-42267-0/proceedings  
354 pp. + index/ill./1986  
\$59.50 (\$71.40 outside US & Canada)

**ADVANCES IN  
MICROBIAL ECOLOGY**

**Volume 9**

edited by K. C. Marshall

A major source of information for microbial ecologists. Volume 9 covers a variety of new techniques and new research.

0-306-42184-4/393 pp. + index/ill.  
1986/\$65.00 (\$78.00 outside US & Canada)

**THE TOGAVIRIDAE AND  
FLAVIVIRIDAE**

edited by Sondra Schlesinger and Milton J. Schlesinger

Examines the structure and replication of these viruses.

0-306-42176-3/442 pp. + index/ill.  
1986/\$59.50 (\$71.40 outside US & Canada)

**VIRUSES, IMMUNITY,  
AND  
IMMUNODEFICIENCY**

edited by Andor Szentivanyi and Herman Friedman

Of special interest in view of the AIDS crisis, contributions to this book focus on cellular and hormonal immune mechanisms in viral resistance, specific viral infections and immunity, tumor virus infections and immune responses, mechanisms of virus-associated immunoregulation, and immune restoration in virus infections.

0-306-42235-2/proceedings  
358 pp. + index/ill./1986  
\$55.00 (\$66.00 outside US & Canada)



**Plenum Publishing Corporation**

233 Spring Street  
New York, N.Y. 10013

In the United Kingdom:  
88/90 Middlesex Street  
London E1 7EZ, England

with the Copenhagen interpretation brought it widespread acceptance.

In 1935, "a bolt from the blue" arrived in the form of the Einstein-Podolsky-Rosen (EPR) paradox, which apparently showed a violation of causality by quantum mechanics and was, in the authors' view, in conflict with everyday experience ("EPR reality"). This paradox and its later "delayed-choice" elaborations are discussed in the centenary volume by V.D. Mermin and P.J. Kennedy, respectively. Today we know empirically that quantum coherence exists on a macroscopic scale, not only at the atomic level. Laboratory experiments verifying the quantum mechanical result questioned by EPR are now carried out over metres, so that these phenomena must now be regarded as part of our everyday reality. In other words, the "EPR paradox" was simply due to the incompleteness of "EPR reality", which did not embrace the fact of quantum coherence in our everyday world. Of course, most of us still find such coherence an almost incredible fact, but this is only a reflection of our personal limitations. We need another Bohr to reshape our way of looking at things, but probably the next generation of physicists will see no difficulty in all of this.

With the discovery of the neutron in 1932, and the early exploration of nuclear reaction processes, Bohr was drawn into the problems of nuclear physics, the third phase of his life, covered here mainly by R.H. Steuwer. Bohr's contributions — simple, convincing and deep — were typical of the man. He related the sharpness observed for nuclear levels excited by slow neutrons to the many degrees of freedom of the nucleons within a nucleus, illustrating this by a wooden model with balls (nucleons) lying in a depression (the nuclear well). This led him naturally to the idea of "the compound nucleus" as an essential intermediate state in all nuclear processes. However, Bohr over-estimated its range of validity and used it to discourage speculations about nuclear shell-models, thereby delaying their development by two decades. At high energies, nuclear matter proved to be far less opaque to nucleons than he guessed; even at intermediate energy, many important nuclear processes do not proceed through a compound nucleus. Bohr understood at once the implications of the Hahn-Meitner discovery of nuclear fission in 1938, also realizing that the slow-neutron fission they observed was due to capture by the isotope  $^{235}\text{U}$ . With J.A. Wheeler, he then began a major calculation of the mechanism of nuclear fission, based on the liquid drop model of the nucleus, and by December 1939 was already speaking publicly of the possible liberation of nuclear energy on a practical scale.

Bohr allowed the possibility that every next step might require some quite revolutionary

idea. His reply to a far-out idea proposed tentatively by Pauli was characteristic: "Yes, but unfortunately it is not crazy enough". Twice he proposed energy nonconservation as necessary to explain some new phenomenon, quickly withdrawing the idea as soon as some less revolutionary explanation was seen to be adequate (for example, when Pauli's neutrino hypothesis predicted the beta-decay spectrum observed).

In a 1932 lecture, "Light and Life", reprinted in the book, Bohr expressed some unusual ideas about biology which he did not qualify until 1962. Life was an additional mystery, he implied; measurement might kill a living system and this new factor might require an extension of complementarity in biology, and some modification of the physical laws acting there. Bohr's views motivated more than one physicist (M. Delbrück and G.S. Stent, certainly) to move on to biological problems\*; ex-physicists did indeed cause a revolution in molecular biology, although not for the reasons foreseen by Bohr. Stent (*Science* 160, 390; 1968) has re-examined Bohr's early views (apparently unaware of Bohr's 1962 qualifications of them) in the light of the later history of biology, concluding that no hint of phenomena inexplicable within the established physical laws has ever emerged.

Late in 1943, Bohr joined the atomic bomb project at Los Alamos because he felt that mankind faced a crucial challenge, where failure would lead to an appalling step backwards. Since the project was then far advanced, he concerned himself primarily with its long-term political implications. He sought to discuss these with the political leaders in Britain and the United States, but without much effect. Churchill regarded him as positively dangerous, for Churchill's concern was still to win the War, not to contemplate future problems, as M. Gowing and R.V. Jones recount. In this last, political, phase of his life, Bohr tried again in 1950, with his "Open Letter to the United Nations" which is reprinted in the book. The timing, however, was unfortunate; the Korean War broke out a few days later and the world paid little attention to it.

This volume brings together accounts of many different aspects of Bohr and his work in a coherent way, presenting them attractively, with many interesting photographs. It is much enlivened by the extracts of material from various sources which appear in the large margins of its pages. Altogether, a wide audience will find it to be a very stimulating book. □

R.H. Dalitz is Royal Society Research Professor in the Department of Theoretical Physics, University of Oxford, 1 Keble Road, Oxford OX1 3NP, UK.

\* A biography of Delbrück, by Peter Fisher, will be reviewed in *Nature* on 17 April.

## Inside the workings of the brain

Oliver Braddick

**Functions of the Brain.** Edited by Clive Warwick Coen. Clarendon:1985. Pp.209. £15.

"THE brain is quite simply the most complicated object known." In a well-turned introduction, Clive Warwick Coen points out that research on this complicated object is in an exuberant but disorderly state. People from heterogeneous scientific backgrounds are simultaneously at work, using a variety of techniques to address multiple levels of explanation that have a habit of spilling over into each other. The brain itself has a diversity of functions, ranging from thermoregulation to planning sentences, which does not map at all tidily onto the divisions between scientific disciplines or their different methods of study. It follows that in planning a lecture series to provide an overview of current brain research, and assembling it into a book, it would be difficult and probably misleading to seek an ordered unfolding of some intellectual ground-plan. Better to arrange a kind of scientific pot-luck supper, to which a set of enthusiastic cooks each brings his own dish, be it spicy or subtle, a filling casserole or a fluffy confection. *Functions of the Brain* provides quite a satisfying buffet of this kind; the essays in it have some division by the brain functions they consider, but also illustrate their authors' very different scientific methods, objectives and styles.

H.B. Barlow's elegant discourse on perception illustrates how this area of neuroscience has come closest to possessing mature theoretical and experimental subsections of the sort that a physicist would recognize. Barlow argues that the visual system transmits signals about patterns of light in ways which optimize the efficiency of these neural representations; this helps us to understand the known forms of neural codes and their development in terms of the statistical properties of the visual environment, and it suggests principles of cortical organization which have yet to be experimentally tested.

Patrick Wall, who writes about pain, similarly uses his essay to develop a particular line of argument. He challenges what he characterizes as the dualist view, that deterministic sensory pathways supply information to a distinct, conscious central entity. His challenge comes from evidence that the subjective quality of painful sensation has a relation to events in sensory nerves that is very far from one-to-one, and that this is a consequence of the intimate two-way interaction of peripheral and central events in the ner-

vous system. Wall's path through this argument, and his view of its historical context, is more discursive and less focused than Barlow's, but his support of his philosophical approach by discussions of hypnosis, questionnaires in casualty clinics and President Reagan's gunshot wound is likely to intrigue a body of non-technical readers.

J.F. Stein's chapter on control of movement has a less personal tone than either of these two, but does give a clear account of the relations between structure and function in the multiple levels of motor control. Moreover, it provides a nice mirror image of Wall's message by emphasizing that, just as sensory processing is not a one-way flow of information from periphery to centre, motor actions cannot be understood as the hierarchical execution, via lower level reflexes, of centrally enunciated neural commands.

Barlow, Wall and Stein represent different facets of a tradition which, while based in detailed analysis at the neuronal level, likes to muse on the large-scale organizing principles of brain function. The molecular neurobiology of Craig Bailey and Eric Kandel has a much stronger smell of the laboratory bench, where there is little time to look back at intellectual history given the wealth of information that comes tumbling from new electrophysiological and ultrastructural techniques, and where an invertebrate lies waiting whose neuronal interconnections can be mapped completely by scientists with sufficient energy and insight. Bailey and Kandel's work on *Aplysia* brings together the global phenomena of habituation and conditioning with events occurring within identifiable synapses. We do not yet know whether the impressive ability to unite understanding of these levels in a simple organism will help in leaping the much more daunting chasms between subcellular and behavioural phenomena in higher vertebrates; students of mice and men must watch this space in anticipation.

George Fink, on neuroendocrine function, also has a molecular perspective, and like Bailey and Kandel he presents a good deal of experimental detail. Unfortunately he does not have as tightly concentrated a scientific story to tell, and so the non-specialist reader is likely to be dazed rather than carried forward by his table of 24 neuropeptides or his illustrations of the homologies in their amino-acid sequences. However, one compelling impression that remains, in particular from the figures in this chapter, is of the stunning armoury of techniques which the histo-chemically sophisticated researcher can now draw upon to look inside the nervous system.

Norman Geschwind's chapter represents yet another tradition, the oldest in the study of the brain, and one which he

eloquently defends. His recent death deprived us of one in the line of literate and audacious neurologists who extend their close and purposeful clinical observations into imaginative views of brain function. On occasion the breadth of Geschwind's narrative, offering keys to dyslexia, emotional expression and creative impulses, may sweep the reader over issues where those raised in more experimental traditions might want to pause and quibble. However, the approach of clinical neurology, which has recently been married with great effect to the systematic testing methods of cognitive neuropsychology, offers at present almost the only route for linking neural mechanisms with the specially human abilities of language, reasoning and spatial representation.

The chapters on specific topics are topped and tailed by essays from J.Z. Young and Colin Blakemore, respectively, both of whom adopt a more contemplative and philosophical stance. The issues they address — Young on the place of brain function in our broader view of life, Blakemore on what kind of explanation brain scientists should look for — are significant, yet neither really carries the sense of scientific mastery and clarity that marks the best of the other chapters (or, indeed, that can mark these authors when expounding their own work).

Not every active branch of brain research is well portrayed in the book. I would have welcomed more on the rich advances stemming from the combination of sophisticated behavioural techniques and electrophysiological recording in alert (and even mobile) animals, and from the renaissance in the anatomical study of cerebral pathways. Developmental neuroscience is also poorly represented. There is, too, understandable variation in the accessibility of the contributions: some (Wall's and Geschwind's, and perhaps Barlow's) can be read by the layman; others (for example Stein's, and Bailey and Kandel's) are heavier on technical detail and will be of more benefit to those in adjacent disciplines. Nonetheless *Functions of the Brain* is a creditable and often stimulating sampler of what we know — and don't know — about the brain.

Oliver Braddick is a Lecturer in the Department of Experimental Psychology, University of Cambridge, Downing Street, Cambridge CB2 3EB, UK.

### New in paperback

- *Princes and Peasants: Smallpox in History*, by Donald R. Hopkins. Publisher is University of Chicago Press, price is \$12.95, £10.95. For review see *Nature* 310, 608 (1984).
- *Wandering Lands and Animals: The Story of Continental Drift and Animal Populations*, by Edwin H. Colbert, which first appeared in 1973. Publisher is Dover, New York/Constable, London, price is \$7.95, £7.55.

## BOOK REVIEWS

**Ada and the engines**

Richard Gregory

**Ada: A Life and a Legacy.** By Dorothy Stein. MIT Press: 1985. Pp. 321. \$19.95, £17.50.

ADA, daughter of Byron, was born in 1815. Her mother, Annabella Milbanke, left Byron, who himself left England the following year — never to see his offspring again. In 1835 Ada married Lord King, who became the Earl and she the Countess of Lovelace in 1838.

Five years earlier, in 1833 (not long, incidentally, before she attempted to elope with her still unidentified tutor), Ada had first met Charles Babbage. They formed a lasting friendship in which she worked with and for him in the development of the first computers: the Difference Engine for computing tables and the general-purpose programmable Analytical Engine, which was never completed. It is for her association with Babbage that Ada is principally remembered, to the extent that she is said to have been the world's first computer programmer.

In her rich study of human drama and social history at the birth of the modern world, Dorothy Stein gives due accord to Ada's organizing abilities and her work in

translating and adding to Menabrea's monograph on the calculating engines. She does not, however, regard her as a major originator. The key historical questions revolve around the use of Jacquard punched cards to program the Analytical Engine. Dorothy Stein writes (p. 93):

For the modern reader the important distinction . . . is that the Difference Engine followed an unvarying computational path (except for the parlour games Babbage played for the benefit of visitors such as Lady Byron), while the Analytical Engine was to be truly programmable and capable of changing its path according to the results of intermediate calculations or processes. Yet this was a feature mentioned by Ada only in passing . . . For Ada — as for Babbage — the calculating machine was a metaphor as well as a harbinger of economic and scientific progress. For example, the theme stressed in presenting the 'illustrations' or programs was that they demonstrate how certain lengthy, laborious, and complex calculations can be most efficiently executed . . . by the machine into recurrent cyclical groups. The same set of operations can then be repeated over and over by the engine, with only the starting and stopping points indicated by the instructions.

Ada, it seems, saw the programs, and her own hard-won knowledge and skills, in contemporary economic terms as *capital* to save labour and increase enterprise. But this interpretation hardly reduces her achievement: she clearly made a notable contribution to the working out of Babbage's ideas and to what at that time was (and perhaps still is) the metaphysics of computing, asking such questions as: "How can a machine handle imaginary

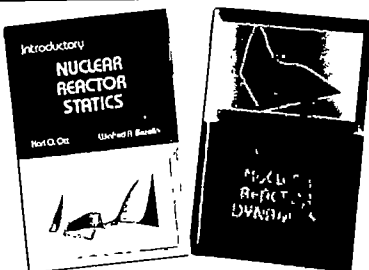


The young Ada — "gifted with intense imagination".

numbers?". It appears, though, that Babbage (born in 1792) was generally a couple of decades ahead of her in questions and answers, and infinitely ahead of everyone else. He himself remains a shadowy but dominating figure in Dorothy Stein's account.

Ada comes remarkably alive in this book, passionate but at times neurotic, with almost too much self-awareness, and falling into disasters ranging from illness and accident to losses on the horses — all this is wonderfully preserved in her correspondence and is most ably presented here. She was gifted with intense imagination. But she had but intermittent perseverance, even for bringing into being the calculating engines she had the wit to see were to be of such immense significance. □

*Richard Gregory is a Professor in the Brain and Perception Laboratory of the Department of Anatomy, Medical School, University of Bristol, University Walk, Bristol BS8 1TD, UK.*

**NEW TITLES  
BY ANS**

"Introductory Nuclear Reactor Statics"  
by Karl O. Ott  
Winfred A. Bezzella

Recommended as an undergraduate or graduate textbook. Valuable source book for reactor analysis and design.

"Introductory Nuclear Reactor Dynamics"  
by Karl O. Ott  
Robert J. Neuhold

Examines fundamental principles of Nuclear Dynamics. Companion volume to Nuclear Reactor Statics, published in 1983.



For additional information write:  
American Nuclear Society  
555 North Kensington Avenue  
La Grange Park, IL 60525 USA

**Glycans explored**

Tim Hardingham

**Glycoprotein and Proteoglycan Techniques.** By J.G. Beeley. Elsevier: 1985. Pp. 462. Hbk Dfl. 295, \$109.25; pbk Dfl. 85, \$31.50.

CARBOHYDRATE structures can be one of the great turn-offs of student days. Be that as it may, the rise in interest in all aspects of the biological functions of glycoproteins and proteoglycans means that there is an ever-widening audience of people keen to get to grips with them. This book does much to help, for not only does it provide a compendium of useful laboratory techniques but also succeeds in conveying some of the essential flavour of research in this area; it gives a good, broad perspective on the variable and yet ordered structures shown by glycoproteins and proteoglycans, and a thorough chemical overview of what can and cannot be done to the intact glycoproteins and their isolated glycopeptides.

The early sections deal with largely tra-

ditional chemical methods of structural analysis. It is, however, the later parts, which review the use of specific enzymes and include sections on the battery of approaches possible with lectins and radioactive labelling techniques, that will be particularly useful. The range covered includes good examples of the variety of approaches that are possible for isolation, purification and structural analysis. Here, too, the author also addresses some of the problems frequently encountered when the supply of starting material is limited, as in characterizing products from cell culture.

The content is not beyond criticism — some of the newer approaches are not mentioned — but the emphasis on techniques accessible to any reasonably equipped laboratory means that the book will be ideal for those just starting up. Moreover it should enable both experienced and inexperienced readers to assimilate with much greater insight the wealth of current publications in this field.

*Tim Hardingham is Deputy Head of the Division of Biochemistry, Kennedy Institute of Rheumatology, Hammersmith, London W6 7DW, UK.*

# The ethics of human gene therapy

from LeRoy Walters

*The correction of single-gene defects in humans by gene therapy is in sight, increasing the need for a solid framework for ethical evaluation.*

WITHIN the next twelve months, it is likely that a proposal to perform gene therapy in humans will be submitted to local and national review bodies in the United States. The proposing research group will be based in one of the eight to ten laboratories in the world now pursuing molecular genetic approaches to the correction of selected inborn errors of metabolism. The hereditary disorders for which gene therapy will initially be attempted are quite rare—adenosine deaminase (ADA) deficiency, which produces severe combined immune deficiency, and Lesch-Nyhan syndrome, which leads to mental retardation and self-mutilation in children.

While gene therapy may sound revolutionary as an approach to human genetic disease, the techniques likely to be used in the near future closely resemble those of conventional medical practice. Thus, gene therapy for ADA deficiency can accurately be described as 'autologous bone marrow transplantation with an extra step'. That extra step will involve not the repair of a malfunctioning gene, but, rather, the addition of a properly functioning gene to as many target cells as possible, thereby compensating for the malfunction caused by the defective gene in those cells.

## First steps

The early attempts at gene therapy will involve only somatic cells, especially the stem cells found in the bone marrow. Molecular genetic modification of germ cells in laboratory animals is still inefficient, and no research groups are currently contemplating the deliberate introduction of genetic alterations into the human germ line. Thus, fears about the transmission to future generations of intentionally induced genetic changes are misplaced, just as they would be after a kidney transplant. For the time being, moreover, only the simplest kinds of genetic defects are considered to be good candidates for gene therapy. These are single-gene defects which are recessively inherited and which result in the lack of an essential enzyme. The production of such enzymes is almost a mechanical function, necessary to be sure, but shared by humans with many other members of the

animal kingdom. Thus, any allegation that current gene therapy efforts represent 'tampering' with 'distinctively human characteristics' is simply fallacious.

## Risk assessment

Ethical questions about gene therapy as now planned are of two kinds, substantive and procedural. The substantive questions can be further subdivided, with some oversimplification, into technical and non-technical questions. The chief technical questions surrounding gene therapy involve the comparison of potential benefits and harms, or, in contemporary language, risk assessment. The assessment process begins with an evaluation of the genetic disease to be treated. At this stage the central question is: What kinds of morbidity and what mortality rates are associated with the disease? If the disease is severe for the individuals affected by it, one can proceed to consider existing therapies and their effectiveness. If dietary or current medical therapies provide reasonable control for disease victims, the disease may not be a good early candidate for gene therapy. On the other hand, if no effective therapy exists or if the therapy cannot be used with some categories of patients, molecular genetic approaches to treatment may be a reasonable alternative to merely palliative measures.

Like the development of all innovative medical therapies, the pursuit of gene therapy as an alternative therapeutic mode involves preclinical studies in animal models and tissue cultures. At this stage the risk assessment process must seek to determine and evaluate the probable safety and effectiveness of the new technique. Here, researchers attempting to develop gene therapy techniques face a special, but by no means unique, problem: there are few laboratory animal models for the single-gene defects that afflict humans, and, in particular, there are no known non-human models for the enzyme-deficiency diseases which are likely to be judged appropriate early candidates for human gene therapy. Researchers may be able to insert a new gene into appropriate animal cells and monitor the expression of the gene, but they are unlikely to be able to demonstrate

a clinical 'cure' in a diseased laboratory animal.

From a safety standpoint, one advantage of a gene therapy approach that uses bone marrow cells is that the cells are treated outside the body, *in vitro*. If a particular experiment goes awry, the cells are simply not returned to the laboratory animal or, in the clinical context, to the patient. But other safety questions are matters of continuing concern. The new genes will probably be carried into the stem cells by carefully designed retroviruses from which much of the native genetic information has been deleted. These defective retroviruses will function as vectors for the new gene. It is possible, but not likely, that the retroviral vectors will recombine with undetected viruses or endogenous DNA sequences in the cells and so become infectious. It is also possible that the vector/gene combinations, because they integrate randomly into the chromosomes of the cells, will activate previously dormant proto-oncogenes or disrupt essential, properly functioning genes. On the question of efficiency, it is still not clear whether sufficiently high levels of expression can be achieved in primates to offer a reasonable hope of clinical benefit.

## Other ethical issues

Non-technical questions about human gene therapy, while apparently less amenable to verification by laboratory data, are nonetheless important. These questions derive in part from the recent history of clinical innovation, from renal dialysis in the early 1960s, the first heart transplants in 1967 and recent experience with the artificial heart and xenografting. They are also based on codes of ethics in research published between the late 1940s and the present.

In the early years of renal dialysis, one major issue was the selection of a few patients from among many candidates for life-saving treatment. In Seattle, Washington, a special committee was established to make these decisions. Commentators on the Seattle committee's experience have noted how difficult it is to avoid making judgements about the comparative social worth of patients when not all patients can be offered treatment<sup>1</sup>. With

rare genetic diseases, although the potential patient pool will be small, choices will need to be made from among multiple candidates for experimental gene therapy. Thus, fairness in the selection of subjects may be an important issue even in the earliest trials of human gene therapy.

Informed consent will almost certainly also be an important issue. To be adequately informed about their decisions, prospective patients will need to have, or have imparted to them, basic information about bone marrow transplantation and gene therapy techniques. If, as seems likely, parents or guardians are asked to make decisions on behalf of infants or young children, the consent process will be even more complex. Properly informed, potential research subjects or their proxies will be made aware that they are embarking on essentially uncharted territory. This awareness should help to temper their hope—and that of the investigators, also—that they are participating in a major therapeutic breakthrough.

Questions of privacy and confidentiality may also arise. The pioneer recipients of heart transplants and the artificial heart are known to us by name; in contrast, the newborn recipient of a baboon heart, Baby Fae, remained at least partially anonymous until her death in late 1984. With gene therapy, one hopes for a reasonable balance between familial privacy and the desire of the public and the media to know. Researchers will bear the primary responsibility for informing patients and their families of the public interest in gene therapy and for shielding patients from excessive media exposure. If, as seems likely, the earliest patients are infants or young children who are incapable of expressing their own views regarding publicity, they will deserve special protection.

## Guidelines

In the Declaration of Helsinki and similar codes of ethics in research, biomedical researchers have proposed general standards for human experimentation. The revised Declaration of Helsinki<sup>2</sup>, adopted by the World Medical Association in 1975, includes ethical guidelines on research design, risk-benefit analysis, informed consent, privacy and accuracy in reporting research results. In most developed nations, local committees, variously called 'ethics committees' or 'institutional review boards', rely on these international standards and derivative national rules in reviewing individual research protocols. However, when major therapeutic innovations are initially proposed, this carefully evolved approach to the review of proposed human experimentation may need to be supplemented by more specific ethical standards and, possibly, by custom-tailored review mechanisms. *In vitro* fertilization is an example of a new biomedical technology that has been the

object of special scrutiny in several countries, including the United Kingdom, Australia and Canada.

During the past two-and-a-half years, a framework for the ethical evaluation of human gene therapy has been developed in the United States. This framework includes a publicly discussed set of questions, called *Points to Consider in the Design and Submission of Human Somatic-Cell Gene Therapy Protocols*<sup>3</sup>, and a public national review process. The *Points to Consider* reflect a national and perhaps international consensus on the most important areas of concern surrounding human gene therapy. Major areas identified in the central section of the document are the following:

(1) Objectives and rationale of the proposed research.

(2) Research design, anticipated risks and benefits: (i) structure and characteristics of the biological system; (ii) pre-clinical studies; (iii) clinical procedures, including patient monitoring; (iv) public health considerations; (v) qualifications of investigators and adequacy of facilities.

(3) Selection of patients.

(4) Informed consent.

(5) Privacy and confidentiality.

A series of questions is posed about each area of concern, and great latitude is left to investigators in formulating responses to the questions. For example, on the subject of preclinical studies with laboratory animals, investigators are asked: "Has a protocol similar to the one proposed for a clinical trial been carried out in non-human primates and/or other animals? What were the results?"

The *Points to Consider* document was drafted by the Working Group on Human Gene Therapy, an interdisciplinary subcommittee of the NIH Recombinant DNA Advisory Committee (RAC). The Working Group includes three laboratory scientists, three clinicians, three ethicists, three attorneys, two public-policy specialists, and a lay member. The document represents an attempt to distill 15 years of ethical discussion in published articles and books<sup>4-15</sup>, at public symposia<sup>16-18</sup>, and in government hearings and reports in the United States and Europe<sup>19-22</sup>. *Points to Consider* was published twice for public comment in the United States *Federal Register* and was revised to take into account the suggestions made by respondents.

As a complement to the confidential review of new biological compounds conducted by the federal Food and Drug Administration, a special public review mechanism has also been established to evaluate proposals to perform gene therapy in humans, at least during the early years. This review mechanism was created by the NIH RAC and is modelled after the review process employed by RAC during the early years of recombinant DNA research. After review by local ethics

committees, RAC and its subcommittee, the Working Group on Human Gene Therapy, will provide public national review of each gene therapy proposal that is to be supported by NIH funds. All interested persons will therefore have ready access to information about gene therapy proposals, to the review process itself and to its outcome.

When gene therapy has not yet cured a human patient of disease, it may seem premature to discuss questions that may emerge if human gene therapy is successful. Yet, one role of ethics is to provide timely consideration of future questions for public policy. Several issues may arise.

## Genetic diagnosis

At present, attempts to describe 'the morbid anatomy of the human genome' are outpacing gene therapy by a considerable margin<sup>23</sup>. Within the past year, new markers for several major genetic diseases have been described, among them cystic fibrosis<sup>24-26</sup>, polycystic kidney disease<sup>27</sup> and Duchenne muscular dystrophy<sup>28</sup>. At the prenatal stage, early diagnosis of genetic defects presents couples with a decision about selective abortion, but applied to children or adults, the new tests will provide early notice of a tendency to develop a particular disease (such as atherosclerosis<sup>29</sup>) or of the presence of a gene that will cause a late-onset disorder (such as Huntington's disease<sup>30</sup>).

The 'early notice' aspect of the new genetic tests will raise difficult ethical questions in its own right. For example, which children or adults should be tested, and what should they be told about the results of the tests? Moreover, one can anticipate that insurance companies, employers and perhaps even prospective marriage partners, will have a keen interest in securing detailed genetic profiles of particular individuals. The primary implication of these screening techniques for gene therapy is that they may identify additional groups of candidates for curative or pre-emptive intervention.

## Commercial considerations

Commercially oriented biotechnology companies have been leading participants in the quest for DNA-based diagnostic techniques but seem, at present, relatively uninterested in DNA-mediated approaches to the cure of disease. This lack of interest may reflect the fact that, in the near future at least, human gene therapy will be a labour-intensive procedure, akin to bone marrow transplantation. Each university-based research team involved with gene therapy also seems to be tailoring its own vector/gene combinations to suit its specific purposes. It is possible that there may emerge commercial interest in producing vectors or vector/gene kits for particular diseases, but, given the rarity of the diseases thought to be the likeliest candi-

dates for early attempts at gene therapy, commercial incentives are currently quite weak.

### Gene replacement

Present approaches to gene therapy can quite literally be described as gene addition. Properly functioning genes, introduced into the appropriate cells, will, it is hoped, compensate for malfunctioning or nonfunctioning genes. This approach holds great promise for the somatic-cell treatment of recessive genetic disorders, but for the treatment of dominant disorders such as Huntington's disease, it may be necessary to inactivate the disease-causing gene or even to remove and replace it with a gene that functions properly. Techniques for this kind of precisely targeted molecular microsurgery have not yet been developed for mammals and will probably not emerge for decades.

### Germline therapy

No aspect of gene therapy is more highly charged than that of germline or germ-cell therapy; it might seem, therefore, politically prudent to avoid the subject. But what is politically prudent may not be ethically responsible. In fact, timely ethical discussion of this issue, before germline gene therapy in humans is technically feasible, may assist future policymakers in their deliberations.

The principal rationale for germline human gene therapy, when it becomes a technical possibility, will be a simple argument from efficiency. If somatic-cell therapy becomes a successful cure for single-gene defects of high prevalence, such as cystic fibrosis and sickle-cell anaemia, phenotypically normal patients will grow to adulthood and presumably be capable of reproducing. They will then constitute a new group of homozygous 'carriers' of genetic disease, who can transmit malfunctioning genes to their offspring. Affected offspring could presumably be treated by means of somatic-cell gene therapy in each succeeding generation, but some phenotypically cured patients would probably consider it more efficient to prevent the transmission of specific malfunctioning genes to their offspring, if the option were available.

A second rationale for the germline approach is that some genetic diseases may be treatable only by this method. For example, because of the blood-brain barrier, the brain cells involved in hereditary central nervous system disorders may be inaccessible to somatic-cell gene therapy. Early intervention that affects all the cells

of the future organism, including the germ cells, may be the only means available for treating cells or tissues which are not amenable to genetic repair after birth.

Genetic changes have been introduced into the germ lines of several species of laboratory and domestic animals<sup>31-34</sup>, but the method for producing such transgenic animals is unlikely to be used with humans. Because the foreign DNA is inserted into the pronuclei of mammalian embryos before the pronuclei fuse and the new genome is established, one would not know in most cases whether a particular embryo were destined to have a genetic disease. A more likely approach in humans is the genetic repair of sperm or egg cells, either *in vivo* or, more probably, *in vitro*. Methods for reliably introducing properly functioning genes into germ cells and for verifying their successful introduction would need to be developed. As simple gene addition would allow the transmission of known malfunctioning genes to future generations, the techniques of gene inactivation or gene replacement would probably be used, if available.

### Economic issues

Given that the first-year costs of cardiac transplantation approximate \$90,000 per patient (1983 dollars) in the United States<sup>35</sup>, it may reasonably be asked whether gene therapy will be another expensive half-way technology. If employed with bone marrow transplantation, human gene therapy will be labour-intensive and will entail sizeable initial costs. But even if one does not assign an economic value to improvement in the quality of cured patients' lives, the one-time cost for gene therapy may be considerably less than the cost of repeated hospitalization for the treatment of sickle-cell anaemia or cystic fibrosis. In short, for patients suffering from many, if not most, genetic diseases caused by single-gene defects, gene therapy may become a cost-effective method of care.

In the more distant future, the prospects for, and possible approaches to, human gene therapy are not yet clear. But if the link between gene therapy and bone marrow transplantation can be broken, gene therapy may become available to a wider circle of patients. For example, if vectors specific for particular target cells can be developed, vector/gene combinations can perhaps be administered intravenously to outpatients. At that stage, if it is ever reached, medicine will stand at the threshold of a new era in treating the more than 3,000 genetic disorders that afflict our species.

I acknowledge research support from the NSF and the National Endowment for Humanities (RII-8309871) and from the Joseph P. Kennedy Jr Foundation. I thank W. French Anderson, Lori B. Andrews, Stanley Barban and Robert M. Cook-Deegan for their helpful comments on earlier drafts of this paper.

*LeRoy Walters is Director of the Center for Bioethics at the Kennedy Institute of Ethics, Georgetown University, Washington, DC 20057, USA. He has been a member of the NIH Recombinant DNA Advisory Committee from 1976 to 1980 and again from 1984 to the present. He chairs RAC's Working Group on Human Gene Therapy.*

1. Ramsey, P. *The Patient as Person*, 239-275 (Yale University Press, New Haven, Connecticut, 1970)
2. World Medical Association *Declaration of Helsinki* revised edn (1975); repr. in *Contemporary Issues in Bioethics* (eds Beauchamp, T. L. & Walters, L. I. 511-512 (Wadsworth, Belmont, California, 1982)
3. *Federal Register* 50, 33463 (1985); repr. in *Recomb DNA tech. Bull.* 8, 116-122 (1985).
4. Davis, B. D. *Science* 170, 1279-1283 (1970)
5. Friedmann, T. & Roblin, R. *Science* 175, 949-955 (1972)
6. Howard, T. & Rifkin, J. *Who Should Play God?* (Dell, New York, 1977).
7. Shinn, R. in *Encyclopedia of Bioethics* Vol. 2 (ed. Reich, W. T.) 521-527 (Free Press-Macmillan, New York, 1978).
8. Anderson, W. F. & Fletcher, J. C. *New Engl J Med* 303, 1293-1297 (1980).
9. Motulsky, A. *Science* 219, 135-140 (1983)
10. Friedmann, T. *Gene Therapy—Fact and Fiction* (Cold Spring Harbor Laboratory, New York, 1983)
11. Fletcher, J. C. *Virginia Law Rev.* 69, 515-546 (1983)
12. Baskin, Y. *The Gene Doctors* (William Morrow, New York, 1984).
13. Anderson, W. F. *Science* 226, 401-409 (1984).
14. Anderson, W. F. *J. med. Phil.* 10, 275-291 (1985)
15. Fletcher, J. C. *J. med. Phil.* 10, 293-309 (1985).
16. Hamilton, M. (ed.) *The New Genetics and the Future of Man*, 109-175 (William B. Erdmans, Grand Rapids, Michigan, 1971).
17. Lappé, M. & Morison, R. S. *Ann. N.Y. Acad. Sci.* 265, 59-65, 141-169 (1976).
18. Research with Recombinant DNA: An Academy Forum, 7-9 March 1977 (National Academy of Sciences, Washington, DC, 1977).
19. Council of Europe, Parliamentary Assembly. Recommendation 934 (1982) on Genetic Engineering, in *Texts Adopted by the Assembly* (Council of Europe, Strasbourg, 1982).
20. US President's Commission for the Study of Ethical Problems in Medicine and Biomedical and Behavioral Research. *Splicing Life* (US Govt. Printing Office, Washington, DC, November 1982).
21. US Congress, House Subcommittee on Investigations and Oversight. *Human Genetic Engineering* (97th Congr., 2nd Sess., 16-18 November 1982).
22. US Congress, Office of Technology Assessment *Human Gene Therapy: Background Paper* (OTA, Washington, DC, December 1984).
23. McKusick, V. A. *Clin. Genet.* 27, 207-239 (1985)
24. Knowlton, R. G. et al. *Nature* 318, 380-382 (1985)
25. White, R. et al. *Nature* 318, 382-384 (1985)
26. Wainwright, B. J. et al. *Nature* 318, 384-385 (1985)
27. Reeder, S. T. et al. *Nature* 317, 542-544 (1985)
28. Monaco, A. P. et al. *Nature* 316, 842-845 (1985)
29. Joyce, C. *New Scientist* 108, 34 (1985)
30. Gusella, J. F. et al. *Nature* 306, 234-238 (1983)
31. Palmiter, R. D. & Brinster, R. L. *Cell* 41, 343-345 (1985)
32. Hammer, R. E. et al. *Nature* 315, 680-683 (1985)
33. Brinster, R. L., Chen, H. Y., Trumbauer, M. L., Yagel, M. K. & Palmiter, R. D. *Proc. natn. Acad. Sci. U.S.A.* 82, 4438-4442 (1985)
34. Stout, J. T., Chen, H. Y., Brennand, J., Caskey, C. I. & Brinster, R. L. *Nature* 317, 250-252 (1985)
35. Evans, R. W. et al. *The National Heart Transplantation Study: Final Report* Vol. 3, 28-46 (Battelle Human Affairs Research Center, 1984)

# Transitional field behaviour from Southern Hemisphere lavas: evidence for two-stage reversals of the geodynamo

Kenneth A. Hoffman

Physics Department, California Polytechnic State University, San Luis Obispo, California 93407, USA

*Palaeomagnetic records from Australasian basalts provide a rare view of transitional field behaviour, as seen from mid-southern latitudes. These data suggest that a geomagnetic reversal is accomplished in two steps, separated by an interval of relative dynamo quiescence. A potentially long-lived field configuration, developed early, is observed to be the 'stepping stone' from which both successful and unsuccessful reversal attempts are made. Several aborted attempts involving the same intermediate field geometry may precede an actual polarity transition.*

WHILE the number of palaeomagnetic records of polarity transitions obtained from sites in the Northern Hemisphere has steadily increased<sup>1-8</sup>, the need for Southern Hemisphere records has become more apparent. Although one of the first detailed accounts of palaeofield behaviour during a complete reversal comes from South Africa<sup>9</sup>, few additional records from sites south of the Equator have since been reported<sup>10,11</sup>. Nevertheless, it is clear that any meaningful determination of field morphology during transitions, a major constraint on any complete model of the reversing geodynamo, requires contemporaneous records of intermediate field behaviour from sites scattered about both hemispheres<sup>12-14</sup>.

To help rectify this situation, three mid-southern-latitude Cenozoic shield volcanoes which were the focus of magnetostratigraphic studies some fifteen years ago<sup>15,16</sup> were revisited (Fig. 1a). Specifically, the sampled sites are:

- Liverpool Volcano ( $31.7^{\circ}$ S,  $150.2^{\circ}$ E), New South Wales, Australia, where a continuous Oligocene sequence of approximately 59 flows records a series of 4 geomagnetic events, L1 to L4.
- Akaroa Volcano ( $43.8^{\circ}$ S,  $173.0^{\circ}$ E), Banks Peninsula, New Zealand, where a Miocene lava sequence records intermediate field behaviour through two sequential reversals, A1 and A2.
- Mt Kaputar ( $30.2^{\circ}$ S,  $150.2^{\circ}$ E), New South Wales, Australia, where a late Miocene excursion (K1) is recorded.

The data from these palaeomagnetic events have been corrected for any subsequent tectonic rotation of the sites and have been reduced to site palaeolatitudes consistent with the age of the lavas. Both corrections are deduced from the averaged full-polarity data for each site. The volcanic structures appear to be flat-lying, so that correction for tectonic tilt was unnecessary.

## Recorded field behaviour

**Liverpool Volcano, Australia.** This volcano, potassium-argon dated at  $33.7 \pm 0.7$  Myr (ref. 15), is built of alkali olivine basalts. Previously reported palaeomagnetic data from several lava flows have been interpreted as showing a series of three polarity reversals<sup>15</sup>; however, we find that only one complete transition, involving a polarity change from reverse-to-normal (R-N), is recorded at Liverpool. We believe that this discrepancy is caused by a small number of palaeomagnetic directions recorded by an unusual magnetic carrier mineral<sup>17</sup>.

Approximately 300 cores were drilled over  $\sim 360$  m of continuous vertical section exposed along Yarraman Creek and two of its tributaries. A dense and sometimes redundant sampling procedure was used to ensure that the magnetic record had no gaps. Each site was examined carefully to verify that the flows

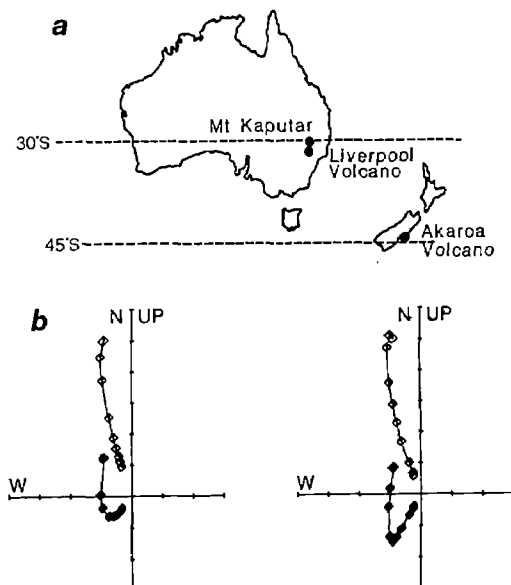


Fig. 1 a, Location of Cenozoic volcanoes sampled for this study. b, Orthogonal plots of remanence behaviour during stepwise alternating field (AF) demagnetization to 20 mT (left) and stepwise thermal demagnetization to 320 °C (right) conducted on typical specimens from flow YC21 from Liverpool Volcano. This flow was chosen because it possesses the most intermediate primary palaeofield direction of all flows reported in this study. Solid (open) symbols denote projections on the vertical (horizontal) plane.

were definitely *in situ*. In all, 59 individual flows and flow groups were sampled in detail.

Palaeomagnetic analysis involved both alternating field (AF) demagnetization and thermal cleaning, sometimes in combination. At no time was single-step or 'blanket' demagnetization employed. For each specimen, the direction of primary thermoremanent magnetization (TRM) was determined from the observed behaviour during stepwise demagnetization (see Fig. 1b).

In Fig. 2a, declination (*D*) and inclination (*I*) are plotted in chronological flow order; the flows in this sequence provide a record of field behaviour spanning a single R-N transition.

Inspection of Fig. 2a reveals that nearly the entire reversal appears to take place between two successive extrusions, but that a large number of flows in the sequence, before and after the primary transition, display intermediate palaeodirections. Lack of information regarding the absolute timing of lava extrusion means that we cannot tell what time-span is involved.

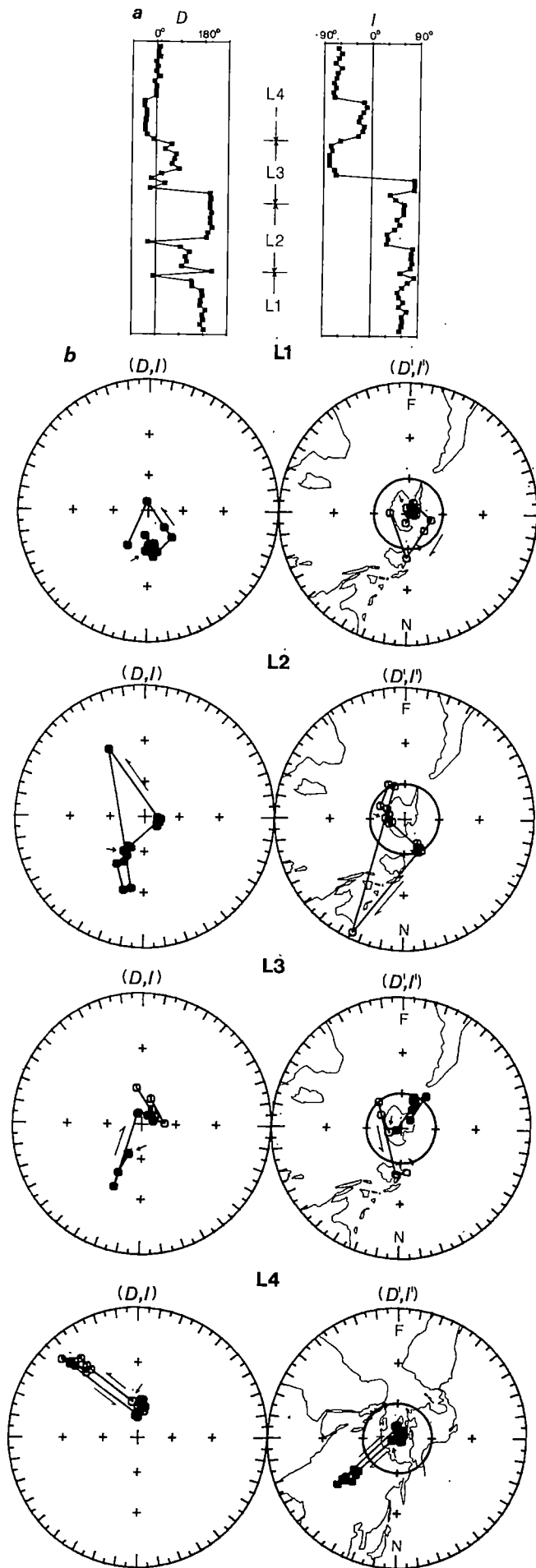


**Fig. 2** AF- and thermally demagnetized mean flow directions from a continuous sequence of basalts from Liverpool Volcano, Australia. *a*, Declination (*D*) and inclination (*I*) from transitional events L1 (R-R; the oldest), L2 (R-R), L3 (R-N) and L4 (N-N). *b*, Polar stereographic plots in (*D*, *I*)-space (left) and in rotated (*D'*, *I'*)-space<sup>18</sup> (right). Solid (open) symbols correspond to palaeodirections on the lower (upper) hemisphere. The four events are displayed chronologically. (*D'*, *I'*) plots present palaeodirectional movement as if one were looking down the normal polarity dipole field direction; the angular distance to any point from the centre is a direct measure of the angular distance from the axial dipole field direction corresponding to this site in Oligocene times. The small circle represents a 30° departure and the small plus signs represent a 60° departure. 'N' ('F') indicates perfectly near-sided (far-sided) rotated directions. The double-headed arrow indicates the oldest datum of each sequence. Broken lines are used to indicate unknown directional paths of large angular extent. Those (*D'*, *I'*) directions corresponding to virtual geomagnetic poles (VGPs) lying on the coastlines of the continents are indicated. In this way one can observe the VGP path in this directional space.

In Fig. 2*b*, the Liverpool data are displayed as vector paths in (*D*, *I*)-space and rotated (*D'*, *I'*)-space<sup>18</sup>. Before the actual change in polarity, three departures of the field vector from full polarity are seen (Fig. 2*b*, events L1-L3). The first directional swing (L1) involves a maximum recorded angular displacement from the axial dipole field direction of ~35° in the north/south-up/down plane, to subvertical (downwards), and is an almost perfectly near-sided<sup>12,13</sup> direction. The second swing (L2), also strongly near-sided, has a maximum recorded extent of about 90° from full polarity. Note that this single-flow result is preceded by a direction similar to that associated with the first swing and, moreover, that this recurring, strongly near-sided palaeofield orientation remained virtually stationary during the extrusion of several flows.

Interestingly, the third directional swing (L3) again proceeds to a strongly near-sided intermediate direction, very similar to the other such directions noted. This time, three successive flows record this palaeofield orientation. Immediately following these intermediate directions is the (possibly rapid) transition to normal polarity. After a final directional swing (L4), marginally near-sided, to a position ~45–60° from the direction associated with the (now normal-polarity) axial dipole field, the palaeofield appears to 'settle' into a long-term normal polarity state.

**Akaroa Volcano, New Zealand.** The Miocene sequence of alkaline lavas at Akaroa Volcano, K-Ar dated at ~8.5 Myr, contains a number of polarity boundaries<sup>16</sup>. In our resampling, approximately 250 cores were drilled over ~160 m of section exposed along Lighthouse Road. Figure 3 shows the data from two sequential transitions (a N-R transition followed by a R-N transition).

Although the record from this shield volcano appears to be less detailed than that from the Liverpool sequence, both transitions do contain intermediate palaeofield directions. Specifically, each reversal record contains a single, localized set of intermediate directions; in the case of the R-N reversal (Fig. 3, event A2), these directions remained nearly invariant during the extrusion of seven lavas. As at Liverpool Volcano, the R-N transition recorded at Akaroa Volcano includes intermediate directions which deviate by up to 45° in the north/south, up/down plane from the reverse-polarity axial dipole field direction; however, in contrast to the Liverpool record, this intermediate orientation is almost perfectly far-sided. That is, while the Liverpool field behaviour during events L1-L3 is dominated by a steepening in inclination, that recorded at Akaroa during event A2 exhibits a shallowing. The intermediate field directions recorded during the apparent onset of the preceding N-R transition (Fig. 3, event A1) also deviate from the axial dipole field direction by about 45°; however, for this event the orientation of the directional swing is far from the north/south-up/down plane.

Between the recorded N-R and R-N transitions, the Akaroa lavas may have recorded as many as three R-R palaeofield

excursions. Unfortunately, two of these possible events are each observed in only one lava. The remaining event is recorded in five lavas; however, the magnetic remanence properties of the three oldest flows of this sequence are atypical and require further examination. The two youngest flows, which exhibit no unusual remanence properties, possess palaeofield directions which are very close to the intermediate directions seen in the subsequent R-N transition. Such an occurrence is reminiscent of the Liverpool data.

**Mount Kaputar, Australia.** Previously reported palaeomagnetic results from the Mt Kaputar lava sequence, K-Ar dated at  $\sim 17.5$  Myr, suggested the presence of a single, normal-polarity geomagnetic excursion<sup>15</sup>. Our sampling confirmed this event; Fig. 4 shows the excursion to be almost perfectly far-sided, involving a directional change from full polarity to sub-vertical (upwards). Moreover, as at both Liverpool and Akaroa, this event consists of a single characteristic direction recorded in several successive lavas. It is not known whether event K1 is ultimately followed by a full polarity transition.

### Recurring intermediate directions

Whether associated with a geomagnetic excursion or with a polarity transition, the intermediate behaviour of the palaeomagnetic field revealed in the above mid-southern-latitude records appears to be dominated by an angular displacement to a position between  $30^\circ$  and  $60^\circ$  from the initial axial dipole field direction. Figure 5 summarizes the intermediate directional data reported here, plotted in  $(D', I')$ -space. The almost complete lack of intermediate directions deviating by more than  $60^\circ$  from the initial axial dipole direction is striking; indeed, only one of the 31 flows possesses such a direction.

The similarity in directional behaviour recorded during these events raises the possibility that most of them, perhaps all, have their origin in the same type of dynamo process in the Earth's core. The data suggest that the geomagnetic reversal process is characterized at its onset by an essentially stationary intermediate field geometry which, at least at mid-southern-latitude sites, is associated with vector directions less than  $\sim 60^\circ$  from that of the immediately preceding axial dipole field. In particular, the palaeofield behaviour recorded in the Liverpool lavas appears to possess a 'memory', insofar as each of a series of three departures is apparently dominated by essentially the same intermediate field geometry (Fig. 2b, events L1-L3). This observation of a recurring transitional direction strongly suggests a temporal dominance of the reversing field by a stationary or quasi-stationary transitional configuration. This interpretation of the Liverpool data does not rely on any assumptions regarding the mean extrusion rate or degree of eruptive clustering.

These data demonstrate a clear observational link between successful polarity transitions and the occurrence of at least some geomagnetic excursions (abortive field reversals). Moreover, the Liverpool results indicate that the initial core process associated with field reversals is the same regardless of whether a given attempt is successful or unsuccessful.

Another instance of a recurring intermediate field geometry (this time probably not associated with an ultimately successful polarity transition) can be found in the literature. Reporting on a palaeomagnetic investigation of Brunhes-age lavas from Amsterdam Island, situated at mid-southern latitudes ( $37.8^\circ$  S,  $77.5^\circ$  E), Watkins and Nougier<sup>19</sup> note that two distinct basalt sequences (containing two and three flows, respectively) display nearly the same intermediate palaeodirection. They then argue that the geomagnetic field vector recorded at Amsterdam Island changed from full normal polarity to the same intermediate direction on two separate occasions. Interestingly, these intermediate Brunhes directions are found to lie between  $30^\circ$  and  $45^\circ$  from the initial (normal polarity) axial dipole field direction and, moreover, are strongly far-sided. In fact, this intermediate behaviour corresponds to a near-vertical (upwards) vector field

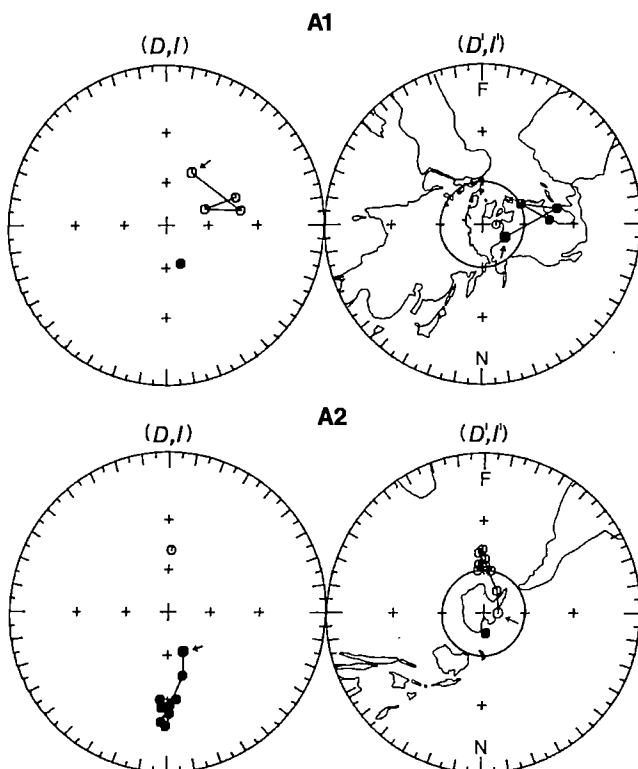


Fig. 3 Demagnetized directional data from two transitional events from Akaroa Volcano, New Zealand: A1 (N-R; the older) and A2 (R-N). See Fig. 2b legend.

direction at the site, strikingly similar to that found in the (normal) Miocene lavas at Mount Kaputar and nearly antipodal to the (reverse) Oligocene lavas from Liverpool Volcano. The Amsterdam Island events are included in Fig. 5 (Am1, 2).

These younger Southern Hemisphere data, taken together with those from Australia and New Zealand, suggest that the core process responsible for these intermediate-field events has possessed similar characteristics throughout the Cenozoic. Moreover, when considered in this light, the Amsterdam data indicate that at least some unsuccessful reversal attempts have occurred during the Brunhes normal epoch. It seems likely that such attempts have characterized the behaviour of the geodynamo throughout geological time.

With regard to field geometry, Fig. 5 indicates strikingly near-sided or far-sided intermediate directions to be present during all four recorded events involving reverse-polarity fields, as well as three of the five events involving normal polarity. Of these seven departures from full polarity consistent with a strongly axisymmetric, apparently stationary intermediate field geometry (namely, L1-3, A2, K1 and Am1, 2), six are associated with an inclination steepening, while event A2 alone indicates an inclination shallowing. The two remaining normal polarity departures (namely, L4 and A1) are associated with significant non-zonal field characteristics. Hence, although many of these data suggest largely axisymmetric fields of varying harmonic content during the onset of reversals, while the field is transitional and essentially stationary, such a geometrical aspect may not always be associated with the core process.

The lack of intermediate directions deviating by more than  $60^\circ$  from the initial axial dipole field direction during, in particular, the three successful transitions suggests that field changes are rapid during the hypothesized second stage of the reversal process. The first (onset) stage may also be rapid, but in view of the lack of knowledge regarding the recurrence time between any two extrusions, these suggestions must be considered statistically. In this sense, however, the summary display of the Southern Hemisphere basalt data (Fig. 5) is quite compelling.

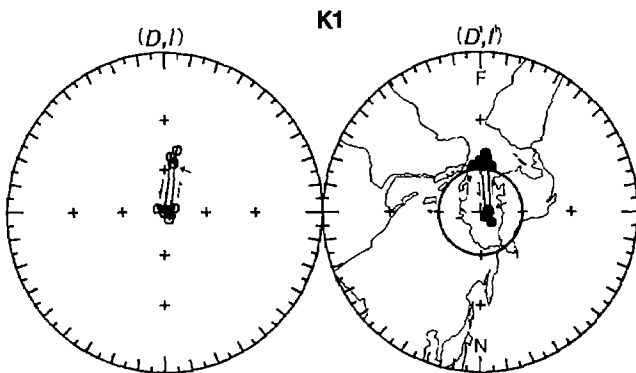


Fig. 4 Demagnetized directional data from event K1 (N-N) from Mt Kaputar, Australia. See Fig. 2b legend.

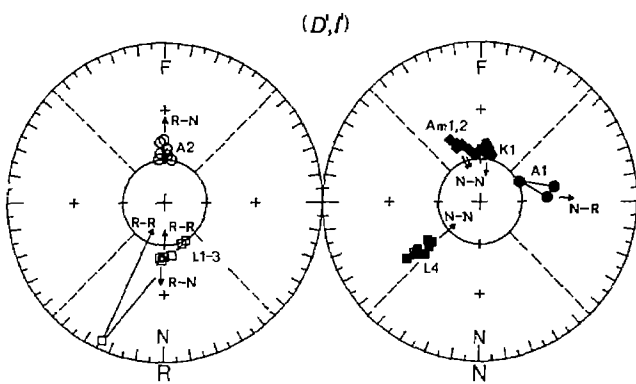


Fig. 5 Summary plot in  $(D', I')$ -space of all intermediate directions reported in this study. Data corresponding to two Brunhes-aged excursions (Am1, 2) from Amsterdam Island, Indian Ocean<sup>19</sup> are also plotted. Events starting from a reverse (normal) polarity field appear at left (right). The diagonal dashed lines are the boundaries between directional quadrants consistent and inconsistent with axisymmetric field dominance<sup>18</sup>. See Fig. 2b legend.

### Comparison with Northern Hemisphere records

The question that arises is: to what degree are palaeomagnetic transition records from the Northern Hemisphere compatible with these Southern Hemisphere data in suggesting the existence of a two-step reversal process?

The literature contains several apparently highly reliable Cenozoic records from igneous structures consistent with our Southern Hemisphere findings. A dramatic record of this kind is the Icelandic 'R3-N3' transition record<sup>20</sup>, which consists almost exclusively of a large number of systematically varying, intermediate palaeodirections residing less than  $90^\circ$  from the reverse-polarity axial dipole field direction<sup>18</sup>. Reporting the measurement of strong palaeointensities in a few of these intermediate-directed lavas, Shaw<sup>20,21</sup> proposed that a third metastable state of the geomagnetic field, in addition to normal and reverse polarity, may exist. We return to this hypothesis later.

More recently, Bogue and Coe<sup>3,22</sup> have investigated two sequential reversals obtained from lava sequences on Kauai, Hawaii. They report the existence of clustered, marginally intermediate directions at the onset of the reversals (especially for the R-N transition), but find a complete lack of strongly intermediate directions at other times during the polarity transitions. From these data, Bogue and Coe argue that the bulk of the directional changes associated with both transitions occurred rapidly.

The recently reported reinvestigation of the very detailed Miocene R-N record from the mid-northern-latitude basalts comprising Steens Mountain, Oregon<sup>8</sup>, reveals that the core process is characterized by stop-and-go behaviour. The authors<sup>8</sup>

consider such behaviour to be a consequence of a succession of 'geomagnetic impulses' in the core. In particular, the authors note a large and regular change in direction at the onset of the reversal to an intermediate orientation which remains essentially unchanged during the extrusion of several flows. There follows an apparently rapid change (an impulse) to full normal polarity and then, before the completion of the reversal, a 'rebound' to the same intermediate field direction<sup>8</sup>.

Stronger supporting evidence comes from intrusions, because of their capability to record in a more continuous fashion than lava sequences. In particular, the detailed records of two Miocene R-N transitions obtained from intrusions in the Pacific north-west of the United States<sup>23</sup>, which differ in age by several Myr, display strikingly similar palaeofield behaviour<sup>1,23</sup>. Specifically, both records indicate a quite rapid and marked change in inclination at the onset of the transition. The field is then observed to maintain a loosely stationary intermediate geometry, apparently for quite some time before the completion of each reversal. One record (Tatoosh intrusion) contains a rebound from normal polarity to this same field configuration<sup>23</sup>, much as is seen in the Steens Mountain record. Given that these records were derived from slowly cooled igneous bodies and are thus considered to be continuous, such time-dependent interpretations of directional movements are highly credible.

Particular high-resolution reversal records obtained from sedimentary structures in the Northern Hemisphere also display field behaviour consistent with our findings from southern latitudes. The two most striking examples are the Matuyama-Brunhes record from the Boso Peninsula, Japan<sup>24</sup>, and the Gauss-Matuyama record from Searles Valley, California<sup>5</sup>. Both records suggest the reversal onset to be characterized by a movement to an intermediate palaeodirection which remains essentially stationary. In the younger (R-N) transition, the intermediate field configuration displays strong zonal symmetry<sup>1</sup>, however, the intermediate field recorded during the older (N-R) transition is without question non-zonal.

### The geomagnetic reversal process

Clearly, a significant fraction of available transition data from both hemispheres supports the idea of a reversal process in the core which is rather discontinuous. We believe that the findings from Southern Hemisphere volcanics presented here further clarify the core mechanism. Specifically, these data suggest that a potentially long-lived, intermediate field state is developed near the onset of the transition process. From this stationary or quasi-stationary configuration, a rapid change to either polarity is indicated.

It seems reasonable to suspect that geomagnetic reversal attempts start locally in the core<sup>25</sup>, perhaps caused by a form of short-range, hydrodynamic disturbance. Moreover, the repetitive field behaviour recorded at Liverpool Volcano may indicate that a succession of nearly identical disturbances can occur at the same location in the core over a relatively short interval of time, or alternatively, that a single disturbance can fluctuate significantly in intensity during its existence. The developed intermediate field geometry associated with a given attempt may be considered metastable as first proposed by Shaw<sup>20,21</sup>. However, according to the Southern Hemisphere data, the particular geometry is likely to vary from one series of events to the next, perhaps linked to the location in the core where the reversal-causing disturbance initiates. At this point in the process the reversal attempt may abort. It is not known just what conditions are required for the dynamo to undergo a successful transition in polarity.

As we have seen, available high-resolution transition data often suggest quite rapid directional movement to be a feature of the reversing geodynamo. Indeed, one conclusion from the Steens Mountain study<sup>8</sup> is that a small number of geomagnetic impulses, characterized by extremely large angular rates of change of the vector field, occurred during this reversal. Such

rapidity indicates that reversal attempts are in large part 'fluid-driven'; that is, associated with changes dominated by frozen-in flux<sup>26,27</sup> in a changing velocity field. On the other hand, the process of magnetic flux diffusion must become significant over longer intervals of time. This may explain the observation, certainly a feature of much of the Southern Hemisphere data, of apparent axisymmetry of the stationary or quasi-stationary transitional field geometry developed between the two stages of more rapid change. Specifically, as the duration of a reversal-causing hydrodynamic disturbance increases, so too may the zonal symmetry of the perturbed field produced by the affected local fluid source. In an  $\alpha\omega$ -dynamo<sup>28,29</sup> this may result from flux diffusion as the  $\omega$ -process spreads the altered field azimuthally. The data, however, cannot eliminate the possibility that those cases of apparent zonal dominance are produced from the outset by latitudinal 'flooding'<sup>12,13,22</sup> or by diffusive decay of an axially symmetric field<sup>30</sup>. Neither can the recorded events, each having been obtained from a single site, provide any quantitative measure of the relative importance of zonal and non-zonal harmonic content.

We emphasize that no compelling information is gained from the Southern Hemisphere data regarding the nature of configurational changes throughout the reversal process. Hence, any suggestion of axisymmetry associated with a given event cannot be extrapolated, especially to times after the development of the apparently stationary intermediate field configuration. Indeed, the data suggest the return to full polarity during successful attempts to be accomplished by one; or a series of<sup>8</sup>, rapid, fluid-driven events. Such are not

likely to be associated with axially symmetric fields<sup>27</sup>.

The Southern Hemisphere transition data clearly suggest that a stationary or quasi-stationary intermediate field configuration may dominate an entire reversal. This interpretation of the data, if valid for most polarity reversal attempts, implies that the corresponding global field geometry associated with a given event is quantifiable, provided that the same feature is recognized in contemporaneous, distant records. When the appropriate data become available, such a determination will constitute a major step forward in our understanding of the spatial characteristics of the reversal mechanism in the Earth's core.

I thank M. W. McElhinny and D. V. Christoffel for helping to make this project possible during my sabbatical leave in Australia and New Zealand; B. J. J. Embelton and P. W. Schmidt for field support through the CSIRO; Mark Huddleston, M. McFadden and D. Edwards for assistance with sampling; P. McFadden for his interest and assistance in the field; S. Weaver and P. Wellman for helpful discussions; the New South Wales National Park Service and A. W. Benton for permission to sample state-owned and private lands, respectively, and M. Prévost for reviews. D. Alexander, C. Callahan, M. Garrison, L. Hewey, K. Lubliner, A. Lyon, B. Lyons and G. P. Scandalas assisted in the laboratory; K. Norville assisted in both field and laboratory. This project was supported through NSF grant EAR80-8018791 (funded in part through the US-Australia Cooperative Science Program), NSF grant EAR82-12766, the Research School of Earth Sciences, Australian National University and the Physics Department, Victoria University of Wellington, New Zealand.

Received 23 July 1985; accepted 23 January 1986.

1. Fuller, M. *et al.* *Rev. Geophys. Space Phys.* **17**, 179–203 (1979).
2. Valet, J.-P. & Laj, C. *Earth planet. Sci. Lett.* **54**, 53–63 (1981).
3. Bogue, S. W. & Coe, R. S. *Nature* **295**, 399–401 (1982).
4. Clément, B. M. *et al.* *Phil. Trans. R. Soc. A306*, 113–119 (1982).
5. Liddicat, J. C. *Phil. Trans. R. Soc. A306*, 121–128 (1982).
6. Williams, I. & Fuller, M. *J. geophys. Res.* **87**, 9408–9418 (1982).
7. Valet, J.-P. & Laj, C. *Nature* **311**, 552–555 (1984).
8. Prévost, M. *et al.* *Nature* **316**, 230–234 (1985).
9. Van Zijl, J. S. *et al.* *Geophys. J. R. astr. Soc.* **7**, 169–182 (1962).
10. Clement, B. M. & Kent, D. V. *J. geophys. Res.* **89**, 1049–1058 (1984).
11. Clement, B. M. & Kent, D. V. *Phys. Earth planet. Int.* **39**, 301–313 (1985).
12. Hoffman, K. A. *Science* **196**, 1329–1332 (1977).
13. Hoffman, K. A. & Fuller, M. *Nature* **273**, 715–718 (1978).
14. Williams, I. S. & Fuller, M. *J. geophys. Res.* **B6**, 11657–11665 (1981).
15. Wellman, P. *et al.* *Geophys. J. R. astr. Soc.* **18**, 371–395 (1969).
16. Evans, A. L. *Geophys. J. R. astr. Soc.* **21**, 163–183 (1970).
17. Hoffman, K. A. *Geophys. Res. Lett.* **11**, 681–684 (1984).
18. Hoffman, K. A. *J. geophys. Res.* **89**, 6285–6292 (1984).
19. Watkins, N. D. & Nouguier, J. *J. geophys. Res.* **78**, 6050–6068 (1973).
20. Shaw, J. *Geophys. J. R. astr. Soc.* **40**, 345–350 (1975).
21. Shaw, J. *Geophys. J. R. astr. Soc.* **8**, 263–269 (1977).
22. Bogue, S. W. & Coe, R. S. *J. geophys. Res.* **89**, 10341–10354 (1984).
23. Dodson, R. *et al.* *Geophys. J. R. astr. Soc.* **53**, 373–412 (1978).
24. Niitsuma, N. *Tohoku Univ. Sci. Rep. 2nd Ser. (Geology)* **43**, 1–39 (1971).
25. Hoffman, K. A. *Earth planet. Sci. Lett.* **44**, 7–17 (1979).
26. Benton, E. R. *Eos* **63**, 653 (1982).
27. Gubbins, D. & Roberts, N. *Geophys. J. R. astr. Soc.* **73**, 675–687 (1983).
28. Levy, E. H. *Astrophys. J.* **171**, 635–642 (1971).
29. Levy, E. H. *Astrophys. J.* **175**, 573–581 (1972).
30. Hide, R. *Nature* **293**, 728–729 (1981).
31. Levy, E. H. *Astrophys. J.* **175**, 573–581 (1972).
32. Hide, R. *Nature* **293**, 728–729 (1981).

## Transfer of specificity by murine $\alpha$ and $\beta$ T-cell receptor genes

Zlatko Dembić, Werner Haas, Siegfried Weiss, James McCubrey, Hansruedi Kiefer, Harald von Boehmer & Michael Steinmetz

Basel Institute for Immunology, Grenzacherstrasse 487, CH-4005 Basel, Switzerland

*T-cell receptor  $\alpha$ - and  $\beta$ -chain genes were isolated from a class I major histocompatibility complex-restricted cytotoxic T-cell clone and transferred by protoplast fusion into another cytolytic T-cell clone of different specificity. Expression of the transfected  $\alpha$  and  $\beta$  genes endowed the recipient cell with the specificity of the donor cell.*

In the immune system of vertebrates, T cells recognize foreign structures on cell surfaces in the context of glycoproteins encoded by the major histocompatibility complex (MHC) (for review see ref. 1). The molecule that recognizes the foreign antigens and MHC determinants—the T-cell receptor—is composed of at least two polypeptide chains,  $\alpha$  and  $\beta$ , which

contribute to the specificity of the cell (see refs 2, 3 for a review). The  $\alpha$ - and  $\beta$ -chains are associated on the cell surface with additional molecules, notably the T3 molecule, which might be important for certain effector functions<sup>4,5</sup>. Furthermore, the Lyt 2/T8 and L3T4/T4 surface glycoproteins are thought to stabilize the binding of T cells to their targets<sup>6–8</sup>. It is assumed that these

additional interactions are especially important for receptors with low affinity as the blocking effect of antibodies directed against L3T4 can be reversed by increasing the density of the target antigen<sup>7,8</sup>.

The genes encoding the  $\alpha$ - and  $\beta$ -chains of the T-cell receptor have been cloned and characterized<sup>9-11</sup>; they are composed of genetic segments which rearrange during T-cell development to generate T cells with clonally distributed receptors containing variable (V) and constant (C) regions. In the mouse, the variable regions of the  $\alpha$ - and  $\beta$ -chains are encoded by about 20  $V_\alpha$ , 2  $D_\alpha$  (diversity), 12  $J_\alpha$  (joining), at least 50  $V_\beta$ , and over 20  $J_\beta$  gene segments, while a single  $C_\alpha$  and two almost identical  $C_\beta$  genes encode the constant regions<sup>12-23</sup>. A third gene family,  $\gamma$ , is closely related to the  $\alpha$  and  $\beta$  genes and shows specific rearrangements in T cells<sup>24-26</sup>. The protein product of the  $\gamma$  gene has not yet been identified and the function of the  $\gamma$  gene is unknown.

Various elegant experiments have addressed the question of whether the  $\alpha$ - and  $\beta$ -chains are sufficient to endow a T cell with both antigen and MHC specificity<sup>27,28</sup>. Perhaps the most straightforward way to investigate this question is by gene transfer between T cells of different specificities. Here we show that T-cell receptor  $\alpha$ - and  $\beta$ -chain genes, isolated from a cytotoxic T cell, are sufficient to transfer that cell's MHC-restricted antigen specificity to another T cell.

### Isolation of $\alpha$ - and $\beta$ -chain alleles

The cytotoxic T-cell clone BDFL 1.1.3 (called BDFL), isolated from a (C57BL/6  $\times$  DBA/2)F<sub>1</sub> mouse shows specificity for the hapten fluorescein (FL) and the MHC class I antigen D<sup>d</sup>. We constructed complementary DNA and genomic DNA libraries for BDFL using  $\lambda$ gt11 and cosmid vectors, respectively. From the cDNA library we isolated two  $\alpha$ -chain and four  $\beta$ -chain cDNA clones using  $\alpha$ - and  $\beta$ -chain constant-region hybridization probes that have been described elsewhere<sup>29,30</sup>. Sequence determination of the cDNA clones revealed that the two  $\alpha$  and all four  $\beta$  clones were derived from a single, presumably functional,  $\alpha$ - and  $\beta$ -chain allele, respectively. Northern blot analysis of BDFL poly(A)<sup>+</sup> RNA with  $\alpha$ - and  $\beta$ -chain constant-region probes revealed 1.5-kilobase (kb) and (less abundant) 1.2-kb  $\alpha$ -chain transcripts and a 1.3-kb  $\beta$ -chain transcript (Fig. 1). The  $\alpha$ -chain cDNA clones correspond to the larger transcript, as shown using the V-region-specific hybridization probe  $V_{BDFL\alpha I}$  (Fig. 1).

Cosmid clones were isolated from the genomic library<sup>29</sup> using  $\alpha$ - and  $\beta$ -chain constant-region probes as well as the  $V_{BDFL\alpha I}$  variable-region probe. The  $V_{BDFL\alpha I}$  probe detects only a single V gene segment in germline DNA (data not shown). Based on overlapping restriction maps, these clones could be ordered into four clusters defining the two  $\alpha$ - and the two  $\beta$ -chain alleles of BDFL (Fig. 2). Comparison of the cloned genes with germline DNA sequences for  $\alpha$ - and  $\beta$ -chain genes<sup>14,22</sup> revealed that all four alleles had undergone DNA rearrangements.

### Identification of functional alleles

To characterize the four alleles, we determined their DNA sequences around the points of rearrangement. The  $\alpha I$  and  $\beta I$  alleles are functionally rearranged genes while the  $\alpha II$  and  $\beta II$  alleles contain nonfunctional rearrangements. All four genes possess rearranged V gene segments (Fig. 3).

The two  $\alpha$  alleles have been formed by rearrangement of two V gene segments, termed  $V_{BDFL\alpha I}$  and  $V_{BDFL\alpha II}$ , with  $J_\alpha$  gene segments located 40 and 10 kb upstream of  $C_\alpha$ , respectively (Figs 2a, b and 3). The two  $V_\alpha$  and the  $J_{BDFL\alpha I}$  gene segments have not been described previously, whereas the  $J_{BDFL\alpha II}$  gene segment has been found<sup>20</sup> in an  $\alpha$ -chain cDNA clone. We also sequenced the  $J_{BDFL\alpha II}$  gene segment in a germline clone derived from BALB/c DNA (Figs 2a, 3).

The BDFL $\alpha I$  allele contains an open reading frame throughout the V gene and a splice site at the expected position

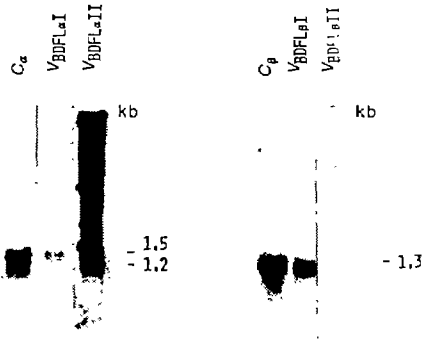


**Fig. 1** Northern blot analysis of T-cell receptor genes of the cytolytic T-cell clone BDFL. Poly(A)<sup>+</sup>-selected RNA (2  $\mu$ g per lane) was separated on a 1% formaldehyde gel, transferred to a nitrocellulose filter and hybridized with the probes indicated. The  $C_\alpha$  probe is identical to probe 2 described previously<sup>29</sup>. The  $V_{BDFL\alpha I}$  probe is an *Rsa*I-EcoRI fragment of the  $\alpha$ -chain cDNA clone pTBD1.9, isolated from the BDFL cDNA library. This probe contains 200 bp of the BDFL $\alpha I$  V region and 25 bp of the  $C_\alpha$  region. The  $V_{BDFL\alpha II}$  probe is a 4-kb *Bam*HI fragment containing the  $V-J_{BDFL\alpha II}$  exon from cosmid clone BDFL9.3 (compare with Fig. 2). The  $C_\beta$  probe is the 300-bp insert of the  $\beta$ -chain cDNA clone 4.4 described previously<sup>30</sup>. The  $V_{BDFL\beta I}$  probe is a 200-bp EcoRI-PstI fragment of a  $\beta$ -chain cDNA clone isolated from the BDFL cDNA library. The  $V_{BDFL\beta II}$  probe is a 1.2-kb *Sal*I-*Bam*HI fragment from cosmid clone BDFL3.2 (compare with Fig. 2). **Methods.** RNA was isolated by guanidinium isothiocyanate and CsCl gradient centrifugation<sup>39,40</sup>. Blots were hybridized with oligo-labelled probes as described previously<sup>29,41</sup>. The cDNA library was constructed in the  $\lambda$ gt11 vector as described elsewhere<sup>42</sup>. RNA relative molecular masses ( $M_r$ s) were determined using DNA fragments of known lengths run on the same gel. The blot obtained with the  $V_{BDFL\alpha II}$  probe is overexposed to show the 1.2-kb  $\alpha$  gene transcript.

at the end of the J gene segment. The V-region sequence is identical to the BDFL  $\alpha$ -chain cDNA clone (Fig. 3). This identifies the  $\alpha I$  gene as the functional allele. It is interesting to note that the V gene has an unusually long intron of 430 base pairs (bp) between the leader and the V exon. The BDFL $\alpha II$  allele is nonfunctional. The frame in which the V and J gene segments have been joined results in a premature termination codon at the end of the V region. The  $\alpha II$  allele is also transcribed, although at a lower level than the  $\alpha I$  allele, giving rise to the 1.2-kb RNA molecule (Fig. 1). We do not know why this unusually short transcript is produced.

The BDFL $\beta I$  allele shows a  $V-D-J_\beta 2.5$  rearrangement which deleted the  $C_\beta I$  constant-region gene (Figs 2c, 3). BDFL $\beta I$  is the functional  $\beta$  allele because it has an open reading frame and is identical to the four  $\beta$ -chain cDNA clones isolated. Interestingly, this  $\beta$  gene contains the same V gene segment (E1) previously identified<sup>15</sup> in a trinitrophenol (TNP)-specific helper T-cell clone restricted to I-A<sup>d</sup>. Thus, as found previously<sup>18,31,32</sup>, the same V gene segment can be used by MHC class I and class II-restricted T cells. The BDFL $\beta II$  allele is characterized by a rearrangement of a V gene segment to  $D_\beta I$  and  $J_\beta 1.2$  (Figs 2d, 3); the rearrangement has fused the gene segments such that a premature termination codon is encountered in the C region. On the basis of these criteria, the BDFL $\beta II$  gene is nonfunctional. Also, it does not produce a  $\beta$ -chain transcript detectable by Northern blot analysis (Fig. 1). The BDFL $\beta II$  V gene segment has not been described previously<sup>15,18,19</sup>. Thus, at present, 17  $V_\beta$  gene segments have been identified in the mouse genome.

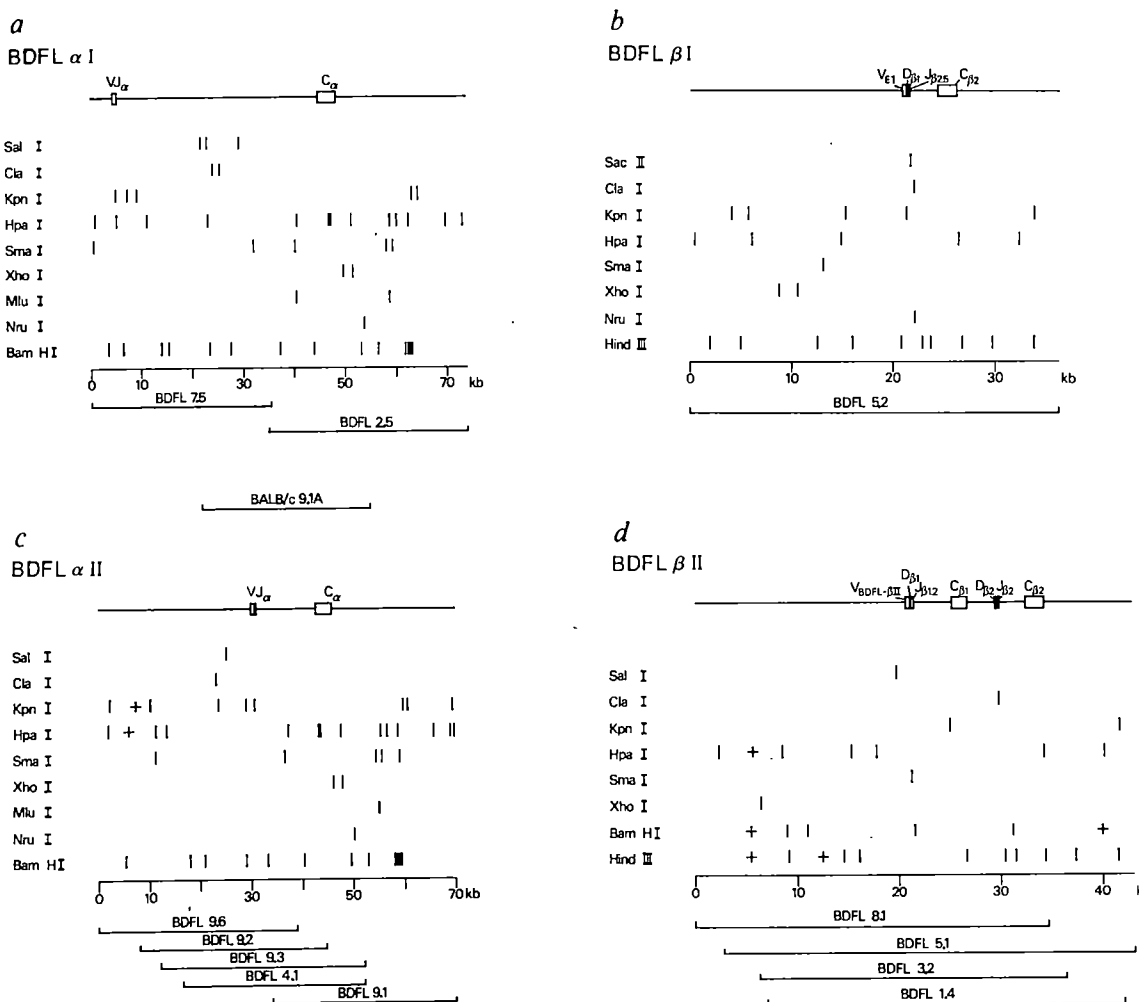


**Fig. 2** Molecular maps of rearranged T-cell receptor  $\alpha$ - and  $\beta$ -chain alleles from BDFL. Boxes indicate the location and approximate size of the  $V$  and  $C$  gene segments; their positions were deduced from sequence determinations (compare with Fig. 3) and by Southern blot hybridization using the  $V$ - and  $C$ -region probes described in Fig. 1 legend. The  $D_{\beta}2-J_{\beta}2$  rearrangement in the BDFL $\beta$ II gene was deduced from smaller restriction fragments in this region, compared with germline restriction maps<sup>14</sup>, but has not been sequenced. Restriction enzyme sites are indicated by vertical bars. + Indicates the presence of unassigned sites for the same enzyme in the segment marked. *a*, The BDFL $\alpha$ I allele is defined by two overlapping cosmid clones derived from the DBA/2 chromosome (compare with ref. 29); as these overlap by less than 0.5 kb of DNA, a germline cosmid clone, BALB/c9.1A, was isolated from a BALB/c cosmid library<sup>43</sup> to confirm the overlap. *b*, The BDFL $\alpha$ II allele is defined by five overlapping cosmid clones derived from the C57BL/6J chromosome (compare with ref. 29). *c*, The BDFL $\beta$ I allele is defined by one cosmid clone. No site for *Sal* I was found. *d*, The BDFL $\beta$ II allele is defined by four overlapping cosmid clones.

**Methods.** The BDFL cosmid library was constructed and screened with oligo-labelled  $C_{\alpha}$ ,  $C_{\beta}$  and  $V_{BDFL\alpha}$ I probes (see Fig. 1 legend) as described previously<sup>29</sup>. The probe used to isolate the cosmid clone BALB/c9.1A was a 2-kb fragment extending from the left-most *Bam* HI site to the left end of cosmid clone BDFL2.5. All cosmid were analysed by restriction enzyme digestion and hybridization as described previously<sup>44,45</sup>.

## Transfection of functional alleles

To transfer the BDFL $\alpha$ I and  $\beta$ I alleles into another T cell, we constructed the cosmid molecule BD7 containing both genes in the same transcriptional orientation together with the neomycin-resistance gene as a positive selection marker (Fig. 4). Briefly, 30 kb of the large intervening sequence between the exons encoding the  $V$  and  $C$  regions of the  $\alpha$ -chain were excised so that

the  $\alpha$  gene together with the  $\beta$  gene would fit into the cosmid vector. The deletion in the intron ends 10 kb upstream of the  $C_{\alpha}$  gene and therefore leaves at least one functional  $J_{\alpha}$  gene segment<sup>22</sup> behind. We reasoned that if the T-cell receptor  $\alpha$  gene contains a tissue-specific enhancer element in a similar position to that in immunoglobulin heavy and light-chain genes<sup>33–35</sup>, it should be located downstream of the most 3' functional  $J_{\alpha}$  gene segment and would therefore be retained in our construct. The

**Fig. 3** (Opposite) Nucleotide and predicted amino-acid sequences of the T-cell receptor  $\alpha$ - and  $\beta$ -chain  $V$  genes and cDNAs from BDFL. *a*,  $\alpha$ I; *b*,  $\alpha$ II; *c*,  $\beta$ I; *d*,  $\beta$ II. The leader (L),  $V$ ,  $D$ , and  $J$  regions are indicated. In BDFL $\alpha$ I and BDFL $\alpha$ II, broken arrows indicate unknown locations of boundaries and possible extra nucleotides between  $V$  and  $J$ . Dashes indicate where cDNA sequences are identical to genomic sequences.  $g_{\alpha}^{II}$  in *b* is the sequence of the germline  $J_{BDFL\alpha}$ II gene segment on cosmid clone BALB/c9.1A (compare with Fig. 2). Proposed nonamer and heptamer recognition sequences for DNA rearrangement are indicated by the respective numbers. Conserved splice donor sites at the 3' end of the  $J$ -gene segments are underlined.

**Methods.** The BDFL $\alpha$ I and BDFL $\beta$ I cDNAs were excised from  $\lambda$ gt11 and subcloned into the *Eco*RI site of pUC9 or M13mp18. Relevant restriction enzyme fragments were isolated from cosmid clones (see below) and subcloned into pUC9 or M13mp18/19. DNA sequences were obtained using deletion subcloning<sup>46</sup>, chemical degradation<sup>47</sup> and dideoxynucleotide chain termination<sup>48</sup> techniques. Primers used for dideoxynucleotide sequencing were either purchased (universal M13 primer) or synthesized<sup>49</sup>. The following fragments were isolated and subcloned for sequencing (compare with Fig. 2): a 3-kb *Bam*HI from cosmid clone BDFL7.5 containing the  $V_{BDFL\alpha}$ I gene (this clone was designated pV $\alpha$ -1); a 4-kb *Bam*HI fragment from cosmid clone BDFL9.3 containing the  $V_{BDFL\alpha}$ II gene; a 1.2-kb *Hind*III-*Clal* fragment from cosmid clone BDFL5.2 containing  $V_{BDFL\beta}$ I; a 1.2-kb *Sal*I-*Bam*HI fragment from cosmid clone BDFL3.2 containing  $V_{BDFL\beta}$ II; and a 9-kb *Bam*HI fragment from cosmid clone BALB/c9.1A containing the unrearranged  $J_{BDFL\alpha}$ II gene segment.

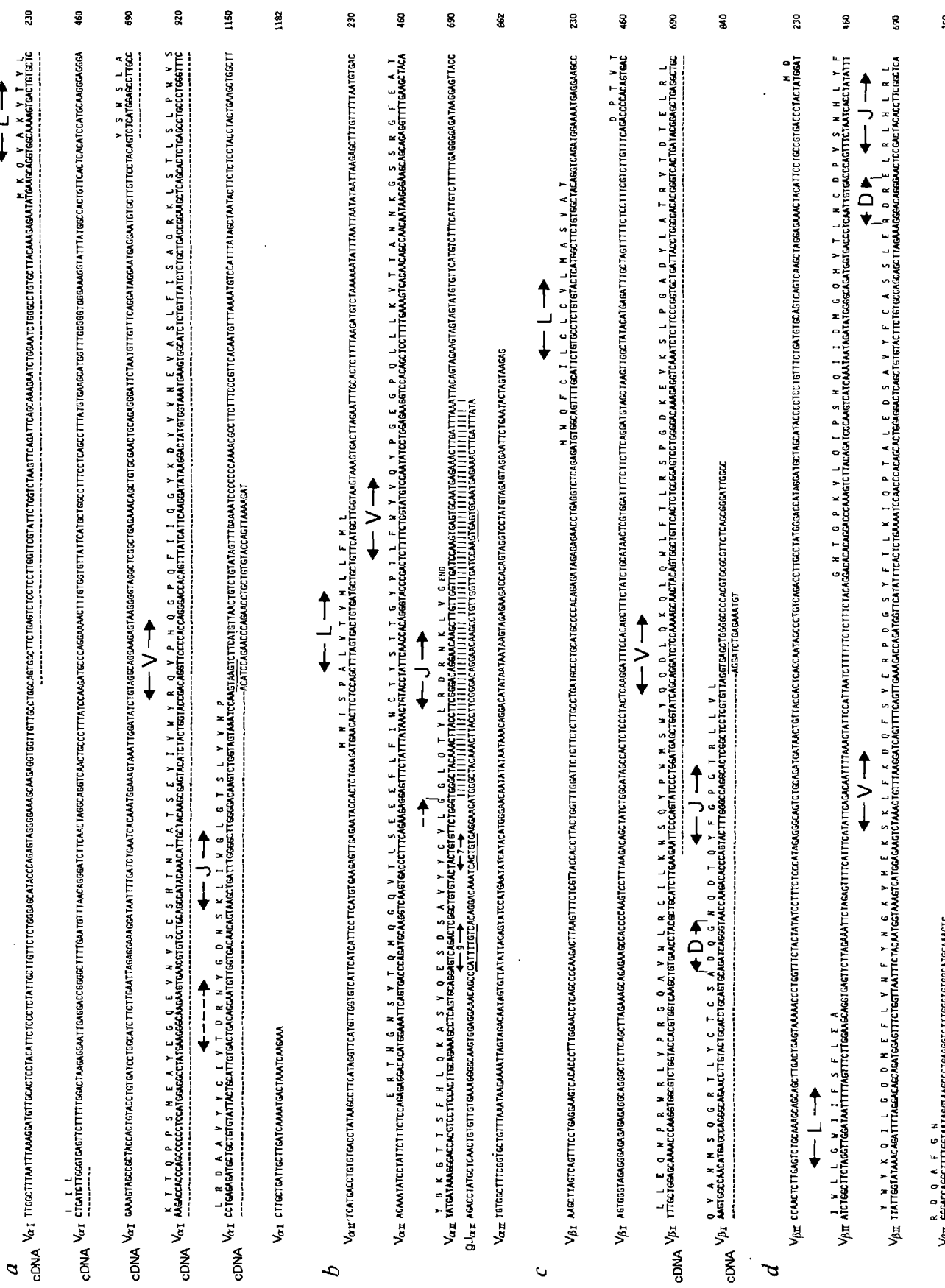


**Figure 3**

shortened  $\alpha I$  gene on an 18-kb fragment was then inserted, together with a 24-kb fragment containing the  $\beta I$  gene, into the cosmid vector pTCF containing the G418-resistance gene with simian virus 40 (SV40) promoter and enhancer sequences. In this construct the  $\alpha I$  and  $\beta I$  genes retained 1 and 8 kb of 5'-flanking sequence, respectively.

The BD7 construct was then transfected by protoplast fusion into the cytolytic T-cell hybridoma SPH (ref. 36), which recognizes the hapten 3-(*p*-sulphophenylidazo)-4-hydroxyphenylacetic acid (SP) and the K<sup>k</sup> MHC class I molecule. The T-cell hybridoma SPH was obtained by fusion of a CBA-derived cytotoxic T cell with the AKR thymoma BW5147.

From four independent protoplast fusion experiments with BD7, we isolated 41 G418-resistant clones. Of these clones, 22 had retained the antigen and MHC-specific cytolytic activity of the recipient T-cell hybridoma (data not shown); 12 of these were analysed further.

### Clone BD7-S17 transcribes transfected genes

We analysed transcription of the transfected BDFL  $\alpha$  and  $\beta$  genes, since no anti-idiotypic antibody directed against the T-cell receptor of the BDFL killer cell was available. Initially, RNA dot-blot experiments were carried out on all 12 transfectants. Using the  $V_{BDFL\alpha I}$  and  $V_{BDFL\beta I}$ -specific probes only one transfectant (BD7-S17) showed high levels of BDFL $\alpha I$  gene transcription, while two transfectants (BD7-S17 and BD7-S19) showed high levels of BDFL $\beta I$  gene transcription (not shown). Northern blot analysis confirmed that the BD7-S17 transfectant contained high levels of  $\alpha$  and  $\beta$  transcripts hybridizing to the BDFL  $V$ -region probes (Fig. 5a). The BD7-J9 transfectant showed intermediate levels of  $\beta$ -gene transcripts but no  $\alpha$  transcripts (Fig. 5a).

In contrast to the  $V_{BDFL\alpha I}$  probe, the  $V_{BDFL\beta I}$  probe hybridized weakly with RNA from the SPH recipient T cell (Fig. 5a), indicating that the same or a closely related  $V_\beta$  gene segment was transcribed in SPH. We therefore performed RNase protection experiments to show unequivocally that proper  $\alpha$ - and  $\beta$ -gene transcripts were derived from the introduced BDFL $\alpha I$  and  $\beta I$  genes, respectively, in the transfectants.

As probes for the RNase protection experiments, we used labelled 'anti-sense' RNA transcripts derived *in vitro* from the coding strands of the  $V_{\alpha I}$  and  $V_{\beta I}$  genes (Fig. 5b). These probes were annealed with RNA from BDFL, SPH, BD7-S17 and BD7-J9 cells, digested with RNase and analysed on a 6% sequencing gel. As shown in Fig. 5b, BDFL and BD7-S17 RNA protected 352-nucleotide (nt)  $V_{\alpha I}$  and 351-nt  $V_{\beta I}$  RNA fragments. BD7-J9 RNA protected the 351-nt  $V_{\beta I}$  RNA fragment but showed no protection of the  $V_{\alpha I}$  probe. SPH RNA did not protect the  $V_{\alpha I}$  RNA but it (as well as RNA from the two transfectants) did protect a 291-nt fragment of the  $V_{\beta I}$  RNA probe, again indicating that the same or a very similar  $V_\beta$  gene segment is transcribed in the SPH and BDFL cells. Because of the difference in size between the  $V_\beta$  fragments protected by SPH and BDFL RNA, at least the sequences around the  $D$  regions must be different in the  $\beta$ -chain genes of BDFL and SPH.

The results of the RNase protection experiments confirm that the introduced BDFL  $\alpha I$  and  $\beta I$  genes are transcribed and spliced in clone BD7-S17 while only the BDFL  $\beta I$  gene is transcribed and spliced in BD7-J9. We have not found a major protected band for the 5'-untranslated regions and the leader sequences of the  $\alpha$  and  $\beta$  genes, possibly because of premature termination of most of the *in vitro*-synthesized RNA molecules.

Figure 5c shows an analysis of the RNAs of the two transfectants, the donor and the recipient T cells, using an oligonucleotide probe specific for the  $V_{BDFL\beta I}$  gene. With this probe transcripts of the same size were found in the transfectants and the BDFL donor cell, while no hybridization was observed with RNA from SPH recipient cells. We conclude, therefore, that the BDFL  $\alpha$  and  $\beta$  gene transcripts were correctly initiated, spliced and terminated in the transfectants.

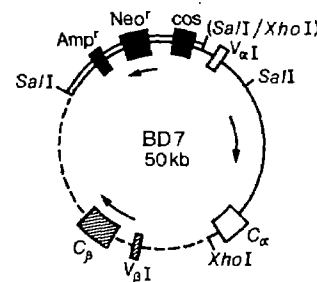


**Fig. 4** Structure of the BD7 T-cell receptor gene construct. The cosmid BD7 was derived by subcloning the BDFL $\alpha I$  and BDFL $\beta I$  genes into the cosmid vector pTCF, described in ref. 50. □, ▨:  $V$  and  $C$  genes of BDFL $\alpha I$  and BDFL $\beta I$ , respectively. Amp', the  $\beta$ -lactamase gene of pBR322; Neo', the aminoglycosyl 3'-phosphotransferase gene from Tn5; cos, cos site of phage  $\lambda$ . Arrows indicate the orientation of transcription. The double-lined segment represents the vector; the segment indicated by a single line was derived from parts of cosmids BDFL7.5 and BDFL2.5; the segment represented by a broken line was derived from cosmid BDFL5.2 (see below). Restriction enzyme sites used in the construction are shown. Parentheses indicate that the respective sites were inactivated during the cloning.

**Methods.** The construction involved several subcloning steps: (1) in pV $\alpha$ -1 (see Fig. 3 legend) the unique  $SalI$  site of the pUC9 vector was converted into a  $XbaI$  site by linker insertion. (2) The insert of pV $\alpha$ -1, excised with  $SalI$  and  $XbaI$ , was subcloned into the  $SalI$  site of the cosmid vector pTCF. One of the resulting clones, pTCFV $\alpha$ -C, contained the desired unique  $SalI$  site 3' of the  $V_{BDFL\alpha I}$  gene (the other  $SalI$  site was not regenerated because of ligation of  $SalI$  and  $XbaI$  sticky ends). (3) A 15-kb  $SalI-XbaI$  fragment from cosmid BDFL2.5, together with a 24-kb  $SalI-XbaI$  fragment from cosmid BDFL5.2D (derived from cosmid clone BDFL5.2 after conversion of the unique  $SalI$  site into a  $XbaI$  site; compare with Fig. 2), was inserted into the  $SalI$  site of pTCFV $\alpha$ -C. From the resulting clones, cosmid BD7, with one  $XbaI$  and two  $SalI$  sites, was selected for transfection experiments. BD7 was transferred to SPH hybridoma cells by protoplast fusion as described elsewhere<sup>51,52</sup>.

### Specificity of BD7-S17 transfectant

To determine whether the introduced and transcribed BDFL  $\alpha I$  and  $\beta I$  genes enabled the BD7-S17 transfectant to recognize the same target cells as BDFL, we tested its effect on H-2<sup>d</sup>- and H-2<sup>k</sup>-positive cells coupled with either fluorescein or SP. We used two different types of target cells: B-cell blasts and L-cell fibroblasts. We shall first describe the results obtained with B-cell blasts. Figure 6a shows that the BD7-S17 transfectant was able to lyse H-2<sup>k</sup>-positive B-cell blasts coupled with SP, but could not lyse H-2<sup>d</sup>-positive B-cell blasts coupled with FL. Thus, the transfectant had retained the cytolytic specificity of the SPH recipient cell but had not gained the specificity of the BDFL donor cell when tested on B lymphocytes.

It has been argued that T cells which display a relatively low avidity for MHC and antigen require accessory molecules (such as Lyt 2 and L3T4) to strengthen the interaction with target cells<sup>6,8</sup>. The need for L3T4 to stabilize the T-cell/target cell interaction can be overcome by increasing the concentration of antigen on the surface of the target cell<sup>7,8</sup>. For unknown reasons, T-cell hybridomas derived from fusion experiments using BW5147 as the thymoma parent, do not express Lyt 2 molecules<sup>37</sup>. Thus, a possible explanation for the failure of the BD7-S17 transfectant to lyse B-cell blasts is that it requires Lyt 2 which was not expressed on the recipient SPH hybridoma (not shown). Indeed we found that the cytotoxic activity of BD7 cells can be blocked with anti-Lyt 2 antibodies (Fig. 6a). Thus we hoped to overcome the requirement for Lyt 2 by using target cells expressing larger amounts of the D<sup>d</sup> antigen.

## ARTICLES

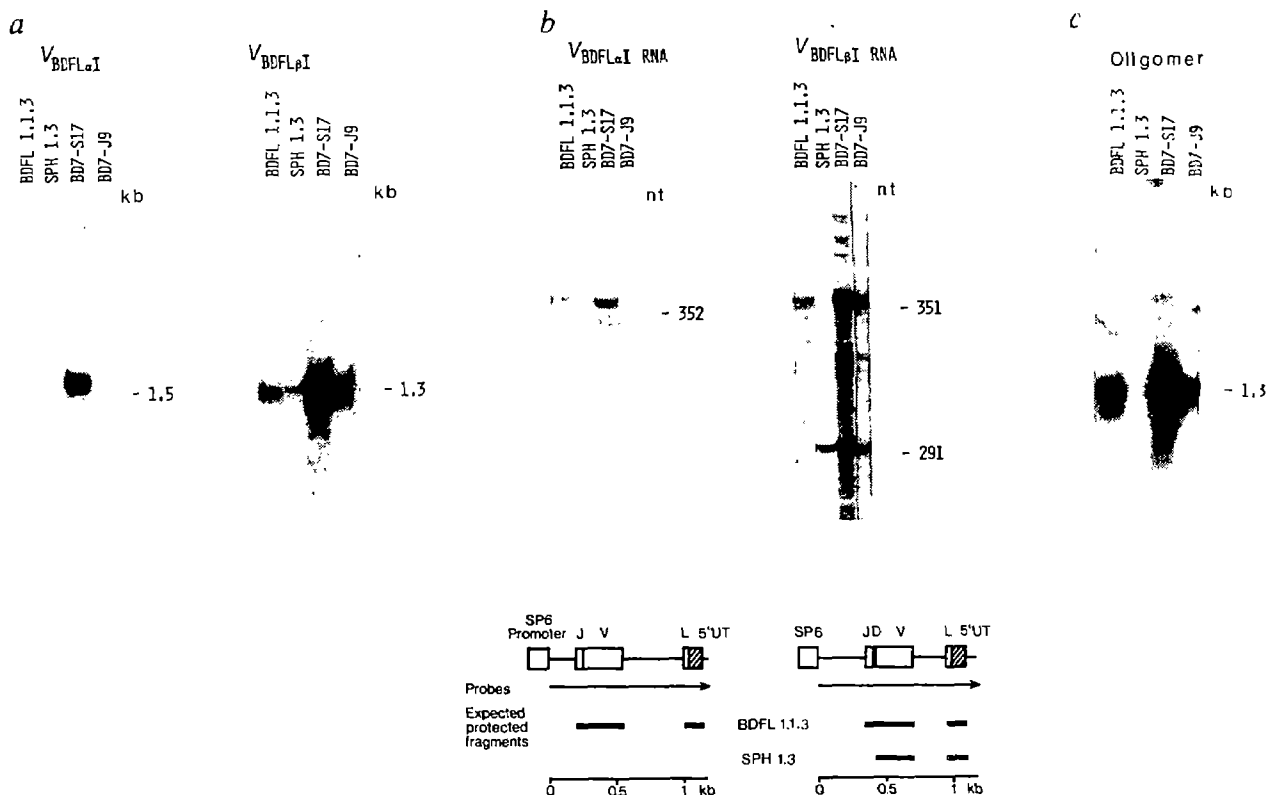


**Fig. 5** Analysis of transfectants by Northern blotting and RNase protection. **a**, Northern blot analysis. Blots were obtained and hybridized with the  $V_{BDFL\alpha I}$  and  $V_{BDFL\beta I}$  probes as described in Fig. 1 legend. **b**, RNase protection experiment. DNA fragments containing the  $\alpha I$  and  $\beta I$  V-region genes were subcloned into the pSP6 vector, labelled and hybridized with poly(A)<sup>+</sup> or total RNA isolated from the indicated T cell as described elsewhere<sup>53</sup>, using a commercially available RNA synthesis kit (Amersham). The  $V_{\alpha I}$  RNA probe was derived from the 1.2-kb insert of a deletion subclone of pV $\alpha$ -1 (see Fig. 3 legend); the  $V_{\beta I}$  RNA probe was derived from the 1.2-kb *Hind*III-*Cla*I fragment of cosmid clone BDFL5.2 (see Fig. 3 legend). The sizes of the protected RNA fragments were determined on 6% polyacrylamide/urea sequencing gels by co-migration with DNA sequence ladders. The sizes of the expected protected RNA fragments are shown in the diagram at the bottom. Open boxes indicate the SP6 promoter region as well as the exons of the  $\alpha$  and  $\beta$  genes. **c**, Northern blot analysis. Northern blots as in **a** were hybridized with a 33-nt oligonucleotide probe specific for the 3' end of the BDFL $\beta I$  V-region gene (positions 729–761 in Fig. 3). The oligomer was synthesized<sup>49</sup>, labelled with T4 polynucleotide kinase and hybridized as described elsewhere<sup>29</sup>.

Next, as target cells we used two different L-cell fibroblasts expressing high levels of either D<sup>d</sup> or K<sup>k</sup> MHC molecules (Fig. 6b). L cells expressing high levels of D<sup>d</sup> antigen (L-D<sup>d</sup>↑; 5–7-fold more than the B-cell lymphoma A20) have been obtained by gene transfection<sup>8</sup>. As L cells are derived from C3H mice, the transfected L cells also express K<sup>k</sup> antigen. L cells expressing large amounts of K<sup>k</sup> antigen (L-K<sup>k</sup>↑; about the same amount as D<sup>d</sup> and about 10-fold more K<sup>k</sup> antigen than on L-D<sup>d</sup>↑) were obtained by selection (see Fig. 6 legend). Both L-cell lines were coupled with either FL or SP and tested with the donor, recipient and transfected cytotoxic T cells.

As shown in Fig. 6b, the BDFL donor T cells lysed only FL-coupled L-D<sup>d</sup>↑ targets well and produced some background lysis on the other targets. The SPH recipient T cells lysed the SP-coupled L-K<sup>k</sup>↑ targets well and showed a low level of lysis above background on SP-coupled L-D<sup>d</sup>↑ targets. The BD7-S17 transfectants lyse both FL-coupled L-D<sup>d</sup>↑ and SP-coupled L-K<sup>k</sup>↑ targets well; they also showed a low level of cytotoxic activity on SP-coupled L-D<sup>d</sup>↑ targets, as did the recipient cells.

We believe that the lysis of SP-coupled L-D<sup>d</sup>↑ targets by the recipient and the transfected T cells results from recognition of the endogenously expressed K<sup>k</sup> antigens and SP on the target cells (the specificity of the recipient). If one subtracts the background lysis of uncoupled L-D<sup>d</sup>↑ target cells, there is about 10% specific lysis by the transfectant and 6% specific lysis by the recipient of the SP-coupled L-D<sup>d</sup>↑ target cells. As these two values are not significantly different there is no evidence for the generation of receptors with mixed specificities on the surface of the transfectant. Thus, the lysis of FL-coupled L-D<sup>d</sup>↑

targets is the only novel specificity detected for the transfectants, which is the result expected if the MHC-restricted antigen specificity of the donor cell is expressed on the transfectants. In agreement with this result, lysis of FL-coupled L-D<sup>d</sup>↑ cells by the transfectant was significantly inhibited by anti-D<sup>d</sup> antibodies (Fig. 6c).

The inability of the BD7-S17 transfectant to lyse FL-coupled B-cell blasts expressing 'normal' levels of D<sup>d</sup> can be explained by the absence of Lyt 2 molecules on the transfectant. Apparently, and in agreement with previous findings<sup>7,8</sup>, this deficiency can be compensated for by over-expression of target antigens. Transfer of the recently isolated Lyt 2 gene<sup>18</sup> into BD7-S17 should allow us to test this explanation.

The low killing efficiency of the BD7-S17 transfectant might also be explained in other ways: for example, other cell surface molecules (possibly the T-cell receptor-related  $\gamma$ -chain of the donor cell) might be important in stabilizing the interaction with target cells. Also, a low concentration of the donor-derived  $\alpha/\beta$  heterodimer on the transfectant could explain the killing inefficiency. The latter possibility can be tested by immunoprecipitation and two-dimensional gel electrophoresis to distinguish between the various  $\alpha$ - and  $\beta$ -chains.

In contrast to BD7-S17, the BD7-J9 transfectant, transcribing the BDFL  $\beta I$  but not the  $\alpha I$  gene, does not lyse FL-coupled L-cell targets expressing high levels of the D<sup>d</sup> class I molecule. Thus, it is unlikely that the  $\beta$ -chain alone can transmit specificity as tested in our system. We have not tested any transfectants expressing the BDFL $\alpha I$  chain alone. Therefore, we conclude that in our system the T-cell receptor  $\alpha$ - and  $\beta$ -chains are

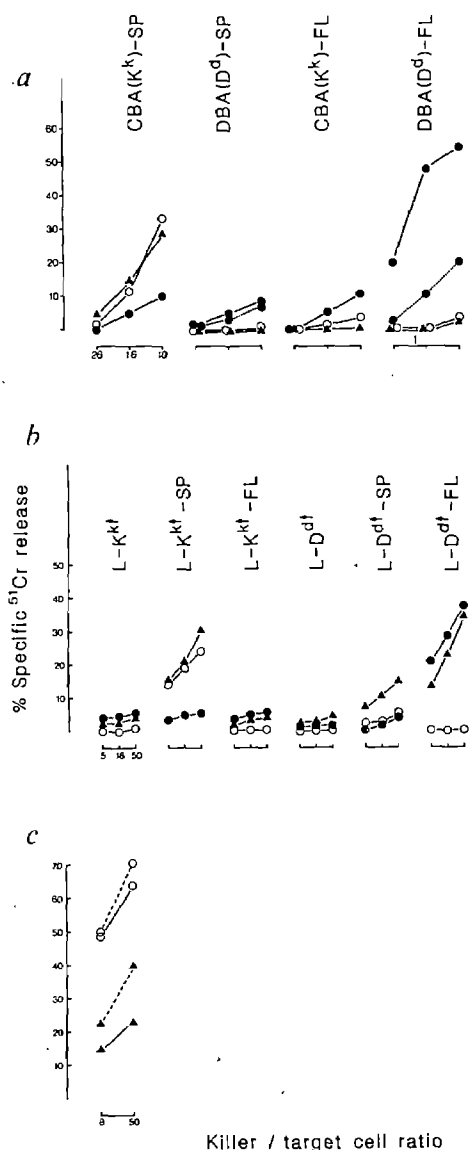


**Fig. 6** *a*, Cytolytic activity of SPH (recipient), BDFL (donor) and BD7-S17 (transfected) T cells on lipopolysaccharide (LPS)-stimulated B-cell blasts coupled with either the hapten 3-(*p*-sulphophenylidazo)-4-hydroxy-phenylacetic acid (SP) or fluorescein (FL). ●—●, BDFL 1.1.3 (FL+D<sup>d</sup>); ○—○, BDFL 1.1.3 plus anti-Lyt 2 antibodies; ○, SPH 1.3 (SP+K<sup>k</sup>); ▲—▲, BD7-S17. The target LPS blasts were labelled with <sup>51</sup>Cr and specific <sup>51</sup>Cr release was determined in a <sup>51</sup>Cr-release assay<sup>54</sup>. For inhibition with anti-Lyt 2 antibodies (53–6.72; 100 µg ml<sup>-1</sup>), cytolytic T cells were incubated with purified antibodies for 15 min before addition of target cells. *b*, Cytolytic activity of SPH (recipient, ○), BDFL (donor, ●) and BD7-S17 (transfected, ▲) cells on L-cell fibroblasts coupled with either SP or FL. L-K<sup>k</sup>↑ cells are LS5 cells (Flow Laboratories) derived from the L929 cell line; they were selected for their high expression of K<sup>k</sup> antigens. L-D<sup>d</sup>↑ cells are Ca 25.8.1 cells transfected with a D<sup>d</sup> class I MHC gene (provided by B. Malissen); this cell line expresses about one-tenth of the level of K<sup>k</sup> antigens expressed by the LS5 cells. As assessed by fluorescence-activated cell sorter analysis, the amount of K<sup>k</sup> antigens expressed by the LS5 cells is slightly higher than the amount of D<sup>d</sup> antigens expressed by the Ca 25.8.1 cells (as tested using monoclonal antibodies H0-100-5/28 (anti-K<sup>k</sup>) and 34-7-23 (anti-D<sup>d</sup>) at a concentration of 100 µg ml<sup>-1</sup>). *c*, Inhibition of cytolytic activity of BD7-S17 (transfected) T cells by preincubation of L-D<sup>d</sup>↑-FL cells with anti-D<sup>d</sup> (34-7-23) antibodies (100 µg ml<sup>-1</sup>) for 15 min before addition of the cytolytic T cells. As a control we used FLH cells whose specificity is not restricted by polymorphic MHC determinants<sup>55</sup>. ○—○, FLH; ○—○, FLH plus anti-D<sup>d</sup>; ▲—▲, BD7-S17; ▲—▲, BD7-S17 plus anti-D<sup>d</sup>.

sufficient to transfer the MHC-restricted antigen specificity to recipient cells.

### Conclusion

These results provide the first definite proof that the T-cell receptor α- and β-chain genes can transmit a functional specificity from one cytotoxic T cell to another. The ability to transfer T-cell receptor specificities by gene transfection opens up new ways of studying, by *in vitro* manipulation, the molecular interactions that enable T cells to recognize both MHC and foreign antigen, genetic elements important for T-cell receptor gene regulation and the development of the T-cell receptor repertoire during ontogeny.

We thank B. Malissen for the L-cell clone CA25.8.1; B. Bogen, F. Melchers and R. Snodgrass for helpful suggestions and constructive criticism; J. Mathur-Rochat, K. Schubiger, O. Nikkanen and R. Schulze for technical help; L. Pomeroy and H. P. Bider for artwork; and C. Brügger and J. Hossmann for preparation of the manuscript. The Basel Institute for Immunology was founded and is supported by F. Hoffmann-La Roche, Ltd.

Received 19 November 1985; accepted 31 January 1986.

- Schwartz, R. H. A. *Rev. Immun.* **3**, 237–261 (1985).
- Hannum, C., Freed, J. H., Tarr, G., Kappler, J. & Marrack, P. *Immun. Rev.* **81**, 161–176 (1984).
- Meuer, S. C., Acuto, O., Hercend, T., Schlossman, S. F. & Reinherz, E. A. *Rev. Immun.* **2**, 23–50 (1984).
- Pessano, S., Ottgen, H., Bhan, A. K. & Terhorst, C. *EMBO J.* **4**, 337–344 (1985).
- Allison, J. P. & Lanier, L. L. *Nature* **314**, 107–109 (1985).
- MacDonald, H. R., Glasebrook, A. L., Bron, C., Kelso, A. & Cerottini, J. C. *Immun. Rev.* **68**, 89–115 (1982).
- Marrack, P. *et al.* *J. exp. Med.* **158**, 1077–1091 (1983).
- Greenstein, J. L., Malissen, B. & Burakoff, S. J. *J. exp. Med.* **162**, 369–374 (1985).
- Davis, M. M. *A. Rev. Immun.* **3**, 537–560 (1985).
- Mak, T. W. & Yanagi, Y. *Immun. Rev.* **81**, 221–233 (1984).
- Robertson, M. *Nature* **317**, 768–771 (1985).
- Chien, Y., Gascoigne, N. R. J., Kavaler, J., Lee, N. E. & Davis, M. M. *Nature* **309**, 322–326 (1984).
- Gascoigne, N. R. J., Chien, Y., Becker, D. M., Kavaler, J. & Davis, M. M. *Nature* **310**, 387–391 (1984).
- Malissen, M. *et al.* *Cell* **37**, 1101–1110 (1984).
- Patten, P. *et al.* *Nature* **312**, 40–46 (1984).
- Saito, H. *et al.* *Nature* **312**, 36–40 (1984).
- Chien, Y. *et al.* *Nature* **312**, 31–35 (1984).
- Barth, R. K. *et al.* *Nature* **316**, 517–523 (1985).
- Behlik, M. A. *et al.* *Science* **239**, 566–570 (1985).
- Arden, B., Klutz, J. L., Siu, G. & Hood, L. E. *Nature* **316**, 783–787 (1985).
- Hayday, A. C. *et al.* *Nature* **316**, 828–832 (1985).
- Winoto, A., Mjolsness, S. & Hood, L. *Nature* **316**, 832–836 (1985).
- Becker, D. M. *et al.* *Nature* **317**, 430–434 (1985).
- Saito, H. *et al.* *Nature* **309**, 757–762 (1984).
- Hayday, A. C. *et al.* *Cell* **40**, 259–269 (1985).
- Heifl, J. S. *et al.* *Nature* **317**, 68–70 (1985).
- Ohashi, P. S. *et al.* *Nature* **316**, 606–609 (1985).
- Yague, J. *et al.* *Cell* **42**, 81–87 (1985).
- Dembic, Z., Bannwarth, W., Taylor, B. A. & Steinmetz, M. *Nature* **314**, 271–273 (1985).
- Snodgrass, H. R., Dembic, Z., Steinmetz, M. & von Boehmer, H. *Nature* **315**, 232–233 (1985).
- Acuto, O. *et al.* *J. exp. Med.* **161**, 1326–1343 (1985).
- Rupp, F., Acha-Orke, H., Hengartner, H., Zinkernagel, R. & Joho, R. *Nature* **315**, 425–427 (1985).
- Gillies, S. D., Folson, V. & Tonegawa, S. *Cell* **33**, 717–728 (1983).
- Picard, D. & Schaffner, W. *Nature* **307**, 80–82 (1984).
- Bergman, Y., Rice, D., Grosschedl, R. & Baltimore, D. *Proc. natn. Acad. Sci. U.S.A.* **81**, 7041–7045 (1984).
- Haas, W. & Kisielow, P. *Eur. J. Immun.* **15**, 755–760 (1985).
- Silva, A., MacDonald, H. R., Conzelmann, A., Corthésy, T. & Nabholz, M. *Immun. Rev.* **76**, 105–129 (1983).
- Zamoyska, R., Voilmer, A. C., Sizer, K. C., Liaw, C. W. & Parnes, J. R. *Cell* **43**, 153–163 (1985).
- Chirgwin, J., Przybyla, A., MacDonald, R. & Rutter, W. *Biochemistry* **18**, 5294–5299 (1979).
- Glisin, V., Crkvenjakov, R. & Byus, C. *Biochemistry* **13**, 2633–2637 (1977).
- Feinberg, A. M. & Vogelstein, B. *Analyt. Biochem.* **132**, 6–13 (1983).
- Goridis, C. *et al.* *EMBO J.* **4**, 631–635 (1985).
- Steinmetz, M. *et al.* *EMBO J.* **3**, 2995–3003 (1984).
- Steinmetz, M. *et al.* *Nature* **300**, 35–42 (1982).
- Steinmetz, M. *et al.* *EMBO J.* **1**, 1–19 (Academic, New York, 1985).
- Frischau, A. M., Garoff, H. & Lehrach, H. *Nucleic Acids Res.* **8**, 5541–5549 (1980).
- Maxam, A. M. & Gilbert, W. *Meth. Enzym.* **65**, 499–560 (1980).
- Sanger, F., Nicklen, S. & Coulson, A. R. *Proc. natn. Acad. Sci. U.S.A.* **74**, 5463–5467 (1977).
- Kiefer, H. R. & Bannwarth, W. in *Immunological Methods* Vol. 3 (eds Lefkovits, I. & Pernis, B.) 69–83 (Academic, New York, 1985).
- Grosfeld, F. G. *et al.* *Nucleic Acids Res.* **21**, 6715–6732 (1982).
- Ochi, A., Hawley, R. G., Sculman, M. J. & Hozumi, N. *Nature* **302**, 340–342 (1983).
- McCubrey, J., McKearn, J. P. & Köhler, G. *Eur. J. Immun.* **15**, 1117–1124 (1985).
- Zinn, K., D'Mario, D. & Maniatis, T. *Cell* **34**, 865–879 (1983).
- Haas, W., Mathur-Rochat, J., Pohlit, H., Nabholz, M. & von Boehmer, H. *Eur. J. Immun.* **10**, 828–834 (1980).
- Haas, W. & Kisielow, P. *Eur. J. Immun.* **15**, 751–755 (1985).

## LETTERS TO NATURE

## Very Large Array observations of rapid non-periodic variations in OJ 287

J. W. Dreher\*, D. H. Roberts† &amp; J. Lehár\*†

\* Physics Department, Massachusetts Institute of Technology, Cambridge, Massachusetts 02139, USA

† Physics Department, Brandeis University, Waltham, Massachusetts 02254, USA

Time variations in compact extragalactic objects can be used to constrain both their emission mechanisms and models for their geometry. In particular, periodic variations constrain the popular black hole model for these sources<sup>1,2</sup>. There have been many reports of the presence (and absence) of both periodic<sup>3–8</sup> and non-periodic<sup>9</sup> variability in the BL Lacertae object OJ 287 = 0851+202, from the optical and infrared through centimetre radio wavelengths (Table 1). The apparent consistency of the reported periodicity near  $P = 15.7$  min and the absence of variations in other sources observed in the same way lends some credence to these variations, even though they are only a few per cent of the mean intensity. We observed OJ 287 with the Very Large Array (VLA) at 5, 15 and 22 GHz several times in early 1983. The 5-GHz data, taken coincident with the 22-GHz observations of Valtaoja *et al.*<sup>8</sup>, show OJ 287 to have decreased in flux by about 1.8% in an irregular way over a span of about 7 h, and to have fluctuated by about 0.5% on a timescale of about 15 min. Brightness temperatures derived from causality constraints range between  $10^{16}$  and  $10^{20}$  K. Fourier spectra of the time series were analysed using a novel one-dimensional complex CLEAN algorithm to remove the effects of the data sampling. At 5 GHz there was no harmonic component to the intensity of OJ 287 which exceeded 0.1% of the mean for any period between 80 and 5,000 s. The limits at 15 and 22 GHz were 2% and 0.8%, respectively.

The 5-GHz observations were made in the standard hybrid C-D configuration of the VLA over the UT interval 1983 May 23.859 to 1983 May 24.171, using both right and left circular polarizations in a 50-MHz bandwidth centred at 4.8851 GHz. To provide an internal check on the observations and to give continuous time coverage on each object, the VLA was divided into two independent subarrays which observed OJ 287 and the calibrator 0839+187 for 6 min 20 s each in two alternating sequences 180° out of step (except for a short period during which the subarrays inadvertently became synchronized). This calibrator is a steep-spectrum, unresolved source (class P in the VLA nomenclature) which lies 3.2° away from OJ 287. The subarrays had 13 and 14 antennas, selected to occupy alternate stations of the array so that the two subarrays had nearly-identical, interlocking spatial configurations. Each subarray also

Table 1 Suggested periodicities in OJ 287

Period (min)	Previously-reported harmonic amplitude (%)					
	5 GHz	15 GHz	22 GHz	37 GHz	Optical	Ref.
42.2	—	—	—	—	2.2	6
40.5	—	—	—	—	4.0	4
39.2	—	—	—	—	0.6	3
22.8	—	—	—	—	2.8	6
15.7	—	—	0.5	0.5–5.0	D	7, 8
13.0	—	—	0.4	D	—	7, 8
12.0	—	—	—	—	0.6	6
19.0–148.0	—	—	—	—	<0.15	5
Upper limits from this work (%)						
Period (min)	5 GHz	15 GHz	22 GHz	37 GHz	Optical	Ref.
1.3–83.3	<0.1	<2.0	<0.8	—	—	—

The symbol D signifies a reported detection at an unspecified level.

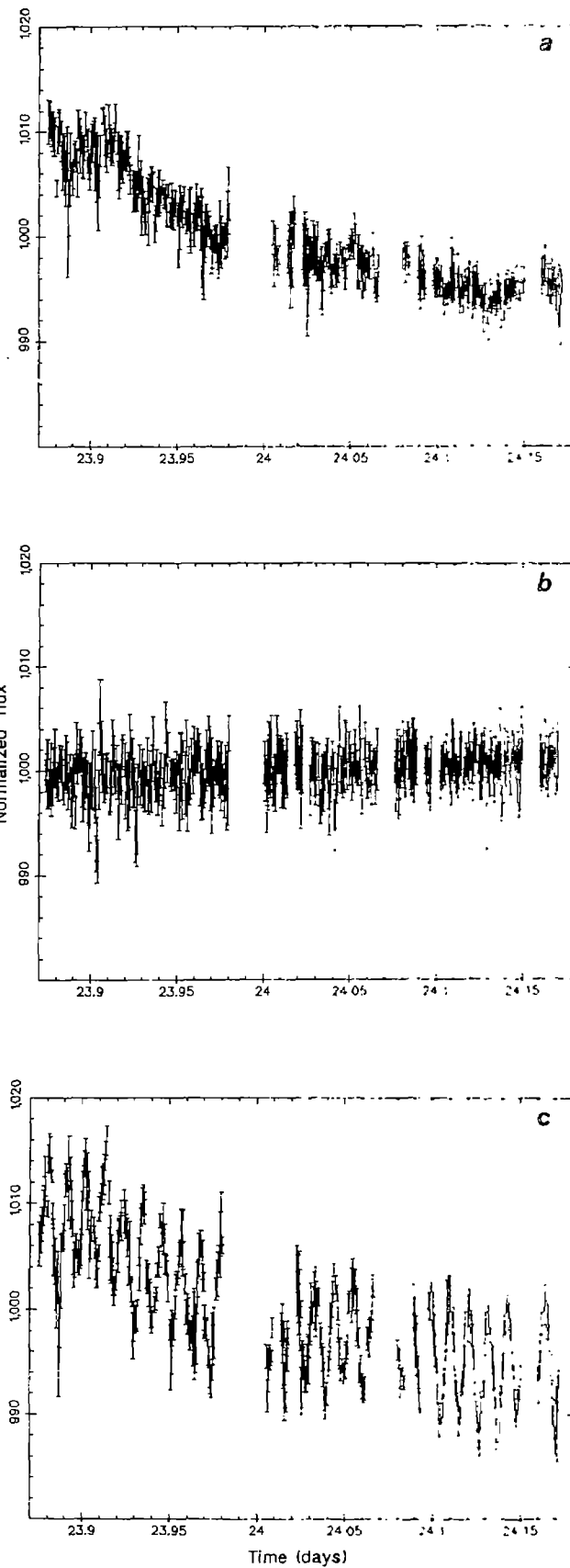


Fig. 1 Normalized flux densities of OJ 287 (a) and 0839 + 187 (b) obtained at 5 GHz by the VLA on 23–24 May 1983, combining the two subarrays and averaging the two polarizations. Artificial data consisting of an amplitude  $p = 0.5\%$  harmonic component with period 15.7 min superimposed on our actual data for OJ 287 are shown in c.

made two short observations of 3C286 (assumed flux 7.41 Jy) to determine the flux scale, and two of OJ 287 in pointing mode to check the pointing of all the antennas. The observations took place in the afternoon, with scattered clouds and winds of  $<6 \text{ m s}^{-1}$ . The phase stability on the longest spacings ( $\sim 2 \text{ km}$ ) was  $\sim 20^\circ$  r.m.s. over 6 min; shorter baselines had significantly better phases.

The visibility data for each subarray and polarization were corrected for the amplitude and phase gains of each antenna using the standard methods, as detailed below. Despite stringent standards, only a few data were edited out. By comparison with 3C286 the flux of 0839+187 was found to be 0.943 Jy, with an internal agreement among antennas of better than 1%. The average flux of OJ 287 was 4.47 Jy. The amplitude gain of each antenna as a function of time was derived on the assumption that 0839+187 had a constant flux; these scan-averaged gains were applied to observations of both 0839+187 and OJ 287 by linear extrapolation over approximately 13 min. The phase gain of each antenna as a function of time was determined by assuming that each source was unresolved and calibrating each source on itself using visibility data vector-averaged over 20 s. A gain table with 1-min intervals was used in all cases. These procedures effectively eliminate systematic pointing errors, atmospheric attenuation, instrumental gain drifts and baseline errors as possible causes of any apparent flux variations in OJ 287.

The same program that solves for the gains (ANTSOL) was then used to extract the time behaviour of OJ 287. The code assumes that the flux  $S$  of OJ 287 is a constant, and solves for the amplitude gain of each antenna  $g_i(t)$  required to adjust the visibility data to make this so. Since the visibilities were amplitude-calibrated for a nominal flux of 4.47 Jy, the resulting power gain  $g_i^2(t)$  of each antenna measures the ratio [ $S(t)/4.47 \text{ Jy}$ ]; the normalization is such that a flux of 4.47 Jy yields a power gain of 1,000. This procedure was applied to both OJ 287 and the calibrator, using 40-s vector averages of the data. Errors in the gain calibration are expected to be associated almost exclusively with the individual antennas, so the degree of internal agreement among the fluxes determined from the different antennas provides valuable information on the accuracy of the measurements.

Bad data points were removed from the time series of each source by excluding those points which deviated from 'provisional means' by more than three 'provisional standard deviations'. A provisional mean for each 40-s segment was found by averaging the 2/3 of the individual antenna data points nearest to their median, and the provisional standard deviation was computed from the 2/3 of the points nearest to it. Only 1,809 of 12,167 data points were removed for OJ 287, and 1,721 of 12,509 for 0839+187. The filtered data were re-scaled so that the overall average for each antenna was 1,000, and from these a mean flux and standard deviation of the mean were produced every 40 s for each subarray and polarization separately. Figure 1a and b shows the resulting flux histories of OJ 287 and 0839+187 obtained by combining the two subarrays and averaging the two polarizations. The breaks occur where there were interruptions in the data-taking. For comparison, artificial data consisting of a 0.5%-amplitude sinusoidal component with period 15.7 min = 943 s (similar to the variation reported at 22 GHz by Valtaoja *et al.*<sup>7</sup> for the same day) added to our actual data for OJ 287 are shown in Fig. 1c.

Errors in these fluxes can arise from numerous sources. The 40-s polarization-averaged mean fluxes for the calibrator showed r.m.s. fluctuations of 0.27% about the long-term average flux; as the thermal noise for each subarray for each 40-s mean is expected<sup>10</sup> to be  $\sim 1.1 \text{ mJy}$ , corresponding to 0.11% r.m.s. for 0839+187, there were other sources of amplitude noise. This conclusion is supported by the fact that the fractional 'noise' for OJ 287 was nearly as great as for 0839+187 despite the fact that OJ 287 is a factor of five stronger. Our estimates of various sources of error in flux determination are summarized in Table

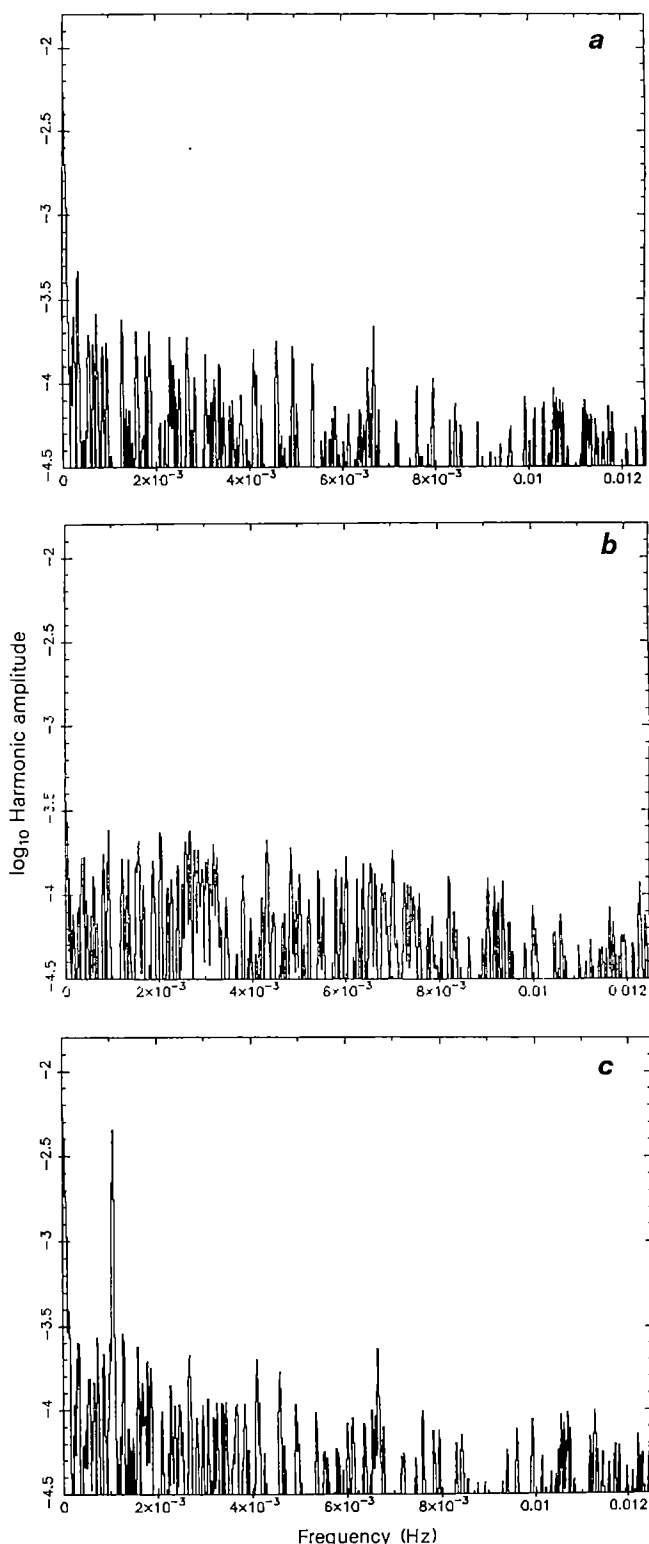
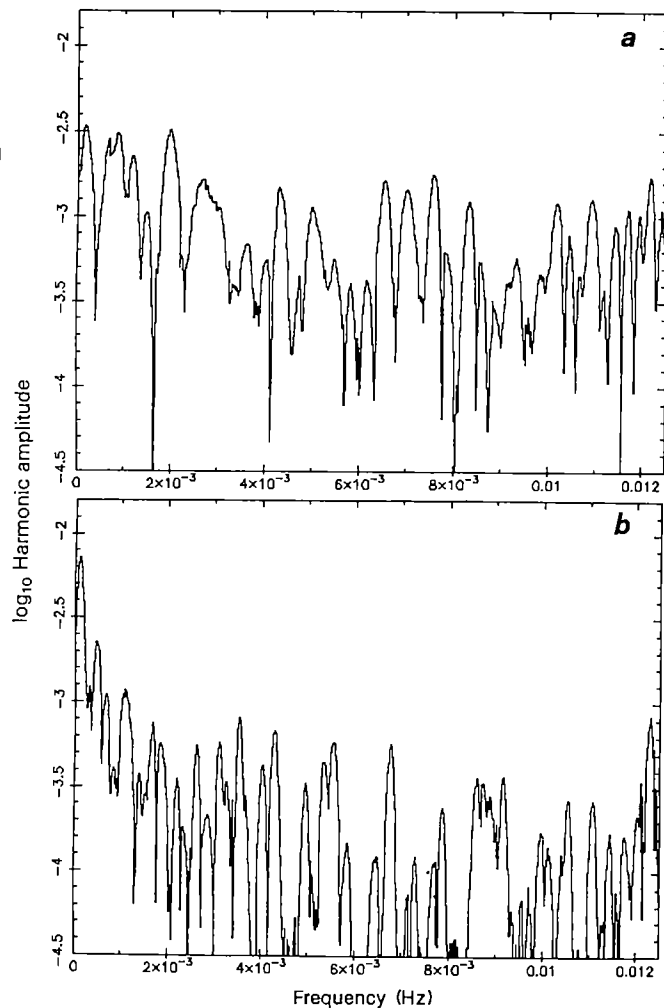


Fig. 2 Harmonic amplitudes of OJ 287 (a), 0839+187 (b), and the artificial data for OJ 287 (c), derived from the time series of Fig. 1, on a logarithmic scale. A conservative upper limit on harmonic variability of OJ 287 with periods between 80 s and 83 min is an amplitude of 0.1% of the mean.

2. The pointing observations showed an array-averaged systematic pointing error of roughly 18 arc s (root sum square of both axes), probably reflecting the well-known effect of sunlight on the antenna mounts. The pointing errors of the individual antennas varied about this mean with an r.m.s. of 23 arc s. While these



**Fig. 3** Harmonic amplitudes of OJ 287 at 15 GHz on 21 May 1983 (a) and at 22 GHz on 17 March 1983 (b) on a logarithmic scale. Conservative upper limits to harmonic variability with periods between 80 s and 83 min are amplitudes of 2% and 0.8% of the mean, respectively.

errors slightly reduce the antenna gains (typically by 0.3%), they are dominated by effects that vary over hours in time and radians on the sky; thus the resulting gain errors are almost totally removed by the calibration. We estimate that short timescale (minutes) pointing errors, which cannot be corrected, were less than 15 arc s; numerical simulations show that at a mean offset of 18 arc s from the beam axis these contribute r.m.s. amplitude fluctuations <0.18% per antenna, or 0.05% per subarray. Assuming a 1-km pathlength through a fair-weather cumulus cloud which covers an entire subarray for minutes, the resulting variations in opacity could give amplitude fluctuations as large as 0.2% per subarray<sup>11</sup>. Rapid variations of atmospheric phase can erratically reduce apparent fluxes by decorrelation of the fringes; to reduce the flux measured by one antenna by 0.1% requires a phase change of 9° over 20 s, which seems implausible for our observing conditions. ‘Closure’ errors arise from limitations in the assumption that the gains are strictly antenna-based; typical values are 1% in amplitude for each correlator. For the mean fluxes these errors should be reduced (by roughly the square root of the total number of correlators) to <0.1%. Rapidly varying errors in the antenna delays can also produce apparent amplitude fluctuations. Although not yet well understood, these variable delay errors are believed to be <0.3 ns, which, combined with constant delay offset errors of ~1 ns, could result in a reduction of <0.3% in apparent flux

**Table 2** Sources of error in VLA 5-GHz flux measurements

Source of error	Magnitude of error	
	One antenna	Subarray of 12
Thermal noise of system (2 pols, 40 s)	2.5 mJy	0.8 mJy
As fraction of 0839+187	0.27%	0.08%
As fraction of OJ 287	0.06%	0.02%
Rapidly varying pointing errors (~15'')	0.2%	0.05%
Opacity of a 1-km fair-weather cumulus cloud drifting over the whole array	0.2%	0.2%
Phase winding within 20-s visibility averaging (at 10° per min)	0.01%	0.00%
Correlator closure errors (1% in amplitude)	0.2%	0.09%
Rapidly varying delay errors of <0.3 ns	<0.3%	<0.09%
Finite resolution of VLA AGC system	<0.1%	<0.03%
ANTSOL printout accuracy	0.05%	0.01%
Maximum root sum square error		
For 0839+187	0.54%	0.26%
For OJ 287	0.47%	0.25%

per antenna and <0.09% for a subarray. Finally, errors arising from the automatic gain control (AGC) system of the VLA and from certain approximations used in our reductions add a combined error that we estimate is <0.03% for each subarray flux measurement. We conclude that the precision of an individual 40-s subarray flux measurement is limited by known random and systematic errors to ~0.3%, in good agreement with the calibrator observations.

The time series for OJ 287 showed a decline of ~1.8% over the ~7 h of data. This change corresponds to a formal timescale of  $\tau = S/|dS/dt| \leq 16$  days, a short but not atypical interval for actively variable sources. The more rapid ‘dip’ of ~0.5°, which occurred over ~15 min near  $t = 23.89$  days has  $\tau \leq 2$  days. These variations were seen in both circular polarizations of all antennas in both subarrays and appear highly significant in terms of the known errors. We feel, therefore, that these variations were real, but experience using the VLA to measure fluxes to an accuracy of <1% is as yet too limited to provide absolute certainty.

Simple causality arguments which limit the size  $R$  of a source to  $R < c\tau/(1+z)$  may be combined with the angular size distance of OJ 287 (770 Mpc for  $z = 0.306$ ,  $H_0 = 75 \text{ km s}^{-1} \text{ Mpc}^{-1}$ , and  $q_0 = 0.5$ ) to infer lower limits to the brightness temperature of  $1 \times 10^{16} \text{ K}$  for a 1.8% change in 7 h and  $6 \times 10^{17} \text{ K}$  for a 0.5% change in 15 min. If the part of the source which contributes the variable flux  $\delta S$  is physically separate from that which provides the steady flux  $S$ , the brightness temperature of the varying region is increased by a factor as large as  $(S/\delta S)$ , leading here to  $6 \times 10^{17}$  and  $1 \times 10^{20} \text{ K}$ , respectively. Such extraordinary inferred brightness temperatures would seem to require either a coherent emission mechanism, unprecedented Doppler boosting, or strong centimetre-wavelength scattering.

In order to search for periodic variations in the intensity of OJ 287, separate temporal spectra for each subarray and polarization were constructed by discrete complex Fourier transform after subtraction of the means. A fast Fourier transform was not used in order that the data need not be binned. These spectra are sensitive to harmonic fluctuations with periods between 1 data span (~7 h, corresponding to  $\sim 4.0 \times 10^{-5} \text{ Hz}$ ) and twice the sample period (80 s, corresponding to  $1.25 \times 10^{-5} \text{ Hz}$ , the Nyquist frequency). The effects of the data window (artefacts and distortion due to the sampling of the data) were removed by performing a one-dimensional complex CLEAN deconvolution analogous to the (two-dimensional) technique widely used on aperture synthesis images (refs 12, 13 and D.H.R., J.L. and J.W.D., in preparation). Since half of the power in this spectrum occurs at negative frequencies, a pure harmonic signal with amplitude a fraction  $p$  of the mean appears as a spectral ampli-

tude of  $p/2$  in the positive-frequency domain. However, for clarity we use the harmonic amplitude  $p$  in our discussion.

The harmonic amplitudes for OJ 287 and 0839+187 are shown in Fig. 2a, b; these are derived from the averages of the separate CLEANed spectra of the two polarization-averaged subarrays. The Fourier spectrum of the artificial data of Fig. 1c shows the anticipated amplitude of  $p = 0.5\%$  at the induced period of 943 s (Fig. 2c); this shows how easily we would have detected such a signal, even in the presence of the intrinsic, low-frequency, non-periodic fluctuations and the random amplitude noise. The spectrum of the calibrator has no peak above  $p = 0.039\%$ . The spectrum of OJ 287 shows no peak near the previously reported period of 943 s ( $1.06 \times 10^{-3}$  Hz). Because the noise is not gaussian, and because the detectability of a signal depends on the sampling as well as the signal-to-noise ratio, it is not possible to give a simple criterion for the smallest detectable harmonic signal. Thus we determined upper limits by processing artificial data sets with decreasing harmonic amplitudes until the signal was lost. At 5 GHz this conservative limit is 0.1% of the mean.

A significant broad component at the level  $p = 0.53\%$  is seen for OJ 287 in the lowest-frequency bins ( $4 \times 10^{-5}$ – $1.5 \times 10^{-4}$  Hz), corresponding to periods between  $\sim 2$  and  $\sim 7$  h. This reflects the power in the nonperiodic fluctuations apparent in Fig. 1a. For 0839+187, such components (if present) should have been removed by the calibration; they appear in the spectrum (Fig. 2b) at a level of only  $p = 0.04\%$ .

Due to scheduling constraints, poor weather, computer failures, and severe instrumental problems only a limited number of useful data were obtained at higher frequencies. Observations at 15 GHz in the C-D array on 21 May 1983 yielded  $\sim 5$  h of rather poor data. At 22 GHz, 2.5 h of data were obtained in the C array on 17 March 1983. The resulting power spectra are shown in Fig. 3, from which we place conservative upper limits on periodic variability of OJ 287 at 15 and 22 GHz of 2% and 0.8% respectively. With more time and better luck these figures could be substantially reduced.

Our observations lend no support to the reports of periodic variability in OJ 287. At 22 GHz our upper limit for periodicity is substantially less than the reported ‘consistent’  $\sim 2.5\%$  amplitude variation found at Metsahovi during 1981 to 1983, but remains (barely) compatible with the 0.5% amplitude found on a single day with the 140-foot telescope at the National Radio Astronomy Observatory<sup>7,8</sup>. This latter observation occurred simultaneously with our 5-GHz observations; if the periodic variation reported at 22 GHz is correct, then our upper limit implies that the spectrum of the varying component must rise remarkably steeply ( $\alpha > +1.7$  where  $S_\nu \propto \nu^\alpha$ ) between 5 and 22 GHz. Only prolonged flux monitoring of very high sensitivity and reliability can ultimately decide whether periodic variations occur in OJ 287.

This research was supported in part by NSF under grants AST82-10966 (J.W.D.) and AST83-15945 (D.H.R.). The NRAO is operated by AUI, Inc., under contract from NSF. We are grateful to Drs A. G. deBruyn and K. Sowinski for discussions and to Dr T. J. Pearson for the use of his graphics routines. Part of this work has been submitted by J.L. in partial fulfillment of the requirements for a BA degree at Brandeis University.

Received 31 October 1985; accepted 9 January 1986.

1. Abramowicz, M. A. & Nobili, L. *Nature* **300**, 506–507 (1982).
2. Elliot, J. L. & Shapiro, S. L. *Astrophys. J.* **192**, L3–L6 (1974).
3. Visvanathan, N. & Elliot, J. L. *Astrophys. J.* **179**, 721–730 (1973).
4. Frolich, A., Goldsmith, S. & Weistrop, D. *Mon. Not. R. astr. Soc.* **168**, 417–425 (1974).
5. Kiplinger, A. J. *Astrophys. J.* **191**, L109–L110 (1974).
6. Carrasco, L., Dultzin-Hacyan, D. & Cruz-Gonzalez, I. *Nature* **314**, 146–148 (1985).
7. Valtaoja, E. *et al.* *Nature* **314**, 148–149 (1985).
8. Valtaoja, E. *et al.* *Univ. Turku Rep. Ser. TURKU-FTL-R* **26** (1982).
9. Wolstencroft, R. D., Gilmore, G. & Williams, P. M. *Mon. Not. R. astr. Soc.* **201**, 479–485 (1982).
10. Napier, P. J. & Crane, P. C. *Aperture Synthesis Workshop* (eds Thompson, A. R. & D'Addario, L. R.) Ch. 3 (National Radio Astronomy Observatory, Green Bank, 1982).
11. Crane, R. K. in *Methods of Experimental Physics* Vol. 12B (ed. Mees, M. L.) 178 (Academic, New York, 1976).
12. Hogbom, J. A. *Astr. Astrophys. Suppl.* **15**, 417–426 (1974).
13. Lehár, J. thesis, Brandeis Univ. (1985).

## Are cometary nuclei primordial rubble piles?

Paul R. Weissman

Earth and Space Science Division, Jet Propulsion Laboratory, Pasadena, California 91109, and Institute for Advanced Study, School of Natural Sciences, Princeton, New Jersey 08540, USA

Whipple's<sup>1</sup> icy conglomerate model for the cometary nucleus has had considerable success in explaining a variety of cometary phenomena such as gas production rates and nongravitational forces. However, as discussed here, both observational evidence and theoretical considerations suggest that the cometary nucleus may not be a well-consolidated single body, but may instead be a loosely bound agglomeration of smaller fragments, weakly bonded and subject to occasional or even frequent disruptive events. The proposed model is analogous to the ‘rubble pile’ model suggested for the larger main-belt asteroids<sup>2</sup>, although the larger cometary fragments are expected to be primordial condensations rather than collisionally derived debris as in the asteroid case. The concept of cometary nuclei as primordial rubble piles is proposed as a modification of the basic Whipple model, not as a replacement for it.

The growing recognition of the importance of comets in understanding the origin of the Solar System has resulted in far more intensive study and observation of them in recent years. Observations made at greater heliocentric distances, at higher resolutions and with new techniques have occasionally produced results which cannot be easily explained with the conventional icy conglomerate or ‘dirty snowball’ model. Although Whipple did not specifically address the subject of the large-scale structure of the cometary nucleus, a single, well-consolidated body was clearly implied. It is worthwhile to ask how the Whipple model could be modified in order to explain these new and different phenomena.

Radar observations of comet IRAS-Araki-Alcock (IAA)<sup>3</sup> indicated that the nucleus was “very rough on a scale larger than the radar wavelength” (3.5 and 12.9 cm), that there was a substantial departure from sphericity, and that 25% of the radar cross-section came from a slowly expanding fan of debris around the nucleus. This last observation, in particular, suggests large particles (dimensions greater than the radar wavelength) breaking free of the nucleus, despite the fact that such large particles are expected to be too heavy to be lifted off the nucleus surface by the low activity observed in IAA. The radar observations also showed evidence of ‘radar-bright’ features on the surface of the rotating nucleus, which might be interpreted as facets on a highly irregular surface topography.

Additional observations give evidence for substantial, slow-moving debris clouds associated with cometary nuclei. Comet Bowell at large heliocentric distance showed a nearly constant coma with expansion velocity  $< 1 \text{ m s}^{-1}$ , and an absence of sub-millimetre particles<sup>4,5</sup>. IRAS (Infrared Astronomy Satellite) images have revealed dense meteoroid streams in the orbits of some short-period comets<sup>6</sup>, an unexpected result because meteoroid streams were presumed to be too dispersed to be detectable with IRAS. Observations of disturbances in the solar wind from the Pioneer Venus spacecraft have been correlated with possible outgassing from a debris stream in the orbit of asteroid 2201 Oljato<sup>7</sup>, an Apollo asteroid which is a likely candidate for an extinct cometary nucleus.

Whipple<sup>8</sup> has suggested that a pair of outbursts in comet P/Holmes may be the result of a grazing collision followed by impact of an orbiting nucleus satellite. Doublet or multiple craters on planetary surfaces<sup>9</sup> may be the result of cometary nuclei which disintegrated at the planet's Roche limit, or were already discrete ‘swarms’ of particles (or satellites) before they

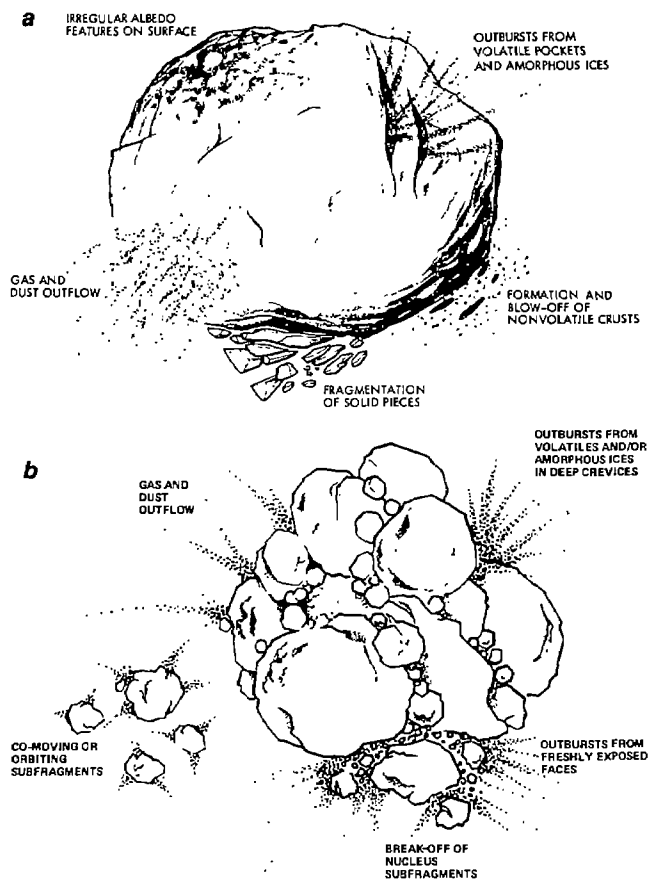


**Fig. 1** *a*, Conceptual illustration of the conventional (icy-conglomerate) cometary nucleus model showing a single, well-consolidated nucleus and some sublimation-related processes which may be acting on the nucleus surface. *b*, Conceptual illustration of the rubble-pile model showing a nucleus made up of many smaller fragments, weakly bonded by local melting at contact interfaces, and perhaps surrounded by orbiting debris. A range of surface processes somewhat different from those shown in *a* nonetheless lead to similar observed phenomena from the comet.

came within the planet's sphere of influence<sup>10</sup>. de Pater *et al.*<sup>11</sup> found evidence for 'clumpy' OH emission in the coma of comet Halley, possibly indicative of multiple sublimation sources.

These observations all suggest the existence of large fragments broken off the cometary nucleus, too large to be rapidly swept into different orbits by radiation pressure or Poynting-Robertson effects. The former process affects micrometre-size dust particles, the latter centimetre-size particles. Thus, the fragments appear to have dimensions ranging from tens of centimetres to perhaps hundreds of metres, and are either orbiting or co-moving with the cometary nuclei.

The very weak gravity fields of cometary nuclei, with an escape velocity of the order of  $2.2 \text{ m s}^{-1}$  for a 3-km-radius nucleus like that of Halley, are not expected to be able to retain large fragments in near-nucleus orbits. Differential Keplerian motion should slowly disperse unbound large particles into different solar orbits. On the other hand, the large particles may behave according to the 'fluidized bed' model of Brin<sup>12</sup>, being briefly levitated off the nucleus by outbursts or spin-induced fragmentation, before settling back slowly in the very weak gravity field. The larger particles might even 'bounce' several times before coming to rest on the nucleus, perhaps mimicking the behaviour of the nucleus satellite suggested for P/Holmes.

Figure 1*a* is a conceptual illustration of an icy-conglomerate cometary nucleus<sup>13</sup>, showing some sublimation-related processes which may be acting on the nucleus surface. The nucleus

is envisaged as a well-consolidated, irregularly shaped, heterogeneous mixture of ice and dust, rotating about some rapidly precessing axis as it loses material through a variety of surface processes. Figure 1*b* is a similar conceptual illustration of the icy-conglomerate rubble-pile model proposed here. Although many of the proposed surface processes are the same as in Fig. 1*a*, some of the others vary somewhat in detail; nevertheless, they will produce similar observed phenomena, and will perhaps aid in explaining some of the anomalous observations described above.

One of the strongest arguments for the rubble-pile model comes from observations of cometary disruption events; that is, comet splitting. Observed statistics show that  $\sim 10\%$  of dynamically new comets from the Oort cloud split on their first return, compared with  $\sim 4\%$  of all long-period comets, and only about  $1\%$  of short-period comets<sup>14</sup>. The disruption events appear to occur randomly with respect to time of perihelion, heliocentric distance and distance from the ecliptic plane. It appears that disruption is associated with some intrinsic instability within the nucleus, so that comets which are likely to split do so rather rapidly, while those disinclined to split are able to survive for many returns, as is necessary if they are to evolve dynamically to short-period orbits.

Observations of splitting events shows that they typically involve small fragments (compared with the total nucleus dimensions) breaking off from the main nucleus, and that multiple fragments are occasionally produced<sup>15</sup>. Comet West in 1976 was one of the best examples of this, ejecting three subfragments near perihelion, two of which persisted for 5 months or more. The separation velocities of the fragments are typically very small, on the order of  $1 \text{ m s}^{-1}$  or less, and outbursts are frequently associated with the splitting event.

It seems logical that disruption events may result from the breaking-free of weakly bonded fragments from the nucleus as the comet approaches the Sun and the thermal wave penetrates to volatile ices at fragment interfaces. Depending on the exact nature of the nucleus, its composition and its past thermal evolution, the solar energy may penetrate either rapidly or slowly, resulting in largely random observed times for disruption events relative to perihelion.

Also, the changing moments of inertia of the nucleus as material is lost asymmetrically from its surface will result in rapid precession of the rotation axis, centrifugally stressing fragment bonds that may not have been stressed on an earlier apparition, or even earlier in the same perihelion passage.

Is the primordial rubble-pile model consistent with the generally accepted picture of cometary origin? Comets are believed to have formed as icy planetesimals in the outer planetary region<sup>16,17</sup>, certainly in the Uranus-Neptune zone<sup>18</sup>, and probably also in an extended solar accretion disk extending out to hundreds of AU or more<sup>19</sup>. Greenberg *et al.* have recently reviewed the topic<sup>20</sup>.

In the basic model, icy grains settle to the equatorial plane of the protosolar nebula. Larger grains settle more rapidly and grow as they settle, reaching sizes of up to tens of metres<sup>21</sup> by the time they arrive at the central plane. Some additional growth may occur before the density of material in the plane becomes high enough to result in gravitational instabilities<sup>22</sup>, which force the disk to disintegrate into many bodies with typical dimensions of 1–10 km.

Some authors have suggested that comets formed at larger solar distances, in subfragments of the protosolar nebula or perhaps even pre-solar interstellar clouds<sup>23,24</sup>. Although the low densities in interstellar clouds would seem to preclude this idea, what follows would be just as true for those models as for the nebula-accretion-disk hypothesis described above.

The accretion and collapse occur at low velocity, as no large bodies have yet grown in the accretion disk to stir up the velocities of the nebular condensates and/or planetesimals. The total gravitational potential energy for assembling a 3-km-radius

comet from infinity is  $1.5 \times 10^4$  erg g<sup>-1</sup>, not enough to raise the mean temperature of the nucleus by 0.01 K.

Low-velocity collisions between fragments are likely to result in some local crushing and melting at the contact surfaces, helping to form a bond at these points, but are unlikely to destroy the individual structure of the fragments. The resulting nucleus would have substantial voids between fragments, and would preserve the great range of fragment sizes.

Storage at large solar distance in the Oort cloud<sup>25</sup>, the lack of substantial internal heat sources<sup>26</sup>, and the very weak cometary gravity field would probably result in little change in this nucleus structure over the history of the Solar System. The comet would be too cold and too small for any substantial mass migration.

In many ways the proposed model reflects on a macroscopic scale the proposed microscopic model of Daniels and Hughes<sup>27</sup>, in which the nucleus is a heterogeneous aggregate of ice and dust grains with substantial voids. That model has also been scaled up<sup>28</sup> to give an aggregate model for cometary nuclei very similar to the rubble-pile model proposed here. There is also some similarity with an earlier comet model by O'Dell<sup>29</sup>, although he emphasized the possibility that comets might be gravitationally bound collections of nonvolatile cores with volatile coatings acquired at large solar distance. The view expressed here is that comets are agglomerations of smaller icy-conglomerate bodies, weakly bound by local melting at contact surfaces.

The question arises as to whether the spacecraft flybys of comet Halley in March 1986 will be able to discriminate between the conventional nucleus model and the rubble-pile model proposed here. Even with high-resolution imaging, the rubble-pile nature of the nucleus may be hidden by the collection of cometary debris near contact interfaces, hiding the true nucleus structure.

The resolution of the narrow-angle cameras of the spacecraft Vega 1 and 2 at 10<sup>4</sup> km distance is expected to be 400 m per line pair, able to discriminate only the gross structure of the nucleus. It is likely that the Halley nucleus may still appear rough at this scale, but individual nucleus fragments with typical dimensions of tens of metres could not be resolved. (The option to send Vega 2 to a closer flyby distance may make resolution of large fragments possible.)

On the other hand, the Giotto spacecraft is targeted for a 500-km flyby with an expected camera resolution of 10 m. This certainly might be able to discriminate individual subfragments of the Halley nucleus. But if Halley is actively ejecting subfragments of metre or even centimetre size, in greater quantity than would be expected from extrapolating our knowledge of micrometre-size particles to the centimetre or greater size range, then it is unlikely that Giotto will survive to reach its minimum approach distance.

I thank Richard Greenberg for useful discussions, David Hughes for many helpful comments, and Piet Hut and John Bahcall of the Institute for Advanced Study for support as a Visiting Member. This work was also supported by the NASA Planetary Geology and Geophysics Program and was done, in part, at the Jet Propulsion Laboratory under contract with NASA.

Received 9 December 1985; accepted 25 February 1986.

1. Whipple, F. L. *Astrophys. J.* **111**, 375–394 (1951); **113**, 464–474 (1950).
2. Davis, D. R., Chapman, C. R., Weidenschilling, S. J. & Greenberg, R. *Icarus* **62**, 30–53 (1985).
3. Goldstein, R. M., Jurgens, R. F. & Sekanina, Z. *Astr. J.* **89**, 1745–1754 (1984).
4. Jewitt, D. *Icarus* **60**, 373–385 (1984).
5. Sekanina, Z. *Astr. J.* **87**, 161–169 (1982).
6. Sykes, M. V., Greenberg, R., Hunten, D. M. & Low, F. J. *Bull. Am. astr. Soc.* **17**, 704 (1985).
7. Araghvani, M. R., Russell, C. T. & Luhmann, J. G. *Adv. Space Res.* **4**, 255–259 (1984).
8. Whipple, F. L. *Icarus* **60**, 522–531 (1984).
9. Oberbeck, V. R. & Aoyagi, M. *J. geophys. Res.* **77**, 2419–2432 (1972).
10. Hut, P. & Weissman, P. R. *Bull. Am. astr. Soc.* **17**, 690 (1985).
11. de Pater, I., Palmer, P. & Schenewerk, M. *IAU Circ.* No. 4142 (1985).
12. Brin, G. D. *Astrophys. J.* **237**, 265–279 (1980).

13. Weissman, P. R. & Kieffer, H. H. *Icarus* **47**, 302–311 (1981).
14. Weissman, P. R. *Astr. Astrophys.* **85**, 191–196 (1980).
15. Sekanina, Z. in *Comets* (ed. Wilkening, L. L.) 251–287 (University of Arizona Press, 1982).
16. Cameron, A. G. W. *Icarus* **1**, 13–69 (1962).
17. Safronov, V. S. *Evolution of the Protoplanetary Cloud and Formation of the Earth and the Planets* (Nauka, Moscow, 1969).
18. Fernandez, J. A. & Ip, W.-H. *Icarus* **47**, 470–479 (1981).
19. Cameron, A. G. W. in *The Origin of the Solar System* (ed. Dermott, S. F.) 49–75 (Wiley, New York, 1978).
20. Greenberg, R., Weidenschilling, S. J., Chapman, C. R. & Davis, D. R. *Icarus* **59**, 87–113 (1984).
21. Weidenschilling, S. J. *Icarus* **44**, 172–189 (1980).
22. Goldreich, P. & Ward, W. R. *Astrophys. J.* **183**, 1051–1061 (1973).
23. Cameron, A. G. W. *Icarus* **18**, 407–450 (1973).
24. Donn, B. & Hughes, D. W. *Bull. Am. astr. Soc.* **17**, 689 (1985).
25. Oort, J. H. *Bull. astr. Insts. Neth.* **11**, 91–110 (1950).
26. Lewis, J. *Icarus* **15**, 174–185 (1971).
27. Daniels, P. A. & Hughes, D. W. *Mon. Not. R. astr. Soc.* **195**, 1001–1009 (1981).
28. Donn, B., Daniels, P. A. & Hughes, D. W. *Bull. Am. astr. Soc.* **17**, 520 (1985).
29. O'Dell, C. R. *Icarus* **19**, 137–146 (1975).

## Deuterium in the outer Solar System: evidence for two distinct reservoirs

T. Owen\*, B. L. Lutz† & C. de Bergh‡

\* Department of Earth and Space Sciences, State University of New York at Stony Brook, Stony Brook, New York 11794, USA

† Planetary Research Center, Lowell Observatory, Mars Hill Road, 1400 West, Flagstaff, Arizona 86001, USA

‡ Laboratoire d'Astronomie Infrarouge, Observatoire de Paris, Section de Meudon, 92195 Meudon Principal Cedex, France

We have just completed a series of determinations of the CH<sub>3</sub>D/CH<sub>4</sub> ratio in the atmospheres of Saturn<sup>1,2</sup>, Titan<sup>3,4</sup> and Uranus<sup>1,3</sup>. These results, coupled with the work of other investigators, suggest that the Solar System contains at least two distinctly different primordial reservoirs of deuterium: that contained in gaseous hydrogen and that contained in the volatiles which have been maintained at low temperatures or isolated from hydrogen; for example, trapped in cold, solid material. Both of these reservoirs were established before the formation of the Solar System.

Figure 1 summarizes the D/H ratios observed in the methane component of the atmospheres of each of the outer planets and Titan. The values shown are derived from measurements of the CH<sub>3</sub>D/CH<sub>4</sub> ratio according to stoichiometry: D/H = 1/4[CH<sub>3</sub>D/CH<sub>4</sub>]. All of our work used the 3ν<sub>2</sub> overtone band near 1.6 μm observed with the Fourier transform spectrometer on the 4-m telescope at Kitt Peak National Observatory<sup>1–5</sup>. We have supplemented our results with the average equivalent value of D/H in methane for Jupiter derived from ground-based (D/H = (3.6 ± 0.6) × 10<sup>-5</sup>) (refs 6, 7) and Voyager (D/H = (3.7 ± 1.8) × 10<sup>-5</sup>) (refs 8, 9) observations of the ν<sub>2</sub> and ν<sub>6</sub> fundamental vibration bands of CH<sub>3</sub>D in the 5- and 10-μm windows, respectively. The value of D/H in methane for Saturn is the mean of our determination (D/H = (1.7<sup>+1.7</sup><sub>-0.8</sub>) × 10<sup>-5</sup>) and that derived from analysis of the Voyager spectra (D/H = (2.2<sup>+1.8</sup><sub>-1.7</sub>) × 10<sup>-5</sup> at 8.6 μm (ref. 10)). This good agreement between the ground-based and spacecraft observations and the excellent internal consistency among the results obtained by different observers using different bands, both in emission and absorption, adds to our confidence in the D/H values displayed in Fig. 1. The error bars shown there are our best estimate of the maximum ranges associated with each value and correspond to between ±2 and ±3 standard deviations (s.d.).

The largest reservoir of deuterium in the Solar System consists of the deuterium in gaseous hydrogen that has been preserved in an unaltered state since the formation of the solar system. The value of D/H in this reservoir should be close to 2 × 10<sup>-5</sup>, the value deduced for the primordial solar nebula from studies of <sup>3</sup>He in meteorites and the solar wind<sup>11–14</sup>. This is indeed the value deduced from the average of the measurements of D/H

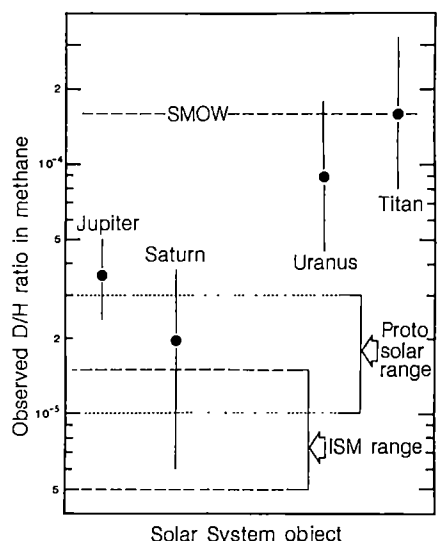
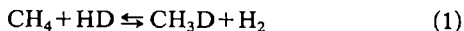


**Fig. 1** Stoichiometric D/H ratios in the methane component of the atmospheres of Jupiter, Saturn, Uranus and Titan ( $D/H = 1/4 [CH_3D/CH_4]$ ). The values for Uranus and Titan are taken from our analysis of  $CH_3D$  in their spectra at  $1.6 \mu m$  (refs 1, 3, 4); Saturn's value is a mean of our value<sup>1,2</sup> and that derived from the Voyager observations<sup>10</sup>; Jupiter's value is a mean of ground-based<sup>6,7</sup> and Voyager<sup>8,9</sup> results. See text for a discussion of the fractionation factor needed to relate these values to equilibrium D/H in the hydrogen component. For comparison, the value for Standard Mean Ocean Water (SMOW) is presented along with recent estimates for the interstellar medium<sup>21</sup> (ISM), and the primitive solar nebula<sup>11-14</sup> (Protosolar).

in methane in the atmospheres of Jupiter and Saturn, where it is mixed with a nearly cosmic abundance of warm hydrogen gas.

To measure this value directly, a small correction must first be applied to the D/H ratio given in Fig. 1, to account for deuterium fractionation between the hydrogen and methane. Fractionation leads to a slight enrichment of deuterium in methane over that in the hydrogen reservoir according to a series of exchange reactions summarized by:



Beer and Taylor<sup>15</sup> considered this problem in detail for Jupiter and found that the internal temperatures and rates of convection are high enough to support equilibrium in this exchange sequence. They estimated that the D/H ratio in methane should be enhanced relative to that in hydrogen by a factor of 1.37 (ref. 15). Homologous arguments lead to a similar result for Saturn. Application of this correction factor to the mean D/H ratio in methane on Jupiter and Saturn,  $3.0 \times 10^{-5}$ , yields a D/H ratio in gaseous hydrogen of  $2.2 \times 10^{-5}$ , in excellent accord with the  $^3He$  results.

Current estimates of the present-day abundances of  $H_2$  and HD in the Jupiter and Saturn atmospheres<sup>17-19</sup> are not consistent with this fractionation picture. The published D/H ratios are near  $5 \times 10^{-5}$ , and recent work suggests that these numbers should be closer to  $10^{-4}$  (W. H. Smith, personal communication). Possible causes for the discrepancy may include the underestimation of the effects of scattering processes which affect the very weak ( $< 1$  mA) lines of HD and the presence of very weak methane absorption in the same spectral region. We favour the value for D/H in the hydrogen component of these atmospheres that is deduced from measurements of  $CH_3D$ , as this value is in good agreement with the primordial D/H ratio estimated from  $^3He$  and thus provides a more consistent picture of the reservoir of deuterium in the protosolar gaseous hydrogen. A protosolar value of D/H near  $10^{-4}$  also seems to be incompatible with standard models of galactic evolution that must convert this ratio to the present local interstellar medium value of  $(1 \pm 0.5) \times 10^{-5}$  in  $4.55 \times 10^9$  yr<sup>20,21</sup>.

The second, much smaller reservoir of deuterium consists of deuterium in volatiles that were trapped in or frozen onto the cold, solid materials in the protosolar nebula, without ever reaching temperatures above 450 K. This temperature is the lower limit required for the reactions represented by equation (1) to reach equilibrium in  $4.55 \times 10^9$  yr. This reservoir is represented in the outer Solar System by unequilibrated gases derived from these solids. The methane in the atmosphere of Titan provides a good example. Our value of D/H in methane for Titan,  $D/H = (1.65^{+1.65}_{-0.8}) \times 10^{-4}$ , is in good agreement with the revised value of  $\sim 2 \times 10^{-4}$  obtained by Kim and Caldwell (ref. 22 and personal communication) from an analysis of the  $8.6-\mu m$   $CH_3D$  band in Voyager spectra. (The revision is required by corrections to the temperature-pressure profile of Titan's atmosphere and new broadening coefficients for the  $\nu_6$  band of  $CH_3D$ .) The difference between D/H in methane on Titan and on Jupiter appears to be significant at the level of 2-3 s.d. The Titan value is similar to that found in the terrestrial oceans (Fig. 1) and in the hydrogen-containing compounds in meteorites<sup>11</sup>.

A thorough analysis of the possible processes that could enhance the D/H ratio in methane on Titan subsequent to the satellite's formation<sup>23</sup> suggests to us that the observed deuterium enrichment predates Titan's origin. In this analysis, Pinto *et al.* found the maximum enrichment factor to lie between 1.7 and 4.4. The high values depend on isotope exchange between methane and hydrogen promoted by a hypothetical catalysis which requires metallic grains in the proto-Saturnian nebula at a temperature near 500 K. In the absence of this unlikely process (neither the high temperatures nor the bare metallic grains are very probable in this environment), the maximum enrichment is 2.2, caused primarily by dissociation of methane and escape of hydrogen from Titan<sup>23</sup>. It thus appears that the enhancement of Titan's D/H ratio by a factor of  $8^{+8}_{-4}$  relative to the primordial, solar-nebula value is significantly larger than can be expected from processes acting during or after formation of the satellite.

The upper limit of 1% on the neon abundance in Titan's atmosphere set by the Voyager observations<sup>24</sup> indicates that the atmosphere is secondary, not captured<sup>25</sup>. Consequently, the deuterium-enriched methane must have been outgassed from the solids, primarily the ices, in the satellite's interior. Thus, within a factor of  $\sim 2$ , the D/H ratio in Titan's methane must correspond to the D/H ratio in the cold methane gas and methane already trapped in solid materials in the protosolar nebula from which the satellite accreted. It represents a reservoir of primordial deuterium that is distinctly different from the reservoir characterized by the methane in the atmospheres of Jupiter and Saturn. The methane on these giant planets has equilibrated with warm atmospheric hydrogen after the formation of these bodies, but evidently this equilibration never occurred during the formation of Titan. We suggest that the high enrichment found in Titan's methane was caused by ion-molecule reactions in the interstellar medium before the formation of the solar system. Such reactions proceed rapidly even at low temperatures and are known to produce even higher enrichments in some molecules<sup>26,27</sup>.

This second reservoir of deuterium may also exist in the cores of all the outer planets, which similarly formed out of the rock-ice component of the protosolar nebula. Additional evidence for it may be found in the atmospheres of Uranus and Neptune, where, in contrast to Jupiter and Saturn, the outgassed deuterium-enriched methane would not be so diluted by fractionation equilibrium with the hydrogen envelope<sup>28</sup>. The value of D/H in methane,  $D/H = 9^{+9}_{-4.5} \times 10^{-5}$ , derived for the atmosphere of Uranus, is a factor of  $4.5^{+4.5}_{-2.3}$  higher than the nominal D/H ratio ascribed to the gaseous hydrogen reservoir, and the only plausible process which can explain this enhancement is the outgassing of methane from a deuterium-enriched rock-ice core. Within the uncertainties we cannot distinguish this value from that found on Titan, although our preferred values suggest that enhancement of the D/H ratio in methane may be slightly

less on Uranus. This would indeed be expected in the absence of comparable hydrogen escape, or from partial dilution through exchange with atmospheric hydrogen.

As was true for Jupiter and Saturn, the existing observations of the HD/H<sub>2</sub> ratio in the uranian atmosphere<sup>17–19,29</sup> are too uncertain to provide an independent evaluation of D/H in the atmospheric hydrogen. It seems unlikely, however, that fractionation equilibrium (equation (1)) could have produced a measurable increase in the D/H ratio in the atmospheric hydrogen of Uranus compared with the primordial hydrogen reservoir, because the methane mixing ratio is only 0.01–0.1 (ref. 30). But a substantial enrichment of deuterium in the hydrogen component would result if much of the hydrogen itself is actually secondary, coming from the dissociation of methane. In this case the atmosphere would be deficient in helium, but might be enriched in N<sub>2</sub>. The Voyager 2 encounter in January 1986 should test these latter consequences.

In either case, the enhancement of the D/H ratio in the atmospheric methane on Uranus is independent evidence of a second reservoir of deuterium in the protosolar nebula, which is distinct from the gaseous hydrogen reservoir and enriched by a factor of ~10. It also supports core-accretion models for outer planet formation. In their comprehensive review of deuterium enrichment in the Solar System, Geiss and Reeves<sup>13</sup> found that the available evidence was inadequate to determine whether the observed enrichments occurred before or after Solar System formation. Our new data strongly support enrichment in the interstellar medium before formation of the solar nebula. A further test of this conclusion will come from the observation of deuterium in comets. Based on the scenario outlined here, we predict D/H ratios near 10<sup>-4</sup> in the major hydrogen-bearing volatiles subliming from a cometary nucleus, values that are

2.5 × 10<sup>-2</sup> lower than the current upper limit reported by A'Hearn *et al.*<sup>31</sup> for OD/OH. Observations of comet Halley now underway both from the ground and from spacecraft may provide this test.

We thank Drs Yuk Yung and Hubert Reeves for discussions. This research was partially supported by NASA grants NSG 7499 and NGR 33015141.

Received 3 September 1985; accepted 15 January 1986.

1. de Bergh, C., Lutz, B. L., Owen, T., Brault, J. & Chauville, J. *Astrophys. J.* (in the press).
2. de Bergh, C., Lutz, B. L., Owen, T. & Chauville, J. *Astrophys. J.* (in the press).
3. Lutz, B. L., de Bergh, C., Maillard, J. P., Owen, T. & Brault, J. *Astrophys. J. Lett.* **248**, L141–L145 (1981).
4. de Bergh, C., Lutz, B. L., Owen, T. & Chauville, J. *Astrophys. J.* (submitted).
5. Lutz, B. L., de Bergh, C. & Maillard, J. P. *Astrophys. J.* **273**, 397–409 (1983).
6. Knacke, R. F., Kim, S. J., Ridgway, S. T. & Tokunaga, A. T. *Astrophys. J.* **262**, 388–395 (1982).
7. Bjoraker, G. L. thesis, Univ. Arizona (Tucson) (1985).
8. Kunde, V. G. *et al. Astrophys. J.* **263**, 443–467 (1982).
9. Drossart, P. *et al. Icarus* **49**, 416 (1982).
10. Courtin, R., Gautier, D., Marten, A. & Beuzard, B. *Astrophys. J.* **287**, 899–916 (1984).
11. Geiss, J. & Reeves, H. *Astr. Astrophys.* **18**, 126–132 (1972).
12. Black, D. C. *Geochim. cosmochim. Acta* **36**, 347–375 (1972).
13. Geiss, J. & Boschler, P. *4th Solar Wind Conf. Burghausen* (1979).
14. Geiss, J. & Reeves, H. *Astr. Astrophys.* **93**, 189–199 (1981).
15. Beer, R. & Taylor, F. W. *Astrophys. J.* **179**, 309–327 (1973).
16. Beer, R. & Taylor, F. W. *Astrophys. J.* **219**, 763–767 (1987).
17. McKellar, A. R. W., Goetz, W. & Ramsay, D. A. *Astrophys. J.* **207**, 663–670 (1976).
18. Macy, W. Jr. & Macy, W. Jr. & Smith, W. H. *Astrophys. J. Lett.* **222**, L73–L75 (1978).
19. Cochran, W. D. & Smith, W. H. *Astrophys. J.* **271**, 859–864 (1983).
20. Gautier, D. & Owen, T. *Nature* **302**, 215–218 (1983).
21. Vodar-Madjar, A. *et al. Astr. Astrophys.* **120**, 58–62 (1983).
22. Kim, S. J. and Caldwell, J. *Icarus* **52**, 473–489 (1982).
23. Pinto, J. P., Lunine, J. I., Kim, S. J. & Yung, Y. L. *Nature* (submitted).
24. Broadfoot, A. L. *et al. Science* **212**, 206–211 (1981).
25. Owen, T. J. *Planet. Sci.* **30**, 833–838 (1982).
26. Solomon, P. M. & Wolff, N. J. *Astrophys. J.* **180**, L89–92 (1973).
27. Watson, W. D. *Rev. mod. Phys.* **48**, 513 (1976).
28. Hubbard, W. B. & MacFarlane, J. J. *Icarus* **44**, 676–682 (1980).
29. Trafton, L. & Ramsay, D. A. *Icarus* **41**, 423–429 (1980).
30. Wallace, L. *Icarus* **43**, 231–259 (1980).
31. A'Hearn, M. F., Schleicher, D. G. & West, R. A. *Astrophys. J.* (in the press).

## Direct laboratory determination of the <sup>187</sup>Re half-life

M. Lindner, D. A. Leich, R. J. Borg, G. P. Russ,  
J. M. Bazan, D. S. Simons\* & A. R. Date†

Lawrence Livermore National Laboratory, Livermore,  
California 94550, USA

\*Center for Analytical Chemistry, National Bureau of Standards,  
Gaithersburg, Maryland 20899, USA

†British Geological Survey, 64–78 Gray's Inn Road,  
London WC1X 8NG, UK

The long-lived, naturally occurring radionuclide <sup>187</sup>Re is important in geochemistry and cosmology as a nucleochronometer. Until now there have been no direct laboratory measurements which have avoided the difficulties of both low-energy β-counting and dependence on radiometric ages of rocks and meteorites. We report here a half-life of  $(4.35 \pm 0.13) \times 10^{10}$  yr, based on the growth of <sup>187</sup>Os over a 4-yr period into a large source of osmium-free rhenium. Since our result agrees with the best geochemically determined values, no significant revision of the present galactic age limits based on the geochemical values is necessary. The agreement at the 5% level of the decay rates determined on laboratory and meteorite-age timescales places a tight constraint on cosmological models in which fundamental 'constants' are allowed to vary. In particular, the fine-structure constant, α, must have changed by less than one part in  $10^5$  over the past  $4.5 \times 10^9$  yr.

Geochemists<sup>1</sup> and astrophysicists<sup>2</sup> have recognized that the isobaric pair <sup>187</sup>Re–<sup>187</sup>Os could provide terrestrial, Solar System and cosmic chronologies. For these, the <sup>187</sup>Re half-life is a necessary parameter. Recent determinations, which indicate a probable value of  $\sim 4 \times 10^{10}$  yr, rely on accepted ages for meteorites and rocks. Analysis of molybdenites of known age

by Hirt *et al.*<sup>3</sup> yielded an average of  $(4.3 \pm 0.5) \times 10^{10}$  yr. With similar techniques applied to meteorites, Luck and Allègre<sup>4</sup> deduced a half-life of  $(4.56 \pm 0.12) \times 10^{10}$  yr. Naldrett<sup>5</sup> determined a half-life of  $(3.5 \pm 0.4) \times 10^{10}$  yr by counting the β-particles emitted from a known quantity of a pure rhenium compound dissolved in a liquid scintillator. His value is significantly lower than the geological<sup>3</sup> and meteoritic<sup>4</sup> values. The results from these different experiments need not agree, since the counting experiment does not detect decays to the bound states of the daughter <sup>187</sup>Os. However, the half-life from the counting experiment should be larger, rather than smaller, than that determined from rocks or meteorites.

Our investigation determined the sum of the β-decays of <sup>187</sup>Re to the bound and unbound states of <sup>187</sup>Os by measuring the growth of <sup>187</sup>Os atoms in a series of 100-g sources of osmium-free perrhenic acid (HReO<sub>4</sub>) solution. Each source differed only in the time interval allowed before osmium removal and measurement. Traces of residual osmium were first removed from 1 kg of concentrated perrhenic acid by exhaustive reflux-distillation. Thus the initial <sup>187</sup>Os/HReO<sub>4</sub> ratio of  $5 \times 10^{-8}$  was reduced to  $7 \times 10^{-12}$ .

The rhenium was 'spiked' with independent gravimetrically prepared solutions of isotopically enriched <sup>190</sup>Os (98%) and <sup>192</sup>Os (99%). The rhenium solution was then frozen at  $-65^\circ\text{C}$  for about 2 yr, thawed at  $-35^\circ\text{C}$  just long enough to remove a 10% aliquot, and refrozen. Osmium was then distilled from the aliquot, purified, and concentrated for isotopic analysis. The thawing and sampling cycle was repeated on the perrhenic acid three times over a 1.5-yr interval following the first sampling. Thus, a single kilogram of rhenium provided a series of <sup>187</sup>Os growth points relative to the two independent 'spikes'. Since the <sup>187</sup>Re/<sup>190</sup>Os and <sup>187</sup>Re/<sup>192</sup>Os ratios were fixed by the spike additions at the onset of growth, we needed only to determine the rate of change of the <sup>187</sup>Os/<sup>190</sup>Os and <sup>187</sup>Os/<sup>192</sup>Os ratios in the rhenium solution from the isotopic analyses of the osmium samples.

**Table 1** Osmium isotope ratios from perrhenic acid source\*

Sample no.	Growth time (days)	$^{187}\text{Os}/^{190}\text{Os}$		$^{187}\text{Os}/^{192}\text{Os}$	
		LAMMA†	ICP-MS‡	LAMMA†	ICP-MS‡
1	670	$1.360 \pm 0.018$	$1.359 \pm 0.013$	$1.418 \pm 0.019$	$1.428 \pm 0.014$
2§	691	$1.387 \pm 0.022$	$1.405 \pm 0.011$	$1.445 \pm 0.021$	$1.481 \pm 0.016$
3	883	$1.672 \pm 0.021$	$1.682 \pm 0.015$	$1.750 \pm 0.022$	$1.761 \pm 0.016$
4	1,236	$2.177 \pm 0.054$	$2.178 \pm 0.027$	$2.258 \pm 0.047$	$2.290 \pm 0.034$

\* Uncertainties expressed as 1 s.d.

† Corrected for isobaric interferences and estimated mass bias, with no uncertainty added. Additional systematic uncertainties of  $\pm 1.5\%$  for  $^{187}/^{190}$  and  $\pm 1.8\%$  for  $^{187}/^{192}$  should be assigned for these corrections.

‡ Corrected for mass bias and for contamination with natural osmium. Uncertainties in these corrections have been included.

§ Correction of  $(2.50 \pm 0.25)\%$  applied for  $^{187}\text{Os}$  content of radioactive  $^{185}\text{Os}$  tracer added in this sample.

In order to monitor chemical yields in one of our samples, we added  $^{185}\text{Os}$  radioactive tracer, made by bombarding tungsten with 65-Mev  $\alpha$ -particles. Since the bombardment produced a spectrum of stable osmium isotopes, which we measured independently<sup>6</sup>, a small correction was made for the  $^{187}\text{Os}$  introduced into the sample with the  $^{185}\text{Os}$  (see Table 1).

Osmium isotopic analyses were performed with two different types of mass spectrometer: a laser microprobe mass analyser (LAMMA), which combines a pulsed-laser ablation ion source with a time-of-flight mass spectrometer<sup>7</sup>, and an inductively coupled plasma mass spectrometer (ICP-MS), which uses an RF-excited argon plasma torch as the ion source for a quadrupole mass spectrometer<sup>8</sup>.

The LAMMA has high sensitivity but it has two limitations<sup>9</sup>. The first is a low threshold for saturation effects in the detector, the second the imprecision of the waveform digitizer in the detector system. These effects limit the ultimate precision of LAMMA isotope ratios. However, we were able to obtain mass abundance ratios with a standard deviation of  $\sim 1\%$  by accumulating large numbers ( $\sim 100$ ) of individual spectra, performing channel-by-channel summation of all spectra and taking ratios of the resulting summed peak areas. Corrections for molecular-ion contributions and uncertain mass-bias effects<sup>10</sup> increase the uncertainty by another estimated 1–2%.

Figure 1 shows the summation of 100 selected LAMMA spectra of the osmium sample isolated from the first 100 g of rhenium. Apart from small amounts of platinum (masses 194 to 196), and an even lower level of molecular-ion contaminants, the three expected osmium peaks stand out clearly. Significantly, the 'signal' at mass 185 is the smallest of any shown in Fig. 1. Interpreted as  $^{185}\text{Re}$ , this implies that no more than a few parts in  $10^{13}$  of the parent rhenium aliquot were carried into the final osmium sample.

In contrast, the ICP-MS was somewhat less sensitive than LAMMA, even with the osmium response strongly enhanced by introduction of the osmium as the tetroxide vapour into the argon torch<sup>11</sup>. However, the combination of ion counting and mass scanning over a relatively stable osmium ion beam, essentially free of isobaric interferences, resulted in mass spectra of better quality than those from LAMMA. Mass fractionation was substantial ( $\sim 1.8\%$  per mass unit), but it was determined with adequate precision by bracketing each run with natural osmium isotopic standards. For the isotopic abundances of natural osmium, we used the values reported by Nier<sup>12</sup>.

Isotope ratio data from both techniques are given in Table 1. Although two of the four ICP-MS measurements showed instrumental contamination with natural osmium, we used a two-

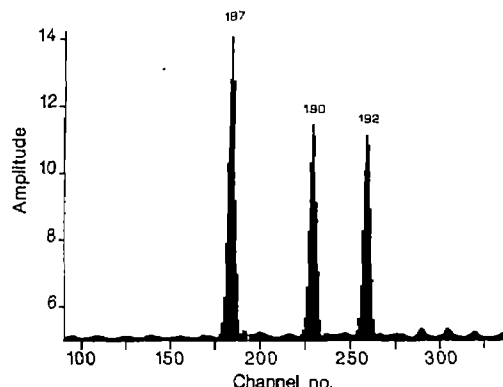


**Fig. 1** Mass spectrum of osmium region; LAMMA data. The osmium sample was isolated from 100 g of perrhenic acid after a growth period of nearly 2 yr.

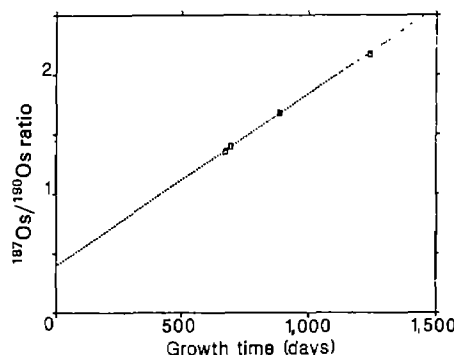


**Fig. 2** Time dependence of the  $^{187}\text{Os}/^{190}\text{Os}$  ratio; ICP-MS data. The dotted line is the least-squares fit.

component analysis to determine the experimental osmium composition. Figure 2 shows the time dependence of the isotope ratio  $^{187}\text{Os}/^{190}\text{Os}$  for the ICP-MS data. The dotted line is the least-squares fit. The non-zero intercept indicates that  $\sim 8$  ng of  $^{187}\text{Os}$  had not been removed before the onset of growth. The slope of the least-squares-fit line in Fig. 2 determines the half-life from the expression

$$t_{1/2} = \left( \frac{^{187}\text{Re}}{^{190}\text{Os}} \right) \frac{\ln 2}{\text{line slope}}$$

in which  $^{187}\text{Re}$  and  $^{190}\text{Os}$  are derived from the gravimetric standardizations of the solutions. Similarly, independent half-life determinations on LAMMA and ICP-MS were made from the  $^{192}\text{Os}$  spike. These results are summarized in Table 2.

We find a 3–4% systematic difference between the measured  $(^{190}\text{Os}/^{192}\text{Os})$  ratios and the values calculated from the

**Table 2**  $^{187}\text{Re}$  half-life values ( $10^{10}$  yr)

Method	$^{190}\text{Os}$ spike	$^{192}\text{Os}$ spike
LAMMA	$4.27 \pm 0.23$	$4.44 \pm 0.24$
ICP-MS	$4.29 \pm 0.19$	$4.41 \pm 0.21$

The weighted average value is  $(4.35 \pm 0.13) \times 10^{10}$  yr.

gravimetric data for the standard solutions of  $^{190}\text{Os}$  and  $^{192}\text{Os}$ . However, X-ray fluorescence analyses of both solutions confirm the absolute values of the gravimetric determinations within the current 5% uncertainty of the X-ray method (F. Bazan, personal communication).

Our half-life value agrees with that of Hirt *et al.*<sup>3</sup> and is only slightly lower than the determination of Luck and Allègre<sup>4</sup>. The

agreement at the  $(5 \pm 6)\%$  level (estimated 95% confidence interval) of the meteoritic half-life value and our laboratory determination can be used to place limits on the possible variation of the fine-structure constant  $\alpha$ , predicted by some cosmological models<sup>13</sup>. Following Dyson<sup>14</sup>, we calculate the average rate of change over the past  $4.55 \times 10^9$  yr to be

$$\left\langle \frac{\dot{\alpha}}{\alpha} \right\rangle = (-1 \pm 2) \times 10^{-15} \text{ yr}^{-1}$$

Due to the small decay energy of  $^{187}\text{Re}$ , these are the tightest limits on the possible variation of  $\alpha$  currently allowed by analysis of  $\beta$ -decay data. However, much tighter limits ( $|\dot{\alpha}/\alpha| < 10^{-17} \text{ yr}^{-1}$  (ref. 15) and  $|\dot{\alpha}/\alpha| < 2 \times 10^{-18} \text{ yr}^{-1}$  (ref. 16)) over the past  $2 \times 10^9$  yr have been claimed from analysis of  $^{149}\text{Sm}$  neutron-capture depletion in the Oklo natural reactor.

With regard to the question of the age of the elements, our half-life value is so close to the one assumed by Clayton<sup>2</sup> that his proposed age limits for galactic nucleosynthesis ( $11-18 \times 10^9$  yr) are still valid.

We thank Dr Barry Berman for pointing out the need for an accurate half-life value for  $^{187}\text{Re}$  in geochemistry and cosmology, and for many discussions in the early stages of this work. We also thank Professor D. D. Clayton for encouragement, Dr G. B. Hudson for discussions on cosmological implications, and

Edith Delucchi and Mr F. Bazan for assistance in solving many chemical and analytical problems. This work was performed by the Lawrence Livermore National Laboratory under the auspices of the Office of Basic Energy Sciences of the US Department of Energy under contract W-7405-Eng-48. Enquiries should be sent to M.L.

Received 1 July 1985; accepted 28 January 1986.

1. Hirt, B., Herr, W. & Hoffmeister, W. *Proc Symp Radioactive Dating*, 35-43 (IAEA, Vienna, 1963).
2. Clayton, D. D. *Astrophys. J.* **139**, 637-663 (1964).
3. Hirt, B., Tilton, G. P., Herr, W. & Hoffmeister, W. in *Earth Science and Meteoritics* (eds Geiss, J. & Goldberg, E. D.) 273-280 (North-Holland, Amsterdam, 1963).
4. Luck, J. M. & Allègre, C. J. *Nature* **302**, 130-132 (1983).
5. Naldrett, S. N. *Can. J. Phys.* **62**, 15-19 (1984).
6. Lindner, M., Delucchi, E. S. & Leich, D. A. *Radiochim. Acta* (submitted).
7. Denoyer, E., Van Grieken, R., Adams, F. & Natusch, D. F. S. *Analyt. Chem.* **54**, No. 1, 26A-41A (1982).
8. Houk, R. S. *et al. Analys. Chem.* **52**, 2283-2289 (1980).
9. Simons, D. S. *Int. J. Mass Spectrom. Ion Processes* **55**, 15-30 (1983/84).
10. Leich, D. A., Lindner, M., Russ, G. P. & Simons, D. S. *33rd Conf. Mass Spectrometry and Allied Topics*, San Diego, 613-614 (American Society for Mass Spectrometry, 1985).
11. Russ, G. P., Bazan, J. M., Date, A. R. & Leich, D. A. *27th Rocky Mountain Conf.*, Denver (Society for Applied Spectrometry, 1985).
12. Nier, A. O. *Phys. Rev.* **S2**, 885 (1937).
13. Dicke, R. H. *Science* **129**, 621-624 (1959).
14. Dyson, F. J. in *Aspects of Quantum Theory* (eds Salam, A. & Wigner, E. P.) Ch. 13 (Cambridge University Press, 1972).
15. Shlyakhter, A. I. *Nature* **264**, 340 (1976).
16. Irvine, J. M. *Phil. Trans. R. Soc. A* **310**, 239-243 (1983).

## Evidence of changing concentrations of atmospheric $\text{CO}_2$ , $\text{N}_2\text{O}$ and $\text{CH}_4$ from air bubbles in Antarctic ice

G. I. Pearman\*, D. Etheridge†, F. de Silva\* & P. J. Fraser\*

\* Atmospheric Research, CSIRO, Private Bag No. 1, Mordialloc, Victoria 3195, Australia

† Antarctic Division, Department of Science, Kingston, Tasmania 7150, Australia

Atmospheric carbon dioxide ( $\text{CO}_2$ ) levels before the industrial revolution were  $\sim 260-280$  p.p.m.v. (parts per  $10^6$  by volume) as determined from studies of air trapped in ice<sup>1,2</sup>. We report here similar results, using Antarctic ice, for the  $\text{CO}_2$  levels during the seventeenth and eighteenth centuries, which suggest an average concentration of 281 (standard deviation  $\sigma = 7$ ) p.p.m.v. The data constrain the net release of biospheric carbon to the atmosphere over the past 200 yr, to  $\sim 5 \times 10^{10}$  tonnes of carbon, mostly during 1850-1900. Measurements of two other 'greenhouse' gases, methane ( $\text{CH}_4$ ) and nitrous oxide ( $\text{N}_2\text{O}$ ), show increases of about 90 and 8% respectively since 1600. This  $\text{CH}_4$  increase is similar to the recently reported<sup>3-6</sup> doubling over the same period, and the  $\text{N}_2\text{O}$  increase, the first direct evidence of historical changes in  $\text{N}_2\text{O}$ , is consistent with releases due to expanding anthropogenic combustion processes<sup>7</sup>.

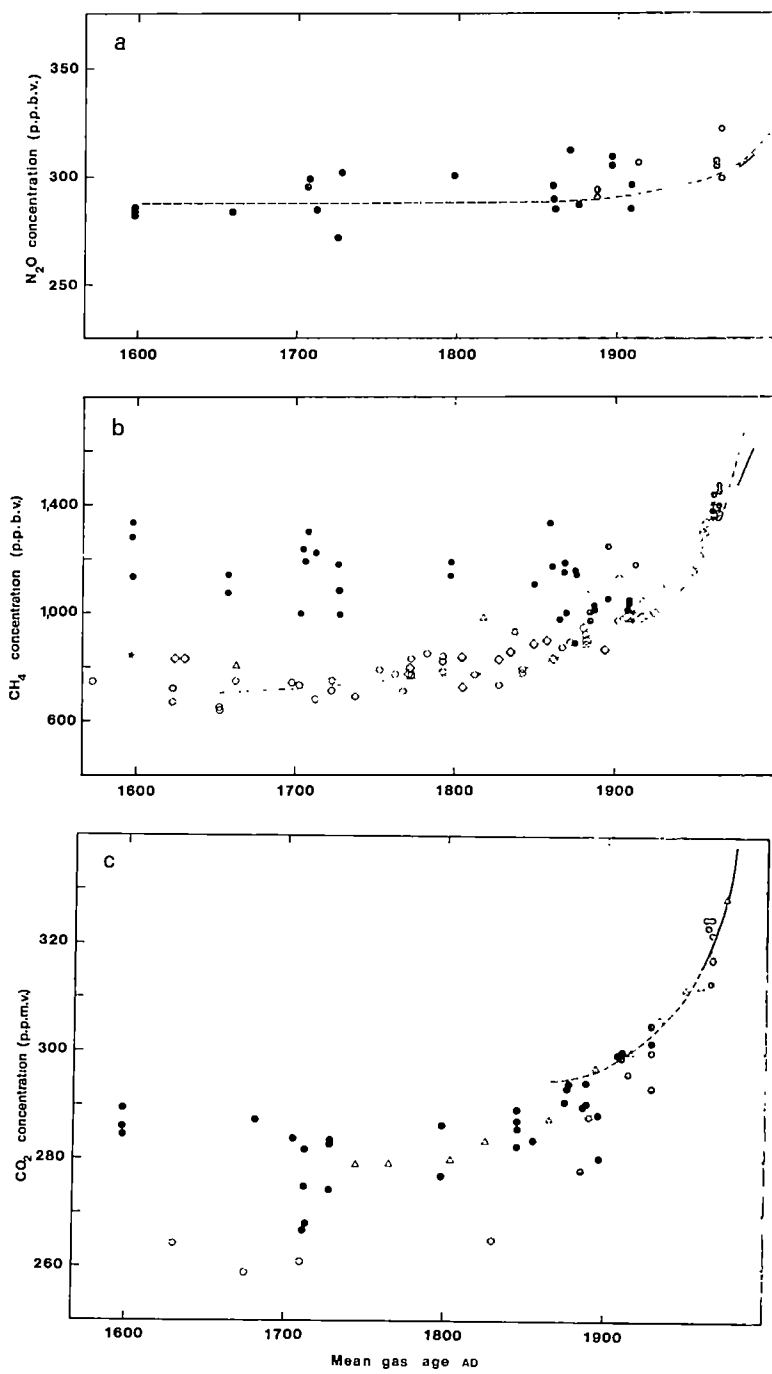
The ice core (BHD) used was thermally drilled to a depth of 473 m near the summit of Law Dome, Antarctica ( $66^\circ 43' \text{S}$ ,  $112^\circ 50' \text{E}$ ; 1,375 m) by the Australian National Antarctic Research Expedition in 1977. High precipitation rates ( $0.65 \text{ m yr}^{-1}$ ), lack of melting at the firm surface (annual average temperature =  $-22^\circ \text{C}$ ), a simple flow regime and small snow dunes all combine to make Law Dome an ideal location for ice-gas composition studies. Although accurate ice dating ( $\pm 2$  yr at 1912,  $\pm 6$  yr at 1850) has been achieved using oxygen isotope stratigraphy<sup>8</sup>, the age of the ice is not the same as that of the occluded air bubbles. However, using recently reported relationships between date of occlusion and ice density for a similar site<sup>9</sup>, the ice is deduced to be 67 yr older than the enclosed air

with 80% of the gas being trapped over the relatively short period of 13 yr.

A complete description of gas extraction and analysis methods used in this study will be given elsewhere. Briefly, a dry extraction technique was developed to crush defect-free and trimmed (0.5-5 cm) core samples (0.5-1.4 kg) to fine powder in  $\sim 4$  min at  $-80^\circ \text{C}$ , releasing approximately  $90 \text{ cm}^3$  of air per kg at STP. The released air was dried ( $-100^\circ \text{C}$ ) and condensed into stainless steel traps at liquid helium temperature. The latter were warmed and agitated for 24 h to ensure uniform mixing. Gas chromatography was used to determine  $\text{CO}_2$  and  $\text{CH}_4$  concentrations to precisions of 0.5 p.p.m.v. and 10 p.p.b.v. (parts per  $10^9$  by volume) respectively using flame-ionization detection, and  $\text{N}_2\text{O}$  to 2 p.p.b.v. using electron-capture detection. To demonstrate whether the technique affected trace gas concentrations in air released from ice, air of known composition was exposed to freshly crushed, evacuated ice, and then re-analysed.  $\text{CO}_2$  and  $\text{N}_2\text{O}$  concentrations were retrieved to within 0.5%, with no bias, while returned  $\text{CH}_4$  concentrations averaged 20 p.p.b.v. or 1.5% high. The  $\text{CH}_4$  data reported here are corrected for this effect. A similar test, involving the crushing of small ice samples (15 g) in the presence of air of known composition, showed similar results for  $\text{CO}_2$  and  $\text{N}_2\text{O}$ , but substantial  $\text{CH}_4$  enhancement. The data represent averages of 1-4 chromatographic analyses.

A total of 75 core samples were crushed and analysed, although due to the availability of the equipment, not all three gases were measured on all samples. There were 44, 69 and 74 samples measured for  $\text{N}_2\text{O}$ ,  $\text{CH}_4$  and  $\text{CO}_2$  respectively. On examination of the data, it was found that sections of the core, exhibiting visible evidence of post-coring melting (PCM), yielded concentrations that were variable and significantly lower than average for  $\text{CO}_2$  and  $\text{N}_2\text{O}$  and higher for  $\text{CH}_4$ . For  $\text{N}_2\text{O}$ , samples exhibiting severe signs of PCM were rejected, leaving 27, with a further sample removed because its concentration was 100 p.p.b.v. less than the average of all the remaining selected data (average 295;  $\sigma = 12$  p.p.b.v.). For  $\text{CH}_4$ , 44 samples survived the PCM examination; two of the remaining samples yielded  $\text{CH}_4$  concentrations 450 and 570 p.p.b.v. higher than the average pre-1920 data (1,115;  $\sigma = 116$  p.p.m.v.), and were therefore rejected. While extremely low  $\text{CO}_2$  concentrations were related to extremes of PCM, it appeared that  $\text{CO}_2$  variability

**Fig. 1** Historical record of atmospheric  $\text{N}_2\text{O}$ ,  $\text{CH}_4$  and  $\text{CO}_2$  concentrations based on measurements of air trapped in the BHD ice core from Law Dome, Antarctica (●). *a*, Solid line, modern data for the South Pole, 1976–79 (ref. 7), and from Cape Grim, Tasmania, 1978–84 (ref. 14). Dashed line, a global tropospheric average concentration for a model incorporating constant non-combustion and growing combustion sources of  $\text{N}_2\text{O}$  (ref. 7).  $\text{N}_2\text{O}$  data are relative to secondary standards<sup>15</sup> provided by R. A. Rasmussen, multiplied by 0.92 to convert to absolute concentration. *b*, Measurements made after elimination of  $\text{CH}_4$  enhancement due to metal-metal friction (★). The other data (●) are believed to require correction downwards by ~400 p.p.b.v. in the fifteenth to sixteenth centuries, the correction decreasing to negligible amounts for modern samples (see text). Modern data are from Cape Grim, 1978–84 (solid line) (refs 16, 17), and from the Northern Hemisphere, 1965–81 (dashed line) (ref. 18). Data from other studies ( $\Delta$ , ref. 4; ○, ref. 5; and  $\diamond$ , ref. 6) are included for comparison. Dotted line, a global tropospheric average concentration from a model incorporating constant natural and growing anthropogenic sources of  $\text{CH}_4$ , and decreasing levels of atmospheric OH (ref. 11).  $\text{CH}_4$  data are relative to NBS standards through Rasmussen secondary standards<sup>15</sup>. *c*, Solid line, modern data for the Mauna Loa Observatory<sup>19</sup>. Data from other ice studies, ( $\Delta$ , ref. 1; ○, ref. 2) are included for comparison. Dashed line, back-extrapolation from the observed concentration in 1959 assuming a constant airborne fraction of 0.57 (ref. 20), using the fossil fuel release data of Rotty<sup>21</sup>.  $\text{CO}_2$  data are reported in the World Meteorological Organization 1981  $\text{CO}_2$  calibration scale.



was associated with subtle and less easily quantified evidence of PCM. Thus for  $\text{CO}_2$ , a datum was selected if its concentration was within 7 p.p.m.v. of at least one other sample of comparable age ( $\pm 5$  yr). This criterion resulted in the selection of 42 samples, 30 of which showed little or no evidence of PCM. The remaining 12 had more than 2 cm of outer ice removed before crushing and this may have explained their apparent independence of PCM.

The selected  $\text{N}_2\text{O}$  data are shown in Fig. 1*a*. The ice data for recent times agree with modern measurements and a linear regression of the whole record shows that concentrations have increased by 6 ( $\sigma = 2$ ) p.p.b.v. per 100 yr over the past 300 yr. This is the first evidence of changing atmospheric  $\text{N}_2\text{O}$  levels on this timescale. The current trend of 0.5–1.8 p.p.b.v.  $\text{yr}^{-1}$  (refs 7, 10) is not characteristic of the 400-yr ice record.  $\text{N}_2\text{O}$  averaged 289 ( $\sigma = 10$ ) p.p.b.v. between 1600 and 1800 compared with modern Southern Hemisphere values of about 310 p.p.b.v. A similar pre-industrial concentration was deduced by Weiss<sup>7</sup>

(Fig. 1*a*) using a combustion source model to fit modern  $\text{N}_2\text{O}$  concentrations and their rate of change with time.

The selected  $\text{CH}_4$  data are shown in Fig. 1*b*, together with results from other ice studies. Again, there is reasonable agreement between modern measurements and the recent ice core records. The new data suggest that atmospheric  $\text{CH}_4$  levels over the period 1600–1900 averaged 1,115 ( $\sigma = 116$ ) p.p.b.v., 40% lower than current concentrations, with the most significant changes occurring during this century. The results are in contrast to other studies which showed that  $\text{CH}_4$  concentrations have doubled since the seventeenth century or earlier<sup>4–6</sup>, with a rapid rise starting in the early nineteenth century. This discrepancy led us to investigate and demonstrate the production of  $\text{CH}_4$  in our apparatus by frictional contact between metal surfaces, as has been observed elsewhere<sup>6</sup>. Subsequent analyses of a further five core samples (see Fig. 1*b*), with this friction eliminated during ice crushing, show good agreement with other studies. These limited results suggest that  $\text{CH}_4$  production is greater with

old ice than with more modern ice. The calibration tests involving ice crushing showed that for gas samples of low CH<sub>4</sub> concentration (~700 p.p.b.v.), the contamination was significant (~400 p.p.b.v.). At higher concentrations (1,800 p.p.b.v.) the CH<sub>4</sub> enhancement was significantly less. Thus, metal-to-metal friction in our apparatus has enhanced CH<sub>4</sub> concentrations observed in ice-cores containing fifteenth to sixteenth century air by ~400 p.p.b.v., while the effect on modern air samples has been negligible. Correcting for this effect would bring our CH<sub>4</sub> data into approximate agreement with previous studies, but the variability in our data caused by variations in the amount of CH<sub>4</sub> produced by friction cannot be allowed for. Improvements to the crushing device have since eliminated the problem.

The selected CO<sub>2</sub> data are presented in Fig. 1c, together with the Swiss<sup>1</sup> and French<sup>2</sup> data. As with N<sub>2</sub>O and CH<sub>4</sub>, the agreement between modern atmospheric measurements and air trapped recently in ice is encouraging. The data indicate CO<sub>2</sub> levels of about 290–295 p.p.m.v. during the last two decades of the nineteenth century, which are supported by chemical measurements made at that time<sup>12</sup>. As with the Swiss data the results suggest that mid-nineteenth-century and earlier concentrations were lower, averaging 281 ± 7 p.p.m.v. for the period 1600–1800, and 288 ± 5 p.p.m.v. for the nineteenth century. This suggests that a rapid increase in atmospheric CO<sub>2</sub> of about 13 p.p.m.v. (294–281) occurred during the second half of the nineteenth century or early twentieth century, that cannot be explained by the small amount of fossil fuel consumed during this period. Assuming an airborne fraction of 0.57 this indicates a net CO<sub>2</sub> source, presumably largely biospheric, of  $4.8 \times 10^{10}$  tonnes. More precise estimates of this source will be possible using a global carbon-cycle model<sup>13</sup>, when the concentration history is better defined.

We are confident that other sections of this core, when transported to Australia in more controlled conditions, will yield additional, better quality data on these and other gaseous constituents. Such data are invaluable in understanding the biogeochemical cycles and abundance of these species in the atmosphere, and assessing their potential role in past climate change.

We thank several people for support during the period of the development of techniques: in particular, we thank Professor W. F. Budd (Melbourne University), Mr V. I. Morgan, Mr I. Allison and Mr D. Jones (Antarctic Division) for their long-term support for the project, Dr I. G. Enting (CSIRO) for advice on gas dating, the workshop staff of CSIRO and Antarctic Division/Glaciology for assistance in the equipment construction, Mr R. Horan, Mr K. Hall (Monash University), Mr R. Kemp (CSIRO) and Professor G. Opat (University of Melbourne) for the supply of and advice on liquid helium, and Professor R. A. Rasmussen (Oregon Graduate Center) for CH<sub>4</sub> and CO<sub>2</sub> gas chromatographic equipment.

Received 23 September 1985; accepted 6 January 1986.

1. Neftel, A., Moor, E., Oeschger, H. & Stauffer, B. *Nature* **315**, 45–47 (1985).
2. Raynaud, D. & Barnola, J. M. *Nature* **315**, 309–311 (1985).
3. Khalil, M. A. K. & Rasmussen, R. A. *Chemosphere* **11**, 877–883 (1982).
4. Craig, H. & Chou, C. C. *Geophys. Res. Lett.* **9**, 1221–1224 (1982).
5. Rasmussen, R. A. & Khalil, M. A. K. *J. geophys. Res.* **89**, 11599–11605 (1984).
6. Stauffer, B., Fischer, G., Neftel, A. & Oeschger, H. *Science* **229**, 1386–1388 (1985).
7. Weiss, R. F. *J. geophys. Res.* **86**, 7185–7195 (1981).
8. Morgan, V. I. *Climat. Change* **7**, 415–419 (1985).
9. Schwander, J. & Stauffer, B. *Nature* **311**, 45–47 (1984).
10. Khalil, M. A. K. & Rasmussen, R. A. *Tellus* **35B**, 161–169 (1983).
11. Khalil, M. A. K. & Rasmussen, R. A. *Atmos. Environ.* **19**, 397–407 (1985).
12. Pearman, G. I. *Search* **15**, 42–45 (1984).
13. Enting, I. G. & Pearman, G. I. *Proc. 6th ORNL Life Sci. Symp. The Global Carbon Cycle*, Knoxville, Tennessee, (in the press).
14. Fraser, P. J., et al. in *Baseline 1983–84* (eds Francey, R. J. & Forgan, B.) (Australian Department of Science and Technology, in the press).
15. Rasmussen, R. A. & Lovelock, J. E. *J. geophys. Res.* **88**, 8369–8378 (1983).
16. Fraser, P. J., Khalil, M. A. K., Rasmussen, R. A. & Steele, L. P. *J. atmos. Chem.* **1**, 125–135 (1984).
17. Fraser, P. J., Hyson, P., Rasmussen, R. A., Crawford, A. J. & Khalil, M. A. K. *J. atmos. Chem.* (in the press).
18. Rasmussen, R. A. & Khalil, M. A. K. *J. geophys. Res.* **86**, 9826–9832 (1981).
19. Keeling, C. D. in *Numeric data package NDP001* (Carbon Dioxide Information Centre, Oak Ridge, Tennessee, 1984).
20. Pearman, G. I. & Beardmore, D. J. *Tellus* **36B**, 1–24 (1984).
21. Rotty, R. M. *J. geophys. Res.* **88**, 1301–1308 (1983).

## Palaeotemperatures still exist in the Greenland ice sheet

D. Dahl-Jensen\* & S. J. Johnsen†

\* Department of Glaciology, Geophysical Institute, University of Copenhagen, Haraldsgade 6, DK-2200 Copenhagen N, Denmark

† Science Institute, University of Iceland, Dunhagi 3, IS-107 Reykjavik, Iceland

**The temperature distribution through the Greenland ice sheet at the Dye 3 borehole is a record of the past climatic changes in the Arctic. The numerical model of the temperature distribution now presented reproduces the observed temperature distribution within 0.03 K, and shows that the basal ice is still cooled 5 K by the cold ice-age climate. The results suggest a mean ice-age temperature of  $-32 \pm 2$  °C, which is 12 K colder than the present temperature, and a precipitation rate  $50 \pm 25\%$  of the present rate. Calculations of a more detailed temperature history through the present interglacial period reveal evidence of the AD 1920–50 maximum, the little ice age, and the Atlantic period.**

The temperature distribution (Fig. 1a) in the 2,037-m deep, liquid-filled borehole at Dye 3 (65° N, 44° W) was measured in 1980, in 1982 and twice in 1983<sup>1</sup>. The 1982 and 1983 temperatures were identical, within the calibration accuracy (0.03 K) of the thermistors used. The disturbances induced by the core drilling in 1979–81 have obviously disappeared, and the 1983 temperature profile therefore represents the steady-state hole temperature. The hole temperature reproduces the undisturbed ice temperatures; deviations caused by small convection cells<sup>1</sup> in the liquid-filled hole are small and are neglected in this work. The bottom temperature is  $-13.22$  °C, so no melting occurs at the base.

Dye 3 is situated 40 km east of the local ice divide of the ice sheet. The flow leading to the borehole is reasonably well known from surface elevations<sup>2,3</sup>, strain rates<sup>4</sup>, surface velocities<sup>5</sup>, precipitation rates and model calculations<sup>6–8</sup>. In outline, the ice flow follows the local ice divide northward from South Dome (64° N, 45° W) and turns at an angle of 60° to the ice divide towards the Dye 3 site. The surface velocity at Dye 3 is as high as  $13 \text{ m yr}^{-1}$  and any temperature model must therefore take into account horizontal advection and internal deformation heating.

The model presented here considers 2,000 m of ice on top of 3,000 m of rock. The heat transfer equation for non-steady state may be written:

$$\frac{\partial T}{\partial t} = k \nabla^2 T - v \nabla T + \frac{f}{\rho c} + \left( \frac{\partial k}{\partial T} + \frac{k}{c} \frac{dc}{dT} \right) \left( \frac{\partial T}{\partial z} \right)^2 \quad (1)$$

where  $T$  is the temperature,  $t$  the time,  $z$  the depth,  $v$  the ice velocity,  $\rho$  the ice density and  $f$  the internal deformation heating.  $k$  and  $c$ , the thermal diffusivity and specific heat capacity of ice, are treated as in ref. 9.

Solutions to equation (1) are calculated numerically with the following assumptions: (1) The problem is assumed to be two-dimensional (flow direction,  $x$ , versus depth,  $z$ ). (2) The ice thickness and the surface lapse rate have remained constant in time. (3) The velocity profiles are adequately represented by the Dansgaard–Johnsen model<sup>10</sup> with a 300-m-thick bottom shear-layer, which approximates the velocity profiles revealed from measurements of the tilting of the Dye 3 borehole<sup>1</sup>. The velocity profiles are assumed to change with time in such a way that the ice sheet maintains mass balance. (4) The horizontal temperature gradient  $\partial T / \partial x$  is assumed to be proportional to the thinning of the annual layers with depth<sup>11</sup>, and the horizontal heat conduction  $k \partial^2 T / \partial x^2$  is negligible. (5) The geothermal heat flux is constant at the base of the 3,000 m of rock, at a value typical for Precambrian shield.

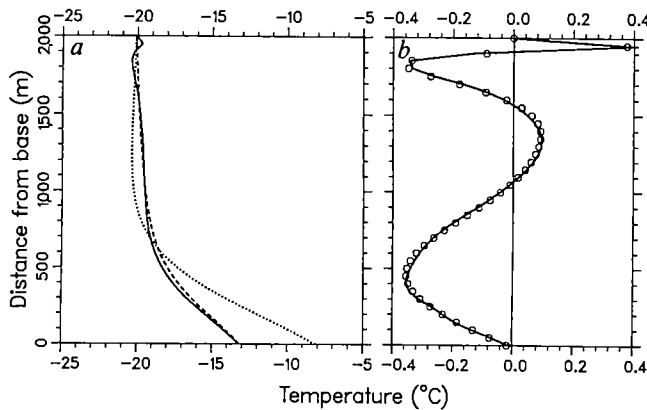


**Fig. 1** *a*, Solid line, measured temperature distribution from the Dye 3 borehole. Dotted line, steady-state temperature distribution calculated for present climatic conditions. Dashed line, calculated non-steady-state temperature distribution. The smoothed climate history used in this calculation is as shown in Fig. 2 with ( $T_{ice}$ ,  $\lambda_{ice}$ ,  $Q_{geo}$ ) values ( $-32^{\circ}C$ ,  $0.245 \text{ m yr}^{-1}$ ,  $38.6 \text{ mW m}^{-2}$ ). *b*, The deviations between the measured (solid line) and the calculated (dashed line) temperature distributions from *a* are shown by the solid line. The deviations represent the more detailed temperature history of the present interglacial period and the circles show the calculated fit to these deviations using the temperature variation on Fig. 5 (solid line). The deviations between this fit and the measurements are  $<0.03 \text{ K}$ .

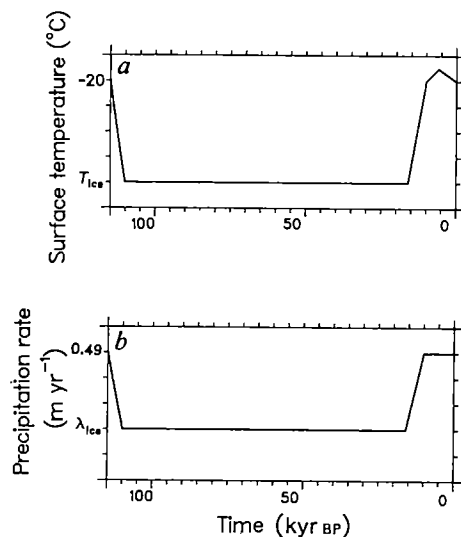


**Fig. 2** The smoothed climate history used to calculate the temperature distribution shown on Fig. 1*a*. *a*, The temperature variation through the 115-kyr glacial cycle.  $T_{ice}$  is the ice-age temperature. *b*, The precipitation rate variation through the cycle.  $\lambda_{ice}$  is the ice-age precipitation.

An initial steady-state temperature profile was calculated for present conditions; that is, using the present surface temperature and precipitation rates. The profile deviates considerably from the observed (Fig. 1*a*). This is seen most clearly at the base, where the steady-state temperature is 5 K too high, indicating that the temperature distribution in the borehole is far from a steady-state distribution. The colder bottom temperature is a remnant from the cold ice-age climate.

A non-steady-state solution can now be calculated by applying a simplified climate history (that is, surface temperature and precipitation rate) as input to the model. The climate history throughout the last glacial cycle, the past 115 kyr BP, is repeated 7–10 times, until the initial state is ‘forgotten’ and the tem-

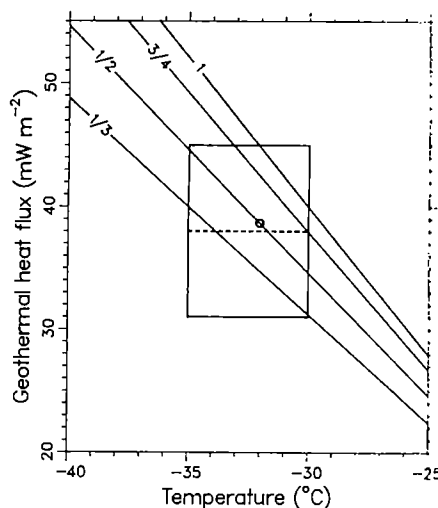


**Fig. 3** The curves represent the parameter combinations ( $T_{ice}$ ,  $\lambda_{ice}$ ,  $Q_{geo}$ ) which give temperature distributions similar to the observed one. The ice-age precipitation rate ( $\lambda_{ice}$ ) relative to the present ( $0.49 \text{ m yr}^{-1}$ ) is shown. The circle is the parameter choice used in the further calculations. ( $T_{ice}$ ,  $\lambda_{ice}$ ,  $Q_{geo}$ ) = ( $-32^{\circ}C$ ,  $0.245 \text{ m yr}^{-1}$ ,  $38.6 \text{ mW m}^{-2}$ ).

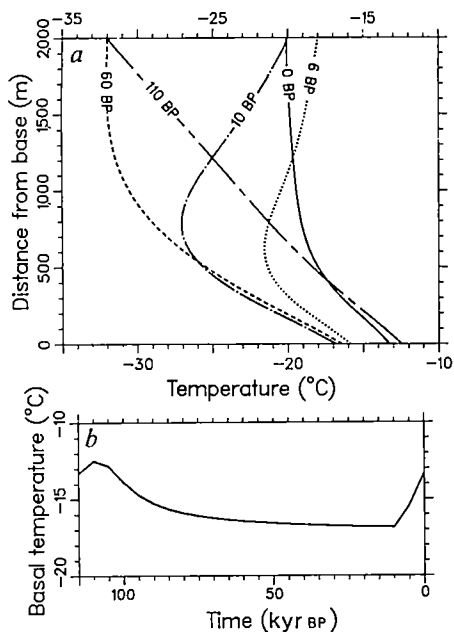
perature profile responds periodically to the periodic forcing.

Figure 2 shows a smoothed version of the 115-kyr-long glacial cycle. The mean ice-age temperature,  $T_{ice}$ , and the mean ice-age precipitation-rate,  $\lambda_{ice}$ , are considered as unknown. Solutions are calculated for a variety of ( $T_{ice}$ ,  $\lambda_{ice}$ ) values. In each case, the geothermal heat flux  $Q_{geo}$  is adjusted so as to make the resulting temperature profiles fit the observed temperature distribution (Fig. 1*a*). The results are presented on Fig. 3. Obviously, a wide span of ( $T_{ice}$ ,  $\lambda_{ice}$ ) values might represent reasonable parameter choices, because the geothermal heat flux in Greenland is poorly known. However, the mean geothermal heat flux for Precambrian shield is  $38.7 \text{ mW m}^{-2}$  (ref. 12), and this is adopted below.

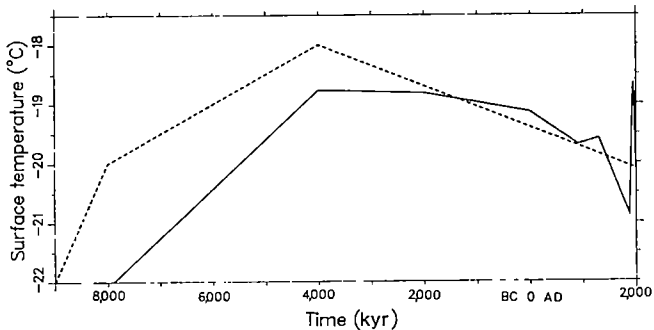
As for  $T_{ice}$ , the mean ice-age temperature at Dye 3 is believed to lie in the range from  $-35$  to  $-30^{\circ}C$ . The upper limit  $-30^{\circ}C$  represents a cooling of 10 K from the present surface temperature. This must be a minimum because the present cooling of the bottom ice is 5 K. The  $\delta^{18}\text{O}$  profile along the Dye 3 deep core<sup>13</sup> has a 7% shift at the Pleistocene/Holocene transition. Many uncertainties are connected with the conversion of this  $\delta$ -shift to a temperature shift, but it is believed to correspond to no less than 10 K. The CLIMAP reconstruction<sup>14</sup> of the Last Glacial Maximum (LGM) climate has a maximum sea-surface temperature anomaly in the North Atlantic. This anomaly between modern and LGM conditions is 14 K, and the anomaly at Dye 3 is not believed to exceed this maximum, so the lower limit of the mean ice-age temperature is probably  $-35^{\circ}C$ .

Figure 3 shows that the curves with a mean precipitation rate,  $\lambda_{ice}$ , 33–75% of the present are the most realistic. This conclusion agrees with the measurements of the radioisotope  $^{10}\text{Be}$  in the deep core<sup>15</sup>.

The calculated variation of the temperature profile throughout the glacial cycle is shown in Fig. 4. The cold glacial climate cooled the surface from 115 kyr BP, but the warming of the basal ice continues to 110 kyr BP. It was only at 65 kyr BP, that is, 50 kyr after the onset of the glaciation, that the basal temperature reached a minimum and the temperature profile got close to a steady-state solution for glacial conditions. The surface temperature variation of 12 K is damped to 5 K at the base. The variation of the temperature distribution, and the time (50 kyr) required to reach a steady-state profile clearly demonstrates the necessity of using a non-steady-state model.



**Fig. 4** *a*, Variation of the temperature distribution through the 115-kyr glacial cycle shown on Fig. 2. *b*, Variation of the basal temperature through the glacial cycle.



**Fig. 5** Solid line, the more detailed temperature variation through the past 10 kyr BP, derived from the observed temperature distribution at the Dye 3 bore-hole. Dashed line, smoothed temperature history also shown on Fig. 2a.

The deviations between the smoothed and the observed temperature profiles are shown on Fig. 1*b*. These deviations are used to calculate a more detailed atmospheric temperature history through the past 10 kyr, the present interglacial period. A least-squares method is used, and the detailed temperature variation is added to the last 115-kyr glacial cycle, used as an input to the non-steady-state model. The temperature trend curve in Fig. 5 results in a calculated temperature profile along the deep hole which deviates <0.03 K from the measured profile (Fig. 1*b*). A study shows that the calculations through the past 10 kyr are rather independent of the 'ice-age solution', that is, the choice of ( $T_{ice}$ ,  $\lambda_{ice}$ ) used to calculate the smoothed temperature profile along the deep core.

The calculated temperature record in Fig. 5, particularly through the recent millennia, agrees well with what is known of post-glacial temperature trends in the Arctic troposphere<sup>16,17</sup>. The AD 1920–50 maximum, the little ice-age (AD 1400–1900), the medieval warm period (AD 900–1400); the cold period in early medieval times, and the warm Roman time are recorded in most of the Northern Hemisphere. The onset of the warm Atlantic period is also revealed at 4000 BC, but its termination around 1000 BC is missing. However, note that the time resol-

ution and the accuracy of the climate history revealed by the Dye 3 deep hole decrease backward in time, because the temperature variations in the borehole are gradually smoothed with increasing depth in the ice sheet.

The numerical modelling shows that the temperature distribution in the ice sheet contains considerable information on past climatic conditions. The information is most detailed in the past 10 kyr, because the resolution in the ice is better and the ice flow and precipitation were similar to the present well-known conditions. The glacial climate can be estimated by the model. The results in Fig. 3 demonstrate that a range of solutions are acceptable. This fact, combined with the unknown ice thickness and ice flow<sup>18</sup> in glacial conditions, limits the resolution of the ice-age climate.

This work has been funded by the Danish Natural Science Research Council, the Commission for Scientific Research in Greenland, Nordic Research Courses (Nordic Council of Ministers) and the European Economic Communities, XII Directorate General (contract CLI.067.DK).

Received 22 August 1985; accepted 10 January 1986.

1. Gundestrup, N. S. & Hansen, B. L. *J. Glaciol.* **30**, 282–288 (1984).
2. Zwally, H. J., Bindshadler, R. A., Brenner, A. C., Martin, T. V. & Thomas, R. H. *J. geophys. Res.* **88**, 1589–1596 (1983).
3. Overgaard, S. & Gundestrup, N. S. *Am. geophys. Un. geophys. Monogr.* **33**, 49–56 (1985).
4. Whillans, I. M., Jezek, K. C., Drew, A. R. & Gundestrup, N. S. *Ann. Glaciol.* **5**, 185–198 (1984).
5. Reeh, N. & Gundestrup, N. S. *J. Glaciol.* **31**, 198–200 (1985).
6. Reeh, N., Johnsen, S. J. & Dahl-Jensen, D. *Am. geophys. Un. geophys. Monogr.* **33**, 57–66 (1985).
7. Dansgaard, W., Clausen, H. B., Dahl-Jensen, D. & Gundestrup, N. S. *Proc. Symp. on EEC Climatology Programme* (1984).
8. Dahl-Jensen, D. *J. Glaciol.* **31**, 92–98 (1985).
9. Dansgaard, W. & Johnsen, S. J. *J. geophys. Res.* **74**, 1109–1110 (1969).
10. Dansgaard, W. & Johnsen, S. J. *J. Glaciol.* **8**, 215–223 (1969).
11. Budd, W. F., Young, N. W. & Austin, C. R. *J. of Glaciol.* **16**, 99–110 (1974).
12. Lee, W. H. K. & Uyeda, S. *Terrestrial Heat Flow* (ed. Lee, W. H. K.) (American Geophysical Union, Washington, DC, 1965).
13. Dansgaard, W. *et al. Geophys. Monogr.* **29** (1984).
14. CLIMAP Project Members, *Geological Society of America Map and Chart Series MC—36* (1981).
15. Beer, J. *et al. Ann. Glaciol.* **5**, 16–17 (1984).
16. Hammer, C. U., Clausen, H. B. & Dansgaard, W. *J. Volcan. geotherm. Res.* **11**, 3–10 (1981).
17. Lamb, H. H. *Climate History and the Modern World* (Methuen, London, 1982).
18. Reeh, N. *Nature* **317**, 797–799 (1985).

## Geophysical modelling of the thermal history of foreland basins

M. A. Kominz & G. C. Bond

Lamont-Doherty Geological Observatory, Columbia University, Palisades, New York, 10964, USA

Rapid subsidence and sedimentation in active foreland basins produces negative thermal anomalies within the sediments and the lithosphere. We have developed a one-dimensional conductive heating model to simulate the thermal effects of subsidence in foreland basins. Application of the model to data from a well in the Alberta Basin suggests that negative thermal anomalies can delay hydrocarbon maturation by a few million years. The thermal anomaly is larger within the lithosphere than in the sediments. As the anomaly is removed by conductive heating the rheological properties of the lithosphere are modified, causing an apparent reduction of plate rigidity. The thermal anomaly in the lithosphere also results in a positive buoyancy force which acts against the mechanical loading of the plate and produces thermally driven uplift when active loading ceases.

We have modelled the subsidence of foreland basins as the response of an elastic or a viscoelastic plate to loading during orogenic compression<sup>1–3</sup>. A relationship has been shown to exist between the thermal state of the continental lithosphere and its

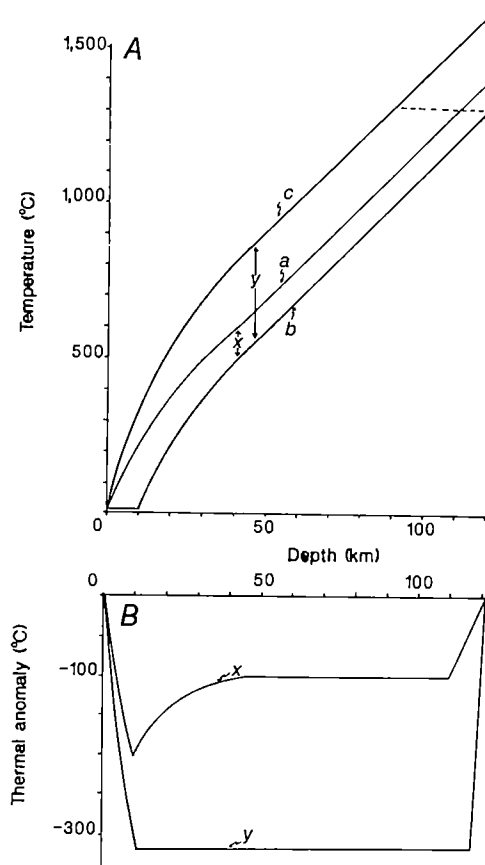


**Fig. 1** The thermal anomaly resulting from a single 10-km episode of subsidence of continental lithosphere. *A*, The original, post-instantaneous-subsidence and final equilibrium thermal gradients are *a*, *b* and *c*, respectively. The difference between the initial and final equilibrium gradients (*y* minus *x*) is the result of thermal blanketing of the added sediments. *B*, The thermal anomalies are *x*, the anomaly resulting from depression of the slab, and *y*, the anomaly resulting from both the depression of the slab and the thermal blanketing effect of the sediments.

response to mechanical loading<sup>3-5</sup>. Rapid deposition of cold, low conductivity sediments results in the formation of negative thermal anomalies (the difference between actual temperatures and equilibrium temperatures) within the sediments and underlying lithosphere. As a result of thermal blanketing, the sediments will equilibrate with a new, generally hotter, equilibrium geothermal gradient, which adds to the negative anomaly (Fig. 1). In our model, the temperature of the asthenosphere during deposition of each increment of sediment is set equal to the equilibrium temperature resulting from the deposition of that increment of sediment. Thus, a sharp temperature change occurs at the interface between the lithosphere, which is not in thermal equilibrium, and the underlying asthenosphere (Fig. 1).

In foreland basins of western North America (Fig. 2), the subsidence resulting from thrusting in the Cordilleran orogenic belt occurs in multiple, rapid episodes with sedimentation rates sufficient to keep the basins nearly filled<sup>6</sup>. This mechanically driven subsidence began between 200 and 160 Myr ago and ended ~50 Myr ago, and was synchronous with thrusting in the adjacent Cordillera. The magnitude of subsidence decreases with distance from the mountain belt, as is shown by the subsidence curves (Fig. 2). Each episode of subsidence, presumably resulting from a distinct phase of thrusting<sup>1,2</sup>, produces negative thermal anomalies. Because heat conduction is slow relative to the frequency and magnitude of the subsidence episodes, a portion of the thermal anomalies resulting from each subsidence episode will be present at the initiation of the next episode.

Thus, non-equilibrium conditions form the initial conditions for all thermal calculations after foreland basin subsidence begins. The thermal evolution is calculated using a one-dimensional finite difference method modified from ref. 7, and we assume that all heat transfer is conductive. A one-dimensional calculation produces an acceptable approximation of the thermal history because foreland basins tend to be broad features in which lateral temperature gradients are likely to be small.

The record of subsidence preserved in the stratigraphy of the foreland basin forms the primary input for our thermal model. Sediment compaction is estimated by the method of Bond and Kominz<sup>8</sup> which was modified to include present-day porosity in the basin strata. Density, specific heat and concentration of radioactive material are calculated as the arithmetic mean of these properties for the appropriate mix of various sediment types and water<sup>9</sup>. We assume that porosity varies with both lithology and depth<sup>8</sup>. Sediment conductivity is calculated according to the Maxwell diffusion equation<sup>10</sup> treating the sediments as a dispersed phase in water. The thermal model is independent of uncertainties in parameters such as palaeo-water depth (or height above sea level), palaeo-sea level (the definition of a fixed base level) and the flexural response of the lithosphere-to-sediment loading. This is because the origin of the thermal gradient is taken to be the sediment-air (water) interface. Thus, the calculated equilibrium and disequilibrium temperatures are a function only of the sedimentation rate and the thermal properties of the sediment column, which can be estimated from the stratigraphic record.

The flow of water through porous sediments affects their thermal history but is not taken into account in our model. Fluids move laterally and upward in a sedimentary basin as a result of compaction. This effect is not significant relative to conductive heating for the Illinois basin<sup>11</sup>, which has sedimentation rates comparable with those in the Alberta Basin. On the other hand, gravity-driven groundwater flow may have a significant effect on sediment temperatures<sup>12</sup>. The topography and water table of subaerial foreland basins slope gradually away from the deformation front toward the craton. The resulting flow pattern depresses the thermal gradients near the mountains and increases them at the cratonic limit of the basin<sup>13</sup>. Steady-state finite element models have been developed to estimate the effects of gravity-driven groundwater flow in the Alberta Basin<sup>14,15</sup>. The thermal perturbations resulting from gravity-driven fluid flow are significant relative to the conductive effects of rapid subsidence and must be taken into account when modeling subaerial phases of subsidence. In the Alberta Basin subsidence is characterized by submarine and mixed submarine to non-marine sediments. Thus, a conductive heating model should yield a reasonably accurate thermal history during active subsidence, but would not be expected to yield an accurate picture of the present-day heat flow regime because of today's groundwater flow. A comprehensive model of the thermal history and present temperatures in the Alberta basin must include the effects of non-steady-state fluid flow as well as rapid sedimentation.

We have applied the thermal model to data from the Getty Union Oyster well in the Alberta Basin. The basin was produced by flexural bending in response to compressional tectonism between the Jurassic and Eocene. Before initiation of the foreland basin, the Hudsonian basement beneath the Alberta Basin was probably not affected by thermal events younger than ~1,700 Myr. Thus, the lithosphere can be assumed to have been in thermal equilibrium at the initiation of thrusting. The equilibrium gradient within the lithosphere is assumed to be  $24\text{ }^{\circ}\text{C km}^{-1}$  at the surface of the crust. Radioactivity within the lithosphere is assumed to be distributed exponentially with a surface value of  $2.5\text{ }\mu\text{W m}^{-3}$  and a decay constant (characteristic depth) of 14 km, resulting in a temperature at the top of the asthenosphere of  $1,375\text{ }^{\circ}\text{C}$  for a 125-km thick lithosphere. These values are consistent with average continental lithospheric

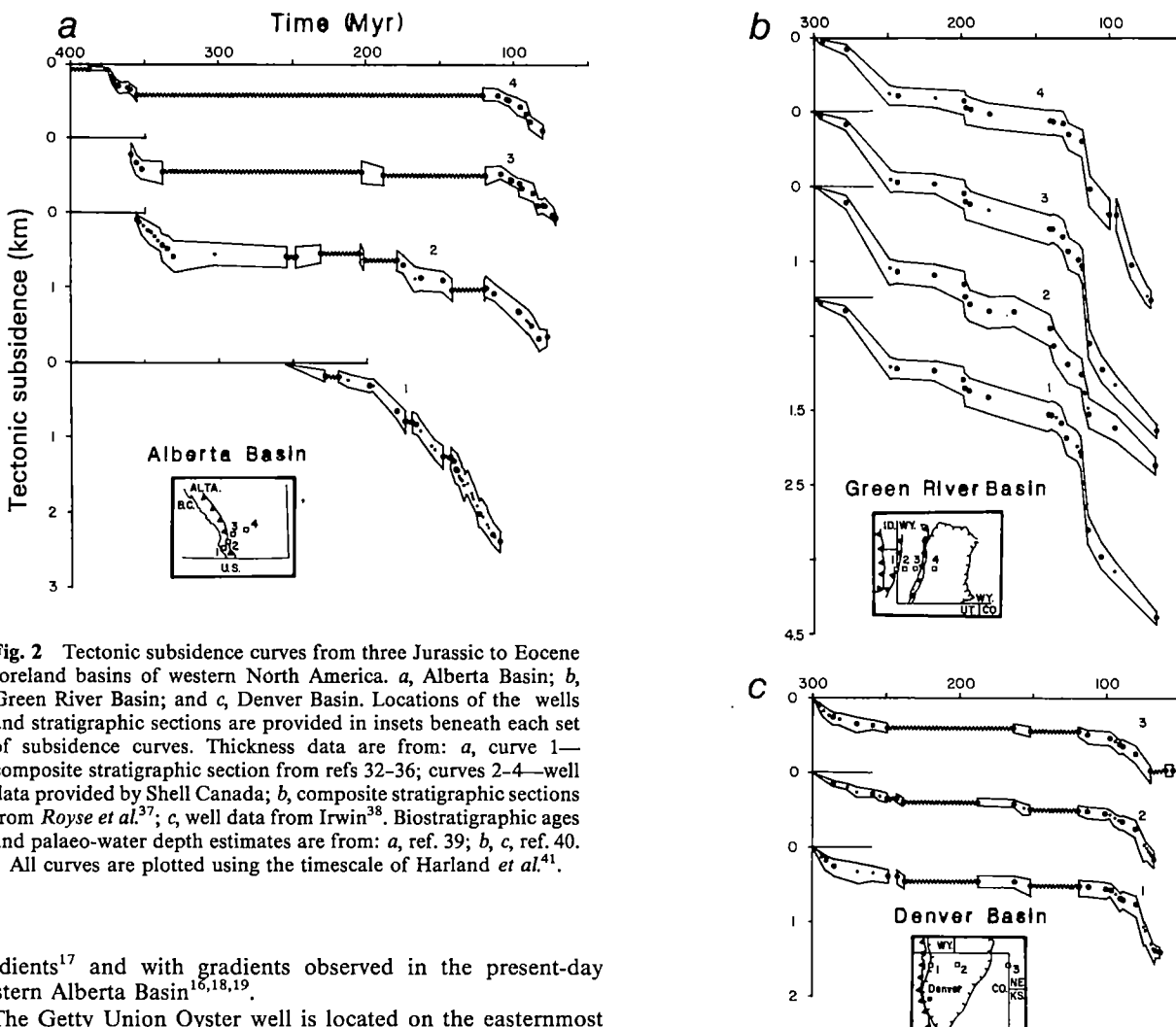


**Fig. 2** Tectonic subsidence curves from three Jurassic to Eocene foreland basins of western North America. *a*, Alberta Basin; *b*, Green River Basin; and *c*, Denver Basin. Locations of the wells and stratigraphic sections are provided in insets beneath each set of subsidence curves. Thickness data are from: *a*, curve 1—composite stratigraphic section from refs 32–36; curves 2–4—well data provided by Shell Canada; *b*, composite stratigraphic sections from Royse *et al.*<sup>37</sup>; *c*, well data from Irwin<sup>38</sup>. Biostratigraphic ages and palaeo-water depth estimates are from: *a*, ref. 39; *b*, *c*, ref. 40. All curves are plotted using the timescale of Harland *et al.*<sup>41</sup>.

gradients<sup>17</sup> and with gradients observed in the present-day western Alberta Basin<sup>16,18,19</sup>.

The Getty Union Oyster well is located on the easternmost edge of the thrust and fold belt (Fig. 2, curve 2). Subsidence of the foreland began in the late Jurassic<sup>20,21</sup> and ended at the end of the Cretaceous when thrusting overran this part of the basin. Because our model required that each sediment package be at least 100 m thick it was necessary to begin the modelling at the base of the middle Jurassic sediments (Fernie group); ~3.75 km of sediments accumulated between the middle Jurassic and the end of the Cretaceous (Fig. 3a). Our model predicts that the subsidence caused a negative thermal anomaly to grow through time to a maximum of ~−60 °C in the lithosphere and −11 °C within the sediments (Fig. 3b, c). Our model further predicts that after thrusting and subsidence ceased, the thermal anomaly would have decayed to −20 °C in the lithosphere.

The thermal anomaly within the sediments has an important effect on the calculation of maturation history within the deepest sediments modelled. The time-temperature index (TTI) of Waples<sup>22</sup>, calculated from the results of our thermal model, is lower than the TTI calculated assuming that thermal equilibrium is maintained throughout the subsidence history (Fig. 4a). The lower TTI values imply that the timing of peak oil generation would be delayed by ~4 Myr relative to that for equilibrium thermal gradients. The surface gradients are higher than predicted by the results of Hacquebard<sup>23</sup> and Majorowicz *et al.*<sup>19</sup>, who suggest that the gradient for the westernmost Alberta basin in Eocene time was about 22 °C km<sup>−1</sup>. The calculation of the equilibrium and the time-dependent temperature histories from our model imply a higher degree of maturation than that which would be calculated using a constant temperature gradient of 22 °C km<sup>−1</sup>. In general, the assumption of constant gradients through time in foreland basins<sup>19,24</sup>, based on the present thermal gradients, is likely to yield maturation values that are too low

in the deeper parts of a foreland basin and too high in the shallower parts. Calculation of thermal gradients based on current maturation values in the western Alberta Basin by Beaumont *et al.*<sup>25</sup> yielded slightly higher gradients (26 °C km<sup>−1</sup>) than those predicted for the Getty Union Oyster well by our model. Their thermal gradients yield correct final maturation values but may not accurately predict the timing of earlier maturation phases. Our modelling indicates that, in calculating maturation, it is not reasonable to assume that thermal gradients were constant throughout the history of foreland basin subsidence.

The decay of the thermal anomaly predicted by our model leads to thermal expansion and lower density within the crust and upper mantle. During subsidence of the basin the increasing buoyancy requires an increase in the driving force which produces subsidence. (The driving force is defined as the difference between the force required for the observed subsidence and the force exerted by the sediments.) The force is probably that portion of the downward force of the thrust loads which, because of the rigidity of the lithospheric plate, is transmitted to the location of the well being modelled. For the Getty Union Oyster well, the driving subsidence increases to ~122% of that which seems to be necessary in the absence of the thermal effects (Fig. 4b). In contrast to the calculation of thermal history, the driving force is dependent on several poorly constrained factors including palaeo-water depth, palaeo-sea level and the flexural response of the lithosphere to the sediment load. Of these effects, only paleo-water depths have been included in the modelling. From middle Jurassic to late Cretaceous, the sea level was rising<sup>26</sup>. Ignoring this change, therefore, results in an overesti-

mate of the subsidence resulting from the driving force. The reverse is the case when sea level fell from late Cretaceous to the present. Ignoring the flexural response of the lithosphere to sediment loading results in an underestimate of the driving force in the deeper part of the basin (the location of the Getty Union Oyster well). Airy isostasy overestimates the force of the sediments acting on the lithosphere directly beneath the greatest loads because the sediment load in the deepest parts of the basin is supported not only by the lithosphere directly beneath it but also by the adjacent lithosphere. Although the driving force is dependent on these corrections (sea level, flexural rigidity and water depth), the thermal history predicted by the model is not, and any correction made to the loading force curve calculated by the thermal model must also be made for the curve which ignores the temperature effect. Thus, the effect of the thermal history of the foreland basin on the buoyancy force, which is illustrated in the difference between the two curves in Fig. 4*b*, is independent of these uncertainties.

During depositional hiatuses and after cessation of loading, the heating of the lithosphere as the thermal anomalies decay will cause thermal expansion and uplift of the basin. In the Getty Union Oyster well, an uplift of ~5 m is predicted during the 6-Myr hiatus in the early Cretaceous. About 115 m of uplift is predicted since the end of subsidence (Fig. 4*c*). This accounts for only 12% of the present-day regional tilt from the foothills to the cratonic edge of the Alberta Basin. The remainder of the uplift may be derived from erosion of the mountain load. Alternatively, it could result from a decoupling of the load from the down-bent plate resulting from regional lithospheric heating in western North America<sup>27</sup>. At the Getty Union Oyster well site, complete decoupling would require the removal of the total driving force (per unit area),  $30.5 \times 10^7$  dynes cm<sup>-2</sup>, resulting in 945 m of uplift. With the addition of thermal expansion, the total uplift is 1,060 m. This amount of uplift is quite close to the observed difference in elevation between the foothills and the cratonic edge of the basin<sup>24,28,29</sup>. A decoupling of the load with the basin is consistent with the gravity modelling of McNutt<sup>30</sup>. Her residual gravity anomaly map shows no paired anomaly in the Alberta foreland region, indicating that only local isostasy operates.

The heating of the lithosphere as the negative thermal anomaly decays also affects the temperature-dependent mechanical properties of the lithosphere. As the lithosphere gets hotter, its rigidity is reduced. The original thickness of the mechanical plate is assumed to have been 41 km. This is the apparent elastic thickness of old oceanic lithosphere<sup>31</sup> and is also the elastic plate thickness used to model the Green River Basin<sup>2</sup>. Our model predicts that heating of the lithosphere over the course of foreland subsidence reduces the elastic plate thickness by ~8 km (Fig. 4*d*). Because elastic rigidity is proportional to the cube of the elastic thickness, this result implies a 47% loss of flexural rigidity. Thus, the response of the lithosphere to loading is significantly affected, causing the plate to appear less rigid as subsidence continues. The magnitude of the loss in rigidity caused by heating is less than that predicted by the viscoelastic model of Beaumont<sup>1</sup> for the Alberta Basin but is similar in magnitude to that predicted by the thermally controlled creep model of Quinlan and Beaumont<sup>4</sup>. In our model the magnitude of the apparent viscosity of the lithosphere diminishes with distance from the load, resulting in a plate of variable rigidity. The effects of heating in foreland basin settings are complex and would be expected to result in a significant time-dependence in the response of the lithosphere to loading which should be taken into account in mechanical modelling of foreland basins. Neither the thermal heating nor any viscoelastic models predict the total loss of rigidity indicated by the current regional topography of the Alberta Basin. This implies that some event, not related to foreland basin formation, has subsequently affected the Alberta Basin.

In conclusion, our modelling of the thermal effects of episodic

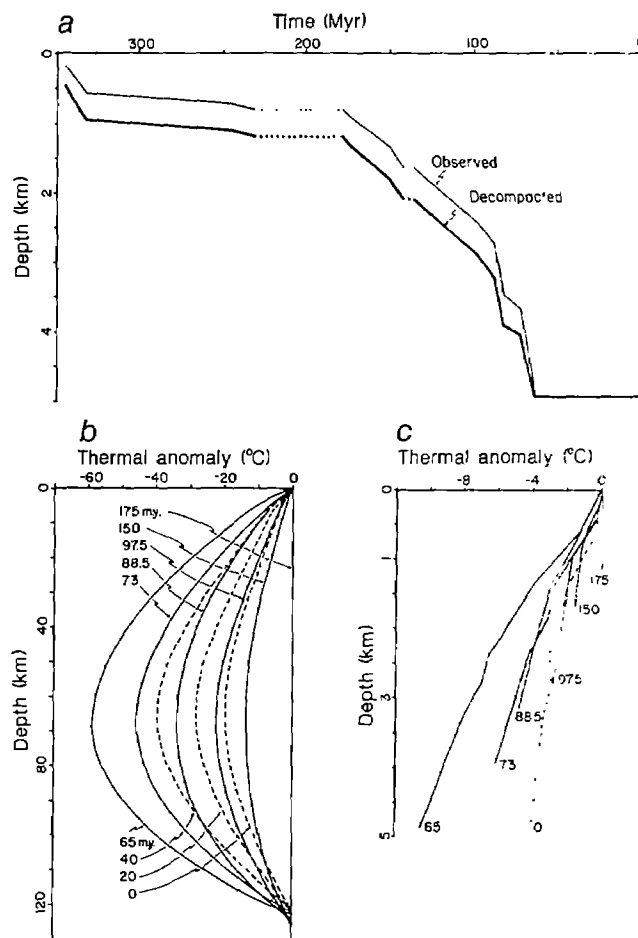


**Fig. 3** *a*, Observed and decompacted subsidence history of the Getty Union Oyster well. The observed curve is a plot of cumulative thicknesses of the present-day sediments. The decompacted subsidence curve shows the subsidence of the basin with compaction of sediments taken into account. The decompacted subsidence curve specifies the subsidence history of the basin at the well, and serves as input for the thermal model. Profiles of thermal disequilibrium in the lithosphere (*b*) and the sediments (*c*) are plotted for specific times during and after active foreland basin subsidence. Foreland basin subsidence begins at 175 Myr, at which time there is no thermal anomaly. The thermal anomaly grows with time during foreland basin subsidence and decays after cessation of thrusting (65–0 Myr).

subsidence in a foreland basin shows that significant thermal anomalies are formed. The episodic subsidence history of the westernmost Alberta Basin, in which 3.75 km of sediments were deposited in 110 Myr, led to a thermal anomaly of  $-60^\circ\text{C}$  in the lithosphere and an anomaly of  $-11^\circ\text{C}$  in the sediments. While the anomaly in the sediments is small, and may be overwhelmed by local variations in temperature, it does represent a systematic effect which has been shown to be sufficient to reduce the final maturation level of the sediments. An implication of our model is that the heating of the lithosphere caused by the decay of the thermal anomaly is sufficient to modify significantly the results of the purely mechanical models that have been proposed for foreland basins. The growth and removal of the thermal anomaly within the lithosphere results in an increase in the force necessary to cause subsidence by ~22%. The buoyancy force is manifested as thermally driven uplift during periods in which loading is not active, possibly causing basin-wide unconformities. Uplift of 115 m, after cessation of subsidence, is predicted for the Alberta Basin. A decrease in the rigidity of the plate by ~47% would appear as an apparent viscous relaxation of the plate. In many foreland basins, the

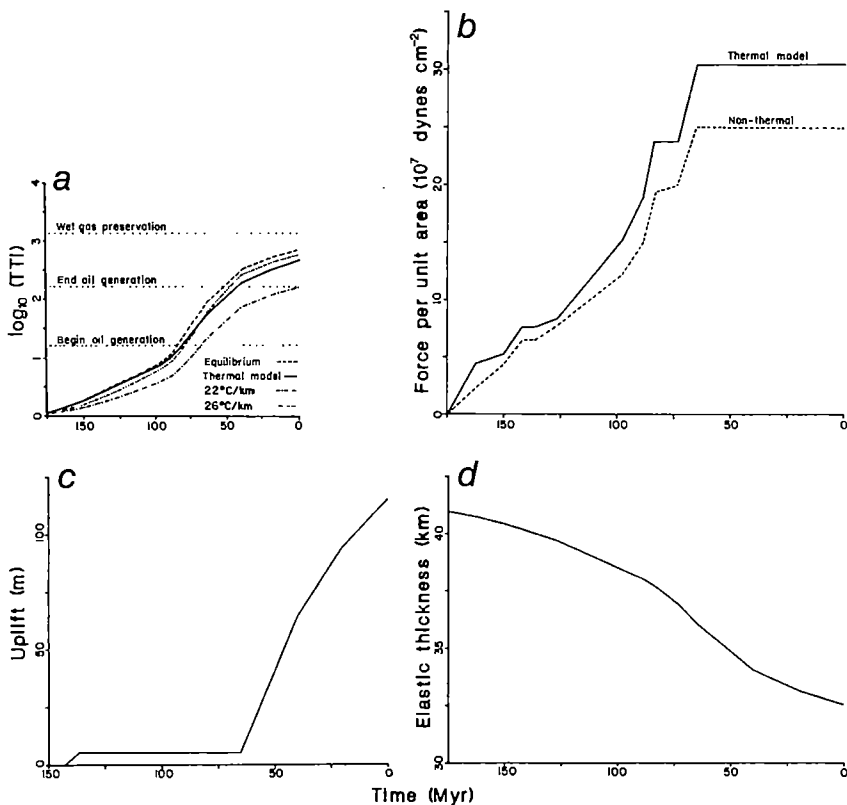


**Fig. 4** *a*, Hydrocarbon maturation history predicted for Carboniferous strata in the Getty Union Oyster well, log TTI, as calibrated by Waples<sup>22</sup>, is plotted as a function of time. Solid (dotted) line, model result, taking (not taking) into account the thermal effects of rapid subsidence. *b*, The driving force per unit area applied to the lithospheric slab beneath the Getty Union Oyster well is shown for the case in which the thermal effects of subsidence are ignored and for the case in which the buoyancy force resulting from heating of the thermal anomaly is included. *c*, During times in which loading is not active, the buoyancy force causes uplift of the basin. The uplift during a 6-Myr depositional hiatus and after cessation of subsidence are plotted for the Getty Union Oyster well. *d*, Depth to the base of the elastic plate, assuming an initial elastic plate thickness of 41 km. The elastic thickness of the plate decreases over time as the negative thermal anomaly decays.

rates and/or magnitudes of subsidence are greater than those preserved in the Getty Union Oyster well. In such basins, the thermal anomalies and associated effects would be larger than those predicted for southwestern Alberta.

This work was supported by funding from Texaco USA, ARCO Oil and Gas Company and the American Association of Petroleum Geologists Grants-in-Aid program. Well data from the Alberta Basin were provided by Shell Canada Resources Ltd. We thank W. C. Pitman III, M. Langseth, N. Christie-Blick and A. B. Watts for critical reading of the manuscript. Lamont-Doherty Geological Observatory contribution no. 3947.

Received 10 June 1985; accepted 10 January 1986.

1. Beaumont, C. *Geophys. J. R. astr. Soc.* **65**, 291–329 (1981).
2. Jordan, T. E. *Bull. Am. Ass. Petr. Geol.* **65**, 2506–2520 (1981).
3. Karner, G. D. & Watts, A. B. *J. geophys. Res.* **88**, 10449–10477 (1983).
4. Quinlan, G. M. & Beaumont, C. *Can. J. Earth Sci.* **21**, 973–996 (1984).
5. Karner, G. D., Steckler, M. S. & Thorne, J. A. *Nature* **304**, 250–253 (1983).
6. Kominz, M. A. & Bond, G. C. *Geol. Soc. Am. Abstr.* **14**, 534 (1982).
7. Clauzing, A. M. in *Advanced Heat Transfer* (ed. Chao, B. T.) 156–216 (Univ. Illinois Press, 1969).
8. Bond, G. C. & Kominz, M. A. *Bull. geol. Soc. Am.* **95**, 155–173 (1984).
9. Gretener, D. W. *Edus Course Note Ser.* No. 17 (Am. Assoc. Pet. Geol., Tulsa, 1981).
10. Beck, A. E. *Geophys. J. astr. Soc.* **70**, 667–715 (1976).
11. Bethke, C. G. thesis, Univ. Illinois (1985).
12. Smith, L. & Chapman, D. S. *J. geophys. Res.* **88**, 593–608 (1983).
13. Hitchon, B. *Bull. Am. Ass. Petr. Geol.* **68**, 713–743 (1984).
14. Garven, G. & Freeze, R. A. *Am. J. Sci.* **284**, 1085–1124 (1984a).
15. Garven, G. & Freeze, R. A. *Am. J. Sci.* **284**, 1125–1174 (1984b).
16. Majorowicz, J. A. & Jessop, A. M. *Tectonophysics* **74**, 209–238 (1981).
17. Slater, J. G., Jaupart, C. & Galson, D. *Rev. Geophys. Space Phys.* **18**, 269–311 (1980).
18. Deroo, G., Powell, T. G., Tissot, B. & McCrossan, R. G. *Bull. geol. Surv. Can.* **262**, 1–136 (1977).
19. Majorowicz, J. A., Ragman, M., Jones, F. W. & McMillan, N. J. *Bull. Can. Petr. Geol.* **33**, 12–21 (1985).
20. Bally, A. W., Gordy, P. L. & Stewart, G. A. *Bull. Can. Petr. Geol.* **14**, 337–381 (1966).
21. Porter, J. W., Price, R. A. & McCrossan, R. G. *Am. Ass. Petr. Geol. Memoir* **9**, 1238–1284 (1982).
22. Waples, D. W. *Bull. Amer. Ass. Petr. Geol.* **64**, 916–926 (1980).
23. Haquebard, P. A. *Bull. geol. Surv. Can.* **262**, 11–23 (1977).
24. Moshier & Waples, D. W. *Bull. Am. Ass. Petr. Geol.* **69**, 161–172 (1985).
25. Beaumont, C., Boutilier, R., MacKenzie, A. S. & Rulkötter, J. *Bull. Am. Ass. Petr. Geol.* **69**, 546–566 (1985).
26. Vail, P. R., Mitchum, R. M. & Thompson III, S. *Mem. Am. Ass. Petr. Geol.* **26**, 83–97 (1977).
27. Sass, J. H. et al. *Physical Properties of Rock and Minerals* (eds Touloukian, Y. S., Judd, W. R. & Roy, R. F.) (McGraw-Hill, New York, 1981).
28. Gussow, W. C. “Regional geological cross sections of the Western Canadian sedimentary cover.” 1:1013760 scale; 6 sections on 1 sheet.
29. Magara, K. *Dev. Petr. Sci.* **9**, 11–46 (1978).
30. McNutt, M. J. *geophys. Res.* **85**, 6377–6396 (1980).
31. Watts, A. B., Bodine, J. H. & Steckler, M. S. *J. geophys. Res.* **85**, 6369–6376 (1980).

32. Weihmann, I. *Bull. Can. Petr. Geol.* **12**, 587–599 (1964).
33. Gibson, D. W. *Bull. Can. Petr. Geol.* **25**, 767–791 (1977).
34. Irish, E. W. *J. Bull. Can. Petr. Geol.* **18**, 125–155 (1970).
35. Norris, D. K. *Bull. Can. Petr. Geol.* **12**, p. 512–535 (1964).
36. Wall, J. H. & Rosene, R. K. *Bull. Can. Petr. Geol.* **25**, 842–867 (1977).
37. Roys, F., Jr., Warner, M. A. & Reese, D. L. *Rocky Mount. Ass. Geol. 1975 Guidebook* 41–54 (1975).
38. Irwin, D. *Rocky Mount. Ass. Geol. Spec. Publ.* No. 2 39 (1975).
39. McCrossan, R. G. & Glaister, R. P. *Geological History of Western Canada*, 232 (Alberta Society of Petroleum Geology, Calgary, 1966).
40. Rocky Mountain Assoc. Geologists *Geologic Atlas of the Rocky Mountain Region, USA* (Hirschfeld, Denver, 1972).
41. Harland, W. B. et al. *A Geologic Time Scale* (Cambridge University Press, 1982).

## <sup>36</sup>Cl in a halite layer from the bottom of the Dead Sea

M. Magaritz\*, A. Kaufman\*, Y. Levy\*, D. Fink†,  
O. Meirav† & M. Paul†

\* Isotope Department, Weizmann Institute of Science, Rehovot 76100, Israel

† Racah Institute of Physics, Hebrew University, Jerusalem, Israel 91904

Stable and radiogenic isotope compositions are commonly used to identify the solution from which minerals such as sulphate, carbonate and silicate were crystallized. Both the sources and the ages of evaporite deposits can be determined by measuring radioactive <sup>36</sup>Cl concentrations using new developments in accelerator mass spectrometry. Halite crystals found in saline sediments, which could not be measured by isotope techniques until this method was developed, are usually assumed to have precipitated from the lake water during former dry periods. In the case of the Dead Sea we tested this assumption by comparing the abundance of <sup>36</sup>Cl isotopes in a shallowly buried halite layer with that in the overlying water. We found that the <sup>36</sup>Cl/Cl ratio is significantly lower in the halite, which indicates that the salt did not crystallize from this water but from a solution originating from the Tertiary diapir underneath the sea or that the salt represents the top of the Mt Sdom formation diapir.

The two stable chlorine isotopes ( $^{35}\text{Cl}$  and  $^{37}\text{Cl}$ ) show a small isotope effect of the order of 3% (ref. 1) which can be used in studies of both recent and ancient evaporite deposits. A third isotope,  $^{36}\text{Cl}$ , which is cosmogenic with a half-life of 301,000 yr, can be used not only as a tracer of the depositional environment but also as the basis of a dating method for halite in the Pleistocene<sup>2</sup>.

The determination of  $^{36}\text{Cl}$  in natural water has already been used to demonstrate the influence of 'ancient' salts on present water systems<sup>3</sup>. Old salt sources (older than several half-lives) are characterized by very low  $^{36}\text{Cl}/\text{Cl}$  ratios<sup>4</sup> (these may be  $<0.5 \times 10^{-15}$ ). The ratio probably never falls below this value because of a second mode (non-cosmogenic) of  $^{36}\text{Cl}$  generation involving the capture of neutrons originating from the interaction of  $\alpha$  particles on light elements. In some cases the ratio can be higher because of local enrichment of uranium and thorium<sup>4</sup>.

The Dead Sea is located in the Jordan rift zone, which is the northern extension of the Syro-African Rift system. We found a layer of massive halite<sup>5-7</sup> under a thin layer of soft sediments in the northern Dead Sea. Although the thickness of the halite layer was not determined, its continuity was demonstrated by extensive coring, the almost homogeneous distribution of trace elements<sup>8</sup> and by seismic profiles (Z. Ben Avraham, Y.L. and J. K. Hall, in preparation).

We analysed a halite sample recovered from the bottom of a 0.4-m-long core taken near Ein Gedi at a depth of 250 m. Associated with the sample was a carbonate mud (70% aragonite, 30% calcite) which yielded a  $^{14}\text{C}$  age of  $500 \pm 500$  yr BP (taking into account that present-day Dead Sea water has an apparent age of 2,000 yr; ref. 6).

The halite was dissolved in water and its  $\text{Cl}^-$  precipitated with  $\text{Ag}^+$  and purified by dissolution in  $\text{NH}_3$  before the final reprecipitation as  $\text{AgCl}$ . We measured  $^{36}\text{Cl}$  in the  $\text{AgCl}$  target using the accelerator mass spectrometer system at the Rehovot 14UD Pelletron Tandem Laboratory<sup>9</sup>. Two samples run on different days yielded  $^{36}\text{Cl}/\text{Cl}$  values of  $6 \pm 3$  and  $7 \pm 5 \times 10^{-15}$ . These values should be compared with those of Dead Sea water and recent (1981) halite which precipitated on a rope suspended in the Dead Sea water column (Table 1).

The distinct difference between the  $^{36}\text{Cl}/\text{Cl}$  ratios in the samples obtained from Dead Sea water and in those of the salt sampled from the halite layer at the bottom of the Dead Sea exclude the possibility that it precipitated from Dead Sea brine either recently or during the past few tens of thousands of years. Yet the age of the chlorine in the water column was found to be between 19,000 and 25,000 yr, based on the  $^{36}\text{Cl}$  concentration and an input model presented by Paul *et al.*<sup>3</sup>. On the other hand, the  $^{36}\text{Cl}/\text{Cl}$  ratio is very similar both to that of Mt Sdom halite taken from a depth of 2,000 m and that of the Ashlag Springs, which represent solutions associated with the Mt Sdom formation (Table 1). Although the last three values in Table 1 are

higher than ratios measured in some old deposits<sup>4</sup>, they are the lowest determined in our laboratory. These values can be explained either by local enrichments of U-Th as mentioned above, or by experimental effects such as cross-contamination during sample preparation or ion source operation.

Several models can be proposed to explain the origin of the halite layer based on its  $^{36}\text{Cl}/\text{Cl}$  ratio and on other geochemical and geophysical evidence: (1) The halite is the topmost layer of a salt diapir<sup>10</sup>. Neev and Hall<sup>10</sup> believe that the diapiric structures detected in seismic profiles indicate the occurrence of rock salt masses of the Mt Sdom formation in different areas of the northern basin of the Dead Sea. (2) The salt was deposited recently from interstitial chloride-bearing solutions that diffused upward from the underlying Mt Sdom formation and not from the contemporary Dead Sea brine. This model can explain the co-occurrence of 'old' salt with sediments whose young age ( $500 \pm 500$  yr BP) is indicated by the  $^{14}\text{C}$  dating of the carbonate fraction. If one accepts this model and the observations of Ben Avraham *et al.* (in preparation) that the salt layer covers most of the floor of the northern Dead Sea, one has to postulate that a brine is diffusing upwards under most of the present-day Dead Sea bottom sediments. According to this model, most of the chlorine dissolved in the present-day Dead Sea brine is derived from the dissolution of rock salt. This is consistent with the findings of Paul *et al.*<sup>3</sup>, based on Cl and  $^{36}\text{Cl}$  balances, that the ratio of the  $\text{Cl}^-$  derived from rocks to the  $\text{Cl}^-$  derived from rain is 100 for the Dead Sea. (3) The halite layer was precipitated following an event during which concentrated saline solutions<sup>11</sup> of the Ashlag Spring type flowed to the bottom of the Dead Sea in large quantities and remained there because of their high density. Table 1 demonstrates that such solutions are characterized by low  $^{36}\text{Cl}/\text{Cl}$  ratios.

These models cannot be differentiated by geochemical methods because in all three, the halite is either part of the Mt Sdom formation or derived from a solution of its salt. Another geochemical parameter that has been suggested as an indicator of the salt's origin is the  $\text{Cl}/\text{Br}$  ratio. This ratio, found to be 3,500–5,300 in the halite layer, is similar to that in Mt Sdom salt and significantly different from the value (1,100) found in halite precipitating from modern Dead Sea water<sup>8</sup>. On the basis of such evidence, Bloch and Picard<sup>12</sup> suggested a Neogene age (the age of Mt Sdom salt) for the halite layer. However,  $\text{Cl}/\text{Br}$  ratios alone are no more than indicative, as halite is known to lose some of its bromide during diagenetic changes.

We can conclude that: (1) the halite does not represent a Dead Sea water precipitate; (2) the halite is associated with Mt Sdom salt, either by being part of the Mt Sdom formation or by originating from a solution whose  $\text{Cl}^-$  is derived from Mt Sdom salt; and (3) the association of the old salt and young  $\text{CaCO}_3$  in the halite layer may favour the second or third hypothesis. Further measurements of  $^{36}\text{Cl}$  in interstitial water and in additional halite samples may elucidate the processes that led to the formation of the halite layer studied.

This work was supported in part by the Bat-Sheva Foundation for Science and Technology and by the Minerva Foundation.

Table 1 Results of  $^{36}\text{Cl}$  determination of samples from the Dead Sea area

	$^{36}\text{Cl}/\text{Cl}^*$ ( $10^{-15}$ )
Dead Sea	
Surface	$17 \pm 4$
80 m†	$17 \pm 2$
310 m	$20 \pm 4$
Ashlag Spring	$4 \pm 2$
Mt Sdom salt	$5 \pm 2$
Halite layer (Dead Sea core)	$6 \pm 3$

\* The value shown is the weighted mean of independent measurements  $\pm$  variance of the mean.

† From halite crystals deposited on a rope suspended in Dead Sea water.

Received 23 September 1985; accepted 15 January 1986.

- Kaufman, R., Long, A., Bentley, H. & Davis, S. *Nature* **309**, 50–52 (1984).
- Phillips, F. M., Smith, G. I., Bentley, H. W., Elmore, D. & Grove, H. E. *Science* **222**, 925–927 (1983).
- Paul, M. *et al.* *Nature* (submitted).
- Bentley, H. W., Phillips, F. M. & Davis, S. N. in *Handbook of Environmental Isotope Geochemistry* Vol. 2 (eds Fritz, P. & Fontes, J. C.) (Elsevier, Amsterdam, in the press).
- Volcani, B. E. in *The Microorganisms of the Dead Sea*, 71–85 (Stern Research Institute, Rehovot, 1944).
- Neev, P. & Emery, K. O. *Bull. geol. Surv. Israel* **41** (1967).
- Beyth, M. in *Developments in Sedimentology* (ed. Nissenbaum, A.) 155–164 (Elsevier, Amsterdam, 1980).
- Levy, Y. *Rep. geol. Surv. Israel GSI/48/84* (1984).
- Fink, R. *et al.* *Nucl. Instrum. Meth. Phys. Res.* **135**, 123–125 (1974).
- Neev, D. & Hall, F. K. *Sed. Geol.* **25**, 209–238 (1979).
- Benton, Y. K. *Geochim. cosmochim. Acta* **25**, 230–260 (1961).
- Bloch, M. R. & Picard, L. Z. *dt. Geol. Ges. Sonderh. Hydrogeol. Chem.*, 119–128 (1970).

## Carbon-isotope events across the Precambrian/Cambrian boundary on the Siberian Platform

Mordekai Magaritz\*, William T. Holser† & Joseph L. Kirschvink‡

\* Isotopes Department, Weizmann Institute, Rehovot 76100, Israel

† Department of Geology, University of Oregon, Eugene, Oregon 97403, USA

‡ Division of Geological and Planetary Sciences, The California Institute of Technology, Pasadena, California 91125, USA

Variations of marine isotopes with time have been observed through the Phanerozoic<sup>1,2</sup>, in association with some period boundaries: Pleistocene/Holocene<sup>3</sup>, Cretaceous/Tertiary<sup>4</sup>, Permo-Triassic<sup>5,6</sup> and Frasnian/Famennian<sup>7</sup>. Most of these changes are associated with extinction events, reflecting changes in life on Earth. One of the major biological changes in Earth's history occurred near the end of Proterozoic time, with widespread increase of biomineralization and the appearance of shelly fauna<sup>8–10</sup>. We present here an initial survey of carbon isotope ratios in a section on the Siberian Platform that spans the Proterozoic/Palaeozoic boundary. After a high of  $\delta^{13}\text{C} = +3.4\text{\textperthousand}$ , 15 m below the boundary,  $\delta^{13}\text{C}$  drops sharply in two cycles across the boundary, to  $\delta^{13}\text{C} = -2\text{\textperthousand}$  near the end of the Tommotian Stage. These variations suggest an initial bloom of biomass in late Vendian time corresponding to the dramatic diversification that must have preceded the widespread appearance of new taxa in the Cambrian fossil record.

The section studied comprises 250 m of carbonate rocks that include the Yudoma Formation of late Vendian age and the Pestrotsvet Formation of Tommotian age along the Aldan River (Dvortsy section, 57.47° N, 129.30° E, 650 km south of Yakutsk) on the Siberian Platform in Yakutia<sup>11–13</sup>. The Vendian/Tommotian boundary, close to the top of the Yudoma Formation, is a candidate for designation as a stratotype of the Precambrian/Cambrian boundary<sup>14</sup>. Arguments have been advanced against this selection<sup>15–17</sup>, but our concern here is with the fossil record rather than the formalities of stratigraphy. Consequently in the following discussions we will informally refer to the Vendian/Tommotian boundary as the Precambrian/Cambrian (P/C/C) boundary. The Dvortsy sequence is transgressive over a shelf of the Archaean Aldan Shield, and this is part of a worldwide transgression that continues through Tommotian time<sup>18</sup>. The rocks range from very fine (<10  $\mu\text{m}$ ) pelletal dolomite to medium-coarse (100–150  $\mu\text{m}$ ) xenomorphic dolomites. Part of the topmost Vendian sequence is dolomite replacing earlier oolitic sediments. As one approaches the suggested P/C/C boundary from below, de-dolomitization and staining with iron oxide indicate an unconformity, suggested by Khomentovsky *et al.*<sup>11</sup>. Our Cambrian samples were also dominantly dolomite, although this section is often described as limestone<sup>11</sup>.

Our samples were obtained as part of IGCP Project 29, and were collected in a similar fashion to a previous set of Tommotian samples from along the Lena River, studied for magnetostratigraphy by Kirschvink and Rozanova<sup>19</sup>. Palaeomagnetic studies of the new samples are in progress by Kirschvink.

$\text{CO}_2$  for mass spectrometry was generated by the method of Magaritz and Kafri<sup>20</sup>.  $\text{CO}_2$  generated by calcite in the dedolomite was removed, and then the remaining dolomite reacted to provide the measured sample. Although the section has suffered dolomitization, probably in an early diagenetic stage, we know from much younger dolostones that the dolomite preserves the original  $\delta^{13}\text{C}$  values<sup>21,22</sup>.

From the base of the Dvortsy section  $\delta^{13}\text{C}$  becomes gradually more positive, from  $\delta^{13}\text{C} = -4$  to  $+3.4\text{\textperthousand}$  (Fig. 1). The most

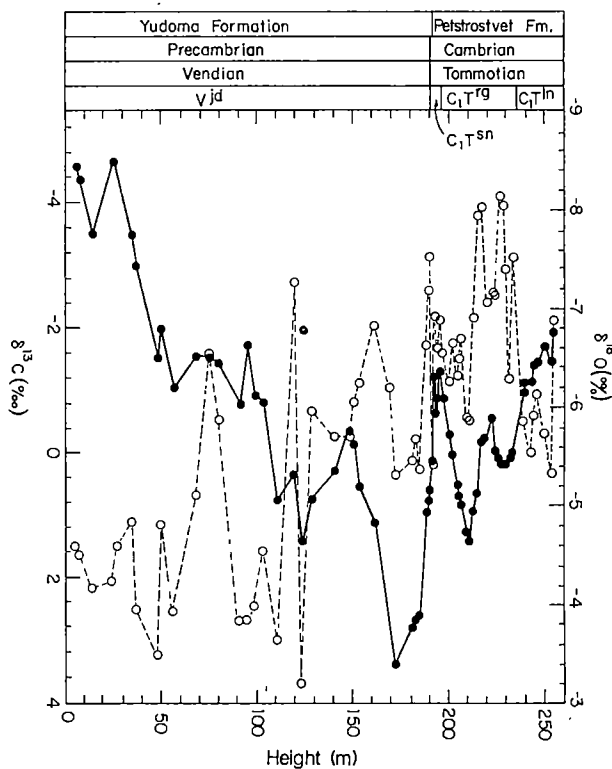


Fig. 1 Profiles of  $\delta^{13}\text{C}$  (●, solid line) and  $\delta^{13}\text{O}$  (○, dashed line) at the Dvortsy section, Aldan River, Yakutia. The metre scale corresponds to the standard scale scribed on the outcrop, which starts at an arbitrary zero about 10 m above the unconformity on the Archaean; the isotope profile begins at +10 m on that scale, or about 20 m above the unconformity. Stratigraphical zone symbols<sup>11</sup>: Vjd, Vendian Yudoma Formation; C<sub>1</sub>T<sup>sn</sup>, Cambrian Tommotian Pestrotsvet Formation, *A. sunnaginiulus* zone; C<sub>1</sub>T<sup>rg</sup>, *D. regularis* zone; C<sub>1</sub>T<sup>ln</sup>, *D. lenaicus* zone.

positive samples are found at about 170 m, 15 m below the P/C/C boundary. From this point, a decline of  $\delta^{13}\text{C}$  to a minimum of  $\delta^{13}\text{C} = -1.3\text{\textperthousand}$  crosses the P/C/C boundary, as well as the rest of the Yudoma Formation and the *Aldanocyathus sunnaginiulus* zone (Fig. 1: C<sub>1</sub>T<sup>sn</sup>, of lower Tommotian age) of the Pestrotsvet Formation. From this point,  $\delta^{13}\text{C}$  rises sharply by 2‰ within a 15-m section of the *Dokidocyathus regularis* zone (Fig. 1: C<sub>1</sub>T<sup>rg</sup>, of middle Tommotian age), and then decreases by 3.3‰ to the end of the analysed section about 10 m below the Tommotian/Atdabanian boundary.

The rise of 7.5‰ in  $\delta^{13}\text{C}$  (Fig. 1) within the Vendian, is at an average rate of change of  $0.04\text{\textperthousand m}^{-1}$ . The second rise, in the *D. regularis* zone (C<sub>1</sub>T<sup>rg</sup>) is of the order of  $0.2\text{\textperthousand m}^{-1}$ , about five times as fast as in the late Vendian, on the admittedly tenuous assumption of a uniform sedimentation rate. The drop of  $\delta^{13}\text{C}$  across the P/C/C boundary is at a faster rate, of  $0.5\text{\textperthousand m}^{-1}$ . Part of this section may be missing at the unconformity, which may mean that the drop is at a similar rate to the previous Vendian increase. Because each of these changes continues over a thick sequence, it is likely that none of them is caused by an instantaneous mechanism. The carbon isotope variations reflect corresponding variations of  $\delta^{13}\text{C}$  in  $\text{HCO}_3$  in shelf waters, which presumably equals that of the surface ocean water mass. Several models have been proposed to explain variations of  $\delta^{13}\text{C}$  in surface ocean waters. For this case, we can ignore those models dependent on the mass of land flora. The remaining models are: (1) changes in biological productivity in the surface ocean<sup>23</sup>; (2) changes in vertical circulation rate for the whole ocean<sup>24</sup>; (3) changes in the fractional preservation of organic carbon on the sea floor, caused by expansion and contraction of the oxygen-minimum zone<sup>25</sup>.

Although we have only a single profile, previous experience with profiles of  $\delta^{13}\text{C}$  at other boundaries suggests that at least the general trends of variation represent worldwide oceanic events, rather than simply basinal changes.

The number and size of phosphorite deposits near the P/C boundary is unequalled at any other time in the geological record<sup>12,26,27</sup>. Phosphorite deposition suggests increased biological productivity, which (model (1)) should increase  $\delta^{13}\text{C}$  in these surface waters. Cook and Shergold<sup>26</sup> connect this burst of phosphorite deposition with the explosive faunal diversification in early Cambrian times, including taxa with phosphatic skeletons. Their time control for the phosphate event(s) is necessarily imprecise, and carbon isotope profiles may eventually refine this course of events. In accordance with the above model, the two periods of increased  $\delta^{13}\text{C}$  correspond to increases in biological activity. The first rise of  $\delta^{13}\text{C}$  occurs in the Vendian system, which has little skeletal fauna and may correspond to a time of diversification, the descendants of which appeared at once in the early Cambrian. This general development was probably interrupted by a decline of productivity, revealed by the reversal across the P/C boundary, which recovered only in the *D. regularis* zone (middle Tommotian). A second decline continued to the top of our record of  $\delta^{13}\text{C}$  (Fig. 1).

The changes of  $\delta^{13}\text{C}$  in Fig. 1 probably represent a final episode of a long record of generally high  $\delta^{13}\text{C}$  in late Proterozoic time, as displayed in thick sections in Svalbard and Greenland (A. H. Knoll, personal communication). In that view, the low  $\delta^{13}\text{C}$  with which our shorter section begins would have been only a temporary drop to a low value.

On a section that is still shorter than ours,  $\delta^{13}\text{C}$  across a zone designated as the P/C boundary at two localities in China shows a sharp negative excursion within 20 cm of the boundary, associated with a possible iridium anomaly<sup>28,29</sup>. However, the levels at which the P/C boundary has been placed in China and Siberia are probably not stratigraphically correlative. In any case, our sampling would probably have missed so sharp an excursion as found in China.

The  $\delta^{18}\text{O}$  values in Fig. 1 have a negative trend, from a mean of  $-4\text{\textperthousand}$  in the first 150 m of our Vendian section, to about  $\delta^{18}\text{O} = -7\text{\textperthousand}$  in the rest of our Vendian and Cambrian section. No major change occurred at the P/C boundary. The correlation of  $\delta^{18}\text{O}$  with  $\delta^{13}\text{C}$  is  $-0.36$ , whereas a positive correlation would have been expected if both  $\delta^{13}\text{C}$  and  $\delta^{18}\text{O}$  had been distorted by freshwater diagenesis. As with other dolomites, one cannot be sure that they preserve an original record of  $\delta^{18}\text{O}$ . Further analyses, especially of phosphate  $\delta^{18}\text{O}$  (ref. 29), may help to explain the variations in  $\delta^{18}\text{O}$ .

This research was funded in part by NSF research grant 8400222 to the University of Oregon, and 8121377 to the California Institute of Technology. This article is a contribution to IGCP Project 29: Precambrian/Cambrian Boundary, and to IGCP Project 199: Rare Events in Geology. A. Yu. Rozanov provided expert guidance to Kirschvink in the field. We thank T. Galin, R. Selnikov and M. Feld for mass spectrometry measurements. A. H. Knoll contributed helpful discussion on Proterozoic geology, palaeontology, and geochemistry.

**Note added in proof:** The recent paper by Tucker<sup>31</sup> gives a carbon isotope profile across the P/C boundary in the Anti-Atlas of Morocco. In that section the boundary is undefined within a 200-m section, which in turn forms part of a 300-m interval for which Tucker has no  $\delta^{13}\text{C}$  data. But Tucker's  $\delta^{13}\text{C}$  values rise from  $-3\text{\textperthousand}$  below this interval to  $+2.5\text{\textperthousand}$  above this interval, which probably corresponds to the late Vendian rise in Fig. 1 above. A more complete profile of  $\delta^{13}\text{C}$  in the Moroccan section may give a precise correlation with the Siberian section.

Received 23 September; accepted 30 December 1985.

1. Veizer, J., Holser, W. T. & Wilgus, C. K. *Geochim. cosmochim. Acta* **44**, 579–587 (1980).
2. Saltzman, E. S., Lindh, T. B. & Holser, W. T. *Geol. Soc. Am. Abstr. Prog.* **14**, 607 (1982).
3. Shackleton, N. J., Imbrie, J. & Hall, A. *Earth planet. Sci. Lett.* **65**, 233–244 (1983).

4. Perch-Nielsen, K., McKenzie, J. & Qizhang He. *Geol. Soc. Am. Spec. Pap.* **190**, 353–371 (1980).
5. Holser, W. T. & Magaritz, M. *Jhb. Geol. Bundesanst. Wien* **128**, 75–82 (1985).
6. Chen J., Shao M., Huo W. & Yao Y. *Scient. Geol. Sinica* **1984**, 88–93 (1984).
7. Playford, P. E., McLaren, D. J., Orth, C. J., Gilmore, J. S. & Goodfellow, W. D. *Science* **226**, 437–439 (1984).
8. Brasier, M. D. *Systematics Ass. Spec. Vol.* **12**, 103–159 (1979).
9. Lowenstam, H. A. and Margulis, L. *Biosystems* **12**, 27–41 (1980).
10. Jiang Zhiwen *Geol. Mag.* **123**, 185–188 (1984).
11. Khomontovsky, V. V., Rozanov, A. Yu., Nuzhnov, S. V. & Fradkin, G. S. (Directors). *Int. Geol. Congr., 27th, Moscow, Guidebook 052-055*, 174–199 (1984).
12. Rozanov, A. Yu. *Episodes*, **7**, 20–24 (1984).
13. Rozanov, A. Yu. & Rozanov, A. Yu. *Litol. Polez. Iskop.* no. 5, 106–111 (1973) [transl: *Lithol. Min. Res.* **8**, 613–617 (1974)].
14. Cowie, J. W. & Rozanov, A. Yu. *Geol. Mag.* **120**, 129–139 (1983).
15. Savitsky, V. E. *Geol. Mag.* **115**, 127–130 (1978).
16. Luo H. et al. *Sinian-Cambrian boundary stratotype section at Meischucun, Jining, Yunnan, China* (People's Publishing House, Yunnan, 1984).
17. Cowie, J. W. *Episodes* **8**, 93–97 (1985).
18. Brasier, M. D. *Precamb. Res.* **17**, 105–123 (1982).
19. Kirschvink, J. L. & Rozanov, A. Yu. *Geol. Mag.* **121**, 189–203 (1984).
20. Magaritz, M. M. & Kafri, U. *Sedim. Geol.* **28**, 29–41 (1984).
21. Degens, E. T. & Epstein, S. *Am. Ass. petrol. Geol. Bull.* **46**, 534–542 (1962).
22. Magaritz, M. M. *Sedim. Geol.* **45**, 115–122 (1985).
23. Broecker, W. S. *Geochim. cosmochim. Acta* **46**, 1689–1706 (1982).
24. Bass, G. W., Southam, J. R. & Peterson, W. H. *Nature* **296**, 620–623 (1982).
25. Scholle, P. A. & Arthur, M. A. *Am. Ass. petrol. Geol. Bull.* **64**, 67–87 (1980).
26. Cook, P. J. & Shergold, J. H. *Nature* **308**, 231–236 (1984).
27. Brasier, M. D. *J. Geol. Soc. Lond.* **137**, 695–703 (1980).
28. Zheng Qin-wen et al. *Int. Geol. Correl. Proj. 99 Conf.*, Gwatt, Switzerland (1985).
29. Hsu, K. J. et al. *Nature* **316**, 809–811 (1985).
30. Kolodny, Y., Luz, B. & Naven, O. *Earth planet. Sci. Lett.* **64**, 398–404 (1984).
31. Tucker, M. E. *Nature* **319**, 48–50 (1986).

## Radiolarian and silicoflagellate response to oceanographic changes associated with the 1983 El Niño

Nicklas G. Pisias, David W. Murray  
& Adrienne K. Roelofs

College of Oceanography, Oregon State University, Corvallis, Oregon 97333, USA

Strong seasonal signals in fluxes and composition of siliceous microfossils have been recorded in sediment traps from two sites in the equatorial Pacific, deployed from December 1982 to March 1984. During the early part of the sampling period, the 1982–83 El Niño event had a profound effect on the radiolaria and silicoflagellates within these two areas. During the El Niño, the radiolarian trap assemblages at Site C ( $1^{\circ}$  N,  $139^{\circ}$  W) most resembled faunal assemblages in western equatorial Pacific sediments, whereas the trap assemblages resembled equatorial divergence sediments in the latter half of the period. At Site S ( $11^{\circ}$  N,  $140^{\circ}$  W), the radiolaria and silicoflagellate species can be correlated with organic carbon fluxes. In general, silicoflagellate shell fluxes are correlated to total opal fluxes where radiolarian fluxes do not exhibit this relationship. Approximately 20–25% of the total count of radiolaria in traps are not present in underlying sediments with a significant loss of the weakly silicified forms. However, the comparison of trap sample assemblages with underlying sediments reported here shows that dissolution does not alter relative abundances of the fossil species used in palaeoclimatic reconstructions. A significant difference is observed between the silicoflagellate trap assemblage and the underlying sediment assemblage.

The samples used in this study were collected with the Oregon State University single-cone traps equipped with five-cup sample changers<sup>1</sup>. The sampling period was 7 days for the first cup and ~100 days for each of the other four cups. At Site C the traps were deployed at 1,095, 1,895 and 3,495 m, at Site S, 700, 1,600 and 3,400 m. Microfossil assemblages were examined to determine the changes in the fluxes and species abundance associated with the marked changes in organic carbon fluxes measured in the sediment traps. In addition, we wanted to determine if the known distributions of radiolaria and silicoflagellates in surface sediments of the equatorial Pacific could be used to infer the

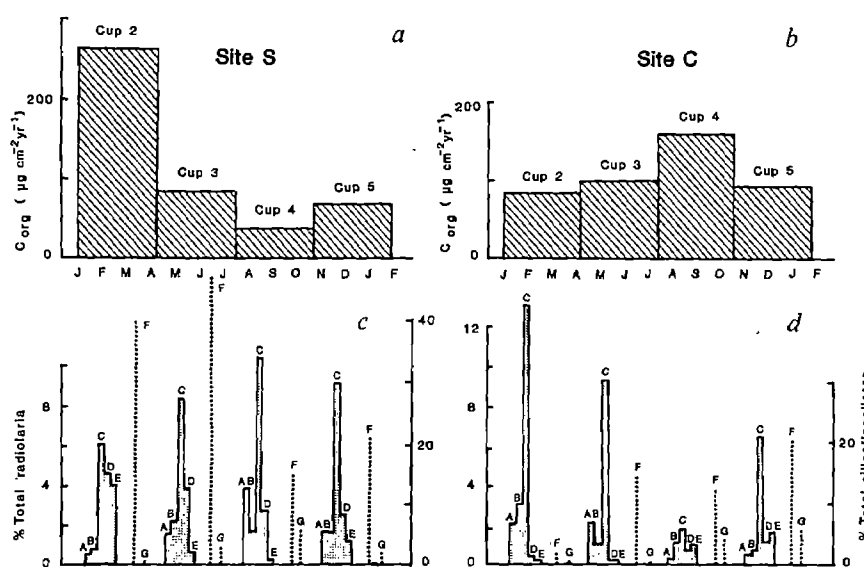


Fig. 1 Organic carbon fluxes at: a, Site S; and b, Site C for 1983; months abbreviated as single letters. Relative abundances of radiolarian (labelled A to E) and silicoflagellate (F and G) species at Site S (c) and Site C (d). Scale for radiolaria is to the left of frames c and d, silicoflagellates to the right. A, *H. entacanthum*; B, *D. tetrathalamus*; C, *T. octocantha/O. stenozena*; D, *P. minythora*; E, *B. auritus-australis*; F, *D. pulchra*, and G, *D. calida*.

nature of oceanographic conditions associated with changes in organic carbon transported to the deep sea.

The  $>63 \mu\text{m}$  fraction from sample splits was used to make quantitative radiolarian microfossil slides using a technique described elsewhere<sup>2</sup>. The average total count of radiolaria in each of the 24 trap samples was 750 with 142 species identified. The  $<63 \mu\text{m}$  fraction from each of the samples was used for preparing silicoflagellate slides. Approximately 250 silicoflagellates were counted in each sample with three species identified.

The estimated fluxes of radiolarian shells in the  $>63 \mu\text{m}$  fraction range from 65 to 332 shells  $\text{cm}^{-2} \text{yr}^{-1}$  at Site S and from 89 to 558 shells  $\text{cm}^{-2} \text{yr}^{-1}$  at Site C. These fluxes are a factor of 3–10 less than those measured by Takahashi<sup>3</sup> who studied radiolaria in both the coarse and fine fractions at stations in the tropical Pacific and Atlantic. Comparison of individual radiolarian species fluxes estimated in the Site S and C traps and those of Takahashi<sup>3</sup> are in good agreement. For example, the maximum fluxes measured for the species *Heliodiscus asteriscus*, *Spongaster tetras* and *Pterocorys zancleus* are 2, 6, and 18 shells  $\text{cm}^{-2} \text{yr}^{-1}$  as compared with other trap experiment values for these species of 1–2, 1–2 and 7–26 shells  $\text{cm}^{-2} \text{yr}^{-1}$  respectively<sup>3</sup>.

The organic carbon flux data used in this study is from ref. 4. The flux of organic carbon shows a marked response to the oceanographic events of 1982–83. During the early part of the trap deployment, organic carbon flux was at a minimum at Site C (Fig. 1). This would be expected from the general picture of reduced equatorial circulation associated with the El Niño event of 1983. However, the carbon flux measured at Site S at  $11^\circ\text{N}$  was extremely high ( $\sim 270 \mu\text{g cm}^{-2} \text{yr}^{-1}$ ). This flux is one of the highest 3-month values measured in the open ocean by the OSU trap programme (J. Dymond, personal communication). As the year progressed, organic carbon flux in the Site S traps fell dramatically to levels below  $80 \mu\text{g cm}^{-2} \text{yr}^{-1}$ , whereas at Site C, the carbon flux increased to a maximum value (Fig. 1). On an annual basis, the carbon flux was higher at Site S than at Site C. This is contrary to the expectation that Site C, within the equatorial divergence, would have the higher organic carbon flux as compared with Site S at the edge of the equatorial productivity belt.

We have found that the relationship between the fluxes of either total radiolarian shells or individual species fluxes is not as closely related to the flux of organic carbon ( $r^2 = 0.04–0.49$ ) as the relationship between radiolarian species composition and organic carbon fluxes ( $r^2 = 0.17–0.87$ ). Thus, we present here only the results from the comparison of radiolarian species composition and trap-measured organic carbon flux.

The results from the analysis of radiolarian species composition in the sediment trap samples are also shown in Fig. 1. The percentages of five radiolarian species are displayed for each of the four seasonal samples. The five species of radiolarian were selected for detailed study based on their distribution in surface sediments from the equatorial Pacific<sup>5,6</sup>, and all are important components of the deep-sea sediment thanatocoenoses.

*Tetrapyle octocantha/Octopyle stenozena* (counted together in both sediment traps and surface sediment samples) are one of the more abundant species of the equatorial region with highest abundances found in the eastern subtropical Pacific. *Hexactinum entacanthum* is found in the eastern equatorial Pacific in lower abundances than *T. octocantha/O. stenozena*, and also in the California Current region. *Didymocystis tetrathalamus* is also a tropical species but, unlike the previous two species, is found in highest abundances in sediments of the western Pacific.

Two other species were examined because of their association with eastern boundary currents and the equatorial divergence zone. *Pterocorys minythora* is found in highest abundance in the eastern equatorial Pacific and Peru Current region and in minor percentages off the southern coast of Baja California and Central America. *Botryostrobus auritus-australis* is found in the Peru and California Currents and in a narrow band along the Equator<sup>6</sup>. Thus, we hypothesize that increased equatorial divergence and its associated productivity would favour the increased abundance of these two radiolaria as compared with the other

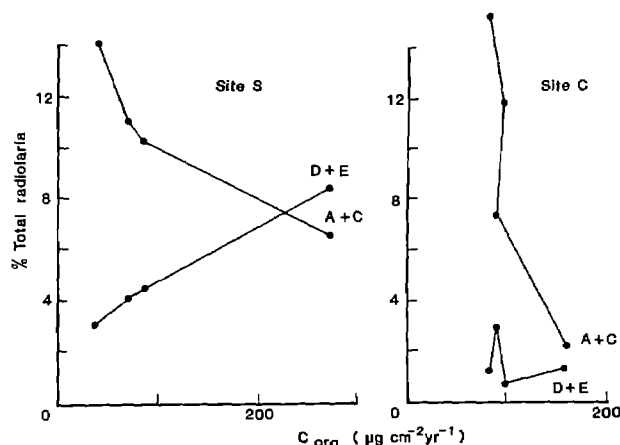
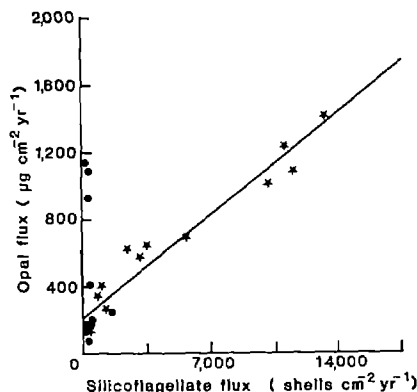


Fig. 2 Relative abundance of radiolarian species versus organic carbon flux in the near surface traps at Site C and Site S. Letters represent the same species as in Fig. 1.



**Fig. 3** Combined biogenic silica flux from all traps at all depths versus the total flux of silicoflagellates. ★, Site C; ●, Site S. Correlation coefficient of data (excluding the very high opal flux from cup 2 at Site S) equals  $r^2 = 0.94$ .

subtropical forms. The differing radiolarian fauna found in the eastern equatorial and western Pacific would also be useful in identifying different circulation patterns associated with the unusual oceanographic events of 1983 (refs. 7–9).

The data from the trap deployments support these hypotheses. A simple relationship is observed between the percentages of the inferred 'productivity' species *P. minytorax* and *B. auritus-australis* and the flux of organic carbon with increased percentages of these species corresponding to increased organic carbon flux (Fig. 2). The species *T. octacantha*/*O. stenozena* decreases in abundance with increasing organic carbon flux. A forced negative correlation between these species is not likely for two reasons. First, these species make up <20% of the total radiolarian count in which 142 species were identified. Second, up to 20% of the total count was not identified. Thus, at Site S, the marked changes in organic carbon flux due to the El Niño even of 1983 are reflected by changes in species abundance (Fig. 2).

At Site C, the relationship between carbon flux, radiolarian fauna and oceanographic events differs from that at Site S. The changes in the 'productivity' species shows very little correlation with the organic carbon flux ( $r^2 = 0.11$ ). We feel that this reflects the marked faunal abundance change which occurred during the sampling period. Twenty-five species, including *T. octacantha*/*O. stenozena* and *D. tetrathalamus*, have their highest abundance in cup 2 at Site C.

Sea-surface temperatures at Site C show a marked warm anomaly during the early part of the deployment, returning to near normal conditions by July of 1983 (ref. 4). This anomalously warm water, which was observed at the Equator throughout the Pacific<sup>7–9</sup> (but not at Site S), was a result of anomalous eastward transport along the Equator. The relative abundance of radiolaria at Site C indicates the presence of western Pacific waters during the early part of 1983. Comparison of the radiolarian fauna with surface sediment distributions shows that the sediment samples most similar to the fauna found in cups 2 and 3 of Site C are from the far western equatorial Pacific (Table 1). The fauna in cups 4 and 5 of Site C and all the cups of Site S most resemble samples from the eastern equatorial Pacific and Panama Basin (Table 1). Thus, at Site C where a major abundance change in the fauna occurred during the deployment, less correlation is found between the radiolarian fauna and organic carbon flux changes.

Silicoflagellates also demonstrate a marked response to the El Niño event. Seasonal silicoflagellate fluxes ranges from 73 to 1,277 shells  $\text{cm}^{-2} \text{yr}^{-1}$  at Site S and 365 to 14,600 shells  $\text{cm}^{-2} \text{yr}^{-1}$  at Site C (Fig. 3). A similar range in fluxes has been reported in traps from the eastern equatorial Pacific<sup>10</sup>.

In general, silicoflagellates are a minor constituent (~1%) of the opal flux. This is especially true at Site S where the <63 µm

**Table 1** Comparison between sediment trap and surface sediment radiolarian assemblages

Trap sample	Surface sediment*	Similarity measure†
Site S (700 m) (11° N 140° W)		
Cup 2	Y71-9-85 (5° S 087° W)	0.89
Cup 3	V24-046 (1° N 087° W)	0.95
Cup 4	Y71-9-91 (6° S 115° W)	0.93
Cup 5	V18-324 (8° N 107° W)	0.89
Site C (1,095 m) (1° N 139° W)		
Cup 2	RC13-23 (0° N 175° W)	0.97
Cup 3	RC10-136 (10° S 154° E)	0.96
Cup 4	V21-207 (0° N 100° W)	0.69
Cup 5	RC10-249 (7° N 087° W)	0.91

\* Samples listed are surface sediment samples which had the highest similarity value with the listed trap sample. Samples were selected out of a set of 191 samples. Thirty-four species were used and the average sediment count was 550 radiolarians per sample.

† The  $\cos \theta$  measure of similarity was used. This index ranges in value from 0.0 to 1.0 with a value of 1.0 indicating that all inter-species ratios in the two samples being compared are identical.

fraction and opal flux are dominated by diatoms. However, at Site C there is a marked increase in the silicoflagellate to diatom ratio in the fine opal fraction as compared with Site S. Unlike the flux of radiolaria shells in the coarse fraction, the flux of silicoflagellates are highly correlated ( $r^2 = 0.95$ ) with the flux of biogenic silica (Fig. 3). The very high opal flux measured in cup 2 of Site S is the result of a large increase in the diatom species *Thalassionema bacillaris* and *Thalassiothrix longissima*, and is not reflected by an increase in silicoflagellates.

The silicoflagellate assemblage at both sites is dominated by *Dictyocha messanensis*, a species common throughout the North Pacific<sup>11</sup>, *Distephanus pulchra*<sup>12</sup> and *Dictyocha calida*. *Distephanus pulchra*, a species associated with high productivity in the Gulf of California<sup>13,14</sup>, is ~15% of the assemblage at Site C and 30–50% at Site S, mirroring the shift of 'productivity' species in the radiolarian results.

The succession of the silicoflagellates at both sites supports the results of the radiolarian studies. At Site S, the three dominant equatorial silicoflagellate species are present throughout the deployment period. Variations in *D. calida*, typical of the warmer waters of the equatorial Pacific<sup>11</sup>, follows the temperature patterns observed at this site. During the early part of the year when temperatures were at a minimum, *D. calida* is found in lowest abundance (Fig. 1). As temperatures increased during the spring and summer this species increased in relative abundance. The species *D. pulchra*, associated with high productivity, is found in highest abundance in cup 3, which has the highest organic carbon flux (Fig. 1). The percentage of this species decreases 50% in the latter part of the year.

At Site C, there is a marked change in the silicoflagellate assemblage during the sampling period. *Dictyocha calida* is not found during the first half of the sampling period and reaches abundances similar to that at Site S in cup 5 (Fig. 1). *Distephanus pulchra* is also found in very low abundances in cup 2 (<2%) as compared with the latter sampling intervals. Thus, the oceanographic events of 1983 are reflected in significant faunal and floral change within the equatorial band but not at 11° N.

Results from the analysis of the Sites S and C traps differ from previous studies in two important ways. It has been suggested that dissolution does not significantly alter the sinking radiolarian population<sup>3</sup> but comparison of trap and surface sediment populations showed that there were significant differences between the two<sup>15</sup>. We found that up to 25% of the settling radiolaria are rare in the underlying sediments and significant loss of these weakly silicified species was noted within the vertically distributed traps. Three species (*Dictyophimus* spp., *Lithomelissa thoracites* and *Peridium* spp.) account for most of the weakly silicified fraction with a combined average of 14% of the total count at Site S and 17% at Site C. These three species are important components of the radiolarian assemblage found in sediments in the Gulf of California<sup>16</sup> but are not common in sediments from the equatorial Pacific. More importantly to palaeoclimatic and palaeoceanographic studies, dissolution does not seem to alter selected microfossil components within the radiolarian thanatocoenoses. Comparison of our trap sample species abundances and an adjacent surface sediment sample from core RC11-210 (1° N 140° W) using only species studied in palaeoclimate reconstructions<sup>5,17</sup> shows very high similarity. The comparison was made by taking a weighted sum (weights were set equal to the radiolarian flux in each sample) of radiolarian species abundance in the four samples from the shallowest trap at Site C. The calculated similarity with a near surface sample of core RC11-210 was 0.91. Samples from the Site S traps could not be compared with sediments from the deployment area as this region of the Pacific is characterized by extensive sediment reworking so that Eocene to late Miocene radiolarian species are found in the near surface sediments.

In contrast, silica dissolution has a significant impact on the silicoflagellate assemblage. *Distephanus pulchra* is an important component in both the Site S and Site C traps. However, this species is not found in the surface sediment at either of the two sites studied and Poelchau<sup>11</sup> and D.M. (unpublished data from Manop Sites H and M) only found it in high abundance in northeastern equatorial Pacific sediments beneath areas of high opal sedimentation rates. This indicates that the distribution of *D. pulchra* in deep-sea sediments is controlled largely by dissolution, and ecological interpretation of this species from deep-sea sediments must be made with caution.

This study supports the contention that sediment trap studies provide important information about the transfer of biogenic components from their production in the near surface ocean to final burial in deep-sea sediments. Also, the study of microfossils in traps not only provides valuable information about the ecology and surface ocean conditions reflected in the fossil species preserved in deep-sea sediments, but in turn microfossil studies provide important information needed to interpret processes controlling the transfer of organic components to the deep-sea.

This research was supported by NSF grants ATM83-19371 and OCE83-15471 to Oregon State University. We appreciate comments and support from J. Dymond and R. Collier.

Received 5 July 1985; accepted 9 January 1986.

1. Moser, J. C. et al. *Limnol Oceanogr.* (in the press).
2. Roclofs, A. & Pisias, N. *Micropaleontology* (in the press).
3. Takahashi, K. *Mar. Micropaleontol.* 8, 171-182 (1983/84); thesis MIT/Woods Hole Oceanographic Institution (1981).
4. Dymond, J. & Collier, R. *Nature* (in the press).
5. Moore, T. C. Jr. *Mar. Micropaleontol.* 3, 229-266 (1978).
6. Lombari, G. & Boden, G. *Cushman Foundation Spec. Publ.* No. 16A-125 (1985).
7. Cande, M. *Science* 222, 1189-1195 (1983).
8. Ramusson, E. & Wallace, J. *Science* 222, 1195-1202 (1983).
9. Barber, R. & Chavez, F. *Science* 222, 1203-1210 (1983).
10. Takahashi, K. *Geol. Soc. Am. Abstr. Prog.* 16, 673 (1984).
11. Poelchau, H. *Mar. Micropaleontology* 22, 164-193 (1976).
12. Ling, S. & Takahashi, K. *Mar. Micropaleontology* 31, 76-81 (1979).
13. Murray, D. & Schrader, H. *Mar. Micropaleontol.* 7, 517-539 (1982/83).
14. Schrader, H. & Baumgartner, T. *Coastal Upwelling* (eds Theide, J. & Suess, E.). Part B, 247 (Plenum, New York, 1983).
15. Takahashi, K. & Honjo, S. *Deep Sea Res.* 30, 543-568 (1983).
16. Pisias, N. *Mar. Micropaleontol.* (in the press).
17. Moore, T. C. et al. *Mar. Micropaleontol.* 5, 215-248 (1979).

## A new prokaryote containing chlorophylls *a* and *b*

T. Burger-Wiersma\*, M. Veenhuis†, H. J. Korthals‡,  
C. C. M. Van de Wiel\* & L. R. Mur\*

\* Laboratorium voor Microbiologie, University of Amsterdam, Nieuwe Achtergracht 127, 1018 WS Amsterdam, The Netherlands

† Laboratorium voor Electronenmicroscopie, University of Groningen, Biological Centre, Kerklaan 30, 9751 NN Haren, The Netherlands

‡ Limnological Institute De Vijverhof, Rijksstraatweg 6, 3631 AC Nieuwersluis, The Netherlands

**Prochlorophyta**, suggested as a new division of prokaryotes<sup>1</sup>, lack phycobilin pigments characteristic of cyanobacteria, but contain chlorophyll *b* as well as chlorophyll *a*, characteristic of green algae and higher plants. Since the description of *Prochloron didemni* as the type species for this division<sup>2</sup>, no other genera or species have been added to the group. The only published accounts of *Prochloron* are obligate symbionts of didemnid ascidians<sup>3</sup>, which are difficult to grow in the absence of their hosts<sup>4</sup>. Consequently, research on their cell composition and physiology has been handicapped. Here, we report a second prochlorophyte. This organism is one of the dominant species in the shallow eutrophic Loosdrecht lakes in The Netherlands, from which it was isolated in 1984. Unlike *Prochloron*, the newly isolated species is filamentous and planktonic. Detailed investigation of its cell structure, composition and physiology is possible as it can easily be grown in a mineral medium.

Batch cultures of the strain were maintained on an orbital shaker at 20 °C in a mineral medium<sup>5</sup> at a photon-flux density of 30  $\mu\text{E m}^{-2} \text{s}^{-1}$  (warm, white fluorescent lamps) and an alternating light/dark regime of 16 h : 8 h. The strain was characterized by pigment analysis, electron microscopy and growth response in the presence of antibiotics.

Pigment analysis by HPLC (ref. 6) shows the distinct peak and retention time characteristic of chlorophyll *b* (Fig. 1A). After fractional separation, spectrophotometric analysis confirmed the presence of chlorophyll *b*, with absorption maxima at 454 and 643 nm and an absorbance ( $A_{454}/A_{643}$ ) ratio of 2.82 (Fig. 1B)<sup>7</sup>.

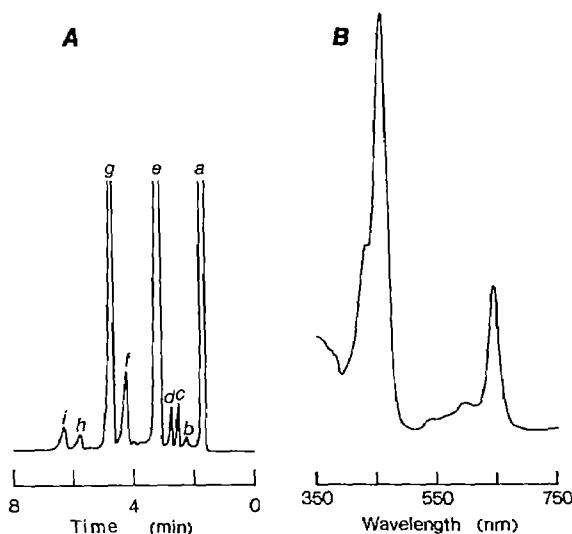
Chlorophyll *a* contents determined from turbidostat cultures vary between 6 and 36 mg per g dry weight, depending on irradiance level. Preliminary results indicate that the chlorophyll *a/b* ratio is rather constant at photon-flux densities ranging from 4 to 150  $\mu\text{E m}^{-2} \text{s}^{-1}$ . The chlorophyll *a/b* ratio varies between 8.1 and 9.0 and is relatively high compared with the ratio commonly found for green algae (2-3)<sup>8</sup> and for *Prochloron* (4-7)<sup>9</sup>.

Table 1 Pigment composition determined by HPLC

	Dry weight ( $\mu\text{g mg}^{-1}$ )
<i>a</i> $\beta$ -Carotene	4.1
<i>b</i> Phaeophytin <i>a</i>	0.8
<i>c</i> Not identified*	ND
<i>d</i> Chlorophyll <i>a'</i>	0.7
<i>e</i> Chlorophyll <i>a</i>	24.0
<i>f</i> Chlorophyll <i>b</i>	3.0
<i>g</i> Zeaxanthin	3.5
<i>h</i> Not identified†	ND
<i>i</i> Not identified†	ND

Letters in left-hand column refer to peaks in the absorbance chromatogram of Fig. 1A. ND, not determined as there is no available standard.

\* Probably canthaxanthin; † probably derivatives of zeaxanthin.



**Fig. 1** *A*, Absorbance (440 nm) chromatogram obtained by HPLC (normal phase, 1,200 p.s.i., semi-preparative column, eluent: 25% acetone in hexane) of an extract of the Loosdrecht isolate. *a-i*, Peaks of individual pigments listed in Table 1. *B*, Absorption spectrum of compound *f*.

No water-soluble pigments could be detected using the extraction technique described by Tandeau de Marsac<sup>10</sup>. In attempts to stimulate the formation of phycobilin pigments, cultures were grown in green light or at a low photon-flux density ( $4 \mu\text{E m}^{-2} \text{s}^{-1}$ ), but in neither case were phycobilin pigments found.

The carotenoid composition (Table 1) resembles that of cyanobacteria as no  $\alpha$ -carotene and lutein were detected by HPLC (Fig. 1A). Lutein is usually found to be the major carotenoid in green algae, zeaxanthin and  $\beta$ -carotene being less abundant, whereas the latter two pigments are often dominant in cyanobacteria<sup>11</sup>. Echinenone, a characteristic carotenoid for most cyanobacteria, although not found in *Anacystis nidulans*<sup>11,12</sup>, is absent in this organism.

Cytology of the cells, including the photosynthetic membranes, was best preserved after pre-fixation in glutaraldehyde and post-fixation in  $\text{KMnO}_4$  (ref. 13) (Fig. 2A). Thin sections of filaments fixed by this method indicate that the thylakoid membranes are present only at the periphery of the cells. Phycobilisomes are not present (Fig. 2C) and the photosynthetic membranes are not separated from the cytoplasm by a bounding membrane, that is, chloroplasts are not present. We did not observe other membrane-bound organelles. In cells fixed by glutaraldehyde/ $\text{OsO}_4$ , a nucleoplasmic region surrounded by

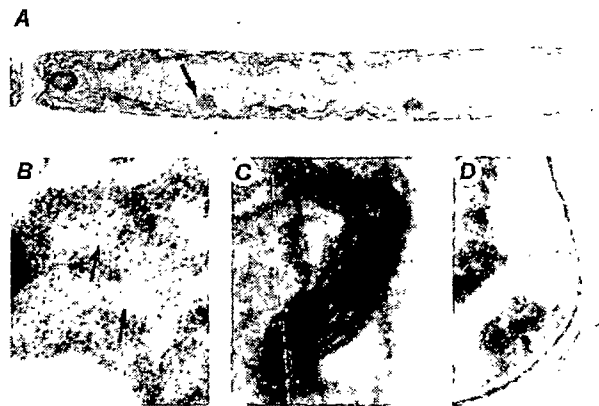


**Fig. 2** *A*, Survey of a cell, fixed in glutaraldehyde/ $\text{KMnO}_4$ , to show overall morphology. The thylakoid membranes are localized close to the cell wall. Arrow, cytoplasmic polyhedral bodies.  $\times 11,520$ . *B-D*, Details of cells to show the presence of DNA (arrows) in the cytoplasm (*B*, glutaraldehyde/ $\text{OsO}_4$ ;  $\times 49,920$ ), the substructure of the thylakoid membranes (*C*, glutaraldehyde/ $\text{KMnO}_4$ ;  $\times 76,320$ ) and the cell wall (*D*, glutaraldehyde/ $\text{OsO}_4$ ;  $\times 28,800$ ).

ribosomes can be distinguished in the central region (Fig. 2B). Another characteristic of prokaryotes is the presence of polyhedral bodies (Fig. 2A), which are thought to represent carboxysomes<sup>14</sup>.

The cell wall resembles that of cyanobacteria and Gram-negative bacteria (Fig. 2D). The thick electron-dense layer adjacent to the plasmalemma is probably peptidoglycan<sup>15</sup>. No mucilaginous sheath was found.

Growth inhibition experiments confirm the prokaryotic nature of the cells. We added cycloheximide (Boehringer), chloramphenicol (Sigma) or cephalosporin (Eli Lilly) to freshly diluted batch cultures of the new organism, of the prokaryote *Oscillatoria agardhii* and of the eukaryote *Scenedesmus protuberans*. Cycloheximide is known to inhibit eukaryotic protein synthesis by blocking the action of 80S ribosomes. Table 2 shows that cycloheximide inhibited growth of *S. protuberans* at a concentration of  $1 \text{ mg l}^{-1}$ , whereas  $20 \text{ mg l}^{-1}$  of cycloheximide was only slightly inhibitory to the growth of *O. agardhii* and of the new prochlorophyte. Chloramphenicol inhibits protein synthesis on 70S ribosomes, not only those present in prokaryotes, but also those in chloroplasts and mitochondria of eukaryotes. However, chloramphenicol does not inhibit the growth of eukaryotes if it is applied in low concentrations, as we demonstrated in control experiments with *S. protuberans*, which still grew at a chloramphenicol concentration of  $20 \text{ mg l}^{-1}$ . For both *O. agardhii* and the new Loosdrecht isolate, growth was inhibited over the whole range of inhibitor concentrations. Cephalosporin acts as an inhibitor of cell-wall synthesis in prokaryotes<sup>16</sup>. Table 2 shows that no growth occurred in batch cultures of *O. agardhii* and of the Loosdrecht isolate after addition of cephalosporin. The growth of *S. protuberans* was not affected by cephalosporin.

Thus, the newly isolated organism seems to be a 'normal' prokaryote with respect to its cytoplasmic ultrastructure, cell-wall structure and its response to antibiotics. We have shown that a photosynthetic apparatus consisting of chlorophylls *a* and *b* is not strictly restricted to eukaryotic algae and higher plants, and thereby have confirmed the earlier observation of Lewin<sup>1</sup>. With regard to structure and pigment composition, the alga is comparable to *Prochloron*.

The discovery of a second prokaryote containing chlorophyll *b* contributes to the taxonomic and phylogenetic discussion on Prochlorophyta, particularly as the newly isolated species can easily be grown in batch as well as continuous cultures.

**Table 2** Inhibition of growth of batch cultures of the Loosdrecht isolate (LI), *O. agardhii* and *S. protuberans*

Antibiotic	Concentration ( $\text{mg l}^{-1}$ )	LI	<i>O. agardhii</i>	<i>S. protuberans</i>
Cycloheximide	1	G		I
Cycloheximide	2	G	G	
Cycloheximide	20	G/I	G/I	
Chloramphenicol	0.2	I		
Chloramphenicol	2	I	I	
Chloramphenicol	20	I	G	
Cephalosporin	3	I		
Cephalosporin	30	I	I	G
Cephalosporin	300	I		

I, inhibition; G, growth.

We thank Ralph A. Lewin, Anton F. Post, Gijs Kraay and Jacco C. Kromkamp for help, and the Dutch Ministry of Public Housing, Physical Planning and the Environment for support.

Received 18 November 1985; accepted 20 January 1986.

1. Lewin, R. A. *Nature* **261**, 697–698 (1976).
2. Lewin, R. A. *Phycologia* **16**, 217 (1977).
3. Lewin, R. A. *Phycologia* **23**, 203–208 (1984).
4. Patterson, G. M. & Withers, N. W. *Science* **217**, 1934–1935 (1982).
5. Van Liere, L. & Mur, L. R. *Mitt. int. Verein. theor. angew. Limnol.* **21**, 158–167 (1978).
6. Korthals, H. J. & Steenbergen, C. L. M. *FEMS Microbiol. Ecol.* **31**, 177–185 (1985).
7. Strain, H. H. & Svec, W. A. In *The Chlorophylls* (eds Vernon, L. P. & Seely, G. R.) 21–66 (Academic, New York, 1966).
8. Hager, A. & Stransky, H. *Archs Microbiol.* **72**, 66–83 (1970).
9. Withers, N. W. *et al.* *Proc. natn. Acad. Sci. U.S.A.* **75**, 2301–2305 (1978).
10. Tandeau de Marsac, N. *J. Bact.* **130**, 82–91 (1977).
11. Stransky, H. & Hager, A. *Archs Microbiol.* **72**, 84–96 (1970).
12. Hertzberg, S., Liaaen-Jensen, S. & Siegelman, H. W. *Phytochemistry* **10**, 3121–3127 (1971).
13. Van Dijken, J. P., Veenhuis, M., Kreger-Van Rij, N. J. W. & Harder, W. *Archs Microbiol.* **102**, 41–44 (1975).
14. Codd, G. A. & Marsden, W. J. N. *Biol. Rev.* **59**, 389–422 (1984).
15. Drews, G. & Weckesser, J. In *The Biology of Cyanobacteria* (eds Carr, N. G. & Whitton, B. A.) 333–358 (Blackwell Scientific, Oxford, 1982).
16. Franklin, T. J. & Snow, G. A. In *Biochemistry of Antimicrobial Action*, 22–55 (Chapman & Hall, London, 1975).

## Serial and parallel processing of visual feature conjunctions

Ken Nakayama & Gerald H. Silverman

Smith-Kettlewell Eye Research Foundation,  
Pacific Presbyterian Medical Center, San Francisco,  
California 94115, USA

Treisman and others<sup>1–3</sup> have reported that the visual search for a target distinguished along a single stimulus dimension (for example, colour or shape) is conducted in parallel, whereas the search for an item defined by the conjunction of two stimulus dimensions is conducted serially. For a single dimension the target 'pops out' and the search time is independent of the number of irrelevant items in the set. For conjunctions, the search time increases as the set becomes larger. Thus, it seems that the visual system is incapable of conducting a parallel search over two stimulus dimensions simultaneously. Here we extend this conclusion for the conjunction of motion and colour, showing that it requires a serial search. We also report two exceptions: if one of the dimensions in a conjunctive search is stereoscopic disparity, a second dimension of either colour or motion can be searched in parallel.

Visual search experiments were conducted with the aid of a Commodore 64 microcomputer and colour television monitor. Two types of experiment were performed, those where the observer's task was to see the unique target which differed from all others in one dimension only (simple); and those where the observer had to find the unique target which was defined by two dimensions (conjunction). The stimulus consisted of a variable size array containing either 15, 25 or 35 targets (see Fig. 1). Each of these targets was a random pattern containing 16 picture elements or pixels. Depending on the experiment (see Fig. 2), the targets were clearly distinguishable either in terms of colour (red versus blue), motion (up versus down) or stereoscopic depth (either in the fixation plane or in front). In the case of stimulus motion, each target formed a rectangular 'aperture' behind which a continuous array of random dots could be moved, either up or down.

The observer was aware of the particular dimension(s) to be searched before the beginning of each block of trials; the task was to press a button as soon as the target was seen. To eliminate false-positives, the array remained visible for an additional 800 ms after the response. This enabled the observer to scrutinize the display and to verify whether his identification was correct.

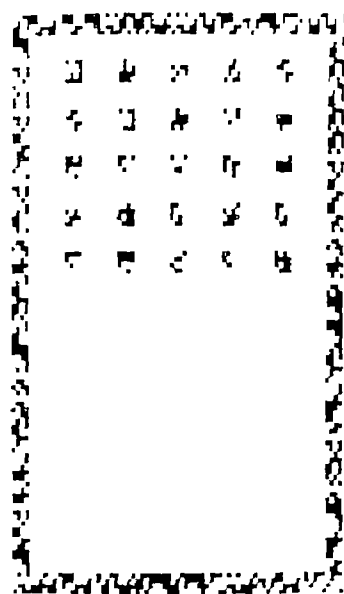


**Fig. 1** The stimulus array contained either 35 targets (7 rows), 25 targets (5 rows) or 15 targets (3 rows) and was bordered with a frame to ensure stereoscopic fusion in the binocular experiments. For observer K.N., the stimuli had the following parameters: target size  $0.4 \times 0.5^\circ$ , frame size  $7.5 \times 13^\circ$ , vertical spacing of targets ( $1.0^\circ$ ), horizontal spacing of targets ( $1.2^\circ$ ), disparity 20 arc min, velocity  $3.75^\circ \text{ s}^{-1}$ . All stimulus parameters were 25% smaller for observer J.S.

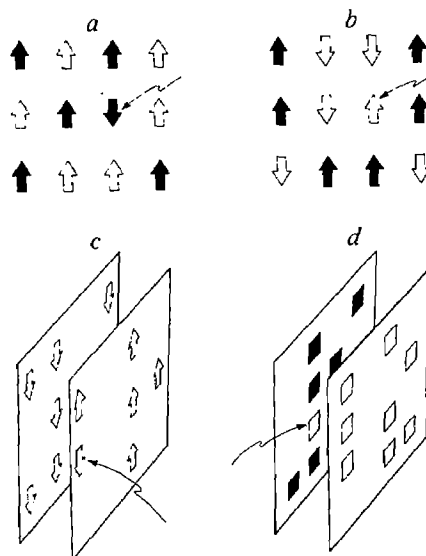
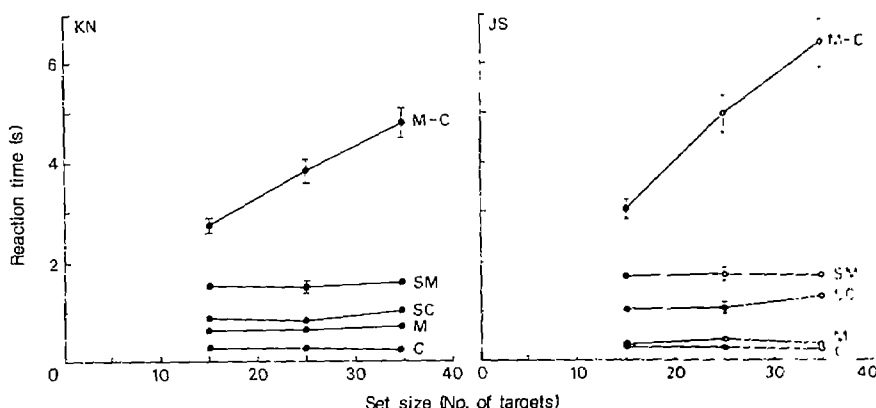


**Fig. 2** *a*, Schematic description of the simple one-dimensional search for a discrepant motion. The observer must find the single target that has the anomalous motion with respect to all motions, targets are randomly coloured. *b*, Conjunctive search for colour and motion. Blue distractors move down, red distractors move up. The target breaks this pattern and is either a blue moving up or a red moving down. *c*, Conjunctive search for stereo and motion. All distracting targets in the front plane are moving up and those in the back plane are moving down. Relevant target either is in front and moves down or in back and moves up. *d*, Conjunctive search for stereo and colour. Distracting targets in the front plane are blue and those in the back plane are red. Relevant target is either red in front or blue in back. Open symbols, blue colours; filled symbols, red colours. Target to be found is marked by small pointer.

The data associated with mistakes were discarded.

Each set of experiments had the same overall design and differed only in the choice of stimulus dimensions to be searched. In any given experiment, two stimulus dimensions were used: motion-and-colour (M-C); stereo-and-motion (SM), or stereo-

**Fig. 3** Reaction times plotted as a function of the number of elements in the set to be searched. Results from two classes of experiments are shown. Conjunction: motion-colour (M-C), stereo-motion (SM), stereo-colour (SC). Simple: colour (C), motion (M), stereo (S). Note that for the conjunctive search of M-C, the anomalous target becomes more difficult to find as set size increases. This is not the case for the conjunction of SM or SC. All plotted reaction times represent the mean of at least 40 separate trials, preceded by at least 40 unscored practice trials.



and-colour (SC). For the simple search, the observer was required to find the target that was distinguished by a unique feature along a single dimension. In the case of motion (M) it was the target which moved in the opposite direction to all others, with colour being randomly assigned to all targets on an equiprobable basis (Fig. 2a). For the case of stereo (S), it was the single target which had a different binocular disparity from all other targets, with colour being randomly assigned to the targets on an equiprobable basis. For the case of colour (C), it was the single target which had the odd colour with the different directions of motion being randomly assigned.

Our first set of experiments extend and confirm previous work<sup>1,2</sup> showing that the search for a single feature is conducted in parallel. Reaction times are short and remain constant as the set size increases. Lower reaction time functions designated C, S and M (Fig. 3) refer to the simple search for colour, stereo and motion, respectively. All indicate that for the single-dimensional search, the processing is pre-attentive and effortless.

Conjunctive search, however, has been shown to require serial processing. We therefore expected that a search requiring the conjunction of motion and colour would also be conducted in serial. The irrelevant targets (distractors) for this experiment were coloured either red or blue on a random equiprobable basis, with upwards motion linked to the red distractors and downwards motion linked to the blue. The relevant target broke this pattern, so it could be either a red moving down or a blue moving up (Fig. 2b). Compared with the simple search, observers found this task to be extremely difficult—they were unable to perform a parallel search for the anomalous motion over a given colour. Instead, they resorted to searching very small portions of the display, almost target by target. These subjective impressions were amply supported by the reaction time functions. The M-C function rose steeply (>100 ms per item) for increasing set sizes, confirming our expectation that the conjunctive search for motion-and-colour is indeed serial (Fig. 3).

In our final set of experiments we introduced the conjunction of stereoscopic disparity with either motion or colour. We generated two separate images on the television monitor and used crossed-polaroid filters to obtain the necessary dichoptic separation to produce the stereograms. The fixation plane was defined by a rectangular border which enclosed the targets and was always visible between trials. The individual targets were randomly assigned to either depth plane with equal probability. For the case of stereo-and-motion, the distractors in the front plane were always moving up and those in the back plane were always moving down. The target to be found was either moving down in the front plane or moving up in the back plane (Fig. 2c). For the case of stereo-and-colour, the distractors in the front plane were always blue and those in the back plane were always red. The target to be found was either a red in the front plane or a blue in the back plane (Fig. 2d).

In comparison with the case of motion-and-colour, these conjunctive tasks were qualitatively different and much easier. The observer had the distinct impression that each plane could

be searched almost effortlessly, in turn. Correspondingly, the reaction time functions for each of these searches are constant over set size, never rising to the high values of reaction time which we found for the M-C search. This can be seen in the functions for SM and SC in Fig. 3. It seems that the visual system can perform a parallel search in one depth plane without interference from target-like distractors in another depth plane.

Our data suggest that the visual system can sequester processing or restrict attention in the spatial dimension (see refs 4, 5) but not to other visual dimensions such as colour and motion. Treisman<sup>2</sup> found that observers can attend to different two-dimensional loci in a complex visual scene, serially, yet perform a search within a given two-dimensional region, in parallel. We show that an analogous process occurs with different stereo-depth planes. Each depth plane can be processed in turn, allowing a parallel search within each plane.

We speculate that retinal disparity in addition to retinal locus has priority when compared with other visual stimulus dimensions; perhaps they constitute a set of primary indices to which the other visual attributes are linked<sup>6</sup>. As such, the results can be related to the anatomical organization of visual cortical projection areas, suggesting a segregation and duplication of visual features according to disparity. Thus, visual features of motion and colour at one disparity could be separately encoded and duplicated at other disparities. This notion of conjunctive parallel processing for dimensions linked to disparity finds a neurophysiological correlate in visual cortex area MT for the case of stereo motion<sup>6</sup> where single cells are selectively tuned to both direction and disparity. The existence of comparable cells selective for both colour and disparity has yet to be reported.

Conversely, the serial search associated with the conjunction of motion and colour seems to preclude the existence of single units selectively tuned to both motion and colour, consistent with recent evidence regarding the functional segregation of colour and motion information within cortical area V2 (refs 7–10) as well as their separate corresponding target destinations in V4 and MT. Cells in V4 are sensitive to wavelength differences but not to the direction of motion<sup>11</sup>, whereas MT cells are sensitive to motion and not to wavelength<sup>12</sup>.

This work was supported in part by grants 5P 30-EY01186 and EY05408 from NIH and (83-0320) from AFOSR.

Received 24 October 1985; accepted 13 January 1986.

1. Treisman, A. *Cogn. Psychol.* **12**, 97–136 (1980).
2. Treisman, A. J. exp. Psychol. **2**, 194–214 (1982).
3. Walters, D. B., Biederman, I. & Weissstein, N. *Invest. Ophthalmol. vis. Sci. Suppl.* **23**, 193 (1983).
4. Downing, C. & Pinker, S. in *Attention and Performance Vol. 11* (eds Posner, M. I. & Marin, O. S. M.) 171–187 (Erlbaum, Hillsdale, New Jersey, 1985).
5. Hillyard, S. A. & Munte, T. F. *Percep. Psychophys.* **36**, 185–193 (1984).
6. Ballard, D. H. *Tech. Rep. No. 133* (Univ. Rochester, 1984).
7. Maunsell, J. H. R. & van Essen, D. C. *J. Neurophysiol.* **49**, 1148–1167 (1983).
8. Ship, S. & Zeki, S. *Nature* **315**, 325–325 (1985).
9. Hubel, D. H. & Livingstone, M. S. *Nature* **315**, 325–327 (1985).
10. DeYoe, E. A. & Van Essen, D. C. *Nature* **317**, 59–61 (1985).
11. Maunsell, J. H. R. & van Essen, D. C. *J. Neurophysiol.* **49**, 1127–1147 (1983).
12. Zeki, S. M. *Cold Spring Harb. Symp. quant. Biol.* **40**, 591–600 (1975).

## Homing behaviour of axons in the embryonic vertebrate brain

William A. Harris

Department of Biology, University of California San Diego, B-022, La Jolla, California 92093, USA

In embryonic nervous systems, growing axons must often travel long distances through diverse extracellular terrains to reach their postsynaptic partners. In most embryos, axons grow to their appropriate targets along particular tracts or nerves, as though they were following guidance cues confined to specific pathways<sup>1-3</sup>. For example, in all vertebrates, axons from the retina invariably grow to the tectum along the well-defined optic tract<sup>4-6</sup>. Yet, transplant experiments demonstrate that retinal axons make tectal

projections even though they enter the brain at locations which are distinctly off the optic tract<sup>7-11</sup>. Only recently has it become possible to label discreet growing projections in the embryonic vertebrate brain<sup>12</sup>. Thus, it is not yet known whether displaced retinal axons grow directly towards the tectum or find it accidentally, through random extension. To resolve this question, pioneering axons from normal and transplanted eyes in embryonic *Xenopus* were labelled using a short-survival horseradish peroxidase (HRP) method<sup>4</sup>, and their orientation during growth was quantitatively assessed. The finding that the ectopic fibres head towards their distant targets implies that guidance cues are not restricted to specific pathways but are distributed throughout the embryonic brain. The significance of this result is discussed with respect to the ontogeny and evolution of the visual pathway.

*Xenopus* embryos at ~24 h post-fertilization (PF) (Nieuwkoop and Faber<sup>13</sup> (NF) stage 24) were prepared for surgery in modified Ringer's solution with anaesthetic (0.01% tricaine) and antibiotics (25 µg ml<sup>-1</sup> gentamycin). Eye primor-

**Fig. 1** *a-c*, Whole-mounts of normal embryonic *Xenopus* brains with labelled optic pathways, viewed laterally (*a* at stage 33/34, *c* at stage 35/36). *b*, Growth cones from *a* at higher magnification. *d-h*, Camera lucida drawings of brains fixed at stages 33/34-40, during which time the retinotectal projection normally develops. Dotted lines in *c* and in most of the camera lucida drawings show the three major subdivisions of the brain: Fo, forebrain; Mi, midbrain; Hi, hindbrain (see *g*). *h*, The protocol for estimating the coordinates of the central tectal neuropil (Tn): a line was drawn from the area of the chiasm (*y*) to the midpoint of the dorsal midbrain (*y'*); at right angles to this, a second line was constructed from the boundary between the midbrain and hindbrain (*x*) to the dorsal-most boundary between the forebrain and midbrain (*x'*). These lines were normalized and served as axes in a cartesian coordinate system. Next, in this stage-40 embryo, a star was placed on the area of most dense midbrain innervation, the tectal neuropil (as determined from visual inspection), and the coordinate pair that best represented this estimated tectal centre was recorded. In this case the respective (*x*, *y*) values were (0.57, 0.70). This procedure was repeated for seven animals at stages 39 and 40 and yielded an average result of (0.55 ± 0.06, 0.73 ± 0.03; mean ± s.d.). These average values were used as the location of the estimated tectal neuropil (ETn) in all experimental animals (see Figs 2, 3) and in normal embryos at stages when retinal axons had not yet reached the target, as shown in *a* and *d*. This quantitative method of estimating the location of the tectal neuropil was necessary because there are no visible independent markers of this structure at early stages. The high reproducibility of the coordinate values in control animals indicates that this method gives a very reasonable, if imprecise, location of the target area. Ch, chiasm; Te, telencephalon; Di, diencephalon; Tcm, tectal cell mass; Pi, pineal; Hy, hypothalamus.

**Methods.** To label embryonic retinal projections, HRP was injected locally using the following procedure. The cornea and lens were removed from anaesthetized and restrained animals and a glass pipette with a terminal bore of ~30 µm, partially filled with a solution of 20% HRP in 2% lyssolecithin, was inserted into the lens cavity. By application of gentle pressure at the back of the pipette, the label was forced onto the vitreal surface of the retinal cup. After about 5 min of superfusion of the retina, the embryo was allowed to recover for 15-30 min, after which it was again anaesthetized and then immersed in ice-cold fixative (1.5% glutaraldehyde and 2% paraformaldehyde in 0.1 M phosphate buffer). After 1 h of fixation, the embryo was rinsed overnight in buffer, and the brain was dissected out and treated histochemically with diaminobenzidine to allow visualization of HRP. The brains were then dehydrated and mounted in methyl salicylate or Fluoromount for examination as whole-mounts.

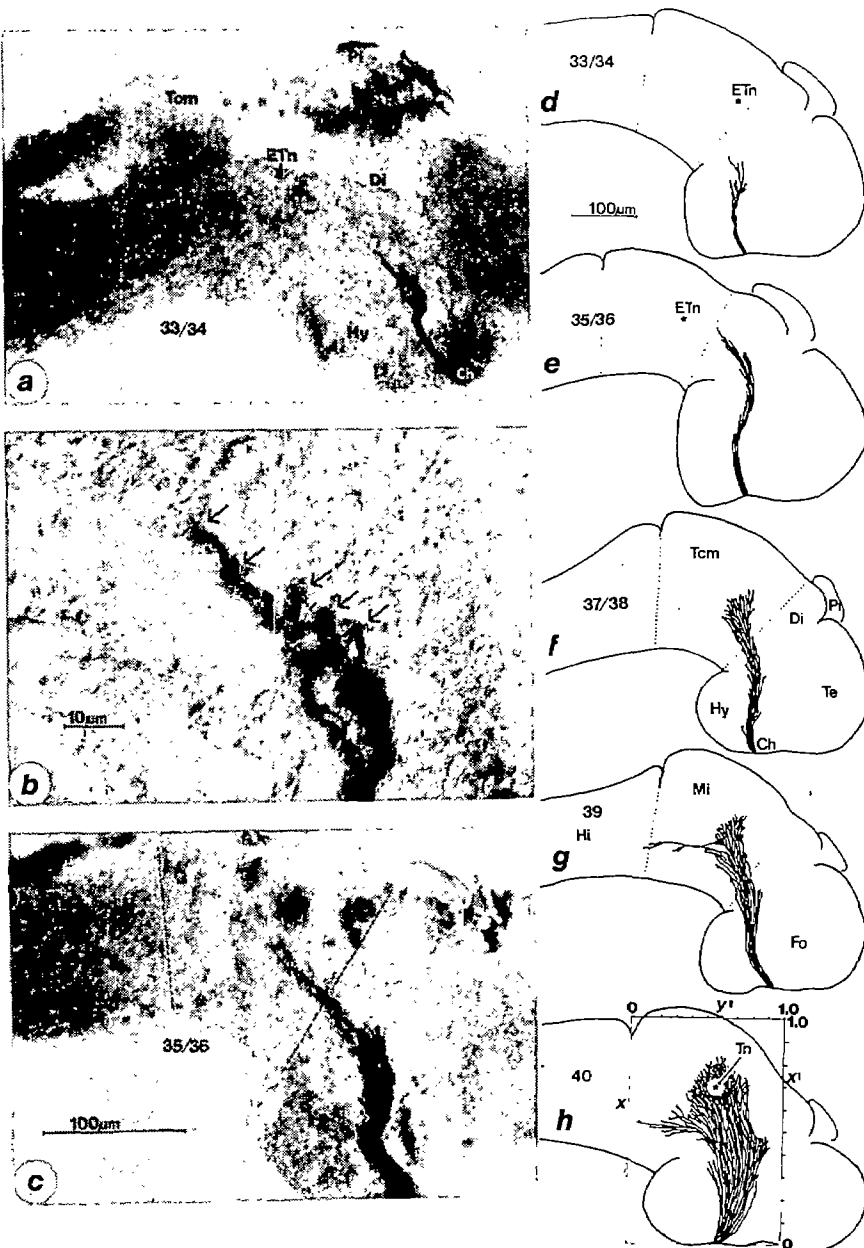
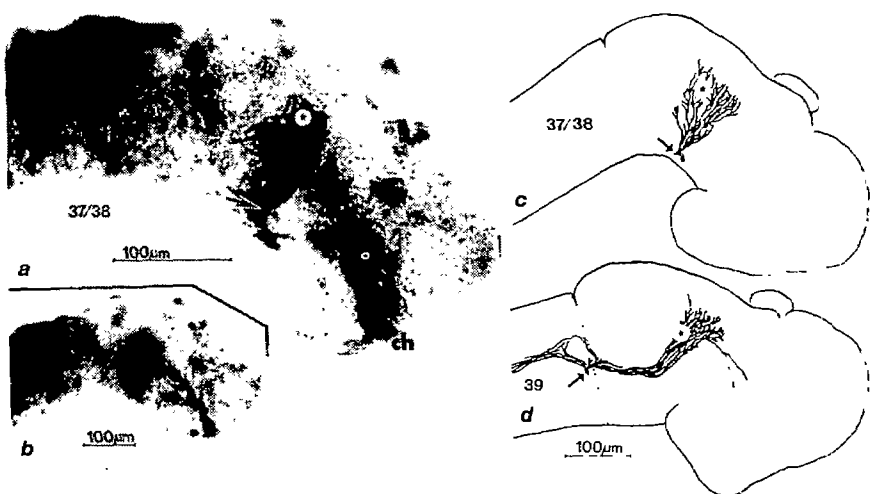


**Fig. 2** Ectopic projections at the time of fibre arrival in the tectum in three animals at stages 37/38 and 39. *a, b*, Photograph of the same stage 37/38 whole-mount (arrow marks entry point); *c, d*, camera lucida drawings of two other cases. Stars indicate the estimated tectal neuropil (see Fig. 1). Note that the ectopic axons migrate to this location. *b*, The control pathway in same animal as *a*. The brain was photographed from the other side and the print made from the reversed negative; this gives the impression that we are focusing through the brain. Note that in *b* the shadow of the ectopic pathway is still visible and can be compared directly with the normal optic pathway. The only overlap is at the tectal neuropil, indicating that the ectopic fibres have reached the normal target by a novel pathway. The entry points (arrows) of the transplanted optic fibres in both *a* and *c* are within the midbrain, and the projection is almost entirely to the ipsilateral tectum. In *d*, the transplanted nerve entry point is near the junction between midbrain and hindbrain and, in this case, some fibres travel down the spinal cord while the rest travel to the tectum.



dia, including epidermis and optic stalk, were excised and inserted into an excavation in the other side of the head of the same embryo. Usually the eye contralateral to the excised one was left in place to ensure that the optic stalk of the transplant healed into the brain at a separate location from that of the control eye. In these cases the embryo developed with two eyes on the same side of its head, a sort of artificial flounder. In some instances, the contralateral eye was removed because it obstructed a desired ectopic transplant site. After the transplant had healed into place ( $\sim 10$ –30 min) the embryo was removed to a 10% Holtfreter's<sup>14</sup> solution where it remained until the stages at which the normal retinal axons invaded the brain and grew towards the tectum (NF stages 33/34–40; 44–66 h PF). At these stages the retinotectal projections of both normal and experimental animals were labelled with HRP (see Fig. 1 legend). The orientation of the displaced axons with respect to their target was assessed using a quantitative method for estimating the location of the tectal neuropil (see Fig. 1 legend), combined with the construction of an orientation index (see Table 2 for details).

The development of the retinotectal projections in whole-mounts of the *Xenopus* brain was examined in 46 normal and 25 experimental embryos. The normal cases (Fig. 1) showed that by stage 33/34 (44 h PF, Fig. 1*a, d*), leading axons are usually in the ventral or mid-diencephalon and climbing towards the tectum. At stage 35/36 (50 h PF, Fig. 1*c, e*) the axons arrive at the dorsal diencephalon, and the first axons reach the tectum at about stage 37/38 (53 h PF, Fig. 1*f*). During stages 39 (56 h PF) and 40 (66 h PF, Fig. 1*g, h*) the innervation of the tectum becomes more dense<sup>12,15</sup>. When the pathway is being forged, the pioneering axons are capped with enlarged growth cones (Fig. 1*b*). Often many such axons, slightly separated from each other, were seen in a single preparation, suggesting that each of the early growing axons may be navigating to the tectum independently. This is consistent with the recent demonstration that the first axons to travel the pathway from eye to tectum, the ones originating from the dorsal retina, do not serve as necessary pioneers for the later-growing axons from the ventral retina<sup>15,16</sup>. The notion of independent navigation is also consistent with the finding for ectopic axons presented below.

To determine whether ectopic axons grow directly to the tectum and innervate it, 14 of the experimental embryos were examined at stages 37/38–40, by which time normal optic axons would have just reached the tectum. To determine whether these ectopic axons orient towards the target from a distance, the other 11 embryos were fixed at stages 33/34–35/36, before optic axons normally reach the tectum.

All 14 of the transplants examined at stages 37/38–40 sent major projections directly to the ipsilateral tectum, where most of the fibres ended in a dense arborization (Fig. 2). In a few cases, where the ectopic entry point into the brain was near the normal optic tract, an additional bundle of fibres was seen travelling through the chiasm region and towards the contralateral tectum, the side of origin of the transplant. When the transplanted optic nerve penetrated the brain near the medulla, some fibres travelled down the spinal cord (Fig. 2*d*). These different secondary projections were expected, as previous studies have shown that ectopic optic nerves entering the diencephalon often send projections to both the ipsilateral and contralateral tectum<sup>17</sup>, and optic fibres entering the hindbrain in frogs and salamanders travel down the spinal cord in a dorsolateral tract<sup>18</sup> (Table 1). A significant feature of the cases reported here is that the ectopic projections were examined at the earliest stages that fibres could have innervated the tectum even in normal animals. The fact that there were no unusual projections implies that these fibres did not head out in arbitrary directions at early stages. Rather, almost all of the ectopic fibres appeared to have advanced directly towards their targets. The present results also show that ectopic axons did not first seek the path where the optic tract would normally lie, and from there navigate on the normal pathway; they appeared instead to run along nearly straight lines between the entry point and

**Table 1** Projections of ectopic optic nerve fibres at the time of reaching the tectum (stage 37/38–40 embryos)

Entry point of optic nerve	Site of projection			
	Ipsilateral tectum and chiasm	Ipsilateral tectum only	Ipsilateral tectum and spinal cord	Other
Forebrain (n = 3)	3	—	—	—
Midbrain (n = 6)	—	4	2	—
Hindbrain* (n = 5)	—	1	4	—

All transplants with central projections sent fibres to the ipsilateral tectum. In addition, those cases in which the ectopic entry point was in the forebrain sent an additional fascicle of fibres into the optic chiasm whereas those that entered the rostral hindbrain sent fibres down the spinal cord as well as to the tectum (see Fig. 2*d*).

\* Entries in this row were all very near to the junction between midbrain and hindbrain.

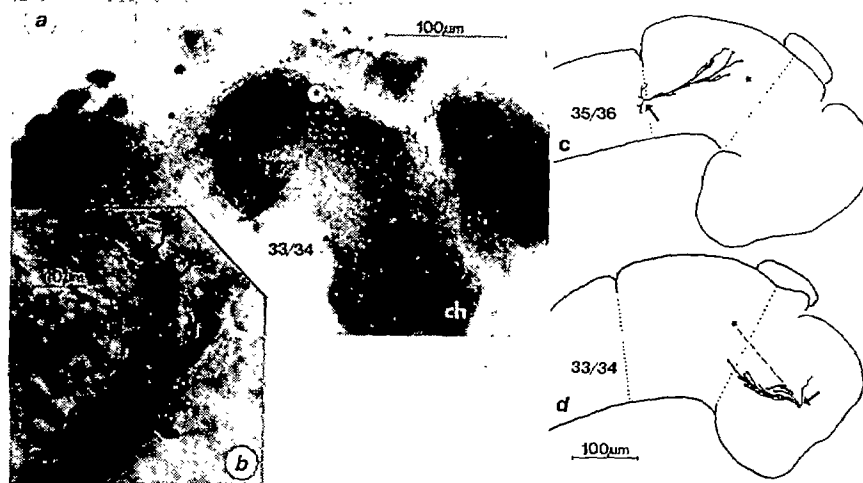


**Fig. 3** Ectopic projections before the fibres have reached the tectum in three animals (stage 33/34-35/36). *a*, Whole-mount of a stage-33/34 animal viewed laterally. Arrows mark entry points and stars indicate the estimated tectal neuropils (calculated as described in Fig. 1 legend). *b*, A higher magnification of growth cones (arrowheads) from *a*, *c*, *d*. Camera lucida drawings of two other cases. Note that the fibres are heading directly for their estimated targets. In *d* the broken line constructed between the entry point and the estimated tectal neuropil serves as the  $0^\circ$  line for the polar orientation graph shown in Fig. 4*a*.

the target, often overlapping with the normal pathway only at the tectum (Fig. 2*b*).

To examine the orientation of displaced axons at stages before normal optic fibres would have reached the tectum, experimental projections were labelled in even younger embryos. Ectopic axons proved similar to normal ones in that at stages NF 33/34 and NF 35/36, though they had not yet reached the tectum, they were growing towards it. In the experimental embryos, ectopic fibres oriented towards the ipsilateral tectum (Fig. 3). A quantitative measure of fibre orientation (the orientation index, *OI*; see Table 2 for details) was obtained by considering the abnormal entry point into the brain as the origin in a polar coordinate system, with a line directly to the estimated tectal neuropil serving as the  $0^\circ$  angle (Fig. 3*d*). When the growth cone-tipped fibres (Fig. 3*b*) were traced by camera lucida techniques onto

such polar graphs and their orientations analysed statistically it became clear that these axons were nonrandomly heading for the tectum (Fig. 4, Table 2).

The finding that displaced axons orient towards their central target suggests that guidance cues in the vertebrate brain are not restricted to particular pathways, but appear to be broadly distributed, so that axons accidentally veering off course can perseveringly 'home-in' on their proper targets. This implies resilience in the development of neural connections, and can explain both transplant results and sizeable variations in the projections of normal optic axons to the tectum (Figs 1*d, e* and 4*e, f*). A distributed guidance mechanism may also have evolutionary significance. For example, if variants occur that slightly alter the placement of the eye primordium, as appears to have happened throughout vertebrate phylogenesis, th-

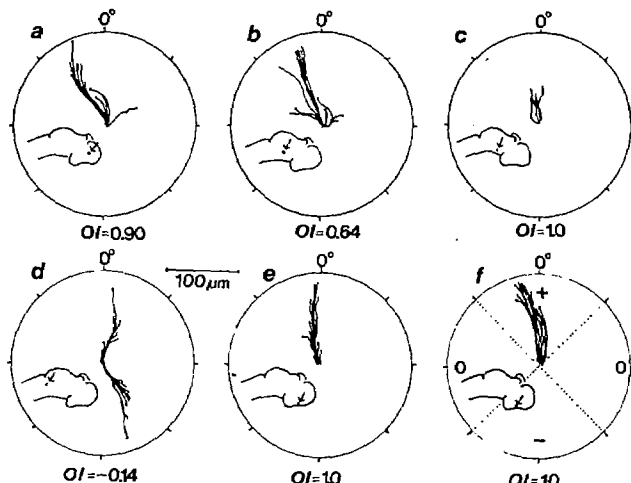


**Fig. 4** Orientation graphs of ectopic (*a-d*) and normal (*e, f*) axons at stages 33/34 and 35/36. Using the ectopic entry point (or in normal animals the chiasm) as the origin, camera lucida drawings of the fibres were made on polar coordinates with  $0^\circ$  indicated as the direct line between the entry point and the estimated tectal neuropil. *a*, Same animal as in Fig. 3*d*; the rest are different cases. In *f*, dotted lines divide the circle into four quadrants (+, 0, - and 0). That most of the fibres in these cases are restricted to the (+) quadrant (see also Table 2) indicates that normal and ectopic retinal fibres seem to orient towards their targets from a distance. In case *d* a major group of fibres is also heading into the (-) quadrant; the entry point in this case is near the midbrain-hindbrain junction and these fibres are running towards the spinal cord. The schematic insets show the approximate entry points of the fibres into the central nervous system for each case. *OI*, the orientation index, which describes a weighted proportion of fibres heading towards their targets (see Table 2 for definition of *OI*).

**Table 2** Orientation of optic nerve fibres before they have reached the tectum (stage 33/34 and 35/36 embryos)

Entry point of optic nerve	Orientation index
Chiasm (normal animals, $n=10$ )	$1.0 \pm 0.0$
All ectopic entry points ( $n=11$ )	$0.41 \pm 0.18$
Ectopic entry points in forebrain and midbrain only ( $n=8$ )	$0.69 \pm 0.16$

The orientation of projections from both normal and ectopic retinal fibres was analysed by assigning an orientation index (*OI*) to each labelled projection. This was done using the polar graphs shown in Fig. 4. Each individual fibre receives a score of +1 if it enters the (+) sector (towards the target), 0 if it enters either of the (0) sectors (neither towards nor away from the target), and -1 if it enters the (-) quadrant (away from the target). The total *OI* for an animal is taken as the sum of scores for the individual fibres divided by the total number of fibres counted. Thus, an *OI* of 1.0 indicates perfect orientation found in normal animals; a score of 0 would indicate no preference, and negative values would indicate that fibres tend to orient away from the tectum. The average score of 0.4 for all the ectopic projections means that optic fibres entering the brain anywhere (within the scope of those represented here) are more likely to orient towards the tectum [(+) quadrant] than run in any other direction [(0) or (-) quadrants]. If one considers only optic fibres that enter the forebrain or midbrain (eliminating all spinal cord projections) the *OI* rises to near 0.7. The reason that the *OI* is higher when hindbrain entry points are excluded is that a number of fibres entering in the hindbrain may be attracted to the alternative target the spinal cord. Thus, for example, the *OI* of -0.14 in Fig. 4*d* belie the obvious orientation of a bundle of fibres heading towards the tectum in this case. A  $\chi^2$  analysis, used to test the random orientation of fibres (that is, 25% to each quadrant) showed that this possibility could be excluded at the  $P < 0.005$  level. Similarly, a one-tailed student's *t*-test showed that the percentage of fibres found in the (+) quadrant was significantly greater than the 25% random expectation ( $P < 0.005$ ). Values shown are mean  $\pm$  s.e.m.

would not jeopardize the formation of a central visual pathway. Such 'long-range' or distributed guidance mechanisms may also account for the remarkable ability of various brain transplants in embryonic or neonatal mammals to make functional connections<sup>19</sup>. There are, however, limits to the range of these guidance cues, for if displaced by too great a distance, ectopic axons may fail to project to their normal targets. For example, when the optic nerve enters the medulla or cord, spinal rather than tectal projections are often made<sup>17,18</sup>. The present results suggest that the cues for appropriate optic fibre guidance must be distributed at least throughout the diencephalon and mesencephalon. The molecular nature of these guidance cues is unknown. One might suspect a chemotactic mechanism<sup>20,21</sup> with the tectum acting as a source of a diffusible attractant. *In vitro* studies have demonstrated trophic effects of soluble factors from the tectum on retinal ganglion cell survival and neurite elongation, yet there has been no *in vitro* demonstration of chemotactic guidance in this system<sup>4,22-24</sup>. This raises the possibility that growth cones can detect cell surface molecules which signal positional information throughout the entire brain<sup>25,26</sup>.

This work was supported by NIH grant HD-14490.

Received 5 November 1985; accepted 2 January 1986.

1. Singer, M., Norlander, R. H. & Egger, M. *J. comp. Neurol.* **185**, 1-22 (1979).
2. Goodman, C. S. *Bioscience* **34**, 300-306 (1984).
3. Lance-Jones, C. & Landmesser, L. *Proc. R. Soc. B* **214**, 1-18 (1981).
4. Harris, W. A., Holt, C. E., Smith, T. A. & Gallen, N. J. *Neurosci. Res.* **13**, 101-122 (1985).
5. Shatz, C. J. & Kliot, M. *Nature* **300**, 525-529 (1982).
6. Thanos, S. & Bonhoeffer, F. *J. comp. Neurol.* **219**, 420-430 (1983).
7. Hubbard, E. *Expl. Neurol.* **19**, 350-356 (1967).
8. Sharma, S. C. *Nature new Biol.* **238**, 286-287 (1972).
9. Hubbard, E. & Ornberg, R. L. *Expl. Neurol.* **50**, 113-123 (1976).
10. Constantine-Paton, M. & Capranica, R. R. *J. comp. Neurol.* **170**, 17-32 (1976).
11. Harris, W. A. *J. Neurosci.* **2**, 329-353 (1982).
12. Holt, C. E. & Harris, W. A. *Nature* **301**, 150-152 (1983).
13. Nieuwkoop, P. D. & Faber, J. *Normal Tables of Xenopus laevis* (North-Holland, Amsterdam, 1956).
14. Rugh, R. *Experimental Embryology* (Burgess Publishing Co., Minneapolis, 1962).
15. Holt, C. E. *J. Neurosci.* **4**, 1130-1152 (1984).
16. Ferguson, B. A. *Soc. Neurosci. Abstr.* **9**, 759 (1983).
17. Harris, W. A. *J. comp. Neurol.* **194**, 319-333 (1980).
18. Constantine-Paton, M. & Capranica, R. R. *J. comp. Neurol.* **170**, 17-32 (1976).
19. Sladek, J. R. & Gash, D. M. *Neural Transplants: Development and Function* (Plenum, New York, 1984).
20. Gunderson, R. W. & Barrett, J. N. *J. Cell Biol.* **87**, 546-554 (1980).
21. Lumsden, A. G. S. & Davis, A. M. *Nature* **306**, 786-788 (1983).
22. Carri, N. A. & Ebendal, T. *Dev. Brain Res.* **6**, 219-229 (1983).
23. Nurcombe, V. & Bennett, M. R. *Expl. Brain Res.* **44**, 249-258 (1981).
24. Sarthy, P. V., Curtis, B. M. & Catterall, W. A. *J. Neurosci.* **3**, 2532-2544 (1983).
25. Gierer, A. *Biol. Cybern.* **42**, 69-78 (1981).
26. Bonhoeffer, F. & Hui, J. *EMBO J.* **1**, 427-431 (1982).

## Pathway selection by growth cones of identified motoneurones in live zebra fish embryos

Judith S. Eisen, Paul Z. Myers & Monte Westerfield

Institute of Neuroscience, University of Oregon, Eugene, Oregon 97403, USA

**How is the adult pattern of connections between motoneurones and the muscles that they innervate established during vertebrate development? Populations of motoneurones are thought to follow one of two patterns of development: (1) motor axons initially follow stereotyped pathways<sup>1</sup> and project to appropriate regions of the developing muscle<sup>2-4</sup> or (2) motor axons initially project to some regions that are incorrect, the inappropriate projections being eliminated subsequently<sup>5-9</sup>. Here we observed individually identified motoneurones in live zebra fish embryos as they formed growth cones and as their growth cones navigated towards their targets. We report that from axogenesis, each motor axon followed a stereotyped pathway and projected only to the specific region of the muscle appropriate for its adult function<sup>10</sup>. In addition, the**

peripheral arbor established by each motoneurone was restricted to a stereotyped region of its own segment and did not overlap with the peripheral arbor of the other motoneurones in that segment. We conclude that the highly stereotyped pattern of innervation seen in the adult is due to initial selection of the appropriate pathway, rather than elimination of incorrect projections.

Zebra fish embryos offer several advantages as a system in which to study neuronal development. The embryos are optically clear, and development occurs rapidly, so we can follow a neurone in a single individual from the time it is first recognizable until its axon reaches its targets. Here we observed the growth of live motoneurones in trunk segments 6-15 (Fig. 1a, b) with Nomarski (Fig. 1c) or fluorescence (Fig. 1d, e) optics.

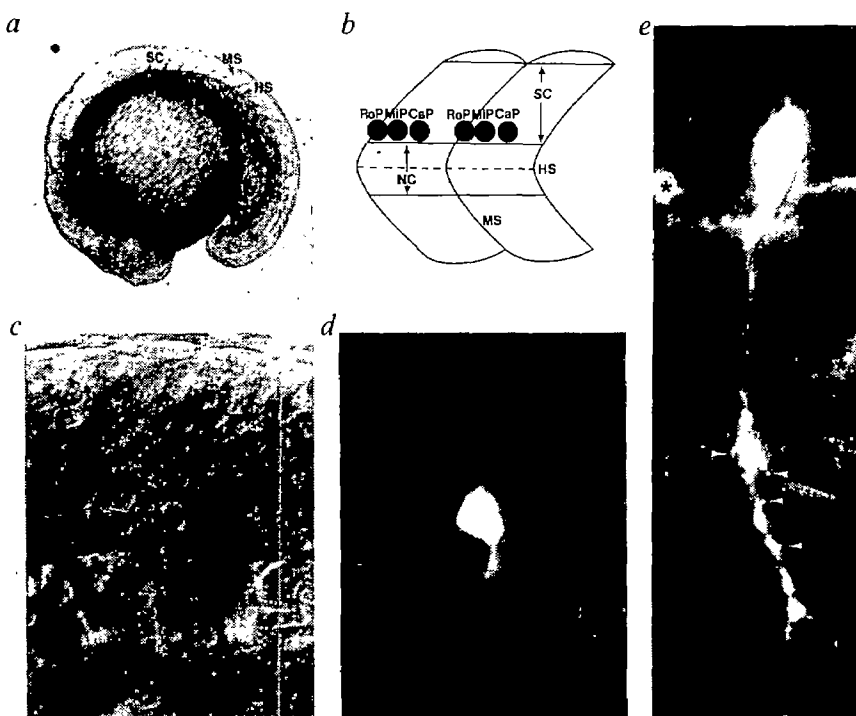
Initially there were three motoneurones on each side of the spinal cord in each segment (Fig. 1b). These cells were recognizable as primary motoneurones<sup>11,12</sup> even prior to axogenesis by their large diameter ( $9.8 \pm 0.9 \mu\text{m}$  (mean  $\pm$  s.d.); 10 cells, 3 animals) and characteristic ventro-lateral positions within the spinal cord. Each primary motoneurone occupied a specific location in the spinal cord, and we have named them according to this feature (caudal primary, CaP; middle primary, MiP; rostral primary, RoP) (Fig. 1b).

Two independent lines of evidence show that the CaP growth cone in each segment leaves the spinal cord before the growth cones of the other primary motoneurones, thus acting as a 'pioneer' in establishing the ventral root. First, using Nomarski optics (Fig. 1c), we found that the earliest growth cone we could observe in each segment was from CaP (50 segments; 19 animals). Second, in four animals, two or all three of the primary motoneurones within a single segment were fluorescently labelled; in all of these cases the CaP growth cone left the spinal cord first. Although the MiP and RoP growth cones consistently left the spinal cord later than the growth cone of the CaP motoneurone in the same segment, our results did not allow us to determine whether the CaP always initiates an axon before MiP and RoP or whether the CaP growth cone leaves the spinal cord first because it has the shortest distance to grow.

Each primary motor axon follows a stereotyped pathway (Fig. 2) characteristic of its cell type. Each CaP axon (Fig. 2a) had a prominent growth cone that grew directly ventrally, along the medial surface of the muscle. At the region of the horizontal septum the CaP growth cone typically paused for about an hour ( $0.9 \pm 0.7 \text{ h}$ ;  $n = 7$ ). When the growth cone continued ventrally, a prominent varicosity remained at the region of the horizontal septum. The CaP growth cone also typically paused and formed varicosities at the bottom of the notochord and at intervals along the length of the growing axon. Branches formed later at some of these varicosities and grew along the medial surface of the muscle.

In contrast, the MiP growth cone (Fig. 2b) grew caudally within the spinal cord, exited at the ventral root, and followed the pathway established by the CaP axon. In segments in which both CaP and MiP motoneurones were labelled ( $n = 4$ ), the two axons appeared to fasciculate. Like CaP growth cones, MiP growth cones grew along the medial surface of the muscle to the region of the horizontal septum. MiP growth cones also typically paused for about 30 min ( $0.6 \pm 0.5 \text{ h}$ ;  $n = 8$ ) at the horizontal septum. Unlike CaP growth cones, however, MiP growth cones did not cross the horizontal septum. Instead, each growth cone sprouted a branch that grew caudally and dorsally, entering the dorsal portion of the segment. MiP axons typically (8 out of 10) retracted their ventral branches as they grew dorsally, although some cells (the remaining 2 out of 10) retained the ventral branch for up to 48 h post-fertilization (PF). RoP growth cones (Fig. 2c) initially followed the pathway described for MiP growth cones. RoP growth cones grew caudally within the spinal cord, exited at the ventral root, and grew directly to the region of the horizontal septum. From this point, they followed a third pathway, growing laterally within the horizontal

**Fig. 1** *a*, Zebra fish embryo at 18 h post-fertilization (PF). The axial musculature is segmented, and the segments are separated by transversely oriented myosepta (MS), and divided into dorsal and ventral regions by the horizontal septum (HS). The chevron-shaped segments are transparent and thus the spinal cord (SC) and the notochord (NC) can be visualized directly. We confined our observations to motoneurones in segments 6–15. In this figure rostral is to the left, and dorsal to the top; all other figures are of the same orientation. Scale bar, 225 µm. *b*, A drawing of two adjacent segments (abbreviations as in *a*). The solid circles represent the positions of the three primary motoneurones in each segment. Caudal primary (CaP) is located in the middle of the segment, at the level of the ventral root; rostral primary (RoP) is located at the rostral end of the segment; and middle primary (MiP) is located between CaP and RoP. Scale bar 33 µm. *c*, Nomarski photomicrograph of a CaP motoneurone (large arrow) with a growth cone (small arrow) in a live embryo at 20.5 h PF. Scale bar 10 µm. *d*, Fluorescence photomicrograph of a living labelled CaP motoneurone (20.5 h PF). Although early growth cones can readily be observed with Nomarski optics, this technique is inadequate for later observations because the development of striations in the muscle fibres obscures axons. Thus, we have also labelled neurones with fluorescent dyes to observe axons and watch their development in live embryos. To label developing primary motoneurones, we injected their early precursor cells with fluorescent dye (fluorescein or rhodamine) conjugated to dextran<sup>19–21</sup>. We injected single blastomeres in developing blastulae at the 32–512-cell stage; as the cells continued to divide, the label was passed on to all of the progeny of the injected blastomere. The descendants of the injected blastomere scattered during gastrulation<sup>21</sup>, so that individual labelled motoneurones were observed at later developmental stages relatively unobscured by other labelled cells. To observe the development of the motoneurones without causing photodamage<sup>22</sup>, we used low levels of epifluorescence, monitored the cells with a silicon-intensified-target camera (SIT camera, GE 57)<sup>23,24</sup> and recorded the image on videotape (VHS) for later analysis. The CaP motoneurone shown was photographed from the face of the video monitor. Scale bar, 10 µm. *e*, CaP motoneurone in a live embryo at 27 h PF (segment 11). The fluorescence optics showed side branches (arrowheads) and varicosities which were present along the length of the axon at these later developmental times. The body of the main growth cone was also clearly visible although filopodia were usually not resolved. In this cell the growth cone bifurcated shortly before the photograph was taken. The asterisks mark fluorescently labelled cells that were out of focus on the other side of the embryo. Scale bar, 10 µm.



septum, and forming horizontal branches that extended from the medial surface of the muscle to the lateral surface.

The peripheral arbor of each primary motoneurone is characteristic of its cell type, being restricted to a stereotyped region of the ipsilateral muscle of its own segment. The same three types of motoneurones have been observed in larvae and adults<sup>12,13</sup>. The branches of CaP motoneurones were confined within the ventral musculature (Fig. 3*a*) in all but a single case (64 out of 65 motoneurones examined until 48 h PF; the remaining CaP motoneurone had a small branch extending into an adjacent segment). In contrast, the branches of MiP motoneurones (Fig. 3*b*) were confined to the dorsal musculature of their own segment (all of 15 motoneurones; 48 h PF). The branches of RoP motoneurones (Fig. 3*c*) also were confined to their own segment, but were restricted to a unique region flanking the horizontal septum (all of 4 motoneurones; 48 h PF).

What factors could be responsible for confining the growth cones of the primary motoneurones within their own segments? One possibility is that the myosepta are barriers to axonal growth, but this seems unlikely as a later-developing class of motoneurones, the secondary motoneurones, have axons that cross these myosepta<sup>10,13</sup>.

A rostro-caudal gradient in the time of axonal outgrowth within a class of motoneurones might be another possible determinant of segmental specificity; a motoneurone from a caudal segment could not innervate muscle in a more rostral segment, because that muscle would already be innervated. However, two independent observations fail to support this notion. First, in

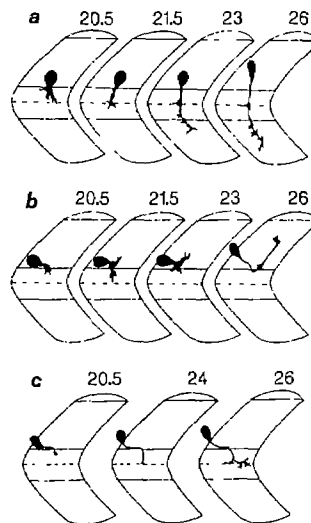


**Fig. 2** The axons of the three primary motoneurones of each segment follow divergent pathways. Drawings from the face of the video monitor of fluorescent motoneurones from live animals at the indicated developmental stages (h PF) superimposed on outlines of the segments. *a*, A single CaP motoneurone at four different times; *b*, a single MiP motoneurone at three different times. (See Fig. 3 for three-dimensional drawings of motoneurones at a later developmental stage.)

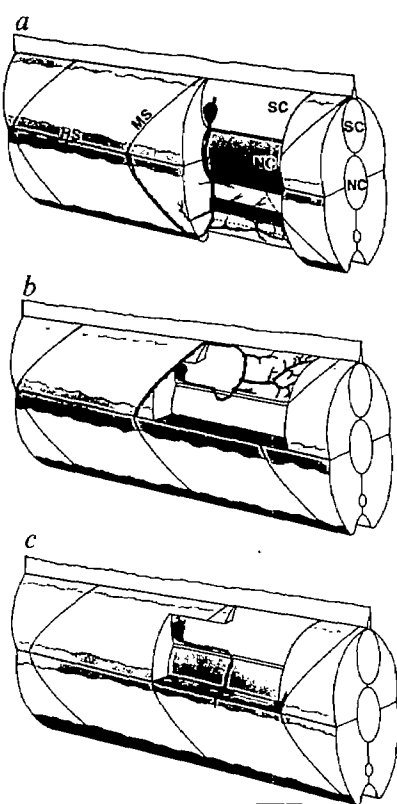


**Fig. 3** Each of the three primary motoneurones in a segment has a unique peripheral arbor, as shown by three-dimensional drawings of the arbors of the primary motoneurones at 48 h PF. A portion of the muscle overlying the spinal cord (SC) and notochord (NC) in each part of the figure has been omitted, to show the underlying pattern of the axonal branches. Each motoneurone projects exclusively to muscle fibres within its own segment, and to an exclusive region of its own segment. HS, horizontal septum; MS, myoseptum. Scale bar, 20  $\mu\text{m}$ . *a*, After the CaP growth cone reached the ventral edge of its segment, it turned laterally and rostrally, and grew dorsally along the lateral surface of the muscle, in the rostral myoseptum, to the level of the horizontal septum. Varicosities formed along the lateral branch at regular intervals, giving it the appearance of a string of beads. *b*, The axon of the MiP motoneurone extended along the medial surface of the dorsal muscle, in the middle of the segment. When the axon reached the dorsal edge, it turned laterally and rostrally, and grew along the lateral surface of the muscle in the rostral myoseptum, to the level of the horizontal septum, elaborating a string of varicosities along the lateral portion of the axon. *c*, The arbor of the RoP motoneurone extended from the medial surface to the lateral surface along the horizontal septum.

animals in which several primary motoneurones of the same type were labelled in more than one segment (Fig. 4), axons in caudal segments preceded axons in rostral segments in half of the cases (38 segments, 7 animals). Second, observations of initial outgrowth of CaP axons using Nomarski optics showed that any trunk segment could be the first to have a CaP growth cone<sup>14</sup> and the appearance of growth cones in other segments did not follow any particular sequence. Thus, rostro-caudal timing seems to be an unlikely explanation of segmental specificity, as axonal outgrowth of a primary motoneurone in any particular segment may precede or follow axonal outgrowth of the primary motoneurone of the same type in adjacent segments.

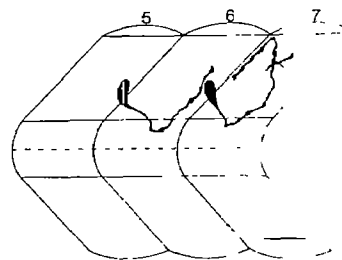


**Fig. 4** Axon outgrowth does not occur in a strict rostral-caudal sequence. Two MiP motoneurones were labelled in adjacent segments in the same animal. The growth cone of the caudal MiP (segment 7) grew out of the spinal cord at 19 h PF. The rostral MiP (segment 6) first sprouted a growth cone 1.5 h later. This drawing of the two cells made at 25 h PF shows that the axon of the caudal MiP had already grown into the myoseptum while the rostral axon was still traversing the dorsal muscle. In other animals the opposite order of outgrowth was seen. Scale bar, 25  $\mu\text{m}$ .

After leaving the spinal cord, all three types of motor growth cones initially followed the same pathway to the horizontal septum, where they paused and then selected neurone-specific pathways. Although pausing at particular locations is behaviour typical of growth cones, the wide range of durations involved suggested that pausing itself may not be a crucial component of proper pathfinding. The choice of divergent pathways at the horizontal septum by these growth cones is reminiscent of the choice of neurone-specific pathways by the growth cones of G and C cells in embryonic grasshoppers<sup>15</sup>. This type of behaviour is consistent with a 'labelled pathways' hypothesis<sup>16</sup> in which growth cones recognize specific molecular factors, along the axonal pathway, that provide guidance cues to them as they navigate towards their targets. Our results suggest that such labelled pathways may be present in vertebrates.

Some of this work has appeared elsewhere in abstract form<sup>17</sup>.

This study was inspired by the pioneering work of Speidel<sup>18</sup>. We thank David Brumbley, Harrison Howard, James McMurray and Rachel Warga for technical assistance, and Corey Goodman, Charles Kimmel, Lynn Landmesser and Walter Metcalfe for comments on earlier versions of the manuscript. This work was supported by NIH grants NS21132 and NS17963, the Oregon MRF, and an MDA postdoctoral fellowship to J.S.E.

Received 4 December 1985; accepted 8 January 1986.

1. Lance-Jones, C. & Landmesser, L. *Proc. R. Soc. B* **214**, 1–18 (1981).
2. Hollyday, M. *Curr. Topics Dev. Biol.* **15**, 181–215 (1980).
3. Hollyday, M. in *Limb Development and Regeneration* (eds Fallon, J. F. & Caplan, A. I.) 183–193 (Liss, New York, 1983).
4. Landmesser, L. A. *Rev. Neurosci.* **3**, 279–302 (1980).
5. Pettigrew, A., Lindeman, R. & Bennett, M. R. J. *Embryol. exp. Morph.* **49**, 115–137 (1979).
6. Lamb, A. H. *Devil Biol.* **54**, 82–99 (1976).
7. Lamb, A. H. *Brain Res.* **134**, 145–150 (1977).
8. Lamb, A. H. *Devil Biol.* **71**, 8–21 (1979).
9. McGrath, P. A. & Bennett, M. R. *Devil Biol.* **69**, 133–145 (1979).
10. Westerfield, M., Myers, P. Z. & Eisen, J. S. *Soc. Neurosci. Abstr.* **10**, 371 (1984).
11. Blight, A. R. *J. comp. Neurol.* **180**, 679–690 (1978).
12. Myers, P. Z. *Soc. Neurosci. Abstr.* **9**, 848 (1983).
13. Westerfield, M., McMurray, J. & Eisen, J. S. *J. Neurosci.* (in the press).
14. Eisen, J. S., Myers, P. Z. & Westerfield, M. *Soc. Neurosci. Abstr.* **11**, 586 (1985).
15. Raper, J., Bastiani, M. J. & Goodman, C. S. *J. Neurosci.* **3**, 20–30 (1983).
16. Raper, J., Bastiani, M. J. & Goodman, C. S. *J. Neurosci.* **3**, 31–41 (1983).
17. Eisen, J. S., Myers, P. Z. & Westerfield, M. *Soc. Neurosci. Abstr.* **10**, 371 (1984).
18. Speidel, C. C. *J. Anat.* **52**, 1–79 (1933).
19. Weisblat, D. A., Zackson, S. L., Blair, S. S. & Young, J. D. *Science* **209**, 1538–1541 (1980).
20. Kimmel, C. B. & Law, R. *Devil Biol.* **108**, 78–85 (1985).
21. Kimmel, C. B. & Law, R. *Devil Biol.* **108**, 94–101 (1985).
22. Miller, J. P. & Silverston, A. I. *Science* **206**, 702–704 (1979).
23. Kater, S. B. & Hadley, R. D. in *Cytological Methods in Neuroanatomy*, ed. Chan-Palay, V., 441–459 (Liss, New York, 1982).
24. Kater, S. B. & Hadley, R. D. *Trends Neurosci.* **5**, 80–82 (1982).

## A T3-like protein complex associated with the antigen receptor on murine T cells

Hans C. Oettgen, Carolyn L. Pettey, W. Lee Maloy\*  
 & Cox Terhorst

Laboratory of Molecular Immunology, Dana Farber Cancer Institute, Harvard Medical School, 44 Binney Street, Boston, Massachusetts 02115, USA

\* Laboratory of Immunogenetics, National Institute of Allergy and Infectious Diseases, National Institutes of Health, Bethesda, Maryland 20205, USA

**Antigen recognition by human T lymphocytes and initiation of T-cell activation are mediated by a group of integral membrane proteins, the T-cell antigen receptor (TCR) and the T3 complex<sup>1-8</sup>.** The polypeptides which comprise T3 (a  $\gamma$ -chain of relative molecular mass ( $M_r$ ) 25,000 (25K), and  $\delta$  and  $\epsilon$  chains of 20K each) are physically associated with the TCR chains<sup>9-12</sup>. Surface expression of the complex requires the presence of all the component T3 and TCR proteins<sup>13</sup>. In contrast to the human system, murine T3 has not been identified using antibodies. Here we describe a murine T3-like protein complex. It appears to be more complicated than human T3, containing three monomeric glycoproteins (21–28K), two of which have *N*-linked carbohydrate side chains and a novel family of TCR-associated homo- and heterodimers. The 28K protein is identified as the murine T3  $\delta$ -chain. The 21K protein is phosphorylated on cell activation with concanavalin A (Con A).

Given the significant structural and functional association of T3 with the human TCR, we expected that T3-like proteins

would be present on murine T cells. Recently, a murine complementary DNA clone homologous with the cDNA sequence encoding one of the human T3 chains (T3 $\delta$ ) has been described<sup>14</sup>. We attempted to identify murine T3-like proteins by isolating polypeptides associated with TCR.

For this purpose, it was necessary to improve the methods for extraction of the protein complex, as immunoprecipitation from conventionally prepared lysates of labelled human T cells with anti-TCR ( $\alpha$  and  $\beta$ ) reagents results in only a minimal co-isolation of the T3 $\gamma$ ,  $\delta$  and  $\epsilon$  chains (see Fig. 1A, lane 1). Figure 1A (lanes 3 and 4) shows that when a digitonin-based extraction procedure is used, both anti-T3 and an anti-TCR reagent precipitate the complete series of T3 and TCR polypeptides— $\alpha$  (49K),  $\beta$  (40K),  $\gamma$  (25K) and  $\delta/\epsilon$  (20K)—from  $^{125}$ I-radiolabelled cells of the human T-cell leukaemia line HPB-ALL.

Using this method, proteins associated with the murine TCR were isolated from  $^{125}$ I-labelled 2B4 cells, a pigeon cytochrome-c-specific, I-E<sup>k</sup>-restricted T-T hybridoma<sup>15</sup>. As shown in Fig. 1B (lane 2), TCR prepared from Nonidet P-40 (NP40)-solubilized cells appears as a single band of 85–90K. The TCR immunoprecipitate from the digitonin lysate (Fig. 1B, lane 6), however, contains an additional set of six specific bands with apparent  $M_r$ s of 34K, 31K, 27K, 25K, 22K and 20K. None of these bands has the same mobility as Thy-1 (Fig. 1B, lane 8) nor do any of them co-precipitate with Thy-1. This control was included because G7, the anti-Thy-1 reagent used for precipitation, causes T-cell proliferation, which suggests that Thy-1 represents the murine homologue of T3 (ref. 16). Studies with another murine T-cell hybridoma, DO-11.10, which is specific for ovalbumin peptides and is I-A<sup>d</sup>-restricted<sup>2</sup>, gave the same result using two different TCR-specific antibodies (Fig. 1C). The proteins are not recovered if antibody against major

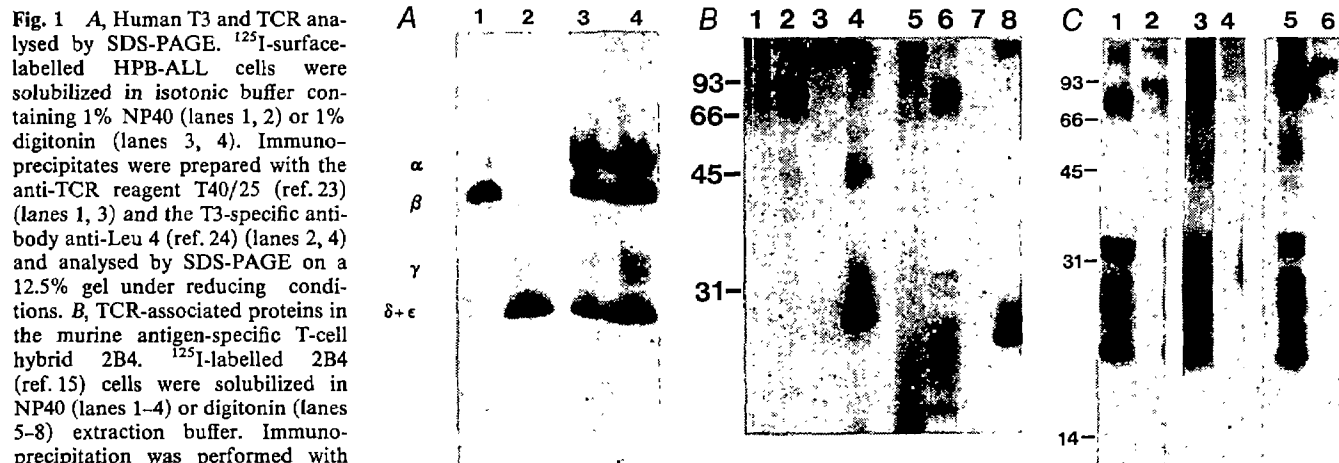


**Fig. 1** *A*, Human T3 and TCR analysed by SDS-PAGE.  $^{125}$ I-surface-labelled HPB-ALL cells were solubilized in isotonic buffer containing 1% NP40 (lanes 1, 2) or 1% digitonin (lanes 3, 4). Immunoprecipitates were prepared with the anti-TCR reagent T40/25 (ref. 23) (lanes 1, 3) and the T3-specific antibody anti-Leu 4 (ref. 24) (lanes 2, 4) and analysed by SDS-PAGE on a 12.5% gel under reducing conditions. *B*, TCR-associated proteins in the murine antigen-specific T-cell hybrid 2B4.  $^{125}$ I-labelled 2B4 (ref. 15) cells were solubilized in NP40 (lanes 1–4) or digitonin (lanes 5–8) extraction buffer. Immunoprecipitation was performed with non-immune mouse serum (lanes 1, 5), normal rat serum (lanes 3, 7), A2B4-2 (anti-TCR)<sup>15</sup> (lanes 2, 6), and G7 (anti Thy-1)<sup>16</sup> (lanes 4, 8), and samples were analysed under non-reducing conditions on a 12.5% gel. The positions of standard protein markers are indicated on the left ( $M_r \times 10^{-3}$ ). *C*, TCR-associated proteins on the T-cell hybrid DO-11.10. Digitonin extracts of  $^{125}$ I-labelled DO-11.10 cells<sup>2</sup> were immunoprecipitated with the clone-specific anti-TCR antibody KJ1-26.1 (ref. 2) (lane 1), non-immune mouse serum (lane 2), the anti-TCR-allotype reagent KJ16-133 (ref. 25) (lane 3) and non-immune rat serum (lane 4). A2B4-2 (lane 5) and normal mouse serum (lane 6) immunoprecipitates from digitonin-extracted 2B4 cells are shown for comparison.

**Methods.** HPB-ALL cells<sup>26</sup> and the murine T-cell hybrids 2B4 and DO-11.10 were cultured in RPMI 1640 medium supplemented with 10% fetal calf serum (FCS). Cells ( $50 \times 10^6$ ) were labelled with  $^{125}$ I (2 mCi, NEN) at room temperature in a 200- $\mu$ l volume of phosphate-buffered saline (PBS) containing 4 IU lactoperoxidase (Sigma); 10  $\mu$ l of 0.05% H<sub>2</sub>O<sub>2</sub> was added at 5-min intervals over a reaction period of 20 min. Cells were washed once in PBS and suspended at 0 °C for 15 min in 300  $\mu$ l extraction buffer (10 mM triethanolamine, 0.15 M NaCl, pH 7.8 with the protease inhibitors: 10 mM iodoacetamide, 1 mM EDTA, 1 mM phenylmethylsulphonyl fluoride and 1  $\mu$ g ml<sup>-1</sup> each of leupeptin, pepstatin, antipain and chymostatin) containing 1% NP40 or 1% digitonin. Digitonin (Aldrich) was prepared as a 2% stock solution. The solid detergent was added to boiling water, which was stirred for 2 min, cooled, allowed to stand at room temperature for 1 week and then filtered<sup>27</sup>. The cell extract was centrifuged at 13,000g for 15 min and the supernatant at 100,000g for 30 min before pre-clearing for 16 h with 10  $\mu$ l of a 10% suspension of *Staphylococcus aureus*. Immunoprecipitation was performed by incubating the extract for 2–4 h with a 10- $\mu$ l packed volume of protein A-Sepharose beads (Pharmacia) precoated with antibody (200  $\mu$ l of hybridoma culture supernatant or 5  $\mu$ l of ascites). Beads coated with rat antibodies were precoated with rabbit anti-rat immunoglobulin. Immunoprecipitates were washed five times in the same buffer used for cell extraction and subjected to SDS-PAGE, using the method of Laemmli<sup>28</sup>.

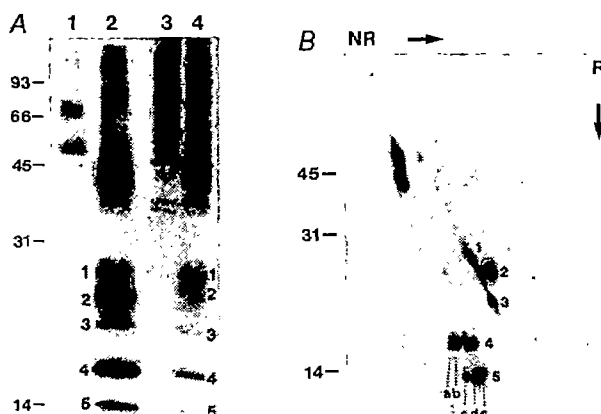


**Fig. 2** *A*, Analysis of murine TCR-associated proteins under reducing conditions. DO-11.10 cells were labelled with  $^{125}\text{I}$ . 2B4 cells ( $2 \times 10^8$ ) were incubated at 37 °C for 16 h with 1 mCi each of  $^{35}\text{S}$ -cysteine and  $^{35}\text{S}$ -methionine (Amersham) in 100 ml cysteine/methionine-free RPMI 1640 medium with 10% dialysed FCS. Immunoprecipitates were prepared from digitonin extracts of the DO-11.10 (lanes 1, 2) and 2B4 (lanes 3, 4) cells using normal rat serum (lane 1), normal mouse serum (lane 3) and the anti-TCR reagents KJ16-133 (lane 2) and A2B4-2 (lane 4), and analysed by SDS-PAGE under reducing conditions. *B*, Two-dimensional non-reducing/reducing SDS-PAGE analysis of murine TCR-associated proteins. An A2B4-2 immunoprecipitate from digitonin-extracted  $^{125}\text{I}$ -labelled 2B4 cells was applied to a 12.5% SDS-polyacrylamide tube gel and electrophoresed under non-reducing conditions. The gel was then equilibrated for 15 min at room temperature in reducing sample buffer containing 5% 2-mercaptoethanol before application to a 12.5% slab gel.

histocompatibility complex (MHC) class I antigen ( $\text{K}^k$ ) or an inappropriate anti-TCR reagent is used (data not shown). We conclude that the murine TCR is associated with a complex group of proteins, some of which may be murine homologues of the human T3 chains.

When analysed under reducing conditions, five TCR-associated proteins—28K (1), 25K (2), 21K (3), 17K (4) and 14K (5)—were found (Fig. 2A, lane 2). This result was also obtained after biosynthetic labelling with  $^{35}\text{S}$ -cysteine and  $^{35}\text{S}$ -methionine (Fig. 2A, lane 4). The 31K and 34K proteins present under non-reducing conditions (Fig. 1B, C) were absent and two new small polypeptides of 14K and 17K (4 and 5) were observed. To determine the relationship between the proteins seen in non-reducing conditions (Fig. 1B) and those recovered after reduction (Fig. 2A, 1–5), we performed a two-dimensional non-reducing/reducing SDS-polyacrylamide gel electrophoresis (PAGE) analysis (Fig. 2B). Proteins composed of disulphide-linked subunits appear below the diagonal on such a gel. A series of 17K and 14K spots corresponding to bands 4 and 5 seen under reducing conditions was observed below the diagonal; these spots were aligned such that they appeared to be derived from two 17K homodimers (which we designate *a* and *b*), two heterodimers (14K+17K; *c* and *d*) and a 14K homodimer (*e*). The 21K, 25K and 28K monomeric proteins, seen as bands 1, 2 and 3 on reducing SDS-PAGE analysis of the TCR-associated proteins, were observed as three spots lying on or near the diagonal. The position of protein 2 above the diagonal may be the result of reduction of internal disulphide bonds. We conclude that the murine T3-like complex consists of five proteins, three monomers and two small subunits which form a family of homo- and heterodimers.

The presence of carbohydrate in the T3-like proteins was assayed by labelling with  $^3\text{H}$ -mannose. In addition to the TCR- $\alpha$ - and  $\beta$ -chains, three bands corresponding to the three TCR-

associated monomers (1, 2 and 3) contained the carbohydrate label (Fig. 3A, lane 4). The dimers containing the 14K and 17K subunits (4 and 5) were not labelled. To confirm the presence of oligosaccharide side chains, the enzyme endoglycosidase F (Endo-F), which hydrolyses the second glycosidic bond of *N*-linked oligosaccharides, was used to digest the purified TCR-associated proteins. Treatment of both the 21K and 28K bands (bands 1 and 3) gave rise to 16K products (Fig. 3B, lanes 2, 6). The bulk of the 25K protein (2) was not altered by Endo-F (Fig. 3B, lane 4). As expected, the 17K subunit (Fig. 3B, lane 7) was unaffected by the deglycosylating enzyme (lane 8). Sufficient amounts of pure 14K protein (band 5) for analysis could not be obtained but in digestions of the unseparated mixture of TCR-associated proteins its mobility had been observed to be unaltered (data not shown). We conclude that proteins 1 and 3, seen as 28K and 21K bands under reducing conditions, contain *N*-linked carbohydrate. Although the 25K protein was not digested, we hesitate to rule out the presence of *N*-linked glycans; incorporation by the 25K protein of  $^3\text{H}$ -mannose, a sugar rarely present in *O*-linked carbohydrate, suggests that it may contain *N*-linked glycosylation that is resistant to enzyme digestion. The 14K and 17K subunits appear to be unglycosylated.

The identity of the T3  $\delta$ -chain among the murine TCR-associated proteins was determined by immunoblotting using a rabbit antiserum specific for a 17-residue synthetic peptide corresponding to the amino-acid sequence deduced for a murine T3 $\delta$  cDNA clone<sup>14</sup>. The serum bound specifically to a 28K membrane protein (Fig. 3C, lanes 3, 4). No binding was observed in the presence of competing peptide (lane 5). Pretreatment of the membrane proteins with Endo-F resulted in a decrease in size of the band from 28K to 16K (Fig. 3C, lanes 6, 7). A preparation of  $^{125}\text{I}$ -labelled TCR-associated proteins was run in parallel (lane 2). In the microslab system used in this analysis, the 25K and 28K proteins (bands 1 and 2) were not resolved but were seen as a single band of the same size as the specifically immunoblotted protein. Given that the protein detected by antiserum to a T3 $\delta$  peptide and the 28K protein (band 1), but not the 25K protein (band 2), are Endo-F-sensitive and have 16K protein backbones, we conclude that the 28K TCR-associated protein represents murine T3 $\delta$ ; this is in agreement with the presence of three sites for *N*-linked glycosylation indicated by the murine T3 $\delta$  cDNA sequence.

In view of the putative role of T3 in signal transduction and the involvement of protein kinases in cellular proliferation, we examined the possibility that one of the T3-like chains is phosphorylated. A TCR-associated phosphoprotein has been described previously by Samelson and colleagues<sup>15</sup>. We were interested to determine whether this polypeptide corresponded to one of the  $^{125}\text{I}$ -labelled proteins of the T3-like complex that we had observed.  $^{32}\text{P}$ -loaded 2B4 cells either treated with Con A or left unstimulated were solubilized in digitonin and anti-TCR immunoprecipitates were prepared (Fig. 4). Although the background bands were of similar intensity in treated and untreated cells, a 20K  $^{32}\text{P}$ -labelled protein which aligned with the 20K  $^{125}\text{I}$ -labelled band (band 3) was seen in the anti-TCR immunoprecipitate from the lysate of stimulated cells alone (Fig. 4, lane 4). Whether this observation indicates that band 3 is a protein kinase is being investigated.

We have identified a T3-like complex of proteins associated with TCR in murine T-cell hybrids. The three glycosylated monomers, the smallest of which is phosphorylated on activation, are similar in size and in their TCR-association to the human T3 $\gamma$ ,  $\delta$  and  $\epsilon$  chains and may constitute their murine homologues. The largest of these monomers appears to be the murine T3 $\delta$  chain. Two of the proteins reported here may correspond to the 24K and 29K proteins isolated with TCR from a murine lymphoma line treated with a crosslinking reagent before solubilization<sup>18–20</sup>. A 23K protein occasionally observed to co-precipitate with TCR from 2B4 cells, which appears to

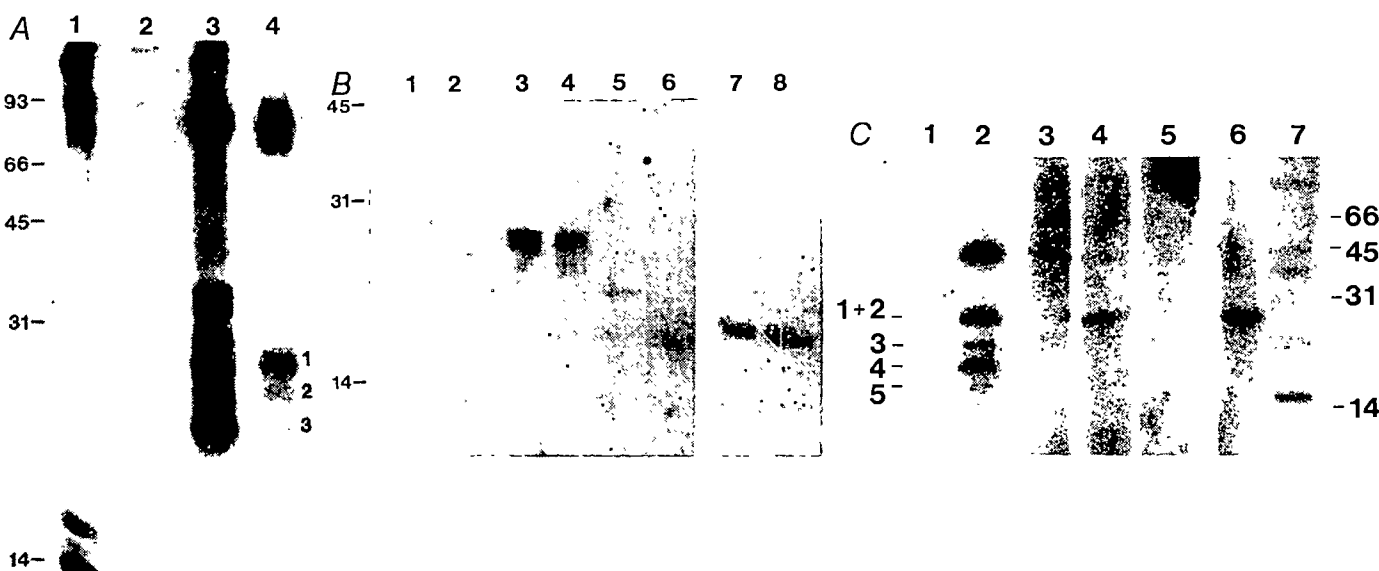


**Fig. 3** *A*, Glycosylation of the murine TCR-associated proteins. 2B4 cells surface-labelled with  $^{125}\text{I}$  as described in Fig. 1 (lanes 1, 3) or biosynthetically labelled with  $^3\text{H}$ -mannose by incubating  $5 \times 10^7$  cells for 16 h at  $37^\circ\text{C}$  in 10 ml of glucose-poor RPMI (containing  $100 \text{ mg l}^{-1}$  glucose and 10% dialysed FCS) with 1 mCi  $^3\text{H}$ -mannose (Amersham) (lanes 2, 4) were extracted in 1% digitonin solubilization buffer. Normal mouse serum (lanes 1, 2) and A2B4-2 anti-TCR (lanes 3, 4) immunoprecipitates were analysed under non-reducing conditions on a 12.5% gel. The sugar was not metabolically converted to amino acids during the overnight incubation because murine H-2 heavy chain but not  $\beta_2$ -microglobulin (nonglycosylated) was labelled by  $^3\text{H}$ -mannose (data not shown). *B*, Endo-F digestion of individual murine TCR-associated proteins. 17K, 21K, 25K and 28K proteins were recovered from lane 2 of the gel in Fig. 2A by electroelution<sup>29</sup>, lyophilized and suspended in 60  $\mu\text{l}$  of 100 mM Tris-HCl pH 6.8, 0.5% SDS, 10 mM EDTA and 1% 2-mercaptoethanol. After heating to  $100^\circ\text{C}$  for 3 min, NP40 was added to 1% and protease inhibitors (see Fig. 1 legend) were added. Endo- $\beta$ -N-acetylglucosaminidase-F (Endo-F)<sup>30</sup> (from Dr J. Kaufman) was added to half of each sample and digestion was allowed to proceed for 4 h at  $37^\circ\text{C}$ . 6  $\mu\text{l}$  of 10% SDS, 50% glycerol, 40% 2-mercaptoethanol and 0.1% bromophenol blue were added to the treated and untreated samples before application to a 12.5% gel. Lane 1, 28K minus Endo-F; lane 2, 28K + Endo-F; lane 3, 25K - Endo-F; lane 4, 25K + Endo-F; lane 5, 21K - Endo-F; lane 6, 21K + Endo-F; lane 7, 17K - Endo-F; lane 8, 17K + Endo-F. *C*, Immunoblot analysis of murine T-cell membrane proteins with an anti-T3 $\delta$  serum. Immunoprecipitates prepared from digitonin-extracted  $^{125}\text{I}$ -labelled DO-11.10 cells using normal mouse serum (lane 1) and the anti-TCR reagent KJ16-133 (lane 2) were separated by SDS-PAGE under reducing conditions on a 12.5% microslab gel<sup>31</sup>. Plasma membrane proteins from the murine thymoma line, EL-4, were run in lanes 3-6. Lane 7 contains Endo-F-digested EL-4 membrane proteins. The proteins were transferred to nitrocellulose<sup>32</sup>. The strips corresponding to the lanes containing T-cell membrane proteins were blocked in 1.5% gelatin, then incubated with preimmune rabbit serum (lane 3) or rabbit antiserum directed against a synthetic peptide based on the deduced amino-acid sequence (residues 126-142) of the murine T3 $\delta$  cDNA (lanes 4-7). Excess free peptide was included in one incubation (lane 5). Nitrocellulose strips were developed with  $^{125}\text{I}$ -goat F(ab')<sub>2</sub> anti-rabbit immunoglobulin (NEN).

cause an increase in the size of TCR after crosslinking of surface proteins, has been reported by Samelson and Schwartz<sup>21</sup>. On the basis of its TCR association and  $M_r$ , the 23K protein probably corresponds to one of the monomeric T3-like polypeptides of 2B4 cells described here. In addition to the monomers, which appear to be similar to the human T3 chains, we have described a novel family of TCR-associated homo- and heterodimers. It is of interest to note that although both the 14K and 17K subunits are easily surface-labelled with  $^{125}\text{I}$  using lactoperoxidase or biosynthetically labelled with  $^{35}\text{S}$ -amino acids, only the 17K polypeptide incorporates the hydrophobic-partitioning, photoactivatable label 3-[trifluoromethyl]-3-[m-iodophenyl]-deazirine<sup>22</sup> (TID), suggesting that it contains a hydrophobic domain that is absent from the 14K protein (data not shown). The possibility that the 14K protein is derived from the 17K protein by *in vivo* or *in vitro* proteolysis remains to be investigated. We believe that a comparison of the structure, biosynthesis and regulation of gene expression of these TCR-associated polypeptide chains in both species will help to elucidate the molecular events involved in TCR function.

We thank Dr Edgar Haber for suggesting the use of digitonin; Dr L. Samelson for providing the T-cell hybrid 2B4 and A2B4-2, the anti-TCR reagent for 2B4 cells; Dr P. Marrack for the hybrid DO-11.10 and the anti-TCR antibodies directed at DO-11.10; Dr Ethan Shevach for the anti-Thy-1 rat monoclonal antibody, G7; Drs Hildegunde Ertl, Ken Rock and David Ucker for their critical review of the manuscript; and Debora Ma for assistance. This work was supported by NIH grant AI 15066. H.C.O. is supported by a Medical Scientist Training Program Grant 2-T32-

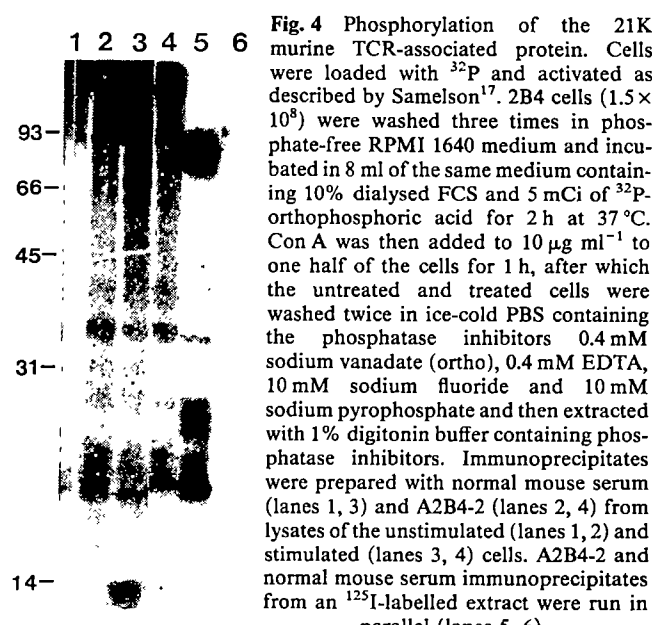


**Fig. 4** Phosphorylation of the 21K murine TCR-associated protein. Cells were loaded with  $^{32}\text{P}$  and activated as described by Samelson<sup>17</sup>. 2B4 cells ( $1.5 \times 10^8$ ) were washed three times in phosphate-free RPMI 1640 medium and incubated in 8 ml of the same medium containing 10% dialysed FCS and 5 mCi of  $^{32}\text{P}$ -orthophosphoric acid for 2 h at  $37^\circ\text{C}$ . Con A was then added to 10  $\mu\text{g ml}^{-1}$  to one half of the cells for 1 h, after which the untreated and treated cells were washed twice in ice-cold PBS containing the phosphatase inhibitors 0.4 mM sodium vanadate (ortho), 0.4 mM EDTA, 10 mM sodium fluoride and 10 mM sodium pyrophosphate and then extracted with 1% digitonin buffer containing phosphatase inhibitors. Immunoprecipitates were prepared with normal mouse serum (lanes 1, 3) and A2B4-2 (lanes 2, 4) from lysates of the unstimulated (lanes 1, 2) and stimulated (lanes 3, 4) cells. A2B4-2 and normal mouse serum immunoprecipitates from an  $^{125}\text{I}$ -labelled extract were run in parallel (lanes 5, 6).

GM07753-06. C.L.P. is a fellow and C.T. a scholar of the Leukemia Society of America.

**Note added in proof:** Since submission of this letter, Samelson and colleagues have reported similar findings concerning T3-like polypeptides on murine T cells<sup>33</sup>, although they differ from us in their interpretation of the protein representing the murine T3δ chain.

Received 9 September; accepted 30 December 1985.

1. Meuer, S. C. et al. *Science* **222**, 1239–1242 (1983).
2. Haskins, K. et al. *J. exp. Med.* **157**, 1149–1169 (1983).
3. Kung, P., Goldstein, G., Reinherz, E. & Schlossman, S. F. *Science* **206**, 347–349 (1979).
4. Borst, J., Alexander, S., Elder, J. & Terhorst, C. *J. biol. Chem.* **258**, 5135–5141 (1983).
5. van Wauwe, J. P., De Mey, J. R. & Goossens, J. G. *J. Immun.* **124**, 2708–2713 (1980).
6. Kaye, J., Porcelli, S., Tite, J., Jones, B. & Janeway, C. A. *J. exp. Med.* **158**, 836–856 (1983).
7. Imboden, J. B. & Stobo, D. *J. exp. Med.* **161**, 446–456 (1985).
8. Oettgen, H. C., Terhorst, C., Cantley, L. C. & Rosoff, P. M. *Cell* **40**, 583–590 (1985).
9. Meuer, S. C. et al. *J. exp. Med.* **157**, 705–719 (1983).
10. Oettgen, H. C., Kappler, J., Tax, W. J. P. & Terhorst, C. *J. biol. Chem.* **259**, 12039–12048 (1984).
11. Borst, J. et al. *Nature* **312**, 455–458 (1985).
12. Brenner, M. B., Trowbridge, I. S. & Strominger, J. L. *Cell* **40**, 183–190 (1985).
13. Ohashi, P. et al. *Nature* **315**, 765–768 (1985).
14. van den Elsen, P., Shepley, B. A., Cho, M. & Terhorst, C. *Nature* **314**, 542–544 (1985).
15. Samelson, L. E., Germain, R. N. & Schwartz, R. H. *Proc. natn. Acad. Sci. U.S.A.* **90**, 6972–6976 (1983).
16. Gunter, K. C., Malek, T. R. & Shevach, E. M. *J. exp. Med.* **159**, 716–730 (1984).
17. Samelson, L. E., Harford, J., Schwartz, R. H. & Klausner, R. D. *Proc. natn. Acad. Sci. U.S.A.* **82**, 1969–1973 (1985).
18. Allison, J. P. & Lanier, L. L. *Nature* **314**, 107–109 (1985).
19. Allison, J. P. et al. *Immun. Rev.* **81**, 145–160 (1984).
20. Allison, J. P., McIntyre, B. W., Ridge, L. L., Gross-Pelose, J. & Lanier, L. L. *Fedn Proc.* **44**, 2870–2873 (1985).
21. Samelson, L. E. & Schwarz, R. H. *Immun. Rev.* **81**, 131–144 (1984).
22. Brunner, J. & Semenza, G. *Biochemistry* **20**, 7174–7181 (1981).
23. Kappler, J. et al. *Cell* **35**, 295–302 (1983).
24. Ledbetter, J. A. et al. *J. exp. Med.* **153**, 310–323 (1981).
25. Haskins, K. et al. *J. exp. Med.* **160**, 452–471 (1984).
26. Morikawa, S., Tatsumi, E., Baba, M., Harada, T. & Yasu, K. *Int. J. Cancer* **21**, 166–170 (1978).
27. Bridges, C. D. B. *Vision Res.* **17**, 301–302 (1977).
28. Laemmli, U. K. *Nature* **227**, 680–685 (1970).
29. Hunkapiller, M. W., Lujan, E., Ostrander, F. & Hood, L. R. *Meth. Enzym.* **91**, 227–236 (1983).
30. Kornfeld, R. & Kornfeld, S. *A Rev. Biochem.* **45**, 217–237 (1976).
31. Matsudaira, P. T. & Burgess, D. R. *Analyt. Biochem.* **87**, 386–396 (1978).
32. Towbin, H., Stachelin, T. & Gordon, J. *Proc. natn. Acad. Sci. U.S.A.* **76**, 4350–4354 (1979).
33. Samelson, L. E., Harford, J. B. & Klausner, R. D. *Cell* **43**, 223–231 (1985).

## Retrovirus-mediated transfer and expression of drug resistance genes in human haematopoietic progenitor cells

Randy A. Hock & A. Dusty Miller

Fred Hutchinson Cancer Research Center, 1124 Columbia Street, Seattle, Washington 98104, USA

**Patients with certain genetic disorders can be cured by bone marrow transplantation<sup>1,2</sup>.** However, as prospective donors do not exist for most patients with potentially curable genetic abnormalities, an alternative treatment for such patients involves the transfer of cloned genes into the patient's haematopoietic stem cells followed by re-infusion of the treated cells<sup>3</sup>. Retroviral vectors provide an efficient means for transferring genes into mammalian cells and have been used to transfer genes into mouse haematopoietic cells<sup>4–8</sup>. We have now produced amphotropic retroviral vectors containing either the bacterial gene for neomycin resistance or a mutant dihydrofolate reductase gene that confers resistance to methotrexate and have used these vectors to infect and confer drug resistance to human haematopoietic progenitor cells *in vitro*. Transfer could be demonstrated in the absence of helper virus by using an amphotropic retrovirus packaging cell line, PA12 (ref. 9). These studies are an important step towards the eventual application of retrovirus-mediated gene transfer to human gene therapy and for molecular approaches to the study of human haematopoiesis.

The haematopoietic system consists of a hierarchy of cells with differing capacities for self-renewal, proliferation and

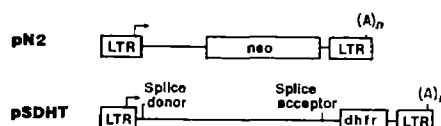


**Fig. 1** Retrovirus vectors. The *dhfr*-containing virus pSDHT (ref. 16) contains the coding region for a MTX-resistant *dhfr* gene<sup>15</sup> inserted into a clone of a spleen focus-forming virus in place of the gp52 envelope gene. The messenger RNA encoding *dhfr* is presumably a spliced message, as is the envelope mRNA. The *neo*-containing virus pN2 (ref. 7) contains a neomycin resistance gene<sup>14</sup> inserted between the long terminal repeats (LTRs) and viral replication signals from Moloney murine leukaemia virus. Arrows indicate promoters, (A)<sub>n</sub> indicates a polyadenylation signal. High-titre amphotropic retrovirus stocks were generated from these constructs as described previously<sup>16</sup>. Briefly, Psi-2 ecotropic retrovirus packaging cells<sup>22</sup> were transfected with viral DNA, and virus was collected after 2 days and used to infect PA12 amphotropic retrovirus packaging cells. Drug-resistant clones were isolated and screened for virus production. Helper virus was assayed using the S<sup>+</sup>L<sup>−</sup> assay<sup>9</sup>. The *dhfr*-virus stock was also tested for the presence of helper virus by infecting NIH 3T3 cells with 1 ml of the virus, passaging the cells for 1 month and assaying these cells for production of *dhfr*-virus and helper virus. In two separate experiments, no virus was detected. Vector titre (CFU ml<sup>−1</sup>) and helper virus titre (focus-forming units per ml) were, respectively,  $5 \times 10^6$  and  $>10^3$  (helper virus titre increased with passage of this cell line) for pN2 and  $2 \times 10^6$  and  $<1$  for pSDHT.

differentiation. Haematopoietic stem cells are primitive cells that undergo both self-renewal and commitment to form progenitor cells<sup>10</sup>. Through extensive proliferation and differentiation of these progenitor cells, a large number of diverse blood cells is formed. Progenitor cells that can be grown *in vitro* include those which give rise to granulocyte/monocyte colonies (CFU-GM)<sup>11</sup>, erythroid colonies (BFU-E)<sup>12</sup> and mixed colonies containing both erythroid and myeloid elements (CFU-MIX)<sup>13</sup>. Certain haematological disorders, such as adenosine deaminase deficiency, purine nucleoside phosphorylase deficiency and the haemoglobinopathies, are potentially curable by transferring normally functioning genes into pluripotent haematopoietic stem cells of patients with such disorders. An important step towards this type of therapy is the demonstration that genes can be efficiently transduced into human haematopoietic cells. Although gene transfer into pluripotent haematopoietic stem cells cannot be measured *in vitro*, we expect that successful transfer into haematopoietic progenitor cells will be indicative of our ability to infect stem cells.

We used retroviral vectors (Fig. 1) containing either a neomycin resistance gene (*neo*)<sup>14</sup> or a mutant dihydrofolate reductase gene (*dhfr*)<sup>15</sup>, dominant-acting selectable genes that confer resistance to the antibiotic G418 or the antifolate methotrexate (MTX), respectively, in mammalian cells. High-titre amphotropic retrovirus stocks were generated from these vectors by transfer into PA12 cells as described previously<sup>16</sup>. Several PA12-SDHT cell lines produced *dhfr*-containing virus at  $2 \times 10^6$  colony-forming units (CFU) ml<sup>−1</sup> in the absence of helper virus. Several PA12-N2 cell lines produced *neo*-containing virus in excess of  $2 \times 10^6$  CFU ml<sup>−1</sup>, but these lines also produced amphotropic helper virus. Helper virus production by these cells was unexpected because the PA12 packaging cells do not produce helper virus when other vectors are used (refs 9, 16, and unpublished results). Helper virus production was apparently due to a recombination event between homologous overlapping sequences in the *neo*-virus and the virus packaging system which are not present in most vectors<sup>16</sup>.

We next determined the concentrations of MTX and G418 which would completely inhibit the growth of human haematopoietic colonies *in vitro*. In agreement with previous reports<sup>17</sup>, little inhibition of CFU-GM colony growth was seen with MTX concentrations of  $10^{-4}$  M when either dialysed or undialysed fetal bovine serum was included in the incubation

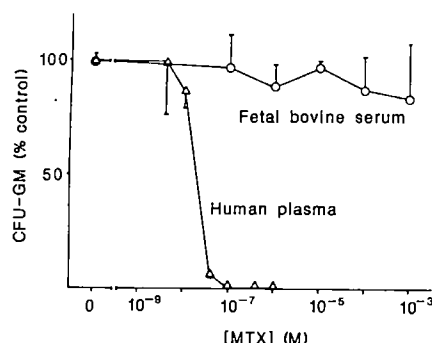


**Fig. 2** Effect of methotrexate on CFU-GM colony growth. Human bone marrow samples were obtained from adult volunteers who were donating their marrow for allogeneic bone marrow transplantation. The bone marrow was fractionated by density gradient centrifugation on Ficoll-Hypaque<sup>23</sup>. The mononuclear cell fraction was removed and washed with Dulbecco's modified Eagle's medium (DMEM) containing 10% fetal bovine serum (FBS). Bone marrow cells ( $1 \times 10^5$ ) were incubated in 35-mm dishes containing 1 ml of Iscove's modified Dulbecco's medium with 40  $\mu$ l ml<sup>-1</sup> placental conditioned medium<sup>24</sup>, 0.3% agar, either 20% heat-inactivated (1 h, 56 °C) FBS (○) or 20% heat-inactivated human AB plasma (△) and MTX as indicated. After incubation for 10–14 days, colonies containing >40 cells were counted using an inverted phase microscope. The total number of colonies from duplicate (FBS-containing plate) or quadruplicate wells (human AB plasma-containing plates) were counted and the results are expressed as a percentage of control plates not receiving MTX ( $\pm$ s.d.). Values are representative of several experiments.

mixture. However, when human plasma was used as the source of serum growth factors, the growth of colonies containing both granulocytic and monocytic elements was stimulated and complete inhibition of colony growth was seen at 10<sup>-7</sup> M MTX (Fig. 2), which correlates with the clinical observations showing bone marrow suppression with MTX serum levels of 10<sup>-7</sup> M (ref. 18). Methotrexate did not consistently inhibit BFU-E and CFU-MIX growth, however, probably because of the complex nature of the medium required for their growth. In contrast, complete growth inhibition of all colony types was demonstrable with G418 at a concentration of 2 mg ml<sup>-1</sup> for CFU-GM and 1 mg ml<sup>-1</sup> for BFU-E and CFU-MIX.

Efficient gene transfer into mouse haematopoietic cells has been achieved only when the bone marrow cells have been co-cultivated with virus-producing cells. Co-cultivation of human bone marrow cells with *neo*- or *dhfr*-virus-producing cells resulted in conversion of 3–10% of the CFU-GM to drug resistance (Table 1). No drug-resistant colonies were seen when bone marrow cells were co-cultivated with parental PA12 cells, which produce viral particles lacking viral RNA. Resistant colonies contained mixtures of myeloid elements including granulocytes and monocytes/macrophages, as confirmed by Wright-Giemsa staining of individual colonies after their removal from agar. Co-cultivation of bone marrow cells with monolayers of *neo*-virus-producing cells conferred G418 resistance to ~20% of the BFU-E. In addition, co-cultivation of marrow cells with the *neo*-virus-producing cells conferred G418 resistance to CFU-MIX, demonstrating that this marrow progenitor cell can also be infected. However, the scarcity of this marrow progenitor cell prevented us from obtaining an accurate estimate of the frequency of infection. As with the CFU-GM, co-cultivation with parental PA12 cells did not confer drug resistance to BFU-E or CFU-MIX.

The presence of helper virus in the *neo*-virus preparation used here (Fig. 1) allowed us to confirm the presence of the *neo*-virus in G418-resistant haematopoietic colonies by rescue of *neo*-virus from these cells. For assay of *neo*-virus release, individual CFU-GM colonies were removed from agar, dispersed by pipetting and co-cultivated with NIH 3T3 (thymidine kinase-negative) cells. After overnight incubation, the culture medium was

**Table 1** Efficiency of gene transfer into CFU-GM, BFU-E and CFU-MIX using retroviral vectors

Progenitor cell	CFU-GM		
Selective agent	G418		
Co-cultivation with:	PA12	PA12/N2	PA12/SDHT
Totals	0/1,320 (0%)	73/1,624 (4.5%)	69/1,168 (5.9%)
Progenitor cell	CFU-GM		
Selective agent	MTX		
Co-cultivation with:	PA12	PA12/N2	PA12/SDHT
Totals	0/246 (0%)	26/256 (10%)	11/331 (3.3%)
Progenitor cell	BFU-E		
Selective agent	G418		
Co-cultivation with:	PA12	PA12/N2	PA12/SDHT
Totals	0/3,188 (0%)	658/3,332 (20%)	33/282 (12%)
Progenitor cell	CFU-MIX		
Selective agent	G418		
Co-cultivation with:	PA12	PA12/N2	PA12/SDHT
Totals	0/7 (0%)	1/9 (11%)	1/4 (25%)
	0/3 (0%)	2/4 (50%)	0/— (0%)
	0/10 (0%)	4/17 (24%)	4/17 (24%)

Control fibroblasts (PA12) and virus-producing fibroblasts (PA12/N2 and PA12/SDHT) were trypsinized and seeded at  $5 \times 10^5$  per 6-cm dish the day before use. Bone marrow cells, enriched for mononuclear cells as described in Fig. 2 legend, were co-cultivated with fibroblasts for 16 h at 37 °C in 4 ml of fresh medium (DMEM supplemented with 10% FBS). Fibroblasts were irradiated (caesium source, 0.459 Gy min<sup>-1</sup> for 5 min) before addition of the bone marrow cells, to ensure that fibroblast colonies would not grow in soft agar culture and be confused with haematopoietic colonies. After co-cultivation, the non-adherent cells were removed and collected by centrifugation (400g, 5 min). The assays described in Fig. 2 legend were used to detect G418- and MTX-resistant CFU-GM. BFU-E and CFU-MIX colonies were grown in Iscove's modified Dulbecco's medium containing 30% FBS (Hyclone, heat-inactivated), 1% beef embryo extract (Gibco), 1% bovine albumin (Armour), 5  $\times$  10<sup>-5</sup> M 2-mercaptoethanol, 100 U ml<sup>-1</sup> penicillin, 100  $\mu$ g ml<sup>-1</sup> streptomycin, 0.1 mg ml<sup>-1</sup> NaHCO<sub>3</sub>, 5  $\mu$ l ml<sup>-1</sup> placental conditioned medium, 0.9% methylcellulose and 1 IU ml<sup>-1</sup> human urinary erythropoietin, essentially as described previously<sup>12,13</sup>. CFU-E were assayed in the absence or presence of either 2 mg ml<sup>-1</sup> G418 or 10<sup>-7</sup> M MTX. BFU-E and CFU-MIX were assayed in the absence and presence of 1 mg ml<sup>-1</sup> G418. After incubation for 14 days, colonies were counted using an inverted microscope. The number of colonies per 10<sup>5</sup> mononuclear cells was 25–100 for CFU-GM, 50–190 for BFU-E and 0.5–2 for CFU-MIX. Each set of paired values is from a separate experiment and represents the number of colonies from quadruplicate wells. The number of drug-resistant colonies is listed first, followed by the number of colonies which grew in the absence of drug.

replaced with medium containing 2 mg ml<sup>-1</sup> G418 and after 7 days the plates were scored for G418-resistant colonies. Of 12 G418-resistant colonies previously exposed to *neo*-virus, 3 induced G418-resistant NIH 3T3 colonies, demonstrating the presence of the *neo*-virus in these colonies. We were not surprised that only a few colonies produced *neo*-virus, for it means that these colonies have been infected with both helper virus and *neo*-virus, which may be a rare event. Thus, the transfer of the *neo* gene into human bone marrow progenitor cells was demonstrated by two criteria, the conferral of drug resistance to CFU-GM, BFU-E and CFU-MIX and the recovery of *neo*-virus from the individual CFU-GM colonies.

These results show that retroviral vectors can be used to transfer genes into normal human haematopoietic progenitor cells. Co-cultivation of bone marrow cells with virus-producing cells results in drug-resistant human CFU-GM with an efficiency (3–10%) similar to those observed for mouse (10–20%)<sup>7</sup> and dog (10–25%)<sup>19</sup> marrow. As the same vector (N2) was used to infect progenitor cells from all three species, we conclude that the efficiency of infection of human marrow is comparable to that of other animals. Because we have been able to infect all specimens examined so far (from over 15 individuals) using these vectors, we also conclude that marrow from most individuals should be susceptible to gene transfer by amphotropic retroviral vectors.

For studies of human haematopoiesis using retroviruses and for eventual application of retroviruses to human gene therapy, it is important to transfer genes in the absence of helper virus, because this prevents replication and spread of the vector following transfer and eliminates the possibility of helper virus-induced disease. The *dhfr*-virus used here was free of replication-competent helper virus by two stringent criteria (Fig. 1) and conferred resistance on CFU-GM with a similar efficiency to the helper virus-containing *neo*-virus. We conclude that replication-defective vectors can successfully mediate gene transfer in human haematopoietic cells in the absence of helper virus. In addition, we assayed all progenitor cells for drug resistance immediately after short-term exposure to virus, therefore drug resistance is due to the initial infection of these cells and not to viral spread, even in the case of the helper virus-containing *neo*-virus. Gene transfer into human CFU-GM has previously been demonstrated only after long-term culture of haematopoietic cells with virus vectors containing helper virus<sup>20,21</sup>.

The finding that the *dhfr*-virus confers MTX resistance on haematopoietic progenitor cells at levels of MTX which affect haematopoiesis *in vivo* suggests that selection for the presence of the vector *in vivo* will be possible. Cells infected with viruses containing the *dhfr* gene linked to a non-selectable gene may similarly be enriched *in vivo*. Hence, even though infection may not be 100% efficient, selection pressure *in vivo* may greatly increase the number of cells containing and expressing the transduced genes.

We thank Drs Eli Gilboa and David Trauber for providing the retroviral plasmids pN2 and pSDHT, respectively, and Drs Irwin Bernstein and Robert Andrews for help with the progenitor cell assays. A.D.M. is a fellow of the Leukemia Society of America. This study was supported by a grant from the Cooley's Anemia Foundation and by NCI grants CA41455 and CA09351.

Received 14 January; accepted 31 January 1986.

- Bortin, M. M. & Rim, A. A. *J. Am. med. Ass.* **238**, 591–600 (1977).
- Thomas, E. D. *et al.* *Lancet* **ii**, 227–229 (1982).
- Anderson, W. F. *Science* **226**, 401–409 (1984).
- Joyner, A., Keller, R. A., Phillips, A. & Bernstein, A. *Nature* **305**, 556–558 (1983).
- Miller, A. D., Eckner, R. J., Jolly, D. J., Friedmann, T. & Verma, I. *Science* **225**, 630–632 (1984).
- Williams, D. A., Lemischka, I. R., Nathan, D. G. & Mulligan, R. C. *Nature* **310**, 476–480 (1984).
- Dick, J. E., Magli, R. C., Huszar, D., Phillips, R. A. & Bernstein, A. *Cell* **42**, 1–79 (1985).
- Keller, G., Paige, C., Gilboa, E. & Wagner, E. F. *Nature* **318**, 149–154 (1985).
- Miller, A. D., Law, M. F. & Verma, I. M. *Molec. cell. Biol.* **5**, 431–437 (1985).
- Quesenberry, P. & Levitt, L. *New Engl. J. Med.* **301**, 755–760, 819–823, 868–872 (1979).
- Pike, B. L. & Robinson, W. A. *J. cell. Physiol.* **76**, 77–84 (1970).
- Stephenson, J. R., Axelrad, A. A., McLeod, D. L. & Shreeve, M. M. *Proc. natn. Acad. Sci. U.S.A.* **68**, 1542–1546 (1971).
- Fausch, A. A. & Messner, H. A. *Blood* **52**, 1243–1248 (1978).
- Colbère-Garapin, F., Horodniceanu, F., Kourilsky, P. & Garapin, A. C. *J. molec. Biol.* **150**, 1–14 (1981).
- Simonsen, C. C. & Levinson, A. D. *Proc. natn. Acad. Sci. U.S.A.* **80**, 2495–2499 (1983).
- Miller, A. D., Trauber, D. R. & Baltimore, C. *Somatic Cell molec. Genet.* **12**, 175–183 (1986).
- Koizumi, S. *et al.* *Expl. Hematol.* **8**, 635–640 (1980).
- Chabner, B. & Young, R. C. *J. clin. Invest.* **52**, 1804–1811 (1973).
- Kwok, W. H., Schuening, F., Stead, R. B. & Miller, A. D. *Proc. natn. Acad. Sci. U.S.A.* (in the press).
- Rothstein, L., Pierce, J. H., Klassen, V. & Greenberger, J. *Blood* **65**, 744–752 (1985).
- Gruber, H. E. *et al.* *Science* **230**, 1057–1061 (1985).
- Mann, R., Mulligan, R. C. & Baltimore, D. *Cell* **33**, 153–159 (1983).
- Andrews, R. G., Torok-Storb, B. & Bernstein, I. D. *Blood* **62**, 124–132 (1983).
- Schlunk, T. & Schleyer, M. *Expl. Hematol.* **8**, 179–184 (1980).

## Structural alteration of viral homologue of receptor proto-oncogene *fms* at carboxyl terminus

Lisa Coussens, Charles Van Beveren\*, Douglas Smith, Ellson Chen, Richard L. Mitchell\*, Clare M. Isacke\*, Inder M. Verma\* & Axel Ullrich

Department of Molecular Biology, Genentech, Inc., 460 Point San Bruno Boulevard, South San Francisco, California 94080, USA

\* Molecular Biology and Virology Laboratory, Salk Institute, PO Box 85800, San Diego, California 92138, USA

A role for proto-oncogenes in the regulation and modulation of cell proliferation<sup>1,2</sup> has been suggested by the findings that the B-chain of platelet-derived growth factor (PDGF) is encoded by the proto-oncogene *sis*<sup>3–7</sup> and that the *erb-B* oncogene product is a truncated form of the epidermal growth factor (EGF) receptor<sup>8–10</sup>. Furthermore, the product of the proto-oncogene *fms* (*c-fms*) may be related or identical to the receptor for macrophage colony-stimulating factor (CSF-1)<sup>11</sup>. *v-fms* is the transforming gene of the McDonough strain of feline sarcoma virus (SM-FeSV)<sup>12,13</sup> and belongs to the family of *src*-related oncogenes which have tyrosine-specific kinase activity. Furthermore, nucleotide sequence analysis of the *v-fms* gene product revealed topological properties of a cell-surface receptor protein<sup>14</sup>. To elucidate the features involved in the conversion of a normal cell-surface receptor gene into an oncogenic one, we have now determined the complete nucleotide sequence of a human *c-fms* complementary DNA. The 972-amino-acid *c-fms* protein has an extracellular domain, a membrane-spanning region, and a cytoplasmic tyrosine protein kinase domain. Comparison of the feline *v-fms* and human *c-fms* sequences reveals that the proteins share extensive homology but have different carboxyl termini.

A λgt10 cDNA library of  $\sim 2 \times 10^6$  clones prepared from total human term placental poly(A)<sup>+</sup> RNA was screened at moderate stringency using a radioactively labelled *Cla*I/*Bgl*II (2.66 kilobases; kb) fragment of *v-fms* (pSM-FeSV) as a hybridization probe (see Fig. 1 legend). Seventeen clones were isolated which were derived from the same messenger RNA, as indicated by restriction analysis and sequence homology to *v-fms*. Figure 1 shows the complete nucleotide sequence of overlapping cDNA clones and translation of the longest open reading frame initiating with methionine. The 3,992-nucleotide sequence is divided into 300 bases of 5'-untranslated sequence, 2,916 nucleotides of coding sequence, and a 716-nucleotide 3'-untranslated region containing a poly(A) addition signal (ATTAAA) 16 base pairs (bp) upstream from the poly(A) tail of several independent clones. Two other cDNA clones (*λc-fms* 32 and *λc-fms* 5) have extended 3'-untranslated regions and contain another poly(A) addition signal 47 bp upstream of the poly(A) tail (not shown). The human placenta thus contains at least two species of *c-fms* mRNAs which have different 3' ends. The longest cDNA sequence is 4,291 nucleotides, which is close to the size determined for the mRNA on Northern blots (4.3 kb), and may well contain all of the *c-fms* mRNA sequence.

The 972-amino-acid primary translational product of *c-fms* sequence contains features characteristic of cell-surface glycoprotein receptors. These include an amino-terminal, predominantly hydrophobic stretch of 23 amino acids, starting with the putative initiator methionine at nucleotide positions 301–303. The sequence surrounding the methionine codon matches the criteria for a likely initiation codon (GCCATGG; ref. 15). An in-frame termination codon (TGA) is found 252 bp upstream from this putative initiation codon, with no alternative ATG in between. Met 1 is thus likely to be the *c-fms* initiation methionine.

**Fig. 1** Nucleotide sequence of *c-fms* cDNA. The nucleotide and amino-acid numbers are shown on the left. In the coding domain, the amino-acid numbers are shown above the nucleotide number. The 5' in-frame termination codon, TGA, is indicated by thin underlining; the sequence at the recombination junction between FeLV and the *v-fms* gene is underlined with a wavy line; the putative signal sequence is indicated with a thicker line followed by a broken line; cysteine residues are shaded; putative *N*-linked glycosylation sites are shown by open boxes; the transmembrane region is emphasized by a black bar; two direct repeats are bracketed; the poly(A) addition signal is underlined and marked by an arrow.

**Methods.** Total poly(A)-containing RNA was isolated from frozen human term placenta. Using the  $\lambda$ gt10 vector system<sup>26</sup>, a cDNA library containing  $1.5 \times 10^6$  recombinants was constructed<sup>8</sup>. Initial screening of this library used a radiolabelled<sup>27</sup>, 2.15-kb *Cla*I/*Bgl*III fragment isolated from the *v-fms* clone pSM-FeSV/*Cla*I/BamHI (2.66 kb)<sup>12</sup>. Two plaque pure positive phage were characterized by Southern blot hybridization and sequenced<sup>28,29</sup>. A 1.5-kb *Eco*RI fragment from phage  $\lambda$ c-fms 32 was then used to rescreen the library and detected 151 putative positive phage. This pool was then screened with a 5'-proximal 130-bp fragment (*Cla*I/*Hinc*II) from *v-fms* pSM-FeSV/*Cla*I/BamHI. The longest of the 27 phage isolated,  $\lambda$ c-fms 102, was sequenced and found to contain the entire pre-*c-fms* coding sequence preceded by an open reading frame.  $\lambda$ c-fms 305 was found to extend further 5' and to contain an in-frame stop codon.

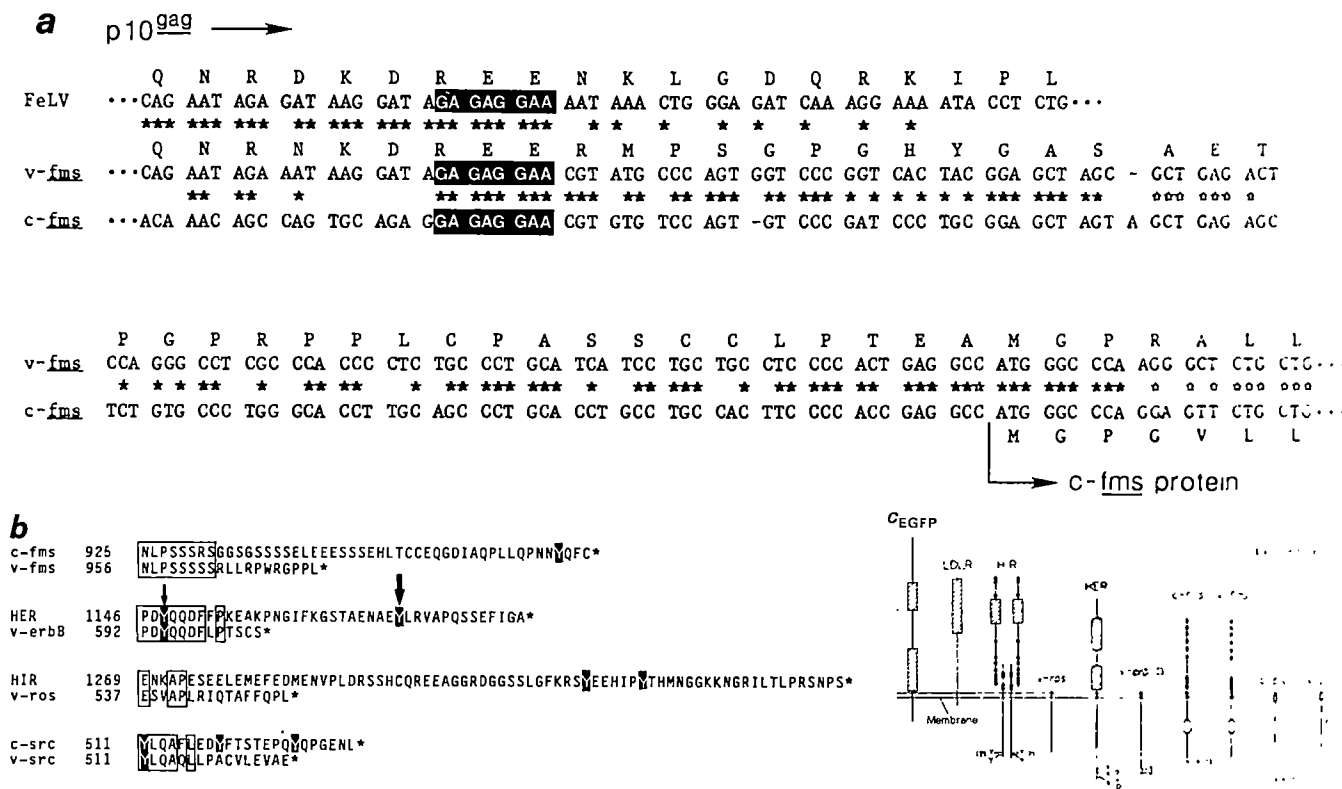


**Fig. 2** *a*, *v-fms* and *c-fms* recombination junction. The sequence around the putative recombination junction of FeLV<sup>30</sup> and *c-fms* (Fig. 1) used to generate *v-fms* is shown. Eight common nucleotides are boxed. The reading frame in FeLV and *v-fms* is translated in single-letter code. Nucleotide sequence homologies are indicated by asterisks. The putative initiation codon of the *c-fms* coding sequence is indicated. *b*, Carboxy-terminal sequence differences between receptors and their oncogenic derivatives. The carboxy-terminal sequences of human *c-fms* and feline *v-fms*, human epidermal growth factor receptor (HER) and avian *v-erbB*<sup>8</sup>, and avian *c-src* and *v-src*<sup>24</sup> are shown. Open boxes indicate homology; tyrosine residues are indicated by solid boxes. Arrows on tyrosine residues indicate phosphorylation sites; the solid filled arrow denotes the major autophosphorylation site of human EGF receptor<sup>23</sup>. *c*, Schematic comparison of structural features of cell-surface receptors and oncogene products. Regions of high-Cys concentration are shown as hatched boxes and single Cys residues as filled circles. The open box in *v-fms* and *c-fms* represents a 70-amino-acid substitution in the tyrosine-kinase domain. The position of carboxy-terminal tyrosine residues is shown. EGFP, epidermal growth factor precursor; LDLR, low-density lipoprotein receptor; HIR, human insulin receptor; HER, human epidermal growth factor receptor.

ine, followed by an ~19–23-amino-acid signal sequence, required for transfer of the nascent polypeptide chain into the lumen of the endoplasmic reticulum<sup>16</sup>. The predicted relative molecular mass ( $M_r$ ) of the unglycosylated *c-fms* polypeptide is 105,000 and 106,000 for the 949- or 953-residue protein, respectively.

During its transport to the cell surface, the feline *c-fms* protein is glycosylated to yield a 165,000- $M_r$  glycoprotein<sup>17</sup>. Eleven *N*-linked glycosylation target sites are found within the 512-residue amino-terminal half of the human *c-fms* sequence (Fig. 1), which represents the extracellular ligand binding domain of this glycoprotein receptor. The *c-fms* extracellular domain lacks the cysteine-rich repeat units<sup>18</sup> found in the cell-surface receptors for EGF<sup>8</sup>, insulin<sup>19</sup> and low-density lipoprotein (LDL)<sup>20</sup>. Although the cysteine content is much lower in *c-fms*, six amino-proximal residues are regularly spaced and are flanked by related sequences, which suggests the possibility of a symmetrically folded conformation within the extracellular ligand binding domain. Hydropathicity analysis of the *c-fms* sequence reveals a fivefold, 90–100-amino-acid repeat of hydropathicity markers, which may indicate the presence of five similarly folded subdomains in this part of the *c-fms* polypeptide (not shown).

A stretch of 25 amino acids characteristic of a membrane-spanning anchor domain separates extracellular and cytoplasmic parts of the sequence. At its carboxyl terminus, the transmembrane sequence is followed by a highly polar and basic

stretch of residues (Tyr-Lys-Tyr-Lys-Gln-Lys-Pro-Lys-Tyr), which may function as a 'stop transfer' sequence and possibly interact with negatively charged phospholipid headgroups on the cytoplasmic surface of the membrane. No threonine or serine residues are found in this region, which could correspond to threonine 654 of the EGF receptor, thought to be involved in protein kinase C modulation of that receptor's activity<sup>6</sup>. The closest potential target for protein kinase C interaction is located at Ser 555, eight residues downstream from the target in the human EGF receptor, Thr 654.

The cytoplasmic domain of the *c-fms* protein is about 530 amino acids long, and shares extensive homology with members of the family of tyrosine-protein kinases<sup>7</sup>. These homologies include the probable ATP binding domain at positions 587–596 and lysine at 616. The homology in the kinase domain is interrupted by a 70-amino-acid insertion in *c-fms* at residue 670, and fades around residue 910 towards the carboxyl terminus. Interestingly, the spacing between the transmembrane and the protein kinase domains is identical to that observed in EGF receptor and insulin receptor<sup>8,19</sup>. The *c-fms* protein from macrophages has been shown to be phosphorylated at tyrosine residues on addition of its presumptive ligand, CSF-1 (ref. 21).

Comparison of the human *c-fms* cDNA and derived amino-acid sequences with corresponding feline *v-fms* sequences reveals a high degree of sequence conservation, especially when one considers the evolutionary distance between these species. The 972-amino-acid *c-fms* sequence is 84% homologous with

v-fms. The most significant differences are found at both the amino-terminal and carboxy-terminal ends. Extracellular sequences display the lowest level of homology (75%) and cytoplasmic domain sequences the highest homology (95%), until c-fms and v-fms diverge completely, shortly before the carboxyl terminus at residue 933 (see Fig. 1). The sequence differences in the extracellular domain include two in-frame deletions in v-fms of one and two codons, respectively (positions 348, 349 and 455). It remains possible that the sequence differences in this domain, of which ~60% are non-conservative, result in altered ligand affinity or specificity.

The open reading frame encodes the 972-amino-acid c-fms protein and extends 249 nucleotides beyond the putative initiation codon into the 5'-untranslated sequence. This region includes a ~150-residue purine-rich sequence that starts about 100 nucleotides upstream from the beginning of the coding sequence and contains short sequence repeats such as GAAGA or GGAAG (Fig. 1). Sequence comparisons revealed that an 8-nucleotide sequence (GAGAGGAA) at the point of divergence between c-fms and gag-v-fms was also found in the relevant position of the gag gene sequence of feline leukaemia virus (FeLV-B)<sup>30</sup> (Figs 1, 2a). This sequence may mark the point where a homologous recombination event generated the gag-v-fms gene. This event truncated the gag gene, and fused it in-frame with the pre-c-fms sequence. 5'-Untranslated sequences of c-fms were thus converted into gag-v-fms coding sequences.

Although Hampe *et al.*<sup>14</sup> have previously proposed that a leader sequence required to generate a glycosylated gag-encoded protein acts as a signal sequence for the gag-fms-encoded protein, our data suggest the alternative, that the signal sequence of c-fms acts as an internal signal for membrane translocation in the gag-v-fms fusion polypeptide. This also offers a possibility for the as yet unknown processing mechanism of gp180<sup>gag-fms</sup> to generate p55<sup>gag</sup> and gp120<sup>fms</sup> by signal peptidase cleavage at the end of the c-fms leader sequence.

We have localized the 3' junction between c-fms and FeLV to the pol gene at a point 595 nucleotides upstream from the env gene initiation codon (results not shown), by comparison with sequences of FeLV-B (J. Elder, personal communication). This is consistent with previous observations that the env gene product of SM-FeSV is intact<sup>12,13</sup>. No homologous or overlapping sequences were discerned when v-fms or c-fms sequences were compared with ~500 nucleotides constituting the 3' end of the feline pol gene and 5' end of the env gene. Inspection of v-fms and c-fms sequences reveals that the two diverge completely at amino acid 933. The c-fms protein extends for 40 additional amino acids, while the v-fms coding sequence terminates after 11 unrelated codons of unknown origin (Figs 1, 2b).

The region in which the carboxyl termini of v-fms and c-fms sequences diverge is flanked by two GCAGCAGCAG repeats (Fig. 1) which may have been involved in sequence truncation by recombination. When the sequence of another fms-containing retrovirus, HZ5-FeSV, was compared with the v-fms and c-fms sequences described here, the point of sequence divergence between the two v-fms sequences was identical to that shown in Fig. 1. Homology between c-fms and the HZ5-FeSV v-fms gene continues beyond the point of divergence between c-fms and the SM-FeSV v-fms genes (P. Besmer, personal communication). The carboxyl terminus of the v-fms protein of HZ5-FeSV is also altered, but differs from that of SM-FeSV, thus excluding the possibility that the carboxyl-termini differences are due to species-specific divergence. As two c-fms-derived oncogenes have undergone structural alterations at their carboxyl termini, this may represent an important event in the conversion of the cellular fms/CSF-1 receptor gene into a gene capable of causing transformation *in vitro* and tumours *in vivo*.

Figure 2b, c compares the tyrosine-kinase family oncogenes, v-erb-B, v-fms and v-src and their cellular relatives, the EGF receptor, c-fms/CSF-1 receptor and c-src. All three viral

oncogenes have an altered carboxyl terminus compared with their putative cellular cognate. The v-ros gene product<sup>22</sup>, which is closely related to the insulin receptor, also has an altered carboxyl terminus compared with the c-ros gene product (L.-H. Wang, personal communication). In all cases the carboxyl termini of cellular cognates contain tyrosine residues, which have an important role in signal transduction. A tyrosine residue is found at position 969 of c-fms in a location similar to that for the EGF receptor tyrosine 1,173, which is a major autophosphorylation substrate for the ligand-induced tyrosine-autophosphorylation activity<sup>23</sup>. Interestingly, the corresponding tyrosine is also missing from the deduced v-fms protein encoded by either SM-FeSV or HZ5-FeSV. This is also true of Tyr 527 in the c-src protein, which is missing from v-src because of an altered carboxyl terminus<sup>24</sup>.

Oncogenes of the transmembrane tyrosine kinase type (v-ros, v-erb-B, v-fms) differ in their extracellular domains (Fig. 2c). v-ros and v-erb-B are related to polypeptide hormone receptors that possess cysteine-rich sequence repeats in their extracellular ligand-binding domains<sup>8,19</sup>. This family includes the non-tyrosine-kinase LDL receptor<sup>20</sup>, as well as the EGF precursor, which may be a receptor for an unknown ligand in addition to being the precursor for EGF<sup>18,25</sup>. Both v-ros and v-erb-B lack most of these extracellular ligand-binding domain sequences, including the cysteine-rich repeats. In contrast, c-fms retains the entire putative ligand-binding domain of c-fms/CSF-1 receptor. Interestingly, this glycoprotein is not a member of the receptor family containing the cysteine-rich clusters. This difference between v-fms and v-ros/v-erb-B may reflect alternative mechanisms used by the respective receptor molecules to control transmembrane signal generation. Double truncation of cellular ros and erb-B proto-oncogenes may be necessary to generate a transforming gene, while a single carboxyl-terminal truncation of the c-fms gene may yield the same result.

We thank Alane Gray and Thomas Dull for technical assistance, Jeanne Arch and Carolyn Goller for preparation of the manuscript, Drs S. Pfeffer and T. Hunter for helpful suggestions and critical reading of the manuscript, Dr J. Elder for the unpublished sequences of FeLV genome, and Dr Charles Sherr for v-fms probes and encouragement. R.L.M. was supported by an NIH postdoctoral fellowship; C.M.I. was supported by a Damon Runyon-Walter Winchell fellowship (DRG 775). Work in the laboratory of I.M.V. was supported by funds from ACS and by NIH grants.

Received 1 November 1985; accepted 16 January 1986.

- Bishop, J. M. *Cell* **42**, 23–28 (1985).
- Muller, R. & Verma, I. M. *Curr. Topics Microbiol. Immunol.* **112**, 73–115 (1984).
- Doolittle, R. F. *et al.* *Science* **221**, 275–277 (1983).
- Waterfield, M. D. *et al.* *Nature* **304**, 35–39 (1983).
- Devare, S. G., Reddy, E. P., Law, J. D., Robbins, K. C. & Aaronson, S. A. *Proc. natn. Acad. Sci. U.S.A.* **80**, 731–735 (1983).
- Hunter, T. *Trends biochem. Sci.* **10**, 275–280 (1985).
- Van Beveren, C. & Verma, I. M. *Curr. Topics Microbiol. Immunol.* **123**, 73–98 (1985).
- Ullrich, A. *et al.* *Nature* **309**, 418–425 (1984).
- Xu, Y.-H. *et al.* *Nature* **309**, 806–810 (1984).
- Lin, C. R. *et al.* *Science* **224**, 843–848 (1984).
- Sherr, C. J. *et al.* *Cell* **41**, 665–676 (1985).
- Donner, L., Fedele, L. A., Garon, C. F., Anderson, S. J. & Sherr, C. J. *J. Virol.* **41**, 489–500 (1982).
- Heisterkamp, N. *et al.* *Virology* **126**, 248–258 (1983).
- Hampe, A., Gobet, M., Sherr, C. J. & Galibert, F. *Proc. natn. Acad. Sci. U.S.A.* **81**, 85–89 (1984).
- Kozak, M. *Microbiol. Rev.* **47**, 1–45 (1983).
- Wickner, W. T. & Lodish, H. F. *Science* **230**, 400–407 (1985).
- Rettenmier, C. W. *et al.* *Science* **228**, 320–322 (1985).
- Pfeffer, S. & Ullrich, A. *Nature* **313**, 184 (1985).
- Ullrich, A. *et al.* *Nature* **313**, 756–761 (1985).
- Yamamoto, T. *et al.* *Cell* **39**, 27–38 (1984).
- Morgan, C. J. & Stanley, E. R. *Biochem. biophys. Res. Commun.* **119**, 35–41 (1984).
- Neckameyer, W. S. & Wang, L.-H. *J. Virol.* **53**, 879–884 (1985).
- Downward, J., Parker, P. & Waterfield, M. D. *Nature* **311**, 483–485 (1984).
- Takeya, T. & Hanafusa, H. *Cell* **32**, 881–890 (1983).
- Gray, A., Dull, T. J. & Ullrich, A. *Nature* **303**, 722–725 (1983).
- Huang, T. *et al.* *Practical Approaches in Biochemistry* (ed. Grover, D.) (Information Retrievable Ltd, Oxford, 1984).
- Taylor, J. M. *et al.* *Biochim. biophys. Acta* **4**, 324–330 (1976).
- Southern, E. J. *molec. Biol.* **98**, 503–517 (1975).
- Messing, J., Crea, R. & Seuberg, P. H. *Nucleic Acids Res.* **9**, 309–321 (1981).
- Laprevotte, I., Hampe, A., Sherr, C. J. & Galibert, F. *J. Virol.* **50**, 884–894 (1984).

## Genomic diversity correlates with clinical variation in Ph'-negative chronic myeloid leukaemia

Christine M. Morris\*, Anthony E. Reeve†,  
Peter H. Fitzgerald\*, Peter E. Hollings\*,  
Michael E. J. Beard‡ & David C. Heaton‡

\* The Cancer Society of New Zealand Cytogenetics Unit, Christchurch Hospital, Christchurch, New Zealand  
† Molecular Carcinogenesis Laboratory, Department of Biochemistry, University of Otago, Dunedin, New Zealand  
‡ Department of Haematology, Christchurch Hospital, Christchurch, New Zealand

The Philadelphia chromosome (Ph') is found in the blood cells of about 90% of patients with chronic myeloid leukaemia (CML) and usually results from the reciprocal chromosome translocation t(9; 22)<sup>1,2</sup>. This translocation relocates the proto-oncogene c-abl, normally found on chromosome 9q34, to within the breakpoint cluster region (bcr) on chromosome 22q11 (refs 3–8). The juxtaposition of c-abl and the 5' portion of bcr appears to be the critical genomic event in CML and results in a novel 8-kilobase (kb) fused abl/bcr transcript<sup>9,10</sup> and a c-abl-related protein of relative molecular mass 210,000 (ref. 11). About 10% of adult patients diagnosed as CML lack the Ph' chromosome; they represent a heterogeneous group of disorders which are difficult to diagnose precisely<sup>12</sup>. We have examined five patients with CML whose leukaemic cells have a normal karyotype. We report here that two of the patients showed the same genomic change as occurs in Ph'-positive CML, but the change resulted from a mechanism other than chromosomal translocation. The remaining three patients showed no genomic rearrangement. This genomic diversity correlated with the clinical differences between the patients.

The abl oncogene is located on chromosome 9 and previous *in situ* hybridization studies have shown that it is translocated to the Ph' chromosome in CML<sup>3–6</sup>. In *situ* hybridization of an <sup>3</sup>H-labelled v-abl probe<sup>13</sup> to metaphase cells of a Ph'-negative patient (patient 1) resulted in specific labelling of the terminal

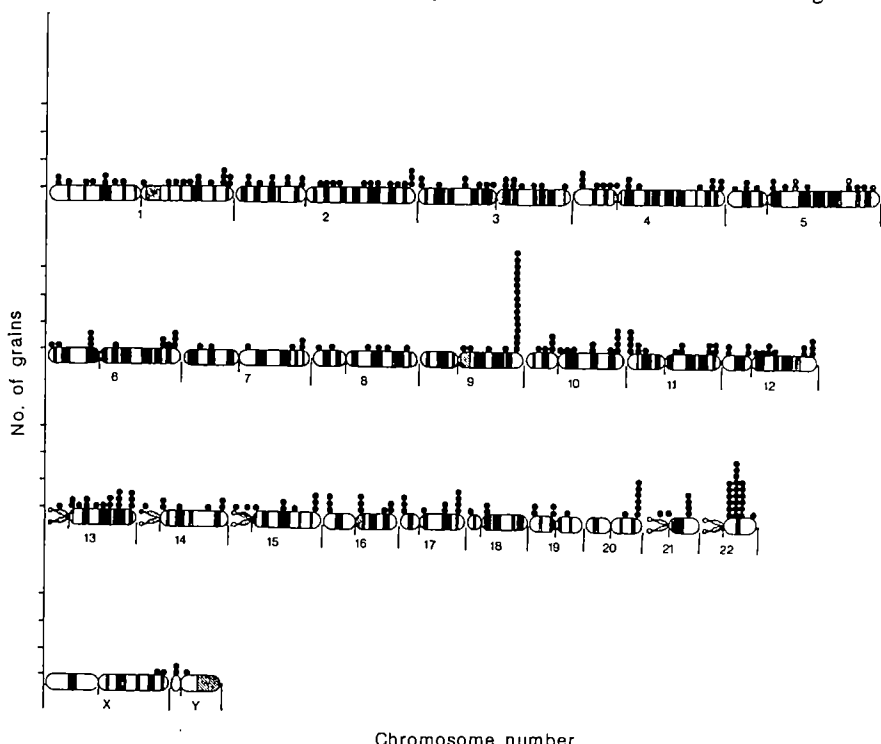
region of chromosome 9q and the proximal half of chromosome 22q. Figure 1 shows the distribution of labelled sites in 138 metaphase cells, representing the combined result of two *in situ* hybridizations to cultured leukaemic blood cells. All G-banded and R-banded cells had a normal karyotype. Sixteen cells were labelled at band 9q34 of chromosome 9, and 21 cells were labelled in the proximal half of chromosome 22q. The probability of each of these distributions was <0.1% on the basis of unit chromosome length and also on the basis of the number of grains per labelled chromosomal site. This is the same oncogene shift as occurs in the standard Ph' translocation, but the chromosomes 22 of our patient showed no morphological evidence of translocation and this was confirmed by *in situ* studies which showed that c-sis remained on chromosome 22 (Fig. 2). In Ph'-positive CML, c-sis is translocated from chromosome 22 to chromosome 9 (ref. 14). Furthermore, a bcr probe which has homology with the 3' end of bcr was also present on chromosome 22 and not translocated to chromosome 9q (Fig. 2) as in the standard t(9; 22)<sup>7,8</sup>. These results suggest an insertion of DNA carrying c-abl in an otherwise normal chromosome 22.

Restriction enzyme analysis of DNA from patient 1, using the 3' bcr (*Hind*III-*Bgl*II) plasmid probe<sup>7</sup>, showed the presence of a new fragment in *Bam*HI, *Bgl*II and *Bgl*II-*Xba*I digests of leukaemic DNA compared with control DNA from the same patient (Fig. 3, lanes 1–2, 5–6 and 9–10, respectively). *Hind*III and *Bgl*II-*Sac*I digests were identical in leukaemic and control DNA (Fig. 3, lanes 3–4, 7–8). These results suggest the presence of a break in the bcr gene ~0.6 kb downstream of exon 3 and between the *Xba*I and *Sst*I restriction sites (Fig. 5); such a break separates the 5' and 3' portions of bcr and would allow, in our patient, insertion of c-abl adjacent to the 5' portion of bcr, a position that appears to be characteristic of CML and essential for production of the 8-kb hybrid abl-bcr RNA transcript<sup>9,10</sup>.

Restriction enzyme analysis of leukaemic DNA from patient 2 using the same bcr probe showed rearrangements in *Hind*III, *Bam*HI and *Eco*RI digests (Fig. 4, lanes 1, 2, 4), but not in a *Bgl*II digest (Fig. 4, lane 3). A *Bgl*II-*Sac*I digest also demonstrated a bcr rearrangement (data not shown). We conclude that in patient 2 a breakpoint occurred within the bcr gene between the *Hind*III and *Bgl*II sites (Fig. 5). Both patients 1 and 2 showed the same type of rearrangements as occur in the 5.8-kb bcr region following the relocation of c-abl to the bcr region in

**Fig. 1** Distribution of sites labelled with the v-abl probe in leukaemic cells from patient 1. Major clusters of grains occur on chromosome 9 at 9q34 and on chromosome 22 at 22q11–12. A small cluster of grains was also observed at band 20q12 ( $P < 1\%$ ), suggesting that cross-hybridization to c-src had occurred; the c-src probe shows a similar cross-hybridization to c-abl (ref. 24).

**Methods.** Leukaemic cells were cultured and mitoses synchronized by the method of Yunis<sup>25</sup> and G-banded<sup>26</sup>. All cells had a normal karyotype. The psub-9 v-abl probe<sup>13</sup> was labelled by nick-translation to a specific activity of  $1.6 \times 10^7$  d.p.m.  $\mu$ g<sup>-1</sup> using <sup>3</sup>H-dATP and <sup>3</sup>H-dCTP. *In situ* hybridization procedures were essentially as described elsewhere<sup>27</sup>. The metaphase cells scored had an average number of two grains (upper range 5) over the chromosomes, and approximately the same numbers on the background.



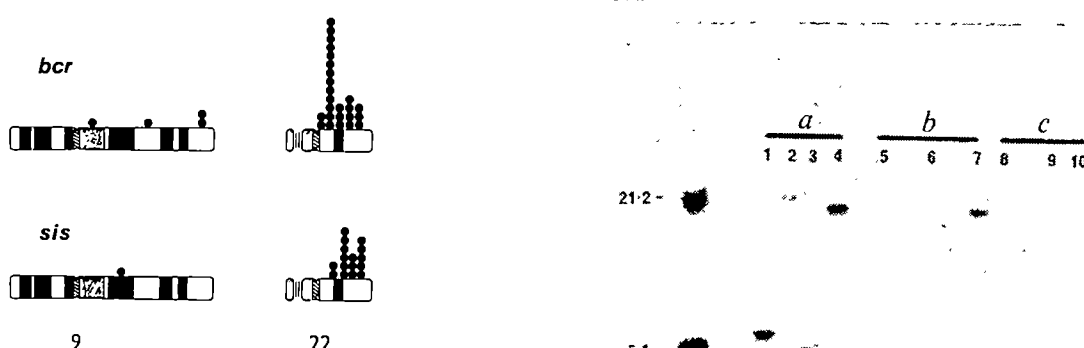


**Fig. 2** Distribution of sites labelled with the 3'-*bcr*<sup>7</sup> and v-*sis* probes<sup>28</sup> on chromosomes 9 and 22 of leukaemic cells from patient 1. <sup>3</sup>H-labelling of probes and *in situ* hybridization were done as described in Fig. 1 legend.

Ph'-positive CML<sup>7,8</sup>, yet the leukaemic cells of both patients 1 and 2 were Ph'-negative and had normal karyotypes.

Three further Ph'-negative patients were studied and none of them showed the gene rearrangements characteristic of Ph'-positive CML. Hybridizations using the *bcr* probe showed no rearrangements in *Hind*III, *Bam*HI or *Eco*RI digests of leukaemic DNA from patient 3 (Fig. 4, lanes 5–7) or in *Hind*III, *Bam*HI and *Bgl*II digests from patient 4 (Fig. 4, lanes 8–10). *In situ* hybridization of the <sup>3</sup>H-labelled v-*abl* probe to chromosomes of leukaemic cells from patient 5 showed specific labelling only at the terminal region of chromosome 9q—the same result as that obtained for a normal control (data not shown).

Two of our Ph'-negative CML patients showed the same genomic changes as occur in Ph'-positive CML; the other three patients did not. This genomic heterogeneity correlated with the clinical variation shown by patients presently diagnosed as being

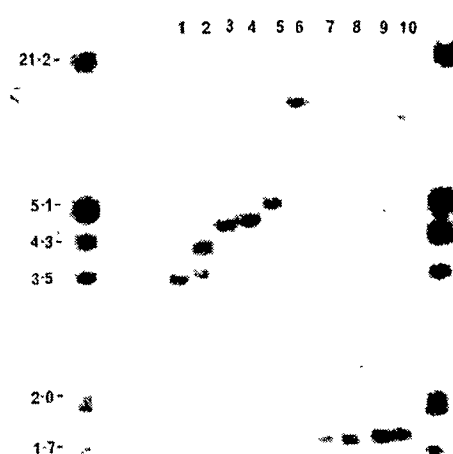


**Fig. 3** Southern blot hybridization of the *bcr* probe to DNA from leukaemic cells of patient 1. Control DNA from Epstein-Barr virus-transformed lymphocytes of patient 1 is shown in the odd-numbered lanes and leukaemic DNA in even-numbered lanes. The DNA samples were digested with the following enzymes: *Bam*HI (lanes 1, 2), *Hind*III (lanes 3, 4), *Bgl*II (lanes 5, 6), *Bgl*II-SacI (lanes 7, 8), and *Bgl*II-XbaI (lanes 9, 10). Southern blots were prepared<sup>29</sup> and hybridized with a nick-translated<sup>30</sup> 1.2-kb *Hind*III-*Bgl*II *bcr* insert<sup>7</sup>. Filters were washed at 68 °C in 0.1×SSC, 0.5% SDS. λ markers (*Hind*III-*Eco*RI) are indicated on the left (in kb). Further studies indicated that the 5.1-kb bands in lanes 9 and 10 were the result of modification of the XbaI site rather than partial digestion.

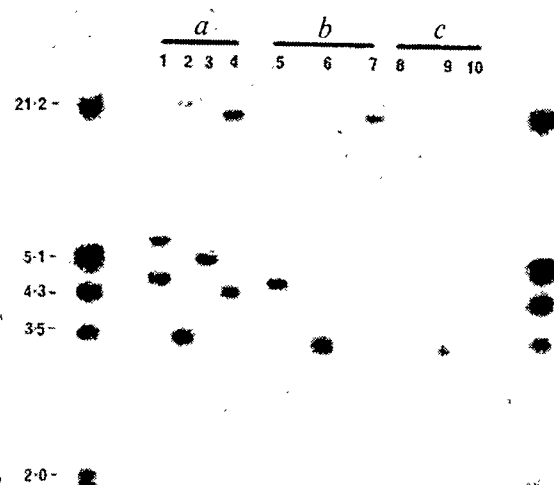


**Fig. 4** Southern blot hybridization of a *bcr* probe to DNA from leukaemic cells of patients 2–4 (a–c, respectively). DNA samples were digested with *Hind*III, *Bam*HI, *Bgl*II and *Eco*RI (a, lanes 1–4 respectively); *Hind*III, *Bam*HI and *Eco*RI (b, lanes 5–7); and *Hind*III, *Bam*HI and *Bgl*II (c, lanes 8–10). Southern blots were prepared and processed as described in Fig. 3 legend.

Ph'-negative<sup>12</sup>. These patients usually present at an older age, have monocytosis, thrombocytopenia, a poor response to chemotherapy and a shortened survival, but a subgroup of Ph'-negative CML patients show clinical and haematological features which are indistinguishable from patients with the Ph' chromosome<sup>15–18</sup>. Our patients 1 and 2 were of the latter type, and it is significant that these patients showed essentially the same genomic rearrangement as occurs in Ph'-positive cases, while retaining an apparently normal karyotype. The clinical courses of patients 1 and 2 have not differed in any way from that seen in Ph'-positive CML. These patients, who are 26 and 49 yr old, are in the chronic phase of CML (6 yr and 4 yr respectively after diagnosis). Both also showed cell colony growth characteristic of CML when buffy coat blood cells were plated on soft agar with colony-stimulating factor (CSF)<sup>19</sup>. Our remaining three patients (3–5) represented the more usual type of Ph'-negative CML: all three were  $\geq 70$  yr old at diagnosis and had a monocytosis in the blood of  $4–14 \times 10^9 \text{ l}^{-1}$ . All responded poorly to treatment with progressive thrombocytopenia and none survived for more than 10 months. Blood cells of patients 3 and 4 did not show the distinctive CML pattern in soft agar with CSF<sup>19</sup> (patient 5 was not tested). These three patients differed clinically and genetically from true CML patients and they probably were suffering from a different haematological disease: a case can be made for their inclusion in the myelodysplastic syndrome<sup>12,20</sup>.

True CML is characterized by the juxtaposition of c-*abl* and *bcr*, and the use of molecular probes will allow the accurate diagnosis of CML patients, whether or not they have a visible chromosomal translocation. Movement of c-*abl* from chromosome 9q to chromosome 22 has been demonstrated not only in the standard Ph' translocation t(9; 22), but also in several variant and complex translocations<sup>4–6,21</sup>. Some of the cases with complex translocations appear to be Ph'-negative, but they carry 'masked' Ph' chromosomes<sup>21–23</sup>. Our results show that c-*abl* and *bcr* can be associated in Ph'-negative CML without apparent chromosomal translocation, but as the result of a separate mechanism which relocates DNA within the cell.

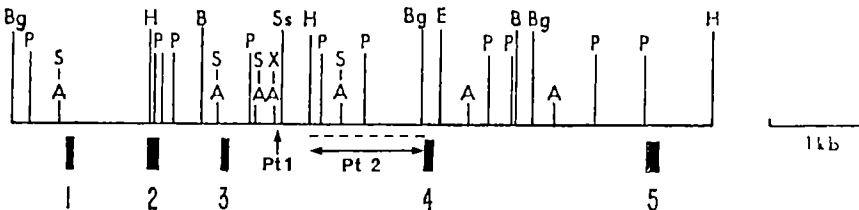
## LETTERS TO NATURE

**Fig. 5** Restriction enzyme map of the breakpoint cluster region (*bcr*) of chromosome 22 after Heisterkamp *et al.*<sup>8</sup>. The sites of breakpoints found in patients 1 and 2 are indicated. The broken line represents the location of the 1.2-kb *bcr* probe used in these experiments. Enzymes used to construct the map were: *Ava*I (A), *Bam*HI (B), *Bgl*II (Bg), *Eco*RI (E), *Hind*III (H), *Pst*I (P), *Sma*I (S), *Sst*I or *Sac*I (Ss) and *Xba*I (X).<sup>8</sup>

This work was supported by the Cancer Society of New Zealand, the Canterbury-Westland and Otago-Southland Divisions and the Blackburn-Mobil Trust.

Received 8 November 1985; accepted 3 February 1986.

1. Rowley, J. D. *Nature* 243, 290–293 (1973).
2. Prakash, O. & Yunis, J. J. *Cancer Genet. Cytogenet.* 11, 361–367 (1984).
3. Heisterkamp, N. *et al.* *Nature* 299, 747–750 (1982).
4. de Klein, A. *et al.* *Nature* 300, 765–767 (1982).
5. Heisterkamp, N. *et al.* *Nature* 306, 239–247 (1983).
6. Bartram, C. R. *et al.* *Nature* 306, 277–280 (1983).
7. Groffen, J. *et al.* *Cell* 36, 93–99 (1984).
8. Heisterkamp, N. *et al.* *Nature* 315, 758–761 (1985).
9. Gale, R. P. & Canaan, E. *Proc. natn. Acad. Sci. U.S.A.* 81, 5648–5652 (1984).
10. Shitelman, E., Lifshitz, B., Gale, R. P. & Canaan, E. *Nature* 315, 550–554 (1985).
11. Konopka, J. B. *et al.* *Proc. natn. Acad. Sci. U.S.A.* (in the press).
12. Pugh, W. C., Pearson, M., Vardiman, J. W. & Rowley, J. D. *Br. J. Haemat.* 60, 457–467 (1985).
13. Goff, S. P., Gilboa, E., Witte, O. N. & Baltimore, D. *Cell* 22, 777–785 (1980).



14. Bartram, C. R. *et al.* *Blood* 63, 223–225 (1984).
15. Edzini, E. Z., Sokal, J. E., Crosswhite, B. S. & Sandberg, A. A. *Ann. intern. Med.* 72, 175–182 (1970).
16. Mintz, U., Vardiman, J., Golomb, H. M. & Rowley, J. D. *Cancer* 43, 411–416 (1979).
17. Sandberg, A. A. *The Chromosomes in Human Cancer and Leukemia*, 2nd (Ed. Leive), New York, 1980.
18. Lawler, S. D. *Semin. Haemat.* 19, 257–272 (1982).
19. Moore, M. A. S. *Clinics Haemat.* 6, 97–112 (1977).
20. Bennett, J. M. *et al.* *Br. J. Haemat.* 51, 189–199 (1982).
21. Hagemeyer, A. *et al.* *Cancer Genet. Cytogenet.* 13, 1–16 (1984).
22. Bartram, C. R. *et al.* *EMBO J.* 4, 683–686 (1985).
23. Hagemeyer, A. *et al.* *Cancer Genet. Cytogenet.* 18, 95–104 (1985).
24. Le Beau, M. M., Westbrook, C. A., Diaz, M. O. & Rowley, J. D. *Nature* 312, 70–71 (1984).
25. Yunis, J. J. *Cancer Genet. Cytogenet.* 7, 43–50 (1982).
26. Cannizzaro, L. A. & Emanuel, B. S. *Cytogenet. Cell Genet.* 38, 308–309 (1984).
27. Harper, M. E. & Saunders, G. F. *Chromosoma* 83, 431–439 (1981).
28. Eva, A. *et al.* *Nature* 295, 116–119 (1982).
29. Maniatis, T., Fritsch, E. F. & Sambrook, J. *Molecular Cloning* (Cold Spring Harbor Laboratory, New York, 1982).
30. Rigby, P. W. J., Dieckmann, M., Rhodes, C. & Berg, P. *J. biol. Chem.* 113, 234–251 (1974).

## Sequence homology of the yeast regulatory protein ADR1 with *Xenopus* transcription factor TFIIIA

Toinette A. Hartshorne, Hal Blumberg & Elton T. Young

Department of Biochemistry, University of Washington, Seattle, Washington 98195, USA

Classical yeast genetics coupled with the cloning of regulatory genes by complementation of function<sup>1,2</sup> is a powerful means of identifying and isolating *trans*-acting regulatory elements<sup>3–6</sup>. One such regulatory gene is *ADR1* which encodes a protein required for transcriptional activation of the glucose-repressible alcohol dehydrogenase (*ADH2*) gene<sup>7,8</sup>. We now report the nucleotide sequence of *ADR1*; it encodes a polypeptide chain of 1,323 amino acids, of which the amino-terminal 302 amino acids are sufficient to stimulate *ADH2* transcription. This active amino-terminal region shows amino-acid sequence homology with the repetitive DNA-binding domain of TFIIIA<sup>9</sup>, an RNA polymerase III transcription factor of *Xenopus laevis*<sup>10</sup>. Similar domains are found in proteins encoded at the *Krüppel*<sup>11</sup> and *Serendipity*<sup>12</sup> loci of *Drosophila melanogaster*. We discuss the implications of this structural homology and suggest that a similar domain may exist in other yeast regulatory proteins such as those encoded by *GAL4* (ref. 13) and *PPR1* (ref. 14).

Figure 1 shows the complete nucleotide sequence of *ADR1* and the predicted amino-acid sequence of the encoded protein. In addition to 3,969 base pairs (bp) of coding-region DNA, 610 bp of 5'-noncoding and 1,560 bp of 3'-noncoding sequence were determined. The presumed initiator methionine codon is flanked by sequences favourable for initiation of translation in eukaryotes<sup>15,16</sup> and is preceded by two TAA termination codons in the same reading frame. The DNA sequence of *ADR1* encodes a polypeptide of 1,323 amino acids with a calculated relative molecular mass of 150,985.

Table 1 illustrates the codon usage for the *ADR1* gene. In *Saccharomyces cerevisiae* a correlation is observed between high levels of gene expression and a bias towards preferred codons which are complementary to the anticodons of the major isoacceptor transfer RNA species<sup>17</sup>. The calculated codon bias index for *ADR1* is very low, 0.076, indicating a lack of preferred

codons and predicting a low level of expression.

Several features of the predicted *ADR1* protein are noteworthy. The amino-acid composition of the amino-terminal region of the protein is highly basic: residues 62–256 are 21% lysine + arginine and only 7% glutamate + aspartate. One portion of this region, residues 203–228, is 41% lysine + arginine. Chou and Fasman conformational parameters<sup>18</sup> predict that residues 214–254 could form an  $\alpha$ -helical structure. There are five cysteines between residues 106 and 140, a region that shows striking homology to TFIIIA<sup>19</sup>, as described below. Three potential sites of phosphorylation are found in the amino-terminal 230 amino acids of *ADR1*; there are none in the rest of the protein. The sequence Arg-Arg-Ala-Ser at residues 227–230 fits one of the two main patterns of acceptor sites for phosphorylation of the serine residue by bovine type II cyclic AMP-dependent protein kinase<sup>20</sup>. The sequences Arg-Lys-Asn-Ser at residues 177–180 and Arg-Lys-Ala-Ser at residues 209–212 are also potential phosphorylation sites but have reduced affinity for the type II cyclic AMP-dependent protein kinase<sup>21</sup>.

The most interesting feature of *ADR1* is the apparent structural homology to TFIIIA, a transcription factor for RNA polymerase III from *X. laevis*<sup>22</sup>. TFIIIA promotes formation of a stable transcription complex by binding to the internal control region of 5S genes<sup>10</sup>. The predicted amino-acid sequence of *ADR1* was used in a homology search conducted for us by Dr Russell Doolittle, using an updated version of the NEWAT database<sup>23</sup>; the only significant match was to TFIIIA. The region of sequence homology with *ADR1* is in a region of TFIIIA which binds 5S genes<sup>24</sup> (Fig. 2). TFIIIA contains a 30-amino-acid motif repeated nine times in tandem in the DNA-binding domain<sup>9</sup>. The most conserved residues of a repeat unit are two cysteines, two histidines and three invariant hydrophobic residues: tyrosine, phenylalanine and leucine. An acidic residue is present between the cysteines, and basic residues, or residues with DNA-binding side chains, are positioned in the 12-residue stretch between the cysteines and histidines. *ADR1* contains two repeat units at positions 98–126 and 127–155 which match the TFIIIA consensus sequence. The conservation of residue type and position suggests that *ADR1* may have a function similar to that of TFIIIA. It is possible that *ADR1* binds to the upstream activation site (UAS) of *ADH2* (refs 8, 25) through this region of the protein, and establishes a functional transcription complex.

*ADR1* and TFIIIA have another feature in common. Following the postulated repeated structure in each protein there is a

-688 -598 -588 -578 -568 -558 -548 -538 -528 -518 -508 -498  
TCGATAGTTACCGCTTGTGAACTAATAAAACTGATATTTCCTGTTCTTCTGGTTGGCGGTGTTTCATTTGTTCATGTTTACTTCGCCACAGGTTTCAAGAACAAAC  
-488 -478 -468 -458 -448 -438 -428 -418 -408 -398 -388 -378  
GCCTTAAAAAATAGGAAACCGTTTCGCTACAGGTCTTATTATCTGTTCTGCTGTTCTTATTCGCTATACTTGCTTATTCGACTTCCGATCCGAATTTCCTCCCT  
-368 -358 -348 -338 -328 -318 -308 -298 -288 -278 -268 -258  
TGAAGACCTTCAAGAACACAGTTATATATCATTGATCTGAATTTCAGGCTATTTCAAAATTCATACCTCCTTATTCACATTTGCTGACTATAGAAAAGCCTTATCTT  
-248 -238 -228 -218 -208 -198 -188 -178 -168 -158 -148 -138  
TTATCTTGAAAGAAAAGGAGTGTATGCAAAACTTATTGTTACTCTGTTTGATATCTCCCTTATTCGTTGAACTATAAGATGATTTGCAATAATTAAACCAATCATTG  
-128 -118 -108 -98 -88 -78 -68 -58 -48 -38 -28 -18  
CTACTTCCCCTTCCCTTATATATAACCTTCAGAAAATTCGCTACTATTCTGACTATAAGAATTCTGTTCCAAAAGAAAATATAAAAATAATCATA  
8 10 20 30 40 50 60 70 80  
TCTATTACT ATG GCT AAC GCA GAA AAA CCA AAC GAT TGT TCA GCC TTT CCC GTT GTC AAC TTG AAT TCG TCC TTT TCT AAC GGC TTC AAT  
Met Ala Asn Val Glu Lys Pro Asn Asp Cys Ser Gly Phe Pro Val Val Leu Asn Ser Cys Phe Ser Asn Gly Phe Asn  
90 100 110 120 130 140 150 160 170  
AAT GAG AAA CAA GAA ATA CAA ATG GAA AGC GAT GAT TCA CCC ATT TTA TTA ATG TCA TCA GCT TCC AGA GAA AAC TCA AAC ACT TTC  
Asn Glu Lys Glu Ile Glu Met Glu Thr Asp Asp Ser Pro Ile Leu Leu Met Ser Ser Ala Ser Arg Glu Asn Ser Asn Thr Phe  
180 190 200 210 220 230 240 250 260  
TCT GTG ATA CAG AGG ACC CCA GAT GGA AAG ATC ATT ACC ACA AAT AAT AAT ATG AAC TCC AAG ATT AAC AAG CAA CTG GAC AAG TTG CCC  
Ser Val Ile Glu Arg Thr Pro Asp Gly Lys Ile Ile Thr Asn Asn Asn Ser Lys Ile Asn Ser Lys Glu Leu Asp Lys Leu Pro  
270 280 290 300 310 320 330 340 350  
GAA AAT TTG AGG CTT AAT GGT AGA ACC CCC AGT GGG AAA CTA AGG TCA TTT GTT TGC GAC GGT TGT AGC AGA CGG TTC GCA AGA CAA GAG  
Glu Asn Leu Arg Leu Asn Gly Arg Thr Pro Ser Gly Lys Leu Arg Ser Phe Val Cys Glu Val Cys Thr Arg'Ala Phe Ala Arg Glu  
360 370 380 390 400 410 420 430 440  
CAC TTG AAA AGA CAT TAC AGA TCC CAT ACA ATT GAA AAA CCT TAT CCC TGT GGC CTC TGC AAC AGA TGC TTT ACT AGG AGG GAC TTA CTC  
His Leu Lys Arg His Tyr Ser His Thr Asn Glu Lys Pro Tyr Pro Cys Gly Leu Cys Asn Arg Cys Phe Thr Arg Arg Asp Asp Lys Leu  
450 460 470 480 490 500 510 520 530  
ATC AGG CAT CCT CAA AAA ATC CAT AGT GGT ATT TTA GGG GAA AGC ATT TCC CAT ACC AAC AGG AAA GTG TCG AGA ACT ATA ACT AAA GCT CGG  
Ile Arg His Ala Glu Ile His Ser Gly Asn Leu Glu Thr Ile Ser His Thr Lys Lys Val Ser Arg Thr Ile Thr Lys Ala Arg  
540 550 560 570 580 590 600 610 620  
AAA AAT TCT GCA TCC TCA GTC AAG TTT CAA ACT CCA ACC TAT GGT ACT CCA GAT ATT GGT ATT TTT TTG ATT CGC ACT ACT CCC ATT ACA  
Lys Asn Ser Ala Ser Ser Val Lys Phe Glu Thr Tyr Glu Thr Pro Asp Asn Gly Asn Phe Leu Asn Arg Thr Thr Ala Asn Thr  
630 640 650 660 670 680 690 700 710  
AGA AGA AAA GCA ACC CCT CAA GCT ATT CTT AAA CGT AGG TAC TTG AAA AAA CTG AGC CGC AGG GCT TCA TTT AGC GCA CAA TCA GCA TCC  
Arg Arg Lys Ala Ser Pro Glu Ala Asn Val Lys Arg Lys Tyr Leu Lys Leu Thr Arg Arg Ala Ser Phe Ser Ala Glu Ser Ala Ser  
720 730 740 750 760 770 780 790 800  
AGC TAT CCT TGC GAC CAA TCT TCG CTA GAA CAA CAT CCA AAG GAT CGT GTT AAA TTT TCT AGC CCT GAA TTA GTT CCA CTT GAC TTG  
Ser Tyr Ala Leu Pro Asp Glu Ser Ser Leu Glu His Pro Lys Asp Arg Val Lys Phe Ser Thr Pro Glu Leu Val Pro Leu Asp Leu  
810 820 830 840 850 860 870 880 890  
AAG AAT CCT GAA CTT GAC TCT TCG TTT GAC CTG ATT AGC ATT CTA GAT ITA AAC CTA ATT CTA GAT TCC ATT TAC ATT ATA GCA TTA GCA  
Lys Asn Pro Glu Leu Asp Ser Ser Phe Asp Leu Asn Met Asn Leu Asp Leu Asn Leu Asp Ser Asn Phe Asn Ile Ala Leu Asn  
900 910 920 930 940 950 960 970 980  
GGT TCT GAT TCT TGT GCA ACA ATG ATT TTG GAT ATT AAA TTG CCC GAA TCA GCA ATT AAC TAC ACA ATT TCT TCC GGC TCA CCA ATT  
Arg Ser Asp Ser Ser Glu Ser Thr Met Asn Leu Asp Tyr Lys Leu Glu Ser Ala Asn Asn Tyr Thr Tyr Ser Gly Ser Pro Thr  
990 1000 1010 1020 1030 1040 1050 1060 1070  
CGC GCA TAT GTC GCC CCT AAC ACG ATT TCT AAG AAC CCT TCA TTT ATT GAC GCA GAC TTA TTG TCG TCG TCG TCG ATA AAA GCC ATT  
Arg Ala Tyr Val Gly Ala Asn Thr Asn Ser Lys Asn Ala Ser Phe Asn Asp Ala Asp Asp Leu Ser Leu Ser Ser Tyr Ile Lys Asn Tyr  
1080 1090 1100 1110 1120 1130 1140 1150 1160  
AAT GAT CAT TGT TTT TCA GTC TCT GAA AGT GAT GAA ACT TCT CCA ATG AAC TCT GAA ATT AAC GAC ACT AAA TTA ATC GTC CCA ATT  
Asn Asp His Leu Phe Ser Val Ser Glu Ser Asp Glu Ser Asp Pro Met Asn Ser Glu Leu Asp Asp Thr Lys Leu Ile Val Pro Asp He  
1170 1180 1190 1200 1210 1220 1230 1240 1250  
AAA TCC ACT ATA CAT CAT ATT TGT AAG GAT TCA AGC TCC TCC TCT TGG ACT GTT GCT ATT GAT ATT AAT AGC ATT AAC ATT AAG GTC TCA GAC  
Lys Ser Thr Ile His His Leu Lys Asp Ser Arg Ser Ser Ser Trp Thr Val Ala Ile Asp Asn Asn Ser Asn Asn Asn Lys Val Ser Asp  
1260 1270 1280 1290 1300 1310 1320 1330 1340  
AAC CAA CCT GAT TTC CTC GAT ATT CAA GAA CTG CTG GAT ATT GAT ACT TTA GGT ATT GAT TGT TIA GAC ACC ACT CCC GTT TTA AAA GAA  
Asn Glu Pro Asp Phe Val Asp Phe Glu Leu Leu Asp Asn Asp Thr Lys Leu Glu Asn Asp His Pro Asn Ser Asn Arg Glu  
1350 1360 1370 1380 1390 1400 1410 1420 1430  
TTT GAA CCT TTA CAT GAT GAT GTC ATA AGT GCT ACC CCC ACC TCA ATT GAG ATT GAC CTT TCC CAT TGT AAC CTA TCA AAC TCT CCA ATT  
Phe Glu Leu Leu His Asp Asp Ser Val Ser Ala Thr Ala Ser Asn Ile Asp Leu Ser His Leu Asn Ser Asn Ser Asn Asn Asn Lys Val Ser Asp  
1440 1450 1460 1470 1480 1490 1500 1510 1520  
TCT CCT CAT AAG TTA ATT TAT AAC ATT AAA GAG CGG ACC ATT GAC GAT ATT GTC ATT TGT TCC GGA CCT GAT CAT CCT CCT AAC CCC GAA  
Ser Pro His Leu Leu Ile Tyr Lys Asn Lys Glu Gly Thr Asn Asp Asp Met Leu Ile Ser Phe Glu Leu Asp His Pro Ser Asn Arg Glu  
1530 1540 1550 1560 1570 1580 1590 1600 1610  
GAT GAT CTG GAT AAC CTA TGT ATT ATG ACC AGA GAT GTT CAA GCC ATA TTC ACT CAA ATT TGT AAA GCA GAA GAG TCT AAA CCA TCC CTC  
Asp Asp Leu Asp Lys Leu Cys Asn Met Thr Arg Asp Val Gln Ile Ala Phe Ser Glu Ile Asp Leu Ser His Leu Asn Ser Asn Ser Leu  
1620 1630 1640 1650 1660 1670 1680 1690 1700  
GAA GAC TTT TTA TCA ACC TCA AAC AGG AAA GAA AGG CCA GAT ACC AAC TAT ACT TTT ATT GCG TTA GAT TGT TTA AGC TTA TCG AAA  
Glu Asp Phe Leu Ser Thr Ser Asn Arg Lys Glu Lys Pro Asp Ser Glu Asn Tyr Phe Tyr Glu Asp Cys Leu Thr Leu Ser Lys  
1710 1720 1730 1740 1750 1760 1770 1780 1790  
ATA TCA AGA CCT CTG CGG CCC TCC ACT GTG AAC AAC ATT CAG CCA TCC CAT TCC ATA GAA TCA AGT CTA TTT ATT GAA CCA ATG AGA ATT  
Ile Ser Arg Ala Leu Pro Ala Ser Thr Val Asn Asn Asn Gin Pro Ser His Ser Ile Glu Ser Lys Leu Phe Asn Glu Pro Met Arg Asn  
1800 1810 1820 1830 1840 1850 1860 1870 1880  
ATG TCC ATT AAA GTG CTT AGA TAC ATT GAA AGG TTC AGT CAT GAT AGT AGC GAT CTC ATG TCC TCT ATT CCA AAC TTC CTG TCC AAA  
Met Cys Ile Lys Val Leu Arg Tyr Tyr Lys Leu His Ser His Asp Ser Val Ser Glu Ser Val Met Asp Ser Asn Pro Asn Leu Leu Ser Lys  
1890 1900 1910 1920 1930 1940 1950 1960 1970  
GAA TTG TTA ATG CCA CCT GTG ACT GAA TAT TTA GAT CTT TCC AGG ATT TCC AAA ATC GTC ATT CCC CAT TCC CCT ATT ATT CAC CCA  
Glu Leu Leu Met Pro Ala Val Ser Glu Tyr Lys Leu Asn Glu Tyr Lys Leu Asp Asn Phe Leu Pro His Pro Ile Ile His Pro  
1980 1990 2000 2010 2020 2030 2040 2050 2060  
AGC TTG CCT GAT TTG GAT TTG GAT ACC TTG CAA CGA TAT ACT ATT GAG GAT CGG ATT GAT GAC GCT GAA AAC GCG CAG TTG TTT GAT CCA  
Ser Leu Leu Asp Leu Asp Ser Asp Ser Glu Ile Arg Tyr Thr Asn Glu Asp Gly Tyr Asp Asp Ala Glu Asn Ala Glu Ser Phe Asp Arg  
2070 2080 2090 2100 2110 2120 2130 2140 2150  
TTA ACT CAA GGG ACA GAT AAA GAA TAT GAT TAC GAG CAC TAT CAA ATC ATT TCC ATT TCC AAA ATC GTC ATT CCC TCA ATT TTG AGC TTC ATG GGC  
Leu Ser Glu Glu Thr Asp Lys Glu Tyr Asp Tyr Glu His Tyr Glu Ile Leu Ser Ile Ser Lys Ile Val Cys Leu Pro Phe Met Ala  
2160 2170 2180 2190 2200 2210 2220 2230 2240  
ACA TTT GGT TCT TTG CAT AAC TTC GGT TAC AAA TCT CAA ACA ATA GAA TTC ATT GAG AGT AGA AGA ATT CTA CAT TCT ATT TTG GAG  
Thr Phe Gly Ser Leu Leu His Lys Phe Gly Tyr Lys Ser Glu Ile Leu Tyr Glu Met Ser Arg Arg Ile Leu His Ser Phe Leu Glu  
2250 2260 2270 2280 2290 2300 2310 2320 2330  
ACT AAA AGA AGG TGT CGC ACT ACA ACA GAA ATT GAC ACT TAT CAG AAC ATT TGG TTG ATG CAA TCC CTA ATA TTG AGC TTC ATG TTC GCT  
Thr Lys Arg Arg Cys Arg Ser Thr Thr Val Asn Asp Ser Tyr Glu Asn Ile Trp Leu Met Glu Ser Leu Ile Leu Ser Phe Met Phe Ala

**Fig. 1** Nucleotide sequence of the *ADR1* gene and the predicted amino-acid sequence of the encoded protein. The amino-acid sequence of the *ADR1* open reading frame is given below the nucleotide sequence starting with the putative initiation codon, which is designated +1, and ending with a TGA termination codon at +3,970. Two TAA termination codons are present 18 and 27 bp upstream of the ATG initiation codon and define the 5' boundary of the open reading frame. Translation termination codons are found in the other two reading frames within 55 nucleotides of the termination codon of the open reading frame. The 610 nucleotides of 5'-untranslated and 1,560 nucleotides of 3'-untranslated sequence contain no large open reading frames on either strand. Potential phosphorylation sites in the amino-acid sequence are indicated by thin lines. TFIID-like repeats are indicated by thick lines.

**Methods.** DNA sequence analysis was derived from plasmid YRp7-ADR1-411 (ref. 5). Small overlapping DNA fragments were cloned into the replicative form of M13mp

phages<sup>34</sup>. Host strain JM103 was used for transformation by recombinant DNAs<sup>34</sup>. Sequence analysis by the dideoxy chain terminator method was initiated with the *Eco*RI fragment (+54 to +1,005) known to lie within the *ADR1* functional region<sup>3</sup> and extended in both directions to include the *ADR1* open reading frame and 5' and 3' flanking sequences shown. Approximately 80% of the contiguous DNA sequence was derived from both strands of DNA. Where only one orientation of DNA provided unambiguous data, the sequence was determined from two or more different clones. Fidelity of the analysis was checked by cleaving the DNA with most of the restriction enzymes having 6-base recognition sites which were predicted to cut the DNA within the coding region. As another check on the sequence, the *ADR1* gene was fused at the *Bgl*II site at codon 642 to the *lacZ* gene. A fusion protein of the predicted size was made (data not shown), demonstrating that the predicted reading frame was used in yeast.

Table 1 Codon usage in *ADR1*

	Phe	TTT	49	Ser	TCT*	41	Tyr	TAT	34	Cys	TGT*	14
		TTG*	26		TCC*	24		TAC*	16	TGC		8
Leu	TTA	47		TCA	38	och	TAA	0	opa	TGA	1	
	TTG*	49		TCG	17	amb	TAG	0	Trp	TGG	4	
Leu	CTT	18		Pro	CCT	14	His	CAT	28	Arg	CGT	6
	CTC	2			CCC	10		CAC*	9	CGC		6
	CTA	16			CCA*	20	Gln	CAA*	31	CGA		5
	CTG	14			CCG	4		CAG	6	CGG		1
Ile	ATT*	37		Thr	ACT*	27	Asn	AAT	83	Ser	AGT	21
	ATC*	18			ACC*	17		AAC*	36	AGC		11
	ATA	20			ACA	14	Lys	AAA	51	Arg	AGA*	27
Met	ATG	29			ACG	14		AAG*	34	AGG		16
Val	GTT*	23		Ala	GCT*	18	Asp	GAT	63	Gly	GGT*	13
	GTC*	7			GCC*	11		GAC	23	GGC		10
	GTA	9			GCA	22	Glu	GAA*	53	GGA		10
	GTG	9			GCG	9		GAG	22	GGG		12

och, ochre codon; amb, amber codon; opa, opal codon.

\* Codons preferred by highly expressed genes in yeast<sup>17</sup>.

region that is rich in lysine + arginine (up to 40% per protein); this region of TFIIIA is thought to interact with other transcription factors or with RNA polymerase III as loss of this region reduced activation of transcription but did not affect DNA binding<sup>24</sup>. A mutant allele of *ADR1*, *ADR1-5'*, which confers partial constitutivity on *ADH2* expression, is located in this basic region (C. Denis, personal communication) but the reason for its effect is unknown.

An elegant model of TFIIIA structure has been proposed which attempts to account for the passage of RNA polymerase III through an internal promoter containing a stable transcription complex<sup>9</sup>. Each 30-amino-acid domain is proposed to form a loop or finger of ~12 amino acids. The base of the loop is formed by a Zn<sup>2+</sup> bound by the cysteine and histidine residues which flank the 12 amino acids. The amino acids in the finger are suggested to bind DNA, with each finger interacting with one half-turn of the helix so that all nine fingers would be in contact with the internal control region of 5S DNA. The conserved hydrophobic residues (Tyr 6, Phe 17, Leu 23) might form a structural core of the multi-domain protein. The multiple independent binding domains of TFIIIA are postulated to allow passage of RNA polymerase III through the internal control region without dislodging the stable transcription complex.

The importance of the finger-like domains of *ADR1* (Fig. 2) for activating *ADH2* expression is suggested by experimental data in addition to its homology with TFIIIA. Previous experiments indicated that a 2.6-kilobase (kb) *ADR1* fragment allowed partial derepression of *ADH2* in a strain containing the *adr1-1* allele<sup>5</sup>. The sequence data presented in Fig. 1 demonstrate that this fragment of *ADR1* would encode only the amino-terminal 302 amino acids of the protein. To determine which region of the *ADR1* protein is required for *ADH2* derepression, a series of 3'-deleted *ADR1* genes was constructed in the yeast/*Escherichia coli* shuttle vector pMW5 (Table 2). The *ADR1* plasmids were introduced into strain 521-6-Δ1 in which the 5'-flanking region and 2 kb of coding sequence of *ADR1* have been replaced by the *LEU2* gene of yeast (data not shown). In this strain *ADR1* structure/function relationships can be assessed in an *adr1-null* genetic background which eliminates the possibility of intragenic complementation between two defective *ADR1* genes.

As shown in Table 2, an amino-terminal 150-amino-acid *ADR1* peptide is unable to derepress *ADH2*. A 302-amino-acid *ADR1* peptide can derepress *ADH2* but is only 20% as active as the entire protein. *ADR1* proteins containing the amino-terminal 505 amino acids are as active as the entire protein. These results suggest that a domain required for *ADR1* function exists between amino acids 150 and 302 and that sequences located between amino acids 302 and 505 may be required for full *ADR1* activity. Therefore, most of the *ADR1* protein (amino

TFIIIA consensus	1	6	8	13	17	23	26	30
	TGEK*P(Y)V(C)	..	DG(C)DKR(F)TKK	..	(L)K*R(H)	..	H	
<i>ADR1</i> repeat 1	98	SGKLRS(F)V(C)--EV(C)TRA(F)ARQEHL(K*)R(H)YR*S(H)		126				
repeat 2	127	TNEK*P(Y)P(C)--GL(C)NRC(F)TRRDL(L)I*R(H)AQKIH		155				
<i>GAL4</i>	3	LLSSIEQ(A)C--DI(C)RLKKLKCSKEKPK(C)AK*-C		31				
<i>PPR1</i>	26	GISKSRTA(C)--KR(C)RLKKIKCDQEFPSC(KR*-C)		54				

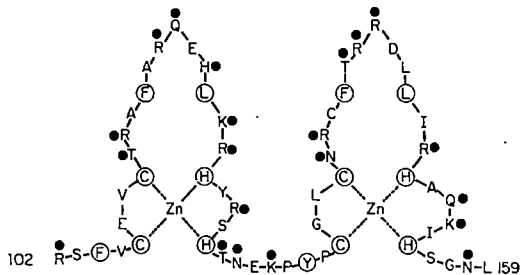


Fig. 2 The amino-acid sequences of the TFIIIA 30-residue repeat compared with amino-acid sequences of yeast regulatory proteins and the proposed 'finger' structure of *ADR1*. The TFIIIA consensus sequence was compiled by Miller *et al.*<sup>9</sup> from the nine contiguous repeat units in the TFIIIA protein. The invariant residues are circled. The numbers above the TFIIIA sequence refer to the amino-acid position in the consensus sequence, not in the TFIIIA polypeptide chain. The numbers adjacent to the other sequences refer to the position of the amino acid in the polypeptide chain. In the consensus sequence, dots mark variable positions in the sequence, and asterisks indicate where insertions sometimes occur in the normal pattern. In the other sequences, a dash (-) indicates a gap introduced for alignment. Each repeat is postulated to form a finger-like structure wherein the two cysteine (C) and two histidine (H) residues bind a Zn<sup>2+</sup> in a tetrahedral arrangement<sup>9</sup>. The hydrophobic residues tyrosine (T), phenylalanine (F) and leucine (L), are proposed to form a structural core for the multiple domains<sup>9</sup>. The region between the second cysteine and the first histidine residue may form a DNA-binding loop. TFIIIA repeat number 7 (ref. 9) has the same gap alignment between its cysteine residues as the *ADR1* repeats. Bottom, the proposed finger structures of *ADR1*, drawn according to the model proposed by Miller *et al.*<sup>9</sup>. Residues with probable DNA-binding side chains [lysine (K), histidine, glutamine (Q), asparagine (N), threonine (T) and arginine (R)] are indicated by solid circles.

acids 505–1,323) is not required for its role in *ADH2* transcriptional activation.

The shortest *ADR1* protein that retained *ADH2*-stimulating activity (containing 302 amino acids) contained the finger region as well as the adjacent Lys + Arg-rich region. The next smaller *ADR1* protein (containing 150 amino acids) was inactive; it lacked the very basic region and retained only the first finger and one-half of the second. Thus a single finger alone may not be sufficient to derepress *ADH2* expression, but whether this is due to loss of the second finger, loss of the very basic region, or both, cannot be distinguished at present. Additional genetic evidence that this finger region of *ADR1* is functionally important derives from DNA sequence analysis of mutants of *ADR1* (C. Denis, personal communication). Two mutants which derepress *ADH2* very poorly contain single amino-acid changes in the finger region of *ADR1*. Neither mutation alters an invariant residue of the TFIIIA consensus sequence. These alterations provide strong evidence, consistent with the deletion analysis reported here, that the finger region is essential for *ADR1* function. By analogy with the proposed structure of TFIIIA, this region would be required for DNA binding. The analysis suggests that one DNA-binding finger is insufficient for *ADR1* activity.

It seemed unlikely that *ADR1* would be the only yeast protein with structural homologies to TFIIIA. The nucleotide sequences of several yeast regulatory proteins have been reported recently<sup>13,14</sup>, including the proteins encoded by *GAL4* and *PPR1* which contain a basic, cysteine-rich amino terminus (Fig. 2). In

**Table 2** Functional characterization of *ADR1* genes containing variable-length 3'-terminal deletions

Relevant yeast genotype	Plasmid	ADH activity ( <i>dr</i> )
<i>adr1-Δ1</i>	pMW5	25
<i>adr1-Δ1</i>	YEp150ADR1	20
<i>adr1-Δ1</i>	YEp302ADR1	1,400
<i>adr1-Δ1</i>	YEp505ADR1	6,500
<i>adr1-Δ1</i>	YEp1323ADR1	6,500
<i>ADR1</i>	pMW5	2,000

**Plasmid constructions:** All constructions used the yeast *E. coli* shuttle vector pMW5, which is the same as plasmid MA56 but lacks the *ADH1* promoter fragment<sup>31</sup>. This plasmid contains the 2μ origin of replication and *TRP1* gene for selection in yeast, as well as the pBR322 sequences necessary for growth and ampicillin-resistance selection in *E. coli*. Plasmid DNA was prepared by the method of Birnboim and Doly<sup>32</sup> and *E. coli* strain RR1 was used for transformation. The restriction enzyme digests of pMW5 and *ADR1* plasmids used to construct the series of 3'-deleted *ADR1* genes are described below. To construct YEp150ADR1 and YEp505ADR1, p411-B (which contains a 5-kb *Bam*HI fragment from clone YRp7-ADR1-411)<sup>5</sup> was digested with *Bam*HI plus *Sph*I (YEp150ADR1), or *Bam*HI plus *Nru*I (YEp505ADR1). To construct YEp302ADR1, p311 (ref. 5) was digested with *Bam*HI and *Pvu*II. YEp1323ADR1 was constructed by excising a 9-kb *Eco*RV fragment from p411 (ref. 5). The appropriate-sized fragment was isolated in each case and ligated with pMW5 cut with the following restriction enzymes. YEp302ADR1 and YEp505ADR1: *Bam*HI plus *Pvu*II; YEp150ADR1: *Bam*HI plus *Sph*I; YEp1323ADR1: *Pvu*II. **Yeast transformation:** Yeast transformations were done using the lithium acetate procedure<sup>33</sup> on 521-6 (*mata adh1-11 ADH2 adh3 ADR1 trp1 ura1 leu2*) and 521-6-Δ1 (*mata adh1-11 ADH2 adh3 adr1-Δ1::LEU2 trp1 ura1 leu2*). ADH assays were performed as described previously<sup>5</sup>. Derepressed cultures (*dr*) were grown in yeast complete medium containing either 3% ethanol or 1% ethanol plus 3% glycerol. Assays were done in triplicate for at least two independent transformants. The values are the means for six assays. Derepressed values in strain 521-6-Δ1 carrying YEp1323ADR1 were corrected for the number of cells that had lost plasmid since plasmid loss occurred at a higher frequency in these strains than in the other transformants.

this region, two pairs of cysteines are separated by 13 amino acids, similar to *ADR1* and *TFIIIA* repeat sequences. Thus, a finger of similar size could be formed with four cysteines acting as ligands for Zn<sup>2+</sup> rather than two cysteine and two histidine residues.

The evidence that a common structure could exist in transcription factors from such divergent species as yeast and frog, which are active with different RNA polymerases, suggested that similar structures might exist in other proteins with DNA-binding activity. Several complementary DNA clones and genes from *D. melanogaster* have recently been found to have this same repeated sequence motif (refs 11, 12 and J. Lengyel, personal communication). One of these genes is derived from *Krüppel*<sup>11,26</sup>, a locus affecting early *Drosophila* development; several of the others are either derived from or are adjacent to blastoderm-specific genes. All these *Drosophila* genes might thus have roles that are important in development, for example as tissue- or gene-specific transcription factors.

The best-characterized protein structure which is involved in DNA binding is the helix-turn-helix motif found in a variety of prokaryotic regulatory proteins<sup>27</sup>, in the yeast MATα2 repressor<sup>28,29</sup> and in the homoeo box region of several eukaryotic proteins<sup>30</sup>. The data presented here suggest that there may be a second structural motif of DNA-binding proteins in eukaryotes typified by the 30-amino-acid repeat found in *TFIIIA* and *ADR1*. The structural homology between *ADR1* and *TFIIIA* suggests that the factors regulating transcription by the different RNA polymerases have been under strong selective pressure to maintain basic structures and functions required for interaction with RNA polymerase and DNA.

We thank Dr Russell Doolittle for his computer-aided analysis of the amino-acid sequence of *ADR1* which revealed the homology between *ADR1* and *TFIIIA*; Dr Clyde Denis for his communication of the nucleotide changes in *ADR1* mutants; Dr Jeff Shuster for pointing out to us the potential phosphorylation sites in *ADR1*; Dr Richard Palmiter for critical reading of the manuscript; and Kate Roudybush for careful preparation of the manuscript. Support for this research was provided by the USPHS (GM26079) and PHS NRSA 5 T32 GM07270 from NIGM.

Received 11 December 1985; accepted 27 January 1986.

- Williamson, V. M., Bennetzen, J., Young, E. T., Nasmyth, K. A. & Hall, B. D. *Nature* **283**, 214-216 (1980).
- Nasmyth, K. A. & Reed, S. I. *Proc. natn. Acad. Sci. U.S.A.* **77**, 2119-2123 (1980).
- Johnston, S. A. & Hopper, J. E. *Proc. natn. Acad. Sci. U.S.A.* **79**, 6971-6975 (1982).
- Laughon, A. & Gesteland, R. F. *Proc. natn. Acad. Sci. U.S.A.* **79**, 6827-6831 (1982).
- Denis, C. L. & Young, E. T. *Molec. cell. Biol.* **3**, 360-370 (1983).
- Penin, M. D., Thireos, G. & Greer, H. *Molec. cell. Biol.* **4**, 520-528 (1984).
- Denis, C. L., Ciricay, M. & Young, E. T. *J. molec. Biol.* **148**, 355-368 (1981).
- Beirer, D. R., Sledziewski, A. & Young, E. T. *Molec. cell. Biol.* **5**, 1743-1749 (1985).
- Miller, J., McLachlan, A. D. & Klug, A. *EMBO J.* **4**, 1609-1614 (1985).
- Engelke, D. R., Ng, S. Y., Shastry, B. S. & Roeder, R. C. *Cell* **19**, 717-723 (1980).
- Rosenberg, B. U. et al. *Nature* **319**, 336-339 (1986).
- Vincent, A., Colot, H. V. & Rosbash, M. *J. molec. Biol.* **186**, 149-166 (1985).
- Laughon, A. & Gesteland, R. F. *Molec. cell. Biol.* **4**, 260-267 (1984).
- Kammerer, B., Guyonvarch, A. & Hubert, J. C. *J. molec. Biol.* **180**, 239-250 (1984).
- Kozak, M. *Nucleic Acid Res.* **9**, 5233-5252 (1981).
- Dobson, M. J., Tuitt, M. F., Roberts, A. J., Kingsman, S. M. *Nucleic Acid Res.* **10**, 2625-2637 (1982).
- Bennetzen, J. L. & Hall, B. D. *J. biol. Chem.* **257**, 3018-3025 (1982).
- Chou, P. Y. & Fasman, G. D. *Biochemistry* **13**, 211-245 (1974).
- Ginsberg, A. M., King, B. O. & Roeder, R. G. *Cell* **39**, 479-489 (1984).
- Krebs, E. G. & Beavo, J. A. *A. Rev. Biochem.* **48**, 923-959 (1979).
- Kemp, B. E., Graves, D. J., Benjamin, E. & Krebs, E. G. *J. biol. Chem.* **252**, 4394 (1977).
- Korn, L. J. *Nature* **295**, 101-105 (1982).
- Doolittle, R. F. *Science* **214**, 149-159 (1981).
- Smith, D. R., Jackson, I. J. & Brown, D. D. *Cell* **37**, 645-652 (1984).
- Shuster, J. et al. *Molec. cell. Biol.* (in the press).
- Knipplie, D. C., Seifert, E., Rosenberg, U. B., Preiss, A. & Jackle, H. *Nature* **317**, 40-44 (1985).
- Anderson, W. F., Ohlendorf, D. H., Takeda, Y. & Matthews, B. W. *Nature* **290**, 744-754 (1981).
- Shepherd, J. C. W., McGinnis, W., Carrasco, A. E., DeRobertis, E. M. & Gehring, W. J. *Nature* **310**, 70-71 (1984).
- Johnson, A. D. & Herskowitz, I. *Cell* **42**, 237-247 (1985).
- Laughon, A. & Scott, M. P. *Nature* **310**, 25-31 (1984).
- Ammerer, G. *Meth. Enzym.* **101**, 192-201 (1983).
- Birnboim, H. C. & Doly, J. *Nucleic Acid Res.* **7**, 1513-1523 (1979).
- Ito, H., Fukuda, Y., Murata, K. & Kimura, A. *J. Bact.* **153**, 163-168 (1983).
- Messing, J. *Meth. Enzym.* **101**, 20-78 (1983).

## Eukaryotic ribosomes that lack a 5.8S RNA

Charles R. Vossbrinck\* & Carl R. Woese†

\* Department of Entomology, 320 Morrill Hall, and

† Department of Genetics and Development, 515 Morrill Hall, University of Illinois, Urbana, Illinois 61801, USA

The 5.8S ribosomal RNA is believed to be a universal eukaryotic characteristic<sup>1</sup>. It has no (size) counterpart among the prokaryotes, although its sequence is homologous with the first 150 or so nucleotides of the prokaryotic large subunit (23S) ribosomal RNA. We report here an exception to this rule. The microsporidian *Vairimorpha necatrix* is a eukaryote that has no 5.8S rRNA. As in the prokaryotes, it has a single large subunit rRNA, whose 5' region corresponds to the 5.8S rRNA.

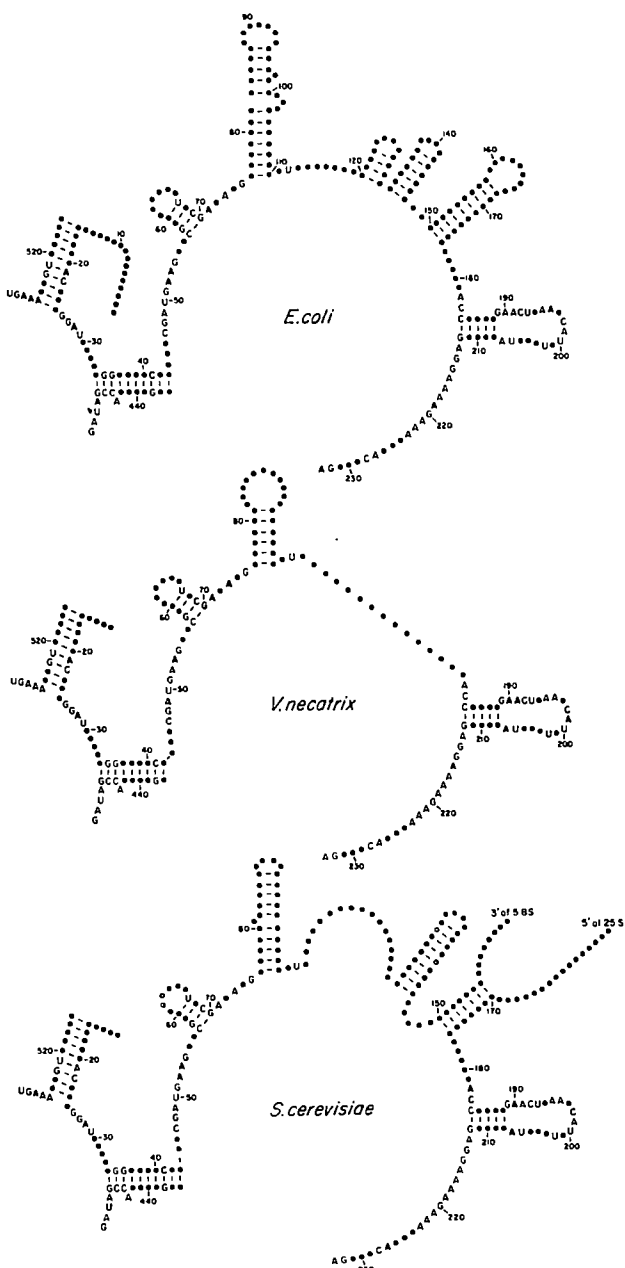
Microsporidia, of which *V. necatrix* is representative, are parasitic eukaryotes with various interesting life cycles<sup>2</sup>. Microsporidian species infect virtually all types of animals, from invertebrates to man<sup>3</sup>. Their ribosomes and rRNAs have been reported to be prokaryotic in size; the ribosome is a 70S (not 80S) particle that comprises 30S and 50S (not 40S and 60S) subunits, which in turn contain 16S and 23S rRNAs<sup>4,5</sup>. While isolating *V. necatrix* RNAs, we observed not only these unusual prokaryotic electrophoretic mobilities, but an unexpected absence of a 5.8S RNA. This fact can be explained in several

pos.(001-100)  
*E. coli* GGUUAACCGA CUAACCGUAC ACCGGUGGAUG CCCUGGCAGU CAGAGGCCAU GAAGGACGUG CUAAUCUGCC AUAGCGUCC GUAAGGUGAU AUGAACGUU  
*V. necatrix* ----- nnnnCCCAC aCaUGGGAUAC aAuAGGAUAC CA-UaACgAU GAAGGUCGu AuAAUACG A-AAGUAAU ----- UAUUUaCCUG  
*S. cerevisiae* ----- AACCUUCA ACAACGGAU UCUGGUUCU CGC-AUCCAU GAAGAACGCA CGGAAUUCGG AUACGUAAUG UGAAUUGCAG --AAUUCGU

pos.(101-180)  
*E. coli* AUAAACGGCG AUUUCGAAU GGGGAAACCC AGUGUGU--UUC- -GACACACUAU CAUUAACUGA AUC-----CAUAGGU UAAUGAGGG  
*V. necatrix* -AUAAAUAU UUUaA--- -UGUAUUGA U-----  
*S. cerevisiae* GAAUCAUCGA AUCUUUGAAC GCACAU-UGC CCCCUUGGUAAU CCAGGGGCAU GCCUGUUUGA GCGUCAUUUxxUGACCUAAU CAGGUAGGAG

pos.(181-250)  
*E. coli* AACCGGGGA ACUGAAACAU CUAAGUACCC CGAGGAAAAG AAAUACCCG AGAUUCCCC AGUAGCGGG  
*V. necatrix* uACCCUUUGA ACUUAAGCaU AUCuUUnAAA GGAGGAAAAG AAACUuACUu GGAAUUCUUU aGUAGCAGCG  
*S. cerevisiae* UACCCCGUGA ACUUAAGCAU ATCAAUAAGC GGAGGAAAAG AAACCAACCG CGAUUGCCIU AGUACGGCC

**Fig. 1** Sequence alignment for the initial portion of the 23S-like ribosomal RNAs from *Escherichia coli*<sup>9</sup>, *Saccharomyces cerevisiae*<sup>10</sup> and *Vairimorpha necatrix*. The alignment procedure was that used in ref. 8. Numbering is according to the *E. coli* 23S rRNA sequence. Positions where composition is uncertain are shown in lower case, using 'n' if the composition is undetermined. Dashes (inserted for alignment purposes) signify gaps in a given sequence. The join between the yeast 5.8S and 25S rRNAs is indicated by 'xx'.



# Agglutination methods for rapid analysis

from Mel Thomas

*Tests making use of carrier-bound antibodies can identify bacteria in less than five minutes, with results visible to the naked eye.*

USING one of the first microscopes, Antony Van Leeuwenhoek observed and described 'animalcules' in 1676. His drawings record the chief forms of bacteria — cocci, rods, filaments and spirochaetes. Hence Van Leeuwenhoek has been dubbed the 'father of bacteriology'.

More than two hundred years later, Robert Koch developed solid nutrient media and staining methods that made growth and observation of these bacteria much easier<sup>1</sup>. These fundamental discoveries spawned a system for bacterial isolation and identification which is still in use today. It involves growing bacteria in primary culture, subculturing onto varied specialized media and observing patterns of substrate utilization. These biochemical identification tests are reliable and specific, but take at least two days and sometimes several weeks to provide results. The need for more rapid and less laborious identification methods led to the development of coagglutination and latex agglutination testing.

In 1973, Göran Kronvall at the University of Lund, Sweden, reported a unique method for typing *Streptococcus pneumoniae* which was not only rapid, but also very easy to perform<sup>2</sup>. Kronvall called his method 'coagglutination'. Later that same year Christensen *et al.* described the use of coagglutination for the serological grouping of streptococci<sup>3</sup>. This research demonstrated that pathogens from overnight cultures could be identified in minutes instead of days.

## The lattice link

Coagglutination is an immunodiagnostic technology that utilizes antibodies in a reagent to detect specific bacterial antigens. The reagent consists of a suspension of non-viable staphylococci onto which specific antibodies are adsorbed. Recently the same principle has also been applied to polystyrene particles as carriers for latex agglutination. When a sample containing the homologous antigen is mixed with the reagent, an antigen-antibody linkage occurs which forms a lattice visible to the naked eye.

Pharmacia Diagnostics AB obtained commercial rights to the technique and began marketing its own improved pathogen identification tests in 1975. Now test kits can diagnose streptococci groups A, B, C, D, F and G, gonococci, meningococci, pneumococci and encapsulated types of *Haemophilus*.

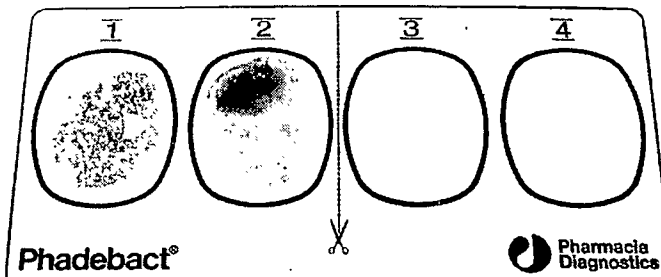


Fig. 1 If a sample tests positive, a fine precipitate visible to the naked eye forms from the lattice linkage of antibodies and antigens.

The original method for the preparation of coagglutination reagents has been published<sup>3</sup>. *Staphylococcus aureus* (strain Cowan I) is grown overnight in tryptic soy broth kept at 35°C and aerated. The harvested bacteria are washed twice with phosphate-buffered saline (PBS: 0.15 M NaCl, 0.01 M phosphate, pH 7.4), and suspended in 0.5 per cent formaldehyde in PBS at room temperature for 3 hours. The formaldehyde-treated suspension is then washed four times in PBS, and adjusted to a final concentration of 10 per cent (v/v).

Protein A, which binds IgG class antibodies to staphylococcus cells by their Fc fragments only, will be stable for several weeks using the above protocol. Heat treatment at 80°C for 2 hours kills the bacteria and extends stability to months if the reagent is stored at 4°C. Finally, the formaldehyde- and heat-treated staphylococci are mixed with a specific antiserum. After washing and resuspension in PBS containing 0.1 per cent sodium azide, the reagent is ready for testing.

To perform the test, a drop of reagent is added to a white slide on which either a smear from a primary culture, or a direct sample, has been placed. The slide is rocked gently back and forth as the reaction proceeds. If the result is positive, a fine precipitate will form within 2 minutes (see Fig. 1).

## A latex alternative

Latex agglutination is similar to coagglutination in that it employs a carrier, latex, to which specific antibodies are adsorbed. The preparation of latex reagents is also well-documented<sup>4</sup>. One part of 0.81 µm polystyrene latex particles is combined

with one part antiserum which has been diluted to an empirically defined optimal reactivity concentration. The suspension is incubated at 37°C for 2 hours. Then, two volumes of glycine-buffered saline (1.0 M glycine and 1 per cent NaCl, pH 8.2) containing 0.1 per cent bovine serum albumin is added. The sensitized latex reagent is stored at 4°C.

Antibody adsorption on staphylococci and latex particles is quite different. Protein A, present on treated staphylococci but not on latex, orients the antibodies so that the Fab structures are open for reaction; latex, however, adsorbs antibodies randomly, as shown in Fig. 2. Hence a portion of the antibodies adsorbed on latex are rendered useless for immuno-diagnostic purposes. This does not mean that latex agglutination is a less sensitive technique than coagglutination. It does mean, however, that different antibody concentrations may be needed, as well as some form of sample preparation, for instance an extraction process.

## Collective benefits

The advantages of coagglutination and latex agglutination are many. Because testing a primary culture takes less than 5 minutes, specific antibacterial therapy can be initiated at the earliest possible moment, perhaps preventing morbidity and mortality due to infection. Agglutination methods do not require living organisms for testing, and so avoid the problems of bacterial identification associated with live cultures.

Direct testing is also possible on certain specimens using coagglutination or latex agglutination. Cerebrospinal fluid, serum

and urine can be used directly in tests for *Streptococcus pneumoniae*, *Haemophilus influenzae*, *Neisseria meningitidis* and *Streptococcus* group B. Recently, agglutination tests for the identification of *S. pyogenes* (*Streptococcus* group A) directly from throat swabs have been introduced. In this case, rapid bacterial identification has a real benefit in that it protects patients who do not have group A streptococcal pharyngitis from the needless use of antibiotics.

The simplicity of coagglutination and latex agglutination testing cannot be over-emphasized. Testing is done by hand,

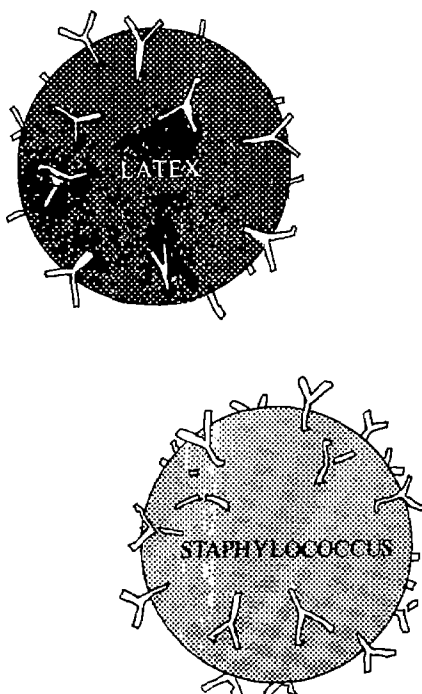


**Fig. 2** Antibodies adsorb randomly to latex, but the protein A coating staphylococci anchors antibodies by their Fe fragments.

without the need for expensive and complicated equipment. No special training is required, and the final cost of bacterial identification can be much less than that of prolonged biochemical procedures.

What of the future? Agglutination technology is taking advantage of highly specific monoclonal antibodies, and tests are being developed for viruses as well as additional bacteria. The areas of development are limited only by the levels of sensitivity that can be achieved. That which was started by Van Leeuwenhoek and Koch has gained new impetus from Kronvall and his successors. □

*Mel Thomas is at Pharmacia Diagnostics, Piscataway, New Jersey 08854, USA.*

1. Zinsser *Microbiology*, 14th edn (Meredith, New York, 1968).
2. Kronvall, G. *Med. Microbiol.* 6, 187-190 (1973).
3. Christensen, P., Kahlmeter, G., Jonsson, S. & Kronvall, G. *Inf. Immun.* 7, 881-885 (1973).
4. *Manual of Clinical Microbiology*, 4th edn (American Society for Microbiology, Washington, DC 1985).

## Taking a closer look at microbiology

*Bacteria, fungi and yeast have captured a degree of attention that belies their dimensions. This week's review examines microbial techniques from the fermenter to the autoclave.*

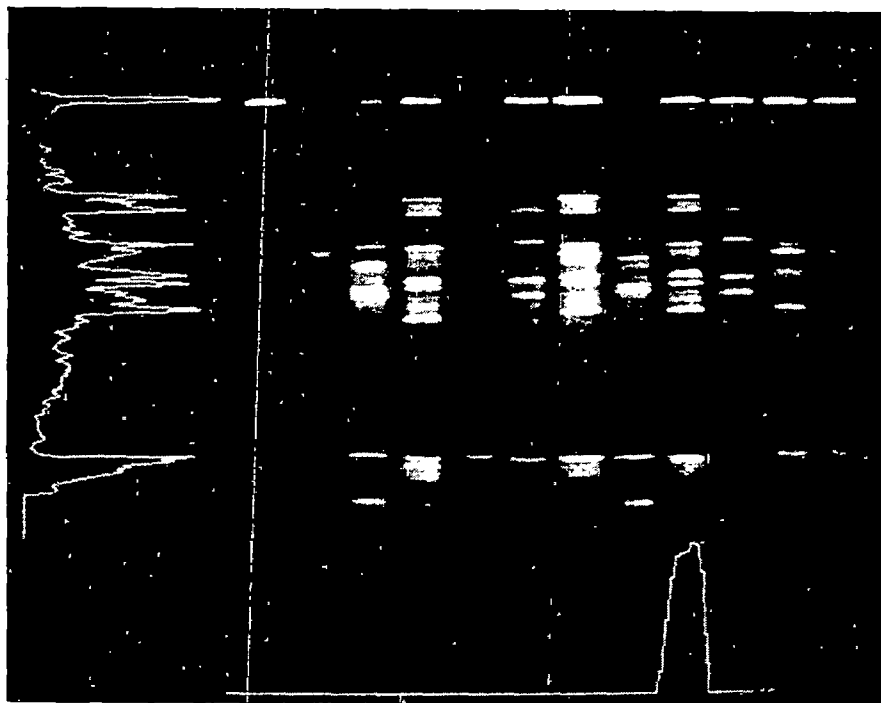
A NON-RADIOACTIVE DNA probe to rival avidin-biotin methods has emerged from the laboratories of Biotech Research (Reader Service No. 100). Beginning in May, Biotech will offer testing kits for viral and bacterial infection based on **hapten-antibody binding**. Because the system is chemical rather than enzymatic, Biotech expects to be able to sell the kits for one-half to one-third the cost of most non-radioactive probes. The company is developing both 'do-it-yourself' kits for customizing probes, and kits for specific viral and bacterial genes.

Back on the avidin-biotin front, Enzo Biochem Inc. have refined their **DNA probe system** in Pathogene II kits that even an amateur can use (Reader Service No. 101). The non-radioactive assay kits are available for infectious agents including *Chlamydia trachomatis*, herpes simplex virus, Epstein-Barr virus, cytomegalovirus (CMV) and adenovirus 5. Step-by-step instructions and all the reagents and buffers for 20 assays come in one package, priced at \$135 (US), except for the \$155 CMV kit.

The two-dimensional AMBIS beta scanning system was originally created to

quantitate the gel patterns Robert Silman used to 'fingerprint' bacteria. When Automated Microbiology Systems Inc. set out to market the identification system, they recognized a need for a fast, convenient scanner that would display the scan in autoradiograph form. Now their AMBIS system can do that, and much more. The scanner will quantitate beta-emitting isotopes from thin-layer chromatography plates, transfer membranes and whole body sections as well as gels, in as little as 15 to 30 minutes (Reader Service No. 102). An IBM PC/AT with a 20-megabyte hard disk and Hercules graphics stores the results and makes data extraction and quantitation simple. The scanner sells for \$24,000 (US), or \$29,000 with the computer included.

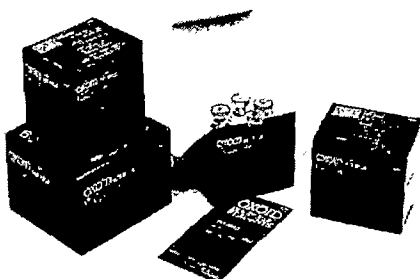
A **gene identification system** for Gram-negative bacteria promises to make matching mutant phenotypes to mutated genes a little easier (Reader Service No. 103). The system relies on a transposon in the plasmid vector that tags the region at which the vector DNA became incorporated into the recipient genome, causing mutation. Allelix Inc. in Canada will license to or undertake collaborative work with interested firms or organizations.



*The AMBIS system scans all lanes simultaneously to assemble a composite image.*

## PRODUCT REVIEW

In cases where finding a bacterial toxin is more important than detecting the bacteria itself, **toxin identification kits** may be



Toxin detection via latex agglutination.

the best bet. Oxoid Ltd. recently launched four such kits that employ the reversed passive latex agglutination (RPLA) technique for detection (Reader Service No. 104). Their sensitivity is as low as 1 or 2 ng of toxin per ml because the Oxoid's antibodies are highly purified. Kits are available for staphylococcal enterotoxins A, B, C and D, *Vibrio cholerae* enterotoxin/*E. coli* heat labile enterotoxin, *Clostridium perfringens* enterotoxin and staphylococcal toxic shock syndrome toxin. Each kit provides for 20 tests; costs vary.

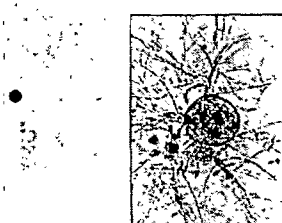
Culture media formulated for the selective isolation of microbial species is one way to be sure what's growing where. Selectatab media for *Campylobacter* and *Yersinia* isolation are the latest additions to Mast Laboratories Ltd's media list (Reader Service No. 105). The products come in packs of 25 tablets for less than £15 each, and each tablet is suited for 250 ml of the appropriate medium. All tablets have a shelf life of two years.

## Culture counts

If supplies of filamentous fungi and yeasts are running low, check the updated ATCC Catalogue of Fungi/Yeasts for more than 1,450 brand new strains (Read-

### • ATCC UPDATE FUNGI/YEASTS

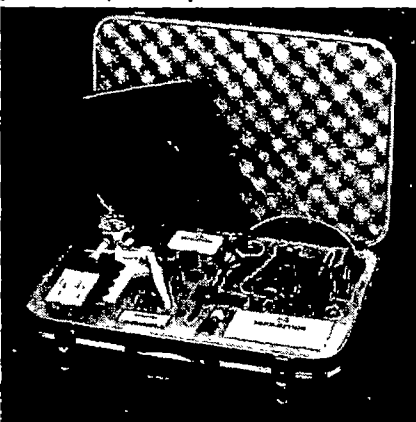
A SUPPLEMENT TO THE 1984 FUNGI CATALOGUE - NOVEMBER 1985



Over 1450 strains indexed alphabetically by species name  
Alphabetical listings provide easy access in the ATCC's latest catalogue.

er Service No. 106). The American Type Culture Collection has added strains that are useful in biological control, degradation, production, resistance/sensitivity, testing and assays, including controls for antibiotic sensitivity tests. ATCC also provides information on special applications, genotypes, pathogenicity, recommended media and growth conditions wherever possible.

The EpiCount kit from Nucleopore performs counts of liquid-borne microorganisms in less than 30 minutes (Reader Service No. 107). The Epicount procedure involves trapping microbes on a black polycarbonate membrane with a 10 µm pore size (ordinary cellulose membranes



Nucleopore's epifluorescent counter uses an acridine orange stain.

have pore sizes between 150 and 200 µm). The small pore size creates a surface capture effect which, in combination with the dark background, improves the accuracy of epifluorescent counting. The essential elements for Nucleopore's system, except the microscope, come in a \$695 (US) kit.

**Fluorescence activated cell sorters** (FACS) can pick out a microbe in a million, and the more parameters specified, the more particular the selection. Becton Dickinson have upgraded the options on their FACS 440 dual laser bench flow cytometers to include five-parameter status (Reader Service No. 108). A new £19,000 (UK) He-Ne laser is suitable for two- and three-colour immunofluorescence for antibody marking, as well as forward and 90 degrees light scatter analysis to indicate size and granularity. The 5 watt laser provides 32 mW of power at 633 nm with a typical tube life of 20,000 hours.

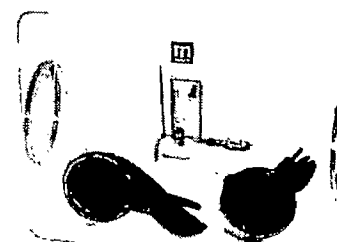
## Chamber choices

Even heating and minimum deviation make Gallenkamp's air jacket incubators reliable laboratory companions (Reader Service No. 109). Indirect heating with the air jacket design eliminates the need for mechanical convection, while a sophisticated electronic thermostat keeps temperature steady. Gallenkamp uses adjustable



With built-in protection systems temperatures in Gallenkamp incubators never stray more than 2° stainless steel shelves to allow flexible interior space. The incubators, available in 93 and 153 litre capacities, run £825 and £1,006 (UK) respectively, and each has a temperature range from 5 to 60°C.

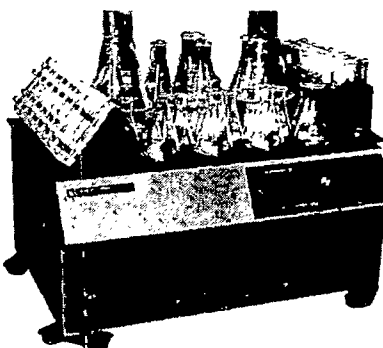
Manostat Corp. presents an economical way to get into controlled environments with their new glove box, priced under \$1,500 (US) (Reader Service No. 110). Options available with the box include bare hand entry, air lock and a selection of



Two or more Manostat glove boxes can be connected with a coupling sleeve.  
different gloves. Plexiglass construction makes customization easy for special attachments such as valves or hose ends.

## Shaken and stirred

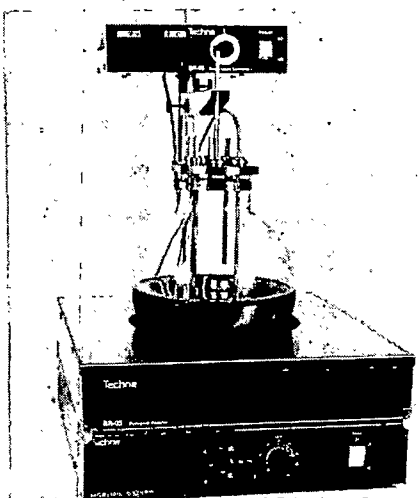
Switching flask or test tube sizes in biological shakers often means changing platforms as well. But New Brunswick Scientific have perforated their 'universal' plat-



A New Brunswick shaker's drive mechanism is unfazed by unbalanced or heavy loads.

form with over 200 holes, to accommodate up to 12 different sizes of Erlenmeyer flasks at one time or hold slant and test tube tracks (Reader Service No. 111). Flasks can range from 25 ml to 6 litres; test tubes, from 13 to 25 mm. The 18 × 30 inch platform is priced at \$400 (US).

By floating an impeller on top rather than using a sunken spin bar, Techne Inc. say they've improved the rate of solution of oxygen by 50 to 80 per cent in their latest bioreactor (Reader Service No. 112). The



The BR-05 bioreactor is all glass with a stainless steel multi-port cap.

2.5-litre BR-05 has a spherical shape that increases the ratio of surface area to volume over that of a comparable cylinder.

#### ADVERTISEMENTS

<b>PHORBOL ESTERS</b> Co-Inducer of Interferon Cat. #M4600 ..... 5mg / \$81.06	<b>MEZEREIN</b> Co-Inducer of Interferon Cat. #M4600 ..... 5mg / \$81.06
<b>LC SERVICES CORPORATION</b> 165 New Boston Street Woburn, MA 01801 (617) 938-1700	

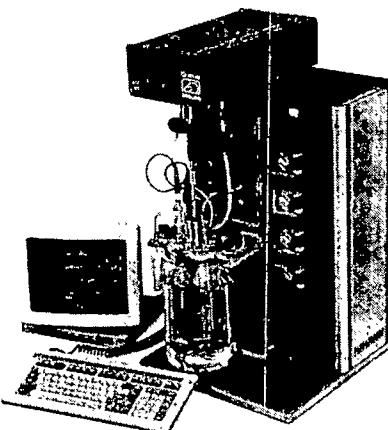
Reader Service No.38

<b>Yeast?</b> <b>Tetrad Analysis?</b> <b>SINGER</b> MICROMANIPULATOR MK III Patented	
Perfect control in 3 Dimensions from a single joystick. Continuous variable reductions to suit all magnifications. No after sales maintenance needed.	
<b>Details from:</b> <b>Singer Instrument Co. Ltd.,</b> Treborough Lodge Roadwater, Watchet Somerset TA23 0QL England. Tel. (0984) 40226 Telex: 337492 Comcab G.	

Reader Service No.37

cylindrical vessel. That feature disperses oxygen in the bioreactor without forming air bubbles. The \$3,500 (US) unit comes with a platinum temperature sensor (to be submerged in the medium), stirrer and speed control.

An integrated bioreactor system from Queue Systems can perform both fermentation and cell culture with individual



Data from the integrated Queue Mouse fermenter can be sent to a printer or another computer.

control of up to 21 variables (Reader Service No. 113). Complete with pre-programmed software, the Queue Mouse works in batch, feed batch and continuous culture applications, as well as hollow fibre, mechanically agitated and airlift bioreactors. For about \$20,000 (US), the Mouse system offers flexibility as its strong point.

Computer-controlled gradient feed technology has enabled Battelle to produce recombinant *E. coli* cells in concentrations of over 80 grams (dry weight) per litre (Reader Service No. 114). The fermentation know-how is available from Battelle in a technical manual, a computer software package and follow-up technical services for under \$15,000 (US). The company expects that their system will also be applicable to genetically modified *Bacillus subtilis*, other bacteria and yeasts.

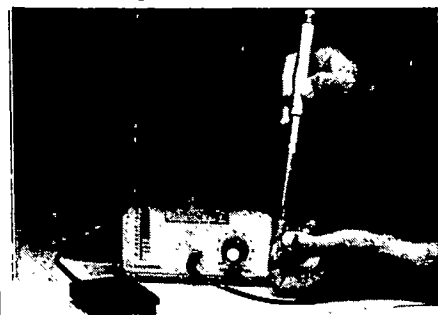
Applikon's series of small and middle-range fermenters runs the gamut of fermentation unit size and specificity (Reader Service No. 115). They offer fermenters suited for cell or continuous cultures in round bottom, flat bottom or jacketed glass vessels and stainless steel bioreactors. Each has plenty of ports on the headplate. Applikon's stirrer assemblies were designed to avoid contamination, in double lipseal or magnetic-coupled stirrer versions. Prices vary depending on the choice of unit and options.

## The end of the line

When it's time to wrap up an experiment, Riese Enterprises has a combination

waste disposal/sterilization indicator bag designed for biohazardous waste (Reader Service No. 116). Bright red, melt-resistant BioSure bags integrate time, temperature and pressure to signify, by means of a migrating blue chemical, when contents have been safely autoclaved. The bags come in packs of 100 and cost \$78 (US) for the 19 × 24 inch size and \$85 for the 24 × 36 inch bags.

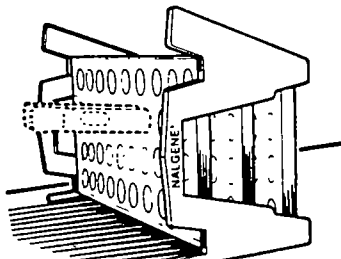
Bacteria and viruses are easy prey for Kontes' micro ultrasonic cell disrupter (Reader Service No. 117). The disrupter will produce rapid and reproducible results with micro- to millilitre sample volumes. Monitor circuitry maintains the displacement amplitude of the probe tip under widely varying loads, and an LED indicator displays the load imposed by the



A tiny probe from Kontes makes for small-scale cell disruption.

sample. The combination of these two features ensures reproducible figures, with a \$1,230 (US) price tag.

Nalgene's 1986 labware catalogue covers over 400 of their plastic lab products in 118 pages (Reader Service No. 118). The catalogue leaves no stone unturned, listing full product specifications, prices, chemical resistance/physical properties data and care and use instructions for every item. In addition to routine illustrations, this year's booklet contains a 14-page colour section featuring Nalgene's new disposable filter units. Test tube and vial



Every product gets a picture in Nalgene's new catalogue.

racks, centrifuge bottles and laboratory jars, carboys and Petri plates are offered for the microbiologist's inspection. □

These notes are compiled by Karen Wright from information provided by the manufacturers. To obtain further details about these products use the reader service card bound inside the journal.

A. S. Alter  
24-6-85

## Chirac's newly won winning ways

*In the aftermath of the French election the consequences for science of the demise of the ministry for research may be overestimated.*

THE new Prime Minister of France, M. Jacques Chirac, is inevitably less demonstrative a supporter of the French research and development establishment than was his predecessor, M. Laurent Fabius, who had succeeded to that post from his earlier appointment as minister of research. So much was widely predicted in the weeks preceding the election, when M. Chirac's advisers were forever saying that the research bureaucracy had become a natural target for their cost-cutting decentralizing zeal (*Nature* 319, 729; 1986). Even so, it will have come as a shock to many people that these widely flagged intentions could have implied anything so radical as the abolition of the ministry of research (see page 295). Henceforth, unless M. Chirac changes tack, research will be no better distinguished from the other routine matters with which governments are concerned than it is, for example, in Britain. Is this not a sign that the new government intends for science the policies of malign neglect on which previous governments in Paris have habitually relied? And will not the result be that the resurgence of the past five years will be more rapidly put into reverse?

Fears such as these will be widely expressed in the next few weeks, but it is too soon to take them seriously. M. Chirac may intend to keep his election promise to let the French ministry of research go into limbo. It remains to be seen whether he will have the courage (some would say gall) also to reorganize along the lines of his manifesto the agencies by which French research has been supported over the past five or even fifty years, the research councils of which the Centre National de la Recherche Scientifique (CNRS) is the chief. Before the election, M. Chirac's advisers were promising that the agricultural and medical research councils would be transferred to the corresponding ministries and that CNRS, by far the largest, would be broken into smaller pieces. To some extent, the motivation of these policies is doctrinal, born of the conviction more common on the right than the left that governments may create the framework for industrial innovation but can have no substantial (or useful) part to play in the execution of industrial strategy. Yet there is no suggestion that the French agricultural and health research councils will be much transformed by what M. Chirac plans for them. The crucial issues are not administrative but financial.

### Tradition

The future of CNRS is bound to be more difficult to decide. Traditionally, even before the Second World War, CNRS had several distinct but parallel functions. In recent decades, CNRS has become best known as the agency by which major efforts in basic science are undertaken, in fields as different as high-energy physics and geochemistry. Innovations of this kind have spawned the distinctive French efforts in space research and oceanography, now administratively independent. But CNRS is also the traditional partner, with the universities, in the conduct of academically based research, but in a manner that is interestingly distinct from that practised almost everywhere else. Most of its work in support of university research is channelled through the full-time CNRS employees who work alongside academics in university laboratories, exciting both the admiration of colleagues and their envy. On the face of things, it would

not be a disaster if some of this activity were transformed into that more familiar elsewhere in Western Europe and North America, the provision of research funds to university researchers by means of the familiar competition for research grants. Siting the administration of CNRS within the ministry of education in Paris will make it easier for M. Chirac and his colleagues to contemplate a change along these lines. Provided that the contemplation is serious, not a token prelude to predetermined and prejudiced reorganization, there may even be benefits to be won from change in this direction. Robbing CNRS of its role as the chief sponsor of major projects in basic research would be a more dangerous step to contemplate at this early stage.

### Change

The other obvious consequences of the post-election reorganization of the French government are inevitably harder to assess, if only because of the novelty (and ambiguity) of the arrangement that has harnessed a socialist president to a right-wing executive in the constitution of the government. President Mitterrand will be anxious to ensure that the executive and the French Assembly do not chip away at his constitutional authority over French foreign policy, which will make the whole area of French collaboration with other countries a potential no-man's land in the months ahead. The chances are that the President will be able to sustain those French policies stemming from his personal enthusiasm for European collaboration in high technology. It would not be surprising if the Prime Minister, as a *quid pro quo*, were to succeed in aligning France with Britain in scepticism about the need for continued investment in collaborative high-energy physics through the agency of CERN, the high-energy physics laboratory at Geneva. Provided that both partners in this uneasy government alliance acknowledge that the immense benefits that have accrued to France in the past five years are a prize that cannot be lightly thrown away, even developments such as these need not spell doom.

Newly elected governments tend to brim over with enthusiasm better suited to routine matters of public administration than to the proper care for sensitive parts of public life, among which research may be the most delicate. It is one thing to nationalize (or denationalize) a string of banks or other businesses, replacing one bunch of shareholders by another, and quite another to pretend to know what decisions should be made, and how, in a field in which even the practitioners are at a loss to tell just what needs doing. So what M. Chirac must keep clearly in mind, during the first few heady weeks when enthusiasm may get the better of his colleagues' judgement, is that France has done extremely well in basic research during the past decade for reasons which are not sufficiently explained by the way in which money has been thrown at some researchers during the past five years. During the same period, for reasons which are probably quite separate, the French telecommunications network has ceased to be a joke and become something of a marvel instead. Nobody's interest would be served if the new government, by pretending that it knows not merely the questions but the answers, were to make a mess of this beneficent development. □

# Japan eager to join in the star wars fray

*Tokyo*

JAPAN is sailing steadily towards taking part in the US Strategic Defense Initiative (SDI), and the opposition that was expected to wreck participation has altogether failed to materialize. At the end of this week, 46 representatives and engineers from 21 of Japan's high-technology companies, accompanied by nine government officials, will set off to the United States for a 10-day tour of institutes and companies where SDI research is taking place. This is the first time that industry has been involved in SDI missions to the United States, and completes the groundwork for industrial participation.

Executives of high-technology companies are already happy to admit that they have been contacted by government officials encouraging them to look for SDI contracts. What is worrying industry now is not whether they will be allowed to participate but, as the head of one small electronics company put it, "the extent to which the government is intending to try to control affairs from behind the scenes".

Keeping direct government involvement, and research in government laboratories, out of sight looks like the last concession that will be made to those who oppose SDI. So far, the opposition has in any case been remarkable for its silence. Neither the principal opposition parties nor the media have attempted to make a major political issue out of SDI, despite the extremely emotive nature of defence issues in Japan.

One reason is that the opposition has much bigger problems to think about. In the next few months, Prime Minister Yasuhiro Nakasone will begin the break-up of the state-owned Japan National Railways (JNR) into six regional private companies, plus companies to run the "bullet" train and freight services. The aim is to get JNR's almost unbelievable debt — in excess of the foreign debt of Mexico — off the public shoulders and to shed almost 40 per cent of its third of a million staff. The principal opposition party, the Japan Socialist Party, and the unions have enough to do opposing privatization without worrying about SDI.

Opposition to SDI participation may also arise through factional struggles within the ranks of Nakasone's own Liberal Democratic Party (LDP). The Prime Minister seems clearly to be aiming at calling elections for both upper and lower houses of the Diet in June. At that time, he should be at the peak of his popularity. He will have visited the United States in April and hosted the summit of industrial

nations in Tokyo in June, both of which are certain to heighten his image as Japan's first truly international statesman. If a resounding victory in the elections follows, he will be in a position to call for a change in the LDP rules that will allow him to stay on for a third two-year term as LDP leader, and thus Prime Minister.

Naturally enough, other contenders for the LDP leadership who now begin to see that the end of Nakasone's fixed term of

*Yup, we sure could have done with a few of those beauties above Pearl Harbor...*



office may be a mirage are less than happy. Among them, Foreign Minister Shintaro Abe is known to be cool towards SDI participation: so internal feuds within LDP could still lead to a change of course.

The only other serious barrier to participation is a 199 all-party Diet resolution banning the military use of space. The resolution has been taken seriously and

has been invoked, for example, to try to stop the self-defence forces using Japanese-launched commercial satellites for military communications. But lawyers already believe that loopholes can be found.

Next week's mission to the United States is plainly aimed at looking for commercial possibilities. It will include engineers from virtually all of Japan's big electronics companies — Fujitsu, Hitachi, NEC, Sony, Oki and Sumitomo — as well as from large self-defence force contractors such as Mitsubishi Heavy Industries. The industrial representatives will split into three groups according to their fields of commercial expertise. They will visit the Lincoln Laboratory of MIT, the Los Alamos National Laboratory and the US Army Strategic Defense Command as well as several industrial companies.

Worries that Japan's lack of anti-spionage laws might limit participation seem also to have been dispelled. US Defense Secretary Caspar Weinberger said last week that Japan would not have to be bound by special confidentiality agreements to carry out SDI research, given the "high level of trust between the two nations".

At the end of the day, however, there is still no doubt that many researchers in industry would prefer to have little to do with SDI. Some, who remember the Second World War, find any involvement with the military regrettable. Others attribute Japan's economic miracle to its refusal to waste talent or money on the development of military rather than consumer technology. They fear they are gradually going to be dragged down into the same hole in which the United States finds itself.

**Alun Anderson**

## Waving the star (wars) and stripes

*Washington*

No expense was spared, no detail too small at a Washington banquet and award ceremony held last week for heroes of the Strategic Defense Initiative (SDI). Even jaded regulars at defence contractor bashes were flabbergasted when a full-colour guard in revolutionary war uniforms marched to the podium to the beat of fife and drum, bearing the stars and stripes and military flags festooned with campaign streamers.

The Hollywood-style ceremony was held by the American Defense Preparedness Association (ADPA), a defence contractor organization, as part of a two-day classified symposium on SDI at the National Academy of Sciences. The first two recipients of the ADPA Strategic Defense Award were Dr James Fletcher, recently nominated as administrator of the National Aeronautics and Space Administration and chairman of a key early study that supported SDI, and Dr George Keyworth,

a fervent SDI advocate who was until recently director of the White House's Office of Science and Technology Policy. Medallions bearing the ADPA seal were presented to the proud winners by no less than Lt General James Abrahamson, director of the SDI organization.

Banquet guests were then treated to five-minute film clips capturing dramatic high-points of the public-consumption experiment spectacles. The US Army's SDI team and the Lockheed Missile and Space Company took home the ADPA Strategic Defense Technical Achievement Award, for the successful homing overlay experiment in which a dummy missile was intercepted and destroyed in space. Runners-up were Dr Richard Briggs of Lawrence Livermore Laboratory (free electron laser), and Itek Optical Systems Division (atmospheric compensation system, tested on television during a shuttle flight last year).

**Tim Beardsley**

## French elections

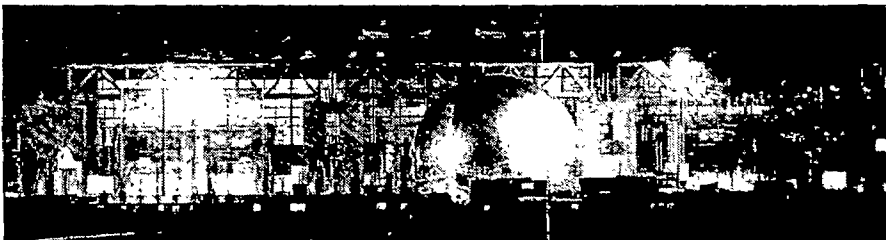
## Research loses its ministry

THE French general elections last week, which led to the appointment of a new right-wing French government, have also produced a slap in the face for the research establishment. For M. Jacques Chirac, the new prime minister, has failed to appoint a minister to head the Ministère de la Recherche et de la Technologie (MRT), the nerve centre of the previous government's strategy on research. Last week, staff at the ministry were in limbo, as ministerial appointments were announced which ignored the existence of MRT.

Even worse, the new prime minister, the mayor of Paris and leader of the minority Rassemblement pour la République (RPR) party, has not mentioned research or technology in a list of five priority issues for the future, although the outgoing socialist government would almost certainly have done so. For Chirac, precedence goes to issues such as de-nationalization, law and order and a return to transferable voting (a system which President François Mitterrand threw out in favour of proportional representation in a successful bid to complicate the right's hold on the present parliament).

According to the plans of Chirac's science advisers, responsibility for technology policy and the overall distribution of the French government research budget will be given to a prime-ministerial office one-tenth the size of the present MRT, which would be faster acting and more flexible than the socialists' ministry. But by late last week, no announcement had been made about the setting-up of such a body.

This turn of events presents one big question-mark for Eureka, the programme for European cooperation in high-technology innovation which was created with a great flourish by President Mitterrand last year. Anomalously, Mitterrand remains president until the next presidential elections (which must take place by 1988). Constitutionally, he will retain major powers over foreign and defence policy, and already he has vetoed one of Chirac's nominees for the job of foreign minister — ostensibly because the candidate was too much in favour of the US Strategic Defense Initiative (SDI). Eureka will fall slap into the centre of this turmoil, as the programme was born as a response to the US call for European participation in SDI, and involves foreign, defence and research policy in high degree. Yet the ministry which has been overseeing the programme (MRT) is no longer to exist: conflict between Chirac and Mitterrand on foreign policy seems inevitable.



THE "Cité des Sciences et de l'Industrie", France's giant leap into modern interactive exhibition methods for science and technology, is now open to the public. Originally commissioned by the previous French president, M. Giscard d'Estaing, the Cité has grown out of a gigantic and failed abattoir built to serve the whole of the Paris region.

The redesigned building includes two "domes" on the roof which will follow the

As for research, M. Chirac's actions so far are entirely consistent with statements made by his science advisers before the election. The only mention of research in Chirac's new, slimmed-down administration is at the ministry of education, where one of three junior ministers assisting the principal education minister will be responsible for "the universities and research". If the previously advertised programme is carried through, this new "delegate minister", theoretical chemist M. Alain Devaquet, will now take control of the major French research council, the Centre National de la Recherche Scientifique (CNRS), and begin to dismantle parts of it in order to decentralize policy-making and to give university researchers more direct power over their laboratories.

Devaquet himself, however, is less

feared by some of the architects of the previous government's science policy than others Chirac might have chosen. A 43-year-old professor at the University of Paris (South), he studied chemistry at the École Normale Supérieure de St Cloud from 1962 to 1966, and has worked in North America at Cornell University and the University of Western Ontario. He is a member of a respected CNRS "laboratoire associé", one of the many CNRS laboratories jointly supported by the universities and by CNRS. Many such laboratories, however, have a sense of having suffered from CNRS policies of concentration, which are claimed to have favoured the CNRS's fully-owned "laboratoires propres", and this factor may shape some of Devaquet's own thinking.

Robert Walgate

feared by some of the architects of the previous government's science policy than others Chirac might have chosen. A 43-year-old professor at the University of Paris (South), he studied chemistry at the École Normale Supérieure de St Cloud from 1962 to 1966, and has worked in North America at Cornell University and the University of Western Ontario. He is a member of a respected CNRS "laboratoire associé", one of the many CNRS laboratories jointly supported by the universities and by CNRS. Many such laboratories, however, have a sense of having suffered from CNRS policies of concentration, which are claimed to have favoured the CNRS's fully-owned "laboratoires propres", and this factor may shape some of Devaquet's own thinking.

Robert Walgate

## Nuclear energy

## Weizsäcker changes his mind

## Hamburg

CARL FRIEDRICH von Weizsäcker, the physicist and philosopher whose brother, Richard von Weizsäcker, is West German president, has changed his mind about the place of nuclear energy in the fuel economy of West Germany. As director of the Max-Planck Institute of Future Research until his retirement in 1980, von Weizsäcker judiciously balanced his opposition to nuclear weapons with the opinion that peaceful nuclear energy is a necessity. But now, in a foreword to a book to be published shortly, he announces that he has changed his mind.

Although now 74, von Weizsäcker's opinion is still influential in West Germany. His revised opinion accompanies a book *Die Grenzen der Atomwirtschaft* (The limitations of the nuclear economy) by Klaus Michael Meyer-Abich, a Hamburg state senator, and Bertram Scheffold, a Frankfurt economist.

Von Weizsäcker has been influential in

the West German debate on nuclear energy since at least 1957, when he organized the "declaration of the Göttingen eighteen" in which a number of distinguished West German physicists declared their opposition to nuclear weapons. In 1983, he was the adviser on national security policy to the social democratic candidate for federal chancellor, Hans-Jochen Vogel.

According to the unpublished foreword, von Weizsäcker has changed his mind because of the "sleepless nights" he endured worrying about the problem of the protection of civil nuclear power plants from attack, either by terrorists or in time of war. He says that he has come to prefer that the development of solar energy should now take precedence because of his fear of "outrages", and that he does not dispute the possibility that, in a peaceful world, nuclear energy could again "render mankind an important service".

Jürgen Neffe

## Japan's research

# Industry imitating life tomorrow

**Tokyo**

A SMALL team inside Japan's Ministry of International Trade and Industry (MITI) is busy preparing the framework for a major research programme — "the human frontier project" — that will try to create a new interface between basic biological research and technological development. With luck, the programme could be launched during the summit of the leaders of the Western industrial nations in Tokyo in May.

The human frontier programme takes its fanciful name from part of a report submitted to MITI's Agency of Industrial Science and Technology by a special advisory panel. Among its members were Leon Esaki, Nobel prizewinner and head of IBM's Tokyo Research Center. The report, entitled *Technological Development and International Exchange for the 21st Century*, makes the customary criticisms of Japan as a "free rider" on the West's basic research endeavours. It goes on to propose the "human frontier" plan in that curious mixture of officialese and hyperbole, studded with fashionable high-tech words taken from the English, that seems to characterize the workings of small advisory groups. Among other things it calls for "researchers with centripetal force (!) to be collected in one place so that through repeated *burainsutomingu* (brain storming), *tema* (themes) and *conseputo* (concepts) can be clarified . . .". As with other MITI research projects, however, exotic titles and preliminaries are no guide to the seriousness of the contents.

What is being suggested is a long-term (perhaps twenty-year) programme aimed at carrying out basic research in the biological sciences but with very close attention to possible technological applications. MITI research projects, which have always been partly carried out in government research institutes and partly in industrial companies, seem just the format for this approach. And if it seems unlikely that industrial companies would be interested in basic biological research, it is worth remembering that both NEC and Mitsubishi Electric are running invertebrate neurophysiology programmes on the grounds that better computers can be built by studying the way living organisms transmit and process information.

That idea is behind one of the three main areas proposed for the human frontier programme: an attempt to imitate functioning of brain and nerve networks to find new ways of information management and control circuitry that could be implemented in new kinds of electronic materials. A second area is the imitation of chemical processes taking place within

living things. The aim is to build better industrial catalysts, carry out reactions using less energy and to trap light energy with artificial photosynthesis systems. Imitation of muscles and sinews of living organisms comes third, with the aim of building energy-efficient "physiological machines". The overall philosophy is of basic research for the sake of its applications, contrasting with the popular Western concept of basic research for the sake of "the advancement of knowledge"!

The human frontier programme is not the only new project to be aired in recent weeks. A separate private advisory panel to the Prime Minister, the Advisory Group on Structural Economic Adjustment for International Harmony, is expected shortly to call for a Japanese

version of the European Eureka high-technology development project. Artificial intelligence, new materials, optoelectronics and robotics are likely to be its key themes and international collaboration is to be invited.

What in part makes thoughts of such projects possible is the dramatic drop in Japan's oil bill. Two-thirds of Japan's energy needs are met by oil and every drop of it is imported. The halving of crude oil prices (not yet passed on to the consumer) gives the government an unparalleled opportunity to spend money in new ways. A second factor is the problem of Japan's participation in the US Strategic Defense Initiative (SDI) (see page 294). Public opposition to military research in Japan is strong and it is thought that major, non-military international research might sweeten the involvement in SDI that the government is clearly aiming at.

**Alun Anderson**

## Japanese space programme

# Abundance of satellites planned

**Tokyo**

NEW and revised plans for Japan's space programme were announced last week by the Space Activities Commission (SAC). Altogether the launch of some eleven satellites plus a couple of space experiments have been fixed for the next five fiscal years, along with development of new and more powerful launch vehicles.

SAC is a part of the Prime Minister's Office responsible for overall coordination of the space programme's two arms: the scientific programme run by the Institute of Space and Astronautical Science (ISAS) and the applications programme run by the National Space Development Agency (NASDA). On the academic side, the chief news is that a magnetosphere observation satellite "Geotail" will be launched by the end of the 1990 fiscal year. The satellite is due to be launched by the space shuttle in a cooperative programme with the United States and will make observations on the structure and dynamics of the long magnetic tail formed on the night side of the Earth.

In the nearer future, two other Japanese experiments are due to be taken up by the space shuttle. No changes in their dates have yet been announced by the US National Aeronautics and Space Administration as a result of the explosion of the Challenger. From ISAS come Space Experiments with Particle Accelerator (SEpac). The idea is to inject charged particles from electron and ion beam accelerators into the Earth's ionosphere and magnetosphere to generate an artificial aurora which will aid understanding of the behaviour of space plasma and the generation of auroral lights. NASDA aims at a more practical application with

its First Material Processing Test, to be carried on Spacelab. Various experiments for producing materials under gravity-free conditions are under development.

Three other important missions will come from ISAS. As had been expected. Astro-C will be launched this fiscal year to continue ISAS's highly successful series of X-ray observation satellites. Heavier and bigger than its two predecessors launched in 1981 and 1982, it should be able to observe X-ray sources in more distant galaxies as well as in the Milky Way. Following that, Exos-D will be launched in fiscal year 1988 to continue the series of satellites observing the upper atmosphere and aurora. Next, in fiscal year 1989, the "Muses" interplanetary probe programme will begin with the launch of Muses-A, a satellite designed to test the orientation, control and data-transmission systems needed to make possible a flight to the Moon.

The SAC plan also reveals that NASDA's H-II rocket should be ready for its maiden flight in fiscal year 1991. Using almost entirely home-developed technology, it will have two liquid hydrogen/liquid oxygen stages and be capable of putting a two-ton satellite into geostationary orbit. But before that its predecessor, the H-I, capable of handling only a 550-kg payload, should, between fiscal years 1987 and 1989, have launched six satellites. Success will of course depend upon the conclusion of the current development of the H-I's second-stage liquid hydrogen/liquid oxygen engine. Before H-I comes into operation, one more satellite will be launched by the last of the N-II liquid fuel rockets, the Mos-I marine observation satellite. **Alun Anderson**

## US research costs

# Pressure builds in Congress

Washington

RESPONDING to howls of indignation from US universities and Congress, the White House's Office of Management and Budget (OMB) now says it is willing to delay implementing new regulations for compensating universities for the indirect costs associated with federal grants.

Joseph Wright, deputy director of OMB, made the offer to postpone implementation until 1 July at a meeting of the House of Representatives subcommittee on science research and technology to consider the planned changes. Members of the subcommittee were dismayed by OMB's "haste" to make sweeping changes to Circular A-21, the document providing the blueprint for cost reimbursement. The proposed revisions would limit the reimbursement for administrative costs to a fixed percentage of the total amount of a grant; 26 per cent in 1986, dropping to 20 per cent in 1987.

OMB estimates the move will save \$300 million over the next two fiscal years. OMB published its proposed changes in the *Federal Register* on 12 February, with a comment period of only 30 days. The revisions were to take effect from 1 April, although individual agencies were allowed to delay implementation for up to a year, and most had said they would need at least until 1 July to change their procedures.

Even before the new regulations were announced, the university community was seething over rumours of OMB's plans (see *Nature* 319, 346; 1986). The complaints were that OMB was making the changes without consulting those affected, and that the 26 per cent figure was arbitrary, not reflecting varying needs in different institutions. When the changes were finally announced, universities were indignant at the short period allowed for comment, complaining that OMB could not be very interested in what they had to say.

Since 12 February, university presidents and their allies in Congress have unleashed a flood of letters to OMB protesting the changes. Forced into a conciliatory posture before the subcommittee, Wright was nonetheless unwilling to extend the 30-day comment period. He did, however, agree to meet Dale Corson, chairman of the Government/University/Industry Roundtable, to establish an agenda for discussions in the coming weeks. In addition, subcommittee chairman Doug Walgren (Democrat, Pennsylvania) indicated that his committee would continue to take testimony on the amendments, and would require OMB to respond to them.

Joseph Palca

## British astronomy

# Time for Greenwich to move

A DECISION has finally been made about the fate of the two ground-based observatories in Britain. The Science and Engineering Research Council (SERC), which supports the Royal Greenwich Observatory (based, since 1948, at Herstmonceux in Sussex) and the Royal Observatory, Edinburgh, announced last week that the Royal Greenwich Observatory (RGO) will be moved yet again. A final decision will be made in June between the three sites now under consideration: "in order of priority", Edinburgh and the Universities of Cambridge and Manchester.

The need for some decision arises from the steady replacement of British-based optical instruments by more advanced equipment at overseas observatories, chiefly at La Palma in the mid-Atlantic and Hawaii. Although the two British observatories have provided technical and managerial support for the overseas observatories, the role of RGO in this connection will be much reduced from 1990, with the completion of the 4.3-m John Herschel reflector at the La Palma observatory. Although SERC plans to decide on the eventual location of RGO at its meeting in June, the move will not take place until 1990.

Plainly, SERC has found its decision about the location of RGO exceedingly difficult to make. The need for some reorganization has been apparent for some five years, and has been an urgent issue since November 1984, when SERC put in hand a reappraisal of its pattern of spending. But a working party under the previous chairman of SERC, Sir John Kingman, which produced a list of options for the council in January of this year, was apparently unable to decide between them. It will not be possible to confirm rumours that the Kingman group recommended a continuation of the status quo because, according to Professor E.J.W. Mitchell, now the chairman of SERC, its report will not be published.

At the same time, the possibility of British withdrawal from the Anglo-Australian Telescope has been postponed, at least until 1990. This became a live issue roughly a year ago, when continued British collaboration at the Australian site, which costs SERC £1.5 million a year, was given a low priority by the Astronomy and Space Board of SERC. Australians were quick to point out that the collaboration is regulated by a formal treaty between Britain and Australia with no break clause. Now, it seems, discussions are under way with other potential partners, including Japan, which may lead to a change of status for the Anglo-Australian Telescope, but not before the end of the decade.

SERC's intention is that the move of

RGO from the Herstmonceux site will be self-financing, at least so far as capital costs are concerned. The chief, but still uncertain, element in any such calculation is the value of the fifteenth century castle which dominates the observatory's site in Sussex. One imponderable is the likely value of the building on the open market. Another is whether SERC would be allowed by the British Treasury to keep the whole proceeds of a successful sale.

According to Mitchell last week, the intention is that RGO should retain its separate identity even when it has moved to another site. To the extent that both RGO and Edinburgh provide instrumental and engineering support for overseas telescopes, the two large optical instruments at La Palma and the infrared and millimetre-wave telescopes in Hawaii (the second of which is now nearing completion), the advantages of a merger at Edinburgh are plain. But SERC is also aware of the benefits of siting RGO at a university where astronomy is already strong. One of SERC's disappointments in the present arrangements is plainly that the connection between RGO and the University of Sussex, 20 miles away, is "not the kind of interaction we are looking for", according to Mitchell.

For the time being, there are no firm plans to save recurrent costs by the proposed move, although the Astronomy and Space Board is already committed to reducing its expenditure by £1.5 million a year in the interests of SERC's flexibility. Steps have already been taken to consult trades unions representing staff at RGO.

Among the complications of the move now foreseen are the need to continue the work of the Nautical Almanac Office to which RGO now makes only a nominal contribution. The work of the laser-ranging unit based at RGO will be continued if suitable arrangements can be reached with the Ministry of Defence and with the Department of Trade and Industry. SERC seems conscious of the need to preserve and make accessible the archive of RGO, but not necessarily at the site to which RGO as a whole will move.

By the time the eventual location of RGO is decided in June, more may be known of the long-term relationship between SERC and the National Space Centre established last year by the British government, but still largely a paper entity. The possibility that SERC might become one of the contributors to this organization, which would be used as a vehicle for carrying through space research projects now under the wing of the Astronomy and Space Research Board, is being considered, but negotiations have not yet been completed. □

## US Office of Naval Research

# More money means more trouble

Washington

THE US Office of Naval Research (ONR) celebrates its fortieth anniversary this year, but its biological research managers have their eyes to the future. The \$40 million spent this year by ONR's life sciences directorate supports some of the most long-term basic research in the federal budget. But as the federal budget for military research has increased in recent years in relation to the civilian budget, the role of ONR seems to be changing. It plans to support more training and education as well as research. Some academics have misgivings.

Almost all the life sciences research supported by ONR (about 15 per cent of the total) is carried out under contracts with universities. ONR uses the newest techniques of molecular biology and biotechnology to produce protein adhesives, deuterated lubricants and other surfactant molecules. Priority research topics include enzymes from organisms that inhabit extreme environments, the interplay of the central nervous system with immune function and the modelling of neural circuits with the aim of understanding "biological intelligence".

ONR selects among research proposals at least partly by independent review. All the bioscience research is unclassified. But there the similarity with a civilian research agency ends. In the words of Dr Steven Zornetzer, associate head of ONR's life sciences directorate, research supported by ONR "should have, or could have down-the-line" applications for the US Navy. That condition is one of the reasons behind a recent controversial ONR decision to close its Naval Biosciences Laboratory at Oakland, California. It has also caused dissent at the Massachusetts Institute of Technology (MIT), where biology faculty have voted once to refuse up to \$4 million per year of ONR support for a new biotechnology training programme.

The Naval Biosciences Laboratory, managed by the School of Public Health of the University of California (UC) at Berkeley, had a total budget of \$5.7 million in 1985 (mostly from ONR) and a staff of about 100. Research there focuses on gene expression in different systems and on "slow" viruses. In 1984, the School of Public Health and the laboratory together inaugurated a molecular parasitology research group, headed by acting laboratory director Dr Nina Agabian, which grew rapidly and now represents about half of the laboratory's staff. But, despite "extraordinarily high marks" at a May 1985 external review, Agabian says that the laboratory was told abruptly last September that the site must be vacated by Septem-

ber 1987. Feelings are still running high.

ONR cites two reasons for the decision. First, the converted Second World War barracks that house the laboratory are outdated, and modification would not be cost effective. And, second, molecular parasitology with potential medical applications should be the responsibility of the US Army rather than ONR in accordance with an inter-service agreement that the army should support infectious disease research. Agabian's group now expects to be rehoused in a new building as part of an inter-campus parasitology effort with UC San Francisco. The relationship with ONR seems over.

The navy clearly had reason other than mere lack of interest in the laboratory's dominant research area for its decision. The laboratory's contractual position is unusual (although not unique). Other non-competitive research contracts were modified at the same time.

Worries that basic research may be skewed towards military objectives underlie in part the vote by MIT's biology faculty last month not to apply to ONR for support for its planned biotechnology training programme. ONR announced last January that (together with the Defense Advanced Research Projects Agency) it proposed to spend an additional \$25 million in fiscal year 1986 on 5-year block research grants worth up to \$4 million. The increase represents ONR's share of the Pentagon's University Research Initiative, which comes on stream this year. One of the eligible grants, for marine bioengineering, would support graduate student research training in molecular biology of marine organisms, with special reference to bio-fouling and drag reduction.

MIT's plans for an interdisciplinary biotechnology training programme had been held up by lack of funds so that the new ONR grant seemed a godsend. But the biology faculty objected to applying (albeit at a poorly-attended meeting), although the other faculties that would be involved have raised no objection. The biology faculty is expected to reverse its decision in a second vote this week.

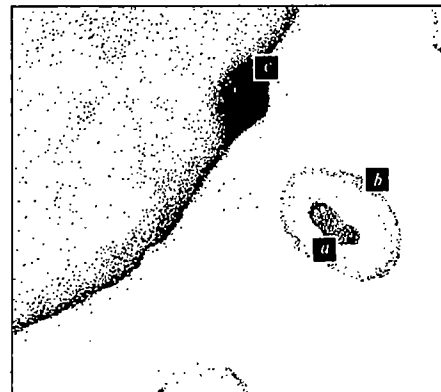
ONR already supports some researchers in the MIT biology faculty, but opponents of ONR support distinguish between individuals who accept specific ONR research grants and MIT as a whole accepting that a whole course should be supported ultimately by the Department of Defense.

Dr Maury Fox, chairman of the biology department, who does not oppose the idea that ONR might support the course, would also prefer educational programmes funded by non-military sources.

# No help on AIDS

THE illustration below is the only one in a full-page advertisement headed ARE YOU AT RISK FROM AIDS? which was placed by the Department of Health and Social Security in British newspapers last week. Its caption runs: "a, AIDS nucleoid containing the biological message to cause damage (sic). b, Lipid membrane (very fragile). Packages virus and allows movement between cells. c, T helper cell/white cell."

The text of the advertisement, which is admirably expressed in plain English, does not mention nucleoids, lipids, virus packaging, T helper cells or white cells. Asked



why such an enigmatic illustration and confusing legend should have been allowed to mar an otherwise excellent message, a spokesman for the department said it was included to relieve the monotony of the text. Asked what a nucleoid was, she came back with the definition "a granular or fibrillar substance in certain erythrocytes which resembles a nucleus". That is indeed one dictionary definition (for example *McGraw-Hill Nursing Dictionary*). But the appropriate definition is "A term used by electron microscopists to describe the electron-dense centrally placed region observed in certain viruses" (*A Dictionary of Virology*, Blackwell).

Fox believes, however, that that is a matter for national policy and "I'll have to live with it". Others are unconvinced. Frank Solomon, assistant professor of biology at MIT, opposes ONR block grants and believes the Pentagon would not hesitate to classify "biosludge" research that turned out to have important weapons applications. And he is opposed in principle to the military supporting and controlling a larger proportion of US basic research, selecting topics on other than exclusively scientific merit.

Others fear that the "increased collaboration with ONR" mentioned with the grant prospectus might increase opportunities for military direction of the work. Whatever the outcome of the MIT debate, similar questions may be asked on other campuses as defence research dollars spread further.

Tim Beardsley

## Medical Research Council

## NEWS

# Government blamed for decay

FORCED to lay bare its plans for the next five years, the British Medical Research Council (MRC) has identified several areas of research into which it intends to pump money but is much less categorical about where the money will come from.

MRC's first "Corporate Plan", published last week, has been produced in response to a request by ministers and the Advisory Board for the Research Councils for each council to explain how it intends to cope with the decline in the overall funds for research that are forecast for the next five years. In a grudging introduction to its plan, MRC asks how it can plan for five years when its budget is the result of an annual bid with an uncertain outcome, made worse by late decisions.

In general terms, the plan states that MRC cannot simply opt out of some areas of medical research. So it will have to raise the threshold for providing funds in all areas of research. At the same time, there is a need for concentration of resources within certain areas in order for the research to be internationally competitive.

The one such area of research that is clearly identified in the plan is neurobiology. This comes as no surprise, since MRC has repeatedly stressed that British neurobiology is in a poor state but has failed to do much about it. "There is a need for a large centre where the development, interactions and molecular biology of nerve cells and their supporting com-

ponents can be studied... in order to retain in this country a number of our most gifted workers", says the report. Additionally it identifies an urgent need to establish at least one major new centre in Alzheimer's disease and a large new facility of parasitology, particularly since spending on tropical medicine in Britain "can only be described as derisory".

Other priorities include a new MRC unit to study disorders of movement and balance, an expansion of support for protein engineering and a need for strong centres for the clinically led study of infectious diseases.

The problem is how to support the new initiatives. MRC uses its plan to say that while remaining alert to ways of increasing its income from commercial resources — which accounted for less than £2 million of the £123.5 million income last year — the generation of income will not become a guiding purpose of its research programmes. Nor does the council intend to become a fund-raising organization.

Even without the need to finance new initiatives, the plan identifies the need for extra spending. First, the salaries that can be offered are already uncompetitive in some key areas of research. Second, there is a pressing need to increase the number of research studentships and training fellowships to avoid the loss to research of many gifted graduates. And, third, there is the severe problem of outdated equip-

## British farm research

# Downbeat plan for agriculture

THE British Agricultural and Food Research Council (AFRC), which has seen the British government wash its hands of responsibility for agricultural research in the past five years, has now produced a corporate plan for the years ahead which is reciprocally dismissive of what it can expect from government. The chief message is that, within a budget that will have shrunk by some 26 per cent (if inflation works out at an average of 5 per cent a year) between 1983 and 1991, the council will somehow manage to increase its spending on university research grants to more than £8 million a year.

The council goes further than its predecessors to acknowledge why the British government has been beastly towards AFRC by noting that the success of European agricultural research, which is manifested by the large surpluses of commodities accumulated under the Common Agricultural Policy, are a proof that merely increasing production is no longer a sufficient objective for research. But the plan says that while consideration such as

the nutritional value of the public diet are now of greater importance than in the past, it remains the case that the production of high-value crops at low cost is an important objective of research.

The plan also marks out, as a new direction for its research, the better integration of agriculture with environmental considerations, an issue raised two years ago by a report of the House of Lords Select Committee on Science and Technology which was generally critical of farmers.

The corporate plan shows that most areas of AFRC research will decline in the years ahead, but that there will be a growth (to 14.2 per cent by value) of food research. It says that it hopes to raise funds from other than government sources to increase what it has available for research, but is plainly uncertain how to calculate what may be available given the government's intention to support a substantial part of the cost of British agricultural research by levies on those sections of the farming industry that can be made to pay for the service. □

ment in MRC research establishments.

To meet all these demands, MRC is to impose higher standards in judging whether to continue an existing research unit upon the departure of its director, and to encourage all directors not to replace staff who leave. It intends also to introduce compulsory retirement "on grounds of reduced efficiency" for its scientists and to be tougher in assessing the cost-effectiveness of research it supports.

Lacking any real solution to its financial problems, however, MRC uses its corporate plan repeatedly to attack government policy. Reduction of public expenditure is a legitimate aim, it implies, but "the cuts have been made too rapidly for any sensible accommodation... there has been little appreciation of the damage this is causing to the nation's research capability".

Peter Newmark

## West German environment

# Greens bite back in Hesse

## Hamburg

HERR Joschka Fischer has begun to make his mark as the first member of the environmentalist Green party to hold office as a regional government minister. At the beginning of the month, Fischer made public his first set of regulations, intended to improve water quality of the rivers Main and Rhine, which will bear most directly on the operations of Farbwerke Hoechst, the largest chemical manufacturer in West Germany.

Fischer owes his post as a minister in the Hesse government to the failure of the Social Democrats (SPD) to retain their majority in the Hesse parliament. The Hesse Greens were at first divided over the proposal that they should form a coalition with the SPD, but eventually a "red-green" alliance was formed.

Far from being a stranger to politics, Fischer won acclaim during his two years in the federal parliament (Bundestag) as an eloquent speaker. He was required to retire from the Bundestag when the Greens decided that their representatives would be rotated every two years.

In fact the pollution limits so far decreed are likely to cause Hoechst very little trouble. Apparently relieved that the regulations are not more worrying, the company says that it will need no new equipment to keep its daily discharge of mercury below 1.125 kg and cadmium below 0.6 kg (a fourfold reduction in each case). The daily discharge of all acid is to be reduced from 150 to 10 tonnes. However, Fischer does not conceal his intention, in collaboration with Hoechst, that pollution should be further reduced when the new regulations expire in 1987.

Jürgen Neffe

## Polish agriculture

# Plans for foundation impeded

POLAND'S controversial "agricultural foundation", sponsored by the Roman Catholic Church, which plans to raise money in the West to inject new technology into Polish agriculture, has run into further trouble. The original scheme would have benefited only private farmers, since the 25 per cent of land in the "socialized" sector has for many years received massive government investment. But Polish sources now report that the government is pressing for a proportion of the fund to go to socialized agriculture.

Since the idea of the foundation was first mooted four years ago, government negotiators have shown every sign of trying to block progress. Meetings with Church representatives have been postponed on every conceivable excuse, ranging from the "wars of the Crosses" (protests by secondary school children about the removal of crucifixes from their classrooms) to the murder of Father Jerzy Popieluszko.

Even after the enabling legislation for the foundation was passed in autumn 1984, the wrangling continued. Under the terms of the foundation, an initial \$28 mil-

lion so created would eventually be used for in-country investments such as artesian wells and for improving the social infrastructure in rural areas.) The Church wished the imports to be duty-free; the State pressed for the payment of the full rate of duty. Shortly before the parliamentary elections last autumn, the government seemed prepared to concede this point, with the unspoken *quid pro quo* that the Church would not encourage the calls for a boycott of the elections. When the bishops themselves stayed away from the elections, the attitude of the government hardened perceptibly.

By the beginning of this year, a new point of contention was raised. The gov-

ernment hinted that the \$200,000 pledge to it by Mr Lech Walesa (his 1982 Nobel peace prize winnings) would "politicize the fund irretrievably". A face-saving formula was worked out by which the organizing committee "relieved Mr Walesa of the moral obligations he undertook when he donated the prize to the foundation and Walesa himself decided to withdraw his winnings."

A Vatican Radio communique which announced the organizing committee's decision at the end of February was couched in terms suggesting that, once this matter is resolved, the foundation could implement the pilot projects. But the next demand that "socialized agriculture should have a share of the fund suggests that the Polish government is still set on prolonging the negotiations as long as possible.

Vera Ric

## US agriculture

# More food, but fewer farms

### Washington

THE new biotechnology should allow the United States to continue meeting domestic food requirements and to contribute significantly to world food demand over the next 20 years, according to a new report\* by the Office of Technology Assessment (OTA). But the same technologies could also exacerbate a trend towards fewer and larger farms, unless Congress takes action to prevent it.

OTA estimates that a 1.8 per cent annual increase in world food production is needed to meet demand by the year 2000, and 83 per cent of this increase has to be from increased production through new technology. OTA agrees with other studies that animal production is likely to be the first to benefit from genetic engineering and other new techniques; plant biotechnology will also benefit, while information technology should allow improved crop and herd management.

Under the most likely assumptions, including application of new technology, OTA estimates that food production could increase by 2 per cent per year. But if the utilization of new technology were significantly less than that OTA thinks most likely, the goal necessary to meet world demand would not be met.

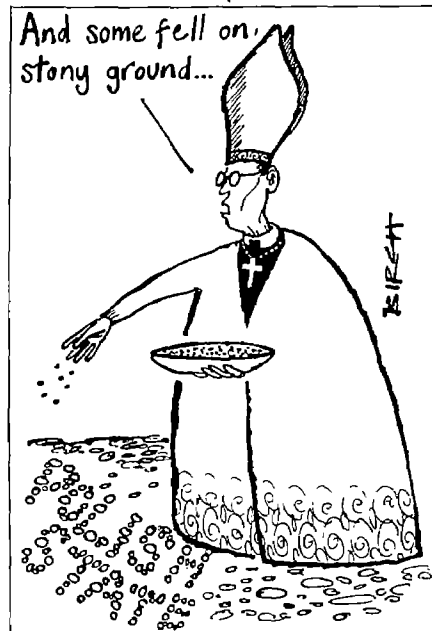
The very detailed report appears to have received a favourable reaction in the US Department of Agriculture. But its most controversial conclusions — because they have immediate consequences for domestic policy — are those relating to different types of farms. OTA argues that very large farms (annual sales of more than \$250,000) will be well able to apply the new technologies by themselves, whereas moderate and small farms will be less able to do so without targeted help from the government. As a result, the

relative competitive advantage enjoyed by large farms will increase as technological advances. OTA predicts that the number of farms will fall from 2.2 million in 1982 to 1.2 million by the year 2000. The number of small farms (less than \$100,000 annual sales) would fall from 60 to 50 per cent.

Some have questioned this prediction. Dr William Brown, chairman of the National Academy of Sciences' Board on Agriculture, believes that the rate of disappearance of small farms is exaggerated in the report.

The report is timely: Congress is in the process of considering the administration's proposed agriculture research budget for the coming fiscal year. Research and development in the Department of Agriculture would (in dollar terms) be hit harder under the proposed budget than almost any other department; however, the reductions are concentrated in the extension services and in programmes targeted to local problems which the administration has long held should be paid for by local and State governments. Competitive grants in the agricultural research service — which addresses long-term research — are protected. Congress has previously resisted attempts to cut local agricultural applied research and the House of Representatives' subcommittee dealing with appropriations for agriculture last week made clear its concern about the extent of proposed reductions: some programmes would take cuts of 60 per cent, others would disappear completely. But with the Gramm-Rudman deficit reduction act in place, bets are off over how Congress will act.

Tim Beardsley



lion was raised for pilot studies, and ten projects were worked out, including water development, agricultural field services, milk production and tractor repairs. But the government was reluctant to let work begin on any of these until the whole cost of the planned rescue operation (\$1,800 million over five years) had been raised.

Another cause of dispute was the foundation's plan to import agricultural machinery and supplies, purchased for hard currency, and to sell them to farmers at current market prices, but for zloty, partly on a deferred payment basis. (The zloty

\*Technology, public policy and the changing structure of American agriculture. Office of Technology Assessment, 1986.

## Soviet education

## Helping towards better careers

THE Soviet Union has introduced new rules for admission to higher education, designed to make university training more job-orientated. Instead of students being assessed simply on the sum of marks gained in their entrance examinations, an additional set of marks will also be awarded on the basis of interviews. The interview panel will assess each applicant's chances of success in his or her proposed field of study, and will provide guidance as to career choice. Commenting on the new procedures, the Moscow daily *Pravda* noted that they will give a clear advantage to young people who have begun to prepare themselves for their future profession while still attending secondary school.

The new admission rules are thus a continuation of the policy, introduced in the general education sector two years ago, of making study more closely related to future work.

In practical terms, the new rules will reduce the work-load on the entrants. Instead of having to offer four subjects, they will now only have to offer three: Russian language and literature (non-Russians may offer their native language if that is to be their language of tuition), a choice of mathematics, biology or social science (according to the student's chosen field) and the subject that the student eventually hopes to pursue.

Furthermore, it will be easier for would-be entrants to make applications to more than one university or institute. Until now, except for a handful of elite Moscow institutions, which held their entrance examinations in July, all examinations took place during August. As the Soviet Union has no national clearing-house system, this meant, effectively, that students keen to secure a place would aim at an institution rumoured to be easy on admissions. (This was particularly true of young men wanting to defer military service until after graduation). As a result many of the more cautious applicants set their sights rather lower than was necessary.

Now, according to *Pravda*, all higher education establishments in Moscow city, Moscow *oblast* and Leningrad will, "as an experiment", hold their entrance examinations in July. This move, *Pravda* pointed out sententiously, "will allow those who did not pass the entrance examinations to one of the Central higher educational institutions to apply their efforts to gain entrance to a higher educational institution in some other town".

Vera Rich

## NEWS

## Environmental pollution

## US suit charges cancer causation

## Washington

In what may become a landmark personal injury case, the families of seven childhood cancer victims from Woburn, Massachusetts, are suing two large US corporations said to be responsible for the illnesses by polluting the local drinking water. Some 40 expert witnesses have been lined up by both sides to argue whether an excess of acute lymphocytic leukaemia and other conditions in east Woburn could be due to halogenated hydrocarbons that were found in two polluted wells in 1979.

The case is one of the first in which it has been claimed that specific chemicals in drinking water caused specific illnesses. The wells, whose water mainly supplied east Woburn, tapped a different aquifer from Woburn's other wells. They were first used in 1967 and were closed in 1979 when trichloroethylene and tetrachloroethylene were found in the water at 200 parts per billion ( $10^9$ ) and 20 parts per billion respectively; other pollutants included (1,1,1)-trichloroethane, (1,2)-trans dichloroethylene and chloroform. The plaintiffs claim that the chemicals came from dumping or accidental spills at nearby plants owned by W.P. Grace and Company and Beatrice Foods. A third company, Unifirst, a dry-cleaning company, has already settled for \$1 million.

A local clergyman apparently first drew attention to a suspected leukaemia cluster in east Woburn, and the town's high incidence compared to national rates was subsequently confirmed in a study by the Massachusetts department of health. Nineteen cases were found where only six would have been expected; and renal cancer was also significantly elevated. The department concluded, however, that the "hypothesis suggesting that the increase in leukaemia incidence was associated with environmental hazards in Woburn . . . is neither supported nor refuted by the study findings".

But a more recent study by S.W. Lagakos, B.J. Wessen and M. Zelen of Harvard School of Public Health and Dana-Farber Cancer Institute does find a positive statistical association between access to water from the polluted wells and childhood leukaemia, as well as perinatal deaths and some congenital abnormalities. This study, in press with the *Journal of the American Statistical Association*, does not compare incidences in Woburn with those elsewhere, but establishes that within Woburn the diseases are found predominantly among those who drank more of the polluted water.

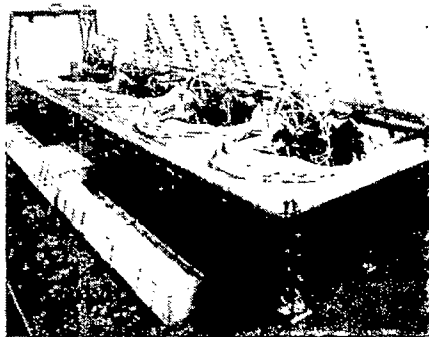
One of the pollutants, trichloroethane, is said recently to have been shown to cause leukaemia in rats. But a major

weakness in the plaintiffs' case is that nothing is known about the nature and degree of pollution of the wells at any time other than 1979, when they were immediately closed. The known carcinogens that were then in the water supply were present in far lower concentrations than have been shown to cause cancers in laboratory animals and in human occupational health studies. But it is argued that the fetus may be more susceptible to carcinogens than the adult, and that plaintiffs are basing much of their case on recent immunological tests indicating abnormalities in the blood of the plaintiffs' families.

The trial, which is in its third week, is expected to last for several months. First it will be decided whether the defendants contributed to groundwater contamination; medical questions will be examined only if the answer to the first question is yes. Beatrice Foods is refusing to comment on detailed aspects of the litigation, although it is pointed out that the accusation is that the company allowed pollution of ground it owns adjacent to its plant. W.P. Grace says that its plant, which manufactures stainless steel food processing equipment, may have leaked small quantities of cleaning agents and degreasers onto its own property, but that investigations (including drilling 50 test wells) had shown this would not have found its way into the wells.

Tim Beardsley

## Europe's optical telescope for 1990



STILL just a model, this is the 16-metre optical telescope, the "Very Large Telescope", planned for the European Southern Observatory (ESO) in Chile. ESO technical committees are now meeting to establish exact specifications for the new instrument with the aim of presenting plans for a DM 300 million project to ESO member countries in time for work to start in 1987. The VLT is to be sited at an altitude of 2,400m, and the human figures in the above photograph put its size into perspective.

## CORRESPONDENCE

## Sakharov's achievements

SIR—Ernest B. Glinér's letter "Another reason for saving Sakharov" (*Nature* 318, 513; 1985) notes only his work on gravitation. His major contributions in particle physics, fusion research and cosmology provide additional evidence that Sakharov's scientific contributions will be remembered, like those of Galileo, long after the names of those who persecuted him are forgotten. Perhaps the new Soviet leaders will note that their grandchildren may study the work of this great Russian physicist and wonder about the role of their grandfathers in his persecution.

In 1950 Sakharov proposed a solution to fusion's major problem: how to contain the reaction at its enormously high temperatures where no known materials can survive. Sakharov's "magnetic bottle", called the "tokomak" (ref. 1, p.49), which uses magnetic forces to contain the hot fusion fire, is currently the front-line approach to fusion reactors and may go down in history as man's answer to the energy crisis.

Sakharov's two remarkable 1966 papers on particle physics were far ahead of their time. Sakharov and Ya. B. Zeldovich (ref. 1, p.271; ref. 2) obtained relations between masses of different known particles in surprising agreement with experiment by assuming the new quark theory of matter which built all these particles from the same three basic building blocks arranged in different combinations, and held them together by forces which, although unknown, were always the same in different particles. Sakharov's work was ignored because the physics establishment did not take quarks seriously at that time.

Even more remarkable was Sakharov's resolution in 1966 of the apparent contradiction between the "big bang" theory of the origin of the Universe and the failure of astrophysical observations to reveal any trace of antimatter in the Universe. In his theory, the antimatter created in equal amounts with matter in the big bang decayed more rapidly than matter, leaving the observed excess matter. Sakharov demonstrated (ref. 1, pp.147, 151) three necessary conditions for this mechanism: (1) the recently discovered CP violation asymmetry between the interactions of particles and antiparticles; (2) a departure from thermal equilibrium; (3) violation of the law of baryon number conservation. This required the proton to be unstable and to decay into electrons and mesons, but so slowly that proton decay would not have been detected in any experiments.

His theory was not accepted because of a number of assumptions ridiculed as crazy at the time: (1) the existence of new very heavy boson particles; (2) the existence of quarks and of new interactions between quarks, electrons and these new

heavy bosons; (3) violation of the sacred principle of baryon conservation.

Today Sakharov's theory is the accepted view on the antimatter problem, his crazy assumptions are now a central part of the standard theories, and his three conditions are accepted as necessary for any cosmological model. Quarks, new heavy bosons which allow protons to change into electrons, violation of the law of baryon conservation and predictions that the proton must decay are all essential ingredients of the new "grand unification" theories. Many large expensive experiments are searching for Sakharov's predicted proton decay.

Even in his isolation in Gorki he has managed to continue the development of his 1966 ideas into new work on the quark theory of matter<sup>3</sup> and the cosmology of the early Universe<sup>4</sup>. His continual hopes for freedom in the Soviet Union and an end to the nuclear arms race seem like wild dreams. But we can all hope that once again Andrei Sakharov is right and only 10 years ahead of his time, and that the new Soviet leaders will allow him to return to Moscow with free access to scientific libraries, institutes and personal contacts so that he can pursue his work freely for the benefit of all mankind.

HARRY J. LIPKIN

*High Energy Physics Division,  
Argonne National Laboratory,  
9700 South Cass Avenue,  
Argonne, Illinois 60439, USA*

1. Sakharov, A.D. *Collected Scientific Works* (eds Ter Haar, D., Chudnovsky, D.V. & Chudnovsky, G.V.) (Dekker, New York, 1982).
2. Lipkin, H.J. *Ann. N.Y. Acad. Sci.* 452, 79 (1985).
3. Sakharov A.D. *Zh. eksp. teor. fiz.* 78, 2112 (1980), 79, 350 (1980); *Soviet Phys. JETP* 51, 1059 (1980), 52, 175 (1980).
4. Sakharov, A.D. *Zh. eksp. teor. fiz.* 79, 689 (1980); *Soviet Phys. JETP* 52, 349 (1980).

## Open house

SIR—In your article "What price freedom?" (*Nature* 319, 608; 1986), you say that "IUPPS is affiliated to a UNESCO umbrella organization which advocates an academic boycott of South Africa". This point needs to be clarified. The International Union of Prehistoric and Protohistoric Sciences (IUPPS) is affiliated to the International Council for Philosophy and Humanistic Studies (CIPSH). CIPSH has considered itself bound by UNESCO policy and will not give funds either for activities taking place in South Africa or to persons falling under the jurisdiction of South Africa.

CIPSH, however, believes that international congresses should be open to all bona fide scholars, irrespective of domicile, race, religion or belief. This policy was set out in an exchange of correspondence between the secretary-general of CIPSH and the secretary-general of

IUPPS in August 1985, specifically in response to Professor Ucko's enquiry to the latter as to the official attitude of IUPPS and CIPSH towards the participation of persons working in South Africa in the activities of IUPPS. Moreover, the CIPSH bureau, at its meeting in Istanbul about the beginning of December 1985, reiterated this CIPSH policy and indicated that the organizers of the Southampton congress should take every precaution to ensure the free participation of all in their activities.

Failing such arrangements, the bureau resolved, the organizers of the congress would be entitled to cancel the holding of the meeting, since it would not be able to ensure completely free participation and academic freedom.

In this attitude, then, it does not seem that the policy of CIPSH "advocates an academic boycott". On the contrary, its policy towards international congresses seems to square with that of the International Council of Scientific Unions (ICSU): both parties favour the free circulation of scientists and an "open house" participation in international congresses.

PHILLIP V. TOBIAS

*Department of Anatomy,  
University of the Witwatersrand  
Medical School,  
York Road, Parktown,  
Johannesburg 2193, South Africa*

## Too many fourth states of matter?

SIR—In the short period of time between May and October last year, I see that the "fourth state of matter" was referred to in *Nature* in two book reviews, one on plasma physics<sup>1</sup> and the other on polymers<sup>2</sup>. The same phrase has been used in connection with the discovery of icosahedral symmetry.

Physicists should realize that if there is such a thing as the fourth state of matter, there can be only one of it. Moreover, physicists should be aware that in 1940 the attribution was used to describe the superfluidity of helium-3 (refs 5, 6). But the phrase has also been used to describe other kinds of superfluidity such as in the superconducting state of electrons<sup>7</sup>.

Is there a danger that this practice will get out of hand?

J.M. GOLDSCHVARTZ  
*Clavecimbellaan 273,  
2287 VK Rijswijk zh,  
The Netherlands*

1. Lashmore-Davis, C.N. *Nature* 315, 162 (1985).
2. Eisenberg, H. *Nature* 317, 773 (1985).
3. Allen, J.F. & Misener, A.D. *Proc. R. Soc. A172*, 467 (1939).
4. Kapitza, P.L. *J. Phys. Moscow* 5, 59 (1941).
5. Osheroff, D.D., Richardson, R.C. & Lee, D.M. *Phys. Rev. Lett.* 28, 885 (1972).
6. Osheroff, D.D., Gully, W.J., Richardson, R.C. & Lee, D.M. *Phys. Rev. Lett.* 29, 920 (1972).
7. London, F. *Superfluids*, Vol.2 (Dover, New York, 1960).

# New ways with crystal growth

*Computer simulations of the aggregation process are fashionable because the problems are complicated. But mathematics still has a place.*

THAT crystal growth is a complicated process requires no formal proof: how, otherwise, runs the conventional argument, would snowflakes have such a shape? One consequence of considerations such as these is the wealth of numerical simulations which there have been, in the past few years, of how elementary particulates may be added to the surface of a growing aggregate by diffusion from the exterior. This fashion is a reaction to earlier disappointments, and particularly to the recognition that earlier macroscopic models of the growth of aggregates, which distinguished between the various positions on an extending surface only by their macroscopic properties and especially their curvature, have given only poor accounts of what really happens. So it may be a salutary lesson for all concerned that there should now have appeared an analytical calculation of the changing shape of a surface growing by aggregation; people who have been learning how to program increasingly complicated computer machinery may yet find themselves mugging up on differential equations again.

To be fair, the question that has arisen is only part of the whole complicated problem, and may be put like this. In the earliest stages of the growth of a crystal or other aggregate, chance adhesion will be the rule, so that small particles will tend to be rough particles. Given time to reach equilibrium, of course, the roughnesses will become smooth as particles in exceptional positions find less energetically exposed sites at which to settle down, but there will also be circumstances in which a surface growing at a modest rate will become smoother in the course of time as added particles find their way preferentially to the gaps left in the growing surface. To account for the irregularity of snowflakes, either microscopically (by numerical simulation) or macroscopically (by allowing for the extra energy of elements added at places where the curvature is great using the language of surface tension), boils down to supposing that the circumstances are dynamic, not static. The rapidly growing tip of a snowflake crystal is, because of its geometry, exposed to a greater volume of the environment from which further elements may be accreted than would be a re-entrant part of the snowflake surface, while the speed with which newly accreted elements may readjust their positions is so much less than

that with which new elements are added  
that aberrations are, so to speak, frozen.

The new development is surprisingly straightforward, and the product of the cosmopolitan collaboration of Mehran Kardar of Harvard University, Giorgio Parisi from the University of Rome and Yi-Cheng Zhang from the Brookhaven National Laboratory (*Phys. Rev. Lett.* **56**, 889; 1986). The question they set out to answer is that of how a surface accreting extra elements will grow in the course of time, allowing that the circumstances are midway between those which determine the behaviour of a growing snowflake, where there is no opportunity for newly added particles to readjust their positions, and those that dominate the macroscopic growth of solids which are predisposed towards the emergence of globules of one form or another.

The simplest starting point is the assumption that the normal to a surface will determine the direction in which it will grow locally. There follows a geometrical construction of what happens at the surface, beginning with the assumption that it is possible to measure the distance of the surface as a function of time from some fixed plane; the distance might, for example, be the height of the surface of a growing crystal from the bottom of a vessel in which it is allowed to settle. At any point, the rate of change of the height with time will therefore be determined by the rate of growth normal to the surface and by the square of the gradient of the surface at that point. From this it follows naturally and very simply that the rate of change with time of height from the reference plane is proportional, first, to the curvature of the surface at that point and, second, to the square of the gradient of the surface at that same point. The first term is that which represents the effect of surface tension. The second, which makes the differential equation non-linear, allows for lateral growth. For completeness, the specification of the problem requires that there should be an element of noisiness, represented by a third term, in the gaussian function in time and space, whose only important property is that its average should be zero.

Mathematicians will quickly observe that this non-linear equation describing the evolution of an accreting surface can be converted into a linear form that of a diffusion process. Indeed, in this form the equations are similar to those which des-

cribe the behaviour of branched polymer molecules in which the surrounding environment discriminates against over-extended forms.

The interest of this formulation of the problem of the growth of accreting surfaces is that, in principle, it allows of a global view of what may be happening. If the noisiness of the problem is left out of account, the equations suggest that a one-dimensional growing surface will consist of a sequence of parabolic segments which, as time goes on, will grow at each others' expense, the larger segments swallowing the smaller. If the surface is two-dimensional, there will be patches on the surface which form a comprehensive network covering the whole which again, with the passage of time, allow the larger to swallow the smaller. Specifically, for one-dimensional surfaces, the size of the parabolic segments increases with the  $2/3$  power of the time, which is what the numerical simulations suggest.

The noisiness of the problem cannot, in reality, be ignored, but cannot as easily be described in words. But a degree of randomness turns out to be a physical benefit in suggesting analogies with what may happen in other physical circumstances, those of quantum mechanics for example. Indeed, the cleverness of this treatment of the problem of growing surfaces lies in the way it can be transformed from a problem in the solution of differential equations to one much more familiar in quantum electrodynamics, that of describing the time-evolution of a system by the effect of operators on some starting function.

The result, in the surface problem, is a set of simple rules that may describe the simple scaling properties of the problem. That such must emerge follows from the simple observation that, in the case of a one-dimensional surface, a structure which is made up from a sequence of parabolic segments transforms itself in the course of time to another sequence of parabolic segments whose average size has grown by a factor which is some fractional power of the time elapsed. The authors are quick to point out that their model agrees with several of the numerical simulations which have been carried out in circumstances when comparisons are possible. But the importance of this novel treatment is as a physical insight into the aggregation problem when simulations can provide only answers, not understanding.

## Model crystals

# Penny plain, tuppence coloured

from Robert W. Cahn

A FLOURISHING community of theoreticians seeks to clarify processes in crystals—phase transformations, critical phenomena, radiation damage, melting and vitrification — by simulating them in powerful computers. The latest attempts to model crystals realistically are reported in two papers elsewhere in this issue<sup>1,2</sup>.

Physical modelling of crystals began in the late 1940s with the two-dimensional soap-bubble raft of Bragg, Nye and Lomer. Given the right bubble radius, such rafts reproduced well the interatomic force law typical for metals, and were used to simulate the motion of dislocations under shear stress. They were also used to model metallic glasses, but for this purpose, two populations of bubbles of different radii were essential to inhibit 'crystallization'. Such rafts have been well used, notably by Argon<sup>3</sup>, to interpret mechanical properties of metallic glasses.

In the 1960s, Bernal produced his influential liquid model with monosized steel balls kneaded in a football bladder, which was later extended to imitate metallic glass structures. In contrast to the bubble raft, Bernal's model suffered from the fact that the balls were hard and could not imitate the 'soft' interatomic force laws appropriate for alloys; this inadequacy was overcome, both literally and metaphorically, by the introduction of software to allow relaxation of a Bernal model via computer simulation.

More recently, a new family of 'macro-particulate' crystals has appeared in the form of colloidal crystals<sup>4</sup>, regular assemblies of equal submicron-sized spheres, typically of a polymer or of silica. These crystals were not intended as models: their study grew from observations of natural macroparticulate crystals — the crystalline viruses and opal<sup>5</sup> (which consists of regular arrays of monosized amorphous silica spheres). The first artificial macroparticulate crystals to be made, gem-quality opals, were made by gravity-induced sedimentation of colloidal silica suspensions by Pierre Gilson at his factory in northern France<sup>6</sup> and in commercial production since 1974. How these opals are stabilized after sedimentation (sintering or low-temperature adhesion) is a commercial secret.

The study of silica (and polymeric) macroparticulate crystals has accelerated rapidly since then (although it is doubtful whether many of the physicists concerned know of Gilson's early triumph). The use of macroparticulate crystal assemblies of ceramic microspheres as 'green' precursors for sintering has now been proposed

and a promising start has been made with silica<sup>6</sup> (as discussed in these columns<sup>7</sup>).

One of the papers in this issue<sup>1</sup> follows the colloidal approach to crystal simulation: Pusey and van Megen used monosized polymethylmethacrylate spheres, 0.3 μm in diameter and stabilized in suspension by a thin coating of another polymer. The organic suspensions were of high volume fractions, ranging from 0.39 to 0.53. After mechanical homogenization, each suspension was allowed to settle. In the volume fraction range 0.44–0.50, polycrystalline structures have bright opalescence; suspensions below 0.41 do not crystallize at all; whereas in the range 0.41–0.44, a stable liquid-plus-crystal two-phase state forms. But the really novel feature occurs in volume fractions above 0.50, where the viscous suspension remains in a 'glassy' form indefinitely: in effect, this is a kinetically metastable random dispersion which is too dense, and therefore too immobile, to order. Unlike two-dimensional bubble rafts, therefore, in three dimensions it is possible to create a glass from a population of monosized spheres. (Whether this is possible depends on the mobility of the units; be they macroparticles or atoms, pure metals cannot be prevented from crystallizing even at cooling rates in excess of  $10^{12}$  K s<sup>-1</sup>.) Pusey and van Megen's method could be used to make a form of artificial opal if a way to stabilize the crystals against accidental randomization can be found.

Pusey and van Megen's suspensions differ radically from another kind which also show unexpected properties: Clark and Ackerson<sup>10,11</sup> demonstrated that very dilute (0.1 per cent) suspensions of highly charged polymer spheres can 'crystallize' into body-centred cubic crystals while remaining suspended, but randomize (melt) after vigorous shear deformation — an observation which could shed light on mechanical instability models of melting for ordinary atomic crystals.

The other paper in this issue<sup>2</sup>, by Georges *et al.*<sup>2</sup>, exploits bubble rafts to simulate, in two dimensions, a microhardness indentation test. A conical indenter is simulated by a suitably shaped (poly)crystalline raft; the test object is a large monosized polycrystalline raft covered by an amorphous 'coating' consisting of a mix of two bubble sizes. The authors do not explain why they chose to test a glass-coated crystalline-simulated sample, but in the light of some recent tests on real glassy wear-resistant coatings, it was a happy choice. The simulated coating proves extremely resistant to penetration, but its

behaviour is intimately affected by its crystalline substrate, which undergoes a largely elastic deformation. On unloading, this elastic distortion recovers and the form of the indentation recovers with it, so much so that the end-result is a small mound instead of an indentation.

This model system with its properties is of considerable interest in relation to recent work on the use of an ultramicrohardness tester, the nanoindenter, invented and named by W.C. Oliver<sup>12,13</sup>. This instrument is extremely sensitive, using measurements of the vertical displacement of the indenter (as small as 20 nm) to evaluate the residual indentation. (Direct measurement of such minute features would require scanning electron microscopy.) The instrument allows the increase in effective hardness for indents less than 100 nm deep to be confirmed and interpreted<sup>12</sup>. It was also found that considerable elastic recovery of the indentation takes place, and that this is essentially caused by a recovery of the 'hinterland' of the indentation, just as in the bubble simulation. But nanoindentations in real crystals do not invert and finish up as mounds.

Oliver and his collaborators have also studied the nanohardness of coated (ion-implanted) metals<sup>13</sup>. Of relevance to the present discussion is the behaviour of steel ion-implanted with both titanium (Ti) and carbon (C). If the concentrations of both are sufficient, the coating is very hard and wear-resistant. Such Ti/C implants are known to be amorphous, and the excellent mechanical properties of the layers are directly correlated with their vitreous nature. Georges *et al.*<sup>2</sup> agree with these findings in the sense that their amorphous simulated coating proved impenetrable, being always pushed ahead of the moving indenter, but disagree in the sense that the yield stress they observed for the coating was lower than that for the crystalline substrate. Amorphous Ti/C coatings are stronger, harder and more wear-resistant than the underlying steel. □

1. Pusey, P.N. & van Megen, W. *Nature* **320**, 340 (1986).
2. Georges, J.M., Meille, G., Loubet, J.L. & Tolen, A.M. *Nature* **320**, 342 (1986).
3. Simpson, A.W. & Hodkinson, P. *Nature* **337**, 320 (1972).
4. Argon, A.S. & Kuo, H.Y. *Mater. Sci. Engng.* **39**, 101 (1979).
5. Pieranski, P. *Contemp. Phys.* **24**, 25 (1983).
6. Darragh, P.J., Gaskin, A.J. & Sanders, J.V. *Scient. Am.* **234** (4), 84 (1976).
7. Anderson, B.W. *Gem Testing* 9th edn (Butterworth, London, 1980).
8. Sacks, M.D. & Tseng, T.-Y. *J. Am. Ceram. Soc.* **67**, 526 (1984).
9. Calvert, P.D. *Nature News and Views* **317**, 201 (1985).
10. Clark, N.A., Hurd, A.J. & Ackerson, B.J. *Nature* **281**, 57 (1979).
11. Ackerson, B.J. & Clark, N.A. *Phys. Rev. Lett.* **46**, 123 (1981).
12. Pethica, J.B., Hutchings, R. & Oliver, W.C. *Phil. Mag.* **A48**, 593 (1983).
13. Pethica, J.B., Hutchings, R. & Oliver, W.C. *Nucl. Instrum. Meth.* **209/210**, 995 (1983).

Robert W. Cahn is currently Fairchild Distinguished Scholar in the Keck Engineering Laboratories, California Institute of Technology, Pasadena, California 91125, USA.

## Somatic mutation

# Do plants evolve differently?

from William J. Sutherland and Andrew R. Watkinson

It has recently been stressed that single plants may consist of a mosaic of genetically different parts<sup>1,2</sup>. If this is true, then the usual explanations for the operation of natural selection on animals may be insufficient to account for the process of genetic change in many plant populations. The relative importance of somatic and gametic mutations in plants cannot be assessed until the necessary measurements are made. But it is clear that somatic mutation could be important in many plant species.

Modern genetics is based on Weissmann's<sup>3</sup> distinction between the cell line and the germ line. Mutations within cells may be expressed but are not passed on to further generations; mutations in the germ line are both expressed and transmitted to descendants. In Weissmann's theory, changes in the germ line are the sole means of evolutionary change. But Weissmann was a zoologist and applied his fundamental principle only to animals. In plants there is no distinction between the germ line and the soma. Growth occurs through the iteration of structural units (modular growth) by one or (usually) many growing points; as a consequence a mutation in a meristem may be expressed in subsequent growth and will then be contained in the pollen or ova. Thus, in plants (and some colonial animals) there is the possibility of genetic variation within an individual and, as a consequence, variation in fitness between modules.

There have been few attempts to measure genetic variability within plants, although there are indications that it may be a widespread phenomenon. Chimaera are common in two species of fern, *Mattuccia struthiopteris* and *Onoclea sensibilis*<sup>4</sup>; 10 out of 56 of the former and 16 out of 37 of the latter possess mutants. The rates of these mutations are high, with 0.0177 and 0.0341 mutations, respectively, per apical cell per generation. In the herbaceous perennial spring beauty (*Claytonia virginica*) 68 per cent of the population show differences in chromosome number within a plant<sup>5</sup>; of 8,000 plant varieties cultivated in Europe in 1899, 5,000 originated as somatic mutations<sup>6</sup>.

Once genetic differences exist between parts of the same plant there is the opportunity for natural selection to modify the gene frequencies within an individual by the process of differential growth. If the parts possessing the mutation grow faster the mutation may spread; if the mutation prevents successful growth then it will be eliminated — anyone possessing an

ornamental plant with variegated leaves knows that it is essential to remove branches containing normal unvariegated leaves which grow more quickly and would eventually dominate the plant.

The importance of differential growth is also shown in the case of the white clover (*Trifolium repens*) in north Wales. There is considerable genetic diversity within populations<sup>7</sup> and the growth rate of different genotypes depends on the surrounding vegetation<sup>8</sup>. Those genotypes that grow with the grass *Holcus lanatus* produce more ramets when cultivated among *H. lanatus* than when placed among other grasses; other genotypes respond similarly to other species. Thus, the abundance and distribution of different genotypes is determined by differential growth.

In principle it is clear that evolutionary change in a population may originate from somatic mutations. It is essential that somatic mutations should be inherited both sexually and asexually and also that there is differential growth of different genotypes within the same plant. But the importance of somatic mutations is in dispute. Some argue<sup>9</sup> that the role of somatic mutations is trivial, although the model on which this assertion is based does not take differential growth into account. A later model<sup>10</sup> supports the notion that somatic mutations will produce enough variability to prevent pathogens and herbivores from adapting to all branches on individual host

trees. This model also shows that somatic mutation may be an important source of variation within trees and tree populations. It seems likely that this mechanism is unimportant for species with relatively few meristems (such as peas and maize) but more important for long-lived and extensive species. Thus, individual clones of the aspen (*Populus tremuloides*) can cover 200 acres, be comprised of 47,000 trees and may date back to the Pleistocene<sup>11</sup> — it would be incredible if each of these clones was genetically homogeneous.

Although trees provide obvious examples of large, long-lived species, somatic mutation and differential growth could also be important in stoloniferous and rhizomatous plants. Most trees are restricted by a unified architecture that limits the potential for differential growth of branches, whereas in stoloniferous species (such as clover and creeping buttercup) the individual plant fragments as it grows, thus allowing a favourable mutant to spread rapidly. □

1. Whitham, T.A., Williams, A.G. & Robinson, A.M. in *A New Ecology* (eds Price, P.W., Slobodchikoff, C.N. & Gaud, W.S.) 15 (Wiley, New York, 1985).
2. Gill, D.E. & Halverson, T.G. in *Evolutionary Ecology* (ed. Shorrocks, B.) 105 (Blackwell, Oxford, 1984).
3. Weissmann, A. *On Heredity* (Clarendon, Oxford 1883)
4. Klekowski, E.J. *J. Evolution* 38, 417 (1984)
5. Lewis, W.H., Oliver, R.L. & Luijken, T.K. *Science* 172, 564 (1971).
6. Cramer, P.J.S. *Nature* 3 Vers Vol. 6 (Wetenschappelijke Haarlem, The Netherlands, 1907).
7. Cahn, M.A. & Harper, J.L. *Heredity* 37, 309. (1976).
8. Turkington, R. & Harper, J.L. *J. Ecol.* 67, 245 (1979).
9. Slatkin, M. in *Evolution in Honour of John Maynard Smith* (eds Greenwood, P.J., Harvey, P.H. & Slatkin, M.) 19 (Cambridge University Press, 1984).
10. Antolin, M.F. & Stroebel, C. *Am. Nat.* 126, 52 (1985).
11. Kemperman, J.A. & Barnes, B.V. *Can. J. Bot.* 54, 2603 (1976).

William J. Sutherland and Andrew R. Watkinson are at the School of Biological Sciences, University of East Anglia, Norwich NR4 7TJ, UK.

## Palaeoclimatology

# Bears versus beetles

from Peter D. Moore

THE INTERNATIONAL Geological Correlation Programme recently stated the view that there were two separate warm periods during the last (Ipswichian) interglacial period, and that they can be defined on the basis of their mammalian fauna<sup>1</sup>. The final (Devensian) glaciation is generally believed to have reached its maximum geographical extent 18,000 years ago (18,000 bp) and by 14,000 years ago Britain was essentially deglaciated. But there are many problems in elucidating the climatic sequence of the previous 200,000 years.

Fossil mammalian bones are an important source of evidence in Quaternary palaeoecology, but their use in climatic reconstruction raises some problems. Such material can be identified with con-

siderable accuracy but compared with other types of fossil evidence, such as pollen, diatoms and beetles, mammalian bones are rare. This means that sufficiently large populations of bones to allow statistical analysis at any site are infrequent, whereas smaller and more abundant fossils, such as pollen grains, lend themselves to this approach. Climatic conclusions from mammalian fossils are also complicated by the relatively large range of tolerance of mammals compared with cold-blooded invertebrates. Thus, one can argue that beetles are better climatic indicators than bears. But some aspects of climatic reconstruction in the late Quaternary are now under debate as a result of finds of mammal bones in Britain.

Until recently it was thought that the

Ipswichian was the only interglacial during the 200,000 years preceding the Devensian, but there are increasing difficulties in reconciling the evidence from various sites presumed to be of this age<sup>1</sup>. Fossil assemblages in Britain at sites such as Bobbitshole, Suffolk<sup>2</sup> and Trafalgar Square, London<sup>3</sup> contained a typically warm climate fauna, including hippopotamus, and lacked any steppic species, such as horse.

At other British sites, such as Marsworth, Buckingham and Stanton Harcourt, Oxford, deposits with a similar pollen spectrum and therefore assumed to be Ipswichian yield fossils such as mammoth and horse, indicative of colder conditions. There is evidence that these mammoth-bearing strata are separated from those containing warm, hippopotamus fauna by a very cold intervening phase. The mammoth/horse episode is the earlier of the two and can be correlated with oxygen isotope stage 7. The hippopotamus event has been dated by uranium and thorium isotopes to between 135,000 and 114,000 BP at Victoria cave in Yorkshire<sup>5</sup>, which corresponds to oxygen isotope substage 5e.

Precisely what happened between the time when hippopotami were wallowing in the British wetlands and the intense glaciation of 18,000 years ago is still uncertain. There is evidence of a warm climate about 60,000 years ago at Chelford, Cheshire, when pine, birch and spruce were the major dominants of the pollen flora<sup>6</sup>. But the radiocarbon dating of this site is not entirely satisfactory as it extends beyond the timescale in which the method is reliable.

Pollen data showing the increasing cold nature of the flora following the Ipswichian Interglacial are available from a site at Wing, Leicester<sup>7</sup>, and a marine pollen sequence has been produced from Fjøsanger Fjord in western Norway<sup>8</sup>. The latter site shows an abrupt decline in forest vegetation and a spread of grassland as the last glacial episode began.

Further evidence concerning the early part of the last glacial has now been obtained from another cave deposit in Yorkshire, only 23 km away from the Victoria cave site. The Stump Cross cave<sup>9</sup> has been found to contain bone remains of wolf, reindeer and wolverine, which constitute a distinctly tundra or boreal mammal assemblage. In many respects the assemblage resembles that found in the mammoth-bone houses of the Ukraine<sup>10</sup>, dating from the end of the last glaciation, although no mammoth bones are found at Stump Cross. The Stump Cross bones are associated with calcite deposits that have been subjected to uranium-series radiometric dating and provide dates ranging between 84,000 and 81,000 BP which, if taken at their face value, places the bone collection in the younger part of

oxygen isotope stage 5, between the hippopotamus fauna of Victoria cave and the spruce forest of the Chelford Interstadial.

There must have been a considerable fall in temperature between 120,000 and 85,000 BP to account for this change of fauna, but closer interpretation in climatic terms is not simple. The three major animal species were probably inter-related as predators and prey, the wolf and the wolverine preying on reindeer. But damage to the bones by splintering and chewing suggest that the bone hordes were accumulated by wolverines that also preyed on wolves and even on one another. The physical and biological setting of this drama is difficult to reconstruct precisely because wolverines and the other species represented are found not only in open tundra areas, but also in the coniferous forest (taiga) zone. So, on the basis of evidence from mammalian bones, it is still not possible to determine whether the earliest phase of the Devensian was colder than the conditions in the Chelford Interstadial. It does not provide an answer to the origin of the till underlying the Chelford deposits, which may belong to an earlier glaciation<sup>11</sup>. Climatic deterioration since the day of the hippopotamus had clearly

been substantial, but was it sufficient to result in a pre-Chelford glaciation in the British Devensian?

The story has now become even more complicated by a report earlier this month from Bacon Hole, Wales<sup>12</sup> of sediments dated at 81,000 BP that contain a clearly warmth-demanding fauna including straight-tusked elephant (*Palaeoloxodon*), rhino (*Dicerorhinus*) and hyaena (*Crocuta*). This will certainly cast the interglacial cats among the periglacial pigeons. Perhaps the beetles will still have the last word. □

1. Shotton, F.W. *Quat. Newslett.* **45**, 28 (1985).
2. ICP Project 24 *Quat. Newslett.* **39**, 20 (1983).
3. West, R.G. *Phil. Trans. R. Soc. B241*, 1 (1957).
4. Franks, J.W. *New Phytol.* **59**, 145 (1960).
5. Gascoyne, M., Currant, A.P. & Lord, T.C. *Nature* **294**, 652 (1981).
6. Simpson, I.M. & West, R.G. *New Phytol.* **57**, 239 (1958).
7. Hall, A.R. *Phil. Trans. R. Soc. B289*, 135 (1980).
8. Mangerud, J., Sønstebo, E. & Sejrup, H.-P. *Nature* **277**, 189 (1979).
9. Sutcliffe, A.J. *et al. Quat. Res.* **24**, 73 (1985).
10. Müller-Beck, H. in *Paleoecology of Beringia* (eds Hopkins, D.M., Matthews, J.V., Schweger, C.E. & Young, S.B.) 329 (Academic, London, 1982).
11. West, R.G. *Pleistocene Geology and Biology* 2nd Edn 295 (Longman, London, 1977).
12. Stringer, C.B., Currant, A.P., Schwartz, H.P. & Colclough, S.N. *Nature* **320**, 59 (1986).

*Peter D. Moore is Reader in Ecology at the Department of Biology, King's College (KQC), 68 Half Moon Lane, London SE24 9JF, UK.*

### Igneous petrology

## Archaean mantle models

from E.G. Nisbet

ONE of the chief interests of igneous petrology lies in establishing the nature and the history of the Earth's mantle, the region below the differentiated crust and above the central core. We know very little about its composition and structure, how the continents become differentiated from it and how it has evolved thermally. In the past few years new data have allowed petrologists to produce an exotic array of speculative models of the state of the mantle in Archaean time (before  $2.5 \times 10^9$  years ago). Many of these models are based on inferences drawn from komatiites (magnesian lavas that erupted at temperatures up to  $1,650^\circ\text{C}$ ). Recently, Herzberg and O'Hara<sup>1</sup> and Walker<sup>2</sup> have used experimental data on the melting behaviour of natural samples to suggest that the upper mantle (shallower than about 670 km) has a very unlikely composition which is best explained if it originated as a melt, leaving the lower mantle as residue.

Recent experimental work<sup>3,4</sup> on 'fertile' nodules from great depths in South African diamond pipes<sup>5,7</sup> shows that the solidus and liquidus temperatures (the temperatures at onset and completion of melting) converge at pressures of 100–150 kbar (equivalent to depths of 300–450 km). If the fertile nodules are representative of mantle composition, then the

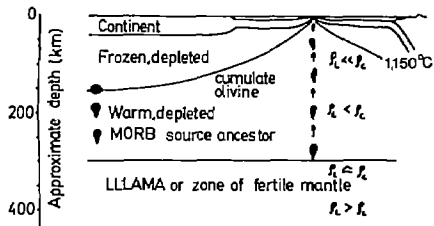
close approach of solidus and liquidus has major implications. Walker<sup>2</sup> has shown that such an approach to convergence is most improbable if the upper mantle is a random aggregate of crystals collected during accretion or as a residue from melting. More likely is that the upper mantle samples show convergence of solidus and liquidus because they were themselves once liquid compositions produced by high-pressure congruent crystal-liquid interaction. If the samples are indeed representative of the upper mantle, the implication is that the upper mantle was itself a melt, derived either by the accumulation of melts from the lower mantle, as suggested by Herzberg and O'Hara<sup>1</sup>, or from a vast globe-encircling magma ocean<sup>6</sup>.

How definite are these conclusions? There are, of course, experimental uncertainties: errors in the measurement of temperature are probably fairly large, but not large enough to undermine the convergence of solidus and liquidus. More important is how representative the nodule samples are of the upper mantle. Diamonds are known to be very old, and have been held in the cool continental lithosphere for up to  $3 \times 10^9$  years at depths of about 150 km. Possibly the fertile nodules were kept there with the diamonds, and may thus represent liquids

## NEWS AND VIEWS

that ascended and were trapped by being frozen into the base of the continents in mid-Archaean time, since being reworked by metasomatism and the accidents of eruption. If so, the nodules may not be particularly good guides to bulk mantle compositions.

There are other lines of evidence that help to elucidate the nature of the upper mantle. Komatiites erupted in many locations on the Earth's surface in Archaean time, and must have been derived from a mantle source. It is possible that they come from a source similar to the fertile nodules, and it has also been suggested<sup>3</sup> that they were produced by very small degrees of partial melt of material similar to the nodules, at pressures in excess of 70 kbar. But, the near-chondritic composition of the trace elements in the lavas suggest instead that they originated as fairly high degrees of melt of a mantle parent. One possible model of the early Archaean mantle<sup>6</sup> is based on the prediction that at great depth komatiite liquids are denser than the coexisting olivine. If this is the case, it is possible that large



Model of the possible structure of the Archaean mantle. All depths very poorly constrained. Blobs, rising melt;  $\rho_L$ , density of liquid;  $\rho_c$ , density of crystals; Some blobs erupt as komatiite or derived liquids with varying degrees of contamination, others are trapped and frozen into the continental lithosphere.

laterally linked magma accumulations (LLLAMAs) existed in the Archaean Earth, trapped by chemistry and density as a magma ocean whose top surface was at a depth of about 250–300 km (depending on the level of the supposed density crossover). Such a magma ocean would act as a source for komatiitic liquids.

Isotope evidence also provides an interesting picture of the Archaean upper mantle. The mafic lava sequences typically seem to have come from sources which had positive  $\epsilon_{\text{Nd}}$  values, something that is normally thought to imply that the source region had previously undergone extraction of a magma enriched in incompatible elements. Arndt (personal communication) has pointed out that a magma ocean source would probably be little depleted and thus is an implausible direct source of the parent liquid for Archaean mafic lavas. Furthermore, there is considerable variation in the compositions of komatiites, which is difficult to reconcile with the notion that they all have a common source.

Very little is yet known about the com-

position of the early upper mantle. If the experimental data from nodules is indeed a good guide, then the mantle may have been extensively molten or perhaps a serial accumulation of melts. But the nodules may not be representative. Similarly, the komatiites may imply the presence of a magma ocean, but is this consistent with their chemical variation and the isotopic evidence for a depleted source?

A speculative reconstruction is shown in the figure: possibly the mantle was stratified, with a depleted light layer over a magma ocean. Komatiites may have

been derived in various ways from the ocean or from the depleted layer, or could have been isotopically and chemically contaminated on ascent. □

1. Herzberg, C.T. & O'Hara, M.J. *Geophys. Res. Lett.* **12**, 541 (1985).
2. Walker, D. *Contrib. Mineral. Petrol.* (in the press).
3. Takahashi, E. & Scarfe, C.M. *Nature* **315**, 566 (1985).
4. Scarfe, C.M. & Takahashi, E. *EOS* **66**, 1130 (1985).
5. O'Hara, M.J., Saunders, M.J. & Mercy, E.I.P. *Phys. Chem. Earth* **9**, 571 (1975).
6. Nisbet, E.G. & Walker, D. *Earth planet. Sci. Lett.* **60**, 105 (1982).
7. Richardson, S.M., Erlank, A.J. & Hart, S.R. *Earth planet. Sci. Lett.* **75**, 116 (1985).

E.G. Nisbet is in the Department of Geological Sciences, University of Saskatchewan, Saskatoon S7N OW0, Canada.

## Tropical plant ecophysiology

## Research in South-East Asia

from Barry Osmond

HUMAN activities in the tropics are responsible for large-scale and rapid ecological changes. In South-East Asia the clearing of forests threatens to eliminate or seriously reduce the populations of many commercially and scientifically valuable plant species within the next two decades. These threatened species must be maintained in managed ecosystems which contribute to the economic well-being of the region, and not solely in reserves dedicated to the conservation of genetic resources. Whole new ecological systems, based on agroforestry and mixed cropping, are being constructed (Torquebiau, E.F. *Agroforestry Systems* **2**, 103; 1984). All of these activities are taking place in a near-vacuum so far as understanding of the functional relationships within tropical plant communities is concerned. A recent international conference in Bogor, Indonesia\* focused on the needs and opportunities for plant ecophysiological research in South-East Asia, and established a regional network of ecologists, agronomists and foresters to promote these studies.

Two main themes emerged. First, the understanding of temporary environmental change and the biological response to this change in tree seedlings following gap formation is primarily relevant to forest management (A. Mohammed, Forest Research Institute, Kepong). Second, understanding the problems of plant stress physiology in permanently changed, often degraded, grassland and cultivated land is relevant to the productivity of indigenous and introduced crops, most of which perform poorly under tropical conditions (F. Muhamidir, Research Institute for Food Crops, Bogor).

Many of the foundations of tropical

plant ecophysiology were laid in South-East Asia by early botanical explorers such as Schimper in the late nineteenth century, and by pioneering experimentalists like Stocker who worked in the Bogor botanical gardens in the 1920s. Unlike the American tropics, investigation of plant biology in South-East Asia was in the hands of botanists, rather than naturalists, and there is now a large body of ecological data for the region (for example, Whitmore, T.C. *Tropical Rainforests of the Far East* 2nd edn; Clarendon, Oxford, 1984). However, the rate of exploitation has far outstripped our understanding of functional relationships in tropical vegetation, all of which is summarized in one slim volume (Medina, E., Mooney, H.A. & Vazquez-Yanez, C. (eds) *Physiological Ecology of Plants of the Wet Tropics* Junk, The Hague, 1984). Our ignorance of vegetation dynamics and the principles of plant/environment interactions in tropical systems has led to coexistence of contradictory theory and practice — to management based on faith rather than fact.

Many tropical plant biologists now believe that understanding of forest systems hinges on vegetation responses to gap formation, called patch dynamics (Watt, A.S.J. *Ecol.* **35**, 1; 1947). It is now known that leaves of trees grown in the shade possess an astonishing ability to use light flecks of 30–60 seconds' duration which depends both on prior light experience and on significant post-illumination CO<sub>2</sub> fixation. These induction and capacitance components of light-fleck use (R.W. Pearcy, University of California at Davis) are drastically modified during the sustained increase of light which follows gap formation. It was previously thought that plants of deeply shaded habitats were excluded from open habitats by photo-destruction of the photosynthetic apparatus (photo-inhibition), and their inability to acclimate to high light. However, it

\*SEAMEO-BIOTROP South-East Asian Regional Center for Tropical Botany, 4–6 December 1985, supported by IDRC, Canada; ICSU International Biosciences Networks; and UNESCO, and organized by Dr Wongchan Wongkaew, Botany Department, Kasetsart University, Bangkok Bangkok.

now seems that tree seedlings on the forest floor, and understorey shade plants such as *Alocasia*, persist in bright light by maintaining a dynamic compromise between limited acclimation and chronic photo-inhibition.

New, simplified techniques, which bring the diagnosis of photosynthetic acclimation and photo-inhibition within easy reach, will permit ecophysiological analyses of these factors in vegetation dynamics. For example, disk O<sub>2</sub> electrodes originally developed for studies of photosynthetic induction at the Research Institute for Photosynthesis, University of Sheffield, have been adapted to measure quantum yield and room-temperature fluorescence (Walker, D.A. & Osmond, C.B. *Proc. R. Soc. B*, in the press). In training courses before the conference, the electrodes were applied to assess the lack of acclimation and extent of photo-inhibition in ratan, an important forest product of South-East Asia which is very fastidious with regard to light. The same system has been used to probe the light responses of photosynthesis in tropical forest epiphytes, which may have a role in branch fall and gap formation. Many of these epiphytes carry out CO<sub>2</sub> fixation via crassulacean acid metabolism (more commonly associated with succulent plants in high-light, desert habitats), which, with intrinsically high quantum yields, appears to confer photosynthetic advantages under conditions of low light and high temperature (Winter, K., Osmond, C.B. & Hubick, K.T. *Oecologia* **68**, 224; 1986).

Integration of these insights into the performance of tropical plants with key ecological observations, such as leaf phenology pattern (R. Corlett, National University of Singapore) will help to define the productive structure of natural, disturbed and managed forest systems. The same ecophysiological approaches are needed to understand the role of environmental stresses, such as high temperature, inadequate nutrition and water, in limiting the productivity of agriculture of cleared land in the tropics. Even crops of tropical origin, such as maize and sorghum, perform poorly compared with temperate regions, whereas their wild counterparts such as *Imperata* are very aggressive. It is increasingly clear, for example, that high light intensities exaggerate the effect of stress on the photosynthetic apparatus. The light-avoiding movements of leaves of the tropical legume Siratro, which mitigate water and high temperature stress (Ludlow, M.M. & Björkman, O. *Planta* **161**, 508; 1984), is but one example of the ecophysiological insights that could provide a guideline for improvement of indigenous and introduced crops in the tropics. □

Barry Osmond is Professor of Environmental Biology at the Australian National University, Box 475, Canberra City, ACT 2601, Australia.

## Creationism

# On the tracks of men and money

from Tony Thulborn

In their attempts to discredit the theory of evolution, creationists have made one claim that captures the public's imagination like no other — the claim that humans coexisted with dinosaurs. The evidence for this notion is said to reside in the Cretaceous limestones (about 120 million years old) of the Paluxy River, Texas, where markings alleged to be human footprints are preserved alongside the tracks of dinosaurs. These dubious 'man-tracks' figure prominently in creationist literature and have even been featured in several films, including the widely distributed *Footprints in Stone*. There is no doubt that the tale of the man-tracks is one of the most popular draw-cards held by the creationists. Consequently it is surprising to learn that the tale has now been publicly renounced by a leading American creationist.

On 7 January, John D. Morris, author of a standard creationist text on the man-tracks (*Tracking those Incredible Dinosaurs and the People who Knew Them* CLP, San Diego, 1980) made a startling confession: in a lecture at the University of New South Wales, he admitted that he could find no scientifically acceptable evidence of human tracks in the Paluxy limestones and agreed that it would be improper for creationists to continue citing man-tracks as evidence against evolution. Morris repeated his conclusions in a leaflet published by the Institute for Creation Research (*Impact* **151**, 1; 1986) and has also announced that *Footprints in Stone* will be withdrawn.

These welcome retractions came during the course of the 1986 Creation Science Summer Institute, a creationist symposium organized by Australia's Creation Science Foundation (CSF). Why did Morris change his mind? Apparently many of the man-tracks in the Paluxy River have now been weathered to such a degree that their true nature is becoming embarrassingly obvious: the vaguely elliptical markings heralded as human footprints have gradually weathered into the unmistakable outlines of three-toed dinosaur tracks. In the course of his lecture Morris expressed astonishment that the clarity of fossil footprints could improve, rather than deteriorate, as a consequence of natural weathering. This process is well known by professional palaeontologists but was unfamiliar to Morris, who suspected that fanatical anti-creationists had been defacing the evidence.

Morris chose to make his retraction at a crucial moment in the history of Australia's creationist movement. His forthright

confession may go some way towards restoring the public image of CSF, which has suffered an onslaught of damaging criticism in past weeks. The most destructive criticisms appeared in a book (*Creationism, an Australian Perspective* Australian Skeptics, Melbourne, 1986) that was published only 72 hours before CSF began its summer institute. The editors of the book, Martin Bridgstock (Griffith University) and Ken Smith (Queensland University), present a series of short essays explaining the scientific and intellectual bankruptcy of CSF's arguments. More unusually, they also delve into the organization's financial dealings, based on a search of the Corporate Affairs Office in Brisbane.

The financial statements of CSF for the years 1983–84 and 1984–85 contain some intriguing facts and figures. It appears that CSF disposed of more than \$A92,000 under the heading of an 'extraordinary item' (sic). CSF still declines to give a detailed explanation of where the money went. Next, it transpires that CSF does not spend much money on scientific research. The statement for the year ending 31 March 1983 lists an outlay on research of \$A398; in the following year research expenditure soared to \$A860, less than 0.2 per cent of the organization's half-million dollar income.

Most remarkable of all is the discovery that CSF received federal government funding to the amount of \$A24,698 during the two-year period. The fact that federal funds were delivered to CSF in the form of an 'export market development grant' raises an interesting question: what does the organization intend to export? The obvious answer is that it plans to export religious materials, which is evident from the fact that CSF officially declares its principal business to be: "The preaching of the Gospel, Christian Education, the accumulation and presentation of scientific evidence relevant to Creation, publication of a magazine and the sale of books, tapes and filmstrips".

If it can be demonstrated that the exports of CSF are religious in nature it is likely that its federal funding will be ruled unconstitutional. An article in the *Melbourne Age* (4 January 1986) reports that lawyers are now investigating the possibility of a challenge under section 116 of the Australian constitution, which expressly prohibits the government from establishing a religion. □

Tony Thulborn is in the Department of Zoology, University of Queensland, St Lucia, Brisbane, Australia 4067.

## Colloid chemistry

## Applications of microemulsions

from B.H. Robinson

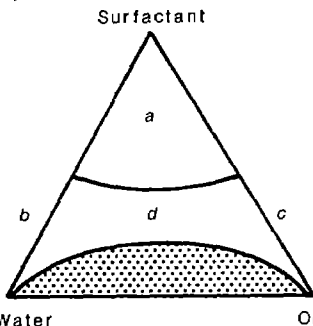
It is well known that oil and water do not mix. However, if a chemical dispersing agent, known variously as a surface-active agent, surfactant or detergent, is added then a 'microemulsion' liquid dispersion may well form. The surfactant, located at the interface between the two phases, dramatically lowers the oil-water interfacial tension. The dispersions are optically transparent and are generally thought to be thermodynamically stable. Until recently, physicists and physical chemists interested in the properties of the liquid state did not regard such systems worth serious study, believing that they were far too complex and irreproducible in their behaviour. But this situation is now changing rapidly and microemulsions are attracting wide interest in both industrial and academic research laboratories. On page 338 of this issue<sup>1</sup>, and in a preceding paper<sup>2</sup>, J. Tabony reports the results of a structural study of a surfactant-stabilized dispersion containing equal volumes of oil and water that indicates the presence of well-defined structural domains.

Most experimentalists have avoided the composition region in the middle of the triangular phase diagram (see figure), favouring the simpler 'precursor' systems along the water-oil and oil-surfactant sides of the triangle. In the absence of oil, surfactants spontaneously self-organize in water at low concentrations to form micelles, and as the surfactant concentration is increased, a variety of lyotropic liquid crystalline structures are formed. These soap-water systems are of great importance in detergency and are now quite well understood. In a similar way, certain surfactants, including phospholipids, form inverted micelles, which can readily take up water to form microstructural domains in which water is dispersed in oil in the form of essentially monodisperse aqueous droplets. Their size can be precisely controlled by varying the amounts of water and surfactant. In contrast, previous studies in the composition region (*d* of the figure) suggest the existence of open 'bicontinuous' sponge-like structures in which the surfactant forms an interface of rapidly fluctuating curvature but in which the net curvature (time- or space-averaged) is near zero<sup>3</sup>.

The results reported by Tabony in this issue were obtained using one of a range of neutron-scattering instruments which are available for structural and dynamic studies at the Institute Laue Langevin, Grenoble. Much new information on size, structure and motion of a whole range of colloidal dispersions is now becoming

available as a result of the successful exploitation of the Grenoble facility, and research will continue also at the pulsed-neutron source in the UK.

Neutrons are particularly useful for studies on liquid dispersions because the method of contrast variation (selective deuterium labelling of a component of the system) can reveal the internal structure of an individual droplet and motions of particular components. The accessible wavelength range is such that inter-droplet interactions are also readily studied using small-angle scattering methods<sup>4</sup>. Molecular motions on a very short (nanosecond) timescale can also be probed



Schematic triangular phase diagram of an oil-water-surfactant system. Shaded region, water-oil immiscibility region (2-phase); *a*, liquid-crystalline phases; *b*, micelles in aqueous solution; *c*, reversed-micelles in oil; *d*, concentrated single-phase microemulsion domain.

using inelastic scattering techniques.

Many detailed triangular phase diagrams for a range of surfactants are already available (for example, ref. 5) and furthermore, water can be substituted by several other polar solvents, for example, glycerol and formamide. Theoretical papers have stressed the importance of the shape of the surfactant molecule (and its natural curvature when adsorbed at the oil-water interface) in influencing the structures which form<sup>6</sup>, so we can now predict structures more effectively.

Why is industry interested in such microemulsions? There are a number of reasons. For example, the oil industry is keen in the longer term to exploit surfactant-enhanced tertiary oil recovery methods for which rheological properties of the microemulsion are important, and to explore the possibilities of gasoline substitutes based on liquid blends with alcohol. There are obvious applications in the food and cosmetics industries, particularly using phospholipid surfactants. Single component thermotropic (low molar mass) liquid crystals have already found wide application as electro-optic

display devices in watches and calculators. Applications of the lyotropic analogues, based on surfactant-water systems, have not been so forthcoming but the extra dimension introduced by the oil component produces a rich diversity of structures with potentially interesting rheological and electrical properties. Characterization of structure and interactions at the molecular level is the first step towards the exploitation of such new materials.

The possibility of precisely controlling the size and stability of the microstructure domains suggests interesting applications for liquid-membrane technology, and the compartmentalized liquid structures of high surface area provided by the oil-water dispersions suggest their use as a novel and versatile medium for chemical synthesis. The potential in this field is indicated in a recent review on enzyme processes in microemulsions<sup>7</sup>. Enzymes retain their activity in such dispersions and in an oil-rich medium the thermodynamic equilibrium of reactions is shifted in such a way that the possibility exists for catalysing reactions in the reverse direction to that favoured in aqueous solution, a process known as reverse enzyme synthesis. In this way, esters can be synthesized rapidly under mild conditions from carboxylic acids and alcohols, or oligopeptides can be prepared from amino acids.

Another potential use of the fluid but structured microdomains of the type reported by Tabony is in the preparation of microscopic particles of a desired size or shape reflecting the structure within the liquid dispersion. Small spherical metallic particles of, for example, platinum<sup>8</sup> and cobalt boride have already been prepared successfully in water-oil microemulsion systems using this approach and the preparation of particles of other shapes should be possible in microemulsions which have a long-lived non-spherical microstructure. Such particles show catalytic activity in selective hydrogenation reactions<sup>9</sup>. J.H. Fendler has stressed the wide range of chemical processes, such as artificial photosynthesis, that may be facilitated by reaction at interfaces<sup>10</sup>. Microemulsions and the so-called 'liquid crystal microemulsions' as described by Tabony look to have considerable potential for exploitation in the near future.

1. Tabony, J. *Nature* 320, 338 (1986).
2. Tabony, J. *Nature* 319, 400 (1986).
3. Gennes, P.G. & Taupin, C. *J. phys. Chem.* 86, 2294 (1982).
4. Ottewill, R.H. (in Goodwin, J.W. ed) *Colloidal Dispersions* R.S.C. Spec. Pub. 43, 143; 1982).
5. Ekwall, P. *Adv. Liquid Cryst.* 1, 1 (1975).
6. Israelachvili, J.N., Mitchell, J.D. & Ninham, B.W. *J. Faraday Trans.* 72(2), 1525 (1976).
7. Luisi, P.L. *Ang. Chemie, Int. Ed.* Engl. 24, 439 (1984).
8. Boutonet, M., Kizling, M., Stenius, P. & Marz, G. *Colloids Surf.* 5, 209 (1982).
9. Lufimpadio, N. et al. *Surfactants in Solution* (eds Mittel, K.T. & Lindman, B.) Vol. 3, 1483 (Plenum, New York 1983).
10. Fendler, J.H. *Chem. Engng. News* 2 January, 25 (1984).

B.H. Robinson is in the Chemical Laboratory, University of Kent, Canterbury CT2 2NH, UK

## Visual cortex

# What layer 6 tells layer 4

from Simon LeVay

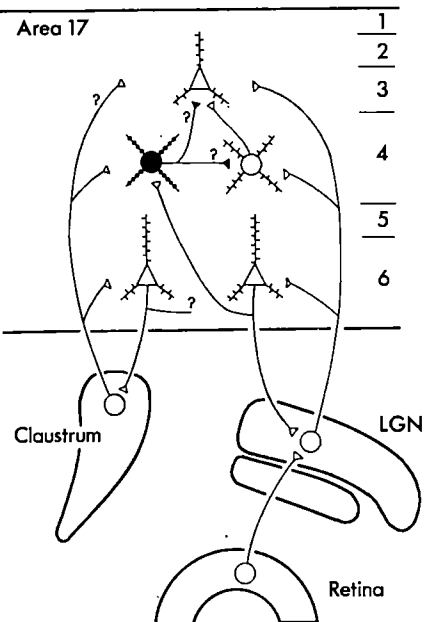
THE primary visual cortex (area 17) of the cat has been the object of intense study since Hubel and Wiesel's pioneering work, first published 24 years ago (*J. Physiol., Lond.* **160**, 106; 1962). As a result, we now know the characteristic shapes and connections of many of the major cell types, have categorized the visual responses of neurones in area 17 and matched morphological and functional cell types using intracellular recording and staining techniques. Taken together, these data allow increasingly precise hypotheses about the generation of specific response properties of cortical neurones. Elsewhere in this issue, J. Bolz and D.C. Gilbert put forward one such hypothesis and provide experimental support for it (*Nature* **320**, 362; 1986).

Most neurones in area 17 are orientation-selective, that is, a neurone responds best to an elongated bar of light at a particular orientation that is swept broadside across its receptive field. Many cells have specific requirements with respect to the length of the bar (its dimension along the orientation axis). Some cells respond increasingly well as the stimulus length is increased up to some optimal value (typically 1–3 degrees of visual angle), but respond less well, or cease to respond completely, if the stimulus is lengthened further. The output of these 'end-inhibited' cells thus conveys information about both the orientation and the length of the stimulus. End-inhibited cells are common in the upper cellular layers of area 17 (layers 2, 3 and 4) but are rare in layer 6, the deepest layer. Layer 6 contains many cells which respond poorly to short bars; instead they respond increasingly well as the length of the bar is increased to quite high values (4–16 degrees). Bolz and Gilbert suggest that the activity of these cells is responsible for the end-inhibition of cells in the upper layers.

The circuitry by which this could be achieved is illustrated in the figure. Many pyramidal neurones in layer 6 have axonal branches that ascend to layer 4, where they terminate predominantly on the varicose dendrites of spinefree stellate cells. The spinefree cells are thought to be inhibitory neurones whose axons may contact the spiny dendrite stellate cells, which comprise the major neuronal type of layer 4. (It is known that the output of the spiny dendrite stellate cells is largely to the pyramidal neurones of layers 2 and 3.)

According to Bolz and Gilbert's hypothesis, presentation of a short bar (say 2 degrees long) activates layer 4 cells but has little effect on layer 6 cells, whereas pre-

sentation of a long bar (say 8 degrees) activates layer 6 cells, which excite the spinefree cells of layer 4 and suppress the response of the spiny dendrite cells, producing end-inhibition. For this scheme to work the connections must be specific to sets of neurones sharing a common orientation preference — this is taken care of by the fact that interlaminar connections are predominantly vertical and cells sharing a common orientation preference are organized into vertical columns.



Some intrinsic and subcortical connections of area 17 that may be involved in the generation of end-inhibition. Retinal neurones drive neurones in the lateral geniculate nucleus (LGN), which in turn provide input to neurones in cortical layers 3, 4 and 6. Many layer 6 cells have ascending branches which contact spinefree stellate cells (shown in black) in layer 4. These cells are thought to inhibit the spiny stellate cells of the same layer and/or the pyramidal cells of layer 3. Descending axons from layer 6 neurones innervate the LGN and the claustrum. Claustral neurones send a return projection to area 17 that ends in all layers, but most heavily in layer 4. All the cortical neurones drawn here lie in the same orientation column. Uncertain connections are indicated by the question marks.

To test their model, Bolz and Gilbert recorded from cells in the upper cortical layers while reversibly inactivating a patch of layer 6 cells immediately below by direct injection of the inhibitory neurotransmitter  $\gamma$ -aminobutyric acid. During the block, which lasted for a few minutes after each injection, most upper-layer cells lost all or part of their end-inhibition — that is, they responded to long as well

as to short bars. Other properties of the neurones (orientation and direction selectivity) should be largely unaffected.

In terms of the history of ideas about the laminar organization of the cortex, Bolz and Gilbert's results suggest something of a compromise. Earlier workers stressed the notion of reverberating interlaminar circuits or of sequential processing of visual signals from layer to layer. According to these ideas, inactivation of a single layer should largely or totally disable cortical function. In contrast, more recent observations suggest a surprising degree of functional independence of the layers. For example, layer 4, long thought to be the major input layer of area 17, can be silenced without seeming to affect responses in layers 2 and 3 (Malpeli, J.G. *J. Neurophysiol.* **49**, 595; 1983). Bolz and Gilbert show that inactivating a single layer can eliminate a single aspect of cortical function while leaving other aspects intact, and their results illustrate how columnar organization, at least in the orientation domain, simplifies the elaboration of response properties.

What is the specific wiring responsible for these processes? As well as sending axons to layer 4, layer 6 neurones also provide the descending arms of two loops that connect area 17 with subcortical nuclei, the lateral geniculate nucleus and the claustrum (see figure), therefore these descending pathways are also silenced by the  $\gamma$ -aminobutyric acid injections. The cortico-claustral loop has previously been implicated in the generation of end-inhibition in area 17 (Sherk, H. & LeVay, S. *J. Neurosci.* **3**, 2121; 1983), although its contribution is only partial. The role of the massive descending pathway to the lateral geniculate nucleus is something of a mystery. But geniculate neurones have an antagonistic centre-surround type of receptive-field organization, which gives them some degree of end-inhibition when they are stimulated with elongated bars. There are hints that the cortico-geniculate pathway could modulate this effect (Tsumoto, T. *Expl. Brain Res.* **32**, 345; 1978) thus providing another route by which layer 6 cells could indirectly influence end-inhibition in the upper cortical layers. More precise experiments are required to elucidate the contributions of these pathways to end-inhibition.

To what extent can Bolz and Gilbert's findings be extended to other cortical areas or to other species? The almost total lack of data allows free rein for speculation. Perhaps the general role of layer 6 is to determine whether increased local cortical activity is matched by heightened activity of neighbouring regions, and, if so, to suppress the activity of upper layer cells. This would be equivalent to the lateral inhibition seen at early levels of

## BOOK REVIEWS

# A place for teleology?

William H. Press

**The Anthropic Cosmological Principle.** By John D. Barrow and Frank J. Tipler. Clarendon: 1986. Pp. 706. £25, \$29.95.

TELEOLOGY, we recall, is the doctrine that natural phenomena are guided not only by immediate causal forces, but also by certain pre-determined, distant goals. It is an understatement to say that teleology has been out of fashion in science in the past century, and probably not much of an exaggeration to say that the present scientific paradigm rejects the teleological hypothesis vehemently, categorically and usually with contempt. If the Darwinian revolution was not about the rejection of teleology, then what was it about?

Now there comes a book — no crackpot tract, but a scholarly, philosophically sophisticated and mathematically high-brow monograph — that says we've all made a big mistake; there really is a place for teleology and related concepts in today's science. At least (the authors ask), give us a chance to present arguments, drawn in the main from modern theoretical cosmology, which may convince the reader of an astounding claim: there is a grand design in the Universe that favours the development of intelligent life. This claim, in certain variations (as we shall see in a moment), is the "anthropic cosmological principle".

The immediate dilemma is whether or not to take such a book seriously at all. There are several good reasons to do so. First, it is a magnificently quixotic quest that the authors are undertaking, and they approach it with style, erudition and panache, though not without some sly reliance on debaters' tricks. Second, as the rest of us putter around in the basement of currently accepted scientific beliefs, it is not a bad thing to be prepared to defend those beliefs — and this book surely offers a dangerous (but in the end, I think, rebuttable) challenge to them.

Third, although Barrow and Tipler try valiantly to cloak their thesis in the garb of heavy philosophy and impenetrable (and sometimes misused) mathematics, there lurks within the book a delightful, wide-ranging and provocative exploration of their own hodge-podge of broad intellectual interests. These centre on modern relativistic cosmology (in which the authors do hold established credentials) and range from there with enthusiasm, and greater or lesser competence, into biochemistry

and the origin of life, into space travel and extraterrestrial intelligence, into many-world interpretations of quantum mechanics, into critical analysis of the work of Jesuit mystic Teilhard de Chardin and the Humean rejection of design arguments for the existence of God, and much, much more. It would be quite a challenge to find another book whose "B" index entries include Boshongo creation myths, the auto-



catalytic role of beryllium-8 in the helium-burning reaction and Bianchi type VII universes.

So what business have a couple of mathematical cosmologists poking around in places such as this? Barrow and Tipler have found themselves a kind of intellectual magic carpet, which transports them effortlessly through parochial disciplinary barriers into any field they want to get into. The anthropic principle is that magic carpet. Under its present name, it has been talked about by (mostly) cosmologists for something more than a decade; Barrow and Tipler trace it, and its forerunners and precursors, back through several centuries.

A weak, and not very controversial, form of the anthropic principle is the notion that observational selection biases should be accounted for in cosmology, just as they are accounted for in less grandiose fields of observational or natural science. As the authors put this:

The observed values of all physical and cosmological quantities are not equally probable but they take on values restricted by the require-

ment that there exist sites where carbon-based life can evolve and by the requirement that the Universe be old enough for it to have already done so.

In other words, we know that we are here (Bishop Berkeley, Descartes: these authors have you all figured out), so we might as well rule out physical theories and cosmological models that are incompatible with that "observation". Taken this way, the weak anthropic principle (WAP) is little more than an application of Bayes theorem of probabilities, letting a little bit of *a posteriori* knowledge (the existence of life on Earth) intrude into an assessment of the likelihood of *a priori* theories.

There is only the faintest whiff of teleological dogma in the WAP. By accepting it, one gains intellectual dominion over a whole set of territories which would otherwise lie outside the scope of science. "Why" do the physical constants have the values that they do? "Why" is the Earth the size and temperature that it is? And so on. The meat of this book is the exploration of consequences of the WAP in cosmology, astrophysics, planetary physics and evolutionary biology. But the seductive trap that the authors are setting is already clear: as soon as we accept the "why" formulation of questions that the WAP allows us to address, we have entered a receptive state of mind for the strong anthropic principle (SAP): "The Universe must have those properties which allow life to develop within it at some stage in its history". Or, more extreme yet, John Archibald Wheeler's participatory anthropic principle (PAP): "Observers are necessary to bring the Universe into being". Barrow and Tipler coyly avoid saying that they want us to believe in one of these stronger statements, but one cannot read their book without feeling that they do, that they are earnest, wide-eyed, proselytizing believers themselves. One can almost see them handing out flowers in airports or train stations.

It is at this point that, not without reluctance, I have to bail out of their plane and parachute to safety. Barrow and Tipler have given us an engaging book, practically a universal education in both the history of modern science and the history of the Universe. (In a short review one cannot do justice to the diversity of their topics and the fascinating historical titbits that they have unearthed and recorded.) This book will be much quoted, much debated and much praised. It deserves a place on the shelf of any serious scholar of science, and it will be found on a

good many coffee tables as well. Nevertheless, in my opinion, there is some fundamental intellectual dishonesty here, some snake oil being peddled. The authors are trying desperately to be taken seriously, and they do not always play fair with their readers.

While there is a lot of good scientific exposition in the book, there is too a distressing amount of what seems to be mathematical flim-flam, that is, quotation of precise results in a manner designed to mislead less-mathematical readers and cause them to jump to the authors' desired (usually non-mathematical) conclusion. For example, after some rather woolly discussion of Penrose conformal diagrams, Barrow and Tipler conclude "A Penrose diagram allows us to define rigorously 'an achieved infinity', a concept whose logical consistency philosophers have been doubtful about for thousands of years". This is a silly assertion, but it is put forth with the utmost gravity, in such a way that many readers will be taken in. And it is only one of many such cases.

Nor do the authors always play fair with other workers in their field. They have a tendency to bury footnote references to the work of their colleagues in and among a plethora of erudite footnotes to nineteenth- and twentieth-century precursors. This becomes particularly disturbing when, as is sometimes the case, the exposition mirrors other authors' papers practically sentence by sentence. The casual reader will come away mistakenly crediting Barrow and Tipler for ideas that they have, in fact, only nicely summarized. The serious scholar should take their bibliographical research and attributions (an immense amount of work on their part) as indicative, not definitive.

The book's flaws, I think, can be traced back to a single cause: the authors badly want to be the founding doctrinal theorists of a "new" resurgence of teleological belief in science. They bring to their cause an impressively broad knowledge of scientific exotica, but the factual content of the book is only their means to an end that (in my opinion) is threatening to the modern scientific enterprise. That end is nothing less than the fusion of matters of science with matters of individual faith and belief. It has taken us a long time to separate these matters, each to its own legitimate arena in human affairs. We should not lightly allow them to become once again jumbled, least of all by a book that now and then cuts corners in getting to its own pre-determined, distant goals. This is a fascinating and entertaining book, one to read and think about. But it is also one whose extra-scientific agenda most of us will, ultimately, wish to reject. □

*William H. Press is Professor of Astronomy and Physics at the Center for Astrophysics, Harvard University, 60 Garden Street, Cambridge, Massachusetts 02138, USA.*

## What do intermediate filaments do?

*Keith Burridge*

**Intermediate Filaments: A Review.** By Peter Traub. Springer-Verlag: 1985. Pp. 266. DM 168.

FOR SEVERAL years people interested in intermediate filaments have looked over their shoulders with envy at those studying microtubules and microfilaments. While there is ample evidence for the importance of microtubules and microfilaments in generating cellular movements, the function of intermediate filaments remains elusive. Because no obvious motility function has been apparent, some sort of skeletal or structural role has been generally, if begrudgingly, accepted, but this concept has not been embraced with the kind of enthusiasm that gives a field new momentum.

Anyone examining the function of intermediate filaments has some puzzling experimental observations to consider. Some cells exist, apparently quite happily, without them. Similarly, the intermediate filaments within a cell can be collapsed by microinjection of antibodies without detectable effects on the cell's behaviour. From these observations one might conclude the intermediate filaments are not very important, or, alternatively, that they have a subtle function which has been missed because the assays have been inappropriate. This latter argument is the one adopted by Peter Traub. He proposes that the idea that intermediate filaments have a structural role is essentially the consequence of depending on structural techniques, such as immunofluorescence and electron microscopy, to study them. Traub uses the final chapter of his book to present his own, novel ideas about possible functions; rather than being skeletal elements within cells, he suggests, intermediate filaments are involved in signal transduction from the plasma membrane or cytoplasm to the nucleus.

Traub first became entangled in this field accidentally. Working as a virologist, he became intrigued with a protein that was binding to some viral RNA. Only later did he realize that this protein had been discovered previously and was vimentin, the subunit of one of the main types of intermediate filament. At this point others might have dropped the subject, attributing the binding to irrelevant coincidence, but Traub and his colleagues have pursued the matter. They have shown under physiological conditions that the subunit proteins of several classes of intermediate filament have a specificity for binding to DNA rather than to RNA. From the work of others, it has been

known for some time that intermediate filaments are very susceptible to proteolytic cleavage by a calcium-activated protease in the cytoplasm, and again Traub has demonstrated that the fragments generated from the different classes of filament by this protease retain the selective DNA-binding activity.

These biochemical observations form the basis of Traub's theory. He suggests that calcium elevated in the cytoplasm in response to external signals activates the protease. This, in turn, cleaves the intermediate filament subunits, which can no longer assemble, and which are transported back to the nucleus. Here they interact with DNA or chromatin, probably in conjunction with other proteins, in a regulatory manner. When I first read about this idea I was sceptical. I still am, but Traub assembles a considerable body of evidence that is consistent with the proposal. Certainly, an advantage of his hypothesis is that it suggests many experiments by which it could be tested. On the other hand, the idea that intermediate filaments have primarily a skeletal function is a difficult concept to establish or to destroy.

Only the last chapter of the book is dedicated to this unorthodox but refreshing concept. Regardless of whether or not one accepts it, the book as a whole provides an excellent review of intermediate filaments. Almost every aspect of the subject is covered, with references up until about 1984, ranging from heterogeneity, structure and assembly, to the interaction of intermediate filaments with other elements, secondary modification and response to normal and pathological stimuli. Given how vast and labyrinthine the field has become, this is quite an accomplishment. The only area in which Traub has not attempted to be comprehensive is the increasing clinical use of intermediate filaments for tumour typing.

The book should be useful both for specialists and for the many cell biologists who, like myself, have a peripheral interest in intermediate filaments. It is well organized, well indexed and has a bibliography of some 60 pages. I anticipate that it will be the standard work for many years. If it also stimulates some novel experiments that help to unravel the knot of intermediate filament function, then Traub should be well pleased with having provided a double service to the field. □

*Keith Burridge is in the Laboratories for Cell Biology, Department of Anatomy, University of North Carolina at Chapel Hill, 111 Swing Building 217H, Chapel Hill, North Carolina 27514, USA.*

- Two recent books on the cytoskeleton are *Molecular Biology of the Cytoskeleton* (G.G. Borisy et al., eds), published by Cold Spring Harbor Laboratory, and *The Cytoskeleton: An Introductory Survey* (by M. Schliwa), published by Springer-Verlag.

## Temper out of time

J.S. Jones

**The Evolutionary Process: A Critical Review of Evolutionary Theory.** By Verne Grant. Columbia University Press: 1985. Pp. 499. \$40.

One of the pleasures of being an evolutionist is that one's colleagues are such a cantankerous lot. They have, of course, a great deal to be cantankerous about. Each one of Darwin's precepts — that there exists extensive genetic diversity which reflects variation in fitness, that most polymorphism is subject to natural selection and that the gradual accumulation of favoured variants leads to the origin of species — has been disputed since they were first stated, and molecular biology has given new heart to those whose chief pleasure is in attacking the Darwinian edifice.

This book treats evolutionary theory from the viewpoint of an author who has grown up with the subject. Grant comes from that generation of biologists, now almost extinct, which sees evolution in the context of a deep understanding of the world of living animals and plants rather than as experts in a newly invented (and somewhat nebulous) science of "evolutionary biology". He discusses many of the classics of the field; gene flow, population structure and patterns of speciation in *Drosophila*, industrial melanism, genetic load, adaptive radiation and human evolution. Many of his examples come from plants, with sequoias as exemplars of population structure, the origin of corn as an instance of the power of selection and the annual herb *Gilia* as an illustration of reproductive isolating mechanisms.

There is, too, space for the grinding of a few private axes. Kin selection has, apparently, only slight explanatory power and a great ability to cause confusion of thinking. The same is true of speciation in continuous populations. However, many of the book's themes are acceptable to the most conventional evolutionist: the vast majority of new mutations are deleterious, natural selection always has the last word in determining the fate of a newly arisen variant and macroevolution can be explained as the summation of many microevolutionary events.

For all the strengths of a treatment of this sort, the book suffers from its concentration on convention. Traditional explanations will, no doubt, explain many of the patterns of morphological evolution which we see in nature. However, most of the recent excitement in evolutionary theory has arisen from the discoveries of molecular biology. It is now clear that there is a staggering amount of genetic diversity in DNA structure and that, at

this level, some of the patterns of genetic differentiation among closely related species are very difficult to explain in terms of mutation and selection. Grant's subtitle is *A Critical Review of Evolutionary Theory*, but it is not easy to be critical in a review which omits many of the ugly facts which now threaten Darwin's beautiful theory. Molecular evolution does get a mention, but its wider implications are scarcely discussed. As a result the book conveys little of the genuine bad temper which is such an attractive feature of modern evolutionary biology.

This, then, is a gentleman's book, which deals largely with the controversies of yesterday. It may well be that these will be the controversies of tomorrow; but what is needed is a fuller discussion of their relevance to the discoveries of today. □

J.S. Jones is a Lecturer in the Department of Genetics and Biometry, University College London, 4 Stephenson Way, London NW1 2HE, UK.

## Views of the virus

P.J.G. Butler

**Virus Structure and Assembly.** Edited by Sherwood Casjens. Jones and Bartlett: 1985. Pp. 295. \$45, £45.

VIRUSES are studied not only as interesting microorganisms in their own right, but also for what they can tell us about the host cells which they infect. Because many of them have small genomes, coding for few proteins (sometimes only three, including the coat protein for packaging new virions), they have to suborn many cellular functions for synthesis and even sometimes assembly of their components. Even in viruses with large genomes, such as bacteriophage T4 which codes for many enzymes, a fair proportion of the genes duplicate functions already available in the host cell and are inessential except in unusual hosts. Thus a virus-infected cell carries out many of its normal functions, but to a grossly exaggerated extent, and with a narrower range of products, which facilitates research into these processes.

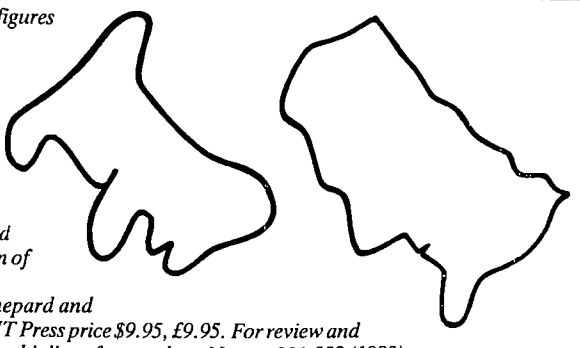
Ambiguous shapes: these two figures are each open to different interpretations according to whether they are mentally rotated 45° clockwise or 45° anticlockwise (one of them, for instance, can be seen as a man in a chef's hat or, alternatively, as a dog). The illustrations are reproduced from the new paperback edition of Mental Images and Their Transformations, by R.N. Shepard and L.A. Cooper, published by MIT Press price \$9.95, £9.95. For review and discussion of the issues raised by this line of research see Nature 301, 353 (1983).

There are many reviews of specific areas of virus structure and assembly aimed at specialist audiences, but no attempt has been made recently to cover the whole field in a single volume. A book such as the present one is therefore to be welcomed and it is all the more regrettable that it is in the area of all-round coverage that *Virus Structure and Assembly* is at its weakest; it is, perhaps, the difficulty of covering such a vast amount of information which has deterred others from attempting the task. The editor has gallantly contributed the two general chapters, "An Introduction to Virus Structure and Assembly" and "Nucleic Acid Packaging", himself. The second of these occupies a full quarter of the book, but despite its relative length I feel that it falls short of the mark. Inside Casjens's own areas of expertise the subject is well handled, but in dealing with less-familiar material he has resorted to a simple listing of published views with little attempt to assess their merits or significance.

The book contains several excellent chapters, which are both enjoyable and informative, but in the main these cover areas close to the editor's research interest (that is, bacteriophage). While I must declare an interest in the topic, it is inadequate to try to summarize tobacco mosaic virus, for which the most detailed information for any virus is available on both structure and assembly, in just four pages. In comparison, an entire chapter is devoted to the tailed bacteriophages, which also take large parts of two further chapters. While they demonstrate the power of genetic analysis, we have little understanding of their detailed interactions as there are no high-resolution structures known.

On the topics which are given adequate space this book does a good job, but it fails to meet the objective which the editor sets out in his preface; it would be wrong for anyone outside the field to be deceived by the title into thinking that it gives an overall picture of our knowledge of virus structure and assembly. It is, nonetheless, certainly worth reading. □

P.J.G. Butler is in the Medical Research Council's Laboratory of Molecular Biology, Hills Road, Cambridge CB2 2QH, UK.



## BOOK REVIEWS

# An image of science and business

Peter Newmark

**A Machine Called Indomitable.** By Sonny Kleinfield. *Times Books, New York: 1985.* Pp. 250. \$16.95.

RAYMOND Damadian, the main subject and inspiration for this book, could, it seems, have chosen to make a career as a violinist or a tennis player had he not chosen to study science and later medicine. By the end of Sonny Kleinfield's rather shallow account, his subject has become a business man, grown rich by selling the nuclear magnetic resonance (NMR) scanner that he had pioneered. But this is much less a story of how the son of some poor Armenian immigrants made good in the great American tradition, than how a misfit in the conventional world of medical research was forced into business to support himself.

Damadian's problems with his fellow researchers seem to have been catalysed by his early association with Gilbert Ling, a physiologist who believes that the interior of cells comprises multiple polarized layers of water molecules which account for phenomena such as those otherwise interpreted as a sodium pump in the cell membrane. Falling under the spell of Ling — who remains a voice in the wilderness — Damadian first reasoned that the water structure of cancer cells would differ from that of normal cells, and then came across NMR as a means of detecting that difference: "One afternoon, peering at the pool... Damadian went off into his own mind. Gradually, swirling like smoke, visions emerged. Perhaps some sort of giant NMR machine might be just the device that could be used to scan his stomach (which was still acting up)..." (p.27). In the style of the reporter (for the *New York Times*) that he is, Kleinfield recounts how the dream of 1970 became the prototype machine of 1977, and the business of today.

Damadian's first "mistake" was to outline in *Science* his vision of using NMR to detect tumours on the basis of their abnormal water structure. The paper seems to have been the subject of a good deal of derision, from which its author never really recovered in the eyes of many of his peers. The result was a continual struggle for money to support his work and a growing contempt and fear of his rivals, especially Paul Lauterbur at the University of New York at Stony Brook, whose paper on NMR imaging (for which he coined the unused term *zeugmatography*) was published in *Nature* in 1973. Damadian was incensed that the paper contained no reference to his own work; he was, however,

inspired by Lauterbur's achievement to switch his own efforts to imaging.

Perhaps Damadian's character is best illustrated by his financial struggles. When his first grant application was turned down he wrote directly to President Nixon: "The rejection of my grant by the National Institutes of Health is a colossal stupidity [which] reflects only the enduring ignorance and the complete absence of vision of the men who decide". Urged by NIH to reapply, he received a three-year grant with which he bought his first NMR machine. When that grant ran out and the "appallingly disgusting" peer review system failed him again, he raised money privately with the help of a brother-in-law

Reasoning that his fatness was the problem, he put pressure on his only slim associate to be scanned by the machine — by then christened Indomitable. Persuasion took two months, the scan itself four and three-quarter hours. But the result was an image. And a press conference. And more hostility.

Failing to get recognition, promotion or papers published, and once again without the money to proceed, it was then that Damadian decided to go into business. He also decided to switch from a superconducting magnet, with its problematical requirements for cooling by liquid helium, to a permanent magnet, which weighs 3,000 g in the latest machines. They now

## Tumor Detection by Nuclear Magnetic Resonance

**Abstract.** Spin echo nuclear magnetic resonance measurements may be used as a method for discriminating between malignant tumors and normal tissue. Measurements of spin-lattice ( $T_1$ ) and spin-spin ( $T_2$ ) magnetic relaxation times were made in six normal tissues in the rat (muscle, kidney, stomach, intestine, brain, and liver) and in two malignant solid tumors, Walker sarcoma and Novikoff hepatoma. Relaxation times for the two malignant tumors were distinctly outside the range of values for the normal tissues studied, an indication that the malignant tissues were characterized by an increase in the freedom of tissue water

Cause of controversy: the opening lines of Damadian's paper in *Science*, 19 March 1971.

through a Citizens' Campaign for New Approaches to Cancer. There followed a large National Cancer Institute grant (and a patent) but again no renewal. Later, in desperation, Damadian travelled to Plains, Georgia, to try and persuade the newly-elected President Carter of his case. Hugh Carter, a cousin, did his best on Damadian's behalf but no money was forthcoming. In the end it was a wealthy businessman who came to the rescue.

Despite financial problems, Damadian was making progress in the construction of a human NMR scanner. But the lack of money meant that much labour and ingenuity had to be spent on building everything, including the superconducting magnet, from scratch and often from junk. He was driven to a considerable extent by the fear that Lauterbur, or one of the British groups that had entered the field, would be the first to produce NMR images of the human body, in which case Damadian foresaw that he would lose any remaining chance of getting the credit for his invention. Lauterbur, however, seems not to have been concerned. A research associate at the time is quoted as saying "He didn't think Damadian was capable of producing an image. He thought he was some crazy doctor".

Whereas Lauterbur and others were busy imaging lemons, green peppers and even rats, Damadian was going for broke. Finding no volunteer among his colleagues to be the first human to be NMR scanned — there was some apprehension about the possible effects of a long exposure to a strong magnetic field — Damadian became his own guinea pig in May 1977. The result was not even a lemon.

sell for more than \$1.6 million and have to compete with similar machines from at least a dozen rival companies.

Kleinfield's book has its attractions. It provides a plausible picture of a man who suffered the results of allowing his enthusiasm to get the better of him when the rules of the game demand a more measured approach. It is easy to see both why he became almost paranoid about his peers and why they took him less than seriously. It is, however, hard to be too enthusiastic about a writer who can say (p.8): "Two of the important substances that get reabsorbed [in the kidney] are sodium and potassium; they are the secret to biological electricity, which is the foundation of life. It allows us to move our arms and legs and to breathe". Also, even though the book does not pretend to be a balanced account of the development of NMR imaging, it would have benefited from a less Damadian-dominated version of the story. The author talked to Lauterbur and some of the British rivals, but one learns little of the former and next to nothing of the latter.

Ironically, NMR scanners are still of little use in detecting tumours, the point of departure for Damadian's quest. Undaunted, Damadian now foresees the development of Indomitable into a tumour-killing device. And, indomitably, he still believes that in cancer "the real event that's taking place is that the water is becoming more and more disorganized and less structured in the cell". For better or for worse there is probably more room for such characters in business than in science. Or even in music or tennis. □

Peter Newmark is Deputy Editor of *Nature*.

# The management of sea-level rise

from Walter S. Newman and Rhodes W. Fairbridge

*Man can regulate the hydrological cycle by diverting ocean-bound fresh water into reservoirs, subsurface storage and interior basins, and by diverting sea water into continental depressions. Between 1957 and 1982, human intervention stored as much as  $0.75 \text{ mm yr}^{-1}$  of sea level rise potential in reservoirs and irrigation projects.*

TIDE gauge studies reveal that the trend of sea level in this century has been generally upwards along most of the world's coastlines. For most of this century, the mean rise has been more than  $1 \text{ mm yr}^{-1}$  (refs 1–4). Meier<sup>5</sup> believes that the wasting of mid-latitude glaciers by 'greenhouse-effect' warming is in part responsible for the modern sea-level rise, whereas Gornitz *et al.*<sup>1</sup> find the 'steric effect' (expansion of near-surface water due to temperature increase) explains much of the remainder of the current rise.

In the past few years, several independent reports (for example, refs 6, 7) have presented rather alarming scenarios predicting a greenhouse-effect sea-level rise on the order of 0.6 to 3.5 m by the end of the next century<sup>8</sup>. Although the CO<sub>2</sub> models may be controversial, the tide-gauge evidence is qualitatively correct. Whatever might be the ultimate cause of the contemporary sea-level rise, the continuing marine inundation poses a major threat to the world's littoral population.

## Options

The problem can be addressed in several ways: by evacuation and retreat from the contemporary littoral (including legislated withdrawal from coastal habitations and investments), defence of the shore by a variety of engineering schemes, as practised, for example, in the Netherlands, and/or manipulation of the hydrologic cycle. On a worldwide basis, we have no means of estimating the cost of either the evacuation or the defence options. For most littoral states, either of these options would presumably consume an appreciable portion of their gross national products.

We examine here a third option: anthropogenic management of the hydrologic cycle. A eustatic sea-level rise of  $1.25 \text{ mm yr}^{-1}$  equals an annual increase in ocean volume of nearly  $500 \text{ km}^3 \text{ yr}^{-1}$ . We assume that these figures are a conservative approximation of the observed trends. The crux of the problem of regulating sea level is then how to interrupt the hydrological cycle so that each year we can intercept and dispose of, or store,  $\sim 500 \text{ km}^3$  of additional water volume apparently being added to the ocean mass.

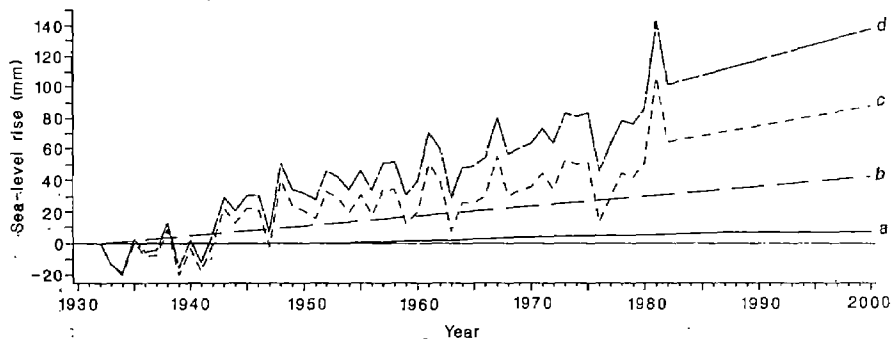


Fig. 1 Sea-level volume suppression since 1932 due to reservoir and irrigation project storage. The global sea-level plot (c) to 1982 is based on data by Gornitz and Lebedeff<sup>22</sup>, thereafter an assumed volume increase of  $500 \text{ km}^3 \text{ yr}^{-1}$  is used to extrapolate the sea-level rise to the year 2000. Trace a shows the growth of the known storage capacity of the world's 107 largest reservoirs<sup>9</sup> (capacity  $\geq 1 \text{ km}^3$ ); b is our estimate of water volume detention in small reservoirs and irrigation projects. Trace d adds the anthropogenically-stored water (a plus b) to trace c, to generate what would have been the trace of sea level unsuppressed by continental storage. Note that this trace does not include the effect, if any, of groundwater mining.

In fact, we already store an appreciable volume of water on the continents. The Soviet hydrologist M. I. L'vovich<sup>9</sup> estimates that mankind now regulates 15% of the Earth's annual river discharge. Figure 1 (trace a) shows the rate of growth of the water storage capacities of the world's 107 largest reservoirs<sup>10</sup>. The total quantity already stored or planned for storage by the end of the century is  $\sim 3,100 \text{ km}^3$ . These data imply that since 1932, sea-level rise has been suppressed by reservoir storage.

Figure 1 also shows the 'noisy' rise of sea level since 1932 (trace c). This trace is derived from an updated and expanded database of tide-gauge measurements and late Holocene sea-level indicators assembled by Gornitz and Lebedeff<sup>22</sup> and used by them to obtain a global average sea-level rise of  $1.2 \pm 0.3 \text{ mm yr}^{-1}$ . We used their data for the interval 1932–1982 and extrapolated the slope of their data ( $1.25 \text{ mm yr}^{-1}$ ) to the year 2000.

The water stored in large reservoirs would otherwise have been responsible for an appreciable annual increment in modern sea-level rise. For the time interval 1957–82, the mean rate of suppression has been about  $125 \text{ km}^3 \text{ yr}^{-1}$  (equal to a potential rise in sea level of  $0.25 \text{ mm yr}^{-1}$ ). This volume does not include the construction and closing of millions of smaller reservoirs which might double the rate of sea-

level-rise suppression to  $0.5 \text{ mm yr}^{-1}$  ( $250 \text{ km}^3 \text{ yr}^{-1}$ ). Nor does this volume include irrigation water, some of which infiltrates into aquifers, although at least half of it is transpired and evaporated and most of the remainder runs off again towards the world ocean<sup>11</sup>. We estimate that about  $125 \text{ km}^3 \text{ yr}^{-1}$  of some  $3,000 \text{ km}^3 \text{ yr}^{-1}$  of consumed irrigation water infiltrates to the subsurface, or remains as soil moisture and is more or less permanently stored in association with irrigation projects. We suggest that since 1932, all forms of reservoir storage plus irrigation projects have been storing  $\sim 375 \text{ km}^3 \text{ yr}^{-1}$  of water, equivalent to a potential sea-level rise of  $\sim 0.75 \text{ mm yr}^{-1}$ . The estimated rate of small reservoir and irrigation storage since 1932 and extrapolated to the year 2000 is shown as trace b in Fig. 1.

In contrast to water currently being withdrawn from the hydrological cycle is water formerly in storage but now being recycled. The USSR Committee for the International Hydrologic Decade has estimated<sup>12</sup> a sea-level rise of  $0.8 \text{ mm yr}^{-1}$  due to decrease in groundwater storage, and Gornitz *et al.*<sup>11</sup> believe that land storage is probably not a major cause of sea-level change because new storage is being balanced by groundwater mining. Both of these estimates are based on extrapolations of water mined from the Great Plains

Ogallala aquifer that extends north from western Texas through to the Dakotas. However, the lateral transmissivity of the Ogallala is very low because of the variability of the sediments in this alluvial formation<sup>13</sup>. It is therefore probable that their estimates of withdrawal are excessive by an order of magnitude or more. For example, Nace<sup>13</sup> wrote that "Pumpage from the Ogallala formation has reduced storage by nearly 110 km<sup>3</sup>, and annual withdrawals in recent years have been about 6.2 km<sup>3</sup>." Furthermore, Ambrogi<sup>14</sup> insists that the annual rate of irrigation storage clearly exceeds groundwater mining in arid areas. The total quantity of mined groundwater is difficult to determine, but probably amounts to less than 100 km<sup>3</sup> yr<sup>-1</sup>. Groundwater mining, if real and appreciable, would require a subtraction from reservoir and irrigation storage water accumulation in Fig. 1.

Trace *d* in Fig. 1 shows the result of adding the storage capacities of large and small reservoirs and irrigation projects (traces *a* and *b*) to the observed and extrapolated sea-level rise since 1932 (trace *c*). The result is a sea-level curve as it might have evolved had it not been for the several classes of anthropogenic continental water storage. The difference between the observed and projected sea-level curves *c* and *d* represents our estimate of the suppression of the 'true' sea level trajectory by continental water storage.

In addition to freshwater storage, it is also feasible to channel sea water into some of the world's great interior drainage basins which lie well below present sea level. Such potential sinks include the Imperial Valley of California, the Qattara Depression of northwestern Egypt, the Dead Sea rift valley of Israel and Jordan, the Salina Gaulicho of Argentina and the Eritrea (Lake Assale) depression in Ethiopia. All of these schemes also possess appreciable hydroelectric power potential. Marine diversion engineering feasibility studies already exist for the Dead Sea Basin and the Qattara Depression<sup>15,16</sup>. We estimate the storage potential of each of these depressions to be on the order of 1,000 km<sup>3</sup> or more.

The site with the greatest potential for freshwater storage is the Aral-Caspian depression, which lies within the Eurasian landmass. The Caspian Sea surface is at an elevation of -28 m and falling. Raising the level of the Caspian Sea by only 10 m would store 4,420 km<sup>3</sup> of water, which represents eight years of sea-level rise at 1.25 mm yr<sup>-1</sup>. The Soviet Union is already diverting water from the north-flowing Vychegda and Pechora rivers in European Russia, but this will serve only to reduce somewhat the rate of fall of Caspian Sea level<sup>17,18</sup>. The three northern Siberian rivers (Ob, Yenisey and Lena) discharge about 1,500 km<sup>3</sup> yr<sup>-1</sup>. Soviet engineers are

planning the diversion of these rivers towards the south for irrigation and hydroelectric power as well as the maintenance of the Caspian and Aral Sea levels<sup>19</sup>. Additional water will be retained in smaller upstream reservoirs as well as in soils and subsurface aquifers. The central Eurasian project is thus certainly a key element in sea-level management.

Still other major and minor sinks offer considerable water storage potential and other benefits. Examples include the Great Artesian Basin of Queensland and New South Wales in Australia, and the middle Niger and upper Zaire valleys (with spillways into the Chad Basin) in North Africa. The several-decades-old NAWPA (North America Water and Power Alliance) plan to divert surplus water from Canada into the United States<sup>20</sup> would store about 1,000 km<sup>3</sup> of fresh water in the Rocky Mountain Trench, equal to ~2.0 yr of sea-level rise at 1.25 mm yr<sup>-1</sup>. The plan also envisaged additional storage by the damming and partial revival of ancient proglacial lake basins and recharging of subsurface water aquifers. With water and sediment loading, isostatic downwarping of all these reservoirs would gradually increase their capacity by an estimated ten per cent, although some seismic risk is always involved with such continental crustal loading.

### Consequences

The major benefit of sea-level regulation is the mitigation of the damage inevitably caused by continuing littoral zone inundation. A cost-benefit estimate requires close study of the potential savings offered by the sea-level management option as compared to the money that would otherwise be invested in shoreline protection, the evacuation of populations and the abandonment of 'hopeless cases'. Note that there has already been considerable (if inadvertent) capital investment in sea-level management projects.

Major river diversion and storage will certainly have an impact on ocean dynamics and chemistry<sup>21</sup>. The potential oceanographic alterations are difficult to assess and the ecological consequences of our suggested hydrological cycle interruptions are largely unknown.

The 107 largest freshwater reservoirs already (or will before the end of this century) impound nearly 3,100 km<sup>3</sup> of fresh water (Fig. 1), and probably a similar quantity is already stored in the many smaller reservoirs. All this suggests that ~6,000 km<sup>3</sup> of water has been temporarily stored in surface reservoirs and prevented from flowing into the world ocean. This would be equivalent to 15.0 mm of sea-level rise or a 12-year lag in sea-level rise at 1.25 mm yr<sup>-1</sup>. In addition, irrigation projects have absorbed by infiltration ~125 km<sup>3</sup> yr<sup>-1</sup> since 1932, corresponding to nearly 7,000 km<sup>3</sup> of subsurface water

and equal to about 14 years of sea-level rise. Thus reservoir and irrigation storage have caused sea-level rise to lag about 26 years behind its projected uncontrolled rate of rise (Fig. 1). Mankind has thus unwittingly been exercising an appreciable control on sea-level rise. For the past 25 years, continental storage might account for a reduction of as much as 0.75 mm yr<sup>-1</sup> in eustatic sea-level rise.

For the immediate future, human ingenuity can undoubtedly find additional capacity to expand storage to accommodate 50 years of sea-level rise. An additional 5 mm of sea-level equivalent could be budgeted to correspond to the increased absolute humidity due to evaporation from all these reservoirs. We project that mankind will exhaust cost-effective water storage capacity near the middle of the next century, thus requiring the emergence of some other means of sea-level-rise management technology.

Although the unintentional sea-level management projects already completed and underway are indeed impressive, further sea-level management will require international cooperation on an unprecedented level. To prevent worldwide littoral disaster, new projects must be planned immediately, and be well underway by the end of this century. All littoral nations must work out some system of contributing to a fund to support these projects. Sea level rise joins 'death and taxes' as the inexorable fate of mankind. This 'fact of life' must be addressed and soon!

Dr Albert Kleine Bornhorst and Dr Michael Siebenhuner of Hannover, and Professor Dov Nir of Jerusalem provided helpful guidance concerning the Qattara and Dead Sea Projects. Dr David H. Speidel provided valuable data and welcome direction to sources of information. Earlier versions of this paper were read by David H. Speidel, Michael R. Rampino, Les Marcus, Sergej Lebedeff, Shaike Bornstein, Ann Kelly and Leonard J. Cinquemani. Considerable input came from our colleagues at the Goddard Institute for Space Studies where W.S.N. was a National Research Council Visiting Senior Research Associate in 1980-81 and has since continued his affiliation. Shaike Bornstein programmed and executed the figure. The research was supported by the Research Foundation of the City University of New York. This paper is a contribution to IGCP-200.

Walter S. Newman is at the Department of Geology, Queens College of the City University of New York, Flushing, New York 11367, USA. Rhodes W. Fairbridge is at the Department of Geological Sciences, Columbia University, New York, New York 10027, USA.

1. Gornitz, V. S., Lebedeff, S. & Hansen, J. *Science* **215**, 1611-1614 (1982).
2. Barnett, T. P. *Climatic Change* **5**, 15-85 (1983).

## REVIEW ARTICLE

3. IAPSO Advisory Committee on Tides and Mean Sea Level *Eos* 66, 754–756 (1985).
4. Fairbridge, R. W. & Krebs, D. A. *Geophys. J. R. astr. Soc.* 6, 532–545 (1962).
5. Meier, M. F. *Science* 266, 418–421 (1984).
6. Nierenberg, W. A. et al. eds *Changing Climate: Report of the Carbon Dioxide Assessment Committee*, 1983 (National Academy Press, Washington, 1983).
7. Barth, M. C. & Titus, J. G. (eds) *Greenhouse Effect and Sea Level Rise* (Van Nostrand Reinhold, New York, 1984).
8. Hoffman, J. S. in *Greenhouse Effect and Sea Level Rise* (eds Barth, M. C. & Titus, J. G.) 79–103 (Van Nostrand Reinhold, New York, 1984).
9. L'vovich, M. I. *World Water Resources and their Future* (American Geophysical Union, Washington, 1979).
10. Tilley, J. M. *Major Dams, Reservoirs and Hydroelectric Plants—Worldwide* (U.S. Bureau of Reclamation, Engineers and Research Center, Denver, 1983).
11. Postel, S. in *State of the World: 1985* (ed. Brown, L. R.) 42–72 (Norton, New York, 1985).
12. Korzun, V. I. (ed.) *World Water Balance and Resources of the World* (UNESCO, Moscow, 1978).
13. Nace, R. L. in *Water, Earth, and Man* (ed. Chorley, R. J.) 285–294 (Methuen, London, 1969).
14. Ambrogi, R. P. *Scient. Am.* 230, (5), 21–27 (1977).
15. Steering Committee for the Projected Inter-seas Water Conduit *Interim Report* pts 1, 2 (State of Israel, Ministries of Energy and Infrastructure and Finance, 1980).
16. Joint Venture Quattara *Quattara Depression Study Feasibility Report* (Lahmeyer International GmbH, Frankfurt, 1981).
17. Micklin, P. P. *Can. Geogr.* 13, 199–215 (1969).
18. Kelly, P. M., Campbell, D. A., Micklin, P. P. & Tarrant, J. R. *GeoJournal* 7 (3), 201–214 (1983).
19. Rich, V. *Nature* 317, 758 (1985).
20. The Ralph Parsons Co., North American Water and Power Alliance, Brochure 606–2934–19 (1967).
21. Holt, T., Kelly, P. M. & Cherry, B. S. B. *Ann. Glaciol.* 5, 61–85 (1984).
22. Gornitz, V. S. & Lebedeff, S. Spec. Publs Soc. econ. Palaeont. Miner. (in the press).

## REVIEW ARTICLE

**Transition region of the Earth's upper mantle****Don L. Anderson\* & Jay D. Bass†****\* Seismological Laboratory, California Institute of Technology, Pasadena, California 91125, USA****† Department of Geology, University of Illinois, Urbana, Illinois 61801, USA**

*The transition region of the Earth's upper mantle, 400–650 km deep, appears to be mineralogically and chemically distinct from both the shallow mantle and lower mantle. It contains most of the basalt fraction of the Earth's mantle.*

*"The transition layer appears to hold the key to a number of major geophysical problems"* (ref. 1).

THE Earth's mantle is conventionally divided into three major subdivisions: the shallow mantle, the transition region and the lower mantle. High seismic velocity gradients extend from 400 km, the top of the transition region, to ~800 km. The relatively homogeneous part of the lower mantle starts near 800 km and extends to within several hundred kilometres of the core-mantle boundary. Major changes in mantle mineralogy occur near 400 and 650 km (refs 2–6). The question of whether these represent equilibrium phase boundaries in a homogeneous mantle<sup>2,6,7</sup> or changes in chemistry<sup>8–13</sup> is fundamental to many problems in earth sciences. There is abundant evidence that the Earth as a whole is a differentiated body and is inhomogeneous on many scales. For example, the extreme concentration of trace elements in the continental crust requires efficient extraction of these elements from all or most of the mantle<sup>14,15</sup>. Nonetheless, the chemistry of the mantle remains a controversial issue which can be reduced to three basic questions: (1) is the mantle homogeneous in composition or is it chemically stratified? (2)

Is the major-element chemistry of the mantle more similar to upper mantle peridotites or to chondrites? (3) What is the composition of the source region of basalts erupted at mid-ocean ridges? We address each of these questions using data from cosmochemistry, geochemistry, petrology, seismology and mineral physics.

**Chondritic Earth**

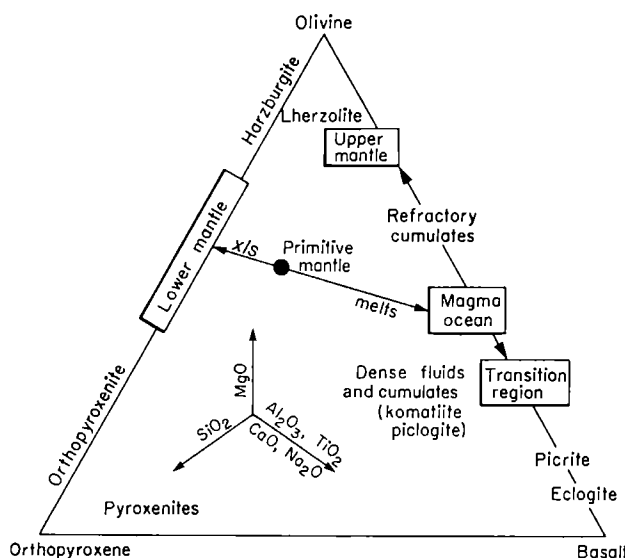
There is no *a priori* reason to believe that the major and refractory elements were not accreted into the Earth in cosmic (or solar) proportions. But several complicating factors need to be considered; for instance, meteorites and, presumably, the terrestrial planets are depleted to varying degrees in volatile elements such as Na, K, Rb and S. In igneous processes the most refractory crystals are MgSiO<sub>3</sub> (Ca-poor pyroxene) and (Mg, Fe)<sub>2</sub>SiO<sub>4</sub> (olivine) and the more fusible (basaltic) components are rich in CaO, Al<sub>2</sub>O<sub>3</sub> and TiO<sub>2</sub> and the incompatible trace elements, both refractory and volatile. Melting and melt separation fractionate the major elements, separate peridotite (olivine plus pyroxene) from basalt (Ca and Na-rich pyroxene plus an Al-rich phase), and concentrate the incompatible elements into the liquid fractions. Consequently, extensive melting during accretion separates materials having different crystallization temperatures and densities.

As it turns out, the assumption that the Earth has chondritic abundances of the major rock- and core-forming elements, with oxygen as the light element in the core, provides an excellent fit to the first-order parameters of the Earth such as mean density and size and density of the core (Table 1). The predicted size of the core is remarkably close to the actual size (32 wt%). The composition Fe<sub>2</sub>O for the core not only has the appropriate density<sup>16</sup> but also represents the amount of FeO that can be dissolved in molten Fe at core pressures<sup>17,18</sup>. The core will be slightly larger if it contains chondritic abundances of Ni and some S or if the mantle is less FeO-rich than assumed. Fe<sub>2</sub>O, being approximately the eutectic composition of melt in the Fe–FeO system at high pressure<sup>18</sup>, has a low melting point and drains to the core. This exercise supports the concept of a chondritic Earth for the major elements, which implies a pyroxene-rich mantle.

**Table 1** Estimates of cosmic abundances of the major refractory elements (expressed as wt% oxides) and estimates of the average composition of the subdivisions of the mantle

Cosmic abundances <sup>98</sup> mantle	Shallow mantle (average lherzolite) <sup>19</sup>	Transition region (piclogite) <sup>22</sup>	Lower mantle (cosmic- 20%) lherzolite- 10% piclogite)
MgO	36.6	42.2	36.8
Al <sub>2</sub> O <sub>3</sub>	3.67	2.05	3.4
SiO <sub>2</sub>	50.8	44.2	53.2
CaO	2.89	1.92	2.4
FeO	6.08	8.29	4.8
Core			
Fe <sub>2</sub> O	30.1		

The mantle Fe/Mg ratio is assumed for cosmic abundances<sup>98</sup>.



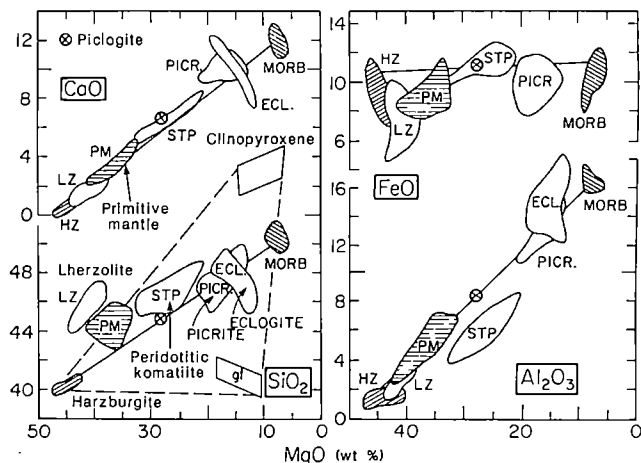
**Fig. 1** Schematic illustration of differentiation of primitive mantle (chondritic) during accretion (low-pressure melting) into melts (magma ocean) and refractory residue (x/s). Crystallization of the magma ocean separates minerals according to their crystallization temperature and density, giving a chemically stratified upper mantle.

Figure 1 illustrates the accretional differentiation of a chondritic Earth. Gravitational energy is delivered to the surface of a planet and melting and melt-crystal separation are, at least initially, low-pressure processes. A melt layer, or magma ocean, crystallizes refractory, low-density olivine, which is concentrated in the shallow mantle, in peridotite and lherzolite. The dense mineral garnet,  $(\text{Mg}, \text{Fe}, \text{Ca})_3(\text{Al}_2, \text{MgSi}, \text{FeSi}, \text{CaSi})\text{Si}_3\text{O}_{12}$ , crystallizes later and sinks. Residual fluid freezes to a clinopyroxene-garnet-rich mixture with some olivine, an assemblage we term piclogite.

Figure 2 gives the chemistry of a 'cosmic' mantle and several terrestrial rock types. The fields PM are estimates of upper mantle chemistry<sup>7,19,20</sup> including pyrolite, a hypothetical mixture of basalt and peridotite<sup>7</sup>. Piclogite is the inferred composition of the transition region from seismic data<sup>21,22</sup>. Most mantle rocks and magmas fall in the garnet-clinopyroxene-harzburgite (mainly olivine) field. Lherzolite and cosmic compositions have an orthopyroxene component. Piclogite falls approximately on the tie line between mid-ocean ridge basalts (MORBs) (and picrite) and harzburgite, thus satisfying a standard assumption about the basalt source region<sup>7,23</sup>; that is, the source of MORB contains both basaltic and refractory fractions. Piclogite is close in composition to komatiite, a common Precambrian rock type.

Primitive mantle, with cosmic ratios of refractory elements, contains the equivalent of 50% peridotite, 36% orthopyroxene and 9–14% MORB (Table 2). If basalts form by melting in the shallow mantle, where melt segregation can occur at relatively low degrees of melting, the MORB reservoir may contain only a small amount of basalt, ~20%. If this reservoir is deeper than 200 km, melt segregation is more difficult<sup>24,25</sup> and extensive melting can occur, resulting in instability of the source region, adiabatic ascent and extensive melting before eruption at mid-ocean ridges or intrusion into the shallow mantle. In this case basalt may represent a much larger fraction of the reservoir. The transition region, which we argue later is MORB plus up to 30% olivine, represents 11% of the mantle. The basalt fraction of the mantle may not be uniformly dispersed because the transition region itself could accommodate most of the basalt of the Earth.

Basaltic melts are buoyant at low pressure but are denser than olivine and pyroxene below some 200 km (ref. 24). Crystallization of basalt at high pressure yields dense eclogite. The original



**Fig. 2** Chemistry of primitive mantle and various products of mantle differentiation. Data from refs 15, 19, 20, 22. Piclogite, similar in composition to komatiites, satisfies the seismic data for the transition region<sup>22</sup>. Picrite may be the parent magma for MORBs (ref. 23). The lower mantle is the result of removal of lherzolite and picrite from cosmic abundances. The fields labelled PM refer to petrological models of the upper mantle (refs 7, 19, 20). Lherzolite (LZ) and harzburgite (HZ) are representative of shallow mantle peridotites. PICR, picrite; ECL, eclogite; STP, spinifex-textured peridotites. The shaded areas represent the most abundant rock types. Dashed lines enclose the HZ, Cpx, garnet field. The oxides (ordinate) are plotted against MgO (abscissa).

stratigraphy of the mantle would therefore be, from the top down, basalt, peridotite, eclogite and, at great depth, olivine orthopyroxenite, the high-pressure residual of the original differentiation. This is a gravitationally stable configuration except that when eclogite partially melts it becomes buoyant because of the elimination of garnet.

If the upper 400 km of the mantle is lherzolite<sup>19</sup> and the transition region is piclogite<sup>21,22</sup>, the composition of the lower mantle (Table 1) is considerably enriched in Si compared with lherzolite. The lower mantle in this model is 85 wt%  $\text{MgSiO}_3$  and 7.4 wt% (Mg, Fe)O. Upper mantle lherzolite, by contrast, has 22.2 wt% (Mg, Fe)O.

The measured Mg/Si ratio of peridotite is higher than in any meteorite class. This has been attributed to volatility and net depletion of the mantle in Si (ref. 26). However, basalt extraction causes an increase in Mg/Si and a decrease in density of the residue; this residue will therefore concentrate in the shallow mantle<sup>27–30</sup>. Ca-Al-rich chondrites are depleted in volatiles but still have a lower Mg/Si ratio than lherzolites. There is no reason to suppose that the Earth's mantle is depleted in Si but several reasons to suspect that upper mantle lherzolites have been depleted in Si by removal of basalt. Chondritic ratios of Ca/Al and Al/Mg limit the amount of basaltic material. Orthopyroxenite, a possibly important constituent of the lower mantle, is required to achieve chondritic ratios of Mg/Si.

The mantle + crust is depleted in volatile elements relative to carbonaceous chondrites<sup>14,15,31</sup>. Assuming that refractory elements occur with cosmic ratios, it is possible to estimate the

**Table 2** Components of primitive mantle (wt%) that yield chondritic ratios of refractory lithophiles

	Model 1	Model 2
Continental crust	0.55	0.55
Peridotite	52.2	49.2
Orthopyroxenite	38.0	35.4
Basalt (MORB)	9.3	14.4
Kimberlite	0.19	0.17

Composition of components from refs 15, 19, 79.

Table 3 Composition of primitive mantle based on multi-component petrological models

	Cosmic	Mantle		% Of element in:			
		Model 1	Model 2	Model 1		Model 2	
				Crust	MORB	Crust	MORB
Mg (%)	21.3	21.1	21.4	0.1	2.6	0.1	4
Al (%)	1.9	1.9	1.9	2.8	46	2.4	69
Si (%)	23.1	22.9	23.3	0.6	9.5	0.7	15
Ca (%)	2.0	2.0	2.0	1.5	43	0.9	67
Ti (%)	0.1	0.08	0.12	3.4	56	1.7	58
Sr (p.p.m.)	17.3	13.3	13.4	17	36	21	56
Ba (p.p.m.)	4.9	6.2	8.0	31	6	49	7
La (p.p.m.)	0.51	0.60	0.57	18	16	27	26
Yb (p.p.m.)	0.35	0.37	0.26	3	42	3	93
Th (p.p.m.)	0.06	0.064	0.051	41	4	55	8
U (p.p.m.)	0.02	0.019	0.015	35	9	47	19
Li (p.p.m.)	3.4	2.0	2.6	3	56	2	67
Na (%)	1.1	0.12	0.13	12	33	13	49
K (%)	0.12	0.035	0.017	19	8	56	27
Rb (p.p.m.)	4.97	0.41	0.50	56	4	68	5
Cs (p.p.m.)	0.41	0.02	0.01	62	1	67	2
Ratios							
Mg/Si	0.92	0.92	0.92				
Ca/Al	1.07	1.07	1.03				
Mg/Al	11.3	11.4	11.1				
La/Yb	1.48	1.61	2.19				
Ce/Yb	3.87	3.43	4.31				
Rb/Sr	0.288	0.031	0.037				

p.p.m., parts per  $10^6$ .

major- and trace-element chemistry of the mantle from various observed products of mantle differentiation<sup>15</sup>. Attempts to do this with three-component systems (crust, basalt and peridotite for major elements<sup>32</sup>, or crust, depleted mantle and primitive mantle in isotope studies<sup>33,34</sup>) fail to give chondritic ratios for all refractory lithophile elements or for key major-element ratios as Mg/Si. To span the trace-element and isotope chemistry of basalts and the major-element chemistry of ultramafic rocks, it is necessary to involve at least four components<sup>15</sup>. The crust is also an essential component of primitive mantle. We therefore treat primitive mantle as a five-component system (crust, basalt (MORB), enriched magma (kimberlite or ocean-island basalt), Iherzolite and pyroxenite) and solve for the mixing ratios which give chondritic ratios for the refractory lithophile elements. Typical solutions are given in Table 2. The peridotite component varies from ~47 to 60% depending on its fertility (that is, Al<sub>2</sub>O<sub>3</sub> and CaO content). The enriched component is ~0.2% if it is similar to kimberlite and somewhat more if it is similar to ocean-island basalts or recycled crust. The MORB content of primitive mantle ranges up to 14 wt%, the amount depending, again, on the fertility (or basalt content) of the peridotite.

The continental crust contains >30% of the large and high-valence ions (Table 3). MORB is complementary to continental crust, being depleted in the very incompatible elements and enriched in Ca, Al, Hf, Yb, Y and other elements that substitute for Al and Ca in garnet. The enriched mantle component, required because of the enriched nature of ocean-island basalts<sup>35</sup>, xenoliths<sup>36</sup> and kimberlites<sup>37,38</sup>, may represent subducted crust or material left over from inefficient melt removal from the mantle. We use kimberlite to model this material but, for most elements, continental crust or ocean-island basalts would serve as well. Table 3 gives results from two mass-balance calculations, including the fraction of various elements contained in the crust and in the basalt part of the MORB reservoir. The extreme enrichment of some elements in the continental crust provides strong evidence against a substantial primitive, undifferentiated reservoir in the mantle. The whole mantle must be processed to obtain these enrichments; most of the mantle must therefore be depleted in these elements. The most efficient way to accomplish this separation is during the melting and vaporization associated with accretion. Stripping incompatible

elements out of the mantle by subsequent melting is much less efficient—the last fraction of melt is difficult to remove. The concentration of W, Cs, Rb and Th in the continental crust is such that >50% of the mantle must have been completely stripped of these elements. The MORB source contains a large fraction of the mantle's inventory of Al, Ca, Ti, Sr, Li, Na and the heavy rare-earth elements (HREE) and high concentrations of the light rare-earth elements (LREE), Sr, Y, Zr, Hf, Na, Li, U and Ta. These elements are presumably sequestered at depth in clinopyroxene and garnet, the major minerals of eclogite. The continental crust is excessively enriched in elements with large ionic radius or high charge, whereas MORB is enriched in elements with ionic radii between Al<sup>3+</sup> and Ca<sup>2+</sup>.

These results strongly suggest an extensively differentiated Earth, probably involving a deep magma ocean in early Earth history. In contrast to the Moon, the terrestrial crust is trivial in volume. It does not contain most of the Ca<sup>2+</sup> and Al<sup>3+</sup> of the planet and it is deficient in elements which can be removed from a melt by the crystallization of garnet and clinopyroxene. MORBs are enriched in these elements, suggesting that they are melts from a deep eclogite-rich layer, the terrestrial equivalent of the thick lunar crust. The fact that the roots of mid-ocean ridges can be traced by seismic techniques to depths of the order of 400 km<sup>39-42</sup> and that the transition region appears to be garnet-rich rather than olivine-rich<sup>21,22,43</sup>, support the notion that the transition region is the major basalt reservoir. The transition region would then contain much of the mantle inventory of the HREE, Al, Ca, Ti, Sr, Li and Na, leaving a lower mantle depleted in Ca, Al, Ti and incompatible elements including U, Th and K. If the shallow mantle is predominantly residual or cumulate olivine, the most refractory mantle mineral at low pressure, the lower mantle will be even more pyroxene-rich than primitive mantle. Trace element-modelling (including rare-earth elements, REE) of MORB genesis requires that most of the garnet and clinopyroxene in the source be consumed by the melting process<sup>27-30</sup>.

### Upper mantle and 400-km discontinuity

The upper mantle includes the seismic lithosphere, which averages ~40 km in thickness under ocean basins<sup>44</sup> and 150 km under stable shields<sup>45</sup>. The shield lithosphere and the top of the

oceanic lithosphere have seismic properties consistent with peridotite<sup>46</sup>. The lower oceanic lithosphere may be garnet- rather than olivine-rich<sup>8,46</sup>. The 150-km-thick shield lithosphere is probably buoyant with respect to oceanic lithosphere and the underlying mantle, which explains its long-term stability<sup>46</sup>.

Seismic velocities decrease at 20–50 km under oceans and 150 km under shields, indicating a change in mineralogy and, for some regions, the presence of a melt phase. Seismic velocities are so low in some regions that partial melting is implied to depths at least as great as 300 km (ref. 46). Under some mid-ocean ridges low velocities extend to 400 km (refs 39–42).

Seismic velocities increase abruptly at 400 km, which is usually attributed to the olivine-spinel phase change. However, the velocity jump associated with this transformation<sup>47,48</sup> is ~20% and is spread over an appreciable depth interval<sup>5,49,50</sup> whereas the observed jump is 4–5% and is rather abrupt. The other important minerals of the mantle, pyroxenes, transform to garnet solid-solution assemblages (garnetite), primarily between 350–400 km for orthopyroxene<sup>50–52</sup> and somewhat greater depth for clinopyroxene<sup>53</sup>. The associated velocity increase is greater than for the olivine-spinel transformation<sup>61,62</sup>; this places an upper bound on the olivine plus orthopyroxene content of the mantle near 400 km. Garnet and possibly jadeite ( $\text{NaAlSi}_2\text{O}_6$ ) survive to high pressures<sup>54</sup>, dilute the effects of the other minerals and reduce the size of the discontinuity. If the mantle above 400 km is mostly olivine and orthopyroxene, the 400-km discontinuity must involve a change in chemistry.

### Transition region

In early seismological models the transition region was characterized by a rapid but smooth increase in seismic velocities between 400 and 1,000 km depth. As the quality of seismic data improved, the transition region was found to be more complex than originally thought. Abrupt changes in velocity were found at ~400 and 650 km (refs 55–60). Recent models<sup>41,42,45</sup> have velocity jumps of 4–6% at each discontinuity, high gradients between the discontinuities and below the deeper one to ~750 or 800 km (refs 41, 42, 44).

The major minerals in shallow mantle peridotites are olivine [ $(\text{Mg}, \text{Fe})_2\text{SiO}_4$ ] and orthopyroxene [ $(\text{Mg}, \text{Fe})\text{SiO}_3$ ]. Olivine collapses to the  $\beta$ -spinel structure at ~400 km, with a large increase in density and elastic properties, and to  $\gamma$ -spinel at ~500 km, with a small change in physical properties<sup>47</sup>. Phases with lower seismic velocities are required to satisfy the seismic constraints. Garnet and clinopyroxene, a solid solution of diopside [ $\text{Ca}(\text{Mg}, \text{Fe})\text{Si}_2\text{O}_6$ ] and jadeite, have the appropriate characteristics, but these are minor minerals in peridotite. Orthopyroxene transforms to a garnet-like phase, majorite, starting at ~300 km. The modulus of majorite<sup>61</sup> is much higher than garnet or spinel and the modulus in the transition region<sup>21,22,62</sup> would exclude a spinel-majorite mineralogy (but see ref. 100).

The seismic properties of  $\beta$ - and  $\gamma$ -spinel are similar<sup>47,48</sup> and only a small discontinuity would result from the  $\beta$ - $\gamma$  transformation. The orthopyroxene-majorite transition is complete at depths of the order of 400 km (refs 50–53). The only further transformation expected at transition-zone pressures is the garnetite-to-ilmenite structure phase change, which probably gives a slight increase in velocity. Aside from a change in chemistry the only way to explain the low velocities and high gradients in the transition zone is that clinopyroxene transforms to a Ca-rich garnet-like phase analogous to majorite. This transition is spread out over a broad pressure interval and is much deeper than the corresponding transition in orthopyroxene<sup>53</sup>. Thus, the velocities, the velocity gradient and the great depth of the mixed-phase region all argue for a clinopyroxene-garnet-rich transition region, with the clinopyroxene gradually changing to a Ca- and Si-rich garnet. Whether the above inferences are plausible depends on the high-pressure stability of clinopyroxene and garnet.

There have been several attempts to model the seismic

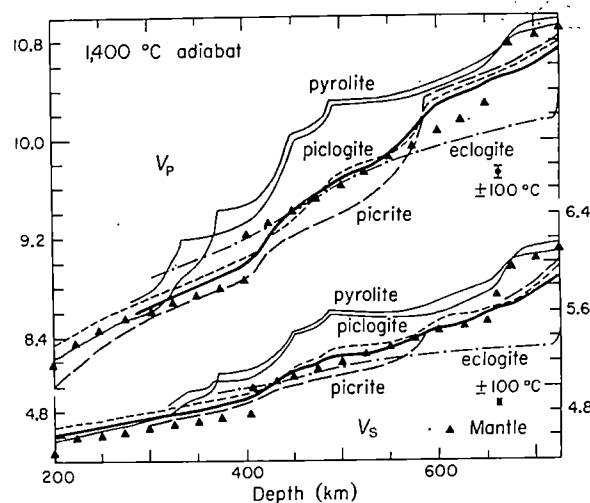


**Fig. 3** Compressional ( $V_p$ ) and shear ( $V_s$ ) velocity as a function of depth for PREM (triangles<sup>95</sup>) and for various petrological models, using finite strain theory<sup>64</sup> and parameters summarized in refs 22 and 50. Phase relations modified from refs 5, 50, 52, 53, including the pressure correction of ref. 50. The rapid increases in velocity are caused primarily by orthopyroxene-majorite, olivine-spinel, clinopyroxene-majorite, spinel to perovskite plus magnesiowustite and garnet-majorite to perovskite. The garnet-ilmenite transition is ignored. Piclogite contains more olivine and less garnet than picrite and eclogite. Heavy solid lines, piclogite; thin solid lines, pyrolite; long dashed lines, picrite; dot-dashed lines, eclogite; short dashed lines, a garnet pyroxenite. If the new  $K_s$  value for majorite (ref. 100) is used instead of the Jeanloz value (ref. 61) then the velocities in pyrolite are lower but the shape and gradient are still wrong. PREM, preliminary reference Earth model.

velocities in the transition region for olivine- and orthopyroxene-rich (for example, peridotite) compositions<sup>21,62</sup> using mineral physics and phase-equilibrium data<sup>2,3,10,21,22,62</sup>. The velocities, gradients and discontinuities are not well matched by homogeneous peridotite models. Using current estimates of appropriate phase diagrams<sup>22,49–53</sup> and finite strain theory<sup>63,64</sup> we have calculated seismic velocities for several mineralogical assemblages (Fig. 3). Picrite and eclogite are garnet- and clinopyroxene-rich rocks with different garnet/clinopyroxene ratios. The composition of piclogite is given in Table 1 and Fig. 2. It is clear that the velocities in pyrolite are higher than observed. The heavy solid line, piclogite (Fig. 3), results from an attempt to satisfy the velocities between 200 and 650 km by a single, homogeneous mineralogy. Note that the 400- and 650-km discontinuities are not well matched. It seems therefore that neither of them can be modelled as equilibrium phase boundaries. Eclogite and piclogite, with appropriate garnet/clinopyroxene ratios, satisfy the data between 400 and 550 km. In the eclogite model the 400-km discontinuity would be a chemical change from peridotite to eclogite. In the piclogite model the discontinuity is mostly caused by the olivine- $\beta$  transition. Piclogite contains 30 wt% olivine.

Weidner<sup>65</sup> calculated seismic velocities in the transition region and his results apparently support the pyrolite model for depths between 400 and 500 km. He assumes, however, that majorite has the same shear modulus,  $G$ , as garnet despite the fact that the bulk moduli,  $K_s$ , differ by >20%. Our estimate of  $K_s/G$  for majorite, 1.86, is similar to other garnets and in the typical range for Fe-poor silicates. Weidner's value, 24% greater, is representative only of Fe-, Co-, Cd- and Ge-rich compounds, but these have very low  $K_s$  compared with majorite. Fe-poor and high- $K_s$  oxides and silicates all have  $K_s/G < 1.9$ . Weidner's model also has appreciable orthopyroxene, a low-velocity phase, present to depths as great as 500 km, whereas orthopyroxene has transformed to majorite by 400 km in our calculations. Below 500 km the two studies agree in that the compressional velocity

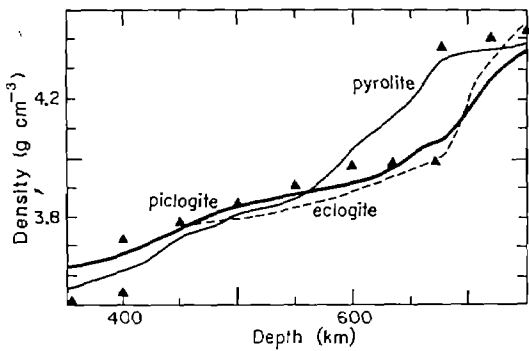


Fig. 4 Density versus depth calculated for various petrological models along the 1,400 °C adiabat. Note that piclogite and eclogite are gravitationally stable in the transition region and olivine-rich assemblages, such as pyrolite, are stable in the shallow mantle. ▲, PREM. Heavy solid line, piclogite; thin solid line, pyrolite; dashed line, eclogite.

for pyrolite exceeds the seismic values. Even if majorite has elastic properties similar to garnet<sup>100</sup> the velocities in pyrolite would be too high below 400 km.

It is interesting to compare the density profiles for pyrolite, piclogite and eclogite (Fig. 4). Eclogite and piclogite have low densities to ~670 km and approach lower mantle values near 750 km. The seismic resolution of density is poor but the strong reflector near 650 km implies an abrupt jump in density as well as in velocity. None of the isochemical models has this characteristic, but a chemical change from eclogite or piclogite to  $MgSiO_3$ -perovskite would have the correct magnitude of jump. The density jump in a pyrolite mantle is large but diffuse, and the changes in elastic properties are also probably diffuse. Therefore, phase changes in pyrolite do not explain the 650-km discontinuity. Note that piclogite and eclogite are less dense than pyrolite and the mantle between 670 and 750 km. Eclogite-rich assemblages will therefore be unable to sink into the lower mantle. Ringwood<sup>66</sup> reached the opposite conclusion because of the large amount of stishovite (a dense polymorph of  $SiO_2$ ) in his quartz eclogite and because he assumes that  $CaSiO_3$  forms perovskite, rather than garnet-majorite, and that it is denser than the lower mantle. It is more likely that  $CaSiO_3$  is present in diopside or garnet rather than as an isolated phase. Refractory peridotite is less dense than fertile peridotite or piclogite and will concentrate in the shallow mantle. The bulk of the material subducting into the transition region may be eclogitic, possibly an important constituent of the lower oceanic lithosphere.

The main disagreement between piclogite and seismic data is the increase of the velocity anomaly  $V_p$  in piclogite at a depth of 550 km caused by the garnet-perovskite phase change. It is probable that garnet transforms to perovskite via an intervening field of lower-velocity ilmenite. A thermal boundary layer at 650 km combined with a positive Clapeyron slope would also increase the depth of this phase change. The mineralogy implied by the seismic velocities can be used to calculate the density contrasts across the 400- and 650-km transitions. These are 3 and 10%, respectively. The effect of temperature, including phase changes and partial melting, can reverse the density contrast at 400 km but is unlikely to be able to do so at 650 km. A chemical change at 650 km, perhaps depressed to 720 km under subduction zones<sup>67</sup> and elevated to 620 km in warmer parts of the mantle<sup>68,69</sup>, is consistent with the abrupt termination of seismic activity<sup>70</sup>, the focal mechanisms of deep earthquakes<sup>71,72</sup> and the deep resistance encountered by slabs<sup>73</sup>.

### Lower mantle mineralogy

The 650-km discontinuity was discovered and characterized<sup>55-60</sup> in the 1960s and is therefore one of the most recently mapped major features of the mantle. In the context of an olivine-rich mantle the discontinuity was interpreted as a phase change from

the spinel form of olivine to a hypothetical post-spinel phase, with silicon in octahedral coordination and an increase of FeO content<sup>2,3</sup>. Thus, from the beginning, there has been an element of both a phase change and a chemical change associated with the interpretation of this boundary. Uncertainties in crystal structures and elastic properties of high-pressure phases, however, made it difficult to exclude a purely equilibrium-phase boundary. This interpretation required a strongly negative Clapeyron slope for the reaction<sup>2</sup> and a particularly high density and bulk modulus for the post-spinel phase<sup>3,7</sup>. Later work showed that the density and elastic properties of the lower mantle were higher than the post-spinel phase. A lower mantle stoichiometry closer to pyroxene than to olivine, and closer to chondritic than to peridotitic, was proposed<sup>3,8-13,63</sup>. Although it is difficult to estimate the FeO content of the lower mantle<sup>6,8,74</sup>, variations in the  $SiO_2$  content have large effects on the seismic velocities<sup>11</sup>, whether the  $SiO_2$  is in stishovite or perovskite<sup>8,11-13</sup>.

The 650-km discontinuity is a good reflector of short-period seismic energy. To be a good reflector requires a large increase in density and velocity over a small fraction of a wavelength, perhaps 3–4 km (refs 62, 68, 75, 76). Most phase changes in mantle silicates are second order and are spread over 20 km or more<sup>50</sup>. Reflections and conversions of seismic waves have been reported from depths ranging from ~590 to 720 km (refs 67–69, 75). Thus, there is a possible range of 130 km in the depth of the 650-km discontinuity.

Earthquake activity terminates abruptly near 670 km. Detailed studies indicate that the Tonga–Fiji slab encounters a barrier at 670 km, then shortens and thickens<sup>71</sup>. The transition to horizontal shear in the deepest part of the seismic zone is evidence of the strong resistance experienced by subducted material at the discontinuity. Material appears to move laterally rather than vertically at the base of the seismic zone<sup>71</sup>. High velocities below some deep-focus earthquakes in the Kuriles<sup>77</sup> could be caused by anisotropy, with high velocities in the flow plane, or to deformation of the interface (ref. 78; B. Marsh and B. Hager, personal communication) and detachment of a boundary layer at the top of the lower mantle.

In a cold slab the stable form of orthopyroxene below some 570 km is the ilmenite rather than the garnet structure<sup>79</sup>. Ilmenite is remarkably anisotropic<sup>80</sup> (16% for  $V_p$ , 34% for  $V_s$ ). If it crystallizes with its principle axes in the plane of the slab, then seismic waves travelling down dip and along strike will be very fast compared with waves that travel along the slow intermediate directions or exit the slab early to enter the warmer adjacent mantle with lower velocity and more isotropic phase assemblages. This would give residuals having similar characteristics to a deeply penetrating slab. Craeger and Jordan<sup>77</sup> use observations on olivine-rich rocks to dismiss the importance of anisotropy, but olivine, of course, is not stable at the required depths. Ilmenite differs from olivine in the manner required to explain the observations, in particular in the magnitude and orientation of the S-anisotropy, without requiring slab penetration into the lower mantle. The deep slab penetration model<sup>77</sup> requires a large (5%) velocity anomaly in the slab at great depth, much larger than found at shallower depths<sup>81</sup>. Actually, slab material may be less dense and have slower seismic velocities than the lower mantle (Fig. 4), particularly if ilmenite is present. The high gradient of seismic velocity between 650 and 750 or 800 km implies a high density gradient. Slabs may therefore penetrate ~100 km into the lower mantle before they become buoyant. A similar amount of depression of the boundary by the cold slab is also possible. Crumpling of the slab at 650 km (ref. 71) will destroy its slab-like character even if it can sink into the lower mantle. The correlation of geoid highs with subduction regions also indicates a strong resistance of slab material to penetration into the lower mantle<sup>73</sup>. The 650-km discontinuity may be composed of two reflectors 40 km apart<sup>69</sup>, which may be further evidence for a slab lying on the discontinuity<sup>71,72</sup>.

There is general agreement that a change in mineralogy (that is, change in crystal structure or phase) occurs near 650 km. Early thermochemical models viewed the discontinuity as an equilibrium phase boundary between olivine in the spinel structure and a homogeneous post-spinel phase having the properties of the constituent oxides. The nature of this post-spinel phase was unknown. Analogue and shock-wave data ultimately lead to the proposal that  $(\text{Mg}, \text{Fe})\text{SiO}_3$  (perovskite) and  $(\text{Mg}, \text{Fe})\text{O}$  are the dominant phases<sup>82-84</sup>. Perovskite is stable at depths  $>750$  km and at lower pressure if the Clapeyron slope is negative<sup>82-94</sup>. Perovskite was predicted to have a slightly higher bulk modulus than the mixed oxides<sup>8-11</sup> and this is confirmed by recent measurements<sup>85</sup>. The lower mantle, below 800 km, had velocities in excess of those predicted for peridotite and conclusions regarding a pyroxene-rich mantle were supported<sup>8,11</sup>. The conclusion that the lower mantle is pyroxene-rich is independent of the mineralogy, that is, perovskite +  $(\text{Mg}, \text{Fe})\text{O}$  or  $(\text{Mg}, \text{Fe})\text{O}$  + stishovite. The uncertainties in the elastic properties of the two assemblages overlap.

Three methods have been used to infer lower mantle composition: (1) extrapolation of laboratory data to lower mantle conditions<sup>9,10</sup>; (2) comparison of seismic and shock-wave data<sup>8,12</sup>; and (3) extrapolation of seismic data to standard conditions<sup>3,11,63</sup>. The last method is the most accurate and involves the fewest assumptions. The seismic data themselves are used to estimate density, elastic properties and pressure derivatives and to test for adiabaticity and homogeneity.

The seismic parameter  $\Phi = K_s/\rho = V_p^2 - (4/3)V_s^2$ , inferred from seismic, compression and ultrasonic data, is a useful diagnostic of crystal structure and  $\text{SiO}_2$  content ( $K_s$ ,  $\rho$ ,  $V_p$  and  $V_s$  are the bulk modulus, density, compressional and shear velocities, respectively.) The variation of  $\Phi$  with depth in most of the lower mantle is consistent with the assumptions of homogeneity and adiabaticity<sup>11,95</sup> which are required to extrapolate to pressure ( $P = 0$ ) to obtain  $\Phi_0$  and  $\rho_0$ . The major minerals of the lower mantle can have similar densities<sup>12,86</sup> but quite different  $\Phi$ .

Si coordination and the Si-O bond distance are the same for perovskite and stishovite<sup>94</sup>. Therefore,  $K_s$  and  $\Phi$  of the lower mantle depend on  $\text{SiO}_2$  content and are nearly independent of details of the mineralogy.  $\text{SiO}_2$ , whether in perovskite or stishovite, increases  $\Phi$  whereas  $\text{CaO}$ ,  $\text{FeO}$  and  $\text{MgO}$  decrease it. Tables 4 and 5 give  $\Phi$  values for possible lower mantle assemblages including lherzolite, undepleted and depleted cosmic mineralogies and pure  $\text{MgSiO}_3$  (perovskite). Also given is the seismic  $\Phi$  corrected for temperature and pressure;  $\Phi_0(P=0)$  is  $54 \pm 2 \text{ km}^2 \text{ s}^{-2}$ . Assuming an adiabat (temperature  $T_0 = 1,400-1,800^\circ\text{C}$ ) yields  $\Phi_0$  in the range  $62 \pm 3 \text{ km}^2 \text{ s}^{-2}$ . Olivine, with equal molar proportions of  $\text{MgSiO}_3$  (perovskite) and  $(\text{Mg}_{0.8}\text{Fe}_{0.2})\text{O}$ , gives  $52 \text{ km}^2 \text{ s}^{-2}$ . Pure perovskite gives  $63 \text{ km}^2 \text{ s}^{-2}$ . Clearly,  $\Phi_0$  for an olivine or lherzolite lower mantle is too low; the pyroxene and cosmic models, with  $\text{SiO}_2 > 52$  wt %, provide a good fit. The differentiated cosmic model is cosmic composition minus a lherzolite shallow mantle and a piclogite transition region. Barren cosmic is calculated by removing all of the basaltic fraction from primitive mantle. The increase in  $\Phi$  associated with phase changes in lherzolite ( $\gamma$ -spinel + majorite) to the post-spinel phases is too small to be consistent with the observed increase unless the  $K_s$  (majorite) of ref. 61 is too high.<sup>100</sup> There is a trade-off between the effects of composition and temperature<sup>12,50,87</sup>, but the low value of thermal expansion implied for perovskite in a pyrolite model<sup>87</sup> is unlikely<sup>88</sup>. Thus, the composition of the lower mantle is consistent with a differentiated chondritic Earth model.

### Surface-wave tomography

Surface-wave tomography<sup>39,40,96</sup> has put regional seismic studies into a global context. The low-velocity layer is not a uniform global layer of constant thickness. It rises to the near surface under young oceanic, back-arc and extensional regions and is

Table 4 Seismic parameter  $\Phi$  at  $P = 0$

	$\Phi$ ( $\text{km s}^{-1}$ ) <sup>2</sup>
Lower mantle	
High temperature	53.4
Corrected for temperature	$63 \pm 2$
Perovskite	$62 \pm 6$
$\text{Al}_2\text{O}_3$	63.4
$\text{SiO}_2$ (stishovite)	73.7
$\text{MgO}$	47.4
$(\text{Mg}_{0.8}\text{Fe}_{0.2})\text{O}$	40.8

Data from refs 11, 12, 50, 61, 87, 94, 99.

Table 5 Composition and seismic parameter  $\Phi$  for minerals, mineral assemblages and the lower mantle

	$\text{SiO}_2$	$\text{MgO}$ wt %	$\text{Al}_2\text{O}_3$	$\Phi$ ( $\text{km s}^{-1}$ ) <sup>2</sup>
Transition region minerals				
$\gamma$ -Spinel	43	57	0	50.3
Majorite	60	40	0	$62.5^*$
Lower mantle assemblages				
Iherzolite	44.8	42.8	2.08	55.2
Post-spinel	43	57	0	55.4
Perovskite	60	40	0	53.4
Cosmic				
Undifferentiated	50.8	36.6	3.67	58.3
Differentiated	52.4	38.7	2.64	59.2
Barren	50.4	44.3	0	58.0
Lower mantle observed				$63 \pm 2$

\* Ref. 61.  $\Phi = 45.5$  from ref. 100.

deep,  $>150$  km, and less pronounced under shields. In many regions low velocities can be traced down to the transition region, although the global pattern below 400 km bears little relation to surface tectonics. Partial melting is implied for the slower regions<sup>46</sup>. The low velocities associated with magmatic centres seem to be broad upwellings originating at depths at least as great as 400 km.

The most pronounced regions of inferred upwelling in and above the transition region are: North Atlantic, Darwin Rise, North-East Africa and South-East Asia. Most of these have low velocities at the top of the lower mantle<sup>97</sup>, lie in geoid highs and have high average elevations. The correlation with velocities at the top of the lower mantle indicates that material could be rising through the 650-km discontinuity or that hot regions in the lower mantle control the locations of hotspots in the upper mantle.

Thus, seismic tomography has provided both the first global view of the structure of the mantle and evidence that it is not a simple layered system. Heterogeneities in velocity and anisotropy imply that magmas are generated from reservoirs deep in the upper mantle or transition region. The recognition that mid-ocean ridges are deeply rooted suggests that entrainment and melting of shallow mantle, and magma mixing, could be associated with the uplift of the MORB source or ascent of its separated magma. The view that emerges is of broad, deep upwellings, some of which are associated with ridges and continental rifts. Oceanic crust and other extrusives probably represent only a small fraction of the molten material delivered to the upper mantle. The rest presumably spreads laterally and is available for off-ridge volcanism and underplating of the lithosphere. The oceanic lithosphere may, in fact, thicken by underplating of material similar to the parent magma of oceanic basalts, giving a dense, eclogite lower lithosphere. The view of a homogeneous partially molten peridotitic asthenosphere extending to  $\sim 200$  km and passively providing basalts to mid-

ocean ridges clearly must be abandoned. The MORB source is much deeper but the shallow mantle may be the holding tank for large amounts of picritic material and the repository for light differentiation products of all ages, including peridotite.

## Discussion

There are no inconsistencies with a chondritic Earth when the major and refractory elements are considered. The silicon deficiency hypothesis is unnecessary. Seismic data are consistent with a differentiated Earth having a peridotite shallow layer, a basalt-rich transition region, a pyroxene-rich lower mantle and a dynamically stratified upper mantle. Isotope data show that mantle inhomogeneities are ancient, possibly developing during the accretion of the Earth and its high-temperature early history. The energy of accretion is adequate to melt or even vaporize the infalling material. A thick early atmosphere and buoyant insulating layers in the upper mantle would delay crystallization of melts trapped at depth and promote gravitational stratification during accretion, cooling and crystallization.

Much of the discussion of whole mantle against layered convection focuses on the roles of viscosity, mean atomic weight and phase changes. These effects alone can probably not prevent whole-mantle convection. On the other hand, an isoviscous mantle with constant mean atomic weight can be chemically stratified. For example, a differentiated planet with a feldspar-rich crust, an olivine-rich shallow mantle, a garnet-rich transition region and a perovskite lower mantle is gravitationally stable. Variations in  $\text{SiO}_2$ ,  $\text{MgO}$  and  $\text{Al}_2\text{O}_3$ , which have similar mean relative molecular mass, control the stable mineral assemblages which, in turn, determine the intrinsic density and seismic properties.

Chemical stratification of the mantle is a natural consequence of melting and melt-solid separation. Basalts and cumulates are examples of these processes; the crust and core are more global manifestations. Convective stirring to maintain or regain homogeneity is a process for which there is little support. A chemically stratified mantle does not imply that each layer is isotopically homogeneous on a global basis. Mixing and homogenization may take place in a given convection cell or between adjacent cells but there is little communication between opposite sides of the Earth. In a dynamically stratified Earth the shallow mantle is enriched at various times by subduction of sediments and altered oceanic crust, and by upward migration of melts. A deeper reservoir may provide the bulk of the material erupting at oceanic islands, mid-ocean ridges and mid-plate environments.

A garnet- and clinopyroxene-rich region is stable at depth when it is cold but is buoyant when it is hot or partially molten. Therefore, it can be responsible for both radial and lateral inhomogeneity in the upper mantle. The broad stability field of garnet-majorite prevents it from converting to perovskite and sinking into the lower mantle. Although the lower mantle may be convecting, it can be isolated chemically, but not thermally, from the upper mantle because of its high intrinsic density. In contrast, the density differences between the shallower layers can be reversed by high temperature, partial melting and phase changes.

Differentiation of the Earth leads to boundaries which separate materials differing in both mineralogy and composition. Basaltic melts rise until they become neutrally buoyant or until trapped by the lithosphere. Subducted basalt and melts intruded at depth convert to eclogite and sink. Phase changes in basalt-eclogite occur at different depths from those in olivine- and orthopyroxene-rich materials. Thus, if the 650-km discontinuity were initially an equilibrium-phase boundary in a homogeneous mantle, subducted eclogite or a piclogite cumulate would not be able to sink through the boundary if the transformation of  $\text{CaO-Al}_2\text{O}_3-\text{Na}_2\text{O}$ -rich garnetite to denser phases occurs at greater pressure or results in less-dense minerals than involved in the original equilibrium phase boundary.

We refer to the mantle as dynamically stratified in contrast to the static layering which is the ultimate fate of a cooling planet. When the intrinsic density difference between reservoirs is smaller than temperature-induced variations in density, overturn can occur. These density variations are caused by thermal expansion and by phase changes such as basalt-eclogite, exsolution of pyroxene and partial melting. Thus, piclogite or fertile peridotite is denser than residual peridotite when cold but can be less dense when hot. Adiabatic ascent of the deeper material can cause melting in both layers, entrainment and mixing leading to a lumpy shallow mantle, and magmas which span a large chemical and isotope range. Crystal fractionation of hybrid magmas before eruption induces even more spread in their geochemical characteristics. These phenomena, as well as subduction, create isotope heterogeneities in the shallow mantle. A dynamically stratified mantle and a shallow mantle, heterogeneous on all scales, can coexist. The high density of cold eclogite, and the low density of hot eclogite or basalt, however, means that material of basaltic chemistry will eventually separate from material of peridotite chemistry with only the smaller basaltic accumulations being potentially trapable in the shallow mantle.

We thank B. Hager, E. Stolper, B. Marsh, M. O'Hara and S. Maaloe for stimulating discussions and R. Jeanloz, D. Yuen and D. Weidner for preprints. This work was supported by NSF grants EAR-8115236 and EAR-8317623, and NASA grant NSG-7610. Contribution 4206, Division of Geological and Planetary Sciences, California Institute of Technology.

1. Birch, F. *J. geophys. Res.* **57**, 227–286 (1952).
2. Anderson, D. L. *Science* **157**, 1165–1173 (1967).
3. Anderson, D. L. *Miner. Soc. Am. Spec. Pap.* **3**, 85–93 (1970).
4. Ringwood, A. E. *Phys. Earth planet. Inter.* **3**, 109–155 (1970).
5. Akimoto, S., Matsui, Y. & Syono, Y. in *The Physics and Chemistry of Minerals and Rocks* (ed. Strens, R.) 327–364 (Wiley, New York, 1976).
6. Anderson, D. L. *Geophys. Res. Lett.* **3**, 347–349 (1976).
7. Ringwood, A. E. *Composition and Petrology of the Earth's Mantle* (McGraw-Hill, New York, 1975).
8. Anderson, D. L. *Adv. Earth planet. Sci.* **5**, 179–202 (1977).
9. Gaffney, E. S. & Anderson, D. L. *J. geophys. Res.* **78**, 7005–7014 (1973).
10. Burdick, L. J. & Anderson, D. L. *J. geophys. Res.* **80**, 1070 (1975).
11. Butler, R. & Anderson, D. L. *Phys. Earth planet. Inter.* **17**, 147 (1978).
12. Watt, J. P. & Ahrens, T. J. *J. geophys. Res.* **87**, 5631–5644 (1982).
13. Sawamoto, H. in *High Pressure Research* (eds Manghnani, M. & Akimoto, S.) 219–244 (Academic, New York, 1977).
14. Gast, P. in *The Nature of the Solid Earth* (ed. Robertson, E. C.) 19–40 (McGraw-Hill, New York, 1972).
15. Anderson, D. L. *J. geophys. Res.* **88**, B41–B52 (1983).
16. Bullen, K. E. *The Earth's Density* (Chapman & Hall, London, 1975).
17. Ohtani, E. & Ringwood, A. E. *Earth planet. Sci. Lett.* **71**, 85–93 (1984).
18. Ohtani, E., Ringwood, A. & Hibberd, W. *Earth planet. Sci. Lett.* **71**, 94–103 (1984).
19. Maale, S. & Aoki, K. *Contr. Miner. Petrol.* **63**, 161–173 (1977).
20. Basaltic Volcanism Study Project *Basaltic Volcanism on the Terrestrial Planets* (Pergamon, New York, 1981).
21. Bass, J. D. & Anderson, D. L. *Geophys. Res. Lett.* **11**, 237–240 (1984).
22. Bass, J. D. & Anderson, D. L. (in preparation).
23. Stolper, E. M. *Contr. Miner. Petrol.* **74**, 13–27 (1980).
24. Rigden, S., Ahrens, T. & Stolper, E. *Science* **226**, 1071–1074 (1984).
25. Nisbet, E. & Walker, D. *Earth planet. Sci. Lett.* **60**, 105 (1982).
26. Ringwood, A. E. in *Advances in Earth Sciences* (ed. Hurley, P.) 287–356 (MIT Press, Cambridge, 1966).
27. Anderson, D. L. *Science* **213**, 82–89 (1981).
28. Anderson, D. L. *Adv. Earth planet. Sci.* **12**, 301–318 (1982).
29. Anderson, D. L. *Earth planet. Sci. Lett.* **57**, 13–24 (1982).
30. Anderson, D. L. *Earth planet. Sci. Lett.* **57**, 1–12 (1982).
31. Morgan, J. W. & Anders, E. *Proc. natn. Acad. Sci. U.S.A.* **77**, 6973 (1980).
32. Ringwood, A. E. *Origin of the Earth and Moon* (Springer, New York, 1979).
33. DePaolo, D. J. & Wasserburg, G. J. *Proc. natn. Acad. Sci. U.S.A.* **76**, 3056–1979.
34. Jacobsen, S. B. & Wasserburg, G. J. *J. geophys. Res.* **84**, 7411–7427 (1979).
35. Menzies, M. & Murthy, V. R. *Nature* **283**, 634 (1980).
36. Frey, F. & Prinz, M. *Earth planet. Sci. Lett.* **38**, 129–176 (1978).
37. McCulloch, M. T., Jaques, A., Nelson, D. & Lewis, J. *Nature* **302**, 400 (1983).
38. Anderson, D. L. in *Proc. 3rd int. Kimberlite Conf.* (ed. Komprobst, J.) 395–403 (Elsevier, New York, 1984).
39. Nataf, H.-C., Nakanishi, I. & Anderson, D. L. *Geophys. Res.* **11**, 109–112 (1984).
40. Anderson, D. L. & Dziewonski, A. *Science* **251** No. 4, 60–68 (1984).
41. Walck, M. *Geophys. J.R. astr. Soc.* **76**, 697–723 (1984).
42. Given, J. W. & Helmberger, D. V. *J. geophys. Res.* **85**, 7183–7194 (1980).
43. Anderson, D. L. *Science* **223**, 347–355 (1984).
44. Regan, J. & Anderson, D. L. *Phys. Earth planet. Inter.* **35**, 227–263 (1984).
45. Grand, S. & Helmberger, D. V. *J. geophys. Res.* **89**, 11,465–11,475 (1984).
46. Anderson, D. L. & Bass, J. D. *Geophys. Res. Lett.* **11**, 637–640 (1984).
47. Sawamoto, H., Weidner, D., Sasaki, S. & Kumazawa, M. *J. geophys. Res.* **89**, 7852–7860 (1984).
48. Sawamoto, H., Weidner, D. J., Sasaki, S. & Kumazawa, M. *Science* **224**, 749–751 (1984).
49. Akimoto, S. *Tectonophysics* **13**, 161–187 (1972).

50. Jeanloz, R. & Thompson, A. B. *Rev. Geophys. Space Phys.* **21**, 51–74 (1983).  
 51. Ringwood, A. E. & Major, A. *Earth planet. Sci. Lett.* **12**, 411–418 (1971).  
 52. Akagi, M. & Akimoto, S. *Phys. Earth planet. Inter.* **15**, 90–106 (1977).  
 53. Akagi, M. & Akimoto, S. *Phys. Earth planet. Int.* **19**, 31–51 (1979).  
 54. Liu, L. in *The Earth: Its Origin, Structure and Evolution* (ed. McElhinny, M. W.) 177–202 (Academic, New York, 1979).  
 55. Anderson, D. L. & Toksoz, M. N. *J. geophys. Res.* **68**, 3483–3500 (1963).  
 56. Niazi, M. & Anderson, D. L. *Bull. seismol. Soc. Am.* **58**, 339–366 (1968).  
 58. Johnson, L. R. *J. geophys. Res.* **72**, 6309–6325 (1967).  
 59. Archambeau, C. B., Flinn, E. A. & Lambert, D. G. *J. geophys. Res.* **74**, 5825–5866 (1969).  
 60. Kanamori, H. *Bull. Earthq. Res. Inst. Tokyo Univ.* **45**, 657–678 (1967).  
 61. Jeanloz, R. *J. geophys. Res.* **86**, 6171–6179 (1981).  
 62. Lees, A. C., Bukowinski, M. S. T. & Jeanloz, R. *J. geophys. Res.* **88**, 8145 (1983).  
 63. Anderson, D. L., Sammis, C. & Jordan, T. *Nature of the Solid Earth* (ed. Robertson, E.) 41–66 (McGraw-Hill, New York, 1972).  
 64. Sammis, C., Anderson, D. L. & Jordan, T. *J. geophys. Res.* **75**, 4478–4480 (1970).  
 65. Weidner, D. *Geophys. Res. Lett.* **12**, 417–420 (1985).  
 66. Ringwood, A. *J. Geol.* **90**, 611–643 (1982).  
 67. Bock, G. & Ha, J. *Geophys. J.R. astr. Soc.* **77**, 593–615 (1984).  
 68. Whitcomb, J. H. & Anderson, D. L. *J. geophys. Res.* **75**, 5713–5728 (1970).  
 69. Sobel, P. thesis, Univ. Minnesota (1978).  
 70. Richter, F. M. *J. geophys. Res.* **84**, 6783–6795 (1979).  
 71. Giardini, D. & Woodhouse, J. H. *Nature* **307**, 505–509 (1984).  
 72. Isacks, B. & Molnar, P. *Rev. Geophys. Space Phys.* **9**, 103–174 (1971).  
 73. Hager, B. H. & Richards, M. A. *J. geophys. Res.* **89**, 5987–6002 (1984).  
 74. Liebermann, R. C. & Ringwood, A. E. *J. geophys. Res.* **78**, 6926–6932 (1973).  
 75. Adams, R. D. *Bull. seismol. Soc. Am.* **61**, 1441–1451 (1971).
76. Richards, P. G. *Z. Geophys.* **38**, 517–527 (1972).  
 77. Creager, K. & Jordan, T. *J. geophys. Res.* **89**, 3031–3050 (1984).  
 78. Christensen, V. & Yuen, D. *J. geophys. Res.* **89**, 4389–4402 (1984).  
 79. Kato, T. & Kumazawa, M. *Nature* **316**, 803–805 (1985).  
 80. Weidner, D. *Phys. Earth planet. Inter.* **40**, 65–70 (1985).  
 81. Hirahara, K., Ishikawa, Y. *J. Phys. Earth* **32**, 197–218 (1984).  
 82. Ringwood, A. E. *Origin of the Earth and Moon* (Springer, New York, 1979).  
 83. Ito, E. & Matsui, Y. *Earth planet. Sci. Lett.* **38**, 442–450 (1978).  
 84. Liu, L. *Geophys. Res. Lett.* **1**, 277–280 (1974).  
 85. Mao, H., Yagi, T. & Bell, P. *Yb. Carnegie Instn Wash.* **76**, 502–504 (1977).  
 86. Ito, E., Takahashi, E. & Matsui, Y. *Earth planet. Sci. Lett.* **67**, 238–248 (1984).  
 87. Jackson, I. *Earth planet. Sci. Lett.* **62**, 91–103 (1983).  
 88. Knittle, E. & Jeanloz, R. *Nature* (in the press).  
 89. Ringwood, A. E. *J. geophys. Res.* **67**, 4005–4010 (1962).  
 90. Reid, A. & Ringwood, A. E. *Geophys. Res.* **80**, 3363–3370 (1975).  
 91. Ahrens, T. J., Anderson, D. L. & Ringwood, A. E. *Rev. Geophys.* **7**, 667–707 (1969).  
 92. Davies, G. F. & Anderson, D. L. *J. geophys. Res.* **76**, 2617–2627 (1971).  
 93. Liu, L. *Phys. Earth planet. Inter.* **11**, 289–298 (1976).  
 94. Yagi, T., Mao, H. K. & Bell, P. M. *Phys. Chem. Miner.* **3**, 97–110 (1978).  
 95. Dziewonski, A. M. & Anderson, D. L. *Phys. Earth planet. Inter.* **25**, 297–356 (1981).  
 96. Woodhouse, J. H. & Dziewonski, A. M. *J. geophys. Res.* **89**, 5853 (1984).  
 97. Clayton, R. & Comer, R. *EOS* **64**, 776 (1983).  
 98. Anders, E. & Ebihara, M. *Geochim. cosmochim. Acta* **46**, 2363–2380 (1982).  
 99. Weidner, D., Bass, J., Ringwood, A. & Sinclair, W. *J. geophys. Res.* **87**, 4740–4746 (1982).  
 100. Yagi, Y., Akagi, M., Shimomura, O., Tami, H. & Akimoto, S. *U.S. Japan Seminar, High-Pressure Research in Geophysics and Geochemistry, Program with Abstracts, January 13–16, 1986*, 62–63 (1986).

## ARTICLES

## Spatial restriction in expression of a mouse homoeo box locus within the central nervous system

Alexander Awgulewitsch\*, Manuel F. Utset†, Charles P. Hart\*, William McGinnis‡ & Frank H. Ruddle\*

Departments of \* Biology, † Human Genetics and ‡ Molecular Biophysics and Biochemistry, Yale University, New Haven, Connecticut 06511, USA

*A common feature of Drosophila homoeo box genes appears to be their spatially restricted expression patterns during morphogenesis. Using Northern blot analysis and in situ hybridization to mouse tissue sections, the spatially restricted expression of a newly identified mouse homoeo box locus, Hox-3, within the central nervous system of newborn and adult mice has been demonstrated.*

THE morphogenetic events which result in the segmented body plan of the fruit fly *Drosophila melanogaster* have been subjected to detailed genetic analyses. The genes controlling the segmentation processes and the identity of different segments are referred to as segmentation and homoeotic genes, respectively<sup>1–3</sup>. The recent cloning of some of these genes located in the bithorax (BX-C) and *Antennapedia* (ANT-C) gene complexes<sup>4–6</sup> has allowed the study of their molecular structure. One outcome of these structural analyses has been the detection of cross-homology between different homoeotic and segmentation genes. The best characterized cross-homology is known as the homoeo box, which encodes a highly conserved protein domain<sup>7–11</sup> that appears to be preferentially localized in the *Drosophila* genome within loci controlling fly morphogenesis. How this conserved sequence is related to the homoeotic or segmentation functions of these morphogenetic loci is not yet known.

Highly conserved copies of homoeo box sequences are found in a wide variety of animals, including mammals<sup>7,12–14</sup>. The possibility that the mammalian and fly genes might perform similar morphogenetic functions is so far supported only by superficial similarities in their time of expression during embryogenesis<sup>15–21</sup>, their tissue-specific expression during embryonic<sup>20</sup>, postnatal<sup>21</sup> and adult stages<sup>19–21</sup>, their transcriptional activity in differentiated embryonic carcinoma cells from mouse and man<sup>16,17,19</sup>, as well as in the clustered organization of homoeo box genes in both *Drosophila* and mammals<sup>15,17,19,21</sup>. In *D. melanogaster*, the transcripts encoded by different homoeo box genes accumulate in regionally localized subsets of cells during

embryonic and larval development<sup>10,22–27</sup>. The detection of similar patterns of mouse homoeo box gene expression during embryogenesis would be expected should the genes perform functions analogous to those of the *Drosophila* homoeo box gene family.

We report here the structural analysis of a murine homoeo box which we have mapped to chromosome 15. Analysis of the transcriptional activity of this newly identified homoeo box locus provides evidence for spatially restricted expression in a specific anterior-posterior region of the mouse central nervous system.

### Isolation and structure of clone

A library of mouse genomic DNA in λ Charon 28 was screened under reduced stringency conditions with homoeo box-containing probes derived from the *Antennapedia* (*Antp*) and *Ultrabithorax* (*Ubx*) genes of *Drosophila*<sup>7</sup>. Nine separate recombinants were isolated after screening  $10^6$  λ clones (approximately three genome equivalents). The results presented here concern one of these clones, originally named λ Mo-EA. A restriction map of this clone obtained with six different restriction endonucleases is shown in Fig. 1a. The 2.2-kilobase (kb) *Bam*HI-*Eco*RI restriction fragment at the left end of the phage insert contains the homoeo box homology and was subcloned in the pSP64 vector system. The subclone, designated pMo-EA, was analysed for further restriction sites with two additional restriction enzymes, *Hae*III and *Hinf*I (Fig. 1a). The homology to the homoeo box sequences from *Drosophila* (*Ubx* and *Antp*) is confined to a 320-base-pair (bp) *Hae*III-*Hae*III fragment in

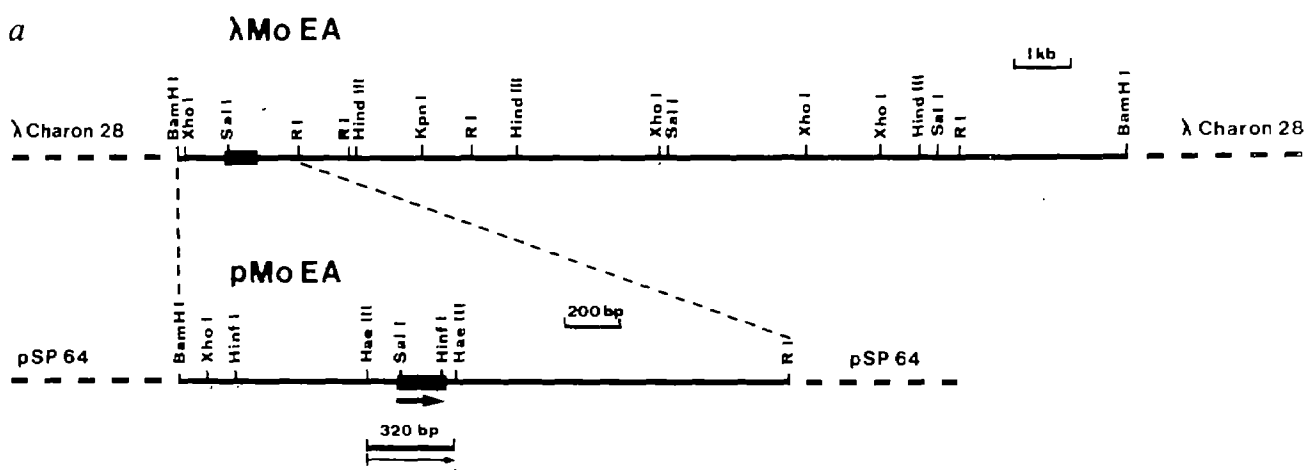


**Fig. 1** *a*, Restriction site maps of the recombinant  $\lambda$  clone and the pSP64 subclone containing the Mo-EA homoeo box. The clone was isolated by screening a  $\lambda$  phage library of mouse genomic DNA (BALB/c mouse embryo DNA inserted into Charon 28; the library was kindly provided by Dr P. Leder) with the *Antp* and *Ubx* homoeo box plasmids under reduced stringency conditions<sup>7</sup>. The black box indicates the region homologous to the *Antp* and *Ubx* homoeo box clones from *Drosophila*. The presumed direction of transcription is from left to right (bold arrow) based on the conserved open reading frame. The *Hae*III-*Hae*III restriction fragment of 320 bp in length (bottom) was used as a probe for Northern blot and *in situ* hybridizations and for sequence analysis (thin arrows at the bottom) using the chain termination method<sup>28</sup>. RI = *Eco*RI. *b*, DNA sequence of the Mo-EA (*Hox-3*) homoeo box. The DNA sequence of Mo-EA is aligned (5' to 3') with homologous regions from *Antp*<sup>7</sup> and *Ubx*<sup>10</sup> from *Drosophila* and Mo-10<sup>29</sup> and m6<sup>16</sup> from mouse. The sequence is shown from position -42 (42 bp upstream of the homology) to position 201 (21 bp downstream of the homology). The codons of the common open reading frame are aligned. The black bars indicate nucleotide homology between all five homoeo box sequences. *c*, Conceptual translation of the conserved homologous open reading frame in the Mo-EA homoeo box (Fig. 1*b*). The amino-acid sequence is shown in comparison with the *Antp*<sup>7</sup>, *Ubx*<sup>10</sup> and Mo-10<sup>29</sup> and m6<sup>16</sup> homoeo domains. The region of homology extends from positions 1 to position 60. The black bars indicate amino-acid homology between all five homoeo domains.

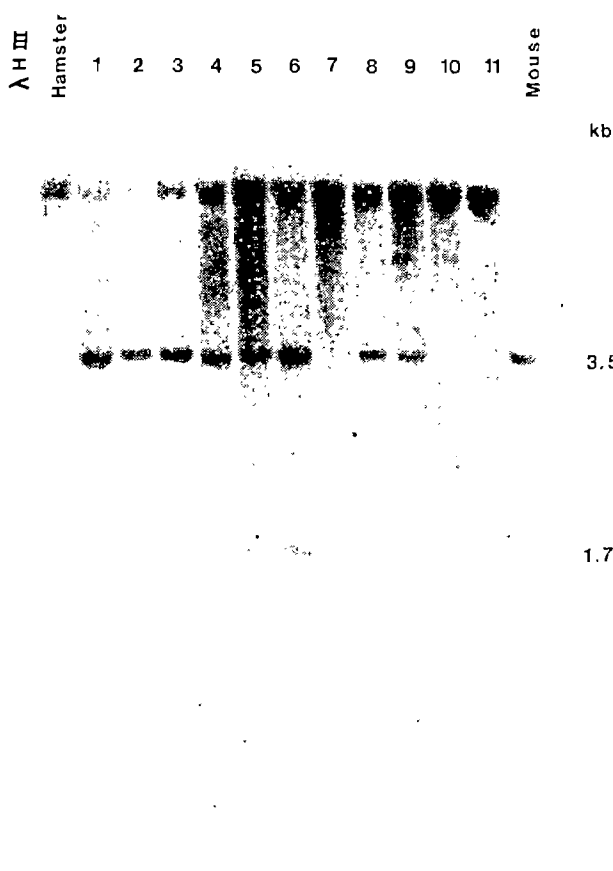


**Fig. 2** Southern blot hybridization of mouse, hamster and mouse $\times$ hamster hybrid cell line DNAs with the *Hox-3* DNA probe, pMo-EA. Approximately 15  $\mu$ g of *Pst*I-digested DNA was loaded per track. The probe was nick translated in the presence of  $^{32}\text{P}$ -dCTP to a specific activity of  $10^8$  c.p.m.  $\mu\text{g}^{-1}$  and hybridized as reported previously<sup>29</sup>. Bacteriophage  $\lambda$  DNA digested with *Hind*III ( $\lambda$  HIII) was used for relative molecular mass determinations and the sizes of the mouse-specific hybridizing fragments are shown on the right. Hybrids listed from 1-11 are 2-1, 2-1-1, 2-1-7, 12G7, 4B31, 2a2c2, R44, EcM4, 10bs2, Mae32 and CEC, respectively. They are described in McGinnis *et al.*<sup>29</sup> and Pratcheva *et al.*<sup>39</sup>.

the middle of the pMo-EA insert. This fragment was cloned in M13 mp11 in both orientations and the nucleotide sequence was determined using the dideoxy chain termination method<sup>28</sup>. The 180-bp DNA sequence of the mouse EA homoeo box with 42-bp flanking sequence upstream and 21-bp sequence downstream is shown in Fig. 1b. Identification of the *Sal*I and *Hinf*I restriction endonuclease sites close to the 5' end (*Sal*I, base positions 11-16) and near the 3' region (*Hinf*I, base positions 150-154) within the homoeo box allows the 5' $\rightarrow$ 3' orientation on the restriction map (Fig. 1a). Comparison with the *Antp* and *Ubx* homoeo box DNA sequences from *Drosophila*<sup>7,10</sup> shows ~73% and ~68% homology, respectively, while the homology to mouse 10 (ref. 29) and m6 from mouse<sup>16</sup> is considerably lower, ~56% and ~66%, respectively.

The conceptual translation of the mouse EA homoeo box and its comparison with *Antp*<sup>7</sup>, *Ubx*<sup>10</sup>, mouse-10 (Mo-10)<sup>29</sup> and m6<sup>16</sup> are shown in Fig. 1c. The homology of the amino-acid sequence of mouse EA to each of the four other homoeo domains is 83% to *Antp*, 80% to *Ubx*, 62% to Mo-10 and 78% to m6. The striking conservation in the amino-acid sequence is restricted to the homoeo domain, encoded by nucleotides 1-180. Out of 60 amino acids, 35 are identical at all five loci from mouse and fly.

### Chromosomal mapping

Twenty-five mouse $\times$ hamster hybrid cell lines were screened for the presence or absence of mouse sequences cloned in pMo-EA. These cell lines contain the entire complement of hamster chromosomes and differing subsets of mouse chromosomes. The presence of a particular mouse chromosome is determined by

a combination of isozyme, DNA marker and karyotypic analyses.

Southern blot hybridizations using pMo-EA as a probe and mouse, hamster and mouse $\times$ hamster hybrid cell line DNAs digested with a variety of restriction endonucleases identified *Pst*I as an enzyme that distinguished the mouse EA hybridizing fragments from the cross-hybridizing hamster fragments. pMo-EA hybridizes with 3.5-kb and 1.7-kb *Pst*I fragments in a mouse genomic Southern blot. Cross-hybridizing bands of approximately 10 kb and 12 kb are present in the hamster genome using the mouse probe. A representative Southern blot is shown in Fig. 2. Scoring the mouse $\times$ hamster hybrid cell lines for the presence of the mouse-specific fragments assigns this genomic locus to mouse chromosome 15. A summary of the hybrid cell line blot hybridization results is shown in Table 1. The chromosomal location of mouse EA is different from the position of

**Table 1** Southern blot hybridization results for mouse $\times$ hamster hybrid cell line DNAs probed with *Hox-3* probe pMo-EA

Mouse chromosome	Concordant			Discordant		
	+/-	-/-	Total	+/-	-/+	Total
1	12	6	18	1	6	7
2	13	5	18	2	3	5
3	11	7	18	0	4	4
4	13	5	18	2	5	7
5	6	6	12	1	12	13
6	13	6	19	1	5	6
7	16	3	19	4	2	6
8	12	7	19	0	6	6
9	10	4	14	3	7	10
10	14	6	20	0	5	5
11	0	7	7	0	18	18
12	15	3	18	4	2	6
13	4	3	7	0	2	2
14	5	6	11	1	13	14
15	6	3	9	0	0	0
16	3	2	5	1	3	4
17	17	4	21	3	3	6
18	1	6	7	1	10	11
19	8	5	13	2	6	8
X	8	2	10	5	7	12

The murine chromosomal complement of the 25 hybrid cell lines was determined by karyotyping and/or the analysis of isozyme and DNA markers. The presence or absence of mouse chromosome 15 is concordant with the presence or absence of the *Hox-3* diagnostic mouse bands.

two other homoeo box loci identified previously, *Hox-1* on chromosome 6<sup>29</sup>, and *Hox-2* on chromosome 11<sup>30,31</sup>. Keeping the same scheme of nomenclature, we call the newly identified mouse EA locus on chromosome 15, *Hox-3*.

### *Hox-3* encodes tissue-specific transcripts

The expression of homoeo box genes in *D. melanogaster* follows a spatially and temporally restricted pattern. This has been most effectively demonstrated by *in situ* hybridizations to serial sections of embryos and larvae using genomic or complementary DNA probes<sup>10,22-27</sup>. At mid-to-late stages of embryogenesis, different homoeotic transcripts are expressed in distinct regions of the fly central nervous system.

We have used both Northern blot analysis and *in situ* hybridization to histological sections to test transcript distributions in different tissues and in different anterior/posterior positions in the mouse body. In the first experiment, transcription from the *Hox-3* locus was tested at different stages of embryonic development. Poly(A)<sup>-</sup> and poly(A)<sup>+</sup> RNAs were isolated from total embryos at 11, 12, 13, 16, 19 and 21 days post coitum and hybridized with the nick-translated pMo-EA probe from *Hox-3*.

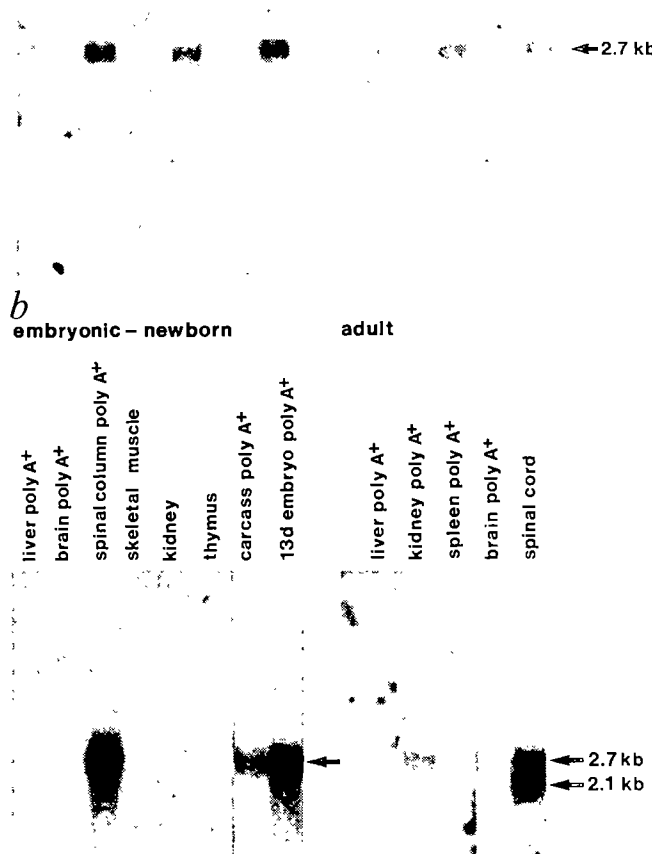
**Fig. 3** *a*, Northern blot hybridizations of *Hox-3* to poly(A)<sup>-</sup> and poly(A)<sup>+</sup> RNAs (shown as A<sup>-</sup> and A<sup>+</sup>) isolated from whole mouse embryos of different gestation stages, starting with day 11 (11d). At gestation stage day 21 (21d) the mice were born and the newborn mice were used for the experiment. *b*, Northern blot hybridizations of *Hox-3* to poly(A)<sup>+</sup> and total RNAs isolated from liver, brain, spinal column, skeletal muscle, kidney, thymus and carcass dissected from newborn CD-1 mice (left), and to poly(A)<sup>+</sup> RNAs from liver, kidney, spleen, brain and spinal cord (total RNA) from adult male and female CD-1 mice (right). Poly(A)<sup>+</sup> RNA from whole embryos of gestation stage day 13 (last track on the left) served as a positive control.

**Methods.** The breeding of mice (CD-1), the dissection of embryos and tissues and the isolation of RNA using the guanidinium thiocyanate-CsCl method<sup>40</sup> were done essentially as described previously<sup>15</sup>. The spinal column from newborn mice was dissected by cutting it directly behind the skull and by separating it from limbs and ribs on either side. Most of the muscle and connective tissue was removed before the RNA was isolated. For the isolation of RNA from the spinal cord of adult animals, the spinal column was first dissected in the same way. The spinal cord was separated from the vertebrae by nicking the spinal column with 5–10 transverse cuts set along its anterior-posterior axis, and by pulling the vertebrae off the cylindrical nerve cord in the longitudinal direction. By this procedure it was possible to prepare the entire nerve cord from the atlas region to the region of the sacral vertebrae. Carcass (*b*) means the whole body of a newborn mouse after removal of the spinal column. Eight µg of each poly(A)<sup>-</sup> and poly(A)<sup>+</sup> RNA sample (*a*) and 8 µg of poly(A)<sup>+</sup> RNA or 20 µg of total RNA (*b*) were separated in formaldehyde gels and transferred to nitrocellulose gels according to Maniatis *et al.*<sup>41</sup>. The RNA filters were prehybridized for 8–15 h at 42 °C in 50% formamide, 5×SSC, 50 mM sodium phosphate (pH 6.6), 0.1% SDS, 5×Denhardt's solution<sup>42</sup> and 100–200 µg ml<sup>-1</sup> of denatured sonicated salmon sperm DNA (Sigma). The hybridization with nick-translated plasmid DNA (pMo-EA) was carried out under the same conditions with 10% dextran sulphate added for 20–24 h. The concentration of denatured <sup>32</sup>P-labelled probe DNA (specific activities ~2×10<sup>8</sup> c.p.m. per µg DNA) was about 3–5 ng ml<sup>-1</sup>. The filters were washed in 3×SSC, 0.1% SDS at room temperature for 2×10 min and in 0.2×SSC, 0.1% SDS at 65 °C for 3×20 min. The filters were autoradiographed with XAR-5 film from Kodak and an intensifying screen for 2 days at -70 °C. As a control (*b*) the filters were stripped with boiling 0.1×SSPE, 0.1% SDS and hybridized with a <sup>32</sup>P-labelled cDNA clone of the human hypoxanthine phosphoribosyl transferase (*hprt*) gene<sup>43</sup>. Each RNA sample displayed a single band at the same position, but of different intensity, indicating the integrity of the RNAs.

The results show an abundant transcript of approximately 2.7 kb in size, present only in the poly(A)<sup>+</sup> RNA fractions of all these embryonic stages (Fig. 3*a*). No hybridization signals were detectable with the poly(A)<sup>-</sup> RNAs even after longer autoradiographic exposures. Embryonic stages earlier than day 11 post coitum have not yet been tested.

In order to investigate the tissue distribution of the *Hox-3* transcript(s), we prepared RNA blots using RNA isolated from a number of different tissues and organs from newborn and adult animals, and hybridized them with the pMo-EA probe (Fig. 3*b*). Analysis of the RNAs from newborn mice (Fig. 3*b*, left) showed that the strongest hybridization signal was obtained with the poly(A)<sup>+</sup> RNA isolated from the spinal column, indicating that at this stage of development a major site of *Hox-3* transcript accumulation is in cells of the spinal column. The size of the hybridizing transcript of 2.7 kb is identical to the size of the abundant transcript in 13-day embryos. A less abundant transcript of the same size is present in the RNA samples from kidney and from the carcass remaining after removal of the spinal column. The weak signal with the kidney was obtained with total RNA, while the stronger signal with the carcass was obtained with poly(A)<sup>+</sup> RNA. Since there was no hybridization signal detectable with the RNAs from the other tissues and organs tested, including liver, brain, skeletal muscle and thymus, we suspect that much of the hybridization signal in the carcass is due to kidney-specific expression of the *Hox-3* locus.

<i>a</i>	11d	12d	13d	16d	19d	21d
	A <sup>-</sup>	A <sup>+</sup>	A <sup>-</sup>	A <sup>+</sup>	A <sup>-</sup>	A <sup>+</sup>



The distribution of *Hox-3* transcripts in RNA samples from adult tissues (Fig. 3*b*, right) is consistent with our data concerning *Hox-3* expression in newborn mice and allows us to draw additional conclusions. While liver, spleen, skeletal muscle (data not shown) and brain appear to be negative for *Hox-3* expression, the kidney and the spinal cord are positive. A strong signal is obtained with the unfractionated total RNA from the spinal cord, in contrast to the weaker hybridization signal obtained with the poly(A)<sup>+</sup> RNA from the kidney, suggesting a much higher level of *Hox-3* expression in the adult spinal cord than in the adult kidney. The data allow us to assign a specific part of the central nervous system—the spinal cord—as at least one major site for *Hox-3* expression in adult mice. Although the tissue distribution of *Hox-3* transcripts appears to be the same in newborn and adult, in adult spinal cord an additional transcript of about 2.1 kb in size appears to be present in a higher copy number than the 2.7-kb transcript. This 2.1-kb transcript is not detectable in the other RNA samples.

#### Localized accumulation of *Hox-3* transcripts

If the *Hox-3* locus functions in a manner similar to *Drosophila* homoeotic genes, one would expect spatial restrictions of the transcripts that we have detected within the spinal cord. We have tested this prediction by two different experimental approaches: first by using Northern blot analysis of RNA isolated from three distinct regions of both the newborn spinal

column and the adult spinal cord, and second, by using *in situ* hybridization to tissue sections.

For the Northern blot hybridizations we used the 320-bp *Hae*III fragment which contains the entire *Hox-3* homoeo box and 140 bp of flanking sequences (Fig. 1a, b). In mRNA samples from the whole spinal column of newborn mice and from the spinal cord of adults (Fig. 4c, tracks Se+Sa, top) the 2.7-kb transcript was detected in both newborn and adult tissue, and the 2.1-kb RNA only in adult.

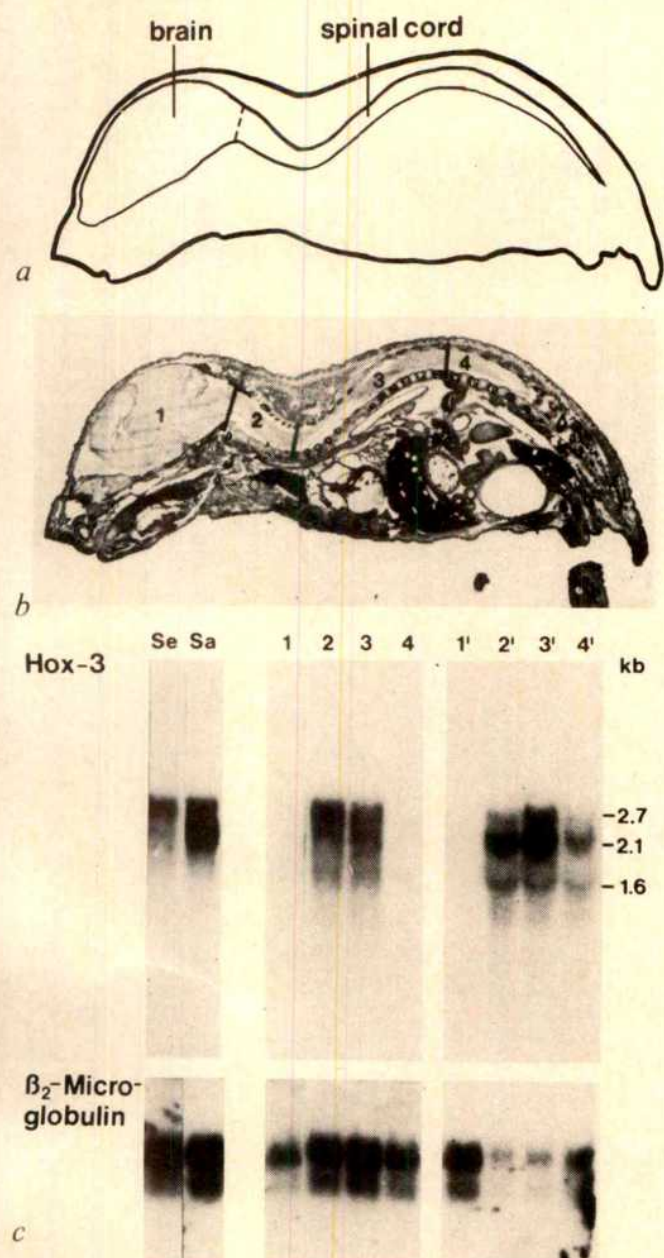
The results obtained with RNA samples from the newborn brain and from the cervical, the thoracic, and the lumbar/sacral/caudal regions of the newborn spinal column are shown in Fig. 4c, tracks 1–4. The photograph of a sagittal section of a newborn mouse (Fig. 4b) and a schematic drawing of this photograph (Fig. 4a) depict the regions of the central nervous system or spinal column from which the four different RNA samples were isolated (Fig. 4 legend). Strong hybridization signals were obtained with the RNA samples from the cervical and thoracic regions (tracks 2 and 3 in Fig. 4c, top), while the hybridization to the samples from the brain and lumbar region (tracks 1 and 4) appeared to be either negative (brain) or weak (lumbar). In the control experiment (Fig. 4c, bottom) carried out with the same filter and using a mouse  $\beta_2$ -microglobulin probe<sup>32,33</sup>, all three RNA samples from the newborn spinal column showed roughly equal signals, while the signal with the RNA from newborn brain was considerably weaker, though easily detectable. These data suggest a spatially restricted accumulation of *Hox-3* transcripts in the anterior regions of the spinal column from newborn mice. In addition to the 2.7-kb transcript, two other RNAs, 2.1 kb and 1.6 kb in size, were detected (Fig. 4c, tracks 2, 3). The 2.1-kb RNA presumably corresponds to the transcript also detected in the adult spinal cord (Figs 3b; 4c, track Sa, top), where it is the most abundant *Hox-3* transcript. The weak signal at the 1.6-kb position was not detected in the experiments described above (Figs 3a, b; 4c, tracks Se, Sa, top). Since we see a relatively stronger signal at the corresponding position by hybridizing the 320-bp *Hae*III fragment from *Hox-3* to total RNAs from adult spinal cord (Fig. 4c, tracks 2'–4', top), but not upon hybridization to the poly(A)<sup>+</sup> RNA from adult spinal cord (Fig. 4c, track Sa, top), it is possible that these bands result from hybridization to heterogeneous RNA fragments which have been compressed into this region close to the 18S ribosomal RNA<sup>26</sup>.

The spatial restriction of *Hox-3* transcripts in the central nervous system of adult mice was also tested by RNA blot analysis. A messenger RNA sample from the brain and samples of equal amounts of total RNA from the cervical, thoracic and lumbar regions of adult spinal cord were probed with the 320-bp *Hae*III fragment containing the *Hox-3* homoeo box (Fig. 4c, tracks 1'–4', top). No hybridization to the mRNA from the brain is detected, while all three RNA samples from the different spinal cord regions show hybridization to the 2.7- and 2.1-kb transcripts. High signal intensities are detected with the RNAs from the cervical and thoracic regions of the spinal cord, in contrast to the considerably weaker hybridization signals obtained with the RNA sample from the lumbar region. The significance of these signal intensity differences is supported by the control hybridization with the  $\beta_2$ -microglobulin probe (Fig. 4c, tracks 1'–4', bottom), showing equal intensities in the tracks corresponding to the cervical, thoracic and lumbar regions, which indicates equal amounts of RNA in each of these tracks.

We have also examined the spatial restriction of *Hox-3* expression in newborn mice by hybridizing the 320-bp homoeo box probe to whole body serial sections (Fig. 4d, e). As a control we used a probe containing sequences from the mouse  $\alpha$ -fetoprotein (AFP) gene, which is strongly expressed in newborn mouse liver<sup>34</sup> (Fig. 4f, g). Comparison of an autoradiograph of a sagittal section hybridized with the *Hox-3* probe (Fig. 4e) with a photograph of the stained section (Fig. 4d) indicates that

**Fig. 4 (opposite)** *a*, Schematic drawing of a sagittal section of a newborn mouse shown in *b*. *b*, Photograph of a Giemsa-stained sagittal section of a newborn mouse. For the isolation of RNAs from different regions of the central nervous system (CNS), the spinal column was separated from the brain and cut into three different sections as indicated by the black lines. The numbers label the separated regions of the CNS or the spinal column, respectively, from which RNAs have been isolated and refer directly to the labels used for the RNA blot hybridizations with the *Hox-3* probe in *c*; 1, brain; 2, cervical region; 3, thoracic region; 4, lumbar/sacral region. *c*, Top, Northern blot hybridization of *Hox-3* to RNA samples from the brain, and from different sections of the newborn spinal column and the adult spinal cord. The different tracks represent the following RNAs with the amounts ( $\mu$ g) determined by  $A_{260}$  measurement; Se, poly(A)<sup>+</sup> RNA from whole newborn spinal column (8  $\mu$ g); Sa, poly(A)<sup>+</sup> RNA from whole adult spinal cord (8  $\mu$ g); 1–4, poly(A)<sup>+</sup> RNAs from the newborn brain (1) and from the cervical (2), the thoracic (3) and the lumbar/sacral/caudal (4) region of the newborn spinal column (8  $\mu$ g each); 1', poly(A)<sup>+</sup> RNA from the adult brain (8  $\mu$ g); 2'–4', total RNAs from the cervical (2'), thoracic (3') and lumbar/sacral (4') region of the adult spinal cord (40  $\mu$ g each). Bottom, control hybridization of the RNA blot represented on the top with a mouse  $\beta_2$ -microglobulin probe (kindly provided by Dr P. Leder). *d*, Bright-field view of a sagittal section of a newborn mouse that was hybridized with the *Hox-3* probe. *e*, Autoradiograph obtained after exposure of the section in *d* to Kodak XAR-5 film for 20 days. The arrow indicates the hybridization signal resulting from *Hox-3* transcripts in the spinal cord. The apparent signal in the head region is due to a fold in the section at that position. The artefactual labelling of the thymus is discussed in the text. *f*, Bright-field view of a sagittal section of a newborn mouse that was hybridized with a mouse AFP gene probe (kindly provided by Dr S. Tilghman). *T*, thymus. *g*, Autoradiograph obtained after exposure of the section in *f* to Kodak XAR-5 film for 20 days. The arrow indicates the hybridization signal resulting from AFP transcripts in the liver. *T*, thymus.

**Methods. Dissections of nervous tissues, RNA isolations and Northern blot hybridizations:** The dissection of the brain and spinal column or the preparation of the spinal cord in the case of adult animals was done as described in Fig. 3 legend. The three different sections of the cervical, thoracic and lumbar/sacral/caudal region of the spinal column were obtained by cutting behind the 7th and 20th vertebrae from anterior to posterior as indicated in *b*. The isolation of RNAs, electrophoresis, blotting to nitrocellulose and hybridizations were carried out as referred (Fig. 3). The *Hox-3* probe was the 320-bp *Hae*III fragment shown in Fig. 1a; the  $\beta_2$ -microglobulin gene probe has been described previously<sup>32,33</sup>. **In situ hybridization.** The *in situ* hybridization to frozen sections of newborn mice was performed by a modification of the technique of Lawrence and Singer<sup>44</sup>. Briefly, newborn mice were killed with chloroform and quick-frozen in OCT embedding medium (Miles Laboratories) on a cryostat specimen holder by immersing the holder into liquid nitrogen. After warming to  $-20^{\circ}\text{C}$ , the frozen blocks were sectioned at 8–10  $\mu\text{m}$  on a SLEE cryostat. The sections were picked up onto acid-cleaned microscope slides subbed according to Gall and Pardue<sup>45</sup>, except that 0.3% gelatin was used. The sections were then fixed and dehydrated according to the method of Hafen *et al.*<sup>46</sup>. The plasmid pAFP-440, a pSP65 derivative, contains ~130 bp of AFP coding sequences within a 440-bp *Hinc*II fragment of mouse genomic DNA. pAFP-440 and the 320-bp *Hae*III fragment of *Hox-3* were labelled to specific activities approaching  $1 \times 10^8$  d.p.m. with  $^{35}\text{S}$ -labelled deoxyribonucleotide 5'-( $\alpha$ -thio)triphosphates (Amersham) as follows. Three parallel nick-translation reactions with increasing concentrations of DNase I (Sigma) were set up for each probe. In each reaction, 0.5  $\mu\text{g}$  of DNA was suspended in 30  $\mu\text{l}$  1  $\times$  nick-translation buffer<sup>41</sup> containing  $\sim 50 \mu\text{Ci}$  each of  $^{35}\text{S}$ -labelled dATP and dCTP, and 20  $\mu\text{M}$  each of unlabelled dGTP and dTTP. DNase I concentrations used were 0.5  $\text{ng ml}^{-1}$ , 1.0  $\text{ng ml}^{-1}$  and 2.0  $\text{ng ml}^{-1}$ . 20 units of DNA polymerase I (Boehringer) were added and the reaction mixes were incubated at room temperature for 60 min. The reactions were stopped by the addition of 100  $\mu\text{l}$  of 0.1 M NaCl, 10 mM Tris-HCl (pH 8.0), 2 mM EDTA and 0.02% SDS, and the probes were separated from the unincorporated nucleotides by passage through a Sephadex-G50 spin column<sup>41</sup>. The probes were then boiled for 1 min and stored at  $-20^{\circ}\text{C}$ . Just before hybridization, the probes were suspended at a concentration of 1 ng  $\mu\text{l}^{-1}$  in freshly prepared hybridization buffer containing 0.5  $\text{ng ml}^{-1}$  *Escherichia coli* transfer RNA, 1  $\times$  Denhardt's solution<sup>42</sup>, 50% deionized formamide, 0.75 M NaCl, 10 mM Tris-HCl (pH 7.5), 2 mM EDTA, 10% dextran sulphate, and 10 mM dithiothreitol. 50  $\mu\text{l}$  of hybridization solution was applied to each newborn mouse section and covered with 24  $\times$  40-mm coverslip. The coverslips were sealed with rubber cement, and then the slides were heated to  $80^{\circ}\text{C}$  for 2 min to denature the probe<sup>47</sup>. Hybridization was carried out in a moist chamber at  $37^{\circ}\text{C}$  for 4–5 h. The sections were washed by first removing the rubber cement and then allowing the coverslips to float off in a solution of 2  $\times$  SSC, 50% formamide, and 0.1% 2-mercaptoethanol. The sections were then incubated for at least 30 min in the same buffer at  $37^{\circ}\text{C}$ , followed by at least 30 min in 1  $\times$  SSC, and 50% formamide at  $37^{\circ}\text{C}$ , and finally by at least 30 min in 1  $\times$  SSC at room temperature with gentle shaking. The sections were then dehydrated in 70% and 95% ethanol (2  $\times$  5 min, each), air dried and exposed to Kodak XAR-5 film for 20 days. The sections were then immersed in Kodak NTB-2 emulsion as described by Hafen *et al.*<sup>46</sup>, except that the emulsion was diluted 1:1 with  $\text{H}_2\text{O}$ , and autoradiography was allowed to proceed for 15 days at  $4^{\circ}\text{C}$  in a dry, light-tight box. The slides were developed in Kodak D-19 developer for 2 min, rinsed briefly in  $\text{H}_2\text{O}$ , and fixed in Kodak rapid-fix for 4 min, all at about  $15^{\circ}\text{C}$ . The sections were stained with Giemsa and examined by light microscopy.



*Hox-3* transcripts accumulate in cells of the spinal cord. In numerous serial sections that have been probed in this manner, *Hox-3* transcripts have been detected throughout the posterior region of the spinal cord, with an anterior limit of transcript accumulation observed at approximately the level of the third cervical vertebra. A close-up view of this region of the spinal cord is depicted in Fig. 6. Note the decrease in specific signal over cell bodies anterior to the C-3/C-4 region. No obvious morphological transition occurs at this expression boundary. The highest signal levels are always observed adjacent to the boundary in the cervical region and in the thoracic region of the spinal cord. No signals forward of this boundary in any part of the central nervous system have been observed at any section depth. The cells of the thymus are also strongly labelled with the *Hox-3* probe, but this signal is apparently artefactual because the AFP probe labelled the thymus as strongly as the *Hox-3* probe (Fig. 4f, g), and because Northern blots of thymus RNA indicate no accumulation of *Hox-3* transcripts (see Fig. 3b). We observed no detectable labelling of kidney cells with the *Hox-3*

probe, presumably due to the relative insensitivity of the *in situ* method versus Northern blot analysis.

To better characterize the localization of transcripts in the newborn spinal cord and to confirm the presumed direction of transcription, single-stranded probes were used for *in situ* hybridizations to cross-sections of three different regions of the newborn spinal column: just posterior to the second, sixth and twentieth vertebrae (Fig. 5). For these experiments, the homoeo box-containing 320-bp *Hae*III fragment cloned in the Gemini vector system was used as a template for the synthesis of  $^{35}\text{S}$ -labelled RNA transcripts from both strands. A strong specific signal was obtained only from hybridizations to cross-sections of the spinal cord region just posterior to the sixth vertebra and only using the probe detecting transcripts synthesized in the direction predicted by the orientation of the homoeo box (Fig. 5b'). Comparing the autoradiograph with the stained section (Fig. 5b) indicates an accumulation of *Hox-3* transcripts in the centre of the spinal cord, whereas the spinal ganglia do not appear specifically labelled.

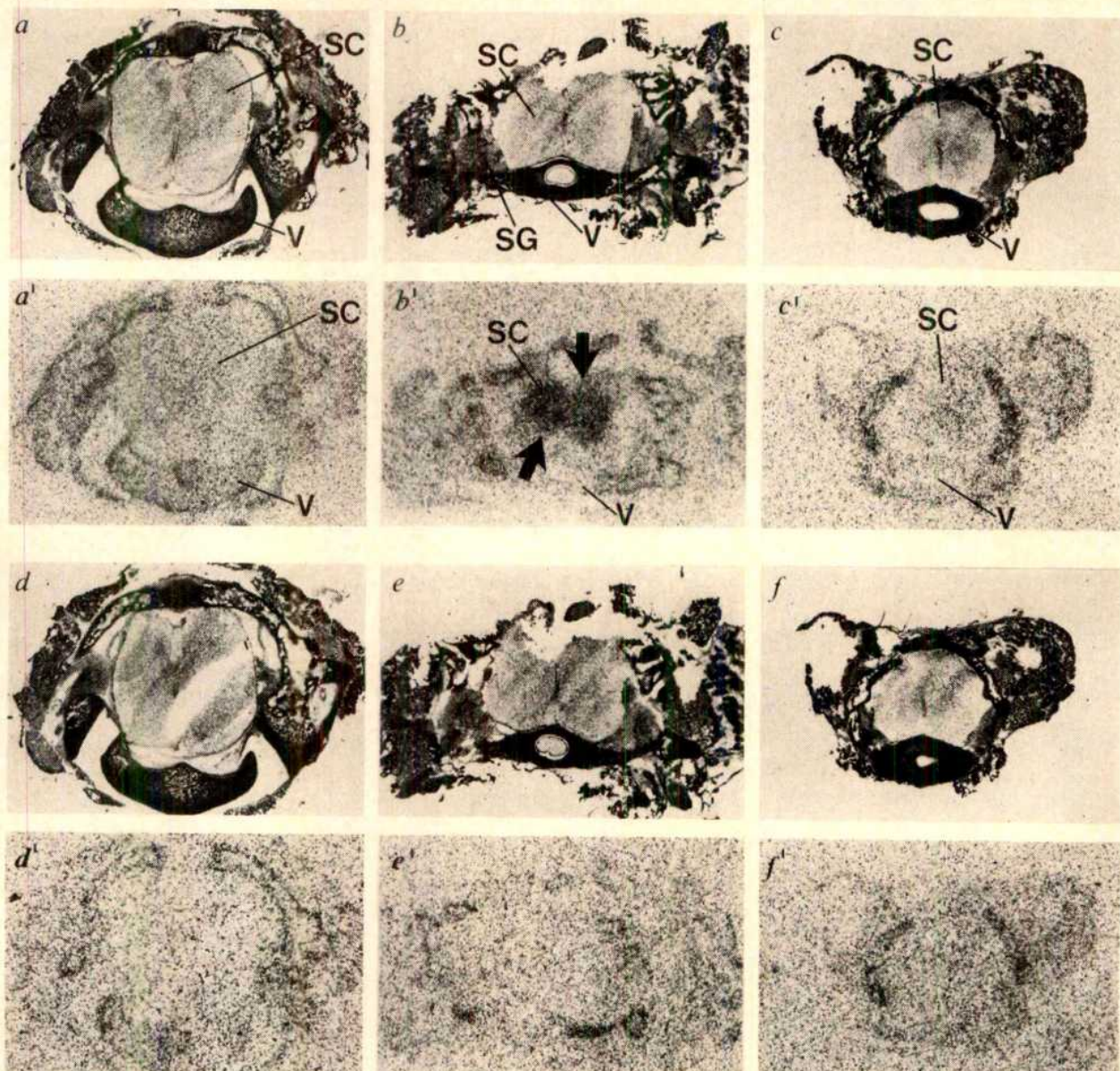


**Fig. 5** *a-c*, Bright-field views of Giemsa-stained sections of the newborn spinal cord from regions just posterior to the 2nd (*a*), 6th (*b*) and 20th (*c*) vertebrae hybridized with <sup>35</sup>S-labelled RNA complementary to the coding strand of *Hox-3*. All three sections were hybridized on the same microscope slide. The dorsal side is at the top of each photograph. V, vertebral body; SC, spinal cord; SG, spinal ganglion. *a'-c'*, Autoradiographs obtained after exposure of the sections shown in *a*, *b*, *c* to Kodak RP-5 film for 48 h. The arrows in *b'* (spinal cord region just posterior to the 6th vertebra) point to the specific signal in the centre of the spinal cord. The surrounding nonspecific labelling is mainly concentrated over dense cartilaginous tissue. *d-f*, Bright-field views of Giemsa-stained cross-sections of the newborn spinal cord from regions just posterior to the 2nd (*d*), 6th (*e*) and 20th (*f*) vertebrae, hybridized with <sup>35</sup>S-labelled RNA complementary to the anticoding strand of *Hox-3*. All three sections were hybridized on the same microscope slide and are from the same animal as those in *a*, *b* and *c*. *d'-f'*, Autoradiographs obtained after exposure of the sections in *a*, *b*, *c* to Kodak XRP-5 film for 48 h.

**Methods.** The 320-bp *Hae*III fragment (Fig. 1*a*) was cloned into the poly-linker region of pGem4 (Promega Biotech) by standard methods. High specific activity RNA transcripts ( $\sim 10^8$  c.p.m.  $\mu\text{g}^{-1}$ ) complementary to coding and anticoding strands were prepared essentially as described by Cox *et al.*<sup>48</sup>, as modified by the manufacturer. Labelled nucleotide, <sup>35</sup>S-labelled UTP (400 Ci mol<sup>-1</sup>, Amersham), was used at a concentration of 12  $\mu\text{M}$  in the synthesis reaction. Hybridizations were performed for 6 h at 50 °C with a probe concentration of 0.25  $\mu\text{g ml}^{-1}$ , essentially as described by Cox *et al.*<sup>48</sup>. After allowing the coverslips to float off in a solution of 2  $\times$  SSC, 50% formamide, and 0.1%  $\beta$ -mercaptoethanol, wash conditions were as follows: 2  $\times$  SSC, 50% formamide, 0.1%  $\beta$ -mercaptoethanol, 50 °C; 20  $\mu\text{g ml}^{-1}$  RNase, 0.5 M NaCl, 10 mM Tris-Cl (pH 8.0), 37 °C; 2  $\times$  SSC, 50% formamide, 0.1%  $\beta$ -mercaptoethanol, 50 °C; 1  $\times$  SSC, 50% formamide, 0.1%  $\beta$ -mercaptoethanol, 50 °C; all for at least 30 min. Slides were then dehydrated and exposed to X-ray film.

## Conclusions

If mouse homoeo box genes direct specific morphogenetic functions during embryonic development, one would predict spatial localization of their expression to specific body regions of the developing mouse. Studies from several laboratories have already demonstrated differential expression of individual homoeo box genes in different mouse tissues at several developmental stages<sup>19,20,21</sup>. For example, *Hox-2.1* transcripts are abundant in the embryonic, newborn and adult central nervous system<sup>20,21</sup>. As shown in this study, *Hox-3* transcripts also accumulate in the newborn and adult central nervous system,

and more importantly, *Hox-3* transcript abundance displays a striking spatially restricted localization along the longitudinal axis of the central nervous system (Figs 4, 5). The highest level of *Hox-3* transcript accumulation occurs in the posterior cervical and anterior thoracic region of the spinal cord. We detect no expression more anteriorly and only weak expression in more posterior regions of the central nervous system.

One of the distinguishing characteristics of many of the homoeo box-containing homoeotic genes of *Drosophila* is their localized expression within discrete regions of the ventral nerve cord of the developing fly<sup>23,27</sup>. For the *Antp* gene, this restricted pattern of expression persists at least until the third instar larval

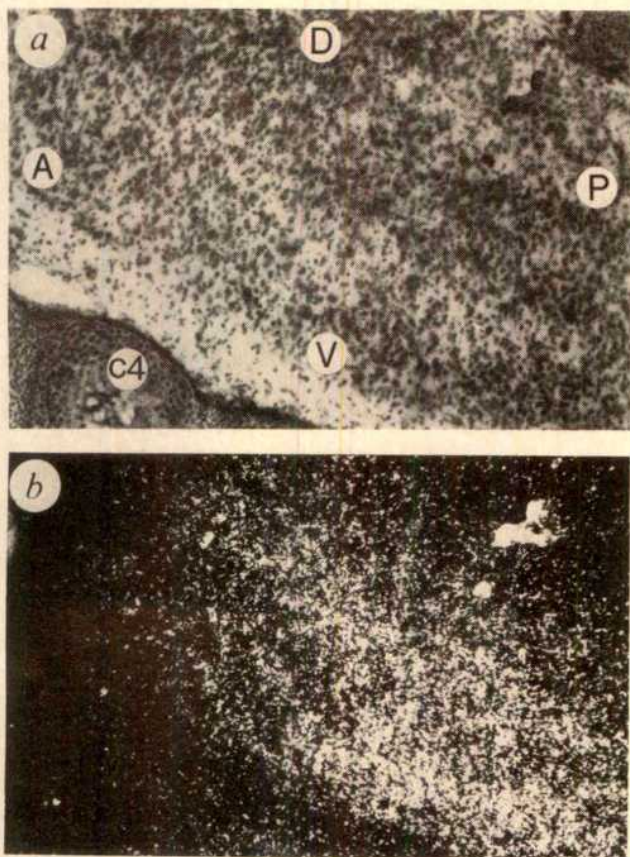


**Fig. 6** Bright-field (*a*) and dark-field (*b*) views of the anterior-most region of specific labelling of the spinal cord of the section depicted in Fig. 4*d*. A, anterior; D, dorsal; P, posterior; V, ventral; C4, fourth cervical vertebra. ( $\times 69.3$ ).

stage<sup>35</sup>. By Northern blot analysis *Antp* products can still be detected in late pupal stages and also in the adult fly<sup>6</sup>.

Although attempts to draw functional parallels between the pattern of *Hox-3* expression in newborn and adult mice and the patterns of expression of homoeotic genes during fruit fly embryogenesis are still admittedly speculative, the similarity of these patterns is dramatic. In addition, preliminary observations indicate that the observed localization of *Hox-3* expression occurs at least as early as the 13th day of embryogenesis (M.F.U. *et al.*, unpublished data). We therefore conclude that the observed patterns of expression of *Hox-3* and *Drosophila* homoeo box sequences within the respective central nervous systems of mice and flies is consistent with a developmental role for *Hox-3* within a specific region of the mouse body plan.

Received 6 November 1985; accepted 7 February 1986.

1. Nusslein-Volhard, C. & Wieschaus, E. *Nature* **287**, 795–801 (1980).
2. Garcia-Bellido, A. *Am. Zool.* **17**, 613–629 (1977).
3. Lewis, E. B. *Nature* **276**, 565–570 (1978).
4. Bender, W. *et al.* *Science* **221**, 23–29 (1983).
5. Garber, R. L., Kuroiwa, A. & Gehring, W. J. *EMBO J.* **2**, 2027–2036 (1983).
6. Scott, M. P. *et al.* *Cell* **35**, 763–776 (1983).
7. McGinnis, W., Garber, R. L., Wirz, J., Kuroiwa, A. & Gehring, W. J. *Cell* **37**, 403–408 (1984).
8. Scott, M. P. & Weiner, A. J. *Proc. natn. Acad. Sci. U.S.A.* **78**, 1095–1099 (1984).
9. Poole, S. J., Kauvar, L. M., Drees, B. & Kornberg, T. *Cell* **40**, 37–43 (1985).
10. Fjose, A., McGinnis, W. & Gehring, W. J. *Nature* **313**, 284–289 (1985).
11. Regulski, M. *et al.* *Cell* **43**, 71–80 (1985).
12. Carrasco, A. E., McGinnis, W., Gehring, W. J. & DeRobertis, E. M. *Cell* **37**, 409–414 (1984).
13. Muller, M. M., Carrasco, A. E. & DeRobertis, E. M. *Cell* **39**, 157–162 (1984).
14. McGinnis, W. *Cold Spring Harb. Symp. quant. Biol.* **50**, 263–270 (1985).
15. Hart, C. P., Awgulewitsch, A., Fainsod, A., McGinnis, W. & Ruddle, F. H. *Cell* **43**, 9–18 (1985).
16. Colberg-Poley, A. M., Voss, S. D., Chowdhury, K. & Gruss, P. *Nature* **314**, 713–718 (1985).
17. Hauser, C. A. *et al.* *Cell* **43**, 19–28 (1985).
18. Joyner, A. L., Kornberg, T., Coleman, K. G., Cox, D. R. & Martin, G. R. *Cell* **43**, 29–37 (1985).
19. Colberg-Poley, A. M. *et al.* *Cell* **43**, 39–45 (1985).
20. Jackson, I. J., Schofield, P. & Hogan, B. *Nature* **317**, 745–748 (1985).
21. Ruddle, F. H. *et al.* *Cold Spring Harb. Symp. quant. Biol.* **50**, 277–284 (1985).
22. Akam, M. E. *EMBO J.* **2**, 2075–2084 (1983).
23. Levine, M., Hafen, E., Garber, R. L. & Gehring, W. J. *EMBO J.* **2**, 2037–2046 (1983).
24. McGinnis, W., Levine, M., Hafen, E., Kuroiwa, A. & Gehring, W. J. *Nature* **308**, 428–433 (1984).

Morphogenetic loci might also be expected to show specific temporal patterns of transcriptional activity during development. *Hox-3* is transcriptionally active at all developmental stages tested so far, spanning the time between the 11th day of gestation and the adult mouse. With the *Hox-3* probe pMo-EA, we detected an abundant transcript of 2.7 kb at all of these stages (Fig. 3*a, b*). Although no obvious temporal differences in *Hox-3* expression were detected during gestation, a difference in *Hox-3* expression between newborn and adult mice was detected. This difference is indicated by a shift in the relative abundance of the 2.1-kb and 2.7-kb transcripts in RNA samples from newborn spinal column versus adult spinal cord (Figs 3*b, c*). We also detected relatively low levels of the 2.7-kb *Hox-3* transcript in RNA samples from newborn and adult kidney (Fig. 3*b*).

A number of previously identified genes controlling morphogenesis in *Drosophila*, such as *Deformed*, *infra-abdominal 2*, *infra-abdominal 7* (refs 11, 36) and *engrailed*<sup>10</sup>, have been isolated by virtue of their cross-homology to homoeo box probes. Attempting to correlate homoeo box genes with known morphogenetic loci in the mouse is much more difficult because of the relatively small number of murine mutations known to disrupt morphogenesis, and the low resolution of cytogenetic mapping. However, it may eventually be possible to reveal the suspected morphogenetic functions of murine homoeo box genes by analysing their genetic linkage to the known developmental mutations in mouse. In contrast to the previously characterized mouse homoeo boxes which are located on chromosomes 6<sup>29</sup> and 11<sup>30,31</sup>, the *Hox-3* locus maps to mouse chromosome 15. In light of the expression of *Hox-3* in the spinal cord, it is interesting to note that the semi-dominant mutation *velvet coat* (*Ve*), which in the homozygous state disrupts neural tube formation<sup>37</sup>, also maps to this chromosome<sup>38</sup>.

The results reported here are entirely consistent with a morphogenetic role for the *Hox-3* locus. However, because of the descriptive and comparative nature of our data, this view must remain conjectural. The next stage of analysis must involve direct experimentation to test this hypothesis.

We thank Nadine McGinnis and Lois Nichols for technical assistance, Marie Siniscalchi for typing the manuscript, Suzy Pafka for photographic assistance, and Drs Howard Lieberman and Abraham Fainsod for reviewing the manuscript. We also thank Drs Phil Leder and Shirley Tilghman for cloned DNA, Dr Dimitrina Pravtcheva for hybrid cell line DNAs, and Dr Michael Levine for advice on *in situ* hybridization methodologies. M.F.U. received financial support from the Life and Health Insurance Medical Research Fund and the Medical Scientist Training Program. C.P.H. was supported by an NIH predoctoral training grant. This work was supported by NIH grant GM09966 to F.H.R. and NSF grant DCB8501822 to W.M.

25. Kornberg, T., Siden, J., O'Farrell, P. & Simon, M. *Cell* **40**, 45–53 (1985).
26. Akam, M. E. & Martinez-Arias, A. *EMBO J.* **4**, 1689–1700 (1985).
27. Harding, K., Wedeen, C., McGinnis, W. & Levine, M. *Science* **239**, 1236–1242 (1985).
28. Sanger, F., Nicklen, S. & Coulson, A. R. *Proc. natn. Acad. Sci. U.S.A.* **74**, 5463–5467 (1977).
29. McGinnis, W., Hart, C. P., Gehring, W. J. & Ruddle, F. H. *Cell* **38**, 675–680 (1984).
30. Rabin, M. *et al.* *Nature* **314**, 175–178 (1985).
31. Joyner, A. L. *et al.* *Nature* **314**, 173–175 (1985).
32. Parnes, J. R. & Seidman, J. G. *Cell* **29**, 661–669 (1982).
33. Kelly, K., Cochran, B. H., Stiles, C. D. & Leder, P. *Cell* **35**, 603–610 (1983).
34. Tilghman, S. M. & Belawsky, A. *Proc. natn. Acad. Sci. U.S.A.* **79**, 5254–5257 (1982).
35. Hafen, E. *thesis*, Univ. Basel (1983).
36. Karch, F. *et al.* *Cell* **43**, 81–96 (1985).
37. Diwan, S. & Stevens, L. C. *Mouse News Lett.* **51**, 25 (1974).
38. Green, M. C. *Genetic Variants and Strains of the Laboratory Mouse* (Fischer, Stuttgart, 1981).
39. Pravtcheva, D. D., Ruddle, F. H., Ellis, R. W. & Scolnick, E. M. *Somat. Cell Genet.* **9**, 681–686 (1983).
40. Chirgwin, J. M., Przybyla, A. E., MacDonald, R. J. & Rutter, W. J. *Biochemistry* **18**, 5294–5299 (1979).
41. Maniatis, T., Fritsch, E. F. & Sambrook, J. *Molecular Cloning: A Laboratory Manual* (Cold Spring Harbor Laboratory, New York, 1982).
42. Denhardt, D. T. *Biochem. biophys. Res. Commun.* **29**, 641 (1966).
43. Jolly, D. J. *et al.* *Proc. natn. Acad. Sci. U.S.A.* **80**, 477–481 (1983).
44. Lawrence, J. B. & Singer, R. H. *Nucleic Acids Res.* **13**, 1777–1799 (1985).
45. Gall, J. G. & Pardue, M. L. *Meth. Enzym.* **21**, 470–480 (1971).
46. Hafen, E., Levine, M., Garber, R. L. & Gehring, W. J. *EMBO J.* **2**, 617–623 (1983).
47. Brigati, D. J. *et al.* *Virology* **126**, 32–50 (1983).
48. Cox, K. H., DeLeon, D. V., Angerer, L. M. & Angerer, R. C. *Devl Biol.* **101**, 485–502 (1984).

## First light from a young star?

Bo Reipurth\* & John Bally†

\* Copenhagen University Observatory, Øster Voldgade 3,  
DK-1350 Copenhagen K, Denmark

† AT&T Bell Laboratories, Holmdel, New Jersey 07733, USA

The early phases of stellar evolution are frequently characterized by vigorous interaction between the nascent star and its environment, resulting in the formation of molecular outflows, highly collimated jets, Herbig-Haro objects and small emission or reflection nebulae. A deep survey of such small nebulae around young stars in the Orion molecular clouds has recently been completed<sup>1</sup>. We report here the sudden appearance of a highly variable, conical nebula (Object 50) 1.5 arc min south of a  $250L_{\odot}$  infrared source in the southern part of the L1641 cloud in Orion. The nebula coincides with the edge of the approaching lobe of a  $10^5$ -yr-old bipolar molecular outflow. Variability of the infrared source generates light pulses observed to propagate through the surrounding ambient cloud, producing a fluctuating illumination pattern. This emission may represent the first optical radiation to have emerged from this newborn star.

Object 50 is a large (1 arc min wide), luminous and structured nebula located in one of the most opaque regions of the Orion clouds. It is readily visible on a SERC-J Schmidt plate obtained in 1979, but examination of the blue and red Palomar Schmidt plates from 1955 shows nothing at this location. Obviously a highly time-dependent phenomenon is taking place here. A search at 2.2  $\mu\text{m}$  with the ESO 1-m telescope at La Silla, Chile, has shown that Object 50 itself is not directly associated with a

star, but is a reflection nebula of an intense near-infrared source located ~1.5 arc min to the north, and coinciding with a faint star-like nebulosity on the Schmidt plate. This source has also been detected by the Infrared Astronomy Satellite (IRAS). Positions measured on the 1979 Schmidt plate are listed in Table 1.

Broad-band CCD (charge-coupled device) images have been obtained of the region with the Danish 1.5-m telescope at La Silla on three occasions in the past few years. Figure 1a shows the region as it appeared on 20 December 1982, through a filter transmitting from 8,500 Å to the CCD cut-off at almost 1,100 Å. Object 50 itself shows a well-defined edge towards the infrared source, an intricate pattern of lighter and darker areas, and a faint tail stretching away from the source. About 1.5 arc min north of Object 50, at the location of the infrared source, two unequal nebulosities (the eastern and western lobes) are visible, separated by an opaque bridge. The position of the infrared source, as determined by IRAS and from ground-based near-infrared observations, coincides with the western lobe to within a few arc s. The eastern lobe is the more luminous and it shows a hint of a very faint structure pointing towards the south-east. A similar image, taken at the same time, but through a broadband filter centred on 6,500 Å, shows the same morphology, but the lobes around the infrared source are significantly fainter, demonstrating that there is little H $\alpha$  emission. Figure 1b shows an image in all respects similar to Fig. 1a (same instrumentation, exposure time, filter, seeing, reduction procedure), but obtained two years later, on 9 January 1985. Dramatic changes have occurred in the intervening period. While the western lobe has faded considerably, the faint structures associated with the eastern lobe have evolved into a highly collimated beam, 25 arc s long, with two knots. The length of the beam seen in January 1985 is almost 3 light-months if the scattering surface is located in the plane of the sky. The beam is directed 180° away from the axis connecting the infrared source with the centroid of the redshifted portion of the molecular outflow (see below). The

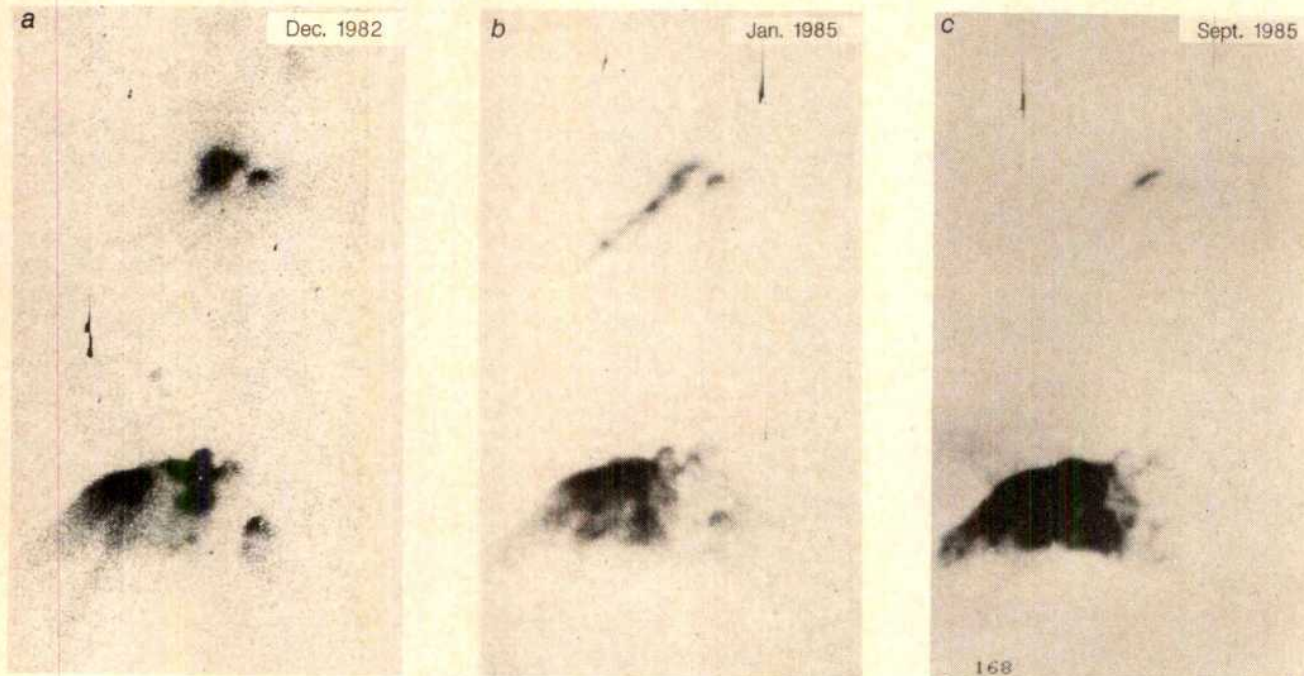


**Fig. 1** Three CCD images showing Object 50, taken through broad-band filter (from ~8,500 Å to almost 1,100 Å) with the Danish 1.5-m telescope at La Silla, Chile, on 20 December 1982 (a), 9 January 1985 (b) and 23 September 1985 (c). This nebula appeared after 1955, as nothing is visible on the Palomar Sky Survey plates taken of this region. The field shown is 1.75 arc min in right ascension and 3 arc min in declination; north is at the top and east at the right of each image. The intense and variable infrared source IRAS05380-0728 is situated at the small nebulosity in the upper part of the field. A pulse of light, presumably emitted in late 1984, illuminates the 'jet' seen in the January 1985 image and is observed to propagate 1.5 arc min to the south by September 1985. The faint pattern in the background is residual interference of sky emission lines in the CCD chip.

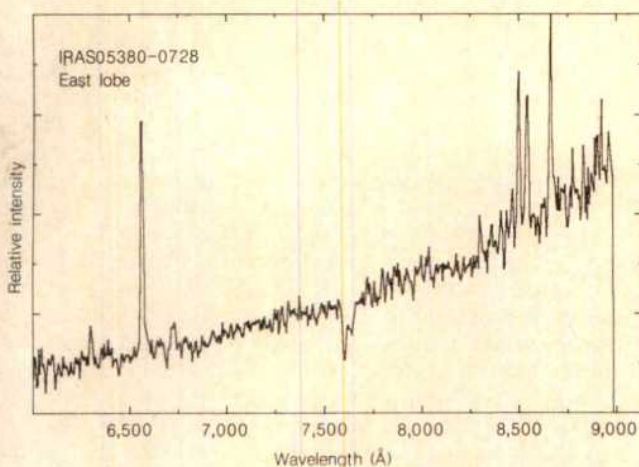


**Fig. 2** A low-resolution red spectrum of the nebulosity around the infrared source, obtained on 27 January 1985 with the 4-m telescope at Cerro Tololo by J. A. Graham, using a Boller and Chivens spectrograph and CCD detector. The low extinction inferred from the red continuum indicates that there is much less obstructing material toward the reflection nebula than along our line-of-sight. The spectrum indicates that the hidden star is of low or intermediate mass.

overall morphology of Object 50 is retained, but its luminous pattern has changed completely. Figure 1c shows the region as it appeared on 23 September 1985, displayed with intensity levels roughly similar to Fig. 1a, b; the beam of light extending from the infrared source has all but disappeared, leaving only a faint and diffuse illuminated patch. A faint extended nebulosity is now seen to surround Object 50 and may represent the same pulse of light which produced the beam 9 months earlier. A comparison of the three CCD images shows a gradual fading of the western nebulosity, where the infrared source is located.

Near-infrared photometry of the infrared source IRAS05380-0728, obtained through a 15-arc-s diaphragm on 31 January 1985, is given in Table 2 together with the IRAS fluxes. Comparison with observations made in April and December 1983 reveals considerable variability in the source, with a decrease of  $\sim 20\%$  in near-infrared luminosity from 1983 to 1985. For an assumed distance to the L1641 cloud of 460 pc, the luminosity in 1985 between 1.2 and 4.8  $\mu\text{m}$  is  $\sim 27L_\odot$ , the IRAS luminosity between 12 and 100  $\mu\text{m}$  (without colour correction factors) is  $\sim 120L_\odot$ , and an interpolation between 4.8 and 12  $\mu\text{m}$  yields roughly another  $100L_\odot$ . Altogether, the luminosity of the source is  $\sim 250L_\odot$ ; this is considerably less than that observed for massive embedded stars, but fairly luminous compared with the average low-mass pre-main-sequence star. Except for the IRAS catalogue, the source is not listed in catalogues of infrared sources. The source FIRSSE101 is only 2.5 arc min away<sup>2</sup>, one-third of the way towards the equally bright source IRAS05375-0731. Since FIRSSE101 was detected with a 10-arc-min beam, it is probably an unresolved blend of the two sources.

We have explored the nature of the infrared source through optical and infrared spectroscopy of the reflected light. Figure 2 shows a low-resolution red spectrum of the luminous eastern

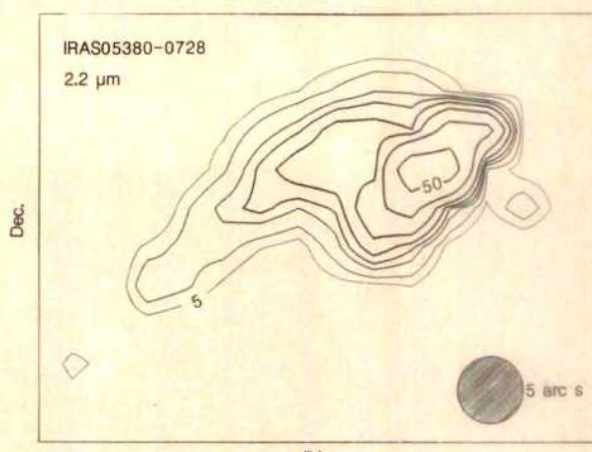


**Fig. 3** A 2.2- $\mu\text{m}$  map of the infrared source and its immediate surroundings, obtained with a 5-arc-s diaphragm through the ESO 1-m telescope at La Silla on 9 February 1985. The contour levels are at 5, 7, 10, 12, 15, 20, 30 and 50 (arbitrary units). The source is clearly extended along the axis determined by the source and the centre of the redshifted CO lobe. The contours of the infrared reflection nebula correspond very well to the optical appearance of the object at the same time. The ruled circle shows the size of the aperture stop used to make the map; it corresponds to a 5-arc-s diameter circle on the sky.

lobe east of the infrared source, obtained on 27 January 1985 at the CTIO 4-m telescope with a Boller and Chivens spectrograph and a CCD. The spectrum shows a slightly reddened continuum with purely terrestrial absorption features and only a few emission lines: mainly H $\alpha$  and the calcium triplet, as well as weak line of [O I] and [S II]. This appearance is very different from that of the more massive pre-main-sequence stars<sup>4</sup>. In accordance with the luminosity estimate, the spectroscopic

**Table 2** Infrared observations

	J	H	K	L	M
31 January 1985 (mag.)	13.8 (0.25)	10.74 (0.05)	8.33 (0.01)	3.72 (0.01)	2.47 (0.03)
	12 $\mu\text{m}$	25 $\mu\text{m}$	60 $\mu\text{m}$	100 $\mu\text{m}$	
IRAS (Jy)	28.3	89.6	186.6	225.0	

evidence suggests that the infrared source and the source of illumination of Object 50 is a low- or intermediate-mass pre-main-sequence star. The sudden appearance of Object 50 implies an abrupt brightening of the infrared source reminiscent of FU Ori eruptions<sup>5</sup>. However, following an outburst, FU Ori stars do not show H $\alpha$  emission, at least not strong enough to be visible in low-resolution spectra. Moreover, the 2.0–2.2- $\mu\text{m}$  wavelength range in these objects is characterized by a suppression caused by the 1.9- $\mu\text{m}$  H<sub>2</sub>O absorption band. Our 2.0–2.5- $\mu\text{m}$  circular variable filter (CVF) spectrum shows no such absorption, only a red continuum with no lines. A 2.8–4.2- $\mu\text{m}$  CVF spectrum shows a pronounced 3.07- $\mu\text{m}$  ice absorption band.

We obtained a map of the source at 2.2  $\mu\text{m}$  on 9 February 1985, with the ESO 1-m telescope and a 5-arc-s diaphragm, by taking data at 3-arc-s intervals in right ascension and declination (Fig. 3). The infrared source is extended in a NW-SE direction, with a structure closely mimicking the optical beam seen in Fig. 1b. The linear optical and near-infrared feature is seen to emanate from the eastern side of the stellar source which lies at or slightly west of the western optical knot. The axis defined by the linear feature points directly toward the centre of the redshifted lobe of the bipolar CO outflow located to the northwest of the infrared source. The prototype of such infrared nebulae is located in Chamaeleon<sup>6,7</sup>.

**Table 1** Positions measured on the 1979 Schmidt phase

Object	RA (1950)	Dec. (1950)
Object 50	5 h 39 min 05.0 s	-7° 30' 26" a
Object 50 IRS (optical position)	5 38 03.4	-7 29 04 b
Object 50 IRS (IRAS position)	5 38 02.7	-7 28 59

IRS, infrared source; a, approximate central position; b, brightest eastern lobe.

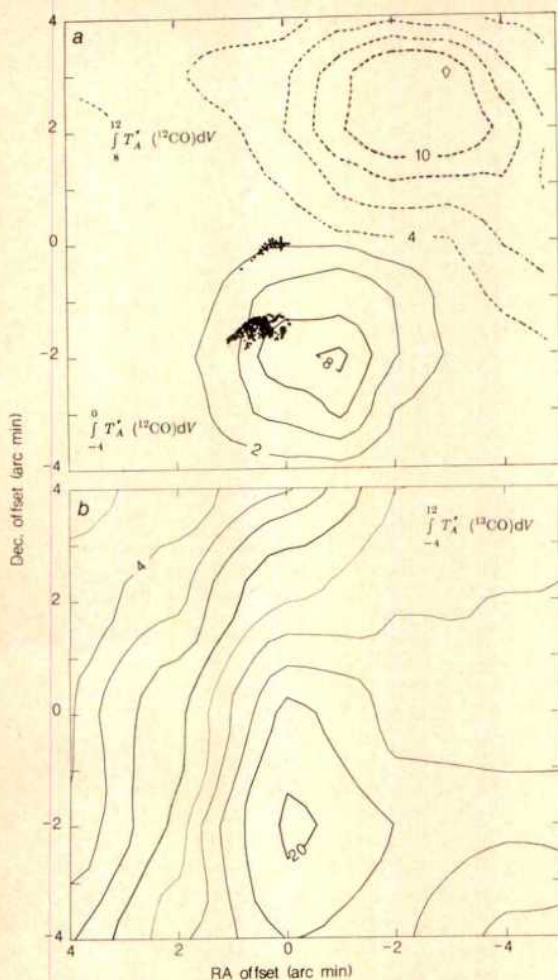


**Fig. 4** *a*, A  $^{12}\text{CO}$  map made with the 7-m millimetre-wave antenna at Crawford Hill in New Jersey, showing the redshifted (broken contours) and blueshifted (solid contours) lobes of the bipolar flow associated with Object 50. Contour interval:  $2 \text{ K km s}^{-1}$ . The + symbol at (0, 0) marks the position of the infrared source. The position of the optical nebula is indicated by the dotted pattern. *b*, A  $^{13}\text{CO}$  map showing the distribution of total emissivity (which is roughly proportional to the column density of molecular gas) in the region surrounding Object 50. Contour interval:  $2 \text{ K km s}^{-1}$ .  $T_A^*$  is the observed antenna temperature corrected for atmospheric attenuation.  $V$  is the velocity (in  $\text{km s}^{-1}$ ) with respect to the local standard of rest.

A  $10 \times 10$ -arc-min field was mapped in the  $^{12}\text{CO}$  and  $^{13}\text{CO}$  species with the AT&T Bell Laboratories 7-m millimetre-wave antenna located in Holmdel, New Jersey. The beam size of this antenna at 110 GHz is 100 arc s. An 8-arc-min-long, bent bipolar outflow (Fig. 4*a*) is centred near the infrared source. The velocity of the outflow is low; the full width of the high-velocity emission at the 0.2-K level is only  $\sim 16 \text{ km s}^{-1}$ . As we do not know the inclination of the source with respect to the line-of-sight, the true flow velocity is impossible to determine; however, a reasonable guess is that it is in the range  $4\text{--}8 \text{ km s}^{-1}$ . Using the observed isotopic intensity ratio,  $^{12}\text{CO}/^{13}\text{CO} = 20$  in the wings, we estimate the observed flow mass to be  $\sim 2.5M_\odot$ . About this much mass may be present at velocities hidden by the cloud core and is thus unobservable. Therefore, a good estimate for the total flow mass is  $5M_\odot$ . The flow dynamic lifetime is  $R/V_{\text{flow}} = 10^5 \text{ yr}$ , making this one of the older bipolar outflows known<sup>8</sup>. The mechanical luminosity in the flow is  $0.6L_\odot$ , the energy of the flow is  $2 \times 10^{45} \text{ erg}$ , and the momentum is  $30M_\odot \text{ km s}^{-1}$ . These values are characteristic of a highly evolved outflow associated with a star of intermediate luminosity.

The  $^{13}\text{CO}$  observations (Fig. 4*b*) show that the infrared source is located at the northern end of a high-column-density region centred at  $V_{\text{LSR}}$  (velocity with respect to the local standard of

rest) =  $4 \text{ km s}^{-1}$ . We believe that the blueshifted portion of the CO outflow has been deflected to the west by the north-south ridge of gas. The optical nebulosity is situated at the extreme eastern edge of the blueshifted portion of the bipolar flow and is possibly a protrusion of high-density gas directly illuminated by the star through the cavity excavated by the outflow. This feature may be part of the structure responsible for the deflection of the blueshifted flow. Evidently this is the first place where the flow has punched a hole in the ambient foreground cloud, allowing scattered light from the infrared source to escape towards our line-of-sight.

The abrupt appearance of Object 50 within the past 30 years may indicate a sudden brightening of the infrared source, similar to an FU-Orionis eruption. Variability of reflection nebulae has been observed before, notably in Hubble's variable nebula (NGC2261)<sup>9</sup>, PV Cep<sup>10,11</sup>, and R CrA (ref. 12 and J. A. Graham and A. C. Phillips, in preparation), but not on the spectacular scale reported here. We believe the underlying mechanism operating both in the present region and in the above objects is time variability of the light output from a young embedded star, possibly modulated by the movement of opaque masses very close to the star, causing patterns of light and shadow to move over the surrounding cloud. The extended cavities through which the light is transmitted to the reflecting surfaces have been produced recently by a bipolar outflow from the newborn star. This is probably a common phenomenon for all stars that are emerging from their parental clouds. In view of the sudden appearance of Object 50, we may here be seeing the first light emerging from this young star.

We thank John Graham for the optical spectrum, Patrice Bouchet for giving us observing time to obtain the  $2.2\text{-}\mu\text{m}$  map, and Leif Hansen for a CCD image. This study was supported in part by the Danish Astronomical Board and the Danish Space Agency.

Received 9 December 1985; accepted 6 February 1986.

- Reipurth, B. *Astr. Astrophys. Suppl.* **61**, 319–330 (1985).
- Price, S. D., Murdoch, L. P. & Shivanandan, K. *Far Infrared Sky Survey Experiment. Final Report AFGL-TR-83-0055* (NASA, Washington, DC, 1983).
- McGregor, P. J., Persson, S. E. & Cohen, J. G. *Astrophys. J.* **286**, 609–629 (1984).
- Herbig, G. H. & Soderblom, D. R. *Astrophys. J.* **242**, 628–637 (1980).
- Herbig, G. H. *Astrophys. J.* **217**, 693–715 (1977).
- Schwartz, R. D. & Heinze, K. G. *Astr. J.* **88**, 1665–1669 (1983).
- Cohen, N. & Schwartz, R. D. *Astr. J.* **89**, 277–279 (1984).
- Bally, J. & Lada, C. J. *Astrophys. J.* **265**, 824–847 (1983).
- Hubble, E. P. *Astrophys. J.* **44**, 190–197 (1916).
- Cohen, M., Kuhf, L. V. & Harlan, E. A. *Astrophys. J.* **215**, L127–L129 (1977).
- Cohen, M., Kuhf, L. V., Harlan, E. A. & Spinrad, H. *Astrophys. J.* **245**, 920–926 (1981).
- Knox-Shaw, H. *Mon. Not. R. astr. Soc.* **76**, 646–647 (1916).

## Occurrence of liquid-crystalline mesophases in microemulsion dispersions

J. Tabony

CEA-IRDI-DESICP, Département de Physico-Chimie, Centre d'Etudes Nucléaires de Saclay, 91191 Gif-sur-Yvette, Cedex, France

Although microemulsion dispersions have compositions which are related to lyotropic liquid crystals, their possible structures are not normally considered to be crystalline. As described here, small-angle neutron diffraction spectra have been obtained from some oil-water microemulsion dispersions, and display peaks which correspond to lamellar, hexagonal and cubic arrangements, similar to those observed in lyotropic liquid crystals. The formation of these liquid crystal mesophases (mesomorphic phases) seems to be a general feature of microemulsion compositions and not an isolated example.

Surfactant molecules in aqueous solution self-aggregate in various ways<sup>1–4</sup>. At surfactant concentrations of less than about 20–30 wt%, micellar solutions are formed, which comprise small

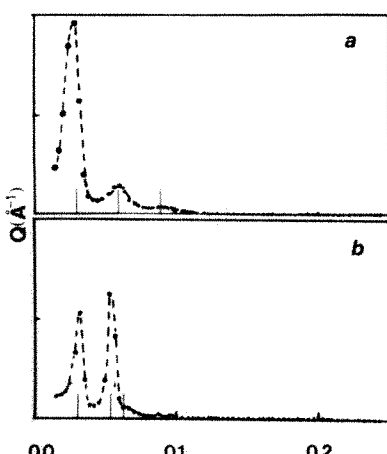


**Fig. 1** Neutron small-angle diffraction patterns from microemulsions with the compositions given in the text. *a*, Composition A; *b*, composition B. The vertical lines indicate the expected positions<sup>9</sup> for *a*, a lamellar structure with 185-Å spacing and *b*, a hexagonal structure with a 200-Å unit cell.

quasi-spherical aggregates, with a radius approximately the size of the surfactant chain length<sup>3,4</sup>. Little or no long-range order exists between these micelles. At higher surfactant concentrations the micelles often increase in size, becoming rods or plates; long-range order is established and the well known lamellar, hexagonal and cubic liquid crystalline mesophases occur<sup>1,2</sup>. Solubilization of hydrocarbons in these surfactant-water binary mixtures is often limited, but is considerably enhanced by the addition of a co-surfactant such as a short-chain alcohol like pentanol or butanol.

The resulting oil and water dispersions, commonly termed microemulsions<sup>5</sup>, are frequently fluid, transparent and optically isotropic. Often such microemulsion dispersions can be formulated over a wide range of oil and water volume fractions. For small concentrations of oil or water the structure has frequently been found to be a dispersion of oil droplets in water or water droplets in oil<sup>6</sup>. The droplets are stabilized by an interfacial film of surfactant and co-surfactant and may be considered to be swollen micelles.

Microemulsion dispersions are not normally thought to form liquid-crystalline mesophases. However, since in surfactant-water binary mixtures micelles precede the appearance of liquid-crystalline phases, and since some microemulsion dispersions resemble swollen micelles, then under some circumstances, such as an increased volume fraction of swollen micelles, the oil or water droplets may rearrange in such a way that liquid-crystalline materials result. Recently, a neutron diffraction pattern consistent with a cubic structure has been obtained from a microemulsion containing approximately equal volumes of oil and water<sup>7</sup>. Here I present neutron diffraction spectra from microemulsion dispersions which are characteristic of lamellar and hexagonal structures. Unlike the cubic phase mentioned above, these liquid-crystalline phases occur for low as well as high volume fractions of dispersed oil or water. These liquid crystalline materials differ from ordinary surfactant-water lyotropic liquid crystals in that the surfactant concentrations are much lower (10 wt% or less) than those normally used (~50 wt%). This results in lattice spacings (200–1,000 Å) considerably larger than those found in surfactant-water binary systems (20–100 Å). One way of accounting for this difference in behaviour is the following: if in binary surfactant-water liquid crystals, the liquid-crystalline phases are derived from small surfactant micelles (radius ~20 Å), then in microemulsions they will arise from the larger swollen micelles (radius 100–200 Å). Hence in the latter case not only will the crystal spacings be much greater, but because the bulk of the swollen micelle is comprised of either oil or water, the amount of surfactant in the dispersion

will be much less than for the binary surfactant-water case. Moreover, as the bulk of the surfactant is situated at the oil–water interface, the ratio of the quantities of surfactant to oil or surfactant to water will control the dimensions of the crystal spacings. Such a simplistic explanation does not, however, explain why such liquid crystals arise. They may no longer be microemulsions in the strict sense of the word, and the use of this term may be misleading. Here I shall continue to call them liquid crystal microemulsions, although oil–water liquid crystals might be a more appropriate name.

Figure 1 shows neutron diffraction spectra obtained from two liquid crystal microemulsions, which display lamellar and hexagonal structures. The spectra were obtained on the small-angle neutron diffractometer, D16, at the Institut Laue-Langevin, Grenoble<sup>8</sup>.

The microemulsion compositions were: A (lamellar), tetradecyl trimethylammonium bromide (0.58 g), pentanol (0.65 ml), cyclohexane (0.35 ml), D<sub>2</sub>O (8 ml); B (hexagonal), tetradecyl trimethylammonium bromide (1.42 g), pentanol (0.60 ml), cyclohexane (4.0 ml), D<sub>2</sub>O (4.0 ml). So as to allow comparison, the composition of the cubic phase already reported<sup>7</sup> was tetradecyl trimethylammonium bromide (2.1 g), butanol (1.0 ml), octane (4.0 ml), D<sub>2</sub>O (4.0 ml).

The spectrum from composition A (Fig. 1*a*) shows three equidistant Bragg peaks corresponding to a lamellar<sup>9</sup> structure with a lattice spacing of 185 Å. Although the dispersion contains more than 85% water it is both viscous and optically birefringent. The spectrum from composition B (Fig. 1*b*) shows Bragg peaks for values of the momentum transfer (*Q*) in approximately the ratio 1: $\sqrt{3}$ :2. This is consistent with a hexagonal arrangement with a unit cell of 200 Å. Like the lamellar phase, the dispersion is both viscous and birefringent. As in ordinary lyotropic liquid crystals, the viscosity increases in the order lamellar, hexagonal, cubic: the lamellar phase flows slowly, whereas the cubic phase appears solid, flowing only over a period of days or weeks. None of these materials appears to behave as a newtonian fluid; they form spontaneously on mixing and show no signs of separation either after storage for more than a year or on centrifugation. Hence, they appear to be thermodynamically stable, and probably do not consist of a dispersion of small liquid-crystal particles. If the latter were the case, the resulting Bragg spacings would be much smaller than those observed.

The structure of these phases has not yet been fully elucidated. The lamellar phase probably comprises thin layers of cyclohexane sandwiched between an interfacial film of surfactant and co-surfactant. The amount of cyclohexane in composition A corresponds to approximately one monolayer; given the length of the surfactant molecule, this suggests that the oil-soap sandwich should be approximately 30–40 Å thick. This should be compared with the overall spacing of 185 Å. These mesophases occur over a relatively restricted range of alcohol concentrations. For the lamellar phase this corresponds to a molar ratio of alcohol to surfactant of ~3:1. This observation suggests that in this case the interfacial layer is comprised of a two-dimensional hexagonal arrangement of alcohol molecules with a surfactant molecule in the centre. The proton NMR spectra consist of relatively sharp lines similar to those observed in ordinary lyotropic liquid crystals; this shows that the different molecular components are in a mobile liquid state. It thus seems likely that the interfacial layer of surfactant and co-surfactant has considerable dynamic disorder. Although the lamellar composition (A) contains only a small amount of cyclohexane, much higher cyclohexane concentrations may be used. Lamellar phases have been observed in compositions having equal volumes of oil and water, and even oil-based compositions. It thus appears that the thickness of the oil and/or water layers can be varied almost at will.

In the phase diagram, the lamellar phase of composition A adjoins that of a dispersion of swollen micelles, and changes in the alcohol or surfactant concentration result in a transition to

such a structure. This suggests that the lamellar phase is closely related to a dispersion of droplets. A transition from a dispersion of droplets to a dispersion of plates could result in a lamellar nematic-type phase. The driving force for the transition is clearly related to the alcohol content of the dispersion. Following the interfacial theory (R) presented by Winsor<sup>10</sup>, it can be argued that progressive intercalation of alcohol amongst the paraffinic surfactant chains will tend to reduce the interfacial curvature in the swollen micelle until flat regions are formed which subsequently order in a lamellar manner. This is supported by the observation that in the hexagonal and cubic phases, which have locally non-zero interfacial curvatures, the alcohol-to-surfactant ratio is less than in the lamellar phase.

Although all of the examples presented contain the same surfactant, I have also formulated liquid crystal microemulsions with other surfactants and co-surfactants. Their occurrence hence seems to be a general feature of microemulsion phase behaviour and not an isolated example.

I thank the Institut Laue-Langevin, Grenoble, for providing the neutron beam time, and S. Wilson and L. Braganza for their assistance with the D16 diffractometer.

Received 9 September 1985; accepted 21 January 1986.

- Elkwall, P. in *Advances in Liquid Crystals* Vol. 1 (ed. Brown, G. H.) Ch. 1 (Academic, New York, 1971).
- Tiddy, G. J. T. *Phys. Rep.* **57**, 1–46 (1980).
- Wennerstrom, H. & Lindman, B. *Phys. Rep.* **52**, 1–86 (1979).
- Lindman, B. & Wennerstrom, H. *Topics Curr. Chem.* **87**, 1–84 (1980).
- Prince, L. M. *Microemulsion, Theory and Practice* (Academic, New York, 1977).
- Cebula, D. J., Harding, L., Ottewill, R. H. & Pusey, P. N. *Colloid Polym. Sci.* **258**, 973–976 (1980).
- Tabony, J. *Nature* **319**, 400 (1986).
- Neutron Beam Facilities Available for Users* (Institut Laue-Langevin, Grenoble, 1981).
- Fontell, K. in *Liquid Crystals and Plastic Crystals* Vol. 2 (eds Gray, G. W. & Winsor, P. A.) Ch. 4 (Wiley, New York, 1974).
- Winsor, P. A. in *Liquid Crystals and Plastic Crystals* Vol. 1 (eds Gray, G. W. & Winsor, P. A.) Ch. 5 (Wiley, New York, 1974).

## Phase behaviour of concentrated suspensions of nearly hard colloidal spheres

P. N. Pusey & W. van Megen\*

Royal Signals and Radar Establishment, St Andrews Road, Malvern WR14 3PS, UK

Suspensions of spherical colloidal particles in a liquid show a fascinating variety of phase behaviour which can mimic that of simple atomic liquids and solids. 'Colloidal fluids'<sup>1–4</sup>, in which there are significant short-range correlations between the positions of neighbouring particles, and 'colloidal crystals'<sup>5–7</sup>, which have long-range spatial order, have been investigated extensively. We report here a detailed study of the phase diagram of suspensions of colloidal spheres which interact through a steep repulsive potential. With increasing particle concentration we observed a progression from colloidal fluid, to fluid and crystal phases in coexistence, to fully crystallized samples. At the highest concentrations we obtained very viscous samples in which full crystallization had not occurred after several months and in which the particles appeared to be arranged as an amorphous 'colloidal glass'. The empirical phase diagram can be reproduced reasonably well by an effective hard-sphere model. The observation of the colloidal glass phase is interesting both in itself and because of possible relevance to the manufacture of high-strength ceramics<sup>8</sup>.

The particles studied were colloidal polymethylmethacrylate (PMMA), stabilized sterically by poly-12-hydroxystearic acid<sup>9</sup>. Electron microscopy, light scattering and crystallography showed the radius of the PMMA cores to be  $305 \pm 10$  nm and

the polydispersity (standard deviation of the particle size distribution divided by the mean size) to be about 0.05. The thickness of the stabilizer layer was 10–20 nm, a small fraction of the particle radius. Thus the repulsive potential arising from interpenetration of the polymer coatings of different particles was relatively steep. The suspension medium was a mixture of decalin and carbon disulphide in volume ratio 2.66:1, chosen to match closely the refractive index of the particles, ~1.51 (ref. 10). This provided nearly transparent samples suitable for light scattering measurements as well as for visual observation of processes occurring in the bulk of the samples. Furthermore, index matching is expected to minimize interparticle attractions due to van der Waals forces. Ten samples were prepared from a stock solution of known PMMA weight fraction (determined by drying). They were concentrated by low-speed centrifugation to form a dense sediment, followed by removal of a weighed amount of clear supernatant liquid. Slow tumbling of the samples then redispersed the particles effectively. The fractional volumes  $\phi_C$  of the samples occupied by PMMA cores were calculated using literature values for the densities of PMMA and the liquids.

After extensive tumbling which, we assume, left the particles positionally randomized (that is, showing only local short-range order), samples 2–10 were set up as shown in Fig. 1a and were illuminated obliquely from behind by a broad beam of white light. The most dilute sample (2, on the extreme right of Fig. 1a), with  $\phi_C = 0.393$ , showed no macroscopically observable change with time. Earlier work<sup>10–12</sup> has established that at (and below) this concentration the particles are spatially arranged much like atoms in a dense liquid, exhibiting considerable short-range positional ordering. Although hindered by their neighbours, the particles remain able to diffuse through this colloidal fluid under the influence of brownian motion. After times ranging from minutes to hours, small, Bragg-reflecting crystallites formed homogeneously throughout the volumes of samples 3–7. In samples 3–5 the crystallites settled under gravity within a day to form well-defined boundaries between coexisting polycrystalline and fluid phases. Samples 6 and 7 remained filled with small compact crystallites. In these two samples the state of lowest free energy is evidently a colloidal crystal which grows, by diffusion of the particles, from the randomized metastable state formed by the tumbling process. Once crystallization is complete, the particle motions are largely limited to local brownian excursions centred on sites in the regular crystalline array. The crystal structure was determined by light-scattering crystallography to be face-centred cubic<sup>13</sup>. The coexistence of colloidal fluid and crystal observed in samples 3–5 is analogous to the coexistence of a simple liquid and solid (such as ice and water) at a first-order phase transition. Sample 8 crystallized heterogeneously, starting from the meniscus and cell walls, to form relatively large irregular crystals. The most concentrated ( $\phi_C \geq 0.50$ ), highly viscous samples 9 and 10 exhibited only partial heterogeneous crystallization even when left undisturbed for several months. Although the crystalline state is, presumably, still thermodynamically preferred for these samples, it appears that the concentration is so high that particle diffusion is hindered to the point where crystals do not form on this timescale and the suspensions remain in the metastable amorphous phase created by the tumbling. The different results of homogeneous and heterogeneous nucleation are shown clearly in Fig. 1b.

The observed phase behaviour is summarized in Fig. 2. In the coexistence region we plot the fraction of the sample volume occupied by the crystalline phase against  $\phi_C$ . Not surprisingly, we find a linear (lever-rule) dependence which, when extrapolated to 0 and 100%, provides 'freezing' and 'melting' concentrations.

While there is evidence<sup>13</sup> that, due to interpenetration of their stabilizing polymer coatings, the interaction between the particles is slightly 'soft', it seems simplest to discuss our findings in terms of an effective hard-sphere model; such models for simple

\* Permanent address: Department of Applied Physics, Royal Melbourne Institute of Technology, Melbourne, Australia.

**Fig. 1** *a*, Nearly-hard-sphere suspensions, 4 days after tumbling, illuminated obliquely from behind by white light. The samples are contained in cells of cross-section 1 cm  $\times$  1 cm and are numbered 2–10, in our nomenclature, from the right in order of increasing concentration. Actual concentrations are shown in Fig. 2. Immediately after tumbling, all the samples appeared featureless (see top of sample 2 or bottom of sample 9), reflecting randomization of the particle positions. The text describes the dynamic processes which occurred over 4 days and led to the structures depicted in the photograph. The scattering geometry is such that the first peak in the structure factor of the amorphous phases and the first Bragg reflection of the crystals occur in the red at the right of the picture and in the blue-green at the left. Some overall gravitational settling of the particles has occurred, leading to a small layer of crystals at the bottom of sample 2 (which, it should be emphasized, showed no crystallization in the bulk) and compaction of the crystallites at the bottom of samples 3–7. *b*, Close-up of samples 7–9 under the same conditions as in *a*. Crystallization nucleated homogeneously in sample 7 but heterogeneously in sample 8. The lower part of sample 9 shows clearly the amorphous glassy phase which did not crystallize over several months.



liquids have been extensively studied, both theoretically and by computer simulation<sup>14–17</sup>. Thus we assume that the core volume fraction  $\phi_c^F = 0.407$ , at which freezing starts (see Fig. 2), is equivalent to an effective volume fraction 0.494, the freezing concentration for hard spheres<sup>16</sup>. This implies a hard-sphere interaction radius about 20 nm (roughly the thickness of the stabilizer layer) greater than the core radius, ~305 nm. We therefore include in Fig. 2 a scale appropriate to the effective hard-sphere volume fraction, defined by  $\phi_E = (0.494/0.407)\phi_c$ . With this scaling the melting density  $\phi_E^M = 0.536$  for the colloidal suspension is slightly smaller than the value 0.545 expected for the equivalent hard spheres<sup>16</sup>. Such a slight difference between the observed coexistence region and that expected for hard spheres could be caused by several factors; for example, softness

of the interparticle potential<sup>17</sup>, slight interparticle attractions<sup>17</sup>, particle polydispersity<sup>18</sup>, or, very likely, a combination of these. The effective volume fraction of the most concentrated glassy sample, 10, is close to the value  $\phi_E = 0.637$  expected for the Bernal (random close-packed) hard-sphere glass<sup>14,19,20</sup>.

We conclude that the colloidal suspensions described above should prove useful model 'nearly-hard-sphere' systems for further experimentation. In particular, the rate of transport in these suspensions is many orders of magnitude smaller than that in simple molecular systems, a property which should simplify the study of some kinetic processes<sup>21</sup>. We have already made a number of other measurements, discussed elsewhere<sup>13</sup>. These include: the kinetics of crystallization, light crystallography, rheological measurements in the metastable fluid and

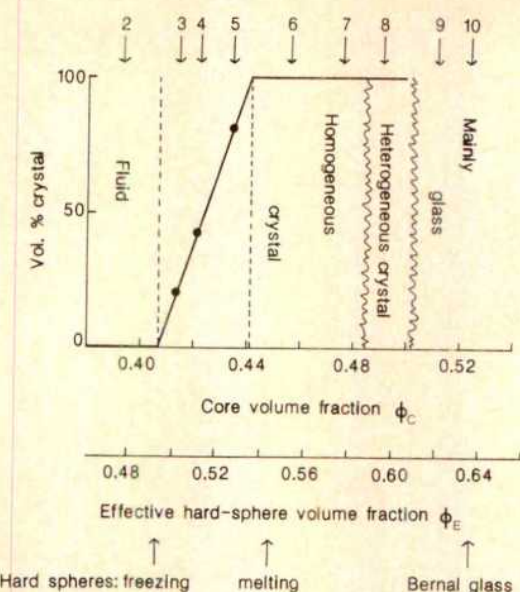


**Fig. 2** 'Phase-diagram' of the samples shown in Fig. 1. Arrows at top indicate the sample concentrations. The two horizontal axes indicate the measured volume fraction of PMMA cores and the effective hard-sphere volume fraction defined in the text. Arrows at the bottom indicate the volume fractions, obtained from computer simulations, for freezing, melting and random close packing ('Bernal glass') of hard spheres.

glassy phases, and measurements by conventional and dynamic light scattering of structure factors and particle diffusion in the fluid, crystal and glassy phases. The discovery of a glass composed of (nearly) equal-sized spheres is especially interesting since, although there has recently been considerable theoretical work (for example, refs 22–25) and computer simulations<sup>14,15</sup> on such model glasses, real glasses composed of spherical units are rare. (Colloidal glasses observed up to now have contained mixtures of spheres of different sizes<sup>26</sup>.) Finally we note current interest<sup>8</sup> in manufacturing industrial ceramics from 'green bodies' composed of particles of uniform size packed densely either at random (a colloidal glass) or in a colloidal crystal; the present work shows how both these structures may be achieved.

We thank Professor R. H. Ottewill and his group at Bristol University for providing the PMMA particles complete with electron-microscopic characterization; Dr L. V. Woodcock for a valuable discussion; and Mr L. Clarke for the photography.

Received 13 November 1985; accepted 5 February 1986.

- Brown, J. C., Pusey, P. N., Goodwin, J. W. & Ottewill, R. H. *J. Phys.* **A8**, 664–682 (1975).
- Dickinson, E. A. *Rep. R. Soc. Chem. C*, 3–37 (1983).
- van Megen, W. & Snook, I. *Adv. Colloid Interface Sci.* **21**, 119–194 (1984).
- Edwards, J., Everett, D. H., O'Sullivan, T., Pangalou, I. & Vincent, B. *JCS Faraday Trans. I* **80**, 2599–2607 (1984).
- Kose, A. & Hachisu, S. *J. Colloid Interface Sci.* **46**, 460–469 (1974).
- Clark, N. A., Hurd, A. J. & Ackerson, B. J. *Nature* **281**, 57–60 (1979).
- Pieranski, P. *Contemp. Phys.* **24**, 25–73 (1983).
- Calvert, P. *Nature* **317**, 201 (1985).
- Antl, L. *et al.* *Colloids and Surfaces* (in the press).
- van Megen, W., Ottewill, R. H., Owens, S. M. & Pusey, P. N. *J. chem. Phys.* **82**, 508–515 (1985).
- Pusey, P. N. & van Megen, W. *J. Phys., Paris* **44**, 285–291 (1983).
- Vrij, A. *et al.* *Faraday Discuss. chem. Soc.* **76**, 19–35 (1983).
- Pusey, P. N. & van Megen, W. in *Proc. Symp. Physics of Complex and Supermolecular Fluids* (ed. Safran, S. A.) (Wiley, New York, in the press).
- Woodcock, L. V. *Ann. N.Y. Acad. Sci.* **37**, 274–298 (1981).
- Angell, C. A., Clarke, J. H. R. & Woodcock, L. V. *Adv. chem. Phys.* **48**, 397–453 (1981).
- Hoover, W. G. & Ree, F. H. *J. chem. Phys.* **49**, 3609–3617 (1968).
- Hansen, J. P. & McDonald, I. R. *Theory of Simple Liquids* (Academic, New York, 1976).
- Dickinson, E. & Parker, R. J. *Phys., Paris* **46**, L229–L232 (1985).
- Bernal, J. D. & Mason, J. *Nature* **188**, 910 (1960).
- Bernal, J. D. *Proc. R. Soc. A280*, 299–322 (1964).
- Hanley, H. J. M., Rainwater, J. C., Clark, N. A. & Ackerson, B. J. *J. chem. Phys.* **79**, 4448–4458 (1983).
- Leutheusser, E. *Phys. Rev. A29*, 2765–2773 (1984).
- Das, S. P., Mazenko, G. F., Ramaswamy, S. & Toner, J. *J. Phys. Rev. Lett.* **54**, 118–121 (1985).
- Singh, Y., Stoessel, J. P. & Wolynes, P. G. *Phys. Rev. Lett.* **54**, 1059–1062 (1985).
- Ullo, J. J. & Yip, S. *Phys. Rev. Lett.* **54**, 1509–1512 (1985).
- Lindsay, H. M. & Chaikin, P. M. *J. chem. Phys.* **76**, 3774–3781 (1982).

## Bubble raft model for indentation with adhesion

J. M. Georges, G. Meille, J. L. Loubet & A. M. Tolen

Laboratoire de Technologie des Surfaces, Ecole Centrale de Lyon, 36 avenue Guy de Collongue, CNRS UA 85, BP 163, 69131 Ecully Cedex, France

Indentation hardness tests are now widely used to measure the mechanical properties of solid surfaces<sup>1–3</sup>. Recent developments of this technique<sup>4,5</sup> permit the analysis of the outermost 10 nm of materials. Experimental and theoretical questions arise regarding the physical and mechanical processes involved in such small indentations. We describe here an indentation experiment on a microscopic scale, using soap bubbles blown onto a water surface. Bubble rafts provide a simple two-dimensional model for indentation behaviour; as for other materials, their behaviour is governed by two principal attraction–repulsion forces<sup>6</sup>, and by geometrical constraints. A crystalline two-dimensional lattice is obtained by using bubbles of uniform size<sup>7–9</sup>, whereas bubbles of two sizes give an amorphous structure<sup>10,11</sup>. Indentation can be represented by the contact between a triangular crystalline raft and a rectangular crystalline raft bordered by an amorphous layer. The flow of the materials, which is dependent on both adhesion and the force between the two rafts, can be analysed during the experiment.

The experimental configuration is shown in Fig. 1. We used a rectangular glass trough, approximately 60 × 30 cm and 15 cm deep, containing a soap solution of surface tension  $\gamma = 6.9 \times 10^{-2}$  N m<sup>-1</sup>. Air at constant pressure was blown through short capillaries with 50-μm and 100-μm bores in order to produce uniform bubbles. The bubble diameter depends on the nozzle size and is independent of the distance of the jet below

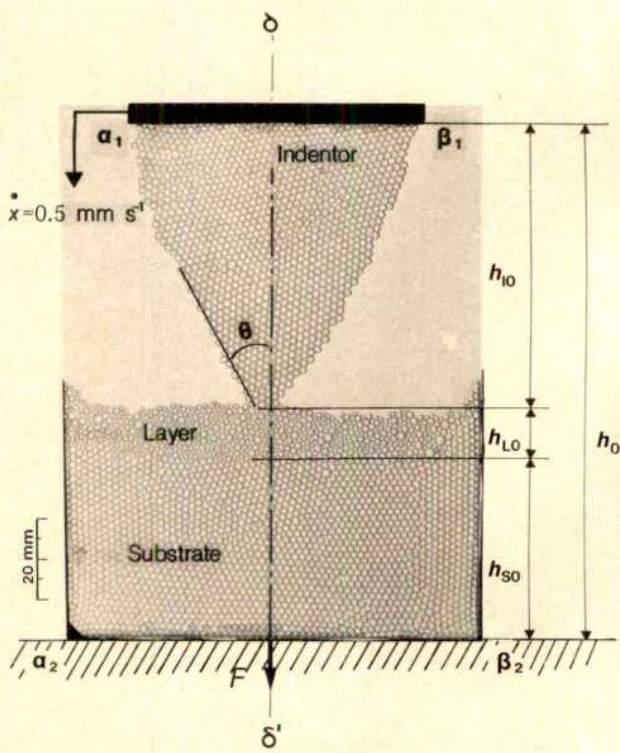


**Fig. 1** Bubble rafts used to model the indentation process. Two-dimensional rafts containing bubbles of 2.3 mm and 1.4 mm diameter are blown onto a water surface. The displacement to frame  $\alpha_1\beta_1$  parallel to frame  $\alpha_2\beta_2$  causes indentation to take place. The force  $F$  is measured in the plane perpendicular to frame  $\alpha_2\beta_2$ .

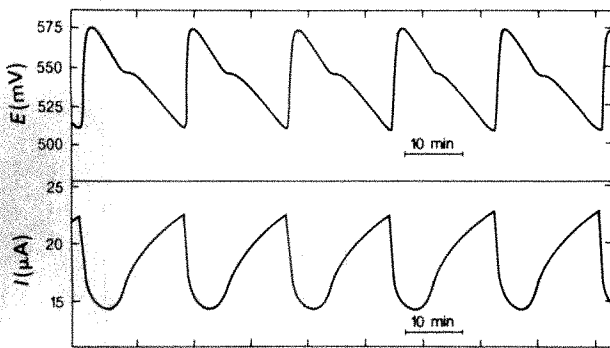


**Fig. 1** Chemical oscillations in the permanganate-hydrogen peroxide system ( $2 \times 10^{-4}$  M  $\text{KMnO}_4$ ,  $3 \times 10^{-4}$  M  $\text{H}_2\text{O}_2$ ,  $10^{-3}$  M  $\text{H}_3\text{PO}_4$ ,  $k_0 = 1.8 \times 10^{-3} \text{ s}^{-1}$ , temperature  $10^\circ\text{C}$ ). The polarographic current was measured with a potential of  $0.0 \text{ V}$  applied to the  $1.0 \text{ M}$  mercurousulphate electrode.

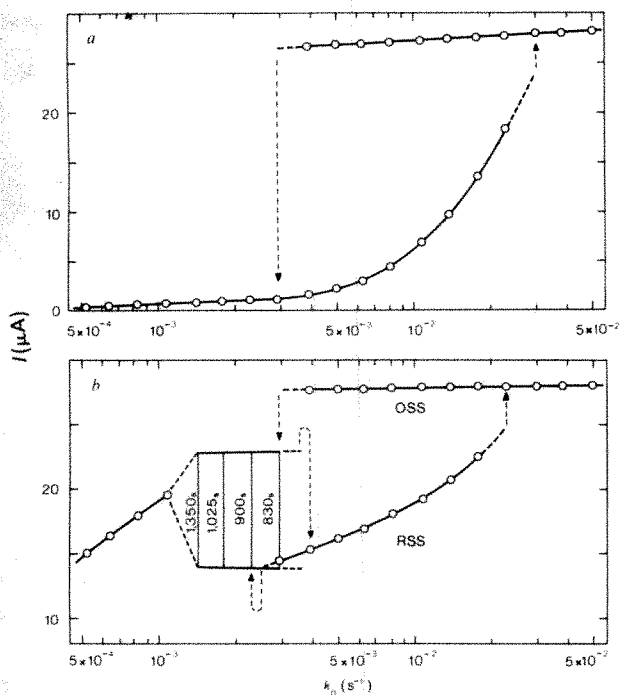
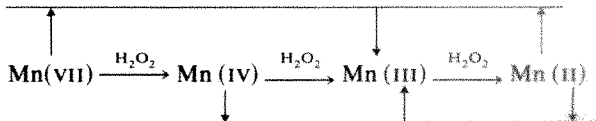


**Fig. 2** Plots of polarographic current ( $I$ ) versus flow rate ( $k_0$ ) for the  $\text{KMnO}_4-\text{H}_2\text{O}_2$  system. In  $a$  ( $2 \times 10^{-4}$  M  $\text{KMnO}_4$ ,  $6 \times 10^{-4}$  M  $\text{H}_2\text{O}_2$ ,  $10^{-3}$  M  $\text{H}_3\text{PO}_4$ , temperature  $10^\circ\text{C}$ ,  $E = 0.0 \text{ V}$ ) the system displays kinetic/bistability; in  $b$  ( $2 \times 10^{-4}$  M  $\text{KMnO}_4$ ,  $3 \times 10^{-4}$  M  $\text{H}_2\text{O}_2$ ,  $10^{-3}$  M  $\text{H}_3\text{PO}_4$ , temperature  $10^\circ\text{C}$ ,  $E = 0.0 \text{ V}$ ) the system has two steady states and an oscillatory state. The system behaviour is described in detail in the text.

highest value of  $k_0$ , the system is in an oxidized steady state. On decreasing  $k_0$  to  $3 \times 10^{-3} \text{ s}^{-1}$ , the system passes from an OSS to an oscillatory state, which persists down to  $k_0 = 1.4 \times 10^{-3} \text{ s}^{-1}$ . On the other hand, on increasing  $k_0$  from  $1.4 \times 10^{-3} \text{ s}^{-1}$  to  $3 \times 10^{-3} \text{ s}^{-1}$ , the system passes from oscillation to a lower set of steady states. The system does not oscillate at  $k_0 = 3 \times 10^{-3} \text{ s}^{-1}$  if returning from the lower set of steady states.

In the conditions described here, the system exhibited sustained oscillations even when the inner wall of the CTR was covered with a film of paraffin. Also, we were able to follow the periodic colour changes of the bulk of the solution even when there was no Pt electrode immersed in the solution. Thus, neither a glass surface nor the presence of platinum was necessary for the chemical oscillations to occur.

The oscillations observed here may arise from the following feedback mechanism:



Further studies are under way in our laboratory on the detailed mechanism of this chemical oscillator, focusing on the role of Mn intermediates and phosphoric acid. We believe we have found the first permanganate chemical oscillator, which might herald the beginning of an era of chemical oscillators based on transition-metal chemistry.

Received 26 November 1985; accepted 14 January 1986.

- De Kepper, P., Ouyang, Q. & Dulos, E. in *Non-Equilibrium Dynamics in Chemical Systems* (eds Vidal, C. & Pacault, A.) 44–49 (Springer, Berlin, 1984).
- Reckley, J. S. & Showalter, K. *J. Am. chem. Soc.* **103**, 7012–7013 (1981).
- Epstein, I. R., Dateo, C. E., De Kepper, P., Kustin, K. & Orbán, M. in *Nonlinear Phenomena in Chemical Systems* (eds Vidal, C. & Pacault, A.) 188–191 (Springer, Berlin, 1984).
- Dallison, A. M., Macer, D. R. J. & Rodley, G. A. *Inorg. chim. Acta* **76**, L219–L221 (1983).
- De Kepper, P., Epstein, I. R. & Kustin, K. *J. Am. chem. Soc.* **103**, 6121–6127 (1981).

## Intensity modulation in SAR images of internal waves

D. R. THOMPSON & R. F. GASPAROVIC

Johns Hopkins University, Applied Physics Laboratory, Laurel, Maryland 20707, USA

During the SAR Signature Experiment<sup>1</sup> (SARSEX), conducted in 1984 in the New York Bight off the eastern coast of the United States, synthetic aperture radar (SAR) images of the ocean surface and concurrent ground-truth measurements were collected in order to test quantitatively various imaging theories. These theories<sup>2–4</sup> predict that the intensity modulations observed in SAR images of internal waves are produced by variations in the small-scale surface roughness induced by spatial variations in the internal-wave surface current field. Analysis of the SARSEX data indicates that the imaging theories can explain the observed modulation for L-band ( $\sim 24\text{-cm}$ ) SAR wavelengths, but under-predict by almost an order of magnitude the observed X-band ( $\sim 3.2\text{-cm}$ ) modulation. To explain this latter discrepancy, we hypothesize a two-step mechanism in which the observed X-band modulation results from additional small-scale roughness produced by the strong perturbation of the metre-scale surface waves by the internal wave current field.

The SARSEX data<sup>1</sup> include L- and X-band SAR images of the ocean surface from various incidence angles and viewing directions, and for the first time, concurrent ground-truth measurements of the wind velocity, surface current velocity and vertical temperature profile for each image. Figure 1 shows typical L- and X-band images of the surface manifestation of a group of internal waves propagating towards the top (range direction) of the image. The SAR incidence angles to these waves range from  $25^\circ$  to  $47^\circ$  which correspond to Bragg wavenumbers  $k_B$  (equal to twice the projection of the radar wavenumber on the horizontal surface) of  $22\text{--}38 \text{ rad m}^{-1}$  for L-band and  $166\text{--}287 \text{ rad m}^{-1}$  for X-band. The research vessels *Bartlett* and *Cape*, seen near the bottom of the images, collected ground-truth data by traversing the waves on parallel tracks towards the top of the scene. Note that both bright and dark bands are associated with each internal wave in the L-band image, but that only bright bands appear at X-band. An acceptable SAR imaging theory, when coupled with the pertinent environmental data, should be able to explain quantitatively the features observed in these images.

For the radar frequencies and incidence angles appropriate to Fig. 1, the radar backscatter from the ocean surface is given by the Bragg scattering limit<sup>5,6</sup>. In this limit, the SAR intensity modulation (or relative intensity) for range-travelling waves is given by

$$M(\mathbf{k}_B, x) = \frac{S(\mathbf{k}_B, x) + S(-\mathbf{k}_B, x)}{S_{eq}(\mathbf{k}_B) + S_{eq}(-\mathbf{k}_B)} \quad (1)$$

where the surface-wave height spectral density  $S(\mathbf{k}_B, x)$  is a function of position ( $x$ ) due to the presence of the surface current field. The quantity  $S_{eq}(\mathbf{k})$  is the equilibrium (no-current) spectrum. The problem is to understand how  $S_{eq}(\mathbf{k})$  is modulated by the surface currents.

As pointed out by Hughes<sup>4</sup> and Alpers<sup>2</sup>, the time and spatial variations of the internal-wave current field are much slower than those of the relevant surface waves, so that a Wentzel, Kramer, Brillouin-type theory<sup>7</sup> may be used to describe their interaction. For this study we adopt an action-balance equation proposed by Hughes<sup>4</sup> of the form

$$\frac{dN(\mathbf{k}; x, t)}{dt} = \beta(\mathbf{k}) N(\mathbf{k}; x, t) \left[ 1 - \frac{N(\mathbf{k}; x, t)}{N_{eq}(\mathbf{k})} \right] \quad (2)$$

where the action spectrum  $N(\mathbf{k}; x, t) = \rho[\omega_0/|\mathbf{k}|]S(\mathbf{k}; x, t)$ ,  $\rho$  is the fluid density,  $\omega_0$  is the intrinsic frequency of a wave in a local rest frame given by  $\omega_0^2 = gk[1 + (k/363)^2]$ , with  $g$  being the gravitational acceleration, and the  $(k/363)^2$  term accounts for surface tension effects. The time dependence of  $k$  and  $x$  in equation (2) is given by the coupled system

$$\begin{aligned} \frac{dx_i}{dt} &= \frac{\partial \omega_0}{\partial k_i} + U_i \\ \frac{dk_i}{dt} &= -k_j \frac{\partial U_j}{\partial x_i} \end{aligned} \quad (3)$$

where  $U_i(x, t)$  is the surface current field, the indices run from 1 to 2, and repeated indices are summed. This system defines trajectories in four-dimensional phase space along which equation (2) is valid. The size of the source term on the right-hand side of equation (2) depends on the function  $\beta(\mathbf{k})$ , the so-called relaxation rate. It is an increasing function of  $k$  and wind speed, but there is considerable uncertainty as to its exact functional form<sup>4,8</sup>. In the present study we use the expression for  $\beta(\mathbf{k})$  given by Hughes<sup>4</sup>. With the relaxation time  $\tau = \beta^{-1}$ , we find, for the conditions of the SARSEX images in Fig. 1, that  $\tau$  ranges from 10 to 20 s at L-band and from 1 to 2 s at X-band.

With the definition  $S(\mathbf{k}, x, t)/S_{eq}(\mathbf{k}) = [1 + P(\mathbf{k}; x, t)]^{-1}$ , we can integrate equation (2) to obtain  $P(\mathbf{k}; x, t)$  in the form

$$P(\mathbf{k}; x, t) = N_{eq}(\mathbf{k}) \int_{-\infty}^t k'_j \frac{\partial U_j(x')}{\partial x'_i} \frac{\partial Q_{eq}(k')}{\partial k'_i} \exp[-\int_{t'}^t \beta(k'') dt''] dt' \quad (4)$$

where  $N_{eq}(\mathbf{k}) = \rho[\omega_0/|\mathbf{k}|]S_{eq}(\mathbf{k})$ ,  $Q_{eq} = 1/N_{eq}$ , and the time dependence of the primed and double-primed variables is given by equations (3). For the results presented below,  $S_{eq}(\mathbf{k})$  is given by a modified Pierson equilibrium spectrum<sup>9</sup>, with a  $\cos^4[(\theta_k - \theta_w)/2]$  angular dependence where  $\theta_w$  is the wind direction. No assumptions concerning the properties of the current fields have been made in obtaining equation (4). For the case where  $|U| \ll \partial \omega_0 / \partial k$  and  $|\partial U / \partial x| \ll \beta$ , it can be shown that equation (4) yields the perturbation given by Alpers<sup>2</sup>.

Experimentally determined surface currents and winds were input to the model described above, and the calculated intensity modulations were compared with those measured from the SAR images. The measured currents were parameterized in the form

$U_0 \operatorname{sech}^2[K(x - C_1 t)]$ , with typical values for the peak current  $U_0$ , phase speed  $C_1$  and peak gradient for the waves shown in Fig. 1 being  $\sim 0.3$ – $0.6 \text{ m s}^{-1}$ ,  $0.65$ – $0.75 \text{ m s}^{-1}$  and  $0.002$ – $0.008 \text{ s}^{-1}$ , respectively. The wind speed was  $6 \text{ m s}^{-1}$  towards  $145^\circ$  with respect to the direction of internal wave propagation.

Figure 2 compares the measured L- and X-band intensity modulations along the track of *Bartlett* over waves 2, 3 and 4 (solid curves) with the predictions from the wave-current interaction model (dashed curves). The measured relative intensities were obtained from the digital SAR imagery by averaging over about 145 m in azimuth, smoothing over 30 m in range and normalizing so that the mean background intensity is unity. As Fig. 2a shows, the general agreement between measurement and prediction at L-band is quite encouraging, although the maximum measured modulation is somewhat under-predicted. Note that the calculated modulation reproduces both the enhancement and reduction in intensity observed in the L-band images. In fact, the computed modulation is roughly proportional to the horizontal current gradient, in agreement with Alpers' theory<sup>2</sup>. Thus, we feel that, within the uncertainties inherent in the ground-truth measurements and the exact value of the relaxation rate, the wave-current interaction theory outlined above can adequately explain the L-band SAR imaging of internal waves.

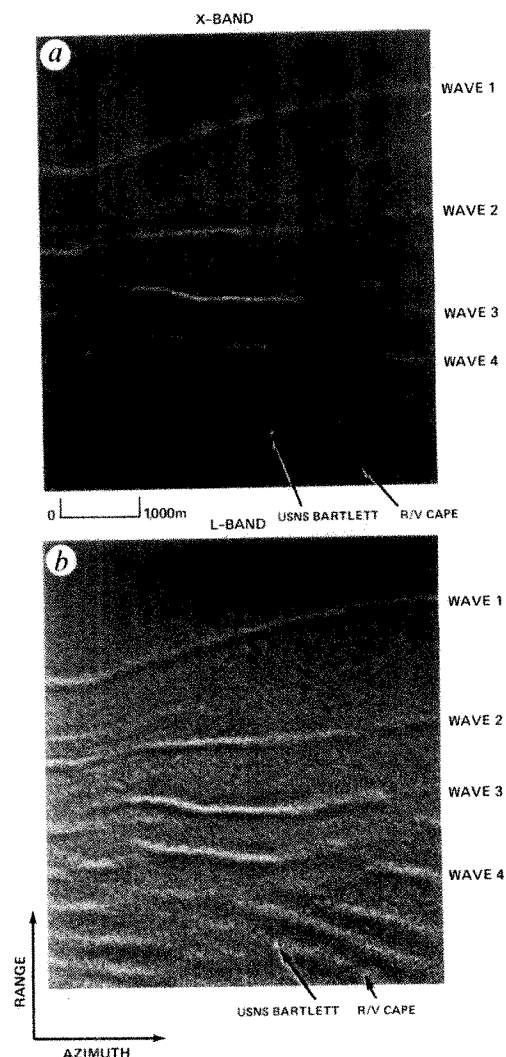
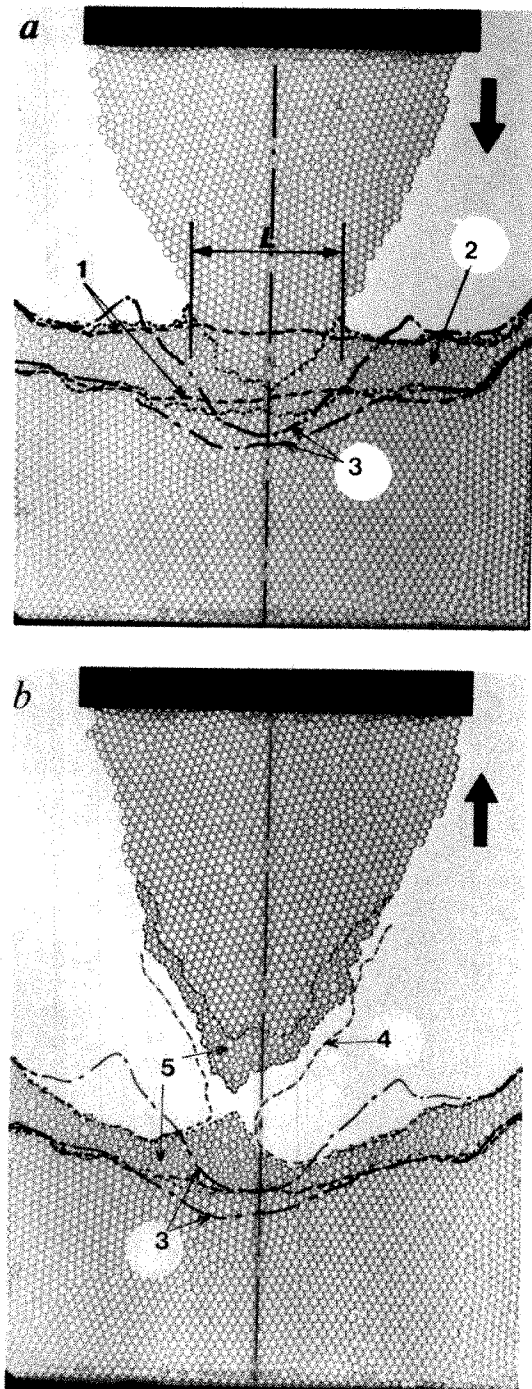


Fig. 1 Concurrent X-band (a) and L-band (b) SAR images of internal waves recorded during the SARSEX.

the surface and the pressure. A raft with uniform bubble diameter (2.3 mm) gives a crystalline structure; a raft with a 40/60 mixture of two diameters (2.3 and 1.4 mm) gives an amorphous structure.

The indenter is a triangular sheet of large bubbles with tip angle  $2\theta = 60^\circ$  which sticks to the frame  $\alpha_1\beta_1$  (Fig. 1). The indented material is a layer of a mixture of two sizes of bubble (thickness  $h_{L0}$ ) on a substrate which is a rectangular sheet of large bubbles (thickness  $h_{S0}$ ) attached to frame  $\alpha_2\beta_2$ . Frame  $\alpha_1\beta_1$  is moved at constant low speed ( $0.5 \text{ mm s}^{-1}$ ) parallel to



**Fig. 2** Examples of deformation during loading (a) and unloading (b). The boundaries of the amorphous layer are shown during the initial (1, dashed lines), intermediate (2, dotted lines) and final (3, dash-dot lines) stages of indentation, and during (4, dashed lines in b) and after (5, dotted lines in b) unloading. In the final configuration (5), note the adherent amorphous layer on the crystalline indenter.

frame  $\alpha_2\beta_2$ , causing an indentation in which a displacement, rather than a load, is imposed. As indentation proceeds, the normal force  $F$  transmitted to  $\alpha_2\beta_2$  is continuously recorded, giving the loading curve (see Fig. 3). The movement is then reversed to obtain the unloading curve.

An enlarged motion picture of the experiment reveals some important aspects of the indentation process (Fig. 2). As the indenter approaches the surface, adhesion occurs between the indenter tip and the amorphous layer. Attractive forces between the two rafts appear well before the two touch, at a distance of about 5 mm. On moving  $\alpha_1\beta_1$  further, repulsive forces appear, and the first displacements occur in the amorphous layer. Then the indenter sinks into this layer, which clearly undergoes considerable plastic flow. In spite of local slips, the substrate does not yield perceptibly under the thrust until the penetration reaches a point where only a small amount of amorphous material (a thickness of 5 or 6 bubbles) is trapped in the interface. It is essential to note that, however far we pushed the indenter into the layer and substrate (3, Fig. 2), we could never penetrate the amorphous layer.

On unloading, the amorphous material sticks to the indenter tip so that tensile flow results in contraction and finally rupture in the glassy structures. Therefore, the 'surface' after testing does not have a regular triangular deformation but a hollow imprint with a protrusion in the middle. The indenter tip has an adhered layer, a fact that should be kept in mind when performing repeated microindentation measurements.

Figure 3 shows the loading and unloading curves, obtained by plotting the load  $F$  against the displacement  $x = h_0 - h$ , where  $h$  is the current distance between the two frames. Repulsive and compressive forces lie above the abscissa; attractive and tensile forces lie below it. The arrowheads indicate the progression of the experiment. As loading begins (A), the initial force is attractive, due to adhesion between the indenter tip and the amorphous layer. With progressive deformation, adhesion becomes less important, and  $F$  increases broadly proportionally to  $x$ ; superimposed on this linear trend are some sudden instabilities caused by grain slips and dislocation movements in the crystalline rafts. Towards the end of the loading the force rises steeply, thus confirming the earlier assumption that loading consists of

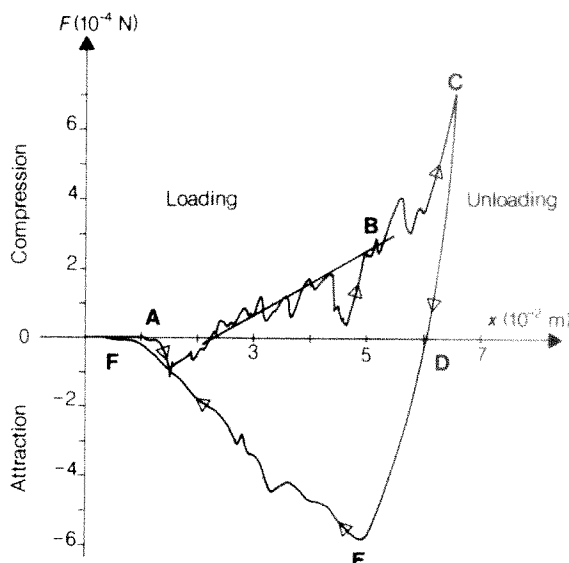


**Fig. 3** Loading and unloading curves for indentation experiment. Loading (A-C): after an initial attractive stage governed by adhesion (A), the force  $F$  increases; first gradually, in proportion to displacement  $x$  (A-B, governed by amorphous layer behaviour), and then more steeply (B-C, governed by substrate behaviour). Unloading (C-D): elastic recovery (C-D) is followed by traction (D-E), and then by contraction of the amorphous layer (E-F).

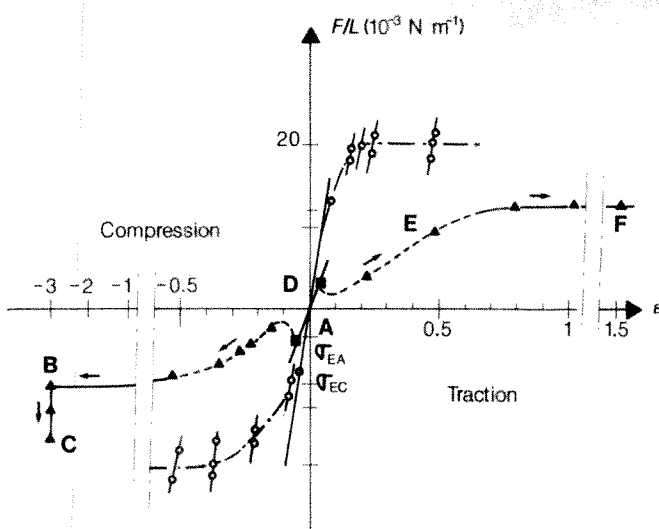


**Fig. 4** Mechanical behaviour of crystalline (○) and amorphous (▲) rafts. Data points lying on solid lines were obtained from the analysis of the indentation process, those on broken lines from additional traction and compression experiments.  $\sigma_{EA}$  and  $\sigma_{EC}$  are the elastic limits of the amorphous and crystal tests, respectively. During the process of indentation, the mechanical behaviour of the amorphous layer follows points A, B, C, D, E, F.

two distinct stages, affecting first the amorphous layer and then the substrate.

On unloading, the first step is elastic recovery (C-D, Fig. 3) of the crystalline rafts. This is followed by traction, transmitted through the amorphous layer (D-E), which finally decreases (E-F) as the amorphous material contracts.

In order to treat the stress and strain data quantitatively we define the mean stress to be the force  $F$  divided by the specimen breadth  $L$  (Fig. 2a). We therefore measure, for each displacement  $x$ , the dimensions  $h_I$  of the indentor,  $h_L$  of the layer and  $h_S$  of the substrate, measured along the symmetry axis  $\delta-\delta'$  (Fig. 1). The values  $\varepsilon_I = (h_{I0} - h_I)/h_{I0} = X_I/h_{I0}$  ( $I = I, L, S$ ) give the uniaxial deformation of each layer. The measurement of the breadth  $L$  of the indentor then yields the two-dimensional stress  $F/L$ .

The above observations suggest that the amorphous material behaviour accounts for the bulk of the stress  $F/L = f(x_I/h_{I0})$  during most of the experiment. To investigate the behaviour of the crystalline raft, a compressive and tensile test curve for a uniform sheet of large bubbles is also plotted (Fig. 4).

We find that the elastic modulus (see also ref. 12) and yield stress of the amorphous material are less than those of the crystalline material. Instabilities are clearly shown in the stress-strain curves of the crystalline material, in accordance with previous work<sup>13</sup>. Finally, the hardness measurement shows that the mean pressure is proportional to the yield value, with the constant of proportionality depending on the shape of the indentor.

Received 1 December 1985; accepted 5 February 1986.

1. Tabor, D. *The Hardness of Metals* (Clarendon, Oxford, 1951).
2. Atkins, A. G. *Metal Sci. J.* **16**, 127–137 (1982).
3. Johnson, K. L. *J. Mech. Phys. Solids* **18**, 115–126 (1970).
4. Pollock, H. M., Maugis, D. & Barquins, M. *IMS/ASTM Microindentation Hardness Testing Symp.* 1984 (ASTM, in the press).
5. Tonck, A., Loubet, J. L. & Georges, J. M. ASLE Preprint no. 85 TC-2A-1, Tribology Conf., Atlanta (1985).
6. Bragg, L. & Nye, J. F. *Proc. R. Soc. A190*, 474–481 (1949).
7. Bragg, L. & Lomer, W. M. *Proc. R. Soc. A196*, 171–181 (1949).
8. Lomer, W. M. *Proc. R. Soc. A196*, 182–194 (1949).
9. Argon, A. S. & Shi, L. T. in *Proc. Fall Meet. Metall. Soc. AIME* (ed. Vitek, V.) 279–303 (1982).
10. Georges, J. M. & Meille, G. *Proc. JSLE int. Tribology Conf., Tokyo*, 885–890 (1985).
11. Maeda, K. & Takeuchi, S. *Phil. Mag. A44*, 643–656 (1981).
12. Simpson, A. W. & Hodkinson, P. *Nature* **237**, 320–322 (1972).
13. Maeda, K. & Takeuchi, S. *Phys. Status Solidi A49*, 685–696 (1978).

## A novel, non-halogen-based chemical oscillator

Arpád Nagy & Ludovít Treindl

Department of Physical Chemistry, Comenius University,  
842 15 Bratislava, Czechoslovakia

Although a kinetic bistability in the reduction of permanganate by hydrogen peroxide<sup>1</sup> as well as in the reduction of permanganate by oxalate<sup>2,3</sup> in a continuous-flow tank reactor (CTR) has recently been observed, a permanganate chemical oscillator has not yet been described. So far, the only oscillator known has been a bromate one containing permanganate,  $Mn^{2+}$  ions and oxalate as a substrate<sup>4</sup>. The discovery of new chemical oscillators which are essentially different from those described previously is of great importance, as it supplies further information concerning the exact mechanistic requirements for chemical oscillations to occur. We report here the conditions under which a permanganate chemical oscillator functions in a CTR.

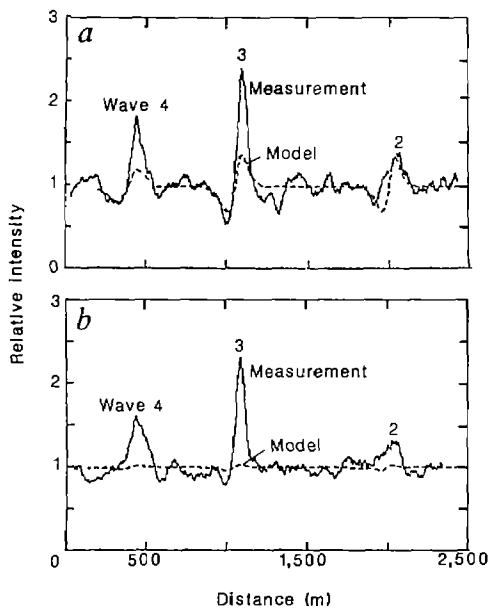
Our novel chemical oscillator consists of an aqueous solution of potassium permanganate, hydrogen peroxide and phosphoric acid. During the reaction in a CTR, the platinum redox-electrode potential and polarographic limiting current oscillate. A periodic change of colour of the bulk of the solution from violet to pink during the oscillation is also observed. Figure 1 shows the typical oscillatory pattern of the Pt redox-electrode potential and of the polarographic limiting current.

We used a glass CTR (40 ml volume) with a mantle connected to a TB 150 ultrathermostat (Medingen), and monitored the oscillatory reaction using a Pt redox electrode (Radelkis, Hungary), or polarographically by means of a static Pt electrode in flowing, well-stirred solution. We applied a potential of 0.0 or +1.0 V to a separated-mercurousulphate (1.0 M) electrode. The polarographic current at a potential of 0.0 V results mostly from the reduction of  $MnO_4^-$  ions; at +1.0 V it results from the anodic oxidation of  $Mn^{2+}$  ions. We were able to monitor the chemical oscillations at both potentials. The experiments were done with a stirring frequency of  $400\text{ min}^{-1}$ . The flow of solution through the CTR was driven by a peristaltic pump, type PP 2-15 (ZALIMP, Poland). The potentiometric and polarographic measurements were made using a precision digital pH meter, OP-208/1, and a polarograph, type OH 102 (Radelkis, Hungary), respectively.

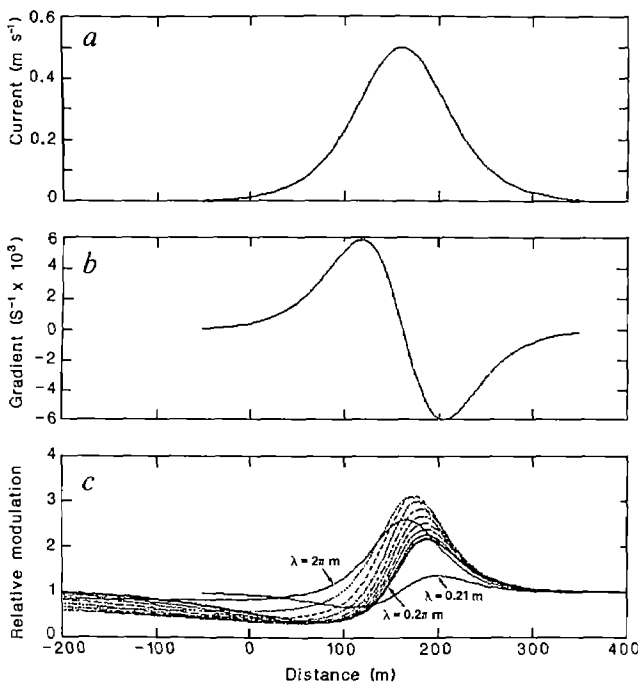
Our system (which comprises aqueous permanganate, hydrogen peroxide and phosphoric acid) exhibits a kinetic bistability either between two stationary states or between an oscillatory and a stationary state (Fig. 2). Following a stationary polarographic limiting current or a Pt redox-electrode potential, a kinetic bistability between two stationary states can be observed (Fig. 2a), if both reactants are in a stoichiometric ratio or if there is excess hydrogen peroxide. This kinetic bistability is similar to that of the permanganate-oxalate system<sup>2</sup>, which we were able to reproduce in our CTR. Following the conventions of De Kepper, Epstein and Kustin<sup>1,5</sup>, we use the terms 'thermodynamic branch' and 'flow branch' to describe the permanganate-hydrogen peroxide bistability. The set of states with low polarographic current (PC) is referred to as the reduced steady state (RSS) because manganese is mainly in its reduced form; this set of states corresponds to the thermodynamic branch. The set of states with high PC is referred to as the oxidized steady state (OSS), as manganese is in its oxidized form,  $Mn^{(VII)}$ . This set of states corresponds to the flow branch. The two branches overlap over a large range of  $k_0$  values. The arrows in Fig. 2 indicate the transitions from one steady state to another.

Figure 2b shows the behaviour of the system when potassium permanganate is in a stoichiometric excess. Starting from the

The situation at X-band is not so clear, however (Fig. 2b). The measured X-band relative intensity maxima have nearly the same values and occur at nearly the same position as the corresponding L-band maxima, but the pronounced regions of reduced intensity observed at L-band are not so apparent. The computed X-band modulations, on the other hand, differ from the background by only a few per cent. This is because the source term on the right-hand side of equation (2) is more effective in forcing the X-band spectral components towards equilibrium. This under-prediction cannot be removed by simply



**Fig. 2** Comparison of the measured (solid curves) and computed (dashed curves) L- and X-band relative intensity for waves 2-4 as discussed in the text. *a*, L-band; *b*, X-band.



**Fig. 3** Comparison of the spatial behaviour of the current and current gradient determined for wave 3 with that of the computed spectral modulation at several different wavelengths. *a*, Surface current; *b*, surface current gradient; *c*, spectral modulation.

adjusting the X-band relaxation rate to a value similar to that at L-band without sacrificing the intuitive feeling that shorter surface waves should respond more quickly to wind forcing than should longer ones. Furthermore, such an adjustment of the X-band relaxation rate would produce significant regions of decreased intensity which are not apparent in the X-band images.

These observations indicate that although the presence of the internal-wave surface current does indeed produce enhanced roughening of the surface at X-band scales, this roughening is not due to direct modulation of X-band Bragg waves as described by equation (2). Since it is well known that steep metre-scale gravity waves tend to lose energy to smaller scales through nonlinear interactions and ultimately through breaking<sup>10</sup>, we propose that the observed X-band modulation is the result of a two-step process in which small-scale roughening is generated due to the perturbation of the longer wind waves by the internal-wave surface current field. Hughes and Gower<sup>3</sup> have alluded to a similar hypothesis as a possible explanation for observed differences in L- and X-band SAR images of internal waves in the Georgia Strait.

For this hypothesis to be credible, the longer wind waves must be substantially modulated by the internal-wave surface current at roughly the same position as are the L-band Bragg waves. We have investigated this point by computing the perturbation of a band of metre-scale waves by the surface current due to internal wave 3. Results are presented in Fig. 3c for wavelengths ranging from  $0.21 \text{ m}$  (L-band Bragg wave) to  $2\pi \text{ m}$ ; the family of curves between  $\lambda = 2\pi \text{ m}$  and  $\lambda = 0.2\pi \text{ m}$  corresponds to wavenumbers between  $1 \text{ rad m}^{-1}$  and  $10 \text{ rad m}^{-1}$  in steps of  $1 \text{ rad m}^{-1}$ . This plot shows that the position of maximum perturbation for the longest waves is near the peak of the internal-wave surface current (Fig. 3a). As the wavelength decreases, the position of the maximum shifts towards the position of the minimum (negative) gradient (Fig. 3b). Moreover, peak modulations of two to three times the equilibrium value occur throughout this region of the internal wave phase. Although we cannot quantify the degree to which the small-scale surface roughness is affected by this modulation of the longer metre-scale waves, it seems likely that it is large enough to cause a significant increase, for example, in the density of parasitic capillary waves or small-scale, locally breaking waves, thereby affecting the X-band SAR return. The region of large modulation occurs at roughly the same location as the maximum L-band perturbation, consistent with the observation from the SAR data. The modulation of the longer waves might also produce additional L-band scatterers which could explain the slight under-prediction of the maxima in the L-band SAR signatures discussed earlier. Finally, we see from Fig. 3 that there is an extended region where the metre-scale waves show a modulation less than unity. In this region, there should be no effect on the small-scale roughness from the two-step process discussed above, and the magnitudes of the X-band Bragg components should therefore be comparable to their equilibrium values. This would explain why no noticeable dark bands, such as those observed at L-band, are visible on the X-band images.

We hope to test these ideas further by analysing additional SAR imagery under environmental and imaging conditions producing a different character for the longer-wave modulations. Such analyses should add significantly to our understanding of the physics governing SAR imaging of ocean currents, and perhaps eventually lead to the development of a tool for general internal wave monitoring.

We thank E. Kasischke (Environmental Research Institute of Michigan) for the SAR data and for discussions; also our colleagues at Johns Hopkins/APL including J. Apel, B. Gotwols and A. Brandt for useful discussions, J. Kerr and B. Raff for processing the SAR images, and N. Curtiss and K. McMakin for preparation of the manuscript. The work was sponsored by the ONR.

Received 7 August 1985; accepted 15 January 1986.

1. Gaspavoric, R. F. & Apel, J. R. *Proc. 1985 int. Geoscience and Remote Sensing Symp.*, IEEE Catalog 85CH2162-6, 1123-1128 (1985).
2. Alpers, W. *Nature* 314, 245-247 (1985).
3. Hughes, B. A. & Gower, J. F. R. *J. geophys. Res.* 88, 1809-1824 (1983).
4. Hughes, B. A. *J. geophys. Res.* 83, 455-465 (1978).
5. Valenzuela, G. R. *Radio Sci.* 3, 1057-1066 (1968).
6. Wright, J. W. *IEEE Trans. Antennas Propagation, AP-14*, 749-754 (1966).
7. LeBlond, P. H. & Mysak, L. A. *Waves in the Ocean* (Elsevier, New York, 1978).
8. Plant, W. J. *J. geophys. Res.* 87, 1961-1967 (1982).
9. Bjerkas, A. W. & Riedel, F. W. *Tech. Mem. TG-1328* (Johns Hopkins University Applied Physics Laboratory, 1979).
10. Phillips, O. M. *The Dynamics of the Upper Ocean* (Cambridge University Press, 1977).

## Direct indication of pore-water advection from pore pressure measurements in Madeira Abyssal Plain sediments

P. J. Schultheiss & S. D. McPhail

Institute of Oceanographic Sciences, Brook Road, Wormley, Godalming GU8 5UB, UK

The difference in pressure between the sea floor and a point in the underlying sediment is an indicator of the velocity of pore-water flow. This differential pore pressure has now been measured at five sites using a free-fall piezometer (pop-up pore pressure instrument, PUPPI) in a distal turbidite province of the Madeira Abyssal Plain. We found that at one of the five sites the pressure was slightly positive, at two others it was effectively zero, but at the remaining two sites the pore pressure was significantly negative ( $-450$  and  $-120$  Pa at 4 m depth). The implication is that at these last two sites water is moving downwards at rates of  $3.1$  and  $0.8$  mm  $\text{yr}^{-1}$  (calculated using laboratory-measured hydraulic conductivities from core samples). If this downward movement is part of a hydrogeological system which includes upward movement of pore water elsewhere, there are obvious implications for schemes to dispose of highly radioactive waste by burial in deep-sea sediments.

Pore pressure measurements in soils and sediments provide an essential component in the evaluation of the effective stress condition which governs the material behaviour. The effective stress is given by  $\sigma' = \sigma - u$ , where  $\sigma$  is the total stress and  $u$  is the pore pressure. Thus pore pressure measurements in ocean sediments are of interest to those concerned with offshore construction. In addition, many geological processes (for example, consolidation, lithification, sediment stability and liquefaction potential) will be influenced by the state of effective stress and hence by the pore pressure. Another process which will be dominated by pore pressure gradients is the mass movement of pore water through the sediments. The PUPPI was designed to investigate the possible advection of pore waters at sites designated as study areas for the feasibility of radioactive waste disposal. Pore-water advection is one of many factors that could potentially accelerate or retard the release of dissolved radionuclides to ocean waters from buried canisters.

It is generally accepted that the anomalously low values of conductive heat flux observed in areas close to active spreading centres can be accounted for by hydrothermal circulation through the highly permeable ocean crust into the sea; this process has been observed to occur in young oceanic crust<sup>1-4</sup>. Evidence for the existence of pore-water advection in deep-sea sediments comes mainly from nonlinear temperature profiles measured at several locations<sup>5-9</sup>. Vertical pore-water advection velocities calculated from such temperature profiles and from pore-water chemistry have been compared at three sites in the equatorial Pacific<sup>10</sup>. It was found that the velocities calculated using sulphate diffusion-convection-reaction models were two to three orders of magnitude lower than velocities calculated from the nonlinear temperature profiles, suggesting that mechan-

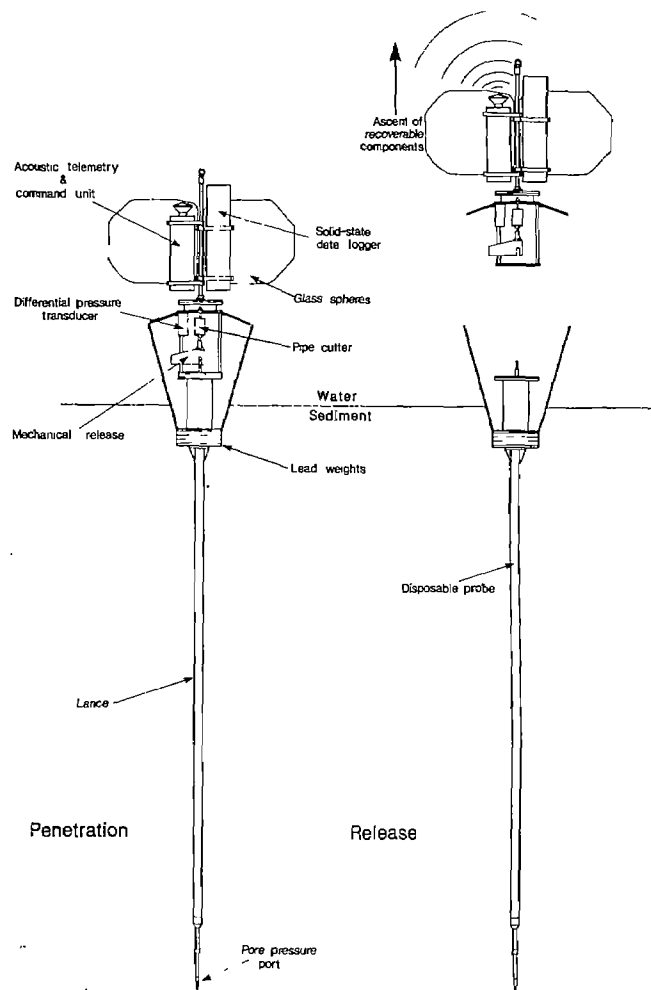


Fig. 1 Schematic diagrams of the pop-up pore pressure instrument (PUPPI): left, after its free-fall through the water column and penetration into the sediments; right, after release from the sea floor, showing recoverable and disposable components.

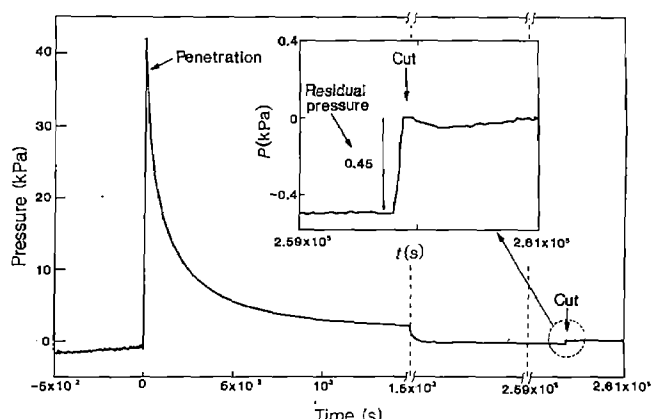
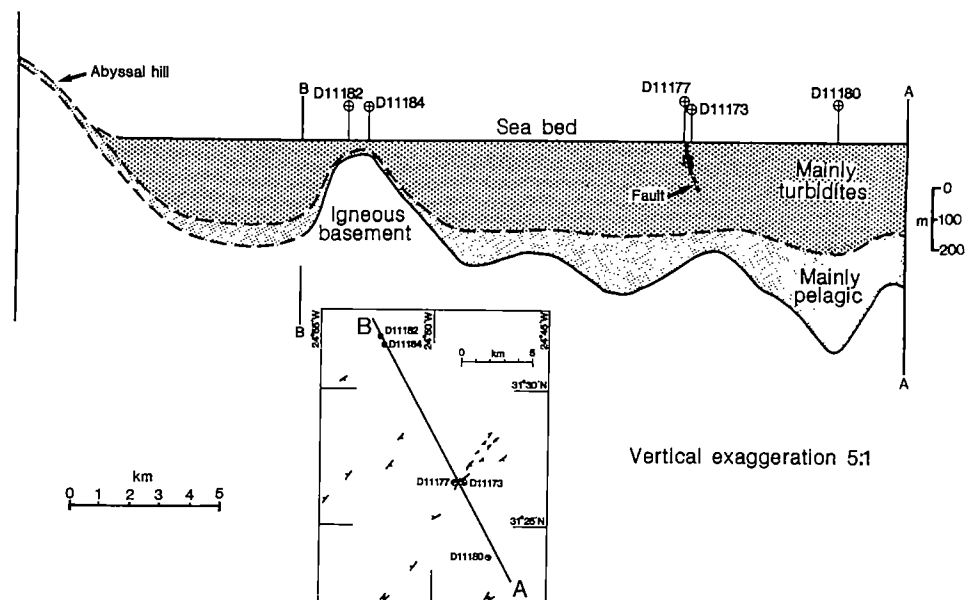


Fig. 2 Pressure-plot for PUPPI station D11184 showing the insertion pressure pulse at zero time (penetration) followed by the decay curve and the cut. Note the changes in the timescale. The inset shows an expanded record around the cut revealing a  $-0.45$ -kPa residual differential pressure.

isms other than pore-water advection are responsible for the profiles<sup>11</sup>. In addition it is unlikely, with currently available techniques, that a resolution of better than  $100$  mm  $\text{yr}^{-1}$  could be obtained using temperature profiles. Studies of pore-water advection relevant to the disposal of high-level radioactive waste must have a resolution of better than  $1$  mm  $\text{yr}^{-1}$ .



**Fig. 3** Section through the Great Meteor East study area showing the location of the five PUPPI sites in relation to faults, basement topography and sediment thickness. Inset shows location of section A-B and station positions.

The movement of water through a permeable medium is described by Darcy's law:  $Q = KA\Delta u/\eta L$ , where  $Q$  is the volume flow-rate of a liquid of viscosity  $\eta$  caused by a pressure difference  $\Delta u$  over a length  $L$  in a cross-section  $A$  of a porous medium with specific permeability  $K$ . When water is the percolant it is customary to define the hydraulic conductivity:  $k = K\gamma g/\eta$ , where  $\gamma$  is the density of the fluid and  $g$  the acceleration due to gravity. The velocity of an element of water in a permeable medium is  $v = Q/A$ ; therefore,  $v = k\Delta u/n\eta gL$ , where  $n$  is the fractional porosity of the sediment. Values of  $k$  and  $n$  can be measured from core samples in the laboratory but the differential pore pressure must be measured *in situ* by a piezometer.

The PUPPI (Fig. 1) was designed at the Institute of Oceanographic Sciences<sup>12</sup> to measure residual pore pressures at a depth of 4 m in soft sediments with a final resolution of 10 Pa. It is a free-fall instrument that can be ballasted to penetrate a range of sediment types in water depths of up to 6,000 m. In its present configuration it has a single pressure port near the end of the lance, connected to a differential pressure transducer (the other port is open to the sea). It therefore measures the pore pressure with respect to sea-bed hydrostatic pressure. A programmable solid-state data logger is used to record the pressure data at a maximum rate of 0.5 sample per s. An accelerometer record of the penetration event enables the depth of penetration to be calculated. Recovery is accomplished using an acoustic command that activates a release mechanism which simultaneously cuts the pipe connecting the pressure port to the transducer. The lance, ballast and cone assembly are left on the sea floor; the buoyant instrument package ascends to the surface for recovery.

A sample pressure-time record is shown in Fig. 2 (note the changes in timescale which are necessary to illustrate the behaviour). When the instrument penetrates the sea floor, a pore-pressure transient (~40 kPa) results from the large radial stress imposed on the sediment by lance insertion and from the small vertical stress due to the submerged weight of the PUPPI (~75 kg). This pressure transient decays with time as the sediment undergoes primary consolidation. After 10 min it has decayed to 10%, and after 3 h less than 1% of the peak value. No detectable decay occurs during the final 24 h; hence it is assumed that the pore pressure caused by the instrument has decayed to zero.

To obtain pore pressure measurements of the required accuracy, the transducer must be accurately calibrated. Laboratory experiments have shown that changes in ambient temperature and pressure cause only a small (<1%) change in the

total range; however, for maximum accuracy an *in situ* zero-calibration method is used. Pressure data are logged rapidly near the time when the pore pressure pipe connecting the transducer to the pressure port is cut. The reading after the cut must be zero and any change in reading near the time of the cut, after averaging to remove the signal from tidal cycles, indicates the existence of a differential pore pressure in the sediments. The data shown in Fig. 2 are plotted with reference to the zero pressure reading obtained after the cut. During the 500 s before penetration, the zero point on the transducer drifted by ~1 kPa as a result of temperature and pressure changes. It drifted a further 0.5 kPa before the pipe was cut 2 days later.

Data were collected on *Discovery* cruise 153 from five sites within an area known as the GME (Great Meteor East) study area. Figure 3 shows a section through the area, based on the interpretation of coring and seismic reflection profiling data<sup>13</sup>. The inset shows the station positions. The area is an abyssal plain, comprising ~90-Myr-old basement overlain by a sequence of pelagic sediments, which are in turn overlain by a series of thick distal turbidites<sup>14</sup>. Within the turbidite sequence there are a large number of faults which are clearly revealed on 3.5-kHz reflection profiles<sup>13</sup>. The PUPPI stations cover three major areas: (1) D11180 is in an area of thick sedimentary cover (~700 m); (2) D11173 and D11177 lie within 50–200 m of the fault line (determined with bottom transponders for navigation); (3) D11182 and D11184 are in an area of thin sedimentary cover (~75 and 50 m) over a sub-bottom basement high that does not outcrop. The results are summarized in Table 1. Two sites show significant negative residual pressure gradients (D11177 and D11184). As shown in Fig. 3, D11177 is ~50 m from a fault, on the downthrown side, whereas D11173 is ~200 m from the same fault on the upthrown side. D11184 lies very close to the peak of the sub-bottom basement high, where there is ~50 m of sediment cover, whereas D11182 lies on the flank, where the cover thickness is ~75 m. One site (D11180) shows a small positive residual pressure, but the instrumental precision is not sufficient to distinguish this result from a differential pressure of zero.

The advection velocities calculated for the two sites which show negative residual pressures (D11177 and D11184) are  $-0.8 \text{ mm yr}^{-1}$  and  $-3.1 \text{ mm yr}^{-1}$  respectively. The negative sign indicates that the movement is downward. These velocities are calculated using laboratory-measured values for the hydraulic conductivity (corrected for *in situ* conditions using density and viscosity data<sup>15</sup>) and porosity (see Table 1).

In these experiments the water which was used to fill the pipe before deployment had a measured density which could exceed

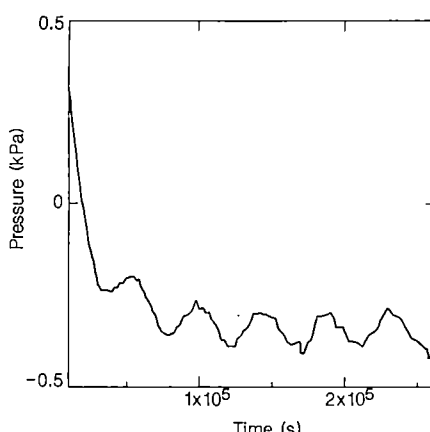


**Fig. 4** Expanded pressure-time plot for PUPPI station D11184, showing the attenuated tidal cycles recorded as a result of the finite compliance of the differential pressure transducer.

that of the bottom water by as much as 0.18%. This density difference could cause an apparent residual pressure of  $-78$  Pa, which translates into an apparent advection velocity of  $-0.5$  mm  $\text{yr}^{-1}$ . The advection velocities listed in Table 1 might therefore have to be increased by up to  $0.5$  mm  $\text{yr}^{-1}$ ; this would not change the overall interpretation of the data.

The largest source of potential error is in the laboratory hydraulic conductivity measurement, and arises not from the technique used but from the possibility of unrepresentative sampling (missing fractures or open burrows) and/or disturbance<sup>16</sup> (closing of open burrows). If this is a source of error, it is most likely that the *in situ* value will be higher than the laboratory measurement, possibly by up to an order of magnitude. If this is the case then the advection velocities at all sites could be much higher. To resolve this uncertainty, we are investigating the accurate *in situ* evaluation of hydraulic permeability. The most promising method involves the observation of an effect caused by tidal variation. Pore pressure measurements suffer from a time lag in their measurement because of the finite compliance of the transducer and the low permeability of the sediments. As a result of this, a tidal cycle appears on the pore pressure record. It is highly attenuated and possibly phase-shifted from the real tidal hydrostatic waveform. Figure 4 shows the tidal cycles observed at station D11184, which have an amplitude of  $\sim 120$  Pa, compared with the tidal amplitude of  $\sim 7$  kPa. The oscillations are only just within the resolution of the instrument but this could be improved by increasing the transducer resolution. A comparison with the actual hydrostatic pressure changes (monitored using a tide gauge) should enable accurate *in situ* values of hydraulic conductivity to be obtained.

The limited hydrogeological data presented for the transect shown in Fig. 3 show a downward flow of water over a sub-bottom basement high and near a fault. The questions that must be addressed for the radioactive waste feasibility study concern

**Table 1** Differential pressures and advection velocities calculated from the equation  $v = k\Delta u / n\gamma g L^*$

PUPPI site no.	$\Delta U$ (Pa)	$V$ (mm $\text{yr}^{-1}$ )
D11173	0	0
D11177	-120	-0.8
D11180	+30	+0.2
D11182	0	0
D11184	-450	-3.1

$\Delta u$ , Measured residual differential pressure;  $v$ , calculated advection velocity.

\*  $k = 7 \times 10^{-9}$  m  $\text{s}^{-1}$ ;  $n = 0.77$ ;  $\gamma = 1,053$  kg  $\text{m}^{-3}$ ;  $g = 9.81$  m  $\text{s}^{-2}$ ;  $L = 4$  m.

the nature of the flow. Is it part of a thermally driven convection cell, and if so what is the scale of the cell and where are the discharge areas? Or is it caused by a consumption of water within the deeper sediments or basement as part of a diagenetic chemical process? Possible discharge areas are from local abyssal hills or over large areas within the thicker sedimentary sequence, but the discharge rates must be below the present resolution of the PUPPI. The positive advection velocity seen at site D11180 may be indicative of such discharge.

We thank B. Hart, A. Packwood, R. B. Whitmarsh and R. E. Kirk for significant contributions and advice during the concept and design phases of the PUPPI, and R. B. Whitmarsh, R. C. Searle, T. J. G. Francis, P. P. E. Weaver, D. Abbott, A. F. Richards and E. James for discussion and helpful criticism of the text. This research has been carried out under contract for the Department of the Environment, as part of its radioactive waste management programme.

Received 8 May 1985; accepted 23 January 1986.

1. Corliss, J. B. *et al.* *Science* **203**, 1073–1083 (1979).
2. RISE Project Group. *Science* **207**, 1421–1433 (1980).
3. Macdonald, K. C. & Luyendyk, B. B. *Earth planet. Sci. Lett.* **48**, 1–7 (1981).
4. Anderson, R. N. *et al.* *Nature* **300**, 589–594 (1982).
5. Anderson, R. N., Hobart, M. A. & Langseth, M. G. *Science* **204**, 828–832 (1979).
6. Langseth, M. G. & Herman, B. M. J. *Geophys. Res.* **86**, 10805–10819 (1981).
7. Becker, K. & von Herzen, R. P. J. *Geophys. Res.* **88**, 1057–1066 (1983).
8. Williams, D. L. *et al.* *Geophys. Res.* **84**, 7467–7484 (1979).
9. Abbott, D. H., Menke, W. & Morin, R. J. *Geophys. Res.* **88**, 1075–1093 (1983).
10. Crowe, J. & McDuff, R. E. *Eos* **60**, 863 (1979).
11. Noel, M. J. *Geophys. J. R. astr. Soc.* **76**, 673–690 (1984).
12. Schultheiss, P. J., McPhail, S. D., Packwood, A. R. & Hart, B. *Inst. oceanogr. Sci. Rep.* no. 202 (1985).
13. Searle, R. C. *et al.* *Inst. oceanogr. Sci. Rep.* no. 193 (1985).
14. Weaver, P. P. E. & Kuijpers, A. *Nature* **306**, 360–363 (1983).
15. Schultheiss, P. J. & Gunn, D. E. *Inst. oceanogr. Sci. Rep.* no. 201 (1985).
16. Weaver, P. P. E. & Schultheiss, P. J. *Nature* **301**, 329–331 (1983).

## Direct dating of the oxygen-isotope record of the last deglaciation by $^{14}\text{C}$ accelerator mass spectrometry

Jean-Claude Duplessy\*, Maurice Arnold\*, Pierre Maurice\*, Edouard Bard\*, Josette Duprat† & Jean Moyes†

\* Centre des Faibles Radioactivités, Laboratoire mixte CNRS-CEA, F-91190 Gif-sur-Yvette, France

† Département de Géologie et Océanographie, Université de Bordeaux 1, Avenue des Facultés, F-33405 Talence, France

Major trends of Quaternary global climate are reflected in the continental ice volume changes which have been reconstructed by oxygen-isotope analysis<sup>1,2</sup>.  $\delta^{18}\text{O}$  records from deep-sea sediments show that the net glacial build-up occurs relatively slowly<sup>3</sup>, but that the end of an ice age occurs quickly, in less than 10,000 yr, implying a nonlinear response<sup>4,5</sup> to simple Milankovitch theory<sup>6</sup>. The latter observation suggests that the cause of the most recent deglaciation was the maximum in summer calorific radiation at the upper latitudes of the Northern Hemisphere centred around 11,000 yr ago, a view supported by early studies<sup>7</sup>. Later work has produced conflicting dates, the main source of confusion being problems with obtaining accurate and reliable dates. Here, by using accelerator mass spectrometry, we have measured  $^{14}\text{C}$  for various species of foraminifera to produce a reliable timescale for the oxygen-isotope record. Our results show that, at the end of the last ice age, continental ice sheets began to melt more than 4,000 yr before the Northern Hemisphere maximum of summer calorific radiation.

The timing of deglaciation has important consequences for the mechanisms of climate change. The earlier work suggesting

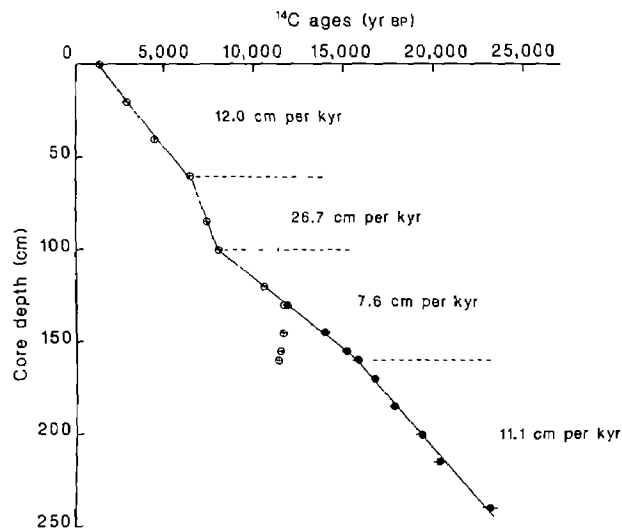


Fig. 1 AMS  $^{14}\text{C}$  ages plotted against sample depth in core CH73-139C for two foraminiferal species, *G. bulloides* (○) and *N. pachyderma* (●).

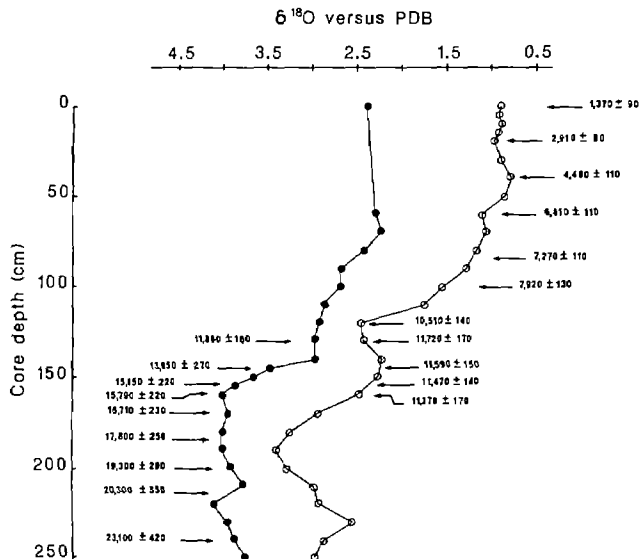


Fig. 2 Oxygen-isotope records and  $^{14}\text{C}$  ages of the two foraminiferal species *G. bulloides* and *N. pachyderma* in the core CH73-139C.

that the maximum rate of ice-sheet disintegration was centred at  $\sim 11,000$  yr ago<sup>7</sup>, implying that ice melting was a direct response to insolation, has been cast into doubt by more recent isotopic analysis of deep-sea sediments deposited with a high sedimentation rate in the northeastern Atlantic Ocean. This suggested that deglaciation occurred in two discrete steps, the first (termination 1a) between 16,000 and 13,000 yr ago and the second (termination 1b) between 10,000 and 8,000 yr ago<sup>8</sup>. This evidence implies that there was no melting of the ice sheets between 13,000 and 10,000 yr ago, the time at which fastest melting should have occurred according to earlier studies. Recent studies add even more confusion: a two-step deglaciation centred at  $\sim 12,500$  yr BP was proposed by Mix<sup>9</sup>. Stacked oxygen-isotope data from foraminifera in tropical Atlantic sediment cores suggested that the last deglacial transition began at 14,000 yr BP<sup>10,11</sup>. Other studies suggested that the deglaciation started 13,000–15,000 yr ago with one to three steps<sup>11–13</sup>. There is thus a 3,000-yr uncertainty concerning the exact timing of the beginning of the last deglaciation.

The main causes of age discrepancies in deep-sea sediment cores are mainly (1) bioturbation, which mixes the upper cen-

timetres of sediment and partially blurs the palaeoclimatic record and which is particularly severe in cores with a low sedimentation rate, and (2) the presence within the North Atlantic sediment either of ice-raftered carbonate or of wind-, river- and current-transported carbonate, which are derived from pre-Pleistocene continental rocks and bias  $^{14}\text{C}$  ages towards older values.

Accelerator mass spectrometry (AMS) provides reliable  $^{14}\text{C}$  ages with only 1–2 mg of carbon; it thus offers a unique opportunity to obtain  $^{14}\text{C}$  ages on pure foraminiferal samples, free of detrital contamination. We present here analyses performed on foraminiferal shells from core CH73-139C, raised from the Rockall Plateau ( $54^{\circ}38' \text{N}$ ,  $16^{\circ}21' \text{W}$ , water depth 2,209 m). This core has a mean sedimentation rate approximately equal to 10 cm per 1,000 yr<sup>8,14</sup>, which reduces (but does not cancel) the effects of bioturbation. Its isotopic and palaeoclimatic records are typical of those of the northeastern Atlantic Ocean<sup>8,15,16</sup>. We determined  $^{14}\text{C}$  ages for individual species of foraminifera using the Tandetron Accelerator in Gif-sur-Yvette<sup>17</sup>; 1,000–2,000 foraminiferal shells were examined under a binocular microscope for the two species *Neogloboquadrina pachyderma* (left coiling), which predominates during cold climatic episodes, and *Globigerina bulloides*, which is a transitional/subpolar species, abundant during interglacial conditions. The foraminiferal shells were cleaned in an ultrasonic bath, then attacked superficially with  $10^{-3}$  M nitric acid to prevent surficial contamination from modern carbonate, and reacted under vacuum with phosphoric acid. The  $\text{CO}_2$  evolved was converted to carbon by reaction with hydrogen in the presence of iron at  $650^{\circ}\text{C}$  (ref. 18). The  $^{14}\text{C}/^{12}\text{C}$  content of the sample was compared with that of a National Bureau of Standards oxalic acid reference sample prepared from the same amount of carbon and with the same amount of iron to prevent fractionation in the accelerator source, depending on the C/Fe ratio. Other fractionations were corrected by comparing the  $^{13}\text{C}/^{12}\text{C}$  ratio of the sample with that of the reference sample<sup>19</sup>. This procedure provides values for the  $^{14}\text{C}/^{12}\text{C}$  ratio that are accurate to better than 1% of the modern  $^{14}\text{C}$  content (M.A. et al., in preparation). Six pre-Quaternary foraminiferal samples prepared according to this procedure had a background contamination of  $0.58 \pm 0.15\%$  of the modern  $^{14}\text{C}/^{12}\text{C}$  ratio, corresponding to an apparent age of 41,500 yr, which is the present limit of dating for the Gif accelerator. This background contribution was subtracted from all the measurements and represents a minor correction. Errors for the  $^{14}\text{C}$  ages, calculated at the  $1\sigma$  level, take into account the statistical error for the counts performed on both experimental and reference samples and the uncertainty on the background (M.A. et al., in preparation). Finally, foraminiferal  $^{14}\text{C}$  ages have been corrected for the apparent  $^{14}\text{C}$  age of surface sea water—that is, 400 years.

Figure 1 plots  $^{14}\text{C}$  ages against depth: in the upper 60 cm of the core,  $^{14}\text{C}$  analyses of *G. bulloides* indicate a mean sedimentation rate of 12 cm per 1,000 yr. Between 60 and 100 cm depth, the beginning of the Holocene is characterized by a high sedimentation rate (26.7 cm per 1,000 yr). Below 160 cm,  $^{14}\text{C}$  analyses of *N. pachyderma* indicate a mean sedimentation rate of 11.1 cm per 1,000 yr during glacial times before 15,100 BP. Between 130 and 160 cm,  $^{14}\text{C}$  ages of *N. pachyderma* indicate a constant mean sedimentation rate of 7.6 cm per 1,000 yr from 12,000 to 15,000 yr BP. Between 100 and 160 cm, the  $^{14}\text{C}$  ages of *G. bulloides* increase with core depth until 130 cm and remain constant from 130 to 160 cm. These constant age values indicate that *G. bulloides* became abundant in the northeastern Atlantic only after 11,600 yr BP and was mixed in older sediment levels by bioturbation. Only a few specimens were found below 160 cm. This abundance was sufficient for an oxygen-isotope analysis but not for  $^{14}\text{C}$  dating. At 100, 120 and 130 cm depth, the  $^{14}\text{C}$  ages of *G. bulloides* coincide with those derived from an extrapolation of the sedimentation rate provided by  $^{14}\text{C}$  analyses of *N. pachyderma*. We therefore assume a constant sedimentation rate of 7.6 cm per 1,000 yr during the whole climatic transition. This

value is lower than both glacial and interglacial values, in agreement with the fall in productivity associated with the deglaciation<sup>15</sup>.

Below 130 cm, bioturbation introduces a strong age difference between the two species which increases progressively to more than 4,000 yr at 160 cm. This result clearly illustrates how a <sup>14</sup>C analysis performed on a mixture of species may be misleading. The age of any given species analysed for stable isotope content may be drastically different from that of the bulk foraminiferal population if the species exhibit important fluctuations in abundance and are mixed with deeper layers in the sediment. AMS thus provides a new means to studying the impact of bioturbation in deep-sea sediments.

Figure 2 shows the oxygen-isotope records of *G. bulloides* and of *N. pachyderma* and the <sup>14</sup>C ages obtained for the same species. The *G. bulloides* data show that termination 1b occurred after 10,500 yr BP, in agreement with the general recognition that this step followed the Younger Dryas cold event<sup>8–10,12,13</sup>. The major development of *G. bulloides* at about 11,600 yr BP in the northeastern Atlantic Ocean coincides with the Allerod warm continental event. This result provides the first evidence that oceanic conditions may have varied during the Bolling/Allerod interstadial complex, which lasted from 13,300 to 11,000 yr BP.

The <sup>14</sup>C ages obtained for *N. pachyderma* samples provide an accurate timescale for termination 1a. As this isotopic record is similar to, and in phase with, the benthic record of the same core within experimental errors<sup>8</sup>, we believe that it reflects changes of continental ice volume during the last deglaciation. Our data show that the first phase of major melting began soon after 15,800 yr BP (level 160 cm;  $\delta^{18}\text{O} = 4.02$ ) and was complete by ~13,300 yr BP (level 140 cm;  $\delta^{18}\text{O} = 2.97$ ). The mid-point of termination 1a is dated at ~14,000 yr BP, which suggests that the speed of deglaciation increased progressively during most of this melting episode and fell sharply to zero by its end. The pause in ice melting until termination 1b is confirmed by consistent ages measured in both of the foraminiferal species during the interval 12,000–10,500 yr BP.

By providing <sup>14</sup>C ages for individuals of the same species as those analysed for  $\delta^{18}\text{O}$ , AMS allows us to minimize the effects of bioturbation and to derive the most accurate timescale for the palaeoclimatic record of deep-sea sediments. For example, the  $\delta^{18}\text{O}$  values of *G. bulloides* exhibit their first decrease at a depth 20 cm below that of *N. pachyderma* in core CH73-139C. AMS <sup>14</sup>C dates demonstrate that this 20-cm lead of the *G. bulloides* record over the *N. pachyderma* record is an artefact of bioturbation. The inconsistency between the two isotopic records disappears when both records are compared with the <sup>14</sup>C ages measured on the same foraminiferal species (Fig. 2). In view of this remarkable age difference between different foraminiferal species in a core with an accumulation rate around 10 cm/kyr, it is not surprising that initial results from a core in the Pacific with an accumulation rate of only ~2 cm/kyr were disappointingly confusing<sup>20</sup>.

The chronology of the last deglaciation that we propose here shows good agreement with the palaeoclimatic record of western Europe, which has a highly maritime climate closely linked to the temperature of the northeastern Atlantic Ocean. The internal coherence of both continental and oceanic evidence suggests that our timescale is probably exact within the uncertainties of the <sup>14</sup>C dates, that is, ~250 yr in this time range.

Our data demonstrate that the first rapid phase of deglaciation occurred before the maximum in summer calorific insolation over the high and middle latitudes of the Northern Hemisphere at 11,000 yr BP, they support the hypothesis that rates of ice melting are not linearly linked to insolation<sup>5,6</sup> and that the deglaciation resulted from the complex interaction of many feedback mechanisms. This early deglaciation suggests that among these feedback mechanisms, atmospheric CO<sub>2</sub> concentrations and ice dynamics may have had a major role. On one

hand, increasing concentrations of atmospheric CO<sub>2</sub> at the end of the glaciation<sup>21,22</sup> may have contributed significantly to the forcing of the deglaciation because a comparison of  $\delta^{13}\text{C}$  and  $\delta^{18}\text{O}$  analyses of planktonic and benthic foraminifera from the Pacific Ocean suggests that the CO<sub>2</sub> increase began before continental ice began to melt<sup>23</sup>. On the other hand, the mechanism of ice dynamics are necessary to explain the disagreement between the two-step isotopic record suggesting a discontinuous volumetric deglaciation, and the variation of the ice sheet are extent between 15,000 and 7,000 yr BP which is more easily explained by a smooth progressive melting of the ice sheet<sup>2</sup>. However, the seasonal disappearance of sea ice in the Norwegian-Greenland Sea soon after 18,000 yr BP<sup>25</sup> may have triggered rapid ice calving into the ocean and the down-draw of the great ice sheets<sup>26</sup>.

We thank J. Labeyrie for introducing AMS at Gif-sur-Yvette. J. Antignac, E. Kaltnecker, B. Le Coat and H. Leclaire for help in the analyses; R. Lesueur, A. Castera and D. de Zertucha for their help in developing AMS; and N. J. Shackleton, L. Labeyrie and W. Dudley for useful discussions and review of the manuscript. This work was supported by CNRS (PNEDC), CEA and EEC grant CLI 085-F. CFR contribution no. 751.

Received 14 October; accepted 30 December 1985.

- Emiliani, C. *J. Geol.* **63**, 538–578 (1955).
- Shackleton, N. J. & Opdyke, N. D. *Quat. Res.* **3**, 39–55 (1973).
- CLIMAP. *Science* **191**, 1131–1137 (1976).
- Hays, J. D., Imbrie, J. & Shackleton, N. J. *Science* **194**, 1121–1132 (1976).
- Imbrie, J. & Imbrie, J. Z. *Science* **207**, 943–953 (1980).
- Milanovitch, M. *R. Serbian Acad. (Beograd) Spec. Publ.* **133** (1941).
- Broecker, W. S., Ewing, M. & Heezen, B. C. *Science* **258**, 429–448 (1960).
- Duplessy, J. C., Delibrias, G., Turon, J. L., Pujol, C. & Duprat, J. *Palaeogeogr., Palaeoclimatol., Palaeoecol.* **35**, 121–144 (1981).
- Ruddiman, W. F. & Duplessy, J. C. *Quat. Res.* **23**, 1–17 (1985).
- Berger, W. H. *Sver. geol. Unders. Afh.* **76**(7c), 270–280 (1982).
- Mix, A. C. & Ruddiman, W. F. *Quat. Res.* (in the press).
- Berger, W. H., Killingley, J. S., Metzler, C. V. & Vincent, E. *Quat. Res.* **23**, 258–271 (1985).
- Samthein, M., Erlerkeusser, H. & Zahn, R. *Bull. Inst. géol. Basin d'Aquitaine, Bordeaux* **3**, 393–407 (1982).
- Pujol, C. thesis, Univ. Bordeaux 1 (1980).
- Ruddiman, W. F. & McIntyre, A. *Palaeogeogr., Palaeoclimatol., Palaeoecol.* **35**, 145–21 (1981).
- Labeyrie, L. D. & Duplessy, J. C. *Palaeogeogr., Palaeoclimatol., Palaeoecol.* **50**, 217–24 (1985).
- Arnold, M., Lesueur, R., Maurice, P. & Duplessy, J. C. *3rd Int. Symp. Accelerator Mass Spectrometry: AMS '84*, Zurich (1984).
- Vogel, J. S., Souton, J. R., Nelson, D. E. & Brown, T. A. *Nucl. Instrum. Meth.* **223**, 289–29 (1984).
- Beukens, R. P. & Lee, H. W. *Symp. Accelerator Mass Spectrometry, Proc. Argonne National Lab. ANL/PHY-81-1n*, 416–425 (1981).
- Andree, M. et al. *Nuclear Instruments and Methods in Physics Research* **B5**, 340–345 (1984).
- Berner, W., Stauffer, B. & Oeschger, H. *Radiocarbon* **22**, 227–235 (1980).
- Delmas, R. J., Ascencio, J.-M. & Legrand, M. *Nature* **284**, 155–157 (1980).
- Shackleton, N. J. & Pisias, N. G. in *The Carbon Cycle and Atmospheric CO<sub>2</sub>: Natural Variations Archean to Present* (eds Sundquist, E. T. & Broecker, W. S.) 303–317 (Am. Geophys. Un., Washington, DC, 1985).
- Paterson, W. S. B. *Rev. Geophys. Space Phys.* **10**, 885–917 (1972).
- Grouset, F. & Duplessy, J. C. *Mar. Geol.* **52**, M11–M17 (1983).
- Denton, G. H. & Hughes, T. *The Last Great Ice Sheets* (Wiley-Interscience, New York, 1981).

## Extensive deposition of banded iron formations was possible without photosynthesis

Louis M. François

Astrophysical Institute, University of Liège, 5 Avenue de Cointe, B-4200 Cointe-Liège, Belgium

Precambrian banded iron formations (BIFs) consist of alternating layers of silica and iron minerals such as haematite, magnetite and siderite<sup>1,2</sup>, but there is controversy as to the origin of the iron. According to one point of view, iron was precipitated from sea water containing Fe(II) ions in solution<sup>3,4</sup>. Because the photodissociation of water vapour in the Precambrian atmosphere would have been too slow to generate enough of the most probable oxidizing agent, oxygen<sup>5</sup>, this process would have had to wait for the evolution of organisms producing oxygen. Cairns-Smith<sup>6</sup> and

Braterman *et al.*<sup>7</sup> alternatively suggested abiotic photodissociation of  $\text{FeOH}^+$ . Through the use of a Precambrian ocean model, I demonstrate here that such a process can quantitatively account for the formation of known BIFs.

The ocean is divided into three regions (see Fig. 1): the mixed layer, the thermocline and the deep-water reservoir, and is composed of the following cations:  $\text{Na}^+$ ,  $\text{K}^+$ ,  $\text{Mg}^{2+}$ ,  $\text{Ca}^{2+}$ ,  $\text{Fe}^{2+}$  and  $\text{H}^+$ ; and anions:  $\text{Cl}^-$ ,  $\text{SO}_4^{2-}$ ,  $\text{HCO}_3^-$ ,  $\text{CO}_3^{2-}$ ,  $\text{OH}^-$  and  $\text{H}_2\text{BO}_3^-$ . These ions can form various complexes. The mixed layer is 100 m thick and is at a temperature of 20 °C. Photo-oxidation of  $\text{FeOH}^+$  occurs in this region. In the thermocline, which is 1,000 m thick, the temperature decreases linearly with depth. Total  $\text{Fe(II)}$  ( $\text{Fe}^{2+} + \text{FeOH}^+ + \text{FeCl}^- + \text{FeSO}_4^0$ ) is transported by diffusion and upward advection (upwelling) throughout the thermocline. The deep-water reservoir is assumed to be homogeneous and has a temperature of 5 °C. Deep-water formation at high latitudes is modelled by a pipe linking the mixed layer to the deep-water reservoir and in which the water circulates downwards with a velocity equal to the advective velocity.

Following Holland<sup>3</sup>, the deep water is assumed to be saturated with respect to siderite. Langmuir<sup>8</sup> reports a temperature-dependent expression for the activity solubility product. At 5 °C, the value  $K_{\text{FeCO}_3} = 1.31 \times 10^{-10} \text{ mol}^2 \text{ kg}^{-2}$  is found for the concentration solubility product, using the activity coefficient of  $\text{Fe}^{2+}$  and  $\text{CO}_3^{2-}$  at an ionic strength  $I = 0.7$ .  $\text{Fe(II)}$  is transported upward from the deep water by advection and diffusion. In the mixed layer,  $\text{Fe(II)}$  is transformed into  $\text{FeOH}^+$ ; this ion is photo-

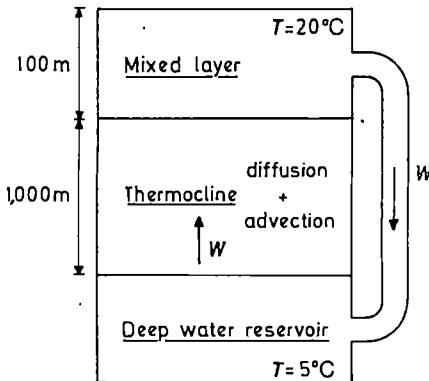


Fig. 1 Vertical structure of the ocean in the model;  $w$  is the advective velocity.

According to Braterman *et al.*<sup>7</sup>, the quantum yield  $\gamma$  of the photo-oxidation reaction lies between 0.01 and 0.05. A mean value of 0.03 is adopted. The calculated photo-oxidation rate is multiplied by 0.5 to account for the day-night alternation.

The photochemical model requires the  $\text{FeOH}^+$  concentration in the mixed layer as an input. It may be obtained from the total  $\text{Fe(II)}$  concentration, provided that the  $p\text{H}$  profile is known. The  $p\text{H}$  is calculated by taking the chemical reactions listed in Table 1 into consideration. The concentrations of the major ions are assumed to be equal to the present concentrations, except for  $\text{Ca}^{2+}$  and  $\text{SO}_4^{2-}$ . The value  $[\text{SO}_4^{2-}] = 10^{-3} \text{ mol kg}^{-1}$  is adopted, based on the discussion of Walker and Brindlecombe<sup>11</sup>. The  $\text{Ca}^{2+}$  concentration is chosen in such a way that the deep water is saturated with respect to calcite.  $[\text{HCO}_3^-]$  and  $[\text{CO}_3^{2-}]$  are calculated from the requirement that the surface water be in equilibrium with the atmospheric  $\text{CO}_2$  pressure, which is a model parameter.

The  $\text{Fe(II)}$  concentration in the mixed layer is linked to its concentration in the deep water (at siderite saturation), by imposing that the upward flux of  $\text{Fe(II)}$  is conserved throughout the thermocline. The upward transport in this layer is due to advection and eddy diffusion. The diffusion coefficient  $K$  is assumed to be  $4,000 \text{ m}^2 \text{ yr}^{-1}$ , its present mean value<sup>12</sup>. The advective velocity  $w$  is a model parameter; for the global ocean, its present value is  $\sim 4 \text{ m yr}^{-1}$ .

Other details of the model will be presented elsewhere (L.M.F. and J.-C. Gérard, in preparation), where chemical oxidation of  $\text{Fe(II)}$  by oxygen will be studied quantitatively and compared with photochemical oxidation.

The model has been run with atmospheric  $\text{CO}_2$  pressures,  $P_{\text{CO}_2}$ , of 1, 10, 100 and 1,000 PAL (PAL, present atmospheric level). Table 2 lists the calculated values of  $\phi_{\text{phot}}$ . The 'standard model' refers to the case  $K = 4,000 \text{ m}^2 \text{ yr}^{-1}$  and  $w = 4 \text{ m yr}^{-1}$ ; that is, it represents the ocean as a whole with conditions close to those pertaining at present. As the atmospheric  $\text{CO}_2$  pressure is increased, two processes act in opposite directions. First, the  $p\text{H}$  in the mixed layer becomes lower so that  $[\text{FeOH}^+]$  and  $\phi_{\text{phot}}$  tend to be reduced. Second, the carbonate ion becomes less abundant and, since the deep water is saturated with respect to siderite, the  $\text{Fe}^{2+}$  concentration increases in the deep water and also in the mixed layer as a result of transport, so that  $\phi_{\text{phot}}$  tends to become higher. In the 'standard model', the second process is dominant and  $\phi_{\text{phot}}$  increases from 0.308 mol  $\text{Fe m}^{-2} \text{ yr}^{-1}$  at 1 PAL to 0.657 mol  $\text{Fe m}^{-2} \text{ yr}^{-1}$  at 1,000 PAL. The effects of varying several parameters of the model have been investigated. Increasing the quantum efficiency to the value  $\gamma = 0.05$  has no appreciable effect on  $\phi_{\text{phot}}$ . Thus, the experimental uncertainty in the value of  $\gamma$  is not important. If the temperature of the deep water is increased from 5 to 20 °C, the rate of photo-oxidation is decreased as a result of lower  $\text{Fe(II)}$  concentrations caused by the lower solubility of siderite, but this decrease is not dramatic. The effect of dividing the absorption coefficient of  $\text{FeOH}^+$  by 13 is marked at high  $P_{\text{CO}_2}$ . However,

Table 1 Reactions considered for the  $p\text{H}$  calculation

	Reactions	log K	Ref.
$K_1$	$\text{Fe}^{2+} + \text{OH}^- \rightleftharpoons \text{FeOH}^+$	3.86	18
$K_2$	$\text{Fe}^{2+} + \text{Cl}^- \rightleftharpoons \text{FeCl}^+$	-0.45	18
$K_3$	$\text{Fe}^{2+} + \text{SO}_4^{2-} \rightleftharpoons \text{FeSO}_4^0$	0.61	18
$K_4$	$\text{H}^+ + \text{SO}_4^{2-} \rightleftharpoons \text{HSO}_4^-$	1.064	19
$K_5$	$\text{HCO}_3^- + \text{Mg}^{2+} \rightleftharpoons \text{MgHCO}_3^+$	0.017	19
$K_6$	$\text{CO}_3^{2-} + \text{Mg}^{2+} \rightleftharpoons \text{MgCO}_3^0$	1.512	19
$K_7$	$\text{HCO}_3^- + \text{Ca}^{2+} \rightleftharpoons \text{CaHCO}_3^+$	0.017	Assumed equal to $K_5$
$K_8$	$\text{CO}_3^{2-} + \text{Ca}^{2+} \rightleftharpoons \text{CaCO}_3^0$	1.512	Assumed equal to $K_6$
$K_9$	$\text{Mg}^{2+} + \text{OH}^- \rightleftharpoons \text{MgOH}^+$	1.58	19
$K_{10}$	$\text{Ca}^{2+} + \text{OH}^- \rightleftharpoons \text{CaOH}^+$	0.25	19
$K_{11}$	$\text{H}_2\text{O} \rightleftharpoons \text{H}^+ + \text{OH}^-$	*	20
$K_{12}$	$\text{H}_2\text{CO}_3 \rightleftharpoons \text{H}^+ + \text{HCO}_3^-$	*	21
$K_{13}$	$\text{HCO}_3^- \rightleftharpoons \text{H}^+ + \text{CO}_3^{2-}$	*	21
$K_{14}$	$\text{H}_3\text{BO}_3 \rightleftharpoons \text{H}^+ + \text{H}_2\text{BO}_3^-$	*	21

\*  $K_{11}$  to  $K_{14}$  are temperature- and salinity-dependent expressions. A salinity of 35‰ has been assumed.

oxidized and gives rise to  $\text{Fe(III)}$  falling particles. In this model, it is assumed that no reduction of  $\text{Fe(III)}$  takes place in the thermocline, so that there is no production or sink of  $\text{Fe(II)}$  in this layer. Some  $\text{Fe(III)}$  may, nevertheless, be reduced to  $\text{Fe(II)}$  in the deep water. As a result, the rate of BIF deposition may be somewhat lower than the photo-oxidation rate  $\phi_{\text{phot}}$ .

The model is composed of three coupled sub-models, the first of which describes the photochemical aspects of the photo-oxidation reaction, the second calculates the  $p\text{H}$  profile and the third deals with ocean dynamics. These various calculations are repeated iteratively until convergence.

In the photochemical model, the photo-oxidation rate  $\phi_{\text{phot}}$  is calculated as a function of the  $\text{FeOH}^+$  concentration in the mixed layer. The solar photons are absorbed in the mixed layer by  $\text{FeOH}^+$  and water. Photo-oxidation occurs for photons with a wavelength between 220 and 460 nm. The molar absorption coefficient  $\epsilon_{\text{FeOH}}^+$  is from ref. 9. However, Braterman *et al.*<sup>10</sup> report an absorption coefficient at 366 nm that is about 13 times less than that found by Ehrenfreund and Leibenguth<sup>9</sup> at the same wavelength. Thus, the effect of dividing the absorption coefficient by this factor (over the whole spectrum) is assessed.

**Table 2** The magnitude of the  $\text{FeOH}^+$  photo-oxidation rate  $\phi_{\text{phot}}$  at various atmospheric  $\text{CO}_2$  pressures

$\phi_{\text{phot}}$ (mol Fe $\text{m}^{-2}$ $\text{yr}^{-1}$ )	$P_{\text{CO}_2}$ 1 PAL	$P_{\text{CO}_2}$ 10 PAL	$P_{\text{CO}_2}$ 100 PAL	$P_{\text{CO}_2}$ 1,000 PAL
(1) Standard model	0.308	0.335	0.440	0.657
(2) $\gamma = 0.05$	0.309	0.337	0.444	0.676
(3) $T_{\text{DEEP}} = 20^\circ\text{C}$	0.203	0.220	0.280	0.406
(4) Modified absorption coefficient	0.301	0.312	0.359	0.361
(5) $T_{\text{DEEP}} = 20^\circ\text{C} +$ modified absorption coefficient	0.198	0.204	0.225	0.215
(6) $w = 0$	0.195	0.213	0.280	0.427
(7) $w = 0 +$ modified absorption coefficient	0.192	0.203	0.245	0.278
(8) $w = 4,000 \text{ m yr}^{-1}$	75.1	42.3	20.7	9.11

(1) Standard model:  $K = 4,000 \text{ m}^2 \text{ yr}^{-1}$ ;  $w = 4 \text{ m yr}^{-1}$ ;  $\gamma = 0.03$ ; temperature of the deep water,  $5^\circ\text{C}$ . (2) Same as the standard model except that  $\gamma = 0.05$ . (3) Same as the standard model except that the temperature of the deep water is  $20^\circ\text{C}$ . (4) Same as the standard model except that the absorption coefficient  $\epsilon_{\text{FeOH}^+}$  of Ehrenfreund and Leibenguth<sup>9</sup> has been divided by 13. (5) Same as model (4) except that the temperature of the deep water is  $20^\circ\text{C}$ . (6) Same as the standard model except that  $w = 0$ . (7) Same as model (4) except that  $w = 0$ . (8) Same as the standard model except that  $w = 4,000 \text{ m yr}^{-1}$ .

even at 1,000 PAL, this variation of  $\epsilon_{\text{FeOH}^+}$  has no great effect on the photo-oxidation rate:  $\phi_{\text{phot}}$  shows a decrease of only <50%. Therefore, it seems that the mean photo-oxidation rate  $\phi_{\text{phot}}$  for the global Archaean ocean could have been as high as  $0.5 \text{ mol Fe m}^{-2} \text{ yr}^{-1}$ .

The effect of the intensity of the ocean circulation is also shown in Table 2. When  $w$  is set equal to zero, the model becomes entirely diffusive and the Fe(II) concentration increases linearly with depth. It is observed that the order of magnitude of  $\phi_{\text{phot}}$  is not greatly affected by such a variation of  $w$ . On the other hand, when  $w$  is increased to  $4,000 \text{ m yr}^{-1}$ ,  $\phi_{\text{phot}}$  can become several hundred times higher.

In the modern ocean, the vertical velocity of upwelling may be as large as several  $\text{km yr}^{-1}$  in areas of strong upwelling<sup>13</sup>. Thus, the model with  $w = 4,000 \text{ m yr}^{-1}$  may be used to describe a restricted basin in such an area. At a  $\text{CO}_2$  pressure of 100 PAL, the rate of photo-oxidation of  $\text{FeOH}^+$  could have been as high as  $20 \text{ mol Fe m}^{-2} \text{ yr}^{-1}$ , that is,  $112 \text{ mg cm}^{-2} \text{ yr}^{-1}$ . This value may be compared with the iron deposition rate of  $20 \text{ mg cm}^{-2} \text{ yr}^{-1}$  in the BIFs of the Hamersley Basin in Australia<sup>14</sup>. Consequently, the possibility that extensive BIF deposits could form without oxygen through photo-oxidation of  $\text{FeOH}^+$  must be considered.

If the area of the Archaean ocean was the same as today, a mean photo-oxidation rate of  $0.5 \text{ mol Fe m}^{-2} \text{ yr}^{-1}$  corresponds to a global flux of  $1.8 \times 10^{14} \text{ mol Fe yr}^{-1}$ . Garrels and MacKenzie<sup>15</sup> report a value of  $12.2 \times 10^{14} \text{ g yr}^{-1}$  (that is,  $0.218 \times 10^{14} \text{ mol yr}^{-1}$ ) for the present-day input of iron to the ocean in the suspended sediments of rivers. On the Archaean Earth, however, the geochemical fluxes of ions into the ocean were probably governed by the interaction of sea water with the basaltic ocean crust<sup>16</sup>. For the present ocean, these fluxes are very poorly known, but according to Wolery and Sleep<sup>17</sup>, the total basaltic crust input of iron to the ocean would fall in the range  $22-39 \times 10^{12} \text{ g Fe yr}^{-1}$ ; that is,  $0.39-0.69 \times 10^{12} \text{ mol Fe yr}^{-1}$ . This basaltic flux of iron was probably several times greater during the Archaean, as a result of a higher rate of volcanic activity. However, this flux was probably not much greater than the present flux of iron suspended in rivers. Thus, a conservative estimate is that the Archaean geochemical input of iron to the ocean was close to  $0.2 \times 10^{14} \text{ mol yr}^{-1}$ . If this assumption is correct, the calculated value of the global photo-oxidation rate of  $\text{FeOH}^+$ ,  $\phi_{\text{phot}}$ , seems to be an order of magnitude too high.

This discrepancy may be explained by one or more of the following hypotheses: (1) The deep water was not saturated with respect to siderite. (2) The absorption of solar light by sea salts in the range 220–460 nm can limit the photo-oxidation rate more efficiently than the absorption by water itself. (3) The Fe(III) produced in the mixed layer reacted with reduced compounds dissolved in the ocean, thus decreasing the rate of BIF deposition. (4) The diffusion coefficient  $K$  and the advective velocity  $w$  were both lower than today.

It would be interesting to refine the ocean model to study possibilities (2) and (3). However, such a task would not be easy in view of our poor knowledge of the Archaean ocean chemistry.

In conclusion, the present model shows that  $\text{FeOH}^+$  photo-oxidation was able to produce BIF deposits as extensive as have been found in the Hamersley Basin. From a global point of view, a total photo-oxidation rate of  $1.8 \times 10^{14} \text{ mol Fe yr}^{-1}$  has been calculated. Since  $\text{FeOH}^+$  photo-oxidation releases hydrogen, such a flux may have had important consequences for the oxidation state of the Precambrian atmosphere. An important question concerns the rate at which Fe(III) would react with the hydrogen released or with any other reduced compound dissolved in the ocean. This point is difficult to analyse quantitatively as neither the kinetics of the reaction nor the composition of Archaean sea water is well known. The model results might also depend slightly on the presence of small amounts of  $\text{O}_2$ . This problem will be examined elsewhere.

This work was supported by a fellowship from the Belgian Institute for the encouragement of Industrial and Agricultural Scientific Research.

Received 19 September 1985; accepted 20 January 1986.

1. Gole, M. J. & Klein, C. J. *Geol.* **89**, 169–183 (1981).
2. James, H. L. *U.S. Geol. Surv. Prof. Pap.* **440-W** (1966).
3. Holland, H. D. *Econ. Geol.* **68**, 1169–1172 (1973).
4. Drever, J. I. *Geol. Soc. Am. Bull.* **85**, 1099–1105 (1974).
5. Walker, J. C. G. *Pure appl. Geophys.* **117**, 498–512 (1978).
6. Cairns-Smith, A. G. *Nature* **276**, 807–808 (1978).
7. Brateman, P. S., Cairns-Smith, A. G. & Sloper, R. W. *Nature* **303**, 163–164 (1983).
8. Langmuir, D. *U.S. Geol. Surv. Prof. Pap.* **650-B**, 180–184 (1969).
9. Ehrenfreund, M. & Leibenguth, J.-L. *Bull. Soc. chim. Fr.* **2494–2505** (1970).
10. Brateman, P. S., Cairns-Smith, A. G., Sloper, R. W., Truscott, T. G. & Craw, M. *Dalton Trans.*, 1441–1445 (1984).
11. Walker, J. C. G. & Brimblecombe, P. *Precambr. Res.* **28**, 205–222 (1985).
12. Oeschger, H., Siegenthaler, U., Schotterer, U. & Gugelmann, A. *Tellus* **27**, 168–192 (1975).
13. Holland, H. D. *The Chemical Evolution of the Atmosphere and Oceans*, 396 (Princeton University Press, 1984).
14. Trendall, A. F. J. *geol. Soc. Aust.* **19**, 287–311 (1972).
15. Garrels, R. M. & Mackenzie, F. T. *Evolution of Sedimentary Rocks*, 112 (Norton, New York, 1971).
16. Veizer, J., Compston, W., Hoefs, J. & Nielsen, H. *Naturwissenschaften* **69**, 173–180 (1984).
17. Wolery, T. J. & Sleep, N. H. *J. Geol.* **84**, 249–275 (1976).
18. Davison, W. *Geochim. cosmochim. Acta* **43**, 1693–1696 (1979).
19. Dyrssen, D. & Wedborg, M. in *The Sea* Vol. 5 (ed. Goldberg, E. D.) 181–195 (Wiley, New York, 1974).
20. Millero, F. J. *Geochim. cosmochim. Acta* **43**, 1651–1661 (1979).
21. Gieskes, J. M. in *The Sea* Vol. 5 (ed. Goldberg, E. D.) 123–151 (Wiley, New York, 1974).

## High levels of natural radionuclides in a deep-sea infaunal xenophyophore

David D. Swinbanks & Yoshihisa Shirayama

Ocean Research Institute, University of Tokyo, 1-15-1 Minamidai, Nakano-ku, Tokyo 164, Japan

While debate continues about the disposal of man-made radioactive wastes in the deep sea, one deep-sea rhizopod is storing naturally occurring radionuclides to high concentrations in its home centimetres below the floor of the Izu-Ogasawara Trench. The hadal infaunal xenophyophore *Occultammina profunda* fills its test, a network of sediment tubes, with spherical micro-packets of waste (stercomes) containing 450–520 d.p.m. per g dry wt of the natural radionuclide  $^{210}\text{Pb}$ . The stercomes are stored in flimsy membrane tubes immediately next to a thread-like protoplasmic body (granellare), which has equally high  $^{210}\text{Pb}$  levels. A model

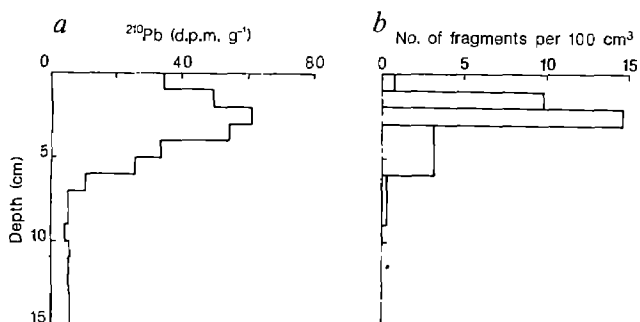


Fig. 1 The vertical distribution of  $^{210}\text{Pb}$  (ref. 5) (a) and fragments of *O. profunda*<sup>8</sup> (b) in the box core of sediment from the Izu-Ogasawara Trench (sample depth 8,260 m). The former distribution is based on one subcore of  $100\text{ cm}^2$  cross-section while the latter is the average distribution of four such subcores (not including that for  $^{210}\text{Pb}$ ). Only fragments of *O. profunda* which contained granellare stained red by Rose Bengal were counted. Each fragment contains on average  $2.4 \pm 2.3\text{ }\mu\text{g}$  dry wt of granellare ( $n = 42$ ).

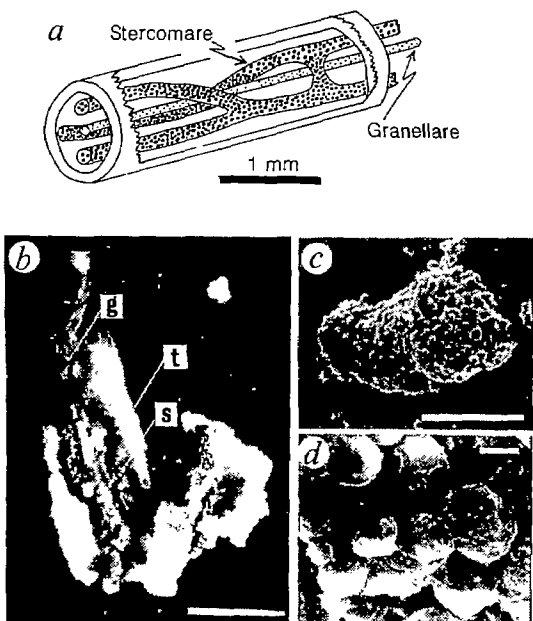


Fig. 2 a, Internal organization of *O. profunda*. b, A fragment of *O. profunda* split open to reveal the granellare (g), stercomare (s) and tubular test (t). Scale bar, 500  $\mu\text{m}$ . c, Scanning electron micrograph of a stercomare showing aggregations of stercomes (pellets) enclosed within a tubular membrane. Scale bar, 170  $\mu\text{m}$ . d, Scanning electron micrograph of stercomes. Scale bar, 8  $\mu\text{m}$ .

of stercome excretion suggests that *O. profunda* grows quickly and can produce transient subsurface peaks in the vertical distribution of  $^{210}\text{Pb}$  in the sediment while causing little, if any, sediment mixing, a finding which could have profound consequences for the  $^{210}\text{Pb}$ -modelling of deep-sea bioturbation (mixing of sediments by organisms). From the barium content of the granellare (21,000 parts per million, p.p.m.) and assuming that the  $^{226}\text{Ra}/\text{Ba}$  ratio in the surrounding sediment and sea water is maintained in the organism, it is inferred that the protoplasmic  $^{210}\text{Pb}$  is supported by 320–350 d.p.m. per g dry wt of  $^{226}\text{Ra}$  concentrated in intracellular barite crystals. Consequently, *O. profunda* and xenophyophores in general are probably subject to unusually high levels of natural radiation (several  $\text{Sv yr}^{-1}$ ), among the highest reported for any living organism.

$^{210}\text{Pb}$  is derived from the decay of  $^{226}\text{Ra}$  in sea water and the Earth's crust<sup>1</sup>. With a half-life of 22 yr,  $^{210}\text{Pb}$  decays to the short-lived  $\beta$ -emitter  $^{210}\text{Bi}$  and thence to the  $\alpha$ -emitter  $^{210}\text{Po}$  which has a half-life of 138 days.  $^{210}\text{Po}$  is often concentrated by marine organisms and unusually high levels of  $^{210}\text{Po}$  have

recently been reported in certain mid-water oceanic shrimp and fish, but  $^{210}\text{Pb}$  activities in organisms are typically much lower (a few d.p.m. per g dry wt at most)<sup>2</sup>. However, very little is known about natural radionuclide levels in deep-sea benthic organisms, a situation that must be rectified if the hazards of radioactive waste disposal are to be properly assessed.

The vertical distribution of  $^{210}\text{Pb}$  in surficial deep-sea sediments has been analysed extensively in attempts to estimate rates of bioturbation<sup>3–7</sup>. The mixing model on which such estimates are based, however, assumes that  $^{210}\text{Pb}$  enters the sediment at the sediment/water interface attached to sinking particulate matter and remains attached to sedimentary particles throughout the mixing process. The possibility that a significant fraction of  $^{210}\text{Pb}$  enters the sediment through the tissue and excretion products of benthic organisms living below the sediment/water interface has not been considered. We decided to examine  $^{210}\text{Pb}$  levels in the infaunal xenophyophore *O. profunda* because an unusual subsurface peak in the vertical distribution of  $^{210}\text{Pb}$  in the sediment, which could not be explained by the standard mixing model<sup>5</sup>, coincided with a peak in the vertical distribution of the xenophyophore at 2–3 cm depth<sup>8</sup>, and we thought the xenophyophore might be responsible for the  $^{210}\text{Pb}$  peak (Fig. 1). Such 'anomalous'  $^{210}\text{Pb}$  distributions can be quite common in the deep sea<sup>6</sup>, and it is becoming increasingly clear that the standard mixing model, which predicts an exponential decrease in  $^{210}\text{Pb}$  activity with depth in the sediment, is 'idealized'.

Xenophyophores are giant deep-sea rhizopod protozoans that live on and in the sediment<sup>8,9</sup> and are closely related to benthic foraminiferans. Deep-sea photography has revealed that epifaunal xenophyophores can be very abundant (~1–10  $\text{m}^{-2}$ ) in certain environments<sup>10</sup>, and the infaunal xenophyophore of the present study, collected from a box core from the Izu-Ogasawara Trench, was the most abundant macrofaunal organism in the core<sup>8</sup>.

The test of *O. profunda* consists of a horizontal network of sediment tubes (500–1,000  $\mu\text{m}$  diameter) that enclose a central granellare string (40–130  $\mu\text{m}$  diameter) surrounded by one to three peripheral stercomare strings (125–160  $\mu\text{m}$  diameter) (Fig. 2a–c)<sup>8</sup>. Both the granellare and stercomare have a thin (<0.5  $\mu\text{m}$ ) organic membrane wall that in the former encloses the multinucleate plasma body and in the latter, stercomes. Stercomes are small black spherical pellets ~10  $\mu\text{m}$  in diameter (Fig. 2d) which are thought to be waste and excretion products, although very little is known about their composition<sup>9</sup>. An unusual feature of xenophyophores is that they contain high concentrations of barium (~10<sup>4</sup> p.p.m.) in the form of intracellular barite crystals called granellae, which are believed to be secreted by the organism<sup>9,11</sup>. In *O. profunda* the granellae are less than 0.5  $\mu\text{m}$  in size (O. S. Tendal, personal communication).

A total of about 160 fragments of *O. profunda* were separated from two subcores of sediment (each  $100\text{ cm}^2$  in horizontal cross-section) which had been stored in a freezer (~10 °C) since collection in March 1980. The top 10 cm of each subcore was sliced horizontally at 1-cm intervals and the sediment washed through a 0.5-mm sieve that retained fragments of the organism. After air-drying on filter paper, the fragments were divided into test, granellare and stercomare, each subcore yielding ~40 mg dry weight of test, 5 mg of stercomare and 0.2 mg of granellare. In addition, comparable amounts of test, stercomare and granellare were obtained from alcohol-preserved specimens of *O. profunda*. Pooled samples of each part of the organism and the sediment at each 1-cm interval were analysed separately for  $^{210}\text{Pb}$  by the  $^{210}\text{Po}$  technique<sup>12</sup> (Table 1).  $^{210}\text{Pb}$  activities were corrected to those at the time of sampling (4–5 yr earlier), assuming that the  $^{210}\text{Pb}$  (half-life 22 yr) was unsupported. Aliquots (10 cm $^3$ ) of the acid-dissolved samples (5 cm $^3$ ) used for  $^{210}\text{Pb}$  analysis were analysed for barium by inductively coupled plasma emission spectrometry<sup>13</sup>.

The  $^{210}\text{Pb}$  content of the sediment peaked at 1.5 cm depth, coincident with a peak in the vertical distribution of *O. profunda*.

**Table 1** Measured  $^{210}\text{Po}$  activities and barium contents of various parts of *O. profunda* and the surrounding sediment, and their estimated  $^{210}\text{Pb}$  and  $^{226}\text{Ra}$  activities

Sample	$^{210}\text{Po}$ (d.p.m. g $^{-1}$ )*	$^{210}\text{Pb}$ (d.p.m. g $^{-1}$ )	Ba (p.p.m.)	$^{226}\text{Ra}$ (d.p.m. g $^{-1}$ )
Granellare (0–6 cm)	450±100†	510±110	21,000	320–350
Stercomare (0–6 cm)	380±60‡	450±70		
1–2 cm	440±50§	490±50	870	13–14
2–3 cm	420±40†	480±50		
Test (0–6 cm)	440±50‡	520±60		
2–3 cm	430±40‡	510±50		
Test (0–6 cm)	42±5	47±6	356	5–6
Sediment (0–6 cm)	52±3	62±4		
	9–57	10–65	329–359	5.2

Samples were digested in acid and  $^{210}\text{Po}$  was spontaneously deposited on one or two silver disks (1 cm diameter) the  $\alpha$ -activities of which were then counted for 1–5 days. A  $^{208}\text{Po}$  tracer was added to the sample for the determination of chemical yield, which ranged between 10 and 85%. Because the  $^{210}\text{Po}$  analysis was performed 4–5 yr after sample collection, it can be assumed that  $^{210}\text{Po}$ , which has a half-life of 138 days, was in secular equilibrium with its grandparent  $^{210}\text{Pb}$  at the time of analysis (that is, the activities of the two radionuclides were the same) and this was confirmed by replating some of the samples after 9–12 months. Errors are based on  $1\sigma$  counting statistics and include, where significant, errors due to blank correction. Counts for chemical blanks were at most one or two counts per day above background, which at counting efficiencies of 24–33% ranged from 0.3 to 7 counts per day depending on the detector used (eight detectors in all).  $^{210}\text{Po}$  counts for the granellare samples, although low due to low sample weight, were more than five times those for the blanks (including background), yielding  $^{210}\text{Po}$  estimates with a 15–20% error as opposed to ~10% error for the other parts of the organism.

\* 1 d.p.m. g $^{-1}$  = 16.7 Bq kg $^{-1}$ .

† Measured 26 March 1984 (frozen samples, collected 3 March 1980).

‡ Measured 27 September 1985 (alcohol-preserved samples, collected 3 March 1980).

§ Measured 15 December 1983 (frozen samples, collected 3 March 1980).

|| Estimated from Ba content assuming a  $^{226}\text{Ra}/\text{Ba}$  ratio of 4.2–4.6 nmol per mol.

¶ Estimated from constant  $^{210}\text{Pb}$  activity below 7 cm depth (Fig. 1).

but the  $^{210}\text{Pb}$  peak was much weaker and 1 cm shallower than in Fig. 1 (Fig. 3a, b). The  $^{210}\text{Pb}$  activity of the xenophyophore's test, which is composed of particles selected from the surrounding sediment, was comparable to, or slightly higher than, the activity of sediment at the same depth (Fig. 3a), whereas the activity of the granellare and stercomare was an order of magnitude higher, at 450–520 d.p.m. per g dry wt (Table 1). In the 1–2- and 2–3-cm layers, where *O. profunda* was most abundant, stercomare showed no significant difference in  $^{210}\text{Pb}$  content between layers, with values of 520 and 510 d.p.m. per g dry wt, respectively. Comparably high levels of unsupported  $^{210}\text{Po}$  have recently been reported in the hepatopancreas of mid-water penaeid shrimp, but the highest levels of  $^{210}\text{Pb}$  previously reported in any organism, which were for benthic amphipods from the Central Pacific, are two orders of magnitude lower than our findings<sup>2</sup>. Preliminary  $^{210}\text{Pb}$  analysis of two epifaunal species of xenophyophore (an unidentified species from a depth of 5,270 m on the Pacific margin of the Japan Trench and *Psammina nummulina* collected from 3,570 m between the Cocos Ridge and East Guatemala Basin) has yielded comparably high levels of  $^{210}\text{Po}$  in their granellare and stercomare, but  $^{210}\text{Pb}$  support has yet to be confirmed (our unpublished data).

There are two possible origins for the  $^{210}\text{Pb}$  in *O. profunda*. One possibility is that the xenophyophore accumulates the radionuclide at the sediment/water interface by feeding on settling particulate matter containing several hundred d.p.m. per g dry wt of  $^{210}\text{Pb}$  (refs 14, 15; for a possible feeding mechanism

in infaunal xenophyophores see ref. 16). Another quite different possible source is  $^{226}\text{Ra}$  within the intracellular granellae. It is well known that the chemistry of barium is very similar to that of radium, its chemical congener in the Periodic Table, and the  $^{226}\text{Ra}/\text{Ba}$  ratio in oceanic sea water maintains a nearly constant value of 4.6 nmol of  $^{226}\text{Ra}$  per mol Ba (ref. 17), very similar to the value estimated for the box-core sediment of the present study (we estimate the ratio to be 4.2 nmol  $^{226}\text{Ra}$  per mol Ba by assuming that the almost constant  $^{210}\text{Pb}$  activity of about 5.2 d.p.m. per g dry wt below 7-cm depth (Fig. 1) equals the  $^{226}\text{Ra}$  activity and by using an average of 335 p.p.m. for the barium content of the sediment (Table 1)). Assuming that the ratio in the surrounding sediment and sea water is maintained in *O. profunda*, as in diatoms<sup>18</sup>, the granellare, which contain about 21,000 p.p.m. of barium (Table 1), are estimated to contain 320–350 d.p.m. per g dry wt of  $^{226}\text{Ra}$  (using values of 4.2 and 4.6 nmol  $^{226}\text{Ra}$  per mol Ba, respectively). If this estimate is of the right order of magnitude, then estimated  $^{210}\text{Pb}$  contents for granellare in Table 1 will require a downward adjustment of ~10% (assuming no radon loss) because in the calculation of the values in Table 1 it was assumed that  $^{210}\text{Pb}$  was unsupported.

The percentage of  $^{210}\text{Pb}$  in the granellare which is derived from  $^{226}\text{Ra}$  in the granellae will depend on the age of the granellae. If, as we suggest below, xenophyophores are short-lived organisms, and if granellae are secreted intracellularly, then the contribution of  $^{210}\text{Pb}$  from granellae will be small, because it requires several half-lives (>100 yr) for  $^{210}\text{Pb}$  to achieve secular equilibrium with  $^{226}\text{Ra}$ . In the case of the stercomare and test, the barium content is much lower, 870 and 356 p.p.m., respectively, corresponding to estimated  $^{226}\text{Ra}$  contents of 13–14 and 5–6 d.p.m. per g dry wt, respectively (Table 1), and thus their  $^{210}\text{Pb}$  is largely unsupported by  $^{226}\text{Ra}$ .

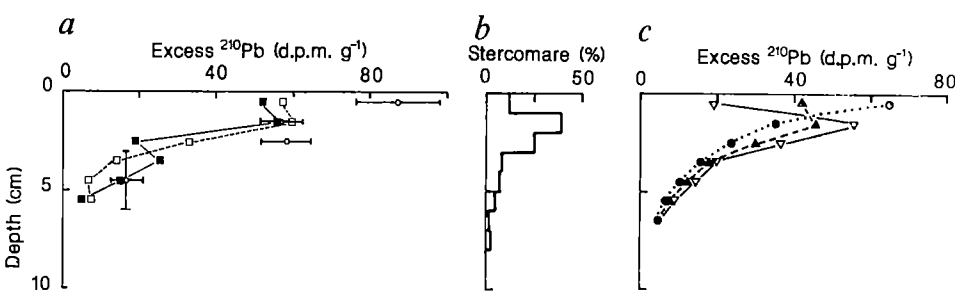
Our  $^{210}\text{Po}$  data and the  $^{226}\text{Ra}$  levels estimated from the barium content suggest that the plasma body of *O. profunda* is subject to an unusually high dose of natural radiation. Considering only  $\alpha$ -radiation and assuming that it has an effective quality factor of 20 (ref. 19), the dose from  $^{210}\text{Pb}$ -supported  $^{210}\text{Po}$  alone is about 0.8 Sv yr $^{-1}$  (using a measured wet/dry ratio of 5.0±0.5 and a  $^{210}\text{Po}$  ( $^{210}\text{Pb}$ ) content of 450 d.p.m. per g dry wt), whereas if the granellare contain 320 d.p.m. per g dry wt of  $^{226}\text{Ra}$  (the lower estimate given above) the radiation dose increases to about 3.0 Sv yr $^{-1}$  (assuming no radon loss and assuming the short-lived  $\alpha$ -emitting descendants of radon, namely  $^{218}\text{Po}$  and  $^{214}\text{Po}$ , contribute to the dose). The latter dose is comparable to that in the hepatopancreas of mid-water penaeid shrimp (3.9 Sv yr $^{-1}$ ), which is the highest natural radiation dose so far reported for any living organism<sup>2</sup>. The dose from  $^{226}\text{Ra}$  for *O. profunda*, however, should be regarded only as an order of magnitude estimate in the absence of measured  $^{226}\text{Ra}$  levels.

In most xenophyophores, the granellae are much larger (2–5  $\mu\text{m}$ ) than in *O. profunda* (<0.5  $\mu\text{m}$ ) and in some species granellae can be so abundant as to obscure the nuclei of the plasma body<sup>9</sup>. If the  $^{226}\text{Ra}/\text{Ba}$  ratio of oceanic sea water is maintained in these crystals, they will contain about 10<sup>4</sup> d.p.m. g dry wt of  $^{226}\text{Ra}$  and the adjacent nuclei of the plasma body will be subject to radiation doses even higher than those estimated above for *O. profunda*.

Although marine organisms are probably less sensitive to radiation than is man<sup>20</sup>, the possibility that these high radiation doses have affected xenophyophores over the long term should be considered. For example, has exposure to high levels of radiation resulted in a high incidence of radiation-induced mutation and/or development of radiation resistance? Studies of the molecular biology of these organisms might answer some of these questions. Turning to the geological record, it has been suggested that the trace fossil *Paleodictyon*, which occurs as far back as the Ordovician, is a fossilized form of infaunal xenophyophore<sup>16</sup>. If this is so, study of *Paleodictyon* could throw light on the evolution of xenophyophores over the past 500 Myr and might provide further insight into the above matters.

**Fig. 3** *a*, Activity of excess  $^{210}\text{Pb}$  in the sediment ( $\square$ , ■) and test ( $\circ$ ) of *O. profunda* as a function of sediment depth. Subcores B (■) and E ( $\square$ ) were separated laterally by 10 cm. All the test samples come from subcore E and covered a 1-cm vertical interval except for that from 3 to 6 cm, which came from a separate subcore not analysed for  $^{210}\text{Pb}$ . Horizontal bars indicate errors in test values. Excess  $^{210}\text{Pb}$  was calculated by

assuming a constant  $^{226}\text{Ra}$  content of 5.2 d.p.m. per g in the sediment and test (estimated from constant  $^{210}\text{Pb}$  activity below 7 cm depth in Fig. 1 and barium content of test in Table 1). *b*, Average vertical distribution of *O. profunda* stercomare (in weight per cent of total stercomare yield) in the two subcores in *a*. *c*, A model of the effects of stercome excretion on the vertical distribution of  $^{210}\text{Pb}$ . The sediment is divided into 1-cm-thick horizontal layers with a horizontal cross-sectional area of  $100\text{ cm}^2$  (as in our subcores) and the activity of excess  $^{210}\text{Pb}$  is maintained at 60 d.p.m.  $\text{cm}^{-2}$  (as in our subcores) by a constant flux of  $^{210}\text{Pb}$  to the sediment/water interface. For simplicity, porosity is assumed to be constant with depth (the average value of 86.5% for 0–7 cm is used) and sedimentation is considered to be negligible during the short time intervals considered. The concentration of excess  $^{210}\text{Pb}$  in stercomare is taken to be constant at 500 d.p.m.  $\text{g}^{-1}$  and the stercomare  $^{210}\text{Pb}$  is assumed to be derived from feeding at the sediment/water interface (all the  $^{210}\text{Pb}$  in stercomare comes from the 0–1-cm layer). In the model, a given amount of stercomare (5, 10 or 20 mg per  $100\text{ cm}^2$  for cases 1, 2 and 3, respectively) is instantaneously formed each month while an equivalent amount decays and releases its  $^{210}\text{Pb}$  to the immediately surrounding sediment. After stercomare decay, it is assumed that the stercomare-derived  $^{210}\text{Pb}$  is not immediately redistributed by bioturbation, an assumption which probably holds for periods of time comparable to the half-life of  $^{210}\text{Pb}$  (22 yr) (ref. 6). If the rate of stercomare formation is  $r$ , then the total inventory of stercomare-derived  $^{210}\text{Pb}$  after time  $t$  will be given by:  $I_t = \int_0^t ar e^{-\lambda t} dt = ar(1/\lambda - 1/\lambda e^{-\lambda t})$ , where  $\lambda$  is the decay constant of  $^{210}\text{Pb}$  and  $a$  is the activity of  $^{210}\text{Pb}$  in stercomare. The inventory is subtracted from the 0–1-cm layer and portions are allotted to the layers of the model according to the depth distribution of stercomare on the left. The effects of the three rates of stercomare formation in cases 1, 2 and 3 are considered. The effects of these rates after various intervals of time are shown by the dashed and solid curves (●, Exponential curve; ▲, case 1, 250 yr; case 2, 22 yr; case 3, 9 yr; Δ, case 2, 250 yr; case 3, 22 yr). For example, the dashed curve can be produced by a rate of 10 mg per  $100\text{ cm}^2$  per month (case 2) acting for 22 yr or by a rate of 20 mg per  $100\text{ cm}^2$  per month (case 3) acting for 9 yr, while the solid curve can be produced by the latter rate acting for 22 yr. Note the similarity of the dashed curve to the curves in *a* and the resemblance of the solid curve to the  $^{210}\text{Pb}$  profile in Fig. 1.



Of more immediate interest, however, is the possible effect of *O. profunda* on  $^{210}\text{Pb}$  distribution in the sediment through the excretion of stercomes rich in unsupported  $^{210}\text{Pb}$ . While it is generally believed that deep-sea organisms grow slowly and live long, there is circumstantial evidence that xenophyophores may grow rapidly. Epifaunal xenophyophores have been observed on freshly formed biogenic mounds (L. A. Levin, personal communication) which elsewhere in the deep sea have been seen to form within a few months (C. R. Smith, personal communication). As xenophyophores are almost certainly immobile, this suggests they may grow on a timescale of months rather than years. If so, a dense patch of *O. profunda* can have a very significant localized effect on the vertical distribution of  $^{210}\text{Pb}$ , as the model in Fig. 3c shows. In this model, we consider only stercome excretion—the contribution of  $^{210}\text{Pb}$  from granular, the weight of which is only 3–4% that of stercomare, is neglected—and it is assumed that all unsupported  $^{210}\text{Pb}$  in stercomare is derived from feeding on particulate matter settling at the sediment/water interface. The particulate matter flux will thus mark an upper limit for the rate of stercomare production. We estimate the former to be ~50–60 mg per  $100\text{ cm}^2$  per month based on a  $^{210}\text{Pb}$  flux of 1.9–2.4 d.p.m. per  $\text{cm}^2$  per yr (ref. 5 and the present study) and an average  $^{210}\text{Pb}$  content for particulate matter of 330 d.p.m. per g (refs 14, 15). At the maximum observed density of 420 *O. profunda* fragments per  $100\text{ cm}^2$ , the density of stercomare is estimated to be ~30 mg per  $100\text{ cm}^2$ , and if this is replaced at a rate between once a month and once a year, local stercomare production will lie between 2.5 and 30 mg per  $100\text{ cm}^2$  per month, well within the above estimated flux of particulate matter.

When stercomare production exceeds ~5 mg per  $100\text{ cm}^2$  per month, the vertical distribution of  $^{210}\text{Pb}$  begins to deviate significantly from the exponential curve expected in the standard diffusion mixing model<sup>3</sup> (compare with Fig. 3c). At a rate of 10 mg per  $100\text{ cm}^2$  per month, a small subsurface peak comparable to that observed in our subcores is formed within 22 yr at the depth of the peak in stercomare distribution (Fig. 3a–c); at a rate of 20 mg per  $100\text{ cm}^2$  per month the same peak is formed

in only 9 yr, after 22 yr it becomes pronounced (compare with Fig. 1) and after 40 yr the 0–1-cm layer is completely lacking in  $^{210}\text{Pb}$ . Thus, a combination of patchy *O. profunda* distribution and rapid stercomare formation could account for both the occurrence of a subsurface  $^{210}\text{Pb}$  peak and the marked subcore variation in the vertical distribution of  $^{210}\text{Pb}$ . Looked at another way, our model and the observed distributions of  $^{210}\text{Pb}$  and *O. profunda* suggest that this xenophyophore grows and excretes rapidly.

The model in Fig. 3c represents a major departure from the usual interpretation of  $^{210}\text{Pb}$  distribution in deep-sea sediments, as it involves highly selective redistribution of  $^{210}\text{Pb}$ -rich material in a non-steady-state fashion with little or no sediment mixing (our observations of stercomes suggest they contain few if any refractory sedimentary minerals). Apart from xenophyophores, many ‘primitive’ monothalamic deep-sea foraminiferans (for example, allogromiids, *Rhizammina*, komokiaceans) accumulate stercomes, and other benthic rhizopod protozoans producing masses of stercomes are extremely abundant in oligotrophic regions of the deep sea<sup>21</sup>. Our model therefore probably applies to wide areas of the ocean floor, and  $^{210}\text{Pb}$  distributions in deep-sea sediments may require substantial reinterpretation.

We thank N. Nozaki for providing advice and facilities for  $^{210}\text{Po}$  analysis, H. S. Yang and M. Yamada for assistance in radionuclide analysis, M. Sugiyama for carrying out the barium analysis, and R. D. Cherry, J. N. Smith, A. J. Gooday and J. Thomson for their review comments. D.D.S. was supported by a postdoctoral fellowship from the Japan Society for the Promotion of Science and the Royal Society of London.

Received 30 December 1985; accepted 28 January 1986.

- Burton, W. M. & Stewart, N. G. *Nature* **186**, 584–589 (1960).
- Cherry, R. D. & Heyraud, M. *Science* **218**, 54–56 (1982).
- Nozaki, Y., Cochran, J. K., Turekian, K. K. & Keller, G. *Earth planet. Sci. Lett.* **34**, 167–173 (1977).
- DeMaster, D. J. & Cochran, J. K. *Earth planet. Sci. Lett.* **61**, 257–271 (1982).
- Yamada, M., Kitaoka, H. & Tsunogai, S. *Deep Sea Res.* **30**, 1147–1156 (1983).
- Smith, J. N. & Schafer, C. T. *J. mar. Res.* **42**, 1117–1145 (1984).
- Cochran, J. K. *Geochim. cosmochim. Acta* **49**, 1195–1210 (1985).
- Tendal, O. S., Swinbanks, D. D. & Shirayama, Y. *Oceanol. Acta* **5**, 325–329 (1982).
- Tendal, O. S. *Galathea Rep.* **12**, 7–99 (1972).

10. Tendai, O. S. & Gooday, A. J. *Oceanol. Acta* 4, 415–422 (1981).
11. Gooday, A. J. & Nott, J. A. J. *mar. biol. Ass. U.K.* 62, 595–605 (1982).
12. Black, S. C. *Hlth Phys.* 7, 87–91 (1961).
13. Sugiyama, M., Matsui, M. & Nakayama, E. J. *oceanogr. Soc. Jap.* 40, 295–302 (1984).
14. Spencer, D. W. et al. *J. mar. Res.* 36, 493–523 (1978).
15. Bacon, M. P., Huh, C., Fleer, A. P. & Deuser, W. G. *Deep Sea Res.* 32, 273–286 (1985).
16. Swinbanks, D. D. *Science* 218, 47–49 (1982).
17. Chan, L. H. et al. *Earth planet. Sci. Lett.* 32, 258–267 (1976).
18. Szabo, B. J. *Geochim. cosmochim. Acta* 31, 1321–1331 (1967).
19. International Commission on Radiological Protection, Publication 26, 53 (Pergamon, Oxford, 1977).
20. Blaylock, B. G. & Trabalka, J. B. *Adv. Radiat. Biol.* 7, 103–152 (1978).
21. Riemann, F. *Oceanol. Acta* 6, 303–311 (1983).

## Perception of apparent motion by commissurotomy patients

V. S. Ramachandran

Department of Psychology, C-009, University of California at San Diego, La Jolla, California 92093, USA

A. Cronin-Golomb & J. J. Myers

Division of Biology, California Institute of Technology, Pasadena, California 91125, USA

**When two spatially separated light spots are flashed in rapid succession, the spot will appear to move between the two locations—an illusion called apparent motion<sup>1,2</sup>. We have presented this display to callosum-sectioned human patients and found that they could correctly report the temporal order of a simple apparent motion sequence presented across the vertical meridian. Hence, the forebrain commissures are not required for this function.**

We investigated motion perception by commissurotomy patients whose corpus callosum, anterior commissure, hippocampal commissure and massa intermedia (when encountered) had been sectioned surgically for the treatment of intractable epilepsy<sup>3,4</sup>. An intact corpus callosum is presumed to be involved in various types of visual integration across the vertical meridian<sup>5,6</sup>. For example, we tested three callosum-sectioned patients (L.B., A.A. and N.G.) and found that they experienced difficulty in matching the orientations of two lines flashed simultaneously on either side of the vertical meridian for 150 ms (ref. 7). When asked to indicate whether the orientations were the same or different, they performed very poorly; even orthogonal lines were sometimes reported to be parallel. Further, callosum-sectioned patients cannot perceive 'midline-stereopsis'<sup>8</sup> because they lack the commissural fibres<sup>9–12</sup> required to match disparate binocular stimuli across the vertical meridian. We therefore wondered whether these individuals could perceive apparent motion of a single light spot jumping across the midline from one hemi-field to the other. The spot subtended 20 arc min and its two successive locations were 9° apart (that is, 4.5° from the midline), so that we were stimulating the long-range rather than short-range motion<sup>13</sup> system. The spot was generated on a Panasonic monitor using an Apple 2c microcomputer. Stimulus duration and inter-stimulus interval (ISI) were held constant at 130 ms and 30 ms, respectively. Trials were generated randomly by the computer so that the spot jumped from either left to right (L-R) or right to left (R-L), or the two spots appeared simultaneously. One experimenter sat behind the cathode ray tube (CRT) screen and carefully watched the subject's eyes, and any trial on which the eyes moved was discarded. Each trial began a short interval after a warning tone. The interval between the tone and the appearance of the first spot was varied randomly. The subject's task was to fixate a central X and to indicate either the presence of simultaneity or the direction of perceived apparent movement by pointing to a card which pictorially depicted the three possibilities (Fig. 1). To ensure that the instructions were clearly understood, we began with 10 'training' trials presented entirely within the appropriate hemi-field alone

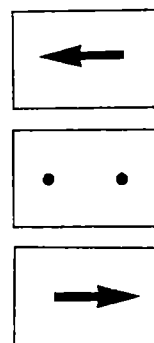


Fig. 1 The illustration shown to the subjects to enable them to point to the perceived direction of movement. The card was always presented in the hemi-field corresponding to the hand that was being used.

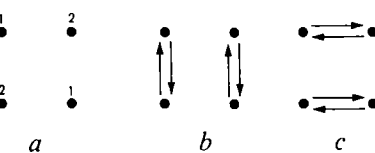


Fig. 2 Fluctuation in perception similar to that seen in Necker cubes can also be observed in an ambiguous apparent motion display (a). The direction of perceived oscillation in this bi-stable display can be influenced by the will only at slow speeds of alternation. Dots in diagonally opposite corners are flashed simultaneously and then switched off and replaced by dots appearing on the remaining two corners. (The numerals indicate order of presentation.) The frames are alternated in a continuous cycle. The two possible percepts (b and c) are also depicted.

(for example, left hemi-field for the left hand). When the actual experimental session began, the subject used one hand alone to indicate the perceived direction for each of 30 trials presented across the vertical meridian in random order. (The card with illustrations was always presented in the hemi-field corresponding to the hand that was being used.) After this, the subject switched hands and was confronted with a new random sequence of 30 trials. Three subjects ( $n = 3$ ) were used in these experiments and in two of them (L.B. and N.G.) we had NMR confirmation of commissurotomy<sup>14</sup> (J. Bogen, personal communication).

The results were clear-cut. L.B. could clearly discriminate L-R from R-L and either of these from simultaneous stimuli. (He was 100% accurate on all 60 trials, 30 with each hand.) N.G. had no difficulty in discriminating L-R from R-L, but she displayed considerable uncertainty with the simultaneous condition. (She was correct on 37 out of the 40 L-R/R-L trials and incorrect on all 20 trials on which the dots appeared simultaneously.) The third subject (A.A.) was accurate on 43 out of 60 trials and had no special difficulty with simultaneous stimuli (in fact, he got 18 correct out of 20). For all three subjects  $P < 0.01$  (two-tailed binomial test). The result with L.B. is especially interesting because previous studies<sup>8</sup> have shown him to lack midline stereopsis.

We were especially concerned about eye movements in this experiment, as the subject could have resorted to the strategy of using eccentric fixation to confine both spots to one hemi-field. To minimize this possibility, we instructed the subject to carefully fixate the central X, and had one experimenter constantly watching the eyes from across the table. As a further precaution, we ran another series of trials with the spots separated by 14° of visual angle instead of 9°. Again, L.B. was accurate on 100% of 30 trials, N.G. was correct on all 20 trials requiring R-L/L-R discrimination and incorrect on all 10 trials on which the spots were simultaneous, and A.A. was correct on 24 trials out of 30 ( $P < 0.01$ ; two-tailed binomial test). In this experiment, the subjects would have had to deviate their fixation by at least 7°

to bring both spots within one hemi-field and this seems highly unlikely.

Thus, the forebrain commissures are not required for correctly discriminating the temporal order of stimuli appearing across the midline in rapid succession. However, were the patients actually seeing movement or were they simply making discriminations based on temporal order *per se*? We questioned them on this point, taking care not to prompt them, and all three replied unhesitatingly that they had seen the dot 'move' or 'jump' rather than merely change location. To confirm this further, we increased the ISI gradually until the subjects (L.B. and A.A.; N.G. was not tested) reported a transition from seeing movement to seeing simple temporal succession. (The duration of each spot was 50 ms and the separation between them 8°.) For A.A. the transition occurred at 456 ms (mean of 8 readings, 4 ascending and 4 descending; s.d. = 46) and for L.B. it occurred at 329 ms (s.d. = 28) for vertical apparent motion along the vertical meridian. For horizontal motion across the vertical meridian, these values were 372 ms (s.d. = 71.5) and 346 ms (s.d. = 49), respectively. Thus, the transition from motion to temporal succession seems to occur at about the same ISI for both vertical and horizontal sequence, suggesting that the patients were indeed seeing movement across the midline when the ISI was appropriate. Interestingly, for the horizontal sequence, when the ISI was too long, they often reported seeing only a single spot flashing on and off and their ability to discriminate temporal order actually deteriorated even though they had more time available. It was almost as though one could switch from a single conscious individual to two individuals by simply increasing the ISI! (This provides another suggestive argument against the involvement of eye movements.) Further experiments are in progress to determine whether Korte's laws<sup>14</sup> of apparent motion would also apply to the 'second' visual system.

We conclude that apparent motion can be seen readily across the midline in spite of total transection of the forebrain commissures; this implies that the effect might be mediated largely by the so-called second visual system<sup>15-19</sup>, which bypasses the lateral geniculate nucleus and relays through the superior colliculus and pulvinar. This phylogenetically older system may be adequate for mediating motion perception but not for stereopsis<sup>20-22</sup> and 'form' perception. But what about more complex effects in motion perception, such as the perception of the ambiguous display depicted in Fig. 2? Does the bi-stability of ambiguous apparent motion displays depend on the cortex and on an intact corpus callosum?

A display similar to Fig. 2a subtending 5° was produced on the CRT and presented completely within one hemi-field alone. Two spots were flashed on opposite corners of a square (frame 1) and then replaced by two spots appearing on the two remaining corners<sup>23</sup>. The display is perceptually reversible (like a Necker cube)<sup>24</sup> and bi-stable in that there are two mutually exclusive percepts, vertical motion and horizontal motion. The two possible percepts (Fig. 2b and c) were explained to each subject (each hemisphere?) and the subject was 'trained' to use the corresponding hand to indicate the direction of perceived movement by simply pointing to an illustration on a card depicting the appropriate direction of movement. Informal testing suggested that each hemisphere could see these alternative percepts quite clearly.

When normal subjects fixate the centre of such a display, there is a slightly greater tendency to see vertical<sup>25,26</sup> rather than horizontal oscillation, although either percept can be seen voluntarily. As this tendency is usually attributed to delays across the midline imposed by the corpus callosum<sup>25,26</sup>, we wondered whether commissurotomy patients would always see exclusively vertical oscillation and we tested this conjecture in L.B., N.G. and A.A. To our surprise, we found that when they fixated a small spot in the centre of the display, they could in fact very easily see either organization at will. A perceptual switch could also be encouraged by momentarily occluding portions of the

display; for example, they could switch from vertical to horizontal oscillation by temporarily occluding the lower half of the display and then removing the occluder.

Next, we measured the tendency to see vertical compared with horizontal motion by changing the breadth/height ratio of the ambiguous figure while the subjects fixated an 'X' in the centre of the display. The height of the figure was varied randomly from trial to trial and on each trial the subject's task was simply to indicate whether he/she saw vertical or horizontal motion (inter-trial interval = 10 s; stimulus onset asynchrony = 150 ms; ISI = 0; the breadth was held constant at 5° and a total of 10 different height/breadth ratios were used, ranging from 0.53 to 2.15). For the normal 'control' subjects, vertical and horizontal motion were equally probable when the height/breadth ratio was 1.37 (mean of 40 readings; 20 readings for each subject). For the three commissurotomy patients, the ratios were 1.39, 1.5 and 1.51 for L.B., N.G. and A.A., respectively (mean of 20 readings for each subject; in N.G. we discarded 3 trials on which there were accidental eye movements). These results suggest that commissurotomy patients can see horizontal oscillations across the vertical meridian almost as easily as could normal subjects. Note that when they were seeing horizontal motion across the vertical meridian, the vertical motion signal must be either inhibited or vetoed at some level. The curious implication is that this inhibition can occur across the midline in the absence of forebrain commissures.

Further experiments are in progress to determine whether apparent motion of more abstract stimuli, such as cyclopean targets<sup>27</sup>, 'subjective contours'<sup>28,29</sup> and coloured spots at isoluminance<sup>30</sup>, can also be mediated by the second visual system in these patients. (Such stimuli are normally thought to require cortical processing.) Also, one wonders whether each hemisphere can independently 'will' a perceptual reversal without involving the other hemisphere, a question that might interest theologians.

We thank R. W. Sperry and E. Ebbesen for providing facilities, and C. Hamilton, V. Inada, J. Bogen, F. H. C. Crick, O. Braddick and J. A. Deutsch for stimulating discussions. The experiments were carried out in the laboratory of Dr R. W. Sperry at Caltech, Pasadena, California. V.S.R. was supported by academic senate and biomedical research grants from UCSD. A.C.-G. was supported by the NIH and by a Del E. Webb Fellowship from the California Institute of Technology.

Received 6 August 1985; accepted 23 January 1986.

1. Wertheimer, M. *Z. Psychol.* **61**, 161-265 (1912).
2. Kokers, P. *Aspects of Motion Perception* (Pergamon, New York, 1972).
3. Bogen, J. E. & Vogel, P. J. in *Les Syndromes de Disconnection Chez l'Homme* (eds Michel, F. & Schott, B.) 227-251 (Hôpital Neurologique, Lyon, 1975).
4. Bogen, J. E. in *Clinical Neuropsychology* (eds Heilman, K. M. & Valenstein, E.) Oxford University Press, 1979).
5. Sperry, R. W. *Am. Psychologist* **23**, 723-733 (1968).
6. Sperry, R. W., Gazzaniga, M. S. & Bogen, J. E. in *Handbook of Clinical Neurology* (eds Vincken, P. J. & Bruyn, G. W.) 273-290 (North-Holland, Amsterdam, 1969).
7. Ramachandran, V. S. & Cobb, S. (in preparation).
8. Mitchell, D. E. & Blakemore, C. B. *Vision Res.* **10**, 49-54 (1970).
9. Choudhury, B. P., Whitteridge, D. & Wilson, M. E. Q. *J. exp. Physiol.* **50**, 214-219 (1965).
10. Hubel, D. H. & Wiesel, T. N. *J. Neurophysiol.* **30**, 1561-1573 (1967).
11. Zeki, S. M. *Brain Res.* **34**, 63-75 (1970).
12. Pettigrew, J., Ramachandran, V. S. & Bravo, H. *Brain Behav. Evol.* **24**, 64-93 (1984).
13. Braddick, O. J. *Vision Res.* **14**, 519-527 (1974).
14. Korte, A. *Z. Psychol.* **72**, 194-296 (1915).
15. Trevarthen, C. B. & Sperry, R. W. *Brain* **96**, 547-570 (1973).
16. Trevarthen, C. B. *Psychol. Forsch.* **31**, 299-337 (1968).
17. Schneider, G. E. *Science* **163**, 895-902 (1969).
18. Weiszcrantz, L., Warrington, E. K. & Saunders, M. *Brain* **97**, 709-728 (1974).
19. Pöppel, E., Held, R. & Frost, D. *Nature* **243**, 295-296 (1973).
20. Barlow, H. B., Blakemore, C. B. & Pettigrew, J. D. J. *Physiol., Lond.* **193**, 327-342 (1967).
21. Hubel, D. H. & Wiesel, T. N. *Nature* **225**, 41-42 (1970).
22. Ramachandran, V. S., Clarke, P. G. H. & Whitteridge, D. *Nature* **268**, 333-335 (1977).
23. Ramachandran, V. S. & Anstis, S. M. *Nature* **304**, 529-531 (1983); *Perception* **14**, 135-143 (1985).
24. Necker, L. A. *Phil. Mag.* **1** (3d s.) 329-337 (1832).
25. Gengerelli, J. A. *J. exp. Psychol.* **38**, 592-599 (1948).
26. Ramachandran, V. S. & Anstis, S. M. *Vision Res.* **23**, 83-85 (1983).
27. Julesz, B. *Foundations of Cyclopean Perception* (University of Chicago Press, 1971).
28. Ramachandran, V. S., Rao, V. M. & Vidyaasagar, T. R. *Vision Res.* **13**, 1399-1401 (1973).
29. Ramachandran, V. S. *Perception* **14**, 127-134 (1985).
30. Ramachandran, V. S. & Gregory, R. L. *Nature* **275**, 55-56 (1978).

## Sampling in spatial vision

Dennis M. Levi & Stanley A. Klein

College of Optometry, University of Houston-University Park,  
4901 Calhoun Boulevard, Houston, Texas 77004, USA

The human visual system is capable of making spatial discriminations with extraordinary accuracy. In normal foveal vision, relative position, width or size can be judged with an accuracy much finer than the size or spacing of even the smallest foveal cones. This remarkable accuracy of spatial vision has been termed 'hyperacuity'<sup>1</sup>. Almost a century ago Ewald Hering proposed that the accuracy of Vernier acuity could be accounted for by averaging of discrete samples along the length of the lines comprising the targets<sup>2</sup>; however, the discovery that Vernier acuity of a few arc seconds could be achieved with dots has rendered the nature and role of sampling in spatial discrimination unclear<sup>3</sup>. We have been investigating the sampling of spatial information in central and peripheral vision (the perifovea) of normal human observers and in observers with strabismic amblyopia. Our results, presented here, show that peripheral vision and central vision of strabismic amblyopes differ qualitatively in their sampling characteristics from those of the normal fovea. Both the periphery and the central visual field of strabismic amblyopes demonstrate marked positional uncertainty which can be reduced by averaging of spatial information from discrete samples.

In the first experiment highly practised observers judged whether a test line presented briefly bisected the interval between two continuously viewed reference lines. The lines were composed of discrete samples (dots), each approximately 1 arc min and separated by inter-sample spaces of variable extent. We varied both the number of dots comprising each line and the inter-space size. The inset in Fig. 1 shows an example of a stimulus in which each line comprised five samples. The vertical separation of the lines was chosen to be optimal for each observer based on preliminary testing (see Table 1, column 2). A signal detection methodology was used to obtain thresholds for this spatial discrimination<sup>4</sup>. Figure 1a shows for two normal observers that foveal thresholds improved only slightly as the number of samples increased from 1 to 5. Additional samples beyond 5 had no further effect on thresholds and with even a single sample, thresholds were smaller than the inter-cone spacing ( $\sim 30$  arc s in the fovea).

Figure 1b shows results at  $2.5^\circ$  in the lower visual field; the data differ both quantitatively and qualitatively from those of the fovea. First, the threshold for a single sample is higher by more than a factor of 10. The threshold for a single sample (in the absence of spatial averaging) may provide an estimate of the intrinsic positional uncertainty of the visual system. What is of special interest here is that the threshold for a single sample is much larger than the inter-cone spacing at  $2.5^\circ$  ( $\sim 70$  arc s), suggesting that it is the cortical sampling grain rather than the cone mosaic which limits position discrimination in the periphery. Second, in the periphery, adding samples has a strong effect on bisection thresholds. For an 'ideal detector' that is limited by the spatial sampling grain, the positional uncertainty would be reduced in proportion to the square root of the number of independent samples; for the log-log axes of Fig. 1 this would mean a slope of  $-0.5$ . A flatter slope (like that of the fovea) would indicate that sparseness of sampling was not the factor limiting spatial discrimination. A higher slope would indicate an effect on the visibility of the targets by luminance summation. Table 1 gives the parameters for the fits to all the data in Fig. 1 (broken lines). While the results for the fovea are not compatible with a slope of  $-0.5$ , those for the periphery are consistent with a decrease in threshold proportional to  $\sqrt{n}$  ( $n$  is the number of discrete samples) up to  $n = 10$ . Beyond this, adding more

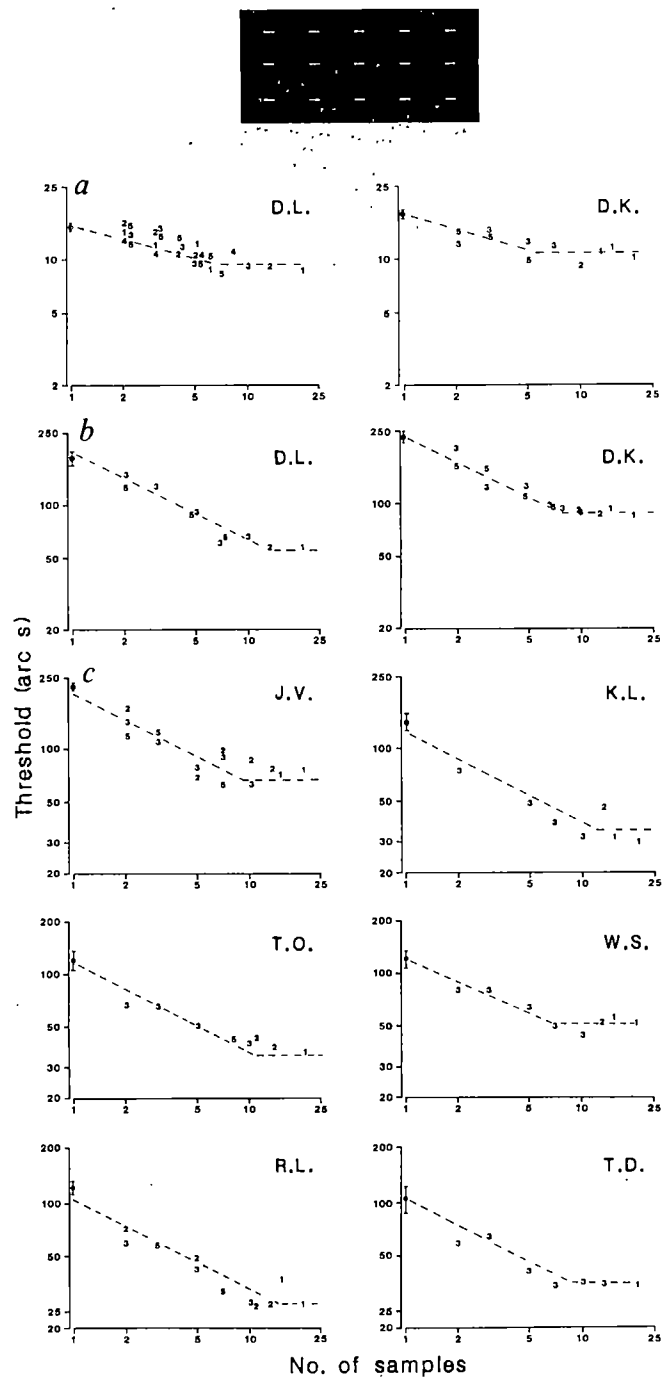


**Fig. 1** Top, a schematic diagram of the 3-line bisection stimulus, with each line composed of five samples (that is, dots  $\sim 1$  arc min) each separated by 2 arc min. The observer's task was to judge the vertical position of the briefly flashed test line (middle line) relative to the bisection point. The vertical separation between the reference lines and bisection point was optimized for each panel and is given in Table 1. Bisection thresholds equivalent to the signal detection parameter,  $d' = 0.675$  (75% correct), are based on 250–600 trials per point, and are plotted as a function of the number of samples for normal foveal vision (a), peripheral vision (b) and the central field of strabismic amblyopes (c). The numbers in each graph represent the sizes of the inter-space intervals in arc min. Each graph has been fitted with two lines. Thresholds decrease as the number of samples increases to  $\sim 5$  for foveal vision and 10 for peripheral and amblyopic vision. A slope of  $-0.5$  (that is, thresholds proportional to the square root of the number of samples) provides a reasonable fit for the data of the periphery and of the strabismic amblyopes. A shallower slope,  $-0.3$ , provides a good fit to the foveal results (see Table 1).

Table 1 Parameters for the fits to the data in Fig. 1

Condition	Vertical separation (min)	Observer	Snellen acuity	Threshold for a single sample (arc s) ( $y_0$ )	Asymptotic no. of samples ( $x_A$ )	Slope ( $r$ )
Normal fovea	3	D.L.	6/4.5	16.4 ± 0.80	7.8 ± 1.7	-0.29 ± 0.04*
	3	D.K.	6/5	17.4 ± 0.65	5.4 ± 1.3	-0.30 ± 0.04*
Periphery (2.5°)	12.4	D.L.	6/21	191.6 ± 11.3	11.1 ± 2.0	-0.48 ± 0.04
	12	D.K.	6/22	233.5 ± 10.6	9.5 ± 0.9	-0.43 ± 0.04
Strabismic amblyopia†	10	J.V.	6/24	219.8 ± 25	5.3 ± 0.9	-0.66 ± 0.11
	5	T.D.	6/8	97.7 ± 10.5	7.0 ± 1.4	-0.52 ± 0.08
	6.7	R.L.	6/12	110.8 ± 8.1	10.0 ± 2.6	-0.58 ± 0.09
	12	T.O.	6/10	104.7 ± 8.3	11.6 ± 2.6	-0.43 ± 0.06
	5	K.L.	6/12	114.8 ± 17.5	16.2 ± 7.8	-0.50 ± 0.07
	10	W.S.	6/13.5	117.5 ± 9.1	7.2 ± 1.7	-0.42 ± 0.07

Values were obtained by nonlinear regression of the form  $\log y = \log y_0 + r \log x$  for  $x < x_A$  and  $y = \log y_0 + r \log x_A$  for  $x \geq x_A$  where  $y$  is the threshold in arc s and  $x$  is the number of samples. The SAS statistical package was used. Fitting all the data with a second model, where  $x$  is the length of samples plus inter-spaces, gave a significantly worse  $\chi^2$  value: 226 as opposed to 172 ( $p < 0.025$ ,  $F$  test with 127 d.f.). Errors represent 1 standard error. All observers were carefully refracted and wore appropriate spectacle corrections if necessary. Extensive practice was given before the actual data collection. D.L. is an author. Snellen acuity (75% correct) was derived from crowded Davidson-Eskridge charts (6/6 corresponds to a 60-arc s feature). \* Not consistent with a slope of -0.5 at the 0.000001 level, whereas all the other data are consistent with a slope of -0.5 at the 0.05 confidence level. † Each of these observers has a constant unilateral strabismus of early onset and reduced acuity in an otherwise healthy eye.

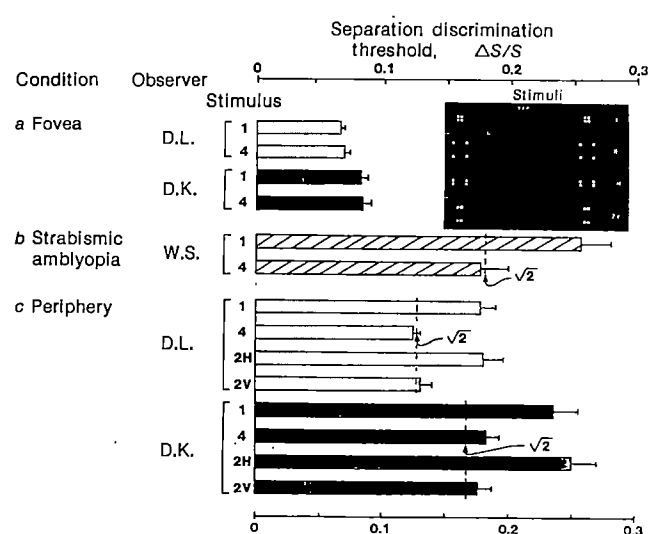
samples has no additional effect on thresholds. The effect of adding samples is not simply explained by luminance summation, as making a single sample seven times brighter in a control experiment did not improve the bisection threshold.

The spatial vision of strabismic amblyopes has previously been compared to that of the normal periphery<sup>5-7</sup>. The data shown in Fig. 1c for the amblyopic eyes of six strabismic amblyopes bear a remarkable similarity to the results for the normal periphery (Fig. 1b). For each of the strabismic amblyopes, as in the normal periphery, position uncertainty is high with only one sample, and thresholds improve in proportion to the square root of the number of discrete samples. Table 1 also shows Snellen acuity for each observer. For the amblyopic eyes and the periphery, the threshold for one sample is approximately equal to Snellen acuity. In foveal vision, on the other hand, the threshold for one sample is about three times better than Snellen acuity (that is, a hyperacuity). Interestingly, the non-amblyopic eyes of strabismic amblyopes were similar to those of the normal observers. For example, J.V., a highly experienced observer who had the most severe amblyopia, showed a threshold with one sample of  $19.0 \pm 0.9$  arc s and a slope of  $-0.24 \pm 0.1$  with his preferred eye.

A second experiment was performed in order to verify our sampling hypothesis and to determine whether information is

sampled only along the length of the lines of the target (that is, orthogonal to the discrimination cue) as originally suggested by Hering<sup>2</sup>. Here, the observers' task was to judge whether the separation between two small boxes was larger or smaller than the standard (12.4 arc min) separation<sup>8</sup>. Each box was actually composed of four tiny dots, illustrated schematically in the inset in Fig. 2 (stimuli 1 and 4). In this experiment, we manipulated the distances between the four dots comprising each of the two boxes. When they were close together (10 arc s) and thus unresolved, they represented a single (bright) sample. When the dots were all separated so that they could be resolved (1.2 arc min for the normal fovea; 2.4 arc min for peripheral and amblyopic vision) they provided four discrete samples. By this device the total luminance of each box stimulus was balanced and was approximately 20 times the observers' detection threshold. Figure 2a shows the separation discrimination threshold for unresolved (one sample) and resolved dots (four samples). For the normal fovea (Fig. 2a) thresholds for the two conditions were identical. For a strabismic amblyopic eye (Fig. 2b) and for the normal periphery (Fig. 2c), thresholds improved noticeably for the resolved dots. We have confirmed these observations on other observers and at different separations. We anticipated that increasing the number of samples from one to four would result in a twofold decrease in threshold (equal to  $\sqrt{4}$ ). However,

Fig. 2 Inset, a schematic diagram of the stimuli for spatial interval discrimination. In an experimental run, the stimulus (two boxes) was presented briefly with one of five closely spaced separations, centred at 12.4 arc min, and the observer judged whether the spatial interval between the two boxes (SEP in inset) was larger or smaller than the implicit standard. Stimulus feedback was given after each trial. Each box actually comprised four tiny bright dots on a dark background. When the dots were closely spaced (10 arc s) and therefore unresolved, there was only one sample per box (stimulus 1). When the dots were separated by 1.2 arc min (fovea) or 2.4 arc min (periphery and strabismic amblyope) they were seen as four discrete samples (stimulus 4). Separating the dots either only horizontally (2H) or only vertically (2V) resulted in two discrete samples. Threshold, equivalent to  $d' = 0.675$ , is specified as a fraction of the base separation (12.4 arc min) for unresolved (stimulus 1) and resolved (4) dots for the fovea of two normal observers (a), a strabismic amblyope (b) and peripheral vision of two observers at 2.5° (c). Each threshold is the mean of four counterbalanced runs (125 trials per run). To test which samples were effective in lowering the threshold, the dots were separated either horizontally or vertically. The results show that two samples separated horizontally (2H) were not significantly better than a single sample, whereas two samples separated vertically (2V) were  $\sqrt{2}$  better than a single sample in lowering the separation discrimination threshold.



surprisingly, the thresholds were in fact reduced by only  $\sim\sqrt{2}$ , suggesting that only two of the samples were effective. To test this possibility, we separated the dots either horizontally only or vertically only (stimuli 2H and 2V in the inset), thus providing two samples either in the same direction as the discrimination cue (horizontal separation) or in the orthogonal direction (vertical separation). Horizontal separation gave thresholds identical to that obtained with a single sample whereas vertical separation gave thresholds which were  $\sqrt{2}$  better. Thus, the two samples in the direction orthogonal to the discrimination cue each contributed effectively to reducing the threshold. This result is consistent with Hering's hypothesis regarding the averaging of discrete samples and suggests that this process is performed by oriented mechanisms.

Our results show that spatial information is indeed sampled discretely along the length of targets as originally proposed by Hering. In normal foveal vision, this process has a relatively small impact on the accuracy of spatial discriminations, presumably because the fovea has little intrinsic positional uncertainty. Thus foveal thresholds are smaller than a cone diameter. However, in the normal periphery and in the central field of strabismic amblyopes, the addition of spatial samples in the direction orthogonal to the discrimination cue reduces thresholds in proportion to  $\sqrt{n}$ , as would be expected in an ideal detector with uncorrelated noise at an early stage of visual processing.

In peripheral vision, the high degree of spatial uncertainty with a few samples can be understood on the basis of the anatomy and physiology of the retina and cortex which results in a sparse neural sampling grain<sup>9</sup>. In strabismic amblyopia, we hypothesize that abnormal binocular interactions result in similar neural consequences—that is, a sparse spatial sampling grain as a result of there being insufficient cortical neurones to provide accurate position signals and/or a scrambling of the neural signals<sup>5</sup>. A sparse sampling grain and/or scrambling of neural signals would introduce positional noise which is uncorrelated between stimulus samples in peripheral and strabismic amblyopic vision.

We thank H. Bedell, B. Breitmeyer, R. Harwerth, R. Manny, E. Smith, S. Steinman, G. Westheimer and Y. Yap for helpful comments, and Alvenia Daniels for preparation of the manuscript. This research was supported by research grants R01EY01728 and R01EY04776 from the National Eye Institute.

Received 23 December 1985; accepted 24 January 1986.

1. Westheimer, G. *Invest. Ophthalmol. vis. Sci.* **12**, 570–572 (1975).
2. Hering, E. *Ber. Math. phys. Classe Königl. Sachs. Ges. Wiss. Leipzig (Naturwiss. Teil)* **16**–24 (1899).
3. Ludvigh, E. *Am. J. Ophthalmol.* **36**, 139–142 (1953).
4. Levi, D. M., Klein, S. A. & Aitsebaomo, A. P. *Vision Res.* **25**, 963–977 (1985).
5. Levi, D. M. & Klein, S. A. *Vision Res.* **25**, 979–991 (1985).
6. Bradick, O. *Nature* **298**, 224–225 (1982).
7. Hess, R. & Bradley, A. *Nature* **287**, 463–464 (1980).
8. Westheimer, G. & McKee, S. P. *Vision Res.* **17**, 940–967 (1977).
9. Dow, B. M., Snyder, R. G., Vautin, R. G. & Bauer, R. *Expl. Brain Res.* **44**, 213–228 (1981).

## Generation of end-inhibition in the visual cortex via interlaminar connections

Jürgen Bolz & Charles D. Gilbert

Laboratory of Neurobiology, Rockefeller University, New York, New York 10021, USA

To understand the mechanisms by which the receptive field properties of visual cortical cells are generated, one must consider both the thalamic input to the cortex and the intrinsic cortical connections. In the cat striate cortex, layer 4 is the main recipient of input from the lateral geniculate nucleus, yet the cells in that layer possess several receptive field properties that are distinct from the geniculate input, including orientation specificity, binocularity, directionality and end-inhibition, the last of which allows cells to respond to edges of a restricted length<sup>1–4</sup>. These properties could be generated by connections within the layer, by its input from the claustrum<sup>5</sup> or by the massive projection that layer 4 receives from layer 6 (refs 6–9). In the present study, we attempted to determine the functional role of the layer 6 to layer 4 projection by reversible inactivation of layer 6 using the inhibitory transmitter  $\gamma$ -aminobutyric acid (GABA). After inactivating layer 6, cells in layer 4 lost end-inhibition. Cells in layer 2+3, which receive their principal input from layer 4, were similarly affected. The elimination of end-inhibition was specific, other receptive field properties, such as direction selectivity or orientation specificity, remaining intact.

Recordings were made in cats maintained on sodium thiopental anaesthesia, paralysed with succinylcholine and artificially respiration with 100% oxygen. At the start of an experiment virtually all of the cells in layers 2, 3 and 4 were end-inhibited to some degree. The oxygen helped maintain the proportion of end-inhibited cells, which otherwise tended to decline during the experiment. The animals' electrocardiogram, electroencephalogram, temperature and expired CO<sub>2</sub> concentration were continuously monitored. A small hole was drilled in the skull above the visual cortex, and the dura and pia opened. To

study the role of the layer 6 to 4 pathway, we inactivated layer 6 by injecting GABA and examined the effect of this treatment on the receptive field properties in layers 2 to 4. A similar approach has been used in other systems with inhibitory transmitters or analogues, local anaesthetics or cobalt<sup>10–12</sup>. The advantage of GABA is that it affects cells and not afferents and the effects are reversible. In initial experiments to determine the area inactivated by GABA injections of various amounts and concentrations, the micropipette was placed about 300  $\mu$ m below the layer 5/6 border and a second tungsten electrode, laterally displaced at various distances from the first electrode, was advanced to approximately the same laminar position as the micropipette. The entrance into layer 6 was recognized by the appearance of cells possessing long receptive fields in this layer<sup>3</sup>. After the penetrations, electrolytic lesions were made to verify the placement of the electrodes histologically and to determine the horizontal displacement between the two electrodes. We found that a 0.1- $\mu$ l injection of 10 mM GABA inactivated an area of  $\sim 700 \mu\text{m}$  in diameter. The inactivation lasted for several minutes and was always reversible.

Having established the conditions for blockade of the activity of layer 6 cells, we recorded from cells in layers 2+3 and 4 while the GABA pipette was in a corresponding topographical position in layer 6. Figure 1 shows response histograms of a simple cell in layer 4. When tested with a stationary flashing bar, the cell's receptive field consisted of a separate 'on' region flanked by two antagonistic 'off' regions. The cell was end-inhibited: its response to a long bar ( $8^\circ$ ) was reduced by 54% compared with its response to a bar of optimal length ( $1^\circ$ ). An injection of 0.1  $\mu$ l of 10 mM GABA in layer 6 had no effect on the cell's response to the short bar, but greatly increased its response to the long bar, so that end-inhibition was completely eliminated. This blockade was reversible, for 3 min after GABA injection the cell's response was again reduced over 50% by end-inhibition.

Cells in the superficial layers showed similar effects to those seen in layer 4. Figure 2 shows response histograms of a layer 2+3 cell with a complex receptive field,  $0.5^\circ \times 1.5^\circ$  in size, and on-off responses to a stationary flashing bar. The cell responded briskly when a bar of optimal length ( $0.5^\circ$ ) was moved across its receptive field, but the response was reduced by 58% when

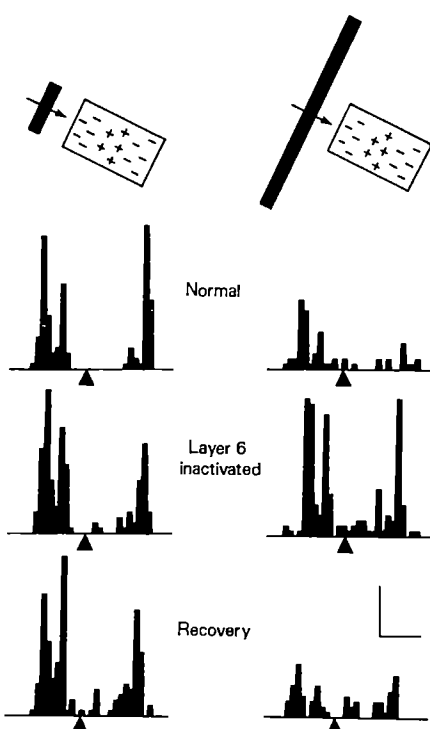


**Fig. 1** Effect of inactivation of layer 6 on a simple cell in layer 4. The cell's receptive field was  $1^\circ \times 1.5^\circ$  and had antagonistic on (+) and off (-) subfields when tested with a stationary flashing bar. Layer 6 was inactivated by pressure injection of  $0.1 \mu\text{l}$  GABA (10 mM in 0.9% saline) using a glass micropipette with an insulated tungsten electrode glued to the side. Recordings were made either through the tungsten electrode or the micropipette, and were used to determine the duration of blockade. The injection pipette was positioned in layer 6 by advancing it until cells with receptive field properties characteristic of the layer were found<sup>3</sup> and then advanced an additional 300  $\mu\text{m}$ . A second tungsten electrode was placed in layer 4, directly over the pipette in layer 6. The positions of the injection pipette and tungsten electrode were later confirmed histologically. Response histograms from 10 stimulus presentations each were made before (top), immediately after (middle) and 3 min after (bottom) GABA injection in layer 6. The triangles under each histogram indicate the point at which the bar reversed direction. The cell was end-inhibited, such that its response to a long bar ( $8^\circ$ ) was 54% less than its response to a bar of optimum length ( $1^\circ$ ). This inhibition was eliminated by inactivation of layer 6 (right column), whereas the cell's response to a short bar was unchanged. Calibration: vertical mark, 10 spikes per bin; horizontal mark, 1 s.

the stimulating bar was lengthened to  $8^\circ$ . The cell showed directional preference, responding 2.3 times more to movement in the optimal direction than to movement in the opposite direction. When layer 6 was inactivated by injecting  $0.2 \mu\text{l}$  of 10 mM GABA, the cell's response to the short bar was unchanged, but its response to the long bar was strongly increased, so that end-inhibition was eliminated. There was no effect on direction selectivity. Thus, end-inhibition was selectively eliminated, decreasing from 58% before GABA injection to 3% during layer 6 inactivation. Seven minutes after GABA injection the cell had almost completely recovered (to 45% end-inhibition).

For most cells, the reduction of end-inhibition after a GABA injection was readily recognized within the first few responses to a long bar swept across the receptive field. The maximal effect lasted 1–5 min and the cell's response then gradually recovered, being complete within 3–40 min. The effects were reversible after several injections. In one case, 11 injections were made without causing permanent changes in the receptive field properties of the recorded cell and without causing damage visible in Nissl-stained sections.

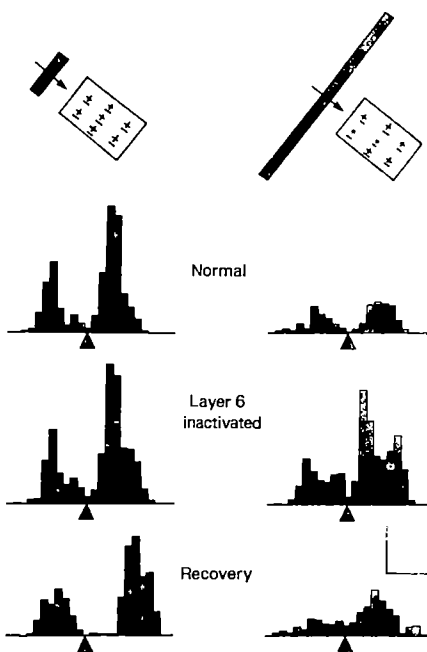


**Fig. 2** Effect of  $0.2 \mu\text{l}$  GABA (10 mM) injection in layer 6 on a complex cell in layer 2+3. Same procedure as in Fig. 1. The cell's receptive field was  $0.5^\circ \times 1.5^\circ$  and gave mixed on (+) and off (-) responses when tested with a stationary flashing bar. When the stimulating bar was  $8^\circ$  long (top right), the cell's response was reduced by 58% of its response to a bar of optimal length ( $0.5^\circ$ , top left). During layer 6 inactivation, the cell was only  $3^\circ$  end-inhibited (middle right). Seven minutes after GABA injection the cell was again 45% end-inhibited (bottom right). Inactivation of layer 6 had no effect on the response to the bar with an optimal length of  $0.5^\circ$  (histograms in left column). Note that inactivation of layer 6 had no effect on the cell's direction selectivity. Each histogram was obtained from 10 stimulus presentations. Calibration: vertical mark, 50 spikes per bin; horizontal mark, 1 s.

To determine the spatial distribution of the effect, we compared length response curves before and during inactivation by producing and reversing the effect many times and obtaining histograms before and during inactivation for each of a number of bar lengths. An example is shown in Fig. 3. The cell showed summation until the stimulating bar was increased up to the full length of the excitatory part of the cell's receptive field, further lengthening of the bar inhibited the cell's response until the response was completely suppressed by a bar  $4^\circ$  in length. Inactivation of layer 6 uncovered a vigorous response to long bars, but had no effect on the response to bars equal in length or shorter than the excitatory portion of the receptive field.

We also investigated the effect of layer 6 inactivation on orientation tuning and directionality. The full range of orientations over which we could elicit a response was determined using a hand-held projector, and we determined this range before and during layer 6 inactivation. While layer 6 was inactivated, the orientation tuning to a long bar was sharper than to a short bar, as it was before the blockade. A few cells showed slight increases in width of orientation tuning, although even when end-inhibition was completely eliminated they were still clearly orientation-selective. For the entire population studied directionality was unaffected during layer 6 inactivation (Fig. 2).

The effect of layer 6 inactivation was examined on a sample of 49 end-inhibited cells from 12 cats. We selected only those cells with moderate to strong end-inhibition, and limited the size of the injection to that required for a clear reduction of end-inhibition, but never applied more than  $0.3 \mu\text{l}$  in a single injection. The reduction of end-inhibition and the time course of the effect depended on the alignment of the two electrodes and the size of the GABA injection. For example, end-inhibition

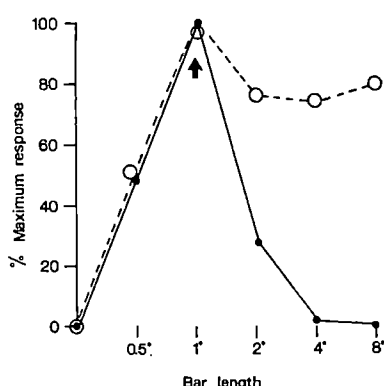


**Fig. 3** Length-response curve for a complex cell in layer 2+3 before (continuous line) and after (dashed line) GABA injection in layer 6. The cell showed summation until the stimulating bar extended for the full length of the excitatory portion of the receptive field, as determined by testing its response to a short bar centred at different positions along its axis of orientation (arrow). Further lengthening of the bar reduced the response of the cell until it was completely inhibited by bars of 4° length or longer. Inactivation of layer 6 revealed a vigorous response to long bars, but had no effects on the response to bars equal in length or shorter than the excitatory portion of the receptive field.

of the cell in Fig. 2 was reduced from 58% to 40% by 0.1  $\mu$ l GABA and abolished by 0.2  $\mu$ l. However, the amount of GABA necessary to reduce end-inhibition was independent of the laminar position of the cell, with complex cells in layer 2+3 requiring the same average dosage as simple cells in layer 4. Out of our sample of 49 cells, end-inhibition was significantly decreased for all but 3 of the cells. For the cells where no effect was seen, later histological reconstruction of the positions of the recording and injection electrodes showed that their horizontal displacement was greater than 500  $\mu$ m. Figure 4 shows the extent of the change in end-inhibition for our sample population of cells in layers 2+3 and 4.

Our experiments suggest that layer 6 is the source of end-inhibition for cells in layers 4 and 2+3. Many layer 6 pyramidal cells have axon collaterals that project to and ramify within layer 4 (refs 6–8). As mentioned above, these cells have long receptive fields, often requiring relatively long bars for activation and showing increased response as the stimulating bar is lengthened up to 8° or more. Cells in layer 4 and above have small receptive fields, and show progressive inhibition as the stimulating bar is lengthened, up to sizes equivalent to the excitatory portion of layer 6 cell receptive fields. A model for generating end-inhibition from cells with long receptive fields was originally suggested by Hubel and Wiesel<sup>13</sup>. The projection pattern and receptive field properties of layer 6 cells led to the hypothesis that these could be the cells responsible for end-inhibition, either by direct inhibitory action or by making contact with inhibitory interneurones within layer 4 (refs 6, 14).

Layer 6 cells are likely to be excitatory, because they take up and transport aspartate, a putative excitatory transmitter<sup>15</sup>, and form asymmetrical synapses with round vesicles, a morphology usually associated with excitatory synapses<sup>16</sup>. However, using serial electron microscope reconstructions, McGuire *et al.*<sup>16</sup> demonstrated that many of the processes that are postsynaptic to layer 6 collaterals belong to either smooth or sparsely spinous cells, which are thought to be inhibitory, as they form symmetrical synapses<sup>17,18</sup> and are GABAergic<sup>19,20</sup>. A role for GABAergic interneurones in end-inhibition is supported by iontophoresis of the GABA antagonist bicuculline while recording from end-inhibited cells in layer 2+3, though usually the

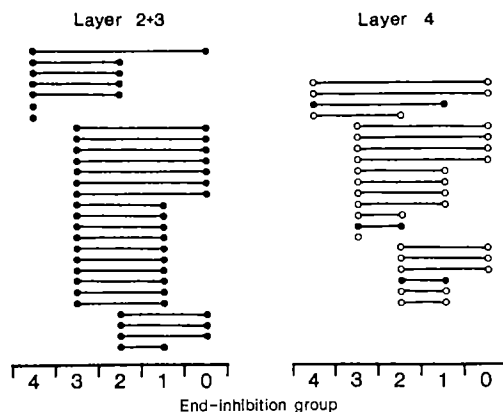


**Fig. 4** End-inhibition of cells in layers 2+3 (left) and 4 (right) before and after GABA injection in layer 6. Degree of end-inhibition was divided into five categories. Cells in group 0 had no end-inhibition (0–10%); in group 1, end-inhibition was weak (11–35%); in group 2, it was medium (36–60%); in group 3, it was strong (61–90%); and in group 4, end-inhibition was very strong (91–100%). For all but three cells, inactivation of layer 6 significantly reduced end-inhibition. Closed circles, complex cells; open circles, simple cells.

effects were weak<sup>21</sup>. The fact that the response to short bars was unaffected by layer 6 inactivation is consistent with our model, in that layer 6 cells are frequently not activated by short bars and therefore are unlikely to influence the response of layer 4 cells to short bars. Finally, this hypothesis predicts that some inhibitory interneurones in layer 4 will have long receptive fields. These neurones may have been missed because interneurones are smaller and less common than principal neurones, and it is difficult to determine the receptive field length without appropriate quantitative methods. However, using intracellular recording and dye injection, A. Humphrey (personal communication) recently found a smooth stellate cell in layer 4 possessing a long receptive field similar to those of layer 6 neurones.

Our findings are comparable to those of Sherk and LeVay<sup>22</sup>, who studied the role of the projection from claustrum to cortex. The claustrum projects to all layers of visual cortex, but most heavily to layer 4 (ref. 5). Cells in the claustrum have similar receptive fields to those in layer 6 (ref. 5), and when the claustrum is lesioned, cortical cells lose some of their end-inhibition<sup>22</sup>. The effects of inactivating layer 6 seen in the present study were stronger than those caused by lesioning the claustrum. Since layer 6 is the source of input to the claustrum and since this pathway is retinotopically organized<sup>23</sup>, inactivating layer 6 could effectively block the claustral input to layer 4 as well as the direct layer 6 to 4 projection, thus removing both sources of end-inhibition with a single injection.

Inactivating layer 6 abolished end-inhibition in layer 2+3 as readily as in layer 4, although layer 6 projects predominantly to layer 4. However, spiny stellate cells in layer 4 have a strong, presumably excitatory projection to layer 2+3 (refs 6, 9). Our results therefore suggest that cells in layer 4 endow layer 2+3 neurones with end-inhibition, an idea which is further supported by the finding that layers 2+3 and 4 have the same proportions of end-inhibited cells<sup>3</sup> showing a comparable degree of end inhibition<sup>3</sup>. This may explain why bicuculline iontophoresis could not eliminate end-inhibition in the superficial layers, since cells to which the bicuculline was applied may not have generated end-inhibition themselves, but instead may have inherited it from cells distant from the iontophoretic pipette. Our findings provide indirect evidence for an excitatory link between layers 4 and 2+3, and suggest that at least one property is transferred

through that pathway. This conflicts with the finding that layer 2+3 cells appear normal when layer 4 is silenced by inactivation of the A laminae of the geniculate, requiring all receptive field properties to be generated anew in each cortical layer<sup>11</sup>. Instead, our results are consistent with the hypothesis of Hubel and Wiesel<sup>1</sup> of a sequence of processing from simple cells to complex cells, representing a functional interaction between cortical layers.

In conclusion, we have shown an association between one

component of the intrinsic cortical circuit and a specific receptive field property. Our results demonstrate how a functionally defined class of cortical cells participates in the transformation of geniculate input occurring within the striate cortex.

We thank Torsten Wiesel for his continuous encouragement and support, Larry Katz for his helpful discussions, and Barbara McGuire and Dan Tso for comments. This work was supported by the Max-Planck-Gesellschaft, NIH grant EY04782 and NSF grants BNS8351738 and BNS8318794.

Received 27 September; accepted 12 December 1985.

1. Hubel, D. H. & Wiesel, T. N. *J. Physiol., Lond.* **160**, 106–154 (1962).
2. Dreher, B. *Invest. Ophthalmol.* **11**, 355–356 (1972).
3. Gilbert, C. D. *J. Physiol., Lond.* **268**, 391–421 (1977).
4. Rose, D. J. *Physiol., Lond.* **271**, 1–23 (1977).
5. LeVay, S. & Sherk, H. *J. Neurosci.* **1**, 956–980 (1981).
6. Gilbert, C. D. & Wiesel, T. N. *Nature* **280**, 120–125 (1979).
7. Lund, J. S., Henry, G. H., MacQueen, C. L. & Harvey, A. R. *J. comp. Neurol.* **184**, 599–618 (1979).
8. Katz, L. C., Burkhalter, A. & Dreyer, W. J. *Nature* **310**, 498–500 (1984).
9. Martin, K. A. C. & Whitteridge, D. J. *Physiol., Lond.* **253**, 463–504 (1985).
10. Malpeli, J. G., Schiller, P. H. & Colby, C. L. *J. Neurophysiol.* **46**, 1102–1119 (1981).

11. Malpeli, J. G. *J. Neurophysiol.* **49**, 595–610 (1983).
12. Newsome, W. T., Wurtz, R. H., Dürsteler & Mikami, A. *Expl Brain Res.* **58**, 392–399 (1985).
13. Hubel, D. H. & Wiesel, T. N. *J. Neurophysiol.* **28**, 229–289 (1965).
14. Wiesel, T. N. & Gilbert, C. D. Q. *Jl exp. Physiol.* **68**, 525–543 (1983).
15. Baughman, R. W. & Gilbert, C. D. *J. Neurosci.* **1**, 427–439 (1981).
16. McGuire, B. A., Hornung, J.-P., Gilbert, C. D. & Wiesel, T. N. *J. Neurosci.* **4**, 3021–3033 (1984).
17. LeVay, S. *J. comp. Neurol.* **150**, 53–86 (1973).
18. Peters, A. & Fairen, A. *J. comp. Neurol.* **181**, 129–172 (1978).
19. Ribak, C. E. *J. Neurocytol.* **7**, 461–478 (1978).
20. Hamos, J. E., Davis, P. L. & Sterling, P. *J. comp. Neural.* **217**, 449–457 (1983).
21. Sililato, A. M. & Versiani, V. *J. Physiol., Lond.* **273**, 775–790 (1977).
22. Sherk, H. & LeVay, S. *J. Neurosci.* **3**, 2121–2127 (1983).
23. LeVay, S. & Sherk, H. *J. Neurosci.* **1**, 993–1002 (1981).

## Retrovirus insertion inactivates mouse $\alpha 1(I)$ collagen gene by blocking initiation of transcription

Stefan Hartung\*, Rudolf Jaenisch\*\*† & Michael Breindl\*

\* Heinrich-Pette-Institut für experimentelle Virologie und Immunologie an der Universität Hamburg, Martinistraße 52, 2000 Hamburg 20, FRG

† Whitehead Institute for Biomedical Research and Department of Biology, Massachusetts Institute of Technology, 9 Cambridge Center, Cambridge, Massachusetts 02142, USA

Mov13 mice carry a single Moloney murine leukaemia virus (MuLV) proviral copy in the first intron of the  $\alpha 1(I)$  collagen gene. Virus insertion interferes with the synthesis of stable  $\alpha 1(I)$  collagen messenger RNA and causes a recessive lethal mutation<sup>1,2</sup>. The virus insertion has induced changes of the methylation pattern<sup>3</sup> as well as the chromatin conformation in the mutated gene. Specifically, a DNase-hypersensitive site which is associated with active transcription of the wild-type collagen gene is not present in the mutant allele<sup>4</sup>. The block of collagen expression could be caused by virus-induced instability of collagen mRNA or by impaired initiation of transcription. To distinguish between these possibilities, we have compared the activity of the  $\alpha 1(I)$  collagen gene promoter in cell lines derived from wild-type and Mov13 embryos by nuclear run-on transcription experiments and S<sub>1</sub> mapping of nuclear RNA. We show here that initiation of transcription of the mutant gene is reduced 20–100-fold. This indicates that the virus-induced change of chromatin structure in the promoter region of the mutant gene prevents RNA polymerase from binding to its DNA template. Our results are consistent with the notion that the promoter-associated DNase-hypersensitive site is a prerequisite for rather than a consequence of gene activity.

To determine the transcriptional initiation at the wild-type and Mov13  $\alpha 1(I)$  collagen gene promoter, we performed nuclear run-on transcription experiments with nuclei from cell lines derived from wild-type or homozygous Mov13 embryos. Undifferentiated P19 embryonal carcinoma (EC) cells, which do not transcribe  $\alpha 1(I)$  collagen mRNA<sup>4</sup>, were used as a control. Nuclei were isolated and RNA was synthesized *in vitro* in the presence of <sup>32</sup>P-UTP and hybridized to a Southern blot of restriction fragments which were derived from a 14-kilobase (kb) clone containing the 5' end of the  $\alpha 1(I)$  collagen gene<sup>1</sup>.

Restriction fragments of a rat  $\alpha$ -tubulin complementary DNA clone<sup>5</sup> served as internal standard. The result of a typical experiment is shown in Fig. 1a. *In vitro* synthesized RNA from all cell lines hybridized with comparable intensity to the  $\alpha$ -tubulin DNA fragment. In contrast, only RNA from wild-type, but not from Mov13 or P19, cells hybridized to the  $\alpha 1(I)$  collagen restriction fragments. (Fragments 1B and 2B, which did hybridize, contain repetitive sequences located 5' of the  $\alpha 1(I)$  collagen gene, see map, Fig. 1c). The intensity of hybridization of the individual fragments was roughly proportional to their size, indicating that sequences derived from different sections of the gene were transcribed *in vitro* with identical frequency. Moreover, hybridization of the 1.1-kb *Bst*EII/*Xba*I fragment 1D, which contains only intron sequences (Fig. 1c), shows that the *in vitro* elongated RNAs used as hybridization probes were primary transcripts and not processed RNA.

The 0.5-kb *Bst*EII/*Bgl*II fragment 2C contains almost exclusively sequences derived from the first exon of the  $\alpha 1(I)$  collagen gene which in Mov13 DNA is located 5' of the viral integration site. The intensity of hybridization of this fragment is therefore a measure of initiation of  $\alpha 1(I)$  collagen mRNA transcription in wild-type as well as in Mov13 cells. Figure 1a shows that fragment 2C hybridized only to RNA from wild-type but not from Mov13 cells. Similarly, no signal was seen with RNA from P19 cells. Even after extended exposure of the autoradiogram (Fig. 1b) the 0.5-kb fragment 2C did not give a visible signal with RNA from Mov13 cells. This shows that in Mov13 cells the absence of  $\alpha 1(I)$  collagen mRNA is due, at least in part, to a reduction of the number of RNA polymerase molecules initiating RNA transcription at the  $\alpha 1(I)$  collagen promoter rather than a premature termination or aberrant splicing of transcripts. Densitometer scans of autoradiograms from several independent experiments (not shown) allowed us to estimate that initiation of  $\alpha 1(I)$  collagen gene transcription in Mov13 cells is at least 20-fold lower than in wild-type cells. However, because of the small size of fragment 2C and the corresponding weak signal produced on the autoradiogram, this is a minimal estimate indicating the limits of detection by this assay rather than the actual extent of transcriptional inhibition.

*In vitro* elongated RNA from Mov13 cells did hybridize to the 4.9-kb fragment 1F (Fig. 1b; a faint hybridization of fragment 1F with P19 RNA was also visible on the original autoradiogram but is not shown). To determine whether Mov13 and P19 cells show residual  $\alpha 1(I)$  collagen promoter activity which was undetectable by the nuclear run-on transcription assay but could account for the hybridization of Mov13 transcripts to fragment

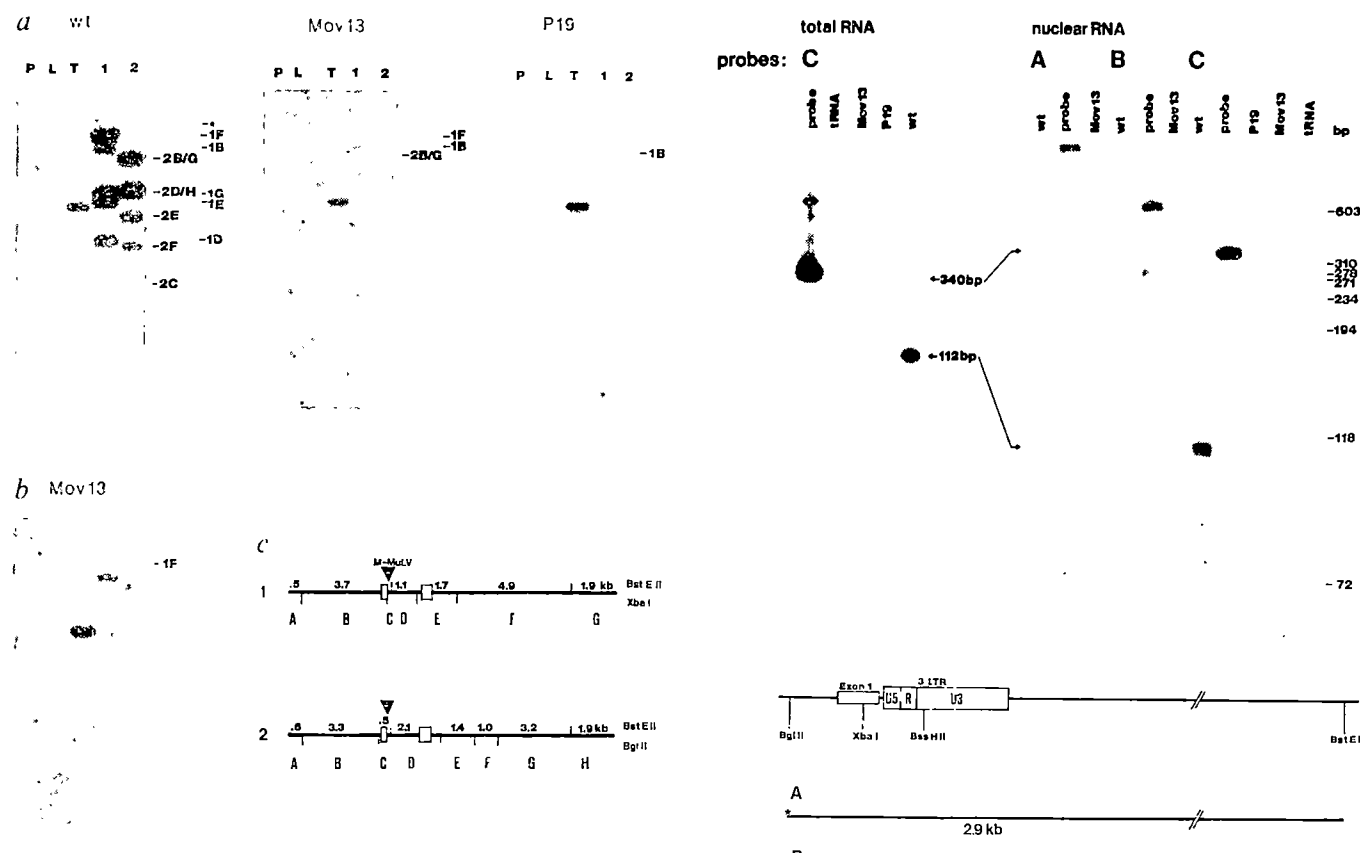


**Fig. 1** Hybridization of *in vitro* elongated RNA to restriction fragments of the mouse  $\alpha 1(I)$  collagen gene. Nuclei were prepared from cell lines derived from wild-type (wt) or homozygous Mov13 embryos<sup>1</sup> and from the EC cell line P19. Nuclear RNA was elongated in the presence of  $^{32}\text{P}$ -UTP, purified and hybridized to nitrocellulose filters containing restriction fragments of a genomic clone of the mouse  $\alpha 1(I)$  collagen gene (lanes 1, 2 and ref. 2), a rat  $\alpha$ -tubulin cDNA clone (lane T and ref. 5), and pBR322 (P) or  $\lambda(L)$  control DNA. The filters were exposed for 1 day (*a*) or 8 days (*b*). A partial restriction map of the mouse  $\alpha 1(I)$  collagen gene<sup>2</sup> is shown in *c*. The first two exons of the gene are shown as open boxes, the M-MuLV integration site in Mov13 DNA as an arrowhead. The restriction sites of the enzymes *Bst*EII, *Xba*I and *Bgl*II are shown which were used to produce the DNA blots shown in *a*. The uppermost band marked with an asterisk in lane 1 is due to a partial digest.

**Methods.** Isolation of nuclei, run-on transcription, purification of labelled RNA, and hybridization were performed according to published procedures<sup>14–16</sup>, with minor modifications. After exposure to X-ray film, the filters were rehybridized with a nick-translated mouse  $\alpha 1(I)$  collagen DNA probe to confirm that all the blots used contained identical amounts of DNA (not shown).

1F, we performed nuclease S<sub>1</sub> mapping experiments with nuclear RNA from wild-type, Mov13 and P19 cells. These RNA preparations showed a ~100-fold enrichment of nuclear RNA sequences, as estimated from the yield of RNA recovered in this fraction relative to total cellular RNA and from an electrophoretic analysis of 45S ribosomal RNA precursor molecules in the nuclear RNA preparations (not shown). Because of the presence of considerable amounts of this latter RNA species, we also expected an enrichment of primary mRNA transcripts in the nuclear RNA fraction and therefore an increased sensitivity of the nuclease S<sub>1</sub> mapping assay.

The probes used in these assays and the results are shown in Fig. 2. Besides a 0.34-kb *Bgl*II/*Xba*I fragment (probe C) which has previously been used for S<sub>1</sub> nuclease mapping of  $\alpha 1(I)$  collagen mRNA<sup>2,4</sup>, we have also used a 0.63-kb *Bgl*II/*Bss*HII fragment (probe B) prepared from a genomic clone of Mov13

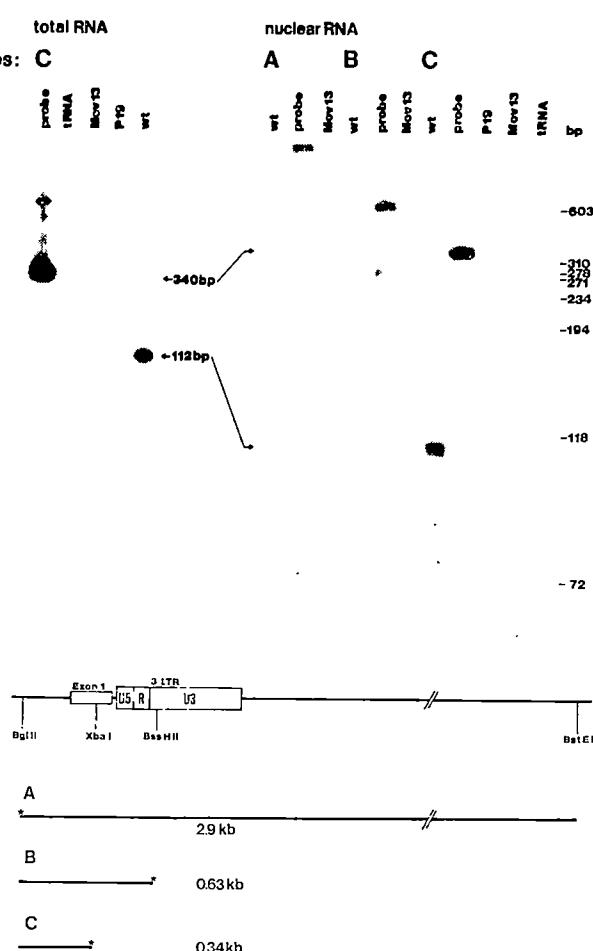


**Fig. 2** Nuclease S<sub>1</sub>-mapping analysis of total and nuclear RNA from wild-type (wt), homozygous Mov13 and P19 cells. The RNAs analysed with probes A, B or C, respectively (compare the map and the text), are indicated at the top of the autoradiograms. **Methods.** Cells were homogenized in hypotonic buffer<sup>4</sup> in the presence of 0.03–0.05% Triton X-100 and nuclei isolated by centrifugation and extracted with phenol-chloroform. RNA was separated from DNA by CsCl gradient centrifugation. Samples of 15  $\mu\text{g}$  of nuclear or 25  $\mu\text{g}$  of total RNA were hybridized to 10–20 ng of each probe, digested with S<sub>1</sub> nuclease and analysed by polyacrylamide gel electrophoresis<sup>2</sup>.

DNA<sup>6</sup>. This fragment, which contains the first exon of the  $\alpha 1(I)$  collagen gene and sequences derived from the 3' long terminal repeat (LTR) of the M-MuLV provirus integrated in Mov13 DNA was used to detect any transcripts initiating at the collagen promoter and continuing into viral sequences. The 2.9-kb *Bgl*II/*Bst*EII fragment (probe A) was labelled at the opposite strand and was included to detect possible transcripts initiating at the viral promoter in the 3' LTR and extending into cellular sequences (that is, anti-sense RNA complementary to the first exon and 5'-flanking sequences of the  $\alpha 1(I)$  collagen gene). Probe C detected the expected 112-base-pair (bp) protected fragment in both total and nuclear RNA from wild-type but not from Mov13 or P19 cells (Fig. 2). Accordingly, probe B did not detect any transcripts in Mov13 nuclear RNA which would have resulted in a protected fragment of 400 bp. This shows that there is no residual  $\alpha 1(I)$  collagen promoter activity in Mov13 cells

which might have escaped detection by the run-on transcription assay. The sensitivity of the S<sub>1</sub> mapping assays was estimated by counting the radioactivity in the corresponding gel slices (not shown). In nuclear RNA from Mov13 and P19 cells we would have been able to detect a 100-fold lower concentration of  $\alpha 1(I)$  collagen transcripts as compared with wild-type cells. Assuming that the nuclear RNA used contained predominantly primary transcripts, we can conclude that initiation of transcription at the  $\alpha 1(I)$  collagen promoter in Mov13 cells is reduced by at least 100-fold relative to wild-type cells and is comparable to P19 cells which normally do not transcribe  $\alpha 1(I)$  collagen mRNA. The hybridization of restriction fragment 1F with *in vitro* elongated RNA from Mov13 cells (Fig. 1b) can therefore not be due to transcripts initiated at the  $\alpha 1(I)$  collagen promoter. It may be the result of activation of cryptic promoter sequences within the  $\alpha 1(I)$  collagen gene due to the provirus insertion, or cross-hybridization of this section of the gene with type III collagen mRNA or with other unknown repetitive sequences. The presence of a member of the mouse *B1* family of middle repetitive sequences in the  $\alpha 1(I)$  collagen gene has in fact recently been shown<sup>7</sup>.

Probe A did not detect any transcripts initiating in the proviral 3' LTR and extending into cellular sequences (Fig. 2). This was not unexpected because indirect evidence indicates that this proviral copy in Mov13 cells is transcriptionally inactive<sup>4</sup>, and because intact retroviral proviruses usually do not use their 3' LTR for initiation of transcription<sup>8</sup>.

Our results show that the provirus-induced change of chromatin structure of the  $\alpha 1(I)$  collagen gene in Mov13 cells inhibits initiation of transcription, probably by preventing RNA polymerase and/or other transcription factors from binding to the DNA template. The most striking difference in chromatin structure of the wild-type and mutant gene is the absence of the transcription-associated DNase-hypersensitive site in the latter<sup>4</sup>. DNase-hypersensitive sites within eukaryotic genes are thought to be regions where transcription factors bind to regulatory DNA sequences<sup>9-12</sup>. They may have an important role in developmental gene activation<sup>13</sup>. Because the virus insertion in Mov13 cells has not changed the DNA sequence containing the presumptive binding site but exerts its effect over a distance of ~500 bp, the binding of such factors must be controlled by structural features of the chromatin rather than DNA sequence alone. Our results therefore suggest that the promoter-associated hypersensitive site is a prerequisite for rather than a consequence of gene activity. The virus seems to cause the mutation by long-range and indirect effects which may prevent correct activation of the  $\alpha 1(I)$  collagen gene by interfering with the developmentally regulated induction of the hypersensitive site.

We thank K. Harbers for the gift of plasmids and C. Dony and U. Chen-Betdeken for advice with the run-on transcriptions. This work was supported by the Deutsche Forschungsgemeinschaft and by grants HD-19015 from NIH and P01-CA38497 from the NCI. The Heinrich-Pette-Institut is supported by Freie und Hansestadt Hamburg and by Bundesministerium für Jugend, Familie und Gesundheit.

Received 9 December 1985; accepted 19 January 1986.

1. Schnieke, A., Harbers, K. & Jaenisch, R. *Nature* **304**, 315-320 (1983).
2. Harbers, K., Kuehn, M., Delius, H. & Jaenisch, R. *Proc. natn. Acad. Sci. U.S.A.* **81**, 1504-1508 (1984).
3. Jähner, D. & Jaenisch, R. *Nature* **315**, 594-597 (1985).
4. Breindl, M., Harbers, K. & Jaenisch, R. *Cell* **38**, 9-16 (1984).
5. Lemischka, T. R., Farmer, S., Racaniello, V. R. & Sharp, P. A. *J. molec. Biol.* **151**, 101-120 (1981).
6. Jaenisch, R. *et al.* *Cell* **32**, 209-216 (1983).
7. Monson, J. B., Friedman, J. & McCarthy, B. *Molec. cell. Biol.* **2**, 1362-1371 (1982).
8. Cullen, B. R., Lomedico, P. T. & Ju, G. *Nature* **307**, 241-245 (1984).
9. Elgin, S. C. R. *Cell* **27**, 413-415 (1981).
10. Wu, C. *Nature* **309**, 229-234 (1984).
11. Emerson, B. M., Lewis, C. & Felsenfeld, G. *Cell* **41**, 21-30 (1985).
12. Dynan, W. S. & Tjian, R. *Nature* **316**, 774-778 (1985).
13. Weintraub, H. *Cell* **42**, 705-711 (1985).
14. Groudine, M., Peretz, M. & Weintraub, H. *Molec. cell. Biol.* **1**, 281-288 (1981).
15. Lacy, E., Hardison, R. C., Quon, D. & Maniatis, T. *Cell* **18**, 1273-1283 (1979).
16. Dony, C., Kessel, M. & Gruss, P. *Nature* **317**, 636-639 (1985).

## The trans-activator gene of HTLV-III is essential for virus replication

Amanda G. Fisher\*, Mark B. Feinberg\*, Steven F. Josephs\*, Mary E. Harper\*, Lisa M. Marselle\*, Gregory Reyes†, Matthew A. Gonda‡, Anna Aldovini\*, Christine Debouk§, Robert C. Gallo\* & Flossie Wong-Staal\*

\* Laboratory of Tumor Cell Biology, Developmental Therapeutics Program, National Cancer Institute, Bethesda, Maryland 20205, USA

† Gene Labs Incorporated, 871 Industrial road, San Carlos, California 94070, USA

‡ Laboratory of Cell and Molecular Structure, National Cancer Institute, Frederick Cancer Research Facility, Frederick, Maryland 21701, USA

§ Department of Molecular Genetics, Smith Kline & French Laboratories, 709 Swedeland Rd, Swedeland, Pennsylvania 19479, USA

Studies of the genomic structure of human T-lymphotropic virus type III (HTLV-III) and related viruses, implicated as the causal agent of acquired immune deficiency syndrome (AIDS), have identified a sixth open reading frame in addition to the five previously known within the genome (*gag*, *pol*, *sor*, *env* and 3' *orf*)<sup>1-4</sup>. This gene, called *tat*-III, lies between the *sor* and *env* genes and is able to mediate activation, in a *trans* configuration, of the genes linked to HTLV-III long terminal repeat (LTR) sequences<sup>5-8</sup>. We now present evidence that the product of *tat*-III is an absolute requirement for virus expression. We show that derivatives of a biologically competent molecular clone of HTLV-III<sup>9</sup>, in which the *tat*-III gene is deleted or the normal splicing abrogated, failed to produce or expressed unusually low levels of virus, respectively, when transfected into T-cell cultures. The capacity of these *tat*-III-defective genomes was transiently restored by co-transfection of a plasmid clone containing a functional *tat*-III gene or by introducing the TAT-III protein itself. As HTLV-III and related viruses are the presumed causal agents of AIDS and associated conditions<sup>10-12</sup>, the observation that *tat*-III is critical for HTLV-III replication has important clinical implications, and suggests that specific inhibition of the activity of *tat*-III could be a novel and effective therapeutic approach to the treatment of AIDS.

Transcriptional activation of viral genes by viral regulatory elements acting in *cis* and *trans* configurations was first described for DNA tumour viruses<sup>13-18</sup>, and *trans*-activator genes have since been found in retroviruses of man<sup>19-21</sup>, cattle<sup>22,23</sup> and sheep<sup>24</sup>. Knowledge that *trans*-acting factors can specifically augment the expression of viral genes has led to intense speculation that *trans*-activator genes may have crucial roles in the biology of these viruses.

The *tat*-III gene, as characterized by functional mapping studies, consists of three exons<sup>6,7</sup>. The first exon is non-coding and extends 287 base pairs from the 5' LTR. The second exon, located between the *sor* (for short open reading frame) and *env* (envelope) genes, encodes 72 amino acids and is crucial for *trans*-activation. The third exon encodes only 14 amino acids and is located within the *env* gene in a different reading frame. To investigate whether *trans*-activation is an essential feature of HTLV-III replication, a panel of HTLV-III plasmid clones containing modifications in the *tat*-III gene were generated (Fig. 1). These constructs were derived from a plasmid clone pHXB2D which contains full-length HTLV-III provirus and produces infectious HTLV-III virions and cytopathic effects when transfected into normal human T lymphocytes<sup>9</sup>. Clone pHXB2gpt, which contains an *Xba*I/*Hpa*I viral DNA fragment from λ HXB2D inserted into plasmid vector pSP65gpt, was used to generate genomic constructs lacking either the major coding region (pHXB2ΔSal-Sst) or the splice acceptor sequences

**Fig. 1** Construction of HTLV-III plasmids and analysis of CAT activity. The precise nature of the deletions shown was confirmed by nucleotide sequence analysis. The nucleotide positions shown correspond to those published for BH10 (ref. 1). Closed boxes depict LTR sequences, cross-hatched boxes depict the *Escherichia coli* xanthine-guanine phosphoribosyl transferase gene (*xgpt*)<sup>29</sup> and open triangles show regions deleted from the HTLV-III genome. Open squares shown in plasmids pCV-1 and pCV-3 (ref. 6) represent adenovirus middle late promoter (MLP) sequences<sup>30</sup>.

**Methods.** An 11.5-kb *Xba*I/*Hpa*I fragment containing full-length HTLV-III proviral DNA was excised from the phage clone λ HXB2-D (ref. 31) and inserted into the *Bam*HI and *Eco*RI sites of the plasmid pSP65gpt. Clone pHXB2gpt contains the viral insert in the same transcriptional orientation as the *E. coli* *xgpt* gene. pHXB2gpt was used for the construction of pHXB2ΔSal-Sst and pHXB2ΔSal-RI plasmids. Construct pHXB2ΔSal-Sst is deleted of nucleotides 5,367–5,580 and hence lacks the entire first coding exon of *tat*-III (exon 2), including the initiating methionine. It was generated from pHXB2gpt by a *Sst*I partial restriction digest followed by digestion to completion with *Sal*I, end repair with T4 DNA polymerase and re-closure with T4 DNA ligase. Plasmid pHXB2ΔSal-RI is deleted of nucleotides 5,323–5,367 and hence lacks the splice acceptor sequence thought to be preferentially used to generate mature *tat*-III mRNA<sup>6</sup>, while the entire *tat*-III coding sequence is unaffected. The clone was constructed by an *Eco*RI partial restriction of pHXB2gpt, followed by complete digestion with *Sst*I, repair with the Klenow fragment of *E. coli* DNA polymerase and re-closure with T4 ligase. Plasmids pCV-1 and pCV-3 contain the complete cDNA of the spliced *tat*-III and 3' *orf* mRNA, respectively<sup>6</sup>. The ability of plasmid clones to *trans-activate* genes linked to HTLV-III LTR sequences was assessed as follows: 10 µg of DNA from the recombinant plasmid pCD12CAT (containing the bacterial gene for CAT under the regulation of the HTLV-III LTR<sup>26</sup>) was mixed with 10 µg of DNA from each test plasmid individually and transfected into 1.1 × 10<sup>7</sup> H9 lymphoid cells. The transfections were performed by incubating the cells in RPMI 1640 media containing 250 µg ml<sup>-1</sup> DEAE-dextran, 50 mM Tris-HCl pH 7.3 for 1 h at 37 °C. Cells were washed with complete media (RPMI 1640, 10% fetal calf serum (FCS) and 50 µg ml<sup>-1</sup> gentamicin) and maintained for 48 h at 37 °C in complete media. The cells were collected, washed in phosphate-buffered saline and resuspended in 1 ml of 0.04 M Tris-HCl pH 7.4, 0.15 M NaCl and 0.001 M EDTA, transferred to Eppendorf tubes and pelleted. Cells were resuspended in 0.25 M Tris-HCl pH 7.8 and lysed by freeze-thawing three times. After pelleting cell debris (5 min in Beckman microfuge), supernatants were transferred to new Eppendorf tubes and heated to 60 °C for 10 min. CAT activity was determined on 20-µl aliquots incubated with <sup>14</sup>C-chloramphenicol and acetyl CoA as previously described<sup>23</sup>. Chloramphenicol and acetylated metabolites were separated by ascending TLC and visualized by autoradiography. Radiolabelled chloramphenicol and derivatives were cut from the plates and quantitated by liquid scintillation counting. CAT activity was determined as counts per min (c.p.m.) of acetylated metabolites of chloramphenicol expressed as a percentage of the total c.p.m. The results shown are the means and standard deviation of three independent co-transfections for each test plasmid. Transfection of RSVCAT<sup>32</sup>, SVOCAT<sup>32</sup> and pCD12CAT alone gave values of 48.0 ± 6.9, 0.31 ± 0.036 and 1.41 ± 0.13, respectively. RSVCAT thus served as a positive control for each experiment, while SVOCAT, which lacks a functional promoter, is a negative control. Levels of CAT activity significantly above the values for pCD12CAT alone were indicative of *trans-activating* activity.

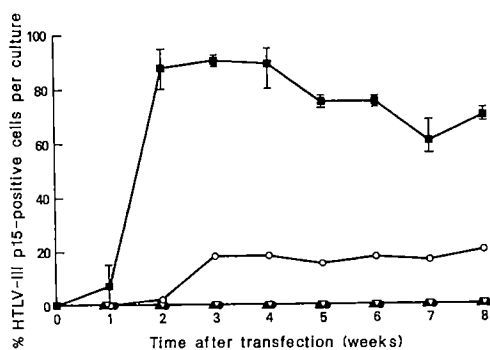
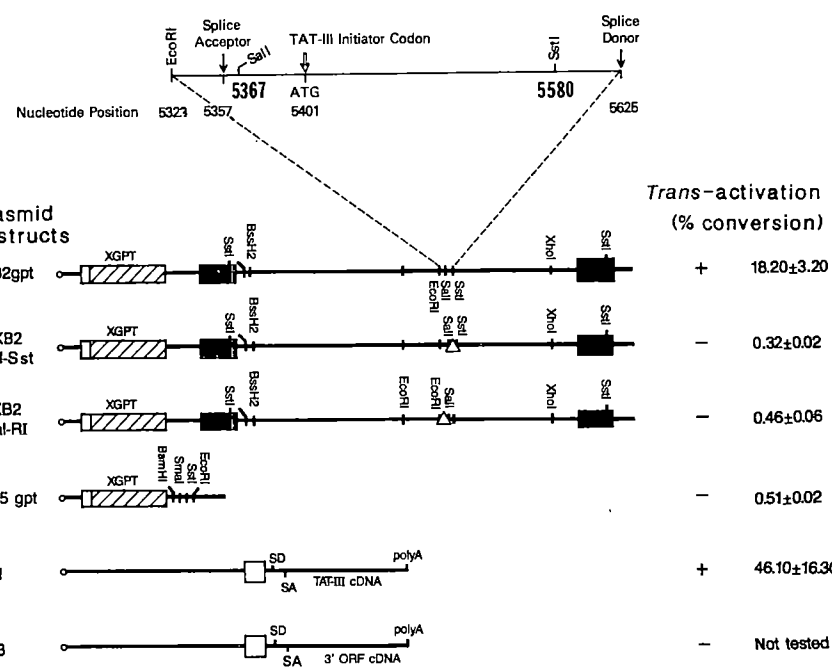


**Fig. 2** Comparison of virus expression in H9 cultures following transfection with HTLV-III plasmid derivatives. The percentage of cells expressing HTLV-III p15 antigen was assessed by immunofluorescence using the monoclonal antibody BT2 and standard protocols<sup>33</sup>. The results shown are the mean value and range obtained following three independent transfections with plasmids pHXB2gpt (■), pHXB2ΔSal-Sst (▲), pSP65gpt (▽) and pHXB2ΔSal-RI (cultures 1 (●), 2 and 3 (○)).

**Methods.** H9 cells (2.5 × 10<sup>6</sup>) were transfected with 10<sup>10</sup> bacterial protoplasts using a protoplast fusion technique<sup>9</sup>. The cells were maintained in culture at a density of 5 × 10<sup>5</sup> to 2 × 10<sup>6</sup> per ml for 8 weeks in RPMI 1640 media containing 20% fetal calf serum/antibiotics, and HTLV-III virus production assayed by electron microscopy 1, 2, 4, 6 and 8 weeks after transfection.

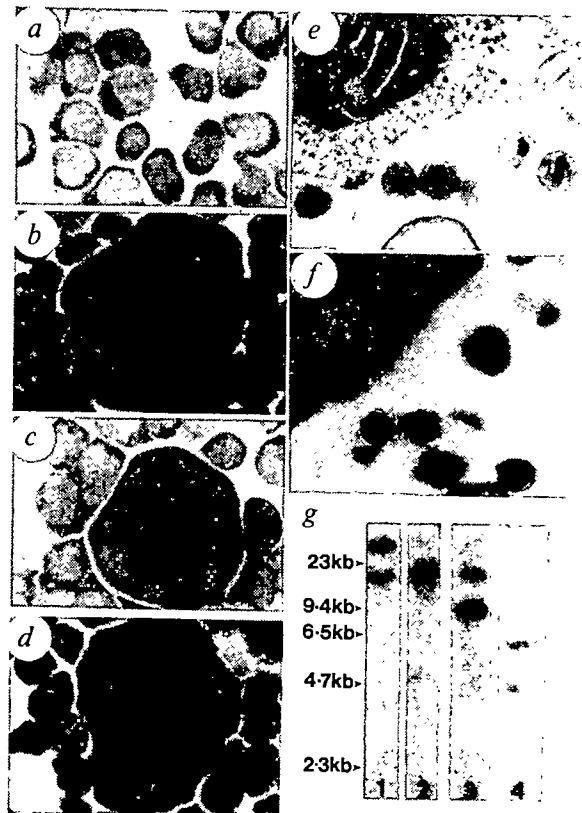


(pHBXB2 $\Delta$ Sal-RI) of *tat*-III. In pHXB2 $\Delta$ Sal-Sst, nucleotides 5,367–5,580 (from the *Sal*I/*Sst*I sites) have been deleted, removing most of the *tat*-III coding sequences of the second exon together with sequences upstream of the *tat*-III initiation codon (position 5,401) (Fig. 1). Plasmid pHXB2 $\Delta$ Sal-RI has lost nucleotides 5,323–5,367 (from the *Sal*I/*Eco*RI sites) and hence lacks the splice acceptor (position 5,357) thought to be preferentially used to generate mature *tat*-III messenger RNA<sup>6</sup>, while the entire coding sequence remains unaffected.

The extent to which these deleted genomes are capable of *trans-activating* genes linked to the HTLV-III LTRs was assessed in a series of DEAE-mediated co-transfection experiments<sup>25</sup> using pCD12CAT as an indicator<sup>26</sup>. Chloramphenicol acetyltransferase (CAT) activity was determined 48 h after transfection as the amount of cytoplasmic <sup>14</sup>C-labelled chloramphenicol converted to acetylated metabolites, expressed as a percentage of the total. Transfection of H9 cells with pHXB2gpt + pCD12CAT significantly augmented CAT activity (18.2%) as compared with transfection using pCD12CAT alone (0.03%) or pCD12CAT + pSP65gpt (0.5%) (Fig. 1), consistent with pHXB2gpt containing a biologically functional *tat*-III gene<sup>26</sup>. Co-transfection of pCD12CAT with pHXB2 $\Delta$ Sal-Sst or pHXB2 $\Delta$ Sal-RI gave values of 0.3% and 0.4%, respectively. Thus, in standard assays, *trans-activation* was not detected using genomes that lacked either the second exon coding sequences or the splice acceptor site of the *tat*-III gene. These results are consistent with reports of the location of *trans-activator* gene of HTLV-III and its normal splicing<sup>6,7</sup>.

To assess the capacity of *tat*-III-defective genomes for productive virus replication, constructs pHXB2 $\Delta$ Sal-Sst and

**Fig. 3** Demonstration of multinucleated cells, virus particles and HTLV-III DNA sequences in cultures transfected with HTLV-III plasmid derivatives. Three to five days after transfection, H9 cells were removed from culture, cytocentrifuge preparations made and stained with Wright-Giemsa stain to reveal nuclear morphology. *a-d*, Samples from cultures transfected with pSP65gpt (*a*), pHXB2gpt (*b*), pHXB2ASal-Sst (*c*) and pHXB2ASal-RI (*d*). Multinucleated cells at frequencies of  $>1$  to 5% of total were observed in samples *b*, *c* and *d*. *e, f*, Electron micrographs of virions produced 2 weeks after transfection with pHXB2gpt and pHXB2ASal-RI, respectively. In the case of pHXB2gpt, the virions had typical HTLV-III morphology, were abundant and budding particles readily observed. In the case of pHXB2ASal-RI, both characteristic HTLV-III virions and particles with abnormal morphology (irregular shape and cores) were evident and very few particles were found. Budding virus was not evident in these cultures 1–4 weeks after transfection but was occasionally demonstrated thereafter. *g*, Southern blots of DNA prepared from H9 cells 2 weeks after transfection with pHXB2ASal-Sst (lanes 1–3) or pHXB2gpt (lane 4). DNA (5  $\mu$ g) was digested separately with the enzymes *Xba*I (lane 1), *Bam*HI (lane 2) or *Sst*I (lanes 3, 4) electrophoresed in 0.8% agarose gels, blotted and hybridized to probe prepared from nick translation of the *Sst*I/*Sst*I fragment of the phage clone  $\lambda$  BHIO<sup>31</sup>. Nitrocellulose acetate filters were washed in 0.5  $\times$  SSC, 0.1% SDS at 65 °C for 2–4 h before exposure. Digestion of H9/pHXB2ASal-Sst DNA with *Xba*I (an enzyme that does not cut the viral genome but has a single site in the plasmid) yields a single band at 17 kb, corresponding to linearized plasmid in these cells, and a high- $M_r$  smear ( $>23$  kb), suggesting integration of the transfected DNA. Digestion with *Bam*HI (an enzyme that cuts at a single site in the HTLV-III sequences of the plasmid) reveals a single 17-kb band, consistent with the presence of plasmid DNA in transfected cells. *Sst*I digestion of DNA from pHXB2ASal-Sst-transfected cultures shows an intense band of 9.5 kb and a less intense band of 17 kb. The former corresponds to the *Sst*I/*Sst*I viral insert which is predicted following the construction of pHXB2ASal-Sst from pHXB2gpt. The latter probably represents residual partially digested plasmid. *Sst*I digestion of H9/pHXB2gpt DNA (lane 4) shows two bands at 5.8 and 3.7 kb, representing the fragments predicted from digestion of unintegrated proviral DNA with this enzyme.



pHXB2ASal-RI, pHXB2gpt and pSP65gpt, were introduced into H9 cells by protoplast fusion. This technique has been used by our own and other laboratories to transfect and stably express genes in lymphoid cells<sup>9,27</sup>. Figure 2 summarizes time-course experiments in which the frequency of cells expressing HTLV-III p15 (gag-related protein) was assessed following protoplast fusion. One week after transfection with pHXB2gpt, 1–15% of H9 cells expressed HTLV-III p15 and extracellular and budding virions were evident. The number of HTLV-III-expressing cells increased to 80–90% within the first 2 weeks and was maintained at a high level throughout the experiment. In contrast, no virus- or p15-expressing cells were detected after transfection with pHXB2ASal-Sst. These results indicate that *tat*-III is crucial for HTLV-III production. Southern blots (see Fig. 3g) prepared from these cells and probed for HTLV-III sequences showed the presence of linearized unintegrated plasmid DNA (a 17-kilobase (kb) band, lanes 1, 2) and integrated HTLV-III sequences (a high relative molecular mass ( $M_r$ ) smear  $>23$  kb, lane 1). Hence, the failure of H9/pHXB2ASal-Sst cultures to produce virus was not due to failure to introduce this DNA into cells. Notably, digestions with enzymes that do not cut in the HTLV-III sequence (*Xba*I, Fig. 3g, lane 1) or cut at a single site in the plasmid (*Bam*HI, lane 2) failed to reveal a 9.5-kb band, corresponding to unintegrated HTLV-III DNA in pHXB2ASal-Sst-transfected cells. The absence of unintegrated viral DNA may be an indication of lack of virus replication.

Transfection of clone pHXB2ASal-RI resulted in virus expression in two of three cases. In these, low-level expression (<2% of cells) of p15 was demonstrated 2 weeks after transfection. Electron micrographs revealed small numbers of exclusively extracellular particles, many of which had unusual morphology compared with typical virions (see Fig. 3f and e, respectively). These aberrant particles may represent true defective particles or simply degenerating virions. The proportion of cells expressing p15 increased to ~30% by week 3 and reached a plateau at 10–20% in successive weeks.

These results have two implications. First, the molecular clone pHXB2ASal-RI is capable of generating HTLV-III virus, but at

markedly reduced levels compared with the parental pHXB2gpt plasmid (we estimate that cultures transfected with the former contained 10 times fewer particles). Hence, we suggest that this clone, deprived of the normal splice acceptor used to generate *tat*-III, is able to use alternative splice acceptor sites in the 5' region of the genome to generate mature *tat*-III mRNA. Alternatively, we can postulate that *tat* is being read off a polycistronic message which includes *sor-tat-3'orf*. Complementary DNA clones corresponding to these sequences have been identified and shown to *trans*-activate in the CAT assay (S. K. Arya *et al.*, in preparation). An apparent inconsistency with these hypotheses is the failure to demonstrate *trans*-activation with plasmid pHXB2ASal-RI. To clarify this point, we performed extended CAT assays on the virus-positive and -negative pHXB2ASal-RI-transfected cultures. Cultures 1 (virus negative) and 2 (virus positive) (Fig. 2), assayed 8 weeks after transfection, gave conversions of  $^{14}\text{C}$ -chloramphenicol of  $0.534 \pm 0.068\%$  and  $52.47 \pm 11.07\%$ , respectively, in 13-h assays. The latter value is significantly greater than the conversion rates seen in uninfected cultures (0.5%), consistent with low levels of *trans*-activation in virus-positive, pHXB2ASal-RI-transfected H9 cultures. Second, the frequency of HTLV-III p15-positive cells in pHXB2ASal-RI-transfected cultures did not increase to approach 100%. Using an *in situ* technique capable of detecting infrequent cells expressing as few as 20–60 HTLV-III RNA transcripts per cell<sup>28</sup>, we determined that 0% and 25% of cultures 1 and 2 (week 8) and 20% of culture 3 (week 4) expressed viral RNA. These results are comparable to immunofluorescence values and support the contention that virus generated from pHXB2ASal-RI is either defective or produced in too low amounts to spread efficiently through the culture. As the splice acceptor deleted in pHXB2ASal-RI may be used to generate *tat*-III and 3'orf mRNA, the reduced infectivity might be attributable to compromising either or both of these genes.

Figure 3c, d demonstrates the capacity of *tat*-III-defective constructs transiently (3–5 days after protoplast fusion) to induce H9 cell multinucleation at frequencies exceeding 1% (1–5%) and suggests that shortly after transfection with

PLASMID USED FOR TRANSFECTION	COMPLEMENTATION PARTNER	RELATIVE FREQUENCY OF HTLV-III EXPRESSING CELLS IN H9 TRANSFECTED CULTURES (time/days after transfection)								
		1	2	3	4	5	6	7	14	21
pHXB2 gpt	None	-	+	++	++	+++	++++	++++	++++	++++
pSP65 gpt	None	-	-	-	-	-	-	-	-	-
pHXB2ΔSal-Sst	None	-	-	-	-	-	-	-	-	-
pHXB2ΔSal-Sst	pHXB2 gpt	-	+	+	++	+++	+++	+++	+++	+++
pHXB2ΔSal-Sst	pCV-1	-	-	-	-	-	-	-	-	-
pHXB2ΔSal-Sst	pCV-3	-	-	-	-	-	-	-	-	-
pHXB2ΔSal-Sst	tat III protein	-	-	-	-	-	-	-	-	-

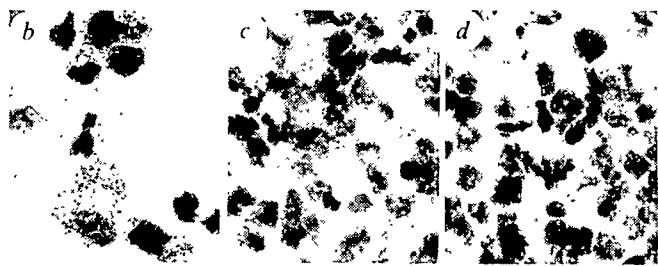


**Fig. 4** Complementation of *tat* activity in H9 cells transfected with HTLV-III plasmids deleted in the *trans*-activator gene. *a*, Time course of relative frequency of HTLV-III-expressing cells in H9-transfected cultures. Expression of viral *gag* protein p15 was assessed on a daily basis and the proportions of expressing cells are indicated on an increasing scale where - = none detected, + = few expressing cells, ++ = 0.1–1.0% positive cells, +++ = 1.0–10% positive cells and ++++ = 10–>99% positive cells. *b–d*, Autoradiographs of transfected cells labelled by *in situ* hybridization for HTLV-III RNA. The number of grains (intensity of labelling per cell) indicates the relative abundance of HTLV-III RNA. *b*, *c*, H9 cell cultures 16 days after transfection with pHXB2ΔSal-RI. In the case of *b*, 48 h before *in situ* assay these cultures were transfected with protoplasts containing TAT-III protein. Comparison with parallel cultures not transfected with TAT-III protein (*c*) shows that expression is clearly elevated in the former, 30% and 1% of cells in cultures, corresponding respectively to *b* and *c*, being judged as positive (>20 grains per cell). H9 cells were also transfected with pHXB2ΔSal-Sst and 14 days later transfected with protoplasts containing TAT-III protein. In this case (*d*), we were unable to detect HTLV-III RNA 48 h later.

**Methods.** *a*, Using the protoplast fusion technique as described previously<sup>9</sup>,  $10^{10}$  bacterial protoplasts containing plasmids pHXB2ΔSal-Sst, pSP65gpt or pHXB2gpt were separately transfected into  $3 \times 10^6$  H9 cells. In addition,  $5 \times 10^9$  protoplasts containing pHXB2ΔSal-Sst were separately combined with equivalent amounts of pCV-1, pCV-3 and pHXB2gpt or bacterial protoplasts containing TAT-III protein, and the mixed preparations fused with  $3 \times 10^6$  H9 cells. Bacterial protoplasts containing TAT-III protein were prepared as follows. *E. coli* strain AR120 carrying the plasmid pOTS-tat-III (ref. 35) were grown exponentially and induced to synthesize TAT-III protein by the addition of  $60 \mu\text{g ml}^{-1}$  nalidixic acid<sup>36</sup>, for 5 h at  $37^\circ\text{C}$ .  $10^{10}$  bacteria were collected, washed, treated with lysozyme to produce protoplasts and fused with H9 cells. The efficiency of TAT-III production following nalidixic acid treatment was checked by subjecting bacterial lysates to SDS-polyacrylamide gel electrophoresis and visualization of the separated proteins by Coomassie brilliant blue staining (data not shown). We estimate that the TAT-III protein accounts for 2–5% of the total cellular protein in the induced bacteria. *b–d*, Cells were cytocentrifuged on to microscope slides, fixed and hybridized *in situ* according to Harper *et al.*<sup>28</sup>. The  $^{35}\text{S}$ -labelled RNA probe was synthesized by transcription of clone pBH10-R3<sup>28</sup> and was specific for the 3' portion (1–2 kb) of the HTLV-III genome.

pHXB2ΔSal-Sst or pHXB2ΔSal-R1, small numbers of cells transcribe HTLV-III envelope genes. This observation can in part be explained by reports that HTLV-III LTRs can act as efficient promoters in lymphoid cells<sup>5,26</sup>, in the absence of *tat*-III.

Complementation experiments were performed to determine whether the failure of TAT-defective clones to generate HTLV-III efficiently could be compensated by the provision of a functional *tat*-III gene or the TAT-III protein itself (see Fig. 4). H9 cells transfected with pHXB2gpt alone or in combination with pHXB2ΔSal-Sst expressed HTLV-III p15 and virus particles 3–4 days after transfection, indicating that the simultaneous fusion of protoplasts containing different plasmids does not alter the efficiency of DNA transfection *per se*. HTLV-III-expressing cells were not detected following transfection of pHXB2ΔSal-Sst alone or in combination with pCV-3. However,

following co-transfection of pHXB2ΔSal-Sst and pCV-1, HTLV-III p15-positive cells were apparent 6 (<0.01%) to 14 (2.8%) days after fusion and HTLV-III RNA-expressing cells confirmed in parallel *in situ* studies. These results show that the capacity for virus expression can be restored to a genome deprived of *tat*-III by the provision of an unlinked, functional *tat*-III gene. No virus-expressing cells were seen in the same cultures 21 days after transfection. This transient expression infers that complementation was achieved in *trans* and that decreased expression was coincident with reduced numbers of cells which stably retained both pHXB2ΔSal-Sst and pCV-1. Analysis of DNA prepared from these cells on day 14 showed that the proviral DNA corresponds exactly to that predicted from clone pHXB2ΔSal-Sst (data not shown), and excludes the generation of a competent virus by recombination.

The introduction of bacterially derived TAT-III protein into H9/pHXB2ΔSal-Sst cultures did not result in virus expression, whereas its addition to H9/pHXB2ΔSal-RI cultures caused a marked increase in virus expression within 48 h; approximately 1% of cells expressed HTLV-III RNA before the introduction of *tat*-III (Fig. 4*c*), compared with 30%, including heavily labelled (>1,000 grains per cell) multinucleated cells, 2 days after its introduction (Fig. 4*b*). Thus, a single introduction of TAT-III protein appears insufficient to restore virus production to a genome devoid of *tat*-III coding sequences, but sufficient to boost virus production in a genome containing a functionally compromised *tat*-III gene. This discrepancy may reflect a short biological half-life of the TAT-III protein. The observation that *tat*-III is essential for HTLV-III replication parallels a report that *tat*-II (otherwise called the *x* or *x-lor* gene of HTLV-II) mediates *trans*-activation of viral genes and is essential for replication of HTLV-II<sup>21</sup>. These data support the notion that *trans*-activation control systems are fundamental to the biology of this newly identified group of retroviruses. In addition, as *tat* activity seems to be essential for virus production, the development of inhibitors that specifically block the activity of these *trans*-acting factors provides a new approach to the treatment of AIDS patients and individuals infected with HTLV-III.

We thank Lynn Simek, Laura Stengl, Mary Lipsky and Marty White for their help in these studies and Dr S. K. Arya for providing the cDNA clones pCV-1 and pCV-3. This work was supported in part by grants to A.G.F. from the Foundation for Advanced Education in the Sciences Inc. and the Lady Tata Memorial Research Fund. M.B.F. is a predoctoral fellow in the Cancer Biology Programme of Stanford University.

Received 8 November 1985; accepted 10 February 1986.

- Ratner, L. *et al.* *Nature* **313**, 277–284 (1985).
- Wain-Hobson, S., Sonigo, P., Danos, O., Cole, S. & Alizon, M. *Cell* **40**, 9–18 (1985).
- Sanchez-Pescador, R. *et al.* *Science* **227**, 484–492 (1985).
- Muesing, M. A. *et al.* *Nature* **313**, 450–458 (1985).
- Sodroski, J. G. *et al.* *Science* **227**, 171–173 (1985).
- Arya, S. K., Guo, C., Josephs, S. F. & Wong-Staal, F. *Science* **229**, 69–73 (1985).
- Sodroski, J. G., Patarca, R., Wong-Staal, F., Rosen, C. A. & Haseltine, W. A. *Science* **229**, 74–77 (1985).
- Rosen, C. A., Sodroski, J. G. & Haseltine, W. A. *Cell* **41**, 813–823 (1985).
- Fisher, A. G., Collalti, E., Ratner, L., Gallo, R. C. & Wong-Staal, F. *Nature* **316**, 262–265 (1985).
- Gallo, R. C. *et al.* *Science* **224**, 500–503 (1984).
- Barre-Sinoussi, F. *et al.* *Science* **220**, 868–871 (1983).
- Levy, J. A. *et al.* *Science* **225**, 69–72 (1984).
- Nevins, J. R., Ginsberg, H. W., Blanchard, J. M., Wilson, M. C. & Darnell, J. E. *J. Virol.* **32**, 727–733 (1979).
- Jones, N. & Shenk, T. *Proc. natn. Acad. Sci. U.S.A.* **76**, 3665–3669 (1979).
- Khoury, G. & May, E. J. *J. Virol.* **23**, 167–176 (1977).
- Brady, J. N., Bolen, J. B., Radonovic, M., Slazman, N. & Khoury, G. *Proc. natn. Acad. Sci. U.S.A.* **81**, 2040–2044 (1984).
- Benoist, C. & Champon, P. *Nature* **290**, 304–310 (1981).
- Nevins, J. R. *Cell* **26**, 213–220 (1980).
- Sodroski, J. G., Rosen, C. A. & Haseltine, W. A. *Science* **225**, 381–385 (1984).
- Sodroski, J. G., Rosen, C. A., Goh, W. C. & Haseltine, W. A. *Science* **228**, 1430–1432 (1985).
- Chen, I. S. Y. *et al.* *Science* **229**, 54–57 (1985).
- Rosen, C. A., Sodroski, J. G., Kettman, R., Burny, A. & Haseltine, W. A. *Science* **227**, 320–322 (1985).
- Darse, D., Caradonna, S. J. & Casey, J. W. *Science* **227**, 317–320 (1985).
- Hess, J. L., Clements, J. & Narayan, O. *Science* **229**, 482–485 (1985).
- Queen, C. & Baltimore, D. *Cell* **33**, 741–748 (1983).
- Seigel, L. *et al.* *Virology* **148**, 226–231 (1986).
- Yoakum, G. H. *Biotechniques* **5**, 24–30 (1984).

28. Harper, M. E., Marselle, L. M., Gallo, R. C. & Wong-Staal, F. *Proc. natn. Acad. Sci. U.S.A.* **83**, 772-776 (1986).  
 29. Muligan, R. C. & Berg, P. *Proc. natn. Acad. Sci. U.S.A.* **78**, 2072-2076 (1981).  
 30. Kaufman, J. R. & Sharp, P. A. *Molec. cell. Biol.* **2**, 1304-1319 (1982).  
 31. Shaw, G. M. et al. *Science* **226**, 1165-1171 (1984).  
 32. Gorman, C. M., Merlino, G. T., Willingham, M. C., Pastan, I. & Howard, B. H. *Proc. natn. Acad. Sci. U.S.A.* **79**, 6777-6781 (1982).  
 33. Veronese di Marzo, F. et al. *Virology* **Proc. natn. Acad. Sci. U.S.A.** **82**, 5199-5202 (1985).  
 34. Maniatis, T., Fritsch, E. F. & Sambrook, J. in *Molecular Cloning: A Laboratory Manual*, 23-233 (Cold Spring Harbor Laboratory, New York, 1982).  
 35. Aldovini, A. et al. *Proc. natn. Acad. Sci. U.S.A.* (submitted).  
 36. Mott, J. E., Grant, R. A., Ho, Y. S. & Plat, T. *Proc. natn. Acad. Sci. U.S.A.* **82**, 88-92 (1985).

## A model of synthetase/transfer RNA interaction as deduced by protein engineering

Hugues Bedouelle\* & Greg Winter

Laboratory of Molecular Biology, Medical Research Council,  
Hills Road, Cambridge CB2 2QH, UK

The recognition of transfer-RNA by their cognate aminoacyl-tRNA synthetases is the crucial step in the translation of the genetic code. In order to construct a structural model of the complex between the tyrosyl-tRNA synthetase (TyrTS) from *Bacillus stearothermophilus* and tRNA<sup>Tyr</sup>, 40 basic residues at the surface of the TyrTS dimer have been mutated by site-directed mutagenesis and heterodimers created *in vitro* by recombining subunits derived from different mutants. As reported here a cluster of basic residues (Arg 207-Lys 208) in the N-terminal domain of one TyrTS subunit interacts with the acceptor stem of tRNA<sup>Tyr</sup> and two separated clusters of basic residues (Arg 368-Arg 371; Arg 407-Arg 408-Lys 410-Lys 411) in the C-terminal domain of the other subunit interact with the anticodon arm. The TyrTS would thus clamp the tRNA in a fixed orientation. The precise alignment of the flexible ... ACCA 3' end of the tRNA for attack on the tyrosyl adenylate is made by contacts closer to the catalytic groups of the enzyme, such as with Lys 151.

TyrTS catalyses the aminoacylation of tRNA<sup>Tyr</sup> in a two-stage reaction. The tyrosine is first activated with ATP to form tyrosyl adenylate and pyrophosphate, then the adenylate is attacked by the 3'-terminal ribose of the tRNA to form Tyr-tRNA<sup>Tyr</sup> and AMP. TyrTS is a dimer which shows 'half-of-the-sites' reactivity, forming one tyrosyl adenylate and binding tightly one tyrosine and one tRNA<sup>Tyr</sup> per dimer in solution. The two subunits are related by symmetry through a 2-fold axis. Each subunit has an

N-terminal domain (residues 1-319), which makes all the interactions with the tyrosyl adenylate and forms the subunit interface, and a C-terminal domain (residues 320-419), which is disordered in the crystal (reviewed in ref. 1). By creating a truncated TyrTS at the level of the gene, Waye et al.<sup>2</sup> have shown that the N-terminal domain of TyrTS catalyses the formation of tyrosyl adenylate with unchanged  $k_{cat}$  and  $K_M$  but does not charge and does not bind tRNA<sup>Tyr</sup>; this shows that the C-terminal domain of TyrTS is essential for tRNA binding.

To identify residues of TyrTS that interact with tRNA<sup>Tyr</sup>, we chose the following strategy: (1) We assumed that basic residues of the synthetase could form salt bridges with the phosphates of the tRNA backbone or hydrogen bonds with the nucleotide bases. (2) Because the *B. stearothermophilus* and *Escherichia coli* TyrTS have homologous sequences and similar properties<sup>3,4</sup>, we considered mainly the conserved basic residues. (3) We changed the arginine and histidine residues to glutamine, and lysine to asparagine; such changes remove the charge but not the hydrophilic character of the residue. We therefore mutated 40 basic residues of the *B. stearothermophilus* TyrTS by oligonucleotide-directed mutagenesis of the encoding gene (*tyrS*) (see Fig. 1 legend).

To test the overall activity of the mutant synthetases, we devised an *in vivo* genetic complementation assay. In this assay, the *B. stearothermophilus* *tyrS* gene is carried by and expressed from a recombinant M13 phage<sup>5</sup>. The host is HB2111, an *E. coli* strain which harbours a thermosensitive mutation in its own *tyrS* gene, which is an essential gene. The HB2111 cells can grow at 42 °C, the non-permissive temperature, only if they are infected by a phage which directs the production of an active *B. stearothermophilus* TyrTS. Most of the 40 mutant phages could complement HB2111 and were therefore eliminated. However, 13 mutants were either unable to complement—KN82, RQ86, KN151, KN208, KN230, KN233, RQ368, RQ407, KN410 and KN411—or did so weakly—RQ207, RQ371 and RQ408 (Fig. 1).

The 13 TyrTS mutants identified from the complementation assay and the wild-type TyrTS were purified from phage-infected cells. All the mutant enzymes were able to form enzyme-bound tyrosyl adenylate, albeit slowly for mutants RQ86 and KN233 (half life,  $t_{1/2} = 8$  and 27 min respectively, compared with 2 s for the wild-type enzyme)<sup>6</sup>. The pyrophosphate exchange assay showed that the mutant and wild-type enzymes had similar activities (4.6 s<sup>-1</sup> at 2 mM ATP, 50 μM Tyr and 2 mM pyrophosphate) except for mutants KN82, RQ86, KN230 and KN233 (<0.23 s<sup>-1</sup>) (see Table 1). Thus, although these four mutants are able to form tyrosyl adenylate and are presumably correctly folded, there is nevertheless a lesion in the activation step. Additional experiments are needed to determine whether the

\* Present address: UPMTG, Institut Pasteur, 28, Rue du Docteur Roux, 75724 Paris, Cedex 15, France.

Table 1 Kinetic parameters for tRNA<sup>Tyr</sup> charging

Mutant	$k_{cat}$ (s <sup>-1</sup> × 10 <sup>3</sup> )	$K_M$ (μM)	$k_{cat}/K_M$ (s <sup>-1</sup> M <sup>-1</sup> × 10 <sup>-3</sup> )	$\Delta G_{app}$ (kcal mol <sup>-1</sup> )	Complementation
Wild type	450	1.4	315	0	+
KN151	3	1.2	2.3	2.9	-
RQ207	ND	>100	19.4	1.7	+/-
KN208	ND	>28	11.3	2.0	-
RQ368	ND	>100	2.4	2.9	-
RQ371	ND	>100	17.1	1.7	+/-
RQ407	ND	>100	11.9	1.9	-
RQ408	ND	>100	16.5	1.8	+/-
KN410	ND	>100	9.3	2.1	-
KN411	ND	>100	12.8	1.9	-

$\Delta G_{app} = -RT\ln(k_{cat}/K_M)_{mut}/(k_{cat}/K_M)_{wt}$  (mut, mutant; wt, wild type)<sup>11</sup>. For genetic complementation assay, see Fig. 1 legend. ND, not determined. Purification of the wild-type and mutant enzymes from phage-infected cells<sup>7</sup>, active-site titration, pyrophosphate exchange and tRNA charging assays<sup>11</sup> were done as described elsewhere. We obtained different values for the wild-type TyrTS with pure *E. coli* tRNA<sup>Tyr</sup> (Boehringer 1,000 pmol of tyrosine incorporation per  $A_{260}$  unit) and crude *E. coli* tRNAs ( $K_M = 1.43$  versus 2.57 μM and  $k_{cat} = 0.45$  versus 1.17 s<sup>-1</sup>). The rate of charging by the wild-type enzyme gave a straight line in the Eadie-Hofstee plot (see ref. 12) only for pure tRNA<sup>Tyr</sup> concentrations less than 6 μM and was inhibited for higher values. We therefore used pure *E. coli* tRNA<sup>Tyr</sup> for the mutant enzymes, in the range 0.375-6 μM.

**Fig. 1** Stereo view of the TyrTS backbone with mutated side chains. Forty basic residues—lysine (K), arginine (R) or histidine (H)—were mutated to asparagine (N) or glutamine (Q). Twenty-seven mutants gave full growth (+) in the genetic complementation assay while 13 mutants gave residual (+/-) or no growth (-): RQ10+, RQ56+, RQ57+, HQ63+, RQ64+, KN82-, KN83+, RQ86-, RQ100+, KN102+, RQ137+, KN141+, HQ142+, KN151-, RQ157+, RQ207+/-, KN208-, KN210+, KA225+, KN230-, KN233-, KN245+, RQ265+, KN268+, RQ286+, KN291+, RQ292+, KN304+, HQ307+, KN367+, RQ368-, RQ371+/-, RQ385+, RQ398+, RQ402+, RQ407-, RQ408+/-, KN410-, KN411-, RQ417+, wild type+. The N-terminal domain (residues 1–319) is represented with bound tyrosyl adenylate. *a*, 22 residues that, when mutated, score as +; *b*, 7 residues that score as +/- or -. From bottom to top of the figure: R207, K208, K151, K82 and R86 on the left, K230 and 233 on the right.

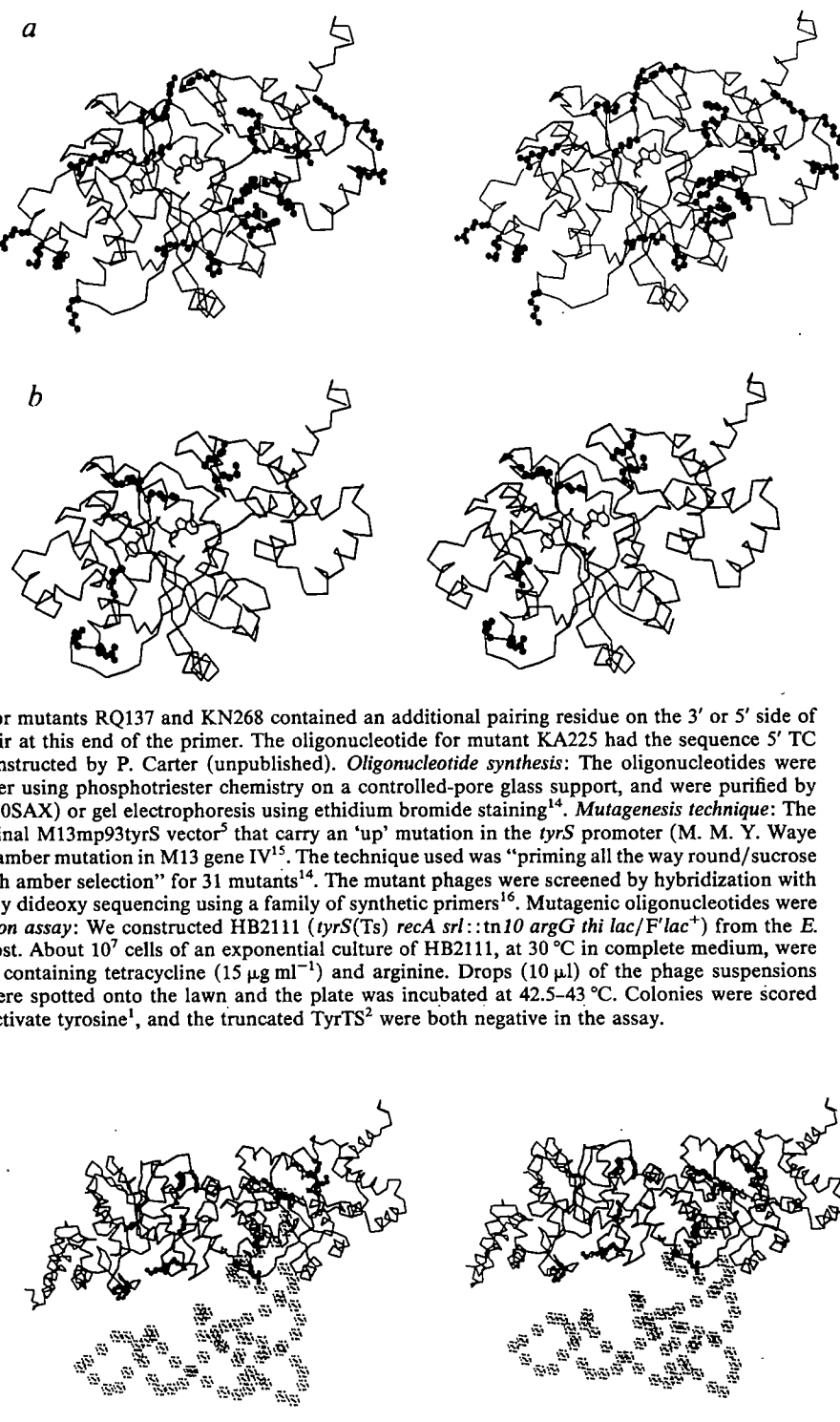
**Methods.** Primer design: In general, we used codons AAC for Asn and CAG for Gln. CAA was used in the mutants RQ64, RQ292 and RQ402 to improve discrimination during the screening of the mutants. In general, the oligonucleotides contained seven pairing residues on each side of the mismatched base(s)

and were 15- or 16-mers. The oligonucleotides for mutants RQ137 and KN268 contained an additional pairing residue on the 3' or 5' side of the mismatch, respectively, to provide a G-C pair at this end of the primer. The oligonucleotide for mutant KA225 had the sequence 5' TC CGC TGC CGT CAC AAG 3'; KA225 was constructed by P. Carter (unpublished). Oligonucleotide synthesis: The oligonucleotides were synthesized by Biosearch SAM1 DNA synthesizer using phosphotriester chemistry on a controlled-pore glass support, and were purified by either HPLC on an ion-exchange resin (Partisil 10SAX) or gel electrophoresis using ethidium bromide staining<sup>14</sup>. Mutagenesis technique: The mutagenesis was done on derivatives of the original M13mp93tyrS vector<sup>5</sup> that carry an 'up' mutation in the *tyrS* promoter (M. M. Y. Waye and G.W., in preparation) and, in some cases, an amber mutation in M13 gene IV<sup>15</sup>. The technique used was "priming all the way round/sucrose gradient" for 9 mutants and "double priming with amber selection" for 31 mutants<sup>14</sup>. The mutant phages were screened by hybridization with the mutagenic oligonucleotides<sup>14</sup> followed by dideoxy sequencing using a family of synthetic primers<sup>16</sup>. Mutagenic oligonucleotides were also used as sequencing primers. Complementation assay: We constructed HB2111 (*tyrS*(Ts) *recA* *srl*::tn10 *argG* *thi* *lac*/F' *lac*<sup>+</sup>) from the *E. coli* K-12 strain 565cN (ref. 17) and used it as host. About 10<sup>7</sup> cells of an exponential culture of HB2111, at 30 °C in complete medium, were spread on a pre-warmed minimal glucose plate containing tetracycline (15 µg ml<sup>-1</sup>) and arginine. Drops (10 µl) of the phage suspensions (~5 × 10<sup>11</sup> plaque-forming units (PFU) ml<sup>-1</sup>) were spotted onto the lawn and the plate was incubated at 42.5–43 °C. Colonies were scored after 48 h. The mutant HN45, which does not activate tyrosine<sup>1</sup>, and the truncated TyrTS<sup>2</sup> were both negative in the assay.

**Fig. 2** Docking of tRNA and synthetase. The figure shows the backbone of the TyrTS dimer with tyrosyl adenylate bound to the right subunit and with the side chains of residues R207, K208, K151, K82, R86, K230 and K233 (for the identification of these residues, see Fig. 1 legend). Only the N-terminal domain (residues 1–319) of each subunit is represented. The structure of tRNA<sup>Phe</sup> is indicated by the van der Waals' spheres of its phosphorous atoms. The flexible 3'-terminus of the tRNA (... ACCA 3') was docked up to the tyrosyl adenylate binding site and the 3'-terminal adenosine could be fitted into the active site so as to attack the tyrosyl adenylate at the scissile bond; however, several rotations of the phosphodiester backbone were required to avoid bad contacts.

wild-type residues at these four positions also interact with the tRNA; in the crystallographic structure, they lie on the rim of the tyrosyl adenylate binding site (Fig. 1).

Table 1 shows the kinetic results for the charging of tRNA by the nine mutants that exchange pyrophosphate at a normal rate. Eight of the nine mutant enzymes have altered  $K_m$  values for tRNA in the aminoacylation reaction, which indicates that most of the contacts between the synthetase and the tRNA are involved in the initial complex formation. The KN151 mutant has a  $K_m$  for tRNA which is identical to that of the wild-type enzyme and a  $k_{cat}$  which is reduced by 150-fold; this indicates that the wild-type residue, Lys 151, is not involved in the initial binding between the synthetase and the tRNA and that TyrTS



and tRNA<sup>Tyr</sup> may make an additional contact, involving Lys 151, in the transition state.

Previously, we have shown that it is possible to form and purify heterodimers between truncated (lacking residues 319–417) and full-length TyrTS enzymes by mixing the two parental homodimers in equimolar amounts, denaturing the mixture with urea, then renaturing it by electrophoresis through a non-denaturing polyacrylamide gel. After renaturation, the two-refolded homodimers and the heterodimer are roughly in the proportion 1:1:2, as theoretically expected. Detailed kinetic studies of purified heterodimers carrying the Asn 45 mutation (which prevents tyrosine activation) in either the full-length or the truncated subunit, have shown that one tRNA molecule

Table 2 Charging activity of TyrTS heterodimers

Mixture	Aminoacylation rate ( $s^{-1} \times 10^3$ )	
	a	b
tr+KN82	270	59
tr+RQ86	277	4
tr+KN151	196	2
tr+RQ207	304	29
tr+KN208	328	25
tr+KN230	297	6
tr+KN233	250	9
tr+RQ368	3	2
tr+RQ371	32	22
tr+RQ407	16	11
tr+RQ408	31	23
tr+KN410	14	11
tr+KN411	20	13
KN151 + RQ368	162	4

The truncated TyrTS (tr)<sup>2</sup> and each of the 13 mutants were mixed in equal molarities (according to active-site titration) before (a) or after (b) the denaturation/renaturation process. A similar experiment was performed with the KN151 and RQ368 mutants. The rates are calculated per input mole of one of the two parental homodimers; calculated in this way, they can reach 100% of the rate of the re-folded wild-type enzyme if there is random reassociation of the monomers. In case a, half of the monomers are theoretically engaged in heterodimer formation and therefore the contribution of the re-folded homodimers should be half the value in b. The rates for the re-folded truncated and wild-type enzymes were 0 and  $421 \times 10^{-3} s^{-1}$  respectively. The rate of charging by the active TyrTS heterodimers (46–75% that of reconstituted wild-type enzyme) implies that the tRNA affects the formation or the hydrolysis of tyrosyl adenylate. Each heterodimer has two potential sites for tyrosine activation and a single site for tRNA binding. However, due to half-of-the-sites reactivity, only one molecule of tyrosyl adenylate is formed per heterodimer. If tyrosyl adenylate is formed on the truncated subunit, it can be attacked by the tRNA (rate  $0.45 s^{-1}$ ; see Table 1) and the enzyme can recycle, whereas if adenylate is formed on the other subunit, it cannot be transferred to the tRNA and also prevents further tyrosine activation at the truncated subunit. In the latter case, the enzyme is blocked until the tyrosyl adenylate hydrolyses (rate  $0.45 \times 10^{-3} s^{-1}$ , ref. 13). If tyrosyl adenylate could form at random at either subunit, the heterodimers would quickly be blocked (50% of the remaining active heterodimers each cycle). Thus, we suspect that either the tyrosyl adenylate forms preferentially on the truncated subunit of the heterodimers (directed by the lie of the tRNA), or the binding of tRNA greatly stimulates hydrolysis of blocking tyrosyl adenylate. The experiments were done in 100 mM Tris-HCl, 44 mM Tris pH 7.78, 10 mM MgCl<sub>2</sub>, 10 mM 2-mercaptoethanol and 0.1 mM phenyl methyl sulphonyl fluoride. For denaturation, the starting solutions (20  $\mu$ l) were 10.4  $\mu$ M in each enzyme; 1  $\mu$ l bovine serum albumin (BSA, 20 mg ml<sup>-1</sup>) was added, then urea until saturation ( $\sim$ 25 mg; volume 40  $\mu$ l, urea 10 M, BSA 0.5 mg ml<sup>-1</sup> final concentration). For renaturation, the urea solutions were diluted using nine steps of 1 M each (15 min at room temperature for each step), keeping BSA at 0.5 mg ml<sup>-1</sup>. Aliquots (2.25  $\mu$ l) of the mixtures were assayed in 100  $\mu$ l of 10 mM Mg-ATP, 20  $\mu$ M <sup>14</sup>C-Tyr (514 mCi mmol<sup>-1</sup>), 5 mg ml<sup>-1</sup> crude *E. coli* tRNA (380 pmol of tyrosine incorporation per mg). The presence of BSA during the denaturation/renaturation process was necessary to recover activity. 73% of the activity of the wild-type TyrTS could be recovered using stepwise dilution of urea whereas only 7% was recovered after a one-step dilution. The addition of urea to the tRNA charging assay resulted in a progressive increase of the rate (2.5-fold maximum at 0.16 M urea).

interacts with both TyrTS subunits<sup>7</sup>. These studies also show that the 3'-terminal adenosine of the tRNA attacks the tyrosyl adenylate in the truncated subunit of the heterodimer.

Here, we have formed heterodimers between the truncated TyrTS and each of the 13 mutants described above by stepwise dilution of the urea. As controls, we also mixed the two parental homodimers after the denaturation/renaturation process. We assayed the final mixtures for charging of tRNA with <sup>14</sup>C-tyrosine (Table 2). The seven mutants carrying a lesion in the N-terminal domain formed active heterodimers with the trun-

cated TyrTS. Similarly, an active heterodimer could be made between the mutant enzymes KN151 and RQ368. Thus, a functional tRNA interaction site can be reconstituted by assembling two inactive monomers, one of which has a wild-type N-terminal domain but lacks the C-terminal domain (or has a lesion therein) and the other having a mutated N-terminal domain but a wild-type C-terminal domain<sup>7</sup>. The results show that tRNA<sup>Tyr</sup> interacts with the residues Lys 151, Arg 207 and Lys 208 (which correspond to mutated residues) in the truncated subunit of the heterodimer and therefore, taking into account our previous results<sup>7</sup>, that it interacts with both tyrosyl adenylate and residues Lys 151, Arg 207 and Lys 208 in the same subunit of the dimer. The six mutants with a lesion in the C-terminal domain did not form active heterodimers with the truncated TyrTS; this result was expected because the C-terminal domain of TyrTS is necessary for tRNA charging<sup>2</sup>.

In the active heterodimers, one of the constitutive monomers lacks the C-terminal domain. Therefore, in the wild-type TyrTS, only one of the two symmetrical copies of the C-terminal domain is essential for tRNA interaction. Similarly, only one of the two monomers has a wild-type N-terminal domain. Therefore, only one of the two symmetrical copies of residues Lys 151, Arg 207 or Lys 208 is essential for interaction with tRNA. These results show that TyrTS can function with only one productive tRNA binding site per dimer.

Model-building studies<sup>4</sup> indicate that tRNA<sup>Tyr</sup> may fold into a structure which is similar to the known structure of yeast tRNA<sup>Phe</sup> (ref. 8). We have attempted a docking of TyrTS<sup>9</sup> with tRNA<sup>Phe</sup> using the computer graphics program FRODO<sup>10</sup>. The 3'-hydroxyl of tRNA<sup>Phe</sup> was held near the tyrosyl adenylate binding site and the tRNA rotated around this fixed point so that the acceptor arm interacted with the tyrosyl adenylate and with residues Lys 151, Arg 207 and Lys 208 on the same subunit. With the path of the tRNA fixed as above, we examined the interaction of the anticodon arm with the second (nonproductive) subunit; this subunit interacts with the tRNA through its disordered C-terminal domain. In the crystallographic map, this domain may correspond to an island of electron density which is located in part on top of the  $\alpha$ -helical domain and of the tyrosyl adenylate binding pocket. It is unlikely that the N-terminal domain of the nonproductive subunit makes important contacts to the tRNA through basic residues, as the heterodimers constructed between the truncated TyrTS and the non-complementing mutants at positions 82, 86, 151, 207, 208, 230 and 233 were all active in tRNA charging (Table 2). The model in Fig. 2 was generated by a more careful docking of the acceptor stem with the productive subunit and suggests that the anticodon arm lies in the plane of the subunits, where it would be in close proximity to the crystallographic island of density mentioned above (Fig. 2).

H.B. thanks the Royal Society and EMBO for long-term fellowships.

Received 8 October 1985; accepted 17 January 1986.

- Fersht, A. R. et al. *Angew. Chem.* **23**, 467–473 (1984).
- Waye, M. M. Y., Winter, G., Wilkinson, A. J. & Fersht, A. R. *EMBO J.* **2**, 1827–1829 (1983).
- Winter, G., Koch, G. L. E., Hartley, B. S. & Barker, D. G. *Eur. J. Biochem.* **132**, 383–387 (1983).
- Brown, R. S. et al. *Nucleic Acids Res.* **5**, 23–26 (1978).
- Winter, G., Fersht, A. R., Wilkinson, A. J., Zoller, M. & Smith, M. *Nature* **299**, 756–758 (1982).
- Fersht, A. R., Mulvey, R. S. & Koch, G. L. E. *Biochemistry* **14**, 13–18 (1975).
- Carter, P., Bedouelle, H. & Winter, G. *Proc. natn. Acad. Sci. U.S.A.* (in the press).
- Robertus, J. D. et al. *Nature* **250**, 546–551 (1974).
- Bhat, T. N., Blow, D. M., Brick, P. & Nyborg, J. *J. molec. Biol.* **158**, 699–709 (1982).
- Jones, T. A. in *Computational Crystallography* (ed. Sayre, D.) 303–310 (Clarendon, Oxford, 1982).
- Wilkinson, A. J., Fersht, A. R., Blow, D. M. & Winter, G. *Biochemistry* **22**, 3581–3586 (1983).
- Fersht, A. R. *Enzyme Structure and Mechanisms* (Freeman, New York, 1985).
- Fersht, A. R. *Biochemistry* **14**, 5–12 (1975).
- Carter, P., Bedouelle, H., Waye, M. M. Y. & Winter, G. *Oligonucleotide Site-directed Mutagenesis in M13: An Experimental Manual* (Anglian Biotechnology, Colchester, 1985).
- Carter, P., Bedouelle, H. & Winter, G. *Nucleic Acids Res.* **13**, 4431–4443 (1985).
- Wilkinson, A. J., Fersht, A. R., Blow, D. M., Carter, P. & Winter, G. *Nature* **307**, 187–188 (1984).
- Barker, D. G. *Eur. J. Biochem.* **125**, 357–360 (1982).

## Upstream activator sequences are present in the promoters of nitrogen fixation genes

Martin Buck\*, Stephen Miller,  
Martin Drummond & Ray Dixon

AFRC Unit of Nitrogen Fixation, University of Sussex,  
Brighton BN1 9RQ, UK

Nitrogen fixation (*nif*) genes in *Klebsiella pneumoniae* are controlled by a transcriptional activation mechanism which requires the *ntrA* gene product acting concert with either the *ntrC* or *nifA* products (reviewed in ref. 1). The *nif* promoters lack the canonical -35, -10 promoter elements and instead their activation requires nucleotide sequences located around -24 and -12 (refs 2-4). We have now identified and characterized a further essential promoter sequence in the *K. pneumoniae* *nifH*, *nifU*, *nifB* and *ORF* promoters, located more than 100 base pairs (bp) from the transcription start site. This promoter element is required for *nifA*- but not *ntrC*-mediated activation and for the inhibition of chromosomal *nif* expression observed when cells harbour multiple copies of certain *nif* promoters<sup>5</sup>. The upstream sequence is conserved among 10 *Rhizobium* and 2 *Azotobacter* *nif* promoters. We show that the positioning and orientation of the upstream sequence is not critical for promoter activity up to a distance of 2 kilobases

(kb) and that the upstream sequence is itself transcriptionally inactive, probably acting in *cis* with the downstream sequences to produce a fully active promoter. Thus, an extended promoter structure is required for *nif* gene expression.

Deletion of nucleotides -72 to -184 in the *K. pneumoniae* *nifH* promoter greatly reduces its transcriptional activation by the *nif*-specific activator *nifA* (ref. 4), and relieves the inhibition of chromosomal *nif* gene expression<sup>2</sup> usually shown by multiple copies of the *nifH* promoter<sup>5</sup>. We have analysed in detail the role of upstream sequences in *nifH*, *nifU* and *nifB* promoter function. Figure 1a shows that upstream sequences are essential for the multicopy inhibitory effect of the *nifH* (pMB1, pSMM4) and *nifU* (pMD1106, pSMM9) promoters (the *nifB* promoter clone shows no multicopy inhibition). The *nifH* promoter can be weakly activated by *ntrC* (ref. 4), but we were unable to detect *ntrC* activation of the *nifU* and *nifB* promoters. The *nifH*, *nifU* and *nifB* promoters require upstream sequences for efficient *nifA* activation, but *ntrC* activation of the *nifH* promoter is independent of the upstream element. Therefore, the upstream element is required only for *nifA* activation, thereby indicating that the deletions do not disrupt a more general property of the promoter, for example secondary RNA polymerase binding sites<sup>6</sup>.

Within sequences deleted from the *nifH*, *nifU* and *nifB* promoters, we have identified a new *nif* consensus sequence that occurs upstream in *K. pneumoniae*, *Rhizobium* and *Azotobacter* *nif* promoters (Table 1). These sequences are delineated to within 8 bp at the 5' end and 4 bp at the 3' end by the deletion

Table 1 Upstream sequences in *nif* promoters

<i>nifH</i> Kp(16)	G C A G G G C G C A A T T G T T C T G T T T C C C A C A T T T G -136
<i>nifU</i> Kp <sup>†</sup>	C G T G T C G T T T C T G T G A C A A A G G C C C A C A A A A C -116
<i>nifB</i> Kp <sup>†‡</sup>	A C T G T G C C T T A T G T G A G A T T C A G G A C A T T T G -143
<i>ORF</i> Kp(16)	T G G T G G C G G C T T T G T C G G C T G T T C A A C A G C T T -147
<i>nifB</i> Kp <sup>†</sup>	C C A G G C G G G A T A G G T C A T A A A G C A C A C A T G C C -119
<i>nifH</i> Rm(17)	A C T G T A G C C C T T G T C G G C T T A G C G A C A C G A G -122
<i>nifH</i> Rt(18)	G T C G T C A C C C T T G T C G G C T T C G T G A C A C G C T * -130
<i>nifH</i> PR(19)	G G T G T G G C C G T T G T T C G T T T C T G A C A G C C G -141
<i>nifDK</i> PR(20)	G C A A A C G C C C G A T G T C G C C T T C G C A A C A A C A A -111
<i>nifHa</i> & <i>b</i> Rp(21)	C G C T T T G T C T G A T C G G C G A C A T T A G * -129
<i>nifH</i> Rj(22)	T T G C G A T T G T T T G T C G T T G T C T G A C A G C C G -140
<i>nifH</i> Rj(22)'	C G G G C A G A T C T T G T C A G A T C C A A A A C A G C C T -111
<i>nifDK</i> Rj(23)	G C A A A G G C G G A G T G T C G C A T T C G C A A C A A C A G -109
<i>nifDK</i> Cowpea R(24) IRC78	C C A A A G C G G T G A T G T C G G G T T C G C A A C A A A T C -113
Rm P <sub>2</sub> (25)	T C C G T C G C C C T C T G T C G G C C C C T C G A C A C A A G -130
Rm P <sub>3</sub> (25)	T T C G T C A C C C T T G T C G G C T T A A C C A C A C A A G -130
<i>nifH</i> Ac. <sup>§</sup>	G A T G T A G G G A C A T G T C G T G T A G C A T A C A C A G A -142
<i>nifH</i> Av.(26)	C A T T G T T C G G T T G T A G C A A T T A C A C A C A T G T * -153
<i>nifE</i> Av.(27)	G G A C G C C T G C T T G T T G C A A A C C T G A C A G G A A * -103
Consensus	G A N <sub>7</sub> T G T N <sub>4</sub> T N <sub>5</sub> A C A
Binding site consensus <sup>7</sup>	T G T G T N <sub>6-10</sub> A C A C A

For comparison, the position of the invariant G of the TGT motif is given, with the C residue of the invariant G-C dinucleotide promoter element designated as -12. Abbreviations used: Kp, *Klebsiella pneumoniae*; Rm, *Rhizobium meliloti*; Rt, *Rhizobium trifoli*; PR, *Parasponium rhizobium*; Rj, *Rhizobium japonicum*; Rp, *Rhizobium phaseoli*; Ac, *Azotobacter chroococcum*; Av., *Azotobacter vinelandii*. The upstream sequence is absent from the *K. pneumoniae* *nifL* promoter<sup>10</sup>. The *nifE* promoter shows partial homology only. A potential upstream promoter element exists in the *nifF* promoter<sup>10</sup>, but at position -263. The upstream element is present in two out of three *Rhizobium phaseoli* *nifH* promoter sequences<sup>21</sup>. The two potential upstream elements present in the *Rhizobium japonicum* *nifH* promoter sequence<sup>22</sup> are shown. The upstream consensus sequence is also found in all three *Rhizobium trifoli* repeated sequence copies described in ref. 28. Both Ac. *nifH* and Av. *nifE* promoters have a TGT-N<sub>10</sub>-ACA upstream sequence; the Av. *nifH* upstream sequence encodes a partially homologous element of the form TGT-N<sub>9/11</sub>-ACA. References are shown in parentheses.

\* Transcription start site has not been determined, but the promoter has been identified by homology with the *nif* consensus -24, -12 promoter sequences.

† J. Beynon, V. Buchanan-Wollaston, M. C. Cannon and F. C. Cannon, in preparation. ‡ M.D., unpublished data. § R. A. Jones, P. Woodley and R. C. Robson, unpublished data.

end points in plasmids pSMM8 and pSMM9 (Figs 3 and 1a, respectively). The conserved sequence conforms to a consensus sequence for protein binding sites on DNA<sup>7</sup> and could be a site at which *nifA* interacts with *nif* promoters. The DNA sequence of the *nifA* gene predicts a potential DNA binding domain in the C-terminal region of the *nifA* protein<sup>8</sup>. The upstream promoter elements identified by us may interact with the *nifA* protein at this domain. The proposed binding sites lie more than 100 nucleotides from the transcription start (where this has been determined) and are characterized by an invariant TGT-N<sub>10</sub>-ACA motif flanked by A+T-rich sequences.

Multicopy inhibition is thought to result from activator titration<sup>9</sup>. We reasoned that, as the upstream consensus conforms to a protein binding site, and as a point mutation in the *nifH* promoter (G→T-136)<sup>2,4</sup> within this sequence relieves multicopy inhibition, *nifA* might bind to the upstream sequence. However, when we assessed the ability of the *nifH* upstream sequence alone to cause multicopy inhibition (Fig. 1b), no inhibition was detected, even when the upstream element was cloned into the very high copy number pEMBL8<sup>+</sup> plasmid. Furthermore, no inhibition was detected from subclones of the *nifH* promoter which retained only the downstream *nif* consensus promoter

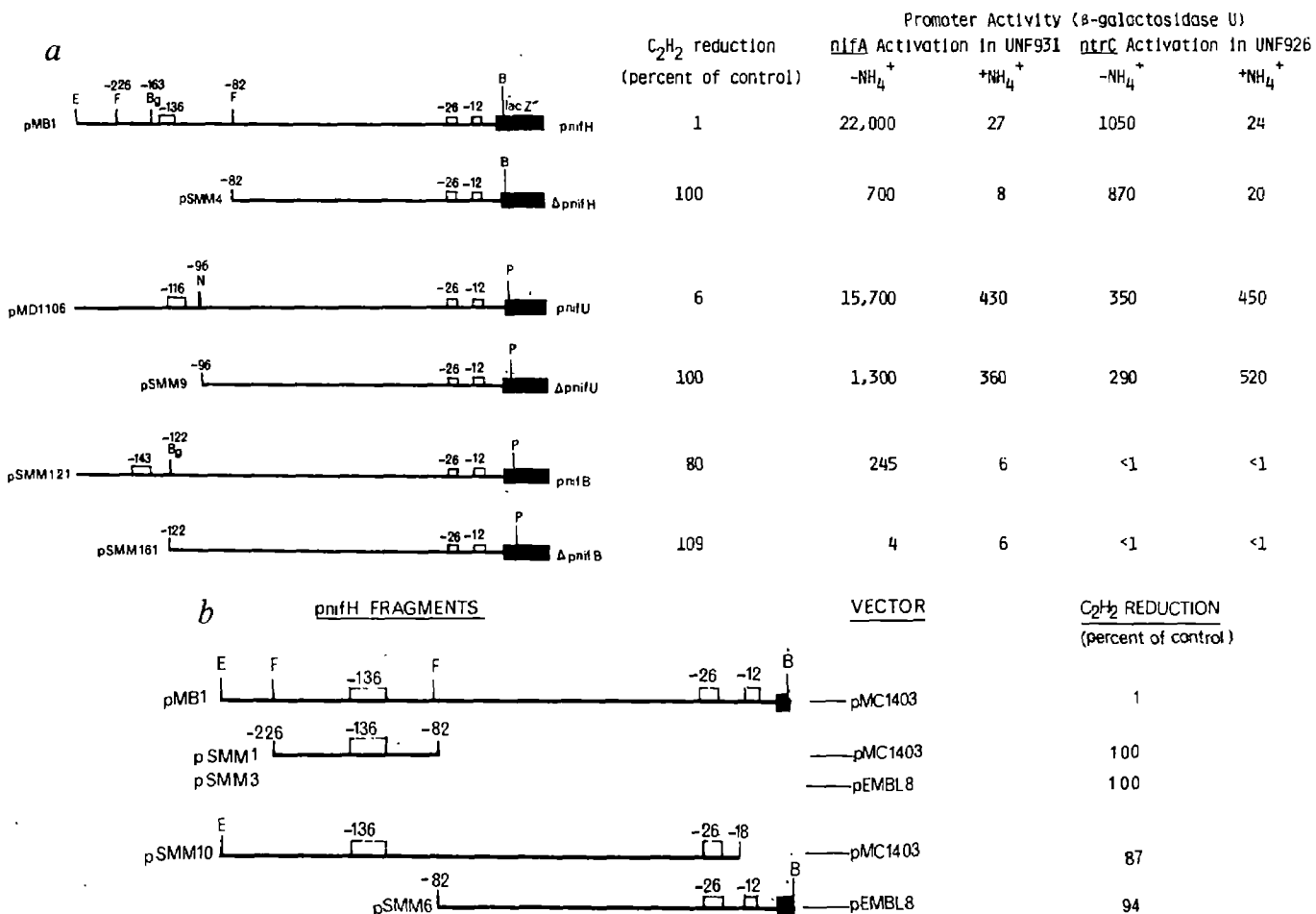


**Fig. 1** *a*, Influence of upstream deletions on the activities of the *nifH*, *nifU* and *nifB* promoters. Each promoter clone (pnif) and the upstream deleted derivative ( $\Delta$ pnif) was assayed for its multicopy inhibitory effect on chromosomal *nif* expression by measuring the acetylene reduction activity of *K. pneumoniae* UNF931 (*ntr*<sup>+</sup> *nif*<sup>+</sup>)<sup>5</sup> carrying pnif and  $\Delta$ pnif. These data are expressed as a percentage of the acetylene reduction activity of UNF931 carrying the promoter cloning vehicle, pMC1403. Transcriptional activation of pnif and  $\Delta$ pnif by *nifA* was assayed in UNF931 and activation by *ntrC* in UNF926 (*ntr*<sup>+</sup>  $\Delta$ his-nif) as described previously<sup>4</sup>. The activators *nifA* and *ntrC* are functionally related proteins and can substitute for one another in the activation of a number of *ntr*-regulated promoters<sup>1</sup>. Activation data are given as units of  $\beta$ -galactosidase. Open boxes at -136, -116 and -143 indicate the position of a conserved upstream sequence (see Table 1). The low level of activator-independent constitutive expression from the *nifU* promoter clones may be attributed to the sequence 5'-AATACA-N<sub>16</sub>-TTAAAT behaving as a typical prokaryotic promoter of the -10, -35 form<sup>29</sup>. Relevant restriction sites shown are: B, *Bam*HI; Bg, *Bgl*II; E, *Eco*RI; F, *Fnu*DII; N, *Nru*I; P, *Pst*I. *b*, Multicopy inhibition from subclones of the *nifH* promoter.

**Methods:** *a*, Plasmids: *nif-lacZ* translational fusions were constructed in the expression vector pMC1403 (ref. 30) or its derivative pMD1405 (ref. 4). The *nifH-lacZ* fusion plasmid pMB1 has been described previously<sup>4</sup>. Plasmid pSMM4 was constructed by cloning the downstream *Fnu*DII-*Bam*HI fragment from pMB1 into *Sma*I-*Bam*HI-digested pMC1403. Plasmids pMD1106 and pGS1103 are *nifU* and *nifB* translational fusions constructed in pMD1045. Deletion of the upstream sequence from the *nifU* promoter was achieved by isolating the shortened promoter as a *Nru*I-*Pst*I fragment and ligating this into *Sma*I-*Pst*I-digested pMD1106 (to retain the reading frame) to yield plasmid pSMM9. Plasmids pSMM121 and pSMM161, which carry the complete and upstream deleted *nifB* promoter respectively, were constructed by isolating the *nifB* promoter as an *Eco*RI-*Pst*I fragment from pGS1103, digesting this with *Eco*RV or *Bgl*I, ligating into *Sma*I-*Pst*I-digested pMD1405, treating with T4 DNA polymerase and religating. *b*, Assays were performed as for *a*. Plasmid pSMM1 was constructed by subcloning the *Fnu*DII restriction fragment carrying the upstream sequence of the *nifH* promoter into *Sma*I-digested pMC1403. The upstream sequence was also cloned into pEMBL8<sup>+</sup> as an *Eco*RI-*Bam*HI fragment from pSMM1, as was the downstream sequence from pSMM4, to yield plasmids pSMM3 and pSMM6, respectively. Sequencing single-stranded template derived from pSMM3 showed that the upstream sequence in pSMM1 was in the same orientation as in pMB1. Plasmid pSMM10 was constructed by restricting the *nifH* *Eco*RI-*Bam*HI promoter fragment from pMB3 with *Rsa*I and ligating this material into *Eco*RI-*Sma*I-digested pMC1403. (Plasmid pMB3 carries a silent point mutation at -18 which creates an *Rsa*I restriction site<sup>4</sup>.)

Table 2 Activities of *nifL* and *nifL-nifH* hybrid promoters

Plasmid	Upstream sequence and orientation	None	Plasmid in <i>trans</i>		Acetylene reduction (%)
			pMC71A ( <i>nifA</i> <sup>c</sup> ) Activity	pMM14 ( <i>ntrC</i> <sup>c</sup> ) ( $\beta$ -galactosidase units)	
pRD531	<i>nifL</i>	50	2,200	2,900	—
pRD535	$\Delta nifL$	70	430	340	100
pSMM535	<i>ORF + nifH</i>	10	2,600	26	50
pSMM536	<i>nifH + ORF</i>	11	1,300	130	37

Activation of *nifL* and *nifH-nifL* hybrid promoters by *nifA* and *ntrC* plasmids. Cultures were grown and assayed as described previously<sup>4</sup>. The strain background for activation assays was *Escherichia coli* ET8894 ( $\Delta(rha-ntrC)1703 rbs gyrA hutC lacZ::IS1 Mucts62$ ). Plasmids pMM14 and pMC71A provide *ntrC* and *nifA* in *trans* constitutively. Multicopy inhibition was assayed in *K. pneumoniae* UNF931 (ref. 4).

Table 3 Influence of spacing and orientation of upstream sequences on activation

Plasmid	Position of upstream elements	Element and orientation (turns of helix)	Activity (% pMBI)	C <sub>2</sub> H <sub>2</sub> reduction (% control)
pMB43	-102	$\overline{H} + \overline{ORF}$ (3.2)	44	75
pMB42	-103	$\overline{ORF} + \overline{H}$ (3.14)	105	48
pSMM48	-124	$\overline{H}$ (1.14)	50	8
pMB1 (wild type)	-136	$\overline{ORF} + \overline{H}$ (0)	100	1
pSMM8	-136	$\overline{H}$ (0)	79	0.3
pSMM15	-155	$\overline{H} + \overline{ORF}$ (1.81)	55	5
pSMM14	-156	$\overline{ORF} + \overline{H}$ (1.9)	46	1
pSMM47	-156	$\overline{H}$ (1.9)	56	3
pSMM142	-168	$\overline{ORF} + \overline{H}$ (3.04)	145	10
pSMM143	-190	$\overline{ORF} + \overline{H}$ (5.14)	51	70
pSMM144	-196	$\overline{ORF} + \overline{H}$ (5.71)	34	70
pSMM146	-200	$\overline{ORF} + \overline{H}$ (6.1)	27	68
pJMW31	-208	$\overline{ORF} + \overline{H}$ (6.9)	34	100
pSMM141	-1,350	$\overline{ORF} + \overline{H}$ —	12	100
pJMW3	-2,150	$\overline{ORF} + \overline{H}$ —	10	100
pSMM4	—	—	3	100

See Fig. 3 legend.

sequence (Fig. 1b), indicating that the upstream element acts in *cis* with sequences at -24 and -12. Evidence for this comes from the finding that when cloned as an *Eco*RI fragment from pSMM13 into pACYC184, and present in *trans* to the upstream deleted plasmid pSMM4, there is no increase in the level of expression or multicopy inhibition from pSMM4 (data not shown). Transcriptional activity of the *nifH* upstream sequence was assessed by cloning it as an *Eco*RI-*Bam*HI fragment from pSMM1 into the transcriptional fusion vector pJEL126. Assays in UNF931 ( $\pm \text{NH}_4$ ) demonstrated that the *nifH* upstream element was transcriptionally inactive in the direction of *nifH* (data not shown). Therefore, all *nifH* transcription is initiated down-

stream and the upstream element cannot act as an independent promoter, but must act with the downstream consensus promoter sequences at -24 and -12 to facilitate multicopy inhibition and efficient transcription.

Upstream sequences are necessary for full expression of the *nifL* promoter but, unlike the *nifH* promoter, these sequences show no specificity towards *ntrC* versus *nifA* activation<sup>10</sup>. Consistent with this is the finding that the *nifL* promoter lacks sequences shown in Table 1. To examine the *nifA*-specific character of the upstream element, a hybrid promoter was constructed carrying the *nifL* downstream elements and upstream sequences from the *nifH* promoter (Fig. 2). Other constructs (see below) had demonstrated that the spacing was not critical for activation. Results (Table 2) show that the *nifH* upstream sequence restored efficient *nifA* activation to a *nifL-lac* promoter (pRD535) lacking *nifL* upstream sequences<sup>10</sup>. Although *nifA* activation was enhanced, *ntrC* activation remained low, confirming the *nifA*-specific character of the upstream element. The hybrid promoters (pSMM535 and 536) inhibited acetylene reduction in UNF931, consistent with the observation that the upstream element is required in the *nifH* and *nifU* promoters for multicopy inhibition and acts in *cis* (Fig. 1).

We constructed several mutant derivatives of the *nifH* promoter in which the spacing between the upstream and downstream elements was altered (Fig. 3, Table 3). The wild-type *nifH* promoter carries an upstream element believed to be associated with the *ORF* promoter (Fig. 3, Table 1). Starting with plasmid pSMM8, which lacks the *ORF* upstream element, we examined both the influence of the *ORF* upstream element and the orientation of the *nifH* upstream element on expression (Fig. 3), and found (Table 3) that: (1) the *ORF* sequence is not required for *nifH* promoter expression (plasmids pSMM8,

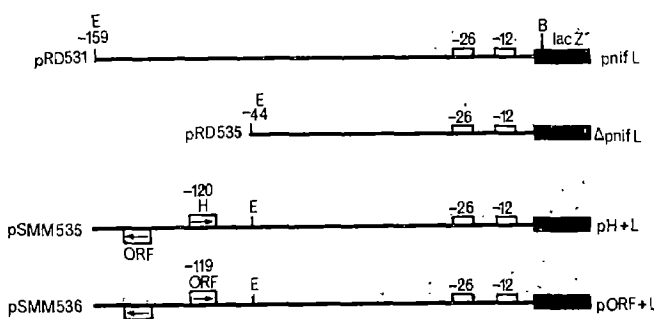
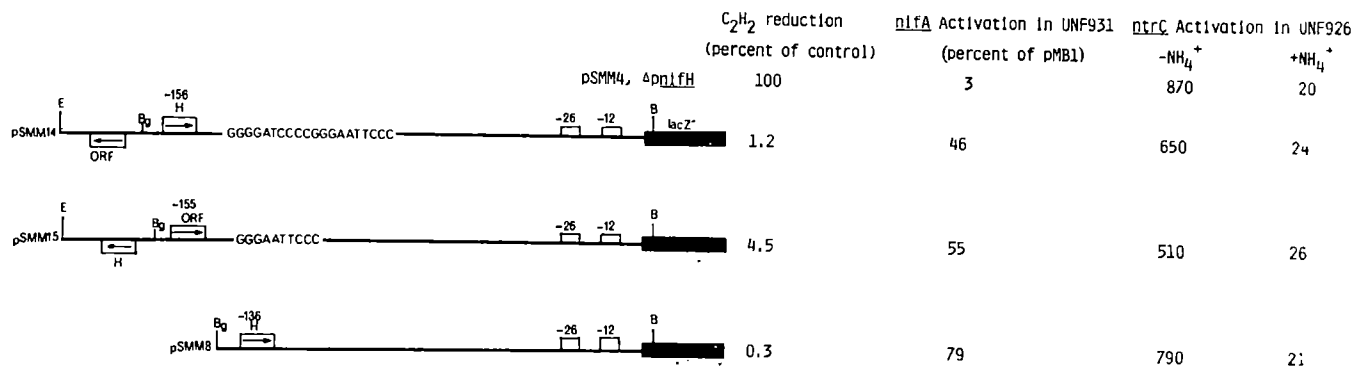


Fig. 2 Construction of hybrid *nifH-nifL* promoters. The upstream element from the *nifH* promoter clone pMB1, which carries both *nifH* and *ORF* upstream sequences, was cloned from pSMM13 (see Fig. 3 legend) as an *Eco*RI restriction fragment into *Eco*RI-linearized pRD535. Plasmid pSMM535 carries the *nifH* upstream sequence proximal to pnifL, pSMM536 carries the *ORF* upstream sequence proximal to pnifL. The position of the G residue of the TGT motif is given for plasmids pSMM535 and pSMM536.



**Fig. 3** Influence of spacer mutations and the *ORF* upstream sequence on *nifH* promoter activity (see also Table 3). Assays of activity were performed as for Fig. 1a, with *nifA* activation data being presented as a percentage of the pMB1 activity. Data from the upstream *nifH* promoter deletion plasmid pSMM4 ( $\Delta p n i f H$ ) are included for comparison. The position of the G residue of the TGT motif is indicated, and the number of turns of the helix by which this is displaced from the wild-type position at -136 is given. Plasmids pSMM14 and pSMM15 were constructed by first cloning the upstream sequence from pSMM1 into pEMBL8<sup>+</sup> on a *PstI*-*BamHI* fragment to yield pSMM13, recovering the upstream element as an *EcoRI* restriction fragment and ligating this in both orientations into pSMM4 linearized using *EcoRI*. The additional DNA gained from these cloning steps is shown. The *ORF* upstream sequence was deleted from pMB1 by treating the *BglII* fragment carrying the *nifH* promoter (and part of *lacZ*) with T4 DNA polymerase, cutting with *BamHI* and ligating into *SmaI*-*BamHI*-digested pMC1403 to yield pSMM8. To obtain the *nifH* upstream sequence on an *EcoRI* fragment in the absence of the *ORF* upstream element, the *EcoRI*-*HindIII* fragment carrying only the *nifH* upstream sequence was subcloned from pSMM8 into *EcoRI*-*SmaI*-digested pMC1403 to yield pSMM81. The *nifH* upstream sequence was then subcloned from pSMM81 as a *PstI*-*BamHI* fragment into pEMBL8<sup>+</sup> to yield pSMM82, permitting its isolation as an *EcoRI* fragment which was then ligated in both orientations into *EcoRI*-linearized pSMM4 to yield plasmids pSMM47 and pSMM48. To increase the spacing between upstream and downstream elements, the kanamycin resistance gene from PACYC177, flanked by an inverted repeat of cloning nests from pEMBL18 (M.D., unpublished), was cloned into the *HincII* fragment into the *SmaI* site of pSMM14 to yield pSMM41. Subsequent deletion of the kanamycin resistance gene by restriction with *Xba*-1, *Sma*-1 or *Asp*-718 yielded plasmids pSMM142, pSMM143 and pSMM144, respectively. Filling in the *Asp*-718 site in pSMM144 using Klenow polymerase yielded pSMM146. Cloning the  $\Omega$  insertion element<sup>31</sup> as a *SmaI* fragment from pHB34 $\Omega$  into the *SmaI* site of pSMM14 yielded pJMW3, and subsequent deletion of the insertion element using the *HindIII* sites yielded pJMW31. Plasmids pMB42 and pMB43 were obtained by cloning the *EcoRI* fragment carrying the upstream sequences from pSMM13 into pMB41. Plasmid pMB41 is deleted for nucleotides through to position -27 and carries a silent T to C transition at -27, being derived from pMB4 (ref. 4). For all upstream spacer mutants, equivalent derivatives of pSMM4 were constructed, thus carrying the packing sequences but no upstream elements. In all cases, derepression assays of these control plasmids in UNF931 produced 400–600 units of  $\beta$ -galactosidase activity.

pSMM47 and pSMM48), (2) the upstream element can activate transcription even when placed 2 kb away from the downstream promoter elements, but has an optimal position around position -136 and (3) when the orientation of the *nifH* upstream element is reversed, it is still active (plasmids pSMM8, pSMM47 and pSMM48). In the last case, the sequence of the element is 5'-CCAAATGTGGGAAACAGAACAAATTGCGC, retaining only those underlined sequences in common with the element in its usual orientation (Table 1). Nucleotides -28 to -80 of the *nifH* promoter are absent from plasmids pMB42 and pMB43, demonstrating that most nucleotides between the upstream and downstream elements are not essential for activation. Multicopy inhibition assays (Table 3) indicate that this parameter of *nifH* promoter activity is more sensitive to changes in the spatial relationship between upstream and downstream elements than is activation. However, the variability associated with the multicopy inhibition assay prevents us from determining whether a low level of inhibition can be attributed to plasmids pSMM141, pJMW3 and pJMW31.

We have suggested that the upstream promoter element is a site at which *nifA* interacts to promote transcription. For several positively controlled promoters, the proximity of activator and RNA polymerase binding sites suggests that transcriptional activators can interact directly with RNA polymerase<sup>11</sup>. Because of the greater distance over which the upstream element can act (Fig. 3), such an interaction seems unlikely in the case of *nif* promoters. Rather, we suggest that if a *nifA*-polymerase interaction is necessary for activation, it could occur either through a tertiary interaction facilitated by a folding in the DNA structure (rather than as a linear protein arrangement), as has been proposed for *araC*- and *galR*-mediated repression<sup>12,13</sup>, or through *nifA* interacting with the upstream sequence and then sliding along the DNA towards proteins located at the downstream sequences. The folding model may require that the faces of the helix containing upstream and downstream sequences

bear a strict spatial relationship to each other in order that proteins interacting with these sequences make contact correctly. However, it is not possible at present to distinguish rigorously between the various mechanistic possibilities.

The upstream sequence seems to reflect a specialization among certain *nif* promoters, not restricted to *K. pneumoniae*, permitting efficient activation by regulatory proteins functionally homologous to *nifA*. Recently, Better *et al.*<sup>14</sup> observed that upstream sequences were required for maximal activation of the *Rhizobium meliloti* *nifHDK* promoter by the *K. pneumoniae* *nifA* gene product. The promoter-down phenotype of these upstream deletions<sup>14</sup> could be attributed to the loss of the *R. meliloti* upstream promoter element (Table 1). A similar requirement for upstream sequences has been found in the expression of the *Rhizobium japonicum* *nifH* and *nifD* promoters (A. Alvarez-Morales and H. Hennecke, personal communication). It is interesting to note the similarities between the properties of the upstream DNA sequence required for activation and those of eukaryotic enhancer sequences, in particular the ability to function over a considerable distance and the independence of orientation<sup>15</sup>.

We thank J. Beynon and F. Cannon for making available unpublished *K. pneumoniae* *nif* sequence data, R. Robson for the *A. chroococcum* *nifH* sequence, W. Cannon for technical support, J. Woodcock for constructing plasmids pJMW3 and pJMW31, M. Merrick for useful discussions, and J. R. Postgate for his critical reading of the manuscript.

Received 16 December 1985; accepted 5 February 1986.

- Dixon, R. A. *J. gen. Microbiol.* **130**, 2745–2755 (1984).
- Brown, S. E. & Ausubel, F. M. *J. Bact.* **157**, 143–147 (1984).
- Ow, D. W., Xiong, Y., Gu, Q. & Shen, S.-C. *J. Bact.* **161**, 868–874 (1985).
- Buck, M., Khan, H. & Dixon, R. *Nucleic Acids Res.* **13**, 7621–7638 (1985).
- Buchanan-Wollaston, V., Cannon, M. C. & Cannon, F. C. *Molec. Genet.* **184**, 102–106 (1981).
- Travers, A. A., Lamond, A. I., Mace, H. A. F. & Berman, M. L. *Cell* **35**, 265–273 (1983).

7. Gicquel-Sanzey, B. & Cossart, P. *EMBO J.* 1, 591-595 (1983).
8. Drummond, M., Whitty, P. & Wootton, J. *EMBO J.* 5, 441-447 (1986).
9. Riedel, G. E., Brown, S. E. & Ausubel, F. M. *J. Bact.* 153, 45-56 (1983).
10. Drummond, M., Clements, J., Merrick, M. & Dixon, R. *Nature* 301, 302-307 (1983).
11. Raibaud, O. & Schwartz, M. A. *Reu. Genet.* 18, 173-206 (1984).
12. Dunn, T. M., Hahn, S., Ogden, S. & Schlief, R. F. *Proc. natn. Acad. Sci. U.S.A.* 81, 5017-5020 (1984).
13. Majumdar, A. & Adhya, S. *Proc. natn. Acad. Sci. U.S.A.* 81, 6100-6104 (1984).
14. Better, M., Ditta, G. & Helinski, D. *EMBO J.* 4, 2419-2424 (1985).
15. Dynan, W. S. & Tjian, R. *Nature* 316, 774-778 (1985).
16. Scott, K. F., Rolfe, B. G. & Shine, J. *J. molec. appl. Genet.* 1, 71-81 (1981).
17. Sundaresan, V., Jones, J. D. G., Ow, D. W. & Ausubel, F. M. *Nature* 301, 727-732 (1983).
18. Scott, K. F., Rolfe, B. G. & Shine, J. *DNA* 2, 149-155 (1983).
19. Scott, K. F., Rolfe, B. G. & Shine, J. *DNA* 2, 141-148 (1983).
20. Weinman, J. J., Fellows, F. F., Gresshoff, P. M., Shine, J. & Scott, K. F. *Nucleic Acids Res.* 12, 8329-8344 (1984).
21. Quinto, C. et al. *Proc. natn. Acad. Sci. U.S.A.* 82, 1170-1174 (1985).
22. Fuhrmann, M. & Hennecke, H. J. *Bact.* 158, 1005-1011 (1984).
23. Kaluza, K. & Hennecke, H. *Molec. gen. Genet.* 196, 35-42 (1984).
24. Yum, A. C. & Szalay, A. *Proc. natn. Acad. Sci. U.S.A.* 81, 7358-7362 (1984).
25. Better, M., Lewis, B., Corbin, D., Ditta, G. & Helinski, D. R. *Cell* 35, 479-485 (1983).
26. Bringle, K. E., Newton, W. E. & Dean, D. R. *Gene* 37, 37-44 (1985).
27. Dean, D. R. & Bringle, K. E. *Proc. natn. Acad. Sci. U.S.A.* 82, 5720-5723 (1985).
28. Schofield, P. R. & Watson, J. M. *Nucleic Acids Res.* 13, 3407-3418 (1985).
29. Hawley, D. K. & McClure, W. R. *Nucleic Acids Res.* 11, 2237-2255 (1983).
30. Casadaban, M. J., Chou, J. & Cohen, S. N. J. *Bact.* 143, 971-980 (1980).
31. Prentki, P. & Krisch, H. M. *Gene* 29, 303-313 (1984).

## Tertiary structural similarity between a class A $\beta$ -lactamase and a penicillin-sensitive D-alanyl carboxypeptidase-transpeptidase

B. Samraoui\*†‡, B. J. Sutton\*†, R. J. Todd\*†,  
P. J. Artymiuk\*‡, S. G. Waley§ & D. C. Phillips\*||

\* Laboratory of Molecular Biophysics, Rex Richards Building,  
South Parks Road, Oxford OX1 3QU, UK

† Laboratoire pour L'utilisation du Rayonnement Electromagnétique  
(LURE), CNRS-Université Paris Sud, 91405 Orsay, France

§ Sir William Dunn School of Pathology, South Parks Road,  
Oxford OX1 3QU, UK

$\beta$ -Lactam antibiotics—the penicillins, cephalosporins and related compounds—act by inhibiting enzymes that catalyse the final stages of the synthesis of bacterial cell walls<sup>1,2</sup>. Recent crystallographic studies of representative enzymes<sup>3,4</sup> are beginning to reveal the structural bases of antibiotic specificity and mechanism of action, while intensive efforts are being made to understand the  $\beta$ -lactamases that are largely responsible for bacterial resistance to these antibiotics<sup>5-8</sup>. It has been suggested that the  $\beta$ -lactamases and  $\beta$ -lactam target enzymes may be evolutionarily related<sup>9</sup> and some similarity of amino-acid sequence around a common active-site serine residue supports this idea<sup>10</sup>. We present here the first evidence from a comparison of three-dimensional structures in support of this hypothesis: the structure of  $\beta$ -lactamase I from *Bacillus cereus*<sup>11</sup> is similar to that of the penicillin-sensitive D-alanyl-D-alanine carboxypeptidase-transpeptidase from *Streptomyces R61*<sup>3</sup>.

$\beta$ -Lactamase I (EC 3.5.2.6) from *B. cereus* 569 is a member of class A, according to the classification of  $\beta$ -lactamases on the basis of amino-acid sequence<sup>12,13</sup>. It was isolated and purified following Baldwin *et al.*<sup>14</sup> and crystals were grown by a vapour-diffusion technique; although small, they diffract to high resolution<sup>15</sup>. They have unit-cell dimensions  $a = 143.0$ ,  $b = 35.8$ ,  $c = 57.2 \text{ \AA}$ ;  $\beta = 97.8^\circ$ . The space group is C2, with one molecule of  $\beta$ -lactamase I per asymmetric unit and about 50% by volume liquid of crystallization. Electron-density maps of the crystal structure have been obtained at 6  $\text{\AA}$  and at higher resolutions

up to 2.5  $\text{\AA}$  by the method of multiple isomorphous replacement combined with the use of anomalous scattering (MIRAS). Three useful heavy-atom derivatives were obtained by soaking the crystals in solutions of  $K_2Pt(C_2O_4)_2$ ,  $Sm(CH_3COO)_3$  and  $CH_3HgCl$ . X-ray diffraction data were collected photographically and, because of the very small size of the crystals, mainly by the use of synchrotron radiation at LURE, France, and at the Synchrotron Radiation Laboratory of the Science and Engineering Research Council, Daresbury. The position of the heavy atom in the Pt derivative was readily derived from isomorphous and anomalous difference Patterson maps and the heavy-atom positions in the other derivatives were obtained from difference-Fourier maps based on Pt phases. The FH<sub>H</sub> (lower estimate) and phase-refinement methods<sup>16</sup> were used to refine the heavy-atom parameters, giving the values at 2.5  $\text{\AA}$  resolution shown in Table 1. The mean figure of merit at 6  $\text{\AA}$  resolution was 0.86 and that at 2.5  $\text{\AA}$  resolution, 0.66.

At low resolution, the boundary of the protein molecule is clear and the protein density includes the rod-like features characteristic of  $\alpha$ -helices (Fig. 1). At 2.5  $\text{\AA}$  resolution, however, the electron density is disappointing, with relatively poor contrast. This is because the derivatives are not ideally isomorphous and is reminiscent of the difficulties encountered in studies of other  $\beta$ -lactamases<sup>5,6</sup>. Taken together, our results prompt consideration of the suggestion that  $\beta$ -lactamases have variable conformations<sup>17</sup>. However, the map at high resolution was much improved by use of the Wang method of density modification<sup>18</sup>, applied to the MIR phases, which clarified much of the helical density and density corresponding to a  $\beta$ -pleated sheet, and this modified map provided a satisfactory basis for determination of the structure through the iterative process of map interpretation, restrained-least-squares refinement<sup>19</sup>, phase calculation and map recalculation based on combined MIRAS and calculated phases<sup>20,21</sup>. The initial model, after least-squares refinement, gave a reliability index of 0.37 and this was reduced to 0.31 in one cycle of the iterative procedure. Figure 2 shows the five-stranded  $\beta$ -pleated sheet in the resultant combined-phase map. At this stage, the elements of secondary structure in the molecule are clearly defined, although the connections between them have not all been firmly established.

The overall dimensions of the molecule, excluding some external loops connecting secondary structures, are approximately  $33 \times 38 \times 49 \text{ \AA}$ . Figure 1a shows the arrangement of  $\alpha$ -helices and  $\beta$ -pleated sheet in the molecule; it may be described as a five-stranded  $\beta$ -pleated sheet with a group of three  $\alpha$ -helices on one side of it and five helices on the other. At this stage the molecule does not appear to consist of separate domains of the distinctness observed, for example, in phosphoglycerate kinase<sup>22</sup>, but regions of different structural types, both  $\alpha$  and  $\alpha/\beta$ , are present.

This arrangement of secondary-structure elements in  $\beta$ -lactamase I shows a striking resemblance to the structure of the penicillin-sensitive D-Ala-D-Ala carboxypeptidase-transpeptidase from *Streptomyces R61*<sup>3</sup> (hereafter referred to as R61-CPase). Figure 1b shows the positions of helices and  $\beta$ -pleated sheet in this enzyme, derived from Kelly *et al.*<sup>23</sup> by the method of Rossmann and Argos<sup>24</sup>, superimposed on the corresponding region of the low-resolution map of  $\beta$ -lactamase I. The arrangement of helices and sheet is clearly similar to that observed in the part of  $\beta$ -lactamase I shown as a heavy line in Fig. 1a and repeated, superimposed on the low-resolution electron density, in Fig. 1c. Helices A, B, C, D and H of the R61-CPase correspond well with helices in  $\beta$ -lactamase I. Furthermore, the general position of the  $\beta$ -pleated sheet is the same in the two molecules, although the sheet seems to be more extensive in  $\beta$ -lactamase I and there is a difference in the orientation of the strands of about  $25^\circ$  relative to the common helices. Three  $\alpha$ -helical regions of the  $\beta$ -lactamase I do not have helical counterparts in the R61-CPase structure, and these lie above the section of electron density shown in Fig. 1c and are shown as a faint line in Fig. 1d.

‡ Present addresses: Department of Biochemistry and Molecular Biology, Harvard University, Massachusetts 02138, USA (B.S.); Department of Biochemistry, Sheffield University, Sheffield S10 2TN, UK (P.J.A.).

|| To whom correspondence should be addressed.

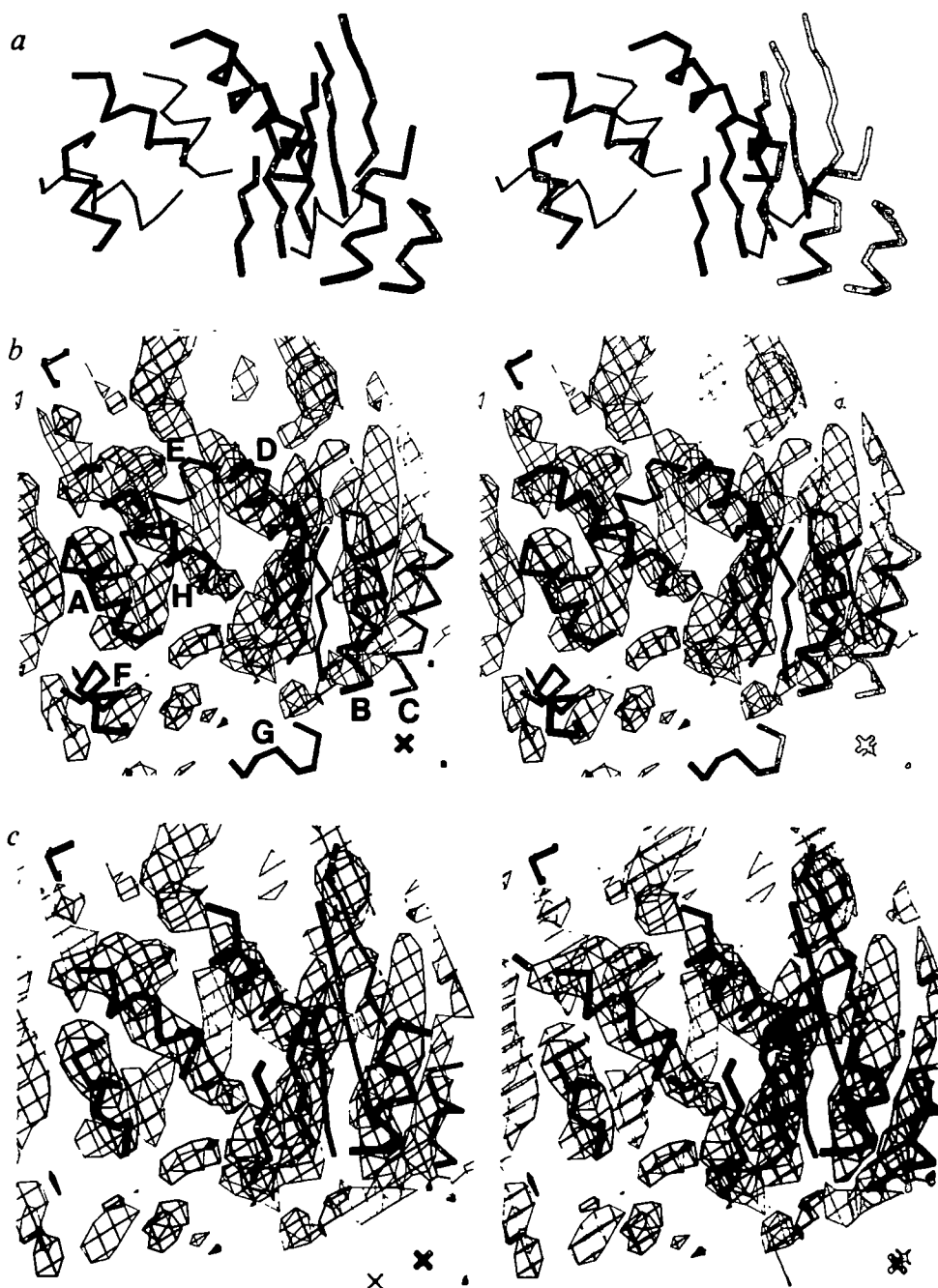


**Fig. 1** *a*, The secondary-structure elements of  $\beta$ -lactamase I derived from analysis at 2.5 Å resolution. Those shown in faint line do not correspond to features in R61-CPase. *b*, A stereo view of part of the electron density in the 6-Å MIRAS map of  $\beta$ -lactamase I with secondary structure elements of the D-Ala-D-Ala carboxypeptidase-transpeptidase from *Streptomyces* R61<sup>20</sup> superimposed. The labelling of the helices is taken from ref. 3; in this more recent model of the structure, the position of helix G is slightly altered (together with the connections between the secondary structures, which are not considered here), but it is clear that there is no electron density in the map of  $\beta$ -lactamase I which corresponds to helices E, F and G of the R61-CPase. *c*, The electron density of *b* with an  $\alpha$ -carbon atom trace of the structure of  $\beta$ -lactamase I derived at high resolution superimposed. Five of the eight  $\alpha$ -helical segments can be seen in this section of the map and model, together with the five-stranded  $\beta$ -pleated sheet.

More detailed comparisons must await a complete interpretation of the  $\beta$ -lactamase map and refinement of both structures, but it is already apparent that there is no density in  $\beta$ -lactamase I corresponding to helices E, F and G in the R61-CPase. This is in accord with the prediction of Kelly *et al.*<sup>3</sup>, made on the assumption of sequence homology between the two molecules in the N-terminal region and the difference between their relative molecular masses, that  $\beta$ -lactamases of class A would lack a part of the carboxy-terminal domain of the R61-CPase. Interestingly, however, helix H, the carboxy-terminal helix of the R61-CPase, has a counterpart in  $\beta$ -lactamase I.

This discovery that a  $\beta$ -lactamase enzyme of class A and a penicillin-sensitive D-Ala-D-Ala carboxypeptidase-transpeptidase enzyme share an extensive region of common tertiary structure suggests very strongly that these two groups of enzymes have evolved by divergence from a common ancestor<sup>25</sup>. This idea was suggested earlier by the weak but significant similarity between sequences surrounding the active-site serine residues

of the class A  $\beta$ -lactamases and two D-alanyl carboxypeptidases from *Bacillus* species<sup>10</sup>, and also the amino-terminal regions of penicillin-binding proteins from *Escherichia coli*<sup>26</sup>. Apart from the fact that the R61-CPase is also a serine enzyme, however, the incomplete sequence data available appear to show no resemblance with the class A  $\beta$ -lactamases<sup>1</sup>. The tertiary structural relationship reported here may therefore provide an example of the persistence of similarities between three-dimensional structures when the similarity between primary structures has disappeared<sup>25</sup>.

R61-CPase shares some characteristics with the class C  $\beta$ -lactamases, which again are serine enzymes<sup>27</sup>: for example, with respect to the relative rates of acylation and deacylation at the active serine residues. Whereas for  $\beta$ -lactamase I, both acylation by benzylpenicillin and deacylation are rapid, for R61-CPase acylation is more than a million times faster than deacylation<sup>2</sup> and the acyl enzyme accumulates, as it does for a class C  $\beta$ -lactamase<sup>28</sup>. The relative molecular mass of R61-CPase is

**Table 1** Refined heavy-atom parameters of the three derivatives for the final 2.5 Å-resolution phase calculation

	Scale factor	Relative occupancy	X	Y	Z	B	$R_K$
Ptb	1.0249	1.8608	0.1800	0.0000	0.2915	10.67	0.07
Ptc	1.0249	1.8559	0.1807	-0.0052	0.2914	3.78	0.08
Sm104	1.0319	0.9832	0.4977	0.3551	-0.0312	62.36	0.16
Sm105	1.0232	0.7653	0.4984	0.3570	0.0189	1.0†	0.19
Sm108	1.0178	1.3591	0.4992	0.3637	0.0194	122.29	0.12
Hg1	1.0270	1.3024	0.1777	0.0122	0.2882	21.79	0.13
Hg2	—	1.2987	0.1662	0.1443	0.4977	82.46	—
Hg3	—	0.4590	0.2315	0.1689	0.7361	55.47	—
Hg4	—	0.2778	0.2468	0.1879	0.8604	6.67	—

Overall mean figure of merit, 0.66.

$$R_K = \sum |F_{PH(obs.)} - F_{PH(cal.)}| / \sum F_{PH(obs.)}$$

where  $F_{PH(obs.)}$  and  $F_{PH(cal.)}$  are, respectively, the observed and calculated heavy-atom derivative structure factor amplitudes<sup>16</sup>. Ptb, Ptc, single-site derivative; two crystals,  $b^*$  and  $a^*$  axis data. Sm104, 105, 108, single-site derivative; three crystals,  $b^*$  axis data. Hg1–4, four-site derivative; one crystal,  $b^*$  axis data.

† Temperature factor fixed.

38,000 and in this respect also it is more similar to a class C (39,600) than to class A (29,000)  $\beta$ -lactamase. Furthermore, there is some similarity between the sequences immediately adjacent to the active-site serines of R61-CPase and class C  $\beta$ -lactamases<sup>3</sup>, as well as between a region beyond the active serine of a class C  $\beta$ -lactamase and the putative corresponding regions in PBPs of *E. coli* and the membrane-bound CPase of *Bacillus subtilis*<sup>2</sup>. There is reason to suspect, therefore, that the CPases and class C  $\beta$ -lactamases have a common evolutionary origin, although additional structural data are clearly needed to establish the relationship<sup>2</sup>. However, no sequence similarity has been detected between the class A and class C  $\beta$ -lactamases and it has been concluded, therefore, that they evolved independently<sup>3</sup>. This conclusion must now be questioned. If the CPases are indeed homologous with the class C  $\beta$ -lactamases and if, as appears from the result reported here, they are also homologous with the class A  $\beta$ -lactamases, then the CPases, the class A and the class C  $\beta$ -lactamases must all have a common evolutionary origin. Consequently, the class C  $\beta$ -lactamases may be expected to share some or all of the tertiary structural features that we have found to be common to the class A  $\beta$ -lactamase I and the R61-CPase enzymes.

Finally, we note that we may shortly be able to compare the zinc-dependent  $\beta$ -lactamase II from *B. cereus*<sup>29</sup>, the structure of which is being determined in this laboratory, with the zinc-dependent CPase from *Streptomyces albus* G (ref. 4). There is no sequence similarity between the two enzymes and the latter is only weakly sensitive to  $\beta$ -lactams, but the relationship suggested here between the serine-dependent  $\beta$ -lactamases and penicillin-sensitive enzymes prompts the thought that the zinc-dependent enzymes may also exhibit a family relationship.

We thank Sheila Gover, David Stuart, John Hellwell, Victor Inzani, V. Knott-Hunziker, Graham Knight and Joan Monks for their help with this work, Dr O. Dideberg for providing the Pt heavy-atom compound, and especially Dr R. Fourme, LURE and the SERC Daresbury Laboratory for their generous provision of synchrotron radiation facilities. This research was supported by the MRC, the E.P. Abraham Cephalosporin Trust (R.J.T.), the Algerian Government (B.S.), the Royal Society (B.J.S.) and the Science and Engineering Research Council. This is a contribution from the Oxford Enzyme Group.

Received 2 December 1985; accepted 7 February 1986.

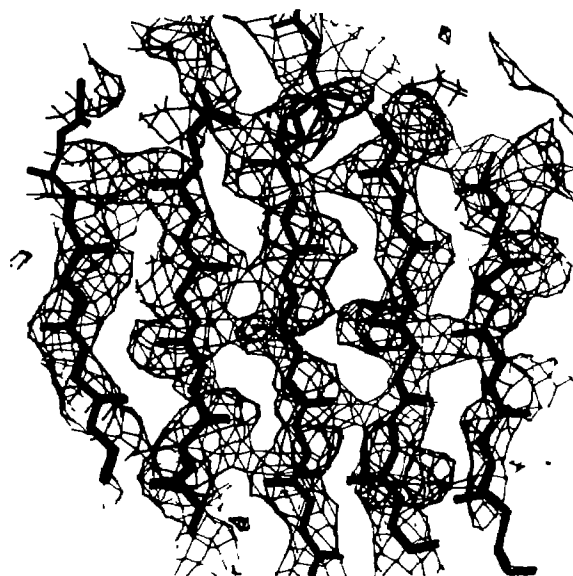


**Fig. 2** Part of the electron-density map of  $\beta$ -lactamase I at 2.5 Å resolution after preliminary refinement. Five strands of  $\beta$ -pleated sheet are shown.

- Frère, J.-M. & Joris, B. *CRC crit. Rev. Microbiol.* **11**, 299–396 (1985).
- Waxman, D. L. & Strominger, J. L. *A. Rev. Biochem.* **52**, 825–869 (1983).
- Kelly, J. A. et al. *J. biol. Chem.* **260**, 6449–6458 (1985).
- Dideberg, O. et al. *Nature* **299**, 469–470 (1982).
- Knox, J. R., Kelly, J. A., Moews, P. C. & DeLucia, M. L. in *Beta-Lactamases*, 127, (Academic, London, 1979).
- Moult, J. et al. *Biochem. J.* **225**, 167–176 (1985).
- Dideberg, O. et al. *J. molec. Biol.* **181**, 145–146 (1985).
- Charlier, P., Dideberg, O., Frère, J.-M., Moews, P. C. & Knox, J. R. *J. molec. Biol.* **171**, 237–238 (1983).
- Pollock, M. R. *Proc. R. Soc. B* **179**, 385–401 (1971).
- Waxman, D. J. & Strominger, J. L. *J. biol. Chem.* **255**, 3964–3976 (1980).
- Kuwabara, S. & Abraham, E. P. *Biochem. J.* **103**, 27c–30c (1967).
- Amblter, R. P. *Phil. Trans. R. Soc. B* **289**, 321–331 (1980).
- Jaurin, B. & Grundstrom, T. *Proc. natn. Acad. Sci. U.S.A.* **78**, 4897–4901 (1981).
- Baldwin, G. S. et al. *Biochem. J.* **191**, 111–116 (1980).
- Aschaffenburg, R. et al. *J. molec. Biol.* **120**, 447–449 (1979).
- Blundell, T. L. & Johnson, L. N. *Protein Crystallography* (Academic, London, 1976).
- Virden, R., Bristow, A. F. & Pain, R. H. *Biochem. biophys. Res. Commun.* **82**, 951–956 (1978).
- Wang, B. C. in *Diffraction Methods for Biological Macromolecules* (eds Wyckoff, H. W., Hirs, C. H. W. & Timasheff, S. N.) 90–112 (Academic, New York, 1985).
- Hendrickson, W. A. & Konnert, J. H. in *Computing in Crystallography* (eds Diamond, R., Ramaseshan, S. & Venkatesan, K.) 13.1–13.26 (Indian Academy of Sciences, Bangalore, 1980).
- Stuart, D. I. & Artyniuk, P. J. *Acta crystallogr.* **A40**, 713–716 (1984).
- Huber, R. et al. *J. molec. Biol.* **89**, 73–101 (1984).
- Banks, R. D. et al. *Nature* **279**, 773–777 (1979).
- Kelly, J. A., Moews, P. C., Knox, J. R., Frère, J.-M. & Ghysen, J.-M. *Science* **218**, 479–481 (1982).
- Rossmann, M. G. & Argos, P. *Acta crystallogr.* **B36**, 819–823 (1980).
- Phillips, D. C., Sternberg, M. J. E. & Sutton, B. J. in *Evolution from Molecules to Men* (ed. Bendall, D. S.) 145–173 (University of Cambridge Press, 1983).
- Waxman, D. J., Amanuma, H. & Strominger, J. L. *FEBS Lett.* **139**, 159–163 (1982).
- Coulson, A. *Biotechnol. genet. Engng Rev.* **3**, 219–253 (1985).
- Knott-Hunziker, V., Petrusson, S., Waley, S. G., Jaurin, B. & Grundstrom, T. *Biochem. J.* **207**, 315–322 (1982).
- Sabath, L. D. & Abraham, E. P. *Biochem. J.* **98**, 11c–13c (1966).

## Estimation of scrapie nucleic acid MW from standard curves for virus sensitivity to ionizing radiation

IN an unusually rancorous communication to this forum<sup>1</sup>, Alper protests Fig. 4 of my letter<sup>2</sup> in which I constructed standard curves for the inactivation of single-stranded (ss) or double-stranded (ds) viruses by ionizing radiation versus their nucleic acid molecular weights (MWs). Extrapolation of either line to the inactivation rate constant ( $D_{37}$ ) of the scrapie virus gave virus-like values for the scrapie genome. This is in sharp contrast to values of 150,000 daltons or less calculated from the 'target theory' by Alper<sup>3</sup> and others<sup>2</sup>.

In defending her target calculation<sup>1</sup>, Alper denounces my use of previous reviews (as a source of data for constructing these curves, incorrectly), asserting that "some of the references are wrong" and that few of the references were checked. She gives the following four examples:

**Yellow fever virus (YFV).** Alper: "Molecular weight too low, about one-tenth of what we took from our independent source. Rohwer's source makes no mention of the MW of this virus." The YFV RNA has been sequenced and has a MW of  $3.7 \times 10^6$  daltons<sup>4</sup>, in good agreement with the value plotted in Fig. 4,  $3.5 \times 10^6$  daltons (as given by) my source<sup>5</sup> (on page 18). The "independent source" preferred by Alper is an ultrastructural study of intact YFV virions. Her value was apparently estimated from the virion core diameter.

**Vaccinia.** Alper: " $D_{37}$  incorrectly quoted by Rohwer from K & M [Kaplan and Moses] who cited McCrea incorrectly." Kaplan and Moses<sup>7</sup> give a range of values for vaccinia obtained from multiple determinations by McCrea<sup>8</sup> and Wilson<sup>9</sup>, both of whom they cite. I plotted the mean of the range. Alper ignores Wilson<sup>9</sup>, selects the single value from McCrea<sup>8</sup> most favourable to her argument, which is also the only determination that appears to have been made under vacuum, and then objects to the use of vacuum.

**Shope papilloma.** Alper: " $D_{37}$  plotted as too high to fit the Lea theory. K & M's source is Syverton *et al.*, who gave the dose for 'total inactivation'—an unknown multiple of the inactivation dose...". Indeed Syverton *et al.*<sup>10</sup> summarize their data in terms of total inactivation rather than inactivation rate constant. However, the rate constant is easily calculated from the data in experiments II–IV and this is the value cited by K & M and plotted in Fig. 4. The identical value was obtained by Lea *et al.*<sup>11</sup> in their analysis of the

completely independent measurements of Friedewald and Anderson<sup>12</sup>.

**Newcastle<sup>12</sup> disease virus (NDV).** Alper: "Inactivation dose too low... Rubin and Temin... irradiated the virus in suspension." NDV has also been irradiated dry<sup>13</sup>, giving a rate constant even smaller than that plotted in Fig. 4. Most investigators, aware that viruses tolerate drying poorly, suspend viruses in broth, serum or tissue homogenates, either wet or frozen, to protect against indirect effects, and for this reason most of the available data have been obtained in suspension. While Alper insists that viruses be irradiated dry, she invokes this argument to discard only the particularly inconvenient NDV point from Fig. 4. If we apply her criteria consistently and consider only the five viruses irradiated dry in Fig. 4 (three from her own laboratory), both the line for the ss viruses and that for the ds viruses closely parallel the original regression lines in Fig. 4 predicting ds scrapie genome of MW  $2.0 \times 10^6$  daltons or a ss genome of  $0.86 \times 10^6$  daltons. These results are consistent with a larger study to be published separately (manuscript in preparation), in which each state, liquid, frozen and dry, was considered separately.

Using these four highly contrived 'examples', Alper alleges that the integrity of Fig. 4 is compromised by the use of previous reviews in documenting the data. *Nature's* succinct format necessitated the use of reviews where possible and did not permit elaboration on individual data points in the two paragraphs of text devoted to Fig. 4.

Alper intimates that low-temperature inactivations may be in error. While it is true that some viruses<sup>14</sup>, but not others<sup>15</sup>, show enhanced protection at liquid nitrogen temperatures ( $-196^\circ\text{C}$ ), the only frozen specimens in Fig. 4 were at dry ice temperatures ( $-78^\circ\text{C}$ ), where the available evidence<sup>15,16</sup>, including that for scrapie<sup>17,18</sup>, suggests virus inactivation kinetics similar to those obtained dry.

Alper's most surprising suggestion is that ss and ds viruses (and even proteins) be regressed as a single group. This is in spite of overwhelming evidence that ss viruses show a 20–40-fold greater sensitivity to inactivation than do ds viruses of similar genome size<sup>7,19–24</sup>. This difference derives in part from the ease with which many otherwise lethal single-strand lesions can be repaired in ds DNA.

As noted by Alper, crude tissue suspensions of the scrapie agent show greater sensitivities to inactivation at ultraviolet wavelengths below the 254 nm maximum typical of some viruses<sup>25</sup>. However, a similar inactivation spectrum is observed for tobacco mosaic virus (TMV)<sup>26</sup> and, to a lesser extent, potato X virus<sup>27</sup>. The absence of other examples may only reflect the limited number of viruses for which an inactivation spectrum has been determined rather than the actual prevalence of this presumed anomaly in nature. It may be noteworthy that TMV and potato X share a filamentous morphology with the scrapie-associated fibril<sup>28</sup>, a candidate structure for the scrapie virus<sup>29</sup>.

Standard curves, such as those in Fig. 4, are the preferred method of measurement in biophysical procedures such as sedimentation and electrophoresis where adequate standards exist. Now that  $D_{37}$  values can be calibrated against exact, sequence-based MWs for dozens of viruses<sup>30</sup>, it no longer makes sense to attempt the estimation of nucleic acid MWs from first principles using the target theory. Moreover, past attempts to do so have seriously misled scrapie investigation.

ROBERT G. ROHWER

Department of Microbiology  
and Immunology,  
311 Lineberger Cancer Research  
Center 237H,  
University of North Carolina,  
Chapel Hill,  
North Carolina 27514, USA

1. Alper, T. *Nature* **317**, 750 (1985).
2. Rohwer, R. G. *Nature* **308**, 658–662 (1984).
3. Alper, T., Haig, D. A. & Clarke, M. C. *Biochem. biophys. Res. Commun.* **22**, 278–284 (1966).
4. Rice, C. M. *et al.* *Science* **229**, 726–733 (1985).
5. Fraenkel-Conrat, H. *Compreh. Virol.* **1**, 18 (1974).
6. Bergold, G. J. & Weibel, J. *Virology* **17**, 554–562 (1962).
7. Kaplan, H. S. & Moses, L. E. *Science* **145**, 21–25 (1964).
8. McCrea, J. F. *Ann. N.Y. Acad. Sci.* **83**, 692–705 (1960).
9. Wilson, D. E. *Radiat. Res.* **14**, 796–802 (1961).
10. Syverton, J. T., Berry, G. P. & Warren, S. L. *J. exp. Med.* **74**, 223–234 (1941).
11. Lea, D., Smith, K. M., Holmes, B. & Markham, R. *Parasitology* **36**, 110–118 (1944).
12. Friedewald, W. F. & Anderson, R. S. *J. exp. Med.* **74**, 463–487 (1941).
13. Woese, C. & Pollard, E. *Archs Biochem. Biophys.* **50**, 354–367 (1954).
14. Hotz, G. *Molec. Biol. Biochem. Biophys.* **27**, 304–311 (1978).
15. Ginoza, W. *Nature* **199**, 453–456 (1963).
16. Ginoza, W. & Norman, A. *Nature* **179**, 520–521 (1957).
17. Alper, T. & Haig, D. A. *J. gen. Virol.* **3**, 157–166 (1968).
18. Gibbs, C. J. Jr, Gajdusek, D. C. & Latarjet, R. *Proc. natn. Acad. Sci. U.S.A.* **75**, 6268–6270 (1978).
19. Terzi, M. *Nature* **191**, 461–463 (1961).
20. Ginoza, W. *Meth. Virol.* **4**, 139–209 (1968).
21. Schambra, F. E. & Hutchinson, F. *Radiat. Res.* **23**, 514–526 (1964).
22. Tessman, I., Tessman, E. S. & Stent, G. S. *Virology* **4**, 209–215 (1957).
23. Ginoza, W. & Miller, R. C. *Proc. natn. Acad. Sci. U.S.A.* **54**, 551–558 (1965).
24. Hotz, G. & Muller, A. Z. *Naturforsch.* **16b**, 282–283 (1961).
25. Latarjet, R., Muell, B., Haig, D. A., Clarke, M. C. & Alper, T. *Nature* **227**, 1341–1343 (1970).
26. McLaren, A. D. *Photochem. Photobiol.* **8**, 521–525 (1968).
27. Kleczkowski, A. & Govier, D. A. *Photochem. Photobiol.* **10**, 53–59 (1969).
28. Merz, P. A., Somerville, R. A., Wisnewski, H. M. & Iqbal, K. *Acta neuropath.* **54**, 63–74 (1981).
29. Merz, P. A. *et al.* *Science* **225**, 437–440 (1984).
30. GenBank (Computer Systems Division, Bolt Beranek & Newman Inc., Cambridge, Massachusetts)

# BOOKS RECEIVED

## Applied Biological Sciences

**Advances in Biotechnological Processes**, Vol. 4. AVSHALOM MIZRAHI and ANTONIUS L. VAN WEZEL (eds). *Alan R. Liss*:1985. Pp.356. ISBN 0-8451-3023-2. £64.

**Alcoholism and Substance Abuse: Strategies for Clinical Intervention**. By THOMAS E. BRATTER and GARY G. FORREST. *Collier Macmillan*:1985. Pp.650. ISBN 0-02-904260-7. £40.

**Annual Reports in Medicinal Chemistry**, Vol. 20. D. M. BAILEY (ed.). *Academic*:1985. Pp.352. ISBN 0-12-040520-2. Np.

**Antibodies: Protective, Destructive and Regulatory Role**. F. MILGROM, C.J. ABEYOUNIS and B. ALBINI (eds). *Karger*:1985. Pp.462. ISBN 3-8055-3990-8. *SwFr*.375, DM 450, \$159.75.

**Atlas of Positron Emission Tomography of the Brain**. By W.-D. HEISS, C. BELL, K. HERHOLTZ, G. PAWLICK, R. WAGNER and K. WIENHARD. *Springer-Verlag*:1985. (*German and English*) Pp.130. *Hbk* ISBN 3-540-15636-4. DM 148.

**"Autistic" Children: New Hope for a Cure**. By N. and E.A. TINBERGEN. *George Allen & Unwin*:1985. Pp.362. *Hbk* ISBN 0-04-157010-3; *pbk* ISBN 0-04-157011-1. *Pbk* £9.95.

**Carcinogenesis: A Comprehensive Survey**. J. CARL BARRETT and RAYMOND W. TENNANT (eds). *Raven*:1985. Pp.461. ISBN 0-88167-116-9. \$70.50.

**Communication Problems in Autism**. ERIC SCHOPLER and GARY B. MESIBOV (eds). *Plenum*:1985. Pp.333. *Hbk* ISBN 0-306-41859-2. Np.

**Comparison of Type I and Type II Diabetes: Similarities and Dissimilarities in Etiology, Pathogenesis, and Complications**. MLA DEN VRANIC, CHARLES H. HOLLENBERG and GEORGE STEINER (eds). *Plenum*:1985. Pp.349. ISBN 0-306-42066-X. Np.

**Contemporary Topics in Immunobiology**, Vol. 15: Immune Complexes and Human Cancer. FERNANDO A. SALINAS and MICHAEL G. HANNA Jr (eds). *Plenum Press*:1985. Pp.280. ISBN 0-306-41955-6. Np.

**Decision-Making in General Practice**. MICHAEL SHELDON, JOHN BROOKES and ALAN RECTOR (eds). *Macmillan, London*:1985. Pp.269. ISBN 0-333-36626-3. £25.

**Dietary Fibre, Fibre-Depleted Foods and Disease**. HUGH TROWELL, DENIS BURKITT and KENNETH HEATON (eds). *Academic*:1985. Pp.433. ISBN 0-12-701160-9. \$64.50, £49.50.

**Directory of On-going Research in Cancer Epidemiology** 1985. C.S. MUIR and G. WAGNER (eds). *International Agency for Research on Cancer, World Health Organization*:1985. Pp.756. *Pbk* ISBN 92-321169-3. £22.

**Encounters with Qi: Exploring Chinese Medicine**. By DAVID EINSENBERG. *W.W. Norton*:1985. Pp.254. ISBN 0-393-02213-7. \$16.95.

**Ethical Issues in Preventative Medicine**. SYPROS DOXIADIS (ed.). *Martinus Nijhoff*:1985. Pp.108. *Hbk* ISBN 90-247-3232-8. Np.

**Evaluation of Large Ruminants for the Tropics**. J.W. COPLAND (ed.). *Australian Centre of International Agricultural Research (ACIAR)*, G.P.O. Box 1571, Canberra, Australia:1985. Pp.178. *Pbk* ISBN 0-949511-09-9. Np.

**Experimental Research on Vinylidene Chloride Carcinogenesis**. CESARE MALTONI et al. (eds). *Princeton Scientific/Wiley*:1985. Pp.229. ISBN 0-911131-38-8. £83.60.

**Familial Cancer**. H.J. MULLER, W. WEBER and T. KUTTAPPA (eds). *Karger*:1985. Pp.292. *Hbk* ISBN 3-8055-4245-3. *SwFr*.185, DM 222, £57.90, \$78.75.

**Free Radicals in Biology and Medicine**. Life Chemistry Reports, Vol. 3, No. 1 and 2. J.V. BANNISTER, B. HALLIWELL and P. O'NEILL (eds). *Harwood Academic Publishers*:1985. *Pbk* ISBN 3-7186-0285-7. \$69.

**Functional Mapping of the Brain in Vascular Disorders**. WOLF-DIETER HEISS (ed.). *Springer-Verlag*:1985. Pp.126. *Pbk* ISBN 3-540-15801-4. DM 56.

**Handbook of Clinical Behaviour Therapy with Adults**. MICHEL HERSEN and ALAN S. BEL-LACK (eds). *Plenum*:1985. Pp.732. ISBN 0-306-41875-4. Np.

**Handbook of Laboratory Health and Safety Measures**. S.B. PAL (ed.). *MTP Press*:1985. Pp.391. ISBN 0-85200-766-3. £59.95.

**Hepatitis**. B. ROBERT J. GERETY (ed.). *Academic*:1985. Pp.470. *Hbk* ISBN 0-12-280672-7. £68.50, \$79.

**Interaction Theory in Forest Ecology and Management**. By ROLFE A. LEARY. *Martinus Nijhoff/Dr W. Junk*:1985. Pp.219. *Hbk* ISBN 90-247-3220-4. Np.

**Interferon**, 6, 1985. IAN GRESSER (ed.). *Academic*:1985. Pp.143. ISBN 0-12-302255-X. \$25, £16.

**Interpretation of Endometrial Biopsies**, 2nd Edn. By ANCEL BLAUSTEIN. *Raven Press*:1985. Pp.304. *Hbk* ISBN 0-88167-120-7. £42.50.

**Interpretation of Negative Epidemiological Evidence for Carcinogenicity**. N.J. WALD and R. DOLL (eds). *International Agency for Research on Cancer*:1985. Pp.232. *Hbk* ISBN 92-832-1165-0. £20.

**An Introduction to Human Ecology Research on Agricultural Systems in Southeast Asia**. A. TERRY RAMBO and PERCY E. SAJISE (eds). *University of the Philippines at Los Baños*:1985. Pp.327. *Pbk* ISBN 0-86638-062-0. Np.

**Iron Fortification of Foods**. FERGUS M. CLYDESDALE and KATHRYN L. WIEMER (eds). *Academic*:1985. Pp.176. ISBN 0-12-177060-5. \$36.50, £32.50.

**Laser Photobiology and Photomedicine**. S. MARTELLUCCI and A.N. CHESTER (eds). *Plenum*:1985. Pp.334. *Hbk* ISBN 0-306-41915-7. Np.

**Leukotrienes in Cardiovascular and Pulmonary Function**. *Progress in Clinical and Biological Research*, Vol. 199. ALLAN M. LEFER and MARLYS H. GEE (eds). *Alan R. Liss*:1985. Pp.270. *Hbk* ISBN 0-8451-5049-9. £32.

**The Meaning of Addiction: Compulsive Experience and its Interpretation**. By STANTON PEELE. *Lexington Books*:1985. Pp.203. ISBN 0-669-02952-1. £25.

**Mechanisms of Resistance to Plant Diseases**. R.S.S. FRASER (ed.). *Martinus Nijhoff/Dr W. Junk Publishers*:1985. Pp.462. *Hbk* ISBN 90-247-3204-2. Dfl. 190, £71.

**The Medical and Biological Effects of Light**. *Annals of the New York Academy of Sciences*, Vol. 453. RICHARD J. WURTMAN, MICHAEL L. BAUM and JOHN T. POTTS Jr (eds). *The New York Academy of Sciences*:1985. Pp.408. *Hbk* ISBN 0-89766-300-4; *pbk* ISBN 0-89766-301-2. Np.

**Metal Ions in Biological Systems**, Vol. 19. *Antibiotics and Their Complexes*. HELMUT SIGEL (ed.). *Dekker*:1985. Pp.429. ISBN 0-8247-7425-6. £85.

**Microsurgery of Cerebral Aneurysms: An Atlas**. By ZENTARO ITO. *Nishimura/Elsevier*:1985. Pp.299. *Hbk* ISBN 90-219-3062-5. Dfl. 600, \$222.25.

**Modern Trends in Leukemia VI: New Results in Clinical and Biological Research Including Pediatric Oncology**. ROLF NETH, ROBERT C. GALLO, MELVYN F. GREAVES and GRITTA JANKA (eds). *Springer-Verlag*:1985. Pp.521. *Pbk* ISBN 3-540-15329-2. DM 198.

**Myelofibrosis: Pathophysiology and Clinical Management**. S.M. LEWIS (ed.). *Marcel Dekker*:1985. Pp.207. ISBN 0-8247-7411-6. £78.

**New Cardiovascular Drugs**, 1985. ALEXANDER SCRABINE (ed.). *Raven*:1985. Pp.308. ISBN 0-88167-114-2. £54.50.

**Nuclear Medicine Annual** 1985. LEONARD M. FREEMAN and HEIDI S. WEISSMANN (eds). *Raven*:1985. Pp.362. ISBN 0-88167-086-3. £70.50.

**The Patient Within the Patient: Problems in Perinatal Medicine**. BRUCE K. YOUNG (ed.). *Alan R. Liss*:1985. Pp.240. *Hbk* ISBN 0-8451-1060-8. £30.

**Pediatric Differential Diagnosis**, 2nd Edn. By STEPHEN H. SHELDON and HOWARD B. LEVY. *Raven Press*:1985. Pp.209. *Pbk* ISBN 0-88167-112-6. Np.

**Pharmaceuticals Among the Sunrise Industries: Proceedings of an Office of Health Economics Symposium**. NICHOLAS WELLS (ed.). *Croom Helm*:1984. Pp.240. ISBN 0-7099-1947-6. £19.95.

**Physical Chemistry: Principles and Applications in Biological Sciences**, 2nd Edn. By IGNACIO TINO CO. JR., KENNETH SAUER and JAMES C. WANG. *Prentice-Hall*:1985. Pp.706. ISBN 0-13-666280-3. £37.40.

**Practice and Theory of Enzyme Immunoassays**. P. TIJSSEN (ed.). *Elsevier*:1985. Pp.549. *Hbk* ISBN 0-444-80634-2; *pbk* ISBN 0-444-80633-4. *Hbk* Dfl. 260, £96.25; *pbk* Dfl. 85, \$31.50.

**Principles of Metastasis**. By L. WEISS. *Academic*:1985. Pp. 425. ISBN 0-12-742820-8. \$52, £52.

**Progress in Applied Microcirculation: Resistance Vessels: Physiology, Pharmacology and Hypertensive Pathology**. M.J. MULVANY et al. (eds). *Karger*:1985. Pp. 226. *SwFr*. 140, DM 168, \$59.75.

**Progress in Clinical and Biological Research**, Vol. 178. **Bluetongue and Related Orbiviruses**. T. LYNNWOOD BARBER and MICHAEL M. JOCHIM (eds). *Alan R. Liss*:1985. Pp.772. ISBN 0-8451-5028-6. £84.

**Progress in Clinical and Biological Research**, Vol. 185A: **EORTC Genitourinary Group, Monograph 2**, Pt A. **Therapeutic Principles in Metastatic Prostate Cancer**. FRITZ H. SCHROEDER and BRIAN RICHARDS (eds). *Alan R. Liss*:1985. Pp.474. ISBN 0-8451-0188-9. £52.

**Progress in Clinical and Biological Research**, Vol. 185B: **EORTC Genitourinary Group, Monograph 2**, Pt B. **Superficial Bladder Tumors**. FRITZ H. SCHROEDER and BRIAN RICHARDS (eds). *Alan R. Liss*:1985. Pp.179. ISBN 0-8451-0189-7. £26.

**The Pyrethroid Insecticides**. J.P. LEAHY (ed.). *Taylor & Francis*:1985. Pp.440. *Hbk* ISBN 0-85066-283-4. £45.

**Radiolabeled Cellular Blood Elements: Pathophysiology, Techniques and Scintigraphic Applications**. **NATO ASI Series**. M.L. THAKUR (ed.). *Plenum*:1985. Pp.434. *Hbk* ISBN 0-306-41935-1. Np.

**Recent Achievements in Restorative Neurology**, Vol. 1: **Upper Motor Neuron Functions and Dysfunctions**. JOHN ECCLES and MILAN R. DIMITRIJEVIC (eds). *Karger*:1985. Pp.345. ISBN 3-8055-4020-5. *SwFr*.279, DM 335, \$118.75, £87.20.

**Surgical Pharmacology of the Eye**. MARVIN L. SEARS and AHTI TARKKANEN (eds). *Raven*:1985. Pp.592. ISBN 0-88167-047-2. \$65.50.

**The Tetracyclines**. J.J. HLAVAKA and J.H. BOOTHE (eds). *Springer-Verlag*:1985. Pp.451. *Hbk* ISBN 3-540-15259-8. Np.

**Toxic Susceptibility: Male/Female Differences**. By EDWARD J. CALABRESE. *Wiley*:1985. Pp.336. ISBN 0-471-80903-9. £61.35.

**Toxicology of Insecticides**, 2nd Edn. By FUMIO MATSUMURA. *Plenum*:1985. Pp.598. *Hbk* ISBN 0-306-419-79-3. \$45.

**Ultrasound Annual** 1985. ROGERS C. SANDERS and MICHAEL C. HILL (eds). *Raven Press*:1985. Pp.381. *Hbk* ISBN 0-88167-143-6. £76.50.

**Your Healthy Heart. A Guide to How the Heart Works and How to Keep it Healthy**. By CHRISTIAAN BARNARD and PETER EVANS. *Macdonald*:1985. Pp.224. ISBN 0-356-10524-5. £12.95.

## Psychology

**Accounting for Aggression: Perspectives on Aggression and Violence**. By GERDA SIANN. *Allen & Unwin*:1985. Pp.294. ISBN 0-04-301188-8. £6.95.

## General

**Analysis of Experiments with Missing Data**. By YADOLAH DODGE. *Wiley*:1985. Pp.499. *Hbk* ISBN 0-471-88736-6. £40.85.

**Aspects of Symmetry: Selected Erice Lectures**. By SIDNEY COLEMAN. *Cambridge University Press*:1985. Pp.402. ISBN 0-521-26706-4. Np.

**Constructing the Universe**. By DAVID LAYZER. *W.H. Freeman*:1985. Pp.313. ISBN 0-7167-5003-1. £27.95.

**Das Phänomen des Polarlichts**. By WILFRIED SCHRÖDER. *Wissenschaftliche Buchgesellschaft, Darmstadt, FRG*:1984. Pp.156. *Pbk* ISBN 3-534-08997-9. *Pbk* DM 37.50.

**Digital Communications and Spread Spectrum Systems**. By ROGER E. ZIEMER and ROGER L. PETERSON. *Collier Macmillan*:1985. Pp.750. *Hbk* ISBN 0-02-431670-9. £38.

## Author Index for Volume 319

### January — February 1986

Issue no.	Issue date	Pagination
6048	2 January	1-84
6049	9 January	85-162
6050	16 January	163-248
6051	23 January	249-342
6052	30 January	343-434
6053	6 February	435-522
6054	13 February	523-606
6055	20 February	607-706
6056	27 February	707-826

- Abe, Y. *See under* Matsui, T., 319, 303  
 Acton, J R. Solving Equations with Physical Understanding, *Book review by* Upstill, C., 319, 820  
 Ada, G L. *See under* Brown, F., 319, 549  
 Agullera, G. *See under* Uedelman, R., 319, 147  
*See under* Holmes, M C., 319, 326  
 Ahmad, S. Observation of a dislocation source in ice by synchrotron radiation topography (with Ohtomo, M, Whitworth, R W) *Letter to Nature*, 319, 659  
 Akyaiye, D E. Aeromagnetic anomalies and tectonic trends in and around the Benue Trough, Nigeria (with Hall, D H, Millar, T W, Verheijen, P J T, Awad, M B, Ojo, S B) *Letter to Nature*, 319, 582  
 Akam, M. Developmental genes: Mediators of cell communication? *News and views*, 319, 447  
*Book review of* From Gene to Animal: An Introduction to the Molecular Biology of Animal Development (by De Pomerai, D.) 319, 806  
 Akyama, T. *See under* Yamamoto, T., 319, 230  
 Alexander, R McN. Human energetics: Making headway in Africa, *News and views*, 319, 623  
 Alexeev, A. *See under* Bregestovski, P., 319, 776  
 Allen, D A. *See under* Sanders, R H., 319, 191  
 Allen, J R L. Principles of Physical Sedimentology, *Book review by* Allen, P., 319, 813  
*Experiments in Physical Sedimentology, Book review by* Allen, P., 319, 813  
 Allen, P. *Book review of* Principles of Physical Sedimentology (by Allen, J R L.) 319, 813  
*Book review of* Experiments in Physical Sedimentology (by Allen, J R L.), 319, 813  
 Allen, R J. Large-scale dissociation of molecular gas in galaxies by newly formed stars (with Atherton, P D, Tilanus, R P J) *Letter to Nature*, 319, 296  
 Alt, F W. *See under* Kohl, N E., 319, 73  
*See under* Zimmerman, K A., 319, 780  
 Amasino, R M. *See under* Furner, I J., 319, 422  
 Ambrose, S H. Reconstruction of African human diet using bone collagen carbon and nitrogen isotope ratios (with DeNiro, M J) *Letter to Nature*, 319, 321  
 Andersen, J L. *See under* Weathers, K C., 319, 657  
 Anderson, A. Japanese public health: New campaign launched against hepatitis B, *News*, 319, 3  
*Japanese communications: What band-rate for psi?*, *News*, 319, 5  
*Japanese technology: First sale overseas of military equipment*, *News*, 319, 87  
*Japanese science budget: Some gains, some losses*, *Opinion*, 319, 252  
*Japanese education: Uncertain future for reform*, *News*, 319, 347  
*Japanese research: Small increase brings big gains*, *News*, 319, 528  
*Japanese broadcasting satellites: Toshiba pays price of failure*, *News*, 319, 613  
*Environmental pollution: Does Japan have acid rain?*, *News*, 319, 711  
*The Japan Prize*, *News*, 319, 714  
*Japan likely to participate in SDI*, *News*, 319, 714  
 Anderson, E. *See under* Morris, R G M., 319, 774  
 Anderson, J R. Cognitive Psychology and its Implications, 2nd Edn., *Book review by* Sutherland, S., 319, 798  
*Book review of* The Evolution of Primate Behaviour, 2nd Edn. (by Jolly, A.), 319, 800  
 Andersson, W H. *See under* Reeves, K R., 319, 94  
 Andersson, K. *See under* Skoglund, U., 319, 560  
 Andersson, M. *See under* Götsmark, F., 319, 589

- André, J J. Molecular Semiconductors: Photoelectrical Properties and Solar Cells, *Book review by* Eley, D D., 319, 458  
 Andrews, R P. Product Review: Automated continuous flow peptide synthesis, *Miscellany*, 319, 429  
 Antoni, F A. *See under* Holmes, M C., 319, 326  
 Arnold, J R. *See under* Nishizumi, K., 319, 134  
*See under* Kubik, P W., 319, 568  
 Arnold, M H. Plant gene conservation (with Astley, D, Bell, E A, Bleasdale, J K A, Bunting, A H, Burley, J, Callow, J A, Cooper, J P, Day, P R, Ellis, R H, Ford-Lloyd, B V, Giles, R J, Hawkes, J G, Hayes, J D, Henshaw, G G, Heslop-Harrison, J, Heywood, V H, Innes, N L, Jackson, M T, Jenkins, G, Lawrence, M J, Lester, R N N, Matthews, P, Mumford, P M, Roberts, E H, Simmonds, N W, Smartt, J, Smith, R D, Tyler, B, Watkins, R, Whitmore, T C, Withers, L A) *Correspondence*, 319, 615  
 Arthaud, F. *See under* Cyaden Scientific Team., 319, 396  
 Asano, S. *See under* Nagata, S., 319, 415  
 Ashcroft, W A. Corrigendum: Major shear zones and autochthonous Dalradian in the north-east Scottish Caledonides (with Kneller, B C, Leslie, A G, Munro, M) *Letter to Nature*, 319, 606  
 Aspden, H. Earnshaw's theorem, *Correspondence*, 319, 8  
 Astley, D. *See under* Arnold, M H., 319, 615  
 Atherton, P D. *See under* Allen, R J., 319, 296  
 Atkins, P W. Physical Chemistry, 3rd Edn., *Book review by* Rigby, M., 319, 820  
 Atkinson, B G. Editor, Changes in Eukaryotic Gene Expression in Response to Environmental Stress, *Book review by* Prosser, C L., 319, 187  
 Attенborough, R. *Book review of* The Descent of Woman: A New Edition (by Morgan, E.), 319, 271  
*Book review of* Myths of Gender: Biological Theories About Women and Men (by Fausto-Sterling, A.) 319, 271  
 Au, C T. Specific role of transient O<sup>2</sup>(s) at Mg(0001) surfaces in activation of ammonia by dioxygen and nitrous oxide (with Roberts, M W) *Letter to Nature*, 319, 206  
 Auerbach, S. *See under* Farley, J., 319, 220  
 Aurora, P E. *See under* Wolff, S M., 319, 270  
 Avravay, B. *See under* Cyaden Scientific Team., 319, 396  
 Azuende, J M. *See under* Cyaden Scientific Team., 319, 396  
 Awab, M B. *See under* Ajakaiye, D E., 319, 582  
 Awramik, S M. Palaeontology: New fossil finds in old rocks, *News and views*, 319, 446  
*The Precambrian-Cambrian boundary and geochemical perturbations*, *Matters arising*, 319, 696  
 Axford, W I. The magnetic field of Uranus (with Vasiliunas, V M) *Scientific correspondence*, 319, 267  
 Azuma, C. *See under* Noma, Y., 319, 640  
 Bada, J L. Isoleucine stereoisomers on the Earth (with Zhao, M, Steinberg, S, Ruth, E) *Letter to Nature*, 319, 314  
 Badgley, C. Estimating the error of age interpolation in sedimentary rocks (with Taube, L, Bookstein, F L) *Letter to Nature*, 319, 139  
 Bahn, P G. *Book review of* On the Track of Ice Age Mammals (by Sutcliffe, A J.) 319, 273  
 Baldwin, A. Animal intelligence, *Correspondence*, 319, 172  
 Bailey, A I. *See under* Hayati, I., 319, 41  
 Balmer, A J. Synapsin I is a microtubule-bundling protein (with Bennett, V) *Letter to Nature*, 319, 145  
 Baker, P F. *Book review of* Calcium in Biological Systems (Rubin, P, Weiss, G B, Putney, J W editors) 319, 22  
 Balajee, S. Phenolic degradation by "dissimilatory plasmid" (with Boominathan, K, Mahadevan, A) *Scientific correspondence*, 319, 728  
 Baltimore, D. *See under* Singh, H., 319, 154  
*Immunoglobulin genes: Inversion for gene construction*, *News and views*, 319, 12  
 Baltz, D. *See under* Baltz, T., 319, 602  
 Baltz, T. Stable expression of two variable surface glycoproteins by cloned *Trypanosoma equiperdum* (with Grun, C, Baltz, D, Roth, C, Raibaud, A, Eisen, H) *Letter to Nature*, 319, 602  
 Bancel, P A. Pauling's model not universally accepted (with Stephens, P W, Goldman, A) *Scientific correspondence*, 319, 104  
 Banks, G. *See under* Rolfe, M., 319, 313  
 Barbacid, M. *See under* Martin-Zanca, D., 319, 743  
 Barber, R T. Ocean variability in relation to living resources during the 1982-83 El Niño (with Chávez, F P) *Review article*, 319, 279  
 Barde, Y-A. *See under* Davies, A M., 319, 497  
 Barkmann, W. *See under* Woods, J D., 319, 574  
 Barrowman, M M. Two roles for guanine nucleotide in the insulin secretion sequence of neutrophils (with Chock, P B, Chock, B D) *Letter to Nature*, 319, 504  
 Bartel, N. VLBI limits on the proper motion of the core of the superluminal quasar 3C245 (with Herring, J A, Rother, M I, Shapiro, I I, Corey, B E) *Article*, 319, 733  
 Barzilai, A. *See under* Weiss, R A., 319, 744  
 Baudry, M. Excitatory amino acids inhibit stimulation of phosphatidylinositol metabolism by amine agonists in hippocampus (with Evans, J, Lynch, G) *Letter to Nature*, 319, 329  
*See under* Morris, R G M., 319, 774  
 Beardsley, T. Remote sensing: US agencies blared for middle News, 319, 4  
*Laboratory animals: US protection act approved*, *News*, 319, 7  
*Bell Labs: From monopoly to competition*, *News*, 319, 90  
*US/Canada acid rain: Envoy's compromise in dispute*, *News*, 319, 168  
*Gramm-Rudman Act: Automatic cuts threatened*, *News*, 319, 264  
*Asbestos ban*, *News*, 319, 345  
 SDI: Software rows, *News*, 319, 345  
*US animal drugs: FDA chastised by Congress*, *News*, 319, 347  
*US research grants: Experiment in informality*, *News*, 319, 349  
*US space research: Nobody knows what will happen next*, *News*, 319, 437  
 SDI on campus, *News*, 319, 437  
*Voyager 2: Uranus is something else again*, *News*, 319, 419  
*EPA expansion urged*, *News*, 319, 443  
*Nuclear safety: Opposition relaxing standards*, *News*, 319, 167  
*Neutron research sources: US ambitions for new machine*, *News*, 319, 167  
*Animal welfare: Tip-off leads to NIH ban*, *News*, 319, 524  
*US budget: Biosciences lose out to defence*, *News*, 319, 526  
*Wright, K: News*, 319, 526  
*Challenger catastrophe: Commission concentrates on suspect rubber sealing rings*, *News*, 319, 609  
*Feynman's physics*, *News*, 319, 609  
*Monkey business: Bolivia asks for animals back*, *News*, 319, 610  
*Pharmaceuticals: NIH retreat from controversy*, *News*, 319, 611  
 Becker, G A. *See under* Kupferman, S L., 319, 474  
 Begon, M E. Ecology: Individuals, Populations and Communities, *Book review by* Smith, R H., 319, 419  
 Begue, B. *See under* Gomard, F., 319, 153  
 Behrensmeyer, A K. Trampling as a cause of bone surface damage and pseudo-cutmarks (with Gordon, K D, Yanagisawa, T) *Letter to Nature*, 319, 768  
 Bell, E A. *See under* Arnold, M H., 319, 615  
 Ben-Ze'ev, A. *See under* Ungar, F., 319, 787  
 Bender, B. Ban on South Africans (with Gledhill, J, Larsen, M, Rowlands, M, Tilley, C) *Correspondence*, 319, 612  
 Bengtson, S. *See under* Morris, S C., 319, 696

- Bennett, V. *See under* Baines, A. J., 319, 145  
 Benveniste, R. E. *See under* O'Brien, S. J., 319, 428  
 Berezin, A. A. Pauling's model not universally accepted, *Scientific correspondence*, 319, 104  
 Berg, J. M. Nucleic acid-binding proteins: More metal-binding fingers, *News and views*, 319, 264  
 Berger, G. W. Dating volcanic ash by ESR, *Matters arising*, 319, 795  
 Berger, L. *See under* Mandelis, N., 319, 751  
 Bergstedt-Lindquist, S. *See under* Noma, Y., 319, 640  
 Bertolini, D. R. Stimulation of bone resorption and inhibition of bone formation *in vitro* by human tumour necrosis factors (with Nedwin, G. E., Bringman, T. S., Smith, D. D., Mundy, G. R.) *Letter to Nature*, 319, 516  
 Betsholtz, C. *See under* Hedin, C.-H., 319, 511  
 Bevan, M. J. *See under* Rammensee, H.-G., 319, 502  
 Bhat, P. N. A very high energy γ-ray burst from the Crab pulsar (with Ramamurthy, P. V., Sreekantan, B. V., Vishwanath, P. R.) *Letter to Nature*, 319, 127  
 Bickle, M. Plate tectonics: Global thermal histories, *News and views*, 319, 13  
 Blakley, K. S. *See under* Knap, A. H., 319, 572  
 Bird, R. J. Metric system, *Correspondence*, 319, 8  
 Bishop, J. M. Oncogenes: Tricks with tyrosine kinases, *News and views*, 319, 722  
 Bittner, P. B. *See under* Martinet, Y., 319, 158  
 Black, K. P. *See under* Frogatt, P. C., 319, 578  
 Blair, D. G. The search for extraterrestrials, *Scientific correspondence*, 319, 270  
 Blakemore, J. S. Solid State Physics, 2nd Edn. revised, *Book review* by Jonscher, A. K., 319, 823  
 Blanc, D. *See under* Möllisen, M., 319, 28  
 Blank, L. W. West German forests: Deterioration, but some recovery, *News*, 319, 529  
 Bleasdale, J. K. A. *See under* Arnold, M. H., 319, 615  
 Bloom, B. R. *See under* Mustafa, A. S., 319, 63  
 Boaden, P. J. S. An Introduction to Coastal Ecology, *Book review* by Hawkins, S., 319, 808  
 Bohm, D. A. Quantum potential approach to the Wheeler delayed-choice experiment: Reply (with Dewdney, C., Hiley, B. H.) *Matters arising*, 319, 699  
 Bohme, D. K. Ionic origins of carbenes in space, *Letter to Nature*, 319, 473  
 Bolis, L. Editor, Design and Performance of Muscular Systems, *Book review* by Simmons, R. M., 319, 188  
 Bolt, B. A. An Introduction to the Theory of Seismology, 4th Edn., *Book review* by Marshall, P. D., 319, 814  
 Bookstein, F. L. *See under* Badgley, C., 319, 139  
 Boominathan, K. *See under* Balajee, S., 319, 728  
 Bordenave, G. Jacques Oudin 1908-1985, *News and views*, 319, 174  
 Bormann, F. H. *See under* Weather, K. C., 319, 657  
 Botet, R. Large computers key to aggregation phenomena (with Julien, R.) *Scientific correspondence*, 319, 454  
 Boulter, D. *Book review* of Principles of Plant Biotechnology: An Introduction to Genetic Engineering in Plants (by Mantell, S. H., Matthews, J. A., McKee, R. A.), 319, 806  
 Boulter, J. Isolation of a cDNA clone coding for a possible neural nicotinic acetylcholine receptor α-subunit (with Evans, K., Goldman, D., Martin, G., Treco, D., Heinemann, S., Patrick, J.) *Article*, 319, 368  
 Bourne, L. E. Cognitive Processes, 2nd Edn., *Book review* by Sutherland, S., 319, 798  
 Bovee, E. C. Editor, An Illustrated Guide to the Protozoa, *Book review* by Cox, F. E. G., 319, 366  
 Bowden, W. B. *See under* Weather, K. C., 319, 657  
 Bowen, B. *See under* Nick, H., 319, 243  
 Boyce, A. L. *See under* Waincoat, J. S., 319, 491  
 Boyd, M. A new method for measuring palaeomagnetic intensities, *Letter to Nature*, 319, 208  
 Boyd, R. Culture and the Evolutionary Process, *Book review* by Kitcher, P., 319, 105  
 Boyer, D. *See under* Pham, V. N., 319, 310  
 Boyle, C. B. Quasi-periodic oscillations from accretion disk coronas (with Fabian, A. C., Guillet, P. W.) *Letter to Nature*, 319, 648  
 Bradbury, A. J. 1-Methyl-4-phenylpyridine is neurotoxic to the nigrostriatal dopamine pathway (with Costall, B., Domenech, A. M., Jenner, P., Kelly, M. E., Marsden, C. D., Naylor, R. J.) *Letter to Nature*, 319, 56  
 Bradford, P. G. *See under* Späth, A., 319, 514  
 Brabec, A. *See under* Hubbard, W. B., 319, 636  
 Brammar, W. J. *Book review* of Genes II (by Lewin, B.), 319, 805  
 Brand, C. R. *Book review* of Personality and Individual Differences: A Natural Science Approach (by Eysenck, H. J., Eysenck, M. W.), 319, 799  
 Brandon, M. T. *See under* Green, A. G., 319, 210  
 Brandt, S. The Picture Book of Quantum Mechanics, *Book review* by Rhodes, W., 319, 821  
 Braumandl, A. *Book review* of Changing Order: Replication and Induction in Scientific Practice (by Collins, H. M.), 319, 274  
 Bregestowski, P. Elevation of intracellular calcium reduces voltage-dependent potassium conductance in human T cells (with Redkozubov, A., Alexeev, A.) *Letter to Nature*, 319, 776  
 Brice, K. A. *See under* Penkett, S. A., 319, 655  
 Bringman, T. S. *See under* Bertolini, D. R., 319, 516  
 Brinster, R. See under Krumlauf, R., 319, 224  
 Britten, R. S. Aleksandrov, Correspondence, 319, 172  
 Britton, W. J. *See under* Mustafa, A. S., 319, 63  
 Broadbent, D. *Book review* of The Mind's New Science: A History of the Cognitive Revolution (by Gardner, H.), 319, 545  
 Brock, D. J. H. The facts on cystic fibrosis testing (with van Heyningen, V.) *Scientific correspondence*, 319, 18
- Broecker, W. S. Editor, The Carbon Cycle and Atmospheric CO<sub>2</sub>: Natural Variations Archean to Present, *Book review* by Whitfield, M., 319, 108  
 Brostoff, J. Immunology, *Book review* by Paul, W. E., 319, 805  
 Introducing Immunology, *Book review* by Paul, W. E., 319, 805  
 Brousse, C. *See under* Dran, J.-C., 319, 485  
 Brown, D. Neuropharmacology: Acetylcholine and brain cells, *News and views*, 319, 358  
 Brown, F. Recombinant vaccinia viruses as vaccines (with Schild, G. C., Ada, G. L.) *Commentary*, 319, 549  
 Brown, G. The Field Description of Igneous Rocks, *Book review* by Cox, K. G., 319, 813  
 Browne, J. *Book review* of Seeds of Change: Five Plants that Transformed Mankind (by Hobhouse, H.), 319, 21  
 Brummer, G. J. A. Planktonic foraminiferal ontogeny and new perspectives for micropalaeontology (with Hemleben, C., Spindler, M.) *Letter to Nature*, 319, 50  
 Brun, J. P. *See under* Cyaden Scientific Team., 319, 396  
 Bryant, P. E. *Book review* of Theories of Development: Concepts and Applications, 2nd Edn. (by Crain, W. C.), 319, 797  
*Book review* of Human Intelligence: Perspectives and Prospects (by Kail, R., Pellegrino, J. W.), 319, 797  
*Book review* of Human Abilities: An Information-Processing Approach (Sternberg, R. J. editor) 319, 797  
 Buffington, A. Cosmic rays: Where do antiprotons come from?, *News and views*, 319, 178  
 Bullen, K. E. An Introduction to the Theory of Seismology, 4th Edn., *Book review* by Marshall, P. D., 319, 814  
 Bunting, A. H. *See under* Arnold, M. H., 319, 615  
 Burgen, A. S. V. Gaddum's Pharmacology, 9th Edn., *Book review* by Jenkins, D., 319, 802  
 Burgoyne, P. S. Sex chromosomes: Mammalian X and Y crossover, *News and views*, 319, 258  
 Burgoyne, R. D. Identification of a secretory granule-binding protein as caldesmon (with Cheek, T. R., Norman, K.-M.) *Letter to Nature*, 319, 68  
 Burleigh, R. Archaeology: Reconstructing ancient diets, *News and views*, 319, 259  
 Burley, J. *See under* Arnold, M. H., 319, 615  
 Bush, M. E. *See under* O'Brien, S. J., 319, 428  
 Butters, N. Editor, Neuropsychology of Memory, *Book review* by Rabbitt, P., 319, 365  
 Byerly, R. G. Stratamatolites from the 3,300-3,500-Myr Swaziland Supergroup, Barberton Mountain Land, South Africa (with Lower, D. R., Walsh, M. M.) *Letter to Nature*, 319, 489  
 Bynum, W. F. *Book review* of The Old Brown Dog: Women, Workers, and Vivisection in Edwardian England (by Lansbury, C.), 319, 546  
 Bywater, R. Metric system, *Correspondence*, 319, 93  
 Cade, T. J. Vertebrate Life, 2nd Edn., *Book review* by Kemp, T., 319, 811  
 Cahn, J. W. Pauling's model not universally accepted (with Gratias, D., Shechtman, D.) *Scientific correspondence*, 319, 102  
 Cahn, R. W. Materials science: Limits to Coulomb's law, *News and views*, 319, 177  
 Calkin, M. G. Minimum energy configurations (with Kiang, D., Tindall, D. A.) *Scientific correspondence*, 319, 454  
 Callen, H. B. Thermodynamics and an Introduction to Thermo statics, 2nd Edn., *Book review* by Guénault, T., 319, 822  
 Callow, J. A. *See under* Arnold, M. H., 319, 615  
 Calzolari, P. *See under* Mandelis, N., 319, 751  
 Cambier, J. C. Immunology: Seeing the way to B-cell growth, *News and views*, 319, 620  
 Cameron, E. M. *See under* Hattori, K., 319, 45  
 Cammack, R. Hydrogenases: From chemistry to legume growth (with Yates, M. G.) *News and views*, 319, 182  
 Camp, S. *See under* Schumacher, M., 319, 407  
 Campbell, J. A. *Book review* of Artificial Intelligence: The Very Idea (by Haugeland, J.), 319, 185  
*Book review* of Introduction to Artificial Intelligence (by Char niak, E., McDermott, D.), 319, 798  
 Campbell, P. Fusion research: US, Europe, Japan collaborate, *News*, 319, 168  
 European particle physics: CERN budget scrutiny planned, *News*, 319, 525  
 Canfield, M. AIDS, *Correspondence*, 319, 716  
 Cantor, C. R. *See under* Smith, C. L., 319, 701  
 Caputo, D. *See under* McKeon, F. D., 319, 463  
 Caroe, G. The Royal Institution: An Informal History, *Book review* by Porter, R., 319, 455  
 Carpino, M. *See under* Milani, A., 319, 386  
 Carter, L. *See under* Frogatt, P. C., 319, 578  
 Cass, D. A. *See under* Weather, K. C., 319, 657  
 Catt, K. J. *See under* Udelsman, R., 319, 147  
*See under* Holmes, M. C., 319, 326  
 Cavagna, G. A. *See under* Maloy, G. M. O., 319, 668  
 Chada, K. An embryonic pattern of expression of a human fetal globin gene in transgenic mice (with Magram, J., Costantini, F.) *Letter to Nature*, 319, 685  
 Challoner, P. B. *See under* Thompson, C. B., 319, 374  
 Champon, P. *See under* Takahashi, K., 319, 121  
 Chan, K. *See under* Koop, B. F., 319, 234  
 Chandra, H. S. X chromosomes and dosage compensation, *Scientific correspondence*, 319, 18  
 Chapman, G. A. Time-integrated energy budget of a solar activity complex (with Herzog, A. D., Lawrence, J. K.) *Letter to Nature*, 319, 654  
 Chapman, V. M. *See under* Krumlauf, R., 319, 224  
 Charlton, T. R. A plate tectonic model of the eastern Indonesia collision zone, *Letter to Nature*, 319, 394  
 Charniak, E. Introduction to Artificial Intelligence, *Book review* by Campbell, J. A., 319, 798  
 Charnock, H. *Book review* of Elements of Dynamic Oceanography (by Tolmazin, D.), 319, 825  
*Book review* of Introductory Physics of the Atmosphere and Ocean (by Hasse, L., Dobson, F.), 319, 825  
 Chávez, F. P. *See under* Barber, R. T., 319, 279  
 Cheah, M. S. C. *See* proto-oncogene mRNA induced in B lymphocytes by Epstein-Barr virus infection (with Ley, T. J., Tronick, S. R., Robbins, K. C.) *Letter to Nature*, 319, 238  
 Cheek, T. R. *See under* Burgoyne, R. D., 319, 68  
 Cheungsong-Popov, R. *See under* Weiss, R. A., 319, 794  
 Chen, C. S. *See under* Mullins, J. I., 319, 333  
 Chernyl, A. I. Scientific Communications and Information Exchange, *Book review* by Garfield, E., 319, 272  
 Chien, J. C. W. Highly conducting acetylene-CO copolymers and limitations of the soliton model: Reply, *Matters arising*, 319, 698  
 Choukroune, P. *See under* Cyaden Scientific Team., 319, 396  
 Chrousos, G. P. *See under* Udelman, R., 319, 147  
 Clemons, R. J. *See under* Dickinson, R. E., 319, 109  
 Clamé, C. AIDS, *Correspondence*, 319, 716  
 Clark, N. N. Fractal harmonics and rugged materials, *Scientific correspondence*, 319, 625  
 Clark, R. W. The Life of Ernst Chain: Penicillin and Beyond, *Book review* by Macfarlane, G., 319, 363  
 Clarke, M. British computing: Cooperative research spends up, *News*, 319, 88  
 British science: Researchers find a voice, *News*, 319, 169  
 Archaeologists: World congress quits Southampton for Mainz, *News*, 319, 251  
 Searle's UK research lab closes, *News*, 319, 251  
 IVF: Another bill bites the dust, *News*, 319, 349  
 Clavden, S. *See under* Weiss, R. A., 319, 794  
 Clegg, J. B. *See under* Waincoat, J. S., 319, 491  
 Clowes, R. M. *See under* Green, A. G., 319, 210  
 Cobbold, P. H. *See under* Woods, N. M., 319, 600  
 Cockcroft, C. S. *See under* Barrowman, M. M., 319, 504  
 Coggan, J. H. Jr. Oncofetal antigens, *Matters arising*, 319, 428  
 Cohen, J. *Book review* of Biology of Fertilization (Metz, C. B., Monroy, A. editor), 319, 20  
 Collins, H. M. Changing Order: Replication and Induction in Scientific Practice, *Book review* by Brannigan, A., 319, 274  
 Collinson, M. Palaeobotany: On folicles and flowers, *News and views*, 319, 723  
 Collum, R. G. *See under* Zimmerman, K. A., 319, 780  
 Coasard, N. J. *See under* Kubik, P. W., 319, 568  
 Cook, L. M. Editor, Case Studies in Population Biology, *Book review* by Usher, M. B., 319, 810  
 Cooke, H. J. *See under* Rouyer, F., 319, 291  
 Cooke, I. M. *See under* Lemos, J. R., 319, 410  
 Cooke, J. Permanent distortion of positional system of *Xenopus* embryo by brief early perturbation in gravity, *Letter to Nature*, 319, 60  
 Cooper, J. P. *See under* Arnold, M. H., 319, 615  
 Cooper, M. D. *See under* Rossant, J., 319, 507  
 Corey, B. E. *See under* Bartel, N., 319, 733  
 Cortiglioni, S. *See under* Mandelis, N., 319, 751  
 Costall, B. *See under* Bradbury, A. J., 319, 56  
 Costantini, F. *See under* Chada, K., 319, 685  
 Côté, S. *See under* Rosenberg, U. B., 319, 336  
 Cottler-Fox, M. *See under* Fox, C. H., 319, 8  
 Cowan, W. M. Molecular Bases of Neural Development, *Book review* by Lund, R. D., 319, 107  
 Cowden, A. *See under* Groves, D. I., 319, 136  
 Cowley, D. J. Protein structure: Polar pocket with nonpolar lining, *News and views*, 319, 14  
 Cox, F. E. G. *Book review* of An Illustrated Guide to the Protozoa (Lee, J. H., Hutner, S. H., Bovee, E. C. editors), 319, 366  
*Book review* of Foundations of Parasitology, 3rd Edn. (by Schmidt, G. D., Roberts, L. S.), 319, 807  
 Cox, H. C. Bicadinane, a C<sub>30</sub> pentacyclic isoprenoid hydrocarbon found in crude oil (with de Leeuw, J. W., Schenck, P. A., van Koningsveld, H., Jansen, J. C., van de Graaf, B., van Geerestein, V. J., Kinters, J. A., Kruck, C., Jans, A. W. H.) *Letter to Nature*, 319, 316  
 Cox, K. G. *See under* Mitchell, C., 319, 131  
*Book review* of Magmas and Magmatic Rocks: An Introduction to Igneous Petrology (by Middlemost, E. A. K.), 319, 813  
*Book review* of Igneous Petrology (by McBirney, A. R.), 319, 813  
*Book review* of The Field Description of Igneous Rocks (by Thorpe, R., Brown, G.), 319, 813  
 Crain, W. C. Theories of Development: Concepts and Applications, 2nd Edn., *Book review* by Bryant, P. E., 319, 797  
 Cristiani, A. *See under* Rammensee, H.-G., 319, 502  
 Croce, C. M. *See under* Kozbor, D., 319, 331  
 Crow, T. J. Division of Japanese psychiatry, *Correspondence*, 319, 172  
 Crum, L. A. Acoustic cavitation generated by microsecond pulses of ultrasound (with Fowlkes, J. B.) *Letter to Nature*, 319, 52  
 Crystal, R. G. *See under* Martinet, Y., 319, 158  
 Cuthbertson, K. S. R. *See under* Woods, N. M., 319, 600  
 Cyaden Scientific Team. Tectonics of the westernmost Gulf of Aden and the Gulf of Tadjoura from submersible observations (with Choukroune, P., Auvergne, B., Francheteau, J., Lepine, J. C., Arthaud, F., Brun, J. P., Auzende, J. M., Sichler, B., Khobay, Y.) *Letter to Nature*, 319, 396  
 Cynader, M. S. *See under* Swindale, N. V., 319, 591  
 Dahmen, H. D. The Picture Book of Quantum Mechanics, *Book review* by Rhodes, W., 319, 821  
 Daneholt, B. *See under* Skoglund, U., 319, 560

- Daniels, V G. AIDS: The Acquired Immune Deficiency Syndrome. *Book review by Tedder, R S.* 319, 457
- Das, A. Quantum Mechanics: A Modern Introduction. *Book review by Rhodes, W.* 319, 821
- Davies, A M. Different factors from the central nervous system and periphery regulate the survival of sensory neurones (with Thoenen, H. Barde, Y-A) *Letter to Nature*, 319, 497
- Davis, J A. Darwin, Freud and creationism. *Correspondence*, 319, 616
- Davis, M M. *See under* Rawley, L A., 319, 383
- Day, P R. *See under* Arnold, M H., 319, 615
- Dayton, A I. *See under* Rosen, C A., 319, 555
- DeBremeccker, J-C. Geophysics: The Earth's Interior. *Book review by McNutt, M.* 319, 815
- de Leeuw, J W. *See under* Cox, H C., 319, 316
- De Pomerai, D. From Gene to Animal: An Introduction to the Molecular Biology of Animal Development. *Book review by Akam, M.* 319, 806
- De Souza, E B. Reciprocal changes in corticotropin-releasing factor (CRF)-like immunoreactivity and CRF receptors in cerebral cortex of Alzheimer's disease (with Whitehouse, P J. Kuhar, M J. Price, D L. Vale, W W) *Letter to Nature*, 319, 593
- de Vries, R R P. *See under* Ottenhoff, T H M., 319, 66
- See under* Ottenhoff, T H M., 319, 427
- de Wit, M Y L. *See under* Ottenhoff, T H M., 319, 66
- See under* Ottenhoff, T H M., 319, 427
- DeAmicis, G. *See under* Mandolesi, N., 319, 751
- Dean, M. *See under* White, R., 319, 160
- Dean, P D G. Editor, Affinity Chromatography: A Practical Approach. *Book review by Parkh, I.* 319, 629
- Delphino, F. *See under* Mandolesi, N., 319, 751
- DeNiro, M J. *See under* Ambrose, S H., 319, 321
- Denis, K A. *See under* Zimmerman, K A., 319, 780
- Dennison, J E. Antarctic and non-Antarctic meteorites form different populations (with Lingner, D W. Lipschutz, M E) *Letter to Nature*, 319, 390
- DePinho, R A. *See under* Kohl, N E., 319, 73
- Dermer, C D. Secondary antiproton production in relativistic plasmas (with Ramaty, R) *Letter to Nature*, 319, 205
- Dermott, S F. Masses of the satellites of Uranus (with Nicholson, P D) *Article*, 319, 115
- Desnuelle, C. *See under* Renaud, J-F., 319, 678
- Desrosiers, R C. Origin of the human AIDS virus. *Scientific correspondence*, 319, 728
- Dessler, A J. Space physics: Does Uranus have a magnetic field?. *News and views*, 319, 174
- Erratum: Does Uranus have a magnetic field?. *News and views*, 319, 721
- Deuser, W G. *See under* Knap, A H., 319, 572
- Devaux, C. *See under* Malissen, M., 319, 28
- DeVita, V Jr. AIDS: Etiology, Diagnosis, Treatment and Prevention. *Book review by Tedder, R S.* 319, 457
- Dewdney, C. *See under* Bohm, D J., 319, 699
- Diamond, J. Extinct animals: The mammoths' last migration. *News and views*, 319, 265
- Dieke, R H. *See under* Kuhn, J R., 319, 128
- Dickinson, A S. Book review of Computational Physics (by Koonin, S E.) 319, 821
- Dickinson, R E. Future global warming from atmospheric trace gases (with Cicerone, R J) *Review article*, 319, 109
- Dikkens, A J. Geology in Petroleum Production: A Primer in Petroleum Geology. *Book review by Wilson, R C L.* 319, 812
- Dinarello, C A. *See under* Wolff, S M., 319, 270
- Dobbs, E R. Electromagnetic Waves. *Book review by Rosser, W G*. 319, 823
- Dobson, F. Introductory Physics of the Atmosphere and Ocean. *Book review by Charnock, H.* 319, 825
- Domeney, A M. *See under* Bradbury, A J., 319, 56
- Domrowski, R L. Cognitive Processes, 2nd Edn. *Book review by Sutherland, S.* 319, 798
- Doumling, D P. Pragmatism is not enough. *Correspondence*, 319, 94
- Dowling, J E. *See under* Sakai, H M., 319, 495
- Downes, A J B. *See under* Dunlop, J S., 319, 564
- Drake, J A. Ecological modelling: Invasions of natural communities (with Williamson, M) *News and views*, 319, 718
- Dran, J-C. Mechanism of aqueous dissolution of silicate glasses yielded by fission tracks (with Petit, J-C. Brousse, C) *Letter to Nature*, 319, 485
- Draper, P. Leprosy vaccine. *Correspondence*, 319, 94
- Dronamraju, K R. Haldane: The Life and Work of J B S. Haldane with Special Reference to India. *Book review by Pirie, N W*. 319, 630
- Duellman, W E. Biology of Amphibians. *Book review by Haliday, T.* 319, 364
- Duff, B G. Fundamental Particles: An Introduction to Quarks and Leptons. *Book review by Gibson, W R.* 319, 823
- Duffett-Smith, P J. *See under* Spinks, M J., 319, 471
- Duncan, M J. The Physiological Ecology of Seaweeds. *Book review by Lewin, R A.* 319, 807
- Dunlap, K. *See under* Holz, G G IV., 319, 670
- Dunlop, J S. A quasar with  $z=3.71$  and limits on the number of more distant objects (with Downes, A J B. Peacock, J A. Savage, A. Lilly, S J. Watson, F G. Longair, M S) *Article*, 319, 564
- Dunn, K. *See under* Gammon, G., 319, 413
- Dynan, W S. Transcription factor Sp1 recognizes a DNA sequence in the mouse dihydrofolate reductase promoter (with Sazer, S. Tjian, R. Schimke, R T) *Letter to Nature*, 319, 246
- Eaton, J S. *See under* Weather, K C., 319, 657
- Eccles, D H. Causes of African famine. *Correspondence*, 319, 715
- Eckern, U. Quantum mechanics: Is the theory applicable to macroscopic objects? *News and views*, 319, 726
- Edelman, G M. Molecular Bases of Neural Development. *Book review by Lund, R D.* 319, 107
- Edwards, R H. Differential RNA splicing predicts two distinct nerve growth factor precursors (with Selby, M J. Rutter, W J) *Letter to Nature*, 319, 784
- Egan, T M. Acetylcholine hyperpolarizes central neurones by acting on an  $M_2$  muscarinic receptor (with North, R A) *Letter to Nature*, 319, 405
- Eisen, H. *See under* Baltz, T., 319, 602
- Eisenberg, D. Solvation energy in protein folding and binding (with McLachlan, A D) *Article*, 319, 199
- Eklund, T. Metric system. *Correspondence*, 319, 716
- Eley, D D. Book review of Molecular Semiconductors: Photoelectrical Properties and Solar Cells (by Simon, J. André, J J.) 319, 458
- Elferink, D G. *See under* Ottenhoff, T H M., 319, 66
- Eller, L-R. *See under* Hubbard, W B., 319, 636
- Elliott, J R. Mapping of general anaesthetic target sites (with Haydon, D A) *Matters arising*, 319, 77
- Ellis, R H. *See under* Arnold, M H., 319, 615
- Ellison, D C. *See under* Kazanas, D., 319, 380
- Elmore, D. *See under* Kubik, P W., 319, 568
- Emanuel, K A. Nuclear winter: Towards a scientific exercise. *News and views*, 319, 259
- Embrey, S H. Too colourful. *Correspondence*, 319, 715
- Enver, T. Gene regulation: Importance of helical periodicity (with Patient, R) *News and views*, 319, 99
- Erlank, A J. *See under* Haggerty, S E., 319, 761
- Esat, T M. Isotope anomalies induced in laboratory distillation (with Spear, R H. Taylor, S R) *Letter to Nature*, 319, 576
- Eshleman, V R. Mode decoupling during retrorefraction as an explanation for bizarre radar echoes from icy moons. *Letter to Nature*, 319, 755
- Evans, J. *See under* Baudry, M., 319, 329
- Evans, K. *See under* Boulter, J., 319, 368
- Eysenck, H J. Book review of Handbook of Intelligence: Theories, Measurements and Applications (Wolman, B B editor) 319, 627
- Personality and Individual Differences: A Natural Science Approach. *Book review by Brand, C R.* 319, 799
- Eysenck, M W. Personality and Individual Differences: A Natural Science Approach. *Book review by Brand, C R.* 319, 799
- Fabian, A C. X-ray astronomy: New results from Exosat. *News and views*, 319, 451
- See under* Boyle, C B., 319, 648
- Falusi, A G. *See under* Waincoat, J S., 319, 491
- Farley, J. Protein kinase C activation induces conductance changes in *Hermissenda* photoreceptors like those seen in associative learning (with Auerbach, S) *Letter to Nature*, 319, 220
- Farmer, C B. *See under* Toon, G C., 319, 570
- Farmer, P B. Editor, The Molecular Basis of Cancer. *Book review by Weinstein, I B.* 319, 803
- Faulstich, H. Trityl lead in rain in the Black Forest (with Stouras, C) *Scientific correspondence*, 319, 17
- Fausto-Sterling, A. Myths of Gender: Biological Theories About Women and Men. *Book review by Attenborough, R.* 319, 271
- Fegley, B Jr. Chemical effects of large impacts on the Earth's primitive atmosphere (with Prinn, R G. Hartman, H. Watkins, G H) *Letter to Nature*, 319, 305
- Feirtinger, M. Fundamental Neuroanatomy. *Book review by Fitzgerald, M.* 319, 801
- Feizi, T. Oncofetal antigens: Reply. *Matters arising*, 319, 428
- Ferl, R J. *See under* Nick, H., 319, 243
- Fernandez, J M. *See under* Lindau, M., 319, 150
- French-Constant, C. Proliferating bipotential glial progenitor cells in adult rat optic nerve (with Raff, M C) *Letter to Nature*, 319, 499
- Field, G B. *See under* Krauss, L M., 319, 748
- Fine, A. Neurochemistry: Peptides and Alzheimer's disease. *News and views*, 319, 537
- Flink, G R. *See under* Serrano, R., 319, 689
- Fitch, F. *See under* Malissen, M., 319, 28
- Fitzgerald, M. Book review of Principles of Neural Science, 2nd Edn. (by Kandel, E R. Schwartz, J H.) 319, 801
- Book review of Progress in Neuroscience: Readings from Scientific American (Thompson, R F editor) 319, 801
- Book review of The Brain: An Introduction to Neuroscience (by Thompson, R F.) 319, 801
- Book review of Fundamental Neuroanatomy (by Nauta, J H. Feirtag, M.) 319, 801
- Fletcher, R J. Molecular Structure: Macromolecules in Three Dimensions. *Book review by Rodger, C D.* 319, 804
- Flint, J. *See under* Waincoat, J S., 319, 491
- Fogg, G E. Ocean ecology: Light and ultraphytoplankton. *News and views*, 319, 96
- Ford-Lloyd, B V. *See under* Arnold, M H., 319, 615
- Fordham, D. Book review of Shackleton (by Huntford, R.) 319, 186
- Forster, A. *See under* Lefranc, M P., 319, 420
- Fowlkes, J B. *See under* Crum, L A., 319, 52
- Fox, C H. AIDS in the human brain (with Cottler-Fox, M) *Correspondence*, 319, 8
- Fox, K. *See under* Milani, A., 319, 386
- Francheteau, J. *See under* Cyaneid Scientific Team, 319, 396
- Francis, D. The pyroxene paradox in MORB glasses — a signature of picritic parental magmas? *Letter to Nature*, 319, 586
- Franks, N P. Mapping of general anaesthetic target sites: Reply (with Lieb, W R) *Matters arising*, 319, 78
- Fremlin, J H. Free will and determinism. *Correspondence*, 319, 352
- Friedmann, T. *See under* Schumacher, M., 319, 407
- Froggatt, P C. An exceptionally large late Quaternary eruption from New Zealand (with Nelson, C S. Carter, L. Griggs, G. Black, K. P) *Letter to Nature*, 319, 578
- Fromm, M E. Stable transformation of maize after gene transfer by electroporation (with Taylor, I P. Walbot, V) *Letter to Nature*, 319, 791
- Frommer, J E. *See under* Wuid, F., 319, 697
- Fukushi, T. *See under* Takatsuki, H., 319, 240
- Fung, I Y. *See under* Tucker, C J., 319, 195
- Furner, I J. An Agrobacterium transformation in the evolution of the genus *Nicotiana* (with Huffman, G A. Amerson, R M. Gerstel, D J. Gordon, M P. Nestor, I W) *Letter to Nature*, 319, 422
- Futrell, D S. Implications of welded breccias in Mount Ngarragon tektites. *Letter to Nature*, 319, 683
- Futuyma, D J. Book review of Evolution: Essays in Honour of John Maynard Smith (Greenwood, P J. Harvey, P H. Stokin, M editors) 319, 19
- Gage, P W. *See under* Krouse, M E., 319, 58
- Gale, G. Book review of Alfred North Whitehead: The Man and His Work, Vol. I 1861-1910 (by Lowe, V.) 319, 521
- Book review of Science and the Modern World (by Whitehead, A N.) 319, 548
- Gall, W E. Molecular Bases of Neural Development. *Book review by Lund, R D.* 319, 107
- Galloway, J N. *See under* Weather, K C., 319, 657
- Gambles, P. Marine science: Proposal for British overseas. *News and views*, 319, 351
- Marine science: Changes afloat. *News*, 319, 433
- Gammie, G. Neonatal T-cell tolerance to maternal immunogenic peptides is caused by clonal inactivation (with Dunn, K. Shultz, N. Oki, A. Wilbur, S. Sceriz, E L) *Letter to Nature*, 319, 313
- Gammie, R H. *See under* Tucker, C J., 319, 195
- Gardner, H. The Mind's New Science: A History of the Cognitive Revolution. *Book review by Broadbent, D*. 319, 545
- Garfield, E. Book review of Scientific Communications and Information Exchange (by Mikhailov, A I. Chernov, A I. Gulyazev, R S.) 319, 272
- Garfinkel, D J. *See under* Furner, I J., 319, 422
- Garrett, R A. Archaeabacterial terminator. *Rept. Scient. corr. correspondence*, 319, 268
- Gaskell, C M. Distant galaxies: Pushing back the redshift limit. *News and views*, 319, 539
- Gee, C E. *See under* Kohl, N E., 319, 73
- See under* Zimmerman, K A., 319, 780
- Geiger, B. *See under* Ungar, F., 319, 757
- Gerlach, T M. Carbon and sulphur isotope composition of Kilauea parental magma (with Thomas, D M) *Letter to Nature*, 319, 421
- Giallongo, J B. *See under* Kozbier, D., 319, 311
- Gillard, D. Horizontal shear flow in the mantle beneath the Tien Shan arc (with Woodhouse, J H) *Article*, 319, 551
- Gibson, W R. Book review of Fundamental Particles: An Introduction to Quarks and Leptons (by Duff, B G.) 319, 823
- Book review of Elementary Particles 2nd Edn. (by Hughes, I S.) 319, 823
- Gilbert, W. *See under* Nick, H., 319, 243
- Origin of life: The RNA world. *News and views*, 319, 611
- Gilchrist, T L. Heterocyclic Chemistry. *Book review by Purcell, K*. 319, 816
- Giles, R J. *See under* Arnold, M H., 319, 615
- Gillarevskii, R S. Scientific Communications and Information Exchange (with Garfield, E) 319, 272
- Gilinsky, A S. Mind and Brain: Principles of Neurocybernetics. *Book review by Young, A.* 319, 799
- Gill, H K. *See under* Mustafa, A S., 319, 63
- Gingerich, O. Vekhovskiy. *Correspondence*, 319, 91
- Gingerich, P D. Early Eocene *Cetus torosus* — oldest primate of modern aspect from North America. *Letter to Nature*, 319, 319
- Ginzburg, L R. Lectures in Theoretical Population Biology. *Book review by Usher, M B.* 319, 810
- Girod, C. *See under* Baltz, T., 319, 602
- Gledhill, J. *See under* Bender, B., 319, 532
- Glover, H E. Light quality and oceanic ultraphytoplankton (with Keller, M D. Guillard, R R L) *Letter to Nature*, 319, 142
- Godal, T. *See under* Mustafa, A S., 319, 63
- Goddard, G V. Learning: A step nearer a neural substrate. *News and views*, 319, 721
- Goh, W C. *See under* Rosen, C A., 319, 555
- Golding, B W. Importance of local mesoscale factors in development of nuclear winter (with Goldsmith, P. MacLean, N. A. Slingo, A) *Letter to Nature*, 319, 301
- Goldman, A I. *See under* Bancel, P A., 319, 104
- Goldman, D. *See under* Boulter, J., 319, 368
- Goldsmith, P. *See under* Golding, B W., 319, 301
- Goldstein, D S. *See under* Udelsman, R., 319, 147
- Golenburg, E M. Lectures in Theoretical Population Biology. *Book review by Usher, M B.* 319, 810
- Gomard, E. Murine cells expressing an HLA molecule are specifically lysed by HLA-restricted avian human T cells (with Bapna, S. Sodoyer, S. Maryanski, J L. Jordan, B R. Levy, J P) *Letter to Nature*, 319, 153
- Gomperts, B D. *See under* Barrowman, M M., 319, 903
- Gong, V. Editor, Understanding AIDS: A Comprehensive Guide. *Book review by Tedder, R S.* 319, 457
- Gooding, D. Editor, Faraday Rediscovered: Essays on the Life and Work of Michael Faraday. 1791-1857. *Book review by Suddick, M.* 319, 628
- Goodman, L S. Editor, Goodman and Gilman's The Pharmacological Basis of Therapeutics, 7th Edn. *Book review by Jenkins, D*. 319, 802
- Goodman, M. *See under* Koop, B F., 319, 234
- Goodman Gilman, A. Editor, Goodman and Gilman's The Pharmacological Basis of Therapeutics, 7th Edn. *Book review by Jenkins, D*. 319, 802

- inson, D. 319, 802  
**Gordon, K.D.** See under Behrensmeyer, A.K., 319, 768  
**Gordon, M.P.** See under Furner, I.J., 319, 422  
**Gorun, S.M.** A new synthetic approach to the ferritin core uncovers the soluble iron (III) oxo-hydroxo aggregate [ $\text{Fe}_{11}\text{O}_6(\text{O}_2\text{CPh})_{15}$ ] (with Lippard, S.J.) *Letter to Nature*, 319, 666  
**Götmark, F.** Flock-feeding on fish schools increases individual success in gulls (with Winkler, D.W., Andersson, M.) *Letter to Nature*, 319, 589  
**Gough, D.** Solar physics: What causes the solar cycle?, *News and views*, 319, 263  
**Grantham, R.** AIDS virus and HTLV-I differ in codon choices (with Perrin, P.) *Scientific correspondence*, 319, 727  
**Gratias, D.** See under Cahn, J.W., 319, 102  
**Green, A.G.** Seismic reflection imaging of the subducting Juan de Fuca plate (with Clowes, R.M., Yorath, C.J., Spencer, C., Kanasewich, E.R., Brandon, M.T., Sutherland Brown, A.) *Letter to Nature*, 319, 210  
**Green, R.M.** *Spherical Astronomy*, *Book review* by McNally, D. 319, 824  
**Greenwood, P.J.** Editor, Evolution: Essays in Honour of John Maynard Smith, *Book review* by Futuyma, D.J. 319, 19  
**Grey, I.E.** See under Haggerty, S.E., 319, 761  
**Griggs, G.** See under Froggatt, P.C., 319, 578  
**Grossi, C.E.** See under Rossant, J., 319, 507  
**Grotendorst, G.R.** See under Martinet, Y., 319, 158  
**Groudine, M.** See under Thompson, C.B., 319, 374  
**Groves, D.I.** Thermal erosion by komatiites at Kambalda, Western Australia and the genesis of nickel ores (with Korkiakoski, E.A., McNaughton, N.J., Lester, C.M., Cowden, A.) *Letter to Nature*, 319, 136  
**Grundy, H.F.** *Feature Notes on Pharmacology*, *Book review* by Jenkinson, D. 319, 802  
**Guénault, T.** *Book review of Thermodynamics and an Introduction to Thermostatics*, 2nd Edn. (by Callen, H.B.) 319, 822  
*Book review of The Theory of Thermodynamics* (by Waldram, J.R.) 319, 822  
**Guilbert, P.W.** See under Boyle, C.B., 319, 648  
**Guillard, R.R.L.** See under Glover, H.E., 319, 142  
**Guth, A.H.** See under Krauss, L.M., 319, 748  
**Haas, M.** See under Ishai, Z.B., 319, 795  
**Haberer, J.** *Book review of Einstein in America* (by Sayen, J.) 319, 20  
**Hadley, N.** The Adaptive Role of Lipids in Biological Systems, *Book review* by Prosser, C.L. 319, 187  
**Hagag, N.** Inhibition of growth factor-induced differentiation of PC12 cells by microinjection of antibody to ras p21 (with Halegoua, S., Viola, M.) *Letter to Nature*, 319, 680  
**Haggerty, S.E.** Metasomatic mineral titanate complexing in upper mantle (with Erlank, A.J., Grey, I.E.) *Letter to Nature*, 319, 761  
**Halduc, I.** Basic Organometallic Chemistry, *Book review* by Taylor, R.J. 319, 817  
**Halegoua, S.** See under Hagag, N., 319, 680  
**Hall, D.H.** See under Ajakaiye, D.E., 319, 582  
**Hall, E.T.** See under Mandelstam, J., 319, 715  
**Hallam, A.** The Pliensbachian and Tithonian extinction events, *Letter to Nature*, 319, 765  
*Book review of The Burgess Shale* (by Whittington, H.B.) 319, 629  
*Book review of Earth and Life Through Time* (by Stanley, S.M.) 319, 811  
**Halliday, D.** Basic Concepts in Relativity and Early Quantum Theory, 2nd Edn., *Book review* by Raine, D.J. 319, 822  
**Halliday, T.** *Book review of Biology of Amphibians* (by Duellman, W.E., Trueb, L.) 319, 364  
**Halstead, B.** *Book review of Palaeontology: An Introduction* (by Nield, E.W., Tucker, V.C.T.) 319, 810  
**Hammer, R.E.** See under Kratulauf, R., 319, 224  
**Harper, J.L.** Ecology: Individuals, Populations and Communities, *Book review* by Smith, R.H. 319, 809  
**Harper, P.G.** Introduction to Physical Mathematics, *Book review* by Uptill, C. 319, 820  
**Harrison, C.** *Book review of Basic Biogeography*, 2nd Edn. (by Pears, N.) 319, 809  
**Harrison, G.A.** See under Mandelstam, J., 319, 715  
**Harrison, P.J.** The Physiological Ecology of Seaweeds, *Book review* by Lewin, R.A. 319, 807  
**Hartman, H.** See under Fegley, B.Jr., 319, 305  
**Harvey, P.H.** Editor, Evolution: Essays in Honour of John Maynard Smith, *Book review* by Futuyma, D.J. 319, 19  
**Harvey, R.C.** See under Mandelstam, N., 319, 751  
**Harwit, M.** Is IRAS cirrus cloud emission largely fine-structure radiation? (with Houck, J.R., Stacey, G.J.) *Letter to Nature*, 319, 646  
**Harwood, J.P.** See under Udelman, R., 319, 147  
**Hastelton, W.A.** See under Rosen, C.A., 319, 555  
**Hasinger, G.** Quasi-periodic oscillations in the X-ray flux of Cyg X-2 (with Langmeier, A., Szajno, M., Trümper, J., Lewin, W.H.G., White, N.E.) *Letter to Nature*, 319, 469  
**Hasse, L.** Introductory Physics of the Atmosphere and Ocean, *Book review* by Charnock, H. 319, 825  
**Hattori, K.** Archaean magmatic sulphate (with Cameron, E.M.) *Letter to Nature*, 319, 45  
**Haugeland, J.** Artificial Intelligence: The Very Idea, *Book review* by Campbell, J.A. 319, 185  
**Hawkes, J.G.** See under Arnold, M.H., 319, 615  
**Hawkes, P.W.** *Book review of Pattern Recognition: Human and Mechanical* (by Watanabe, S.) 319, 107  
**Hawkins, S.** *Book review of An Introduction to Coastal Ecology* (by Boaden, P.J.S., Seed, R.) 319, 808  
**Hay, D.A.** Essentials of Behaviour Genetics, *Book review* by Huntingford, F.A. 319, 800  
**Hayati, I.** Mechanism of stable jet formation in electrohydrodynamic atomization (with Bailey, A.I., Tedros, Th.F.) *Letter to Nature*, 319, 41  
**Haydon, D.A.** See under Elliott, J.R., 319, 77  
**Hayes, J.D.** See under Arnold, M.H., 319, 615  
**Healy, A.F.** Cognitive Processes, 2nd Edn., *Book review* by Sutherland, S. 319, 798  
**Heaney, S.I.** Ecology: Tundra river transformation, *News and views*, 319, 260  
**Heath, J.** *Book review of An Atlas of Immunofluorescence in Cultured Cells* (by Willingham, M.C., Pastan, I.) 319, 547  
**Heathcock, C.H.** Introduction to Organic Chemistry, 3rd Edn., *Book review* by Mann, J. 319, 818  
**Heaton, C.A.** Editor, *The Chemical Industry*, *Book review* by Wilcockson, R.B. 319, 818  
**Heeger, A.J.** See under Wudl, F. 319, 697  
**Heglund, N.C.** See under Maloy, G.M.O., 319, 668  
**Hegner, E.** Nd-Sr-Pb isotope constraints on the sources of West Maui volcano, Hawaii (with Uruh, D., Tatsumoto, M.) *Letter to Nature*, 319, 478  
**Heinemann, S.** See under Boulter, J., 319, 368  
**Heiser, J.B.** *Vertebrate Life*, 2nd Edn., *Book review* by Kemp, T. 319, 811  
**Heldin, C.-H.** A human osteosarcoma cell line secretes a growth factor structurally related to a homodimer of PDGF A-chains (with Johansson, A., Wennberg, S., Wernstedt, C., Betsholtz, C., Westermark, B.) *Letter to Nature*, 319, 511  
**Hellman, S.** AIDS: Etiology, Diagnosis, Treatment and Prevention, *Book review* by Tedder, R.S. 319, 457  
**Hemleben, C.** See under Brummer, G.-J.A., 319, 50  
**Henshaw, G.G.** See under Arnold, M.H., 319, 615  
**Herbst, J.** See under White, R., 319, 160  
**Hernandez, M.** See under Wainscoat, J.S., 319, 491  
**Herring, T.A.** See under Carter, M., 319, 733  
**Herskowitz, I.** See under Mitchell, A.P., 319, 738  
**Hertzlinger, J.** Price of star wars, *Correspondence*, 319, 8  
**Herzog, A.D.** See under Chapman, G.A., 319, 654  
**Heslop-Harrison, J.** See under Arnold, M.H., 319, 615  
**Hetherington, N.** Edwin Hubble: legal eagle, *Commentary*, 319, 189  
**Heywood, V.H.** See under Arnold, M.H., 319, 615  
**Hibberson, W.O.** See under Sekine, T., 319, 584  
**Hiley, B.H.** See under Bohm, D.J., 319, 699  
**Hill, A.** Anthropology: Tools, teeth and trampling, *News and views*, 319, 719  
**Hill, A.V.S.** See under Wainscoat, J.S., 319, 491  
**Hirata, Y.** See under Nagata, S., 319, 415  
**Hirochika, H.** See under Takatsuji, H., 319, 240  
**Hirota, M.** See under Imai, N., 319, 796  
**Hirst, D.M.** Potential Energy Surfaces: Molecular Structure and Reaction Dynamics, *Book review* by Stone, A. 319, 819  
**Hobbs, A.S.** No sexism please, *Correspondence*, 319, 444  
**Hobhouse, H.** Seeds of Change: Five Plants that Transformed Mankind, *Book review* by Browne, J. 319, 21  
**Hoff, M.** See under White, R., 319, 160  
**Holdsworth, G.** Ice shelf creep rates and the flow law of ice, *Scientific correspondence*, 319, 727  
**Hollenbeck, P.** Organelle transport: Moving in different directions, *News and views*, 319, 724  
**Hollingsworth, A.** Weather forecasting: Storm hunting with fractals, *News and views*, 319, 11  
**Holmes, M.C.** Magnocellular axons in passage through the median eminence release vasopressin (with Antoni, F.A., Aguilera, G., Catt, K.J.) *Letter to Nature*, 319, 326  
**Holz, G.G. IV.** GTP-binding proteins mediate transmitter inhibition of voltage-dependent calcium channels (with Rane, S.G., Dumlak, K.) *Letter to Nature*, 319, 670  
**Honjo, T.** See under Noma, Y., 319, 640  
**Hood, L.** See under Malissen, M., 319, 28  
**Hoover, E.A.** See under Mullins, J.I., 319, 333  
**Horridge, A.** *Book review of Model Neural Networks and Behavior* (Selverston, A. editor) 319, 22  
**Houck, J.R.** See under Harwit, M., 319, 646  
**Hsü, K.J.** The Precambrian-Cambrian boundary and geochemical perturbations: Reply, *Matters arising*, 319, 697  
**Hubbard, W.B.** Occultation detection of a neptunian ring-like arc (with Brahic, A., Sicardi, B., Elicer, L.R., Roques, F., Vilas, F.) *Article*, 319, 636  
**Huffman, G.A.** See under Furner, I.J., 319, 422  
**Hughes, D.W.** Astronomy: Hollow meteoroid streams, *News and views*, 319, 718  
**Hughes, I.E.** Learning Pharmacology Through MCQ: A Comprehensive Text, *Book review* by Jenkinson, D. 319, 802  
**Hughes, I.S.** Elementary Particles, 2nd Edn., *Book review* by Gibson, W.R. 319, 823  
**Hughes, S.H.** See under Martin-Zanca, D., 319, 743  
**Hugues, M.** See under Renaud, J.-F., 319, 678  
**Hunter, G.D.** AFRC cuts, *Correspondence*, 319, 256  
**Huntingford, R.** Shackleton, *Book review* by Fordham, D. 319, 186  
**Huntingford, F.A.** *Book review of Essentials of Behaviour Genetics* (by Hay, D.A.) 319, 800  
**Huth, P.** See under Weathers, K.C., 319, 657  
**Hutner, S.H.** Editor, *An Illustrated Guide to the Protozoa*, *Book review* by Cox, F.E.G. 319, 366  
**Iino, M.** See under Shimazaki, K., 319, 324  
**Ikawa, S.** See under Yamamoto, T., 319, 230  
**Ikeda, J.-E.** See under Takatsuji, H., 319, 240  
**Imai, N.** Dating volcanic ash by ESR: Reply (with Shimokawa, K., Hirota, M.) *Matters arising*, 319, 796  
**Innes, N.L.** See under Arnold, M.H., 319, 615  
**Inzani, P.** See under Mandelstam, N., 319, 751  
**Ip, W.H.** Solar wind interaction with Uranus' atmosphere, *Scientific correspondence*, 319, 268  
**Irifuné, T.** See under Sekine, T., 319, 584  
**Irisawa, H.** See under Kimura, J., 319, 596  
**Isaacs, N.S.** *Book review of The Physical Basis of Organic Chemistry* (by Maskill, H.) 319, 816  
*Book review of Pictorial Orbital Theory* (by Tedder, J.M., Nechval, A.) 319, 816  
**Ishai, Z.B.** Lack of HTLV-I antibodies in Africans: Reply (with Haas, M., Jensen, F.C.) *Matters arising*, 319, 795  
**Ivanl, J.** See under Ottenhoff, T.H.M., 319, 427  
**Ivanyi, J.** See under Ottenhoff, T.H.M., 319, 66  
**Jäckle, H.** See under Rosenberg, U.B., 319, 336  
**Jackson, M.T.** See under Arnold, M.H., 319, 615  
**James, F.A.J.L.** Editor, Faraday Rediscovered: Essays on the Life and Work of Michael Faraday, 1791-1867, *Book review* by Shortland, M. 319, 628  
**James, K.** Introducing Immunology, *Book review* by Paul, W.E. 319, 805  
**James, M.N.G.** Molecular structure of an aspartic proteinase zymogen, porcine pepsinogen, at 1.8 Å resolution (with Sielecki, A.R.) *Article*, 319, 33  
**Jans, A.W.H.** See under Cox, H.C., 319, 316  
**Jansen, J.C.** See under Cox, H.C., 319, 316  
**Jayaraman, K.S.** Bhopal disaster: India blames Union Carbide, *News*, 319, 7  
**IVF**: India embraces test-tubes, *News*, 319, 611  
**Indian science:** All change at the top, *News*, 319, 612  
**Jeanloz, R.** See under Knittle, E., 319, 214  
**Jeffrey, L.C.** Feasibility of a low-mass binary source progenitor for PSR1937+214, *Letter to Nature*, 319, 384  
**Jenkins, G.** See under Arnold, M.H., 319, 615  
**Jenkinson, D.** *Book review of Goodman and Gilman's The Pharmacological Basis of Therapeutics*, 7th Edn. (Goodman Gilman, A., Goodman, L.S., Rail, T.W., Murad, F. editors) 319, 802  
*Book review of Lecture Notes on Pharmacology* (by Grundy, H.F.) 319, 802  
*Book review of Learning Pharmacology Through MCQ: A Comprehensive Text* (by Large, B.J., Hughes, I.E.) 319, 802  
*Book review of Gaddum's Pharmacology*, 9th Edn. (by Burgen, A.S.V., Mitchell, J.F.M.) 319, 802  
**Jenner, P.** See under Bradbury, A.J., 319, 56  
**Jennings, J.N.** Karst Geomorphology, 2nd Edn., *Book review* by Williams, P.W. 319, 814  
**Jensen, F.C.** See under Ishai, Z.B., 319, 795  
**Jin, G.Y.** See under Pham, V.N., 319, 310  
**Johnson, W.S.** Editor, Affinity Chromatography: A Practical Approach, *Book review* by Parikh, I. 319, 629  
**Johnson, A.** See under Holdin, C.H., 319, 511  
**Johnson, C.** See under Rouyer, F., 319, 291  
**Jolly, A.** The Evolution of Primate Behaviour, 2nd Edn., *Book review* by Anderson, J.R. 319, 800  
**Jones, E.** See under Woodland, H., 319, 261  
**Jones, J.S.** Human evolution: How small was the bottleneck? (with Rohani, S.) *News and views*, 319, 449  
**Jones, L.** Accidental human vaccination with vaccinia virus expressing nucleoprotein gene (with Ristow, S., Yilmaz, T., Moss, B.) *Scientific correspondence*, 319, 543  
**Jonscher, A.K.** *Book review of Solid State Physics*, 2nd Edn. revised (by Blakemore, J.S.) 319, 823  
**Jordan, B.R.** See under Gomard, E., 319, 153  
**Jukes, T.H.** The fight for science textbooks, *Commentary*, 319, 367  
**Frost resistance and *Pseudomonas***, *News and views*, 319, 617  
**Jullien, R.** See under Botet, R., 319, 454  
**Kaill, R.** Human Intelligence: Perspectives and Prospects, *Book review* by Bryant, P.E. 319, 797  
**Kanasewich, E.R.** See under Green, A.G., 319, 210  
**Kandel, E.R.** Principles of Neural Science, 2nd Edn., *Book review* by Fitzgerald, M. 319, 801  
**Kanters, J.A.** See under Cox, H.C., 319, 316  
**Karato, S.** Does partial melting reduce the creep strength of the upper mantle?, *Letter to Nature*, 319, 309  
**Karpas, A.** Lack of antibodies to adult T-cell leukaemia virus and to AIDS virus in Israeli Falashas (with Maayan, S., Raz, R.) *Matters arising*, 319, 794  
**Kärre, K.** Selective rejection of H-2-deficient lymphoma variants suggests alternative immune defence strategy (with Ljunggren, H.G., Piontek, G., Kiessling, R.) *Letter to Nature*, 319, 675  
**Kazanas, D.** Origin of ultra-high-energy γ-rays from Cygnus X-3 and related sources (with Ellison, D.C.) *Letter to Nature*, 319, 380  
**Kaziro, Y.** See under Nagata, S., 319, 415  
**Keeling, C.D.** See under Tucker, C.J., 319, 195  
**Keene, W.C.** See under Weathers, K.C., 319, 657  
**Keller, M.D.** See under Glover, H.E., 319, 142  
**Kelley, R.** See under Xu, Y., 319, 652  
**Kelly, M.E.** See under Bradbury, A.J., 319, 56  
**Kemp, T.** *Book review of Vertebrate Life*, 2nd Edn (by McFarland, W.N., Pough, F.H., Cade, T.J., Heiser, J.B.) 319, 811  
*Book review of Looking at Vertebrates: A Practical Guide to Vertebrate Adaptations* (by Rogers, E.) 319, 811  
**Kendall, K.** Inadequacy of Coulomb's friction law for particle assemblies, *Letter to Nature*, 319, 203  
**Kettle, S.F.A.** The Chemical Bond, 2nd Edn., *Book review* by Stone, A. 319, 819  
**Khobar, Y.** See under Cyaden Scientific Team., 319, 396  
**Kiang, D.** See under Calkin, M.G., 319, 454  
**Kielland-Brandt, M.C.** See under Serrano, R., 319, 689  
**Kleinlin, A.** See under Rosenberg, U.B., 319, 336

- Klessing, R. *See under Kärre, K.*, 319, 675  
 Kim, S-J. *See under Pinto, J.P.*, 319, 388  
 Kimball, K.D. *See under Weathers, K.C.*, 319, 657  
 Kimura, J. Na-Ca exchange current in mammalian heart cells (*with Noma, A., Irisawa, H.*) *Letter to Nature*, 319, 596  
 Kinashi, T. *See under Noma, Y.*, 319, 640  
 King, C-Y. *Book review of Earthquake Prediction* (*by Mogi, K.*) 319, 547  
 Kint, J. An anniversary for the lipid bilayer (*with Leroy, J.G.*) *Scientific correspondence*, 319, 17  
 Kirschner, M.W. *See under McKeon, F.D.*, 319, 463  
 Kitchen, P. *Book review of Culture and the Evolutionary Process* (*by Boyd, R., Richerson, P.J.*) 319, 105  
 Klatsky, P.R. *See under Ottenhoff, T.H.M.*, 319, 66  
*See under Ottenhoff, T.H.M.*, 319, 427  
 Klatzmann, D. Immunology: Approaches to AIDS therapy (*with Montagnier, L.*) *News and views*, 319, 10  
 Klein, A. Archaeabacterial terminator, *Scientific correspondence*, 319, 268  
 Klein, J. *See under Nishiizumi, K.*, 319, 134  
 Knap, A.H. Synthetic organic chemicals in the deep Sargasso Sea (*with Binkley, K.S., Deuser, W.G.*) *Letter to Nature*, 319, 572  
 Kneller, B.C. *See under Ashcroft, W.A.*, 319, 606  
 Knittle, E. Thermal expansion of silicate perovskite and stratification of the Earth's mantle (*with Jeanloz, R., Smith, G.L.*) *Letter to Nature*, 319, 214  
 Koefoed, H.P. *See under Miller, C.*, 319, 783  
 Kohl, N.E. Human N-myC is closely related in organization and nucleotide sequence to c-myc (*with Legouy, E., DePinho, R.A., Nisen, P.D., Smith, R.K., Gee, C.E., Alt, F.W.*) *Letter to Nature*, 319, 73  
*See under Zimmerman, K.A.*, 319, 780  
 Kolb, B. Fundamentals of Human Neuropsychology, 2nd Edn., *Book review by Young, A.*, 319, 799  
 Konopka, J.B. *See under Kozbor, D.*, 319, 331  
 Koobs, D.H. Creationism, *Correspondence*, 319, 172  
 Koonin, S.E. Computational Physics, *Book review by Dickinson, A.S.*, 319, 821  
 Koop, B.F. Primate  $\eta$ -globin DNA sequences and man's place among the great apes (*with Goodman, M., Xu, P., Chan, K., Slighotom, J.L.*) *Letter to Nature*, 319, 234  
 Korkakoski, E.A. *See under Groves, D.I.*, 319, 136  
 Kozbor, D. Expression of a translocated c-abl gene in hybrids of mouse fibroblasts and chronic myelogenous leukaemia cells (*with Giallongo, J.B., Sierzega, M.E., Konopka, J.B., Witte, O.N., Showe, L.C., Croce, C.M.*) *Letter to Nature*, 319, 331  
 Krauss, L.M. Inflation and shadow matter (*with Guth, A.H., Spergel, D.N., Field, G.B., Press, W.H.*) *Letter to Nature*, 319, 748  
 Krebs, C.J. Ecology: The Experimental Analysis of Distribution and Abundance, 3rd Edn., *Book review by Smith, R.H.*, 319, 809  
 Krouse, M.E. A large anion-selective channel has seven conductance levels (*with Schneider, G.T., Gage, P.W.*) *Letter to Nature*, 319, 58  
 Krusk, C. *See under Cox, H.C.*, 319, 316  
 Krumlauf, R. Differential expression of  $\alpha$ -fetoprotein genes on the inactive and somatic tissues of a transgenic mouse line (*with Chapman, V.M., Hammer, R.E., Brinster, R., Tilghman, S.M.*) *Letter to Nature*, 319, 224  
 Kubik, P.W. Determination of cosmogenic  $^{41}\text{Ca}$  in a meteorite with tandem accelerator mass spectrometry (*with Elmore, D., Conrad, N.J., Nishiizumi, K., Arnold, J.R.*) *Letter to Nature*, 319, 568  
 Kubota, N. *See under Nagata, S.*, 319, 415  
 Kuhr, M.J. *See under De Souza, E.B.*, 319, 593  
 Kuhn, J.R. Solar ellipticity fluctuations yield no evidence of g-modes (*with Libbrecht, K.G., Dicke, R.H.*) *Letter to Nature*, 319, 128  
 Kuhmert, L. A new optical photochemical memory device in a light-sensitive chemical active medium, *Letter to Nature*, 319, 393  
 Kuperfeld, S.L. An intense cold core eddy in the North-East Atlantic (*with Becker, G.A., Simmons, W.F., Schauer, U., Marietta, M.G., Nies, H.*) *Letter to Nature*, 319, 474  
 Ladoy, P. *See under Lovejoy, S.*, 319, 43  
 Lake, J.A. An alternative to archaeabacterial dogma, *Scientific correspondence*, 319, 626  
 Lal, D. *See under Nishiizumi, K.*, 319, 134  
 Lafout, J-M. *See under White, R.*, 319, 160  
 Langmeier, A. *See under Hasinger, G.*, 319, 469  
 Lanier, L.L. Ontogeny of natural killer cells (*with Phillips, J.H.*) *Scientific correspondence*, 319, 269  
 Lansbury, C. The Old Brown Dog: Women, Workers, and Vivisection in Edwardian England, *Book review by Bynum, W.F.*, 319, 546  
 Lanzavecchia, A. Is the T-cell receptor involved in T-cell killing?, *Letter to Nature*, 319, 778  
 Large, B.J. Learning Pharmacology Through MCQ: A Comprehensive Text, *Book review by Jenkins, D.*, 319, 802  
 Larsen, M. *See under Bender, B.*, 319, 532  
 Lawden, D.F. Elements of Relativity Theory, *Book review by Raine, D.J.*, 319, 822  
 Lawrence, J.K. *See under Chapman, G.A.*, 319, 654  
 Lawrence, M.J. *See under Arnold, M.H.*, 319, 615  
 Lazdunski, M. *See under Renaud, J-F.*, 319, 678  
 Lee, J.J. Editor, An Illustrated Guide to the Protozoa, *Book review by Cox, F.E.G.*, 319, 366  
 Lefranc, M-P. Rearrangement of two distinct T-cell variable-region genes in human DNA (*with Forster, A., Rabbits, T.H.*) *Letter to Nature*, 319, 420  
 Leg 104 shipboard scientific party. Ocean Drilling Program: Formation of the Norwegian Sea, *News and views*, 319, 360  
 Leggett, J.K. Is a test ban unrealistic?, *Correspondence*, 319, 716  
 Legouy, E. *See under Kohl, N.E.*, 319, 73  
 Lemos, J.R. Single channels and ionic currents in peptidergic nerve terminals (*with Nordmann, J.J., Cooke, I.M., Stuenkel, E.L.*) *Letter to Nature*, 319, 410  
 Lepine, J.C. *See under Cyaden Scientific Team.*, 319, 396  
 Leppert, M. *See under White, R.*, 319, 160  
 Lerner, C.M. Problems and Solutions in Electromagnetic Theory, *Book review by Rosser, W.G.V.*, 319, 823  
 Leroy, J.G. *See under Kint, J.A.*, 319, 17  
 Lesser, C.M. *See under Groves, D.I.*, 319, 136  
 Leslie, A.G. *See under Ashcroft, W.A.*, 319, 606  
 Lester, R.N. *See under Arnold, M.H.*, 319, 615  
 Ley, J.P. *See under Gomard, E.*, 319, 153  
 Lewin, B. Genes II, *Book review by Brammar, W.J.*, 319, 805  
 Lewin, R.A. *Book review of The Physiological Ecology of Seaweeds* (*by Lobban, C.S., Harrison, P.J., Duncan, M.J.*) 319, 807  
 Lewin, W.H.G. *See under Hasinger, G.*, 319, 469  
 Ley, T.J. *See under Cheah, M.S.C.*, 319, 238  
 Leyhausen, D. Corrigendum: Efficiency of petroleum expulsion from shale source rocks (*with Radke, M., Schaefer, R.G.*) *Letter to Nature*, 319, 427  
 Li, L. *See under Pham, V.N.*, 319, 310  
 Libbrecht, K.G. *See under Kuhn, J.R.*, 319, 128  
 Is there an unusual solar core?, *Letter to Nature*, 319, 753  
 Lieb, W.R. *See under Franks, N.P.*, 319, 78  
 Lightman, S. Neuroendocrinology: Molecular approach appraised, *News and views*, 319, 180  
 Likens, G.E. *See under Weathers, K.C.*, 319, 657  
 Lilly, S.J. *See under Dunlop, J.S.*, 319, 564  
 Lindau, M. IgE-mediated degradation of mast cells does not require opening of ion channels (*with Fernandez, J.M.*) *Letter to Nature*, 319, 150  
 Lingner, D.W. *See under Dennison, J.E.*, 319, 390  
 Lippard, S.J. *See under Gorun, S.M.*, 319, 666  
 Lipkje, J. *See under Rosen, C.A.*, 319, 555  
 Lipschutz, M.E. *See under Dennison, J.E.*, 319, 390  
 Liss, P. *Book review of Environmental Chemistry* (*by O'Neill, P.*) 319, 815  
 Ljunggren, H.G. *See under Kärre, K.*, 319, 675  
 Lo, D. Identity of cells that imprint H-2-restricted T-cell specificity in the thymus (*with Sprent, J.*) *Letter to Nature*, 319, 672  
 Lobban, C.S. *The Physiological Ecology of Seaweeds*, *Book review by Lewin, R.A.*, 319, 805  
 Lockwood, J.G. *World Climatic Systems*, *Book review by Widley, T.M.*, 319, 825  
 Loftus, E.F. Cognitive Processes, 2nd Edn., *Book review by Sutherland, S.*, 319, 798  
 Longair, M.S. *See under Dunlop, J.S.*, 319, 564  
 Lovejoy, S. Fractal characterization of inhomogeneous geophysical measuring networks (*with Schertzer, D., Ladoy, P.*) *Letter to Nature*, 319, 43  
 Lowe, V. Alfred North Whitehead: The Man and His Work, Vol. I 1861-1910, *Book review by Gale, G.*, 319, 548  
 Lower, D.R. *See under Byerly, G.R.*, 319, 489  
 Luemann, J.G. Planetary meteorology: Is there lightning on Venus? (*with Nagy, A.F.*) *News and views*, 319, 266  
 Lund, R.D. *Book review of Molecular Bases of Neural Development* (*by Edelman, G.M., Gall, W.E., Cowan, W.M.*) 319, 107  
 Lunline, J.I. *See under Pinto, J.P.*, 319, 388  
 Lynch, G. *See under Baudry, M.*, 319, 329  
 Lynch, G.S. *See under Morris, R.G.M.*, 319, 774  
 Lynch, J.R. *See under Wainscoat, J.S.*, 319, 491  
 Mayan, S. *See under Karpas, A.*, 319, 794  
 Macdonald, M.H. Is anyone there?, *Correspondence*, 319, 172  
 Macfarlane, G. *Book review of The Life of Ernst Chain: Penicillin and Beyond* (*by Clark, R.W.*) 319, 363  
 Macgregor, R.B. Estimation of the polarity of the protein interior by optical spectroscopy (*with Weber, G.*) *Letter to Nature*, 319, 70  
 Machin, N.A. *See under Golding, B.W.*, 319, 301  
 Mackay, A.L. Pauling's model not universally accepted, *Scientific correspondence*, 319, 103  
 MacPhee-Quigley, K. *See under Schumacher, M.*, 319, 407  
 Maddox, B. Television: Defence of the realm, *News*, 319, 253  
 Maddox, J. Further anxieties about AIDS, *News and views*, 319, 9 Voyager 2 swings by Uranus, *News and views*, 319, 95  
 Newtonian gravitation corrected, *News and views*, 319, 173  
 Growth by cannibalization, *News and views*, 319, 257  
 Galactic voids may be statistical, *News and views*, 319, 445  
 British science: Sir Keith Joseph regrets ..., *News*, 319, 531  
 More tests of special relativity, *News and views*, 319, 533  
 US space spending: United front on basic research, *News*, 319, 714  
*Limits on mass of missing mass*, *News and views*, 319, 717  
 Magram, J. *See under Chada, K.*, 319, 685  
 Mahadevan, A. *See under Balajee, S.*, 319, 728  
 Maitland, D.F. Crabs that breathe air with their legs — *Scopimera* and *Dotilla*, *Letter to Nature*, 319, 493  
 Male, D. Immunology, *Book review by Paul, W.E.*, 319, 805  
 Malissen, B. *See under Malissen, M.*, 319, 28  
 Malissen, M. Direct evidence for chromosomal inversion during T-cell receptor  $\beta$ -gene rearrangements (*with McCoy, C., Blanc, D., Trucy, J., Devaux, C., Schmitt-Verhulst, A-M., Fitch, F., Hood, L., Malissen, B.*) *Article*, 319, 28  
 Maloty, G.M.O. Energetic cost of carrying loads: have African women discovered an economic way? (*with Heglund, N.C., Prager, L.M., Cavagna, G.A., Taylor, C.R.*) *Letter to Nature*, 319, 668  
 Mandelstam, J. South Africa (*with Harrison, G.A., Hall, E.T.*) *Correspondence*, 319, 715  
 Mandelstam, J. South Africa (*with Harrison, G.A., Hall, E.T.*) *Correspondence*, 319, 715  
 Mansfield, S. Identification of Na-Ca exchange current in single cardiac myocytes (*with Pott, L.*) *Letter to Nature*, 319, 597  
 Medvedev, Z.A. Sakharov's scientific legacy, *Correspondence*, 319, 93  
 Mehra, V. *See under Mustafa, A.S.*, 319, 63  
 Meisenheimer, K. Optical synchrotron emission in the southern lobes of 3C33 (*with Röser, H-J.*) *Article*, 319, 454  
 Melissinos, A. Quantum Mechanics: A Modern Introduction, *Book review by Rhodes, W.*, 319, 821  
 Merritt, R.L. The Grand Menhir re-examined, *Scientific correspondence*, 319, 18  
 Message, P.J. Celestial mechanics: Testing Solar System stability, *News and views*, 319, 359  
 Metz, C.B. Editor, Biology of Fertilization, *Book review by Cohen, J.* 319, 20

- Meyers, N. Israeli-Egyptian cooperation: Minor relic of Camp David, *News*, 319, 91
- Michell, B. Inositol phosphates: Profusion and confusion, *News and views*, 319, 176
- Michie, C. A. Bird dropping research continues apace, *Scientific correspondence*, 319, 625
- Middle, F. A. Editor, Affinity Chromatography: A Practical Approach, *Book review* by Parikh, I., 319, 629
- Middlemost, E. A. K. Magnas and Magmatic Rocks: An Introduction to Igneous Petrology, *Book review* by Cox, K. G., 319, 813
- Middleton, R. *See under* Nishiizumi, K., 319, 134
- Mikhailov, A. I. Scientific Communications and Information Exchange, *Book review* by Garfield, E., 319, 272
- Milani, A. Long-term changes in the semimajor axes of the outer planets (with Nobili, A. M., Fox, K., Carpino, M.) *Letter to Nature*, 319, 386
- Millan, M. A. *See under* Udelesman, R., 319, 147
- Miller, T. W. *See under* Ajakaiye, D. E., 319, 582
- Miller, C. Human p53 gene localized to short arm of chromosome 17 (with Mohandas, T., Wolf, D., Prokocimer, M., Rotter, V., Koefler, H. P.) *Letter to Nature*, 319, 783
- Miller, G. Animal model for Epstein-Barr lymphoma, *Scientific correspondence*, 319, 626
- Milligan, R. A. Location of exit channel for nascent protein in 80S ribosome (with Unwin, P. N. T.) *Letter to Nature*, 319, 693
- Minna, J. D. *See under* Zimmerman, K. A., 319, 780
- Mitchell, A. P. Activation of meiosis and sporulation by repression of the RMEI product in yeast (with Herskowitz, I.) *Article*, 319, 738
- Mitchell, C. Are the Falkland Islands a rotated microplate? (with Taylor, G. K., Cox, K. G., Shaw, J.) *Letter to Nature*, 319, 131
- Mitchell, J. F. M. Gaddum's Pharmacology, 9th Edn., *Book review* by Jenkinson, D., 319, 802
- Miyajima, N. *See under* Yamamoto, T., 319, 230
- Mogi, K. Earthquake Prediction, *Book review* by King, C.-Y., 319, 547
- Mohandas, T. *See under* Miller, C., 319, 783
- Monroy, A. Editor, Biology of Fertilization, *Book review* by Cohen, J., 319, 20
- Montaguer, L. *See under* Klatzmann, D., 319, 10
- Moorbath, S. *See under* Whitehouse, M. J., 319, 488
- Moore, P. D. Prehistoric ecology: Clues from the pollen record, *News and views*, 319, 361
- Morgan, E. The Descent of Woman: A New Edition, *Book review* by Attenborough, R., 319, 271
- Mornex, J.-F. *See under* Martinet, Y., 319, 158
- Morris, R. G. M. Selective impairment of learning and blockade of long-term potentiation by an N-methyl-D-aspartate receptor antagonist, AP5 (with Anderson, E., Lynch, G. S., Baudry, M.) *Letter to Nature*, 319, 774
- Morris, S. C. The Precambrian-Cambrian boundary and geochemical perturbations (with Bengtson, S.) *Matters arising*, 319, 696
- Mosalkhani, P. Pair production instabilities as a source of X-ray flares from accreting black holes (with Sikora, M.) *Letter to Nature*, 319, 649
- Moss, B. *See under* Jones, L., 319, 543
- Mould, S. M. PhD theses, *Correspondence*, 319, 616
- Mrosovsky, N. Biological rhythms: Sleep researchers caught napping, *News and views*, 319, 536
- Mullins, J. I. Disease-specific and tissue-specific production of unintegrated feline leukaemia virus variant DNA in feline AIDS (with Chen, C. S., Hoover, E. A.) *Letter to Nature*, 319, 333
- Mumford, P. M. *See under* Arnold, M. H., 319, 615
- Mundy, G. R. *See under* Bertolini, D. R., 319, 516
- Munn, C. A. Birds that 'cry wolf', *Letter to Nature*, 319, 143
- Munro, M. *See under* Ashcroft, W. A., 319, 606
- Murad, F. Editor, Goodman and Gilman's The Pharmacological Basis of Therapeutics, 7th Edn., *Book review* by Jenkinson, D., 319, 802
- Murrell, J. N. The Chemical Bond, 2nd Edn., *Book review* by Stone, A., 319, 819
- Mustafa, A. S. Human T-cell clones recognize a major *M. leprae* protein antigen expressed in *E. coli* (with Gill, H. K., Nerland, A., Britton, W. J., Mehra, V., Bloom, B. R., Young, R. A., Godal, T.) *Letter to Nature*, 319, 63
- Nagata, S. Molecular cloning and expression of cDNA for human granulocyte colony-stimulating factor (with Tsuchiya, M., Asano, S., Kazi, Y., Yamazaki, T., Yamamoto, O., Hirata, Y., Kubota, N., Ohe, M., Nomura, H., Ono, M.) *Letter to Nature*, 319, 415
- Nagy, A. F. *See under* Luhmann, J. G., 319, 266
- Naito, T. *See under* Noma, Y., 319, 640
- Naka, K.-I. *See under* Sakai, H. M., 319, 495
- Nakai, S. *See under* Yamamoto, C., 319, 757
- Nakamura, Y. *See under* White, R., 319, 160
- Nash, W. G. *See under* O'Brien, S. J., 319, 428
- Nau, M. M. *See under* Zimmerman, K. A., 319, 780
- Nauta, J. H. Fundamental Neuroanatomy, *Book review* by Fitzgerald, M., 319, 801
- Naylor, R. J. *See under* Bradbury, A. J., 319, 56
- Nechval, A. Pictorial Orbital Theory, *Book review* by Isaacs, N. S., 319, 816
- Nedwell, D. B. *Book review* of Archaeabacteria. The Bacteria: A Treatise on Structure and Function, Vol. VIII (Woese, C. R., Wolfe, R. S. editors) 319, 273
- Nedwin, G. E. *See under* Bertolini, D. R., 319, 516
- Neffe, J. West German space: Ministers at odds about Hermes, *News*, 319, 92
- West German schools: Teachers swell dole queues, *News*, 319, 255
- German research agency: Ethologist takes the helm, *News*, 319, 345
- Seibold in Europe, *News*, 319, 166
- Nelman, P. E. *See under* Thompson, C. B., 319, 374
- Nelson, C. S. *See under* Frogatt, P. C., 319, 578
- Nelson, E. Quantum Fluctuations, *Book review* by Pearle, P., 319, 456
- Nerland, A. *See under* Mustafa, A. S., 319, 63
- Nesbitt, R. W. Geology: Are komatiitic lavas voracious?, *News and views*, 319, 97
- Nester, E. W. *See under* Turner, J. J., 319, 422
- Newmark, P. Molecular biology in Tokyo, *News and views*, 319, 353
- British clinical research: Shotgun merger proposed, *News*, 319, 442
- MRC attacked, *News*, 319, 442
- Malaria vaccines: Biogen revives forgotten project, *News*, 319, 613
- Which interleukin-4?, *News and views*, 319, 620
- Museums: Expenditure cut to the bone, *News*, 319, 712
- Plant breeding: The seeds of commerce, *News*, 319, 713
- Newton, M. *See under* Schumacher, M., 319, 407
- Nicholson, P. D. *See under* Dermott, S. F., 319, 115
- Nick, H. Detection of cytosine methylation in the maize alcohol dehydrogenase gene by genomic sequencing (with Bowen, B., Ferl, R. J., Gilbert, W.) *Letter to Nature*, 319, 243
- Nield, E. W. Palaeontology: An Introduction, *Book review* by Halstead, B., 319, 810
- Nies, H. *See under* Kuiper, S. L., 319, 474
- Nisen, P. D. *See under* Kohl, N. E., 319, 73
- Nishizumi, K. Production of  $^{10}\text{Be}$  and  $^{26}\text{Al}$  by cosmic rays in terrestrial quartz *in situ* and implications for erosion rates (with Lal, D., Klein, J., Middleton, R., Arnold, J. R.) *Letter to Nature*, 319, 134
- See under* Kubik, P. W., 319, 568
- Nobili, A. M. *See under* Milani, A., 319, 386
- Noma, A. *See under* Kimura, J., 319, 596
- Noma, Y. Cloning of cDNA encoding the murine IgG1 induction factor by a novel strategy using SP6 promoter (with Sideras, P., Naito, T., Bergstedt-Lindquist, S., Azuma, C., Severinson, E., Tanabe, T., Kinashi, T., Matsuda, F., Yaito, Y., Honjo, T.) *Article*, 319, 640
- Nomura, H. *See under* Nagata, S., 319, 415
- Nomura, N. *See under* Yamamoto, T., 319, 230
- Nordmann, J. J. *See under* Lemos, J. R., 319, 410
- Norman, K.-M. *See under* Burgoyne, R. D., 319, 68
- North, F. K. Petroleum Geology, *Book review* by Wilson, R. C. L., 319, 812
- North, R. A. *See under* Egan, T. M., 319, 405
- Norton, R. H. *See under* Toon, G. C., 319, 570
- O'Brien, S. J. Palaeontological and molecular views of panda phylogeny: Reply (with Nash, W. G., Benveniste, R. E., Wildt, D. E., Bush, M. E.) *Matters arising*, 319, 428
- O'Connell, P. *See under* White, R., 319, 160
- O'Neill, P. Environmental Chemistry, *Book review* by Liss, P., 319, 815
- O'Reilly, J. J. *Book review* of Fiber Optics: Technology and Applications (by Personick, S. D.), 319, 366
- Oakley, D. A. Editor, Brain and Mind, *Book review* by Young, A., 319, 799
- Ogura, K. Direct conversion of methane to methanol, chloromethane and dichloromethane at room temperature (with Takamagari, K.) *Letter to Nature*, 319, 308
- Oheda, M. *See under* Nagata, S., 319, 415
- Ohtomo, M. *See under* Ahmad, S., 319, 659
- Ojo, S. B. *See under* Ajakaiye, D. E., 319, 582
- Okera, W. Future UNESCO, *Correspondence*, 319, 444
- Oki, A. *See under* Gammon, G., 319, 413
- Old, J. M. *See under* Waincoat, J. S., 319, 491
- Old, R. W. Principles of Gene Manipulation: An Introduction to Genetic Engineering, 3rd Edn., *Book review* by Oliver, S., 319, 803
- Oliver, S. *Book review* of Principles of Gene Manipulation: An Introduction to Genetic Engineering, 3rd Edn. (by Old, R. W., Primrose, S. B.), 319, 803
- Ono, M. *See under* Nagata, S., 319, 415
- Osbourne, G. C. Infrared detectors: Superlattices point ahead, *News and views*, 319, 618
- Otenhoff, T. H. M. *Mycobacterium leprae*-specific protein antigens defined by cloned human helper T cells (with Klatser, P. R., Ivanyi, J., Elferink, D. G., de Wit, M. Y. L., de Vries, R. R. P.) *Letter to Nature*, 319, 66
- Erratum: *Mycobacterium leprae*-specific protein antigens defined by cloned human helper T cells (with Klatser, P. R., Ivanyi, J., Elferink, D. G., de Wit, M. Y. L., de Vries, R. R. P.) *Letter to Nature*, 319, 427
- Oyeyinka, G. O. Malaria — mitogens or super antigens?, *Scientific correspondence*, 319, 543
- Paczynski, B. Will cosmic strings be discovered using the Space Telescope?, *Letter to Nature*, 319, 567
- Palca, J. US science adviser: McTague fills Keyworth's shoes, *News*, 319, 87
- Viral cancers: AIDS virus at the centre, *News*, 319, 170
- Infection mechanism?, *News*, 319, 170
- Synthetic fuels: US Synfuels narrowly bites the dust, *News*, 319, 89
- Space research: Texas A & M fly space-grant kite, *News*, 319, 252
- Genetic engineering: Frost damage tests blocked, *News*, 319, 254
- Solar System: Voyager passes Uranus, Giotto rescued, *News*, 319, 345
- US research costs: Government to turn screws, *News*, 319, 346
- Panel's prescription, *News*, 319, 346
- SFC defies Congress, *News*, 319, 348
- Animal welfare: OTA squares circle of dissent, *News*, 319, 440
- Guidelines off, *News*, 319, 440
- Trials on ice, *News*, 319, 441
- AIDS: Academy looks for strategy, *News*, 319, 441
- World Archaeological Congress: South African exclusion causes academic schism, *News*, 319, 524
- Pharmaceuticals in Britain: Drug list clouds foreign interest, *News*, 319, 529
- Eureka: Secretariat in search of base, *News*, 319, 530
- Palmer, M. R.  $^{187}\text{Os}^{186}\text{Os}$  in marine manganese nodules and the constraints on the crustal geochemistry of rhenium and osmium (with Turcik, K. K.) *Letter to Nature*, 319, 216
- Parikh, I. *Book review* of Affinity Chromatography: A Practical Approach (Dean, P. D. G., Johnson, W. S., Middle, F. A. editors) 319, 629
- Book review* of Affinity Chromatography: Template Chromatography of Nucleic Acids and Proteins (by Schott, H.) 319, 629
- Partridge, R. B. *See under* Mandelis, N., 319, 751
- Pastan, I. An Atlas of Immunofluorescence in Cultured Cells, *Book review* by Heath, J. 319, 547
- Patient, R. *See under* Enver, T., 319, 99
- Patrick, J. *See under* Boulter, J., 319, 368
- Paul, W. E. *Book review* of Immunology (by Roitt, I., Brostoff, J., Male, D.), 319, 805
- Book review* of Introducing Immunology (by Staines, N., Brostoff, J., James, K.), 319, 805
- Peacock, J. A. *See under* Dunlop, J. S., 319, 564
- Pearle, P. *Book review* of Quantum Fluctuations (by Nelson, E.), 319, 456
- Pears, N. Basic Biogeography, 2nd Edn., *Book review* by Harrison, C., 319, 809
- Pearson, A. J. Metallo-organic Chemistry, *Book review* by Taylor, R. J. K., 319, 817
- Pearson, R. The brain drain is here again, *Employment*, 319, 84
- Breaks in career — What chance for women?, *Employment*, 319, 522
- Pegram, S. *See under* Weiss, R. A., 319, 794
- Pellegrino, J. W. Human Intelligence: Perspectives and Prospects, *Book review* by Bryant, P. E., 319, 797
- Penkett, S. A. Atmospheric chemistry: Hydrogen peroxide in cloudwater, *News and views*, 319, 624
- The spring maximum in photo-oxidants in the Northern Hemisphere troposphere (with Brice, K. A.) *Letter to Nature*, 319, 655
- Perrin, P. *See under* Grantham, R., 319, 727
- Perry, B. D. The real cause of Ethiopia's problems, *Scientific correspondence*, 319, 183
- Personick, S. D. Fiber Optics: Technology and Applications, *Book review* by O'Reilly, J. J., 319, 366
- Petif, J.-C. *See under* Dran, J.-C., 319, 485
- Pham, V. N. Partial melting zones in the crust in southern Tibet from magnetotelluric results (with Boyer, D., Therme, P., Yuan, X. C., Li, J., Jin, G. Y.) *Letter to Nature*, 319, 310
- Phillips, J. H. *See under* Lanier, L. L., 319, 269
- Pinto, J. P. D to H ratio and the origin and evolution of Titan's atmosphere (with Lunine, J. I., Kim, S.-J., Yung, Y. L.) *Letter to Nature*, 319, 388
- Piontek, G. *See under* Kärre, K., 319, 675
- Pirie, N. W. *Book review* of Haldane: The Life and Work of J. B. S. Haldane with Special Reference to India (by Dronamraju, K. R.), 319, 630
- Pirt, S. J. Argentine science: Slow return to openness, *News*, 319, 6
- Pletzer, R. *See under* Mayer, E., 319, 298
- Poole, T. Social Behaviour in Mammals, *Book review* by Roper, T., 319, 800
- Porter, R. *Book review* of The Royal Institution: An Informal History (by Caroe, G.), 319, 455
- Pott, L. *See under* Mechmann, S., 319, 597
- Potts, K. T. *Book review* of Heterocyclic Chemistry (by Gilchrist, T. L.), 319, 816
- Pough, R. H. Vertebrate Life, 2nd Edn., *Book review* by Kemp, T., 319, 811
- Powell, T. G. *See under* Summons, R. E., 319, 763
- Prager, L. M. *See under* Maloy, G. M. O., 319, 668
- Preliss, A. *See under* Rosenberg, U. B., 319, 336
- Press, W. H. *See under* Krauss, L. M., 319, 748
- Price, D. L. *See under* De Souza, E. B., 319, 593
- Price, G. D. Earth sciences: Perovskites and plate tectonics, *News and views*, 319, 175
- Primrose, S. B. Principles of Gene Manipulation: An Introduction to Genetic Engineering, 3rd Edn., *Book review* by Oliver, S., 319, 803
- Prince, D. A. *See under* McCormick, D. A., 319, 402
- Prinn, R. G. *See under* Feigley, B. Jr., 319, 305
- Prokocimer, M. *See under* Miller, C., 319, 783
- Prosser, C. L. *Book review* of Changes in Eukaryotic Gene Expression in Response to Environmental Stress (Atkinson, B. G., Walden, D. B. editors) 319, 187
- Book review* of The Adaptive Role of Lipids in Biological Systems (by Hadley, N.), 319, 187
- Principopoulos, M. How to test special relativity (with Theocharis, T.) *Scientific correspondence*, 319, 269
- Putney, J. W. Editor, Calcium in Biological Systems, *Book review* by Baker, P. F., 319, 22
- Putney, J. W. Jr. *See under* Spät, A., 319, 514
- Rabbitts, P. *Book review* of Neuropsychology of Memory (Squire, L. R., Butters, N. editors) 319, 365
- Rabbitts, T. H. *See under* Lefranc, M.-P., 319, 420
- Radke, M. *See under* Leythaeuser, D., 319, 427
- Raff, M. C. *See under* French-Constant, C., 319, 499
- Raiha, A. *See under* Baltz, T., 319, 602
- Raine, D. J. *Book review* of Basic Concepts in Relativity and Early Quantum Theory, 2nd Edn. (by Resnick, R., Halliday, D.), 319, 822
- Book review* of Elements of Relativity Theory (by Lawden, D. F.)

## AUTHOR INDEX

- 319, 822  
 Rall, T W. Editor, Goodman and Gilman's *The Pharmacological Basis of Therapeutics*, 7th Edn., *Book review* by Jenkinson, D. 319, 802  
 Ramanamurthy, P V. *See under* Bhat, P N., 319, 127  
 Ramaty, R. *See under* Dermer, C D., 319, 205  
 Rammensee, H-G. Restricted recognition of  $\beta_2$ -microglobulin by cytotoxic T lymphocytes (with Robinson, P J., Crisanti, A., Bevan, M J.) *Letter to Nature*, 319, 502  
 Rane, S G. *See under* Holz, G G IV., 319, 670  
 Ratner, M I. *See under* Bartel, N., 319, 733  
 Rawley, L A. Period derivative and orbital eccentricity of binary pulsar 1953+29 (with Taylor, J H., Davis, M M) *Letter to Nature*, 319, 383  
 Raz, R. *See under* Karpas, A., 319, 794  
 Reddy, E P. *See under* Rossen, D., 319, 604  
 Redkozubov, A. *See under* Bregestovski, P., 319, 776  
 Rees, W G. *See under* Spinks, M J., 319, 471  
 Reeves, K R. Bees in SE Asia (with Anderson, W H.) *Correspondence*, 319, 94  
 Relde, I. *See under* Rosenberg, U B., 319, 336  
 Renaud, J-F. Expression of apamin receptor in muscles of patients with myotonic muscular dystrophy (with Desnuelle, C., Schmid-Antomarchi, H., Hugues, M., Serratrice, G., Lazdunski, M.) *Letter to Nature*, 319, 678  
 Resnick, R. *Basic Concepts in Relativity and Early Quantum Theory*, 2nd Edn., *Book review* by Raine, D J., 319, 822  
 Rhodes, W. *Book review of Quantum Mechanics: A Modern Introduction* (by Das, A., Melissinos, A.) 319, 821  
*Book review of The Picture Book of Quantum Mechanics* (by Brandt, S., Dahmen, H D.) 319, 821  
 Rich, A. *See under* Wolff, S M., 319, 270  
 Rich, V. Red greens on Yellow River?, *News*, 319, 5  
 Siberian river scheme: Russian party demands caution, *News*, 319, 88  
 Soviets ask for space, *News*, 319, 88  
 Comecon technology: Plans laid for collaboration, *News*, 319, 92  
 Refusnik scientists: Dissenting dissidents agree, *News*, 319, 169  
 Polish astronomers, *News*, 319, 170  
 Romanian mathematics: Absent guest at Princeton, *News*, 319, 171  
 Soviet Union: Scientists facing redundancy, *News*, 319, 255  
 Poles sentenced, *News*, 319, 346  
 Nuclear power: Yugoslav plans approved, *News*, 319, 350  
 Hungarian dam, *News*, 319, 351  
 Soviet environment: Now pollution on television, *News*, 319, 439  
 Bulgarian identity: Proofs of ethnic purity advanced, *News*, 319, 443  
 Nuclear winter: Soviet researcher's part hyped, *News*, 319, 165  
 Antarctic treaty: Argentina expands research effort, *News*, 319, 166  
 Gorbachev's purge reaches researchers, *News*, 319, 528  
 Shcharanski release triggers hopes, *News*, 319, 611  
 Solar telescope: US and China join with Europe, *News*, 319, 709  
 Hydroengineering: More controversy over Danube, *News*, 319, 710  
 Richards, E G. *Book review of Physical Chemistry: Principles and Applications in Biological Sciences*, 2nd Edn. (by Tinoco Jr., I., Sauer, K., Wang, J C.) 319, 804  
 Richards, W G. *Structure and Spectra of Molecules*, *Book review* by Stone, A., 319, 819  
 Richardson, P J. Culture and the Evolutionary Process, *Book review* by Kitcher, P., 319, 105  
 Rigby, M. *Book review of Physical Chemistry*, 3rd Edn. (by Atkins, P W.) 319, 820  
 Ringwood, A E. *See under* Sekine, T., 319, 584  
 Ristow, S. *See under* Jones, L., 319, 543  
 Robbins, K C. *See under* Cheah, M S C., 319, 238  
 Roberts, E H. *See under* Arnold, M H., 319, 615  
 Roberts, I S. Foundations of Parasitology, 3rd Edn., *Book review* by Cox, F E G., 319, 807  
 Roberts, M W. *See under* Au, C T., 319, 206  
 Robinson, J D. Free will and determinism, *Correspondence*, 319, 352  
 Robinson, P J. *See under* Rammensee, H-G., 319, 502  
 Rodger, C D. *Book review of Molecular Structure: Macromolecules in Three Dimensions* (by Fletterick, R J., Schroer, T., Mateka, R J.), 319, 804  
 Rogers, E. *See under* Kemp, T., 319, 811  
 Rogers, J. Repeated sequences: The origin of retroposons, *News and views*, 319, 725  
 Roitt, I. Immunology, *Book review* by Paul, W E., 319, 805  
 Rolfe, M. Induction of yeast Ty element transcription by ultraviolet light (with Spanos, A., Banks, G.) *Letter to Nature*, 319, 339  
 Roper, T. *Book review of Social Behaviour in Mammals* (by Poole, T.) 319, 800  
 Roques, F. *See under* Hubbard, W B., 319, 636  
 Rosam, A-C. Potent ulcerogenic actions of platelet-activating factor on the stomach (with Wallace, J L., Whittle, B J R.) *Letter to Nature*, 319, 54  
 Rosen, C A. Post-transcriptional regulation accounts for the trans-activation of the human T-lymphotropic virus type III (with Sodroski, J G., Goh, W C., Dayton, A I., Lippke, J., Haseltine, W A.) *Article*, 319, 555  
 Rosen, R. Editor, *Theoretical Biology and Complexity: Three Essays on the Natural Philosophy of Complex Systems*, *Book review* by Segel, L A., 319, 457  
 Rosenberg, S. AIDS: Etiology, Diagnosis, Treatment and Prevention, *Book review* by Teidier, R S., 319, 457  
 Rosenberg, U B. Structural homology of the product of the *Drosophila Krüppel* gene with *Xenopus* transcription factor IIIA (with Schröder, C., Preiss, A., Kienlin, A., Côté, S., Reide, I., Jackle, H.) 319, 822  
*Letter to Nature*, 319, 336  
 Rosenwasser, L J. *See under* Wolff, S M., 319, 270  
 Röser, H-J. *See under* Meisenheimer, K., 319, 459  
 Rossant, J. Clonal origin of haematopoietic colonies in the postnatal mouse liver (with Vlijh, K M., Grossi, C E., Cooper, M D.) *Letter to Nature*, 319, 507  
 Rosser, W G V. *Book review of Electromagnetic Waves* (by Dobbs, E R.) 319, 823  
*Book review of Maxwell's Equations and their Applications* (by Thomas, E G., Meadows, A J.) 319, 823  
*Book review of Problems and Solutions in Electromagnetic Theory* (by Lerner, C M.) 319, 823  
*Book review of Electromagnetic Wave Theory* (by Wait, J R.) 319, 823  
 Rosson, D. Nucleotide sequence of chicken c-myc complementary DNA and implications for myb oncogene activation (with Reddy, E P.) *Letter to Nature*, 319, 604  
 Roth, C. *See under* Baltz, T., 319, 602  
 Rothman, J E. Cell biology: Life without clathrin, *News and views*, 319, 96  
 Rotter, V. *See under* Miller, C., 319, 783  
 Rouhani, S. *See under* Jones, J S., 319, 449  
 Rouyer, F. A gradient of sex linkage in the pseudoautosomal region of the human sex chromosomes (with Simmler, M-C., Johnsson, C., Vergnaud, G., Cooke, H J., Weissenbach, J.) *Article*, 319, 291  
 Rowlands, M. *See under* Bender, B., 319, 532  
 Rowlinson, J S. Physics of liquids: Are diameters rectilinear?, *News and views*, 319, 362  
 Rubenstein, E. *See under* Weiss, R A., 319, 794  
 Rubin, R P. Editor, *Calcium in Biological Systems*, *Book review* by Baker, P F., 319, 22  
*See under* Spät, A., 319, 514  
 Ruth, E. *See under* Bada, J L., 319, 314  
 Rutter, W J. *See under* Edwards, R H., 319, 784  
 Saito, T. *See under* Yamamoto, T., 319, 230  
 Sakai, H M. Ganglion cell dendrites are presynaptic in catfish retina (with Nakai, K-I., Dowling, J E.) *Letter to Nature*, 319, 495  
 Samuel, Viscount. PhD thesis, *Correspondence*, 319, 616  
 Sanders, R H. Is the galactic centre black hole a dwarf? (with Allen, D A.) *Article*, 319, 191  
 Sangree, C H. *See under* Mandolei, N., 319, 751  
 Sapienza, C. 'Brain-specific' transcription and evolution of the identifier sequence (with St-Jacques, B.) *Letter to Nature*, 319, 418  
 Sauer, K. *Physical Chemistry: Principles and Applications in Biological Sciences*, 2nd Edn., *Book review* by Richards, E G., 319, 804  
 Saunders, P A H. Radiation threshold, *Correspondence*, 319, 532  
 Savage, A. *See under* Dunlop, J S., 319, 564  
 Saxon, D H. UK physics, *Correspondence*, 319, 256  
 Sayen, J. Einstein in America, *Book review* by Haberer, J., 319, 20  
 Sazer, S. *See under* Dynan, W S., 319, 246  
 Schaefer, R G. *See under* Leythaeuser, D., 319, 427  
 Schauer, U. *See under* Kupferman, S L., 319, 474  
 Schenck, P A. *See under* Cox, H C., 319, 316  
 Schertzer, D. *See under* Lovejoy, S., 319, 43  
 Schild, G C. *See under* Brown, F., 319, 549  
 Schlimk, R T. *See under* Dynan, W S., 319, 246  
 Schmid, R. Prizes for Germany, *Correspondence*, 319, 256  
 Schmid-Antomarchi, H. *See under* Renaud, J-F., 319, 678  
 Schmidt, G D. Foundations of Parasitology, 3rd Edn., *Book review* by Cox, F E G., 319, 807  
 Schmitt-Verhulst, A-M. *See under* Malissen, M., 319, 28  
 Schneider, G T. *See under* Krouse, M E., 319, 58  
 Schofield, W B. *Introduction to Bryology*, *Book review* by Smith, A J., 319, 807  
 Schott, H. Affinity Chromatography: Template Chromatography of Nucleic Acids and Proteins, *Book review* by Parkh, I., 319, 629  
 Schröder, C. *See under* Rosenberg, U B., 319, 336  
 Schroer, T. Molecular Structure: Macromolecules in Three Dimensions, *Book review* by Rodger, C D., 319, 804  
 Schulze, D J. Calcium anomalies in the mantle and a subducted metaserpentinite origin for diamonds, *Letter to Nature*, 319, 483  
 Schumacher, M. Primary structure of *Torpedo californica* acetylcholinesterase deduced from its cDNA sequence (with Camp, S., Maulet, Y., Newton, M., MacPhee-Quigley, K., Taylor, S S., Friedmann, T., Taylor, P.) *Letter to Nature*, 319, 407  
 Schwartz, J H. Principles of Neural Science, 2nd Edn., *Book review* by Fitzgerald, M., 319, 801  
 Scott, C. *See under* Marks, D., 319, 444  
 Scott, D R. Observations of solitary waves in a viscously deformable pipe (with Stevenson, D J., Whitehead, J A Jr.) *Letter to Nature*, 319, 759  
 Scott, P R. Structure and Spectra of Molecules, *Book review* by Stone, A., 319, 819  
 Sequist, E R. *See under* Taylor, A R., 319, 38  
 Seed, R. *An Introduction to Coastal Ecology*, *Book review* by Hawkins, S., 319, 808  
 Sefton, B M. *See under* Voronova, A F., 319, 682  
 Segel, L A. *Book review of Theoretical Biology and Complexity: Three Essays on the Natural Philosophy of Complex Systems* (Rosen, R editor) 319, 457  
 Seger, J. Asymmetry in the evolution of female mating preferences (with Trivers, R.) *Letter to Nature*, 319, 771  
 Sekine, T. High-pressure transformation of eclogite to garnetite in subducted oceanic crust (with Irfune, T., Ringwood, A E., Hibberd, W O.) *Letter to Nature*, 319, 584  
 Selby, M J. *See under* Edwards, R H., 319, 784  
 Selley, R C. Elements of Petroleum Geology, *Book review* by Wilson, R C L., 319, 812  
 Selverston, A I. Editor, *Model Neural Networks and Behavior*. *Book review* by Horridge, A., 319, 22  
 Semba, K. *See under* Yamamoto, T., 319, 220  
 Sen, R. *See under* Singh, H., 319, 154  
 Sercarz, E E. *See under* Gammon, G., 319, 413  
 Serrano, R. Yeast plasma membrane ATPase is essential for growth and has homology with ( $Na^+$  /  $K^+$ ),  $K^+$  and  $Ca^{2+}$  ATPases (with Kielland-Brandt, M C., Fink, G R.) *Letter to Nature*, 319, 689  
 Serrate, G. *See under* Renaud, J-F., 319, 678  
 Severinson, E. *See under* Noma, Y., 319, 640  
 Shapiro, I I. *See under* Bartel, N., 319, 733  
 Sharp, P A. *See under* Singh, H., 319, 154  
 Sharpe, A G. Inorganic Chemistry, 2nd Edn. *Book review* by McCleverty, J., 319, 819  
 Shashri, N. *See under* Gammon, G., 319, 413  
 Shaw, J. *See under* Mitchell, C., 319, 131  
 Shechtman, D. *See under* Cahn, J W., 319, 102  
 Shepherd, G M. Neurobiology: Microcircuits to see by, *News and views*, 319, 452  
 Shimazaki, K. Blue light-dependent proton extrusion by guard cell protoplasts of *Vicia faba* (with Iino, M., Zeiger, E.) *Letter to Nature*, 319, 324  
 Shimokawa, K. *See under* Imai, N., 319, 79b  
 Shortland, M. *Book review of Faraday Rediscovered: Essays on the Life and Work of Michael Faraday* 1791-1867 (Gibbons, D., James, F A J editors) 319, 628  
 Showe, L C. *See under* Kozbor, D., 319, 331  
 Siccrist, B. *See under* Hubbard, W B., 319, 636  
 Sichtler, B. *See under* Cyaden Scientific Team., 319, 148  
 Sideras, P. *See under* Noma, Y., 319, 640  
 Silecki, A R. *See under* James, M N G., 319, 33  
 Sierzega, M E. *See under* Kozbor, D., 319, 331  
 Sikora, M. *See under* Moskalik, P., 319, 649  
 Silver, B L. *The Physical Chemistry of Membranes: An Introduction to the Structure and Dynamics of Biological Membranes*. *Book review* by Tanford, C., 319, 108  
 Simmler, M-C. *See under* Rouyer, F., 319, 291  
 Simmonds, N W. *See under* Arnold, M H., 319, 615  
 Simmons, R M. *Book review of Design and Performance of Microelectronic Systems* (Taylor, C R., Weibel, E., Botts, L. editors) 319, 182  
 Simmons, W F. *See under* Kupferman, S L., 319, 374  
 Simon, J. *Molecular Semiconductors: Photoelectrical Properties and Solar Cells*, *Book review* by Eley, D D., 319, 453  
 Singh, H. A nuclear factor that binds to a conserved sequence motif in transcriptional control elements of immunoglobulin genes (with Sen, R., Baltimore, D., Sharp, P A.) *Letter to Nature*, 319, 154  
 Sironi, G. *See under* Mandolei, N., 319, 751  
 Skoglund, U. Three-dimensional structure of a specific pre-messenger RNP particle established by electron microscopy tomography (with Andersson, K., Strandberg, B., Danielsson, B.) *Article*, 319, 560  
 Slatkin, M. Editor, *Evolution: Essays in Honour of John Maynard Smith*, *Book review* by Futuyma, D J., 319, 19  
 Slughton, J L. *See under* Koop, B F., 319, 234  
 Slingo, A. *See under* Golding, B W., 319, 101  
 Small, H. *Book review of Scientific Communication and Information Exchange* (by Mikhailov, A I., Cherny, A I., Golovchenko, R S.) 319, 272  
 Smartt, J. *See under* Arnold, M H., 319, 615  
 Smiley, D. *See under* Weatherly, K C., 319, 657  
 Smith, A J E. *Book review of Introduction to Bryology* (b., Schaffel, W B.) 319, 807  
 Smith, C L. Product review: Pulsed-field gel electrophoresis of large DNA molecules (with Cantor, C R.) *Microscopy*, 319, 701  
 Smith, D D. *See under* Bertolini, D R., 319, 516  
 Smith, G L. *See under* Knittle, E., 319, 214  
 Smith, R D. *See under* Arnold, M H., 319, 615  
 Smith, R H. *Book review of Ecology: The Experimental Analysis of Distribution and Abundance*, 3rd Edn. (b., Krebs, C J.) 319, 611  
*Book review of Ecology: Individuals, Populations and Communities* (by Begon, M E., Harper, J I., Townsend, C R.) 319, 599  
 Smith, K. *See under* Kohl, N E., 319, 73  
*See under* Zimmerman, K A., 319, 780  
 Sodoyer, S. *See under* Gomard, E., 319, 153  
 Sodroski, J G. *See under* Rosen, C A., 319, 555  
 Solheim, J E. *See under* Mandolei, N., 319, 751  
 Sørensen, K. Rim syncline volume estimation and salt dispersion, *Article*, 319, 23  
 Danish Basin subsidence by Triassic rifting on a lithosphere cooling background, *Letter to Nature*, 319, 660  
 Spanos, A. *See under* Rolfe, M., 319, 339  
 Späth, A. A saturable receptor for  $^{32}P$ -inositol-1,4,5-triphosphate in hepatocytes and neutrophils (with Bradford, P G., McKinney, J S., Rubin, R P., Putney, J W Jr.) *Letter to Nature*, 319, 414  
 Spear, R H. *See under* Esat, T M., 319, 576  
 Spencer, C. *See under* Green, A G., 319, 210  
 Spergel, D N. *See under* Krauss, L M., 319, 745  
 Spindler, M. *See under* Brummer, G J A., 319, 50  
 Spinks, M J. How old is Cygnus A? (with Rees, W G., Dallett-Smith, P J.) *Letter to Nature*, 319, 471  
 Sprent, J. *See under* Lo, D., 319, 672  
 Squire, L R. Editor, *Neuropsychology of Memory*. *Book review* by Rabbitt, P., 319, 365  
 Squire, P T. Solving Equations with Physical Understanding, *Book review* by Upstill, C., 319, 820  
 Sreekantan, B V. *See under* Bhat, P N., 319, 127  
 St-Jacques, B. *See under* Sapienza, C., 319, 418  
 Stacey, G J. *See under* Harwit, M., 319, 646

- Staines, N. Introducing Immunology, *Book review by Paul, W E.* 319, 805
- Stanley, S.M. Earth and Life Through Time, *Book review by Hallam, A.* 319, 811
- Stannage, W. Catastrophism, *Correspondence*, 319, 444
- Steinberg, S. *See under Bada, J L.* 319, 314
- Stenflo, J O. Global resonances in the evolution of solar magnetic fields (with Vogel, M) *Article*, 319, 285
- Stephens, P W. *See under Bancel, P A.* 319, 104
- Stephenson, G. Partial Differential Equations for Scientists and Engineers, 3rd Edn., *Book review by Upstill, C.* 319, 820
- Worked Examples in Mathematics for Scientists and Engineers, *Book review by Upstill, C.* 319, 821
- Stern, C D. The occurrence of reversible epithelia, *Scientific correspondence*, 319, 728
- Sternberg, R.J. Editor, Human Abilities: An Information-Processing Approach, *Book review by Bryant, P E.* 319, 797
- Stevens, C F. Neurotransmitters: Modifying channel function, *News and views*, 319, 622
- Stevenson, D J. *See under Scott, D R.* 319, 759
- Stewart, I. Mathematics: Demystifying the monster, *News and views*, 319, 621
- Stewart, M. Electron microscopy of frozen-hydrated biological material (with Vigers, G) *Review article*, 319, 631
- Stewart, P J. Eureka!, *Correspondence*, 319, 444
- Stone, A. *Book review of The Chemical Bond*, 2nd Edn. (by Murrell, J N, Kettle, S F A, Tedder, J M.) 319, 819
- Book review of Structure and Spectra of Molecules* (by Richards, W G, Scott, P R.) 319, 819
- Book review of Potential Energy Surfaces: Molecular Structure and Reaction Dynamics* (by Hirst, D M.) 319, 819
- Stouraras, C. *See under Faulkner, H.* 319, 17
- Stowell, H. Homochiral creationism, *Correspondence*, 319, 8
- Strandberg, B. *See under Skoglund, U.* 319, 560
- Streitwieser Jr., A. Introduction to Organic Chemistry, 3rd Edn., *Book review by Mann, J.* 319, 818
- Stuenkel, E L. *See under Lemos, J R.* 319, 410
- Stumpf, E F. West German universities, *Correspondence*, 319, 256
- Subirana, J A. Spanish universities: New law leaves unsolved problems, *News*, 319, 710
- Summons, R E. Chlorobiaceae in Palaeozoic seas revealed by biological markers, isotopes and geology (with Powell, T G) *Letter to Nature*, 319, 763
- Sundquist, E T. Editor, The Carbon Cycle and Atmospheric CO<sub>2</sub>: Natural Variations Archean to Present, *Book review by Whitfield, M.* 319, 108
- Sutcliffe, A J. On the Track of Ice Age Mammals, *Book review by Bahn, P G.* 319, 273
- Sutherland, S. *Book review of Cognitive Psychology and its Implications*, 2nd Edn. (by Anderson, J R.) 319, 798
- Book review of Cognitive Processes*, 2nd Edn. (by Bourne, L E, Dominowski, R L, Loftus, E F, Healy, A F.) 319, 798
- Sutherland Brown, A. *See under Green, A G.* 319, 210
- Suzuki, K. Metric system, *Correspondence*, 319, 716
- Swimbanks, D. Marine satellites: Japan offers free data, *News*, 319, 438
- Pacific volcano: Transient Iwojima calf, *News*, 319, 441
- AIDS: Japan screens donated blood, *News*, 319, 610
- Swindale, N V. Vernier acuity in neurones in cat visual cortex (with Cynder, M S) *Letter to Nature*, 319, 591
- Szebehely, V. *Book review of Celestial Mechanics: A Computational Guide for the Practitioner* (by Taff, L G.) 319, 630
- Szajna, M. *See under Hasinger, G.* 319, 469
- Tabony, J. Formation of cubic structures in microemulsions containing equal volumes of oil and water, *Letter to Nature*, 319, 400
- Tadros, Th F. *See under Hayati, I.* 319, 41
- Taff, L G. Celestial Mechanics: A Computational Guide for the Practitioner, *Book review by Szebehely, V.* 319, 630
- Thi, L C. The riddle of the magnetic doors, *Scientific correspondence*, 319, 544
- Takahashi, K. Requirement of stereospecific alignments for initiation from the simian virus 40 early promoter (with Vignerion, M, Matthes, H, Wildeman, A, Zenke, M, Chambon, P) *Article*, 319, 121
- Takamagari, K. *See under Ogura, K.* 319, 308
- Takatsuji, H. Expression of cauliflower mosaic virus reverse transcriptase in yeast (with Hirochika, H, Fukushi, T, Ikeda, J-E) *Letter to Nature*, 319, 240
- Tanabe, T. *See under Noma, Y.* 319, 640
- Tanford, C. *Book review of The Physical Chemistry of Membranes: An Introduction to the Structure and Dynamics of Biological Membranes* (by Silver, B L.) 319, 108
- Tang, T B. Star colours, *Correspondence*, 319, 532
- Tatsumoto, M. *See under Hegner, E.* 319, 478
- Tauxe, L. *See under Badgley, C.* 319, 139
- Taylor, A R. A radio outburst and jet from the symbiotic star CH Cyg (with Sequist, E R, Mattie, J A) *Letter to Nature*, 319, 38
- Taylor, C R. Editor, Design and Performance of Muscular Systems, *Book review by Simmons, R M*, 319, 188
- See under Maloy, G M O.* 319, 668
- Taylor, G K. *See under Mitchell, C.* 319, 131
- Taylor, J H. *See under Rawley, L A.* 319, 383
- Taylor, L P. *See under Fromm, M E.* 319, 791
- Taylor, M A. Marine reptiles: Lifestyle of plesiosaurs, *News and views*, 319, 179
- Taylor, P. *See under Schumacher, M.* 319, 407
- Taylor, R J K. *Book review of Basic Organometallic Chemistry* (by Haiduc, I, Zuckerman, J J.) 319, 817
- Book review of Metallo-organic Chemistry* (by Pearson, A J.) 319, 817
- Taylor, S R. *See under Esat, T M.* 319, 576
- Taylor, S S. *See under Schumacher, M.* 319, 407
- Tedder, J M. Pictorial Orbital Theory, *Book review by Isaacs, N S.* 319, 816
- The Chemical Bond, 2nd Edn., *Book review by Stone, A.* 319, 819
- Tedder, R S. *Book review of Understanding AIDS: A Comprehensive Guide* (Gong, V editor) 319, 457
- Book review of AIDS: The Acquired Immune Deficiency Syndrome* (by Daniels, V G.) 319, 457
- Book review of AIDS: Etiology, Diagnosis, Treatment and Prevention* (by DeVita, V Jr, Hellman, S, Rosenberg, S.) 319, 457
- See under Weiss, R A.* 319, 794
- Thein, S L. *See under Wainscoat, J S.* 319, 491
- Theocharis, T. *See under Psimopoulos, M.* 319, 269
- Therme, P. *See under Pham, V N.* 319, 310
- Thoenen, H. *See under Davies, A M.* 319, 497
- Thomas, D M. *See under Gerlach, T M.* 319, 480
- Thomas, E G. Maxwell's Equations and their Applications, *Book review by Rosser, W G V*, 319, 823
- Thompson, C B. Expression of the c-myc proto-oncogene during cellular proliferation (with Challoner, P B, Neiman, P E, Groudine, M) *Article*, 319, 374
- Thompson, R F. The Brain: An Introduction to Neuroscience, *Book review by Fitzgerald, M.* 319, 801
- Thompson, R F. Editor, Progress in Neuroscience: Readings from Scientific American, *Book review by Fitzgerald, M.* 319, 801
- Thompson, R N. Earth sciences: Sources of basic magmas, *News and views*, 319, 448
- Thorpe, R. The Field Description of Igneous Rocks, *Book review by Cox, K G.* 319, 813
- Tilanus, R P J. *See under Allen, R J.* 319, 296
- Tilghman, S M. *See under Krumlauf, R.* 319, 224
- Tilley, C. *See under Bender, B.* 319, 532
- Tindall, D A. *See under Calkin, M G.* 319, 454
- Tinoco Jr., I. Physical Chemistry: Principles and Applications in Biological Sciences, 2nd Edn., *Book review by Richards, E G.* 319, 804
- Tjian, R. *See under Dynan, W S.* 319, 246
- Toby, S. Long-running experiments, *Scientific correspondence*, 319, 184
- Tolmazin, D. Elements of Dynamic Oceanography, *Book review by Charnock, H.* 319, 825
- Toon, G C. Detection of stratospheric N<sub>2</sub>O<sub>5</sub> by infrared remote sounding (with Farmer, C B, Norton, R H) *Letter to Nature*, 319, 570
- Torau-Allemand, D. *See under Zimmerman, K A.* 319, 780
- Townsend, C R. Ecology: Individuals, Populations and Communities, *Book review by Smith, R H.* 319, 809
- Tooshimura, K. *See under Yamamoto, T.* 319, 230
- Treco, D. *See under Boulter, J.* 319, 368
- Trivers, R. *See under Seger, J.* 319, 771
- Tronick, S R. *See under Cheah, M S C.* 319, 238
- Tracy, J. *See under Malissen, M.* 319, 28
- Trudgill, S. Limestone Geomorphology, *Book review by Williams, P W.* 319, 814
- Trubel, L. Biology of Amphibians, *Book review by Halliday, T.* 319, 364
- Trumper, J. *See under Häsinger, G.* 319, 469
- Tsuchiya, M. *See under Nagata, S.* 319, 415
- Tucker, C J. Relationship between atmospheric CO<sub>2</sub> variations and a satellite-derived vegetation index (with Fung, I Y, Keeling, C D, Gammon, R H) *Article*, 319, 195
- Tucker, M E. Carbon isotope excursions in Precambrian/Cambrian boundary beds, Morocco, *Letter to Nature*, 319, 48
- Tucker, V C T. Palaeontology: An Introduction, *Book review by Halsted, B.* 319, 810
- Turekian, K K. *See under Palmer, M R.* 319, 216
- Tyler, B. *See under Arnold, M H.* 319, 615
- Udelman, R. Functional corticotropin releasing factor receptors in the primate peripheral sympathetic nervous system (with Harwood, J P, Millan, M A, Chrousos, G P, Goldstein, D S, Zimlichman, R, Catt, K J, Aguilera, G) *Letter to Nature*, 319, 147
- Umakantha, N. A quantum potential approach to the Wheeler delayed-choice experiment, *Matters arising*, 319, 699
- Ungar, F. Cell contact- and shape-dependent regulation of vinculin synthesis in cultured fibroblasts (with Geiger, B, Ben-Ze'ev, A) *Letter to Nature*, 319, 787
- Unruh, D. *See under Hegner, E.* 319, 478
- Unwin, P N T. *See under Milligan, R A.* 319, 693
- Upskill, C. *Book review of Solving Equations with Physical Understanding* (by Acton, J R, Squire, P T.) 319, 820
- Book review of Introduction to Physical Mathematics* (by Harper, P G, Weaire, D L.) 319, 820
- Book review of Partial Differential Equations for Scientists and Engineers*, 3rd Edn. (by Stephenson, G.) 319, 820
- Book review of Worked Examples in Mathematics for Scientists and Engineers* (by Stephenson, G.) 319, 821
- Urban, E W. Space science: First results from Spacelab 2, *News and views*, 319, 541
- Usher, M B. *Book review of Lectures in Theoretical Population Biology* (by Grinburg, L R, Golenburg, E M.) 319, 810
- Book review of Case Studies in Population Biology* (Cook, L M editor) 319, 810
- Vale, W W. *See under De Souza, E B.* 319, 593
- van de Graaf, B. *See under Cox, H C.* 319, 316
- van Geerestein, V J. *See under Cox, H C.* 319, 316
- van Heyningen, V. *See under Brock, D J H.* 319, 184
- van Koningsveld, H. *See under Cox, H C.* 319, 316
- Van Valen, L M. Palaeontological and molecular views of panda phylogeny, *Matters arising*, 319, 428
- Vande Woude, G. *See under White, R.* 319, 160
- Vasiliunas, V M. *See under Oxford, W I.* 319, 267
- Vergnaud, G. *See under Rouyer, F.* 319, 291
- Verheijen, P J T. *See under Ajakaiye, D E.* 319, 582
- Vigors, G. *See under Stewart, M.* 319, 631
- Vignerion, M. *See under Takahashi, K.* 319, 121
- Vijh, K M. *See under Rossant, J.* 319, 507
- Villas, B. *See under Hubbard, W B.* 319, 636
- Neptune's rings, *Correspondence*, 319, 616
- Viola, M. *See under Hagag, N.* 319, 680
- Vishwanath, P R. *See under Bhat, P N.* 319, 127
- Vladutz, G. *Book review of Scientific Communications and Information Exchange* (by Mikhaliov, A I, Chernyi, A I, Giliarevskii, R S.) 319, 272
- Vogel, M. *See under Stenflo, J O.* 319, 285
- Voronova, A F. Expression of a new tyrosine protein kinase is stimulated by retrovirus promoter insertion (with Sefton, B M) *Letter to Nature*, 319, 682
- Wainscoat, J S. Evolutionary relationships of human populations from an analysis of nuclear DNA polymorphisms (with Hill, A V S, Boyce, A L, Flint, J, Hernandez, M, Thein, S L, Old, J M, Lynch, J R, Falusi, A G, Weatherall, D J, Clegg, J B) *Letter to Nature*, 319, 491
- Walt, J R. Electromagnetic Wave Theory, *Book review by Rosser, W G V*, 319, 823
- Walbot, V. *See under Fromm, M E.* 319, 791
- Walden, D B. Editor, Changes in Eukaryotic Gene Expression in Response to Environmental Stress, *Book review by Prosser, C L.* 319, 187
- Waldrum, J R. The Theory of Thermodynamics, *Book review by Guénault, T.* 319, 822
- Walgate, R. French science: CNRS faces political change, *News*, 319, 4
- Space science: British head for French lab, *News*, 319, 5
- Channel tunnel: Rail plan gets go-ahead, *Opinion*, 319, 251
- French science: New role for academy?, *News*, 319, 351
- French nuclear power: Problems of plenty and success, *News*, 319, 350
- Ariane: France waits in the wings, *News*, 319, 438
- Budget of INSERM grows, *News*, 319, 442
- French research strategy: CNRS embraces plans for research networks, *News*, 319, 165
- European neutrinos: British aiming to share costs, *News*, 319, 530
- French science policy: Good effort, but must try harder, *News*, 319, 614
- The end of a great experiment?, *Commentary*, 319, 729
- Walker, J M. Editor, The Molecular Basis of Cancer, *Book review by Weinstein, I B*, 319, 803
- Wallace, J L. *See under Rosam, A-C.* 319, 54
- Walsh, M M. *See under Byerly, G R.* 319, 489
- Wang, J C. Physical Chemistry: Principles and Applications in Biological Sciences, 2nd Edn., *Book review by Richards, E G.* 319, 804
- Wang, J-H. Major groove or minor groove?, *Scientific correspondence*, 319, 183
- Warrick, R A. Carbon cycle: Photosynthesis seen from above, *News and views*, 319, 181
- Watanahe, S. Pattern Recognition: Human and Mechanical, *Book review by Hawkes, P W.* 319, 107
- Watkins, G H. *See under Fegley, B Jr.* 319, 305
- Watkins, R. *See under Arnold, M H.* 319, 615
- Watson, F G. *See under Dunlop, J S.* 319, 564
- Weare, D L. Introduction to Physical Mathematics, *Book review by Upstill, C.* 319, 820
- Weale, R A W S. Stiles (1901-1985), *News and views*, 319, 623
- Weatherall, D J. *See under Wainscoat, J S.* 319, 491
- Weathers, K C. A regional acidic cloud/fog event in the eastern United States (with Likens, G E, Bormann, F H, Eaton, J S, Bowden, W B, Andersen, J L, Cass, D A, Galloway, J N, Keene, W C, Kimball, K D, Huth, P, Smiley, D) *Letter to Nature*, 319, 657
- Webs, A C. *See under Wolff, S M.* 319, 270
- Weber, G. *See under McGregor, R B.* 319, 70
- Weibel, E. Editor, Design and Performance of Muscular Systems, *Book review by Simmons, R M.* 319, 188
- Weinstein, I B. *Book review of The Molecular Basis of Cancer* (Farmer, P B, Walker, J M editors) 319, 803
- Weiss, G B. Editor, Calcium in Biological Systems, *Book review by Baker, P F.* 319, 22
- Weiss, R A. Lack of HTLV-I antibodies in Africans (with Cheingsong-Popov, R, Clayden, S, Pegram, S, Tedder, R S, Barzilai, A, Rubenstein, E) *Matters arising*, 319, 794
- Wellbenbach, J. *See under Rouyer, F.* 319, 291
- Wennergren, S. *See under Heldin, C-H.* 319, 511
- Wenz, C. Academic redundancies: Committee retires in confusion, *News*, 319, 349
- Wernstedt, C. *See under Heldin, C-H.* 319, 511
- Westermark, B. *See under Heldin, C-H.* 319, 511
- Westheimer, F. Erratum: Polyribonucleic acids as enzymes, *Miscellany*, 319, 619
- Westheimer, F H. Biochemistry: Polyribonucleic acids as enzymes, *News and views*, 319, 534
- Wetherill, G W. Meteorites: Unexpected Antarctic chemistry, *News and views*, 319, 357
- Whishaw, I Q. Fundamentals of Human Neuropsychology, 2nd Edn., *Book review by Young, A.* 319, 799
- White, N E. *See under Häsinger, G.* 319, 469
- White, R. Erratum: A closely linked genetic marker for cystic fibrosis (with Woodward, S, Leppert, M, O'Connell, P, Nakamura, Y,

- Hoff, M, Herbst, J, Lalouel, J-M, Dean, M, Vande Woude, G. *Letter to Nature*, 319, 160
- Whitehead, A N. Science and the Modern World. *Book review by* Gale, G. 319, 548
- Whitehead, J A Jr. *See under* Scott, D R., 319, 759
- Whitehouse, M J. Pb-Pb systematics of Lewisian gneisses — implications for crustal differentiation (with Moorbat, S) *Letter to Nature*, 319, 488
- Whitehouse, P J. *See under* De Souza, E B., 319, 593
- Whitfield, M. *Book review of* The Carbon Cycle and Atmospheric CO<sub>2</sub>: Natural Variations Archean to Present (Sundquist, E T, Broecker, W S *editors*) 319, 108
- Whitmore, T C. *See under* Arnold, M H., 319, 615
- Whittington, H B. The Burgess Shale. *Book review by* Hallam, A. 319, 629
- Whittle, B J R. *See under* Rosam, A-C., 319, 54
- Whitworth, R W. *See under* Ahmad, S., 319, 659
- Widley, T M L. *Book review of* World Climatic Systems (by Lockwood, J G.) 319, 825
- Wigan, A L. The Duality of the Mind. *Book review by* Marshall, J C. 319, 186
- Wilbur, S. *See under* Gammon, G., 319, 413
- Wilcockson, R B. *Book review of* The Chemical Industry (Heaton, C A *editor*) 319, 818
- Wilcove, D S. Endangered species: The fate of the California condor (with May, R M) *News and views*, 319, 16
- Wilderman, A. *See under* Takahashi, K., 319, 121
- Wildt, D E. *See under* O'Brien, S J., 319, 428
- Williams, P W. *Book review of* Karst Geomorphology, 2nd Edn. (by Jennings, J N.) 319, 814
- Book review of* Limestone Geomorphology (by Trudgill, S.) 319, 814
- Williamson, M. *See under* Drake, J A., 319, 718
- Willingham, M C. An Atlas of Immunofluorescence in Cultured Cells. *Book review by* Heath, J. 319, 547
- Wilson, R C L. *Book review of* Petroleum Geology (by North, F K.) 319, 812
- Book review of* Elements of Petroleum Geology (by Selley, R C.) 319, 812
- Book review of* Geology in Petroleum Production: A Primer in Petroleum Geology (by Dikkers, A J.) 319, 812
- Winkler, D W. *See under* Götsmark, F., 319, 589
- Withers, L A. *See under* Arnold, M H., 319, 615
- Witte, O N. *See under* Koob, D., 319, 331
- See under* Zimmerman, K A., 319, 780
- Woese, C R. Editor, Archaeabacteria. The Bacteria: A Treatise on Structure and Function, Vol. VIII. *Book review by* Nedwell, D B. 319, 273
- Wolf, D. *See under* Miller, C., 319, 783
- Wolfe, R S. Editor, Archaeabacteria. The Bacteria: A Treatise on Structure and Function, Vol. VIII. *Book review by* Nedwell, D B. 319, 273
- Wolfendale, A. Cosmic rays: A supernova for a neighbour? *News and views*, 319, 99
- Wolff, S M. Clone controversy at Immunex (with Auron, P E, Dinarello, C A, Rosenwasser, L J, Webb, A C, Rich, A) *Scientific correspondence*, 319, 270
- Wolman, B B. Editor, Handbook of Intelligence: Theories, Measurements and Applications. *Book review by* Eysenck, H J. 319, 627
- Wood, B. Glynn Isaac 1937-1985. *News and views*, 319, 15
- Woodhouse, J H. *See under* Giardini, D., 319, 551
- Woodland, H. Developmental biology: Unscrambling egg structure (with Jones, E) *News and views*, 319, 261
- Woods, J D. A lagrangian mixed layer model of Atlantic 18°C water formation (with Barkmann, W) *Letter to Nature*, 319, 574
- Woods, N M. Repetitive transient rises in cytoplasmic free calcium in hormone-stimulated hepatocytes (with Cuthbertson, K S R, Cobbold, P H) *Letter to Nature*, 319, 600
- Woodward, S. *See under* White, R., 319, 160
- Wright, F. Earthquake modelling: Caustics in seismology. *News and views*, 319, 720
- Wright, J. Uncertainty and the Strategic Defense Initiative. *Commentary*, 319, 275
- Wright, K. British biotechnology: Celltech within sight of profit. *News*, 319, 89
- Preaching to converts, *News*, 319, 440
- AIDS protein made, *News*, 319, 525
- See under* Beardsley, T., 319, 526
- US plant science: Monsanto's shock firings, *News*, 319, 612
- US universities: New medical school planned, *News*, 319, 712
- Biotechnology: Will Pharmacia join Fermenta?, *News*, 319, 712
- Wudi, F. Highly conducting acetylene-CO copolymers and limitations of the soliton model (with Heeger, A J, Franssen, J F) *Matters arising*, 319, 697
- Wuebbles, D J. Atmospheric chemistry: Reservoir species discovered in the stratosphere. *News and views*, 319, 535
- Xu, P. *See under* Koop, B F., 319, 234
- Xu, Y. Measuring interstellar dust grains from the haloes of binary X-ray sources (with McCray, R, Kelley, R) *Letter to Nature*, 319, 652
- Yamamoto, O. *See under* Nagata, S., 319, 415
- Yamamoto, T. Similarity of protein encoded by the human c-fms gene to epidermal growth factor receptor (with Ikeda, S, Akiyama, T, Semba, K, Nomura, N, Miyazaki, N, Saito, T, Toyoshima, K) *Letter to Nature*, 319, 230
- Yamanaka, C. Thermonuclear neutron yield of 10<sup>17</sup> achieved with Gekko XII green laser (with Nakai, S) *Letter to Nature*, 319, 787
- Yamazaki, T. *See under* Nagata, S., 319, 415
- Yanagi, G T. *See under* Behrensmeier, A K., 319, 765
- Yancopoulos, G D. *See under* Zimmerman, K A., 319, 780
- Yasota, Y. *See under* Noma, Y., 319, 640
- Yates, M G. *See under* Cammack, R., 319, 182
- Yilma, T. *See under* Jones, L., 319, 543
- Yorath, C J. *See under* Green, A G., 319, 210
- Young, A. *Book review of* Fundamentals of Human Neuropsychiatry, 2nd Edn. (by Kolb, B, Whishaw, I Q.) 319, 782
- Book review of* Mind and Brain: Principles of Neurophysiology (by Gilinsky, A S.) 319, 799
- Book review of* Brain and Mind (Oakley, D A *et al.*) 319, 798
- Young, R A. *See under* Mustafa, A S., 319, 63
- Yuan, X C. *See under* Pham, V N., 319, 310
- Yung, Y L. *See under* Pinto, J P., 319, 388
- Zeiger, E. *See under* Shimazaki, K., 319, 324
- Zenke, M. *See under* Takahashi, K., 319, 121
- Zhao, M. *See under* Bada, J L., 319, 314
- Zimlichman, R. *See under* Udelson, R., 319, 147
- Zimmerman, K A. Differential expression of my family genes during murine development (with Yancopoulos, G D, Cellum, R G, Smith, R K, Kohl, N E, Denis, K A, Nau, M M, Witt, O N, Toran-Alvarez, D, Gee, C E, Minna, J D, Alt, F W) *Letter to Nature*, 319, 780
- Zuckerman, J J. Basic Organometallic Chemistry. *Book review by* Taylor, R J K. 319, 817

## SCIENCE AND TECHNOLOGY

# Whatever the subject... refer to MACMILLAN DICTIONARIES

DESIGNED FOR STUDENTS

The paperback *Macmillan Dictionary Series* combines new and established works of teaching and reference with an attractive series format.

- \* authoritative definitions and explanations of all current terminology written by experts
  - \* lucidly written entries with thorough cross referencing
  - \* regular new editions keep the student up to date with the latest research, practice and technology
  - \* a clear layout for easy reference
  - \* prices range from just £7.95 to £9.95
- NEW IN 1986...*

**MACMILLAN DICTIONARY OF BIOTECHNOLOGY**

JIM COOMBS March 1986 320pp 0 333 40875 6 £9.95

**MACMILLAN DICTIONARY OF THE HISTORY OF SCIENCE**

Edited by W F. BYNUM, E J. BROWNE and ROY PORTER

March 1986 528pp 0 333 34901 6 £8.95

**MACMILLAN DICTIONARY OF PERSONAL COMPUTING AND COMMUNICATIONS**

DENNIS LONGLEY and MICHAEL SHAIN

August 1986 320pp 0 333 42170 1 £8.95

**MACMILLAN DICTIONARY OF PHYSICS**

MARY P. LORD August 1986 320pp 0 333 42377 1 £8.95

**MACMILLAN DICTIONARY OF IMMUNOLOGY**

FRED ROSEN, LISA STEINER and EMIL UNANUE

August 1986 256pp 0 333 39248 5 £8.95

**RECENTLY PUBLISHED...****MACMILLAN DICTIONARY OF LIFE SCIENCES** Second Edition

E A. MARTIN 1985 400pp 0 333 38647 7 £9.95

**MACMILLAN DICTIONARY OF THE ENVIRONMENT**

Second Edition MICHAEL ALLABY 1985 536pp 0 333 37951 9 £8.95

**MACMILLAN DICTIONARY OF INFORMATION TECHNOLOGY**

Second Edition DENNIS LONGLEY and MICHAEL SHAIN

1985 392pp 0 333 37261 1 £8.95

**MACMILLAN DICTIONARY OF MICROCOMPUTING** Third Edition

CHARLES SIPPL 1985 544pp 0 333 37082 1 £8.95

**MACMILLAN DICTIONARY OF DATA COMMUNICATIONS**

Second Edition CHARLES SIPPL 1985 544pp 0 333 37083 X £8.95

**MACMILLAN DICTIONARY OF ENERGY**

Edited by MALCOLM LESSER

1985 314pp 0 333 36867 3 £7.95

**MACMILLAN DICTIONARY OF ASTRONOMY**

VALERIE ILLINGWORTH 1985 320pp 0 333 39243 4 £9.95

Not available in USA.



# NATURE CLASSIFIED

**LONDON OFFICE** Jo Godfrey 4 Little Essex Street, WC2R 3LF Telephone 01-240 1101 (Telex 262024)

**AMERICAN OFFICES NEW YORK** Marianne S. Ettisch 65 Bleeker Street, New York, NY 10012 — Telephone (212) 477 9625  
**CANADIAN OFFICE TORONTO** Peter Drake 17 Pine Crescent, Toronto, Ontario M4E 1L1 (416) 690 2423

**RATES UK** — Rest of world — Display £14 per centimetre. Semi-Display £13 per centimetre. Minimum 3 cm. £2 is charged for a box number.

**CONDITIONS.** The Publisher reserves the right to refuse, amend, withdraw or otherwise deal with all advertisements submitted to him at his absolute discretion and without explanation. The Publishers will not be liable for any loss occasioned by the failure of any advertisement to appear from any cause whatever, nor do they accept liability for printers' errors, although every care is taken to avoid mistakes.

**CANCELLATIONS MUST BE RECEIVED NO LATER THAN 5 p.m. ON THURSDAYS PRIOR TO ISSUE DATE.**

## MEDICAL RESEARCH COUNCIL

Dunn Nutrition Unit, Cambridge

## POSTDOCTORAL SCIENTIST

Required to join Dr A Lucas working in the field of infant nutritional physiology (including premature babies). A principle interest of the group is the use of stable isotopes, calorimetry and, in the future, nuclear magnetic resonance for studying energy metabolism and body composition. Postgraduate experience in biochemistry and/or physiology is essential. The appointment is for a period of 3 years. Salary on the University non-clinical academic staff scales in the range £9,276—£11,653 according to previous experience. Applications should be made to the Director of the Unit, Dr R G Whitehead, Dunn Nutritional Laboratory, Downhams Lane, Milton Road, Cambridge CB4 1XJ. Closing date for applications 18th April 1986. The MRC is an equal opportunity employer. (9163)A

## UNIVERSITY OF OXFORD

### UNIVERSITY LECTURE-SHIP IN NEUROSCIENCE

IN ASSOCIATION WITH SOMERVILLE AND BALLIOL COLLEGES

Applications are invited for the above post tenable from 1 January 1987. Candidates should have carried out research in neuroscience, with competence in neuroscience and cell structure. Stipend according to age on the scale £8,020 to £16,760. The successful candidate may be offered a tutorial fellowship at Somerville College, the statutes of which provide that all fellows shall be women, or, if a man is appointed, at Balliol College. Further details may be obtained from Professor R W Guillory, Department of Human Anatomy, South Parks Road, Oxford OX1 3QX, to whom applications (nine typed copies, or one from overseas applicants) with a full curriculum vitae, summary of research interests and the names of three referees should be sent by 30 June, 1986. (9188)A

## UNIVERSITY OF LIVERPOOL

### DEPARTMENT OF BIOCHEMISTRY

#### TEMPORARY LECTURER

Applications are invited from suitably qualified persons for a temporary Lectureship tenable for 1 year from 1st September 1986. Candidates will be required to assist with undergraduate teaching and conduct research in association with one of the research groups in the Department which has facilities available for many areas of animal, plant, microbial and insect biochemistry.

Salary will be in the range £8,020—£9,495 per annum.

Applications together with the names of three referees should be received not later than 30th April 1986 by the Registrar, The University, P.O. Box 147, Liverpool, L69 3BX from whom further particulars may be obtained. Quote ref: RV/706/N. (9155)A

## UNIVERSITY OF NOTTINGHAM

### DEPARTMENT OF PHYSIOLOGY & ENVIRONMENTAL SCIENCE

#### POST DOCTORAL RESEARCH ASSISTANT

Applications are invited for an AFRC-funded postdoctoral research assistant to investigate the role of cell wall degrading enzymes in abscission. Prospective candidates should have, or expect to complete in the near future, a PhD in Plant Physiology or Biochemistry. Experience in the extraction and handling of nucleic acids would be an advantage.

The post is for 3 years starting as soon as possible, with salary (RA 1a) according to age and experience within the range £8,020—£9,495.

Applications with cv and names and addresses of two referees should be sent to Dr J A Roberts, Department of Physiology and Environmental Science, University of Nottingham, Faculty of Agricultural Science, Sutton Bonington, Nr Loughborough, Leics LE12 5RD. (9185)A

## Senior Faculty Position GERIATRICS

The Ritter Department of Geriatrics and Adult Development of the Mount Sinai Medical Center is seeking an internist qualified for a medical school appointment of Associate Professor or higher and who has an interest in geriatrics for a new City University of New York-supported faculty position. The individual will assume a leadership role in the Department, including research, clinical, and administrative responsibilities, and will be appointed in both the Departments of Geriatrics and Medicine. Candidates for this position should have received recognition in their fields. The Mount Sinai Medical Center is comprised of a 1200 bed tertiary care hospital and a medical school. The Ritter Department is the first department of geriatrics in a U.S. medical school and has assumed a leadership position since its establishment three years ago. Salary is negotiable, with excellent benefits. Position available July or September 1986. Curriculum vitae should be sent to Robert N. Butler, M.D., Professor and Chairman, Ritter Department of Geriatrics and Adult Development, THE MOUNT SINAI MEDICAL CENTER, One Gustave L. Levy Place, Annenberg 13-30, New York, NY 10029.

An Equal Opportunity Employer.

**The Mount Sinai Medical Center**

(NW129)



## —SAUDI ARABIA— PHARMACISTS THERAPISTS

A leading hospital in Dhahran is seeking to maintain its reputation for professionalism through the appointment of the following staff:

**PHARMACISTS** — Full professional qualifications plus three years relevant experience.

**PHYSIOTHERAPISTS** — Must have BSC or HNC in physiotherapy, membership of the chartered society plus two years post certification experience.

**OCCUPATIONAL THERAPIST** — Relevant professional qualifications and two years post certification experience.

In addition to the tax free salaries, free accommodation, London round trip air tickets and generous leave allowances. These one year renewable contracts offer the opportunity of working in a modern, five year old 190 bed hospital staffed at senior level by European and American personnel.

For information about these immediate openings call:

**PETER HALL 01-437-6900  
HAK INTERNATIONAL,  
CHESHAM HOUSE  
136 REGENT STREET,  
LONDON**

(W2782)A

A. Sattler 5/3  
24.6

## No way to welcome spring

*The calculated bad manners towards each other of the two major superpowers may presage better things, as last year, but that is the most optimistic reading of events.*

ONLY a few months ago, the general cheerful opinion was that 1986 would be the year in which the wagon of strategic arms control began to roll again. There were several hopeful signs: the generally constructive meeting of the US and Soviet heads of government at Geneva last November, the apparent belief of both leaders that they can gain from arms control (Mr Gorbachev, economically; President Reagan, politically and in reputation), the encouraging noises at the Stockholm conference on European Security over the past several months and the widespread fear that if things do not get better soon, they may get a lot worse. To be sure, nothing much has happened to put flesh on these hopeful bones, but the Soviet Union has offered (and kept) a unilateral moratorium on nuclear testing (due to expire last weekend) and has proposed an ambitious plan for getting rid of strategic nuclear weapons by the end of the century. The chief response so far from Washington has been ambivalent; President Reagan has been lukewarm but has not rejected the proposals outright, and is plainly anxious to fix a date for this year's summit meeting, but other US officials have been downright cool. The British government, responding to the narrow question of whether British nuclear weapons should be restricted at an early stage, has also been downright cool. And now, in the past few weeks, the two superpowers have taken to public rudeness on a scale that will be hard to sustain.

The cheerful reading of these events is that they are a deliberate smokescreen behind which patient diplomats are hammering out the essence of arms control agreements. It is true that the useful meeting last November was preceded by a bout of almost unprecedented recrimination. So too were the months preceding the first of the important agreements on nuclear arms, the partial test-ban treaty of 1963. One of the impediments now to the optimistic view is that the present period also resembles that at the end of 1980 when the Soviet invasion of Afghanistan helped to put paid to the nearly complete draft of a comprehensive test-ban treaty. The danger in the present climate is that the date for this year's planned summit meeting will not be fixed until it is too late for it to be held, with the mid-term elections due in the United States at the beginning of November.

Yet much of the disagreement between the East and the West on arms control consists, in the broadest sense, of misunderstanding. On many of the measures up for agreement, the two sides tend to blow hot and cold, but rarely simultaneously. In 1980, the US administration was keen on a comprehensive test-ban (but may not have been able to win the agreement of the US Senate and its lobbyists); now the shoe is on the other foot, with the Soviet Union being prepared to accept a degree of on-site inspection while the United States, conscious that new missiles will need new warheads and bemused by the Strategic Defense Initiative (SDI), would prefer to talk about almost anything else (except SDI). The essential difficulty is that which has beggared the arms control process from the outset, that of regarding the outstanding problems from the other side's point of view.

Here are some issues on which heads should be banged

together in the next few weeks.

• **Intermediate missiles.** An agreement should be possible this year, especially now that no account will be taken of medium-range aircraft at the outset. One snag is the Soviet determination to keep some mobile SS-20 missiles in Asia; the Soviet Union appears not to appreciate that to require good faith of the United States that these machines would not be moved westwards predicates agreements that have not yet been reached. Another snag is European discontent at the prospect of a European theatre free from all but tactical nuclear weapons and the British and French nuclear forces; but that objection cannot stand in the way of an agreement, which would merely restore the state of affairs before the decision of the North Atlantic Treaty Organization (NATO), in December 1979, to modernize European nuclear forces in response to the appearance of the SS-20s.

• **Strategic missiles.** The Soviet Union and the United States both seem prepared to contemplate substantial reduction of the present limits (those of the unratified SALT II treaty), perhaps by a half. In this context, long-range bombers are bound to matter. A cap on the British and French forces (and the Chinese?) would be appropriate. The United States should appreciate that Soviet unwillingness to carry a larger proportion of its strategic forces on submarines is rational (too many eggs in one kind of basket); the Soviet Union should understand that a substantial reduction is an indispensable prelude to abolition, Mr Gorbachev's goal for 2000.

• **Comprehensive test-ban.** The needs of SDI apart, the United States is at present at a disadvantage in the utility of its missile forces and an agreement on strategic missiles, almost within grasp, will not come about unless US tests continue for some time: the best may be the enemy of the better.

• **Strategic Defense Initiative.** The United States seems not properly to appreciate why the Soviet Union so resents this scheme. Response, either by emulation or the proliferation of existing missile forces, will be ruinously expensive. Even if an effective multi-layered defence against strategic missiles proves feasible, installing such a system over a period of time that must run into decades would be perhaps ruinously dangerous as well. And there is no doubt that the possession of an effective SDI by one side but not the other would be a basis from which to launch a risk-free pre-emptive strike. But the Soviet Union should clarify its reasons for opposing SDI so vociferously. Is the venture fated to be a technical failure, as many critics in the West insist? Might it succeed, in which case why not be prepared to negotiate phased installation? Or will SDI finish up as a mixture of an early warning system and a terminal defence against some missiles (in which case the Anti-Ballistic Missile Treaty would have to be renegotiated)?

None of these arguments is especially profound. No doubt the professional military people on both sides have more specific but more urgent anxieties about the ways in which their opponents are likely to benefit from arms control agreements. The disappointment of the past few months has been that neither side appears to have been ready to acknowledge that anxiety of this kind is both legitimate and unavoidable.

Yet in the absence of such an understanding, agreement will not be possible or, worse, will be reached and then broken.

Another urgent need is for an open recognition that effective strategic arms control is necessarily a slow process. At any time, such as now, it is usually possible to distinguish between the steps that logically come next and those that can only follow. Mr Gorbachev's proposals earlier this year differ from previous versions in their open recognition of this truth. And in spite of the coolness with which some have greeted them, it is plain that they are also negotiable proposals. Why not at least find out, by attempting to negotiate on them? □

## Nuclear virulence

*Some of the problems of the nuclear industry are illustrated by a book review this week.*

NUCLEAR engineers, others who work in the nuclear industry and, indeed, those who use electricity as a fuel, should take care to read the book review by David Pearce, professor of economics at University College London, which appears on page 403 of this issue. To profit from the exercise, it is not necessary to agree with Pearce, or with the author of the book he is reviewing, both of whom are saying that civil nuclear power in Britain and probably elsewhere is a deception practised on an innocent public and on gullible politicians by a bunch of 1950s scientists and technologists ignorant of the imperatives of the social sciences and incompetent as well. The benefit will be the better understanding of the obstacles that will have to be faced by those who would both breathe new life into national nuclear programmes that have fallen on bad times, or who would ensure improved public safety by the better management of nuclear plants.

Do-gooders of that kind should be the first to know what lies ahead of them, to which end Pearce should be generously forgiven his restraint, despite which his piece of action writing is as salutary a warning as there could be against all things nuclear. That the British decision to build advanced gas-cooled reactors in succession to the first generation of natural uranium reactors turned out to be economically unwise is now well-documented, but he does not need, with the passage of so much time, to spare the blushes of those who took the decision, and who are now mostly dead in any case, by concealing the explanation. The decision was technically unsound and was widely said to be so at the time. The problem, in 1960 or thereabouts, was that people were faced with the familiar problem of not knowing how far ahead to jump in the development of a novel technology. The besetting British sin is to jump too far (with the first supersonic civil airliners and so on), but on this occasion they erred in the other direction.

Pearce is also overkind to British nuclear engineers in ascribing the concealment of the truth about nuclear energy to the cover-up engineers who work in public relations and for lobbying organizations. Why not tell it like it was (and, perhaps, still is) that the founders of the British nuclear industry were woefully ignorant of the basic parameters of their craft, the need to anneal irradiated graphite, the corrosion of magnesium by carbon dioxide and the embrittlement of steel by helium gas, all of which they should have learned about at school (together with the biological effects of ingested plutonium)? But his echo of the contention that the problem of waste management must be "solved" before civil nuclear power is exploited cannot of course be gainsaid, although it would have been helpful to have had an economist's view of what constitutes a solution to such a problem.

What Pearce has done is to provide a vivid illustration of the depth of feeling, even passion, that now attends the nuclear issue even in previously sleepy places such as Britain. Many will be grateful to him, especially those who manage without electricity. □

## Good luck strikes back

*British astronomers should move their surplus observatory to a university.*

LONG delayed decisions become palatable because those most affected by them have been anaesthetized while waiting. This is probably why British astronomers appear unperturbed by the announcement last week that the Royal Greenwich Observatory (RGO), founded as an applied science laboratory to exploit seventeenth-century astronomy for better navigation and which left the site whose name it bears nearly forty years ago, is once again to move, perhaps even to merge with the Royal Observatory, Edinburgh. British astronomers are now thoroughly used to the notion that support services for astronomy must be reduced. As one distinguished committee after another has failed to reach a firm conclusion, the exasperated victims have often been chief among those pleading with the executioner to get on with his task.

On this occasion, remarkably, the need that something should be done is not a mark of failure, recklessness or the lack of funds, but if anything the opposite on all three counts. For the best part of fifteen years, or at least ten, the Science and Engineering Research Council (SERC) has dealt imaginatively, responsibly and generously with optical and near-optical astronomy. Capital investment in new telescopes runs close to £50 million, and there is a substantial community of professional astronomers fighting for time on this equipment. One measure of quality of the equipment available to British astronomers is that a SERC committee seriously considered, a year ago, the abandonment of the excellent partnership with Australia in the Anglo-Australian telescope. The two British-based observatories, meanwhile, have found their usefulness diminish. Each of them has provided important support for the building of the new telescopes, but it has been plain for years that there would be no need for both of them when that work was done, as it will be long before 1990.

Two questions arise, only one of which is of a muck-raking character. Most of the decisions about the construction of new telescopes were taken a decade or more ago, when public funds, although already constrained, were easier to come by than at present. In the past few years, the climate has changed so much that it is unthinkable that the same decisions would be taken now; British astronomers are lucky to have squeezed in under the wire in this way.

So why has there been such diffidence in deciding what to do about RGO? And although SERC has laid down that the move of RGO from its present cloudy site must be "self-financing", why is nothing said about the financial savings that may flow from the decision that RGO should move? If there are none, people will be asking whether the move can be worthwhile.

The second question is raised by the incompleteness of last week's decision. RGO is to move, but will be told only in June where and with whom it will spend the rest of its days. SERC seems to be faced with two choices. A merger of the two ground-based observatories would yield economies of scale and concentration, but SERC judges that an institution based in Edinburgh could not have the close links with academic astronomers that would be fruitful for both sides. This is the spirit in which the research council has invited "expressions of interest" (otherwise known as bids) from universities willing to take in RGO as a kind of paying guest. Cambridge and Manchester are the chief contenders. It should be plain to SERC that the benefits of an academic partnership are huge, and that the university option provides British research institutes with a chance to give back to British universities some of the resources and responsibility of which they have been robbed over the decades. But would it not be invidious to pick one out of two? Maybe, but to settle for a merger would be wrong. □

## AIDS research

# New human retroviruses: One causes AIDS . . .

ACQUIRED immune deficiency syndrome (AIDS) can be caused by a second virus, at least 30 per cent different in sequence from the virus particle, termed HTLV-III in the United States and LAV in France, that is currently implicated in the disease. So claimed Luc Montagnier, head of the French group that discovered LAV at the Institut Pasteur in Paris, at a meeting in Lisbon, Portugal, last week. (HTLV, or human T-lymphotropic virus, was isolated by Robert Gallo and his colleagues at the US National Institutes of Health and Montagnier and his group isolated what they called LAV, or lymphadenopathy virus.)

Montagnier is sending his paper on the

discovery to the *Comptes Rendus* of the French Academy of Sciences, and to *Science*, but was prepared last week to outline what he had said in his Lisbon address. According to Montagnier, the new virus, which he calls LAV-II, was discovered in two patients with AIDS symptoms in a Lisbon hospital. The patients' sera showed no antibodies against LAV (now called LAV-I). There were, however, viruses present that looked just like LAV-I in the electron microscope, and which had the same T-lymphotropic and cytopathic properties.

Nevertheless, DNA probes derived from LAV-I did not hybridize with the DNA from the new virus "in stringent

conditions". Sera from LAV-I patients contained no antibodies for the envelope part of the new virus, although sera from patients infected by the new virus showed a small reactivity with LAV-I core proteins. These data suggested that the new LAV-II virus diverged at least 30 per cent in sequence from LAV-I. Montagnier said.

LAV-II patients also showed some antibodies against the green monkey virus considered similar to LAV-I, "and the interesting question now will be how similar LAV-II is to the simian virus", Montagnier said.

Robert Walgate

## NSF tests mini-supercomputer

Washington

THE National Science Foundation's San Diego Supercomputing Center (SDSC) is gearing up for tests of a mini-supercomputer that could save time and money for thousands of Cray users. The SCS-40 or "Crayette" hardware contains the instruction set of a Cray X-MP and can write or run programs compatible with the mammoth number crunchers. When the machine arrives in July, computer scientists will judge whether the \$600,000 crayette can fill the gap between its \$10 million parent and the average patron.

Scientific Computing Systems in California built the SCS-40 in less than two years to provide an intermediate for local Cray programming and debugging, saving Cray time for the largest calculations. With a quarter of a Cray's capacity, the SCS-40 could also expand the computing power of smaller facilities.

John Connolly, head of the supercomputer project at NSF, says that if the SCS-40 makes the grade it could be added to hundreds of remote facilities for the Crays at Carnegie-Mellon University in Pittsburgh and the University of Illinois at Urbana-Champaign, in addition to the San Diego site. Nearly half of the advanced scientific computing budget is eaten away by the leasing of the Crays installed in these centres. Connolly thinks the auxiliary crayettes would prove to be cost-neutral compared to direct Cray use for programming. The SCS-40s might realize their greatest savings in reduced time spent in labour-intensive programming.

Software simulations of Cray architecture have been devised, but are orders of magnitude slower than the Crays themselves and overwhelm lesser machines. Cray's own attempt to build a mini version was shelved in the prototype stage because the market differed from Cray's established clientele. Several other start-up companies that attempted the project could not rally sufficient support. By 1987, the verdict on the SCS-40 should be in.

Karen Wright

## AIDS research

## . . . and the other does not

Washington

ANOTHER dispute over scientific primacy has erupted between the United States and France about a human retrovirus. Max Essex and Phyllis Kanki of the Harvard School of Public Health in Boston, together with colleagues at Harvard and in France and Senegal, have found a virus related to Simian T-lymphotropic virus type III found in African Green Monkey (STLV-III<sub>AGM</sub>) that can be detected in healthy humans. Essex announced the discovery last week to coincide with an announcement by Luc Montagnier of the Institut Pasteur about another human retrovirus (see above). A paper describing Essex's virus will appear in the 11 April issue of *Science*.

Like human T-lymphotropic virus type-III/lymphadenopathy virus (HTLV-III/LAV), the new virus, termed HTLV-IV, infects helper T-cells. But unlike HTLV-III, it is not cytopathic for T-cells.

Last year, Essex and his colleagues reported finding healthy individuals from West Africa who displayed strong antibody reactivity to all STLV-III<sub>AGM</sub> viral proteins, but reacted weakly with viral proteins from HTLV-III/LAV. They concluded that there was in Africa a human virus more closely related to STLV-III than HTLV-III that either shared a common genetic ancestor or derived directly from the monkey virus.

The Harvard team successfully grew HTLV-IV from serum of three seropositive individuals. Analysis of the new virus shows that it shares many proteins with STLV-III<sub>AGM</sub>, more so than with

HTLV-III/LAV, notably a 32,000 dalton protein suspected to be a transmembrane envelope protein. The analogous protein in HTLV-III/LAV weighs 42,000 daltons. Electron micrograph morphology of HTLV-IV likewise shows greater similarities to the monkey virus than to HTLV-III/LAV.

At a press conference at the American Society of Microbiologists' annual meeting in Washington, DC, Essex said the new virus described by Montagnier "appears to be related" to HTLV-IV. Unlike LAV-II, HTLV-IV does not appear to cause illness, but Essex would not rule out the possibility that infected individuals might develop disease later in life. Essex believes there is a continuum of retroviruses from those closely related to STLV-III to those closer to HTLV-III/LAV, and it may be that LAV-II lies on that continuum.

Essex was prompted to release details of his discovery in advance of its formal publication because of intense pressure from the media both on him and his collaborator Francis Barin in Tours, France, to comment on Montagnier's discovery. Essex maintains he learned of Montagnier's work only on 22 March, and then only at second hand. Essex worried that he would be "raked over the coals" by the press for refusing to comment on his own work at a time of intense public interest in human retroviruses.

US journalists were alerted to the Institut Pasteur discovery by a press release from a New York public relations company.

Joseph Palca

**US patents**

## Doubts on secrecy order

A PROPOSED new secrecy order for controlling militarily sensitive patent applications is starting to worry US high-technology industry. The proposed order, shortly to be published for comment by the US Patent Office, would be used for controlling patent applications containing information that, while not classified, is subject to export control under new authority given to the Department of Defense (DoD). Some fear the new order might make difficulties for US high-technology industries seeking patent protection abroad.

The Patent Office has long had the power to place secrecy orders on patent applications containing information whose publication would harm national security. Two of three new categories of secrecy order now proposed under the 1951 Invention Secrecy Act essentially formalize existing practice. In a nutshell, patent applications are reviewed to determine whether a secrecy order is necessary; if it is, no patent issues while the order is in force, and the inventor is ordered not to disclose the substance of the application to third parties. Patent applications in foreign countries are not permitted while the secrecy order remains in force.

The third new proposed secrecy order, for non-classifiable but export-controlled material, is rather different. It would allow US citizens access to the patent application for legitimate business purposes, and would allow patent applications in foreign countries that have export control rules and reciprocal secrecy agreements with the United States.

Concern that this might make problems for US industry have been raised by the American Association for the Advancement of Science. Although at first reading the new order seems to be a liberalization of existing practice, in fact new authority granted to the Department of Defense in its 1984 authorization

greatly extends its scope to label information sensitive and hence subject to export control. In the past, patent secrecy orders have been used only rarely for inventions arising from privately-funded research. These were the sort of inventions that, had they arisen from government-funded research, would have been instantly classified. But the new "secrecy order and permit for filing in certain countries" could be applied far more often; guidance for classifying technology as export-controllable comes from the militarily sensitive technologies list, which covers a great deal of ground.

A US inventor who found his patent application subject to one of the new orders would be able to manufacture and sell the invention in the United States (this is a "legitimate business purpose") but would risk the invention being copied and "reverse engineered" by competitors overseas while the secrecy order was in force. In the area of electronics, countries on the Pacific rim pose a particular threat. Although the inventor would be confident of ultimate patent protection in the United States and in the other countries named in the secrecy order, by the time a patent issued the market might be flooded with foreign copies. To avoid this, inventors might choose to sit on their inventions until the secrecy order expired and a patent issued, even at the expense of not establishing a captive market.

The Patent Office has said that the new proposals will be published in its official gazette for comment before being brought into force, and believes the congressionally-mandated test of when to impose secrecy orders (possible harm to national security) is unchanged. The Congressional Research Service has raised some doubts about the broad definitions in the order but finds no major legal flaw. Manufacturers' organizations are starting to take notice. Tim Beardsley

## UK Strategic Defense Initiative contracts

Company	Project	Duration of contract (years)	Amount
Ferranti	Optical computing	1	\$142,500
General Electric	Concept definitions	1	\$100,000
General Electric	Kinetic energy weapons	1	\$100,000
Heriot-Watt University	Optical computing	1	\$142,500
UK Atomic Energy Authority	Neutral particle beam	5	\$10,000,000

ALTHOUGH the agreement signed last December for British participation in the Strategic Defense Initiative (SDI) guaranteed no specific sums, British companies had hoped to garner about \$1,500 million-worth of SDI contracts. So far, at

least, that figure is a long way off. The table above is compiled from figures supplied last week by the Federation of American Scientists. The SDI office in Washington will not confirm or deny these figures. □

**Mars mission**

## NASA selects contractors

**Washington**

PLANS for a Mars Observer mission crept toward completion this week with the selection by the National Aeronautics and Space Administration of contractors for the spacecraft and booster components. NASA named RCA Astro-Electronics to build the spacecraft, which has an estimated price of over \$250 million, while Orbital Sciences Corporation will provide the \$20 million propulsion system. But NASA has already been dealt another delay in the form of a bid protest filed by Hughes Aircraft in February.

NASA's Jet Propulsion Laboratory (JPL) directs the Observer mission, which was proposed in 1983. The first in a series of low-cost inner planet probes, the spacecraft will borrow the design of Earth orbiters and is scheduled for launching from the United States's space shuttle in 1990. By 1991, Observer will be circling Mars for a full martian year. The spoils of the mission may prove useful in organizing the manned mission to Mars which, according to the issue of *Aviation Week and Space Technology* for 24 March 1986, will be suggested by the National Commission on Space early in April.

Hughes's protest stems from a JPL announcement on 20 February that NASA had expressed a preference for an independent upper stage booster design, and that proposals for integrated spacecraft-booster designs would not be considered. With this decision, NASA essentially threw out proposals submitted by Hughes, RCA and Ford Aerospace in mid-1985. But each of these companies was still in the running for the spacecraft contract, having also prepared proposals for the spacecraft alone.

Although Hughes will not comment, one NASA official says it believes it would have won the bid on integrated designs. In a statement issued last week, JPL's director Lewis Allen insists that RCA would have been victor.

A conference on 10 April at the General Accounting Office (GAO) will give both sides a chance to air their views, but GAO may not offer a resolution until June.

In the meantime, NASA cannot award a contract to RCA, and contract negotiations are stalled. JPL's confidence in the outcome, however, can be gauged from the laboratory's activity in the midst of the fervour: JPL has begun distributing RCA's spacecraft specifications to potential bidders for the mission's complement of scientific instruments.

**Karen Wright**

## US research

# Smithsonian center to close

**Washington**

ALTHOUGH it was known to be coming, the timing of the Smithsonian Institution decision to close the Smithsonian Environmental Research Center (SERC) in Rockville, Maryland, later this year has prompted cries of outrage from SERC-Rockville employees and their supporters.

Notice of the decision was contained in a memorandum sent to SERC-Rockville director William Klein on 21 March by Smithsonian assistant secretary for science David Challinor. During a visit to SERC-Rockville last February, Challinor told Klein and others that the Smithsonian was thinking of closing the center during the 1987 fiscal year. The March memorandum stated that the facility would close and all positions would be abolished on 14 November 1986, six weeks after the start of the 1987 fiscal year.

While the Smithsonian maintains that some employees will be offered positions at other Smithsonian facilities, that is not the impression left with employees.

What particularly rankles with people at SERC-Rockville is that they feel deci-

sions were made without their involvement. "I have not been consulted about this decision whatsoever", says Klein.

Also annoying has been the Smithsonian's opinion that SERC-Rockville's productivity "was not up to the standards of similar institutions". Those familiar with SERC-Rockville's work concede that the facility could have helped its cause by publishing more frequently.

SERC began in 1929 as part of the Smithsonian Astrophysical Observatory and became an independent bureau in 1969. It now occupies a leased facility in Rockville, a suburb of Washington, DC. The staff consists of 11 scientists and 34 support personnel, with an annual budget of around \$2 million. The centre is primarily devoted to photobiology, with current research projects focusing on blue and red light photoreceptors, accessory pigments and CO<sub>2</sub> photosynthesis. In addition, there is a solar radiation monitoring group and a carbon-dating facility, both likely to be retained elsewhere by the Smithsonian.

Two independent reviews of SERC-Rockville conducted in 1979 and 1981 for the Smithsonian concluded that the labo-

ratory lacked the "critical mass" of people and facilities to perform world class science. The possibility was considered of merging SERC-Rockville with a smaller SERC facility on the Chesapeake Bay, but the \$30 million price tag for a new facility was beyond the institution's budgetary grasp.

Several universities, including Johns Hopkins, Duke and the University of Maryland, expressed an interest in merging with SERC-Rockville, but were unwilling to make the financial commitment that the Smithsonian wanted.

The Smithsonian Institution ultimately decided that it could not afford to support SERC-Rockville at a level it felt was necessary for good science, and the decision to close the centre was hastened by the fact that the lease on the Rockville facility was due to expire in 1990.

Winslow Briggs, head of the department of plant biology at the Carnegie Institution of Washington in Stanford, California, calls SERC-Rockville's work "not terribly fashionable, but terribly important". He expressed disappointment at the Smithsonian's decision, and "outrage" that the closure would take place this year.

The Smithsonian is not blaming budget problems as the primary reason for the closure. Instead, says Ross Simons, programme manager in Challinor's office, the issue is "where Smithsonian science as a whole should be going". Simons says the Smithsonian's scientific strength in the natural sciences is in evolutionary biology, and that is where money saved from the SERC-Rockville closure will be spent.

**Joseph Palca**

## US engineering

# Five more centres named

**Washington**

THE National Science Foundation (NSF) last week announced five more Engineering Research Centers, intended to foster interdisciplinary research and education in selected engineering fields. The five new centres, selected from 102 proposals from 75 institutions, will together receive \$56,300,000 over the next five years.

The first six NSF engineering research centres were announced in May 1985 in response to a widespread sentiment that NSF should be doing more to foster engineering research. Since then, NSF authorizing statutes have been amended to give greater prominence to engineering. But even with the new emphasis (enthusiastically championed by NSF's director Erich Bloch) the number of centers will not reach 25 by the end of fiscal

year 1987, a previously discussed target.

The existing six centres have succeeded in attracting substantial industrial support: \$13 million on top of the original \$10 million from NSF. The newly announced centres are expected to do likewise. Typically, 20–40 faculty members are involved in a centre, and collaboration with industry on engineering problems is mandatory. Observers are encouraged by progress so far. According to Lynn Preston of NSF's cross-disciplinary research directorate, the centres have inspired other universities and industry to establish cooperative research links along NSF lines even without NSF support. Some similar collaborative research centres are proposed to be funded this year by the Department of Defense under its new University Research Initiative.

**Tim Beardsley**

Institution	Subject	Amount (over 5 years) (\$ million)
University of Utah & Brigham Young University	Advanced combustion engineering	9.7
Carnegie-Mellon University	Engineering design technology	14.9
University of Illinois-Urbana	Compound semiconductor microelectronics	11.6
Lehigh University	Large structural systems	10.4
Ohio State University	Net shape manufacturing (direct near-final shape production)	9.7

# EPA bars AGS test

**Washington**

THE Environmental Protection Agency (EPA) has suspended the experimental use permit issued to Advanced Genetic Sciences (AGS) for field trials of genetically altered bacteria on strawberry plants until new data can be reviewed.

EPA will also fine AGS \$20,000, the maximum allowed by law, for testing the genetically altered version of *Pseudomonas syringae* under conditions that could have led to an environmental release of the bacteria. The EPA complaint charges AGS with misrepresentation and falsification of data, as well as use of an experimental substance in a manner not prescribed by agreed protocols.

Last month, AGS admitted that pathogenicity tests on the new bacteria, developed to protect crops from frost damage, were carried out on trees on the roof of its Oakland headquarters (see *Nature* 320, 2; 1986). EPA regulations require such tests to be conducted in an enclosed environment. AGS has now agreed to redo pathogenicity tests on the trees. Joseph Palca

## French science

# Bureaucracy looks to survival

In an extraordinary declaration of the likely directions of the new French government's education policy last week, the new minister of education, René Monory, has announced that he will make no radical alterations to the constructive policy of his socialist predecessor, Jean-Pierre Chevènement.

Monory told journalists that he "wanted to get things moving" and that he agreed with most of the things that Chevènement had been doing. He was particularly happy, he said, with Chevènement's efforts to raise the number of schoolchildren achieving the "baccalauréate" (the high school graduation certificate that guarantees entry to university). "International competition and demography demand it", he said.

Thus Monory has pinned his colours to Chevènement's typically radical efforts to reform the school system, which for Chevènement was too geared toward mathematics and to the entry of the very few into a few élite institutions.

Chevènement's intention was to create new universities of technology and more *grandes écoles* geared to tomorrow's technology. But pre-election advisers to the new Prime Minister, Jacques Chirac, sought to strengthen and return power to the existing university

system, and had been working on legislation to this end. Chevènement's grand plan will not now be torn up. Chirac and Monory may be planning to go easy; Monory is talking of not wishing to "rekindle the battles", said Monory.

The government's policy remains far from clear. Bernard Descombes, who masterminded the previous government's successful attempts to tighten up assessment and research quality in the French universities, was due to meet his new minister for higher education and research, Alain Devaquet, just before the Easter break. Whether the old ministry of research and technology will survive is apparently not yet decided.

Meanwhile, Devaquet occupies not the small office at the ministry of education appropriate to a junior minister but the grand headquarters of the old ministry of research and technology, in the old Ecole Polytechnique on the Montaigne St Genevieve. The switchboard operators are selfconsciously announcing "ministry of higher education and research" to incoming callers. Some on the Montaigne hope that the ministry will not be as radically dismantled as Chirac has been threatening.

Devaquet has also filled the powerful post of cabinet director with Michèle

Legras, who is four years older than her minister and a career administrator of some eminence; she has served under ex-prime minister Raymond Barre and was *chef du cabinet* to a previous (but regrettably forgotten) research minister, Jacques Sourdille, in 1977.

Robert Walgate

## Polish nuclear power

# Safety fears

LOCAL opinion in the district of Lubusz in western Poland is "outraged" by plans to build a nuclear waste dump, according to Zielona Gora local radio. Members of the Sejm (parliament) are accordingly being sent to the area to confer with local officials, although no final decision on where the waste will be stored can be reached until an expert survey is completed in 1990.

At present, a new bill on the nuclear industry is being drafted. Polish media and press agency reports on the bill, during the past two weeks, have stressed that it will make all necessary provisions to protect workers in the nuclear industry and the public at large from radiation hazard. This stress on safety is clearly meant to allay fears not only in Lubusz but also in the vicinity of the planned nuclear power stations at Zarnowiec and Włocławek.

The fears go beyond the usual apprehension of residents of an area where a nuclear installation is planned. Nuclear safety in Poland is by no means well organized, but is at present governed by a regulation dating from 1961 which involves not only the Atomic Energy Commission but four other ministries as well.

In 1973, the second congress of Polish science called for a two to threefold increase in the number of nuclear safety experts, but numbers have instead fallen rapidly (by 45 per cent between 1980 and 1985), while those who remain are mostly approaching retirement age. In May 1985, the academic council of the Institute of Nuclear Chemistry and Technology at Zeran, stated that Polish radiological protection work is in so disastrous a state that its very existence is threatened.

How far the new bill can remedy this situation is unclear. The main need seems to be the training of a new generation of safety experts, which will take several years. But the rapid response of the Sejm to the disquiet in Lubusz, to say nothing of the fact that it was reported in the official media, suggests that the Polish authorities, now irrevocably committed to a programme of nuclear expansion, are anxious that fears over safety should not escalate into the kind of anti-nuclear protest now building up in Yugoslavia.

Vera Rich

# Aleksandrov stays at Soviet academy

ACADEMICIAN Anatoli Aleksandrov, the 83-year-old president of the Soviet Academy of Sciences, has retained his post, in spite of rumours that he was to resign at the annual general meeting on 19 March. Most rumours tipped as his successor Academician Evgeneii Velikhov, a physicist who has recently entered the arena of international politics as head of "Scientists against Nuclear War". Shortly before the meeting, however, Academician Viktor Logonov, the rector of Moscow University and also a physicist, was also mentioned as a possible successor. In the event, in spite of Mr Gorbachev's current policy of retiring eminent but superannuated people, Aleksandrov was not replaced.

Aleksandrov is not in the best of health, and has not for some years attended ceremonial functions abroad. His continuation in office will mean continued diplomatic limelight for the vice-presidents, who depurate for him, which may not be entirely unwelcome to those not eligible for the presidency. Over the past few years, it has become a tradition that the president of the academy is either a mathematician or a physicist.

Apart from Aleksandrov's staying on, this year's meeting brought few surprises. Most speeches dealt with the implementation of the resolutions of the recent party congress, insofar as they affect science.

Aleksandrov himself noted that the role of the academy as a coordinator of all research work in the Soviet Union should be "appreciably enhanced" in the new five-year plan (1986-90), gave the number of researchers in the Soviet Union as around 1.5 million and noted that this year's research budget (presumably for the whole of the Soviet Union) would amount to 29,000 million rubles. Other speakers dealt with the priority areas already outlined in the guidelines for the plan, but Academician Yurii Ovchinnikov complained that although genetic engineering can produce new medicines in six months, the time needed to test and "verify" them (10-12 years) was much too long.

One innovation that seems to have been generated within the academy is the decision to create an interdisciplinary coordination council for the investigation of the "entire package of questions of the study of man".

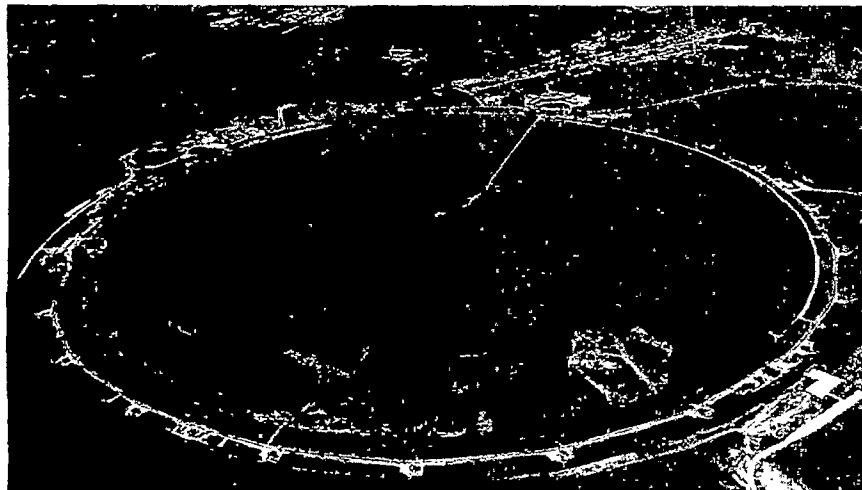
Vera Rich

**Fermilab**

# High-energy physics in a suitcase

**Batavia, Illinois**

PHYSICISTS at Fermi National Accelerator Laboratory (Fermilab) are not the only ones disappointed that the main accelerator beam was shut down for repairs after last fall's successful engineering run that produced the highest energy



proton-antiproton collisions ever. A flock of Canada geese typically spends the cold Illinois winter on one of the cooling ponds for main ring magnets. With the ring's magnets turned off, the ponds are now mostly ice, so that this winter the large flock has had to fight for space in the small area melted by heat from Fermilab's computers.

Fermilab sits on 6,800 acres about 30 miles from downtown Chicago. Despite its relative proximity to one of the largest cities in the United States, a herd of 75 buffalo grazing just beyond the Collider Detection Facility (CDF) serves as a reminder that the city is not that close. Indeed, a conscious effort has been made to minimize the environmental impact of Fermilab's facilities. A project begun nearly a decade ago by Fermilab employees and area residents has now replanted all 800 acres inside the ring, restoring much of the original prairie vegetation.

Fermilab was dedicated in 1974. Today, there are about 2,200 employees, although that number will be allowed to slip to 2,000 under budgetary pressures. There are 400 physicists resident at Fermilab, but there is also a steady stream of visiting physicists from the 325 institutions in the United States and abroad involved in collaborative projects.

**Fermilab budget (\$ million)**

	FY85	FY86	FY87 (estimate)
Operations	122.3	118.8	135.9
Capital equipment	27.5	31.6	30.5
Construction	41.6	19.3	23.7

Most visiting scientists, called "users" by the resident staff, stay at the Fermilab village, once the town of Weston, Illinois. Collaborators on Fermilab projects who still have teaching responsibilities at their home institutions face an itinerant lifestyle. "I have my bags

packed all the time", says Phil Kesten, a postdoctoral fellow at Brandeis University working on software for CDF. Kesten leaves his home in Boston once every 2 to 3 weeks for four-day visits to Fermilab. Some pay even more frequent visits.

While the trip to Chicago takes about an hour by car, many are reluctant to spend the extra travel time. The neighbouring towns of Batavia, Aurora and St Charles are hardly famous for their cultural appeal. "One likes to go out to a nice restaurant once in a while", says Kesten. "After a few trips, you've tried them all".

One bonus from living at Fermilab is the opportunity to visit Chez Leon, a restaurant run by Tita Jensen, wife of physicist Hans Jensen. Chez Leon is open only for lunch on Wednesdays and dinners on Thursdays, but visitors have been known to adjust their schedules to coincide with those times.

Users are not alone in being faced with heavy travel schedules. During this period of tight federal budgets, Fermilab project directors constantly find themselves travelling to Washington to defend their fiscal needs. Two weeks ago, Peter Koehler and Paul Grannis, co-leaders of a new colliding beam detector known as D-Zero, made the pilgrimage to urge Department of Energy officials to release an additional \$1 million to support research and development efforts by the 125 collaborating institutions. While Koehler and Grannis are satisfied with the \$7.1 million allocation in the 1986 budget for D-Zero, they are concerned

that without additional money for their collaborators, work will fall behind schedule. But prospects for this extra money are not good. The Department of Energy has already used up most of its discretionary funds for this fiscal year.

Fermilab director Leon Lederman was also in Washington recently, testifying before a House subcommittee on high-energy physics. Reagan administration budgets have treated Fermilab fairly generously. With the commissioning of the Polarized Proton Beam and Target System, expected within five months, Fermilab will finish a \$25 million upgrade to the fixed beam experiments.

The completion of the major Tevatron construction projects brought Fermilab's budget down to \$169.7 million in 1986 from \$191.4 million in 1985. The government has proposed a 1987 budget of \$190.1 million that will allow improvements to the antiproton Debuncher and Accumulator rings, as well as completion of CDF and continued work at D-Zero.

But Lederman believes that science in general is "trembling at the edge of a decline" like that of 1968. Lederman is especially concerned about the effects of the automatic cuts that may be required by the Gramm-Rudman deficit reduction act. "It will kill American science", says Lederman. He argues that most scientific efforts operate on a pattern of growth, and to apply the brakes suddenly can wreak havoc. Moreover, in a large facility such as Fermilab, many capital

**Leon Lederman**

costs are fixed, and a 15 per cent cut in the overall budget can mean a 40 per cent cut in funds available for research.

For the time being, Lederman believes that Fermilab is "sitting pretty". Until the Superconducting Supercollider is built, and Lederman believes it will be, Fermilab will provide the highest energy window into the particle physics world.

Department of Energy officials concede it will be difficult to obtain the funds budgeted for Fermilab in 1987. But the prospect of losing funds for research is extremely frustrating for high-energy physicists who feel their subject is "incredibly juicy" right now. "It's like being in an attic full of treasures", says Lederman, "and we've opened only one box".

**Joseph Palca**

# West German universities

SIR—With nearly six years experience of the present "democratic" system in one West German university and after working for 10 years in a US university (JVB) and 28 years in a UK university (GE), we believe that Stumpfl (*Nature* 319, 256; 1986) overstates its deficiencies.

The "democratic" committees (on which professors constitute only 50 per cent of the membership, even for the appointment of new professors) are, as he claims, immensely time-consuming and inefficient. However, they provide an opportunity, perhaps the only one, for students to counter the all-pervading attitude that the university exists primarily to support the administration or the teachers rather than to educate the students. It is the rule rather than the exception that professors allow only one hour a week for individual contact with students (the weekly *Sprechstunde*); and there is frequently also little informal contact between professors within one faculty or with the lecturers, there being no equivalent to the regular "lunchtime get-together" or the "common room".

In our experience, the committees are not "...dominated by extreme left-wing activists". The real power lies with one individual in the faculty, the dean and his tiny committee, the *Dekanat*. He is responsible for all administrative duties (for example the teaching programme, financial expenditure, the supervision of the lecturers, the allocation of space, arranging for the appointment of new professors, safety, appeals against examination procedures or results).

Since these duties are so arduous (and incompatible with full-time teaching or research), the office is generally held for only one or two years — hardly long enough to learn how to perform the duties competently. Being ultimately responsible but insufficiently experienced, the dean may indeed adopt "populist measures" or have to "bow to the majority of the less qualified" to obtain committee decisions required to keep the faculty running.

Meanwhile, each professor is explicitly expected by all those who work with/under him to advocate lines of action that will afford maximal gain to his particular section of the faculty; hence, self-interested pleading rather than consideration of the overall good characterizes the interminable committee discussion; and the dean, who may not himself be entirely disinterested, lacks the experience to hold out against merely clever arguing.

On this analysis, it is not the "democratic" system in itself that is at fault. Rather, the purposes of the university have been lost sight of (partly due to the sheer weight of the administrative paper

work); and the day-to-day administration falls to those who do not remain in office long enough to learn to withstand those who push hardest.

JOSEPHINE V. BROWN  
GEORGE ETTLINGER

*University of Bielefeld,  
4800 Bielefeld 1, FRG*

## South Africa

SIR—Would it be too much to hope for a cool and rational discussion of the issues raised by the banning of South Africans from the World Archaeological Congress? While there is indeed an issue of principle involved, as Bender *et al.* insist (*Nature* 319, 532; 1986), the decision about what action to take should be made with a view to what is most likely to be effective.

It is presumably this which lies behind the idea of "historical moments" in the lives of repressive governments, and makes it worth serious consideration. However, it also undermines the attempt of Bender and his colleagues to treat South Africa as uniquely awful because it institutionalizes apartheid. Mandelstam *et al.* (*Nature* 319, 715; 1986) are right to condemn them for failing to address the real issue. But they go on to ridicule the use of the "historical moments" argument against South Africa on the grounds that logically we should apply it to many other regimes as well. Although some of the examples they cite are strange — the only "mass slaughters that take place constantly in the Middle East" that I know of are part of the Iran-Iraq war, and they seem unaware of the recent change of government in Uganda — there is every reason for being prepared to treat other repressive regimes in the same way as South Africa's.

There is no doubt that the attitude to South Africa of the left in Britain has long been distorted by hypocritical double standards. South Africa is very far from being the nastiest country in the world, or even in Africa.

That said, there is a better *prima facie* argument for singling out South Africa at this particular moment than is acknowledged by Mandelstam *et al.* It does have democratic structures and institutions of a kind, and, *pace* Dr Slabbert, a legitimate opposition, and is thus more likely than, say, Paraguay or Syria to respond to boycotts and bans because, unlike them, it has a body politic capable of feeling the pressure.

We should forget the shoddy behaviour and dubious motives characteristic of so many of apartheid's foreign opponents among the fashionable left, and instead concentrate on what is most likely to bring

about desirable change in South Africa, and in the much more vicious regimes to be found in almost every continent.

A. W. ANDERSON

*University of Oxford,  
Department of Biological Anthropology,  
58 Banbury Road,  
Oxford OX2 6QS, UK*

SIR—The recent letter from Bender *et al.* (*Nature* 319, 532; 1986) supporting the Southampton boycott of South African archaeologists is basically a purely political document, apparently expressing the view that the Botha government will tremble in its shoes when enlightened academics stamp their feet. If only this proposition were true. The arguments presented appear to place little value on either scientific or educational considerations. However as the letter comes from a university address, one must presume its writers are educationists, and so should be willing to state their position clearly as regards educational issues.

As a pragmatic scientist and university teacher, it seems to me their position as educationists must be one of the following:

- (1) It is wrong to provide good quality universities in South Africa. If this is the stance, its basis presumably is that black people do not need a university education.
- (2) It is right to provide good quality universities in South Africa, but those who do so should be penalized for their efforts. This stance seems to be straightforwardly contradictory.
- (3) It is all right to provide undergraduate education in South Africa, but post-graduate education and research should not take place there. If this is the stance, it presumably means that the appropriate ceiling for black people is an undergraduate degree — which is just a sophisticated version of Dr Verwoerd's vision that they should be educated so far and no further.
- (4) Both undergraduate and graduate university education should be available to blacks in South Africa, but not to whites. This stance is both racist and eminently unpractical in terms of educational realities. If this is indeed the stand taken, who will do the teaching, and where will the necessary reservoir of high-level academics come from?

In view of the destructive nature of their stance, your correspondents have an obligation to make their position clear. I should very much like to know which of these alternatives they support (or what other view they have of the education that should be available to the populace of this country).

GEORGE F. R. ELLIS

*Department of Applied Mathematics,  
University of Cape Town,  
Rondebosch, Cape 7700,  
South Africa*

## CORRESPONDENCE

## Infectious AIDS

SIR—The letter from the Drs Fox (*Nature* 319, 8; 1986), and your leading article (319, 9; 1986), highlight the recent awareness that the virus known as LAV, HTLV-III, or ARV (hereafter called the AIDS (acquired immune deficiency syndrome) virus) often causes progressive encephalopathy, similar to that in the archetypal slow virus disease of sheep, maedi-visna. However, the generally accepted hypothesis that "the AIDS virus is plainly not particularly infectious" needs to be modified slightly. Under special circumstances the virus is highly infectious.

Infected people are persistently viraemic, and they intermittently shed infected lymphocytes in saliva, semen, bronchial secretions and tears. Serum contains up to 25,000 virions per ml (ref. 1), but virus is largely cell-associated in the other fluids, making them much less infectious than serum. However, AIDS virions remain highly infectious after seven days in water at room temperature, and retain some infectivity when dry for a week<sup>2</sup>. A few AIDS virions injected hypodermically into chimpanzees invariably infects them, and within two weeks their serum becomes persistently infectious.

It is consequently unsurprising that the virus is spread rapidly by repeatedly re-used unsterilized hypodermics, and by sexual manoeuvres that damage the rectal mucosa of people who frequently change partners. Modern medical hypodermics are re-used in poor countries on a very large scale. For example, in four weeks in 1976, the blood-borne virus causing Ebola fever swept through the 120-bed mission hospital in Yambuku, Zaire, because only five needles and five syringes were used each day for all ward patients, and about 400 out-patients<sup>3</sup>. Injection was the preferred route for all medication. A pan of water was used to rinse the hypodermics, which were boiled less than once a day.

With similar practices widespread in Africa, Asia and South America, millions could be infected with the AIDS virus, brought to a continent by a single carrier, before anyone realized that it had arrived. The incubation period to illness lasts years, and early cases are lost amongst the diseases of abject poverty.

Once a critical mass of people have been infected rapidly by highly efficient means of transmitting the virus, then transmission by far less efficient means will inevitably occur increasingly often. These include blood transfusions, perinatal transmission, biologically normal sexual intercourse, needle-stick injuries, chance contact of sores or abrasions with contaminated blood, saliva or sputum, mechanical transmission by blood-sucking insects and flies and routine dental procedures. AIDS patients who have no known "risk factor"

form the third largest "risk group" for AIDS in the United States (6 per cent), the second largest group in Western Europe and the vast majority in Africa. Postulating clandestine homosexuality or heterosexual promiscuity to explain these cases is unnecessarily speculative, given the properties of the virus.

You mention some of the many similarities between the viruses causing AIDS and maedi-visna. If the long-term mortality of infection also turns out to be similar, the AIDS epidemic is more than "a serious problem of public health"; it is the start of a pandemic slow virus disease with the potential to decimate mankind within a couple of decades.

JOHN SEALE

Royal Society of Medicine,  
1 Wimpole Street, London W1M 8AE, UK

- Levy, J.A. et al. *Ann. intern. Med.* 103, 694–699 (1985).
- Barre-Sinoussi, F., Nugeyre, M.T. & Chermann, J.C. *Lancet* ii, 721–722 (1985).
- Report of International Commission *Bull. Wld Hlth Org.* 56, 271–293 (1978).

## Complex forests

SIR—The erroneous idea is becoming widespread that the remarkable forests being destroyed and in danger of extinction round the tropics, subtropics and in a few temperate lands are rain forests, whereas they are often dry sclerophyll woods where the dead leaves crackle underfoot. The essential thing about them is not wetness; it is that they are all coherent communities which are complex multiple aggregations containing many quite different kinds of trees of all shapes and sizes dominated by lofty, often huge trees many centuries old, each bearing a large quantity of timber. Numerous different species of lianes, shrubs and flowering plants hang on the branches adorning the complexity.

The roof of this kind of standing forest is a billowing surface of greatly varied height and shape, frequently overtopped by the crowns of the scattered dominants. Such a kaleidoscopic vegetation takes many centuries to mature, millennia even, and can never be replanted once it is gone. It is surprising that these ancient complex forests have kept the same habits of growth, shape and structure in so many different countries, each with its own unique combination of species. The soil beneath is often poor and exhausted, and after the big trees are cut, the local microclimate changes, and if the surface does not erode and disappear, nothing but weedy scrub will cover its wounds.

Real rain forests blanket many square miles of the Southern Hemisphere among mountains where precipitation rates may reach 450 cm a year, where there is no dry season and everything is sodden. *Nothofagus* trees, all one species in any one place,

grow laced together to a uniform low to medium height, their twisted branches and exposed roots clad in a thick bryophytic wrapping. Many ferns, saplings, shrubs, seedlings and a few flowering plants grace the interior. Such rain forests form a smooth green surface spreading over the country like a carpet, in strong contrast to the bubbling canopies of a complex forest.

These two distinctly structured types of forest, both of which may cover a range of climatic conditions and may abut without ever mixing, are better called "complex" and "blanket". Complex forests are always ancient and if destroyed cannot be reconstituted. Blanket forests in contrast, with a single tree species in any one area, are comparatively short-lived and may generate readily.

GRETA STEVENSON  
Flat 3, Lockwood Court,  
76 Westwood Road, Southampton, UK

## Nature exploiters

SIR—Lord Ashby, in his review of the book *Pesticides and Nature Conservation* (*Nature* 318, 21; 1985), concludes that "there has to be a compromise between those who want to exploit the environment for profit (either by growing crops or making pesticides) and those who want to protect it". He has, however, reversed the roles of the participants.

Those who have become bloated by exploiting the environment for profit are groups such as the Audubon Society, the Sierra Club and the Environmental Defense Fund. They have attained great political clout, huge staffs and bulky portfolios of stocks and bonds financed by the donations of frightened, misinformed citizens who were exposed to the false allegations of pseudoenvironmentalists. Humanity should be included as a part of the environment, and "those who want to protect it" are thus the groups involved in growing crops and preventing illness and death resulting from insect-borne pathogens.

Lord Ashby categorizes John Sheail's book as "a record of missionary work by scientists" who have worked and lobbied on behalf of the environmental movement. Those "missionaries" paid scant heed to the hundreds of millions of human beings who were sacrificed as a result of their efforts, and it might be asked why they resorted to such unscientific methods as deliberately distorting or omitting all the data that refuted their allegations over, for example, the impact of DDT. Lord Ashby is certainly correct: "the story is not over yet".

J. GORDON EDWARDS  
Department of Biological Sciences,  
San Jose State University,  
One Washington Square,  
San Jose, California 95192-0100, USA

## CORRESPONDENCE

## Japanese psychiatry

SIR—As the other visiting scientist named in the article by Alun Anderson entitled "Abuse for visiting scientists" (*Nature* 315, 361; 1985), I would like to add to Kimio Moriyama's response (*Nature* 318, 308; 1985). Dr Moriyama writes that his group did not "intend to visit the smaller meeting at Nagoya". At the smaller meeting, Dr Crow and I were the only two speakers to be scheduled and our presentations were cancelled because the group of psychiatrists and their followers from Tokyo and Gifu were on their way to disrupt the meeting. Previous encounters had led to violent fights between the two groups. I fully agree with Dr Crow (*Nature* 319, 172; 1986). I too am willing to have the abstracts of the cancelled meeting of the Japanese Biological Psychiatric Society, deemed by Dr Moriyama to be unethical, examined by an official Institutional Review Board. I hope that the Japanese psychiatric patients, abandoned by their families, will not be deprived of participation in psychiatric research.

There are apparently some changes now to the betterment of patient rights and patient care in Japan. Changes like that are always too slow. Violent threats and intimidation belong to another era. I do not believe that anyone is served when psychiatrists go into fist fights to disrupt meetings. It will do nothing to remove the stigma attached to the mentally ill or to increase public support for reform. Presumably, we are all involved, because we want to improve our patients' lot and believe in the principle of freedom of scientific information.

DANIEL P. VAN KAMMEN

*Veterans Administration Medical Center,  
Highland Drive,  
Pittsburgh, Pennsylvania 15206, USA*

## Wasting assets

SIR—I recently attended a one-day international meeting concerned with a fundamental aspect of physics. For twenty-four hours I was free to do my proper job of thinking about science and how mankind can better understand the sensible universe. Such is the contrast between this pleasant and productive interlude and what my life otherwise has become that I actually felt guilty at absenting myself from the usual Sisyphean labour of trying to overcome inadequacy of resources, digging away at piles of unproductive paperwork, making meaningless returns and providing unvalidated "indicators" of performance. It was like attending a party in the penthouse of a building while the foundations are crumbling.

A number of overseas colleagues expressed disquiet at the crisis in funding of British science and education, and even more at the crisis in morale resulting from

continual insults and depreciation, and our despair that the nature and importance of what we do will ever be understood. It became apparent that we have come to mistrust our politicians far more than do scientists of other countries. As a transatlantic colleague put it, while US politicians do indeed devote much attention to the need to be re-elected every few years, they are sophisticated enough to understand that pure knowledge and research are the seed-corn of what the culture and industry of their country will need in ten to thirty years' time.

By contrast, we encounter penny-pinching which is squandering a great national asset, once esteemed as among the finest in the world. The whole structure of our institutions concerned with knowledge, from schools through universities to original research, is in disarray. One can hardly doubt that if present policies continue, then even apart from explicit support for research, we shall lack the structures that enable talented people to be educated and become the creative researchers of the future.

In the absence of the new ideas generated by research, we shall lack an essential ingredient needed for industrial prosperity in future decades. This situation has within it the seeds of Britain becoming a third world country, taking its ideas and industrial capital from more developed countries.

The question is not whether we can afford what we spend on schools, universities and research, but how a densely populated island can afford to spend so little on cultivating its intellectual assets. The knowledge base of our culture and industry is in jeopardy so long as we invest less on it than we wager on horses.

PETER FELLGETT

*University of Reading,  
Department of Cybernetics,  
3 Earley Gate, Whiteknights,  
Reading RG6 2AL, UK*

## Creationism

SIR—We have witnessed, again, the basic underlying view of creationism in D.H. Koobs' letter (*Nature* 319, 172; 1986), where he shows four of the methods creationists commonly use during their assaults on science.

First it is claimed that science does not have a complete understanding (which it never can) of important items such as the origin of life or the Universe, that these are some sort of boundaries to reality, that they are impermeable to human scrutiny and that since they are boundaries not crossable by science they are therefore, by default, proof of their presupposed supernatural creator. Nothing is potentially beyond science.

Secondly, Koobs brings science down to the creationists' level by making the

absurd statement that there are areas of science that are to be taken on faith. I have heard many creationists claim it is a greater leap of faith to believe in evolution than it is to believe in creation. These people use that word incorrectly. Faith is a belief without evidence, and in the case of creationism it is a belief in spite of evidence. However, we all know that science accepts nothing on faith.

Thirdly, Koobs gives the impression that reality is manifested by human emotions and desires with this statement: "... who are free to choose which history provides more meaning for life". No comment is necessary.

Finally, misrepresentation runs rampant in creationism. Koobs is obviously referring to punctuated equilibrium when he claims that animals preserved in the fossil record "occurred spontaneously" and trying to equate punctuated equilibrium and spontaneous generation as acts of creation.

Creationism and science will never be two different ways of looking at reality. Creationists do their best to twist, lie, fabricate, misrepresent all they can of reality to deceive their followers and the lay public.

J. RICHARD WAKEFIELD

*385 Main Street,  
Beaverton, Ontario, Canada L0K 1A0*

## Animal deception?

SIR—Several times recently I have read claims (most recently in *Nature* 319, 143–145; 1986) that animals practise deception. There appears to be a strange logic at work here.

First, we have a Cartesian animal, with a limited repertoire of behaviours. There is one behaviour called "alarm call", which the investigator has presumably defined very carefully by extensive observation.

Next, it is reported that the "alarm call" has been used for some other purpose. Instead of concluding that his initial definition of "alarm call" was too narrow, the investigator summons up another animal, one which uses the "alarm call" deceptively. This second, non-Cartesian animal is thus implicitly given credit, or blame, for an act of choice, which invokes a presumption of self-consciousness, even an ethical being.

Ruppell (the author's first citation) may have started this fad with his account of the "lying" mother fox. I believe the investigator is deceiving the investigator here. At the very least, words like "deception", with strong ethical connotations, seem out of place in this sort of context.

HERBERT McARTHUR

*Research Foundation of  
State University of New York,  
State University Plaza,  
Albany, New York 12246, USA*

# Icosahedral frustrations ahead

*The experimenters have been more successful in finding new examples of icosahedral symmetry than the theoreticians have been at interpreting these exciting data.*

In the two years since the discovery of an alloy of manganese and aluminium with icosahedral symmetry by Schechtman, Blech, Gratias and Cahn, most of us have become more knowledgeable about crystallography, but are still perplexed to know what icosahedral symmetry means. This is not to suggest that people have been idle. Making tiny samples of alloys other than the Schechtman alloy, but with the same unexpected symmetry, has been widely practised; electron and X-ray diffraction patterns with five- or tenfold symmetry have become familiar.

People with a feeling for solid geometry have become even more expert at telling how icosahedra may be assembled into the shapes called tricontrahedra, while people like Pauling, with a sixth sense for how crystals are constructed, say the ground is familiar. [Pauling's first statement of this case (*Nature* 317, 512; 1985), which has been disputed, will soon be followed by an elaboration.]

The difficulty remains that ordinary mortals have no way of visualizing the construction of an icosahedral crystal, called a quasicrystal because it must be aperiodic, by placing identical unit cells at the points in space defined by vectors such as those defining ordinary crystal lattices. There is no language in which to search for common ground.

Disappointingly, the most promising candidate has now been used to suggest that the task of telling the true structure of icosahedral crystals is virtually impossible. This is one conclusion of the latest account by Per Bak, of Brookhaven National Laboratory, of his way of regarding icosahedral crystals as the projections on three-dimensional real space of crystal lattices of a more familiar kind constructed in six dimensions (*Phys. Rev. Lett.* 56, 861; 1986). Last year, Bak's account of how structures with only vestigial symmetry — such as the tiling of the two-dimensional plane by two rhombi of different shape — may be related to more symmetrical structures in a higher dimension was one of the most stimulating features of the enquiry.

The argument has general interest. An icosahedron is a solid with 20 faces, each of which is an equilateral triangle. One way of visualizing the figure is to construct a pair of pentagonal pyramids and to bolt them together, one pentagonal base to the other, with a ring of ten equilateral triangles joined head to toe. There are

twelve vertices, all geometrically equivalent, at which the corners of five triangles come together. Icosahedral symmetry is characterized by a total of 120 symmetry operations. For making crystals, icosahedra are unsatisfactory building blocks. For one thing, it is impossible to fill three-dimensional space with them alone. For another, fivefold symmetry is literally incompatible with an underlying lattice structure of the Bravais type. And then there is no simple way of describing such a lattice, even if it could exist, in terms of integral multiples of some set of independent displacement vectors such as normally define the shape of a crystallographic unit cell.

The last difficulty, more than a mere annoyance, is most simply illustrated by a hexagonal lattice in two dimensions as in a sheet of carbon atoms from a graphite crystal. The simplest description is in terms of a pair of vectors of equal length making an angle of 60 degrees with each other. A little scribbling will show that this choice allows the construction of a two-dimensional crystal lattice in which the smallest unit cell is a rhombus whose sides are three times as long as the basic hexagonal sides; each contains two complete hexagons and bits and pieces enough to make a third.

So why not find a more natural description reflecting the inherent hexagonal symmetry? The natural choice of basis vectors would be the set of three equal vectors defined in direction by the three hexagonal sides that meet at every vertex. An arbitrary choice must be made between the two orientations of triple vertices that occur, but the more serious difficulty is that the three vectors are not independent. (If their directions are chosen to point outwards from a triple vertex, their sum will be zero.) In effect, Bak's way of dealing with this difficulty is to pretend that the chosen vectors are in reality independent which, because there are three of them, means that they span three-dimensional space. As in an ordinary crystal, lattice points are then assumed to occur at all points represented by integral multiples of the basis vectors, and the two-dimensional hexagonal pattern will be found by cutting a suitable two-dimensional plane through that three-dimensional lattice.

Last year, Bak successfully applied this technique to the case of icosahedral symmetry, where the natural basis vectors are

a set of six drawn from the centre of the figure to each of the vertices of a pentagonal pyramid chosen at random. (The other six vertices are reached by projecting these vectors backwards.) It does no harm if this set of basis vectors are visualized as orthogonal axes in six-dimensional space. The most general description of this crystal is by means of a function representing the likelihood that matter of a particular kind (manganese or aluminium atoms in the Schechtman case) will occur at some point in space, which must in turn be a periodic function reflecting the repetitiveness of lattice displacements. The underlying icosahedral symmetry is reflected in the way in which this density function can be represented by simple periodic functions such as sines and cosines; symmetrically equivalent Fourier coefficients are identical.

Getting from here to the real world is not so simple. The six-dimensional lattice has icosahedral symmetry, but real three-dimensional space is not related to that pattern in a simple or even unique way. The trick is to classify the different ways in which the symmetry of the six-dimensional symmetry will show up on the three-dimensional "hypersurface" which is the real world. The answer is that the positions of atoms in the real crystal will be determined by the intersection of a sequence of three-dimensional "surfaces" in six dimensions with the real three-dimensional world (itself a hypersurface).

Two conclusions are arresting. First, Bak shows that it is possible to recover the now-familiar Penrose tiling of the two-dimensional plane, and its three-dimensional analogue, as special cases of his six-dimensional construction. But he also shows that there are limitless other ways in which the appearance (in diffraction patterns) of icosahedral symmetry may be generated. The implications of that are stark. There is no "simple mathematical model" of the Schechtman alloy, and no alternative to the complete solution of six-dimensional crystal structures for those who wish to know where the atoms are in these quasi-crystals. But Pauling, who argues for the twinning of unit cells unable otherwise to fill space, will be glad to note that Bak offers the distortion of the "natural" unit cell as one way of looking at icosahedral symmetry. What nobody has yet considered seriously is the energetics of these odd forms.

John Maddox

## Hot stars

# Breaking through the wall

from James B. Kaler

STARS live such long lives that we cannot actually watch one age, even over many human lifetimes. Birth-to-death changes wrought by time must be reconstructed by observing many different stars in varying states of decay, and linking them together by age estimates and theory. The course of stellar evolution has been charted quite successfully: we can recognize young stars; we know what their end products will be; and we can see and understand the natures of many of the intermediate states. Yet there are gaps in the record. The discovery by Atherton, Reay and Pottasch reported in this issue (*Nature* 320, 423; 1986) begins to fill one of the voids, by finally disclosing a member of a theoretically predicted class of extremely hot stars.

The subjects at hand are the stars in the intermediate mass range between about 0.8 and 6–10 times that of the Sun. Below the lower limit, the lifetimes are longer than the age of the Universe, so that none have yet died. Above the very insecure upper limit they explode. Those in the middle lead stable lives for a few billion years as they fuse hydrogen to helium in their cores, then go through a complex series of changes before expiring quietly as the incredibly dense remnants called white dwarfs. When the original hydrogen fuel is exhausted, the core contracts and heats while the outer envelope expands and cools to produce one of the commonly observed red giant stars. When the core temperature gets high enough, the helium created earlier can fuse to carbon, which for a while again stabilizes the star and allows the envelope to contract. On exhaustion of the helium, core contraction resumes, and the envelope expands once again into a giant state. Such a star can be so large (comparable to the inner Solar System) and the surface gravity so low that matter can be expelled in a fierce wind that removes most of the outer envelope, considerably diminishing the stellar mass. A final expulsion of matter reveals a nearly bare core, which is overlain with thin nuclear burning shells of helium and/or hydrogen, topped by a thin, non-reacting hydrogen skin. As this remnant envelope diminishes through winds and nuclear consumption from below, the surface temperature rises, and what is left of the star begins to contract. As it passes 30,000 K it begins to produce enough ultraviolet radiation to ionize the last expanding ejectum, and we now see a planetary nebula, a glowing cloud of gas surrounding a hot blue nucleus.

The stars are predicted to heat at a constant mass-dependent luminosity (Fig. 1)

until they reach a maximum temperature also dependent on mass, whence they cool and dim as they head for their final states among the white dwarfs that abound in

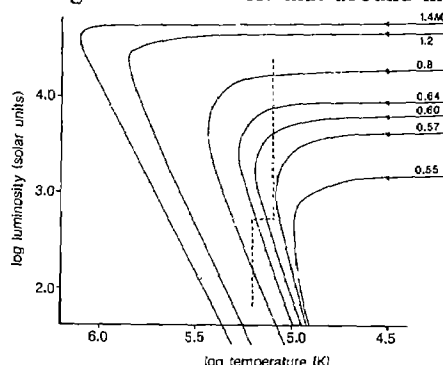


**Fig. 1** Evolution of planetary nuclei in temperature and luminosity as a function of stellar mass (in solar units,  $M_{\odot}$ ). The lowest four curves are from Schönberner (*Astr. Astrophys.* 79, 108; 1979 and personal communication, 1983), the next two from Paczyński (*Acta Astr.* 21, 417; 1971), and the highest is an extrapolation. Dashed lines give the location of Zanstra's wall, the high-temperature limit deduced from conventionally observed stellar magnitudes. (Adapted from R. A. Shaw, thesis, Univ. Illinois, 1985.)

space. This scenario is displayed with real nebulae in Fig. 2, where six planetaries are photographically placed at the same distance and arranged from left to right roughly in order of evolutionary state. The ones at the top are younger and the first three are on the horizontal tracks of Fig. 1. For the middle two we see bright stars in small nebulae, as expected. But as a star heats and produces relatively more ultraviolet photons, its nebula brightens considerably while the optical luminosity diminishes, and the star becomes lost in

the glowing cloud. Thus, we see nebulae with no apparent stars, as has been the case for the fourth object of the top line in Fig. 2, NGC2440, before the new work of Atherton and colleagues. Eventually, a nebula expands to the point where its now-cooling and much dimmer star is again revealed, as shown in the lower two photographs of Fig. 2.

Because most of the stellar radiation is in the far ultraviolet, temperatures from optical spectra are hard to find. Fortunately, we can use the fluorescing nebulae literally to count the number of ionizing photons, which when compared with optical luminosities, yield well-determined measures called Zanstra temperatures. When coupled with estimates of distances we can compute intrinsic luminosities and overlay the results on the theoretical evolutionary tracks to test the theory. With the best available optical stellar magnitudes (apparent luminosities), R.A. Shaw (thesis, Univ. Illinois, 1985) found a high temperature limit near 125,000 K, which he termed Zanstra's wall (outlined in Fig. 1). The stars of lowest mass fall nicely inside the wall, but those of higher mass become so hot that they cannot easily be found until they are quite dim: thus the gap in the observational record.

There have been many false or insecure results that have placed stars beyond the wall. Abell (*Astrophys. J.* 144, 259; 1966), for example, gives temperatures to 250,000 K, but these are grossly inflated because of the unknowing inclusion of nitrogen spectrum lines into the nebular brightnesses used to count stellar photons. Similar results have been derived from old and unreliable magnitudes, many of which seem to be erroneous. Other, indirect, methods use nebular ionization or energy balance to infer high temperatures (for example, see Preite-Martinez A. & Pot-

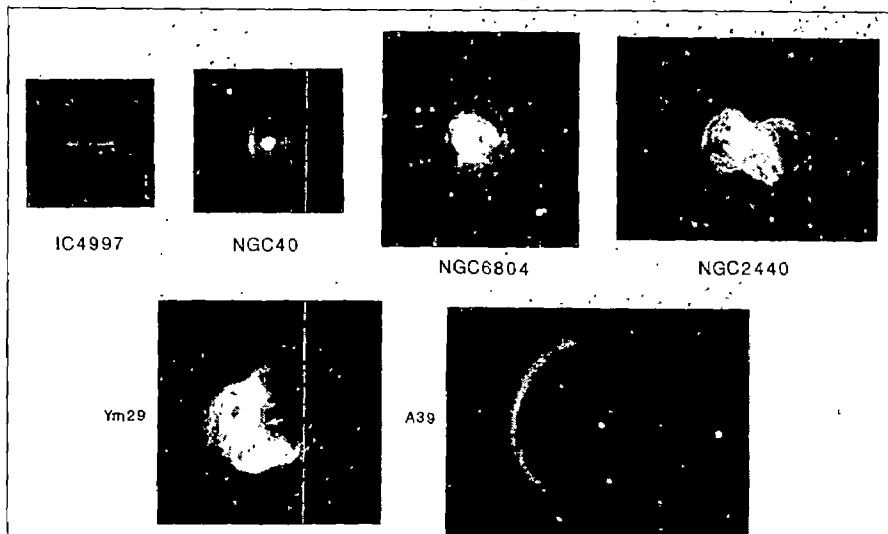


**Fig. 2** Evolution of planetaries illustrated by six nebulae set at the same distance. From left to right the objects proceed in the direction of the arrows in Fig. 1. IC4997, Lick Observatory; NGC40, University of Illinois; NGC2440, Palomar Observatory; others, Kitt Peak National Observatory. (Panel adapted from Kaler, J. B. *Am. Sci.* in the press.)

tasch, S. *Astron. Astrophys.* **94**, 213; 1981), but the stars themselves are not directly examined. Satellite observations in the near ultraviolet indicate some extreme temperatures, but these result from observational error and difficulty in understanding the nature of the radiating stellar atmospheres. Atherton *et al.* (*Astrophys. J.* **232**, 786; 1979) located what may be a star of more than 200,000 K in a nebula similar to NGC2440, NGC7027, but the identification is only tentative.

We see then the significance of the new work by Atherton and colleagues — for the first time such a hot star has been unambiguously seen, and its temperature measured. Now the wall has been truly broken, pioneering the technique necessary to fill in one of the few remaining holes in the paths of stellar evolution. □

*James B. Kaler is in the Department of Astronomy, University of Illinois at Urbana-Champaign, 1011 West Springfield Avenue, Urbana, Illinois 61801, USA.*

### Intracellular signalling

## GTP and calcium release

from P.F. Baker

CALCIUM is an important intracellular signal, key features of the system being the maintenance of a low concentration of free Ca in the cytosol, usually in the region of 100 nM; the existence of pools of Ca, both intracellular and extracellular, at much higher concentrations; mechanisms for transferring Ca from these pools into the cytosol; and, finally, receptors in the cytosol that can respond to changes in free Ca in the 100–1,000 nM range. Although much is known about these receptors and how the various pools of Ca are established, surprisingly little is known about how Ca is permitted to move downhill from these pools into the cytosol. At the plasma membrane the problem seems to be solved by the existence of Ca channels that are gated either chemically or by voltage, and it has always seemed likely that something similar may exist to effect intracellular release; but only recently have possible mechanisms begun to emerge, one of which is presented by Gill *et al.* on page 461 of this issue<sup>1</sup>.

The two major intracellular organelles that bind Ca are the mitochondria and the endoplasmic reticulum. Although their relative importance has long been debated, largely through the application of X-ray microanalysis to fast-frozen tissue, there now seems general agreement that in resting cells mitochondria contain rather little Ca but can sequester massive amounts should the cytosolic Ca begin to rise. In contrast, despite its relatively small Ca-binding capacity, the endoplasmic reticulum looks the stronger candidate for a high-affinity, physiologically relevant, intracellular Ca store. This comes as no surprise to muscle physiologists, who have long recognized that the myofilaments of skeletal and cardiac muscle are surrounded by a highly specialized derivative of the endoplasmic reticulum — the sarcoplasmic reticulum, which serves to regulate the local Ca concentration to which the Ca-sensitive contractile apparatus is exposed. Even in this tissue, however, which is apparently ideal

for experimental investigation, there is still considerable uncertainty about how Ca is released. Likely mechanisms for coupling electrical excitation to Ca release continue to be dominated by variations of the electro-mechanical, charged-plug model first put forward more than 10 years ago by Schneider and Chandler<sup>2</sup>.

The rise to prominence of the endoplasmic reticulum has brought new ideas about Ca mobilization and there now seems to be more known about the mechanism of Ca release from this structure than from the sarcoplasmic reticulum. A major step forward was the discovery by Streb *et al.*<sup>3</sup>, rapidly confirmed in many laboratories, that the water-soluble molecule inositol trisphosphate (IP<sub>3</sub>), a hydrolysis product of the membrane lipid phosphatidylinositol bisphosphate, can release Ca from the endoplasmic reticulum of many cells. In one step, this provided a link between membrane receptors and release of Ca from a major intracellular store. All subsequent work points to the existence in the endoplasmic reticulum of some sort of IP<sub>3</sub>-gated calcium channel. The obvious and very interesting possibility that IP<sub>3</sub> may also be involved in releasing Ca from the sarcoplasmic reticulum of skeletal muscle (see the recent discussion in these columns<sup>4</sup>) received some early and dramatic support but has so far failed to gain general acceptance. A subtle variant however, such as an IP<sub>3</sub>-type molecule as part of the Schneider-Chandler plug acting to release Ca via an IP<sub>3</sub>-type receptor in the sarcoplasmic reticulum is still an open possibility. In addition, by the isolation of nucleotide-gated channels, Smith *et al.*<sup>5</sup> have given new impetus to the search for physiologically relevant, chemically gated Ca channels in the sarcoplasmic reticulum.

Now, Gill *et al.*<sup>1</sup> interpret some very interesting new data in terms of another mechanism. Working with a detergent-permeabilized neuroblastoma cell line, they report that approximately half of the Ca accumulated by a store, presumed to

be the endoplasmic reticulum, can be released by exposure to micromolar concentrations of GTP. This very clear effect is highly specific for GTP and cannot be mimicked by non-hydrolysable analogues suggesting that GTP hydrolysis might be an essential part of the Ca-release process. GTP-dependent release is temperature-dependent and can be inhibited competitively by GDP. The authors make a plausible case for the involvement of a GTP cycle in the control of calcium permeability in the endoplasmic reticulum of neuroblastoma cells. They fail to explain, however, why their system is not permanently activated by the levels of GTP always present inside these cells.

What is the relation between GTP-induced and IP<sub>3</sub>-induced Ca release? The authors claim they are two separate systems. Thus, although IP<sub>3</sub> is active in their cells, its effects are not inhibited by GDP and exhibit a different temperature dependence from GTP-induced release. Although suggestive, these arguments are not compelling and, as the authors admit, it is possible that the IP<sub>3</sub>- and GTP-dependent systems for releasing Ca may prove to be closely related. The finding of Dawson<sup>6</sup> that IP<sub>3</sub>-induced release is strongly stimulated by GTP might be highly significant in this respect. GTP-binding proteins are fast coming to occupy a central position in coupling membrane events and their classic role in coupling occupied receptors to cyclase activation now finds parallels in the activation of phospholipase C and even the opening of channels<sup>7,8</sup>, so there is ample precedent for a similar role in effecting Ca release from the endoplasmic reticulum. According to this view, the preparation of Gill *et al.* may contain an endogenous ligand that can, in the presence of GTP, open Ca channels in the endoplasmic reticulum. The requirement for both GTP and an unknown ligand would both circumvent the tricky question of why physiological levels of GTP do not keep the channels open permanently and focus attention on the nature of the hypothetical intracellular ligand, the binding of which is coupled by GTP to channel opening. If such a ligand exists, it could still be IP<sub>3</sub> or a close relative. The onus seems to be on Gill and his colleagues to prove it does not exist. □

1. Gill, D.L., Ueda, T., Chueh, S.-H. & Noel, M.W. *Nature* **320**, 461 (1986).
2. Schneider, M.F. & Chandler, W.K. *Nature* **242**, 244 (1973).
3. Streb, H., Irvine, R.F., Berridge, M.J. & Schulz, I. *Nature* **306**, 67 (1983).
4. Somlyo, A.P. *Nature News and Views* **316**, 298 (1985).
5. Smith, J.S., Coronado, K. & Meissner, G. *Nature* **316**, 446 (1985).
6. Dawson, A.P. *FEBS Lett.* **185**, 147 (1985).
7. Pfaffinger, P.J., Martin, J.M., Hunter, D.D., Nathenson, N.M. & Hille, B. *Nature* **317**, 536 (1985).
8. Holz, G.G., Rane, S.G. & Dunlap, K. *Nature* **319**, 670 (1986).

*P.F. Baker is Halliburton Professor of Physiology, King's College London, Strand, London WC2R 2LS, UK.*

## Earth sciences

# Growing stromatolites

from Peter J. Smith

CONTRARY to popular belief, terrestrial life did not begin at the start of the Cambrian, about 600 million years (Myr) ago, or even during the few hundred million years immediately preceding it. The Precambrian–Cambrian boundary simply represents the time at which abundant organisms developed hard parts capable of leaving fossil remains. Evidence for what meagre life there was during most of the Precambrian exists not as skeletons and shells but largely as stromatolites, sedimentary structures produced by the activity of blue-green algae. A new discovery by Gomes (*Trans. geol. Soc. S. Afr.* **88**, 1; 1985) reminds us that stromatolites differ from many organisms in the fossil record in that they are still being produced in limited numbers today, giving some insight into the Precambrian conditions under which they developed.

It is highly probable that the most primitive terrestrial organisms originated as long ago as the Hadean, the interval between the creation of the Earth and the formation of the oldest known rocks (about 4,600–3,800 Myr ago): there is certainly evidence for very ancient life in the form of microscopic filaments and cells of bacteria and blue-green algae in South African chert deposits at least 3,200 Myr old. Stromatolites are more important than these insofar as, having hard (albeit inorganic) parts, they have greater survival potential and are thus more common. Walter (*Stromatolites* Elsevier, Amsterdam; 1976) defined them formally as "organo-sedimentary structures produced by sediment trapping, binding and/or precipitation as a result of the growth and metabolic activity of micro-organisms". In other words, they are not fossils at all in the conventional sense in that they are not primary organic remains, although without organisms they would not have been able to form. They are traces of past life much as burrows and tracks are, although more substantial than either.

The organisms involved in the generation of stromatolites are usually blue-green algae which, being filamentous, attract and bind surrounding particles of carbonate into an algal mat. The algae then extend their filaments throughout the newly accreted carbonate layer, attract more particles, and thus expand into thinly laminated structures which can be of considerable overall size. (The largest known forms are mounds hundreds of metres across and tens of metres high.) The algal layers themselves are seldom preserved, of course; but the carbon-

ate accretions often survive in various distinctive forms, such as tabular, domed, branch-like and columnar.

Stromatolites were produced during the Archaean (earlier than 2,500 Myr ago), reached their peak of abundance and diversity during the Proterozoic (2,500–600 Myr), and thereafter declined, although they are sometimes encountered in the Phanerozoic. Indeed, they are still being generated today in a few suitable marine and freshwater environments; modern examples are not so common that new discoveries are of merely routine interest. Despite a resurgence of interest in stromatolites during the past 20 years, the influences on their formation are still unclear, a point worth remembering in view of the many problems to which stromatolite data have been offered as solutions. Claims for the use of such data have been made in almost every branch of the earth sciences and even in astronomy, but as Hofmann (*Earth-Sci. Rev.* **9**, 339; 1973) has pointed out, not all the conclusions rest on sufficiently strong evidence to warrant their acceptance.

The new discovery by Gomes of two types of stromatolite currently growing in South Africa is thus of considerable interest, not least because the study reveals in detail the conditions under which growth is taking place. The site in question is a collapse sinkhole, Wondergat, in dolomite sediments in the western Transvaal. The hole has a cross-sectional area of about 2,000 m<sup>2</sup> and is about 50 m deep at the centre, although two long caves running off from the bottom edge extend the overall depth to about 70 m. More crucially, running off from the side wall at a depth of about 20 m is a smaller cave that has been dissolved into the boundary between the dolomites of the upper 20 m and the dolomitic limestone (with chert bands) underlying them.

The sinkhole contains fresh, clear water at a depth of about 10 m and a temperature of  $21 \pm 4^\circ\text{C}$ . The pH value of the upper 15 m of water (the depths at which stromatolites grow) is between 7.38 and 7.76, the Ca<sup>2+</sup> concentrations vary from 53 to 68 p.p.m. (parts per million) and Mg<sup>2+</sup> concentrations range from 2.7 to 3.4 p.p.m. Water movement is slight, and natural visibility is high at distances of 10–15 km.

It is not possible to tell which of these chemical characteristics are necessary for stromatolite growth. For example, if all other circumstance were to remain unchanged, would stromatolites grow if the pH of the water were, say, 7.2 or 7.9? Or to put the question in a slightly different

way, is the greatest depth of stromatolite growth governed solely by the ability of sunlight to penetrate and hence to allow the photosynthesis necessary for the production of the algae, or is it also defined or limited by one or more of the chemical properties of the water?

As for the stromatolites themselves, tabular 'crinkled' forms grow abundantly on the dolomite side walls of the sinkhole in the upper 15 m of water. They are 15–20 mm thick; light-brown to greenish in colour; soft and spongy; and, apart from the living algae, consist mainly of CaCO<sub>3</sub>. Columnar stromatolites grow on the roof, walls and floor of the first 20 m of the smaller cave and in crevices in the wall of the main sinkhole. These vary in thickness from a few millimetres to a few centimetres; are the same colour as the tabular forms; and similarly consist mainly of CaCO<sub>3</sub>, although they are hard, in contrast to the tabular stromatolites. The form of stromatolite appears to be governed by the range of genera involved, which is in turn influenced by the degree of sunlight available. Tabular forms grow where the light is brightest and columnar forms where it is relatively dim.

One curiosity of the Wondergat stromatolites is that they seem to need permanent submersion for survival and growth. If the water level falls, the exposed stromatolites rapidly desiccate. In this respect they differ from 'typical' stromatolites, which are thought to form with episodic immersions to allow the alternating layers of algae-rich and carbonate-rich material to be built up. There seems little doubt that most known stromatolites were generated in shallow-water zones where tides are the clearly recognizable agents for the periodic transport of sedimentary particles into the algal mats.

There have been previous claims for the discovery of deep-water stromatolites. Achauer and Johnson (*J. sedim. Petrol.* **39**, 1466; 1969), for example, concluded that stromatolites associated with a late Cretaceous reef in Texas must have been generated in deep water. In such a case, the influx of carbonate particles would not necessarily be sedimentary in nature. It is well established that photosynthesis by algal colonies can, by removing CO<sub>2</sub> from the water, increase the pH and accentuate the precipitation of CaCO<sub>3</sub>, which then intermingles with the algae.

Gomes himself makes little comment on the wider implications of his data, which is perhaps wise. Modern stromatolites are quite rare, and freshwater occurrences make up only a very small fraction of the total, calling into question whether the Wondergat find is in fact typical of stromatolites. □

**Molecular biology**

# Transposon tricks revealed

from Andy Flavell

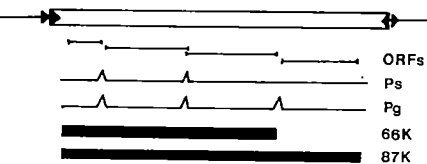
THE mobility of DNA sequences called transposons that can move around within the chromosome of a cell and its progeny has many genetic consequences. One particularly interesting transposon is the P element of the fruitfly *Drosophila melanogaster*, which is transposed (inserted at a new site on the chromosome) at a very high frequency. P elements are especially fascinating because they only transpose in a particular genetic environment; that is to say they are mobilized only when the transposon is placed in an egg that has no P elements already present. Mobilization occurs only in the germ line of the developing embryo (somatic tissue is unaffected). Results reported in two recent papers<sup>1,2</sup> expose the way in which the P element achieves this.

Like all autonomously mobile elements, the P element encodes a transposase enzyme which mediates its transposition. Studies by Rubin's group have shown that P elements contain four open translational reading frames, each of which is necessary for transposase function<sup>3</sup>. It therefore seemed very likely that the entire protein-coding portion of the P element specified a single transposase enzyme. To determine whether the restriction of P transposition to germ tissues is caused by a transcriptional block, Laski, Rio and Rubin<sup>1</sup> have now replaced the P-element promoter with a heat shock protein (hsp 70) promoter known to be active in many tissues. Following the introduction of this construct into the *Drosophila* germ line, massive amounts of P-element RNA are synthesized in somatic tissues of flies descended from transformed parents, but no somatic transposition is observed. Furthermore, a study of natural P-element transcription revealed that the P promoter functions perfectly well in somatic tissues. The authors therefore reasoned that P transposition must be repressed at a post-transcriptional stage.

To resolve this problem the authors embarked on a detailed study of P transcription in somatic tissues (it is technically almost impossible to obtain sufficient quantities of germ cells from *Drosophila* embryos for transcript analysis). They discovered that the first three long open reading frames of the element<sup>1</sup> were spliced to each other as predicted but that no detectable splice existed between the third and fourth open reading frames (see figure). Therefore, a polypeptide synthesized from the RNA would be terminated by a stop codon before reaching the final reading frame, generating a protein of relative molecular mass 66,000 (66K). But

work from the same laboratory<sup>3</sup> had already shown this last reading frame to be essential. Laski, Rio and Rubin<sup>1</sup> therefore hypothesize that the block to P transposition lies in RNA splicing — in somatic tissue only a non-functional downstream truncated protein is synthesized; perhaps in germ tissue the last splice is correctly made to generate active transposase.

To test this hypothesis the authors removed the offending intron at the DNA level by oligonucleotide site-directed mutagenesis. The mutated P element (hsp-PΔ2-3) was then introduced into the *Drosophila* germ line and shown to be functional in both germ and somatic tissues, causing somatic mosaics.



The P element has four long open reading frames (ORFs). The somatic splicing pattern of the P-element RNA (Ps) generates a 66K polypeptide. The putative germ-line splicing of the P element (Pg) generates an 87K protein. The eight base duplications of host DNA (►) flanking the element are marked.

The successful release of P transposase from the shackles imposed on its expression gave Rio, Laski and Rubin<sup>2</sup> the opportunity to study this enzyme. Introduction of hsp-PΔ2-3 into cultured *Drosophila* cells results in the inducible synthesis of large amounts of an 87K protein. The nature of this protein was confirmed immunologically using antisera raised against P open reading frame polypeptides, and enzymatically by an elegant transposition assay using excision of a P element from the *Escherichia coli* β-galactosidase gene on a rescueable shuttle vector. The authors, with commendable modesty, 'tentatively' refer to this polypeptide as the transposase. In line with their earlier interpretation, the element containing a normal complement of introns can only direct the synthesis of a 66K protein that lacks transposase activity.

The possibilities for further study on P transposase are now readily evident. Bulk preparation of active transposase, either from *Drosophila* or bacterial cells, will allow a thorough biochemical study of the enzyme and the *in vitro* dissection of the transposition mechanism. To whet our appetites, Rio *et al.*<sup>2</sup> used the excision products of the rescued shuttle vectors to demonstrate the effect of alterations to the flanking eight-base duplications of the P element on the fidelity of excision. They

discovered that this perturbation yielded only imprecise excisions as opposed to a 25 per cent level of precise excisions of the normal element. The reason for such high imprecise excision of even the normal P element is unknown, but similar results are found in other transposons in plants<sup>4</sup>.

Alternative splicing pathways are well known nowadays, but an all-or-none splicing event is much rarer. What is the function of the 66K protein? Rio *et al.* point out that a tentative DNA-binding domain of this protein is present in both (66K and 87K) proteins and suggest that the 66K protein may inhibit P element transposition by competing with transposase for the termini of the element or by direct protein-protein interaction. The fact that P elements are apparently expressed in somatic tissues as a non-functional polypeptide seems wasteful. Could it have a function in the germ cells? Co-injection of a mutated P element that could produce only the 66K protein, together with a helper-P element, produces germ-line transformants<sup>5</sup>, suggesting that the 66K protein does not completely inhibit transposase function in germ cells. Happily, models for the functions of these proteins can be tested now that they can each be produced in large amounts.

There are several lines of circumstantial evidence to suggest that P elements are not native to *D. melanogaster* but have invaded the organism in the past few hundred years. Many *D. melanogaster* fly stocks lack functional P elements and they are missing from closely related sibling species. But they are present in the distantly related *D. paulistorum*<sup>6</sup>, suggesting a horizontal transmission event. The rampant transposition of this element when introduced into *D. melanogaster* flies lacking the P element suggests that P elements are less fully adapted to their host than the more placid retrotransposons such as *copia* and *gypsy*. Perhaps P elements have not yet developed a germ-line specific promoter but have been able to take advantage of a pre-existing splicing control mechanism to protect the somatic tissues of their host from their ravages.

One final exciting possibility mentioned by the authors is that hsp-PΔ2-3 may transpose in cells from organisms other than *Drosophila*, perhaps even in the germ line and soma of vertebrates. If this turns out to be true then all the advantages given to *Drosophila* genetics by the P element will be available to vertebrate molecular biologists.

1. Laski, F.A., Rio, D.C. & Rubin, G.M. *Cell* 44, 7 (1986).
2. Rio, D.C., Laski, F.A. & Rubin, G.M. *Cell* 44, 21 (1986).
3. Karess, R.E. & Rubin, G.M. *Cell* 38, 135 (1984).
4. O'Hare, K. & Rubin, G.M. *Cell* 34, 25 (1983).
5. Saedler, H. & Nevers, P. *EMBO J.* 4, 585 (1985).
6. Daniels, S.B. *et al.* *Proc natn Acad Sci U.S.A.* 81, 6794 (1984).

Andy Flavell is a lecturer in the Department of Biochemistry, The University of Dundee, Dundee DD1 4HN, UK.

**Immunology**

# Contrasuppressor cells and oral tolerance

from R.B. Taylor

AMONG the subtle regulatory tasks required of the immune system is adjustment of the modality and magnitude of an immune response to suit the anatomical locality in which it is to take place. A good example of this ability is oral tolerance — immune responsiveness to antigens at mucosal surfaces with a much reduced response to systemic challenge with the same antigens<sup>1</sup>. The value of this mechanism is probably to prevent systemic allergic responses to food antigens without compromising local defence of the mucosae. The demands of such subtle functions should have prepared us for the further complexities in immunoregulatory mechanisms that continue to be revealed. One of these, which has now come to stay, is the contrasuppressor circuit<sup>2</sup>. I. Suzuki and co-workers, on page 451 of this issue, now report data implicating contrasuppression in the maintenance of oral tolerance<sup>3</sup>.

As so far defined in mice, this circuit comprises T lymphocytes called contrasuppressor cells whose end function is to neutralize the inhibitory action of T-suppressor cells on the T-helper cell population. One of the cells necessary for contrasuppression has a distinctive surface phenotype and the property of adherence to *Vicia villosa* lectin. These cells have been found in various lymphoid organs including Peyer's patches and seem to play a part in selection of the modality (contact sensitivity or antibody production) of the response to the trinitrophenyl hapten<sup>2,4</sup>. In man there is evidence of contrasuppression in cultures of peripheral blood lymphocytes responding to an antigen from the oral bacterium *Streptococcus mutans*. The cells responsible for this activity were shown to bind antigen and *V. villosa* lectin and carry the surface markers T8, T3 and Ia (see ref. 5 for review).

The work now reported by Suzuki *et al.*<sup>3</sup> builds on the earlier finding in the same laboratory that oral tolerance could be induced in C3H/HeN mice but not in the congenic strain C3H/HeJ which differs at a locus determining the ability to respond to bacterial lipopolysaccharide. In the present work, mice of both strains are subjected to prolonged oral immunization with sheep red blood cells (SRBC). Oral tolerance develops in the C3H/HeN mice but can be broken by transfer of T-cell fractions enriched for contrasuppressor cells taken from the spleens of the C3H/HeJ mice — to result in the development of anti-SRBC antibody-forming cells of all

the major isotypes in the recipient spleen. Very small numbers of contrasuppressor cells ( $5 \times 10^4$ ) are effective. Oral tolerance to SRBC is also shown by C3H/HeN spleen cells *in vitro*, and is similarly abrogated by the inclusion of contrasuppressor cells in the cultures. On the basis of various methods to enrich or deplete the active cells, it was concluded the contrasuppressor cells resemble those originally described. The fact that oral tolerance to SRBC is lost in the presence of contrasuppressor cells indicates clearly that T-helper cells are present but controlled by suppressor cells. If this suppression is neutralized by the contrasuppressor cells then T-helper cells can become active.

The phenomenon of local immune responses in the gut coexisting with oral tolerance has been described as "an island of responsiveness in a sea of suppression".

The challenge now is to find out what elements of the system are sufficiently localized to determine the geography of this island. Restricted migration of contrasuppressor cells from the gut seems unlikely as these cells are found in the spleens of the C3H/HeJ mice after oral immunization. Instead one may need to look at the populations of cells which, once primed, return to the mucosae to function in local immunity. It may be that there is a defect in the return of T-suppressor cells relative to the other types. The growing interest in mucosal immunization is to be welcomed because the mucosal route is after all the commonest, whereas intraperitoneal immunization rarely occurs outside the laboratory — except perhaps in the bull-rings of Seville<sup>6</sup>. □

1. Challacombe, S.J. & Tomasi, T.B. *J. exp. Med.* **152**, 1459 (1980).
2. Green, D.R., Flood, P.M. & Gershon, R.K. *A. Rev. Immun.* **1**, 439 (1983).
3. Suzuki, I., Kiyono, H., Kitamura, K., Green, D.R. & McGhee, J.R. *Nature* **320**, 451 (1986).
4. Ptak, W., Bereta, M., Marcinkiewicz, J., Gershon, R.K. & Green, D.R. *J. Immun.* **133**, 623 (1984).
5. Lehrer, T. *Immun. Today* (in the press).
6. Coutinho, A., Formi, L., Holmberg, D., Ivars, F. & Vaz, N. *Immun. Rev.* **79**, 151 (1984).

R.B. Taylor is in the Department of Pathology, University of Bristol, Bristol BS8 1TD, UK.

**Astronomy**

# A hidden quasar revealed

from C. Martin Gaskell

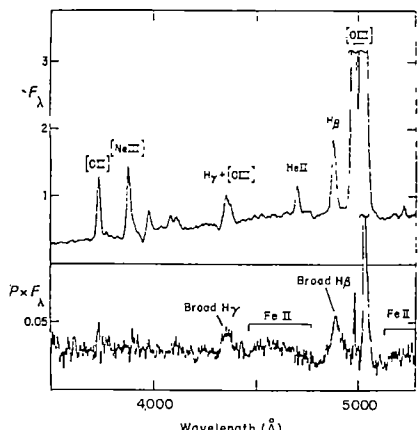
IT has long been realized that the quasar phenomenon encompasses many orders of magnitude in luminosity, ranging from the brightest quasars, which far outshine the galaxies they are in, down to the mildly active nuclei (often called mini-quasars) of relatively normal galaxies like our own, that have luminosities comparable with the brightest stars. Despite the enormous range in energy output (a factor of at least  $10^{10}$ ) there are many features that all these active nuclei possess in common; the most important is a spectrum with (roughly) constant energy per decade of frequency in the entire range from millimetre wavelength radio waves to X-ray (and probably γ-ray) energies. Does this mean that all such 'active' galactic nuclei are manifestations of the same basic quasar mechanism? The answer in recent years has been an increasingly firm yes. And R.R.J. Antonucci and J.S. Miller<sup>1</sup> have now made observations greatly strengthening our belief in the unity of quasar activity.

The quasar family is divided into several genera and species on the basis of the strength and nature of the radio emission and the optical emission line spectrum. One of the more important species is the Seyfert 2 galaxy. A Seyfert galaxy has emission lines whose Doppler broadening

exceeds the velocities of normal interstellar gas and stars in the rest of the galaxy. Khachikian and Weedman<sup>2</sup> sub-divide Seyfert galaxies into two classes: Seyfert 1, where ionized gas moves very rapidly (velocities of a few per cent of the speed of light); and Seyfert 2, where the ionized gas moves only slightly faster than the stars in a typical galactic nucleus (an order of magnitude slower than in Seyfert 1 galaxies). Seyfert 1 galaxies are clearly closely related to the bright quasars. The dense rapidly moving gas producing the strong broad emission lines (the so-called broad-line region) is an intimate part of the quasar phenomenon. It is found at radii as small as a few light days from the energy source in some Seyfert 1 galaxies<sup>3</sup> (only a few times bigger than the Solar System) and is seen in all bright quasars. Why is it not seen in Seyfert 2 galaxies? There are two probable reasons: either the dense gas is somehow hidden; or it is absent, in which case Seyfert 2 galaxies could be fundamentally different from bright quasars.

In the past few years it has been realized that Seyfert 1 galaxies can masquerade as Seyfert 2 galaxies either by temporarily turning off their photoionizing continuum (see, for example, ref. 4) or, in some cases by having a lot of dust obscuring their innermost regions<sup>5,6</sup> (dust is certainly pre-

## NEWS AND VIEWS



Spectra of NGC1068 showing total flux (top) and polarized flux (bottom). The hidden broad lines are only revealed in the polarized light. (Adapted from ref. 1.)

sent in most Seyfert 1 galaxies). But the difference between Seyfert 1 and Seyfert 2 galaxies is more fundamental than the latter simply being turned-off or hidden Seyfert 1 galaxies as the latter have more powerful and extended radio emission<sup>7</sup>.

New optical spectropolarimetric observations of NGC1068 by Antonucci and Miller<sup>1</sup> have gone a long way towards answering the question of what is a Seyfert 2? NGC1068 is the brightest and nearest Seyfert 2 galaxy showing little variability and with no obvious heavy dust obscuration in the nuclei (see figure). It is thus a 'pure' Seyfert 2. Antonucci and Miller have obtained high-quality spectropolarimetric data with the Lick Observatory 120-inch telescope. Looking at only the polarized light they made a remarkable discovery — the light shows the unmistakable spectrum of a Seyfert 1, or quasar, with its high-density rapidly moving gas. This prototypical Seyfert 2 therefore contains a hidden quasar, which is revealed

because, although the light from the innermost region cannot reach us directly, it can scatter off free electrons around the active region. This scattered light, although feeble, is highly polarized.

The photoionizing continuum light that can be observed must be reaching us in the same indirect way, as it shares the same polarization as the hidden broad lines. Antonucci and Miller conclude that the central quasar is probably hidden by a large, thick, doughnut-shaped disk whose hole corresponds to the axis of ejection of the radio-emitting plasma (it has long been known that the optical polarization angle of quasars is related to the orientation of the radio structure<sup>8,9</sup>). Their observations are the best evidence so far that such disks exist.

The Lick Observatory discovery is therefore important for at least two reasons: it tells us a lot about the architecture of Seyfert 2 nuclei; and it also strengthens the case for the basic unity of all species of the quasar family and emphasizes the importance of broad-line regions. What is happening at the centre of NGC1068, as revealed in the ghostly polarized optical spectrum, looks exactly the same as what is going on in any bright quasar. □

1. Antonucci, R.R.J. & Miller, J.S. *Astrophys. J.* **297**, 621 (1985).
2. Khachikian, E. Ye. & Weedman, D.W. *Astrofizika* **7**, 389 (1971).
3. Gaskell, C.M. & Sparke, L.S. *Astrophys. J.* (in the press).
4. Lyutyi, V.M. Oknyanskii, V.L. & Chuvaev, K.K. *Soviet Astron. Lett.* **10**, 335 (1984).
5. Lawrence, A. & Elvis, M. *Astrophys. J.* **256**, 75 (1982).
6. DeZotti, G. & Gaskell, C.M. *Astron. Astrophys.* **147**, 1 (1985).
7. Ulvestad, J.S. & Wilson, A.S. *Astrophys. J.* **285**, 439 (1984).
8. Stockman, H.S., Angel, J.R.P. & Miley, G.K. *Astrophys. J.* **227**, L55 (1979).
9. Antonucci, R.R.J. *Nature* **303**, 158 (1983).

C. Martin Gaskell is in the Department of Astronomy, Ohio State University, Columbus, Ohio 43210, USA

wishing to view it as a quasi-continuous process. The observations receiving most emphasis were those that bore on this question, those relating to the physical conditions of metamorphism and those suggesting that extensional tectonics may be important in the preservation of metamorphic assemblages generated in compressional orogenic belts.

The inference, from the compositions of minerals formed under disequilibrium conditions in transient thermal regimes, of the heat sources for metamorphism is a long-standing problem in petrology, and one that seems to become less tractable as more (and more sophisticated) data become available. Much of the complexity in the metamorphic record results from synto post-tectonic movements (for example, faults, shear zones and doming) on a scale that is much smaller than that of the crust as a whole, and disproportionate attention is paid to such metamorphically complicated regions (B. Hart and T. Dempster, Edinburgh University; A. Thompson and J. Ridley, Federal Institute of Technology, Zürich). These zones of disruption often bound larger regions that record relatively simple metamorphic histories which, although they may be less challenging to the thoroughbred petrologist, are more likely to elucidate the thermal conditions of metamorphism.

The continental lithosphere deforms over regions of hundreds of thousands of kilometres in width, but seismic and geodetic observations show that, within the brittle upper crust, this deformation is broken up on a scale of a few to a few tens of kilometres (J. Jackson, Cambridge University; R. Walcott, Victoria University, Wellington) and metamorphic observations show a similar scale of fragmentation (B. Harte and T. Dempster; A. Thompson and J. Ridley; B.W.D. Yardley *et al.*, Leeds University). Some participants, including M. Parmentier (Brown University) and myself, held that this scale is sufficiently small, compared with the total size of deforming belts, that some understanding of the dynamics could be obtained by treating the continents as continuous media, but much of the discussion (focused by E. Artyushkov, USSR Academy of Sciences, Moscow) found this an oversimplification.

The tectonic history of New Zealand seems to exemplify all the complexity that is claimed for the deforming continents: since the Eocene, relative motion between the Pacific and Australian plates near New Zealand has been accommodated by a combination of compressional, extensional and transcurrent motion over a belt several hundreds of kilometres wide. Yet geodetic observations of the strain during this century indicate that it is continuous when viewed on a scale of about 50 kilometres, and this strain, if it had operated over the past 15 million

## Plate tectonics

## Deformation of continents

from Philip England

ALTHOUGH many geologists now claim at least a broad understanding of the rules governing the global plate-tectonic system, few would be so bold about the dynamics of the large mountain belts that mark the convergence of continental portions of the plates. In contrast to the oceans — where the acquisition of major new sets of data led rapidly to the theory of plate tectonics — the problem in interpreting the geological record on land appears to be an excess of observations, and a lack of a unifying framework in which to view them. In part, this problem arises because the success of plate-tectonic theory in the oceans tempts one to apply the same rules to the continents, but although plate motion is responsible for continental

collision, the resulting deformation does not appear to be explicable by the relative motion of a few rigid plates. Characterizing the deformation in a more useful fashion is difficult because of the number of different perspectives with which mountain belts are viewed.

A recent meeting\* brought together petrologists, structural geologists and geophysicists to discuss theory and observation of orogenic (mountain-forming) belts. The most contentious issue was the configuration of deformation and metamorphism, with most advocating the view that continental tectonics is the relative movement of many rigid blocks, but a few

\*Tectonic Settings of Metamorphism Royal Society Discussion Meeting, 29–30 January 1986.

years, would be consistent with the palaeomagnetically determined rotations of post-middle-Miocene rocks in the region (R. Walcott, Victoria University).

A superficial examination of the thermal conditions beneath the North Island of New Zealand suggests that it is a classic paired metamorphic belt, but in a tectonic setting not usually attributed to these belts: high temperature-low pressure (high  $T$ -low  $P$ ) metamorphism is occurring beneath the central volcanic region, which is extending and subsiding, while low  $T$ -high  $P$  metamorphism is occurring in the Hikurangi Margin to the east, which is uplifting and extending. Thus, a future episode of compression is required before erosion can expose the high  $T$ -low  $P$  metamorphism, whereas the exhumation of low  $T$ -high  $P$  rocks, which is usually thought to require the cessation of subduction, requires no more than the

continuation of the present underplating and extension of the Hikurangi Margin.

A similar process is believed to have operated in the preservation of high-pressure rocks in the Franciscan Formation, Betic Cordillera and Western Alps (J. Platt, Oxford University); large normal faults parallel to the mountain range are also observed in the High Himalaya (J.-P. Burg, Melbourne University). But nobody was prepared to propose such an extensional mechanism for the preservation of a 50-square kilometre area of coesite-bearing rocks that appear to have been metamorphosed at about 30 kilobars in the early stages of the Alpine orogeny (C. Chopin, Ecole Normale Supérieure, Paris).  $\square$

*Philip England is in the Department of Geological Sciences at Harvard University, Hoffmann Laboratory, 20 Oxford Street, Cambridge, Massachusetts 02138, USA.*

## Palaeontology

# How did eurypterids swim?

from D.E.G. Briggs

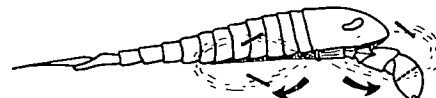
EURYPTERIDS, a group of extinct Palaeozoic arthropods, existed for more than 200 million years from the early Ordovician to the Permian, and were the largest arthropods ever to have evolved—at least half of the eurypterid families included species containing individuals of more than 80 cm long. They became extinct in the most severe mass extinction in the late Permian. A recent report suggests that these large swimming arthropods may have been capable of hovering (Plotnick, R. *Trans. R. Soc. Edinb.* 76, 325; 1985).

Eurypterids had a long streamlined body divided into an anterior prosoma (cephalothorax) and posterior opisthosoma (abdomen). Trace fossil evidence and functional analysis show that eurypterids used the posterior three pairs of prosomal appendages to walk in a hexapodous gait. The last of these, the sixth prosomal appendage, was modified to some extent in all eurypterids, the distal podomeres being commonly flattened and expanded to form a paddle.

Early interpretations of swimming in eurypterids were based largely on comparisons with the horse-shoe crab (*Limulus*), a member of the only major living group of aquatic chelicerates, and envisaged eurypterids as swimming ventral side up, using mainly the opisthosomal limbs (equivalent to the gills of *Limulus*). More detailed studies of the few well-preserved examples (Waterston, C.D. *Fossils and Strata* 4, 241; 1975) showed that eurypterid gills were more similar to the lung sacs of scorpions, consisting of an area or tract on the ventral body wall, rather than appendages modified as book-gills. These

tracts were protected by stiff cuticle and could not have been used for propulsion.

Recent research demonstrates that the paddle provided the primary means of swimming. Paul Selden redescribed the Silurian eurypterid *Baltoeurypterus tetragonophthalmus* (*Trans. R. Soc. Edinb.* 72, 9; 1981) based on the spectacular fossil specimens from the Silurian of Gotland



Hovering in *Baltoeurypterus*. The paddle is moved in a shallow horizontal figure-of-eight, the angle of attack (dashed on the paddle, solid elsewhere) altering to maintain lift. Other prosomal limbs are omitted. This specimen is about 20 cm long.

and Estonia, in the Baltic. The eurypterid cuticle can be isolated from limestone by dissolution in acid and provides information comparable to the exoskeleton of a living arthropod. Most importantly, the mechanics of the joints between the limb podomeres can be reconstructed.

Appendicular swimming may be either predominantly drag-based (the appendages rowing, as oars) or lift-based (the appendages 'flying', as hydrofoils). Selden's analysis of the mechanics of the paddle in *Baltoeurypterus* indicates that the large flat seventh and eighth podomeres could have been alternately expanded to create maximum drag in a power stroke, and then rotated about the paddle and folded to present much less resistance in a recovery stroke. He suggested that the paddles functioned as oars, moving in phase to reduce the likelihood of yawing;

pitching and rolling would have been prevented by the flattened body, tergal projections and outstretched limbs.

But *Baltoeurypterus* was about 20 cm long, a size that exceeds the limit at which drag-based swimming becomes inefficient (at Reynolds numbers of about  $10^2$ ). The limited degree of lift produced by rowing would also be an important consideration if eurypterids were negatively buoyant, as seems probable. Using Selden's detailed analysis of the morphology of *Baltoeurypterus*, Plotnick's new work extends the model of swimming in eurypterids to incorporate a greater element of lift. Plotnick's conclusions are based largely on a study of swimming in portunid crabs, which have a paddle (the fifth pereiopod) strikingly similar to that in eurypterids. Portunids are very manoeuvrable, using a lift-based swimming mechanism that even enables them to hover.

Eurypterids were unable to swim by 'subaqueous flying' (in the manner of penguins) because the nature of the joints prevented up-and-down movement of the paddle at right angles to the direction of progress. But they could move the paddle in a flattened figure-of-eight which, while concentrating the thrust in the backstroke as in rowing, produced lift and a modest degree of thrust in the forestroke. The paddle tapered to a point distally, like a hydrofoil. (It should be noted, however, that the morphology of the paddle is likely to be a compromise between the different requirements of swimming and walking.) Lift-based swimming is more efficient for a large animal than rowing, as a propulsive thrust is produced on both the forestroke and the backstroke and a constant lift is created to counteract the negative buoyancy of the animal. In the eurypterids, the dorsal position of the articulation between podomeres 4 and 5 exaggerated the downward component of the paddle's movement, thus favouring lift.

Not all eurypterids conformed to the morphology of *Baltoeurypterus*. The remarkable late Silurian pterygotids, for example, were more elongate with very slender limbs (including the paddles) and may have been more than 2 metres long. This large size indicates that a lift-based mode of swimming was likely (Selden, P.A. *Spec. Pap. Palaeont.* 32, 39; 1984).

Only a few eurypterids have been subjected to the kind of detailed analyses pioneered by Selden and Plotnick. Although material of the quality of *B. tetragonophthalmus* from the Baltic is rare, research on the biomechanics and hydrodynamics of other well-preserved eurypterids will yield further insights into the functional strategies adopted by these remarkable arthropods.  $\square$

*D.E.G. Briggs is in the Department of Geology, University of Bristol, Wills Memorial Building, Queen's Road, Bristol BS8 1RJ, UK.*

## Outlook brighter on weather forecasts

SIR—Our recent paper "Fractal characterization of inhomogeneous geophysics measuring networks" addressed the fundamental geophysical problem of sparse measuring networks, and pointed to new ways of overcoming longstanding difficulties<sup>1</sup>. Although pleased to have stirred interest in the weather forecasting community, we were therefore somewhat surprised by the pessimistic ("bleak") interpretation given to our findings in Hollingsworth's *News and Views* article<sup>2</sup>. Since this interpretation could be due to a misunderstanding, we would like to clarify our position.

By quantifying the sparseness of the meteorological observing network, we showed that no matter how large, phenomena sufficiently intense and sparse (with fractal dimension  $D < 0.25$ ) would slip through the network undetected. The errors due to this limited dimensional resolution are more subtle than Hollingsworth seems to indicate. We implied neither that the network misses storms, nor the most energetic areas but rather, the most intense regions. Indeed, fundamental characteristics of the various levels of energy density (or more precisely, the flux of energy to smaller scales), are their multiple fractal dimensions which decrease as the intensity level increases. Since any set with  $D < 1$  is a totally disconnected set of points, the regions missed, are the most active cores of storms. These low dimensional (sparse, core) regions play a crucial role in the future evolution of the atmosphere.

Hollingsworth seems to minimize the impact of this lack of dimensional resolution, first by citing the utility of existing forecasts 6–7 days ahead, second, by pointing to the increasing role of satellite data. Let us examine these points one by one.

Hollingsworth admits that even in the vague terms of "economical usefulness" forecasts are limited to periods of one week or less. Even without a precise discussion of predictability and its limits, is it unreasonable to suppose that at least part of our current difficulties are related to our inability to detect sparse but violent events?

Hollingsworth is obviously correct in pointing out the importance of satellite data. Indeed, since remotely sensed data generally have very high dimensional resolutions, our findings add a new argument in their favour. Unfortunately, the satellites themselves, are calibrated by sparse *in situ* networks, and current calibration methods do not recognize the problem of dimensional resolution. Furthermore, the existing four-dimensional data assimilation techniques that are used

to mix *in situ* and satellite data take no quantitative account of the various dimensions involved.

Perhaps, if we abandon the routine ways of dealing with the problem of sparse networks and phenomena, the future can be faced with optimism. New and mushrooming interest in techniques of multi (fractal)-dimensional analysis and simulation may ultimately help clarify basic problems in predictability. In the short term, we may expect rapid development of statistical techniques to provide important corrections to data lacking in dimensional resolution. Improved forecasts over a wide range of timescales could be possible.

SHAUN LOVEJOY

DANIEL SCHERTZER  
PHILIP LADOUX

*Physics Department,  
McGill University,  
3600 University Street,  
Montreal, Québec, Canada H3A 2TB*

*Météorologie Nationale,  
2 Ave Rapp,  
Paris 75007, France*

1. Lovejoy, S., Schertzer, D. & Ladoux, P. *Nature* **319**, 43–44 (1986).

2. Hollingsworth, A. *Nature* **319**, 11–12 (1986).

## Are arguments against archaeabacteria valid?

SIR—Until now we have commented only in passing on Lake's suggestions<sup>1,2</sup> regarding archaeabacterial taxonomy and phylogeny, because their supporting evidence is weak. However, recent correspondence in *Nature*<sup>3–5</sup> and attention elsewhere<sup>6</sup> requires a stronger response.

The upper panel of Fig. 1 is a phylogenetic tree derived by a distance matrix-type analysis of the small subunit rRNAs. It shows the three primary kingdoms as distinct phylogenetic units<sup>7</sup>. (The same branching order results from parsimony analysis<sup>7</sup>.) In contrast, Lake's proposals (lower panel) distribute the various archaeabacteria among three separate 'kingdoms': the 'eocytes' (sulphur-dependent archaeabacteria, such as *Sulfolobus* and *Thermoproteus*), 'photocytes' (extreme halophiles and eubacteria) and methanogens<sup>1,3</sup>.

Two issues are involved here, one scientific (the precise relationships of the other kingdoms to the archaeabacteria) and one semantic (whether Archaeabacteria is a proper taxon). The second issue distinguishes Lake's proposals from those of others, whose phylogenies assume archaeabacteria to be a valid taxon, although possibly paraphyletic<sup>7</sup>.

The factual basis for Lake's proposals is questionable. 'Eocytes' were defined as "a kingdom with a close relationship to

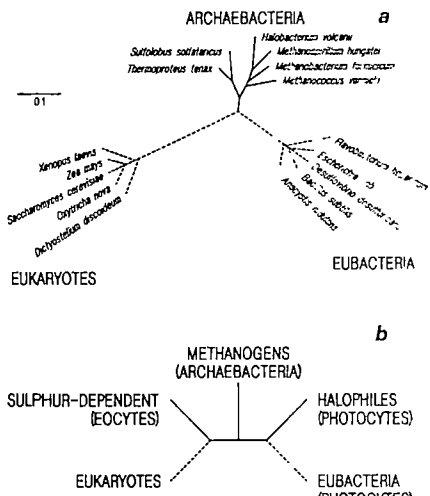


Fig. 1 The alternative views of archaeabacterial taxonomy.

eukaryotes" on the basis of the unusual shape of their 50S ribosomes, a shape ostensibly unique among archaeabacteria. However, a significant fraction of the 50S subunits in *Methanococcus vannielii* have this 'eocyte' shape<sup>8</sup>. Although what underlies these shape differences is not known, it is likely that they reflect relative protein content: subunits from both sulphur-dependent archaeabacteria and the *Methanococcales* have relatively large complements of protein compared with other archaeabacterial ribosomes<sup>9</sup>. Thus, dividing the archaeabacteria on the basis of ribosome type puts methanogens into two separate kingdoms — an untenable classification both phylogenetically and taxonomically.

'Photocytes' were defined on the basis of other perceived similarities in ribosome shape<sup>2</sup>. In this case, too, the defining characteristics are not confined to the defined group<sup>8</sup>. Ribosome shape differences, which have never been shown to be homologous traits, are obviously not reliable determinants of major phylogenetic categories.

The proposals of Lake *et al.* have far too little supporting evidence, and much of this is of little or no phylogenetic value. Their argument rests heavily on the supposed absence of certain traits, which means little when it merely reflects a temporary failure to find them. For example, absence of introns outside the sulphur-dependent archaeabacteria was taken to be significant but introns were subsequently found in the extreme halophiles<sup>7</sup>. Ill-defined similarities, such as "common photosynthetic mechanisms", invoked in grouping eubacteria with the extreme halophiles, are more probably analogies than homologies: the (eu)bacterial chlorophylls have nothing in common with (halophile) bacteriorhodopsin, either structurally or functionally, whereas bacteriorhodopsin is structurally and functionally similar to eukaryotic rhodopsin —

## SCIENTIFIC CORRESPONDENCE

hence its name. By invoking a small number of characters (especially ill-defined ones) one can construct many contradictory taxa: for example, cyanobacteria can be clustered with the extreme halophiles to the exclusion of other eubacteria on the basis of ferredoxin sequences; or, streptomycetes can be grouped with methanogens on the basis of their having coenzyme F420.

Lake's explanation of the rRNA-based tree (Fig. 1a) is that it must be an artefact of the treeing procedure (such procedures have a tendency to group rapidly evolving lines). Although such artefacts do occur, they obviously do not occur in every case involving unequal evolutionary rates. A thorough analysis indicates that the branching order in Fig. 1a does not reflect such an artefact.

Returning to the semantic issue, regardless of whether the archaeabacteria are joined to the two other kingdoms by a single lineage (Fig. 1a) or by two separate lineages (Fig. 1b), archaeabacteria is a taxon of demonstrated predictive and organizational value<sup>7</sup>. It groups together prokaryotes with many characteristic phenotypic features, including composition of membranes, cell walls, rRNAs and tRNAs<sup>10</sup>. Lake's taxa, on the other hand, spread such organisms among several kingdoms (as indicated by the solid lines in the Fig. 1), intermixed with organisms not sharing their common characteristics. Whereas the grouping 'archaeabacteria' easily rationalizes almost all of what is known about these organisms, the Lake taxa are inconsistent with much of the phenotypic evidence and all of the sequence evidence bearing on the issue.

CARL R. WOESE

*Department of Genetics and Development,  
University of Illinois,  
Urbana, Illinois 61801, USA*

NORMAN R. PACE  
GARY J. OLSEN

*Department of Biology,  
Indiana University,  
Bloomington, Indiana 47405, USA*

1. Lake, J.A., Henderson, E., Clark, M.W. & Oakes, M. *Proc. natn. Acad. Sci. U.S.A.* **81**, 3786 (1984).
2. Lake, J.A. et al. *Proc. natn. Acad. Sci. U.S.A.* **82**, 3716 (1985).
3. Lake, J.A. *Nature* **319**, 626 (1986).
4. Zillig, W. *Nature* **320**, 220 (1986).
5. Lederer, H. *Nature* **320**, 220 (1986).
6. Wilson, A.C. *Scient. Am.* **253**(4), 164 (1985).
7. Woese, C.R. & Olsen, G.J. *System. Appl. Microbiol.* (in the press).
8. Stöffler-Meilicke, M., Böhme, C., Strobel, O., Böck, A. & Stöffler, G. *Science* **231**, 1306 (1986).
9. Cammarano, P., Teichner, A. & Londeg, P. *System. Appl. Microbiol.* (in the press).
10. Woese, C.R. & Wolfe, R.S. (eds) *The Bacteria: Archaeabacteria* Vol. 8 (Academic, New York, 1985).

## Link between lamins and intermediate filaments

SIR—Recently McKeon *et al.*<sup>1</sup> reported in *Nature* an exciting result for cell biologists. Lamins, the major proteins of the nuclear envelope, show a striking sequ-

ence and structural homology with the various proteins of the large family of cytoplasmic intermediate filaments (IFs). The complementary-DNA sequence of lamins A and C predicts, however, an insert of 42 amino-acid residues in a coiled-coil domain highly conserved in length in all IF proteins (reviewed in ref. 2). Inspecting the reported lamin sequence I found that this insert starts precisely at a point of a common intron position previously found in several IF genes<sup>2</sup>. The position of most introns of IF genes seems not to be related to the structural subdomains of the proteins<sup>2</sup>. A similar situation was found also for myosin, another fibrous protein built from coiled-coils<sup>3</sup>. Thus, the position of the lamin insert is particularly interesting as it may indicate the evolutionary divergence between IF and lamin genes. This I expect to become more obvious once the entire lamin gene is known.

K. WEBER

*Max-Planck Institute for  
Biophysical Chemistry,  
D-34 Goettingen, FRG*

1. McKeon, F.D., Kirschner, M.W. & Caput, D. *Nature* **319**, 463–468 (1986).
2. Steinert, P.M., Steven, A.C. & Roop, D.R. *Cell* **42**, 411–419 (1985).
3. Karn, J., Brenner, S. & Barnett, L. *Proc. natn. Acad. Sci. U.S.A.* **80**, 4253–4257 (1983).

## The mechanics of visual acuity

SIR—Anyone who needs strongish (positive) reading glasses but does not suffer unduly from astigmatism can see that visual acuity is not just a function of eye-lens quality plus receptor spacing. All that is needed is a red-light-emitting diode behind a square aperture. Looking at this without glasses produces not a single blurred image but an array of about eight red squares, more or less sharply defined. A 'perfect' eye would presumably produce a completely regular array; mine do not, and differ individually.

It follows that the eye–cortex combination acts holographically, in that separate portions of a blurred image give rise to the impression of a sharp image. Furthermore, if instead the image of a point source is properly focused, the system can be expected to give rise to a visual acuity greater than indicated by optical considerations alone.

The compound eyes of insects are known to act in a similar manner, because individual images are too poor to account for bees' discriminatory power, for example. So it is perhaps not surprising that the larger animal eye, producing good optical images, should nevertheless have retained the image-processing power of the cortex representing an earlier stage in the evolution of the eye.

T. NASH

*Bower Chalke,  
Salisbury, Wilts SP5 5BW, UK*

## The human factor in mammoth extinction

SIR—A recent *News and Views* piece by Diamond<sup>1</sup> discusses mammoth hunting and extinction. While I agree that sophisticated hunting techniques must have been available to palaeolithic mammoth hunters, close spearing or hamstringing, as practised by modern Pygmy elephant hunters, is dependent on the possession of razor-sharp iron spearheads<sup>2</sup>; and the existence of a pharmacopoeia of poisons among Palaeolithic hunters is of course undocumented. Trunk snares or weighted hanging spears would seem to depend on the prey moving among rather heavy forest vegetation, whereas the stomach contents of mammoths attest to their inhabiting sparsely forested, open, steppe-like grasslands. Palaeolithic peoples probably trapped mammoths with fire or with footsnares and pitfalls set or dug along regularly used routes. As zoo curators know, a fall of only a metre or even a stumble may be potentially fatal to a large mammal, so a footsnare or pitfall would have been a relatively safe and effective aid to mammoth hunting.

Nevertheless, contrary to Diamond's contention, French and Spanish cave paintings do not unequivocally show these hunting techniques. Tectiform signs in Palaeolithic art are certainly sometimes interpreted as depicting traps and pitfalls, but the interpretation of these signs is subject to debate. They have also been viewed as depicting shelters or maps, or as having a more esoteric symbolic significance.

Finally, Diamond concludes that mammoth extinction is probably the direct result of the proficiency of human hunting. However, the most recent compendium of explanations<sup>3</sup> for Pleistocene megafauna extinctions appears to favour ecological or climatic causes. Certainly the Pleistocene overkill hypothesis originally elaborated by P.S. Martin has not been accepted without debate, and may have lost some potency as an explanatory hypothesis during the past twenty years, even with the introduction of the concept of a blitzkrieg overkill which might explain the paucity of archaeological evidence.

SUSAN CACHET  
*Department of Anthropology,  
Douglas College, Rutgers University,  
New Brunswick, New Jersey 08903, USA*

1. Diamond, J. *Nature* **319**, 265–266 (1986).
2. Coon, C.S. *The Hunting Peoples* (Little, Brown, Boston, 1971).
3. Martin, P.S. & Klein, R.G. *Quaternary Extinctions* (University of Arizona Press, Tucson, 1984).

Scientific Correspondence is intended to provide a forum in which readers may raise points of a rather technical character which are not provoked by articles or letters previously published.

## What's wrong with nuclear power?

David Pearce

**Nuclear Politics: The History of Nuclear Power in Britain.** By Tony Hall. Pelican: 1986. Pp. 200. Pbk £3.95.

THE history of the civilian nuclear power industry in Britain is one of concealment, dubious promises, a reckless approach to technology and naive public relations. The concealment has shown in the attempts to hide the poor safety record of the industry's centrepiece, Sellafield; the dubious promise is revealed in the debatable nature of the comparative economics of nuclear electricity generation; and the recklessness was underlined nearly ten years ago by the Flowers Commission's insistence that waste disposal problems should be solved before, and not after, further expansion of nuclear capacity.

It is, however, in its public relations that the nuclear power industry has made its worst mistakes. With arrogance compounded by naivety the authorities have consistently misread public opinion, with the result that if support has not been forthcoming the public has been treated to a further dose of "education". Such an educational programme demands novel and sympathetic approaches to social acceptability, but the industry is dominated by technologists whose training makes them unequal to the task. The process of decline feeds on this acceptability gap: nuclear power is not just about scientific solutions to scientific problems, it is about the social status of scientists and technologists thrust awkwardly into the political firing line.

It requires only a recent episode to illustrate this lemming-like syndrome. With the accidental discharge of uranium nitrate into the Irish Sea, and admission by the authorities of a separate, internal incident involving plutonium, a newly formed Nuclear Electricity Information Group (itself part of the syndrome—the industry invariably alters titles and names when on the retreat) issued its first advertisements. In one of these, three pub-goers, one looking remarkably like the archetypal university student, reveal that what the common people think of nuclear power is that reactors manufacture acid rain and nuclear electricity produces radioactive light bulbs. Either the advertising agency, and perhaps NEIG, believe these are common misconceptions or the advertisement is a nasty attempt to set up a straw man image of the opposition to nuclear power. Whatever the case, it speaks volumes for the lack of understanding in the nuclear industry of social processes.

Therein lies the clue both to what has gone wrong for nuclear power and

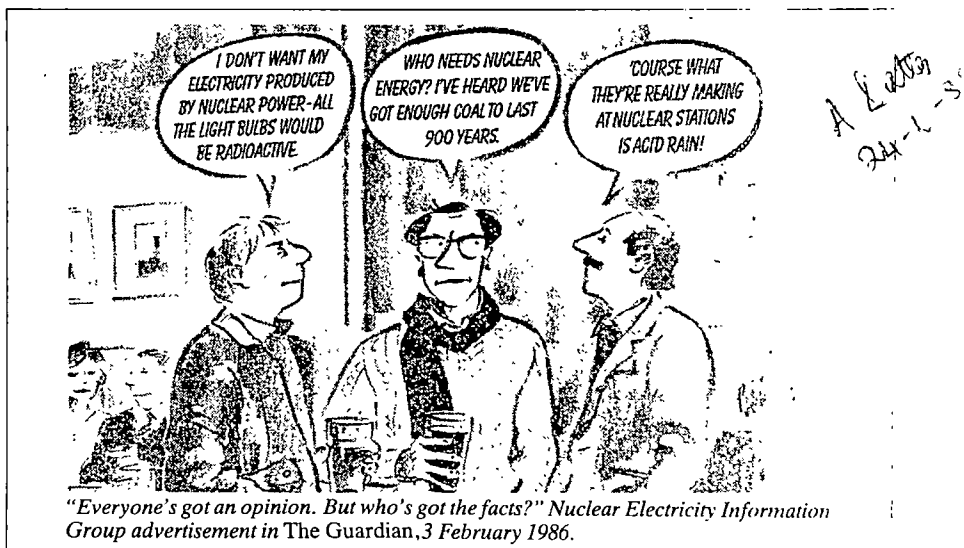
perhaps to the industry's last chance to secure a degree of respectability, at least among the limited groups remaining who are prepared to be even-handed. No information packs for schools, crass advertisements or new shops in towns adjacent to potential waste dumps will substitute for the necessary self-criticism that would arise from asking *why* opposition to nuclear expansion is so fierce and articulate. The days of the early smear campaigns when opponents were branded as Soviet dupes are over. Serious questioning of the fundamental social rationale for nuclear power has found its way into Select Committees, the Monopolies and Mergers Commission, the Royal Commission on Environmental Pollution and many other bodies which cannot be dismissed in the traditional way.

In *Nuclear Politics*, Tony Hall touches on some of the reasons for the focusing of dissent. He is especially detailed and robust on the early years: the links between nuclear power and nuclear weapons, the paranoid secrecy and the distance the industry managed to secure from political control (this being as much due to the ignorance of the politicians as to the propaganda they swallowed). When environmentalism finally became not just a popular but also a respectable political force, the industry had neither the tradition nor the capabilities to handle it. How different the picture might have been if the industry had understood the public perception of risk is hard to say; the mistakes and cover-ups would still have happened, but the effects on public confi-

dence would surely have been less. Instead, the industry reacted in the technological mode. For instance, it persisted with the definition of risk as the probability of death or morbidity, and ignored the concepts rooted in social science which emphasize the nature of both the event and the process leading to the event, as well as the probability. The apotheosis of error in the technological approach to risk was revealed in Lord Rothschild's famous Dimbleby Lecture, warmly applauded by the industry at the time and rightly derided by anyone with a smattering of social understanding. Sadly, Rothschild's thinking still pervades the industry, once again a sad reflection of the absence of a social-science base to pro-nuclear politics.

Tony Hall takes us from the early days to the development of the Magnox programme and on to the AGR "disaster", though strangely omitting any reference here to the damning work of David Henderson in 1977 on the economics, or lack of them, in the AGR programme (a critique which he repeated in last year's Reith Lectures). Hall then outlines the emergence of the opposition to nuclear power, notably the Friends of the Earth and the intellectual spur to respectable criticism from Amory Lovins and Walter Patterson. Missing in this account, however, is mention of the emergence of many doubters in the economics profession—it was never easy to find academic support for the nuclear case, for example. Hall then outlines the famous Windscale Inquiry into the planned new processing plant, now under construction (and under Parliamentary scrutiny). The nuclear industry again misjudged the public view of matters when it greeted so positively the extraordinary bias and eccentricities in the report of the Inquiry. It was almost as if *any* support would do, regardless of its quality.

*Nuclear Politics* is at its weakest in its concluding sections on Sizewell. There is



no summary of the arguments or analysis of the inquiry process, nor any reflection on the attempt to force the demise of the "big" inquiry by the present government, something the industry has always wanted. This is a shame because Tony Hall writes with admirable clarity and skill. The layman's guide to Sizewell will need to be written, while specialists must await Professor O'Riordan's University of East Anglia/Economic and Social Research Council study for the definitive analysis. The other area still to be documented is the role of the regulatory agencies in the fortunes of nuclear power: the Nuclear Installations Inspectorate, the National Radiological Protection Board and the Health and Safety Executive do not have a prominent place in the book.

Nonetheless, Tony Hall has brought together an accurate yet readable mix of the technology and politics of nuclear power in Britain. The pity is that those who need to take on board its lessons will, more likely than not, again fail to do so. □

*David Pearce is a Professor in the Department of Economics, University College London, Gower Street, London WC1E 6BT, UK. He is co-author of Decision Making for Energy Futures: A Case Study of the Windscale Enquiry (Macmillan, London, 1979), and is a member of the National Radiological Protection Board (NRPB). The opinions expressed in the review are personal and should not be taken to reflect those of the NRPB.*

This is a great book,  
and an exciting book...  
readable, worth reading  
and enlightening.

*Sir Karl Popper*

## Cosmology, Physics & Philosophy by Prof Ben Gal-Or

"a master piece... any good library must have a copy of this classical work."

*Ind. J. Phys.*

"... a tour de force... ill be widely read and appreciated... a magnificent and sustained piece of work!"

*Sir Alan Cottrell*

... remarkable... challenging...  
*Am. J. Phys.*

2nd Printing  
Springer-Verlag  
175 5th Ave., N.Y., 10010

Reader Service No.14

## Rich cuttings from a medical life

*Michael Shortland*

**William Hunter and the Eighteenth-Century Medical World.** Edited by W.F. Bynum and Roy Porter. Cambridge University Press: 1985. Pp. 424. £35, \$49.50.

FOR MUCH of its existence, medicine has been the most disreputable of the learned professions — less conspicuous than the law or the church, but its failings for that reason all the more evident. The shady lawyer could lose you a case, the venal priest would sell you a soul, but a visit to your physician might cost you an arm and a leg, and quite possibly your life. Until anaesthetics and antiseptics were developed, the best medicine was no medicine. As Swift put it, the only doctors to be trusted were Doctor Diet and Doctor Quiet.

The defects of medicine were never more visible than during the eighteenth century. Pilloried in the press, ridiculed by satirists and subject to scandal, the physician seemed for a while ready to close shop and hand the keys over to the charlatan pill-pushers who reaped vast profits from the poor soil of conventional physic. These itinerant quacks had one crucial fact in their favour: they might fail to cure your disease, but they did not kill you with their remedies. Early in the century, two rival physicians, Drs John Woodward and Richard Mead met in a duel; supposedly, Mead disarmed his opponent and humanely exclaimed "Take your life". To which Woodward replied "Anything but your potions".

Such an episode may not have been typical, but it was symptomatic. With so few accepted standards of health care and no organization able to police the profession, disputes and disarray were endemic. Lacking a strong self-identity, the doctor found himself aligned, then harangued, with the barber-surgeon and the grocer-apothecary. Moreover, as the second editor of this volume explains, at a time when religion indoctrinated people with a profound belief in the corruptions of the flesh, medicine suffered from a guilt by association. Particularly in branches such as venereology and obstetrics, the humble practitioner was liable to find himself stigmatized by vice and sexual impropriety.

How curious then that William Hunter (1718–1783), whose father intended him for the ministry, should opt instead for a life in medicine. Strange, too, that after a surgical training in provincial Hamilton and then in London, he should gravitate towards obstetrics. But truly astonishing is the discovery, detailed with evident relish

in this collection of essays, that Hunter managed to acquire such eminence and wealth pursuing this doubly-notorious trade. As Porter explains in a brilliant assessment of this apparent misnomer, the gentleman-surgeon, Hunter had to start life in the wrong country (Scotland), in the wrong religion (Presbyterianism) and in the wrong family (large and rough-cut).

Good luck along the way no doubt helped Hunter reach the heights of his adopted profession. But as important was his keen sense of what his potential customers required. From the contributions here on apprenticeship and medical education in Britain and on the continent, it is clear that Hunter made good the relatively dismal opportunities for training by offering private anatomical classes in London hospitals. These were marketed with the same skills he brought to the surgery: precision, efficiency and style. Knowing the opprobrium that attached itself to his line of work, Hunter carefully cultivated contacts and clients. The job of an obstetrician demanded discretion, so he kept a low profile. But he could be showy, exhibitionist and highly visible in different circumstances. In an age when appearances mattered, Hunter could adopt many — in every sphere his skills as a practitioner were enhanced by formidable entrepreneurial acumen.

This is not to belittle his contribution to medical knowledge, though in that domain William's labours were eclipsed by those of his brother John, the famous physiologist and surgeon buried in Westminster Abbey and commemorated by the Hunterian Society. As the final section of this book reveals, William was an innovative and influential male midwife, and a non-interventionist at a time when many of his colleagues saw the recently-designed forceps as the key to the lying-in room.

In this aspect of his career as in others it remains difficult to see whether we are dealing with a remarkable exception to the rule that eighteenth-century medicine was primitive and squalid. It may well be that we should instead view William Hunter as part of the evidence in a general revision of the history of medicine. Certainly, this rich and engrossing volume offers insights into a world very different to that portrayed by Victorian doctors who enjoyed dating all that was proper in medicine to their own time. Whether or not William Hunter fits that particular portrayal is a question which the contributors here tackle from different perspectives and with great subtlety, but the question remains hanging in a promising state of uncertainty. □

*Michael Shortland is in the Department for External Studies, University of Oxford, Rewley House, I Wellington Square, Oxford OX1 2JA, UK.*

## At the frontiers in South America

Norman Myers

**Amazonia.** Edited by Ghillean T. Prance and Thomas E. Lovejoy. *Pergamon:* 1985. Pp. 442. £19.50, \$27.95.

A DOZEN or so scientific books dealing with Amazonia have appeared since 1980. This upsurge in professional interest is heartening, because it reflects a new awareness on the part of the scientific community both within Amazonian nations and elsewhere. After all, there is much to be aware about: with the richest biotic communities on Earth (one fifth of all species), Amazonia represents a kind of frontier for modern biology. Yet we know all too little about what makes it tick, let alone how to keep it ticking.

The region is also a frontier of different sort. The eight nations concerned want to develop it; that is, to exploit it, populate it, do something with it, rather than just leave it "idle" and unoccupied. Lacking science-based models of development, they have tended to employ approaches that owe more to notions of temperate-zone development than to an appreciation of what Amazonia has to offer. Fortunately there are signs of a change in attitude, as governments and international agencies explore the creative challenges of a new frontier in the dual senses.

For all the outburst of writings, no book has reflected the intrinsic complexity of the region, whether seen from the standpoint of the scientist or the developer. Virtually all the material hitherto available is descriptive rather than analytical in style, and traditionally academic in spirit. How pleasing, then, to come across this book, a volume in Pergamon's *Key Environments* series, with its emphasis on relationships and interactions — and not only between biotas and their environs, and so on, but between scientific disciplines with all that should imply for coordination between government departments. The chapter on fish, for instance, reveals not only that Amazonia possesses 3,000 species (15 times as many as Europe), and that commercial fisheries could produce far more animal protein than do the region's cattle ranches; more to the point, we read about entire fish communities, including the 50 species that generate three-quarters of the commercial harvest, and that feed primarily off fruit fallen into the water. This bodes much for plans to turn the alluvial floodplains into rice fields by eliminating riverside forests.

A similar approach characterizes the chapters on soils, vegetation, agriculture, forestry, and useful plants and animals,

among others. The most important chapter of all, however, is probably the one on climate. It shows how the Amazonian forest makes some of its own precipitation, and thus illustrates the ultimately integrative nature of the biospheric sciences; that is, life is not only modified by its environments but it adapts them as well, often to its own long-term benefit. This means that deforestation of part of Amazonia would reduce rainfall for the rest of the region, and thus alter the entire character of the remainder of the forest no matter how well protected it might be. It further implies that rainfall patterns would be affected in southern Brazil as well, this being the country's main crop-growing zone.

So here is a book to applaud. Within its 175,000 words, it encompasses the main components of the great Amazonian ecosystem. Several of the chapters are by Latin Americans, another welcome departure because most scientists interested in the region are still located in North America. My main regret is that there is not more text by the editors. Their two-page Introduction is splendid stuff: all the more pity, then, that they did not include commentaries on each chapter, or at least on the three main sections, with a concluding overview to pull the whole thing together. □

Norman Myers, Upper Meadow, Old Road, Headington, Oxford OX3 8SZ, UK, is a consultant on development and environmental matters.

## Insider's insects

Timothy J. Bradley

**Fundamentals of Insect Physiology.** Edited by Murray S. Blum. *Wiley:* 1985. Pp. 598. \$39.95, £41.40.

DESPITE the number and variety of biology students taking classes on insect physiology, we have hitherto lacked a comprehensive, detailed and up-to-date textbook on the subject. *Fundamentals of Insect Physiology* is a successful attempt to meet that need.

The book contains chapters on most of the traditional areas of physiology, including respiration, circulation, endocrinology, exocrine glands, and metabolism and behaviour, as well as discussion of topics related to neural and muscular function. Both its strengths and its weaknesses derive from the multi-author format. The information is in most part well presented and amazingly free of factual error, as is to be expected when experts are writing about their own specializations. Conversely, while the stylistic differences are not serious, the clarity of writing differs widely and there is little coordination between contributions on related topics.

Some of the chapters will unfortunately be of little use to beginning students of insect physiology. The lengthy account of electrical events in the nervous system is marred by confusing and poorly printed figures, and the examples are drawn largely from experiments using molluscan and mammalian material. More concise explanations of action and receptor potentials are available in basic physiology texts. The chapter on intermediary metabolism presents most of the metabolic pathways as confusing lists of reactions, rather than as pathways connected with arrows; for this topic, students would better be directed to *Insect Physiology* by Mordue *et al.* (Blackwell Scientific, 1980), an excellent but much less comprehensive textbook.

Most of the authors, however, present accurate and readable accounts of their fields. One of the many excellent contributions is the chapter on respiration by T.J. Nation. After a detailed description of morphological adaptations, both in body plan and at the organ and cellular levels, the author proceeds to a mathematical discussion of the physical laws underlying the diffusion of gases, ventilation and the metabolic rate of insects in various physiological states. This is followed by an analysis of specific respiratory adaptations (in pupae, aquatic insects and eggs), with examples of species possessing each type of adaptation. This last feature will be helpful for students faced with the bewildering morphological and taxonomic diversity of insects, for example among those possessing tracheal gills. All of the chapters contain references to review articles and sometimes to the primary literature.

The sequence of material could have been better; for example a discussion of the effects of hormones on behaviour precedes the chapter on endocrinology. Worse, however, is the choice of the opening chapter. My heart goes out to the students who, using this book, begin their acquaintance with insect physiology by reading a rather opaque discussion of the embryology of the insect heart.

The dust jacket indicates that the book is intended "both as a text for courses in insect physiology and as a basic reference for entomologists, zoologists, pest managers and physiologists". We already have an abundance of material in the second role, and it is as a basic text that *Fundamentals of Insect Physiology* has the most to offer. One hopes that later editions will continue to emphasize this aspect. Even as it stands, however, I consider it to be the best such textbook available. □

Timothy J. Bradley is in the Department of Developmental and Cell Biology, University of California at Irvine, Irvine, California 92717, USA.

## Between conservation and catches

T.J. Pitcher

**Marine Mammals and Fisheries.** Edited by J.R. Beddington, R.J.H. Beverton and D.M. Lavigne. *Allen & Unwin:* 1985. Pp. 354. £40, \$55.

INVASION of Earth by powerful, opportunistic and intelligent competitors for its fishery resources would immediately bring calls for their extermination. Yet in this role of conflict with our own species we already have marine mammals, native creatures evolved as part of the delicate balance of ocean ecosystems. Can the management and conservation of marine mammals, many of which by virtue of recent exploitation are rare and endangered species, be reconciled with the optimal control of fisheries? The 20 papers in this timely, readable and well-edited volume arose from a 1981 workshop in La Jolla which addressed the scientific basis of the question, mainly for seals and whales.

Two of the founders of quantitative resource assessment, Sidney Holt in a foreword, and Ray Beverton in Chapter 1, introduce the key issues. Marine mammals may affect catches by eating fish and squid; they may act as intermediate hosts to economically damaging parasitic nematode worms in fish; and they themselves may become lethally entangled in, and damage, fishing gear. Fishery/mammal conflict often brews up despite inconclusive evidence one way or the other, but it is difficult to produce unequivocal scientific analyses because our understanding of the population dynamics of marine mammals is limited: the complex social behaviour of marine mammals makes reproductive and feeding rates hard to predict. Holt considers that this book sets out "where we now are" in this field. I agree, and it does so with admirable clarity.

Beverton looks to technology to solve the entanglement problem, and sets the scene for many of the case studies later in the book. His main contribution, however, is cleverly to modify conventional fishery equations to show how fish stocks are affected by various levels of control imposed on the mammal population, and vice versa. Where the mammal is itself not exploited, his conclusion is that there is no optimal solution allowing coexistence and so the trade-off between fish yields and mammal conservation must be decided using other criteria. Beverton's analysis offers predictions of the consequences of decisions, but not the means for making them.

This theme is taken up in the second chapter by Colin Clark, a leading analyst of resource economics, who concurs that no conventional optimal management criteria favour mammal/fishery coexistence. Clark searches for a pragmatic solution reminiscent of John Pope's "minimum sustainable whinge" fishery strategy, which aims to produce the least dissatisfaction among the interest groups concerned. Maintenance of ecosystem integrity is also one of Clark's goals, although I wonder if ecologists could ever agree how to measure it.

Some time ago, Clark demonstrated how strongly-shoaling fish such as mackerel are easily overexploited because fishermen maintain good catches right up to the last shoal in the sea. Likewise, it pays marine mammals to prey upon these profitable food patches, exacerbating depletion of both mammal and fish populations. Clark advocates careful spatial partitioning of fishery quotas as the only solution.

Both of these opening chapters covering fundamental issues are stimulating and challenging. Twelve case studies, ranging geographically from California to Kerguelen, follow, and although they inevitably vary in approach the net is cast sufficiently wide for the general reader to find something of interest. Three chapters

particularly caught my attention.

Beddington and de la Mare critically describe models aimed at limiting the impact of Southern Ocean krill fisheries on the recovery of Antarctic whales. The role of such strategic simulation models is seen as guiding the acquisition of relevant information, thereby producing insight rather than mere data. Such laudable goals for ecological modelling are rarely achieved and the perceptive review in this chapter could help us get there more often.

Harwood and Greenwood examine dispassionately and in detail the scientific basis of the recent controversial government cull of Scottish grey seals: this chapter will be essential reading for conservationists. The cull had unanticipated and damaging consequences for the seals. Although killing them should increase fish catches, it has so far proved impossible accurately to quantify this effect, whether in numbers, weights or economic terms.

When pole and line capture for tuna changed to mechanized purse seineing in the 1950s, dolphins often associated (for unknown reasons) with tuna schools began to be slaughtered in large numbers. Allen discusses the East Pacific yellowfin tuna fishery where one dolphin dies for every three tonnes of tuna landed. He analyses the costs of concentrating on tuna schools not accompanied by dolphins.

The final section of the book contains six reviews of methods of estimating fish consumption by marine mammals. These, I think, would have been more appropriately published in the specialized literature.

*Marine Mammals and Fisheries* will be indispensable for biologists working on the management of marine resources. It should also attract a wider readership among those concerned to resolve conflicts arising from our exploitation of other species with which we share this planet. □

T.J. Pitcher is a Senior Lecturer in the School of Animal Biology, University College of North Wales, Bangor, Gwynedd LL57 2UW, UK.



Detail of a model of the Cap-Ferret submarine fan, a complex sedimentary body located in the south-eastern part of the Bay of Biscay. (Bathymetric curves are 50m equidistant, scale is c. 12.25km cm<sup>-1</sup>; the numbers refer to features identified in the original.) The illustration is taken from *Submarine Fans and Related Turbidite Systems*, the first volume in a new series, *Frontiers in Sedimentary Geology*, published by Springer-Verlag. Editors of the book are A.H. Bouma, W.R. Normark and N.E. Barnes, price is DM 220.

# Screwworm eradication a grand delusion?

from J. L. Readshaw

*A campaign to eradicate the screwworm, a major pest of livestock in Texas, has cost \$50 million a year. But the claimed success of the programme can be explained by natural variation and new outbreaks may well occur when climatic conditions again favour the pest.*

THE campaign to eradicate screwworm, *Cochliomyia hominivorax* (Coquerel), from the southern United States is the most ambitious entomological programme ever mounted. Its progress over the past 26 years has spawned similar multi-million dollar programmes, aimed at eradicating other major insect pests throughout the world<sup>1</sup>.

The screwworm is a primary parasite of livestock, a tropical species, distributed throughout central and south America and the Caribbean. It extends northward through Mexico and southern Texas, and occasionally spreads throughout southern and central United States causing serious losses to livestock and wildlife<sup>2</sup>.

The adult fly lays batches of eggs on the edges of open wounds. The resulting 'screw-like' maggots burrow into the living flesh, causing myiasis, weakening the animal and occasionally causing death. When mature the maggots leave the wound, drop to the ground, and pupate in the soil—producing adult flies some 10 to 20 days later.

Several generations occur during the warmer months, but the fly has no dormant or protected overwintering stage and thus cannot survive in areas where the average winter temperature drops below about 10 °C (50 °F). Thus the fly normally overwinters only in the extreme south of the United States but reinvades the northern States in spring and summer—the adults being highly mobile.

The eradication programme was conceived by E. F. Knipling in 1938<sup>3</sup>. It is based on the release of millions of artificially-reared sterile males. Male sterility is induced by exposing 5-day-old pupae to  $\gamma$  rays. Because of their superior numbers, the sterile males outcompete the wild males in mating with the wild females. As a result, the wild females lay only sterile eggs; no offspring are produced, and, in theory, the population dwindles to extinction<sup>4</sup>.

The research programme started in 1950, with X-ray and later  $\gamma$ -ray induced sterility<sup>5</sup>. Field trials on the islands of Sanibel and Captiva, off the west coast of Florida, showed promise (G. W. Eddy, A. H. Baumhover, A. J. Graham and F. H. Dudley, unpublished data quotation ref. 6) and, in 1954, a major campaign on Curacao was judged a success<sup>7</sup>. Another

large-scale trial in Florida in 1957<sup>8</sup> provided the impetus for a massive campaign to eradicate screwworm from peninsula Florida, starting in January 1958 and ending with the eradication of screwworm from all the south eastern States by November 1959<sup>9,10</sup>.

Thereafter (1962 to the present) the programme was taken to the south-west states, mainly Texas, New Mexico and Arizona, with a major extension into Mexico in 1976, involving the opening of a new sterile-fly factory at Tuxtla in 1981<sup>11</sup>.

Meanwhile, the 'sterile insect release method' (SIRM) was used to eradicate screwworm from Puerto Rico and the Virgin Islands (1974–75)<sup>12,13</sup>, and to re-eradicate it from Curacao (1977)<sup>14</sup>. Further campaigns are now under consideration for Trinidad and Tobago<sup>15</sup>.

## Flimsy evidence

The scientific basis for screwworm eradication using sterile males rests on only two publications—the first covering the Curacao campaign which lasted less than five months<sup>7</sup>, and the second the Florida trial<sup>8</sup>, which lasted only three months before being overtaken by the Florida campaign. Except for more recent work in Mexico<sup>16,17</sup>, no other systematic data on population levels or sterility have been published. References 7 and 8 are quoted repeatedly in the literature, yet their relevant content occupies only two small tables. Moreover, 'success' of the various campaigns is now accepted as established 'fact'. No cases of screwworm have been reported in Florida since 1972 and only very few in Texas since 1978.

But a recent manuscript by Krafus<sup>18</sup> raises the possibility that screwworm is influenced by climate. This report presents an analysis of the incidence of screwworm cases in Texas in relation to seasonal temperature and moisture conditions during the 1962–82 south-west eradication campaign.

## Historical perspective

Records of screwworm in the United States go back to 1832<sup>2</sup>. In the 1890's it was a serious problem in Texas and the Gulf Coast and subsequently there have been periodic outbreaks, particularly from 1932 to 1935 when massive infestations developed, reaching Florida and the south

eastern States in 1933<sup>19</sup> and extending up to the Great Lakes in 1935.

The progression of this outbreak is interesting. Before early summer 1933, screwworms were not known in Florida, nor in any of the southeastern states. In Florida, the first cases appeared in the extreme north of the state, near Georgia<sup>19</sup>. Earlier, in October 1932, screwworm was common but mild in Mississippi<sup>19</sup>; in 1933 it was present in southern Alabama<sup>20</sup> and Georgia<sup>21</sup>; in 1934 it was a serious problem from the Texas gulf coast, through Louisiana<sup>22</sup>, Mississippi<sup>19</sup>, southern Alabama<sup>20</sup>, Georgia<sup>23</sup> and northern Florida<sup>24</sup>.

This pattern of spread suggests that the screwworm probably reached Florida

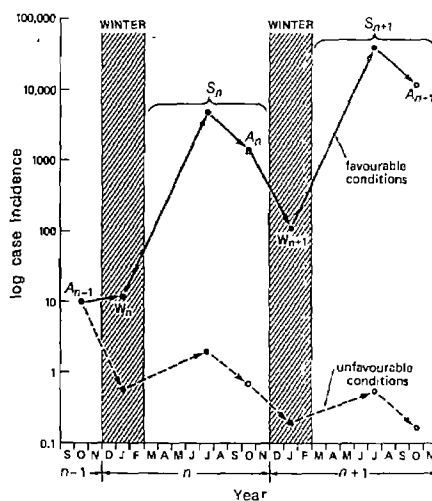
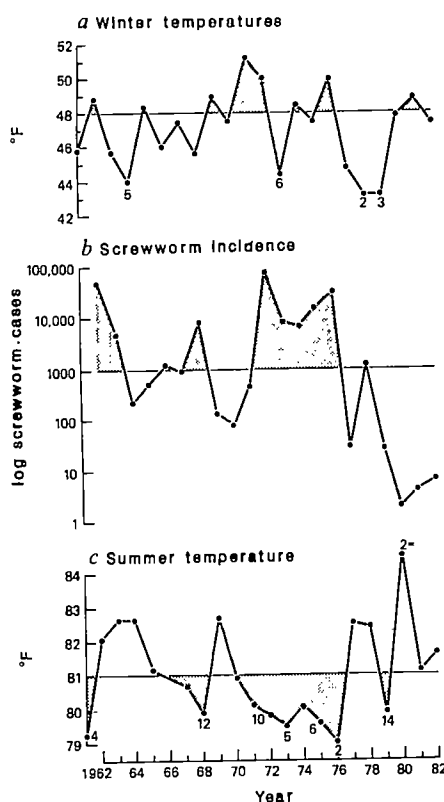


Fig. 1 Hypothetical model illustrating screwworm increase in relation to favourable or unfavourable seasonal conditions.

naturally by eastward movement from Texas and Louisiana during 1932–33, not, as is often claimed, imported on infested stock<sup>6</sup>. In fact Dove and Parman specifically say that the cases in northern Florida occurred *before* the importation of livestock from the drought-stricken western states.

The 1933–35 outbreaks ended throughout the southern States following the very cold winter of 1935–36. The next reports are for 1943, with losses in both the southwestern and southeastern states, following the mild winter of 1942–43. Thereafter, serious outbreaks occurred in association with mild winters in 1945, 1948



**Fig. 2** Correspondence between screwworm case incidence (*b*), winter temperatures (*a*) and summer temperatures (*c*) in Texas between 1962 and 1982. The numbers indicate rank with respect to highest or lowest temperatures during the past 100 years.

and 1949 right across the southern United States<sup>25</sup>. In Florida, another cold winter occurred in 1950–51, “bringing screwworm activity to an end”<sup>25</sup>, but for how long the populations remained low is unclear.

The Florida trial occurred during an outbreak in 1957, following the mild 1956–57 winter, but the eradication campaign was accompanied by the coldest Florida winter on record (records started in 1891)<sup>26</sup>. Similarly, the eradication campaign in the southwest states, starting in 1962, was fortunate in coinciding with two successive cold winters (1962–63 and 1963–64).

During the south-west release programme, outbreaks occurred in 1968 and from 1972 to 1976, with an estimated peak of 2 million cases (equivalent to 29,000 reported cases) in Texas in 1976<sup>27</sup>. Incidentally, two cases were reported from Florida in 1972, but none has been reported there since.

During the past five years there have been very few cases of screwworm anywhere in the United States. Eradication is claimed<sup>11</sup> and the programme has moved into Mexico to create a barrier zone. But eradication has been claimed before: for Texas and New Mexico in 1964, and Arizona and California in 1965<sup>28</sup>.

Thus, it is prudent to ask to what extent is the alleged success of the screwworm

campaign due simply to unfavourable (for the fly) seasonal conditions?

### Texas

The numbers of confirmed cases of screwworms in Texas during the course of the eradication programme are listed in monthly reports of the Texas Agricultural Extension Service<sup>27</sup>. Given these data the following hypothesis can be tested.

The seasonal incidence of screwworm cases in Texas during the eradication campaign was determined in part by: (1) winter temperature, influencing winter survival, and (2) summer temperature and moisture influencing seasonal breeding success.

The hypothesis is illustrated in Fig. 1, with winter cases in year *n* ( $W_n$ ) being derived from the previous autumn's cases ( $A_{n-1}$ ), according to winter temperature conditions ( $wt_n$ ); and with seasonal cases in year *n* ( $S_n$  = spring + summer + autumn cases) being derived from winter cases ( $W_n$ ), according to summer temperatures ( $st_n$ ) and summer moisture ( $sm_n$ ) conditions. The relevant climatic variables for autumn (September–November), winter (December–February) and summer (June–August) for the State of Texas<sup>26</sup> are listed in Table 1, together with the release rates of sterile males during the Texas programme. Also shown is the seasonal incidence of screwworm, which, because of the delay in reporting cases, is expressed on a quarterly basis (winter cases  $W_n$  = January–March and so on).

Adding one to the case data and transforming to natural logarithms, the hypothesis may be expressed by two linear equations:

$$\ln(W_n + 1) = a + b \ln(A_{n-1} + 1) + cwt_n \quad (1)$$

and

$$\ln(S_n + 1) = d + e \ln(W_n + 1) + fst_n + gsm_n \quad (2)$$

where  $W$ ,  $A$  and  $S$  are numbers of screwworm cases reported in years *n* or *n*–1 and  $a$ ,  $b$ , ...,  $g$  are coefficients to be estimated by multiple regression. The analysis shows that the equations

$$\ln(W_n + 1) = -16.24 + 0.45 \ln(A_{n-1} + 1) + 0.34 wt_n \quad (3)$$

and

$$\ln(S_n + 1) = 69.25 + 0.96 \ln(W_n + 1) - 0.80 st_n \quad (4)$$

estimate the actual incidence of winter cases ( $W_n$ ) and seasonal cases ( $S_n$ ) with an accuracy of 74% and 67% respectively (Table 2).

The influence of winter temperature was highly significant ( $c = 0.342 \pm 0.101$ ,  $t = 3.38$ ,  $P < 0.01$ ); summer temperature less so ( $f = -0.803 \pm 0.316$ ,  $t = 2.54$ ,  $P < 0.02$ ); whereas summer moisture, expressed as

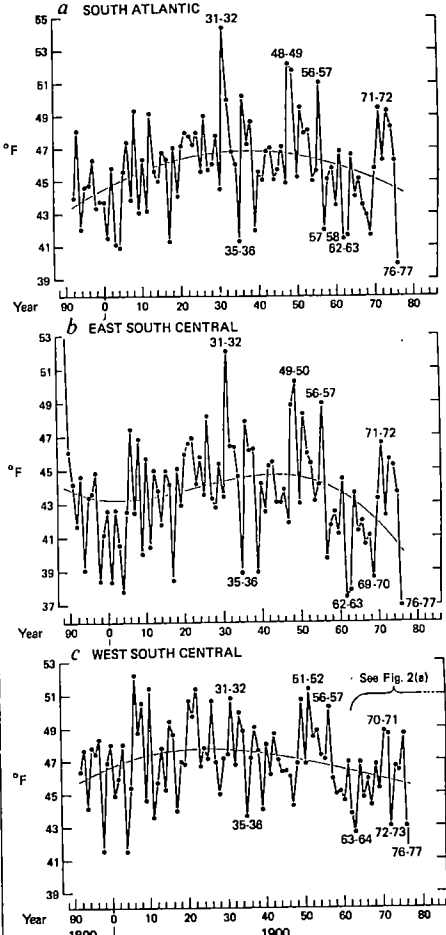


**Fig. 3** Long-term trends in winter temperatures (December–February) since the late 1800s in three contiguous climatic regions of the southern United States. The trend lines are third-order polynomial regression curves. See ref. 29 for more detail and regional boundaries.

either rainfall or the Palmer Drought Severity Index (PDSI) was not significant. However, summer temperature and moisture are negatively correlated such that it is necessary only to include temperature in equation (4).

In other words, given the numbers of autumn cases in Texas in year *n*–1, we can estimate the subsequent numbers of winter cases simply on the basis of winter temperature. Similarly, starting with winter cases, we can estimate the subsequent numbers of seasonal cases on the basis of summer temperature.

The inclusion of sterile male release rates in the model gives an interesting though clearly spurious result. It actually increases the amount of variation accounted for by the model to about  $r^2 = 0.82$  in the case of predicting winter cases from autumn cases, and to  $r^2 = 0.76$  in predicting seasonal cases from winter cases. But in each case the prediction is in the wrong direction as far as the programme's objectives are concerned. The inclusion of release rates gives positive rather than negative regression coefficients equal to +0.245 and +0.403 respectively. This sug-

Table 1 Incidence of screwworm cases in Texas in relation to sterile male release rates and seasonal climatic conditions

Year	Screwworm cases in:			Release rates $\times 10^6$ per day	Winter temperature (°F)	Summer temperature (°F)	Summer rainfall (inches)	PDSI*
	Autumn ( $A_{n-1}$ )	Winter ( $W_n$ )	Season ( $S_n$ )					
1962	?	?	49,363	2.6	47.7	82.1	7.86	?
1963	12,470	217	4,699	6.9	45.7	82.7	5.89	-4.10
1964	2,628	7	216	1.8	44.0	82.7	5.54	-4.04
1965	124	4	462	1.0	48.3	81.2	5.60	-1.72
1966	144	23	1,180	1.7	46.0	80.9	8.54	0.50
1967	855	3	832	2.0	47.4	80.7	6.65	-3.93
1968	551	2	9,266	3.8	45.7	79.9	9.14	3.64
1969	5,577	26	135	2.6	48.8	82.7	5.85	2.05
1970	4	0	92	1.8	47.5	80.9	4.68	-0.54
1971	8	8	436	2.5	51.2	80.2	10.07	-4.34
1972	217	115	90,865	8.4	50.0	79.8	8.73	0.02
1973	19,329	59	8,854	6.4	44.4	79.5	10.60	3.57
1974	5,480	106	6,796	7.9	48.5	80.2	8.82	-2.34
1975	3,321	31	16,733	7.8	47.6	79.6	8.89	4.08
1976	7,383	225	29,016	9.2	50.0	79.0	8.96	1.58
1977	9,266	6	33	6.0	44.8	82.5	5.93	-0.80
1978	4	0	1,236	4.1	43.2	82.4	7.23	-3.40
1979	419	2	30	1.0	43.2	79.9	10.28	3.23
1980	0	0	2	?	47.9	84.5	4.46	-1.76
1981	0	1	4	?	48.8	81.1	11.00	1.54
1982	0	0	6	?	47.4	81.7	6.81	1.98
1983	0	0	0	?	?	?	?	?
1984	0	0	?	?	?	?	?	?

\* PDSI, Palmer Drought Stress Index for Texas during July.

Table 2 Screwworm case incidence in relation to seasonal climatic conditions—analysis of deviance

Winter cases ( $W_n$ )	Sum of squares	d.f.	Mean square	F	$R^2$
Model	48.47	2	24.24	24.48	0.74
Residual	16.89	17	0.99		
Parameter	Estimate	s.e.	t	P	
a (intercept)	-16.24	6.843	3.35	<0.01	
b (autumn cases)	0.451	0.067	6.67	<0.001	
c (winter temperature)	0.342	0.101	3.38	<0.01	
Seasonal cases ( $S_n$ )	Sum of squares	d.f.	Mean square	F	$R^2$
Model	115.78	2	57.89	17.54	0.67
Residual	56.12	17	3.30		
Parameter	Estimate	s.e.	t	P	
d (intercept)	69.25	25.83	2.68	<0.02	
e (winter cases)	0.963	0.244	3.95	<0.001	
f (summer temperature)	-0.803	0.316	2.54	<0.02	

gests that the number of winter cases and the number of seasonal cases actually increased with increasing rates of sterile male release, which is ludicrous. The reason for this curious result lies in the fact that the release rates were positively correlated with the numbers of reported cases ( $r^2 = 0.61$ ,  $P < 0.01$ ) because fly production and hence release rates were increased in an attempt to control the burgeoning screwworm population. The release rates are therefore not included in the model.

Thus, despite the sterile male release programme, screwworm case incidence in Texas appears to have been determined largely by seasonal climatic conditions, especially temperature. The outbreaks occurred in response to favourable conditions, namely, warm winters and cool/wet summers. Conversely, cold winters and hot/dry summers, being unfavourable,

caused case incidence to decrease. This is illustrated in Fig. 1.

The actual coincidence between outbreaks on the one hand and favourable seasonal conditions on the other is shown graphically in Fig. 2.

#### Long-term trends

Having shown a clear relationship between seasonal climatic conditions and screwworm incidence in Texas, it is possible to examine the historical record for the southern United States with greater insight.

Long-term trends in winter temperatures for the relevant contiguous southern regions of the United States—South Atlantic, East South Central and West South Central—stretching westwards from Florida through Mississippi to Texas, as detailed by Diaz and Quayle<sup>29</sup>, are illustrated in Fig. 3.

In respect of the South Atlantic Region, the appearance of the outbreaks in Florida in 1933 and their collapse in 1936 correspond nicely to the exceptionally warm winters of 1931–32, 32–33, and the very cold winter of 33–34 (Fig. 3a). Also the outbreaks between 1945 and 1957 occurred during a succession of warm winters and ended with a very cold winter in 1957–58, which, as noted earlier, fortunately coincided with the Florida eradication campaign. In fact in Florida, the 1957–58 winter was the coldest in nearly 100 years<sup>26</sup>. Since 1958, most winters in Florida have been cold, some exceptionally so (for example, 1976–77 and 1977–78), except for a brief warm period in the early 1970s.

The East South Central temperature pattern (Fig. 3b) is similar but the trend towards colder winters during the past 25 years is even more pronounced. In

particular the cold winters of 1962–63, 63–64, 69–70 and 76–77 stand out.

Finally, the West South Central region (Fig. 3c), which includes Texas, confirms the cool trend, and, in conjunction with Fig. 2, illustrating more recent temperature trends in Texas, shows clearly that climatic conditions have been highly unfavourable for screwworm during the past 8 years, that is since the outbreaks collapsed in 1977. In Texas (see Fig. 2), the winters of 1977–78 and 1978–79 were the second and third coldest on record, whilst the 1980 summer was the second equal hottest on record (see Fig. 2). The 1983–84 winter was also exceptionally cold, killing citrus near San Antonio. The sudden downturn in screwworm case incidence in 1977 and the very low level since is therefore not surprising.

### Predictions

Seasonal weather conditions, especially winter temperature but also summer moisture are often mentioned as important in relation to screwworm activity<sup>30</sup>. Apparently, even in Mexico, hot dry summer weather is a major limiting factor<sup>17</sup>. However, Krafus<sup>18</sup> concludes that climate was not important to the success of the eradication programme but his analytical method is inappropriate.

Past criticism of the programme has centred mostly on other factors such as strain fitness<sup>31</sup>, genetic isolation<sup>32</sup>, application rates and so on, particularly to account for the 1972–76 outbreaks in Texas.

The present analysis is much more damaging. At best it shows that, although the sterile releases may substantially suppress the screwworm population, they cannot prevent outbreaks developing in response to the occurrence of favourable seasonal conditions, at least not in Texas. At worst it suggests that the method may be ineffective and that eradication from the eastern States, namely Florida, occurred naturally because of a succession of very cold winters, combined perhaps with increased vigilance, more effective pesticides and changing land use.

Indeed it is quite possible that the screwworm, which is after all a tropical species, might become exceedingly scarce during periods of unfavourable climate in areas marginal to its normal distribution. It could exist at very low population levels in small isolated pockets provided by waterholes and rivers without being detected by man. Evidence for this exists in the Texas State Program Reports<sup>27</sup> which refer to an estimated ratio of 100:1 actual to reported cases during the 1976 summer season. Clearly zero reported cases does not necessarily mean eradication.

It is also possible that an exceptionally cold winter such as that occurring in Florida in 1957–58, or a succession of cold winters, could actually eradicate the

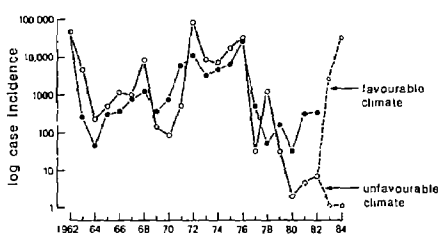


Fig. 4 Observed incidence (○) of screwworm in Texas during the 1962–82 eradication campaign compared with predicted incidence (●) based on actual winter and summer temperatures. Dashed lines represent predictions given favourable and unfavourable conditions.

species from areas isolated from the centre of the flies distribution. In this respect it is significant that the screwworm was not known in Florida before the exceptionally warm winter of 1931–32; that it appears to have reached there by natural progression eastward from Texas and Louisiana; and that winter temperatures in the South Atlantic Region appear to have been favourable for the fly only during the mid 1930s, 1950s and, to a lesser extent, the mid-1970s, in correspondence with the documented outbreaks. Before 1932 and after 1972 the winter climate seems to have been much less favourable for the fly in all the southern and eastern states (Fig. 3).

Admittedly eradication *per se* is virtually impossible to prove. But it is possible to verify the opposite view by making observations over sufficiently long periods of time in favourable potential habitats of the species concerned. In particular, in view of the current work in Mexico and the importance placed on the Tehuantepec barrier, it is imperative that strenuous efforts be made to detect the presence of screwworm in potentially favourable seasons and habitats throughout northern Mexico and southern Texas. Should these efforts fail, then eradication may more

1. Knippling, E. F. in *Sterile Insect Technique and Radiation in Insect Control* 3–23 IAEA, Vienna, 1982.
2. Snow, J. W., Siebenaler, A. J. & Newell, F. G. U.S. Dept. Agric. No. ARM-S-14, 1–32 (1981).
3. Lindquist, A. W. *J. Econ. Entomol.* **48**, 467–469 (1955).
4. Knippling, E. F. *The Basic Principles of Insect Population Suppression and Management* (Agriculture Handbook No. 512, US Department of Agriculture, Washington, 1979).
5. Bushland, R. C. & Hopkins, D. E. *J. Econ. Entomol.* **44**, 725–731 (1951); **46**, 648–656 (1953).
6. Bushland, R. C. *Adv. vet. Sci.* **6**, 1–18 (1960).
7. Baumhover, A. H. *et al.* *J. Econ. Entomol.* **48**, 462–466 (1955).
8. Baumhover, A. H., Husman, C. N., Skipper, C. C. & New, W. D. *J. Econ. Entomol.* **52**, 1202–1206 (1959).
9. Baumhover, A. H. *J. Am. Med. Assoc.* **196**, 240–248 (1966).
10. Bushland, R. C. *Bull. Entomol. Soc. Am.* **21**, 23–26 (1975).
11. Whitten, C. J. in *Sterile Insect Technique and Radiation in Insect Control*, Ed. IAEA (Vienna, 1982), pp. 79–83.
12. Graham, O. H. & Hourigan, J. L. *J. Med. Entomol.* **13**, 629–657 (1977).
13. Williams, D. L., Cartman, S. C. & Hourigan, J. L. *World Anim. Rev.* **21**, 31–35 (1977).
14. Tannahill, F. H., Coppedge, J. R. & Snow, J. W. *J. Med. Entomol.* **17**, 265–267 (1980).
15. Rawlins, S. C., Alexander, F. C., Moe, V., Caesar, E., Moll, K. & Applewhite, L. *J. Econ. Entomol.* **76**, 1106–1111 (1983).
16. Krafus, E. S., Hightower, B. G., Vargas, M. *J. med. Entomol.* **17**, 235–241 (1980).
17. Krafus, E. S. & Hightower, B. G. *J. med. Entomol.* **16**, 33–42 (1979).
18. Krafus, E. S. *Entomol. exp. appl.* **37**, 297–305 (1985).
19. Dove, E. W. & Parman, D. C. *J. Econ. Entomol.* **28**, 765–772 (1935).
20. Robinson, J. M. *J. Econ. Entomol.* **28**, 777–779 (1935).
21. Bissell, Theo, L. *Ga Agric. exp. Stn Bull.* **189**, 3–11 (1935).
22. Laake, E. W. *J. Econ. Entomol.* **28**, 648–649 (1935).
23. Dove, W. E. & Bishop, F. C. *J. Econ. Entomol.* **29**, 1076–1085 (1936).
24. King, W. V. & Bradley, G. H. *J. Econ. Entomol.* **28**, 772–775 (1935).
25. Smith, A. L. & Skipper, C. C. *Fla. Entomol.* **35**, 10–13 (1951).
26. Karl, T. R., Metacalf, L. K., Nicodemus, M. L. & Quayle, R. G. *Statewide Average Climatic History, Texas 1888–1982. Florida 1891–1982*. (Historical Climatology Series 6-1, National Climatic Data Center, Asheville, North Carolina, 1983).
27. Monthly program reports, Texas Agricultural Extension Service (1980).
28. Hightower, B. G. & Graham, O. H. in *Control of livestock insect pests by the Sterile Male Technique* 51–54 (IAEA, Vienna, 1968).
29. Diaz, H. F. & Quayle, R. G. *Mon. Weath. Rev.* **106**, 1393–1421 (1978).
30. Rahn, J. J. & Barger, G. L. *Agric. Meteorol.* **11**, 197–211 (1973).
31. Bush, G. L., Neck, R. W. & Kitto, G. B. *Science* **193**, 491–493 (1976).
32. Richardson, R. H., Ellison, J. R. & Averhoff, A. W. *Science* **215**, 361–370 (1982).
33. Coppedge, J. R. *et al.* *J. Econ. Entomol.* **71**, 579–584 (1978).

safely be assumed, with the corollary that more emphasis be placed on restricting the movements of stock.

If eradication has not been achieved then my analysis leads to the prediction that the outbreaks will return, despite the Mexican programme. Even the additional weaponry known as SWASS (screwworm adult suppression system), an aerially distributed toxic-bait, is unlikely to prevent screwworm increase under favourable climatic conditions<sup>33</sup>.

Figure 4 compares the observed incidence of screwworm cases in Texas over the last 20 years with those predicted by the model—starting with 49,000 cases in 1962 and using the winter and summer temperatures actually experienced in Texas (from Table 1). The model assumes that autumn cases ( $A_n$ ) always represent one-third of the previous year's seasonal cases ( $S_n$ ), an average determined from the actual case records listed in Table 1. The model shows also the expected increase or decrease over two seasons from the observed 1982 level (six cases) in response to either favourable or unfavourable seasonal conditions, based on the extremes observed during the 20-year period. Unfortunately there is no independent set of data on which to test the model, but if it is correct, we may expect screwworm outbreaks to re-occur in Texas in response to the return of favourable climatic conditions—namely, mild winters and cool, moist summers. I sincerely hope not, but my money is on the fly!

Since this manuscript was submitted there has been an outbreak of screwworm comprising “almost 150 reported infestations in northeastern Mexico (as near as 150 miles from the US border) during June and July 1985”. □

*J. L. Readshaw is a Senior Principal Research Scientist with the CSIRO, Division of Entomology, Canberra, ACT, Australia.*

## ARTICLES

# Latest Miocene benthic $\delta^{18}\text{O}$ changes, global ice volume, sea level and the 'Messinian salinity crisis'

David A. Hodell, Kristin M. Elmstrom & James P. Kennett

Graduate School of Oceanography, University of Rhode Island, Narragansett, Rhode Island 02882, USA

Oxygen isotope evidence indicates high but variable  $\delta^{18}\text{O}$  values in benthic foraminiferal calcite during the latest Miocene and earliest Pliocene. These high values may represent increases in global ice volume and associated sea-level fall. The  $\delta^{18}\text{O}$  record resembles glacial/interglacial cycles, but with only one-third the amplitude of the late Pleistocene signal. This variability may reflect instability in the Antarctic ice sheet, and palaeomagnetic correlation points to an isotopic event coinciding with the isolation and desiccation of the Mediterranean basin during the latest Messinian.

DURING the Messinian Age of the late Miocene, the Mediterranean Sea was isolated from the world ocean, and thick and extensive evaporites were deposited in pre-existing basins of the proto-Mediterranean Sea (the 'Messinian salinity crisis'<sup>1</sup>). The closure of the Mediterranean was controlled by a combination of tectonic compression in the western Mediterranean and a global sea level fall during the latest Miocene<sup>1-3</sup>. In 1977, Adams *et al.*<sup>3</sup> stated that "the final severing (between the Mediterranean and Atlantic) may have resulted from glacial-eustatic lowering of the global ocean. Further stratigraphic resolution of late Miocene sea level and ice-volume changes is sought to verify the eustatic-fall hypothesis." We address this question here by examining high-resolution benthic oxygen isotopic data from six sites in the Atlantic and Pacific oceans to determine possible relationships between changes in the benthic  $\delta^{18}\text{O}$  record and deposition of the Messinian evaporites.

The eustatic fall during the latest Miocene has often been attributed to an increase in the volume of ice on Antarctica, but different sets of oxygen isotope data have been found to be contradictory. For example, Shackleton and Kennett<sup>4</sup> proposed an expansion of the Antarctic ice sheet to 1.5–1.8 times its present size, based on a 0.5% increase in oxygen isotopic ratios during the latest Miocene Kapitan Stage at DSDP Site 284, South-West Pacific. The increase at Site 284 is somewhat tenuous, based upon two points only. Furthermore, isotopic analyses of other sections (DSDP Sites 158, 310 and 281) showed no evidence of a single large increase in latest Miocene  $\delta^{18}\text{O}$  values<sup>5-7</sup>. This contradiction led Ciesielski *et al.*<sup>8</sup> to conclude that "further oxygen isotopic studies of late Miocene deep-sea sediments from the southern high latitudes are obviously needed to clarify the true nature of oxygen isotopic change during the latest Miocene."

We have reanalysed Site 284 at a higher sampling frequency to support or reject the  $\delta^{18}\text{O}$  increase reported by Shackleton and Kennett<sup>4</sup>. We have also analysed DSDP Site 516A<sup>9</sup> and three piston cores from Chain Cruise 115 from the Rio Grande Rise in the western South Atlantic. Shackleton and Cita's data from Site 397 in the North Atlantic were included because this site has been correlated to the Messinian salinity crisis<sup>10,11</sup>. From Leg 90 in the South-West Pacific, we analysed Sites 588 and 590<sup>12</sup>, which offer excellent stratigraphic resolution because of high sedimentation rates in the latest Miocene-early Pliocene.

The placement of the Miocene/Pliocene (M/P) boundary is important to this study because its definition is intimately tied to the re-establishment of open marine conditions in the Mediterranean following the Messinian salinity crisis<sup>13</sup>. The boundary stratotype is at the base of the Zanclean Stage at Capo Rosello, Sicily, at the contact between the underlying pyritic

clays and sands of the Arenazzolo unit and overlying Trubi marls. In the latest revision of the Neogene timescale, Berggren *et al.*<sup>14</sup> suggested that the M/P boundary falls just above the Chron 5/Gilbert boundary at 5.3 Myr. The M/P boundary in Site 588 was placed at 107 m, based on the first appearance datum (FAD) of *Globorotalia tumida* and the last appearance datum (LAD) of *Globorotalia conomicoza*<sup>15</sup>. The boundary in Site 588 falls in the lower part of the Gilbert at about 5.0 Myr, or 300,000 yr above the Chron 5/Gilbert boundary. Preliminary cross-correlation of  $^{87}\text{Sr}/^{86}\text{Sr}$  ratios from the base of the Zanclean with magnetostratigraphy from DSDP Site 519 suggests that the base of the Trubi at Capo Rosello is several hundreds of thousands of years above the Chron 5/Gilbert boundary<sup>16</sup>.

## Presentation of data

The benthic oxygen isotope record from Site 588 is shown in Fig. 1. Between 80 and 160 m, we sampled every 70 cm (a sampling interval of 20–25 kyr). The time control is excellent in Site 588 because of palaeomagnetic reversal stratigraphy<sup>17</sup>; the interval of high sampling resolution extends from 6.4 to 3.9 Myr. Oxygen isotopic ratios during the latest Miocene-early Pliocene are clearly marked by high-frequency variation (Fig. 1). The amplitude of the  $\delta^{18}\text{O}$  signal is about 0.5%. In the Quaternary, the maximum difference between glacial and interglacial  $\delta^{18}\text{O}$  values is 1.6–1.8%, the amplitude of the latest Miocene-early Pliocene fluctuations is thus one-third of the late Pleistocene signal.

In Fig. 1, 3- and 5-point running averages of the raw data are presented, to show lower-frequency components of  $\delta^{18}\text{O}$  variation. Oxygen isotopic fluctuations during the latest Miocene-early Pliocene resemble typical glacial-interglacial cycles of the Quaternary, except in their smaller amplitude. The period of these cycles, when the data are plotted against age derived from magnetostratigraphy, is ~400,000 yr. Cyclicity of this period has been reported to dominate late Miocene carbonate records from the Pacific<sup>18</sup>, and may reflect the natural period of 'glacial-interglacial' oscillation in Antarctic ice volume during the late Miocene.

In the following description of the data, we use the terms 'glacial' and 'interglacial' to refer to episodes of net increase and decrease in  $\delta^{18}\text{O}$ , respectively, although we acknowledge that 'cool' and 'warm' are equally applicable because we cannot separate the temperature signal from the ice volume signal in the  $\delta^{18}\text{O}$  record. The intensity of glacial and interglacial cycles appears to increase progressively through the latest Miocene and early Pliocene. The first prominent glacial interval (increased  $\delta^{18}\text{O}$  values) occurs in the younger normal event of Chron 5 between 5.5 and 5.2 Myr. This is followed by a short-

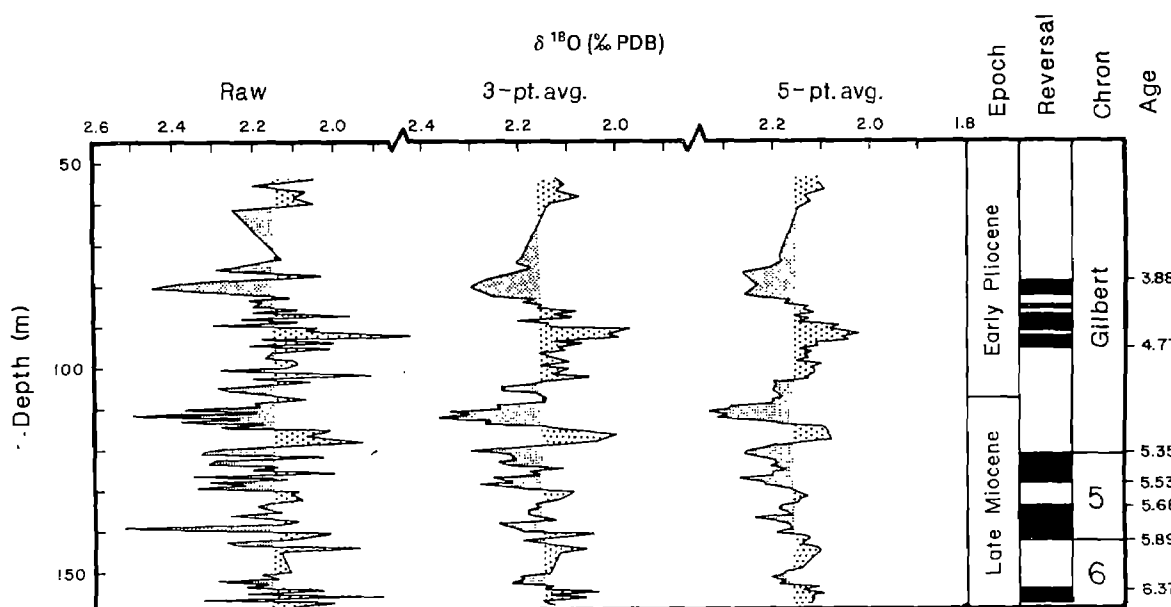


**Fig. 1** Oxygen isotope results from benthic foraminifers *Planulina wuellerstorfi* and/or *Cibicidoides kullenbergi* from Site 588, DSDP Leg 90, South-West Pacific. The sampling interval is 20–25 kyr between 80 and 160 m, or between 6.4 and 3.9 Myr if ages<sup>14</sup> are assigned to the magnetobiostratigraphy of Barton and Bloemendal<sup>17</sup>. The raw  $\delta^{18}\text{O}$  data clearly show that the latest Miocene–early Pliocene was characterized by high-frequency variation in  $\delta^{18}\text{O}$ . The amplitude of variation is  $\sim 0.5\%$  (one-third of the late Pleistocene signal), and the wavelength is  $\sim 400,000$  yr. The 3- and 5-point running averages of the data show the general trends in  $\delta^{18}\text{O}$ , and resemble glacial-interglacial cycles.

term interglacial just above the Chron 5/Gilbert boundary between 5.2 and 5.1 Myr. Oxygen isotopic ratios reach a maximum in the lower Gilbert between 5.1 and 4.8 Myr, reflecting maximum intensity of glaciation or cooling. An interval of lower  $\delta^{18}\text{O}$  values is apparent in the early Pliocene between 4.8 and 4.1 Myr, marking a strong interglacial or warming. The sampling interval decreases above 80 m, but the record indicates that glacial and interglacial events occurred throughout the remaining Pliocene.

Figure 2 is a composite of oxygen isotopic data from six sites (Table 1). The chronology is based on the palaeomagnetic reversal stratigraphy of Sites 588 and 397<sup>17,19</sup>. The other curves were aligned by matching oxygen isotope records between sites. The biostratigraphic position of the M/P boundary is shown for each site, and generally supports the isotopic correlation. The position of the boundary is uncertain by 0.5 Myr (at  $\sim 5.5$ –5.0 Myr), which is reasonable considering the inadequacies of biostratigraphic recognition of the boundary. All sites show an interval of relatively high  $\delta^{18}\text{O}$  values occurring near the M/P boundary. The differences in the character of the  $\delta^{18}\text{O}$  records between sites result from different sampling resolution and sedimentation rates.

The benthic  $\delta^{18}\text{O}$  record at Site 397 is remarkably similar to that at Site 588. Shackleton and Cita<sup>10</sup> reported high-frequency  $\delta^{18}\text{O}$  variation occurring just above and below the position of the Chron 5/Gilbert boundary. Oxygen isotopic ratios increase in late Chron 5, decrease near the Chron 5/Gilbert boundary, increase again in the early Gilbert, and then decrease in the early Pliocene. Maximum  $\delta^{18}\text{O}$  values were calculated to be 0.3% more positive than Holocene values, and the amplitude of the  $\delta^{18}\text{O}$  variation was reported to be about one-third of the late Pleistocene signal<sup>10</sup>.

Site 590 shows high  $\delta^{18}\text{O}$  values in the younger part of Chron 6, and in the very latest Miocene in late Chron 5 and early Gilbert, just before the biostratigraphic position of the M/P boundary. At Site 284, the  $\delta^{18}\text{O}$  increase reported by Shackleton and Kennett<sup>4</sup> is confirmed with more data; however, the increase is no longer single-peaked, but quite broad, spanning the M/P boundary. Following the interval of high  $\delta^{18}\text{O}$

values, oxygen isotopic ratios show a distinct decrease in the early Pliocene. At Site 516A, oxygen isotopic ratios are similar throughout much of the late Miocene and early Pliocene, except for anomalously high  $\delta^{18}\text{O}$  values above and below the biostratigraphic placement of the M/P boundary. These extreme values were reproduced by analysing replicate samples, which gave indistinguishable results within analytical error. Site 516A was sampled every 50,000 yr, and the low resolution of the sampling at this site is probably responsible for the compressed nature of the  $\delta^{18}\text{O}$  increase. Oxygen isotopic ratios at Site 516A show a prominent decrease near the top of the record in the early Pliocene. At *Chain* site (CH) 115, we sampled three piston cores at 10–20-cm intervals to provide higher resolution over the M/P boundary in the South Atlantic. The oxygen isotope record of the individual piston cores (Chain 64, 67 and 86PC) shows similar trends; the data from the three cores were stacked to produce the composite record shown in Fig. 2. The CH 115 data clearly show a distinct interval of higher  $\delta^{18}\text{O}$  values associated with the M/P boundary, followed by a trend toward decreasing  $\delta^{18}\text{O}$  values in the early Pliocene.

All sites show an increase in  $\delta^{18}\text{O}$  values in the latest Miocene, as originally observed by Shackleton and Kennett<sup>4</sup> at DSDP Site 284. But whereas the Shackleton and Kennett data<sup>4</sup> show a single point-increase in  $\delta^{18}\text{O}$ , the higher-resolution records demonstrate that the latest Miocene was marked by high-frequency  $\delta^{18}\text{O}$  variation consisting of several ‘cool-glacial’ and

**Table 1** Sample localities

Site	Latitude	Longitude	Water depth
Chain 115	30°00' S	35°00' W	2,100 m
DSDP 284*	40°31' S	167°41' E	1,066 m
397†	20°51' S	15°11' W	2,900 m
516A‡	30°17' S	35°17' W	1,313 m
588	26°06' S	161°13' E	1,533 m
590§	31°10' S	163°22' E	1,299 m

\* See also ref. 4. † See ref. 10. ‡ See also ref. 9. § See also ref. 12.

## ARTICLES

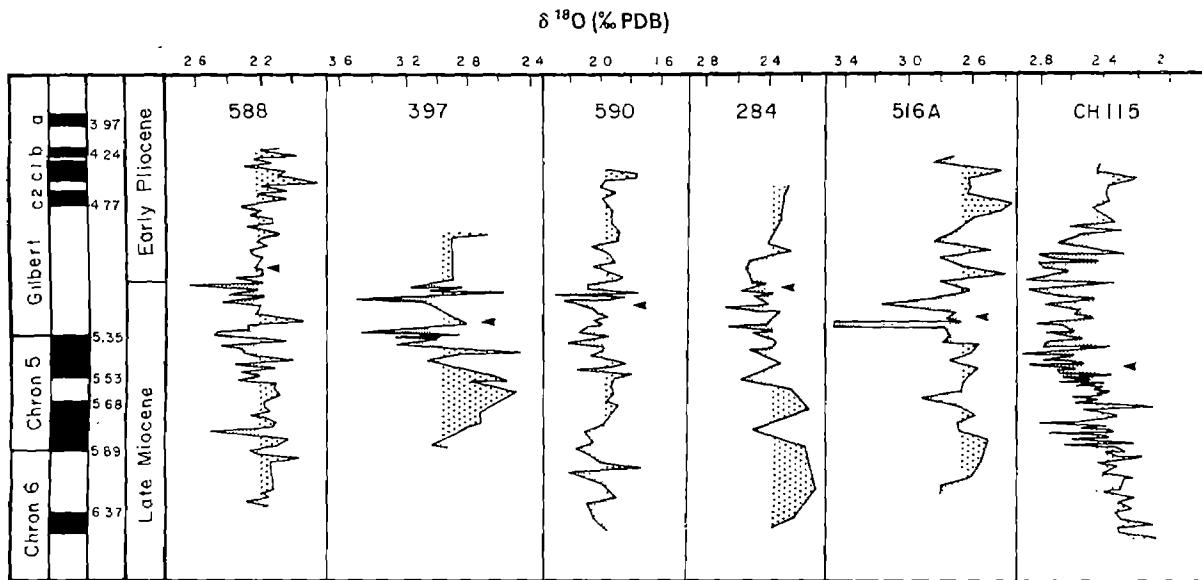


**Fig. 2** Oxygen isotopic results from Sites 588 (South-West Pacific), 397 (North Atlantic), 590, 284 (South-West Pacific), 516A, and CH115 (South-West Atlantic) over the M/P boundary. Oxygen isotopic analyses were generated on the benthic foraminifers *Planulina wuellerstorfi* and/or *Cibicidoides kullenbergi* at Sites 588, 590<sup>12</sup>, 516A<sup>9</sup> and CH 115; several species were run at Site 397 and adjusted to *Uvigerina peregrina*<sup>10</sup>; *Uvigerina* spp. were analysed in Site 284<sup>4</sup>. The palaeomagnetic stratigraphy for Sites 588 and 397 is after Barton and Bloemendal<sup>11</sup> and Hamilton<sup>12</sup>, respectively; ages assigned to magnetic boundaries are after Berggren *et al.*<sup>14</sup>. The M/P boundary was placed in the lower Gilbert at 107 m at Site 588, based on the FAD of *Globorotalia tumida* and LAD of *Globorotalia conomicoza*<sup>15</sup>. The biostratigraphic placement of the M/P boundary is indicated by an arrow. All sites show a general increase in δ<sup>18</sup>O values in the latest Miocene as originally reported by Shackleton and Kennett<sup>4</sup> at Site 284, but the high-resolution record of Site 588 demonstrates that the latest Miocene was also marked by high-frequency δ<sup>18</sup>O changes consisting of several 'cool-glacial' and 'warm-interglacial' episodes.

'warm-interglacial' intervals. The data from Site 588 suggest that maximum δ<sup>18</sup>O values occur during late Chron 5 and early Gilbert. The time interval dominated by high δ<sup>18</sup>O values is ~500,000 yr, brief enough to be easily missed by inadequate sampling, poor core recovery or removal by erosion or dissolution. These factors have undoubtedly contributed to the reported absence of an increase in late Miocene δ<sup>18</sup>O values in other studies<sup>5–7</sup>.

### **Ice volume changes**

The high-frequency δ<sup>18</sup>O variations in the latest Miocene and early Pliocene suggest that ice volume and/or temperature changes occurred throughout this interval. With benthic oxygen isotopic data alone, we cannot deconvolve the isotopic signal into its temperature and ice volume components; however, the fact that we observe similar benthic δ<sup>18</sup>O patterns in six different sites, located at different depths and in different ocean basins, suggests that these changes were at least partially controlled by compositional changes in the δ<sup>18</sup>O of sea water due to fluctuations in global ice volume.

Many authors have suggested an expansion of ice on Antarctica during the latest Miocene, including the development of the West Antarctic ice sheet<sup>8,20–24</sup>. Mercer suggested that ice rafting would abruptly increase its range as ice shelves and floating ice tongues first formed in the Antarctic, because tabular icebergs carry several orders of magnitude more load than do temperate outlet glaciers<sup>25</sup>. During the latest Miocene, the Antarctic Convergence moved northward by 300 km and the distribution of ice-rafterd detritus abruptly expanded equatorward<sup>22,23,26</sup>. For example, ice-rafterd detritus became conspicuous for the first time on the Falkland Plateau at 50°S in the Atlantic<sup>8</sup>. Drewry suggested that conditions suitable for the formation of the marine-based West Antarctic ice sheet did not occur until the late Miocene (4–5 Myr)<sup>21</sup>. Although the age of the Ross Sea disconformity is controversial, several authors suggest that it was formed during the late Miocene to early

Pliocene and indicates the presence of grounded ice in West Antarctica<sup>8,21</sup>.

Ciesielski *et al.* concluded that the sedimentary record of the Maurice Ewing Bank precludes the existence of a West Antarctic ice sheet or extensive ice shelves along the Antarctic margin before the late Miocene<sup>8</sup>. Widespread erosion of the Maurice Ewing Bank in the latest Miocene is inferred to have been caused by the first production of 'true' Antarctic Bottom Water (AABW)<sup>8</sup>, formed by the cooling of surface waters beneath the vast ice shelf that would have extended over much of West Antarctica in the latest Miocene, before the central part of the West Antarctic ice sheet had been grounded.

The mid-latitude history of Southern Hemisphere glaciation supports the general oxygen isotopic trends presented here. The earliest known tills from Argentine Patagonia are latest Miocene in age, and reflect glacial expansion beyond the Andean Mountain front<sup>27</sup>. This glacial evidence provides a minimum age for the initial growth of the West Antarctic ice sheet to the south of South America. The latest Miocene Patagonian glaciation is followed by an interglacial interval during the early Pliocene, and a renewed glacial advance at about 3.6 Myr.

The amplitude and frequency of δ<sup>18</sup>O changes, coupled with ancillary sedimentological and glaciological evidence, suggest that substantial changes occurred in global ice volume during the latest Miocene and early Pliocene. Three possible loci of ice growth and decay exist: East Antarctica, West Antarctica and the Northern Hemisphere. Part of the δ<sup>18</sup>O signal could reflect ice-volume instability resulting from periodic grounding and ungrounding of the West Antarctic ice sheet during the early stages of its formation. Even today the West Antarctic ice sheet is inherently unstable and highly susceptible to small changes in high-latitude summer temperatures<sup>28</sup>. Calculations show that formation of the West Antarctic ice sheet would not dramatically alter the oxygen isotopic composition of sea water because of its small volume ( $1.5\text{--}1.8 \times 10^6 \text{ km}^3$ ) and relatively high δ<sup>18</sup>O (~–20 to –30‰)<sup>8</sup>.

## The Messinian salinity crisis

We suggest a strong correspondence between the trends in the oxygen isotopic data and the deposition of the Messinian evaporites. Correlations between  $\delta^{18}\text{O}$  and evaporite deposition have also been discussed previously<sup>10,29</sup>. The Messinian evaporites were deposited during two discrete stages in late Chron 5 and earliest Gilbert<sup>15,30,31</sup>. The lower evaporite ('Main Salt') unit contains thick halite deposits associated with potassium salts. The great thickness ( $>1\text{ km}$ ) of salt implies a continuous supply of marine waters, and communication between the Mediterranean and the global ocean throughout much of the salinity crisis. Within the Main Salt unit, sedimentological evidence indicates many cycles of marine flooding and evaporative drawdown of water, followed by subaerial erosion<sup>30,31</sup>.

Towards the end of deposition of the Main Salt unit, the supply of brine from the Atlantic was probably cut off because of near-complete isolation of the Mediterranean<sup>30</sup>. This desiccation interval is represented by a widespread unconformity separating the lower and upper evaporite units, and included erosion and recycling of primary salts from the periphery of the basins. This erosional event was followed by an intra-Messinian transgression, when the Mediterranean may have been refilled to the brim<sup>30</sup>. Next, the upper evaporite unit was deposited, consisting of cyclic deposition of marls, stromatolitic carbonates, gypsum, anhydrites and salts. These cycles represent repetition of marine inundation, isolation and evaporative drawdown. Evaporite deposition ceased in the early Pliocene, when tectonic breakage of the dam at Gibraltar and a marine transgression refilled the Mediterranean, resulting in the restoration of deep-water pelagic sedimentation.

The similar character, timing and duration of trends in the oxygen isotopic data and the Messinian salinity crisis imply a causal relationship. The final isolation of the Mediterranean was controlled by long-term tectonic uplift of the western Mediterranean as well as rapid sea-level lowering during the latest Miocene<sup>3</sup>. The relatively high  $\delta^{18}\text{O}$  values in the younger normal event of Chron 5 record an ice-volume increase and eustatic sea-level fall that contributed to the isolation of the Mediterranean. The final connection between the Atlantic and the Mediterranean is believed to have been through the Betic Straits in southern Spain and/or Rif Straits in northern Morocco<sup>3</sup>. Berggren and Haq<sup>32</sup> proposed an abrupt drop in sea level of 50–70 m at 5.5 Myr from benthic foraminiferal assemblage changes in the Andalusian stratotype at Carmona, Spain. The isolation of the Betic Straits at 5.5 Myr coincides with the increase in  $\delta^{18}\text{O}$  values reported here at the base of the younger normal event of Chron 5 (5.6–5.5 Myr).

The lower and upper evaporite units are often separated by an unconformity marking near-complete desiccation of the basin. Marine marls overlie the unconformity in some sections,

and indicate an interval of marine transgression that partly or totally refilled the Mediterranean<sup>30</sup>. This intra-Messinian transgression may be represented by the relatively low  $\delta^{18}\text{O}$  values that occur near the Chron 5/Gilbert boundary in several sites (588, 397, 516A). Increased sampling resolution and examination of the palaeomagnetic stratigraphy of other high-quality sections are needed to confirm this suggested correlation.

Maximum  $\delta^{18}\text{O}$  values occur in the Lower Gilbert (5.1–4.8 Myr), which we correlate with the latest Miocene or uppermost Messinian. These high, variable  $\delta^{18}\text{O}$  values appear to coincide with the cyclic deposition of the upper evaporite unit. The high-frequency variation, superimposed on a lower-frequency component (400,000-yr period), may represent sea-level oscillations that controlled the flux of marine waters across the sills separating the Atlantic and the Mediterranean during the latest Miocene. Periodic inundation of marine waters into a largely desiccated Mediterranean resulted in the cyclic deposition of the upper evaporite unit. During the early Pliocene between ~4.8 and 4.1 Myr, all sites show a decrease in  $\delta^{18}\text{O}$  reflecting a strong interglacial or warming. The early Pliocene has been characterized as a time of global warmth<sup>4,33</sup>, and is transgressive in many shallow marine sequences throughout the world<sup>32,34</sup>. The decrease in  $\delta^{18}\text{O}$  in the early Pliocene coincides with termination of evaporite deposition and restoration of open-marine conditions in the Mediterranean.

As other authors have suggested<sup>1,2,3,11,29,30,35</sup>, we speculate that the isolation and desiccation of the Mediterranean during the latest Miocene was controlled, in part, by glacio-eustatic changes as recorded by benthic oxygen isotopic ratios. Latest Miocene–early Pliocene oxygen isotope records are marked by high-frequency changes that resemble Quaternary glacial-interglacial cycles. The amplitude is about one-third of the late Pleistocene signal, and the wavelength is ~400,000 yr. Increased  $\delta^{18}\text{O}$  values at the base of the younger normal event of Chron 5 coincide with a drop in sea level at 5.5 Myr, recorded in the Carmona Dos-Hermanos section in southern Spain<sup>32</sup>. This eustatic lowering is believed to have severed the final connection between the Atlantic and the Mediterranean, and permitted the onset of evaporite deposition. In some sites, a negative excursion in  $\delta^{18}\text{O}$  occurs near the Chron 5/Gilbert boundary between 5.2 and 5.1 Myr, and may correspond with an intra-Messinian transgression that temporarily refilled the Mediterranean. Maximum  $\delta^{18}\text{O}$  values occur in the Lower Gilbert between 5.1 and 4.8 Myr, and correspond with the deposition of the upper evaporite unit. The evaporites show evidence of distinct cyclicity, which may have been controlled by sea-level changes related to the waxing and waning of latest Miocene ice sheets<sup>2,11,29,30,35</sup>, as suggested by high-frequency  $\delta^{18}\text{O}$  changes. A rapid decrease in  $\delta^{18}\text{O}$  is evident at all sites during the early Pliocene at about 5.0 Myr, marking a glacial retreat and marine transgression that coincided with the termination of the salinity crisis and restoration of open-marine conditions in the Mediterranean.

Received 25 July 1985; accepted 11 February 1986.

1. Hsu, K. J., Cita, M. B. & Ryan, W. B. F. *Init. Rep. DSDP* 13, 1203–1231 (1973).
2. Ryan, W. B. F. in *Messianic Events in the Mediterranean* (ed. Drooger, C. W.) 26–38 (North-Holland, Amsterdam, 1973).
3. Adams, C. G. et al. *Nature* 269, 383–386 (1977).
4. Shackleton, N. J. & Kennett, J. P. *Init. Rep. DSDP* 29, 801–807 ((1975)).
5. Keigwin, L. D. Jr *Earth planet. Sci. Lett.* 45, 361–382 (1979).
6. Loutit, T. S. & Kennett, J. P. *Science* 204, 1196–1199 (1979).
7. Loutit, T. S. *Mar. Micropaleont.* 16, 1–27 (1981).
8. Ciesielski, P. F., Ledbetter, M. T. & Elwood, B. B. *Mar. Geol.* 46, 1–51 (1982).
9. Leonard, K. A., Williams, D. F. & Thunell, R. C. *Init. Rep. DSDP* 72, (1983).
10. Shackleton, N. J. & Cita, M. B. *Init. Rep. DSDP* 47, 433–445 (1979).
11. Cita, M. B. & Ryan, W. B. F. *Init. Rep. DSDP* 47, 447–459 (1979).
12. Elmstrom, K. M. & Kennett, J. P. *Init. Rep. DSDP* 90, 1361–1381 (1986).
13. Cita, M. B. in *Late Neogene Epoch Boundaries* (eds Tsunamasa, S. & Burckle, L. H.) 1–30 (Micropaleontology Press, New York, 1975).
14. Berggren, W. A., Kent, D. V. & Van Couvering, J. A. in *Geochronology and the Geological Record* (ed. Snelling, N. J.) (Geological Society of London, in the press).
15. Jenkins, D. G. & Srinivasan, M. S. *Init. Rep. DSDP* 90, 795–834 (1986).
16. McKenzie, J. A., Mueller, P. & Mueller, D. *Geol. Soc. Am. Abstr. Prog.* 17, 659 (1985).
17. Barton, C. E. & Bloemendal, J. *Init. Rep. DSDP* 90, 1273–1276 (1986).
18. Moore, T. C. Jr Pisias, N. G. & Dunn, D. A. *Mar. Geol.* 46, 217–233 (1982).
19. Hamilton, N. *Init. Rep. DSDP* 47, 463–477 (1979).
20. Kennett, J. P. N. Z. *J. Geol. Geophys.* 10, 1051–1063 (1967).
21. Drewry, D. J. in *Antarctic Glacial History and World Palaeoenvironments* (ed. Van Zinderen Bakker, E. M.) 25–32 (Balkema, Rotterdam, 1978).
22. Hayes, D. E. & Frakes, L. A. *Init. Rep. DSDP* 28, 919–942 (1975).
23. Plasker, G., Bartsch-Winkler, S. & Overshine, A. T. *Init. Rep. DSDP* 36, 857–867 (1977).
24. Mercer, J. H. A. *Rev. Earth planet. Sci.* 11, 99–132 (1983).
25. Mercer, J. H. in *Paleoecology of Africa*, Vol. 8 (ed. Van Zinderen Bakker, E. M.) 885–114 (Balkema, Rotterdam, 1973).
26. Kemp, E. M., Frakes, L. A. & Hayes, D. E. *Init. Rep. DSDP* 28, 909–917 (1975).
27. Mercer, J. H. & Sutter, J. F. *Paleogeogr. Paleoclimatol. Paleoecol.* 38, 185–206 (1982).
28. Mercer, J. H. *Nature* 271, 321–325 (1978).
29. McKenzie, J. A. & Oberhansli, H. in *South Atlantic Paleoceanography* (eds Hsu, K. J. & Weissert, H.) 99–123 (Cambridge University Press, 1985).
30. Hsu, K. J. et al. *Nature* 267, 399–403 (1977).
31. Hsu, K. J. et al. *Init. Rep. DSDP* 42, 1053–1077 (1978).
32. Berggren, W. A. & Haq, B. U. *Paleogeogr. Paleoclimatol. Paleoecol.* 20, 67–129 (1976).
33. Kennett, J. P. et al. *Am. J. Sci.* 279, 52–69 (1979).
34. Kennett, J. P. & Watkins, N. D. *Bull. geol. Soc. Am.* 85, 1385–1398 (1974).
35. Cita, M. B. & Ryan, W. B. F. *Riv. Ital. Paleont. Stratigr.* 84, 1051–1082 (1978).

# A new acute transforming feline retrovirus and relationship of its oncogene v-kit with the protein kinase gene family

Peter Besmer<sup>\*</sup>, John E. Murphy<sup>\*§</sup>, Patricia C. George<sup>\*§</sup>, Feihua Qiu<sup>\*</sup>, Peter J. Bergold<sup>\*</sup>, Lynn Lederman<sup>\*§</sup>, Harry W. Snyder Jr<sup>\*§</sup>, David Brodeur<sup>§</sup>, Evelyn E. Zuckerman<sup>‡</sup> & William D. Hardy<sup>‡</sup>

Laboratories of \* Molecular Oncology, † Viral Oncology and ‡ Veterinary Oncology, Graduate Program in Molecular Biology, Memorial Sloan-Kettering Cancer Center and Cornell University Graduate School of Medical Sciences, New York, New York 10221, USA

*A new acute transforming feline retrovirus, the Hardy-Zuckerman 4 feline sarcoma virus (HZ4-FeSV), has been isolated from a feline fibrosarcoma. The viral genome of HZ4-FeSV contains a new oncogene designated v-kit, has the structure 5' Δagag-kit-Δpol-Δenv 3' and specifies a gag-kit polyprotein of relative molecular mass 80,000. The predicted kit amino-acid sequence displays partial homology with tyrosine-specific protein kinase oncogenes. HZ4-FeSV appears to have been generated by transduction of feline c-kit sequences with feline leukaemia virus.*

VIRAL and non-viral oncogenes can be classified into four distinct groups according to their functional properties—protein kinases, GTPases, nuclear proteins and growth factors, the first of these groups being by far the largest. The functions of the normal cellular counterparts (*c-oncs*) are known for the oncogenes *sis*, *erb-B* and *fms*; the *v-sis* gene of the simian sarcoma virus and the Parodi-Irgens feline sarcoma virus (PI-FeSV) is the homologue of platelet-derived growth factor<sup>1-3</sup>, the *erb-B* protein of avian erythroblastosis virus (AEV) is homologous with the epidermal growth factor receptor<sup>4</sup>, and the *c-fms* protein is related to the receptor for the macrophage colony-stimulating factor CSF-1 (ref. 5). The current notion is therefore that *c-oncs* are components of signal transduction pathways. Many of the known oncogenes were discovered through their association with retroviruses. Oncogenes of acute transforming retroviruses (*v-oncs*) are acquired by transduction of *c-onc* sequences by retroviruses and have been isolated in several vertebrate species from neoplasms of retrovirus-infected animals. Some *v-oncs* have been found in multiple virus isolates of the same species while others have re-emerged in viruses isolated from different species, indicating that the pool of *c-oncs* which can be transduced by retroviruses is limited.

Feline leukaemia virus (FeLV) is transmitted horizontally between domestic cats and is associated with a wide spectrum of neoplastic and blastopenic diseases. Like other retroviruses, FeLV can transduce *c-onc* sequences<sup>6,7</sup>. The rare naturally occurring FeLV-associated feline multicentric fibrosarcomas have been a rich source of acute transforming retroviruses. Nine FeSV strains have been isolated from feline fibrosarcomas: Snyder-Theilen(ST), Gardner-Arnstein(GA), Susan McDonough(SM), Gardner-Rasheed(GR), PI, Theilen-Pederson(TP1) and Hardy-Zuckerman(HZ1 and HZ2)<sup>2,7-15</sup>. Five different oncogenes have been identified in these viruses—*v-fes*, *v-fms*, *v-fgr*, *v-abl* and *v-sis*—indicating that there is no particular specificity for the transduction of *c-oncs* by FeLV<sup>2,15-18</sup>. To investigate further the repertoire of proto-oncogenes that can be transduced by retroviruses, we have isolated and characterized another FeSV strain, the Hardy-Zuckerman 4 feline

sarcoma virus (HZ4-FeSV). This virus contains a unique oncogene, which we have designated *v-kit*, and the predicted *kit* amino-acid sequence displays partial homology with protein kinase oncogenes. We also describe the identification of FeLV *gag* sequences that are preferentially involved in the generation of acute transforming feline retroviruses.

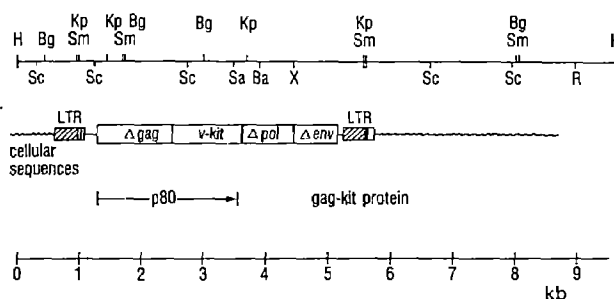
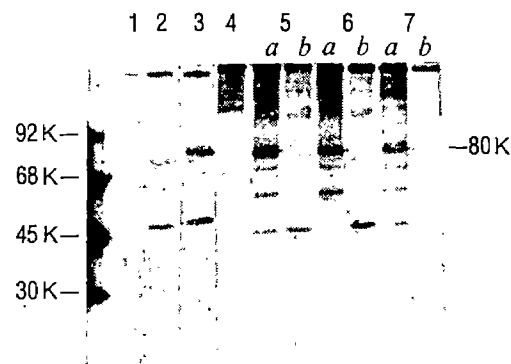
## Isolation of HZ4-FeSV

A 7-yr-old FeLV-infected male domestic cat (SKI 3637) with multiple fibrosarcomas was obtained from a pet household in St Louis, Missouri. The second digit of the right hind leg had been removed because of the presence of a solitary fibrosarcoma. A year after the initial surgery six fibrosarcomas recurred on the right hock and milliary metastases were present in the lungs. The FeLV isolated from the serum and from tumour tissue of cat 3637 was determined as belonging to subgroups A and B (ref. 19). Infection of feline embryo fibroblasts (FEA) and CCL64 mink cells with 0.8 μm filtrate obtained from a homogenate of one of the primary tumours produced distinct foci of transformed cells. Mink HZ4-FeSV virus non-producer cells were obtained from which transforming virus could be rescued by superinfection with amphotropic murine leukaemia virus (MuLV). This result indicated the replication-defective nature of the HZ4-FeSV. HZ4-FeSV non-producer mink cells display characteristic parameters of transformation, that is, they grow in soft agar and they induce fibrosarcomas in nude mice.

## Genetic structure of HZ4-FeSV

The structure of the integrated HZ4-FeSV provirus in the DNA of HZ4-FeSV-infected mink cells was first investigated by Southern blot analysis. A 9.6-kilobase (kb) *Hind*III restriction fragment, presumed to contain the entire HZ4-FeSV provirus, was identified using a FeLV hybridization probe (data not shown), and cloned using the λ vector Charon 30 (Fig. 1 legend). Figure 1A shows a restriction map of the integrated HZ4-FeSV provirus. Restriction fragments containing FeLV-related sequences were identified by hybridization of Southern blots with an FeLV *rep* probe and the genetic structure of the HZ4-FeSV provirus was confirmed by hybridization with probes specific for *gag* and *env* (data not shown). A *Sac*/*Sal* fragment of 0.75 kb (2.75–3.5 kb) was found to lack homology with FeLV sequences, indicating that this fragment contains the HZ4-FeSV *v-onc* sequences. We have designated the HZ4-FeSV-specific sequences *v-kit*. In agreement with the genetic structure of the HZ4-FeSV, a 4.5-kb genome RNA was detected in HZ4-FeSV.

§ Present addresses: Columbia University College of Physicians and Surgeons, New York, New York 10032, USA (J.E.M.); Worcester Foundation for Experimental Biology, Shrewsbury, Massachusetts 01545, USA (L.L.); Pacific Northwest Research Foundation, Seattle, Washington 98104, USA (H.W.S.); Cornell University Medical School, New York, New York, 10021, USA (P.C.G.); Duke University Medical School, Durham, North Carolina 27710, USA (D.B.).

**A****B**

**Fig. 1** Genetic structures of the HZ4-FeSV genome. **A**, Restriction map and genetic structure of the molecularly cloned HZ4-FeSV provirus. The restriction enzymes used to construct this map were EcoRI (R), HindIII (H), SacI (Sc), SmaI (Sm), KpnI (Kp), BglII (Bg), SalI (Sa) and XbaI (X). **B**, Identification of HZ4-FeSV translation product and determination of their immunological relationship with v-fes and v-fms protein products. Extracts of cells labelled with  $^3\text{H}$ -leucine were immunoprecipitated and analysed by SDS-PAGE essentially as described previously<sup>15</sup>. Lane 1, mink CCL64 cells; lanes 2-7, 6B2 HZ4-FeSV mink cells. Lanes 1, 3, rabbit anti-FeLV-p27 serum; lane 2, normal rabbit serum; lanes 5a, b, goat anti-ST-FeSV serum; lanes 6a, b, goat anti-GA-FeSV serum; lanes 7a, b, goat anti-SM-FeSV and serum; lane 4, normal goat serum. The goat sera were used either unabsorbed (lanes 5a, 6a, 7a) or after absorption with excess detergent-disrupted FeLV-A and -B (lanes 5b, 6b, 7b) in order to render them fms- and fes-specific<sup>13</sup>.

**Methods.** The  $\lambda$  phages were grown in *Escherichia coli* K802 and LE392 and their DNA was prepared according to standard procedures. Plasmids were grown in *E. coli* HB101. Plasmid DNAs were prepared essentially according to the cleared lysate method or the SDS-lysis procedure and centrifugation in CsCl-ethidium bromide gradients. Partial library cloning: A partial genomic library of HZ4-FeSV mink non-productive DNA was constructed using the  $\lambda$  vector Charon 30 (ref. 47). HZ4-FeSV mink non-productive cell DNA (150  $\mu\text{g}$ ) was digested with the restriction enzyme HindIII and then fractionated in a salt/sucrose gradient as described elsewhere<sup>47</sup>. The fractions containing the HZ4-FeSV provirus were identified by Southern blot analysis using an FeLV rep hybridization probe. The HZ4-FeSV 9.6-kb DNA fraction was ligated into  $\lambda$  Charon 30 HindIII arms, then packaged *in vitro* to generate viable phage particles. The partial library was screened for FeLV sequences using the method of Benton and Davies with an FeLV rep hybridization probe<sup>47</sup>. The insert of the  $\lambda$  HZ4-FeSV was subcloned into the unique HindIII site of pBR322. Hybridization probes: the entire insert of the plasmid FeLV-B and a 1.0-kb restriction fragment containing 1.13-2.1 kb of the FeLV-B restriction map were used as a FeLV rep and a 5' gag probe, respectively<sup>2</sup>.  $^{32}\text{P}$ -labelled probes were prepared by nick-translation as described previously<sup>11</sup>.

**Fig. 2** Nucleotide sequence of the HZ4-FeSV gag-kit gene. The complete nucleotide sequence of the gag-kit gene sequence was determined by the dideoxynucleotide chain termination method of Sanger following subcloning of fragments into the M13 vectors mp18 and mp19 (refs 22, 49). The predicted amino-acid sequence of the only long open reading frame is shown above using single-letter amino-acid notations. The numbers at the end of each line refer to nucleotides with position +1 defining the beginning of the gag gene. The nucleotides determining the 74-amino-acid gag leader have been assigned negative numbers as proposed by Hampé *et al.*<sup>17</sup>. Junctions between the gag proteins p15, p12 and p30 are indicated as well as the 5' and 3' boundaries of the v-kit sequences. The v-kit nucleotide sequence was determined on both strands and all restriction sites were crossed; the gag nucleotide sequence, on the other hand, was determined at least on one strand. The 5' recombination site between gag and kit sequences was deduced by comparison of the gag-kit sequence with that of the known FeLV gag sequence<sup>17,23</sup>. To determine the 3' recombination site between v-kit and FeLV pol, the gag-kit sequence was compared with the sequence of the GA-FeLV pol gene (*Sma/Kpn* fragment, 4.9-5.1 kb of the GA-FeLV map). The nucleotide sequence of the GA-FeLV *Sma/Kpn* pol fragment was determined on both strands.

Figure 2 presents the nucleotide sequence of the HZ4-FeSV gag-kit gene. The sequence is shown in two strands, top and bottom, with amino-acid translations above the top strand. The sequence starts with a gag leader (negative numbers) and then continues with the gag and v-kit genes. The sequence is aligned with the GA-FeLV pol gene sequence for comparison. The 5' and 3' recombination sites are indicated, along with the 5' and 3' boundaries of the v-kit sequences. The sequence ends with a poly-A tail.

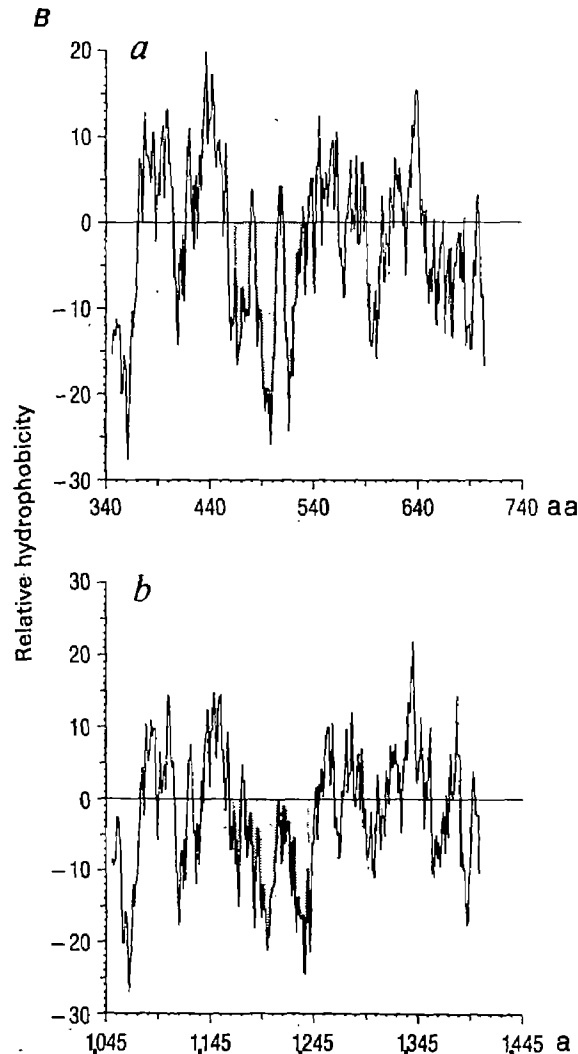
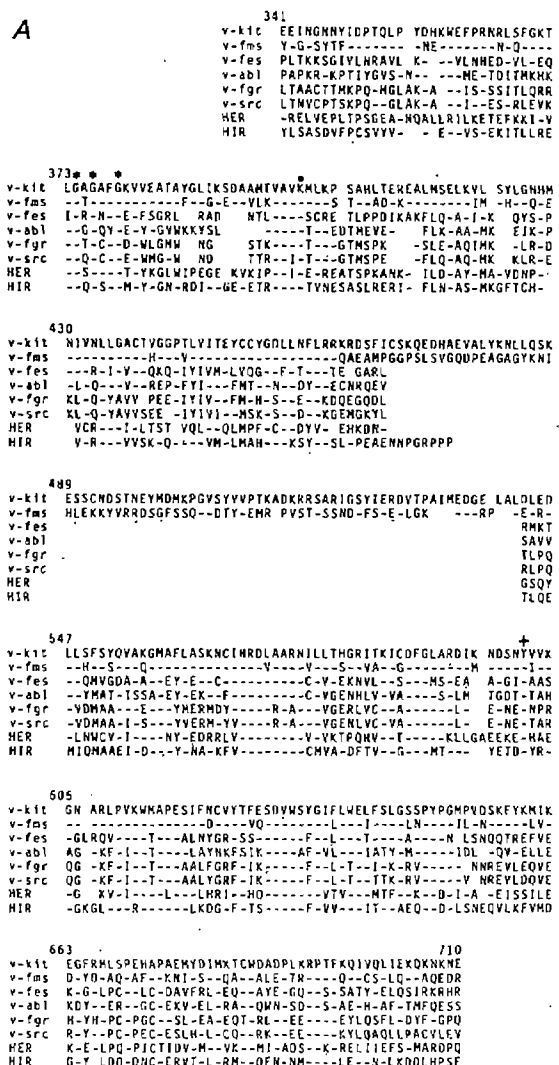


**Fig. 3** Comparison between sequences of *v-kit* and tyrosine kinase. *A*, The predicted *v-kit* amino-acid sequence (amino acids 341–370) is compared with that of the tyrosine kinase genes *v-fms*, *v-fes*, *v-abl*, *v-fgr*, *y-sr*, HER and HIR. The amino-acid alignment was adapted from Ullrich *et al.*<sup>27</sup> with minor modifications. Amino-acid identities are indicated by a dash and gaps as empty space. The sequence signatures of the nucleotide-binding domain GXGXXG at amino acid 374 and Lys 401 are indicated by a star and a solid circle, respectively. Tyr 601 in the phosphorylation domain is indicated by +. *B*, Hydrophobicity analysis of *v-kit* (*a*) and *v-fms* (*b*). The method of Kyte and Doolittle was used with a window of 11 amino acids (aa)<sup>31</sup>. The shaded areas indicate the non-homologous middle domain of *v-kit* and *v-fms*.

infected mink cells that hybridized with FeLV and *kit* hybridization probes (data not shown).

To identify HZ4-FeSV-encoded proteins in HZ4-FeSV-infected mink cells, extracts of metabolically labelled cells were immunoprecipitated with antisera specific for the FeLV structural proteins, and then analysed by polyacrylamide gel electrophoresis (PAGE). The only protein detected was a polypeptide of relative molecular mass ( $M_r$ ) 80,000 (80K), designated p80, which was precipitated with antisera specific for the FeLV gag protein, p27. The genetic structure of the HZ4-FeSV provirus (Fig. 1B) predicts that the p80 protein is composed of both gag and kit sequences.

On transfection of NIH 3T3 mouse cells, the cloned HZ4-FeSV provirus induced foci of transformed cells with an efficiency of  $\sim 10^4$  focus-forming units (FFU) per pmol (ref. 20). Focus-forming virus could be obtained from the transformants by superinfection with amphotropic MuLV ( $10^3$ - $10^4$  FFU ml $^{-1}$ ), indicating that the cells contained the entire provirus. The morphology of the foci of transformed cells obtained by transfection with the pHZ4 DNA was indistinguishable from foci induced by HZ4-FeSV (amphotropic MuLV) pseudotype virus on NIH 3T3 cells (data not shown).

v-kit and protein-tyrosine kinase genes

The relationship between the HZ4-FeSV *v-kit* sequences and those of the known avian and mammalian retroviral oncogenes was determined by hybridizing Southern blots containing the DNA of 18 different oncogenes with  $^{32}$ P-labelled HZ4-FeSV DNA. No homology was found between HZ4-FeSV sequences and sequences of the oncogenes *h-ras*, *k-ras*, *n-ras*, *myc*, *myb*, *ski*, *fos*, *sis*, *src*, *yes*, *ros*, *abl*, *mos*, *fes*, *erb-A*, *erb-B*, *rel* or *raf* (ref. 21). However, a weak hybridization signal was detected with the 1.6-kb *Kpn*/*Bgl*III *v-fms* restricting fragment, although this hybridization was lost on washing at 65 °C in 0.2 × SSC. As both *v-fms* and the HZ4-FeSV *v-kit* sequences are of feline origin, this indicates that HZ4-FeSV does not contain feline *v-fms* sequences. Furthermore, hybridization of blots containing HZ4-FeSV DNA with *v-fms* hybridization probes demonstrated that this homology included sequences of the *v-fms* kinase domain (not shown). Analysis of the immunological relationship between *v-kit* and *v-fms* by immunoprecipitation and SDS-PAGE revealed no immunoprecipitation with a polyclonal *fms*-specific antiserum, indicating that this reagent does not recognize determinants shared by *v-kit* and *v-fms* (Fig. 1*b*).

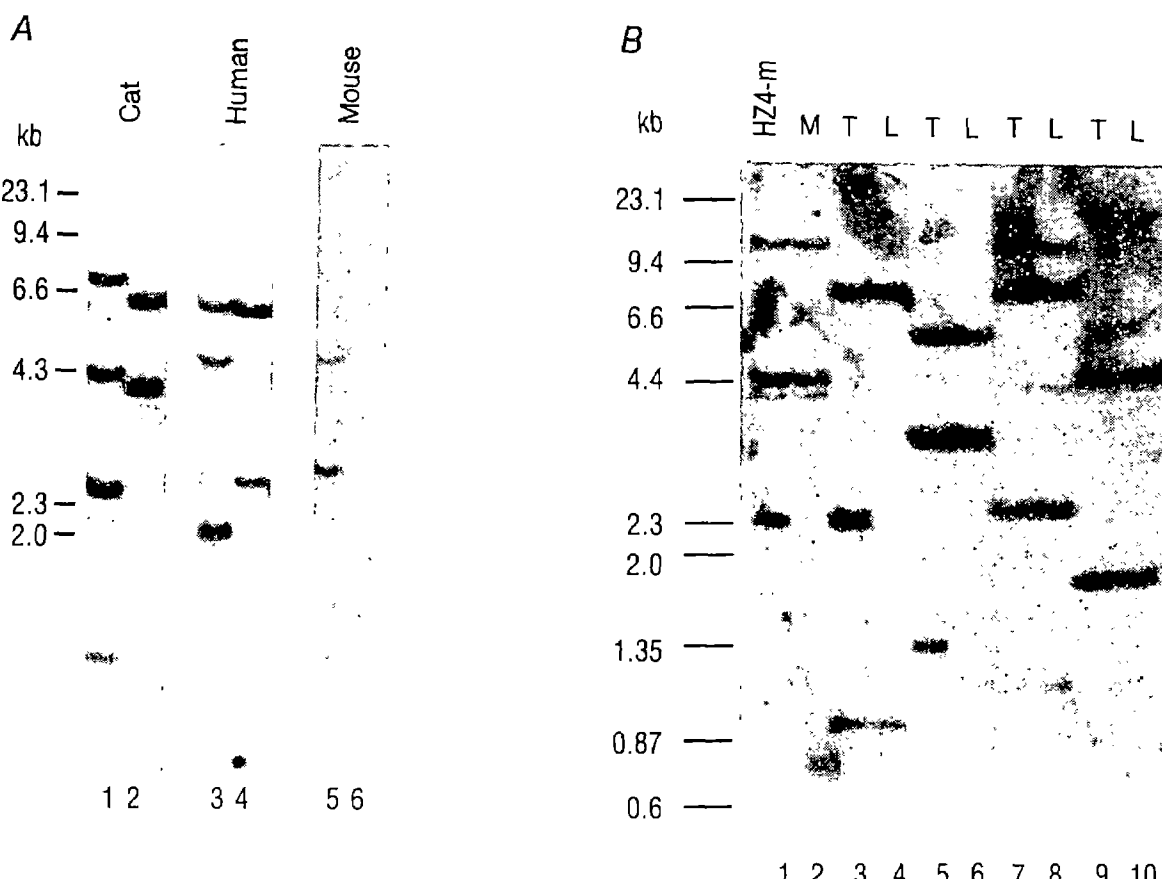


**Fig. 4** *kit* sequences in normal DNA and in DNA from the tumour of cat 3637. **A**, Identification of *c-kit* sequences in normal mammalian DNAs. DNA from the kidney of cat 3590 was prepared from frozen tissue. The tissue (1 g) was homogenized in a Vitris homogenizer in TNE (10 mM Tris pH 8.0, 100 mM NaCl, 10 mM EDTA), nuclei were isolated by differential centrifugation and DNA was prepared from the nuclei as described previously<sup>2</sup>. Aliquots (10 µg) of cat 3590 DNA, NIH 3T3 mouse DNA and human DNA (acute lymphocytic leukaemia line T-ALL-1) were digested with the restriction enzymes *Eco*RI (lanes 1, 3, 5) and *Hind*III (lanes 2, 4, 6) and fractionated in a 1% agarose gel. A Southern blot containing these DNAs was hybridized with a <sup>32</sup>P-labelled v-*kit* probe (2.75–3.5-kb *Sac*/*Sal* fragment) using non-stringent hybridization conditions. Blots were washed at 65 °C in 2×SSC. Migration of *Hind*III λ DNA fragments is indicated in kb. **B**, Identification of the HZ4-FeSV provirus in tumour DNA of cat 3637. DNA was prepared from tumour tissue (T) and from the liver (L) of cat 3637 and digested with restriction enzymes *Sac*I (lanes 9, 10), *Eco*RI (lanes 7, 8), *Bgl*II (lanes 5, 6) and *Kpn*I (lanes 3, 4), and DNA from HZ4-FeSV-infected (HZ4-m) and from uninfected mink cells (M) was digested with *Kpn*I (lanes 1, 2). Southern blots obtained after fractionation of these DNAs in a 1% agarose gel were hybridized with a <sup>32</sup>P-v-*kit* probe (2.75–3.5-kb *Sac*/*Sal* fragment). The blot was washed at 65 °C in 0.3×SSC. Migration of *Hind*III λ DNA and *Hae*III ΦX174 DNA fragments is indicated in kb.

Figure 2 shows the nucleotide sequence of the HZ4-FeSV *gag-kit* gene, determined using the dideoxy chain termination method of Sanger *et al.*<sup>22</sup>. An open reading frame extends from nucleotides -222 to 2,130 which includes 410 amino acids of FeLV *gag* origin, 370 amino acids of *kit* origin and 8 amino acids derived from the *pol* gene. To determine the 5' and 3' recombination sites between FeLV and *kit*, the *gag-kit* sequence was compared with the known FeLV *gag* sequence<sup>17,23</sup>, a segment of FeLV *pol* and Moloney (M) MuLV *pol* sequences (Fig. 2). The 3' recombination site in FeLV *pol* corresponds to M-MuLV *pol* sequences 1.18 kb 5' of the *pol-env* junction<sup>21</sup>.

ST-, GA- and SM-FeSV as well as ST-FeLV encode *gag* leader sequences<sup>17,23</sup>. However, only with SM-FeSV is this sequence thought to be of importance in the biosynthesis of the transforming protein. The predicted amino-acid sequence of *gag-kit* includes the FeLV *gag* leader, a stretch of 70 amino acids containing a hydrophobic signal peptide. The *gag-kit* protein is not glycosylated and probably does not include the leader sequence (H.W.S., unpublished). Therefore, initiation of translation may occur at the ATG at the beginning of the p15 gene at nucleotide 1.

The non-glycosylated *gag* gene products in FeLV are synthesized as a polyprotein of  $M_r$  65K with the structure NH<sub>2</sub>-p15-p12-p30-p10-COOH, which is post-translationally processed

into the individual peptides<sup>24</sup>. The *gag*-derived segment of the HZ4-FeSV *gag-kit* protein consists of 340 amino acids, containing the total sequences of p15 and p12 but only 144 residues of p30. Compared with the sequences of ST-, GA- and SM-FeSV, the HZ4-FeSV *gag* sequences are slightly polymorphic, an unsurprising finding in view of the fact that all known FeSVs originate from naturally occurring tumours in pet cats.

The v-*kit* segment consists of 1,111 nucleotides. The open reading frame extends beyond the *kit* segment into the *pol* gene, where a TGA termination codon is reached 18 nucleotides 3' of the recombination site. The calculated  $M_r$  of 81.5K for the *gag-kit* polyprotein is in good agreement with the observed  $M_r$  80K.

Comparison of the predicted v-*kit* amino-acid sequences with the known tyrosine-specific protein kinases (Fig. 3A) reveals good amino-acid homology between the v-*fms* sequences<sup>17</sup> and v-*kit* (58% overall homology), particularly between amino acids 349–462 and 544–659. On the other hand, there is no obvious homology within amino acids 463–540. Homology also exists, although to a lesser extent, between v-*kit* and v-*fes*, v-*abl*, v-*fgr*, v-*src*, human epidermal growth factor receptor (HER) and human insulin receptor (HIR)<sup>16,18,25–28</sup>. Lysine 401 as well as the configuration GXGXXG at amino acid 374 are characteristic of the nucleotide-binding domain of tyrosine-specific protein

## ARTICLES

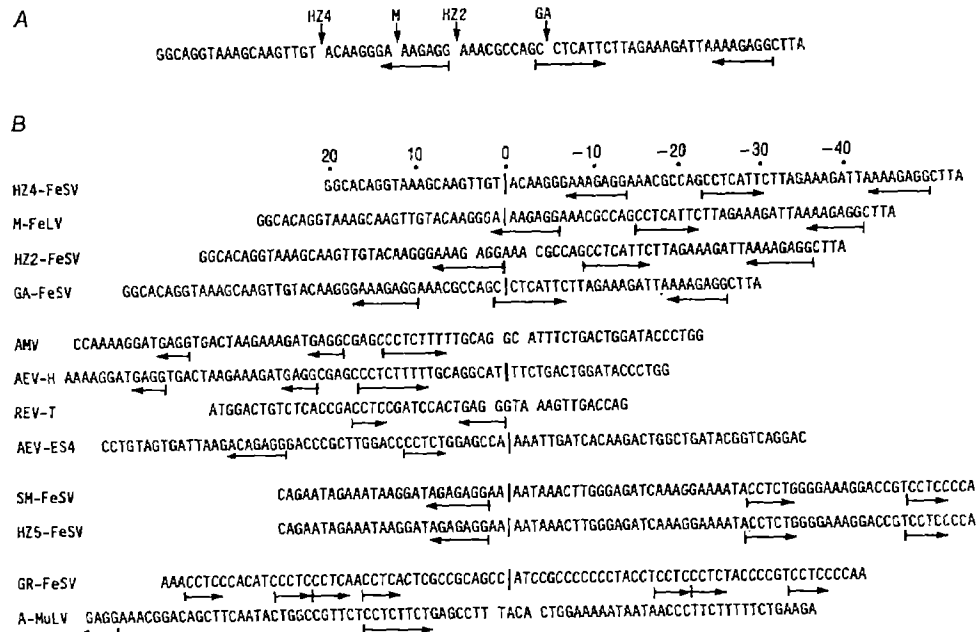


**Fig. 5** Region of preferred 5' recombination sites in the FeLV gag p30 gene. **A**, The gag sequence shown is that found in GA-FeSV and SM-FeSV corresponding to nucleotides 1,568–1,638 (refs 23 and 17, respectively). The AAAGAGG sequence is indicated as ←, and the sequence CCTCTT as →. **B**, GAGG and CCTC consensus sequences at 5'-recombination sites in acute transforming viruses. The retrovirus sequences at 5' recombination sites of the viruses indicated below are aligned. Homologies of retrovirus and c-onc sequences at the recombination site are set off by a space (for example, as in HZ2-FeSV). GAGG and CCTC consensus sequences are indicated as in **A**. The sequences at the 5' recombination site of the following viruses are shown: HZ4-FeSV (this paper), M-FeLV<sup>32</sup>, HZ2-FeSV (this paper), GA-FeSV<sup>16</sup>, SM-FeSV<sup>17</sup>, HZ5-FeSV (this paper), GR-FeSV<sup>18</sup>, Abelson murine leukaemia virus (A-MuLV)<sup>25</sup>, AMV<sup>36</sup>, AEV-H<sup>48</sup> and reticuloendotheliosis virus T (REV-T).

kinases<sup>29,30</sup>. Furthermore, Tyr 601 is the homologue of the tyrosine phosphorylation site 416 of the Rous sarcoma virus v-src protein. Thus, v-kit has all the known structural features of a tyrosine-specific protein kinase. Attempts to identify a gag-kit-associated kinase activity have so far failed, and our structural analysis of kit suggests that this question should be investigated more carefully. The segment containing amino acids 468–542 does not have a counterpart in v-fes, v-abl, v-fgr, v-src, v-yes, HER or HIR, and this is consistent with the interpretation that the nucleotide-binding domain (amino acids 349–462) and the segment containing the phosphorylation site 601 (544–660) are separate functional domains. The corresponding middle domain of v-fms shows no significant amino-acid homology to v-kit, although the v-kit and v-fms middle domains are similarly hydrophilic in nature (Fig. 3B)<sup>31</sup>. It seems likely, then, that these domains are exposed at the exterior surface of the v-kit and v-fms proteins in the cytoplasm. As the middle domains of v-kit and v-fms are embedded between their catalytic domains, they may mediate substrate recognition and thus provide specificity for c-kit- and c-fms-mediated signal transduction.

### Identification of c-kit in cellular DNA

Cellular DNA sequences homologous with the v-kit sequences of HZ4-FeSV were investigated by blot hybridization (Fig. 4A). In normal cat DNA, the v-kit probe (*Sac/Sal*, 0.7 kb) detected EcoRI and HindIII restriction fragments of 7.7, 4.3, 2.4, 1.2 kb and of 6.5, 4.0, 2.0 kb (weak signal, respectively). Human and mouse DNA shows a pattern of hybridization similar to that of cat DNA, the hybridization signal with human DNA being of almost equal intensity to the cat DNA restriction fragments. In contrast, hybridization to mouse DNA is somewhat weaker. These results suggest that there are cellular sequences in normal cat DNA which are homologous to v-kit and that these c-kit sequences are conserved in mammalian genomes. Hybridization of the kit probe detected restriction fragments corresponding to 12–15 kb of DNA, suggesting that c-kit is a large gene or perhaps that the c-kit sequences are derived from multiple loci.

### Origin and oncogenic potential of HZ4-FeSV

To investigate the origin of HZ4-FeSV and its role in the generation of the fibrosarcoma in cat 3637, we used blot hybridization to determine whether the HZ4-FeSV provirus was contained in the tumour DNA (Fig. 4B). In both tumour and normal DNAs, the v-kit probe detected restriction fragments derived from c-kit and, using *Kpn*I and *Bgl*II, tumour-specific fragments of 2.3 and 1.3 kb, respectively, were seen. These fragments are virus internal fragments known from the molecularly cloned HZ4-FeSV provirus (Fig. 1). No tumour-specific restriction fragments were seen with enzymes known to generate fragments involving flanking cellular DNA sequences (*Eco*RI, *Sac*I, a second *Bgl*II fragment of large size would also be expected). The DNA from the tumour of cat 3637 therefore contains the HZ4-FeSV provirus. This not only demonstrates the origin of the virus, but is also consistent with the notion that HZ4-FeSV was involved in the generation of this tumour, although attempts to induce tumours by injection of kittens with HZ4-FeSV (FeLV) pseudotype virus have so far been unsuccessful. Our results also indicate that the tumour is polyclonal, presumably due to virus spread. If tumorigenesis in cat 3637 involved multiple stages, with HZ4-FeSV as an initiator, this did not result in visible clonal outgrowth, as has been seen in other systems<sup>51,52</sup>. However, the virus could have been involved in a late stage of tumorigenesis.

### Preferred recombination site in FeLV gag

The 5' junction between the FeLV and kit sequences in HZ4-FeSV occurs at nucleotide 1,020 of the FeLV gag gene<sup>1,23</sup>. Comparison of this junction with those in GA-FeSV, HZ2-FeSV and the M-FeLV myc virus<sup>16,32</sup> revealed that the 5' recombination sites of these four viruses are clustered within a region of 24 bp in the FeLV gag gene (Fig. 5A). This 24-bp region in FeLV p30 therefore defines a preferred region for recombination which is involved in the generation of acute transforming feline retroviruses.

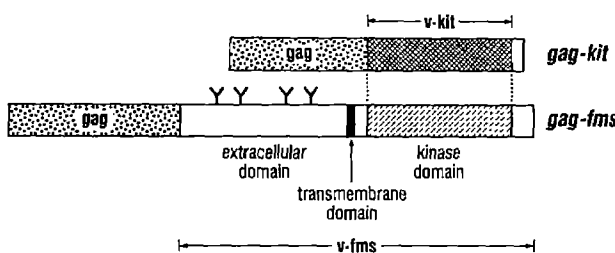


Fig. 6 Schematic comparison of the *gag-kit* and *gag-fms* transforming proteins. Glycosylation sites in the extracellular domain of *v-fms* are indicated by Y.

It seemed possible that the sequences in the FeLV p30 region facilitate the generation of the 5' *gag-onc* junctions and we therefore inspected the nucleic acid sequence around the recombination sites in FeLV p30 to identify sequence motifs characteristic of this region. A heptanucleotide AAAGAGG occurs twice, at nucleotides 1,026 and 1,064, and the complement of this sequence (CCTC(T)TT) occurs once, at nucleotide 1,042, indicating sequence symmetry and potential for secondary structure formation (Fig. 5A). The GAGG and CCTC consensus sequences are found at the 5' junctions of at least 16 of the 28 characterized virus strains, suggesting some link between this sequence and the recombination event (Fig. 5B). Of these viruses, AEV-H and avian myeloblastosis virus (AMV) have junctions that are 2 nucleotides apart and HZ5-FeSV, a new *fms*-containing virus, and SM-FeSV have identical junctions (P.B. and P.C.G., unpublished) (Fig. 5B). In plasmacytomas involving *c-myc* chromosomal translocations, the GAGG sequence motif has been found adjacent to the translocation breakpoints<sup>33</sup>. Thus, events leading to the generation of oncogene-containing retroviruses and chromosomal translocations may involve common recombination mechanisms.

With many acute transforming viruses, the recombinations at the 5' retrovirus-v-onc junctions must result in functional gene fusions, and constraints for expression and function of the transforming proteins may dictate the formation of these junctions. On the other hand, recombination sites in *gag-onc* fusions are known to occur in various regions of the *gag* gene, and *in vitro* alteration of the placement of *onc* sequences within retroviruses can be achieved without loss of function<sup>34,35</sup>. In addition, the recombinations in HZ4-, HZ2- and GA-FeSVs and in M-FeLV involve four different oncogenes. Our observations therefore suggest that the formation of 5' *gag-onc* junctions, which is an early step in the generation of acute transforming viruses<sup>36,37</sup>, may be facilitated by at least two factors, recombinogenic sequences and short sequence homologies between the parental strands at the recombination site described previously<sup>38</sup>.

## Discussion

The present studies demonstrate that HZ4-FeSV is an acute transforming feline retrovirus which, in analogy with other acute transforming viruses, was generated by transduction of feline *c-onc* sequences (which we have designated *kit*). HZ4-FeSV has the structure 5' Δ*gag-kit*-Δ*pol*-Δ*env* 3', and the only gene product we have identified in HZ4-FeSV-infected cells is an 80K protein that contains determinants of FeLV *gag* p15, p12 and p30 as well as *kit* sequences. The *v-kit* amino-acid sequences revealed homology with the tyrosine kinase gene family, its closest relative being *v-fms*.

The *kit* gene resembles *v-fms* not only in significant amino-acid homology, but also in the very distinct domain structure of the protein. *v-fms* has recently been found to have the features of a transmembrane receptor, that is, it consists of an outer cellular domain, a transmembrane domain and an inner cellular domain containing a tyrosine-specific protein kinase; in fact, it

is homologous with the CSF-1 receptor<sup>39,40</sup>. The *v-fms* sequence is 2.9 kb long, while *v-kit* is 1.1 kb. The *v-kit* segment corresponds to *v-fms* sequences of the inner cellular domain, and does not contain a transmembrane domain or sequences of an outer cellular domain. Retroviral oncogenes are thought to represent segments of *c-onc* mRNAs, and it is likely that *v-kit* is only a part of the *c-kit* mRNA; significant portions of *c-kit* coding sequences are probably missing in *v-kit* on both the 5' and 3' sides, although the nature of these sequences is not known. Because of the close relationship between *v-kit* and *v-fms*, it is reasonable to assume that *c-kit* and *c-fms* are closely related genes. Like *c-fms*, then, *c-kit* could encode a transmembrane receptor that is involved in signal transduction.

Most protein kinase oncogenes need to be associated with cellular membranes for function<sup>41,42</sup>, and two different kinds of association are known, association via myristic acid<sup>43</sup> and anchorage in membranes by means of a transmembrane domain<sup>39</sup>. The 65K *gag* polyprotein of mammalian retroviruses and the *gag-onc* fusion proteins of mammalian acute transforming viruses are myristylated at their N-terminus and are thus associated with cellular membranes<sup>44</sup>. As *v-kit* does not have a transmembrane domain like *v-fms*, we predict that, in analogy with other *gag-onc* transforming proteins, the *gag-kit* protein is associated with cellular membranes via *gag*-linked myristylation.

Many different oncogenes have been identified in acute transforming viruses isolated from fibrosarcomas of animals infected by retroviruses. Interestingly, the oncogenes *src*, *yes* and *ros* known from avian retroviruses have not been found in mammalian retroviruses. *kit*, *fms* and *fgr*, on the other hand, have been found only in viruses isolated from feline fibrosarcomas. This inherent specificity of transduction of *c-ons* by FeLV may be due to recombinogenic sequences in the retrovirus and the *c-ons*, as well as functional constraints for the expression of the transforming proteins. It has been proposed that integration of a retrovirus into the cellular DNA may be restricted to transcriptionally active regions of the chromosome<sup>45,46</sup>. Thus, the tissue tropism of a particular virus strain would determine the *c-ons* that can be transduced. Different tissue tropisms of FeLV and avian leukosis virus could therefore also explain the different transduction specificities.

We thank O. Jarrett for the FeLV subgroup determinations; C. Sherr, K. C. Robbins, U. Rapp, I. Verma, S. P. Goff, D. Dina, M. Wigler, R. Ellis, J. M. Bishop, H. Temin and M. Yoshida for DNA reagents used in this study; E. Stavnezer and L. H. Wang for providing unpublished reagents; C. Payne for preparation of numerous plasmids; M. S. Lee for help with the analysis of the tumour DNA; and M. Singhal, K. Brown and R. Markovich for technical assistance. This work was supported by grants from the American Cancer Society (MV-82) and the NIH (CA-32926) to P.B. and (CA-16599) to W.D.H. and H.W.S. H.W.S. was a Scholar of the Leukemia Society of America. P.J.B. was a Horsfall awardee.

Received 16 October 1985; accepted 13 January 1986.

1. Devare, S. G. et al. *Proc. natn. Acad. Sci. U.S.A.* **79**, 3179–3182 (1982).
2. Besmer, P., Snyder, H. W. Jr., Murphy, J. E., Hardy, W. D. Jr & Parodi, A. J. *Virology* **46**, 606–613 (1983).
3. Waterfield, M. D. et al. *Nature* **304**, 35–39 (1983).
4. Downard, J. et al. *Nature* **307**, 521–527 (1984).
5. Sherr, C. J. et al. *Cell* **41**, 665–676 (1985).
6. Hardy, W. D. Jr, Old, L. J., Hess, P. W., Essex, M. & Cotter, S. *Nature* **244**, 266–269 (1973).
7. Besmer, P. *Curr. Topics Microbiol. Immunol.* **107**, 1–27 (1984).
8. Snyder, S. P. & Theilen, G. H. *Nature* **221**, 1074–1075 (1969).
9. Gardner, M. B. et al. *Nature* **226**, 807–809 (1970).
10. McDonough, S. K., Larsen, S., Brodsky, R. S., Stock, W. D. & Hardy, W. D. Jr *Cancer Res.* **31**, 953–956 (1971).
11. Irgens, K., Wyers, M., Morailion, A., Parodi, A. & Fortuny, V. *C. r. hebdo. Séanc. Acad. Sci., Paris* **276**, 1783–1786 (1973).
12. Rasheed, S., Barabid, M., Aaronson, S. A. & Gardner, M. B. *Virology* **117**, 238–244 (1982).
13. Snyder, H. W., Singhal, M. C., Zuckerman, E. E. & Hardy, W. D. *Virology* **132**, 205–210 (1984).
14. Ziemięcki, A. et al. *Virology* **138**, 324–331 (1984).
15. Besmer, P., Hardy, W. D. Jr, Zuckerman, E., Lederman, L. & Snyder, H. S. *Nature* **303**, 825–828 (1983).

## LETTERS TO NATURE

16. Hampe, A., Laprevotte, I., Galibert, F., Fedele, L. A. & Cherr, C. J. *Cell* **30**, 775-785 (1982).
17. Hampe, A., Gobet, M., Sherr, C. J. & Galibert, F. *Proc. natn. Acad. Sci. U.S.A.* **81**, 85-89 (1984).
18. Naharro, G., Robbins, K. C. & Reddy, E. P. *Science* **223**, 63-66 (1984).
19. Sarma, P. S. & Log, T. *Virology* **54**, 160-169 (1973).
20. Graham, E. L. & van der Eb, A. J. *Virology* **52**, 456-467 (1973).
21. Weiss, R., Teich, N., Varmus, H. & Coffin, J. *Molecular Biology of Tumor Viruses* (Cold Spring Harbor Laboratory, New York, 1982).
22. Sanger, F., Nicklen, S. & Coulson, A. R. *Proc. natn. Acad. Sci. U.S.A.* **74**, 5463 (1977).
23. Laprevotte, I., Hampe, A., Sherr, C. J. & Galibert, F. *J. Virol.* **50**, 884-894 (1984).
24. Okazinski, G. F. & Velicer, L. F. *J. Virol.* **22**, 74-85 (1977).
25. Reddy, E. P., Smith, M. J. & Srinivasa, A. *Proc. natn. Acad. Sci. U.S.A.* **80**, 3623-3627 (1983).
26. Schwartz, D. E., Tizard, R. & Gilbert, W. *Cell* **32**, 853-869 (1983).
27. Ulrich, A. *et al.* *Nature* **313**, 756-761 (1985).
28. Ulrich, A. *et al.* *Nature* **309**, 418-425 (1984).
29. Wierenga, R. K. & Hol, W. G. T. *Nature* **302**, 842-844 (1983).
30. Zoller, M. J., Nelson, N. C. & Taylor, S. S. *J. biol. Chem.* **256**, 10837-10842 (1981).
31. Kyte, J. & Doolittle, R. F. *J. molec. Biol.* **157**, 105-132 (1982).
32. Braun, M. J., Deininger, P. L. & Casey, J. W. *J. Virol.* **55**, 177-183 (1985).
33. Piccoli, S. P., Caimi, P. G. & Cole, M. D. *Nature* **310**, 327-330 (1984).
34. Foster, D. A. & Hanafusa, H. *J. Virol.* **48**, 744-751 (1983).
35. Prywes, R., Hoag, T., Rosenberg, N. & Baltimore, D. *J. Virol.* **54**, 123-132 (1985).
36. Klempnauer, K.-H., Gonda, T. J. & Bishop, J. M. *Cell* **31**, 453-463 (1982).
37. Goldfarb, M. & Weinberg, R. J. *J. Virol.* **38**, 136-150 (1981).
38. Wang, J. Y. J. *et al.* *Cell* **36**, 349-356 (1984).
39. Rettenmier, C. W. *et al.* *Cell* **40**, 971-981 (1985).
40. Manger, R., Najita, L., Nichols, E. J., Hakomori, S.-I. & Rohrschneider, L. *Cell* **39**, 327-337 (1984).
41. Peilman, D., Garber, E. A., Cross, F. R. & Hanafusa, H. *Nature* **314**, 374-377 (1985).
42. Roussel, M. F., Rettenmier, C. W., Look, A. T. & Sherr, C. J. *Mol. Cell Biol.* **4**, 1999-2009 (1984).
43. Schultz, A. M., Henderson, L. E., Oroszlan, S., Garber, E. A. & Hanafusa, H. *Science* **227**, 427-429 (1985).
44. Schultz, A. M. & Oroszlan, S. *J. Virol.* **46**, 355-361 (1983).
45. Breindl, M., Habers, K. & Jaenisch, R. *Cell* **38**, 9-16 (1984).
46. Schubach, W. & Groudine, M. *Nature* **307**, 702-708 (1984).
47. Maniatis, T., Fritsch, E. F. & Sambrook, J. *Molecular Cloning: A Laboratory Manual* (Cold Spring Harbor Laboratory, New York, 1982).
48. Yamamoto, T. *et al.* *Cell* **35**, 71-78 (1983).
49. Yanisch-Perron, C., Vieira, T. & Messing, T. *Gene* **33**, 103-119 (1985).
50. Wilhelmson, K. C., Eggleton, K. & Temin, H. *J. Virol.* **52**, 172-182 (1984).
51. Neel, B. G., Hayward, W. S., Robinson, H. L., Fang, J. & Astrin, S. M. *Cell* **23**, 323-334 (1981).
52. Fung, Y. K. T., Lewis, W. G., Crittenden, L. B. & Kung, H. J. *Cell* **33**, 357-368 (1983).
53. Nusse, R., van Oyen, A., Cox, D., Fung, Y. K. T. & Varmus, H. *Nature* **307**, 131-136 (1984).

## LETTERS TO NATURE

## Limits of X-ray variability in active galactic nuclei

P. Barr

Exosat Observatory, European Space Operations Centre,  
Robert Bosch Str. 5, 6100 Darmstadt, FRG

R. F. Mushotzky

Laboratory for High Energy Astrophysics,  
NASA Goddard Space Flight Center, Greenbelt,  
Maryland 20771, USA

Active galactic nuclei (AGN) have been observed to vary in all wavebands on timescales ranging from years to minutes<sup>1-3</sup>. The timescale of variability can yield information about the efficiency of the emission mechanism<sup>4</sup> and the details of the accretion process<sup>5</sup>. Most of the luminosity of Seyfert galaxies and quasars probably occurs in the hard X-ray region, with a cutoff near 1 MeV (ref. 6). (Although there have been reports of high luminosity 'ultraviolet bumps', optical observations of a large sample of objects have shown these to be rare<sup>7,8</sup>.) We show here that there is a significant correlation between the X-ray luminosity and timescale of X-ray variability for Seyfert galaxies and quasars. We interpret this as evidence that the emitting plasma is near the limit of being dominated by electron-positron pairs. BL Lac objects do not follow this pattern; this may be due either to relativistic beaming or to the differing importance of the pair production process.

We have compiled from the literature a sample of Seyfert galaxies and quasars for which the X-ray variability is reliably established, is the fastest variability reported for that particular object, and is time-resolved. Table 1 lists, for each object, name, intensity doubling timescale, 2-10 keV luminosity and object class. Since the temporal behaviour is adequately sampled, the errors in the doubling time are small. Only those sources seen to vary by more than 10% were included. In addition, a number of BL Lacs are included. Because variability in the X-ray emission of BL Lac objects has been less widely reported than in Seyferts, we have dropped the requirement that the BL Lac variations be time-resolved in order to obtain an adequate sample. Figure 1 is a log-log plot of the mean 2-10 keV rest-frame luminosity (assuming Hubble constant  $H_0 = 50 \text{ km s}^{-1} \text{ Mpc}^{-1}$  and deceleration parameter  $q_0 = 0$ ),  $L_x$ , against the time for the source intensity to double,  $\Delta t$ . For Mkn205, OX169 and MCG5-23-16, the amplitude of variation is less than a factor of two and  $\Delta t$  is extrapolated linearly from the observed variability;

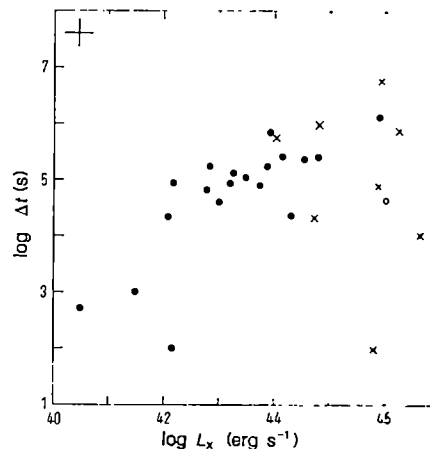


Fig. 1 Plot of  $\log \Delta t$  against  $\log L_x$  for Seyfert galaxies and QSOs (circles) and BL Lac objects (crosses). A typical error bar is shown in the upper left-hand corner.

the other objects exhibited variability by factors between two and six. A typical error bar is shown in Fig. 1. For OX169 and Mkn205,  $L_x$  is extrapolated from the soft X-ray band assuming a power-law spectrum with energy index 0.7 (ref. 9) and purely galactic absorption<sup>10</sup>, the other data are all direct measurements. The BL Lac luminosities are for the 0.5-3.5 keV band, except for Mkn421 (2-17 keV) and 0323+023 (1-20 keV). The 1E1402.3+0416 point represents the lower limit to its luminosity.

For Seyferts and quasars, we find a highly significant correlation between  $\log L_x$  and  $\log \Delta t$ , of the form  $\log L_x = a \log \Delta t + b \text{ erg s}^{-1}$ , with  $a = 0.9 \pm 0.2$ ,  $b = 39 \pm 1$  and linear correlation coefficient  $r_c = 0.7$ . The probability of achieving this by chance from a random sample is  $P < 10^{-3}$  (exclusion of a single point, the Ariel V observation of 3C373, reduces  $P$  to  $10^{-5}$ ). This trend is unlikely to be an observational selection effect; a linear regression of the logarithm of the 2-10 keV intensity against  $\log \Delta t$  yields  $r_c = 0.32$ , while for signal-to-noise ratio versus  $\log \Delta t$ ,  $r_c = 0.2$ . On the other hand, the BL Lac objects obey no such relationship. A linear regression yields correlation coefficient  $r_c = 0.21$ .

We consider first the Seyferts and quasars. Assuming that their hard X-ray spectrum extends to 1 MeV (ref. 6) with energy spectral index 0.7 (ref. 9), a bolometric correction of 1.0 to  $\log L_x$  is indicated. Within the errors the correlation between  $L_x$  and  $\Delta t$  is linear. The hard X-ray luminosity for this sample,  $L_x$ , may thus be written  $\log L_x = \log \Delta t + 40 \text{ erg s}^{-1}$ .

How valid is this treatment? The most homogeneous sampling performed so far has been that by Tennant and Mushotzky<sup>11</sup>,

**Table 1** Doubling time and luminosity of selected Seyfert galaxies, quasars and BL Lac objects

Source	$\log \Delta t$	$\log L_x$	Ref.	Object class
NGC6814	2.00	42.15	11	Seyfert
NGC3031	2.70	40.48	18	Seyfert
NGC4051	3.0	41.48	15	Seyfert
NGC3227	4.33	42.08	11	Seyfert
OX169	4.36	44.30	12	QSO
NGC4151	4.60	43.00	17	Seyfert
3C273	4.65	46.10	13	QSO
NGC7582	4.81	42.78	30	Seyfert
NGC7469	4.90	43.73	13	Seyfert
NGC2110	4.94	43.20	30	Seyfert
NGC5128	4.94	42.17	31	Radio galaxy
MGC5-23-16	5.03	43.48	11	Seyfert
NGC2992	5.11	43.26	13	Seyfert
NGC5506	5.34	42.83	30	Seyfert
NGC526a	5.24	43.87	13	Seyfert
Mkn205	5.35	44.54	12	QSO
3C382	5.41	44.77	*	BLRG
4U0241+62	5.41	44.13	13	QSO
Mkn841	5.84	43.92	32	QSO
1H1820+643	6.11	45.87	33	QSO
PKS0548-32	6.00	44.81	34	BL Lac
3C371	5.78	44.03	35	BL Lac
PKS2155-304	4.90	45.87	36	BL Lac
OJ287	6.78	45.93	37	BL Lac
3C66A	5.88	46.26	38	BL Lac
1E1402.3+0416	4.03	46.63	28	BL Lac
Mkn421	4.33	44.72	13	BL Lac
0323+023	2.00	45.81	29	BL Lac

$\Delta t$ , Time for source intensity to double;  $L_x$ , mean 2–10 keV rest-frame luminosity.

\* P.B. *et al.*, unpublished data.

using HEAO-1 A2 observations of 38 AGN ranging over four decades in intrinsic luminosity. All of their sources for which variability was detected exhibited timescales consistent with our observed correlation. Furthermore, the doubling timescale in individual objects is repeatable at different epochs. The low-amplitude variations of 3C273 found by Einstein Observatory observations<sup>12</sup> imply a doubling timescale similar to that seen in a large-amplitude flare by Ariel V<sup>13</sup>; Einstein<sup>14</sup> and Exosat<sup>15</sup> observations of NGC4051 suggest similar  $\Delta t$ , as do the Ariel V<sup>16</sup> and HEAO-1<sup>17</sup> observations of NGC4151. There are some objects which have not been observed to vary, but AGN are known to experience quiescent epochs between episodes of variability<sup>17,18</sup>. The duty cycle of variability is very poorly determined and it is entirely possible that more extensive observations of the ‘steady’ AGNs may reveal variability.

We know of only one observation of a quasar which diverges strongly from our suggested doubling time-luminosity relationship. This is the remarkable behaviour<sup>19</sup> of 1525+227, which doubled its intensity (initially  $3 \times 10^{44}$  erg s<sup>-1</sup>) in 200 s (a  $4\sigma$  result). If real, this would necessitate relativistic beaming to avoid efficiencies of  $>100\%$ . (Although Bassani *et al.*<sup>20</sup> have attempted a similar treatment, their sample is highly heterogeneous in that the variability timescales used were often taken from infrared, optical or ultraviolet flux measurements and even from optical polarization variations. It is by no means evident that these timescales are relevant to the hard X-ray band in which most of the luminosity arises; indeed, in Seyfert galaxies there is strong evidence that the emission in different wavebands may arise in quite distinct components<sup>21</sup>.)

In the absence of relativistic bulk motions, the characteristic time for the intensity to double must be constrained by the characteristic source size  $R$ . We naively assume  $R \leq c \Delta t$ ; then  $\log L/R \geq 29.6$  erg cm<sup>-1</sup> s<sup>-1</sup>. Defining the dimensionless compactness parameter<sup>22</sup>  $\lambda = L\sigma_T/Rm_ec^3$  (where  $\sigma_T$  is the Thomson cross-section) we have, for the Seyferts and quasars,  $\lambda \geq 10$ . In this regime electron-positron pair production by two-photon

annihilation is important. For  $\lambda > 4\pi$  the plasma would be dominated by the pairs<sup>22</sup>, the compactness parameter cannot be much larger than this because at  $\lambda > 30$  the pairs strongly modify the emergent X-ray spectrum, producing a much steeper soft X-ray continuum than that observed<sup>23</sup>. It is therefore likely that the emitting plasma in this sample of AGN are marginally dominated by electron-positron pairs.

Araki and Lightman<sup>24</sup> have shown that a thermal plasma can be relativistic ( $kT_e \geq 3m_ec^2$ ) only if  $\lambda < 0.15(kT_e/m_ec^2)^{-(1+4\alpha)}$ , where  $\alpha$  is the spectral index of the emergent X-rays. Since  $\alpha \approx 0.7$ , a relativistic thermal plasma would have  $\lambda < 0.01$ , inconsistent with the observations. Therefore, if the plasma is thermal, its temperature is not highly relativistic. If the pairs are nonthermal, Zdziarski and Lightman<sup>25</sup> have shown that, for this likely compactness parameter, inverse Compton scattering of soft photons will produce the hard ( $\alpha \approx 0.7$ ) X-ray power-law spectrum observed.

The Thomson optical depth due to pairs is<sup>26</sup>  $\tau \approx (f_g \lambda)^{1/2}$ , where  $f_g$  is the fraction of primary luminosity radiated above  $2 m_ec^2$ . For  $\lambda \approx 10$  and a primary photon spectrum with an upper cutoff near 1 Mev,  $\tau = 1$ . The efficiency of conversion of matter to energy<sup>4</sup>,  $\eta$ , is  $\geq 5 \times 10^{-43} L/\Delta t$ ; that is,  $\geq 0.5\%$ , where the inequality disappears at  $\tau = 1$ .

Since  $L/R < L_{\text{Edd}}/R_s$ , where  $L_{\text{Edd}}$  is the Eddington limit and  $R_s$  the Schwarzschild radius, a further constraint is  $L > 10^{-3} L_{\text{Edd}}$  (for the classical Eddington limit). However, if the plasma is pair-dominated,  $L_{\text{Edd}}$  is reduced by  $m_p/m_e = 1836$ , the plasma is very near the Eddington limit and pair effects may dominate the hard photon flux for these objects<sup>23</sup>.

If the X-ray emission arises at the surface of an optically thick photosphere, the emissivity  $\epsilon = L/4\pi R^2$ , so that Fig. 1 may be considered to be a plot of luminosity against emissivity, like the Hertzsprung-Russell diagram. For accretion onto a central object of mass  $M$  with  $R/R_s$  fixed for the entire sample, Fig. 1 implies that  $\epsilon \propto 1/M$  and the luminosity per unit mass is constant.

Finally, we note that there is one class of AGN which consistently violate the Seyfert/QSO  $L$ -versus- $\Delta t$  relationship; these are the BL Lac objects. For such objects,  $L/\Delta t$  can be far lower than that implied by the optically thick pair-production limit. White *et al.*<sup>23</sup> have suggested that BL Lacs are in fact AGN with such high luminosities that the emitting plasma is severely pair-dominated, with  $\lambda > 30$ , such that any  $\gamma$ -rays and high energy X-rays are reprocessed to lower energies by two-photon annihilation (and by Compton scattering off the pairs), causing the steep soft X-ray spectra observed.

Conversely, if the observed spectrum of BL Lac objects represents their primary photon spectrum, then, when extrapolated to above 511 keV, it may not yield enough  $\gamma$ -rays to generate pairs; although there are no measurements of the X-ray spectra of BL Lacs above ~20 keV, the observed 2–10 keV spectra appear generally quite soft<sup>27</sup>. In addition, the large optical depths implied by the severely pair-dominated case may be difficult to reconcile with the observed rapid variability. Another possibility is that geometric effects (relativistic bulk motions and anisotropic emission) may obviate the necessity for large values of  $\lambda$  (and associated copious pair production), and in fact are necessary to explain the rapid variability of (and implied high efficiencies in) 1E1402.3+0416 (ref. 28) and 0323+023 (ref. 29). Interestingly, exclusion of the three radio-loud sources in the Seyfert/QSO sample leads to a considerable improvement in the goodness of the fit (from 99.90% to 99.99% significance). It is tempting to speculate that relativistic beaming and/or anisotropic emission mechanisms are also relevant to the X-ray emission from radio-loud quasars, although the evidence so far is, at best, highly circumstantial.

P.B. is affiliated to the Astrophysics Division, Space Science Department, European Space Agency. R.F.M. thanks the Institute of Astronomy, Cambridge, for hospitality extended during 1985.

**Note added in proof:** Recent EXOSAT observations of the Seyfert galaxies NGC3516 (G. Reichert, personal communication), Mkn766 and NGC4593 (P.B. et al., unpublished data) have revealed X-ray variability fully consistent with the suggested doubling time-luminosity relationship.

Received 26 November 1985; accepted 5 February 1986.

1. McHardy, I. *Space Sci. Rev.* **40**, 559–584 (1985).
2. Barr, P. et al. *Mon. Not. R. astr. Soc.* **193**, 549–562 (1980).
3. Glass, I. S. *Mon. Not. R. astr. Soc.* **197**, 1067–1080 (1981).
4. Fabian, A. C. & Rees, M. in *X-ray Astronomy: Proc. Symp. 21st Plenary Meeting of Cospar* (eds Baity, W. A. & Peterson, L. E.) 381–396 (Pergamon, Oxford, 1979).
5. Abromowicz, M. & Nobili, L. *Nature* **300**, 506–507 (1982).
6. Bassani, L. & Dean, A. *Astr. Astrophys.* **122**, 83–87 (1983).
7. Malkan, M. & Sargent, W. L. *Astrophys. J.* **254**, 22–37 (1982).
8. Richstone, D. O. & Schmidt, M. *Astrophys. J.* **235**, 361–376 (1980).
9. Rothschild, R. E. et al. *Astrophys. J.* **269**, 423–437 (1983).
10. Heiles, C. *Astr. Astrophys. Suppl.* **20**, 37–56 (1975).
11. Tennant, A. F. & Mushotzky, R. F. *Astrophys. J.* **264**, 92–104 (1983).
12. Zamorani, G., Giommi, P., Maccacaro, T. & Tannanbaum, H. *Astrophys. J.* **278**, 28–36 (1984).
13. Marshall, N., Warwick, R. & Pounds, K. *Mon. Not. R. astr. Soc.* **194**, 987–1002 (1981).
14. Marshall, F. E., Holt, S. S., Mushotzky, R. F. & Becker, R. H. *Astrophys. J.* **269**, L31–L37 (1983).
15. Lawrence, A., Watson, M. G., Pounds, K. A. & Elvis, M. *Mon. Not. R. astr. Soc.* **217**, 685–699 (1985).
16. Lawrence, A. *Mon. Not. R. astr. Soc.* **192**, 83–94 (1980).
17. Mushotzky, R. F., Holt, S. S. & Serlemitsos, P. *Astrophys. J.* **225**, L115–L118 (1978).
18. Barr, P., Giommi, P., Wamsteker, W., Gilmozzi, R. & Mushotzky, R. F. *Bull. Am. astr. Soc.* **17**, 1608 (1985).
19. Matilsky, T., Schrader, C. & Tannanbaum, H. *Astrophys. J.* **258**, L1–L8 (1983).
20. Bassani, L., Dean, A. J. & Semby, S. *Astr. Astrophys.* **125**, 52–58 (1983).
21. Tanzi, E. et al. *ESA scient. Publ.* **218**, 111–117 (1984).
22. Svensson, R. in *X-Ray and UV Emission from Active Galactic Nuclei* (eds Brinkman, W. & Trumper, J.) 152–163 (MPE Rep. 184, Munich, 1984).
23. White, N. E., Fabian, A. C. & Mushotzky, R. F. *Astr. Astrophys.* **133**, L9–L11 (1983).
24. Araki, A. & Lightman, A. P. *Astrophys. J.* **269**, 49–58 (1983).
25. Ździarski, A. A. & Lightman, A. P. *Astrophys. J.* **294**, L79–L85 (1985).
26. Guibert, P., Fabian, A. & Rees, M. *Mon. Not. R. astr. Soc.* **205**, 593–604 (1983).
27. Urry, M. & Mushotzky, R. F. *Astrophys. J.* **253**, 38–48 (1982).
28. Giommi, P. et al. *Astrophys. J.* **303** (in the press).
29. Doxsey, R. et al. *Astrophys. J.* **264**, L43–L48 (1983).
30. Mushotzky, R. F. *Astrophys. J.* **256**, 92–102 (1983).
31. Lawrence, A., Pye, J. P. & Elvis, M. *Mon. Not. R. astr. Soc.* **181**, 93P–99P (1977).
32. Arnaud, K. et al. *Mon. Not. R. astr. Soc.* **217**, 105–113 (1985).
33. Snyder, W. A. & Wood, K. in *X-Ray and UV Emission from Active Galactic Nuclei* (eds Brinkman, W. & Trumper, J.) 38–47 (MPE Rep. 184, Munich, 1984).
34. Urry, C. M., Mushotzky, R. F., Kondo, Y., Hackney, K. & Hackney, L. *Astrophys. J.* **261**, 12–18 (1982).
35. Snyder, W. A. et al. *Astrophys. J.* **259**, 38–47 (1982).
36. Snyder, W. A. et al. *Astrophys. J.* **237**, L11–L14 (1980).
37. Worrall, D. et al. *Astrophys. J.* **261**, 403–411 (1982).
38. Maccacagni, D., Maraschi, L., Tanzi, E. G., Tareghi, M. & Chiappetti, L. *Astrophys. J.* **273**, 75–80 (1983).

## Detection of the very hot central star in NGC2440

P. D. Atherton\*‡, N. K. Reay† & S. R. Pottasch\*

\* Kapteyn Astronomical Institute, University of Groningen, PB 800, 9700-AV Groningen, The Netherlands

† Astrophysics Group, Blackett Laboratory, Imperial College, London SW7 2BZ, UK

It has been argued<sup>1</sup> that the extremely faint central stars of some planetary nebulae must be very hot, with most of their energy output in the ultraviolet. We now report the detection of the central star of the planetary nebula NGC2440 in a narrow-band continuum image using a CCD (charge-coupled device) camera at the prime focus of the Anglo-Australian telescope. Its visual magnitude has been measured as  $18.9 \pm 0.2$ . Its Zanstra temperature<sup>2,3</sup> is about 350,000 K, so that it is one of the hottest stars ever observed. Its radius corresponds to that of a nearly degenerate star. Theoretical calculations can explain the observed temperature and luminosity if it has a mass of at least  $1.0 M_{\odot}$  and is in its cooling stage, but the predicted age of the nebula is considerably less than that required by the calculations. Furthermore, the present estimates of the progenitor mass of a  $1-M_{\odot}$  white dwarf are brought into question.

‡ Present address: Queensgate Instruments Ltd, 112 Windmill Road, Sunbury-on-Thames, TW16 7HB, UK.

For such a star, all the energy in the Lyman continuum (at wavelengths  $<912 \text{ \AA}$ ) will go into ionizing the surrounding nebular gas, with the energy reappearing at longer wavelengths as recombination and collisionally excited lines. It is possible to estimate the number of ionizing photons emitted by the star because each Lyman photon will (eventually) result in one Balmer photon. The temperature of the central star (the Zanstra temperature) is computed from the ratio of the number of  $H\beta$  photons to the visual continuum emission, assuming either black-body radiation or a model atmosphere. While the total Balmer-line flux from the nebula is easy to measure, the visual magnitude of a hot central star is not. When the central star is not visible on photographs, it is possible to use large-aperture photometry to measure the line and continuum strengths of the nebula and, by applying a theoretical correction to the strength of the nebular continuum, to estimate the contribution to the visual continuum from the star<sup>4,5</sup>. Such a technique is difficult to apply to stars fainter than about  $m_V = 14$  because of the noise from the background night sky and the nebula. A more sensitive search technique<sup>6,7</sup> is to image the nebula using narrow-band filters to exclude all of the nebular emission lines, thus ensuring maximum contrast between the star (which is mainly a continuum source) and the nebula (the spectrum of which is dominated by emission lines).

NGC2440 is a fairly bright nebula lying close to the galactic plane. Shaw and Kaler<sup>8</sup> have derived a lower-limit magnitude of  $m_V = 14.3$  for the central star using the technique of large-aperture photometry. Curtis<sup>9</sup> failed to find the central star on photographs in a survey which went down to  $m_V = 19.5$ , and Pottasch<sup>1</sup> used this lower limit to estimate the central star temperature as  $5 \times 10^5 \text{ K}$ . Kohoutek and Martin<sup>5</sup> have disputed this estimate and claimed the star temperature to be only  $10^5 \text{ K}$ . Reay et al.<sup>7</sup> have given a lower limit of  $m_V = 16$  ( $T = 180,000 \text{ K}$ ).

In order to resolve this controversy we have made new observations with a CCD camera at the prime focus of the Anglo-Australian telescope, using a 10-Å-wide filter centred at 4,788 Å. This wavelength was chosen to exclude any known nebular emission lines, and thus to maximize the contrast of the star against the background.

The images we obtained are shown as contour maps in Fig. 1. Figure 1a shows the central star clearly between the two inner condensations. The seeing for this exposure, determined from the profiles of field stars, was less than 1.0 arc s FWHM. Figure 1b shows an observation taken using the same detector-filter combination one day earlier, when the seeing was 2.0 arc s. The absence of the star is explained entirely by the poorer seeing, as indicated by Fig. 1c, which shows Fig. 1a smoothed to the same spatial resolution as Fig. 1b. The central star is simply drowned by the nebular continuum emission when the seeing is poor.

The magnitude of the central star was determined by interpolating and subtracting the nebular continuum from Fig. 1a and integrating under the stellar profile to determine the total flux. Comparison of this with similar quantities determined for two nearby field stars, the magnitudes and spectral types of which have been determined by Gathier<sup>10</sup>, enabled the visual magnitude of the central star to be determined by making the assumption that it is sufficiently hot to have a Rayleigh-Jeans black-body-like spectrum in the visible and beyond, and assuming the comparison stars have black-body spectra. An independent determination of the magnitude was made by comparison with a standard star (101–281) of known magnitude and spectral type<sup>11</sup>. Again it was necessary to assume that both the central star and standard star have black-body-like spectra in the mid-visible. From these independent calibrations we obtain an average value of  $18.9 \pm 0.2$  for the magnitude of the central star.

The hydrogen Zanstra temperature  $T_Z(H)$  is determined as follows. Using the calibration of Wamsteker<sup>12</sup>, that 0 magnitude in the visual corresponds to  $3.4 \times 10^{-9} \text{ erg cm}^{-2} \text{ s}^{-1} \text{ \AA}^{-1}$ , the magnitude (18.9) of the star is equivalent to a continuum flux

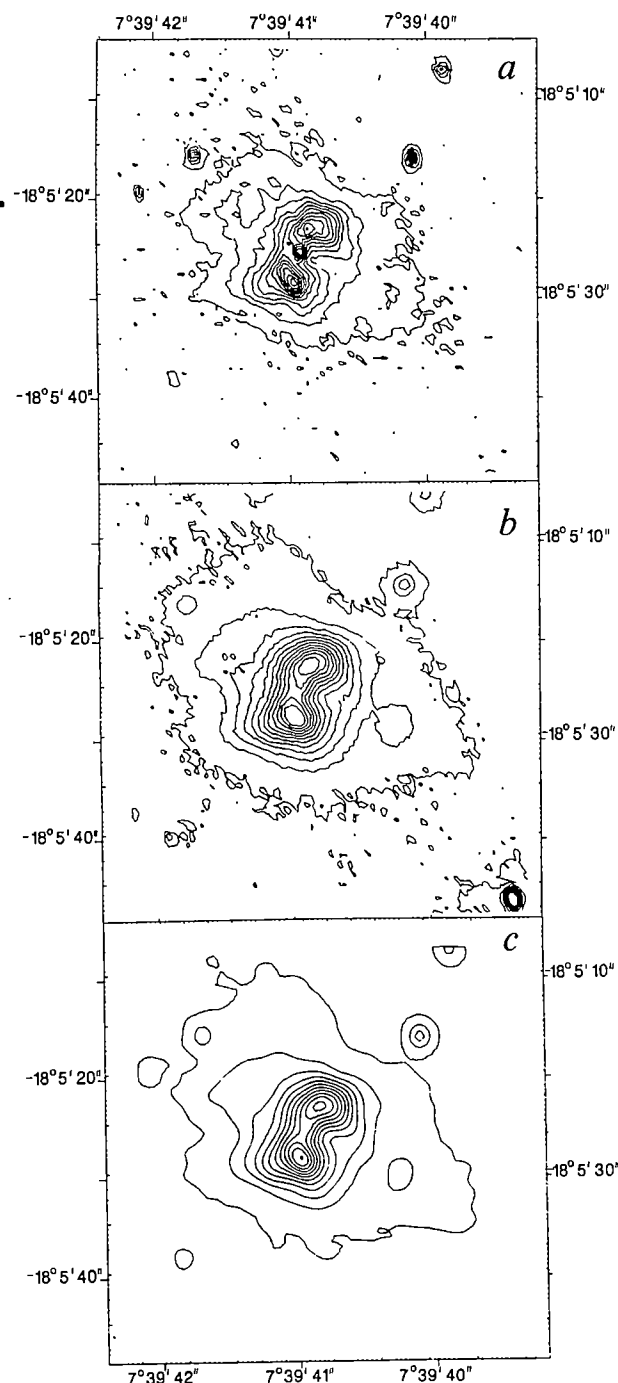


**Fig. 1** Narrow-band CCD images of NGC2440 obtained through a continuum filter centred at  $\lambda = 4,788 \text{ \AA}$ . In *a*, the seeing was 1 arc s, and the central star is clearly visible between the inner pair of condensations. *b*, CCD image recorded on previous night when the seeing was 2 arc s. The star is no longer visible. *c*, Image *a* smoothed to a spatial resolution of 2 arc s. The central star is no longer visible, illustrating the critical importance of seeing conditions to detectability.

of  $1.0 \times 10^{-16} \text{ erg cm}^{-2} \text{ s}^{-1} \text{ \AA}^{-1}$ . The  $H\beta$  flux emitted by the nebula is  $3.6 \times 10^{-11} \text{ erg cm}^{-2} \text{ s}^{-1}$  (ref. 4); the ratio of continuum to  $H\beta$  flux is thus  $2.8 \times 10^{-6} \text{ \AA}^{-1}$  after correction for a reddening of  $E_{B-V} = 0.30$  (ref. 10). This ratio corresponds to  $T_Z(\text{H}) = 4.0 \times 10^5 \text{ K}$ .

The ionized helium Zanstra temperature is computed from the above and the ratio  $\text{He II}(4,686 \text{ \AA})/\text{H}\beta$  of 0.6 (ref. 13). The ratio of continuum to 4,686- $\text{\AA}$  flux,  $4.6 \times 10^{-6} \text{ \AA}^{-1}$ , corresponds to a  $T_Z(\text{He II})$  of  $3.1 \times 10^5 \text{ K}$ . Errors in  $T_Z(\text{H})$  and  $T_Z(\text{He II})$ , due mainly to the error of  $\pm 0.2$  in the stellar magnitude, amount

to  $\pm 25,000 \text{ K}$  and  $\pm 20,000 \text{ K}$  respectively. The difference between  $T_Z(\text{H})$  and  $T_Z(\text{He II})$  is probably due to  $T_Z(\text{H})$  being overestimated because recombination from  $\text{He}^{2+}$  yields more than one photon capable of ionizing hydrogen. On the other hand,  $T_Z(\text{He II})$  is an underestimate for the effective temperature,  $T_{\text{eff}}$ , since some of the photons capable of ionizing  $\text{He}^+$  are actually absorbed by H. These effects become more pronounced at higher temperatures<sup>14</sup>. A good estimate of the effective temperature is  $350,000 \pm 25,000 \text{ K}$ . Notably, in ref. 1 the same effect is reported in NGC7027. These consistent results confirm the assumption that the nebula is optically thick for photons ionizing both hydrogen and helium.

The Zanstra temperature may be compared with that determined from the energy balance method. Preite-Martinez and Pottasch<sup>15</sup> find  $T = 186,000 \text{ K}$  for the central star of NGC2440, but the temperature determination is quite sensitive to the  $\text{He}^{2+}$  abundance. If an abundance ratio  $N_{\text{He}^{2+}}/N_{\text{H}} = 0.053$  is used, which follows from the measurement of Shields *et al.*<sup>13</sup>, the temperature becomes  $T = 230,000 \text{ K}$ . This is slightly lower than the Zanstra temperature. If account is taken of the energy emitted by the nebula in the far-infrared and in ultraviolet transitions not seen by the IUE satellite, then the agreement of the two methods is excellent.

The angular radius can now be computed from the visual flux given above. A correction for extinction must be made: we have used  $E_{B-V} = 0.30$  (ref. 10). The angular radius is then  $R/d = 9.8 \times 10^{-14}$ , where  $R$  is the stellar radius and  $d$  is the distance to the nebula. The value of  $d$  is rather well known<sup>10</sup>; we used  $d = 2.3 \text{ kpc}$ . Thus  $R = 6.8 \times 10^8 \text{ cm} = 0.99 \times 10^{-2} R_\odot$  and the luminosity is about  $2,600 L_\odot$ .

Only one set of evolutionary calculations has been published for stars more massive than  $0.7 M_\odot$ : those of Paczynski<sup>16</sup> for  $0.8 M_\odot$  and  $1.2 M_\odot$ . More recent calculations of the evolution of stars near  $0.6 M_\odot$  (ref. 17) confirm the general trends of the earlier models. As shell nuclear burning proceeds in a star, its temperature increases to a maximum when the shell sources have used up essentially all the available hydrogen and helium, and then begins to decrease. The maximum temperature depends critically on the nebular mass. If the models of Paczynski<sup>16</sup> are correct, it can reach the value observed for NGC2440 only when its mass is  $\geq 1.0 M_\odot$ . The high nitrogen and helium abundances observed in NGC2440 (ref. 3) support our contention that the central star has a mass  $\geq 1.0 M_\odot$ . For a  $1.0-M_\odot$  model, the time remaining until nuclear burning stops is about 300 yr. But the nebula must be considerably older. The age of the nebula can be determined from its diameter and expansion velocity (0.32 pc;  $23 \text{ km s}^{-1}$ ) to be  $\sim 7,000 \text{ yr}$ . But with the present luminosity the cooling time is only  $\sim 1,000 \text{ yr}$ . This discrepancy between the observed and expected age is significant and probably indicates that the theory is incomplete.

Another problem which arises is the following: It is clear that the progenitor of a white dwarf of  $1 M_\odot$  must be quite massive. A recent discussion<sup>18</sup>, based on a study of white dwarfs in open clusters, places this progenitor mass at  $7 M_\odot$ . But the nebular mass in NGC2440 is only  $0.4 M_\odot$  (ref. 3). Thus  $5 M_\odot$  must have been ejected in the course of the evolution of the star, but does not appear to be present in the neighbourhood of the star. While the material could have been ejected at a very early stage in the evolution, this appears unlikely because the most active phase of mass loss appears to be the red giant stage and its transition to a planetary nebula. Thus either the material is in some form which is currently undetectable (molecular hydrogen?) or present estimates of the progenitor mass are much too high.

Received 23 September 1985; accepted 2 January 1986.

1. Pottasch, S. R. *Astr. Astrophys.* **94**, L13-L16 (1981).
2. Zanstra, H. *Publ. Dom. astrophys. Obs.* **4**, 209-260 (1931).
3. Pottasch, S. R. *Planetary Nebula* (Reidel, Dordrecht, 1984).
4. Kaler, J. B. *Astrophys. J.* **210**, 113-119 (1976).
5. Kohoutek, L. & Martin, W. *Astr. Astrophys.* **94**, 365-372 (1981).
6. Atherton, P. D. *et al. Astrophys. J.* **232**, 786-796 (1979).

7. Reay, N. K., Pottasch, S. R., Atherton, P. D. & Taylor, K. *Astr. Astrophys.* **137**, 113–116 (1984).
8. Shaw, R. A. & Kaler, J. B. *Astrophys. J.* **295**, 537–546 (1985).
9. Curtis, H. D. *Univ. Calif. Publ. Lick Obs.* **13**, 57–74 (1918).
10. Gathier, R. thesis, Univ. Groningen (1984).
11. Landolt, A. U. *Astr. J.* **88**, 439–460 (1983).
12. Wamsteker, W. *Astr. Astrophys.* **97**, 329–333 (1981).
13. Shields, G. A., Alter, L. H., Keyes, C. D. & Czyzak, S. J. *Astrophys. J.* **248**, 569–583 (1981).
14. Stasinka, G. & Tyrela, R. *Astr. Astrophys.* (submitted).
15. Preite-Martinez, A. & Pottasch, S. R. *Astr. Astrophys.* **126**, 31–44 (1983).
16. Pacynski, B. *Acta astr.* **21**, 417–435 (1971).
17. Schonberner, D. *Astr. Astrophys.* **103**, 118–130 (1981).
18. Weidmann, V. & Koester, D. *Astr. Astrophys.* **121**, 77–84 (1983).

## Fossil tracks of $\alpha$ -particle interactions in minerals

P. B. Price & M. H. Salamon

Department of Physics, University of California, Berkeley, California 94720, USA

**Fossil tracks of length  $\sim 20 \mu\text{m}$  created by the spontaneous fission of  $^{238}\text{U}$  impurities were discovered in 1962<sup>1</sup> and form the basis of the well-known fission-track dating technique, which is broadly applicable to minerals and natural glasses<sup>2</sup>. Fossil tracks formed by recoil daughter nuclei released in the  $\alpha$  decay of nuclei in the Th and U decay chains were discovered in 1967<sup>3</sup>, but because of their very short ranges ( $< 0.02 \mu\text{m}$ ) have been seen only on cleavage planes of mica crystals. (Artificially produced  $\alpha$ -recoil tracks have also been seen in albite<sup>4</sup>.) During a search for tracks of slow, supermassive magnetic monopoles in large muscovite mica crystals<sup>5,6</sup>, we have discovered a third type of natural track caused by nuclear interactions of  $\alpha$  particles from radioactive impurities with nuclei in mica. These ' $\alpha$ -interaction tracks', with length intermediate between fission tracks and  $\alpha$ -recoil tracks, provide a measure of mild thermal events and are valuable in simulating the appearance and stability of tracks of hypothetical monopole-nucleus bound pairs.**

Price *et al.*<sup>7</sup> showed that a supermassive monopole with speed  $v = 0.001c$  such as is predicted by grand unified theories would produce a detectable radiation-damage track in mica provided

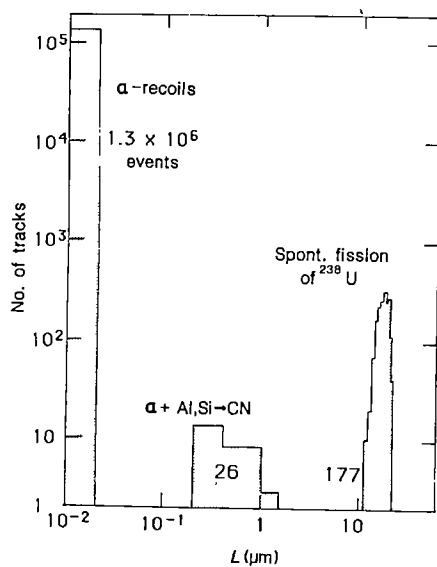


**Fig. 1** Distribution of lengths of naturally occurring tracks intersecting an internal cleavage plane in muscovite mica. To measure the track lengths,  $L$ , we used an etch time of 4 h in 48% HF at 20 °C instead of the 40-h etch used in our monopole search. The track length distribution consists of three distinct peaks, each of which is labelled with the source of the track-forming particles and the number of events observed. CN, compound nucleus.

it first attached to itself a nucleus with a large magnetic moment such as  $^{27}\text{Al}$  while passing through the Earth's crust. In an analysis of measurements<sup>8,9</sup> of the response of mica to accelerated ions of  $^{27}\text{Al}$  and other species, Price *et al.*<sup>7</sup> showed that at low velocities where nuclear stopping dominates over electronic stopping, the rate of etching,  $v_T$ , along the trajectory of an ion in muscovite mica depends on the nuclear stopping power  $S_n$  as:

$$v_T = (0.012 \mu\text{m h}^{-1}) \times (S_n / 1 \text{ GeV cm}^2 \text{ g}^{-1}) \quad (1)$$

for mica etched in 40% HF at 25 °C. To calculate  $S_n$  for a monopole-nucleus bound pair, one simply replaces the mass of the nucleus by the effectively infinite ( $\sim 10^{16}$  AMU) mass of the pair in the semi-empirical expression for  $S_n$  (ref. 10).

In our monopole search<sup>5,6</sup>, we etched for  $t = 48$  h, a much longer time than that used to reveal fission tracks, which ensured that an etch pit of  $\sim 0.25$ – $1.6 \mu\text{m}$  depth would be seen on each cleavage surface if the monopole were bound to a  $^{27}\text{Al}$  nucleus and travelling with speed 0.0002–0.0016c at vertical incidence. Our procedure was to cleave and etch several successive mica sheets, each  $\sim 100 \mu\text{m}$  thick (several times greater than the range of a fission fragment), re-align the layers for viewing in transmitted light, and scan for shallow etch pits that recurred on all cleavage surfaces in a linear array indicating the trajectory of a deeply penetrating particle. As shown in Fig. 1, we found three populations of etch pit pairs, distinctly different in length, which matched on two adjacent cleavage surfaces: (1) As found previously<sup>2,11,12</sup>, fission fragment etch pit pairs have a mean combined length  $\langle L \rangle = 20 \mu\text{m}$  in young, unannealed micas, and a mean length in old micas that is less than 20  $\mu\text{m}$  by an amount which depends on the degree of thermal annealing; (2) shallow etch pits with depths  $\leq 0.02 \mu\text{m}$  as measured with a Tolansky multiple-beam interference device are easily visible in phase contrast and can be discriminated against in a monopole search by using bright-field illumination; (3) etch pairs with combined lengths of  $\sim 0.25$ – $1.5 \mu\text{m}$  measured with the Tolansky device occur at a frequency  $\sim 0.03$ – $0.3$  times the frequency of occurrence of fission tracks. Since the correlation does not continue to adjacent sheets, monopole tracks are ruled out.

The surface density of etch pit pairs of intermediate length is strongly correlated with the densities of fission tracks and  $\alpha$ -recoil pits. We denote surface densities of the three types of

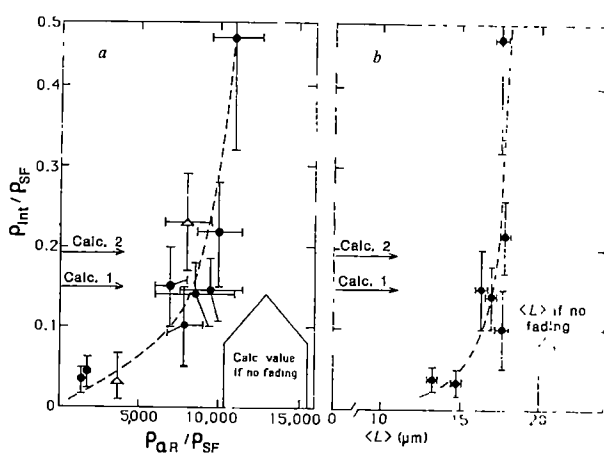


**Fig. 2** *a*, Correlation of the ratio  $\rho_{int}/\rho_{SF}$  with  $\rho_{\alpha R}/\rho_{SF}$  for samples of muscovite with values of  $\rho_{SF}$  ranging from 40 to 1,600 tracks per  $\text{cm}^2$  and with fission track ages of 400–950 Myr. The values of  $\rho_{int}/\rho_{SF}$  labelled 'Calc. 1' and 'Calc. 2' on the ordinate are discussed in the text. The calculated value of  $\rho_{\alpha R}/\rho_{SF}$  indicated by an arrow on the abscissa is taken from ref. 3. *b*, Correlation of  $\rho_{int}/\rho_{SF}$  with mean combined fission track length ( $\langle L \rangle$ ) for various samples of muscovite.

track in number per  $\text{cm}^2$  by  $\rho_{\text{int}}$ ,  $\rho_{\text{SF}}$  and  $\rho_{\alpha R}$  for intermediate, spontaneous fission and  $\alpha$ -recoil respectively. Figure 2a shows the strong correlation of the ratio  $\rho_{\text{int}}/\rho_{\text{SF}}$  with  $\rho_{\alpha R}/\rho_{\text{SF}}$  in large muscovite crystals selected for our monopole search, and in two crystals that we annealed for 1 h at 300 °C and 250 °C (triangles). Figure 2b shows the correlation of  $\rho_{\text{int}}/\rho_{\text{SF}}$  with mean fission track length  $\langle L \rangle$  in the same samples. We note that, despite a factor of 40 variation in  $\rho_{\text{SF}}$  among these micas,  $\rho_{\text{int}}$  correlates closely with  $\rho_{\text{SF}}$  and with  $\rho_{\alpha R}$  in such a way as to suggest strongly that these tracks of intermediate length are related to radiation from either U or Th, that they are much less resistant to thermal annealing than are fission tracks, and that they are somewhat less resistant to thermal annealing than are  $\alpha$ -recoil tracks. The small ratio  $\rho_{\text{int}}/\rho_{\text{SF}}$  in micas with small  $\rho_{\alpha R}/\rho_{\text{SF}}$  and  $\langle L \rangle$  thus seems to be due to partial annealing. Table 1 compares the

Table 1 Natural radiation tracks in mica compared with hypothetical tracks of monopole-nucleus bound pairs

Track type	Z	$\beta$	$dE/dx$ (GeV $\text{cm}^{-2}$ $\text{g}^{-1}$ )	R ( $\mu\text{m}$ )*
Spontaneous fission	~38 and ~52	~0.031–0.046	~25	~20
$\alpha$ Recoil	82–90	0.0013	~15	0.01–0.03
$\alpha$ Interaction	14–15	0.006	~3	0.25–1.6
$^{27}\text{Al}$ -monopole	13	~0.001	~3	$>10^{11}\dagger$

Z, atomic number;  $\beta$ , velocity (units of  $c$ );  $dE/dx$ , rate of energy loss along the track.

\* Sum of ranges of both fragments.

† Although the range is  $>10^2$  km, as a consequence of the low  $v_T$  the etch pits are shallow at every surface traversed.

characteristics of the three types of natural radiation tracks of hypothetical tracks of  $^{27}\text{Al}$ -monopole bound pairs.

We have investigated two candidates for the origin of the etch pits of intermediate length. The first is the recently discovered<sup>13</sup> spontaneous emission of heavy ions by one or more daughter nuclei in the U or Th decay chain. Such an explanation would be viable only if the ratio of decay rates for heavy ion emission relative to spontaneous fission were related to the observed ratios  $\rho_{\text{int}}/\rho_{\text{SF}}$  and to the ratios of etchable range of daughter nucleus following heavy ion emission to fission fragment range  $\langle L \rangle$  as follows:

$$\rho_{\text{int}}/\rho_{\text{SF}} = (\sum \lambda_i C_i R_i) / \lambda_{\text{SF}} C_{238} \langle L \rangle \quad (2)$$

where  $\lambda_i$  is the decay rate for emission of a particular heavy ion from a nuclide with concentration  $C_i$  and etchable range  $R_i$ , and  $\lambda_{\text{SF}}$  and  $C_{238}$  are the spontaneous fission rate and concentration of  $^{238}\text{U}$ . Typically,  $R_i \approx 2\text{--}3 \mu\text{m}$  in mica (only the recoiling daughter, not the energetic heavy ion, has a high enough radiation-damage rate to contribute) and  $\rho_{\text{int}}/\rho_{\text{SF}}$  is observed to be  $\sim 0.1$ , which would require  $(\sum \lambda_i C_i) / \lambda_{\text{SF}} C_{238} \approx 1$  or  $(\sum \lambda_i C_i) / \lambda_{\text{SF}} C_{238} \approx B(\text{HI}/\alpha) \approx 10^{-6}$ , where  $B(\text{HI}/\alpha)$  is the branching ratio for a particular heavy-ion emission mode relative to  $\alpha$ -decay. None of the measured<sup>14</sup> or theoretically predicted<sup>15</sup> values of  $B(\text{HI}/\alpha)$  for radioactive heavy nuclides is as high as  $10^{-9}$ . It seems very unlikely that more than  $\sim 10^{-3}$  of the etch pits of intermediate length could be due to spontaneous heavy-ion emission.

The second explanation, which we believe to be the correct one, is that the etch pits of intermediate length are produced by recoiling compound nuclei resulting from  $(\alpha, n)$  and  $(\alpha, p)$  reactions of  $\alpha$  particles (from the radioactive decay of  $^{232}\text{Th}$ ,  $^{235}\text{U}$  and  $^{238}\text{U}$  and their daughters) with nuclei comprising the mica structure.

Croazaz *et al.*<sup>16</sup> showed by accelerator calibrations that energetic He ions from solar flares could produce short 'interaction tracks' in lunar and meteoritic samples and cosmic dust grains, but did not realize that such tracks could also be produced as

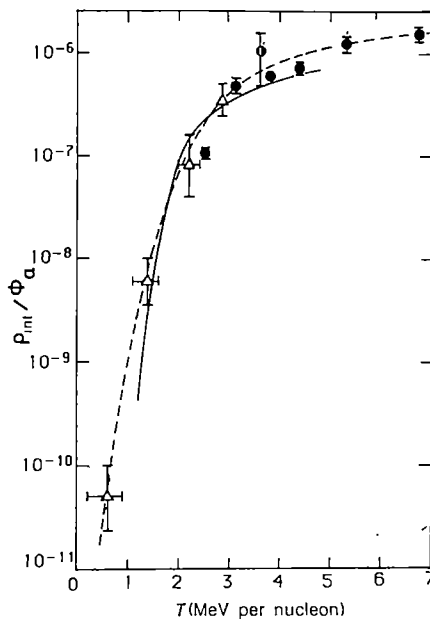


Fig. 3 Production rate of  $\alpha$ -interaction tracks per incident He ion as a function of He ion kinetic energy (T). Experimental points are from ref. 16 (●) and this work (Δ). The dashed line is an empirical fit to the data; the solid line is calculated from the cross-sections for  $(\alpha, p)$  and  $(\alpha, n)$  reactions with Al and Si (equation (3)).

a by-product of  $\alpha$  decay in terrestrial minerals. Figure 3 shows measurements of the ratio of the density of shallow-etch pit pairs on an internal cleavage plane of mica to  $\Phi_{\alpha}$ , the number of He ions per  $\text{cm}^2$ , as a function of He ion kinetic energy (T). The solid points were obtained by Crozaz *et al.*<sup>16</sup>, who slowed a 30-MeV He-ion beam to various energies with absorbers; the open circles are data we obtained at the Lawrence Berkeley Laboratory 88-inch cyclotron using He-ion beams of 11.6 and 14 MeV to bombard partially cleaved mica samples with cleavage planes at depths of  $\sim 20\text{--}60 \mu\text{m}$ . (We annealed the samples for 5 h at 490 °C in air to erase all natural tracks before doing the irradiations.) We calculated the He ion energies at the cleavage planes using a range-energy relation for He ions in muscovite<sup>19</sup>.

We found that, in addition to etch pairs with lengths of  $\sim 0.25\text{--}1.6 \mu\text{m}$ , very faint etch pits, visible only in phase contrast, result from He ion bombardments. Their production rate does not show a threshold at low energies. It is likely that they are simply atoms scattered elastically by the He ions and that their small  $V_T$  is due to their having a smaller charge than the recoiling compound nuclei.

In their study, Crozaz *et al.*<sup>16</sup> found that (1) He ions produced 'interaction tracks' in several minerals in addition to muscovite; (2) the ratio  $\rho_{\text{int}}/\Phi_{\alpha}$  increased rapidly above a threshold at  $\sim 2$  MeV per nucleon (see Fig. 3); (3)  $\rho_{\text{int}}/\Phi_{\alpha}$  was four times higher if the He ions passed through an Al cover foil rather than through a muscovite cover; (4)  $\rho_{\text{int}}/\Phi_{\alpha}$  was  $>100$  times lower for a plastic cover (containing H, C and O nuclei) than for a muscovite cover; (5) the tracks could be annealed out at a much lower temperature than fission tracks. They inferred from the energy threshold that  $\alpha$ -induced nuclear reactions are a more important source than elastically scattered nuclei.

Since the work of Crozaz *et al.*<sup>16</sup>, cross-sections as a function of energy for reactions of He ions with Al and Si targets have been measured<sup>17</sup>, and data on the registration of tracks as a function of Z and velocity in mica have been obtained (refs 8, 9, 18 and P.B.P. and M.H.S., unpublished data). From these

data we have been able to calculate the production rate  $\rho_{\text{int}}/\Phi_\alpha$  as a function of energy, shown by the solid curve in Fig. 3, based on the following expression:

$$\rho_{\text{int}}/\Phi_\alpha = \sum_j C \sigma_j(E) r_j(E) \quad (3)$$

where  $C = C_{\text{Al}} = C_{\text{Si}} = 1.28 \times 10^{22} \text{ cm}^{-3}$  is the number of Al or Si nuclei per  $\text{cm}^3$  in muscovite of composition  $\text{K}_2\text{Al}_4[\text{Si}_6\text{Al}_2\text{O}_{20}]\text{(OH,F)}_4$ ;  $\sigma_j(E)$  is the cross-section for a particular  $(\alpha, p)$  or  $(\alpha, n)$  reaction on Al or Si;  $r_j(E)$  is the recordable range of recoiling residual nuclei following compound nucleus de-excitation; the sum is over both types of reactions and both types of nuclei. Since values of  $r_j$  are typically  $< 1 \mu\text{m}$ , which is much smaller than the range of the  $\alpha$  particles in the beam, the relevant kinetic energy  $E$  can be taken as constant and equal to that of He ions at the cleavage plane. Equation (3) assumes a one-dimensional geometry, which is approximately valid for recoiling compound nuclei emitting a neutron or proton.

Because of their very low etching rate,  $v_T$ , we have ignored contributions of products of He-induced reactions with O and F; in view of the low concentration of K relative to Al + Si, and in the absence of cross-section data, we have ignored He-induced reactions with K. The agreement between the calculated curve and the two sets of data is satisfactory when uncertainties in He-ion energies at the mica cleavage plane and in values of  $r_j$  are taken into account. Therefore, following Crozaz *et al.*<sup>16</sup>, we refer to the etch-pit pairs of intermediate length as  $\alpha$ -interaction tracks.

Table 2 shows the contributions of four of the  $\alpha$ -emitting nuclei in the U and Th decay chains to the concentration of  $\alpha$ -interaction tracks relative to the concentration of spontaneous fission tracks.  $\alpha$  Particles from other nuclides have too low an energy or, in the case of the  $^{235}\text{U}$  chain, too low an abundance to contribute significantly. We used two methods to calculate the ratio  $\rho_{\text{int}}/\rho_{\text{SF}}$ .

The first approach was, for a concentration  $C_i$  and decay rate  $\lambda_i$  of an  $\alpha$ -emitter of species  $i$ , to calculate the flux of  $\alpha$  particles in each interval of residual range seen by Al and Si nuclei located close enough to a cleavage plane to produce  $\alpha$ -interaction tracks crossing that cleavage plane from either side. In the integral in equation (4), the cross-section  $\sigma_j$ , the recordable range  $r_j$  of the recoil product of the compound-nucleus reaction of the  $\alpha$ -particle with Al or Si, and the residual range  $R_i$  of an  $\alpha$  particle from species  $i$  are functions of the residual kinetic energy of the slowing  $\alpha$  particle.

$$\left( \frac{\rho_{\text{int}}}{\rho_{\text{SF}}} \right)_i = \frac{\lambda_i C_i}{\lambda_{\text{SF}} C_{238}} \frac{2C \sum_j \int_0^{R_{\text{max},i}} \sigma_j r_j dR_i}{\langle L \rangle} \quad (4)$$

The sum is over  $(\alpha, p)$  and  $(\alpha, n)$  reactions with Al and Si. The expression for the ratio  $(\rho_{\text{int}}/\rho_{\text{SF}})_i$  has implicitly taken into account an integration over isotropic distributions of directions of  $\alpha$  emission and spontaneous fission, which leads to mean thicknesses  $R_i/2$  for  $\alpha$  emission and  $\langle L \rangle/2$  for fission. Based on calibration data, we take  $r_j$  to be the true range of the recoil minus  $0.15 \mu\text{m}$ , the portion at the end of the range with  $v_T$  too small to be detected. In secular equilibrium the ratio of activities per  $\text{cm}^3$ ,  $\lambda_i C_i / \lambda_{\text{SF}} C_{238}$ , is taken to be  $2.8 \times 10^6$  for all members of the  $^{232}\text{Th}$  decay chain and  $2.2 \times 10^6$  for members of the  $^{238}\text{U}$  chain. The results are shown in the penultimate column of Table

Table 2 Production of  $\alpha$ -interaction tracks by U, Th decay chains

Parent	Daughter	$T_\alpha$ (MeV)	Calc. 1	$\rho_{\text{int}}/\rho_{\text{SF}}$	Calc. 2
$^{232}\text{Th}$	$^{212}\text{Po}$	8.79	0.13	0.13	
$^{232}\text{Th}$	$^{216}\text{Po}$	6.84	0.009	0.018	
$^{238}\text{U}$	$^{214}\text{Po}$	7.69	0.008	0.036	
$^{232}\text{Th}$	$^{220}\text{Rn}$	6.29	0.003	0.009	
Total from all sources			0.15	0.193	

2. The sum of the contributions from the four species gives  $\rho_{\text{int}}/\rho_{\text{SF}} = 0.15$ , which is indicated on the ordinates of Fig. 2 by an arrow labelled 'Calc. 1'.

The second approach was to use the He-ion calibration data for  $\rho_{\text{int}}/\Phi_\alpha$  as a function of energy (Fig. 3) to calculate  $(\rho_{\text{int}}/\rho_{\text{SF}})_i$  for each species  $i$ :

$$\left( \frac{\rho_{\text{int}}}{\rho_{\text{SF}}} \right)_i = \frac{\lambda_i C_i}{\lambda_{\text{SF}} C_{238}} \frac{\int_0^{R_{\text{max},i}} (\rho_{\text{int}}/\Phi_\alpha) dR_i}{\langle L \rangle} \quad (5)$$

The results are shown in the last column of Table 2 and by the arrow labelled 'Calc. 2' on the ordinates in Fig. 2.

The strong correlation of the ratio  $\rho_{\text{int}}/\rho_{\text{SF}}$  with  $\rho_{\alpha R}/\rho_{\text{SF}}$  and  $\langle L \rangle$  for micas varying by a factor of 40 in U concentration, the agreement in length distribution of natural etch pit pairs of intermediate length and of those produced in He-ion irradiations, and the close agreement between the values of  $\rho_{\text{int}}/\rho_{\text{SF}}$  obtained from the two calculations and the value obtained in the majority of the measurements shown in Fig. 2 establish that the naturally occurring etch pit pairs of intermediate length are due to recoil compound-nuclei produced in reactions of  $\alpha$  particles emitted by daughters of U and Th impurities in mica.

Resistance to thermal fading has been shown<sup>2</sup> to depend on radiation damage density associated with a particular type of track. Based on the relative energy deposition rates shown in Table 2, we would expect  $\alpha$ -interaction tracks to be less resistant to thermal fading than  $\alpha$ -recoil tracks, which in turn would be less resistant than fission tracks. This is borne out by the correlations of  $\rho_{\text{int}}/\rho_{\text{SF}}$  with  $\rho_{\alpha R}/\rho_{\text{SF}}$  and  $\langle L \rangle$ , which we have indicated by dashed lines in Fig. 2. All of the micas for which data are presented in Fig. 2 were selected on the basis of their perfection, large size and great age for use in our monopole search. Because of the close similarity in radiation-damage rate for an Al-monopole track and for an  $\alpha$ -interaction track (Table 1), we can use the observed ratio  $\rho_{\text{int}}/\rho_{\text{SF}}$  as a measure of survivability of Al-monopole tracks. We conclude that all but the two samples with  $\rho_{\text{int}}/\rho_{\text{SF}} < 0.1$  would have retained Al-monopole tracks during most if not all of the timespan indicated by their fission track ages.

This work was supported in part by NSF grant PHY-8403710. We thank Dr A. M. Clark (British Museum of Natural History), Dr B. Mason (US National Museum) and Professor Gordon Brown (Stanford University) for supplying mica samples, Ruth-Mary Larimer for assistance with the He-ion irradiations, Dr C. E. Naeser for assistance with fission-track ages, Professor M. Majda for the use of his Tolansky interference device, Dr Eric Norman for a discussion and Michael Solarz for assistance with the etching.

Received 28 October 1985; accepted 6 February 1986.

- Price, P. B. & Walker, R. M. *Nature* **16**, 732–734 (1962).
- Fleischer, R. L., Price, P. B. & Walker, R. M. *Nuclear Tracks in Solids: Principles and Applications* (University of California Press, Berkeley, 1975).
- Huang, W. H. & Walker, R. M. *Science* **155**, 1103–1106 (1967).
- Turkowsky, C. *Earth planet. Sci. Lett.* **5**, 492–496 (1969).
- Price, P. B. & Salamon, M. H. *Proc. 19th int. Cosmic Ray Conf.*, La Jolla **8**, 242–245 (National Aeronautics and Space Administration, Washington, D.C., 1985).
- Price, P. B. & Salamon, M. H. *Phys. Rev. Lett.* (in the press).
- Price, P. B., Guo, S.-L., Ahlen, S. P. & Fleischer, R. L. *Phys. Rev. Lett.* **52**, 1265–1268 (1984).
- Borg, J., Dran, J. C., Langevin, Y., Maurette, M. & Petit, J. C. *Radiat. Effects* **65**, 373–377 (1982).
- Borg, J. thesis, Univ. Paris (1980).
- Wilson, W. D., Haggmark, L. G. & Biersack, J. P. *Phys. Rev. B* **15**, 2458–2468 (1977).
- Bigazzi, G. *Earth planet. Sci. Lett.* **3**, 434–438 (1967).
- Mehta, P. P. & Rama *Earth planet. Sci. Lett.* **7**, 82–86 (1969).
- Rose, H. J. & Jones, G. A. *Nature* **307**, 245–247 (1984).
- Price, P. B. *Phys. Bull.* **36**, 489–490 (1985).
- Poenaru, D., Ivascu, M., Sandulescu, A. & Greiner, W. *Phys. Rev. C* **32**, 572–581 (1985).
- Crozaz, G., Hair, M., Maurette, M. & Walker, R. *Proc. int. top. Conf. Nuclear Track Registration in Insulating Solids and Applications*, Clermont-Ferrand Vol. 2, 41–54 (Laboratoire de Physique Nucléaire, Clermont-Ferrand, 1969).
- Seamster, A. G., Norman, E. B., Leach, D. D., Dyer, P. & Bodansky, D. *Phys. Rev. C* **29**, 394–402 (1984).
- Bibring, J. *et al. Proc. 8th int. Conf. Nuclear Photography and Solid State Track Detectors*, Bucharest Vol. 1, 485–499 (Institute of Atomic Physics, Bucharest, 1972).
- Salamon, M. H. *Lawrence Berkeley Lab. Rep. No. 10446* (1980).

## Incommensurately modulated $\alpha'$ -Sr<sub>2</sub>SiO<sub>4</sub>

L. Stenberg\*, J. R. Sellar\* & B. G. Hyde†

Research School of Chemistry, The Australian National University, GPO Box 4, Canberra, ACT 2601, Australia

The solid-state chemistry of superficially mundane A<sub>2</sub>BX<sub>4</sub> compounds with  $\beta$ -K<sub>2</sub>SO<sub>4</sub>-related structures is 'a can of worms', characterized by prolific polymorphism and, despite careful single-crystal X-ray diffraction studies, persistent uncertainty about exact space groups and atom positions. This is true of Ca<sub>2</sub>SiO<sub>4</sub><sup>1–7</sup>, a major constituent of cement, and Sr<sub>2</sub>SiO<sub>4</sub><sup>8–10</sup> despite 50 years of (confusing) literature. On the other hand, the solid-state physics of some other A<sub>2</sub>BX<sub>4</sub> compounds (for example, K<sub>2</sub>SeO<sub>4</sub>) as well as more exotic charge-density-wave types, involves modulated structures. Similar behaviour could conceivably resolve the structural confusion cited above (wrong structural models may have been refined); to investigate this possibility<sup>11</sup> we have studied the transition  $\beta \rightarrow \alpha'$ -Sr<sub>2</sub>SiO<sub>4</sub> by beam-heating the  $\beta$ -polymorph in an electron microscope. Electron diffraction patterns reveal two sets of incommensurate satellite reflections, indicating distinct modulated structures. Their origin is an asymmetric —Sr—O—Sr—O— chain (common to  $\beta$  and  $\alpha'$ ), with alternating bond lengths which tend to equality as  $T$  increases, but at a cost of reduced total bond strength and energy.

Although the  $\beta$  structures of both Ca<sub>2</sub>SiO<sub>4</sub> and Sr<sub>2</sub>SiO<sub>4</sub> are well characterized, our understanding of the  $\alpha'$ -structure, and hence of the  $\beta \rightleftharpoons \alpha'$  transition, is incomplete. A good refinement of  $\alpha'$ -Ca<sub>2</sub>SiO<sub>4</sub> is not available, and there has been conjecture about its structure. It now seems to be generally agreed that there are two  $\alpha'$ -Ca structures:  $\alpha'_L$  at lower and  $\alpha'_H$  at higher temperatures<sup>5,6</sup>. Both are superstructures of a prototype  $\alpha'$  ( $\beta$ -K<sub>2</sub>SO<sub>4</sub> type, Pmn<sub>b</sub>, Z = 4); but their nature is subject to dispute. For  $\alpha'_L$  some authors deduce 2a × b × 2c<sup>6,12</sup>, others a × 3b × c (ref. 3). On the other hand, the recent, careful single-crystal X-ray study of  $\alpha'$ -Sr<sub>2</sub>SiO<sub>4</sub> (ref. 9) at 110 °C (~25 °C above transition temperature,  $T_{tr}$ ) made no mention of a superstructure (although one would anticipate that Ca<sub>2</sub>SiO<sub>4</sub> and Sr<sub>2</sub>SiO<sub>4</sub> would be similar). The data were analysed in terms of two basic models: (1) an ('ordered') orthorhombic (Pmn<sub>b</sub>) structure with Sr atoms and SiO<sub>4</sub> tetrahedra on (100) mirror planes; and (2) a ('disordered') monoclinic ( $P2_1/n$ , but with  $\beta = 90^\circ$ ) twinned structure with these atoms statistically distributed between two sets of close, (100)-mirror-related positions. Model (2) was preferred:

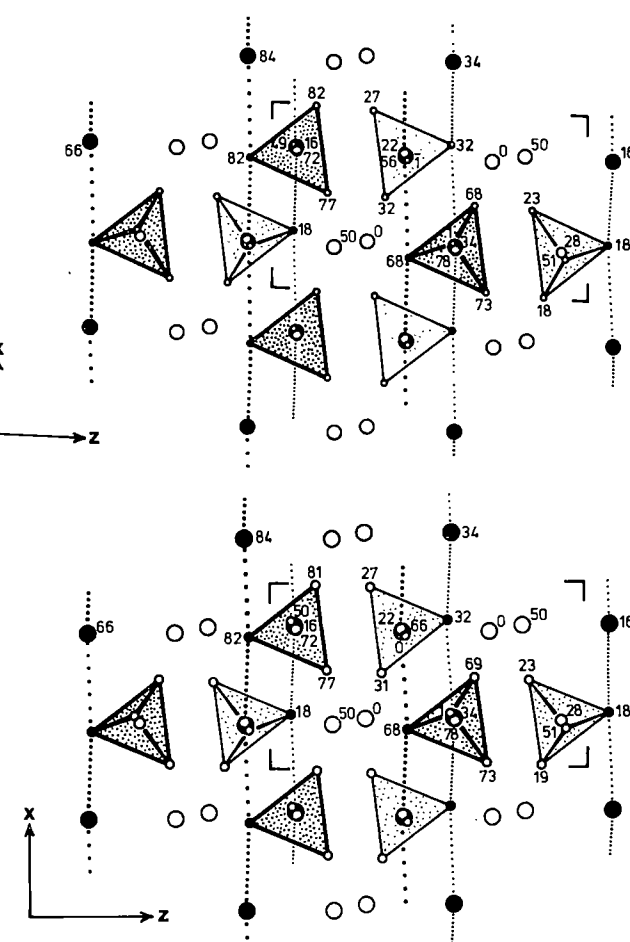


Fig. 2 The structures of  $\beta$ -Sr<sub>2</sub>SiO<sub>4</sub> (ref. 8) (top) and the 'disordered' model of  $\alpha'$ -Sr<sub>2</sub>SiO<sub>4</sub> (ref. 9) (bottom) projected on (010). Large circles, Sr; medium circles, Si; small circles, O atoms. SiO<sub>4</sub> tetrahedra are shown; dotted lines represent —Sr(1)—O(2)— chains, with the dense dots indicating the shorter bond. (The second twin of each is obtained by reflection in (100).)

it strongly resembles the  $\beta$ -Sr<sub>2</sub>SiO<sub>4</sub> structure ( $P2_1/n$ ,  $\beta = 92.67^\circ$ ), crystals of which are always polysynthetically twinned; and  $\alpha'$ -Sr<sub>2</sub>SiO<sub>4</sub> is the para-elastic form of the ferroelastic  $\beta$ . Nevertheless, ambiguity remains.

It is conceivable that an incommensurately modulated structure intrudes into the (displacive)  $\beta \rightleftharpoons \alpha'$  transition and that electron diffraction studies could reveal this<sup>11</sup>. The transition

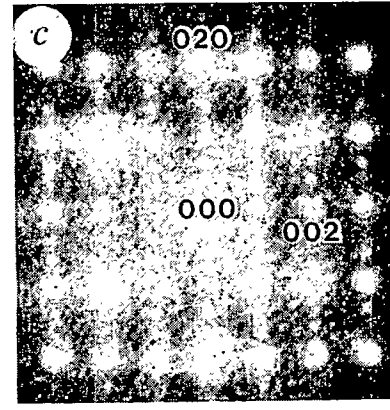
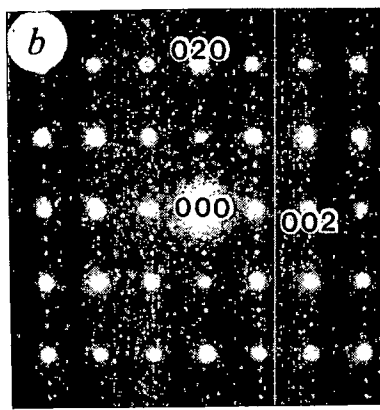
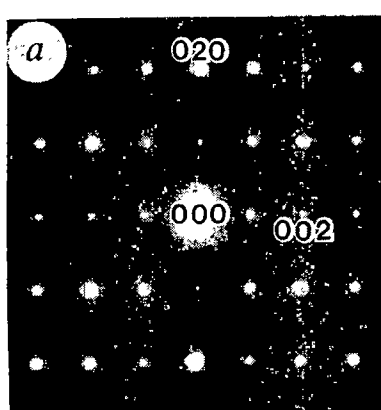


Fig. 1 [100] zone-axis diffraction patterns of *a*,  $\beta$ -Sr<sub>2</sub>SiO<sub>4</sub> (*b*-axis unique); *b*, *c*, beam-heated Sr<sub>2</sub>SiO<sub>4</sub>. The latter two show Bragg reflections similar to those in *a*, but also additional satellite reflections,  $q_1$  in *b* and  $q_2$  in *c*.

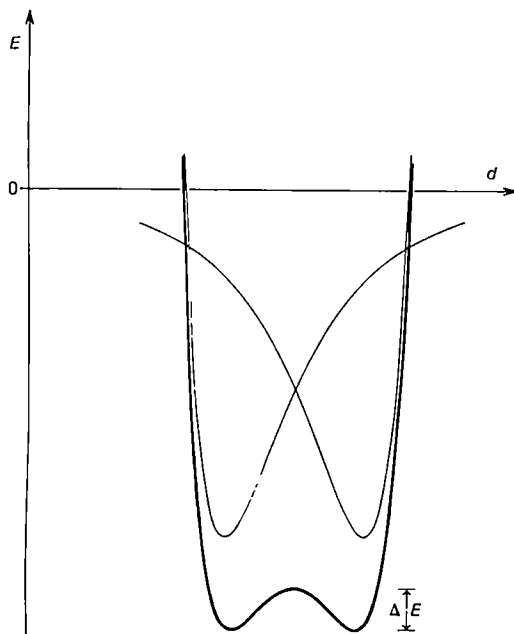


Fig. 3 A schematic representation of the  $\text{Sr}(1)-\text{O}(2)$  bond (potential) energy,  $E$ , as a function of bond length,  $d$ , in the  $-\text{Sr}(1)-\text{O}(2)-$  chains parallel to  $x$ . The thin lines are for adjacent bonds; the solid line is their sum.

temperature is  $\sim 680^\circ\text{C}$  for  $\text{Ca}_2\text{SiO}_4$  (refs 2, 5, 6) but  $\sim 85^\circ\text{C}$  (ref. 13) for  $\text{Sr}_2\text{SiO}_4$ . The lower temperature is more readily accessible in the electron microscope; we have therefore 'beam-heated'  $\text{Sr}_2\text{SiO}_4$ , because a hot stage was not available. An additional advantage of  $\text{Sr}_2\text{SiO}_4$  is that it has no  $\gamma$ -polymorph, so that 'dusting', due to  $\beta \rightarrow \gamma\text{-Ca}_2\text{SiO}_4$ , does not occur. (A previous electron-microscope study of  $\beta \rightarrow \alpha'$ - $\text{Ca}_2\text{SiO}_4$  has been reported<sup>14</sup>, but although micrographs were discussed, diffraction patterns were not.)

Three types of [100] zone-axis diffraction patterns were observed (see Fig. 1). The pattern in  $a$  was obtained with a defocussed beam, and corresponds to the  $\beta$ -phase; for  $b$  and  $c$  a focused (heating) beam was used. In addition to the Bragg reflections observed in  $a$ , patterns  $b$  and  $c$  also contain satellite reflections, the spacing of which is different in the two cases, but apparently incommensurate with the Bragg reflections in both. ( $b$ ,  $q_1 = 0.39b^*$ ;  $c$ ,  $q_2 = 0.30b^*$ .) They correspond to modulations with periodicities of  $\sim 2.56b = 14.5\text{\AA}$  and  $\sim 3.33b = 18.9\text{\AA}$ , respectively. Within the error of measurement, no other  $q$  values have been detected.

The observations are interesting in at least two respects: (1) the multiplicities (2.56 and 3.33) are close to the value of  $3b^*$  reported for an  $\alpha'_L$  superstructure by Saalfeld<sup>3</sup>; (2) the presence of a modulation could well account for the elusive details of the  $\alpha'$ -structure referred to above. While the (relatively weak) satellites are clearly consistent with the single-crystal X-ray diffraction data from  $\alpha'\text{-Sr}_2\text{SiO}_4$  (refs 9, 10), the possibility of modulation appears not to have been considered previously; which is doubly strange as its likelihood was suggested some time ago<sup>15</sup>, although not specifically for alkaline earth silicates. Indeed, the transformations  $Pmn\bar{b} \leftrightarrow \text{incommensurate} \leftrightarrow P2_1/n$  have recently been reported for some other compounds with  $\beta\text{-K}_2\text{SO}_4$ -related structures:  $\text{Cs}_2\text{CdBr}_4$  and  $\text{Cs}_2\text{HgBr}_4$  (ref. 16).

The driving force for this transformation (and related ones) is complex, but its major component is simple and direct. Figure 2 shows (one twin form of each of) the  $\beta$ - and  $\alpha'\text{-SrSiO}_4$  structures<sup>8,9</sup> projected along [010], the pseudo-hexagonal (and unique monoclinic) axis (setting  $P12_1/n$ ) and the modulation direction; in both there are nearly rectilinear chains,  $-\text{Sr}(1)-\text{O}(2)-\text{Sr}(1)-\text{O}(2)-$ , parallel to  $x$ . In these chains, alternate bonds are of different lengths:  $l(\text{Sr}-\text{O}) = 2.56_6$  (denoting uncertainty,  $2.566 \pm 0.00n$ ) and  $3.10_8\text{\AA}$  in  $\beta$  and  $2.68_8$  and

$3.00_4\text{\AA}$  in  $\alpha'$ ; the difference is more marked in  $\beta$  than in  $\alpha'$ . This difference is the principal cause of the well known tilting of the  $\text{SiO}_4$  tetrahedra from a more asymmetrical position in the  $\beta$ -structure to a more symmetrical one in the  $\alpha'$  ( $\alpha'_L$ ?) structure and eventually, at even higher temperatures, to a completely symmetrical one and space group  $Pmn\bar{b}$  in the  $\beta\text{-K}_2\text{SO}_4$ -type ( $\alpha'_H$ ?) structure.

Bond strength calculations<sup>17</sup> yield, for these bonds,  $s = 0.38$  and 0.07 valence units for  $\beta$  and 0.21 and 0.10 for  $\alpha'$ ; so that the sum of the two bond strengths is 0.35 for  $\beta$  and 0.31 for  $\alpha'$ . Clearly the bond energy is higher (and the crystal energy lower) in the former. Equally clearly (and this is emphasized by the invariable polysynthetic twinning of  $\beta$ ), the  $\text{Sr}-\text{O}$  bond energy is a 'double-well' function (Fig. 3). With the difference that the chain is diatomic rather than monatomic, this is the simple situation described by Pynn<sup>18</sup> for incommensurate structures. The modulation can be described as a variation, in the  $b$  direction, of the relative lengths of the two critical  $\text{Sr}(1)-\text{O}(2)$  bonds (which are almost parallel to  $a$ ). As a consequence, the tilt of the  $\text{SiO}_4$  tetrahedra (about an axis sub-parallel to  $b$ , and passing through the Si atoms) varies gradually, and periodically, between two extremes: that in Fig. 2b and its (100)-mirror-related twin.

Similar considerations will almost certainly apply to the analogous calcium silicate, which is now being studied.

Received 25 November 1985; accepted 13 February 1986.

1. Smith, D. K., Majumdar, A. & Ordway, F. *Acta crystallogr.* **18**, 787-795 (1965).
2. Eysel, W. & Hahn, T. Z. *Kristallogr.* **131**, 322-341 (1970).
3. Saalfeld, H. *Am. Miner.* **60**, 824-827 (1975).
4. Moore, P. B. & Araki, T. *Am. Miner.* **61**, 74-87 (1976).
5. Barnes, P., Fentiman, C. H. & Jeffrey, J. W. *Acta crystallogr.* **A36**, 353-356 (1980).
6. Sarkar, S. L. J. *Mater. Sci.* **15**, 1324-1325 (1980).
7. Eysel, W., Höfer, H. H., Keester, K. L. & Hahn, T. *Acta crystallogr.* **B41**, 5-11 (1985).
8. Catti, M., Gazzoni, G. & Ivaldi, G. *Acta crystallogr.* **C39**, 29-34 (1983).
9. Catti, M., Gazzoni, G., Ivaldi, G. & Zanini, G. *Acta crystallogr.* **B39**, 674-679 (1983).
10. Catti, M. & Ivaldi, G. *Acta crystallogr.* **B40**, 537-544 (1984).
11. Barber, J. & Hyde, B. G. *Acta crystallogr.* **B41**, 383-390 (1985).
12. Regourd, M., Bigare, M., Forest, J. & Guinier, A. *5th int. Symp. Chemistry of Cement*, Tokyo, Vol. 1, 44-48 (The Cement Association of Japan, 1968).
13. Catti, M. & Gazzoni, G. *Acta crystallogr.* **B39**, 679-684 (1983).
14. Groves, G. W. J. *Mater. Sci.* **18**, 1615-1624 (1983).
15. Izumi, M., Axe, J. D., Shirane, G. & Shimaoka, K. *Phys. Rev. B15*, 4392-4411 (1977).
16. Altermatt, D., Arend, H., Gramlich, V., Niggli, A. & Petter, W. *Acta crystallogr.* **B40**, 347-350 (1984).
17. Brown, I. D. in *Structure and Bonding in Crystals* Vol. 2 (eds O'Keeffe, M. & Navrotsky, A.) (Academic, New York, 1981).
18. Pynn, R. *Nature* **281**, 433-437 (1979).

## Formation of fractal cracks in a kinetic fracture model

Yves Termonia & Paul Meakin

Central Research and Development Department, Experimental Station, E.I. du Pont de Nemours and Company, Inc., Wilmington, Delaware 19898, USA

Interest is growing in the wide variety of fractal objects<sup>1</sup> found in nature; these include electric discharge patterns<sup>2</sup>, infinite percolation clusters<sup>3,4</sup>, branched polymers<sup>5,6</sup> and surface irregularities<sup>7</sup>. The question of whether surface cracks, such as those that occur in protective coatings, also lead to fractal-like structures is another problem of great interest. Here we study this question theoretically, making use of a molecular model for material failure, introduced previously<sup>8</sup>, which is based on the kinetic theory of fracture<sup>9,10</sup>. The model is applied to a two-dimensional surface stretched in one direction, and our results show that the cracks developing in the material exhibit properties similar to each other, at least at the molecular level. For a wide range of values of the elastic constants of the material, the fractal dimensionality is found to have a universal value,  $D = 1.27 \pm 0.02$ .

The surface is represented by a two-dimensional ( $x$ - $y$ ) network of nodes representing the difficult-to-deform strong parts of the material (Fig. 1). These nodes are joined in the  $y$

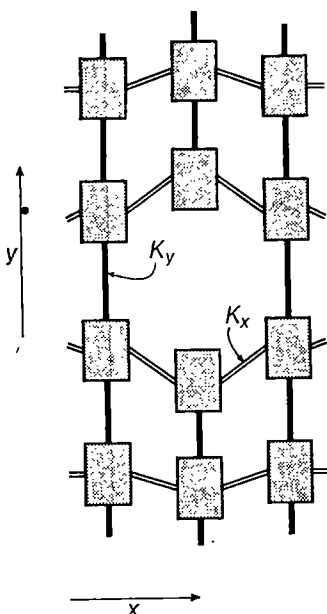


**Fig. 1** Two-dimensional network of nodes with one broken bond along the  $y$ -axis.  $K_y$  and  $K_x$  are the elastic constants for the bonds.

and  $x$  directions by elastic bonds with force constants  $K_y$  and  $K_x$ , representing the easily deformable and easily broken regions. In the case of a fibre that is perfectly ordered and oriented along the  $y$ -axis, the nodes represent the elementary repetition units of the macromolecules, and  $K_y$  and  $K_x$  are the elastic constants for the primary (for example, C-C) and secondary (van der Waals or hydrogen) bonds, respectively. The network is stretched along the  $y$ -axis by a constant strain and the basic events in the network are controlled by thermally activated bond breakages; accumulation of these events leads to crack formation and, ultimately, to network breakdown. The bond breakage process is examined with the help of the following stochastic model. The (unbroken) bonds are subjected at random to a Monte-Carlo lottery which breaks a bond with probability

$$p_i = \exp \{(-U_i + E_i)/kT\}/p_{\max} \quad (1)$$

where  $U_i$  is an activation energy,  $E_i$  is the elastic energy stored in the bond,  $k$  is Boltzmann's constant,  $T$  is the absolute temperature and  $p_{\max}$  is a normalization constant which ensures that the probability of breaking the most stressed bond in the array is unity. We set

$$E_i = (1/2)K_i(\Delta l_i)^2 \quad (2)$$

in which  $K_i$  is the force constant for bond  $i$  and  $\Delta l_i$  is the elongation. As a bond breaks, the two nodes connected through it will move apart (see below). For simplicity, we assume that the motions of the nodes along the  $x$ - and  $y$ -axes are mutually independent<sup>10</sup>, and we focus on their displacements along the  $y$ -axis, where the network is strained. Thus, the  $\Delta l_i$  values (see

equation (2)) are for elongations along the  $y$ -axis and correspond either to an axial tensile force (for a bond along the  $y$ -axis) or to a shear force (for a bond along the  $x$ -axis).

After a very small number of bonds have been broken, the network is relaxed to its minimum energy configuration in a series of steps. At each step, a node  $i$  is visited and its  $y$ -ordinate is adjusted so as to reduce to zero the net residual force ( $R_i$ )

$$R_i = \sum_{[\text{intact bonds } j]} K_j(\Delta l_j) + \sum_{[\text{nodes } i' \text{ in contact}]} R_{i'} \quad (3)$$

acting on that node. The first term on the right-hand side of equation (3) is due to the elastic force acting on the bonds  $j$  originating from node  $i$ , with  $K_j = K_y$  and  $K_j = K_x$  for a bond along the  $y$ - and the  $x$ -axis, respectively.  $\Delta l_j$  is the elongation of bond  $j$ , measured by the difference in the  $y$ -ordinates of the two ends of the bond. The second term on the right-hand side of equation (3) accounts for the external forces acting on node  $i$ , when in contact with any of its two neighbours  $i'$  along the  $y$ -axis. Indeed, we recall our assumption that the nodes are the difficult-to-deform, strong parts of the material.

It is important to note that if the residual force for a node is reduced to zero, it often results in an automatic increase of (the absolute value of) the residuals for the neighbouring nodes. Therefore, the liquidation of all the residuals in the array is a very computer-time-consuming process. For that reason, the liquidation of the residuals has been performed using two well-known computational devices<sup>11</sup>, called overrelaxation and block relaxation, which considerably speed up the convergence of the calculations. Overrelaxation moves a node not simply to the position at which the residual  $R$  is zero, but rather to a position at which the sign of the residual is opposite to that of the average for the neighbouring nodes. The second, and more important, device is known as block relaxation and consists of adjusting the  $y$ -ordinates of more than one node at a time.

We start with an intact network (no broken bonds), stretched by a constant strain of 20%. The stochastic model then proceeds in a series of steps. At each step, 0.1% of the total number of bonds are broken according to equations (1) and (2), after which the network is relaxed towards mechanical equilibrium, using equation (3). These steps are repeated until the network breaks. Typically, a network consists of 60 nodes in the  $y$ -direction and 100 nodes in the  $x$ -direction, with periodic boundary conditions. The small size of the network is dictated by the mechanical relaxation steps which represent the most computer-time-consuming processes in our simulations. A relaxation step was considered to be complete when the net forces measured at the two ends of the network along the  $y$ -axis were equal to within a few per cent. A typical simulation takes 6–8 hours of CPU time on an IBM 3081D. For the calculation of the elongations  $\Delta l_i$  (equation (2)), we set the length of a node along the  $y$ -axis to be equal to 1 unit length (its width being set to 0.2 units). For simplicity, we chose equal activation energies (equation (1)) and took  $kT = 1$ .

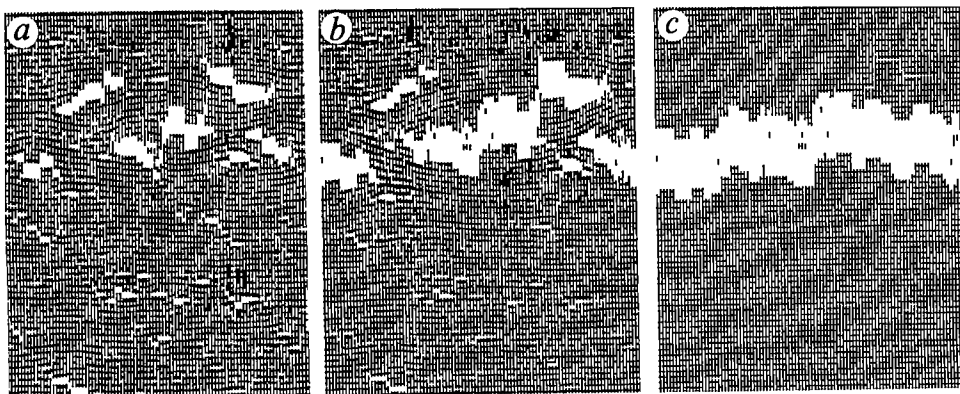


**Fig. 2** Results of the simulations for  $K_x = K_y = 20$  ( $kT = 1$ ,  $U_i$  = constant for all the bonds). *a*, Long before failure; *b*, close to failure; *c*, at failure.

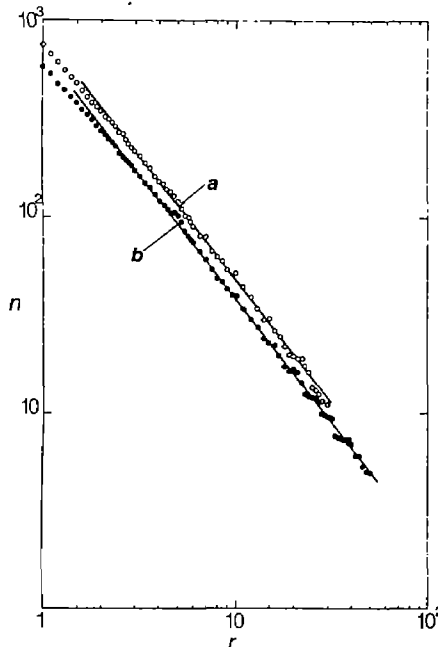


Fig. 3 log-log dependence of  $n$  on  $r$  (see equation (4)), where  $n$  is the number of yardsticks of size  $r$  needed to cover the perimeter of a crack;  $r$  is in units of the width of a node along the  $x$ -axis. Curve  $a$ :  $K_x = K_y = 20$ ; curve  $b$ :  $K_x = 200$ ,  $K_y = 20$ .

Figure 2 shows a two-dimensional network with  $K_x = K_y = 20$ , at different stages of our simulations. Long before failure (Fig. 2a), small cracks are observed which grow in number. As failure is approached (Fig. 2b), these cracks merge together, giving rise to a smaller number of larger cracks. Note that all the cracks at the top of Fig. 2a and b have the same 'dog' shape and already suggest self-similarity properties. At failure (Fig. 2c), only one crack is present, which extends throughout the network along the  $x$ -axis. All the other cracks have either been incorporated into the latter or have been closed through relaxation of the remaining elastic bonds towards their unstretched state. The fraction of broken bonds in Fig. 2c is  $\sim 30\%$ .

The degree of irregularity of a crack perimeter is given by its fractal dimension  $D$  (ref. 1), obtained by measuring the perimeter length using yardsticks of different sizes. The perimeter is a fractal if

$$n \sim r^{-D} \quad (4)$$

where  $n$  is the number of yardsticks of size  $r$  needed to cover the entire perimeter. (Because, in general, one cannot cover the entire perimeter with an integral number of yardsticks, the termination is handled by taking the straight line segment between the current point and the end point of the perimeter. The ratio of the segment length to the yardstick length is then added to the yardstick count<sup>12</sup>.) Curve  $a$  of Fig. 3 shows the log-log dependence of  $n$  on  $r$  for the perimeter of the 'infinite' crack in Fig. 2c. Fitting a straight line in the range  $2 < r < 30$  leads to a slope  $D = 1.27 \pm 0.02$ . A similar value of  $D$ , although for a smaller size range of  $r$ , has been obtained for the perimeters of the finite cracks in Fig. 2b.

An alternative statistical measure of  $D$  for an ensemble of finite cracks examined with the same yardstick size  $r$  is defined by<sup>1</sup>

$$P(r) \sim A(r)^{D/2} \quad (5)$$

where  $P(r)$  is the perimeter and  $A(r)$  is the area (for a given finite crack, the area  $A$  includes all the nodes and groups of nodes completely surrounded by the crack in question<sup>13</sup>). Equation (5) has been applied to the cracks in Fig. 2a and b by determining the value of  $D$  which, for a given  $r$ , minimizes

the standard deviation for the ratios  $P(r)/A(r)^{D/2}$ . In the range  $1 < r < 8$ , we find  $D = 1.31 \pm 0.15$ . Although the statistical error is large because of the small number of cracks investigated, the latter value of  $D$  is consistent with that obtained using equation (4).

The range of  $D$  values achievable by the model can be easily determined. In the limit of large  $kT$ ,  $p_i$  is constant (see equation (1)) and the crack corresponds to a two-dimensional percolation cluster whose exterior perimeter (hull) has a fractal dimension of  $\sim 1.75$ . In the limit  $kT = 0$ , the crack develops horizontally from a small nucleus and  $D = 1$ . For finite  $kT$ ,  $D$  also depends on  $K_x$  and  $K_y$ . Computer simulation results for  $kT = 1$  with  $K_x = K_y = 10$  and  $K_x = 200$ ,  $K_y = 20$  (see Fig. 3, curve b) lead to  $D$  values which are identical, within experimental error, to that ( $1.27 \pm 0.02$ ) found for the initial choice  $K_x = K_y = 20$ . This indicates that for intermediate values of  $kT$ , the fractal dimensionality  $D$  is insensitive to model details and may take on a universal value for all finite, non-zero values of  $kT$ .

Admittedly, our model may be only a crude representation of real experimental systems. For example, the model in its present form does not allow for out-of-plane buckling phenomena or in-plane distortion effects. Nevertheless, we believe that these complications should be minimal in the perfectly ordered and oriented polymeric systems for which the present model was originally devised<sup>8</sup>. Concerning the comparison of our  $D$  values with experimental data, we note that for crushed glass,  $D = 2.35$  (ref. 14), whereas for fractured steel the fractal dimensional increment  $D'$  ( $D' = D - 1$ ) was found to be 1.27 (ref. 15). Although results in two dimensions cannot be extrapolated to three dimensions, it is interesting that the latter experimental values are consistent with our prediction  $D = 1.27$  for a surface, if we assume  $D$  (three dimensions) =  $D$  (two dimensions) + 1.

Received 30 September 1985; accepted 16 January 1986.

1. Mandelbrot, B. B. *The Fractal Geometry of Nature*, 1-468 (Freeman, San Francisco, 1982).
2. Niemeyer, L., Pietronero, L. & Wiesman, H. *J. Phys. Rev. Lett.* **52**, 1033-1036 (1984).
3. Stanley, H. E. *J. Phys. A10*, L211-L220 (1977).
4. Kapitulnik, A., Aharonov, A., Deutscher, G. & Stauffer, D. *J. Phys. A16*, L269-L274 (1983).
5. Family, F. *Phys. Rev. Lett.* **51**, 2112-2115 (1983).
6. Termonia, Y. & Meakin, P. *Phys. Rev. Lett.* **54**, 1083-1086 (1985).
7. Avnir, D., Farin, D. & Pfeifer, P. *Nature* **308**, 261-263 (1984).
8. Termonia, Y., Meakin, P. & Smith, P. *Macromolecules* **18**, 2246-2252 (1985).
9. Kausch, H. H. *Polymer Fracture*, 1-332 (Springer, Berlin, 1978).
10. Dobrodumov, A. V. & El'Yashevitch, A. M. *Sov. Phys. Solid State* **15**, 1259-1260 (1973).
11. de G. Allen, D. N. *Relaxation Methods*, 1-230 (McGraw-Hill, New York, 1954).
12. Farin, D., Peleg, S., Yavin, D. & Avnir, D. preprint, Hebrew Univ. of Jerusalem (1985).
13. Voss, R. F. *J. Phys. A17*, L373-L377 (1984).
14. Avnir, D. & Farin, D. *J. chem. Phys.* **79**, 3566-3571 (1983).
15. Mandelbrot, B. B., Passoja, D. E. & Paullay, A. J. *Nature* **308**, 721-722 (1984).

## Detection of hail by dual-polarization radar

A. J. Illingworth\*, J. W. F. Goddard† & S. M. Cherry†

\* Department of Physics, University of Manchester Institute of Science and Technology, PO Box 88, Manchester M60 1QD, UK

† Rutherford Appleton Laboratories, Chilton, Oxfordshire OX11 0QX, UK

Hail causes considerable damage to property and agriculture and a simple, unambiguous method of determining which convective storms contain hail would be of great use for short-term weather forecasting, and would also find application in the study of the mechanism of hailstone growth. Previous radar methods of hail detection<sup>1-3</sup> have not proved reliable, but here we report results of a new technique based on the measurement of differential reflectivity using dual polarization radar and suggest an additional

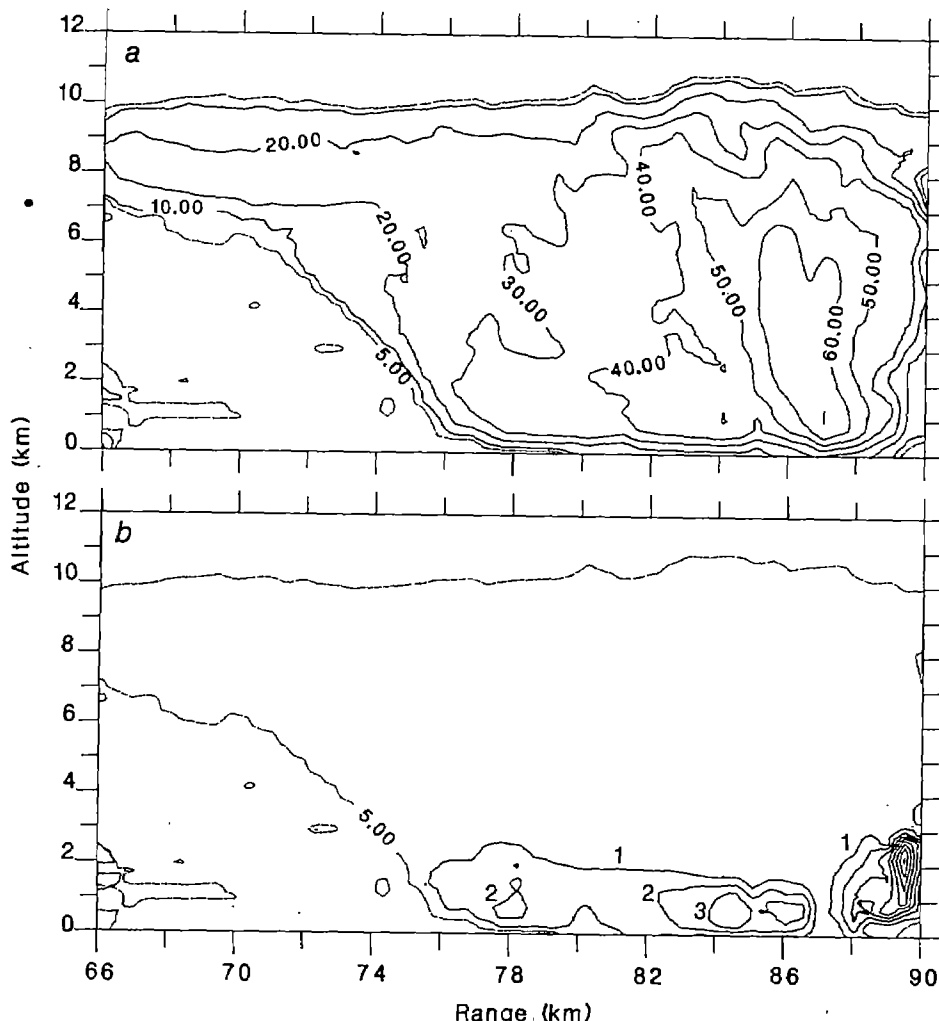


**Fig. 1** Contour plots of reflectivity  $Z$  (*a*) and differential reflectivity  $Z_{DR}$  (*b*) obtained from a vertical scan through an intense convective storm at 13:36 UT, 6 July 1983. *a*, Contours of  $Z$  are drawn every 10 dBZ above  $1 \text{ mm}^6 \text{ m}^{-3}$ , with an additional dotted 5-dBZ contour. *b*, Contours of  $Z_{DR}$  are plotted at 1-dB intervals starting at 1 dB. The dotted 5-dBZ contour from *a* is included, to delineate the extent of the echo. The positive values of  $Z_{DR}$  below 2 km altitude are due to raindrops falling with their horizontal axis larger than the vertical. In contrast to this is a narrow region at 87 km (<1 km wide) at 87 km range where near-zero values of  $Z_{DR}$  extend down to the ground. We believe that this region contains tumbling hail falling to the ground.

criterion for hail recognition. Hail is known to occur in vigorous convective storms in which the effective radar reflectivity,  $Z$ , measured by conventional radar is high. If the hail reaches the ground it is usually restricted to long narrow swathes<sup>4</sup>, often about 1 km wide but up to 50 km long, accompanied by surrounding precipitation in the form of heavy rain. The differential reflectivity technique involves comparing the radar reflectivity factor for horizontally ( $Z_H$ ) and vertically ( $Z_V$ ) polarized radiation; the comparison provides a measure of the mean shape of the precipitation particles. Close to the ground the values of  $Z$  are high for both hail and heavy rain, but because the large raindrops are oblate and fall with their horizontal diameter greater than the vertical, the value of  $Z_H$  in the rain exceeds that of  $Z_V$ . The smaller regions where hail is present can be clearly distinguished from the neighbouring heavy rain because, although individual hailstones may not be spherical, they tumble as they fall and so result in equal values of  $Z_H$  and  $Z_V$ .

For meteorological radars the power scattered back by common precipitation particles is proportional to the sixth power of the particle size and, although the particles may be frozen or liquid and may be non-spherical, it is usual to express the return as the equivalent radar reflectivity factor,  $Z$ , defined as the summation per unit volume of the diameter, raised to the sixth power, of spherical water drops which would scatter the same power as that actually measured.  $Z$  is usually quoted in decibels above  $1 \text{ mm}^6 \text{ m}^{-3}$ . A full review of meteorological applications of radar is provided by Browning<sup>5</sup>.

The new method of hail detection relies on a measurement

of the differential reflectivity,  $Z_{DR}$ , defined in decibels as

$$Z_{DR} = 10 \log_{10} (Z_H / Z_V)$$

The radar used in this study is fully described by Cherry and Goddard<sup>6</sup>. Situated at Chilbolton in southern England, it has an antenna of 25 m diameter, giving a  $0.25^\circ$  beamwidth at the 10 cm operating wavelength. Pulses with horizontal and vertical polarizations are transmitted (and received) alternately with a pulse repetition frequency (PRF) of 610 Hz. The precipitation forms an incoherent target with the values of  $Z$  fluctuating as the hydrometeors reshuffle in space, but this choice of PRF ensures adequate correlation of  $Z$  between sequential samples so that  $Z_{DR}$  may be estimated accurately. Each range-gated data sample comprises a spatial average over 300 m (four pulse volumes), which is time averaged over 64 transmitted pulse pairs. The worst case errors in measuring  $Z$  and  $Z_{DR}$  are estimated to be 0.7 dBZ and 0.2 dB respectively.

A vertical section through a vigorous convective storm is shown in Fig. 1. In Fig. 1*a*, contours of the conventional reflectivity  $Z$  are drawn every 10 dBZ, from 10 dBZ to 70 dBZ above  $1 \text{ mm}^6 \text{ m}^{-3}$ . In Fig. 1*b*, contours of  $Z_{DR}$ , observed simultaneously, are drawn at 1-dB intervals. The dotted  $Z$  contour at 5 dBZ in *a* and *b* delineates the overall extent of the echo. On this day the  $0^\circ\text{C}$  isotherm was at about 3 km altitude, and (as is typical for convective clouds<sup>7</sup>) values of  $Z_{DR}$  at higher altitudes in Fig. 1*b* are very close to zero, indicating randomly tumbling ice particles. Closer to the ground where it is warmer than  $0^\circ\text{C}$ , rain is to be expected, and as the rain intensity

increases the drops become larger and more oblate, leading to larger values of  $Z_{DR}$ ; assuming a Marshall-Palmer raindrop size distribution<sup>8</sup>, calculations show<sup>9</sup> that  $Z_{DR}$  should exceed 1 dB when the  $Z$  value exceeds 35 dBZ. In contrast to this is a region at a range of about 87 km where low values of  $Z_{DR}$  extend down to the ground. For a width of about 600 m (that is, over two neighbouring samples), a  $Z_{DR}$  below 0.5 dB accompanied by a  $Z$  of 65 dBZ extends down to a radar elevation of zero degrees. For monodispersed raindrops this value of  $Z_{DR}$  implies diameters less than 2 mm, which would need to be present in the unrealistic concentration of 500,000 m<sup>-3</sup> to give the observed  $Z$ . This corresponds to rainfall rates of thousands of millimetres per hour, and any other distribution would require even higher concentrations. The only plausible explanation is that the precipitation is hail which is nearly spherical or tumbles as it falls. The hail must be large, and with a high terminal velocity, so that although the surface is wet it has not melted sufficiently to form an oblate-shaped water coating. A similar but less extreme case can be seen in Hall *et al.*<sup>7</sup>.

To monitor hail over a large area, the radar could be scanned in azimuth at low elevation so that in the summer only precipitation at temperatures much above 0 °C is sampled. If regions where  $Z$  is above 45 dBZ are considered, then any region where  $Z_{DR}$  is less than 0.7 dB can be identified as hail reaching the ground. Hail-swaths could be tracked by monitoring the movement, in successive scans, of such low- $Z_{DR}$  cores embedded in regions of both high  $Z$  and  $Z_{DR}$ .

The technique outlined above would not result in false alarms. However, the precise shape and fall-mode of hail is not well known and if aspherical hail falls with a degree of common alignment, then  $Z_{DR}$  might have a local minimum but not fall below the 0.7 dB level. In 1986 the Chilbolton radar will be able to detect the orthogonal return in addition to the co-planar one. This information may provide additional corroborating evidence for hail. The linear depolarization ratio,  $L_{DR}$ , for vertically polarized transmitted radiation is defined as

$$L_{DR} = 10 \log_{10} (Z_{V,H}/Z_V)$$

where  $Z_{V,H}$  is the horizontally polarized return.  $L_{DR}$  values of less than -20 dB have been measured<sup>10</sup> in rain at a 3.2-cm wavelength. The orthogonal return is very low in amplitude because it is believed<sup>11</sup> that raindrops fall with their axes aligned in the vertical, with canting angles of less than 1°. Hail is generally aspherical and computations<sup>12</sup> show that randomly tumbling wet oblate spheroids with an axial ratio of 0.7 should have an  $L_{DR}$  greater than -20 dB. If this is so, the  $L_{DR}$  hail signature is simple: summertime values of  $L_{DR}$  above -20 dB close to the ground must be due to hail. The extreme case of spherical hail would escape  $L_{DR}$ -detection, but would give a clear zero  $Z_{DR}$  signal. At present there are no reports of measurements of  $L_{DR}$  at a 10-cm wavelength, but analysis of data at 3 cm (supplied by P. H. Herzegh, personal communication) confirms that, although propagation problems affect the absolute values of  $L_{DR}$ , a local increase of about 6 dB appears to coincide with a hail shaft.

The presence of hail seems to be the only physically realistic explanation of the localized region of low  $Z_{DR}$  embedded in a more extensive region where both  $Z$  and  $Z_{DR}$  are high. Although it has not been possible to obtain independent ground-based observations in the 500-m-wide region shown in Fig. 1, a long series of comparisons<sup>13</sup> of the radar data with simultaneous raindrop size distributions measured at the ground reveals that such high  $Z$ -low  $Z_{DR}$  combinations are not found in rainfall. More extensive observations with the Chilbolton radar scanning in azimuth at low elevation should enable the tracking of low- $Z_{DR}$  cores and any accompanying anomalous- $L_{DR}$  regions, and thus increase the probability of obtaining independent ground-based confirmation of the hail identification.

We acknowledge support from the Meteorological Office and EOARD through grant AFOSR-85-0188. We thank R. E.

Carbone, P. H. Herzegh, V. N. Bringi and T. A. Seliga for supplying us with  $L_{DR}$  data from the Maypole '84 program.

Received 11 November 1985; accepted 12 February 1986.

1. Geotis, S. G. *J. appl. Met.* **2**, 270-275 (1963).
2. Carbone, R. E. *et al.* *Bull. Am. met. Soc.* **54**, 921-927 (1973).
3. Barge, B. L. *McGill Univ. Sci. Rep.* MW-71 (Montreal 1972).
4. Morgan, G. M. & Towery, N. G. *J. appl. Met.* **14**, 763-770 (1975).
5. Browning, K. A. *Rep. Prog. Phys.* **41**, 761-806 (1978).
6. Cherry, S. M. & Goddard, J. W. F. *URSI Conf.*, Bournemouth 49-54 (RAL, 1982).
7. Hall, M. P. M., Goddard, J. W. F. & Cherry, S. M. *Radio Sci.* **19**, 132-140 (1984).
8. Marshall, J. S. & Palmer, W. J. *Met. S.* **5**, 165-166 (1948).
9. Illingworth, A. J., Goddard, J. W. F. & Cherry, S. M. *Am. met. Soc. 22nd Radar Met. Conf.*, Boston, 145-150 (American Meteorological Society, 1984).
10. Browne, I. C. & Robinson, N. P. *Nature* **170**, 1078-1079 (1952).
11. Beard, K. V. & Jameson, A. R. *J. atmos. Sci.* **40**, 448-454 (1983).
12. Atlas, D., Kerker, M. & Hitschfeld, W. *J. atmos. terr. Phys.* **3**, 108-119 (1953).
13. Goddard, J. W. F. & Cherry, S. M. *Am. met. Soc. 22nd Radar Met. Conf.*, Boston 352-357 (American Meteorological Society, 1984).

## A new geochronometer using lanthanum-138

S. Nakai, H. Shimizu & A. Masuda\*

Laboratory for Rare Earth Element Microanalysis, Department of Chemistry, University of Tokyo, Hongo, Tokyo, 113 Japan

We have applied a new geochronometer, based on the decay of  $^{138}\text{La}$  to  $^{138}\text{Ba}$ , to a sample of Amitsq gneiss from West Greenland. Using a value for the electron-capture decay constant,  $\lambda_{EC}$ , of  $4.44 \times 10^{-12} \text{ yr}^{-1}$ , the resulting age ( $2,408 \pm 24 \text{ Myr}$ ) is in good agreement with that from Sm-Nd systematics ( $2,410 \pm 54 \text{ Myr}$ ). Application of this geological clock is limited to REE (rare earth element)-rich minerals, but its merit is that, for Archaean rocks, the age can be evaluated from one specimen on the assumption that the initial Ba isotope ratios are effectively constant.

$^{138}\text{La}$  decays to  $^{138}\text{Ce}$  and  $^{138}\text{Ba}$  by  $\beta$ -decay and electron capture, respectively. Tanaka and Masuda<sup>1</sup> developed a dating method which employed the  $^{138}\text{La}-^{138}\text{Ce}$  decay. Preliminary trial by Masuda and Nakai<sup>2</sup> demonstrated the possible geochronological utility of the  $^{138}\text{La}-^{138}\text{Ba}$  decay. Our recent access to a better mass spectrometer, and improvement in chemical procedures, have enabled us to advance towards realization of a La-Ba clock.

For REE-rich minerals such as allanite and monazite, in which the La/Ba abundance ratios are higher than  $3 \times 10^2$ , the accumulation of radiogenic  $^{138}\text{Ba}$  from Precambrian times is sufficiently large to let us measure their formation ages using the following equation:

$$(^{138}\text{Ba}/^{137}\text{Ba})_p = (^{138}\text{Ba}/^{137}\text{Ba})_0$$

$$+ \lambda_{EC}/\lambda_{total} \times (^{138}\text{La}/^{137}\text{Ba})_p$$

$$\times [\exp(\lambda_{total} T) - 1]$$

where subscript 'p' refers to present, subscript '0' to the time of formation,  $\lambda_{EC}$  is the electron-capture partial decay constant of  $^{138}\text{La}$  and  $\lambda_{total}$  the total decay constant of the same nuclide. In general,  $(^{138}\text{Ba}/^{137}\text{Ba})_0$  can be regarded as essentially constant, because the contribution of radiogenic  $^{138}\text{Ba}$  to non-radiogenic  $^{138}\text{Ba}$  in ordinary minerals, even after  $4.5 \times 10^9 \text{ yr}$ , is smaller than the range of experimental errors for measurement of  $^{138}\text{Ba}/^{137}\text{Ba}$  ratios and is thus negligible at the present stage of our research. (The cosmic abundance ratio for La/Ba is  $\sim 0.1$  and the isotopic percentage of  $^{138}\text{La}$  with half-life  $\sim 10^{11} \text{ yr}$  is 0.089, while that of  $^{138}\text{Ba}$  is 71.70. If the precision of La/Ba dating is enhanced

\* To whom correspondence should be addressed.

by future progress in mass spectrometry, it may become necessary to admit the dependence of  $(^{138}\text{Ba}/^{137}\text{Ba})_0$  on sample age and composition.) The published values for the half-life of  $^{138}\text{La}$  scatter widely; we have therefore compared our La-Ba ages with Sm-Nd mineral isochron ages for the same samples.

The barium blank from the chemical procedures can be considered as having the same  $^{138}\text{Ba}/^{137}\text{Ba}$  ratio as the initial ratio for the reason mentioned above, which constitutes a unique merit of the dating method under consideration. As noted previously<sup>2</sup>, provided that the experimental procedure is designed to have the same Ba blank effects for both the Ba isotopic composition measurement and the Ba abundance determination, the effect of blank contamination is to move points along the isochron line in the  $^{138}\text{Ba}/^{137}\text{Ba}$  versus  $^{138}\text{La}/^{137}\text{Ba}$  diagram. It follows that no Ba blank corrections are needed for the Ba isotopic ratios and Ba abundances thus obtained. The new geochronometer has been applied to two sets of samples of Precambrian age. The first set of minerals is from the Amitsøq gneiss (GGU110999) of West Greenland, from which allanite, epidote and sphene were used for dating. The second set comprises allanite, apatite and sphene from the Mustikkämäki pegmatite of Finland.

Ba and REE were determined by stable isotope dilution. The Ba blank from the separation procedure was  $\sim 2$  ng. No blank correction was made for the reason previously mentioned. The overall blank for Nd was  $\sim 1$  ng, which is negligible.

Ba and Nd isotopic compositions were measured with a VG 354 mass spectrometer equipped with five Faraday collectors; abundances of Ba, La, Sm and Nd were determined with a JEOL JMS-05RB mass spectrometer. Barium isotopes were measured using Ta-Re-Ta triple filaments. To correct the variation due to mass discrimination, we normalized all the measured isotopic ratios to  $^{136}\text{Ba}/^{137}\text{Ba} = 0.6996$ . The measurements of  $^{138}\text{Ba}/^{137}\text{Ba}$  gave  $6.38969 \pm 12$  ( $2\sigma$ ) for a Merck BaCl<sub>2</sub> reagent (Art 1716),  $6.38997 \pm 22$  ( $2\sigma$ ) for JB-1 standard basalt and  $6.38972 \pm 27$  ( $2\sigma$ ) for BCR-1 standard basalt. The results show the uniformity of Ba isotopic ratios of ordinary rocks within experimental uncertainties, and endorse our suggestion that the initial  $^{138}\text{Ba}/^{137}\text{Ba}$  ratio can be taken as invariable. Our results are nearly in agreement with those of Eugster *et al.*<sup>3</sup> and Lewis *et al.*<sup>4</sup>. (The ratio for reagent Ba,  $6.38969 \pm 12$ , can be taken as representing a 'fixed spot' value.) Neodymium was measured as Nd<sup>+</sup> on Re triple filaments. All the measured isotopic ratios were normalized to  $^{146}\text{Nd}/^{144}\text{Nd} = 0.7219$ . Our  $^{143}\text{Nd}/^{144}\text{Nd}$  ratio for La Jolla Nd standard reagent was  $0.511849 \pm 6$  ( $2\sigma$ ).

Results are shown in Table 1 and Figs 1-3. The isochron lines were fitted using the York method<sup>5</sup>. Uncertainties ( $2\sigma$ ) for  $^{138}\text{La}/^{137}\text{Ba}$  and  $^{147}\text{Sm}/^{144}\text{Nd}$  were estimated at 0.5%. We used  $1.56 \pm 0.05 \times 10^{-11}$  yr for the electron-capture partial half-life ( $\lambda_{EC} = 4.44 \pm 0.15 \times 10^{-12}$  yr<sup>-1</sup>), and  $1.03 \pm 0.02 \times 10^{-11}$  yr for the total half-life of  $^{138}\text{La}$  ( $\lambda_{total} = 6.73 \pm 0.13 \times 10^{-12}$  yr<sup>-1</sup>), as reported by Sato and Hirose<sup>6</sup>. Figure 1 shows a La-Ba isochron plot for the allanite, epidote and whole-rock sample from Amitsøq gneiss specimen GGU110999 (analyses in Table 1). The three data points define an age of  $2,408 \pm 24$  ( $2\sigma$ ) Myr. This

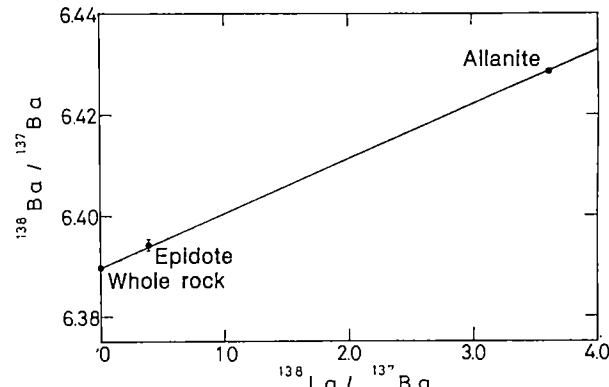


Fig. 1 La-Ba mineral isochron plot for GGU110999 from Amitsøq gneiss, West Greenland. The isochron yields an age of  $2,408 \pm 24$  ( $2\sigma$ ) Myr with an initial  $^{138}\text{Ba}/^{137}\text{Ba}$  ratio of  $6.38968 \pm 28$  ( $2\sigma$ ) ( $\lambda_{EC} = 4.44 \times 10^{-12}$  yr<sup>-1</sup>).

result agrees well with the Sm-Nd mineral isochron age of  $2,410 \pm 54$  ( $2\sigma$ ) Myr (Fig. 2). This agreement is considered not only to prove the validity of La-Ba dating, but also to support the decay constants, and in particular the  $\lambda_{EC}$  value, presented by Sato and Hirose<sup>6</sup>. (The La-Ba age is far more sensitive to  $\lambda_{EC}$  than to  $\lambda_{total}$  or  $\lambda_\beta$ .)

Baadsgaard *et al.*<sup>7</sup> have carried out thorough investigations of mineral isotopic age relationships in Amitsøq gneisses, using U-Th-Pb, Pb-Pb, Rb-Sr and K-Ar systematics. A complicated history of variable mineral response to polymetamorphism is recorded in six rocks, including GGU110999. Based on all the radiometric evidence, it has been concluded that three major metamorphic events affected the Amitsøq gneisses at  $\sim 3,600$ ,  $2,500$  and  $1,550$  Myr. (According to our Sm-Nd data on GGU110999 whole rock, its model Nd age is estimated to be 3,810 Myr.) Our results obtained from La-Ba and Sm-Nd systematics are in keeping with the conclusion of Baadsgaard *et al.*<sup>7</sup> from Rb-Sr mineral analyses, that allanite and sphene appear to have responded to metamorphism most recently at  $\sim 2,200$ -2,600 Myr. The K-Ar ages for biotite and hornblende<sup>7</sup> in GGU110999 are also concordant, at 2,317 and 2,342 Myr, respectively. The concordance of mineral ages is not perfect: the Rb-Sr system in epidote was affected<sup>7</sup> by an event at  $\sim 1,550$  Myr, whereas the GGU110999 epidote falls on the Sm/Nd isochron at 2,410 Myr (Fig. 2), together with allanite and sphene.

We have also investigated the Mustikkämäki pegmatite of Finland. The sphene and allanite from this pegmatite define an isochron age of  $1,694 \pm 42$  ( $2\sigma$ ) Myr. This La-Ba age is younger than the Sm-Nd age,  $1,820 \pm 29$  ( $2\sigma$ ) Myr (Fig. 3). Apparently the geochronology of the Mustikkämäki pegmatite is more complicated than that of the Amitsøq gneiss, but interpretation based on the geological background is difficult at present (O. Kouvo, personal communication). (For the La-Ba age to be strictly consistent with the Sm-Nd age for this pegmatite,  $\lambda_{EC}$  must equal  $4.13 \times 10^{-12}$  yr<sup>-1</sup>, which yields 2,588 in place of

Table 1 La-Ba and Sm-Nd isotopic data

Sample	La (p.p.m.)	Ba (p.p.m.)	$^{138}\text{La}/^{137}\text{Ba}^*$	$^{138}\text{Ba}/^{137}\text{Ba}^\dagger$	Sm (p.p.m.)	Nd (p.p.m.)	$^{147}\text{Sm}/^{144}\text{Nd}^*$	$^{143}\text{Nd}/^{144}\text{Nd}^\dagger$
<b>Amitsøq gneiss (GGU110999)</b>								
Whole rock	11.57	163.1	0.00056	$6.38963 \pm 36$	2,500	13.07	0.1156	$0.510593 \pm 8$
Allanite	$1.680 \times 10^4$	36.65	3.607	$6.42856 \pm 30$	1,236	$1.252 \times 10^4$	0.05964	$0.509725 \pm 11$
Epidote	599.0	11.98	0.3919	$6.39422 \pm 80$	68.85	520.2	0.07997	$0.510045 \pm 8$
Sphene					384.9	1,239	0.1878	$0.511773 \pm 8$
<b>Mustikkämäki pegmatite</b>								
Allanite	$3.218 \times 10^4$	62.34	4.058	$6.42033 \pm 30$	2,010	$1.622 \times 10^4$	0.07489	$0.511101 \pm 8$
Apatite					50.11	187.2	0.1618	$0.512157 \pm 8$
Sphene	187.1	110.2	0.00973	$6.38972 \pm 30$	837.7	1,061	0.4779	$0.515910 \pm 8$

\* Uncertainties are <0.5%. † Errors are  $2\sigma$  of the mean.

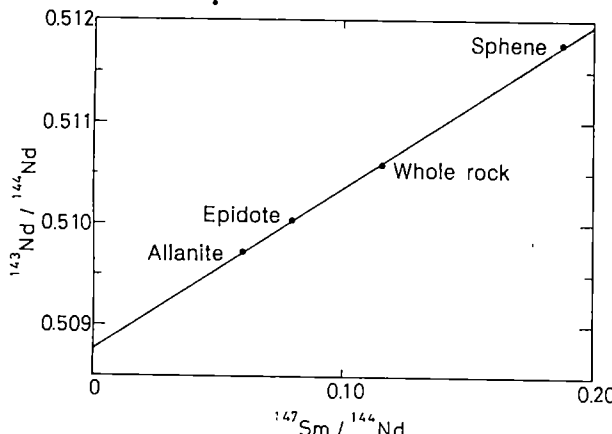


Fig. 2 Sm-Nd mineral isochron plot for 110999 obtained from aliquots of the same sample solution as that used for La-Ba analysis. The isochron yields an age of  $2,410 \pm 54$  ( $2\sigma$ ) Myr with an initial  $^{143}\text{Nd}/^{144}\text{Nd}$  ratio of  $0.508773 \pm 34$  ( $2\sigma$ ) ( $\lambda_\alpha = 6.54 \times 10^{-12} \text{ yr}^{-1}$ ).

2,408 Myr for the GGU110999 La-Ba age.) The above discrepancy between 1,694 and 1,820 Myr is considered to be related to the thermal or metamorphic history of the district concerned and to geochemical mobility of the relevant elements. Some isotopic systems may remain undisturbed through a metamorphic event, while others are disturbed or even completely reset. The response of different isotopic systems is a function of the severity of the metamorphism, and of the geochemical behaviour of the parent and daughter elements in relation to the particular mineral assemblages and reactions associated with the metamorphism.

Apart from the electron capture of  $^{138}\text{La}$ , there are two nuclear reactions which produce  $^{138}\text{Ba}$  in terrestrial minerals. One is the spontaneous fission of  $^{238}\text{U}$  with partial decay constant  $\lambda_f = 8.46 \times 10^{-17} \text{ yr}^{-1}$  (ref. 8), and fission yields for  $^{138}\text{Ba}$  and  $^{137}\text{Ba}$  of 7.2% and 6.6% (ref. 9). Minerals in which the abundance of uranium is  $>400$  times that of barium suffer from the effect of fission and the La-Ba age will change slightly. It is evident that the U contents in our samples are low enough to neglect the fission effect. Another reaction to be considered is the  $\alpha$ -decay of  $^{142}\text{Ce}$ , the effect of which is marginal for La-Ba dating, although the half-life of  $^{142}\text{Ce}$  is not precisely known $^{10-12}$ . If the shortest reported half-life ( $5 \times 10^{15} \text{ yr}$ ; ref. 10) is adopted, the La-Ba ages reported above are  $\sim 0.8\%$  too high. But if the longer half-life ( $>5 \times 10^{16} \text{ yr}$ ; ref. 12) is employed, the  $\alpha$ -decay effect is nearly negligible. (A half-life of  $9 \times 10^{18} \text{ yr}$  has also been reported.)

La-Ba dating is applicable to monazite, allanite, Ba-poor epidote, and other REE-rich minerals. The common occurrence

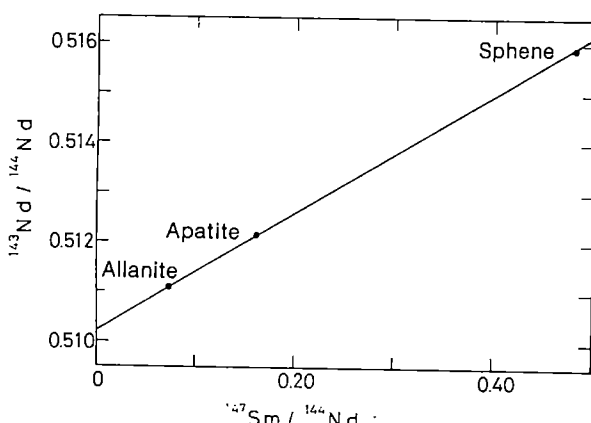


Fig. 3 Sm-Nd mineral isochron plot for the Mustikkamäki pegmatite, Finland. The isochron yields an age of  $1,820 \pm 29$  ( $2\sigma$ ) Myr with an initial  $^{143}\text{Nd}/^{144}\text{Nd}$  ratio of  $0.510207 \pm 26$  ( $2\sigma$ ).

of epidote as a product of low-grade metamorphic events suggests that La-Ba dating may be used to date such events in ancient shield areas. The La/Ba ratios in sphene and apatite appear sometimes to be high enough to allow La-Ba dating. The age of allanite can be determined with one (mm-sized) grain. Although this geochronometer works only for a limited number of minerals, it will have much significance for studies of the evolution of the continental crust, especially in the Pre cambrian.

We thank Professor H. Baadsgaard (University of Alberta) and Dr O. Kouvo (Geological Survey of Finland) for donation of samples, Professor D. Bridgwater (Copenhagen University) for helpful information, and S. Tasaki for help in chemical separation. Permission to publish results on material from the Geological Survey of Greenland (GGU110999) is acknowledged. This research was supported by grant-in-aid for Scientific Research from the Ministry of Education, Science and Culture of Japan.

Received 16 September 1985; accepted 30 January 1986.

1. Tanaka, T. & Masuda, A. *Nature* **300**, 515–518 (1982).
2. Masuda, A. & Nakai, S. *Geochim. J.* **17**, 313–314 (1983).
3. Eugster, O., Tera, F. & Wasserburg, G. J. *J. geophys. Res.* **74**, 3897–3908 (1969).
4. Lewis, R. S., Anders, E., Shimamura, T. & Lugmair, G. W. *Science* **222**, 1013–1015 (1983).
5. York, D. *Can. J. Phys.* **44**, 1079–1086 (1966).
6. Sato, J. & Hirose, T. *Radiochem. radioanalyt. Lett.* **46**, 145–152 (1981).
7. Baadsgaard, H., Lambert, R. St J. & Krupicka, J. *Geochim. cosmochim. Acta* **40**, 513–527 (1976).
8. Gallikler, D., Hugentobler, E. & Hahn, B. *Helv. phys. Acta* **43**, 593–606 (1970).
9. Ishimori, T. *Nippon Genshiryoku Kenkyusho Kenkyu Hokoku* **1102**, 9–97 (1966).
10. Reizler, W. & Kauw, G. Z. *Naturf.* **12A**, 665–666 (1957).
11. Senftle, F. E., Stern, T. W. & Alekna, V. P. *Nature* **184**, 630 (1959).
12. MacFarlane, R. D. & Kohman, T. P. *Phys. Rev.* **121**, 1758–1769 (1961).

## Cosmogenic helium in a terrestrial igneous rock

Mark D. Kurz

Chemistry Department, Woods Hole Oceanographic Institution, Woods Hole, Massachusetts 02543, USA

High  $^3\text{He}/^4\text{He}$  ratios in terrestrial samples are generally interpreted as indicating the presence of primitive or primordial gas<sup>1,2</sup>. Despite the ubiquitous presence of cosmogenic noble gases in meteorites, cosmogenic helium isotopic signatures have never been observed in terrestrial samples<sup>3</sup> and have, for the most part, been considered to be insignificant on the Earth. I present here new helium isotopic measurements on samples from the Kula formation of Haleakala volcano (Hawaii) that are best explained by an *in situ* cosmogenic origin for a significant fraction of the  $^3\text{He}$ . Results from crushing and stepwise heating experiments, and consideration of the exposure age of the sample at the surface and the cosmic-ray fluxes strongly support this hypothesis. Although crustal cosmogenic helium has been proposed previously<sup>4,5</sup>, this represents its first unambiguous identification in a terrestrial sample.

Haleakala volcano, which constitutes the eastern end of the island of Maui, is a shield volcano consisting of tholeiitic lavas unconformably overlain by later alkali basalts<sup>6,7</sup>. The samples discussed here are alkali basalts primarily from the Kula formation, and were erupted between 500,000 and 800,000 yr ago<sup>8,9</sup>. Two of them (H85-10 and H65-4) are drill-core samples<sup>10,11</sup> that are overlain by 160 m of younger Hana formation basalts. The third sample (HS85-3) was collected from the upper 50 cm of a 1.5-m thick surface lava flow at White Hill, near the summit of Haleakala (at elevation 3,200 m); it is a section of the Kula formation that was not buried by the later Hana series<sup>6</sup>. Kaneoka and Takaoka<sup>12</sup> reported high  $^3\text{He}/^4\text{He}$  ratios, up to 37 times the atmospheric value ( $R_a$ ) from the same area, a result that was later confirmed by Rison and Craig<sup>13</sup>. As shown below, these

Table 1 Helium analyses of basalts from Haleakala Volcano

Sample	Description	Depth	Phase analysed	Crushed		Powder heated		1-2 mm grains heated	
				${}^4\text{He}$ (cm <sup>3</sup> STP g <sup>-1</sup> )	${}^3\text{He}/{}^4\text{He}$ (R/R <sub>a</sub> )	${}^4\text{He}$ (cm <sup>3</sup> STP g <sup>-1</sup> )	${}^3\text{He}/{}^4\text{He}$ (R/R <sub>a</sub> )	${}^4\text{He}$ (cm <sup>3</sup> STP g <sup>-1</sup> )	${}^3\text{He}/{}^4\text{He}$ (R/R <sub>a</sub> )
HS85-3	Ankaramite, White Hill Ankaramite with 20% vesicles and 25% phenocrysts. The phenocryst population consists of 60% subhedral clinopyroxene (2-7 mm), and 40% subhedral to euhedral olivine. Zoning and partial resorption of clinopyroxenes is evident in thin section. Phenocrysts contain abundant spinel inclusions and some melt inclusions	Surface	Olivine	$5.76 \times 10^{-9}$	$8.2 \pm 0.2$	$1.82 \times 10^{-9}*$	$417*$	$[7.88 \times 10^{-9}]$	$[106.4]$
			Olivine	$1.22 \times 10^{-8}$	$8.2 \pm 0.1$				
			Olivine						
			Olivine						
			Clinopyroxene	$3.15 \times 10^{-9}$	$8.2 \pm 0.1$	$4.14 \times 10^{-9}*$	$215.2*$	$[3.56 \times 10^{-8}]$	$[32.2]$
			Clinopyroxene					$3.07 \times 10^{-8}*$	$35.6*$
			Matrix (holocrystalline basalt)					$1.66 \times 10^{-8}*$	$26.7*$
H65-4	Drill-core sample	164 m	Olivine	$8.53 \times 10^{-9}$	$8.3 \pm 0.2$			$1.54 \times 10^{-8}$	$8.00 \pm 0.1$
Alkali basalt containing 1% vesicles and 5-6% phenocrysts; the phenocrysts consist of ~70% (2-3 mm) clinopyroxene, 30% (1-2 mm) olivine, and sparse plagioclase (see also refs 10,11).									
H85-10	Drill-core sample	249 m	Olivine	$8.92 \times 10^{-9}$	$8.1 \pm 0.3$	$5.34 \times 10^{-9}*$	$4.89*$		
Alkali basalt containing ~3% 1-3-mm subhedral to euhedral olivine, 2% plagioclase and 1% clinopyroxene (see also refs 10,11)									
H1790-3	Surface		Olivine	$2.38 \times 10^{-8}$	$7.9 \pm 0.1$			$3.56 \times 10^{-8}$	$8.02 \pm 0.2$
Ankaramite from 1790 flow of Haleakala									

Mineral separates were prepared by lightly crushing the sample in a stainless-steel mortar, handpicking the 1-2-mm size fraction, and sonic cleaning in dilute nitric acid, distilled water and acetone. The basalt matrix (sample HS85-3) was handpicked to eliminate any traces of alteration or phenocrysts, but was not treated with solvents (due to the porous nature of the matrix). In several instances, the powder remaining after crushing was recovered from the vacuum vessel, placed in an aluminium foil boat, and subjected to stepwise heating. The procedural blanks for crushing and heating during this study were  $5.2 \pm 0.2 \times 10^{-11}$  ( $\sigma$ , sample standard deviation) cm<sup>3</sup> STP  ${}^4\text{He}$  with  ${}^3\text{He}/{}^4\text{He}$  ratios indistinguishable ( $\pm 20\%$ ) from atmospheric. All samples were devoid of any alteration phases in thin section, hand specimen or in mineral separates.

\* Sum of step-heating experiments (see Table 2). [ ], Sum of 'crushed' and 'powder heated' values from columns 1 and 2.

high  ${}^3\text{He}/{}^4\text{He}$  ratios are due to cosmogenic  ${}^3\text{He}$  within the samples rather than mantle-derived helium as suggested by these authors.

The  ${}^3\text{He}/{}^4\text{He}$  ratios obtained by heating sample HS85-3 (Tables 1, 2) are higher than any previously reported value for terrestrial materials, and considerably higher than primordial meteoritic or even solar-wind helium. Experimental artefacts can immediately be eliminated as an explanation for these high  ${}^3\text{He}/{}^4\text{He}$  ratios. Procedural blanks measured before and after each sample never deviated significantly from the mean blank value. No memory effects could produce the observed results because only terrestrial samples have been analysed in this laboratory, and no anomalous helium has ever been introduced into the furnace, crusher, vacuum lines or mass spectrometer. In addition, samples analysed both before and after HS85-3 (three of which are reported in Table 1) did not display these extreme ratios. Rayleigh fractionation of  ${}^3\text{He}$  and  ${}^4\text{He}$  is also quite unlikely given the large variability observed (between 8 and  $2,600 \times R_a$ ). Finally, eight different analyses of this sample, using three different extraction methods (crushing, heating of powder, and heating of 1-2 mm grains; Table 1), yielded internally consistent results, which would not be produced by any experimental artefacts.

Contamination of the sample by anthropogenic tritium can also be ruled out given the large quantities of tritium that would be required. The amount of excess  ${}^3\text{He}$  in all the HS85-3 mineral separates is  $\sim 1 \times 10^{-12}$  cm<sup>3</sup> STP  ${}^3\text{He}$  g<sup>-1</sup>. To produce this amount of  ${}^3\text{He}$  would require, for example, that the rock consist of 40% water that had a tritium concentration of 1,000 TU (tritium units), which is clearly unrealistic. This possibility is conclusively ruled out by analysis of a surface sample from the 1790 flow on Haleakala (sample H1790-3; Table 1) which does not display anomalous  ${}^3\text{He}$ , but has been exposed to all anthropogenic tritium.

Note also that the total  ${}^3\text{He}/{}^4\text{He}$  ratio data are consistent, in a general way, with results of two other laboratories from the same location<sup>12,13</sup>. Although the ratios reported here are significantly higher, any cosmogenic influence is strongly depth-dependent, being greater nearest the surface, so this difference could easily be explained by sampling geometry.

Several important aspects of the data in Tables 1 and 2 demonstrate why extreme ratios have not been observed previously. First, the extraction methods involved both crushing and heating in vacuum (discussed in detail elsewhere<sup>14,15</sup>), which yield quite different results. In all cases presented here, helium released by crushing phenocrysts was within one standard deviation of 8.2 times atmospheric in  ${}^3\text{He}/{}^4\text{He}$ . However, for sample HS85-3, stepwise heating of the powder remaining after crushing released helium with extremely high  ${}^3\text{He}/{}^4\text{He}$  ratios, up to 2,600 times atmospheric. This extreme internal isotopic variability is clearly illustrated by the step-heating pattern in Fig. 1. The highest  ${}^3\text{He}/{}^4\text{He}$  ratios are released by heating the powder at low to intermediate temperatures. However, at higher temperatures progressively more  ${}^4\text{He}$  is released and the  ${}^3\text{He}/{}^4\text{He}$  decreases, approaching but not quite reaching the  ${}^3\text{He}/{}^4\text{He}$  ratio released by crushing.

The stepwise heating pattern for another sample of Kula age is shown in Fig. 2. This sample differs from HS85-3 primarily in that it is overlain by 160 m of younger Hana basalts and is hence shielded from cosmic rays; the helium released by step-heating never exceeds the  ${}^3\text{He}/{}^4\text{He}$  ratio of the crushing extraction. The release pattern is similar to Fig. 1 in that most of the  ${}^4\text{He}$  is released at 1,350 °C, but in this case, the crushed helium and high-temperature-released helium are isotopically identical at 8  $R_a$ .

The stepwise heating patterns of both olivine powder samples show that the lowest temperature step releases helium having a lower  ${}^3\text{He}/{}^4\text{He}$  ratio than the successive step. The simplest

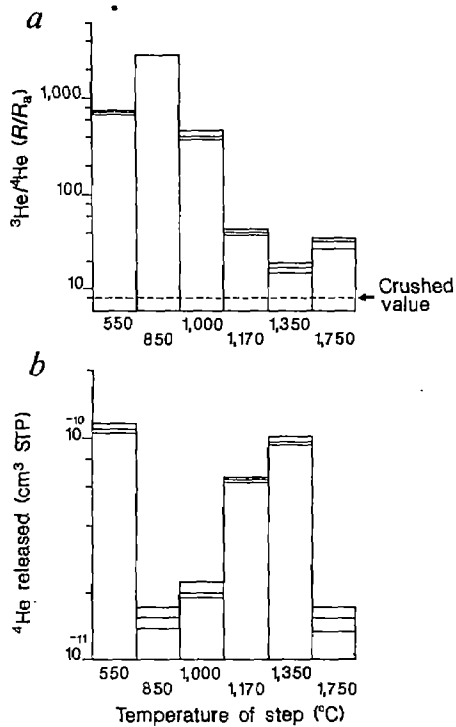


Fig. 1 Stepwise heating of Haleakala surface sample HS85-3, olivine powder. Each step represents the  ${}^3\text{He}/{}^4\text{He}$  (a) and  ${}^4\text{He}$  (b) released at the indicated temperature. The dashed line gives the  ${}^3\text{He}/{}^4\text{He}$  ratio yielded by crushing in vacuo, which is attributed to inherited magmatic helium. The extremely high  ${}^3\text{He}/{}^4\text{He}$  ratios (up to 2,600  $R_a$ ) released at lower temperature are the highest reported terrestrial values, and are attributed to cosmogenic helium. Error bars,  $1\sigma$  uncertainty.

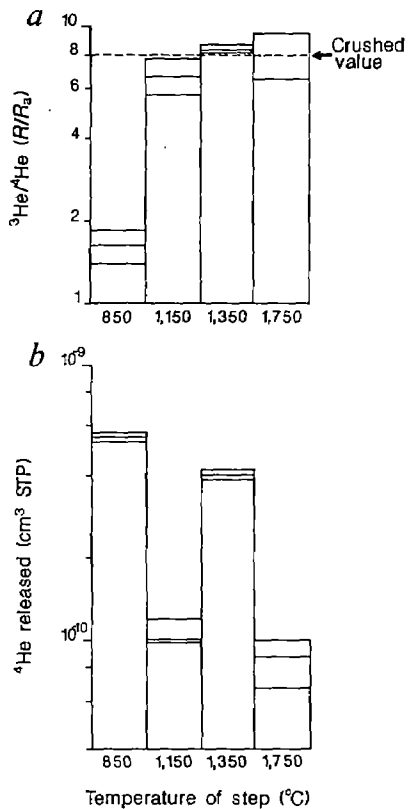


Fig. 2 Stepwise heating of olivine powder from drill-core sample H85-10. The lower  ${}^3\text{He}/{}^4\text{He}$  ratio in the low-temperature step is attributed to radiogenic  ${}^4\text{He}$ . In contrast to the release pattern of Fig. 1, the higher temperature steps are in equilibrium with the  ${}^3\text{He}/{}^4\text{He}$  released by crushing (8  $R_a$ ), which is attributed to the inherited magmatic helium.

explanation for the low-temperature, low- ${}^3\text{He}/{}^4\text{He}$  component is radiogenic helium from the surface of the phenocrysts that are in contact with the basalt matrix, by implantation of  $\alpha$ -particles ( ${}^4\text{He}$ ) from decay of Th and U. Based on the major-element composition of Kula alkali basalt<sup>10</sup>, and assuming a K/U ratio of  $10^4$ , this sample should have a U concentration of  $\sim 0.8$  p.p.m. Assuming Th/U of  $\sim 3$ ,  $\sim 5 \times 10^{-8} \text{ cm}^3 \text{ radiogenic } {}^4\text{He g}^{-1}$  would be produced in 500,000 yr, a minimum age for the Kula formation<sup>8,9</sup>. Therefore, implantation of a very small fraction (<1%) of the matrix radiogenic helium could account for the low-temperature release of  ${}^4\text{He}$ .

The simplest interpretation of Figs 1 and 2 is that the low to intermediate temperatures release the more weakly bound radiogenic and cosmogenic components, and high temperatures release primarily the inherited magmatic component. This explanation is consistent with both the crushing results and the heating patterns in Figs 1 and 2. Most of the helium in the phenocrysts (that contained in melt and spinel inclusions) is released by crushing, and is presumed to be representative of the inherited magmatic component, having a  ${}^3\text{He}/{}^4\text{He}$  ratio of 8  $R_a$ . Because most of the inherited helium is released by crushing, the powder remaining after crushing is most affected by additions of post-eruptive radiogenic and cosmogenic helium. Therefore, heating of olivine powder from sample HS85-3 released the highest  ${}^3\text{He}/{}^4\text{He}$  ratio, up to 2,600 times atmospheric. The extremely high  ${}^3\text{He}/{}^4\text{He}$  released by the low-temperature heating experiments on HS85-3 is most readily explained by the presence of cosmogenic  ${}^3\text{He}$ .

There are several possible mechanisms for producing cosmogenic helium enriched in  ${}^3\text{He}$ : the two most important are capture of thermal neutrons by  ${}^6\text{Li}$  through  ${}^6\text{Li}(n, \alpha)\text{T} \rightarrow {}^3\text{He}$  and spallation reactions on all heavy nuclei to produce T and  ${}^3\text{He}$ . The  ${}^6\text{Li}$  reaction and spallation reactions produce  ${}^3\text{He}/{}^4\text{He}$  of 1 and  $\sim 0.1$  (roughly  $10^6$  and  $10^5$  times atmospheric), respectively. The  ${}^3\text{He}$  production rate by the  ${}^6\text{Li}$  reaction can be readily estimated once the thermal neutron flux is known. The region just below the atmospheric boundary layer will have a higher thermal neutron density due to thermalization of atmospheric fast neutrons<sup>16,17</sup>. Therefore, because of the uncertain sampling depth, a minimum neutron density is given by the production rate within the basalt. The neutron production rate in water at 3 km elevation is roughly  $1.3 \times 10^{-4} \text{ neutrons g}^{-1} \text{ s}^{-1}$  (ref. 18). Scaling according to atomic weight<sup>18</sup>, the neutron production in basalt should be roughly 25% higher than in water. Therefore, a minimum thermal neutron density in the basalt sample is  $\sim 1.6 \times 10^{-4} \text{ neutrons g}^{-1} \text{ s}^{-1}$ , but could be up to five times this value due to thermalization of fast neutrons, depending on the depth below the interface<sup>16,17</sup>.

The fraction of thermal neutrons absorbed by  ${}^6\text{Li}$  is given by  $f = \sigma_{\text{Li}} N_{\text{Li}} / \sum \sigma_i N_i$  where  $\sigma$  is the neutron absorption cross-section (barns, b), and  $N$  is the number of moles of each element ( $i$ ). Using the major- and trace-element composition of Kula alkali basalt<sup>10</sup> for HS85-3,  $\sum \sigma_i N_i = 0.0125 \text{ mol b g}^{-1}$ . Assuming that the Li content is 10 p.p.m. (refs 19, 20),  $f = 8.2 \times 10^{-3}$ , and the  ${}^3\text{He}$  production rate is between 40 and 200 atoms  $\text{g}^{-1} \text{ yr}^{-1}$ . Using the minimum age of the Kula formation ( $\sim 500,000$  yr), this rate would produce between  $7.5 \times 10^{-13}$  and  $3.7 \times 10^{-12} \text{ cm}^3 \text{ STP } {}^3\text{He g}^{-1}$ . Obviously, the depth and age are important unknowns in this calculation, but the  ${}^6\text{Li}$  neutron mechanism alone could readily account for the observed  ${}^3\text{He}$  concentrations ( $\sim 1 \times 10^{-12} \text{ cm}^3 {}^3\text{He g}^{-1}$ ) even if the Li content were a factor of two lower.

The spallation production rate for  ${}^3\text{He}$  can be calculated using the estimates of Yokoyama *et al.*<sup>21</sup> for tritium. Assuming that the  ${}^3\text{He}/\text{tritium}$  production ratio is  $\sim 1$  (ref. 22), and scaling to the atmospheric depth and geomagnetic latitude of Haleakala, the  ${}^3\text{He}$  production rate at the surface is  $\sim 1,100 \text{ atoms g}^{-1} \text{ yr}^{-1}$ . Assuming an attenuation scale of  $180 \text{ g cm}^{-2}$  (M.D.K. *et al.*, in preparation), the production rate at 50 cm would be 630 atoms  $\text{g}^{-1} \text{ yr}^{-1}$  (using a density of  $2 \text{ g cm}^{-3}$ ). These estimates would

Table 2 Stepwise heating experiments

Sample	Temperature (°C)	${}^3\text{He}$ (cm $^3$ STP)	Fraction of total ${}^3\text{He}$	${}^4\text{He}$ (cm $^3$ STP)	Fraction of total ${}^4\text{He}$	${}^3\text{He}/{}^4\text{He}$ ( $R/R_a$ )
<b>HS85-3</b>						
Olivine powder (0.1814 g)	(550) 850 1,000 1,170 1,350 1,750 Total	$1.17 \times 10^{-13}$ $5.65 \times 10^{-14}$ $1.09 \times 10^{-14}$ $3.50 \times 10^{-15}$ $2.33 \times 10^{-15}$ $6.99 \times 10^{-16}$ $1.91 \times 10^{-13}$ $1.05 \times 10^{-12}*$	0.613 0.296 0.057 0.018 0.012 0.004 — —	$1.18 \times 10^{-10}$ $1.56 \times 10^{-11}$ $1.98 \times 10^{-11}$ $6.45 \times 10^{-11}$ $9.66 \times 10^{-11}$ $1.56 \times 10^{-11}$ $3.30 \times 10^{-10}$ $1.82 \times 10^{-9}*$	0.358 0.047 0.060 0.195 0.293 0.047 — —	$714 \pm 12$ $2,600 \pm 235$ $400 \pm 31$ $39 \pm 2$ $17 \pm 2$ $32 \pm 3$ 418 —
1-2 mm olivine (0.1233 g)	850 1,350 1,350 1,350 1,750 Total	$6.90 \times 10^{-14}$ $7.64 \times 10^{-14}$ $9.00 \times 10^{-15}$ $1.83 \times 10^{-15}$ $1.24 \times 10^{-14}$ $1.69 \times 10^{-13}$ $1.37 \times 10^{-12}*$	0.409 0.453 0.053 0.011 0.074 — —	$1.83 \times 10^{-10}$ $7.47 \times 10^{-10}$ $2.29 \times 10^{-10}$ $4.90 \times 10^{-11}$ $5.72 \times 10^{-10}$ $1.78 \times 10^{-9}$ $1.44 \times 10^{-8}$	0.103 0.420 0.129 0.027 0.321 — —	$272 \pm 3$ $73.9 \pm 3$ $28.4 \pm 1.0$ $27 \pm 2.5$ $15.6 \pm 3$ 68.4 —
Clinopyroxene powder (0.1821 g)	(550) 850 850 1,700 Total	$7.75 \times 10^{-14}$ $1.39 \times 10^{-13}$ $3.58 \times 10^{-15}$ $5.15 \times 10^{-15}$ $2.25 \times 10^{-13}$ $1.23 \times 10^{-12}*$	0.344 0.617 0.016 0.023 — —	$2.77 \times 10^{-10}$ $1.55 \times 10^{-10}$ $2.76 \times 10^{-11}$ $2.94 \times 10^{-10}$ $7.54 \times 10^{-10}$ $4.137 \times 10^{-9}*$	0.368 0.206 0.037 0.390 — —	$202 \pm 2$ $649 \pm 7$ $94 \pm 7$ $12.7 \pm 0.4$ 215 —
Matrix (0.1207 g)	(200) (300) (500) 900 1,250 Total	$1.07 \times 10^{-15}$ $3.57 \times 10^{-14}$ $3.42 \times 10^{-14}$ $2.07 \times 10^{-15}$ $1.09 \times 10^{-15}$ $7.41 \times 10^{-14}$ $6.14 \times 10^{-13}*$	0.014 0.482 0.461 0.028 0.015 — —	$8.87 \times 10^{-11}$ $1.07 \times 10^{-9}$ $7.85 \times 10^{-10}$ $3.25 \times 10^{-11}$ $2.92 \times 10^{-11}$ $2.00 \times 10^{-9}$ $1.66 \times 10^{-8}$	0.044 0.534 0.391 0.016 0.015 — —	$8.7 \pm 1.0$ $24.1 \pm 0.3$ $31.5 \pm 0.4$ $46 \pm 3$ $27 \pm 4$ 26.7 —
<b>H85-10</b>						
Olivine powder (0.2128 g)	850 1,150 1,350 1,750 Total	$1.23 \times 10^{-15}$ $9.41 \times 10^{-16}$ $4.54 \times 10^{-15}$ $9.75 \times 10^{-16}$ $7.69 \times 10^{-15}$ $3.62 \times 10^{-14}*$	0.160 0.122 0.591 0.127 — —	$5.52 \times 10^{-10}$ $1.01 \times 10^{-10}$ $3.96 \times 10^{-10}$ $8.68 \times 10^{-11}$ $1.14 \times 10^{-9}$ $5.34 \times 10^{-9}*$	0.486 0.089 0.349 0.076 — —	$1.61 \pm 0.21$ $6.7 \pm 1.0$ $8.3 \pm 0.3$ $8.1 \pm 1.5$ 4.89 —

Temperatures estimated by optical pyrometry; those in parentheses are estimated to be uncertain by 75 °C; all others uncertain by 30 °C. Each temperature step has been corrected for blank  ${}^4\text{He}$  of  $5.2 \pm 0.2 \times 10^{-11}$  cm $^3$  STP and  ${}^3\text{He}$  of  $7.0 \times 10^{-17}$  cm $^3$  STP.

\* cm $^3$  STP g $^{-1}$ .

correspond to  $1.1 \times 10^{-11}$ – $2.0 \times 10^{-11}$  cm $^3$  STP  ${}^3\text{He}$  g $^{-1}$  produced in 500,000 yr, which is significantly greater than both the  ${}^6\text{Li}$  production rate and the observed excess  ${}^3\text{He}$ . Using the calculation method of Reedy and Arnold<sup>23</sup> yields a slightly lower production rate, but is within the uncertainties inherent in the elemental excitation functions and cosmic-ray energy spectrum (details will be given elsewhere).

The other production mechanisms are relatively unimportant for the upper several metres of basalt. The maximum production rate from muon capture processes (see ref. 5) can be estimated by taking the total muon stopping rate<sup>24</sup>, and assuming that the total number of Li atoms reacting is [ $N_{\text{Li}}/N_{\text{total}}$ ]; this mechanism is too low (by a factor of  $\sim 10^5$ ) to be relevant. Takagi<sup>5</sup> has estimated the rates for muon-induced photonuclear processes. Using his  ${}^3\text{He}$  production rate, and a muon flux of 0.01 cm $^{-2}$  s $^{-1}$  (ref. 25), photonuclear processes are also unimportant to the present situation.

Based on these estimates, spallation is the dominant mechanism of cosmogenic  ${}^3\text{He}$  production, although a preliminary report of this work attributed it to the  ${}^6\text{Li}$  reaction<sup>26</sup>. There are several important uncertainties in applying these production rates to sample HS85-3. Both the age and the sampling depth are only known approximately, which can clearly have a large

effect. Also, erosion may have affected the top of the lava flow. The thickness of this lava flow where it was sampled (1.5 m) is quite similar to the thickness at horizons that were later buried<sup>6</sup>, suggesting that erosion has been less than several metres, presumably because of effective drainage near the summit; low erosion rates are also indicated by the presence of intact cinder cones of Kula age<sup>6</sup>. More quantitative discussion of these variables awaits more detailed sampling. Nevertheless, the production rate calculations conclusively show that cosmogenic helium can easily account for the observed excess  ${}^3\text{He}$ .

An additional uncertainty relates to the retention of the cosmogenic helium. The stepwise heating of the phenocrysts released significantly more  ${}^3\text{He}$  than did heating of the basalt matrix. However, the matrix is clearly more susceptible to loss mechanisms because of the smaller grain size of roughly 50  $\mu\text{m}$ , relative to the size of the phenocrysts, which are of the order of several millimetres. For example, if the cosmogenic production rate in the matrix has been similar to that in the phenocrysts,  $\sim 40\%$  has been lost from the matrix. Note also that olivine and clinopyroxene phenocrysts from sample HS85-3 contain roughly the same quantity of cosmogenic  ${}^3\text{He}$  ( $\sim 1.1 \times 10^{-12}$  cm $^3$  STP g $^{-1}$ ; Table 1). This could be explained by the fact that production by spallation is only weakly dependent on composition, with

## LETTERS TO NATURE

virtually all  ${}^3\text{He}$  produced by the major-element targets in the rock (that is, O, Si, Mg, Al). If the  ${}^6\text{Li}$  reaction were the major production mechanism, this uniformity would require that either clinopyroxene and olivine contained equal concentrations of Li, or all the cosmogenic  ${}^3\text{He}$  in the phenocrysts was implanted (as tritium) by the  ${}^6\text{Li}(\text{n}, \alpha){}^3\text{He}$  reactions in the matrix.

Extremely high  ${}^3\text{He}/{}^4\text{He}$  ratios in Kula formation basalt are probably the result of cosmogenic helium, rather than primordial trapped helium<sup>12,13</sup>. Cosmic-ray production rates, exposure ages, and stepwise-heating helium release patterns discussed here are all consistent with this hypothesis. Furthermore, the extremely high  ${}^3\text{He}/{}^4\text{He}$  ratios are not observed in two 'shielded' samples of the same age, or in a historic lava flow (Table 1). A consistent stratigraphical  ${}^3\text{He}/{}^4\text{He}$  trend for Haleakala has been documented<sup>26</sup> that strongly supports the notion that the surface sample contains cosmogenic helium. A more extensive series of samples, spanning the entire range of available ages from Haleakala, yield systematic variability with volcano evolution<sup>26</sup>; all the shielded Hana and Kula series samples have  ${}^3\text{He}/{}^4\text{He}$  ratios indistinguishable from MORB ( $8 R_a$ ).

Cosmogenic helium has been neglected previously, and is clearly important for interpreting helium isotopic results from rock samples that have remained near the surface for long periods of time. In order for cosmogenic helium to be significant, the surface exposure time must be long enough and the initial trapped helium content must be low, factors that must be carefully considered before high  ${}^3\text{He}/{}^4\text{He}$  ratios are attributed to 'primordial' helium. Because the cosmogenic  ${}^3\text{He}/{}^4\text{He}$  ratio is so high, a very small contribution can greatly elevate the measured  ${}^3\text{He}/{}^4\text{He}$  ratio. If some of the uncertainties regarding  ${}^3\text{He}$  production rates and potential loss mechanisms can be resolved, several important geophysical applications will be possible. Cosmogenic nuclides could be used to study ancient cosmic-ray fluxes, terrestrial erosion rates (see refs 27, 28) and possibly exposure ages for terrestrial lava flows.

A result that also has important implications for helium isotope studies is the internal isotopic heterogeneity within olivine and clinopyroxene mineral separates. Although it has generally been assumed that phenocrysts in basaltic lavas reflect the helium isotopic composition of the host magma<sup>12</sup>, the results reported here suggest that this is not necessarily true for older samples, even if cosmogenic helium is absent. Radiogenic helium will tend to lower the  ${}^3\text{He}/{}^4\text{He}$  ratios obtained by total fusion. The combination of crushing in vacuum and stepwise heating techniques provide a valuable experimental protocol for addressing this problem.

I thank M. Garcia, F. Frey and J. Nicholls for providing the samples and for discussing the geology of Haleakala. W. J. Jenkins, R. Reedy and T. Trull provided useful comments and D. Lott and P. O'Brien, laboratory assistance. I also thank Molly Lumpkin for typing, and Marie Johnson and Colleen Hurter for literary assistance. This work was supported by grants NSF-0CE-83-15270 and NASA-ECG-NAG-9-69. This is Woods Hole contribution no. 6059.

Received 25 October 1985; accepted 22 January 1986.

- Tolstikhin, I. N. in *Terrestrial Rare Gases* (eds Alexander, E. C. & Ozima, M.) (Japan Scientific Society Press, Tokyo, 1978).
- Craig, H. & Lupton, J. in *The Sea* Vol. 7 (ed. Emiliani, C.) (Wiley, New York, 1981).
- Bernatowicz, T. J. & Podosek, F. A. in *Terrestrial Rare Gases* (eds Alexander, E. C. & Ozima, M.) (Japan Scientific Society Press, Tokyo, 1978).
- Jeffrey, P. M. & Hagan, P. J. *Nature* **223**, 1253 (1969).
- Takagi, J. *Nature* **227**, 362–363 (1970).
- Stearns, H. T. & MacDonald, G. A. *Hawaii Division Hydrol. Bull.* **7**, 1–344 (1942).
- MacDonald, G. A. & Powers, H. A. *Bull. geol. Soc. Am.* **57**, 115–124 (1946).
- McDougall, I. *Bull. geol. Soc. Am.* **75**, 107–128 (1964).
- Naughton, J. J., MacDonald, G. A. & Greenberg, V. A. J. *Volcan. Geotherm. Res.* **7**, 339–335 (1980).
- Chen, C. Y. & Frey, F. A. *Nature* **302**, 785–789 (1983).
- Chen, C. Y. & Frey, F. A. *J. geophys. Res.* **90**, 8743–8768 (1985).
- Kaneoka, I. & Takaoka, N. *Science* **208**, 1366–1368 (1980).
- Rison, W. & Craig, H. *Earth planet. Sci. Lett.* **66**, 407–426 (1983).
- Kurz, M. D., Meyer, P. & Sigurdsson, H. S. *Earth planet. Sci. Lett.* **74**, 291–305 (1985).

- Kurz, M. D., Jenkins, W. J., Hart, S. R. & Clague, D. *Earth planet. Sci. Lett.* **66**, 338–406 (1983).
- Bethe, H., Korff, S. A. & Glazek, G. *Phys. Rev.* **57**, 573–587 (1940).
- Swetnick, M. J. *Phys. Rev.* **95**, 793–796 (1954).
- Yamahita, M., Stephens, L. D. & Patterson, H. W. *J. geophys. Res.* **71**, 3817–3834 (1966).
- Shaw, D. M., Vatin-Perignon, N. & Muysse, J. R. *Geochim. cosmochim. Acta* **41**, 1601–1607 (1977).
- Bailey, J. C. & Gwodzdz, R. *Lithos* **11**, 73–84 (1978).
- Yokoyama, Y., Reys, J.-L. & Guichard, F. *Earth Planet. Sci. Lett.* **36**, 44–50 (1977).
- Kruger, S. T. & Heymann, D. *J. geophys. Res.* **73**, 4784–4787 (1968).
- Reedy, R. C. & Arnold, J. R. *J. geophys. Res.* **77**, 557–555 (1972).
- Hampel, W. & Kirsten, T. *Proc. 14th int. Cosmic Ray Conf.* **14**, 1895–1909 (1975).
- Rossi, B. *High Energy Particles* (Prentice-Hall, New Jersey, 1952).
- Kurz, M. D., O'Brien, P. A., Garcia, M. O. & Frey, F. A. *Eos* **66**, 1120 (1985).
- Jha, R. & Lal, D. *Proc. 2nd Symp. on Natural Radiation Environment* (eds Vohra, K. G. et al.), 629–635 (Wiley Eastern Limited, New Delhi, 1981).
- Lal, D. & Arnold, J. R. *Proc. Ind. Acad. Sci.* **94**, 1–5 (1985).

## Small non-overlapping offsets of the East Pacific Rise

Rodey Batiza & Steven H. Margolis

McDonnell Center for the Space Sciences, Washington University, St Louis, Missouri 63130, USA

High-resolution bathymetric surveys<sup>1,2</sup> of the East Pacific Rise (EPR) reveal that in addition to overlapping spreading centres (OSCs), the crest of the EPR is offset tiny amounts by smaller features. Recently, Langmuir *et al.* have shown that despite their subtle bathymetric expression, these small offsets, bends and kinks of the EPR, collectively termed deviations from axial linearity (devals), represent important petrological and tectonic boundaries. Some devals are small non-overlapping offsets (SNOOs) that offset the EPR axis by up to a few hundred metres. Bathymetric contours near SNOOs are usually disturbed from their axis-parallel trend in ways that we interpret as evidence for strike-slip faulting and volcanism at high angles to the trend of EPR axis. We offer a model for the formation of SNOOs and their associated faults that invokes independent magma supply, stochastic active spreading and limited non-rigid behaviour of the neovolcanic zone.

Macdonald *et al.*<sup>1</sup> and Lonsdale<sup>2,4</sup> mapped OSCs at the EPR and recognized that bends, kinks and small offsets occur along the EPR axis. Langmuir *et al.*<sup>3</sup> called attention to these smaller features, or devals, because in some cases they represent important petrological boundaries which, along with transform faults and OSCs, define the fundamental petrological and tectonic segmentation of the EPR. Small non-overlapping offsets (SNOOs) are devals which exhibit tiny (up to several hundred metres) lateral offsets of the EPR axis. Unlike OSCs, SNOOs exhibit no overlap. Previously unrecognized is the fact that near SNOOs, axis-parallel depth contours are commonly deflected to be perpendicular, or nearly so, to the EPR axis. We interpret these ridge-normal contour patterns as evidence for strike-slip faults and associated volcanism in the vicinity of SNOOs.

Figure 1 shows an example of a SNOO of the EPR near  $13^{\circ}45' \text{N}$  mapped by Macdonald *et al.*<sup>1</sup>. It is a tiny offset of the EPR that occurs at a local bathymetric low point along the axis. On the south-west side of the SNOO, depth contours swing to the west and are nearly perpendicular to the ridge for several hundred metres away from the ridge crest. Other examples of SNOOs along the EPR can be seen in the published maps of Macdonald *et al.*<sup>1</sup> at  $8^{\circ}42'$ ,  $9^{\circ}00'$ ,  $9^{\circ}02'$ ,  $9^{\circ}04'$ ,  $9^{\circ}06'$ ,  $10^{\circ}20'$ ,  $10^{\circ}31'$ ,  $10^{\circ}42'$ ,  $11^{\circ}16'$ ,  $11^{\circ}45'$ ,  $11^{\circ}58'$ ,  $12^{\circ}10'$ ,  $12^{\circ}17'$ ,  $12^{\circ}27'$ ,  $12^{\circ}34'$ ,  $12^{\circ}36'$ ,  $12^{\circ}39'$ ,  $12^{\circ}50'$ ,  $13^{\circ}46'$ ,  $13^{\circ}47'$ ,  $13^{\circ}57'$ , and  $14^{\circ}12'$ . Lonsdale<sup>2</sup> shows one at  $3^{\circ}48' \text{N}$  and another possible example is present at the Galapagos spreading centre at  $86^{\circ}05' \text{W}$ <sup>5</sup>. Particularly good examples, also known to be petrological boundaries<sup>3</sup>, are at  $11^{\circ}16'$ ,  $12^{\circ}10'$ ,  $12^{\circ}17'$ ,  $12^{\circ}27'$  and  $13^{\circ}47'$  (Fig. 1). These features are commonly: (1) tiny offsets of the ridge axis; (2) located at

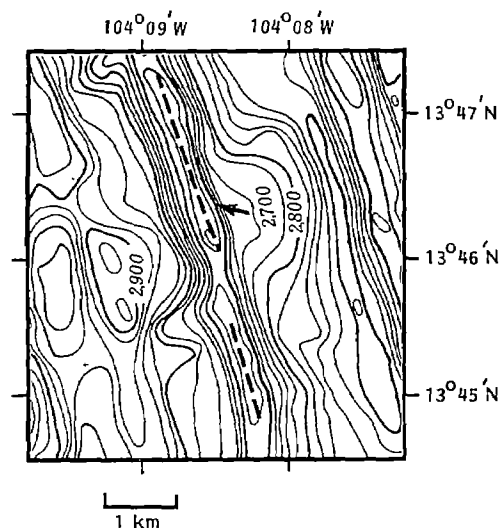


**Fig. 1** Seabeam bathymetry (contour interval 20 m) from ref. 1 showing a small non-overlapping offset (SNOO) at 13°45' N. Note that on the west side of the ridge axis, depth contours veer away and become nearly perpendicular to the ridge. Although subtle bathymetric features like this are found along the ridge at many localities, they are a characteristic feature of SNOOs.

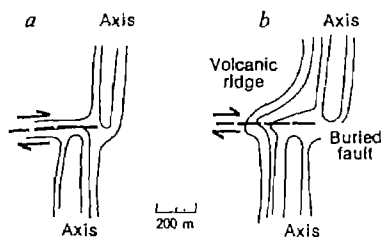


**Fig. 2** Schematic drawing of SNOOs showing our interpretation of the subtle bathymetric disturbances that occur near them. In *a*, the model depth contours (1–5 m contour interval) define a strike-slip fault, expected to have only subtle bathymetric expression. In *b*, the bathymetric expression of the buried strike-slip fault is accentuated by the formation of a volcanic ridge. Both types of SNOO can be seen along the EPR<sup>1,2</sup>. See text for discussion

a bathymetric low point along the axis; and (3) associated with disturbed, ridge-normal depth contours usually on only one side of the ridge. As shown in Fig. 2, we interpret the disturbed contours to represent ridge-normal strike-slip faults and volcanic ridges that, in some cases, bury them. Small submarine strike-slip features without dip-slip movement or volcanism should have only subtle bathymetric expression.

To explain the occurrence of SNOOs and their off-axis disturbed zones (presumed strike-slip faults) we offer a simple model for possible ridge crest behaviour that results in the formation of new SNOOs along previously continuous ridge crest segments. Since SNOOs can be major petrological boundaries, their origin may be linked to magma supply processes<sup>1,3</sup>. Consequently, in our model we assume that the EPR is supplied by discrete magma systems along its length, for which there is a great deal of independent evidence<sup>1,3,6–8</sup>. We also assume that spreading is stochastic. This means that each distinct tectonic and volcanic process associated with plate separation, such as fissuring, extensional normal faulting, dyke injection and deeper magma intrusion is episodic and its rate of occurrence is normally distributed about a mean value<sup>9</sup>. It is not yet known to what extent these distinct tectonic and volcanic processes are correlated, periodic or causally related<sup>10–18</sup>, hence our model is

quite generalized. Finally, we assume that dyke injection or other intrusive processes cause lateral stresses near the surface<sup>19</sup> sufficient to deform the upper parts of the crust. That is, we assume a causal relationship between igneous and tectonic components of spreading. This is speculative, but it is known that intrusion and surface deformation are correlated in some active volcanic rift zones<sup>20,21</sup>.

According to this model, we view the spreading behaviour of adjacent but independently supplied ridge segments as uncorrelated. If a segment actively spreads while adjoining segments do not, offsets between segments will be created in the weak neovolcanic zone. These offsets behave as small ephemeral transform faults except that non-rigid plate deformation is required, which results in relative motion and strike-slip deformation outside the axial rift zone. Consider an initially straight ridge segment as in Fig. 3. Each independently supplied segment has an instantaneous spreading rate  $S_i$ , given by

$$S_i = \bar{S}_i + \sigma_i X \quad (1)$$

where  $i = 1, 2$  for the two segments,  $\bar{S}_i$  and  $\sigma_i$  are the mean and standard deviation of the spreading rate distribution and  $X$  is a standardized normal variable, a random variable with zero mean and unit variance. For simplicity, we assume that the mean spreading rate and standard deviation of each segment are equal (Fig. 3). The instantaneous spreading rate is simply equal to the mean rate plus (or minus) a randomly varying amount. Since each ridge segment selects instantaneous spreading rates episodically (with characteristic time  $\tau$ ) from a distinct, albeit identical, gaussian distribution, offsets between adjoining ridge segments will statistically appear and disappear if the model assumptions are met. The lengthening of these offsets is itself stochastic:

$$S_1 - S_2 = (\bar{S}_1 - \bar{S}_2) + \sqrt{(\sigma_1^2 + \sigma_2^2)} X \quad (2)$$

which can be rewritten

$$S_1 - S_2 - (\bar{S}_1 - \bar{S}_2) = \sigma X \quad (3)$$

where

$$\sigma^2 = (\sigma_1^2 + \sigma_2^2) \quad (4)$$

Next, we use a random walk model<sup>22,23</sup> to consider the distribution of offset lengths after time  $t$ . This is:

$$P(x) = \frac{e^{-\frac{1}{2}(x/\sigma_R)^2}}{\sqrt{2\pi}\sigma_R} \quad (5)$$

where

$$\sigma_R = \sigma\sqrt{\tau} \quad (6)$$

is the standard deviation of the distribution of offset lengths at time  $t \gg \tau$ . The probability of finding an offset larger than  $L$  at time  $t$  is the integral of this distribution:

$$P(x > L) = 2 \int_L^\infty P(x) dx \quad (7)$$

$$= \sqrt{\frac{2}{\pi}} \int_{L/\sigma_R}^\infty e^{-x^2/2} dx \quad (8)$$

Figure 4 shows the probability of occurrence of offsets of various lengths for different values of  $\sigma_R$ . For the EPR, if we choose a mean spreading rate of  $6 \pm 0.7 \text{ cm yr}^{-1}$  and  $\tau = 10^4 \text{ yr}$ , then  $\sigma_R$  is 316 m for  $t = 10^5 \text{ yr}$ . In this example, offsets on the order of 300 m would be expected to develop during a period over which about 6 km of total spreading occurred. Other values may be chosen, since actual values of  $\sigma$  and  $\tau$  for the EPR are not known; however, the values chosen in this example do not seem unreasonable. This model thus shows that observed offsets at SNOOs ( $\sim 10^2 \text{ m}$  in length) can be accounted for by the sort of model we propose.

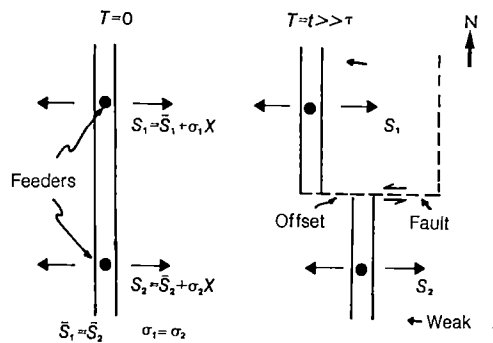


**Fig. 3** Illustration of our proposed model for the origin of SNOOs and ridge-normal structures. At time  $T=0$ , the initially straight ridge segment is fed by two independent feeders and the ridge portions associated with each feeder spread at instantaneous rates of  $S_1$  and  $S_2$  respectively. The mean spreading rates ( $\bar{S}_1$  and  $\bar{S}_2$ ) and the normally-distributed standard deviations from the mean ( $\sigma_1$  and  $\sigma_2$ ) are equal. In these idealized conditions, offsets will develop by deformation of the weak zone near the ridge axis due to tiny stochastic differences in  $S_1$  and  $S_2$  that accumulate after a time interval  $t$ . Although the mean and standard deviation of instantaneous spreading are the same for both ridges, the random component is selected from distinct, albeit identical, distributions. In this example we assume that spreading of segment 2 is fully asymmetric (east flanks weaker than west flank). If symmetric spreading occurred (east and west ridge flanks equally strong) no offset would develop, but strike-slip deformation would occur on both flanks.

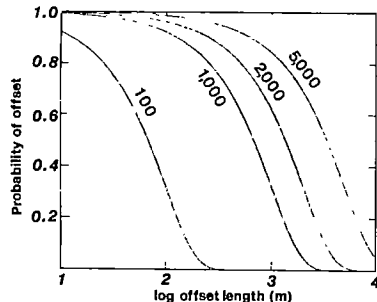


**Fig. 4** Plot of expected offset length between two independently-fed ridge segments ( $\log_{10}$  offset length in metres) versus the probability that it will be observed for several values of  $\sigma_R$ .  $\sigma_R$  is a function of the standard deviation of the mean spreading rate, the duration of spreading ( $t$ ) and  $\tau$ , the characteristic time of the spreading process. Offsets of several hundred metres can develop for  $t \geq 10^5$  yr and reasonable choices of the other variables. See text for discussion.

As shown in Fig. 3, an episodic increment of spreading (intrusion and extension) at a ridge segment while the adjoining segment is quiet can be accommodated in two extreme ways. If both flanks of the rift are equally strong, the relative motion between two adjoining segments could be taken up by strike-slip deformation of both flanks. In this case, no offset between the ridge segments would be created. On the other hand, if one flank is weaker than the other because of local heterogeneity or some other reason, the necessary strike-slip deformation could be confined to one flank. Such behaviour could result in asymmetric spreading as in zero-offset transform faults<sup>24</sup>.

According to our model, SNOOs are newly created as a direct consequence of independent magma supply systems along the EPR. In this regard, our model can be viewed as an extension of the model proposed by Macdonald *et al.*<sup>1</sup> for the behaviour of the EPR. The model has several predictions that can be tested when sufficient data of high resolution are available.

For example, the sea floor in the vicinity of SNOOs should exhibit evidence of strike-slip faulting and/or volcanic eruption along ridge-normal conduits. If evidence of SNOOs and their associated faults is preserved on older ocean floor away from the axis, their distribution could be used to infer the past geometry of magma feeders at the EPR and their temporal stability.

This study was supported by NSF and ONR. We thank the following persons for providing helpful comments on an earlier draft of this paper and for useful discussions: C. Langmuir, J. Bender, K. Macdonald, J. Fox, H. Schouten, R. Hey, P. Lonsdale, J. Allan and D. Wiens. We thank K. Macdonald and J. Fox for kindly providing copies of charts of the EPR.

Received 19 August 1985; accepted 9 January 1986.

- Macdonald, K. C., Sempere, J.-C. & Fox, P. J. *J. geophys. Res.* **89**, 6049–6069 (1984).
- Lonsdale, P. *Bull. geol. Soc. Am.* **96**, 313–327 (1985).
- Langmuir, C. H., Bender, J. F. & Batiza, R. (in preparation).
- Lonsdale, P. *J. geophys. Res.* **88**, 9393–9406 (1983).
- Ballard, R. D., Van Andel, T. H. & Holcomb, R. T. *J. geophys. Res.* **87**, 1149–1161 (1982).
- Whitehead, J. A., Dick, H. J. B. & Schouten, H. *Nature* **312**, 146–148 (1984).
- Schouten, H., Klitgord, K. D. & Whitehead, J. A. *Nature* **317**, 225–229 (1985).
- Crane, K. *Earth planet. Sci. Lett.* **72**, 405–414 (1985).
- Schouten, H. and Denham, C. R. in *Deep Drilling Results in the Atlantic Ocean: Ocean Crust* (eds Talwani, M., Harrison, C. G. & Hayes, D. E.) 151–159 (American Geophysical Union, Washington DC, 1979).
- Atwater, T. in *Deep Drilling Results in the Atlantic Ocean: Ocean Crust* (eds Talwani, M., Harrison, C. G. & Hayes, D. E.) 33–42 (American Geophysical Union, Washington DC, 1979).
- Lister, C. R. B. *EOS* **63**, 1153 (1982).
- Defant, K. S. in *Megatectonics of Continents and Oceans* (eds Johnson, H. & Smith, B. L.) 194–222 (Rutgers University Press, New Brunswick, 1970).
- Anderson, R. N. & Noltman, H. C. *J. R. astr. Soc. Can.* **34**, 137–157 (1973).
- Lachenbruch, A. H. *J. geophys. Res.* **78**, 3395–3417 (1973).
- Lachenbruch, A. H. *J. geophys. Res.* **81**, 1883–1902 (1976).
- Tappronnier, P. & Francheteau, J. *J. geophys. Res.* **83**, 3995–3970 (1978).
- Sleep, N. in *Hydrothermal Processes at Seafloor Spreading Centers* (eds Rona, P. A., Boström, K., Laubier, L. & Smith, K. L.) 71–82 (Plenum, New York, 1983).
- Kappel, E. S. & Ryan, W. B. F. *EOS* **65**, 1110 (1984).
- Spence, D. A. and Turcotte, D. L. *J. geophys. Res.* **90**, 375–580 (1985).
- Björnsson, A., Johnsen, G., Sigurdsson, S. & Thorbergsson, G. *J. geophys. Res.* **84**, 3017–3028 (1979).
- Duffield, W. A., Jackson, D. B. & Swanson, D. A. in *Proc. Symp. Alpine and Arctic Volcanology Problems* 577–587 (Giannini and Figli, Napoli, 1976).
- Feller, W. *An Introduction to Probability Theory and its Applications*, V. I. 1 (John Wiley, New York, 1968).
- Uhlenbeck, G. E. & Ornstein, L. S. *Phys. Rev.* **36**, 823 (1930).
- Schouten, H. & White, R. S. *Geology* **8**, 175–179 (1980).

## The last pluvial climatic episodes in the deserts of southwestern North America

W. Geoffrey Spaulding\* & Lisa J. Graumlich†

\* Quaternary Research Center and Department of Botany, University of Washington, Seattle, Washington 98195, USA

† Department of Ecology and Behavioral Biology, University of Minnesota, Minneapolis, Minnesota 55455, USA

Long-term variations in the effective moisture of deserts are linked both to glacial-interglacial climatic cycles and, through the Milankovitch theory, to orbitally induced changes in solar radiation intensity<sup>1–4</sup>. For southwestern North America, comparison of palaeobotanical data with model predictions of palaeoclimate reveals two distinct pluvial regimes during the late Wisconsin and early Holocene (23–8 kyr BP). Southward displacement of the Aleutian low-pressure centre and strengthened westerlies from ~40° to 30° N were important features of the full-glacial (~18 kyr BP) pluvial maximum. Increased cyclonic storms and weakened monsoons led to a winter precipitation regime, a feature seen both in the fossil record<sup>5,6</sup> and climate models<sup>7,8</sup>. Dominantly zonal flow during this period contrasts with the latest Wisconsin and early Holocene (12–8 kyr BP), when meridional circulation transported maritime tropical air into the desert interior. We now show

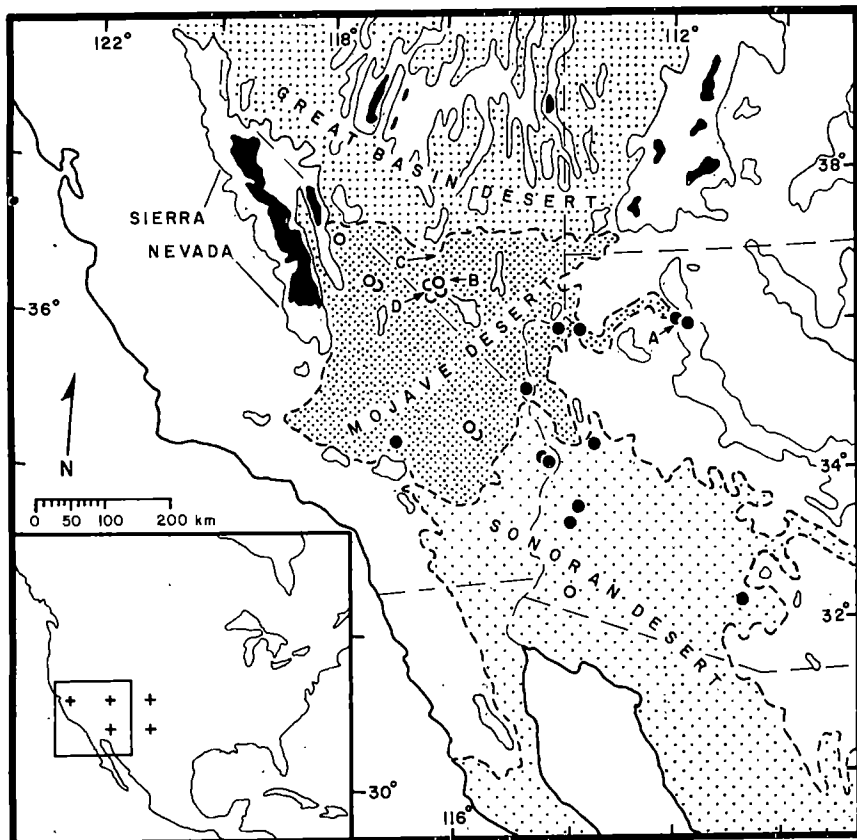


**Fig. 1** The Sonoran, Mojave and southern Great Basin Deserts of North America. Solid lines indicate the 2,000-m contour interval; topography above 3,000 m is shaded. Packrat midden records from below 1,200 m elevation dating from 12 to 8 kyr BP are of desert scrub (open circles) and woodland (closed circles). Other localities mentioned in the text are: A, Grand Canyon; B, Skeleton Hills and Point of Rocks; C, Eleana Range; D, Amargosa Desert. Inset shows the grid points (+) in the Community Climate Model from which area averages were derived for the south-west (Fig. 2).

that plant macrofossil assemblages from packrat (*Neotoma* spp.) middens<sup>9</sup> in the Mojave Desert provide evidence for increased temperatures and summer rainfall during this period<sup>10–12</sup>. The anomalously late persistence (to ~8 kyr BP) of woodland in low-latitude, low-elevation deserts of the south-west<sup>13</sup> is attributed to enhanced monsoonal circulation<sup>3</sup>.

North America's deserts range from the high-latitude steppe of the Great Basin to the subtropical scrub of the Sonoran Desert (Fig. 1). Precipitation seasonality varies: the Great Basin and Mojave Deserts receive <25% of annual precipitation during the summer, whereas the Sonoran Desert has a distinct summer monsoon which accounts for 40–60% of annual precipitation<sup>14,15</sup>. During the full glacial the Sonoran Desert supported widespread woodland characterized by pygmy conifers (*Pinus monophylla*, *Juniperus* spp.), live oaks (*Quercus turbinella*, *Q. dunnii*) and succulents (Agavaceae, Cactaceae). The composition of diverse woodland communities in Sonoran Desert lowlands, and their location more than 600 m below current woodland on nearby mountains, indicates increased annual precipitation (perhaps double today's amounts), reduced summer temperatures and mild winters<sup>5,6</sup>.

North of ~36° N, woodland also occurred far below its current lower altitudinal limit. However, these full-glacial communities did not support the diversity of trees and succulents found farther south. Five low-elevation (<1,200 m), full-glacial Sonoran Desert middens<sup>16,17</sup> provide records of 7 tree species, 14 succulents and 2 steppe shrubs. In contrast, nine low-elevation Mojave Desert sites<sup>10,18</sup> yield only 3 tree species and 6 succulents, but 8 steppe shrub taxa, indicating an effectively drier palaeoclimate. Indeed, the full-glacial Mojave Desert was sufficiently dry to support desert vegetation below 1,000 m elevation<sup>18,19</sup>. Zoned above desert scrub, xerophytic juniper woodland ranged to 1,800 m. Subalpine woodland occurred at higher elevations, dominated by cold-tolerant xerophytic conifers, limber pine (*Pinus flexilis*) and bristlecone pine (*P. longaeva*)<sup>20,21</sup>. Steppe shrubs were widespread not only in desert vegetation, but also in low-elevation and subalpine woodlands<sup>6</sup>.

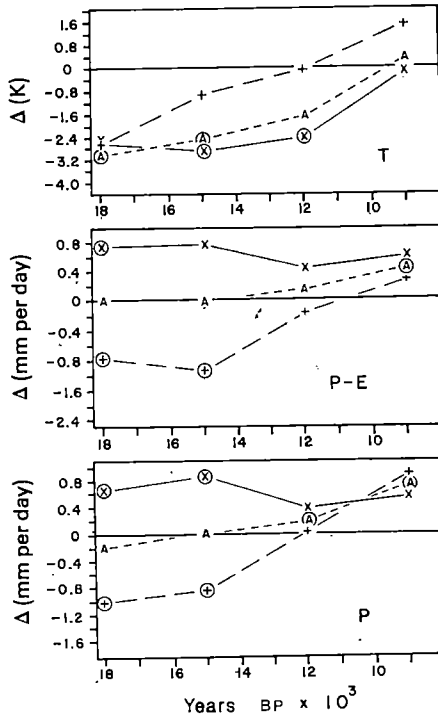


**Fig. 2** Area averages for five land-surface grid points representing southwestern North America (Fig. 1) in the Community Climate Model, programmed for boundary conditions at 3-kyr intervals from 18 to 9 kyr BP. The zero value (horizontal line) in each case represents the result of the control experiment for modern conditions. Model results for temperature (T), precipitation minus evaporation (P-E), and precipitation (P) are expressed in terms of deviations ( $\Delta$ ) for simulations of January (x), July (+) and average annual (A) conditions. Circled symbols represent significant differences from the control result at the 95% level (two-sided  $t$ -test).

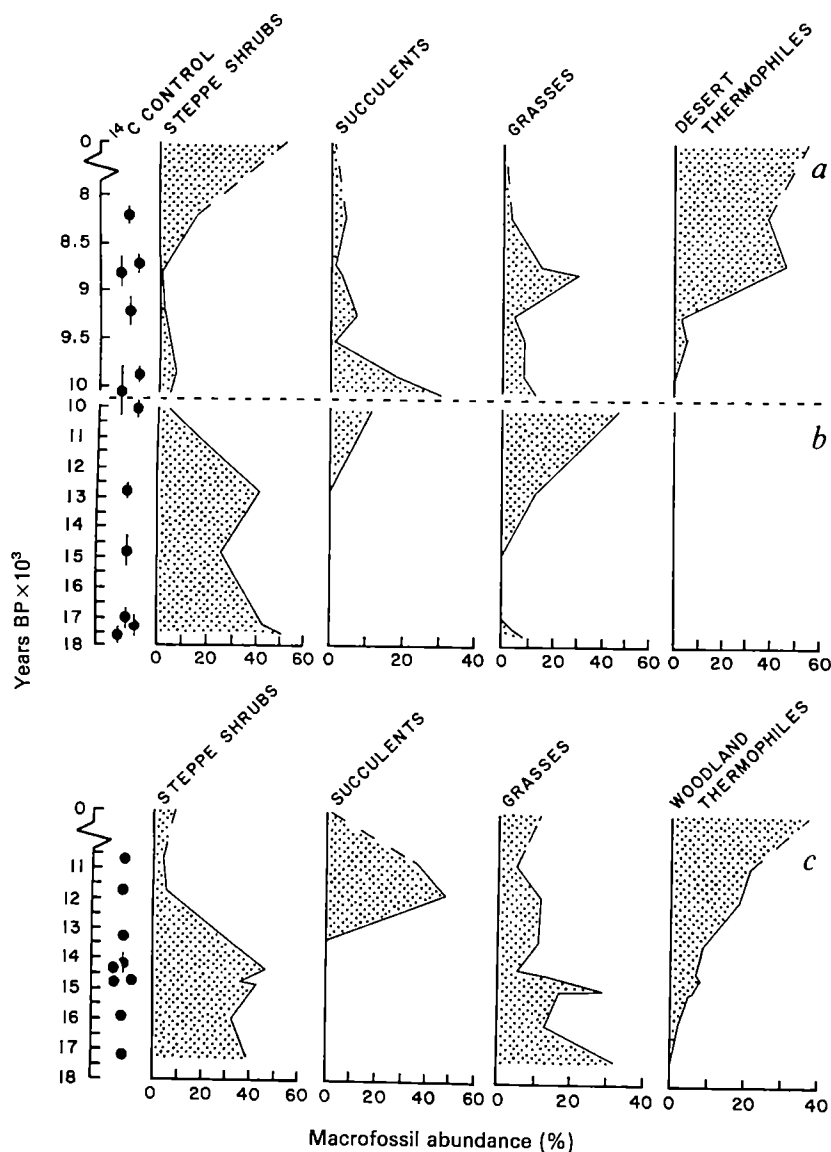


**Fig. 3** Relative abundance of selected plant macrofossils from radiocarbon-dated assemblages collected at three packrat midden sites in the northern Mojave Desert. *a*, Skeleton Hills; *b*, Point of Rocks; *c*, Eleana Range. Macrofossil abundance expressed as percentages of the total number of identified specimens minus the number of specimens of the dominant taxon (NISP-DT). Dashed lines separate the youngest macrofossil assemblages at the Eleana Range-2 and Skeleton Hills-2 sites from the modern control samples collected at those sites. Note changes in the time scale

Mojave Desert macrofossil assemblages reflect a glacial climate distinct from that of the Sonoran Desert. The absence of thermophiles suggests a decline in annual temperatures of  $>6^{\circ}\text{C}$  (ref. 10), contrasting with an estimated decline of  $<4^{\circ}\text{C}$  for the Sonoran Desert<sup>16</sup>. Full-glacial desert scrub and the xerophytic nature of Mojavean woodland accord with a 'pluvial' climate characterized by an increase in annual precipitation of not more than 40%<sup>10,12</sup>. A survey of potential pluvial lake basins in Nevada confirms comparatively dry conditions; many closed valleys in the southern Great Basin have no shoreline features<sup>22</sup>.

The mean position of the winter storm track, now north of  $42^{\circ}\text{N}$  (ref. 23), was shifted south during the full glacial, accounting for pluvial climatic conditions in the south-west<sup>5-7</sup>. Simulations using the US National Center for Atmospheric Research Community Climate Model (CCM) replicate this circulation feature<sup>8,24</sup>. Mesoscale heterogeneity is smoothed by area averages for the south-west (Fig. 2), but these show significant reductions in July precipitation and increases in January precipitation. The transition to relatively dry conditions north of  $36^{\circ}\text{N}$  was topographically controlled. The Sierra Nevada mountain range, reaching altitudes  $>3,000\text{ m}$  north of  $36^{\circ}\text{N}$  (Fig. 1), is a barrier to westerly airflow. In its lee, conditions were relatively dry, while a pronounced pluvial occurred south of  $36^{\circ}\text{N}$ . Such regional variation of palaeoclimate calls into question any single reconstruction put forward to account for palaeophenomena of this subcontinental-scale region.

Decreasing effective moisture is evident by  $\sim 15\text{ kyr BP}$  in the pluvial lake<sup>25-27</sup> and packrat midden record<sup>12</sup>. This late glacial climatic change accentuated regional vegetation differences. Between 10 and 8 kyr BP woodland persisted in the Sonoran Desert<sup>13</sup> but had retreated from most low-elevation sites in the Mojave Desert<sup>28</sup>, a marked anomaly considering that, 2-4° farther south, woodland occurred more than 400 m lower in elevation (Fig. 1). Where desertification might be expected earliest, at low elevations and latitudes in the Sonoran Desert, one finds instead the persistence of woodland long after its demise to the north. The distribution of low-elevation woodland from  $\sim 12-8\text{ kyr BP}$  (Fig. 1) is congruent with the present pattern of summer rainfall dominance in the south-west<sup>23,29</sup>.

Simulations of early Holocene climate<sup>2,8,30</sup> and field evidence from Africa and India<sup>3,31-33</sup> indicate strengthened monsoons at subtropical latitudes. In light of these studies and the following data, we propose that post-glacial woodland persistence in the Sonoran Desert was due to intensified monsoonal precipitation. Strengthened monsoons should be reflected in the fossil record from the summer-dry northern Mojave Desert by increases in succulents and grasses (Poaceae), plants that today are important in areas which receive high proportions of summer rains. Steppe shrubs, typical of winter-rainfall regimes, are expected to be abundant when winter rains dominate.

Assemblages from the Point of Rocks-3 (PR-3) and Eleana Range-2 (ER-2) sites record palaeo-vegetation in distinctly

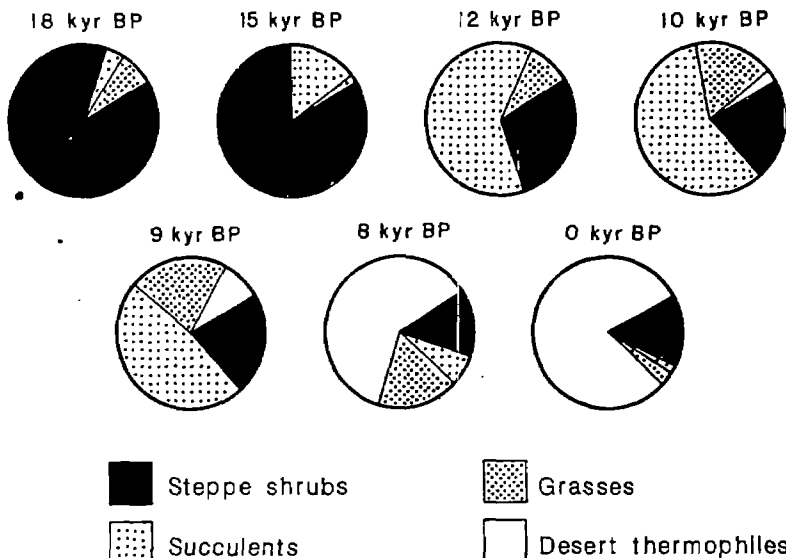


Fig. 4 Averaged relative abundance of selected plant types from macrofossil assemblages at sites below 1,200 m elevation in the Amargosa Desert, an intermontane valley in the northern Mojave Desert (Fig. 1). All packrat midden samples of an age within 1 kyr of the specified age class are considered in averages for that class. Number of sites, with number of samples in parentheses: 18 kyr, 4(6); 15 kyr, 2(3); 12 kyr, 2(5); 10 kyr, 8(14); 9 kyr, 5(12); 8 kyr, 1(3); 0 kyr, 9(9).

different habitats from ~17.5 to 10 kyr BP. PR-3 at 930 m elevation supports xerophytic Mojave Desert scrub, while ER-2 at 1,800 m is at the lower limit of modern woodland. During the full glacial ER-2 supported limber pine and steppe shrubs, while vegetation at PR-3 was dominated by steppe shrubs alone<sup>10,12</sup>. Increasing woodland thermophiles at ER-2 after ~15 kyr BP (Fig. 3) is consistent with CCM-simulated increases in July temperature (Fig. 2). Steppe shrubs decline between 14 and 12 kyr BP (Fig. 3). Samples dating from ~12–10 kyr BP contain abundant succulents and, at the PR-3 site, grasses, indicating summer precipitation. At Skeleton Hills-2, a site similar to PR-3, succulents are important only in samples dated at ~10 kyr BP, suggesting that intensified summer rains ended shortly thereafter (Fig. 3). Steppe shrubs in the modern sample properly reflect winter seasonality of precipitation. Figure 4 summarizes macrofossil data from an intermontane valley in the northern Mojave Desert. Changes in steppe shrub, succulent and grass abundance are those expected from full-glacial winter precipitation dominance, followed by latest Wisconsin and early Holocene summer rainfall dominance.

CCM area averages (Fig. 2) show substantial relative increases in July precipitation during the latest Wisconsin and early Holocene, consistent with fossil data from the Mojave Desert and the Grand Canyon, and attributed to increased summer insolation. The last solar radiation maximum during northern-latitude summer occurred between 11 and 9 kyr BP<sup>35</sup>. Enhanced monsoons also explain the persistence of woodland in the Sonoran Desert, closest to sources of maritime tropical moisture in the Gulf of Mexico and Pacific Ocean. Absence of summer-rain-dependent Sonoran Desert perennials has led to the assertion that monsoons were unimportant at this time<sup>13</sup>. Most Sonoran taxa are frost-sensitive and a CCM area-averaged January temperature for 12 kyr BP is ~2.4 °C below that of the control. The end of this period of relatively cold winter temperatures occurred by ~9 kyr BP (Fig. 2), when desert thermophiles began to increase (Figs 3, 4).

In conclusion, the deserts of southwestern North America lie at higher latitudes, and were in closer proximity to continental ice sheets than those of North Africa and India. Southward deflection of the Pacific westerlies led to a full-glacial pluvial climate. Topographic modulation of airflow created distinct subregional climates. South of the Sierra Nevada, precipitation was greatly enhanced during the full glacial, while in its lee, conditions were drier. Full-glacial CCM area averages do not simulate a decline in July temperature appreciably greater than that for January temperature (Fig. 2), a failure to replicate conditions called for in reconstructions stressing increased equability<sup>5,36</sup>. This is consistent with recent studies indicating substantial lowering of both January and July temperatures<sup>10,12</sup>.

Annual *P – E* (precipitation minus evaporation) simulations for the full glacial approximate modern values (Fig. 2), and conflict with most data indicating increased effective moisture throughout the south-west. This may indicate a deficiency in the model, although results are sensitive to choice of representative grid points. Enhanced monsoons between ~12 and ~9 kyr BP had greatest impact in the Sonoran Desert, explaining delayed desertification there by the overlap of two distinct pluvial episodes. The first, associated with full-glacial climate dynamics, was characterized by lowered temperatures and enhanced winter rainfall. The second, induced by changes in seasonal insolation, was characterized by annual temperatures near the modern mean and enhanced monsoons.

This research was supported by the US Geological Survey, the US Department of Energy, and the NSF. We thank John Kutzbach for discussion and for CCM model results.

Received 15 October 1985; accepted 5 February 1986.

- Berger, A. L. *et al.* (eds) *Milankovitch and Climate* (Reidel, Dordrecht, 1984).
- Kutzbach, J. E. & Otto-Bleisner, B. L. *J. atmos. Sci.* **39**, 1177–1188 (1982).
- Kutzbach, J. E. & Street-Perrott, F. A. *Nature* **317**, 130–134 (1985).
- Davis, O. K. *Science* **225**, 617–619.
- Van Devender, T. R. & Spaulding, W. G. *Science* **204**, 701–710 (1979).
- Spaulding, W. G., Leopold, E. B. & Van Devender, T. R. in *Late Quaternary Environments of the United States*, Vol. 1 (ed. Porter, S. C.) 259–293 (University of Minnesota Press, Minneapolis, 1983).
- Antevs, E. *Amer. Antiquity* **20**, 317–335 (1955).
- Kutzbach, J. E. & Guetter, P. J. *J. atmos. Sci.* (in the press).
- Wells, P. V. *Quat. Res.* **6**, 223–248 (1976).
- Spaulding, W. G. *U.S. Geol. Surv. prof. Pap.* 1329 (1985).
- Cole, K. L. *Science* **217**, 1142–1145 (1982).
- Spaulding, W. G., Robinson, S. W. & Paillet, F. L. *U.S. Geol. Surv. Water Resources Invest. Rpt.* 84-4328 (1984).
- Van Devender, T. R. *Science* **198**, 189–192 (1977).
- Hastings, J. R. & Turner, R. M. *The Changing Mile* (University of Arizona Press, Tucson, 1985).
- Mitchell, V. L. *J. appl. Met.* **15**, 920–927 (1976).
- Van Devender, T. R. thesis, Univ. Arizona, Tucson (1973).
- King, J. E. & Van Devender, T. R. *Quat. Res.* **8**, 191–204 (1977).
- Spaulding, W. G. *Curr. Res. Pleistocene* **2**, 83–85 (1985).
- Wells, P. V. & Woodcock, D. *Madroño* **32**, 11–23 (1985).
- Thompson, R. S. & Mead, J. I. *Quat. Res.* **17**, 39–55 (1982).
- Spaulding, W. G. in *Eighth North American Forest Biology Workshop* (ed. Lanner, R. M.) 42–69 (Utah State University, Logan, 1984).
- Mifflin, M. D. & Wheat, M. M. *Nevada Bur. Mines Geol. Bull.* **94** (1979).
- Bryson, R. A. & Hare, F. K. in *Climates of North America* (eds Bryson, R. A. & Hare, F. K.) 1–48 (Elsevier, Amsterdam, 1974).
- Kutzbach, J. E. & Wright, H. E. *J. Quat. Sci. Rev.* (in the press).
- Scott, W. E. *et al.* *Quat. Res.* **20**, 261–285 (1983).
- Thompson, R. S., Benson, L. V. & Hattori, E. M. *Quat. Res.* **25**, 1–9 (1986).
- Smith, G. I. *U.S. Geol. Surv. prof. Pap.* 1043 (1979).
- Spaulding, W. G. *Quat. Res.* **19**, 256–264 (1983).
- Bryson, R. A. & Lowry, W. P. *Bull. Amer. met. Soc.* **36**, 329–339 (1955).
- Kutzbach, J. E. in *Late Quaternary Environments of the United States* Vol. 2 (ed. Wright, H. E. Jr) 271–277 (University of Minnesota Press, Minneapolis, 1983).
- Bryson, R. A. & Swain, A. M. *Quat. Res.* **16**, 135–145 (1981).
- Talbot, M. R. *et al.* in *Paleoecology of Africa* Vol. 16 (eds Coetzee, J. A. & Van Zinderen Bakker, E. M.) 173–192 (Balkema, Rotterdam, 1984).
- Richie, J. C., Eyles, C. H. & Haynes, C. V. *Nature* **314**, 352–355 (1985).
- Cole, K. L. *Am. Nat.* **125**, 289–303 (1985).
- Berger, A. L. *Quat. Res.* **9**, 139–167 (1978).
- Van Devender, T. R. & Wiseman, F. M. in *Paleoindian Lifeways* (ed. Johnson, E.) 13–27 (West Texas Museum Association, Lubbock, 1977).

## Neuronal cell-cell adhesion depends on interactions of N-CAM with heparin-like molecules

Gregory J. Cole, Arleen Loewy & Luis Glaser

Department of Biological Chemistry, Division of Biology and Biomedical Sciences, Washington University School of Medicine, 660 S. Euclid Avenue, St Louis, Missouri 63110, USA

**Cell-cell interactions are of critical importance during neural development, particularly since the migration of neural cells and the establishment of functional interactions between growing axons and their target cells<sup>1,2</sup> has been suggested to depend upon cell recognition processes.** Neurone-neurone adhesion has been well studied *in vitro*, and is mediated in part by the neural cell adhesion molecule N-CAM<sup>3-7</sup>. N-CAM-mediated cell-cell adhesion has been postulated to occur by a homophilic binding mechanism<sup>8</sup>, in which N-CAM on the surface of one cell binds to N-CAM on a neighbouring cell. Studies in our laboratory have identified a cell surface glycoprotein, now known to be N-CAM<sup>9</sup>, which participates in cell-substratum interactions in the developing chicken nervous system<sup>10-12</sup>. Although this adhesion involves a homophilic binding mechanism, the binding of the cell surface proteoglycan heparan sulphate to the glycoprotein is also required<sup>13</sup>. This raises the question of whether the binding of heparan sulphate to N-CAM is also required for cell-cell adhesion. Here we show that the binding of retinal probe cells to retinal cell monolayers is inhibited by heparin, a functional analogue of heparan sulphate, but not by chondroitin sulphate. Monoclonal antibodies that recognize two different domains on N-CAM, the homophilic-binding and heparin-binding domains, inhibit cell-cell adhesion. The heparin-binding domain isolated from N-CAM by selective proteolysis also inhibits cell-cell adhesion when bound to the probe cells.

The role of the heparin-binding domain of N-CAM in cell-cell adhesion was examined by measuring the binding of <sup>35</sup>S-methionine-labelled probe cells to monolayers of retinal cells, as described by Gottlieb *et al.*<sup>14</sup>. This assay system was selected as we find it gives more reproducible results than the cell aggregation assay. Embryonic day 11 retinal cells added to glass mini-vials derivatized with 3-aminopropyltriethoxysilane form dense retinal cell monolayers and the rate of adhesion of <sup>35</sup>S-methionine-labelled retinal probe cells to this layer can be quantitated. Labelled embryonic day 11 retinal probe cells adhere to the monolayers in a time-dependent manner, with approximately 70% binding after 1 h (Fig. 1).

To examine the effect of heparin (heparan sulphate) on cell-

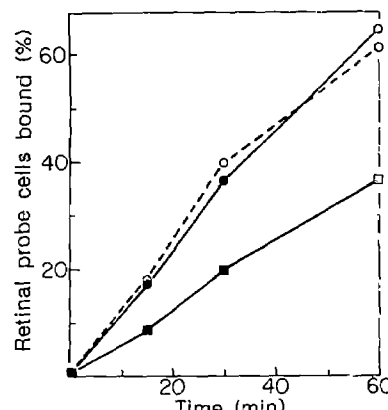


**Fig. 1** Adhesion of metabolically labelled retinal probe cells to retinal cell monolayers. Open circles show the binding of untreated control cells to retinal cell monolayers. The labelled retinal cells bind to the monolayers in a time-dependent manner. Closed circles represent cell to cell adhesion in the presence of  $100 \mu\text{g ml}^{-1}$  chondroitin sulphate (Sigma, grade III mixed isomers), indicating that cell adhesion is not affected by chondroitin sulphate. Closed squares show the adhesion of retinal cells in the presence of  $100 \mu\text{g ml}^{-1}$  heparin (Sigma, No. H-3125). Adhesion is inhibited approximately 40% by heparin at all time points, and suggests that the inhibitory activity of heparin is specific.

**Methods.** Embryonic day 11 chicken retinas were dissociated by incubation for 15 min at  $37^\circ\text{C}$  in 0.05% trypsin in calcium-magnesium-free Hank's solution. The cells were then triturated with a fire-polished Pasteur pipette and incubated overnight in Dulbecco's minimal essential medium containing 15% horse serum to allow recovery of cell surface proteins. Glass mini-vials ( $1.7 \text{ cm}^2$  surface area) were then derivatized with 3-aminopropyltriethoxysilane<sup>12,13</sup> and  $3 \times 10^6$  recovered retinal cells were added to each vial<sup>14</sup>. Cells were coupled to the derivatized surface by centrifugation at 600 g for 5 min, and the vials were then incubated at  $37^\circ\text{C}$  for at least 1 h. Throughout the assay the retinal cells were maintained in Earle's balanced salts solution containing 0.2% albumin. To assay cell adhesion, mechanically dissociated embryonic day 11 retinal cells were pulse-labelled for 1-2 h with  $10 \mu\text{Ci}$  of <sup>35</sup>S-methionine (translation grade, NEN) and approximately  $2 \times 10^5$  cells ( $0.25 \text{ c.p.m. per cell}$ ) were added to each vial. Vials were then incubated at  $37^\circ\text{C}$  on a gyratory shaker (100 r.p.m.). At the indicated times, the assay medium was aspirated and cell adhesion to the monolayer was quantitated by dissolving the cell in 1% Triton X-100, followed by liquid scintillation counting. To assess the effect of chondroitin sulphate or heparin on cell-cell adhesion, assays were conducted with  $100 \mu\text{g ml}^{-1}$  of the glycosaminoglycan present in the assay medium.

cell adhesion, cell adhesion assays were conducted in the presence of various concentrations of heparin or chondroitin sulphate. Heparin, a functional analogue of heparan sulphate, was used in these assays because it is more readily available from commercial suppliers. We have shown previously that cell-substratum adhesion is inhibited with similar efficacy by both heparin and the physiologically relevant ligand heparan sulphate. Chondroitin sulphate was used as a control to rule out any nonspecific inhibition resulting from the charge characteristics of the glycosaminoglycan.

Cell-cell adhesion is not affected by chondroitin sulphate ( $100 \mu\text{g ml}^{-1}$ ), but is partially inhibited by a similar concentration of heparin (Fig. 1). The effect of various concentrations of the glycosaminoglycans on cell-cell adhesion is summarized in Table 1. This adhesion occurred at rates equivalent to control cultures at all concentrations of chondroitin sulphate tested. Increasing concentrations of heparin showed a concentration-dependent inhibition of cell-cell adhesion (Table 1). Only slight (20%) inhibition of cell to cell adhesion was observed with  $50 \mu\text{g ml}^{-1}$  of heparin, even though this concentration abolishes retinal cell attachment to N-CAM linked to a substrate<sup>9,13</sup>, perhaps because a high quantity of cells was used in the cell-cell adhesion assay and  $50 \mu\text{g ml}^{-1}$  of heparin may not be sufficient

**Table 1** Inhibition of cell-cell adhesion by heparin

Treatment	Probe cells bound (%)	Inhibition (%)
Control	$63.5 \pm 3.7$ (6)	—
Chondroitin sulphate	$62.0 \pm 2.6$ (5)	2.4
	$64.1 \pm 5.9$ (2)	0
Heparin	$51.9 \pm 0.6$ (2)	19.3
	$37.0 \pm 2.7$ (5)	41.7
	$22.0 \pm 5.4$ (3)	65.4

Cell-cell adhesion assays were conducted as described in Fig. 1 legend. <sup>35</sup>S-methionine-labelled retinal probe cells were incubated for 1 h at  $37^\circ\text{C}$  with monolayers of retinal cells. The assay medium contained various concentrations of glycosaminoglycans as indicated. After incubation of labelled cells with monolayers, the assay medium was aspirated, cells were solubilized in 1% Triton X-100, and radioactivity quantitated by liquid scintillation counting. Data are expressed as mean  $\pm$  s.d. For each experiment duplicate vials were assayed, and the number of independent experiments conducted is indicated in parentheses.

**Table 2** Inhibition of cell-cell adhesion by anti-N-CAM monoclonal antibodies and heparin-binding domain of N-CAM

Treatment	Probe cells bound (%)	Inhibition (%)
Control	62.3 ± 5.1 (3)	—
• 25K heparin-binding N-CAM fragment	42.3 ± 4.4 (5)	32.1
C <sub>1</sub> H <sub>3</sub> monoclonal	20.2 ± 6.6 (3)	67.6
B <sub>1</sub> A <sub>3</sub> monoclonal in assay	18.4 ± 2.9 (2)	70.5
B <sub>1</sub> A <sub>3</sub> monoclonal, washed	29.8 ± 2.6 (2)	52.2

Cell-cell adhesion assays were conducted as described previously. To assess the effect of heparin-binding domain on cell-cell adhesion, aliquots of <sup>35</sup>S-methionine-labelled probe cells were incubated for 1 h at 4 °C with 50 µg ml<sup>-1</sup> of the heparin-binding domain. The domain was isolated by digesting immunopurified N-CAM with a 1:50 enzyme to substrate ratio of subtilisin protease<sup>9</sup>. The digested protein was then incubated with heparin-agarose, and the heparin-binding domain was eluted with 1 M NaCl<sup>9</sup>. Following incubation of the labelled probe cells with the domain, the cells were added to derivatized vials coated with retinal cells. The effect of anti-N-CAM monoclonals on cell-cell adhesion was determined by incubating the retinal cell monolayers with 0.5 mg ml<sup>-1</sup> of B<sub>1</sub>A<sub>3</sub> Fab fragments or C<sub>1</sub>H<sub>3</sub> monoclonal antibody for 1 h. The monolayers were then washed and labelled probe cells were added. Previous studies have also shown that B<sub>1</sub>A<sub>3</sub> Fab fragments inhibit cell to substratum adhesion more efficiently when present in the assay medium. Therefore, assays were also conducted with 0.5 mg ml<sup>-1</sup> of B<sub>1</sub>A<sub>3</sub> Fab fragments present in the assay medium. In the above experiments, control retinal cell monolayers were also incubated with 0.5 mg ml<sup>-1</sup> of control IgG. When monolayers were treated with anti-retinal cell monoclonal antibodies which do not affect cell-substratum adhesion, no inhibition was observed (data not shown).

to saturate the heparin-binding sites of N-CAM on both the monolayer and the probe cells. The inhibition of adhesion by 65% with 200 µg ml<sup>-1</sup> of heparin is particularly striking, since a similar concentration of chondroitin sulphate does not diminish the rate of cell-cell adhesion. These data suggest that adhesion between retinal cells depends upon cell surface heparan sulphate proteoglycan. It has been shown previously that an antiserum directed against this class of proteoglycan inhibits retinal cell-substratum adhesion<sup>9,13,15</sup>. In view of our previous data demonstrating that N-CAM participates in retinal cell-substratum adhesion and that it possesses a heparin-binding domain<sup>9,13</sup>, we postulate that the binding of cell surface heparan sulphate to N-CAM is required for cell-cell adhesion.

To determine if heparin inhibits N-CAM-mediated cell-cell adhesion, we used both the isolated heparin-binding domain of N-CAM and a monoclonal antibody that recognizes the heparin-binding domain<sup>9</sup> to examine whether heparin-binding by N-CAM is required for cell adhesion. The C<sub>1</sub>H<sub>3</sub> monoclonal antibody inhibits cell-substratum adhesion by a mechanism suggestive of the homophilic binding that has been demonstrated for N-CAM-mediated cell-cell adhesion<sup>8</sup>, but our previous studies implied that heparan sulphate binding to N-CAM was required for homophilic binding to occur<sup>13</sup>. A second monoclonal antibody, B<sub>1</sub>A<sub>3</sub>, recognizes the heparin-binding domain of N-CAM and also inhibits cell-substratum adhesion<sup>9</sup>. Retinal cell monolayers were incubated with these monoclonal antibodies, washed, and incubated with labelled probe cells. In some cases Fab fragments of the monoclonal antibody were present throughout the assay. The C<sub>1</sub>H<sub>3</sub> monoclonal inhibits cell-cell adhesion by approximately 70% (Table 2), which indicates that in this assay system the rate of cell-cell adhesion is to a large extent controlled by N-CAM. Fab fragments of B<sub>1</sub>A<sub>3</sub> also inhibit cell-cell adhesion. We have previously shown that the B<sub>1</sub>A<sub>3</sub> monoclonal inhibits cell-substratum adhesion more efficiently when present in the assay medium<sup>9</sup>. Here we find that the inhibition of cell adhesion was greater, approaching that observed with heparin, when B<sub>1</sub>A<sub>3</sub> Fab fragments were present in the medium than when the retinal cell monolayers were

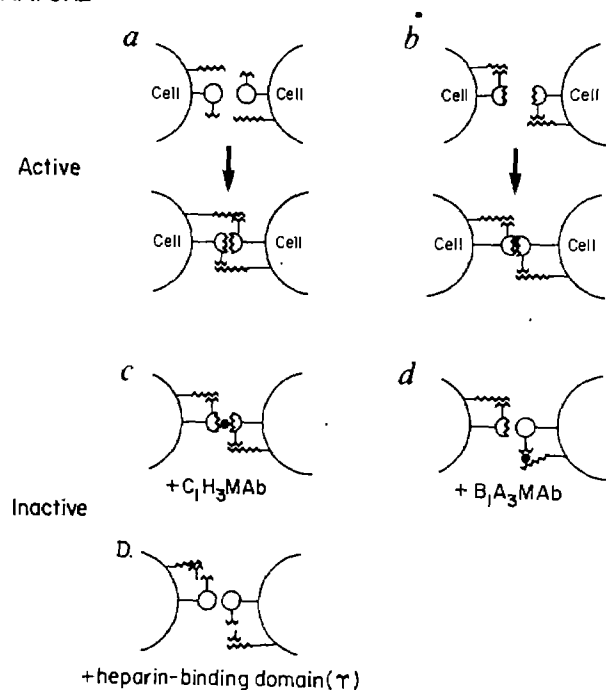


**Fig. 2** Schematic diagram depicting possible mechanisms for the interaction between heparan sulphate and N-CAM in neuronal cell-cell adhesion. The model proposes that N-CAM undergoes a conformational change following heparan sulphate binding<sup>12</sup>, with homophilic binding between N-CAM molecules resulting in cell-cell adhesion. In *a* and *b*, the model indicates that heparan sulphate-N-CAM binding can be *trans* (N-CAM binds to heparan sulphate on opposing cell) or *cis*, although we favour the former mode of binding. *c-e* show possible mechanisms for the inhibition of cell-cell adhesion. *c*, Inhibition by the C<sub>1</sub>H<sub>3</sub> monoclonal, which disrupts homophilic binding; *d*, inhibition by the B<sub>1</sub>A<sub>3</sub> monoclonal, which prevents binding of heparan sulphate to N-CAM and thus the conformational change in the protein; *e*, inhibition by heparin-binding domain of N-CAM, which also prevents the conformational change in N-CAM.

washed after exposure to the antibody. As the B<sub>1</sub>A<sub>3</sub> monoclonal binds to the heparin-binding domain of N-CAM, these observations directly implicate the binding of heparin to N-CAM in retinal cell-cell adhesion.

We also examined whether the heparin-binding domain isolated from N-CAM could inhibit cell-cell adhesion, as this would provide further support for the role of heparin binding to N-CAM in mediating cell to cell adhesion. The heparin-binding domain of N-CAM has been identified by limited proteolysis of immunopurified N-CAM, followed by chromatography on a heparin-agarose column<sup>9</sup>. The isolated heparin-binding domain is a 25,000-dalton fragment that inhibits cell-substratum adhesion when incubated with retinal cells<sup>9</sup> and promotes cell-substratum adhesion when covalently coupled to inert surfaces<sup>9</sup>. In the present study <sup>35</sup>S-methionine-labelled retinal probe cells were incubated with 50 µg ml<sup>-1</sup> of the isolated heparin-binding N-CAM fragment, and then added to mini-vials containing retinal cell monolayers. Cell-cell adhesion was partially inhibited by this polypeptide fragment (Table 2), similar to the inhibition of cell-substratum adhesion previously reported. This implies that the fragment at the concentrations employed<sup>9</sup> does not fully saturate the cell surface heparan sulphate, which is still available to interact with N-CAM in the adherens<sup>15</sup> or on neighbouring retinal cells.

These data still leave open the possibility that the heparin-binding domain of N-CAM is itself not involved in cell-cell adhesion, but binds to cell surface heparan sulphate that interacts with another heparin-binding component participating in cell adhesion. Because the B<sub>1</sub>A<sub>3</sub> monoclonal, which recognizes this polypeptide fragment, inhibits cell-cell adhesion (see

above), it is likely that the heparin-binding domain of N-CAM is an integral component of N-CAM-mediated cell adhesion.

In conclusion, we have demonstrated that cell-cell adhesion in the embryonic chicken neural retina can be inhibited specifically by heparin. A monoclonal antibody that recognizes the heparin-binding domain of N-CAM and a 25,000-dalton heparin-binding polypeptide fragment derived from N-CAM also inhibit cell-cell adhesion. These data suggest that retinal cell adhesion depends upon N-CAM interactions with heparan sulphate, and that these interactions are required for N-CAM homophilic binding. Previous studies in our laboratory have suggested that the binding of heparan sulphate to N-CAM induces a conformational change in the protein<sup>13</sup>, which could modulate homophilic binding between N-CAM molecules. A possible mechanism for the modulation of cell adhesion by heparan sulphate is shown in Fig. 2. Other laboratories have demonstrated that the heparin-binding domains of fibronectin and laminin can promote neurite outgrowth<sup>16,17</sup>. The multiple roles for cell surface proteoglycans require further detailed exploration, in particular to ascertain if other cell adhesion molecules are also able to interact with heparan sulphate, as this would imply that heparan sulphate has a critical regulatory role in a variety of cell interactions during development.

This work was supported by grants GM-81405 and EY-0566 from the National Institutes of Health.

Received 30 October 1985; accepted 13 February 1986.

1. Rakic, P. & Sidman, R. L. *J. comp. Neurol.* **152**, 103–161 (1973).
2. Rutishauser, U., Grumet, M. & Edelman, G. M. *J. Cell Biol.* **97**, 145–152 (1983).
3. Thiery, J. P., Brackenbury, R., Rutishauser, U. & Edelman, G. M. *J. biol. Chem.* **252**, 6841–6845 (1977).
4. Jorgensen, O. S., Delouche, A., Thiery, J. P. & Edelman, G. M. *FEBS Lett.* **111**, 39–42 (1980).
5. Hirn, M., Ghadouri, M. S., Deagostini-Bazin, H. & Goridis, C. *Brain Res.* **265**, 87–100 (1983).
6. Edelman, G. M. *Science* **219**, 450–457 (1983).
7. Rutishauser, U. *Nature* **310**, 549–554 (1984).
8. Rutishauser, U., Hoffman, S. & Edelman, G. M. *Proc. natn. Acad. Sci. U.S.A.* **79**, 685–689 (1982).
9. Cole, G. J. & Glaser, L. *J. Cell Biol.* **102**, 403–412 (1986).
10. Cole, G. J. & Glaser, L. *Proc. natn. Acad. Sci. U.S.A.* **81**, 2260–2264 (1984).
11. Cole, G. J. & Glaser, L. *J. biol. Chem.* **259**, 4031–4034 (1984).
12. Cole, G. J. & Glaser, L. *J. Cell Biol.* **99**, 1605–1612 (1984).
13. Cole, G. J., Schubert, D. & Glaser, L. *J. Cell Biol.* **100**, 1192–1199 (1985).
14. Gottlieb, D. I., Rock, K. & Glaser, L. *Proc. natn. Acad. Sci. U.S.A.* **73**, 410–414 (1976).
15. Schubert, D. & LaCorbiere, M. *J. Cell Biol.* **100**, 56–63 (1985).
16. Edgar, D., Timpl, R. & Thoenen, H. *EMBO J.* **3**, 1463–1468 (1984).
17. Rogers, S. L., McCarthy, J. B., Palm, S. L., Furcht, L. T. & Letourneau, P. C. *J. Neurosci.* **5**, 369–378 (1985).

## Expression of N-cadherin adhesion molecules associated with early morphogenetic events in chick development

Kohei Hatta & Masatoshi Takeichi\*

Department of Biophysics, Faculty of Science, Kyoto University, Kitashirakawa, Sakyo-ku, Kyoto 606, Japan

Selective adhesive properties of cells are thought to have a key role in animal morphogenesis<sup>1</sup>, but the molecular bases underlying these properties remain to be determined. Our studies have demonstrated that cell-type-specific adhesiveness resides in a class of cell-cell adhesion molecules, termed cadherins, which were defined as the molecular components of the  $\text{Ca}^{2+}$ -dependent cell adhesion system (CADS)<sup>2,3</sup>. For example, a cadherin molecule identified in mouse teratocarcinoma cells, termed E-cadherin (this molecule seems to be identical to uvomorulin<sup>4</sup> or cell-CAM 120/80 (ref. 5) and equivalent to chicken L-CAM<sup>6</sup>), was detected only in epithelial cells of various organs<sup>2,3</sup>; it did not cross-react with cadherins on other cell types<sup>7,8</sup>. We recently described a novel type of cadherin, N-cadherin, which is found in mouse cells and whose tissue distribu-

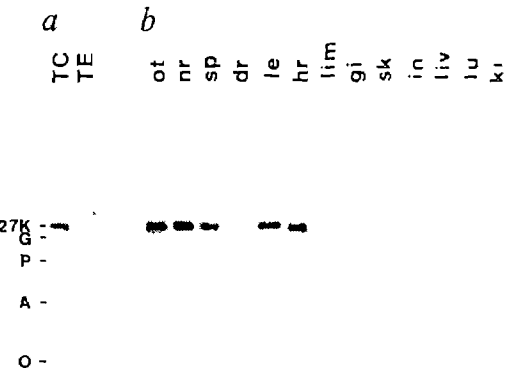


**Fig. 1** Immunoblot analysis of antigens recognized by antibody NCD-2. *a*, Neural retina treated either with a 0.01% trypsin solution containing 10 mM  $\text{CaCl}_2$  (ref. 13) (TC) or with the same trypsin solution containing 1 mM EGTA instead of  $\text{CaCl}_2$  (TE), for 20 min at 37 °C. *b*, Various non-trypsinized tissues: ot, optic tectum; nr, neural retina; sp, spinal cord; dr, dorsal root ganglion; le, lens; hr, heart; lim, limb without skin; gi, gizzard; sk, abdominal skin; in, intestine; liv, liver; lu, lung; ki, kidney. *M*, markers: G,  $\beta$ -galactosidase (116K); P, phosphorylase b (94K); A, serum albumin (68K); O, ovalbumin (43K).

**Methods.** Tissues collected from 6-day-old chick embryos were dissolved in SDS and subjected to SDS-polyacrylamide gel electrophoresis. Proteins were blotted onto nitrocellulose sheets as described elsewhere<sup>2</sup>, then the nitrocellulose sheets were incubated with a culture supernatant of NCD-2 hybridoma, followed by  $^{125}\text{I}$ -labelled anti-rat antibody (Amersham), then processed for autoradiography<sup>2</sup>. NCD-2 was obtained as follows: Neural retina and brain tissues were collected from two 6-day-old chick (White Leghorn) embryos, treated with TC, then homogenized with Freund's complete adjuvant. The homogenates were injected intraperitoneally (i.p.) into a Wistar rat; after 22 days, the rat was given a second i.p. injection comprising the same tissues (collected from six embryos) treated with TC and homogenized with Freund's incomplete adjuvant. Splenocytes of this animal were fused with P3-X63-Ag-U1 myeloma cells 3 days after the second injection. For screening of hybridomas, we used the following immunoblot analysis. Proteins of neural retina treated with TC or TE from 6-day-old chick embryos were electrophoresed and transferred to nitrocellulose sheets. The sheets were cut into thin strips and each strip was incubated with culture supernatants derived from different hybridoma clones. After detection of antigen bands using an appropriate second antibody, the bands detected in TC-treated samples were compared with those detected in TE-treated samples for each hybridoma supernatant. Hybridoma-producing antibodies which reacted with components present only in TC-treated tissue were saved. One such antibody was NCD-2.

tion is distinct from that of E-cadherin<sup>3</sup>. In the present study, we have identified a molecular component of N-cadherin in the chicken and determined its distribution in the tissues of early embryos. The results suggest that expression of this adhesion molecule is associated with separation and sealing of cell layers in morphogenesis.

The  $\text{Ca}^{2+}$ -dependent cell adhesion system displays a unique trypsin sensitivity in that it is removed from cell surfaces by treatment with trypsin in the presence of EGTA (TE treatment) but left intact after treatment with trypsin in the presence of  $\text{Ca}^{2+}$  (TC treatment)<sup>9–12</sup>. We obtained several monoclonal antibodies which react with cell surfaces of chick neural retina dissociated by TC treatment but not with those dissociated by TE treatment. Immunoblot analysis showed that all these antibodies recognize a single component with a relative molecular mass ( $M_r$ ) of 127,000 (127K) (Fig. 1a). We chose one of these monoclonal antibodies (NCD-2) for further studies. NCD-2

\* To whom correspondence should be addressed.

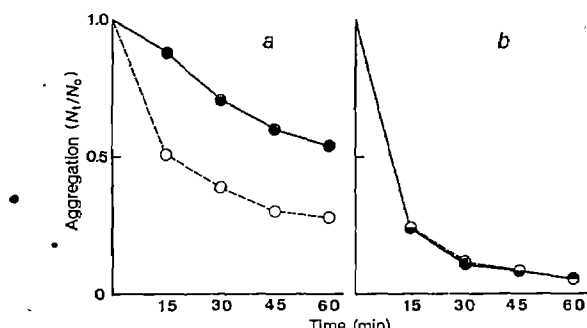


**Fig. 2** Effect of NCD-2 on aggregation of neural retina cells. Tissues were collected from 6-day-old chick embryos and dissociated by treatment with TC (*a*) or LTE<sup>13</sup> (*b*). Cells were allowed to aggregate in either the presence (●) or absence (○) of purified NCD-2 antibody (25 µg ml<sup>-1</sup>). The extent of aggregation was measured using a Coulter counter and is represented by an index  $N/N_0$ , as defined elsewhere<sup>13</sup>. (See ref. 13 for details of the methods of dissociation and aggregation of neural retina cells.) As a control experiment, we tested the effect of a rabbit antiserum raised against whole chicken neural retina, which did not contain antibodies recognizing the 127K protein. Fab fragments of antibodies purified from this antiserum did not inhibit aggregation of TC-treated neural retina cells, although they bound strongly to the surfaces of the cells. (In these studies we did not use Fab fragments of the NCD-2 antibody as even its intact form inhibited cell aggregation. This antibody seems unable to agglutinate cells, therefore the assay of inhibition of cell aggregation by the antibody was not hindered by agglutination. A similar property was observed for the ECCD-1 antibody<sup>2</sup>.)

inhibited the Ca<sup>2+</sup>-dependent aggregation of neural retina cells dissociated by TC treatment, but did not inhibit the Ca<sup>2+</sup>-independent aggregation of neural retina cells dissociated by treatment with a low concentration of trypsin in the presence of EGTA (LTE treatment) (Fig. 2). (The LTE treatment is known to inactivate the CADS but to leave intact the Ca<sup>2+</sup>-independent adhesion system<sup>13</sup>.) These results suggested that NCD-2 specifically recognizes the CADS, and that the 127K protein is a component of this adhesion system.

To provide a rough evaluation of the tissue distribution of the 127K protein, SDS-lysates of various tissues from 6-day-old chick embryos were subjected to immunoblot analysis. Figure 1*b* shows that all nervous tissues tested, for example, optic tectum, spinal cord, dorsal root ganglia as well as neural retina, contained large amounts of 127K protein. Heart and lens were also strongly positive in reaction with NCD-2. On the other hand, limb, gizzard, skin, intestine, liver, lung and kidney were negative or only weakly positive. Immunohistochemical studies showed that essentially all cells in the nervous tissues and lens as well as all myocardial cells in the heart were stained by NCD-2. In the weakly positive tissues, only particular groups of cells, such as mesothelium and ganglion clusters, were stained. These results will be described in detail elsewhere (in preparation). Limbs in embryos at this stage contained only a very small amount of the 127K protein; however, at later stages, when myotubes had differentiated, these multinucleated cells became positive. Thus, the tissue distribution of NCD-2 targets in chicken embryos is similar to that of N-cadherin defined in mouse embryos<sup>3</sup>, suggesting that the 127K protein is the chicken equivalent of mouse N-cadherin. We therefore call this 127K protein chicken N-cadherin.

To investigate the possible morphogenetic role of N-cadherin, we studied the pattern of expression of this adhesion molecule in developing chicken embryos by immunocytochemistry. N-cadherin was not expressed in blastoderm at the blastula stage; it was expressed for the first time at the primitive-streak stage. While the epiblast cells were not stained by NCD-2, cells migrating into the lower layer through the primitive streak did become stained (Fig. 3*a*).

At the head-folding stage, ectoderm cells remained unstained

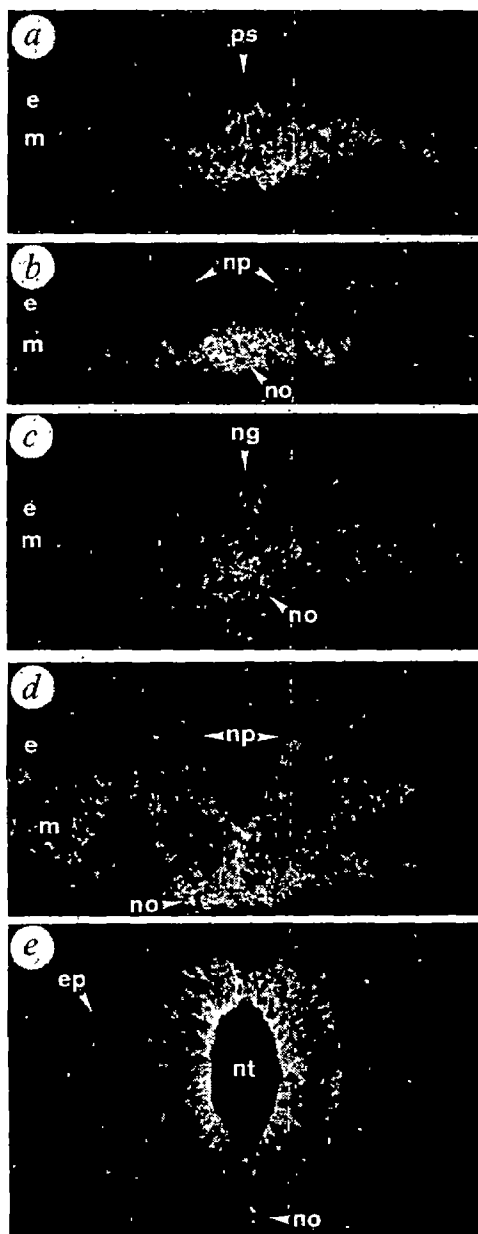
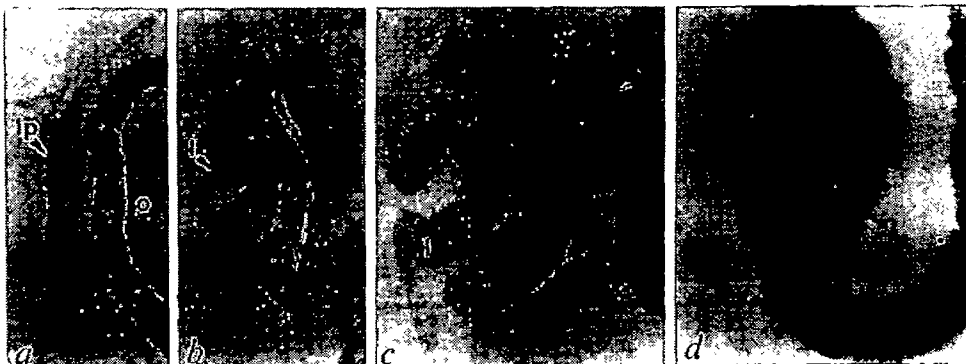


**Fig. 3** Immunocytochemical detection of N-cadherin in early embryos at various stages. *a*, The definitive streak stage. *b*, The head-process stage; sectioned at the neural plate level. *c*, 8-somite stage; sectioned at the level between the 8th somite and Hensen's node. *d*, 11-somite stage; sectioned at a level similar to that in *c*. *e*, 8-somite stage; sectioned at the head region. All specimens were transverse sections. *e*, Epiblast or ectoderm; *m*, mesoderm and endoderm; *ep*, epidermis; *ps*, primitive streak; *np*, neural plate; *ng*, neural groove; *nt*, neural tube; *no*, notochord.  $\times 135$ .

**Methods.** For immunohistochemistry, embryos were fixed in 4% paraformaldehyde in Hanks' solution for 1 h at 4 °C. After incubation in 12–18% sucrose in Hanks' solution for several hours, the samples were layered between abdominal muscle of adult mouse and frozen in isopentane maintained in liquid nitrogen as described by Thieffry *et al.*<sup>14</sup>. Cryostat sections (10 µm thick) were mounted on slides coated with gelatin and dried in air. The samples were incubated successively in the following solutions, with washing at each interval: (1) in 1% bovine serum albumin in HEPES-buffered Hanks' solution (HHS) for 15 min, (2) in culture supernatant of hybridoma for 30 min, (3) in biotinylated anti-rat antibody (Amersham) diluted 1:100 with HHS for 30 min, and (4) in fluorescein-streptavidin (Amersham) diluted 1:400 with HHS for 15 min. After mounting with 90% glycerol-10% HHS containing 0.1% *p*-phenylenediamine<sup>14</sup>, photographs were taken using a Zeiss 18FL microscope. Specificity of antibody binding was checked by comparing the samples with a control that had been treated with ECCD-1 antibody instead of NCD-2. The ECCD-1 antibody also served as a control in the other experiments described here.

**Fig. 4** Immunocytochemical detection of N-cadherin in the developing eye. *a*, Lens placode; *b* and *c*, invaginating lens vesicle; *d*, lens whose formation was complete. *lp*, Lens placode; *l*, lens vesicle or lens; *o*, optic vesicle; *r*, retina. Sections were processed as described in Fig. 2 legend, except that fluorescein-streptavidin was replaced by streptavidin-biotin-peroxidase complex (Amersham). The distribution of the antigen was visualized by means of the peroxidase reaction as described elsewhere<sup>15</sup>.  $\times 135$ .



until folding of the neural plate began (Fig. 3*b*). When invagination of the neural plate had begun, cells in the deepest portion of the neural groove became stained (Fig. 3*c*), and subsequently the stain extended from the bottom to the top of the folding plate (Fig. 3*d*). At the stage when the neural plate had closed, forming a tube, and was detached from the overlying ectoderm, all cells in the tube were stained (Fig. 3*e*), however the ectoderm layer remaining on the body surface did not take up stain. Mesodermal cells at this stage differentiate into various tissues such as notochord, somites and lateral plate, which became more intensely stained, although some cells such as endothelial cells of blood vessels were not stained. The endoderm layer was also stained.

In embryos at later stages, we found that expression of N-cadherin is associated with a variety of morphogenetic events. From among these findings, we describe here an observation on lens formation. Details of other observations will be published elsewhere (in preparation). The lens is formed by invagination of the ectoderm. When the lens placode formed, this thickened part of the ectoderm became stained by NCD-2, while other parts of the ectoderm surrounding the placode remained unstained or were only weakly stained (Fig. 4*a*). Staining of the lens primordium became more intense as invagination proceeded, although the overlying ectoderm contiguous to the lens vesicle was also weakly stained at the ventral portion (Fig. 4*b*, *c*). When lens formation was complete, the lens was heavily stained whereas the overlying ectoderm which differentiated into the corneal epithelium was not stained (Fig. 4*d*). In these studies, we found that, in closing or closed vesicular or tubular structures such as neural tube, somite and lens vesicle, the NCD-2 staining was always more intense in the inner portion of the cell layers (see, for example, Figs 3*e*, 4).

Thus, expression of N-cadherin in chicken embryo coincides with various morphogenetic events—gastrulation, neurulation and lens formation. In these three cases, expression of N-cadherin was initiated in cells undergoing separation from other cell layers (that is, in mesoderm and endoderm cells segregating from the epiblast cell layer, and in the neural tube and the lens vesicle as these tissues separated from the overlying ectoderm). Note that the patterns of N-cadherin expression appear to be complementary to those of L-CAM<sup>6,14</sup>, which is probably the chicken equivalent of mouse E-cadherin<sup>15</sup>. According to Thiery *et al.*<sup>14</sup>, L-CAM is expressed in the epiblast (upper layer) of blastoderm but not in the mesodermal and endodermal cells migrating into the lower layer of the blastoderm during gastrulation. While L-CAM is permanently expressed in the body-surface ectoderm, it disappears from the neural tube and lens vesicle during their invagination from the overlying ectoderm<sup>14</sup>.

Thus, invaginating cells involved in organogenesis of certain tissues begin to express N-cadherin while terminating L-CAM expression. As we reported previously<sup>8</sup>, cells expressing E-cadherin (=L-CAM) do not cross-adhere with cells expressing N-cadherin in a certain cell combination. It seems, therefore, that switches in expression of cadherin from E- to N-type in

the invaginating cells may be an essential step for their segregation from cell layers continuously expressing E-cadherin.

We thank Professor T. S. Okada for his encouragement during this project. This work was supported by research grants from the Japanese Ministry of Education, Science and Culture.

Received 28 June; accepted 21 October 1985.

1. Townes, P. L. & Holtfreter, J. *J. exp. Zool.* **128**, 53–120 (1955)
2. Yoshida-Noro, C., Suzuki, N. & Takeichi, M. *Dev. Biol.* **101**, 19–27 (1984)
3. Hatta, K., Okada, T. S. & Takeichi, M. *Proc. natn. Acad. Sci. U.S.A.* **82**, 2749–2753 (1985)
4. Peyreras, N., Hyafil, F., Louvard, D., Pleeth, H. L. & Jacob, F. *Proc. natn. Acad. Sci. U.S.A.* **80**, 6274–6277 (1983)
5. Damsky, C. H., Richa, C., Solter, D., Knudsen, K. & Buck, C. A. *Cell* **34**, 455–468 (1983)
6. Edelman, G. M., Gallin, W. J., Delouvee, A., Cunningham, B. A. & Thiery, J. P. *Proc. natn. Acad. Sci. U.S.A.* **80**, 4384–4388 (1983)
7. Takeichi, M., Atsumi, T., Yoshida, C., Uno, K. & Okada, T. S. *Dev. Biol.* **87**, 140–149 (1983)
8. Takeichi, M., Hatta, K. & Nagafuchi, A. *UCLA Symp. molec. cell. Biol.* **new ser.** **31**, 223–233 (1985)
9. Takeichi, M. *J. Cell Biol.* **75**, 464–474 (1977)
10. Grunwald, G. B., Geller, R. L. & Lilien, J. *J. Cell Biol.* **85**, 766–776 (1980)
11. Brackenbury, R., Rutishauser, U. & Edelman, G. M. *Proc. natn. Acad. Sci. U.S.A.* **78**, 387–391 (1981)
12. Magnani, J. L., Thomas, W. A. & Steinberg, M. S. *Dev. Biol.* **81**, 96–105 (1981)
13. Urushihara, H., Ozaki, H. S. & Takeichi, M. *Dev. Biol.* **70**, 206–216 (1979)
14. Thiery, J. P., Delouvee, A., Gallin, W. J., Cunningham, B. A. & Edelman, G. M. *Dev. Biol.* **102**, 61–78 (1984)
15. Ogou, S., Yoshida-Noro, C. & Takeichi, M. *J. Cell Biol.* **97**, 944–948 (1984)

## Induction of tolerance by monoclonal antibody therapy

R. J. Benjamin & H. Waldmann

Department of Pathology, University of Cambridge,  
Tennis Court Road, Cambridge CB2 1QP, UK

A major goal in immunology has been to find a means of selectively abolishing an individual's potential to mount an immune response to certain antigens, while preserving responsiveness to others. The facility to induce such specific immunological unresponsiveness in an adult would have major implications for tissue-grafting, the control of allergy and for treatment of autoimmune disease. Classical work has shown that immunosuppressive regimes, such as irradiation, anti-lymphocyte globulin or thoracic duct drainage, may facilitate tolerance induction<sup>1,2</sup>. We describe here a technique by which the immune system of mice can be manipulated to be tolerant to certain protein antigens by administering these during a brief pulse of treatment with a monoclonal antibody directed to the L3T4 molecule on helper T lymphocytes. This technique has the potential to form the basis of a novel generalized means of tolerance induction.

The treatment of mice with the rat monoclonal antibodies YTS 191.1 (ref. 3) and GK 1.5 (ref. 4), directed to the L3T4 molecule on T-helper cells<sup>5</sup>, leads to rapid depletion of this subset from the blood and lymphoid tissues<sup>3,6</sup>, with subsequent immunosuppression of a range of immune functions<sup>3,6,7</sup>. Given that L3T4-depleted animals fail to respond on immunization

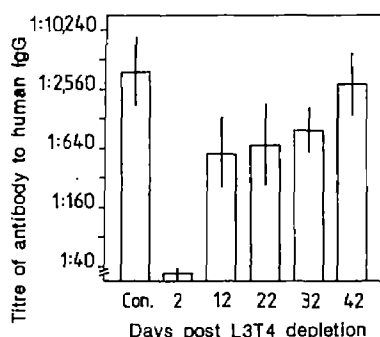


**Fig. 1** Return of immunocompetence after YTS 191.1 treatment in euthymic mice.

**Methods.** Male CBA/Ca mice aged 8–12 weeks were depleted of L3T4-positive T cells by daily injections on days 0 (intravenous (i.v.)), 1 and 2 (intraperitoneal (i.p.)) of YTS 191.1 as 0.2 ml of ascitic fluid from (DA × LOU)F<sub>1</sub> rat enriched for immunoglobulin by precipitation with 50% saturated ammonium sulphate, and equivalent to ~0.4 mg of active monoclonal antibody per dose. Controls received saline by the same protocol. Groups of four mice were randomly selected on various days following treatment and immunized with 0.5 mg heat-aggregated HGG i.v., purified from group O rhesus-positive serum by ammonium sulphate precipitation followed by elution through an ion-exchange chromatographic column (DE 52, Whatman) in 0.01 M sodium phosphate buffer pH 8.0, dialysed into phosphate-buffered saline (PBS) at 10 mg ml<sup>-1</sup>, and then aggregated by heating to 63 °C for 25 min followed by overnight incubation on ice<sup>1</sup>. Mice were bled from their tail veins 11 days after immunization and the sera stored at –20 °C. Serum anti-HGG antibody titres were measured by an enzyme-linked immunosorbent assay (ELISA) as follows. Polyvinyl microtitration trays were coated with purified HGG by incubation of 50 µl per well of 20 µg ml<sup>-1</sup> HGG in PBS for 60 min at 37 °C, washed three times in PBS/0.05% (v/v) Tween 20 (Sigma), and then blocked overnight with 1% (w/v) bovine serum albumin (BSA) in PBS/0.02% (w/v) sodium azide. The trays were then washed and doubling dilutions of test sera in 0.1% BSA/PBS were added to each tray at 50 µl per well and incubated for 60 min at 20 °C. A positive control of peroxidase-linked rabbit anti-human immunoglobulin (Dako) was titrated on each tray. The test samples were followed sequentially, with intervening washes, by species-specific biotinylated sheep anti-mouse immunoglobulin (Amersham) and then biotinylated streptavidin horseradish peroxidase complex (Amersham) both at 1:1,000 dilution in PBS/0.1% BSA and incubated at 50 µl per well for 35 min at 20 °C. Trays were then washed and developed for 5 min with o-phenylenediamine (100 µl per well) and the reaction stopped with 50 µl per well of 0.5 M H<sub>2</sub>SO<sub>4</sub>. Absorbance was read at 490 nm, the results plotted graphically and the titres read relative to the positive control. Data are geometric mean ± s.d. of the antibody titres from four mice.

with protein antigens<sup>6</sup>, we asked whether their immune system maintained any record of such an abortive encounter. This question could be answered by exposing mice to primary antigen challenge during a brief period of anti-L3T4 therapy, and then offering a second challenge dose of the antigen when immunocompetence had been fully re-established. Three responses were possible. First, the animals might appear naive, simply producing a primary-type response. Second, they might have developed memory for a secondary response without exhibiting a primary response. Finally, they might have registered their first encounter with antigen in a negative way and become tolerant.

The experimental design required that we assess the record of antigen encounter in anti-L3T4-treated mice only when full immunocompetence had been restored. Figure 1 shows that mice challenged with heat-aggregated human γ-globulin (HGG) 2 days after L3T4 depletion generated no primary antibody response (as expected). However, challenge at day 12 elicited a strong anti-HGG response and at day 42 this response was

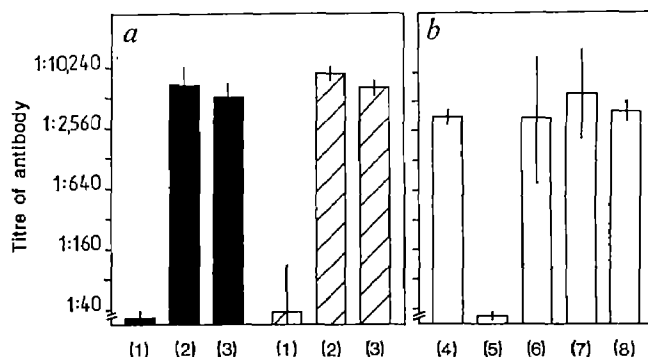


**Fig. 2** YTS 191.1 induces unresponsiveness to its own IgG2b epitopes and to heat-aggregated HGG given concomitantly. *a*, Response to rat IgG2b; *b*, response to HGG.

**Methods.** Adult CBA/Ca male mice in groups of five were pretreated with three injections of YTS 191.1 as in Fig. 1 (groups 1, 4, 5), or as controls received an irrelevant IgG2b monoclonal antibody (YTH 65.3.3, anti-human T200<sup>16</sup>) (groups 2, 6) or saline (groups 3, 7, 8) by the same protocol. In *b*, groups 5, 6 and 7 were then injected on days 2 and 3 with 0.5 mg doses of heat-aggregated HGG prepared as in Fig. 1. Following this pretreatment, mice were maintained on antibiotics (oxytetracycline 50 mg l<sup>-1</sup>, Terramycin; Pfizer) and were free of any obvious disease. On day 12 all mice were bled and the effectiveness of anti-L3T4 treatment was confirmed by the absence of an antibody response to HGG in group 5, as compared with strong primary responses in groups 6 and 7 as measured by an ELISA (data not shown). On days 42 and 52, mice were immunized i.p. with 0.5 mg of the heat-aggregated form of: ■, YTH 3.2.6 (anti-CD7 (Campath 2<sup>10</sup>) IgG2b); ▨, YTH 53.1.4 (anti-human red blood cell (H.W., unpublished data), IgG2b); or □, HGG. YTH 3.2.6 and YTH 53.1.4 were purified from (DA × LOU)F<sub>1</sub> rat ascites by ammonium sulphate precipitation, followed by ion-exchange chromatography in 0.01 M sodium phosphate buffer pH 8.0 (DE 52, Whatman) and then heat-aggregated as above. Mice were bled from their tail veins on day 58 and their sera stored at –20 °C. The serum titres of antibody to the respective immunizing Ag (YTH 3.2.6, YTH 53.1.4 or HGG) were determined by ELISA as in Fig. 1. A mixture of mouse monoclonal antibodies against rat immunoglobulin (Norig 7.16.2, Norig 1.1.6 [both anti-rat IgG2b<sup>17</sup>] and Mar 18.5 [anti-rat light chain<sup>18</sup>]) was used as a reference-positive control for measurement of the anti-rat IgG2b antibody responses. Data are geometric means ± s.d. of antibody titres from five mice.

equivalent to that in untreated controls. Secondary antigen challenge at day 42 after L3T4 treatment would, therefore, give a reliable measure of the immune system's record of its encounter with antigen given under the 'umbrella' of anti-L3T4.

The first test antigen we considered was the anti-L3T4 monoclonal antibody itself. YTS 191.1 and GK 1.5 (both of the rat IgG2b subclass) do not elicit anti-globulin responses *in vivo*<sup>6,8,9</sup>, whereas other rat IgG2b monoclonals with specificity for lymphocytes, all elicit strong responses to themselves<sup>9</sup>. As YTS 191.1 is non-immunogenic, we asked how mice treated with this antibody recorded their encounter with its IgG2b constant-region determinants? In the experiment shown in Fig. 2*a*, mice were pretreated with YTS 191.1, or an irrelevant monoclonal antibody or saline, and then 42 days later were immunized with either of two different heat-aggregated IgG2b monoclonals, having no binding activity for mouse cells (YTH 3.2.6<sup>10</sup> and YTH 53.1.4). No anti-globulin responses could be detected in anti-L3T4-treated mice (group 1) compared with controls (groups 2, 3). Similarly, administration of HGG under the anti-L3T4 umbrella led to later unresponsiveness to rechallenge with this antigen (Fig. 2*b*, group 5). Mice receiving anti-L3T4 but no initial 'recording' dose of HGG (group 4), responded as well as controls (groups 6–8) to the late HGG challenge. Similar results were obtained with HGG derived from a different donor. Later bleeds did not expose immune responses in tolerant mice.

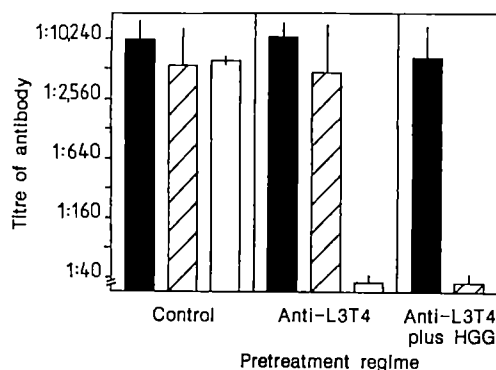


**Fig. 3** Specificity of unresponsiveness to rat IgG2b and HGG. Adult male CBA/Ca mice were rendered unresponsive to rat IgG2b by YTS 191.1 (anti-L3T4 antibody) pretreatment as in group 1 in Fig. 2a, or to HGG by pretreatment with YTS 191.1 plus aggregated HGG (anti-L3T4 antibody plus HGG) as in group 5 in Fig. 2b. On days 42 and 52 after induction of unresponsiveness, these mice and age-matched controls were immunized with 0.5 mg i.p. of the heat-aggregated form of HGG (□), CGG (■) or YTH 3.2.6 (□) (rat IgG2b), and then bled on day 58. Chicken  $\gamma$ -globulin was obtained from Miles Laboratories and heat-aggregated as above. Sera were stored at  $-20^{\circ}\text{C}$  and antibody titres determined by ELISA. Data are geometric means  $\pm$ s.d. of antibody titres from five mice.

This state of unresponsiveness could be shown to be true tolerance by specificity controls. Mice rendered unresponsive to rat IgG2b by administration of anti-L3T4 remained fully responsive to HGG or chicken  $\gamma$ -globulin (CGG) (Fig. 3). Similarly mice made unresponsive to HGG given under the anti-L3T4 umbrella responded normally to CGG (Fig. 3).

We have shown here that mice injected with antigen under the umbrella of an anti-L3T4 antibody maintain a record of the encounter manifesting as tolerance. As a method of tolerance induction it is unique, as we have been able to induce tolerance in normal adult mice with an immunogenic form of an antigen and there is evidence to suggest a special role for anti-L3T4 in permitting tolerance. Other rat IgG2b monoclonal antibodies that deplete lymphocyte populations (such as anti-Thy 1 or anti-Lyt 1) are also immunosuppressive, yet elicit strong anti-globulin responses to themselves<sup>9</sup>, and are therefore unlikely to permit tolerance to other antigens.

T-helper cell depletion by YTS 191.1 may leave up to 10% of the L3T4<sup>+</sup> cells in peripheral lymphoid organs<sup>3</sup>. Why, then, are these remaining cells not primed by antigen to prevent tolerance induction? Perhaps depletion of helper cells is not the only determinant for tolerance induction, and anti-L3T4 monoclonal antibody facilitates tolerance in some other way. Whatever the mechanism, this monoclonal regime has permitted tolerance to rat and human immunoglobulins. However, we have not yet achieved tolerance with heat-aggregated CGG (data not shown). It is likely that this highly immunogenic antigen is able to prime residual T-helper cells and that more aggressive protocols of anti-L3T4 therapy may be necessary to tip the balance of the immunological record towards tolerance.

Our results have direct implications for serotherapy with monoclonal antibodies. First, the anti-globulin response, a major obstacle to any long-term antibody therapy<sup>11</sup>, could be minimized if it were possible to exploit the tolerogenic properties of anti-L3T4 (CD4<sup>12</sup>) monoclonal antibodies in humans. Second, many recent publications have demonstrated the value of anti-L3T4 monoclonals for the treatment of a number of autoimmune diseases in mice and rats<sup>8,13-15</sup>. It is now important to establish whether the benefit of anti-L3T4 therapy in autoimmunity is simply due to blanket immunosuppression or to the creation of a tolerogenic milieu in which the immune system relearns 'self' and no longer pursues its auto-aggressive course. If the latter, then anti-L3T4 therapy may prove to be a preferred means of

treatment of clinical autoimmunity, and perhaps of hypersensitivity in general.

The tolerogenic potential of treatment with anti-L3T4 monoclonal antibodies offers some exciting prospects. Not only do we have a simple model for studying basic mechanisms of tolerance, complementing classical systems using disaggregated proteins<sup>1</sup>, but perhaps with potentiation of the effects described, anti-L3T4 antibodies may have a future as agents for achieving specific tolerance for therapeutic purposes.

We thank Gilly Martin and Mark Frewin for technical assistance and Drs M. Clark and S. Cobbold for helpful advice and discussion. This work was funded by MRC grants and the Oliver Bird Trust. R.J.B. is funded by the Cambridge Livingstone Trust.

Received 9 January; accepted 24 February 1986.

1. Weigle, W. O. *Adv. Immun.* **16**, 61-121 (1973).
2. Shellam, G. R. *Immunology* **17**, 267-270 (1969).
3. Cobbold, S. P., Jayasuriya, A., Nash, A., Prospero, T. D. & Waldmann, H. *Nature* **312**, 548-551 (1984).
4. Dialynas, D. P. *et al.* *J. Immun.* **131**, 2445-2451 (1983).
5. Dialynas, D. P. *et al.* *Immun. Rev.* **47**, 29-56 (1983).
6. Wofsy, D. C., Mayes, J., Woodcock, J. & Seaman, W. E. *J. Immun.* **135**, 1695-1701 (1985).
7. Cobbold, S. P. & Waldmann, H. *Transplantation* (in press).
8. Wofsy, D. & Seaman, W. E. *J. exp. Med.* **161**, 378-391 (1985).
9. Cobbold, S. P., Martin, G., Lovat, P. E. & Waldmann, H. *Adv. exp. Med. Biol.* **186**, 789-795 (1985).
10. Waldmann, H. *et al.* *Adv. exp. Med. Biol.* **186**, 869-875 (1985).
11. Ritz, J. & Schlossman, S. F. *Blood* **59**, 1-11 (1982).
12. Reinherz, E. & Schlossman, S. F. *Cell* **19**, 821-826 (1980).
13. Waldor, M. K. *et al.* *Science* **227**, 415-417 (1985).
14. Ranges, G. E., Sriram, S. & Cooper, S. M. *J. exp. Med.* **162**, 1105-1110 (1985).
15. Brostoff, S. W. & Mason, D. W. *J. Immun.* **133**, 1938-1942 (1985).
16. Bindon, C., Hale, G., Clark, M. & Waldmann, H. *Transplantation* **40**, 538-543 (1985).
17. Hale, G., Clark, M. & Waldmann, H. *J. Immun.* **134**, 3056-3060 (1985).
18. Lanier, L. L., Gutman, G. A., Lewis, D. E., Griswold, S. T. & Warner, N. L. *Hybridsoma* **1**, 125-130 (1982).

## Abrogation of oral tolerance by contrasuppressor T cells suggests the presence of regulatory T-cell networks in the mucosal immune system

Iwao Suzuki\*, Hiroshi Kiyono†, Kyoichi Kitamura\*, Douglas R. Green‡ & Jerry R. McGhee\*

Departments of \* Microbiology and † Oral Biology and Preventive Dentistry, Institute of Dental Research, University of Alabama at Birmingham, University Station, Birmingham, Alabama 35294, USA  
 ‡ Department of Immunology, Faculty of Medicine, University of Alberta, Edmonton, Alberta, Canada T6G 2H7

Continuous ingestion of a thymus-dependent (TD) antigen differentially affects two compartments of the immune system. A secretory IgA antibody response is induced in mucosal tissues, concurrent with a state of antigen-specific systemic unresponsiveness to parenteral challenge<sup>1</sup>, termed oral tolerance<sup>2</sup>. The precise mechanisms whereby gut antigenic exposure induces oral tolerance are unknown, although T-suppressor cells<sup>3,4</sup>, anti-idiotypic networks<sup>5</sup> and immune complex formation<sup>6</sup> have all been proposed. Here we show that the systemic unresponsiveness of mice made orally tolerant to the TD antigen sheep red blood cells (SRBC) is reversed by the adoptive transfer of Lyt-1<sup>+</sup>, 2<sup>-</sup>, *Vicia villosa* lectin-adherent and I-J<sup>+</sup> T cells derived from mice which are genetically resistant to the induction of oral tolerance to SRBC. This T-cell subpopulation has the characteristics of contrasuppressor effector T cells (T<sub>cs</sub>). Small numbers of these T<sub>cs</sub> cells reverse SRBC-specific tolerance both *in vivo* and *in vitro*. This finding offers new insight into the mechanisms of oral tolerance induction and maintenance, and suggests that a network of T cells are involved in the regulation of host responses to ingested antigens.

Prolonged oral immunization of C3H/HeN mice with SRBC induces systemic unresponsiveness, while identically treated

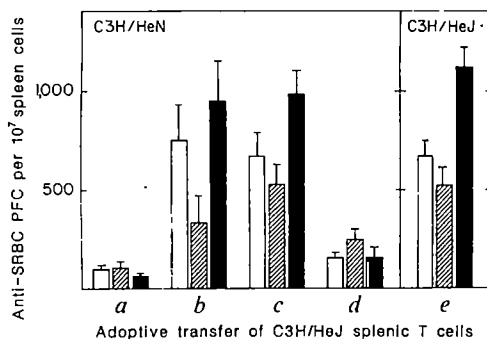


**Fig. 1** Reversal of oral tolerance by adoptive transfer of *V. villosa*-adherent T cells. Groups of 22–28 C3H/HeN (*a*–*d*) and 18–20 C3H/HeJ ( $H-2^k$ ) (*e*) mice were given SRBC daily by GI for 28 days<sup>3,7</sup>. Seven days later, spleen cells from 8–10 C3H/HeJ mice were enriched for T cells by removal of macrophages by adherence to plastic-coated surfaces and B cells by panning on anti-immunoglobulin-coated plates followed by treatment with anti-immunoglobulin and rabbit C (total T cells). T cells were further fractionated by addition to plates coated with *V. villosa* (L-4600 lot #0127F; E.Y. Laboratories, Inc., San Mateo, California) and non-adherent and adherent T cells were collected<sup>13,14</sup>. Approximately 7–9% of the T cells adhere to *V. villosa*. Each T-cell fraction ( $1 \times 10^6$  per mouse) was adoptively transferred to groups of 4–6 orally tolerized C3H/HeN mice and immunized i.p. with SRBC. Four days later, splenic anti-SRBC PFC of the IgM (□), IgG (▨) and IgA (■) isotype were determined<sup>3,7</sup>. *a*, No T cells; *b*, total T cells; *c*, *V. villosa*-adherent T cells; *d*, *V. villosa*-non-adherent T cells; *e*, no T cells. Data are taken from four separate experiments.

C3H/HeJ mice exhibit IgM, IgG and IgA anti-SRBC splenic plaque-forming cell (PFC) responses (Fig. 1)<sup>3</sup>. The inability to induce oral tolerance in C3H/HeJ mice is linked to a defective gene (*Lps<sup>d</sup>*) on chromosome 4 which renders lymphoid cells unresponsive to the endotoxin (lipopolysaccharide, LPS) of Gram-negative bacteria<sup>7,8</sup>. Analysis of the regulatory T cells in the Peyer's patches and spleens of orally immunized LPS-responsive C3H/HeN (*Lps<sup>n</sup>/Lps<sup>n</sup>*) mice identified a predominant T-suppressor ( $T_s$ ) cell activity, while the LPS-nonresponsive C3H/HeJ (*Lps<sup>d</sup>/Lps<sup>d</sup>*) mice were characterized by a predominant T-helper ( $T_h$ ) cell activity<sup>3,7</sup>. This response pattern could result from regulatory T cells in the Peyer's patches of C3H/HeJ mice which render  $T_h$  cells resistant to  $T_s$ -cell activity, and would, therefore, exhibit the  $T_{cs}$ -cell activity described by Gershon, Green and colleagues<sup>9–13</sup>.

To test this possibility, groups of C3H/HeN and C3H/HeJ mice were orally immunized with SRBC<sup>3,7</sup> for 28 consecutive days and purified splenic T cells from the C3H/HeJ animals were then adoptively transferred to orally tolerized C3H/HeN mice. Transfer of  $1 \times 10^6$  C3H/HeJ T cells to the C3H/HeN mice immediately before intraperitoneal (i.p.) challenge abrogated tolerance and allowed the development of IgM, IgG and IgA anti-SRBC PFC responses (Fig. 1). Furthermore, the active T cells could be enriched by adherence to *Vicia villosa* lectin, while the *V. villosa*-non-adherent T cells were not effective at reversing oral tolerance when adoptively transferred to C3H/HeN mice (Fig. 1). Adoptive transfer of *V. villosa* adherent or non-adherent splenic T cells from orally tolerized C3H/HeN mice into the C3H/HeN strain did not reverse oral tolerance. In addition, *V. villosa*-adherent splenic T cells from unimmunized C3H/HeJ or C3H/HeN mice failed to abrogate systemic unresponsiveness when given to orally tolerized C3H/HeN mice. These results suggest that C3H/HeJ mice given SRBC orally develop a subset of splenic T cells which abrogate oral tolerance *in vivo*, and that this T-cell subset shares the property of *V. villosa* binding with the previously described  $T_{cs}$  cells<sup>12,13</sup>.

*V. villosa*-adherent splenic T cells from C3H/HeJ mice were tested over a wide range of cell number ( $1 \times 10^7$ – $5 \times 10^4$ ), and all cell numbers used reversed oral tolerance upon adoptive transfer to C3H/HeN mice (Fig. 2). Higher numbers of *V. villosa*-adherent T cells gave elevated IgM responses, while  $10^5$ – $10^6$  cells supported responses similar to those seen in C3H/HeJ mice (Fig. 2). Interestingly, when the IgA-isotype response was examined, the transfer of graded numbers of *V. villosa*-adherent T cells resulted in a biphasic response. Both high and low numbers of transferred cells abrogated tolerance, while intermediate numbers were less effective. This may suggest that the functional activity observed is due to two distinct populations of  $T_{cs}$  cells, one of which may be IgA-isotype specific.

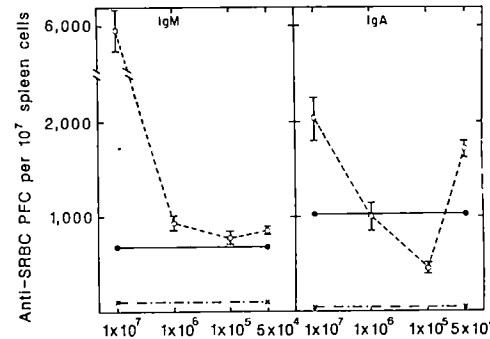


**Fig. 2** Reversal of oral tolerance is achieved with small numbers of *V. villosa*-adherent T cells. Various doses ( $1 \times 10^7$ – $5 \times 10^4$  cells) of *V. villosa*-adherent T cells from spleens of 8–10 C3H/HeJ mice given SRBC by GI for 28 days were adoptively transferred to groups of 4–6 orally tolerized C3H/HeN mice. The animals were immunized i.p. with SRBC and splenic IgM and IgA anti-SRBC PFC were determined 4 days later. As controls, groups of 12 C3H/HeJ and C3H/HeN mice were given SRBC by GI for 28 days followed by systemic injection of this antigen 1 week later; (—●—) for C3H/HeJ and (—○—) for C3H/HeN. Data are taken from three separate experiments.

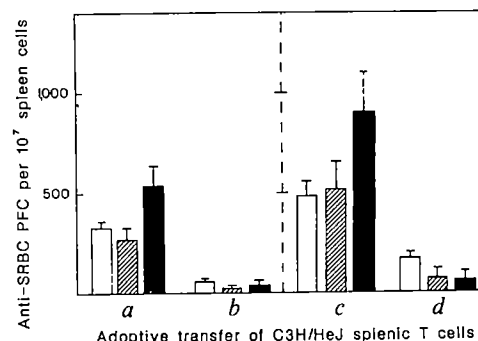


**Fig. 3** Contrerasuppressor T cells mediate reversal of oral tolerance. Splenic T cells from C3H/HeJ mice given SRBC by GI for 28 days were prepared as described in Fig. 1 legend. T cells were further enriched for Lyt-1<sup>+</sup> by treatment with monoclonal anti-Lyt-2 (clone #53-6-72) followed by addition of anti-rat IgG and C. This treatment removed the Lyt-2<sup>+</sup> T-cell population as determined by immunofluorescence staining with fluorescein isothiocyanate-anti-Lyt-2. These Lyt-1<sup>+</sup> T cells were then treated with anti-I-J<sup>k</sup> (Cediranilane) and C. Additional aliquots of Lyt-1<sup>+</sup> T cells were added to *V. villosa* plates and the adherent fractions tested (see Fig. 1 legend). Lyt-1<sup>+</sup>, *V. villosa*<sup>+</sup> T cells were subsequently treated with anti-Lyt-1 (clone #53-7-313) followed by anti-rat IgG and C. Individual T-cell fractions ( $5 \times 10^4$  cells per mouse) were adoptively transferred to groups of 5–7 orally tolerized C3H/HeN mice and immunized i.p. with SRBC. IgM (□), IgG (▨) and IgA (■) anti-SRBC PFC responses were assessed 4 days later. *a*, Anti-Lyt-2+C; *b*, anti-Lyt-2, anti-I-J<sup>k</sup>+C; *c*, anti-Lyt-2+C, *V. villosa* adherent; *d*, anti-Lyt-2+C, *V. villosa* adherent, anti-Lyt-1+C. Data are taken from three separate experiments.

*V. villosa*-adherent T cells gave elevated IgM responses, while  $10^5$ – $10^6$  cells supported responses similar to those seen in C3H/HeJ mice (Fig. 2). Interestingly, when the IgA-isotype response was examined, the transfer of graded numbers of *V. villosa*-adherent T cells resulted in a biphasic response. Both high and low numbers of transferred cells abrogated tolerance, while intermediate numbers were less effective. This may suggest that the functional activity observed is due to two distinct populations of  $T_{cs}$  cells, one of which may be IgA-isotype specific.

Enrichment of Lyt-1<sup>+</sup> T cells from the C3H/HeJ splenic T-cell population by anti-Lyt-2 and rabbit complement (C) treatment gave a cell fraction which abrogated oral tolerance when adoptively transferred to C3H/HeN mice (Fig. 3). This cell fraction contains mature  $T_h$  cells<sup>3,7</sup> and effector  $T_{cs}$  cells, since further

**Table 1** *V. villosa*<sup>+</sup>, Lyt-1<sup>+</sup>, I-J<sup>k+</sup> T cells abrogate the unresponsiveness of spleen cells from orally tolerized mice *in vitro*

Purified T cells added (cell treatment)	Cell no. added†	Anti-SRBC PFC per culture*		
		IgM	IgG	IgA
None	None	65 ± 11	31 ± 12	37 ± 23
Anti-Lyt-2 + C‡	1 × 10 <sup>5</sup>	261 ± 36	126 ± 15	263 ± 26
	5 × 10 <sup>5</sup>	243 ± 35	192 ± 25	332 ± 42
Anti-Lyt-2 and anti-I-J <sup>k</sup> + C‡	1 × 10 <sup>5</sup>	105 ± 14	33 ± 11	71 ± 9
	5 × 10 <sup>5</sup>	40 ± 9	52 ± 7	75 ± 4
Anti-Lyt-2 + C	<i>V. villosa</i> adherent§	1 × 10 <sup>5</sup>	257 ± 24	140 ± 11
		5 × 10 <sup>5</sup>	172 ± 22	184 ± 18
Anti-Lyt-2 and anti-Lyt-1 + C	<i>V. villosa</i> non-adherent§	1 × 10 <sup>5</sup>	92 ± 6	100 ± 8
		5 × 10 <sup>5</sup>	70 ± 8	62 ± 6
Anti-Lyt-2 and anti-Lyt-1 + C	<i>V. villosa</i> adherent§	1 × 10 <sup>5</sup>	94 ± 15	46 ± 8
		5 × 10 <sup>5</sup>	69 ± 11	34 ± 8

Spleen cells ( $5 \times 10^6$ ) from seven to nine C3H/HeN mice orally tolerized with SRBC were cultured in minimal essential medium containing L-glutamine, gentamicin, penicillin, streptomycin, sodium bicarbonate, sodium pyruvate, non-essential amino acids and 10% fetal calf serum and immunized with SRBC ( $2.5 \times 10^6$  per culture) in the presence or absence of added T cells (either  $5 \times 10^5$  or  $1 \times 10^5$  per culture) (see below) and incubated for 5 days<sup>3,7</sup>.

\* Values are the mean IgM, IgG or IgA anti-SRBC PFC per culture per experiment and from three separate experiments. Non-immunized, control cultures gave less than 4 anti-SRBC PFC per culture.

† Aliquots of T cells in various treatment groups were titrated over a range of  $1 \times 10^4$ - $1 \times 10^6$  cells per culture. Representative doses of  $1 \times 10^5$ - $5 \times 10^5$  are included. T cells from normal C3H/HeJ spleen were without effect when added to tolerant C3H/HeN splenic cultures.

‡ Splenic T cells from 10 C3H/HeJ mice given SRBC by gastric intubation (GI) daily for 28 days were prepared as described in Fig. 1 legend. T cells were further enriched into Lyt-1<sup>+</sup> fractions by treatment with anti-Lyt-2 and C (Fig. 3 legend). This treatment removed the Lyt-2<sup>+</sup> T-cell population as determined by immunofluorescence. Aliquots of Lyt-1<sup>+</sup> T cells were treated with anti-I-J<sup>k</sup> and C.

§ Lyt-1<sup>+</sup>-enriched T cells from C3H/HeJ spleen were separated into adherent and non-adherent fractions on *V. villosa* lectin-precoated plates. Additionally, Lyt-1<sup>+</sup> *V. villosa*-adherent T cells were treated with anti-Lyt-1 and C (see Fig. 3 legend).

fractionation of Lyt-1<sup>+</sup> T cells by adherence to *V. villosa* resulted in adherent Lyt-1<sup>+</sup> T cells with tolerance-reversing activity, while non-adherent enriched Lyt-1<sup>+</sup> T<sub>h</sub> cells were without effect (Fig. 3 and data not shown). In addition, treatment of Lyt-1<sup>+</sup>, *V. villosa*-adherent T cells with anti-Lyt-1 and C abrogated reversal of oral tolerance. This suggests that the active T-cell fraction is Lyt-1<sup>+</sup>,<sup>2</sup> and *V. villosa* adherent, all properties of effector T<sub>cs</sub> cells<sup>9-13</sup>.

Previous work has shown that I-J determinants occur on T cells with helper amplifier and contrasuppressor activity<sup>9-13</sup> and on T-cell-derived factors responsible for contrasuppression<sup>9,14</sup>. Although the gene(s) that code for I-J are not known, strong evidence from studies with alloanti-I-J and monoclonal anti-I-J antibodies clearly associate this molecule with T<sub>cs</sub> cells. When splenic Lyt-1<sup>+</sup> T-cell-enriched fractions from C3H/HeJ mice were treated with anti-I-J<sup>k</sup> and C, T<sub>cs</sub>-cell activity was completely lost (Fig. 3). We conclude that reversal of oral tolerance in C3H/HeN mice is mediated by Lyt-1<sup>+</sup>,<sup>2</sup>, *V. villosa*<sup>+</sup>, I-J<sup>k+</sup> effector T<sub>cs</sub> cells.

The T<sub>cs</sub>-cell fractions prepared by the various treatments described above were also effective in restoring tolerant C3H/HeN spleen cells to IgM, IgG and IgA anti-SRBC PFC responses *in vitro*. Lyt-1<sup>+</sup>, *V. villosa*-adherent T cells supported *in vitro* PFC responses of all isotypes, while the *V. villosa*-non-adherent, Lyt-1<sup>+</sup> T<sub>h</sub>-cell-enriched fraction was ineffective (Table 1). Additional treatment of Lyt-1<sup>+</sup> T cells with anti-I-J<sup>k</sup> and C or with anti-Lyt-1 and C eliminated T<sub>cs</sub>-cell activity. Thus, studies *in vitro* confirmed our results with adoptively transferred T cells, and clearly showed that the active T cell is Lyt-1<sup>+</sup>, *V. villosa*-adherent and I-J<sup>k+</sup>.

The present results suggest that regulatory T-T-cell interactions determine the outcome of the host response to systemically administered TD antigen. Mice rendered orally tolerant to SRBC exhibit T<sub>s</sub> cells, which override T<sub>h</sub>-B-cell interactions and result in unresponsiveness<sup>3,7</sup>. The finding that active T<sub>cs</sub> cells from non-tolerant C3H/HeJ mice convert tolerant C3H/HeN mice to responsiveness clearly indicates that oral tolerance to SRBC

is largely mediated by T<sub>s</sub> cells. Implicit in this argument is the presence of T<sub>h</sub> cells in tolerant mice, which fail to function in the absence of T<sub>cs</sub> cells, and T<sub>s</sub>-cell-regulated systemic unresponsiveness ensues. However, T<sub>cs</sub> cells, together with residual T<sub>h</sub> cells, overcome T<sub>s</sub>-cell-mediated tolerance and produce anamnestic-type responses to systemic antigen. Although we do not understand why LPS-nonresponsive C3H/HeJ mice exhibit enhanced T<sub>cs</sub>-cell activity to orally administered SRBC, it is tempting to suggest that endogenous gut LPS diminishes T<sub>cs</sub>-cell induction, perhaps via effects on inducer or transducer precursors of T<sub>cs</sub> effector cells in Peyer's patches of normal LPS-responsive hosts.

Other studies<sup>9,12</sup> have suggested that T<sub>cs</sub> cells act on T<sub>h</sub> cells to render them resistant to suppressor cell influences, and the studies reported here are consistent with this. Our past work has shown that residual T<sub>h</sub> cells occur in both Peyer's patches and spleen of orally tolerant mice<sup>3,7</sup>; however, suppressor T-cell activity was dominant. These T<sub>h</sub> cells, in the presence of effector T<sub>cs</sub> cells, may be able to bypass oral tolerance. Alternatively, it remains possible that T<sub>cs</sub> cells act at the level of T<sub>s</sub> cells and inhibit their function. In this mode, the T<sub>cs</sub> cell would also serve as a suppressor cell whose target is another suppressor cell. This may better explain why small numbers of T<sub>cs</sub> cells can abrogate oral tolerance *in vivo*. In either situation orally induced T<sub>h</sub> cells would function to support anamnestic-type antibody responses in all major isotypes.

We thank Drs J. L. Butler and J. H. Eldridge for critical evaluation of this work and Ms Betty Wells for typing the paper. These studies were supported by USPHS grants AI 19674, AI 18958, DE 04217, New Investigator Research Award AI 21032 (to H.K.) and the Alberta Heritage Foundation (to D.R.G.).

Received 5 November 1985; accepted 28 January 1986.

- Challacombe, S. J. & Tomasi, T. B. Jr *J. exp. Med.* **152**, 1459-1472 (1980).
- Tomasi, T. B. Jr *Transplantation* **29**, 353-356 (1980).
- Kiyono, H., McGhee, J. R., Wannemuehler, M. J. & Michalek, S. M. *J. exp. Med.* **155**, 605-610 (1982).
- Richman, L. K., Chiller, J. M., Brown, W. R., Hanson, D. G. & Vaz, N. M. *J. Immun.* **121**, 2429-2434 (1978).

5. Kagnoff, M. F. *Gastroenterology* **79**, 54–61 (1980).
6. André, C., Heremans, J. F., Vaerman, J. P. & Cambiaso, C. L. *J. exp. Med.* **142**, 1509–1519 (1975).
7. Michalek, S. M., Kiyono, H., Wannemuehler, M. J., Mosteller, L. M. & McGhee, J. R. J. *Immun.* **128**, 1992–1998 (1982).
8. Watson, J., Kelly, K., Largen, M. & Taylor, B. *Ann. J. Immun.* **120**, 422–424 (1978).
9. Green, D. R., Flood, P. M. & Gershon, R. K. *A. Rev. Immun.* **1**, 439–463 (1983).
10. Gershon, R. K. *et al.* *J. exp. Med.* **153**, 1533–1546 (1981).
11. Green, D. R., Gold, J., Martin, S. T., Gershon, R. K. *Proc. natn. Acad. Sci. U.S.A.* **79**, 889–892 (1982).
12. Green, D. R. *et al.* *Eur. J. Immun.* **11**, 973–980 (1981).
13. Iverson, M., Ptak, W., Green, D. R. & Gershon, R. K. *J. exp. Med.* **158**, 982–987 (1983).
14. Yamada, K., Green, D. R., Eardley, D. D., Murphy, D. B. & Gershon, R. K. *J. exp. Med.* **153**, 1547–1561 (1981).

## Superoxide anion is involved in the breakdown of endothelium-derived vascular relaxing factor

R. J. Gryglewski, R. M. J. Palmer & S. Moncada\*

Wellcome Research Laboratories, Langley Court, Beckenham, Kent BR3 3BS, UK

**Endothelium-derived vascular relaxing factor (EDRF)<sup>1</sup>** is a humoral agent that is released by vascular endothelium and mediates vasodilator responses induced by various substances including acetylcholine and bradykinin<sup>2</sup>. EDRF is very unstable, with a half-life of between 6 (refs 3, 4) and 50 (ref. 5) s, and is clearly distinguishable from prostacyclin<sup>6</sup>. The chemical structure of EDRF is unknown but it has been suggested that it is either a hydroperoxy- or free radical-derivative of arachidonic acid or an unstable aldehyde, ketone or lactone<sup>3</sup>. We have examined the role of superoxide anion ( $O_2^-$ ) in the inactivation of EDRF released from vascular endothelial cells cultured on microcarrier beads and bioassayed using a cascade of superfused aortic smooth muscle strips<sup>7</sup>. With this system, we have now demonstrated that EDRF is protected from breakdown by superoxide dismutase (SOD) and  $Cu^{2+}$ , but not by catalase, and is inactivated by  $Fe^{2+}$ . These findings indicate that  $O_2^-$  contributes significantly to the instability of EDRF.

We have recently described a method for the bioassay of EDRF which allows differentiation between the effects of substances on the release, action or stability of EDRF<sup>7</sup>. Briefly, 7–14-day-old cultures of porcine aortic endothelial cells on microcarrier beads are packed into a chromatographic column ( $2\text{--}6 \times 10^7$  cells per column) and perfused with Krebs' solution ( $5 \text{ ml min}^{-1}$  at  $37^\circ\text{C}$ ) gassed with 5%  $CO_2$ /95%  $O_2$  containing indomethacin ( $5 \mu\text{M}$ ) to inhibit the biosynthesis of prostanoids. The column effluent is used to superfuse in cascade<sup>8</sup> two to four spirally cut strips of rabbit thoracic aorta which are denuded of endothelium and contracted with the stable 11,9-epoxy-methane analogue of prostaglandin H<sub>2</sub>, U46619 ( $30\text{--}60 \text{ nM}$ ), or with phenylephrine hydrochloride ( $50\text{--}200 \text{ nM}$ ). The uppermost vascular strip on the bioassay cascade is separated from the cells in the column by a delay of 1 s and the subsequent tissues are separated from each other by delays of 3 s. Nitroglycerin ( $20\text{--}200 \text{ nM}$ ) relaxes all tissues in the cascade when administered over the tissues (OT). This compound is used to standardize the sensitivity of the assay tissues because vascular relaxation induced by nitroglycerin and EDRF, but not by prostacyclin or  $\beta$ -adrenergic agonists, is reported to be mediated via activation of smooth muscle guanylate cyclase (refs 9, 10).

Bradykinin ( $10\text{--}100 \text{ nM}$ ) OT did not affect the tone of the rabbit thoracic aorta preparations, but when infused through the column (TC), it induced the release of EDRF, which in turn relaxed the aorta preparations and disappeared rapidly during passage down the cascade (half-life  $<7 \text{ s}$ , Fig. 1). As authentic EDRF is not available for the construction of standard dose-

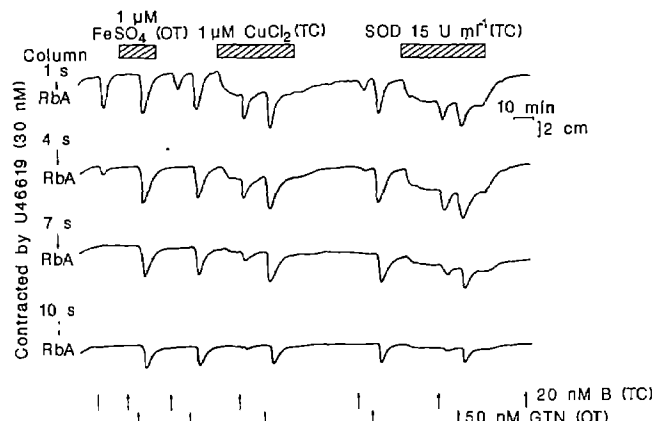


**Fig. 1** Effect of  $Fe^{2+}$ ,  $Cu^{2+}$  and SOD on the relaxation of rabbit aortas (RbA) by EDRF. A column packed with a 7-day-old culture of endothelial cells ( $4.2 \times 10^7$  cells) was perfused with Krebs' buffer ( $5 \text{ ml min}^{-1}$ ). The effluent was used to superfuse a cascade of four rabbit aortas. These preparations, denuded of endothelium and contracted submaximally by U46619 ( $30 \text{ nM}$ ), were separated from the column by delays of 1, 4, 7 and 10 s, respectively. The sensitivity of the rabbit aortas was standardized by administration of nitroglycerin (glyceryl trinitrate, GTN) over the tissues (OT). EDRF was released by 1-min infusions of bradykinin (B,  $20 \text{ nM}$ ) through the column (TC). Infusion of  $Fe^{2+}$  ( $FeSO_4$ ,  $1 \mu\text{M}$ , OT) abolished the vasodilator effect of EDRF without affecting the response to nitroglycerin, indicating the destruction of EDRF by  $Fe^{2+}$ .  $Cu^{2+}$  ( $CuCl_2$ ,  $1 \mu\text{M}$ , TC) caused a relaxation of aorta preparations which diminished down the cascade, revealing the spontaneous release of EDRF. In the presence of  $Cu^{2+}$ , the EDRF released by bradykinin relaxed all the tissues in the cascade. Therefore,  $Cu^{2+}$  increased the survival of EDRF. More than 15 min after the end of the  $Cu^{2+}$  infusions, the uppermost aorta had still not fully recovered from the relaxation. SOD ( $15 \text{ U ml}^{-1}$ ) infused TC produced a similar effect on the basal and bradykinin-induced release of EDRF which, in contrast to that induced by  $Cu^{2+}$ , disappeared within 5 min of terminating the SOD infusion.

response curves, the magnitude of the EDRF-induced relaxations of the vascular strips was expressed as a percentage of that caused by a standard dose of nitroglycerin ( $50 \text{ nM}$ , OT). The relaxation of the first bioassay tissue induced by bradykinin ( $20 \text{ nM}$ , TC)-stimulated EDRF was  $111.7 \pm 7.0\%$  (mean  $\pm$  s.e.m.,  $n = 22$ ) of that of the nitroglycerin standard. These bradykinin-induced vascular relaxations were inhibited 47.3 and 76.5% by haemoglobin ( $10 \mu\text{M}$ , OT;  $n = 2$ ) and  $90.2 \pm 2.0\%$  by methylene blue ( $50 \mu\text{M}$ , OT;  $n = 3$ ), confirming that the substance released was EDRF<sup>10</sup>.

Infusions of SOD ( $5\text{--}30 \text{ U ml}^{-1}$ , TC) caused relaxation of the tissues (Figs 1, 3), the magnitude of the relaxation being greatest in the first assay tissue ( $73.0 \pm 6.6\%$  of the nitroglycerin standard,  $n = 15$ ) and decreasing progressively the farther down the cascade the detector tissue was situated. This relaxation was significantly ( $P < 0.05$ ) attenuated when the infusion of SOD was changed from TC to OT ( $48.2 \pm 7.5\%$  of the nitroglycerin standard,  $n = 6$ ) and was not observed when the assay tissues were superfused with Krebs' solution instead of with effluent from the column. Furthermore, the relaxations caused by either SOD or bradykinin-induced EDRF were inhibited to a similar extent by methylene blue ( $50 \mu\text{M}$ , OT) and haemoglobin ( $10 \mu\text{M}$ , OT). These data suggest that there is a basal release of EDRF from the column which becomes evident when EDRF is stabilized by SOD, so that the release of EDRF induced by bradykinin occurs against a background of continuous release.

The stability of EDRF released by bradykinin was markedly increased by infusions of SOD ( $5\text{--}30 \text{ U ml}^{-1}$ , TC), as shown by the relaxation of the tissues farther down the cascade (Fig. 1). Thus, the relaxations of the first three tissues were increased by  $1.4 \pm 0.07$  ( $n = 11$ ),  $4.05 \pm 1.00$  ( $n = 11$ ) and  $9.3 \pm 1.3$  ( $n = 9$ ) times, respectively. Enhancement of the response of the fourth tissue

\* To whom correspondence should be addressed.

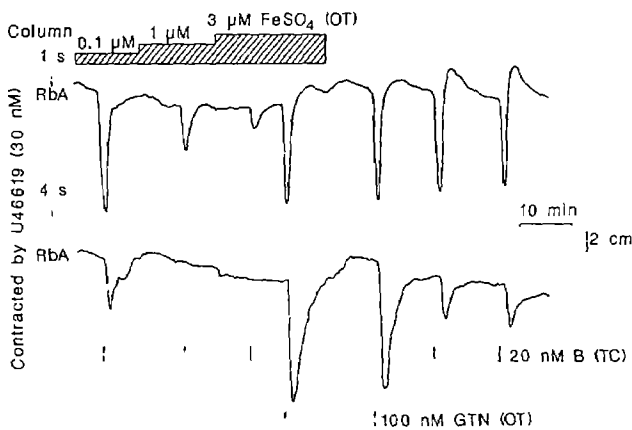


**Fig. 2** Effluent of a column containing endothelial cells (9-day-old culture,  $2.6 \times 10^7$  cells) was used to superfuse two rabbit aorta strips separated by a 3-s delay (as described for Fig. 1). Infusion of increasing concentrations of  $\text{FeSO}_4$  (0.1–3  $\mu\text{M}$ , OT) inhibited the effect of EDRF released by bradykinin (20 nM, TC) without affecting the relaxation induced by nitroglycerin (100 nM, OT). This effect disappeared within 10 min of terminating the infusion of  $\text{FeSO}_4$ .

could not be quantified, as EDRF released by bradykinin in the absence of SOD did not reach this tissue. Bradykinin-induced EDRF was also stabilized when the SOD infusion was changed from TC to OT, although in these conditions SOD was less effective (the responses of the first three tissues were enhanced by  $1.40 \pm 0.16$  ( $n = 5$ ),  $2.70 \pm 0.98$  ( $n = 4$ ) and  $3.74 \pm 0.97$  ( $n = 3$ ) times, respectively). The finding that SOD increases EDRF-induced relaxations when given over the tissue indicates that SOD increases the stability of EDRF; whether it also affects EDRF synthesis or release is unclear. The effect of SOD requires its enzymatic activity, as boiled (1 min) enzyme did not enhance EDRF responses.

Catalase (30 U ml $^{-1}$  OT or TC) did not affect the stability of EDRF when given either alone ( $n = 4$ ) or in combination with SOD ( $n = 3$ ), indicating that  $\text{H}_2\text{O}_2$  or  $\text{H}_2\text{O}_2$ -derived radicals do not contribute to EDRF breakdown. Therefore, it appears that  $\text{O}_2^-$  is a potent inactivator of EDRF and that it is either present or produced in sufficient quantities in our system to inactivate EDRF rapidly.

The idea that the short half-life of EDRF may be a function (at least in part) of the concomitant release of EDRF and  $\text{O}_2^-$  by vascular endothelial cells merits further study. It may explain the reported differences in the half-life of EDRF $^{3,5}$ , as these may in turn be affected by the ratio of EDRF to  $\text{O}_2^-$  in a particular experimental system.

EDRF could also be stabilized by  $\text{Cu}^{2+}$  ( $\text{CuCl}_2$ , 1–3  $\mu\text{M}$ , OT), although less effectively than by SOD. Like SOD,  $\text{CuCl}_2$  was more effective at protecting EDRF released by bradykinin when the infusion was changed from tissue to column; thus, the bradykinin (20 nM, TC)-induced relaxation of the first three tissues was increased by  $1.35 \pm 0.03$  ( $n = 4$ ),  $1.70 \pm 0.65$  ( $n = 4$ ) and  $2.33 \pm 0.90$  ( $n = 3$ ) times and by  $1.50 \pm 0.22$  ( $n = 4$ ),  $2.40 \pm 0.40$  ( $n = 4$ ) and  $4.2 \pm 1.44$  ( $n = 4$ ) times, respectively, by OT and TC  $\text{CuCl}_2$  (1  $\mu\text{M}$ ). In addition, infusions of  $\text{Cu}^{2+}$  alone (TC) caused relaxation of the bioassay tissues (in the uppermost bioassay tissue this relaxation was  $48.0 \pm 7.3\%$  ( $n = 6$ ) of that induced by the nitroglycerin standard) which was smaller the farther the detector tissue was situated from the column, again suggesting a basal release of EDRF in these conditions.  $\text{ZnSO}_4$  (10  $\mu\text{M}$ ) did not affect the stability of EDRF in two experiments. Mammalian cytosolic SODs are copper/zinc enzymes, of which copper is the active species $^{11}$ . Since low-relative molecular mass complexes of  $\text{Cu}^{2+}$  and  $\text{Cu}^{2+}$  itself mimic SOD activity in specific conditions, this effect of  $\text{Cu}^{2+}$  is not unexpected. These results suggest that  $\text{Cu}^{2+}$  acts by dismuting  $\text{O}_2^-$  directly; whether it also

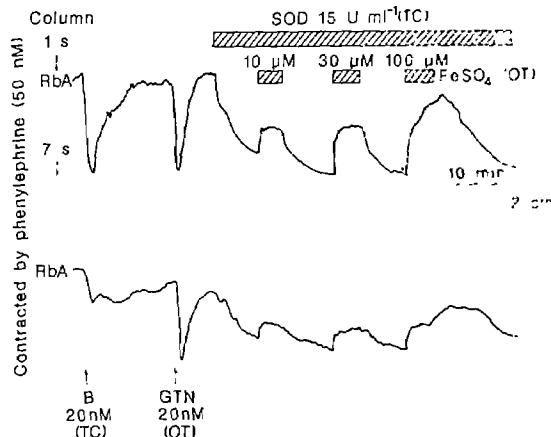


**Fig. 3** Effluent of a column containing endothelial cells (13-day-old culture,  $5.4 \times 10^7$  cells) was used to superfuse two strips of rabbit aorta separated by a 6-s delay (as described in Fig. 1 legend). The tissues were relaxed by bradykinin (20 nM, TC)-induced EDRF and by nitroglycerin (20 nM, OT). Infusion of SOD (15 U ml $^{-1}$ , TC) relaxed the assay tissues. This relaxation could be reversed by infusion of increasing concentrations of  $\text{FeSO}_4$  (10–100  $\mu\text{M}$ , OT).

acts by reactivating $^{12}$  exhausted endothelial SOD $^{13}$  is not clear. However, the finding that the protection of EDRF continues for up to 15 min after the end of  $\text{Cu}^{2+}$  (TC) infusion but not after that of SOD (Fig. 1) supports the latter action. It is interesting that  $\text{Mn}^{2+}$  (10  $\mu\text{M}$   $\text{MnCl}_2$ , TC), the metal ion in SOD from other sources which can also dismute  $\text{O}_2^-$  (refs 14, 15), was inactive in two experiments.

Our hypothesis that  $\text{O}_2^-$  destroys EDRF is further supported by the observation that  $\text{Fe}^{2+}$  is a potent and selective inhibitor of EDRF. Indeed,  $\text{FeSO}_4$  (0.3–10  $\mu\text{M}$ , OT) dose-dependently inhibited the EDRF-induced relaxation of the assay tissues without affecting the response to nitroglycerin (Fig. 2). Thus, 1  $\mu\text{M}$   $\text{FeSO}_4$  OT produced a  $78.2 \pm 9.2\%$  ( $n = 5$ ) inhibition in the response of the uppermost tissue to bradykinin (20 nM, TC)-stimulated EDRF. In addition,  $\text{Fe}^{2+}$  reversed the relaxation of the tissues induced by the basal release of EDRF (observed when SOD was given TC). However, in the presence of SOD (15 U ml $^{-1}$ , TC) 10-fold higher concentrations of  $\text{Fe}^{2+}$  (10–100  $\mu\text{M}$ , OT) were necessary to antagonize the action of EDRF. For example, the relaxation of the uppermost tissue induced by bradykinin-stimulated EDRF was inhibited  $95.5 \pm 0.9\%$  ( $n = 4$ ) by 10  $\mu\text{M}$   $\text{FeSO}_4$  OT in the absence of SOD and  $44.0 \pm 6.5\%$  ( $n = 3$ ) in its presence (15 U ml $^{-1}$ , TC). Since  $\text{Fe}^{2+}$  can catalyse the formation of  $\text{O}_2^-$  in oxygenated phosphate buffer $^{16}$ , these findings suggest that  $\text{Fe}^{2+}$  antagonizes EDRF by inactivating it via the generation of  $\text{O}_2^-$ . Indeed, the pronounced reduction in potency of  $\text{Fe}^{2+}$  in the presence of SOD favours this concept (Fig. 3).  $\text{Fe}^{2+}$  could also inactivate EDRF either directly or by generation of hydroxyl radicals from  $\text{H}_2\text{O}_2$  in Haber-Weiss and Fenton reactions $^{17}$ , although the latter explanation would not be consistent with the lack of effect of catalase on EDRF stability.

The effects of  $\text{Cu}^{2+}$  and  $\text{Fe}^{2+}$  on EDRF stability may indicate a regulatory role for trace elements in the control of the vascular system in health and disease. Both prostacyclin and EDRF have a homeostatic function in vascular integrity. The findings that lipid peroxides and superoxide ions either prevent the synthesis $^{18}$  or destroy the biological activity of these mediators suggest a central role for activated oxygen species in the pathogenesis of vasospasm, thrombosis and atherosclerosis.

We thank Sir John Vane for helpful discussion and Ms L. Pynegar and Mr N. Foxwell for technical assistance.

Since this paper was submitted, we have become aware of a preliminary communication by Vanhoutte and Rubanyi $^{19}$  suggesting that SOD increases the half-life of EDRF.

Received 24 September 1985; accepted 20 February 1986.

1. Furchtgott, R. F. & Zawadzki, J. V. *Nature* **288**, 373–376 (1980).
2. Furchtgott, R. F. A. *Rev. Pharmacol. Tox.* **24**, 175–197 (1984).
3. Griffith, T. M., Edwards, D. H., Lewis, M. J., Newby, A. C. & Henderson, A. H. *Nature* **308**, 645–647 (1984).
4. Cocks, T. M., Angus, J. A., Campbell, J. H. & Campbell, G. R. *J. cell. Physiol.* **123**, 310–320 (1985).
5. Förstermann, U., Trogisch, G. & Busse, R. *Eur. J. Pharmacol.* **106**, 639–643 (1985).
6. Moncada, S., Gryglewski, R. J., Bunting, S. & Vane, J. R. *Nature* **263**, 663–665 (1976).
7. Gryglewski, R. J., Moncada, S. & Palmer, R. M. J. *Br. J. Pharmac.* **87**, 685–694 (1986).
8. Vane, J. R. *Br. J. Pharmac. Chemother.* **23**, 360–373 (1964).
9. Rapaport, R. M., Drizin, M. B. & Murad, F. *Nature* **306**, 174–176 (1983).
10. Martin, W., Villani, G. M., Jothianandan, D. & Furchtgott, R. F. *J. Pharmac. exp. Ther.* **232**, 708–716 (1985).
11. Keele, B. B., McCord, J. M. & Fridovich, I. *J. biol. Chem.* **246**, 2875–2880 (1971).
12. Heikkila, R. E. & Cohen, G. in *Superoxide and Superoxide Dismutases* (eds Michelson, A. M., McCord, J. M. & Fridovich, I.) 367–373 (Academic, London, 1977).
13. Block, E. R., Patel, J. M. & Sheridan, N. P. *J. cell Physiol.* **122**, 240–248 (1985).
14. Epel, B. L. & Neumann, J. *Biochim. biophys. Acta* **325**, 520–529 (1973).
15. Lumsden, J. & Hall, D. C. *Biochem. biophys. Res. Commun.* **64**, 595–602 (1975).
16. Michelson, A. M. in *Superoxide and Superoxide Dismutases* (eds Michelson, A. M., McCord, J. M. & Fridovich, I.) 77–86 (Academic, London, 1977).
17. Freeman, B. A. & Crapo, J. D. *Lab. Invest.* **47**, 412–426 (1982).
18. Moncada, S., Gryglewski, R. J., Bunting, S. & Vane, J. R. *Prostaglandins* **12**, 715–733 (1976).
19. Vanhoutte, P. M. & Rubanyi, G. M. *Clin. Res.* **33**, 523A (1985).

## Dispersed human immunoglobulin κ light-chain genes

E. Lötscher, K.-H. Grzeschik\*, H. G. Bauer,  
H.-D. Pohlenz, B. Straubinger & H. G. Zachau

Institut für Physiologische Chemie der Universität München,  
Goethestrasse 33, 8000 München 2, FRG

\* Institut für Humangenetik der Universität Münster,  
Vesaliusweg 12–14, 4400 Münster, FRG

The gene segments encoding the constant and variable regions of human immunoglobulin light chains of the κ type ( $C_\kappa$ ,  $V_\kappa$ ) have been localized to chromosome 2 (refs 1, 2). The distance between the  $C_\kappa$  and  $V_\kappa$  genes and the number of germline  $V_\kappa$  genes are unknown. As part of our work on the human  $V_\kappa$  locus (refs 3–6 and reviewed in ref. 7), we have now mapped two solitary  $V_\kappa$  gene and a cluster of three  $V_\kappa$  genes to chromosomes 1, 15 and 22, respectively. The three genes that have been sequenced are non-processed pseudogenes, and the same may be true for the other two genes. This is the first time that  $V$ -gene segments have been found outside the  $C$ -gene-containing chromosomes. Our finding is relevant to current estimates of the size of the  $V_\kappa$ -gene repertoire. Furthermore, the dispersed gene regions have some unusual characteristics which may help to clarify the mechanism of dispersion.

To elucidate the human  $V_\kappa$  locus, we prepared hybridization probes for the four known  $V_\kappa$  subgroups<sup>3,8,9</sup> and used them to isolate more than 150 different  $V_\kappa$ -gene-containing cosmids from genomic DNA libraries. Several genomic regions each of about 100 kilobases (kb), altogether about 1,200 kb, comprising 75–80  $V_\kappa$  genes, could be defined with the help of overlapping cosmids and 'genomic walking' experiments (refs 4–6 and H.-D.P. et al. and B.S. et al., manuscripts in preparation). Subclones prepared from the various regions were then hybridized to a panel of digested DNAs from human–rodent cell hybrids. As expected, most of the regions mapped to chromosome 2 but three regions were found on chromosomes 1, 15 and 22, respectively (Figs 1, 2); accordingly, we named them Chr1, Chr15 and Chr22.

Genomic regions Chr1 and Chr15 contain  $V_\kappa$  genes of subgroup I according to comparative hybridization experiments of cosmid digests with probes of different  $V_\kappa$  subgroups. Based on a comparison of their restriction maps with the map of a related gene which has been sequenced (R. Thiebe, unpublished), the  $V_\kappa$ I genes are non-processed genes or pseudogenes. Also, the absence of a  $C_\kappa$ -gene segment from the cosmids of the two regions (and from all our other cosmids) argues against the presence of a processed pseudogene. No other  $V_\kappa$  genes were

found on the cosmids of regions Chr1 and 15 or on cosmids extending these regions in the upstream direction by about 30 kb.

The finding of several hybridizing *Eco*RI fragments in digests of DNA from the chromosome 15-containing cell hybrids (Fig. 2 legend) suggests that chromosome 15 contains several copies either of the whole Chr15 region including the  $V_\kappa$ I gene or of only the region around the search clone used in the hybridization experiment. In the latter case, the  $V_\kappa$ I-gene region must have been inserted in the neighbourhood of one of the copies of this low-repetitive, chromosome-specific sequence.

Region Chr22 contains a cluster of three  $V_\kappa$  genes (Fig. 1). The  $V_\kappa$ I gene (Fig. 3) contains mutations in its start codon and in the conserved heptanucleotide sequence<sup>10–12</sup>. It also carries a 7-base pair (bp) insertion in framework region 3 (FR3), which has probably been created by a duplication. Two stop codons were found in the  $V_\kappa$ II gene; an insertion and a deletion have to be assumed in order to obtain a good fit of the invariant amino acids<sup>13</sup>. Also, the  $V_\kappa$ III gene is a strongly diverged pseudogene. We assign it to this subgroup because it hybridizes weakly with a  $V_\kappa$ III probe (21–4 in ref. 5) and not at all with probes of other subgroups. Also, the invariant amino acids fit this subgroup better than the others. Peculiar T-rich sequences appear at the end of the gene and in the downstream region.

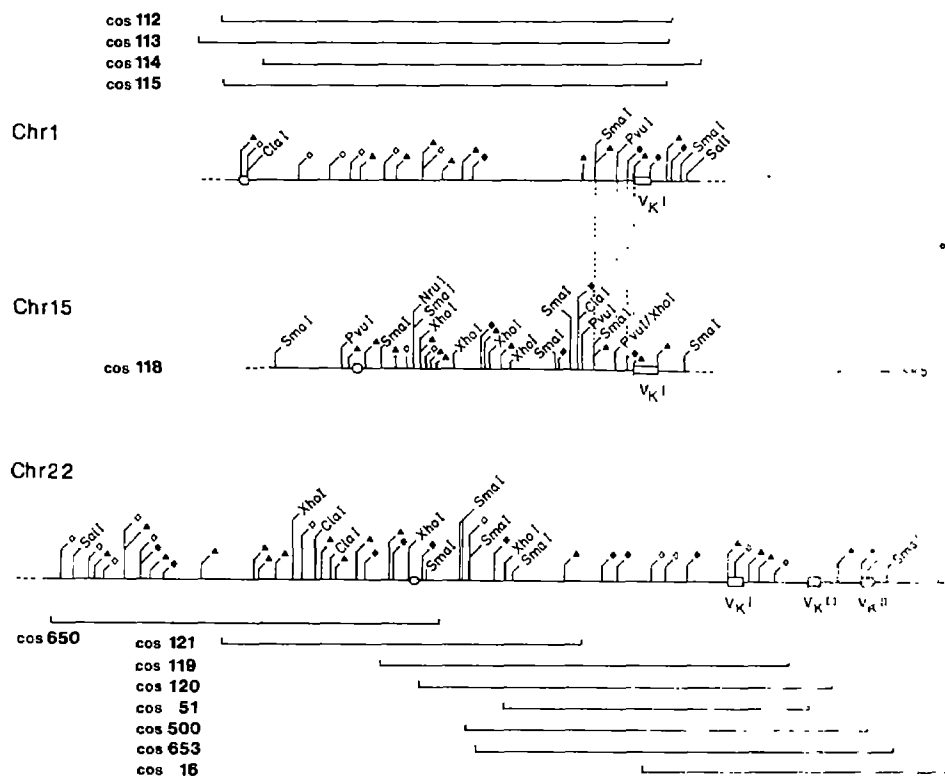
A genomic region containing a cluster of eight  $V_\kappa$  genes which is, at least in part, duplicated within the genome<sup>6</sup> and a  $C_\kappa$ -gene probe were included in the present study for comparison. The localization of  $C_\kappa$  to chromosome 2 (ref. 1) was confirmed and the  $V_\kappa$ -gene region was also located on this chromosome (Fig. 2).

The possibility that the search clone and  $V_\kappa$ -gene regions have become associated artefactually can be excluded for Chr1 and Chr22 because these genomic regions were constructed from several independently isolated cosmids which were identical in the overlapping parts (Fig. 1). Ligation artefacts were extremely rare in the many cosmids that we have isolated from our libraries, and so it is very likely that the Chr15 structure, although based on only one cosmid, also represents a continuous genomic region.

We estimate roughly, based on counting of cloned and chromosomally located genes, that about 10% of the human  $V_\kappa$  genes are located outside chromosome 2. However, the proportion cannot be determined exactly for the following reasons: a fair number of our cloned  $V_\kappa$  genes are still not sufficiently characterized; it is difficult to establish the completeness of library screening experiments; restriction analyses of cosmids containing dispersed  $V_\kappa$  genes suggest that some sequences are present on the respective chromosomes in more than one copy; and finally, the size of the duplicated section of the  $V_\kappa$  locus on chromosome 2 (ref. 6) is not known. A different approach to the question, hybridization of  $V_\kappa$ -gene probes to the panel of human–rodent cell hybrid DNAs, did not yield clear results mainly because of cross-hybridization of the human  $V_\kappa$  genes ( $V_\kappa$ I,  $V_\kappa$ III) with rodent  $V_\kappa$  genes and because of the limits of sensitivity ( $V_\kappa$ II). On the basis of our present data, we conclude that a small but significant fraction of the human  $V_\kappa$  genes is dispersed outside chromosome 2.

In addition to the dispersed  $V_\kappa$  pseudogenes described here, some human  $V_\kappa$  pseudogenes have been found on chromosome 2 (see, for example, refs 4, 6), while others exist which have not yet been mapped to specific chromosomes<sup>3,14</sup>. The dispersed pseudogenes are more widely diverged from the potentially functional genes than are the pseudogenes located on chromosome 2; they are perhaps no longer or less subject to the surveillance by gene conversion-like processes which occurs between adjacent or more distantly located genes of a locus (see, for example, refs 3, 4, 15). Distinct from the non-processed pseudogenes are the processed genes that arise by transcription and retrotranscription events and which are quite common among several gene families (reviewed in ref. 16). Processed human  $J_\lambda C_\lambda$  ( $J$ , joining; ref. 17) and  $C_e$  (refs 18, 19) pseudogenes have also been found, but, notably, no processed  $V$  pseudogenes

**Fig. 1**  $V_{\kappa}$ -gene-containing regions on several chromosomes. The restriction maps of the genomic regions are derived from the cosmids indicated in the figure. All cosmids were isolated from libraries prepared from the same DNA (ref. 4 and H.-D.P., unpublished data). Cosmids are indicated by horizontal lines,  $V_{\kappa}$ -gene regions by boxes, search clone regions by circles. The 5'-3' polarity of regions Chr1 and Chr15 is based on map homology (vertical dashed lines) to another genomic region (not shown) in which the  $V_{\kappa}1$  gene was sequenced (R. Thiebe, unpublished). The search clones (in M13; ref. 21), which were selected for the absence of repetitive sequences, are a 1.0-kb *Bgl*II/*Cla*I fragment (Chr1), a 1.4-kb *Bgl*III/*Bgl*II fragment (Chr15) and a 1.3-kb *Bam*HI/*Xba*I fragment (Chr22). Detailed maps of the subcloned regions and additional map data are reported elsewhere<sup>22-25</sup> and are available on request. Nuclease cleavage sites: ▲, *Bgl*III; ♦, *Bam*HI; ◇, *Kpn*I.



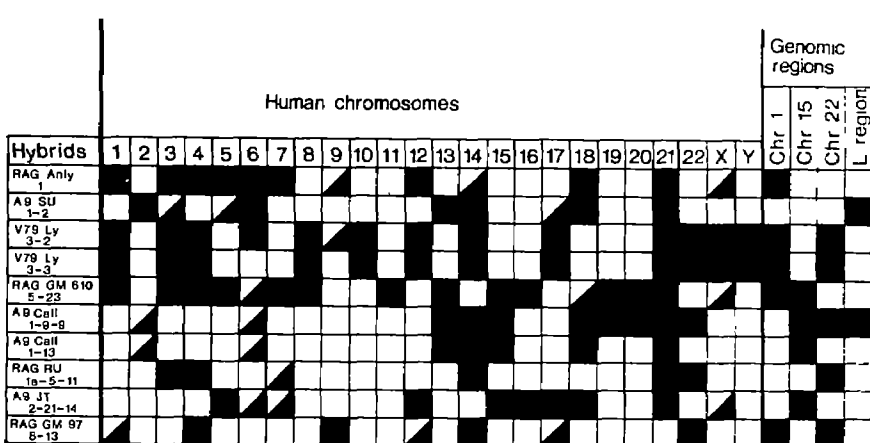
have been detected. This may reflect the fact that *V*-gene segments are probably not transcribed in the germ line.

The mechanism of dispersion of  $V_{\kappa}$ -gene regions is unknown. For other gene families, two mechanisms in addition to retro-transcript insertion and recombinational events have been considered; these are gene conversion-like processes and the dispersion of transposon-like elements (reviewed in ref. 20). The presence of long but imperfect repeats in the flanks of several  $V_{\kappa}$ I genes<sup>4</sup> indicates that such genes may have functioned as transposon-like elements. Also, the evolutionary history of a mixed  $V_{\kappa}$ I,  $V_{\kappa}$ II,  $V_{\kappa}$ III gene cluster is best discussed in terms

of intrachromosomal transposition events<sup>5</sup>. The presence of  $V_{\kappa}$  genes on chromosomes 1 and 15 may be explained by an interchromosomal transposition, although gene conversion-like events cannot be excluded. The transposition of a  $V_{\kappa}$  gene cluster to chromosome 22 is difficult to explain by either mechanism. Perhaps a novel type of recombinational mechanism must be considered in this case. As the dispersed  $V_{\kappa}$  genes do not contribute directly to the repertoire of potentially functional  $V_{\kappa}$  genes, studies on the size of the  $V_{\kappa}$ -gene repertoire must not only count the genes but also determine their chromosomal location.

**Fig. 2** Chromosomal location of  $V_{\kappa}$ -gene-containing regions. The subcloned fragments of regions Chr1, Chr15, Chr22 (Fig. 1) and fragment 21-1 of the region with eight  $V_{\kappa}$  genes (refs 4, 6; called the L region because of the occurrence of the repetitive L sequences next to the  $V_{\kappa}$ I genes<sup>26</sup>) were self-ligated and used as hybridization probes. A panel of 27 mouse-human cell hybrids was generated by fusion of mouse RAG or A9 cells and human fibroblasts originating from various translocation carriers<sup>27-29</sup> and characterized by isozyme and cytogenetic analyses for the presence of human chromosomes and chromosome fragments, as described previously<sup>27</sup>. In addition, two human-chinese hamster cell hybrids generated by fusion of V79 cells with human lymphocytes from a male (46, XY) donor were included in the segregation analysis. Hybrid cell DNAs were digested with EcoRI, separated by

agarose (0.8%) electrophoresis and transferred to Biodyne A membranes (Pall Filtrationstechnik, D-6072 Dreieich). Hybridization of nick-translated probes was as in ref. 5 except that the SDS content of the solutions was 0.5% and the final wash solution contained  $0.5 \times SSC$ . In these conditions, the probes did not hybridize to rodent DNAs. The *EcoRI* fragments of genomic DNA which are detected in the panels have the following lengths (in kb): Chr1, 2.1; Chr15, 6.2, 9, 12, 20, >20 (and 4 weak bands; the 9-kb fragment is derived from the  $V_{\kappa}$ -gene-containing region as represented in cos 118); Chr22, 3.4; L region, 8.2, ~20. All fragments detected by one of the four probes, respectively, segregated concordantly in individual hybrid clones. The segregation analysis of the fragments and human chromosomes in the panel, part of which is shown in the figure, allows the regions detected by the probes to be assigned to chromosomes 1, 15, 22 and 2, respectively. Filled spaces indicate the presence of the chromosome, half-filled spaces indicate that part of the chromosome is present, and empty spaces indicate that the chromosome was not detected by biochemical and cytogenetic analyses. Clone A9 Call 1-9-9 contains a fragment of chromosome 2 (pter-p23) and shows bands with the L-region probe 21-2. Hybrid clone RAG GM 97 8-13 retains the fragment 1pter-q12 and shows the band detected by Chr1. These findings allow us to submap the regions to parts of chromosomes 1 and 2, respectively.



9

This work was supported by Bundesministerium für Forschung und Technologie and Fonds der Chemischen Industrie. K.-H.G. acknowledges the technical assistance of G. Menne. *Note added in proof:* Chr1 was present in two hybrid clones without an intact human chromosome 1 but retaining the fragments 1q12-1pter and 1p13-1qter, respectively; this places region Chr1 between 1p13 and 1q12. Additional cosmids extending the Chr22 region in the 3' direction contain yet another  $V_K$ II and a  $V_K$ I gene or pseudogene; however, the location of these genes on chromosome 22 has not been confirmed directly by experiments with cell hybrids.

Received 14 October 1985; accepted 21 February 1986.

- McBride, O. W. et al. *J. exp. Med.* **155**, 1480-1490 (1982).
  - Malcolm, S. *Proc. natn. Acad. Sci. U.S.A.* **79**, 4957-4961 (1982).
  - Jaenichen, H. R., Pech, M., Lindenmaier, W., Wildgruber, N. & Zachau, H. G. *Nucleic Acids Res.* **12**, 5249-5263 (1984).
  - Pech, M. et al. *J. molec. Biol.* **176**, 189-204 (1984).
  - Pech, M. & Zachau, H. G. *Nucleic Acids Res.* **12**, 9229-9236 (1984).
  - Pech, M. et al. *J. molec. Biol.* **183**, 291-299 (1985).
  - Zachau, H. G. et al. *Hoppe-Seyler's Z. physiol. Chem.* **365**, 1363-1373 (1984).
  - Klobcik, H. G., Solomon, A. & Zachau, H. G. *Nature* **309**, 73-76 (1984).

<i>SurSerLeuGlnFnu</i>	80	<b>Fig. 3 Sequence of the <math>V_{\kappa}</math>I (a), <math>V_{\kappa}</math>II (b) and <math>V_{\kappa}</math>III (c) pseudogenes of the genomic region Chr22.</b>
ABCAGCCTGCAAGCTGCAAGCGT	247	The chain termination method <sup>30</sup> was used with M13mp10 and 11 subclones <sup>21</sup> of cos 120 and 653; both strands were sequenced throughout. The sequencing strategies and additional sequence information (a further 500 bp upstream and 640 bp downstream of the $V_{\kappa}$ I region; 420 bp upstream and 380 bp downstream of the $V_{\kappa}$ III region) are reported elsewhere <sup>25</sup> . The latter information is also being deposited at the EMBL Data Library, Heidelberg. The $V_{\kappa}$ II gene was not sequenced up to the leader region. Sequences underlined are related to the pd and dc boxes <sup>31</sup> , TATA box <sup>10</sup> and the hepta- and non-anucleotide boxes <sup>11,12</sup> as well as the invariant amino acids <sup>13</sup> . A line above amino-acid symbols indicates that an invariant amino acid has been replaced by another amino acid. In the $V_{\kappa}$ II and $V_{\kappa}$ III genes insertions are indicated by brackets and deletions by triangles. *, Stop codon. L, FR and CDR designate leader, framework and complementarity-determining regions, respectively.
CADGGAAAGCAGATGTGTGAGGC	95	
ATTGGAAAATTTGGTAGAAGG	347	
	447	
<i>CTAACATTGAAAAAAATACGTA</i>	-96	
<u>L</u> <u>FR1</u>	2	
<i>lysSerSerGlyAspII</i>	5	
TTTCAGGGTCCAGTGCGGATAT		
7 A R C D E		
<i>AsSerLeuValTyrArgGlyGlu</i>	29	
ACACCCITGATACAGGGGGGAA	105	
<u>FR3</u>	63	
<i>SerAlaValProAspArgLeuS</i>	204	
TCTGCAGGCCAGACAGGGCTCA		
CDR3		
<i>IleGlnAlaLeuGlnThrPhe</i>	95	
ATGCAAGCTCACAACTCTCTCC	334	
CACTCTCAGCAGGGCTCTGGTC	404	
	426	
<i>ABTCCAATGCTTCTTCATGTT</i>	-339	
<u>L</u>	-17	
<u>lysGlnAlaPhe</u>	-239	
CAAGAGAGACTCATGGAAAGCCCC		
	-5	
AACTCTTGTGTTCTCTGACCT	-139	

9. Klobbeck, H. G. *et al.* *Nucleic Acids Res.* **13**, 6515-6529 (1985).
  10. Sakano, H., Hüppi, K., Heinrich, G. & Tonegawa, S. *Nature* **280**, 288-294 (1979).
  11. Max, E. E., Seidman, J. G. & Leder, P. *Proc. natn. Acad. Sci. U.S.A.* **76**, 3450-3454 (1979).
  12. Breathnach, R. & Chamblon, P. A. *Rev. Biochem.* **50**, 349-383 (1981).
  13. Kabat, E. A., Wu, T. T., Bilosky, H., Reid-Miller, M. & Perry, H. *Sequences of Proteins of Immunological Interest* (National Institutes of Health, Bethesda, 1983).
  14. Bentley, D. L. & Rabbits, T. H. *Nature* **288**, 730-733 (1980).
  15. Weiss, E. H. *et al.* *Nature* **310**, 650-655 (1984).
  16. Vanin, E. F. *Biochim. biophys. Acta* **782**, 231-241 (1984).
  17. Hollis, G. F., Hieter, P. A., McBride, O. W., Swan, D. & Leder, P. *Nature* **296**, 321-325 (1982).
  18. Battye, J., Max, E. E., McBride, W. O., Swan, D. & Leder, P. *Proc. natn. Acad. Sci. U.S.A.* **79**, 5956-5960 (1982).
  19. Ueda, S., Nakai, S., Nishida, Y., Hisajima, H. & Honjo, T. *EMBO J.* **1**, 1539-1544 (1982).
  20. D'Eustachio, P. & Ruddle, F. H. *Science* **220**, 919-924 (1983).
  21. Messing, J. *Meth. Enzym.* **101**, 20-78 (1983).
  22. Löttscher, I. thesis, Univ. Munich (in preparation).
  23. Pohlenz, H. D. thesis, Univ. Munich (1986).
  24. Straubinger, B. thesis, Univ. Munich (1986).
  25. Bauer, H. G. thesis, Univ. Munich (1986).
  26. Straubinger, B. *et al.* *Nucleic Acids Res.* **12**, 5265-5275 (1984).
  27. Balazs, I., Purrello, M., Kurnit, D. M., Grzeschik, K. H. & Siniscalco, M. in *Somatic Cell molec. Genet.* **10**, 385-397 (1984).
  28. Camerino, G. *et al.* *Proc. natn. Acad. Sci. U.S.A.* **81**, 498-502 (1984).
  29. Zabel, B. U., Naylor, S. L., Grzeschik, K. H. & Sakaguchi, A. Y. *Somatic Cell molec. Genet.* **10**, 105-108 (1984).
  30. Sanger, F., Coulson, A. R., Barrell, B. G., Smith, A. J. H. & Roe, B. A. *J. molec. Biol.* **143**, 161-178 (1980).
  31. Falkner, F. G. & Zachau, H. G. *Nature* **310**, 71-74 (1984).

## Increased phosphorylation of ribosomal protein S6 following microinjection of insulin receptor-kinase into *Xenopus* oocytes

James L. Maller\*, Linda J. Pike†‡, Gary R. Freidenberg§, Renzo Cordera§, Bradley J. Stith\*, Jerrold M. Olefsky§ & Edwin G. Krebs†

\* Department of Pharmacology, University of Colorado School of Medicine, Denver, Colorado 80262, USA

† Howard Hughes Medical Institute, University of Washington, Seattle, Washington 98195, USA

§ Department of Medicine, University of California, San Diego, La Jolla, California 92093, USA

The protein products of several transforming retroviruses as well as the receptors for several hormones and growth factors, including insulin, have been shown to possess a protein kinase activity *in vitro* specific for tyrosine residues in protein substrates, including themselves (see ref. 1 for a review). In the case of pp60<sup>src</sup> and the insulin receptor, autophosphorylation activates the tyrosine kinase activity towards exogenous substrates<sup>2-4</sup>. Experiments indicate that, *in vivo*, many of these viruses or growth factors induce an increase in cellular phosphotyrosine, as well as an increase in the phosphorylation of serine residues on proteins, including ribosomal protein S6. It seems likely that some of the effects of insulin might be mediated by phosphorylation of intracellular substrates by its receptor. As the  $\beta$  subunit of the receptor is a transmembrane protein<sup>5</sup>, such phosphorylation could occur either while the receptor is still in the membrane or after its internalization. In various cell systems, internalized receptors are degraded, reshelved back to the plasmalemma or maintained in a separate compartment before reinsertion in the membrane<sup>6,7</sup>; shuttling of the insulin receptor could provide the opportunity for it to phosphorylate various intracellular components as part of its mechanism of signal transduction. To approach directly the question of whether the receptor can elicit a signal while acting at an intracellular location, we have microinjected *Xenopus* oocytes with the insulin receptor kinase. The results indicate that an S6 protein-serine kinase is stimulated or an S6 protein-serine phosphatase inhibited by the activity of the insulin receptor, supporting the concept that the insulin receptor acting within the cell can elicit a biological response.

Oocytes possess insulin receptors<sup>8</sup> and respond to insulin by increased intracellular pH, increased phosphorylation of proteins, including ribosomal protein S6, and increased protein synthesis<sup>9-11</sup>. The phosphorylation of serine in S6 is increased in oocytes following the microinjection of purified pp60<sup>v-src</sup>, the protein-tyrosine kinase responsible for transformation by Rous sarcoma virus<sup>12</sup> or the purified protein-tyrosine kinase involved in transformation by Abelson murine leukaemia virus<sup>13</sup>. *Xenopus* oocytes must therefore possess the regulatory pathways utilized by exogenous protein-tyrosine kinases to cause S6 phosphorylation. To obtain further evidence for this, the phosphorylation of S6 was examined after microinjection of insulin receptors into oocytes. The receptor preparation eluted from insulin-Sepharose was highly purified as judged by gel electrophoresis and silver staining (Fig. 1B). (However, this purified form of the solubilized insulin receptor does not necessarily represent the state of the receptor after internalization in a target cell.) Following microinjection of receptors with bound insulin, the phosphorylation of S6 increased rapidly to about threefold that of control oocytes (Fig. 1A). The response is unlikely to be due to leakage of insulin from the injected oocyte because all data

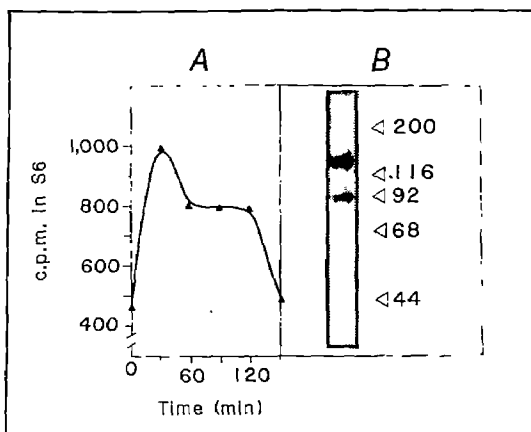


**Fig. 1** S6 phosphorylation following microinjection of insulin-receptor kinase into *Xenopus* oocytes. **A**, Time course of increase in S6 phosphorylation. Insulin receptors purified by affinity chromatography ( $10\text{ }\mu\text{g ml}^{-1}$ ) and incubated with  $100\text{ nM}$  insulin were microinjected into each of 25 oocytes preinjected with  $50\text{ nl}$  of  $^{32}\text{P}_i$  ( $200\text{ mCi ml}^{-1}$ ). Control (0 time) oocytes were injected with  $100\text{ nM}$  insulin,  $1\text{ mg ml}^{-1}$  bovine serum albumin (BSA) in the receptor kinase buffer. At the indicated times ribosomes were isolated and subjected to SDS-gel electrophoresis. The S6 band was identified by autoradiography, excised and counted. **B**, Silver-stained gel of the purified receptor preparation.

Methods. Receptors were purified from a fresh full-term human placenta by a modification of the method reported by Petruzzelli *et al.*<sup>26</sup> Briefly, the placenta was washed in phosphate-buffered saline, diced and homogenized in a Polytron homogenizer for 1 min. Following centrifugation at  $600\text{ g}$  for 5 min, the supernatant was centrifuged at  $50,000\text{ g}$  for 2 h and the membrane pellet resuspended in  $25\text{ mM}$  HEPES pH 7.5,  $0.25\text{ M}$  sucrose,  $1\text{ mM}$   $\text{MgCl}_2$ ,  $0.1\text{ mM}$  phenylmethylsulphonyl fluoride,  $100\text{ mg ml}^{-1}$  bacitracin and  $1\%$  Triton X-100. After 1 h at  $4^\circ\text{C}$ , the membranes were re-centrifuged at  $50,000\text{ g}$  for 2 h and the supernatant was diluted fivefold in  $25\text{ mM}$  HEPES,  $110\text{ mM}$   $\text{NaCl}$ ,  $3\text{ mM}$   $\text{KCl}$ ,  $0.9\text{ mM}$   $\text{MgSO}_4$ ,  $1.4\text{ mM}$   $\text{CaCl}_2$ ,  $2\text{ mM}$  EDTA,  $0.05\%$  Triton X-100 and applied to a 10-ml column of wheat-germ agglutinin-agarose (Vector Laboratories). After extensive washing of the column with the diluting buffer, the receptor was eluted at room temperature with buffer containing  $0.3\text{ M}$  *N*-acetylglucosamine. Fractions were collected in ice cold tubes and those containing receptors were identified on the basis of specific insulin binding and autophosphorylation of a  $95,000\text{-M}_r$  component in the presence of insulin. The pertinent fractions were pooled, dialysed against  $25\text{ mM}$  HEPES pH 7.4,  $5\text{ mM}$   $\text{NaH}_2\text{PO}_4$ ,  $30\text{ mM}$   $\text{NaCl}$ ,  $0.2\%$  Triton X-100,  $10\text{ mM}$  imidazole,  $50\%$  ethylene glycol, and stored at  $-30^\circ\text{C}$ . A typical preparation had an insulin binding activity of  $30\text{ pmol mg}^{-1}$  and a specific activity for phosphorylation of a tyrosine-containing polymer (Glu-Tyr, 1-4) of  $38\text{ pmol per min per mg}$ . For affinity purification, a preparation purified through wheat-germ agglutinin chromatography was adsorbed to and eluted from an insulin-Sepharose column by a modification of the method of Fujita-Yamaguchi *et al.*<sup>27</sup>. The purified receptor was concentrated by adsorption on a small column of DEAE-cellulose and eluted with a small volume of  $40\text{ mM}$  imidazole pH 7.2,  $10\%$  glycerol,  $250\text{ mM}$   $\text{NaCl}$ ,  $0.2\%$  (w/v) Triton X-100 (ref. 14). The receptor had a specific activity for insulin binding of  $3,850\text{ pmol mg}^{-1}$  and for phosphorylation of  $300\text{ nmol per min per mg}$  using as substrate a synthetic peptide corresponding to the autophosphorylation site of pp60<sup>v-src</sup> (ref. 14). The receptor was stored in small aliquots at  $-70^\circ\text{C}$ . Incubation of the preparation with  $[\gamma^{32}\text{P}]ATP$  plus  $\text{Mn}^{2+}$  and  $\text{Mg}^{2+}$  resulted in the phosphorylation of a  $95,000\text{-M}_r$  protein and this phosphorylated material could be immunoprecipitated with antiserum to the insulin receptor (antiserum B9 kindly provided by Dr C. Ron Kahn, Joslin Diabetes Center, Harvard Medical School). For microinjection experiments, the receptor was activated by addition of insulin to  $10^{-7}\text{ M}$  followed by incubation at room temperature for 15 min. Control incubations were with insulin alone in the kinase buffer containing  $1\text{ mg ml}^{-1}$  BSA. After the 15-min incubation, the preparations were kept on ice before being loaded into the microinjection needle. Experiments demonstrated that this procedure activated the tyrosine kinase activity of the receptor as judged by autophosphorylation. Procedures for isolating oocytes and ribosomes are described elsewhere<sup>9</sup>. Silver staining of polyacrylamide gels was carried out using a Bio-Rad silver-stain kit.

are expressed relative to controls injected with insulin in the receptor kinase buffer. Maximal increases in S6 phosphorylation were observed earlier than has been reported for oocytes treated with hormones<sup>9</sup>, and by 3 h after injection, S6 phosphorylation had returned to the basal level. Phosphoamino-acid analysis of S6 from receptor-injected oocytes revealed exclusively phosphoserine while incubation of 40S subunits with the receptor kinase and  $[\gamma^{32}\text{P}]ATP$  *in vitro* produced no S6 phosphorylation (data not shown).

\* Present address: Washington University, Department of Biological Chemistry, Howard Hughes Medical Institute, 660 South Euclid Avenue, St Louis, Missouri 63110, USA.

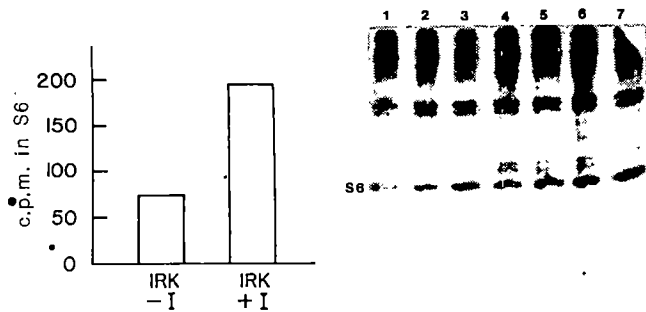


**Fig. 2** Insulin stimulation and dose dependence of S6 phosphorylation by injected receptor kinase A. **A**, Insulin stimulation of S6 phosphorylation by injected receptor kinase. Insulin receptors purified through chromatography on wheat-germ agglutinin agarose were microinjected with or without 100 nM insulin pretreatment into each of 50 oocytes. For insulin pretreatment, the receptor preparation was incubated for 15 min at 22 °C with 100 nM insulin, 1 mg ml<sup>-1</sup> BSA or the BSA vehicle only. S6 phosphorylation was determined as described in Fig. 1 legend except that oocytes were incubated for 4 h with 0.5 mCi ml<sup>-1</sup> <sup>32</sup>P before injection of the receptor instead of being microinjected with <sup>32</sup>P. The use of incubation labelling accounts for the lower level of radioactivity in S6 compared with Fig. 1. The background c.p.m. in S6 (40 c.p.m.) in oocytes injected with buffer containing 100 nM insulin have been subtracted from the values shown. IRK, insulin receptor kinase; I, insulin. **B**, Dose dependence for S6 phosphorylation by injected receptor kinase. Receptors purified through affinity chromatography on insulin-Sepharose were diluted in the kinase buffer (Fig. 1) containing 100 nM insulin plus 1 mg ml<sup>-1</sup> BSA. A 60-nl aliquot of each dilution was injected into each of 30 oocytes and the level of S6 phosphorylation determined by gel electrophoresis and autoradiography as described in Fig. 1 legend. The concentration of insulin receptor injected (μg ml<sup>-1</sup>) was: lane 1, 1; lane 2, 2; lane 3, 5; lane 4, 10; lane 5, 20; lane 6, 50; lane 7, 100.

The insulin receptor possesses appreciable basal protein-tyrosine kinase activity. As Fig. 2A shows, the receptor kinase was able to cause some increase in S6 phosphorylation in the absence of bound insulin, but its activity was doubled after pretreatment with insulin. This degree of stimulation is comparable to the degree of insulin stimulation of the phosphorylation of a synthetic peptide substrate *in vivo*<sup>14</sup>. The increase in S6 phosphorylation was dose dependent (Fig. 2B); receptor preparations diluted more than 100-fold were unable to cause S6 phosphorylation, while maximal change in S6 phosphorylation was induced with the most concentrated form of the receptor.

Although the response to microinjected receptor was very rapid and the receptor was not injected as an endocytotic vesicle, it was important to evaluate the possibility that injected insulin receptors might be rapidly reinserted in the plasma membrane after microinjection. Several types of experiment were carried out to assess this possibility. Previous studies in adipocytes and hepatocytes have demonstrated that insulin receptors photo-labelled with <sup>125</sup>I-NAPA-DP-insulin (2 nitro, 4-azidophenyl-acetyl des-Phe-B1-insulin) can be used to monitor recycling of insulin receptors in target cells<sup>6,15-18</sup>. Such recycling is measured by the loss or reappearance of trypsin-sensitive radioactivity on the intact cell surface as well as by the appearance of degraded forms of immunoprecipitable receptor which migrate on polyacrylamide gels with discrete relative molecular masses ( $M_r$ )<sup>16-18</sup>. Table 1 shows that more than 90% of the injected photo-labelled receptor was resistant to trypsin treatment of intact oocytes when S6 phosphorylation was maximal. Moreover, immunoprecipitation of receptors from injected oocytes revealed no degraded forms (data not shown). When, in other experiments, injected oocytes were homogenized and fractionated by differential centrifugation, less than 2% of the injected receptor was present in the plasma membrane fraction (Table 1). These results make it very unlikely that increased S6 phosphorylation is a result of the action of injected receptors that are reinserted in the plasma membrane.

*In vivo*, S6 exists in multiply-phosphorylated forms containing up to 5 mol phosphate per mol S6. Using a two-dimensional gel system designed for resolution of basic ribosomal proteins, S6 and five of its derivatives corresponding to increasing numbers

**Table 1** Effect of trypsin treatment on insulin receptors in injected oocytes

Source	-Trypsin	+Trypsin
Oocytes	485	450
Oocytes	352	339
Oocytes	407	341
Immunoprecipitate	340	338
Fraction		% Total c.p.m.
P1		6.37 ± 0.16
P2		1.88 ± 0.42
P3		6.40 ± 1.03
S3		85.0 ± 0.58

NAPA-DP-insulin was prepared as described previously<sup>16</sup>. Oocytes (25 per group) were microinjected with <sup>125</sup>I-NAPA-DP-labelled insulin receptors, incubated for 30 min at 24 °C, and some groups were then exposed to trypsin (200 μg ml<sup>-1</sup> final concentration) for 30 min at 4 °C followed by extensive washing and addition of 2 mg ml<sup>-1</sup> soybean trypsin inhibitor. In each of three experiments, injected oocytes were counted in a γ counter before and after trypsin treatment. From a total of 52 trypsin-treated and 52 trypsin-untreated oocytes from two experiments, solubilized material was extracted in a solution containing 2% Triton X-100, 10 mM benzamidine, 2 mM phenylmethylsulphonyl fluoride, 1,000 kIU ml<sup>-1</sup> aprotinin and 2 mg ml<sup>-1</sup> bacitracin, pH 7.4. The labelled insulin receptors were immunoprecipitated by incubation of the soluble extract with anti-insulin-receptor antibody for 16 h at 4 °C followed by a 1-h incubation with protein A. The numbers in the upper portion of the table refer to the c.p.m. with and without trypsin treatment in intact washed oocytes and in immunoprecipitates of receptors from oocytes. In the lower portion, using a photolabelled receptor preparation of higher specific activity, the percentage of injected receptor c.p.m. in different oocyte fractions is presented (± s.e.m., n = 4). P1 is material sedimenting at 1,000g for 15 min, P2 sedimenting at 10,000g for 20 min, P3 sedimenting at 165,000g for 20 min, and S3 material soluble after centrifugation at 165,000g. Fraction P2 has been demonstrated previously to contain nearly all the plasma membrane on the basis of membrane-associated enzyme activities<sup>25</sup>.

of phosphate groups were visualized<sup>10</sup>. Each derivative contains a unique phosphopeptide relative to the preceding derivative, which suggests that phosphorylation of S6 is ordered<sup>19</sup>. Consequently, the distribution of <sup>32</sup>P<sub>i</sub> among the derivatives of S6 gives an indication of its phosphorylation state independent of total <sup>32</sup>P<sub>i</sub> content. In control oocytes injected with insulin (1 μM) alone in buffer, after 90 min most of the phosphorylated S6 was in derivative a (1 mol P<sub>i</sub> per mol S6), with a small amount of b derivative detectable. This is the same pattern as seen in un.injected oocytes. In oocytes injected with insulin receptor kinase, derivative b was the predominant labelled species, with significant amounts of the more highly phosphorylated derivatives c and d visible (Fig. 2B). In order to visualize the derivatives, the autoradiograph in Fig. 2A was exposed for a considerably longer period than in B. Hence the increase in S6 phosphorylation in response to the injected insulin receptor is not apparent in Fig. 3. Following external application of insulin (Fig. 2C) or progesterone (Fig. 2D) until the time of germinal vesicle breakdown (5 h), all the S6 molecules became maximally phosphorylated, as reported previously<sup>9,20</sup>. These results indicate that phosphorylation of S6 in response to insulin receptor kinase reflects the increasing phosphorylation of individual S6 molecules as well as an increase in the number of ribosomes labelled in oocytes.

The experiments reported here support the concept that the insulin receptor can elicit a biological response while acting at an intracellular location, possibly including the inner surface of the plasma membrane. Although the receptors caused an increase in S6 phosphorylation in the absence of insulin pretreatment (Fig. 2), the fact that insulin stimulated peptide phosphorylation and S6 phosphorylation to the same extent (Fig. 2 and ref. 14) suggests that the protein kinase activity of the receptor

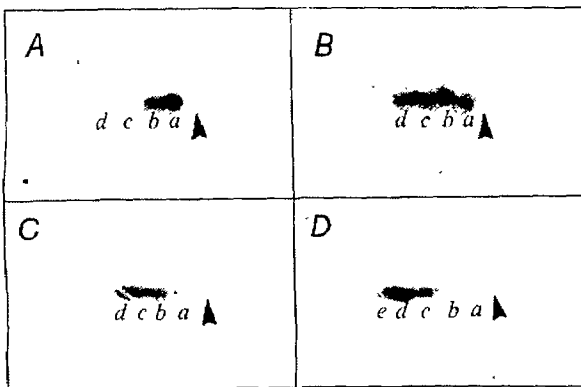


**Fig. 3** Two-dimensional gel electrophoretic analysis of S6.  $^{32}\text{P}$ -labelled oocytes were microinjected with buffer containing 1  $\mu\text{M}$  insulin (**A**) or with insulin receptors eluted from wheat-germ agglutinin-agarose and incubated with 100 nM insulin (**B**), or treated with external insulin (1  $\mu\text{M}$ , **C**) or external progesterone (10  $\mu\text{M}$ , **D**). The arrow marks the position of unphosphorylated S6 and the letters *a*–*e* refer to S6 derivatives containing increasing numbers of phosphate groups.

**Methods.** Ribosomal proteins for two-dimensional gel electrophoresis were extracted as described previously<sup>20</sup>.  $^{32}\text{P}$ -labelled samples for two-dimensional gel electrophoresis were mixed with unlabelled carrier *Xenopus* oocyte ribosomal protein (unphosphorylated S6) and *Xenopus* eggs (phosphorylated S6). Ribosomal species corresponding to the unphosphorylated form (indicated by an arrow) and derivatives corresponding to increasing numbers of phosphate groups (designated *a*–*e* for 1–5 mol phosphate)<sup>10,13,21</sup> were assigned on the basis of the Coomassie blue staining pattern of the co-electrophoresed ribosomal carrier protein.

is responsible for its ability to cause S6 phosphorylation. The fact that S6 is phosphorylated at serine residues while the insulin receptor is a protein-tyrosine kinase, coupled with the finding that *in vitro* the receptor alone was unable to phosphorylate 40S subunits, implies that the activity of a protein-serine kinase or phosphatase may be regulated directly or indirectly by tyrosine phosphorylation. However, we cannot exclude the possibility that some activity of the receptor other than tyrosine phosphorylation is involved in stimulating S6 phosphorylation.

We examined S6 phosphorylation in these studies because it is stimulated by external administration of insulin to oocytes and other cells<sup>9,10,21–23</sup>. The exact function of S6 phosphorylation in protein synthesis is not known, although recent evidence from cultured cells indicates that ribosomes containing maximally phosphorylated S6 are preferentially utilized for polyribosome formation during serum or hormonal stimulation of protein synthesis<sup>21</sup>. Hence, the insulin-induced phosphorylated S6 may be related to the stimulatory effect of this hormone on protein synthesis in the oocyte<sup>10</sup>. In addition to S6 phosphorylation, other insulin effects commonly observed in target cells have been examined in oocytes, including elevation of intracellular pH due to Na/H exchange at the plasma membrane and activation of glycogen synthase, but only intracellular pH was affected by external application of insulin<sup>9,10</sup>. Neither of these activities was affected by microinjection of the insulin receptor kinase (data not shown), which suggests that the mere presence of insulin-receptor kinase inside the cell is insufficient to obtain a complete insulin response. However, in its solubilized form the microinjected receptor kinase may not be accessible to all the cellular compartments necessary to induce the entire set of responses to insulin.

The present results clearly demonstrate that the insulin receptor kinase can elicit at least one insulin effect while acting at an intracellular location. Sequence analysis of the human insulin receptor gene has demonstrated a significant degree of homology with the *src* family of oncogenes<sup>5</sup>, and other studies show that pp60<sup>v-src</sup> and the epidermal growth factor receptor have overlapping substrate specificities *in vitro* with the insulin-receptor

kinase, while antisera to pp60<sup>v-src</sup> are able to immunoprecipitate the insulin-receptor kinase<sup>24</sup>. Since pp60<sup>v-src</sup> is able to cause S6 phosphorylation in oocytes, it is possible that the ability of the insulin receptor to cause S6 phosphorylation in oocytes reflects an overlapping substrate specificity with oncogene protein kinases. The ability of three different protein-tyrosine kinases to cause S6 phosphorylation after injection into oocytes clearly provides a system for investigating whether a common substrate is phosphorylated to increase S6 phosphorylation. Analysis of oocyte substrates for protein-tyrosine kinases and of oocyte S6 protein kinases should elucidate the importance of tyrosine phosphorylation in transduction of the insulin signal and the action of insulin-receptor kinase inside cells.

We thank Diana Smith for assistance with the two-dimensional gel analysis and Eleanor Erikson for a critical reading of the manuscript. This work was supported by grants from the NIH, the Howard Hughes Medical Institute and the Juvenile Diabetes Foundation. J.L.M. is an Established Investigator of the American Heart Association. L.J.P. is an Investigator and E.G.K. a Senior Investigator, Howard Hughes Medical Institute.

Received 9 September 1985; accepted 5 February 1986.

1. Sefton, B. M. & Hunter, T. *Adv. Cyclic Nucleotide Res.* **18**, 195–226 (1984).
2. Rosen, O. M., Herrera, R., Olowe, Y., Petruzzelli, L. M. & Cobb, M. H. *Proc. natn. Acad. Sci. U.S.A.* **80**, 3237–3240 (1983).
3. Yu, K.-T. & Czech, M. P. *J. biol. Chem.* **259**, 5277–5286 (1984).
4. Purchio, A. F., Wells, S. K. & Collett, M. S. *Molec. cell. Biol.* **3**, 1589–1597 (1983).
5. Ullrich, A. *et al.* *Nature* **313**, 756–761 (1985).
6. Heidenreich, K. A. & Olefsky, J. M. in *Molecular Basis of Insulin Action* (ed Czech, M. P.) 45–65 (Plenum, New York, 1985).
7. Simpson, I. A., Hedo, J. A. & Cushman, S. W. *Diabetes* **33**, 13–18 (1984).
8. Maller, J. L. & Koontz, J. W. *Devl. Biol.* **85**, 309–316 (1981).
9. Stith, P. J. & Maller, J. L. *Devl. Biol.* **102**, 72–89 (1984).
10. Stith, B. J. & Maller, J. L. *Devl. Biol.* **107**, 460–469 (1985).
11. Maller, J. L. & Smith, D. S. *Devl. Biol.* **109**, 150–156 (1985).
12. Spivack, J. G., Erikson, R. L. & Maller, J. L. *Molec. cell. Biol.* **4**, 1631–1634 (1984).
13. Maller, J. L., Foulkes, J. G., Erikson, E. & Baltimore, D. *Proc. natn. Acad. Sci. U.S.A.* **82**, 272–276 (1985).
14. Pike, L. J., Eakes, A. T. & Krebs, E. G. *J. biol. Chem.* **261** (in the press).
15. Brandenburg, D., Dracconescu, C., Saunders, D. & Thamm, P. *Nature* **286**, 821–822 (1980).
16. Heidenreich, K., Berthomé, P., Brandenburg, D. & Olefsky, J. M. *Diabetes* **32**, 1001–1009 (1983).
17. Fehlmann, M. *et al.* *Proc. natn. Acad. Sci. U.S.A.* **79**, 5921–5925 (1982).
18. Fehlmann, M. *et al.* *J. Cell Biol.* **93**, 82–87 (1982).
19. Martin-Perez, J. & Thomas, G. *Proc. natn. Acad. Sci. U.S.A.* **80**, 926–930 (1983).
20. Nielsen, P. J., Thomas, G. & Maller, J. L. *Proc. natn. Acad. Sci. U.S.A.* **79**, 2937–2941 (1982).
21. Thomas, G., Martin-Perez, J., Siegmund, M. & Otto, A. M. *Cell* **30**, 235–242 (1982).
22. Wettenhall, R. E. H., Cohen, P., Caudwell, B. & Holland, R. *FEBS Lett.* **148**, 207–213 (1982).
23. Smith, C. J., Wejksnora, P. J., Warner, J. R., Rubin, C. S. & Rosen, O. M. *Proc. natn. Acad. Sci. U.S.A.* **76**, 2725–2729 (1979).
24. Perrotti, N. *et al.* *Science* **227**, 761–763 (1985).
25. Finidori, J., Hanoune, J. & Baulieu, E. E. *Molec. cell. Endocrin.* **28**, 211–227 (1982).
26. Petruzzelli, L. M. *et al.* *Proc. natn. Acad. Sci. U.S.A.* **79**, 6792–6796 (1982).
27. Fujita-Yamaguchi, Y., Choi, S., Sakamoto, Y. & Itakura, K. *J. biol. Chem.* **258**, 5045–5049 (1983).

## Ca<sup>2+</sup> release from endoplasmic reticulum is mediated by a guanine nucleotide regulatory mechanism

Donald L. Gill, Teruko Ueda, Sheau-Huei Chueh & Mark W. Noel

Department of Biological Chemistry, University of Maryland School of Medicine, Baltimore, Maryland 21201, USA

Ca<sup>2+</sup> accumulation and release from intracellular organelles is important for Ca<sup>2+</sup>-signalling events within cells<sup>1,2</sup>. In a variety of cell types, the active Ca<sup>2+</sup>-pumping properties of endoplasmic reticulum (ER) have been directly studied using chemically permeabilized cells<sup>3–6</sup>. The same preparations have been extensively used to study Ca<sup>2+</sup> release from ER, in particular, release mediated by the intracellular messenger inositol 1,4,5-trisphosphate (InsP<sub>3</sub>)<sup>1,2,5,7–12</sup>. So far, these studies and others using microsomal membrane fractions<sup>2,11,13–15</sup> have revealed few mechanistic details of Ca<sup>2+</sup> release from ER, although a recent report<sup>16</sup> indicated that

**InsP<sub>3</sub>-mediated Ca<sup>2+</sup> release from liver microsomes may be dependent on GTP.** In contrast to the latter report, we describe here the direct activation of a specific and sensitive guanine nucleotide regulatory mechanism mediating a substantial release of Ca<sup>2+</sup> from the ER of cells of the neuronal cell line N1E-115. These data indicate the operation of a major new Ca<sup>2+</sup> gating mechanism in ER which is specifically activated by GTP, deactivated by GDP, and which appears to involve a GTP hydrolytic cycle.

Recent detailed studies<sup>6</sup> using N1E-115 neuroblastoma cells permeabilized by brief treatment with 0.005% saponin, have revealed that Ca<sup>2+</sup> is accumulated within ER via a high-affinity (ATP+Mg<sup>2+</sup>)-dependent Ca<sup>2+</sup> pump, which is distinct from that established in earlier studies as functioning in the neural plasma membrane<sup>17-19</sup>. Under approximately physiological intracellular conditions (cytosolic free Ca<sup>2+</sup> (0.1 μM), K<sup>+</sup>, Na<sup>+</sup>, Mg<sup>2+</sup> and pH), the addition of 10 μM GTP induces a large and rapid release of Ca<sup>2+</sup>. Figure 1 shows the remarkable effectiveness of GTP on Ca<sup>2+</sup> release from within N1E-115 cells. In these experiments, cells removed from culture dishes, permeabilized and equilibrated with intracellular medium, were loaded with <sup>45</sup>Ca<sup>2+</sup> to equilibrium for 4 min via operation of the ATP-dependent Ca<sup>2+</sup> pump, as described previously<sup>6</sup>. Addition of 10 μM GTP caused a rapid release of over 50% of the total Ca<sup>2+</sup> accumulated within cells, the effect being almost complete within 20 s (Fig. 1a). Other nucleoside triphosphates (ITP, ATP and CTP) added under identical conditions were ineffective. Moreover, similar experiments revealed that guanosine, GMP, 3',5'-cyclic GMP, 2',3'-cyclic GMP and UTP have no effect at concentrations up to 100 μM. As shown in Fig. 1a, GTP-induced Ca<sup>2+</sup> release was as rapid as that mediated by the Ca<sup>2+</sup> ionophore A23187. However, whereas the ionophore released 85–95% of the total accumulated Ca<sup>2+</sup> from permeabilized cells, the effect of GTP was always partial, consistently releasing 65–75% of ionophore-releasable Ca<sup>2+</sup>. GTP had no effect on either the initial rate or affinity of the (ATP+Mg<sup>2+</sup>)-dependent Ca<sup>2+</sup> pump within permeabilized N1E-115 cells.

Ca<sup>2+</sup> release from permeabilized cells is highly sensitive to GTP. Thus, half-maximal activation of release occurred at ~0.8 μM GTP, the effect being maximal at 10 μM (Fig. 1b). As the incubation mixtures all contained 1 mM ATP (required for Ca<sup>2+</sup> uptake), the effect of GTP is remarkably specific. Identical GTP-sensitivity was observed using either purified muscle GTP or synthetic GTP formed by phosphorylation of purified GMP.

The effects mediated by other guanine nucleotides indicate that the process of Ca<sup>2+</sup> release involves GTP hydrolysis. Thus, as shown in Fig. 2a, the non-hydrolysable analogue of GTP, guanosine 5'-(β,γ-imido)triphosphate (GppNH<sub>P</sub>), at 20 μM was unable to induce Ca<sup>2+</sup> release. Similarly, guanosine 5'-O-(3-thio)triphosphate (GTPγS) up to 100 μM had no effect (see below). In view of this apparent requirement for terminal phosphate hydrolysis, it was perhaps surprising that 20 μM GDP induced an almost maximal release of Ca<sup>2+</sup> (Fig. 2a). However, this occurred over an extended time period (several minutes) and only after a lag of ~30 s before significant Ca<sup>2+</sup> release was observed. This effect is explained by conversion of GDP to GTP catalysed by nucleoside diphosphokinase activity, with the high ATP concentration serving as a phosphoryl donor (see Fig. 2b). Thus, when 1 mM ADP (effective at blocking diphosphokinase activity with an inhibition constant K<sub>i</sub> of 26 μM; ref. 20) was added together with GDP, the action of the latter was completely abolished due to the lack of its enzymatic phosphorylation to GTP. On the other hand, ADP had no effect on GTP-mediated Ca<sup>2+</sup> release, nor did it alter equilibrium Ca<sup>2+</sup> accumulation in the absence of guanine nucleotides. Guanosine 5'-O-(2-thio)diphosphate (GDPβS), a GDP analogue which does not undergo phosphorylation, was also ineffective in inducing significant Ca<sup>2+</sup> release.

Most importantly, GDP is not only ineffective in directly inducing Ca<sup>2+</sup> release, but is in fact a highly effective and specific inhibitor of GTP-mediated Ca<sup>2+</sup> release. Thus, as shown in Fig.

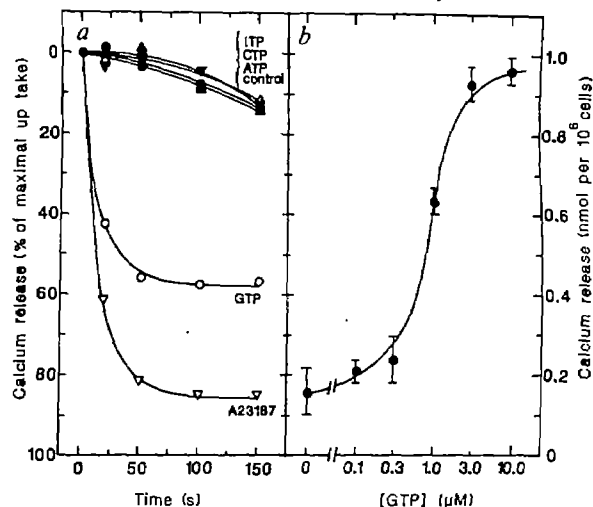


**Fig. 1** Nucleoside triphosphate specificity (a) and GTP-dependence (b) of Ca<sup>2+</sup> release from permeabilized N1E-115 cells. Conditions for the growth, permeabilization and uptake of Ca<sup>2+</sup> for both experiments were similar to those described previously<sup>6</sup>. Briefly, cells cultured in Dulbecco's modified Eagle's medium with 10% fetal calf serum for 12 days, were removed from culture dishes using D<sub>1</sub> medium (137 mM NaCl, 5.4 mM KCl, 58 mM sucrose, 5.5 mM glucose, 0.17 mM Na<sub>2</sub>HPO<sub>4</sub>, 0.22 mM KH<sub>2</sub>PO<sub>4</sub>, pH 6.8) and resuspended in intracellular-like medium (IM; 140 mM KCl, 10 mM NaCl, 2.5 mM MgCl<sub>2</sub>, 10 mM HEPES-KOH, pH 7.0) at 2 × 10<sup>6</sup> cells ml<sup>-1</sup>. After treatment with 0.005% saponin for 10 min at 37 °C, permeabilized cells (comprising 98% of total cells) were washed three times with saponin-free IM. a, Permeabilized cells resuspended at 0.37 × 10<sup>6</sup> cells ml<sup>-1</sup> were incubated at 37 °C in gently stirred vials containing 1.5 ml of 10 μM CaCl<sub>2</sub> (with 80 Ci per mol <sup>45</sup>Ca), 1 mM ATP, 3% PEG (relative molecular mass 6,000) and 48.7 μM EGTA (to give 0.1 μM free Ca<sup>2+</sup>). Mitochondrial inhibitors used previously<sup>6</sup> were omitted as uptake at 0.1 μM free Ca<sup>2+</sup> comprises a negligible mitochondrial component. ATP-dependent uptake of Ca<sup>2+</sup> within the cells proceeded for 4 min, at which time duplicate samples (200 μl each) were immediately removed either before or at the indicated times after addition of 10 μM GTP (○), 10 μM ITP (▲), 10 μM CTP (△), 10 μM ATP (▼), 5 μM A23187 (▽) or IM control (●), each in 1% of the remaining volume. Each 200-μl sample was immediately diluted into 2.5 ml of IM containing 1 mM LaCl<sub>3</sub> at 4 °C, and separated on glass-fibre filters (type 31, Schleicher & Schuell) which were rapidly washed twice with 2.5 ml of La<sup>3+</sup>-containing IM. Results are Ca<sup>2+</sup> release as a percentage of maximal uptake immediately before addition (in this assay, 1.135 ± 0.074 nmol Ca<sup>2+</sup> per 10<sup>6</sup> cells). b, The conditions for Ca<sup>2+</sup> uptake were the same as for a except that cells cultured for 11 days were present in the assay at 0.54 × 10<sup>6</sup> cells ml<sup>-1</sup>, ATP-dependent Ca<sup>2+</sup> accumulation proceeded for 5 min at 37 °C, and release of Ca<sup>2+</sup> after addition of the indicated concentration of GTP was for 4 min in each case. Each result is the mean ± s.d. of six measurements (triplicate determinations taken from two separate vials at each GTP concentration). The mean Ca<sup>2+</sup> accumulation for all vials at the end of the 5-min uptake period was 1.416 ± 0.101 nmol Ca<sup>2+</sup> per 10<sup>6</sup> cells.

2c, 100 μM GDP (a concentration which saturates diphosphokinase activity, and consequently is not significantly converted to GTP) or GDPβS completely blocked the action of GTP. However, at the same high competing concentrations, GppNH<sub>P</sub>, GMP and ITP were all ineffective in blocking the action of GTP, indicating the considerable structural specificity for molecules interacting with the GTP site. The blocking action of GDP further implies that GTP hydrolysis is involved in activation of Ca<sup>2+</sup> release, since, if GDP is formed and remains at least transiently associated with the active site, then a high concentration of added GDP may inhibit GDP release and hence prevent further GTP association. If GTP hydrolysis is required, why does GppNH<sub>P</sub> not block the action of GTP? The answer seems to be that this particular GTP analogue may simply not be recognized by the GTP site. In contrast, GTPγS completely

**Fig. 2** Effect of various guanine nucleotides on the release of  $\text{Ca}^{2+}$  from permeabilized NIE-115 cells. Experiment *a*: ●, buffer control; ○, 10  $\mu\text{M}$  GTP; ▲, 20  $\mu\text{M}$  GppNHp; △, 20  $\mu\text{M}$  GDP; ▽, 5  $\mu\text{M}$  A23187. Experiment *b*, ●, buffer control; ○, 10  $\mu\text{M}$  GTP; △, 10  $\mu\text{M}$  GDP; □, 1 mM ADP; ■, 10  $\mu\text{M}$  GTP with 1 mM ADP; ▲, 10  $\mu\text{M}$  GDP with 1 mM ADP; ▽, 10  $\mu\text{M}$  GDP $\beta$ S; ▽, 5  $\mu\text{M}$  A23187. Experiment *c*, ●, buffer control; ○, 3  $\mu\text{M}$  GTP; △, 3  $\mu\text{M}$  GTP with 100  $\mu\text{M}$  GppNHp; □, 3  $\mu\text{M}$  GTP with 100  $\mu\text{M}$  GDP; ▽, 3  $\mu\text{M}$  GTP with 100  $\mu\text{M}$  GMP; ■, 3  $\mu\text{M}$  GTP with 100  $\mu\text{M}$  ITP; △, 3  $\mu\text{M}$  GTP with 100  $\mu\text{M}$  GTP $\gamma$ S; ▽, 3  $\mu\text{M}$  GTP with 100  $\mu\text{M}$  GDP $\beta$ S; ▽, 5  $\mu\text{M}$  A23187. Total  $\text{Ca}^{2+}$  accumulation in the vials immediately before the additions in experiments *a*-*c* was  $2.162 \pm 0.122$ ,  $1.505 \pm 0.124$  and  $1.316 \pm 0.086$  nmol  $\text{Ca}^{2+}$  per  $10^6$  cells, respectively.

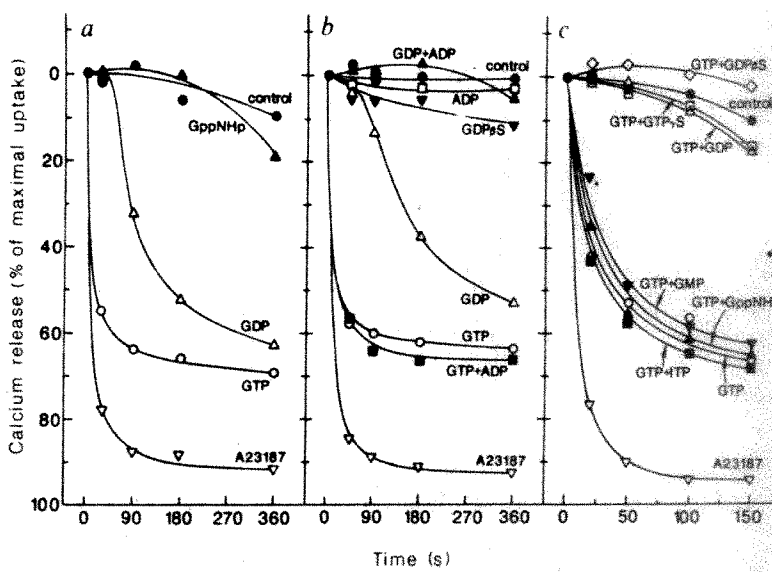
**Methods.** Cells were loaded with  $\text{Ca}^{2+}$  under the conditions described in Fig. 1 legend, except that the incubations contained 9–14-day cultured cells at  $0.24\text{--}0.52 \times 10^6$  cells  $\text{ml}^{-1}$ . Additions were made at the end of 4-min uptake periods, incubations being continued for the times indicated, followed by rapid addition of  $\text{La}^{3+}$ -medium and filtration, as described in Fig. 1 legend.

blocks the action of GTP (Fig. 2c), indicating that this triphosphate can indeed bind to the GTP site, its ineffectiveness substantiating the requirement for terminal phosphate hydrolysis in the activation process.

Support for the contention that GDP interacts with the same site as GTP derives from competition studies (see Fig. 3a). Thus, the effects of two concentrations of GDP (10 and 100  $\mu\text{M}$ ) on the GTP-dependence of  $\text{Ca}^{2+}$  release were examined in the presence of ADP (to inhibit conversion of GDP to GTP). The results show that GDP induces only a decrease in sensitivity to GTP with no change in its maximal effectiveness. Thus, Lineweaver-Burk analysis (Fig. 3a, inset) revealed a change only in the apparent  $K_m$  for GTP ( $\sim 0.75 \mu\text{M}$  in the absence of GDP), indicating a simple competitive inhibition by GDP, with a  $K_i$  of  $3.1 \mu\text{M}$ . The ability of both GTP and GDP to associate with the same site constitutes further evidence that a hydrolytic reaction occurs.

The specific inhibition by GDP provides an important means of determining the relationship between GTP-dependent  $\text{Ca}^{2+}$  release and that mediated by  $\text{InsP}_3$ . Thus, the permeabilized NIE-115 cells demonstrate a rapid  $\text{Ca}^{2+}$  release response to  $\text{InsP}_3$ . As shown in Fig. 3b, the release induced by 10  $\mu\text{M}$   $\text{InsP}_3$  remained unaltered even in the presence of 0.5 mM GDP (Fig. 3b), indicating an important distinction between the two release mechanisms. An even more significant difference is reflected by the temperature-dependence of GTP-induced  $\text{Ca}^{2+}$  release (data not shown) whereby the rate of GTP-mediated  $\text{Ca}^{2+}$  release, normally conducted at  $37^\circ\text{C}$ , was reduced fourfold at  $19^\circ\text{C}$ , and to virtually zero at  $2^\circ\text{C}$ ; this contrasts with the recently described temperature-insensitivity of  $\text{InsP}_3$ -induced  $\text{Ca}^{2+}$  release<sup>21</sup>, and suggests strongly that an enzyme mediates the effects of guanine nucleotides on  $\text{Ca}^{2+}$  release.

From Figs 1–3 it is clear that GTP never mediates 100% release of ionophore-releasable  $\text{Ca}^{2+}$ . There are several possible explanations for this effect, including: (1) reduction in the availability of GTP; (2) a change in the releasability of internal  $\text{Ca}^{2+}$  after GTP addition; (3) refractoriness of the release mechanism; and (4) the existence of discrete subcompartments of ER. The study described in Fig. 4 resolves certain of these possibilities. Thus, the re-addition of GTP after maximal GTP-mediated  $\text{Ca}^{2+}$  release resulted in no further release of  $\text{Ca}^{2+}$  from the cells, whereas application of ionophore at this time released all remaining releasable  $\text{Ca}^{2+}$ . These results indicate first, that lack of GTP is not limiting, and second, that the internal  $\text{Ca}^{2+}$  remains fully releasable. That the release mechanism does in fact remain activated is implied by re-addition of



ATP (to compensate for any ATP loss during the experiment) after GTP-mediated release, whereupon no re-uptake of  $\text{Ca}^{2+}$  was observed. This view is extended by the important observation that addition of GDP after GTP-mediated release reversed the release process and resulted in at least partial re-accumulation of  $\text{Ca}^{2+}$  (Fig. 4, inset). This result indicates that with GDP competing for the regulatory site and preventing either GTP

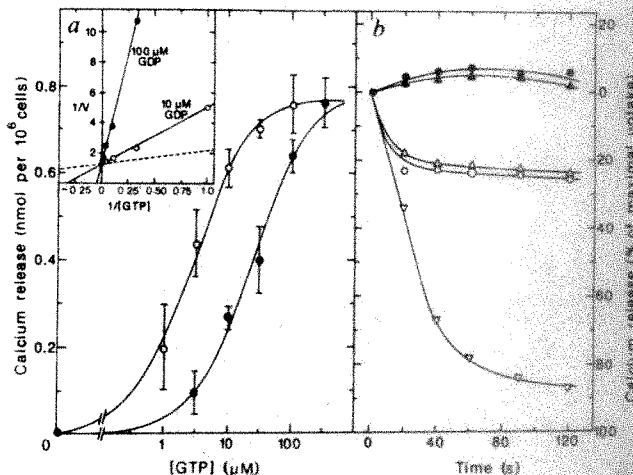


**Fig. 3** Effect of GDP on the concentration-dependence of GTP-mediated  $\text{Ca}^{2+}$  release (*a*) and on  $\text{InsP}_3$ -mediated  $\text{Ca}^{2+}$  release (*b*) from permeabilized NIE-115 cells. Experimental conditions were as described in Fig. 1 legend. *a*, Cells cultured for 8 days were present at  $0.21 \times 10^6$  cells  $\text{ml}^{-1}$ , and  $\text{Ca}^{2+}$  uptake proceeded for 5 min, followed by a 2-min period of  $\text{Ca}^{2+}$  release in the presence of 1 mM ADP and the indicated concentration of GTP, together with either 10  $\mu\text{M}$  (○) or 100  $\mu\text{M}$  (●) GDP. GTP-dependent  $\text{Ca}^{2+}$  release was the difference between  $\text{Ca}^{2+}$  release in the presence and absence of GTP, each result being the mean  $\pm$  s.d. of triplicate determinations. Total  $\text{Ca}^{2+}$  accumulation in each of the vials immediately before guanine nucleotide addition was  $1.544 \pm 0.135$  nmol  $\text{Ca}^{2+}$  per  $10^6$  cells. Inset, Lineweaver-Burk analysis of the data, together with data on GTP-dependence obtained in the absence of GDP (dotted line), for comparison. *b*, 12-day cells were present at  $0.23 \times 10^6$  cells  $\text{ml}^{-1}$ , and  $\text{Ca}^{2+}$  uptake proceeded for 5 min, followed by  $\text{Ca}^{2+}$  release for the indicated times in the presence of: ●, buffer control; ○, 10  $\mu\text{M}$   $\text{InsP}_3$ ; ▲, 0.5 mM GDP; △, 10  $\mu\text{M}$   $\text{InsP}_3$  with 0.5 mM GDP; ▽, 5  $\mu\text{M}$  A23187. Total  $\text{Ca}^{2+}$  accumulation in each vial before additions was  $1.658 \pm 0.060$  nmol  $\text{Ca}^{2+}$  per  $10^6$  cells.

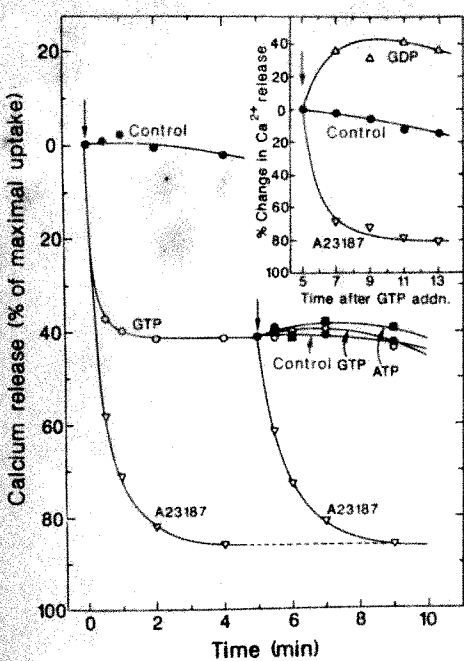


**Fig. 4** Effects of GTP, GDP, ATP and A23187 on  $\text{Ca}^{2+}$  release from permeabilized cells after maximal GTP-mediated  $\text{Ca}^{2+}$  release. Cells cultured for 10 days were present at  $0.66 \times 10^6$  cells  $\text{ml}^{-1}$ , with initial  $\text{Ca}^{2+}$  accumulation proceeding for 5 min. At this time ( $t=0$ )  $\text{Ca}^{2+}$  release was measured after addition of either control buffer (●), 10  $\mu\text{M}$  GTP (○), or 5  $\mu\text{M}$  A23187 (▽), for the times indicated. Additional vials which had been subjected to release with 10  $\mu\text{M}$  GTP for exactly 5 min, received further additions at this time of either control buffer (●), 10  $\mu\text{M}$  GTP (○), 1 mM ATP (■) or 5  $\mu\text{M}$  A23187 (▽), release proceeding for the times indicated. Total  $\text{Ca}^{2+}$  accumulation in each of the vials before the first additions was  $1.170 \pm 0.182$  nmol  $\text{Ca}^{2+}$  per  $10^6$  cells. The inset shows an identical experiment in which maximal release of accumulated  $\text{Ca}^{2+}$  was effected with 10  $\mu\text{M}$  GTP for 5 min, followed by addition of either control buffer (●), 500  $\mu\text{M}$  GDP (△) or 5  $\mu\text{M}$  A23187 (▽). In this experiment cells were present at  $0.93 \times 10^6$  cells  $\text{ml}^{-1}$ , and  $\text{Ca}^{2+}$  uptake before GTP addition was  $0.822 \pm 0.048$  nmol  $\text{Ca}^{2+}$  per  $10^6$  cells.

dissociation and/or GTP reassociation, the release mechanism is returned to an inactive state, allowing  $\text{Ca}^{2+}$  to be retained within the ER.

Thus, the fact that GTP consistently induces only partial release of  $\text{Ca}^{2+}$  with respect to total releasable  $\text{Ca}^{2+}$  probably reflects heterogeneity of the  $\text{Ca}^{2+}$ -sequestering organelles, an effect similar to that observed for  $\text{InsP}_3$ -mediated  $\text{Ca}^{2+}$  release in both permeabilized N1E-115 cells and other cells<sup>1,2,5,8-10</sup>. The profound effectiveness of GTP alone in inducing  $\text{Ca}^{2+}$  release from permeabilized cells contrasts with the apparent lack of effect of the nucleotide on liver microsomes as reported by Dawson<sup>16</sup>, except in the presence of  $\text{InsP}_3$ . This difference is apparently not accounted for by the types of preparation used, as GTP alone also induces substantial  $\text{Ca}^{2+}$  release from N1E-115 cell-derived microsomes, as we recently described<sup>22</sup>. Although differences in the levels of endogenous  $\text{InsP}_3$  could account for such a divergence, the effectiveness of  $\text{InsP}_3$  (half-maximal at 0.5  $\mu\text{M}$ ) in inducing  $\text{Ca}^{2+}$  release from permeabilized N1E-115 cells in the absence of GTP militates against this conclusion. Dawson<sup>16</sup> also showed that in order for GTP to have an effect on  $\text{InsP}_3$ -mediated  $\text{Ca}^{2+}$  release from liver microsomes polyethylene glycol (PEG) must be present. With permeabilized N1E-115 cells, GTP directly activates  $\text{Ca}^{2+}$  release without PEG, however 3% PEG was included in our experiments as its addition enhanced the extent of GTP-mediated  $\text{Ca}^{2+}$  release. Interestingly, GTP-mediated  $\text{Ca}^{2+}$  release from N1E-115 cell microsomes is completely dependent on PEG<sup>22</sup>, suggesting that the release mechanism may involve the interac-

tion of different membrane and/or protein components of ER, which may become dissociated or damaged during homogenization of the cells. Since microtubule assembly is both promoted by PEG<sup>23</sup> and dependent on GTP hydrolysis<sup>24</sup>, one hypothesis was that polymerization or attachment of microtubules might be involved in the  $\text{Ca}^{2+}$ -release mechanism. However, when the microtubule assembly inhibitor colchicine was added to the cell growth medium and/or included in the release assay, it neither blocked nor prevented the GTP-mediated  $\text{Ca}^{2+}$  release.

These results provide direct evidence for a specific guanine nucleotide-regulated  $\text{Ca}^{2+}$  release mechanism in ER which requires GTP, is competitively inhibited by GDP, and probably entails GTP hydrolysis. GTP-induced  $\text{Ca}^{2+}$  release is sufficiently large and rapid to indicate the operation of a channel across the ER membrane. However, the activation of such a channel appears to be controlled by a temperature-sensitive enzymatic reaction involving GTP hydrolysis. Although at present it is unclear whether a simple GTPase activity regulates activation or whether phosphorylation of a regulatory protein occurs via a GTP-dependent kinase reaction, the effect of GDP on reversing the system suggests the former mechanism. Such a mechanism resembles guanine nucleotide regulation of adenylate cyclase activation<sup>25</sup>, with GDP stabilizing a non-activated state, GTP effecting activation (with submicromolar sensitivity), and interconversion between the two states being mediated by a GTPase activity; however, only in the present case is nucleotide hydrolysis required for activation. This mechanism also indicates that the ratio of GTP to GDP may be a determining factor in the opening or closing of  $\text{Ca}^{2+}$  channels within ER, the operation of such channels thus being directly related to the energy charge of the cell. Other regulatory or modifying factors (perhaps controlling the GTPase activity) are likely to be involved in the physiological control of the GTP-mediated release mechanism, particularly as implied by the effectiveness of PEG. Although the GTP-mediated release mechanism has been studied under conditions in which it is functionally distinct from  $\text{InsP}_3$ -mediated release, at least with respect to both GDP-induced inhibition and temperature sensitivity, further experiments are needed to assess the intriguing possibility that the two mechanisms are interrelated.

This work was supported by NIH grant NS19304 by NSF grant DCB-8510225, and by the American Heart Association, Maryland Affiliate. We thank Dr Robin Irvine for supply of  $\text{InsP}_3$ , and Drs Martin Rodbell and Dermot Cooper for helpful discussions and advice.

Received 16 December 1985; accepted 5 February 1986.

- Berridge, M. J. & Irvine, R. F. *Nature* **312**, 315-321 (1984).
- Gill, D. L. *Adv. Cyclic Nucleotide Protein Phosphorylation Res.* **19**, 195-212 (1985).
- Wakasugi, H. et al. *J. Membrane Biol.* **65**, 205-220 (1982).
- Burgess, G. M., McKinney, J. S., Fabiato, A., Leslie, B. A. & Putney, J. W. *J. biol. Chem.* **258**, 15336-15345 (1983).
- Gershengorn, M. C., Geras, E., Purrello, V. S. & Rebecchi, M. J. *J. biol. Chem.* **259**, 10675-10681 (1984).
- Gill, D. L. & Chueh, S. H. *J. biol. Chem.* **260**, 9289-9297 (1985).
- Streb, H., Irvine, R. F., Berridge, M. J. & Schulz, I. *Nature* **306**, 67-69 (1983).
- Burgess, G. M. et al. *Nature* **309**, 63-66 (1984).
- Joseph, S. K., Thomas, A. P., Williams, R. J., Irvine, R. F. & Williamson, J. R. *J. biol. Chem.* **259**, 3077-3081 (1984).
- Hirata, M., Suematsu, E., Hashimoto, T., Hamachi, T. & Koga, T. *Biochem. J.* **223**, 229-236 (1984).
- Joseph, S. K., Williams, R. J., Corkey, B. E., Matschinsky, F. M. & Williamson, J. R. *J. biol. Chem.* **259**, 12952-12955 (1984).
- Prentki, M., Wohlleben, C. B. & Lew, P. D. *J. biol. Chem.* **259**, 13777-13782 (1984).
- Prentki, M. et al. *Nature* **309**, 562-564 (1984).
- Streb, H., Bayerdörfer, E., Haase, W., Irvine, R. F. & Schulz, I. *J. Membrane Biol.* **81**, 241-253 (1984).
- O'Rourke, F. A., Halenda, S. P., Zavoico, G. B. & Feinstein, M. B. *J. biol. Chem.* **260**, 956-962 (1985).
- Dawson, A. P. *FEBS Lett.* **185**, 147-150 (1985).
- Gill, D. L., Grollman, E. F. & Kohn, L. D. *J. biol. Chem.* **256**, 184-192 (1981).
- Gill, D. L. *J. biol. Chem.* **257**, 10986-10990 (1982).
- Gill, D. L., Chueh, S. H. & Whitlow, C. L. *J. biol. Chem.* **259**, 10807-10813 (1984).
- Kimura, N. & Shimada, N. *J. biol. Chem.* **258**, 2278-2283 (1983).
- Smith, J. B., Smith, L. & Higgins, B. L. *J. biol. Chem.* **260**, 14413-14416 (1985).
- Ueda, T., Chueh, S. H., Noel, M. W. & Gill, D. L. *J. biol. Chem.* **261**, 3184-3192 (1986).
- Lee, J. C. & Lee, L. L. Y. *Biochemistry* **18**, 5518-5526 (1979).
- Timasheff, S. N. & Grisham, L. M. *A. Rev. Biochem.* **49**, 565-591 (1980).
- Rodbell, M. *Nature* **284**, 17-22 (1980).

## MATTERS ARISING

### New evidence for the dendrochronological dating of Netherlandish paintings

THE recent paper by Baillie *et al.*<sup>1</sup> resolves a number of long-standing problems in art-historical dendrochronology. One of the first uses of dendrochronology in the history of art dealt with paintings of the Dutch painter Philips Wouwerman who spent all his life in Amsterdam<sup>2,3</sup>. The panels were successfully dated using the South German oak tree-ring chronology<sup>4</sup>, one of only three European long-term oak chronologies in existence at the time. Since the sixteenth/seventeenth century section of the reference series contained timber derived mainly from Hesse in central Germany, the panels were assumed to be from trees cut in the Hessian hills and transported to the Netherlands. Many of these panels had some sapwood remaining, so the felling dates of the oak trees were estimated using an allowance for sapwood of  $20 \pm 5$  years. This figure is of the same order of magnitude as one derived from some 500 oaks from along both sides of the river Rhine<sup>5</sup>.

The problem with art-historical dendrochronology arose when analysis of oak panels used by Rembrandt<sup>6</sup>, Rubens<sup>7</sup> and other painters between the fourteenth and the middle of the seventeenth centuries revealed a new tree-ring pattern which did not cross-match with any of the existing oak chronologies. Since most of the tree-ring series of these panels matched each other extremely well, a floating chronology covering 530 years was established, and this new tree-ring pattern was initially thought to be characteristic for the Netherlands. This assumption was supported by the fact that the panels of English paintings showed an identical pattern<sup>8</sup>, and a growing region along both sides of the Channel was envisaged. It seemed unlikely that the timbers had been imported into the Netherlands since this would mean that trade connections from the fourteenth to the seventeenth century always brought timbers from the same source. But it was striking that no painting from later than around 1650 could be found with the new tree-ring pattern.

In an attempt to tie down this alternative chronology, a complete Netherlands tree-ring chronology was constructed back to AD 1036<sup>9</sup>. However, the alternative tree-ring pattern still failed to crossdate with the Netherlands chronology. It became apparent that two tree-ring chronologies existed for the Netherlands: Type I, relevant to building timbers; and Type II relevant to panel paintings. The position in time of the Type II chronology was assigned on the basis of some ring patterns which appeared to show similarities with both types<sup>10</sup>.

In the meantime a number of new long-oak chronologies have come into

existence, so that from South Sweden through Central to Western Europe a dense grid of reference material is now available<sup>11</sup>. In the light of this new material and with a better understanding of the degree of similarity which can be expected between chronologies from distant localities, the idea that the Type II tree-ring pattern derived from the Netherlands became increasingly untenable.

Within the natural distribution of oak in Europe (Fig. 1) the eastern Baltic coast represents the most likely export source for oak timbers to the Netherlands.

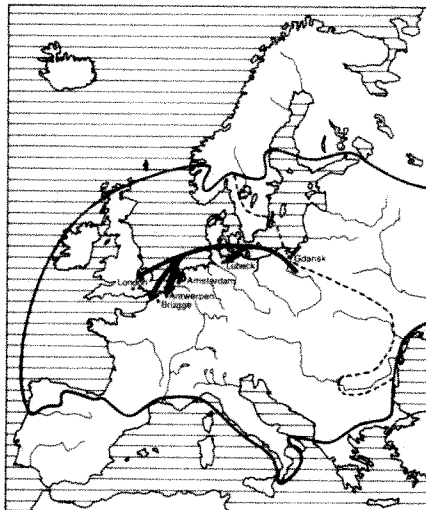


Fig. 1 The areas of the natural distribution of oak. Distribution of *Quercus robur* L. (European oak) is shown as a heavy line, and *Quercus petraea* Liebl. (sessile oak) as an interrupted line. European oak goes further north-east than sessile oak. The source of oak timbers of type II tree-ring pattern and the places of their utilization as panels are indicated (arrows).

According to historical and archival evidence<sup>12-14</sup> the Vistula river (Weichsel) and its tributaries made the large Polish forests accessible. But despite this endemic and the independent investigation of the English Type A art-historical chronologies (which matched with Netherlands Type II) by Baillie *et al.*, which suggested that the timber had derived from Eastern Europe, possibly Poland or Lithuania, a definitive dendrochronological proof was still missing.

In an attempt to finally resolve this question, we have undertaken a study of building timbers from churches and other historical buildings, from art-historical objects and archaeological excavations in North Poland around Gdańsk. A chronology has now been constructed from 1985 back to AD 1000 using some 300 tree-ring series. This chronology matches the Type II chronology with a high 't' value of 6.5 and a percentage of parallel variation of 60%. The Type II chronology now covers the time span from 1115 to 1643 and thus has to be shifted by six years towards the present from our original tentative placement.

With the origin of the Type II timbers resolved it is interesting to trace their occurrence. They are present in Antwerp, Amsterdam<sup>6</sup>, Brussels<sup>15</sup>, Cologne<sup>16</sup> and Lübeck (Eckstein, unpublished data), confirming the trade connections indicated in Fig. 1. Timbers with the Type II ring pattern have only once been found as building timbers in Amsterdam, which supports the view that most of the Baltic oak was exported in the form of planks and boards. An explanation of why Type II timbers are never found after 1650 can be seen in the consequences of the Thirty

Table 1 Ten dendrochronologically dated panels of Rembrandt paintings

Paintings	Time signature	Number of measurable: tree rings altogether	sapwood rings	Dendrochronological felling range of the oak trees	
				before correction with a sapwood allowance of $20 \pm 5$ yr	after correction with a sapwood allowance of 13...15...19 yr
Br. 486 Anna accused by Tobit of stealing the kid	1626	254	5	1622±5	1621...1627
Br. 489 Samson betrayed by Delilah	1628	277	6	1623±5	1622...1628
Br. 2 Self-portrait	1629	132	5	1630±5	1629...1635
Br. 165 Aelbert Cuyp	1632	168	9	1630±5	1629...1635
BR. 152 Old man with a gold chain	1632	132	4	1614±5	1613...1620
Br. 157 A Self-portrait	1632	133	7	1632±5	1631...1637
Br. 159 Portrait of a man	1632	185	4	1633±5	1632...1638
Br. 336 Cornelis Pronck, wife of Aelbert Cuyp	1633	184	3	1632±5	1631...1637
Br. 206 A man in oriental costume	1635	309	11	1626±5	1625...1632
Br. 211 A man in Polish costume	1637	188	7	1634±5	1633...1639

Each dated panel has a time signature; the former and the new range for the felling year of the oak trees are compared taking into account the respective sapwood allowances.

Years War which cut the trade routes across the Baltic Sea. Finally the Second Swedish/Polish War from 1655 to 1660 caused the total breakdown of the Weichsel trade<sup>13</sup>.

With the detection of the provenance for the oak panels new evidence for the sapwood allowance arises. A preliminary analysis of the number of sapwood rings from 180 oaks, from North Poland, results in a median value of 15 with 50% of all values lying between 13 and 19, the lower and upper extremes are 9 and 36, so far. The indication of a west-east gradient of decreasing sapwood rings<sup>1</sup> is thus supported. On the basis of the new placement-in-time and the new sapwood allowance the dating of ten Rembrandt paintings are summarized in Table 1. All ten panels have some sapwood remained and the paintings contain an authentic time signature. Since through the correction a net-shift of only one year resulted, there are no serious art-historical consequences for the respective paintings. All these considerations also apply to the English art-historical objects of the same tree-ring pattern<sup>1</sup>, but not to other art-historical exercises. Thus dates established for oak panels, sculptures<sup>17</sup> and furniture<sup>18</sup> with ring patterns of genuine Dutch<sup>3</sup>, French<sup>9</sup> or West German<sup>16</sup> type are unaffected as are dates for beech panels bearing paintings by artists such as Lucas Cranach<sup>20</sup>, and stringed instruments of spruce<sup>21</sup>.

We thank the Polish Academy of Science (PAN) in Warszawa and the German Academic Exchange Service (DAAD) in Bonn for their generous financial support. This work contains parts of a doctoral dissertation of T.W.

D. ECKSTEIN\*  
T. WAŻNY†  
J. BAUCH\*  
P. KLEIN\*

\* Institute for Wood Biology,  
University of Hamburg, Leuschnerstr. 91  
D-2050 Hamburg 80, FRG  
† Academy of Fine Arts,  
Conservation Faculty,  
Wybrzeże Kościuszki 37,  
00-379 Warszawa, Poland

- Baillie, M. G. L., Hillam, J., Briffa, K. R. & Brown, D. M. *Nature* **315**, 317-319 (1985).
- Bauch, J. *Kunstchronik* **21**, 144-145 (1968).
- Bauch, J. & Eckstein, D. *Stud. Conserv.* **15**, 45-50 (1970).
- Huber, B. & Giertz, V. *Conf. Rep. Austrian Acad. Sci.* **178**, 32-42 (1969).
- Hollstein, E. *Mitteleuropäische Eichenchronologie* (Zabern, Mainz, 1980).
- Bauch, J., Eckstein, D. & Meier-Siem, M. *Ned. Kunsthistorisch Jb.* **23**, 485-496 (1972).
- Bauch, J., Eckstein, D. & Brauner, G. *Jb. Berliner Museen* **20**, 209-221 (1978).
- Fletcher, J. M. *Burlington Mag.* **116**, 250-258 (1974).
- Eckstein, D., Brongers, J. A. & Bauch, J. *Tree-Ring Bull.* **35**, 1-13 (1975).
- Bauch, J. *Br. archaeol. Rep. (Int. Ser.)* **51**, 133-137, 307-314 (1978).
- Eckstein, D. & Wrobel, S. *Dendrochronologia* **1**, 9-20 (1985).
- Raths, R. E. *Der Weichselhandel im 16. Jh.* (Marburg, 1927).
- Krannhals, D. *Danzig und der Weichselhandel in seiner Blütezeit im 16. und 17. Jh.* (Leipzig, 1942).

- Bitvinkas, T. T., Brukshtas, V. & Zukus, V. V. *Ist. Botan. AN Litov. SSR*, 69-73 (1984).
- Klein, P. *5th Int. Seminar Appl. of Science in Examination of Works of Art*, Boston (1983).
- Eckstein, D. & Bauch, J. *Mitt. Deutschen Dendrol. Ges.* **67**, 247-256 (1974).
- Becker, B. *Jahrbuch der staatlichen Kunstsammlungen in Baden-Württemberg* **16**, 28-32 (1974).
- Bauch, J. & Eckstein, D. *Niedersächsische Denkmalpflege* **9**, 116-124 (1978).
- Klein, P. *ICOM 7th Triennial Meeting*, Copenhagen (1984).
- Klein, P. & Bauch, J. *Holzforschung* **37**, 1, 35-39 (1983).
- Klein, P., Mehringer, E. & Bauch, J. *ICOM, 7th Triennial Meeting*, Copenhagen (1984).

from excavations at Lödse on the Gotha River and for 69 trees found means of 16 yr (range 13-21 yr) for trees 100-200 yr old, and 20 yr (range 14-23 yr) for older trees. In contrast to the research on sessile oak referred to by Baillie, and on modern oak in Ireland and north-west England, our experience for pedunculate oak in southern England in Bagley Wood<sup>12</sup> and for mediaeval<sup>8</sup> and Roman<sup>13</sup> times indicates that trees of fast growth—that is, with wide rings—have relatively few sapwood rings.

The interesting suggestions raised by Baillie *et al.* have added to our knowledge, and the long-standing problem of dating Type A chronologies of slow growth has been resolved. The suggestions do not significantly affect our results for Tudor and other paintings on panel, for which our aim has been to derive the probable date to within 15-20 yr.

J. M. FLETCHER

*20 Tullis Close,  
Sutton Courtenay,  
Abingdon, Oxfordshire OX14 4BD, UK*

- Baillie, M. G. L., Hillam, J., Briffa, K. R. & Brown, D. M. *Nature* **315**, 317-319 (1985).
- Fletcher, J. M. & Tapper, M. C. *Medieval Archaeol.* **28**, 112-132 (1984).
- Klein, P. in *Dendrochronology and Archaeology in Europe*, Hamburg, 209-222 (1983).
- Dollinger, P. *The German Hanse* (Macmillan, London, 1970).
- Bitvinkas, T. (ed.) *Climatic Change in Time and Space and Annual Tree Rings* 69-74 (Kaunas, Lithuanian SSR, USSR, 1984).
- Rubner, K. & Reinhold, F. *Das Naturliche Waldbild Europa* (Publisher Paul Parey, Hamburg, 1953).
- Huber, B., Holdheide, W. & Raack, K. *Holz als Roh- und Werkstoff* **4**, 373-380 (1941) 194-221.
- Longman, K. A. & Coutts, M. P. *The British Oak* (Botanical Society of the British Isles, Classey, Faringdon, 1974).
- Cousens, J. E. *Watson* **6**, 161-176 (1965).
- Fletcher, J. M. *Nature* **254**, 506-507 (1975).
- Bräthen, A. *RAA Vol. 1*, 8-124 (National Antiquities & National Historical Museums, Stockholm, 1982); PACT **7**, Pt. I, 27-35 (Second Nordic Conference on Scientific Methods in Archaeology, Copenhagen, 1982).
- Fletcher, J. M. in *The British Oak*, 80-97 (Botanical Society of the British Isles, Classey, Faringdon, 1974).
- Fletcher, J. M. *Trans. Lond. Middx. archaeol.* **33**, 79-84 (1982).

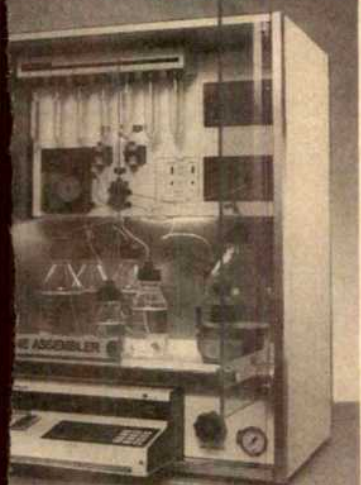
## Matters Arising

Matters Arising is meant as a vehicle for comment and discussion about papers that appear in *Nature*. The originator of a Matters Arising contribution should initially send his manuscript to the author of the original paper and both parties should, wherever possible, agree on what is to be submitted. Neither contributor nor reply (if one is necessary) should be longer than 500 words and the briefest of replies, to the effect that a point is taken, should be considered.

# Familiar sights in fresh relief

New DNA probes hit the mark, pH sensors go micro, and an advanced focused-ion-beam column reveals a startling landscape in even the most ordinary of objects.

Pharmacia has put together a **DNA synthesizer** attuned to tight budgets. The Gene Assembler system includes microprocessor control, a printer, two reaction columns and an absorbance monitor at an introductory price of \$16,499 (US) (Reader Service No. 100). The  $\beta$ -cyanoethyl phosphoramidite reaction effects synthesis with greater than 98 per cent accuracy, producing oligonucleotides longer than 140 bases. Pharmacia managed to keep the system's expense down by incorporating their own chromatographic components and keeping wiring and plumbing in-house. They have also cut corners on the addition cycle time, which is slightly over 10 minutes, and their software does not allow for direct sequence coding of G, T and C. The two-column as-



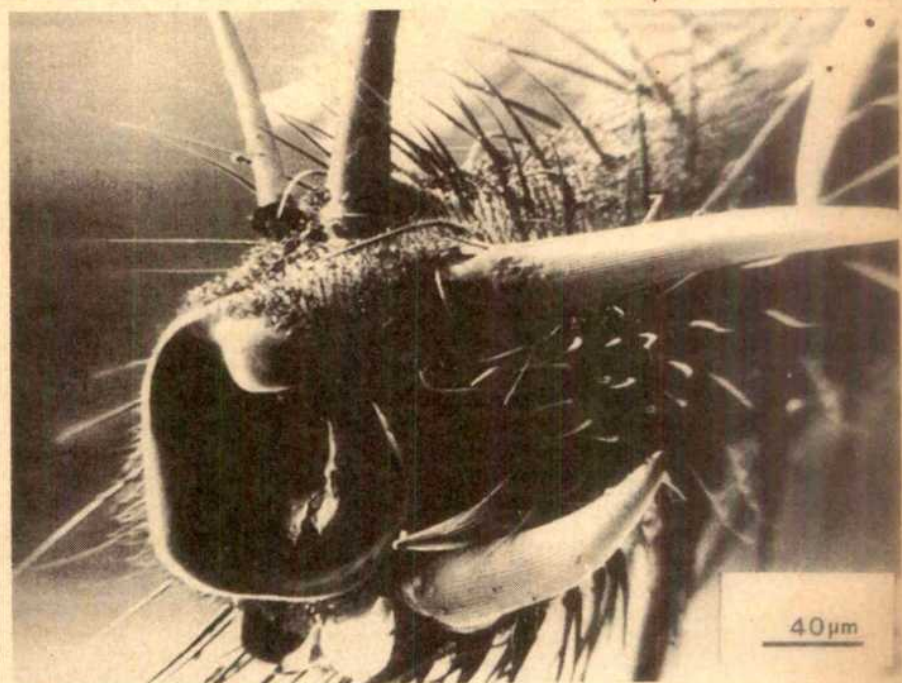
Pharmacia's DNA synthesizer monitors efficiency

sembly, however, is a useful extra that more expensive systems do not offer.

The automated synthesizer from Systec can add up base additions to as little as 5 nmol while maintaining high coupling efficiencies and reagent consumption at a



Systec's new gene machine



It looks like a still from a monster movie, but this image, captured by IBT Dubilier's liquid metal focused-ion-beam column, is just a very close look at a horsefly's foot. The FIB-50 is the first commercially available column of its kind to achieve a resolution below 50 nanometres (Reader Service No. 102). The above micrograph demonstrates the instrument's performance in scanning ion microscopy. Samples, including insulators, require no preparation beyond mounting.

The FIB-50 uses gallium, which melts at

cost of less than \$1.00 per cycle (Reader Service No. 101). Systec's assembler works with any current phosphate or phosphite methods, and any scale from  $1/2$  to 10  $\mu\text{M}$ . Menu-driven software and a colour CRT terminal make the Microsyn-1500 a pleasure to use, but not without a price: Systec's introductory offer for the system is \$28,600 (US). Oligonucleotides well in excess of 100-mers can be constructed and the controlled glass pore columns are reusable. Systec's assembly does not include a monitoring system, however, that would stop the synthesis if an incomplete coupling took place.

## Bits and pieces

Supercoiled nucleic acid markers alleviate the need to digest DNA for sizing. Gibco BRL has increased its range of markers to include supercoiled DNA and RNA 'ladders' in broad size ranges (Reader Service

No. 103). Eleven supercoiled plasmids from 2 to 16 kb long comprise the DNA marker package, and the RNA ladders will size RNA between 0.3 and 9.5 kb. Gibco also sells a single 7.5 kb RNA marker for use in gauging the efficiency of reverse transcription copying. The markers are sold in 25 to 75  $\mu\text{g}$  quantities.

An improvement on nick translation for creating DNA labelling probes is being



Polymeraid makes DNA probes straight from gel fragments

promoted by P & S Biochemicals Ltd. The Polymeraid system, at \$135 (US) per kit,

generates single-stranded probes that incorporate more than  $1 \times 10^6$  c.p.m. per  $\mu\text{g}$  from any size restriction fragment (Reader Service No. 104). Polymeraid uses fragments straight from low melting point agarose gels, eliminating the need for further purification techniques. Each kit contains reagents, buffer and nucleotides for 25 reactions.

Clontech has added several new **cDNA and genomic libraries** to their stock (Reader Service No. 105). The *Saccharomyces cerevisiae* X2180 genome is now available in lambda gt11 for \$360 (US), as is mouse spleen cDNA. Human adrenal and hepatoma cDNA in the gt11 vector can also be purchased for \$450 (US). Clontech supplies human lymphocyte cDNA in gt10 for the same price. The company has many more genomic libraries and rat, bovine and human cDNA pending release on the market.

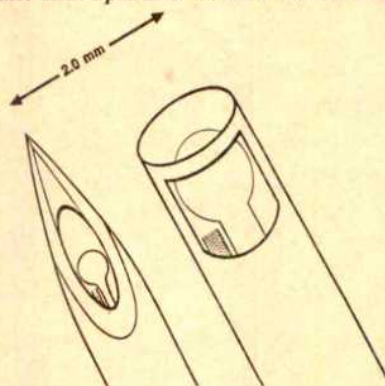
CompuGene's **DNA sequence gel reader** uses a 'talk back' feature to help prevent mistakes in sequence reading (Reader Service No. 106). With a pen to encode the base order, the analyser never has to lift his or her eyes from the gel because CompuGene's machine actually says which base it has recorded. This system hastens scanning considerably, so that 300 nucleotides can be logged in less than 5 minutes. Results from two separate readings can be compared for inconsistencies, and a final verified sequence can be stored in 15 minutes. The gel reader sells for \$4,950 (US) with a reading stand, pen,

digitizer, software and hook-up cables.

*In situ* hybridization with fresh or frozen cells or tissue can be accomplished through autoradiography and Oncor's hybridization kit (Reader Service No. 107). Oncor's kits will **label DNA and RNA targets** with no DNA extraction involved. Formalin-fixed, paraffin-embedded samples will not take to Oncor's method, but almost any other fresh or frozen specimen will. A complete starter kit, including reagents, protocol and equipment, costs £385 (UK) and will service 20 slide hybridizations. Stratech Scientific distributes Oncor's kit in the UK.

## Acid and alkaline

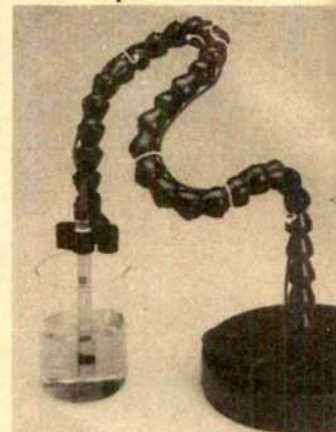
World Precision Instruments markets hand-made **pH microelectrodes** with bulbs



**Big advances for small electrodes** only 300  $\mu\text{m}$  across (Reader Service No. 108). The 'home-brewed' glass WPI uses one-fifth the resistance of the glass

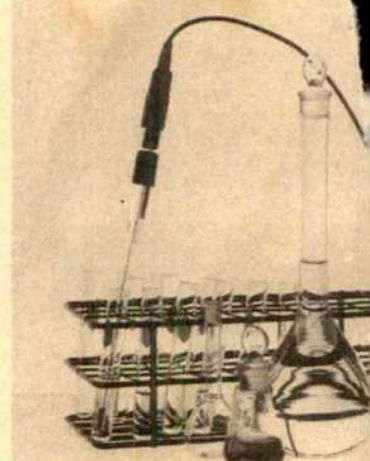
typically used in these applications and improving the quality of microscopic measurements are available in 20-gauge microneedles 0.9 mm in diameter. The ended models with a diameter and a stem length of 100 mm. They cost \$295 (US) and have a s approximately one year.

The Cobra is a flexible yet holder for pH electrodes and o

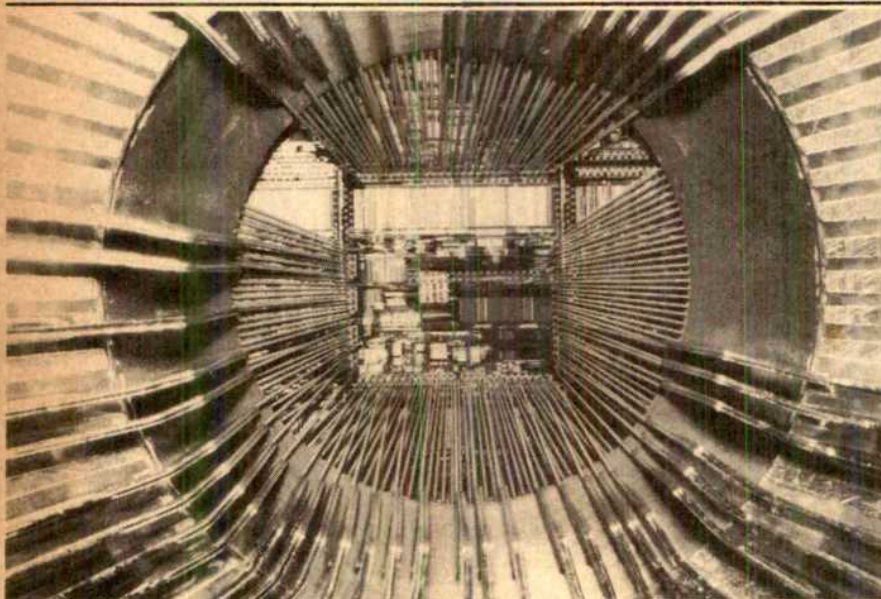


**The Cobra gets a grip on pH electrodes** (Reader Service No. 110). Its base secures a 24-inch arm that bends around corners. Whatman sells extra vertebrae for the \$79 (UK), so that its length can be adjusted. The instrument's design makes the electrode holders seem awkward, may save the occasional solution, takes a spill when a holder decides to go own way.

Beckman Instruments has a **bio-activity electrode** with a Calomel reference half-cell, small enough to fit in test tubes (Reader Service No. 111). The F-1 features a fill solution that will not alter biological and metallic samples. It comes with a one-year warranty, \$1,100 (US). Its size makes it compatible with almost any glassware used by biologists.



**Beckman's electrode won't alter bio-activity**

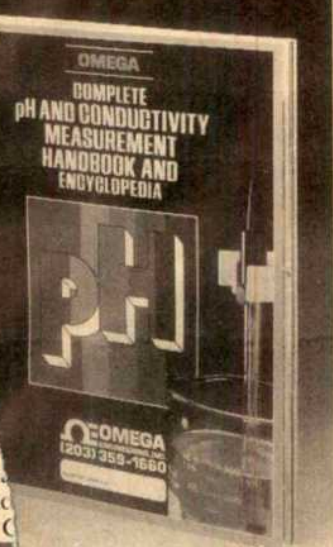


**WITHIN** this 32-bit chip lies the circuitry know-how for IBM's system/370, the most widely used computing instructions for their larger and faster mainframes (Reader Service No. 109). Earlier this year IBM researchers put 370 instructions directly into the microprocessor's read-only mem-

ory (ROM), and tested its operations with the 171 probes radiating from the chip's edges in the above photograph. The miniaturized 'mainframe on a chip' may enable desk-top computers to run off the same software that's the driving force behind IBM's large-scale computer success.

## NEW ON THE MARKET

The 1986 pH and Conductivity measurement Handbook and Encyclopedia from Omega lists hundreds of products in over 100 full-colour pages (Reader Service No. 112).



*...a pH rundown*

No. 112). The catalogue gives specifications, and technical data sheets covering everything from pH electrodes to data acquisition systems. It also offers catalogues on temperature measurement, pressure and flow and level.

### Basics

CASE, the database of the American Chemical Society, will get a 2-million-dollar cost by mid-1986. Chemical Abstracts Service has made plans to re-key its published between 1967 and 1985 which were never rendered in readable form (Reader Service No. 113). AS ONLINE at present covers journals and 6.5 million papers. Some abstracts will be available at no cost. CAS charges an initial fee of \$50 (US), with supplemental charges for access time and

An average. The service includes access speeds to a registry file of 7.6 million minute substances, which can be efficiently name or structure. CAS expects to have a more detailed patent file and a reaction file in place sometime in 1987.

Another reference searching and citation service, Autoscribe Ltd has a program exists to store author, year, title, source, even and key words in any specified format (Reader Service No. 114). The Martz-BIBLIOFILE uses on the strength fields with an upper limit of 100 characters which can be searched. Typically sorted and saved for final use.

In a suitable text editing program, each disk space holds an average

## Laser exchange goes European

WHAT happens to lasers that are no longer wanted? Europe's first laser exchange offers an alternative to abandoned equipment, and to buyers who'd like to benefit from the reduced cost of a system that's already been 'broken in' (Reader Service No. 115). Multic GmbH and its Austrian sister company Physiktechnik began co-ordinating trade deals between laser owners and buyers last summer; since then, Multic's Peter Brandstetter says they have located new homes for over 100 lasers and laser systems. The exchange publishes a newsletter with full descriptions and prices. Transatlantic swaps can be arranged through Laser Resale, the American exchange that inspired European efforts. Commissions averaging about 10 per cent are assessed on the seller at a transaction's completion; otherwise the service is free.

of 400 references, and a single database can be split over two or more disks.

The software costs £250 (UK), and can be used with standard ASCII files in all popular word processors.

Medline and Life Sciences databases are no longer just on-line phenomena. Cambridge Scientific Abstracts has put both collections on compact optical disks for use with IBM PCs (Reader Service No. 116). The disks are updated quarterly and sold as a two-disk set, or separately. Medline, a source for biomedical literature, operates through an agreement with the US National Library of Medicine and the Department of Health and Human Services, to provide indexes for about 20,000 articles every month. The life sciences database indexes more than 98,000 abstracts each year from over 5,000 publications. A two-year subscription to both collections costs \$8,500 (US), including a \$500 charge for purchase of a CD reader. Separately, the Medline database is priced at \$6,350 with a reader, and the Life Sciences disk is \$3,650.

### Methods memos

Ciba Corning Diagnostics has a forty-page brochure that describes the operation and methodology of flame photometry (Reader Service No. 117). A Guide to Flame Photometer Analysis outlines the apparatus, preparation and quantitation of alkali and alkaline earth metals, and describes 22 application methods including the determination of calcium in beer.

Mass detection can be the most useful type of HPLC detection for separations of polymers, resins, lipids and carbohydrates. Applied Chromatography Systems

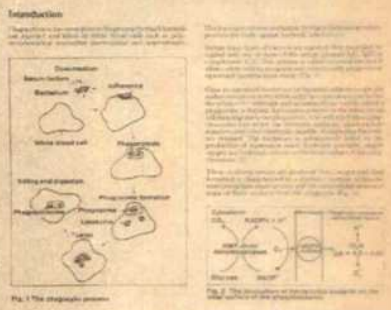
publishes a bibliography of applications for their model 750/14 mass detector (Reader Service No. 118). ACS's detector uses the principle of separating the solvent from the sample, then distinguishing components by light scattering techniques.

To help the potential user judge the feasibility of LC/MS techniques, Kratos Analytical supplies their LC/MS Data Compilation Book (Reader Service No. 119). Kratos' brochure reviews the applications and accomplishments of LC/MS techniques, with attention to typical problems and solutions, and represents the broad range of research that the technique can address.

The measurement of phagocytosis by chemiluminescence has become an important technique in analysing the body's immune response. LKB Instruments discusses the principles of such measurement in their application note 513, entitled *The study of phagocytosis and opsonisation using luminol-enhanced chemiluminescence* (Reader Service No. 120). The note includes exact experimental details on cell preparation, reagent specifications and

### Luminescence TODAY

#### The study of phagocytosis and opsonisation using luminol enhanced chemiluminescence



APPLICATION NOTE 513

Chemiluminescence news from LKB assay equipment. Graphic examples illustrate normal versus defective serum responses.

A new series from Whatman addresses themes in thin layer chromatography and invites contributions from readers (Reader Service No. 121). Past issues of the *Whatman Chromatography Folio* have focused on preadsorbent and high performance TLC, describing how to maximize the usefulness of these methods. The complete folio comprises a reference source for all chromatographers. □

*These notes are compiled by Karen Wright from information provided by the manufacturers. To obtain further details about these products, use the reader service card bound inside the journal.*

# Training for competitiveness

from Richard Pearson

*"The same machines and equipment can be bought by anybody; success in the market goes to those who have a workforce that can use them to best advantage."*

INVESTMENT in people is being seen as the key to economic success once again. The 1960s saw the growing acceptance of the concept of 'human capital' and 'human asset accounting', and in the United Kingdom legislation set up an infrastructure to stimulate and manage training, and to redistribute its costs between the trainers through the Industrial Training Boards. By the late 1970s little progress had been made, the bureaucracies were seen to have taken over, and the incoming Conservative government enacted legislation which led to the demise of most of the training boards. In the mid-1980s training is back in vogue and the publication of *Competence and Competition* (HMSO, 1984; see *Nature* 313, 82; 1985) was part of a new campaign to boost training in the United Kingdom. It highlighted the United Kingdom's 'poor' training performance relative to West Germany, Japan and the US countries where individuals, employers and the state all placed greater value on training, seeing it as necessary capital investment, rather than as a cost.

A survey of UK employers in 1984 showed that while 90 per cent of managers recognized the importance of training, only one in three adults had received any training in the previous year. Private-sector establishments were estimated to have spent over £2,000 million on training adults that year, which averaged £200 per employee or £575 per trainee. Two-thirds of the training was done on-the-job, the rest through courses, with 4 per cent via evening classes and distance learning (Fig. 1).

While the link between training and a company's performance is hard to prove, it was shown that high-performance businesses, defined as those that were profitable, growing and innovating, were twice as likely to be training their staff as were low performers. They also trained twice as many staff and had increased their volume of training by over 25 per cent in the previous five years. By contrast, the low performers had cut their training by as much as 20 per cent over the same period.

The most recent major report in support of the national training campaign is *A Challenge to Complacency: Changing Attitudes to Training* (MSC/NEDO, 1985) which sought to identify the 'why' of our low training performance and hence the scope for encouraging companies to increase their investment in training. The report makes depressing reading. It shows

employers' lack of concern about training and highlights the widespread ignorance among top management as to the scale of resources their organization devoted to training. Decisions about training were predominantly taken by line managers who inevitably focused on short-term needs. In technical areas this is often manifest as a willingness to send people to conferences or short courses to pick up the latest technology, but a neglect or lack of

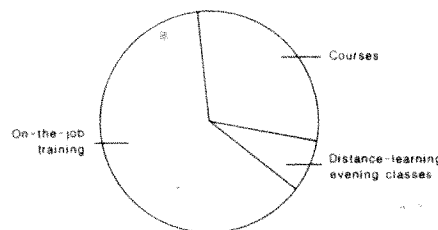


Fig. 1 Types of training. On-the-job training, courses and distance-learning/evening courses annually occupy 34 million, 17 million and 2 million days respectively. (Source: IMS)

interest in the longer-term development of staff. Little attention is paid to the analysis of training needs or evaluation of its results, and training managers and departments have relatively low status. Training is seen as a cost and overhead, to be cut when profits are under pressure, rather than as an investment in the future. In Britain, training was cut in the recession, while in West Germany and Japan the pressure was to increase the level of training given. As the remark made by a West German employer and shown in the introduction reveals, other countries are well aware that competitive advantage can only come through attuning people to a technological world.

The reluctance to invest in training was put down to uncertainties about future prospects and technological change, worries about 'poaching' by other employers and poor experiences with some external trainers. High trainee wage costs were not seen as a problem. At the same time there was little pressure from individual employees or unions, external commentators and investors, or from the government to do better, although the picture is beginning to change.

A number of proposals have been put forward to improve matters. For employers, the preparation and dissemination of case studies showing the links between training and performance are seen to be important. Employers should also be en-

couraged to report regularly on the training. This will require the development of training indicators, initially focusing on inputs such as man days, money invested (not cost!), type of training whether it be on-the-job or off-the-job training staff employed and so on. The process of collecting such data would be a major innovation for many companies and is likely immediately to raise the general awareness of training. In the longer term indicators of training output or performance need to be developed but this will take some time. Individual employees can be an important stimulus for more training; in the United States, for example, it is notable the extent to which individuals seek out and invest in training. In the United Kingdom it is suggested that Individual Training Credits (ITCs) to which individuals and employers contribute, a for occupational pensions, should be set up to pay for approved training. The ITC would need to be transferable so that the could be stored and used to retrain between jobs for example, and could also be used to incorporate grants to individual for example at the start of working life or following redundancy. They could also help share the costs of training more equitably and reduce the fears of loss due to poaching. Of course, if training was at a much higher level overall, there would be less poaching in the first place.

The report also argues the need to improve the operation of the training market, for example by helping colleges to become more responsive to market needs and to improve the working of local labour markets and collaborative training arrangements. Another need is for better information on training availability; at present, many training specialists are confused at the wide variety of training offered and find it difficult to choose the most relevant and effective course. While registers and databases help as to availability, ideally more qualitative assessments are also needed. Many other mechanisms such as grants and fiscal measures are also reviewed in the report.

The analyses of the need to train are getting more frequent, hopefully raising the awareness of its value to employee and employer alike. Time will tell if this translates into an analysis of training needs which is then acted upon.

Richard Pearson is at the Institute of Manpower Studies, Manuell Buildings, University of Sussex, Brighton BN1 9RF, UK.